conference
VPH2026
One society, a whole ecosystem

ABSTRACT BOOK



ASSESSMENT OF THE PREDICTIVE PERFORMANCE OF A FLUID-STRUCTURE-GROWTH MODEL FOR ASCAA

Kexin Yan (1,2,3), Wenfeng Ye (1), Antonio Martínez (1), Leonardo Geronzi (4), Pierre Escrig (2), Jacques Tomasi (2), Michel Rochette (1), Pascal Haigron (2), Aline Bel-Brunon (3)

1. ANSYS, France; 2. Univ Rennes, France; 3. Univ Eiffel, France ; 4. Univ Rome, Italy

1. Introduction

Growth and remodeling models have been developed to compute the evolution of biological structures subjected to alterations of their behaviour or mechanical loading, in their attempt to recover a homeostatic state. In the scope of Ascending Aortic Aneurysm (AscAA), a few studies applied those methods to patient cases [1] but their predictive capability were not assessed. In a previous work [2], we implemented a fluid-structure-growth (FSG) workflow; on one patient case, the model parameters were calibrated to reproduce the observed AscAA growth after two years. In this work, we evaluate the capability of our FSG model to predict the growth four years after the baseline imaging.

2. Materials and Methods

The patient case of this work is a 62 year-old male with a baseline (BCT), 2-year (2YCT), and 4-year (4YCT) Angio-CT scans available. The aortic arch geometry was segmented, remeshed and clipped on each imaging set.

The FSG workflow consists of a Computational Fluid Dynamics simulation (Ansys Fluent) of flow within the aortic arch, from which we extract the distribution of Time-Averaged Wall Shear Stress (TAWSS). The normalized value of TAWSS drives the elastin degradation function within the aortic wall. Then a structural simulation (ANSYS APDL) of growth is performed, starting with the evaluation of prestretch and considering the aortic wall as a mixture of elastin, collagen and smooth muscle cells. The full description of the workflow is available in [2].

To evaluate the FSG workflow predictive ability, we adopted three simulation strategies: (1) simulating 4Y growth maintaining the same conditions and material parameters as for the 2Y simulation, (2) simulating 4Y growth after updating the TAWSS distribution at 2Y through CFD simulation on the 2Y geometry, and (3) simulating 4Y growth after both TAWSS and mechanical support stiffness update after 2Y, to mimic the constraining effect of pericardium.

3. Results

The computed growth after 4Y without update exhibited localized growth (Figure 1); updating TAWSS allowed to better spread growth along the AscAA. Stiffening the mechanical support resulted in controlled growth in the pericardium vicinity.

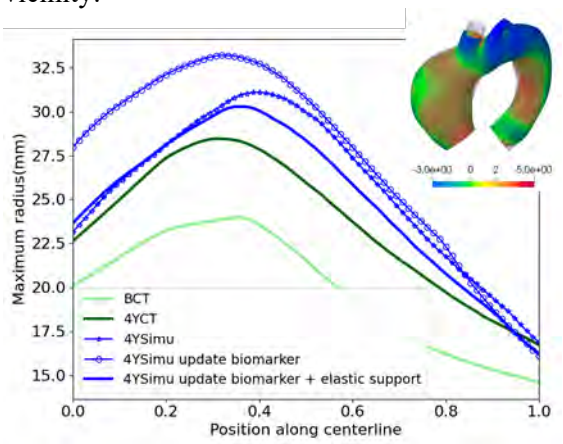


Figure 1: Radius evolution along the AscAA depending on the FSG simulation strategy. Top: Gap between 4YCT (colored) and 4YSimu (transparent) in [mm] for strategy (3)

4. Discussion and Conclusions

This study shows that calibrating FSG models is complex and regular update of the simulation conditions is probably necessary to promote predictive capabilities of these models. Acquiring reliable longitudinal data to assess the FSG model performances is the key to further improvement.

5. References

1. Mousavi SJ et al., Biomech Model Mechan. 18:1895-1913 (2019).
2. Yan K et al., Biomech Model Mechan. 24:405-422 (2025)

Acknowledgements:

This study was partially funded by ANRT (France) under CIFRE Agreement No. 2021/1446.

AN EXPERIMENTALLY VALIDATED INVERSE APPROACH FOR PATIENT-SPECIFIC CHARACTERIZATION OF AAA MECHANICS

Gaia Caruso(1), Andrea Guala(3,4), Lydia Dux-Santoy(3), Gisela Teixidó-Turà(3,5), José F. Rodriguez-Palomares(3,4,5), Mireia Bragulat-Arévalo(3,4), Sergi Bellmunt(5), Marvin García-Reyes(5), Miguel A. Martínez(1,2), Estefanía Peña Baquedano(1,2)

1. Aragón Institute for Engineering Research (I3A), University of Zaragoza, Spain; 2. CIBER-BBN, Centro de Investigación en Red en Bioingeniería, Spain; 3. Vall d'Hebron Institut de Recerca, Barcelona, Spain; 4. Biomedical Research Networking Center on Cardiovascular Diseases, CIBER-CV, Instituto de Salud Carlos III, Madrid, Spain; 5. Department of Vascular Surgery, Hospital Universitari Vall d'Hebron, Barcelona, Spain.

1. Introduction

Current abdominal aortic aneurysm (AAA) rupture risk assessment is primarily diameter-based [1], while patient-specific, non-invasive evaluation of wall mechanics remains limited.

2. Materials and Methods

Four patients with AAA underwent 3D-cine magnetic-resonance (MR). Image-derived systolic-diastolic displacement fields were extracted from segmented luminal geometries. Patient-specific finite element (FE) models incorporating AAA wall and intraluminal thrombus (ILT) domains were developed. The AAA wall was modeled using an anisotropic hyperelastic Gasser-Holzapfel-Ogden formulation [2], while the ILT using a Neo-Hookean model [3]. A Bayesian inverse framework based on Gaussian Process Regression (GPR) was implemented to calibrate wall and ILT material parameters by minimizing the discrepancy between FE-predicted and MRI-derived displacement fields. Model predictions were independently validated against equibiaxial mechanical testing performed on aneurysmal wall specimens of the same four patients harvested during surgery.

3. Results

The Bayesian-calibrated models reproduced patient-specific displacement patterns with good spatial agreement across all cases, with consistently low RMSE values.

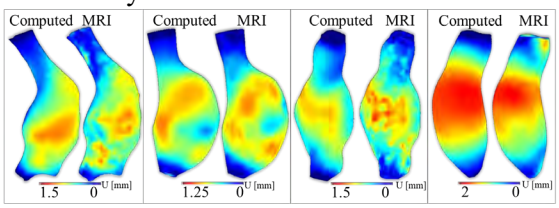


Figure 1: MRI-registered VS FEM computed displacements through AAA inner wall with optimized constitutive materials.

Material parameters identified non-invasively from imaging data yielded equibiaxial stress–stretch responses closely matching experimental measurements.

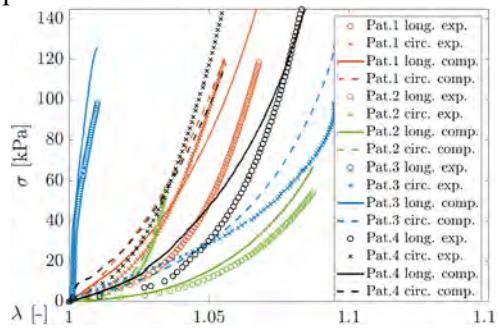


Figure 2: Experimental VS computed equibiaxial test curves (longitudinal, circumferential directions).

4. Discussion and Conclusions

We propose a fully non-invasive, data-driven framework integrating MRI-derived kinematics, nonlinear FE modeling, and Bayesian optimization to calibrate patient-specific AAA mechanics and improve risk stratification.

5. References

1. Choke, E.; *European J. of Vasc. and Endovasc. Surgery*, 2005.
2. Gasser, T.C.; *J. of the Royal Society Interf.*, 2006.
3. Vande Geest, J.P. *J. of Biomechanics*, 2006.

Acknowledgements:

This work is supported by project PID2022-140219OB-I00 funded by MICIU/AEI/ 10.13039/501100011033, by the "European Union NextGenerationEU/PRTR" I00 and the regional Government of Aragón support for the funding of the project T24-20R, by FSE+PRE2023 UZ-18 funded by MICIU/AEI/10.13039/501100011033 and by "ESF Investing in your future", by "ESF+". CIBER Actions are financed by the Instituto de Salud Carlos III with assistance from the European Regional Development Fund.

Predicting Hemodynamics from Aortic Geometry

José Marín (1), Arnau Bayón (2), Francisco Martínez-Gil (1), Pau Romero (1, 3), Miguel Lozano (1), Ignacio García-Fernández (1)

1. CoMMLab – Computational Multiscale Simulation Lab, University of Valencia, Spain; 2. Department of Hydraulic and Environmental Engineering, Universitat Politècnica de València, Spain; 3. Department of Molecular Medicine and Surgery, Karolinska Institutet, Solna, Sweden.

1. Introduction

Wall shear stress (WSS) and pressure distributions in the thoracic aorta are relevant biomarkers for vascular remodeling, aneurysm progression, and atherosclerosis, but their computation through computational fluid dynamics (CFD) is too time-consuming for routine use. This work proposes a deep learning surrogate model that predicts full aortic wall WSS and pressure maps directly from geometry, reducing inference from hours to milliseconds.

2. Materials and Methods

Thoracic aorta geometries were encoded using the Vascular Encoding Framework (VEF), which provides point-to-point correspondence across anatomies through a vessel coordinate system [1]. A PCA-based statistical shape model was built from 32 real cases and used to generate physiologically plausible synthetic aortas by rejection sampling, yielding 780 cases in total [2]. Each geometry was simulated in OpenFOAM under steady incompressible RANS conditions with SST k-ω, using four inlet peak systolic velocities (1.2–1.5 m/s). Geometric descriptors and CFD-derived hemodynamic fields were projected onto 128×128 projection maps. A U-Net received 11 input channels (10 geometric channels plus inlet velocity) and predicted two outputs: wall WSS and pressure. Training used 4-fold cross-validation and a composite loss combining MSE, Smooth L1, gradient, and SSIM terms.

3. Results

Under 4-fold cross-validation, the model achieved mean R^2 = 0.906 for WSS and R^2 = 0.949 for pressure, with SSIM values of 0.832 and 0.876, respectively. Mean RMSE was 0.065 for WSS and 0.051 for pressure. Qualitatively, predicted maps reproduced both global flow patterns and localized high-gradient regions, with pressure being more accurately reconstructed than WSS due to its smoother spatial distribution.

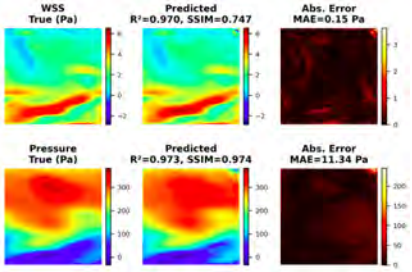


Figure 1: Prediction example from the test set. Images show the true CFD field, the U-Net predicted field, and the absolute error map, with the R^2, SSIM and MAE values annotated on the panel.

4. Discussion and Conclusions

The results show that thoracic aortic hemodynamics can be estimated accurately from geometry alone when anatomy is represented in a spatially consistent way. A key contribution is the use of VEF not only for statistical shape modeling and synthetic data generation, but also for transforming irregular vascular surfaces into aligned projection maps compatible with convolutional architectures. This enables accurate prediction of patient-specific WSS and pressure without running CFD at inference time. Current limitations include steady-state simulations, Newtonian flow assumptions, and restriction to single-branch vessels.

5. References

[1] Romero P, Pedrós A, Sebastián R, Lozano M, García-Fernández I. A robust shape model for blood vessels analysis. Appl Math Comput. 2025;487:129078.

[2] Romero P, Lozano M, Martínez-Gil F, Serra D, Sebastián R, Lamata P, García-Fernández I. Clinically-driven virtual patient cohorts generation: an application to aorta. Front Physiol. 2021;12:713118.

Acknowledgements:

Supported in part by: Generalitat Valenciana Grant AICO/2021/318, CIAICO/2024/247 (Consolidables), PID2020-114291RB-I00 and PID2023-148702OB-I00 funded by MCIN/10.13039/501100011033 and by "ERDF A way of making Europe".

EXPERIMENTALLY VALIDATED COMPUTATIONAL MODELLING OF FLOW REVERSAL IN TYPE B AORTIC DISSECTION

Marco Correnti (1,2)*, Manideep Roy (3)*, Sofia Di Leonardo (1,2), Alessandra Monteleone (1), Ruth P. Lim (4,5), Andrew Ooi (6), Giorgio Micale (2), Suman Chakraborty (3,7) and Gaetano Burriesci (1,2,8)♦

1.Ri.MED Foundation, Palermo, Italy; 2.Engineering Department, University of Palermo, Italy; 3.School of Medical Science and Technology, Indian Institute of Technology Kharagpur, India; 4.Department of Radiology, Austin Health, Australia; 5.Departments of Radiology and Surgery, The University of Melbourne, Australia; 6.Department of Mechanical Engineering, The University of Melbourne, Australia; 7.Department of Mechanical Engineering, Indian Institute of Technology Kharagpur, India; 8.UCL Mechanical Engineering, University College London, UK

*Contributed equally, ♦Corresponding author: Gaetano Burriesci, gburriesci@fondazionerimed.com

1. Introduction

Type B aortic dissection (TBAD) is a severe aortic pathology that splits the vessel into two competing flow channels, known as the true and false lumens [1]. Although computational fluid dynamics (CFD) has been widely employed to investigate the complex haemodynamics associated with this condition, robust experimental validation of these models remains limited [2]. In fact, *in vitro* studies are particularly challenging due to the anatomical and fluid-dynamic complexity of the model [3]. To address this limitation, this work presents a coupled experimental-computational framework to investigate haemodynamics of TBAD under pulsatile flow conditions, with focus on the unsteady flow reversal mechanism within the false lumen.

2. Materials and Methods

An optically transparent silicone phantom was fabricated from computed tomography data using a polyvinyl alcohol (PVA) sacrificial moulding technique [4]. The model was tested under physiological flow conditions in a hydromechanical pulse duplicator (ViVitro, ViVitro Labs, Canada) hosting St. Jude bileaflets mechanical valves. Fluid dynamics was analysed by means of phase-resolved 2D-PIV. Concurrently, CFD simulations were performed via stabilised finite element analysis, with the experimentally measured inflow waveform and calibrated Windkessel models at the outlets.

3. Results

Experimental and computational velocity fields showed strong agreement. Both captured a phase-dependent flow reversal: forward flow was observed in both lumens during peak systole, whereas systolic deceleration induces a localised backward flow that promoted vortex formation near the entry tear. In addition, time-averaged wall shear stress and oscillatory shear index were quantified to assess haemodynamics conditions associated with clinical risk.

4. Discussion and Conclusions

This combined experimental-numerical study investigates TBAD hemodynamics, highlighting a distinct flow reversal in the false-lumen. The validated computational model shows that this phenomenon generates a low-shear, highly oscillatory environment that may promote thrombus formation. Overall, the proposed cyber-physical platform establishes a robust pathway connecting complex flow physics to clinically relevant risk indicators.

5. References

[1] D.P.J. Howard, *et al.*, *Circulation* **2013**, *127*, 2031.

[2] M. Wu, *et al, Journal of Endovascular Therapy* **2025**, *32*, 303.

[3] G. Franzetti, *et al*, *J. Biomech.* **2022**, *134*, 110963.

[4] G. Annio, *et al*, *J. Eng. Sci. Med. Diagn. Ther.* **2020**, *3*.

Acknowledgements:

The authors acknowledge the AIRS Fellowship, SERB (India), the Royal Australian and New Zealand College of Radiologists and the Regione Siciliana (Italy) for financial support. We also thank Emma Hornsey from Austin Health for imaging assistance.

PREDICTING POST-TEVAR ENDOLEAKS: A PRE-OPERATIVE RISK FACTOR FROM FLUID-STRUCTURE INTERACTION SIMULATIONS

Francesca Duca (1), Silvia Tavarone (1), Maurizio Domanin (2,3), Daniele Bissacco (2,3), Santi Trimarchi (2,3), Francesco Migliavacca (1,3), Christian Vergara (1)

(1) LaBS, Dipartimento di Chimica, Materiali e Ingegneria Chimica, Politecnico di Milano, Italy; (2) Department of Clinical Sciences and Community Health, Università degli Studi di Milano, Italy; (3) Section of Vascular Surgery, Fondazione IRCCS Ca' Granda Ospedale Maggiore Policlinico Milano, Italy

Corresponding author: francesca.duca@polimi.it

1. Introduction

To prevent Endoleaks (ELs) formation after Thoracic Endovascular Aortic Repair (TEVAR), adequate stent-graft stability at the Landing Zones (LZs) is essential. In this study, we apply the Fluid-Structure Interaction (FSI) framework proposed in [1] to ten pre-operative patient-specific Thoracic Aortic Aneurysm (TAA) cases, with known post-TEVAR outcomes, aiming to propose a hemodynamic risk factor for predicting type I and III ELs.

2. Materials and Methods

Ten patients are selected for this study and, at the time of the last follow-up, five of them showed an EL. By means of life^X [2], we perform an FSI simulation in each pre-operative scenario to compute the risk factor R:

$$R = \frac{DF_{\perp} \cdot DF_{||} \cdot p_{tortuosity}}{10^6} \qquad (1)$$

where $DF_{\perp}$ and $DF_{||}$ are the drag forces perpendicular and parallel components to the vessel centerline, and $p_{tortuosity}$ is the EL formation probability based on the tortuosity [3]. R is computed for each Proximal (P), Distal (D) and Overlap (O) LZ, and it is then scaled to the interval [0,1]. The patients' cohort is divided into two groups: a calibration set, used to associate specific R values with different risk levels, and a validation set, employed to validate the predictive capability of R.

3. Results

In the calibration set, nearly all LZs affected by ELs exhibit $R \geq 0.94$, while almost all LZs without complications have $R \leq 0.20$ (see Table 1). Thus, we associate low risk of EL formation for LZs with $R \leq 0.33$, moderate risk for those with $0.33 < R \leq 0.67$, and high risk for LZs with $R > 0.67$ (see Figure 1).

Patient	PLZ	DLZ	OLZ-1	OLZ-2
CALIBRATION SET				
PT-09	0.62	0.00	0.00	-
PT-10	0.00	1.00	0.71	-
PT-21	0.94	0.00	0.11	-
PT-22	0.39	0.04	0.14	-
PT-23	0.02	0.18	-	-
PT-50	0.15	0.00	0.00	1.00
PT-51	1.00	0.08	0.96	1.00
PT-78	0.00	0.00	0.01	-
VALIDATION SET				
PT-40	0.00	0.00	0.11	-
PT-67	0.23	1.00	0.06	0.32

Table 1 R values for all patients. Red numbers indicate type I EL cases, while purple numbers type III EL cases.

In the validation set, R predicts the occurrence of a type I EL (see Table 1 and Figure 1).

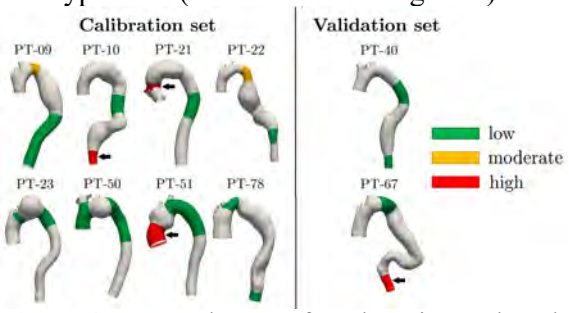


Figure 1 PLZ and DLZ of each patient coloured according to the risk of type I EL formation predicted by R. Black arrows indicate where the EL occurred.

4. Discussion and Conclusions

This study represents a first attempt to investigate a possible relationship between pre-operative hemodynamics and post-TEVAR outcomes.

5. References

1. Duca F et al., J. Physiol; 2025.
2. Africa PC., SoftwareX; 2022; 20:101252.
3. Ueda T et al., AJR; 2011; 197(6):1140-6.

A CFD-LABELLED SYNTHETIC DATASET OF HAEMODYNAMICS IN ABDOMINAL AORTIC ANEURYSM

Vijay Nandurdikar (1), Tejas Canchi (2), Alistair Revell (1), Alejandro F. Frangi (1,3), Ajay B. Harish (1)

1. School of Engineering, University of Manchester, UK
2. University of Sydney, Australia
3. School of Health Sciences, University of Manchester, UK

1. Introduction

Currently, the Abdominal Aortic Aneurysm (AAA) rupture risk stratification relies on maximum diameter alone. Haemodynamic biomarkers, derived from Computational Fluid Dynamics (CFD) simulations, such as wall shear stress (WSS), time-averaged WSS (TAWSS), and oscillatory shear index (OSI) have been shown to have strong correlation to rupture risk [1,5]. However, patient-specific CFD is prohibitively expensive at clinical and cohort scale. Machine learning (ML) surrogates require large annotated datasets that do not currently exist for AAA haemodynamics. In addition, most of the existing datasets contain geometries, largely from men only. We present a CFD-labelled synthetic AAA population designed as a training resource for machine learning surrogates.

2. Materials and Methods

Synthetic population. Statistical distributions were fitted to six anatomical parameters from 258 real AAA patients using maximum likelihood estimation. Demographically stratified sampling produced 182 synthetic geometries spanning males and females across four age bands (50–59 to 80+). Each case was morphed from a reference geometry preserving clinically realistic proportions.

CFD simulations. All 182 geometries were solved in OpenFOAM under pulsatile laminar flow with plug and parabolic inlet profiles (364 simulations total). Six haemodynamic biomarkers were extracted per case alongside eleven geometric descriptors.

ML framework. The usage of the dataset for ML-development is demonstrated through a Bayesian-GNN surrogate which is used to encode each aneurysm as a centreline and surface graph. The Bayesian-GNN enables quick prediction of haemodynamic biomarkers while considering calibrated uncertainty via deep ensembles [3].

3. Results

The proposed framework enables generating synthetic AAA geometries stratified by sex and age group, sampled from patient-derived statistical distributions. Pearson correlations across 364 simulations identified proximal neck diameter as the dominant haemodynamic modulator (WSS_{mean}: $r = 0.77$, $p < 0.001$; $WSS_{95\%}$: $r = 0.58$, $p < 0.001$), while shape compactness (sphericity, convexity) governs oscillatory shear. Maximum diameter primarily determines low-shear area extent rather than peak stress, directly challenging its primacy as a risk surrogate. This fully labelled dataset (182 geometries, 364 simulations, 17 variables per case) now forms the training resource for the proposed GNN surrogate.

4. Discussion and Conclusions

This work contributes the first demographically stratified, CFD-labelled synthetic AAA population designed explicitly as an ML training resource. The GNN surrogate will be, to our knowledge, the first trained on a synthetically generated AAA population; prior GNN haemodynamic surrogates rely exclusively on patient-specific cohorts [2]. GNN surrogate development is underway; full results will be presented at the conference. Future work will target transfer learning from this synthetic cohort to patient-specific geometries to close the domain gap identified in recent benchmarks [4].

5. References

1. Gasser TC, Auer M, Labruto F, Swedenborg J, Roy J. Eur J Vasc Endovasc Surg. 2010;40(2):176–185.
2. Rygiel P, Suk J, Brune C, Yeung KK, Wolterink JM. arXiv:2507.22817. 2025.
3. Lakshminarayanan B, Pritzel A, Blundell C. NeurIPS. 2017;30.
4. Nannini G et al. Comput Biol Med. 2025;195:110477.

5. Nandurdikar V et al. bioRxiv. 2026. doi:10.64898/2026.02.27.708461.

Acknowledgements:
Authors would like to thank The University of Manchester for the funding to Vijay through the Dean's scholarship that supported this work.

BIOMECHANICS OF HUMAN AORTA: SPATIAL AND DEMOGRAPHICAL VARIATIONS

Ankush Aggarwal, Ji-Eun Byun, Andrew McBride

Glasgow Computational Engineering Centre, University of Glasgow, Glasgow United Kingdom

1. Introduction

Biomechanics of the aorta, our main blood vessel that carries blood from the left ventricle to the entire body, plays a key role in the disease development and long-term outcome post treatment. However, it is currently not fully understood and not taken into account in clinical decision making. One challenge in incorporating biomechanics as a clinical tool is its variation: spatial and across the population. The properties of the aortic root, ascending aorta, and descending aorta are known to be different. Moreover, these properties vary substantially from person to person, even in the healthy state. In this study, we present an analysis based on a large dataset with the aim to quantify the trends and variations in mechanical properties of the general population's aorta.

2. Materials and Methods

We used 80,000 MR images from the UK Biobank and used a pre-trained U-Net model [1] to segment the ascending and descending aorta, from which their in-vivo lumen areas and diameters were calculated. From the diameters, the distensibility was derived as:

$$\delta = \frac{D_{\text{sys}} - D_{\text{dias}}}{D_{\text{dias}}} \frac{1}{P_{\text{sys}} - P_{\text{dias}}}$$

Next, we fit a Gaussian-mixture model to determine the probability distribution of aortic area, distensibility, and demographical factors – for both males and females.

$$p(\boldsymbol{\theta}) = \sum_{i=1}^{K} \phi_i \mathcal{N}(\boldsymbol{\mu}_i, \boldsymbol{\Sigma}_i)$$

We used information theory-based metrics (mutual information and conditional mutual information) to quantify global dependence between various factors. Lastly, we combined the in-vivo dataset is combined with ex-vivo dataset of aortic tissue properties via Bayesian inference to infer the distribution of aortic constitutive parameters and stresses in the different aortic layers.

3. Results

The automatic segmentation was effective, and the Gaussian mixture model fit the data with sufficient accuracy. We find that age is a major determinant in the aortic properties, followed by the body surface area. Distensibility and aortic size are also negatively correlated. Even though there is a difference between males and females, this is largely explained by the difference in their body surface areas. With age aorta dilates and becomes stiffer (Fig 1). However, with larger body surface area (height or weight), only the aortic diameter increases, without significant effect on the distensibility. For a given distensibility and aortic diameter, the constitutive parameters of aortic tissue were estimated, which perfectly correlated with the wall thickness. However, a large uncertainty remains in the resulting stresses, which requires more extensive and detailed ex-vivo testing.

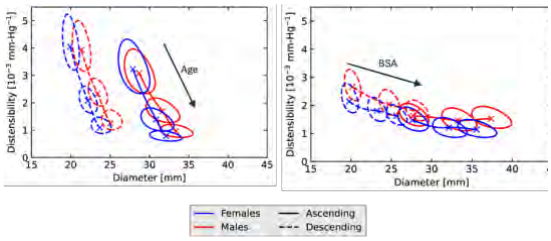


Figure 1: Age-related and body surface area (BSA)-related variation in aortic properties for the ascending and descending aortas.

4. Discussion and Conclusions

The results, for the first time, quantify the trends in aorta's biomechanical properties. The results will help refine clinical planning and improve the treatment options by improving the personalisation offered.

5. References

1. Bai, Wenjia, et al. Nature medicine 26.10 (2020): 1654-1662.

Acknowledgements:

We acknowledge the funding from EPSRC of the UK, through the Impact Acceleration Award scheme.

IN SILICO MODELING OF NEONATAL AORTIC ARCH HYPOPLASIA

Tessa Timmer (1,2), Kirolos Jacob (2), Gregor Krings (2), Mirunalini Thirugnanasambandam (1), Wouter Huberts (1)

1. Eindhoven University of Technology, Netherlands; 2. University Medical Center Utrecht, Netherlands

Correspondence: t.timmer@tue.nl, Biomedical Engineering, Eindhoven University of Technology, Netherlands

1. Introduction

Aortic arch hypoplasia is a congenital heart disease characterized by the underdevelopment of the aortic arch, often occurring with coarctation of the aorta and other congenital heart defects. Surgical repair typically involves proximal arch reconstruction using patch augmentation. However, recurrent coarctation occurs in 20-30% of cases, often requiring reintervention within the first year [1]. This highlights the need to identify patch repair strategies that best optimize aortic arch geometry and post-operative hemodynamics. Understanding the effect of patch repair on the aortic arch requires Fluid-Structure Interaction (FSI) models to capture both flow and wall mechanics. Therefore, the goal of this study is to develop a framework for *in silico* modeling of realistic healthy and hypoplastic neonatal aortic arches.

2. Materials and Methods

A realistic geometry was created by averaging the centerlines of neonates with healthy aortic arches and placing supra-aortic branches and circular cross-sections according to literature and clinical expertise. The hypoplastic aortic arch was derived from this healthy geometry based on the diagnostic criteria. Tetrahedral volume meshes were generated from these geometries, and computational fluid dynamics (CFD) simulations were performed as a first step to assess the geometric effect on hemodynamics. A time-varying parabolic inlet velocity profile derived from a 1D wave propagation model was prescribed [2]. A three-element Windkessel model was placed at each outlet, with parameters tuned to match neonatal blood pressure and the expected outlet flows. The latter varied across geometries due to changes in branch diameters. As the total resistance differed by less than 0.1%, its impact on the results was negligible, and observed differences could therefore be attributed mainly to geometric changes.

3. Results

Preliminary CFD results showed physiological flow patterns in the healthy arch [3], while the hypoplastic arch displayed increased velocity across the narrowed segment and disturbed distal flow (Figure 1). The resulting pressure drop of the hypoplastic arch was approximately 41 mmHg, measured between the proximal and distal points where the diameter is 1.5 times the minimal stenotic diameter. Such a pressure drop is typically considered clinically significant and would prompt consideration for surgical intervention.

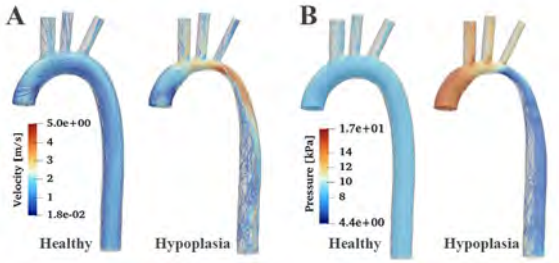


Figure 1: Velocity (A) and pressure (B) during systole for a healthy and hypoplastic neonatal arch.

4. Discussion and Conclusions

The results demonstrated that the workflow yielded hemodynamically realistic models, providing a basis for future FSI studies. However, FSI analyses entail many uncertainties, including neonatal aortic wall and patch material properties and imposed boundary conditions, which are further complicated by the lack of neonatal data. The next steps are therefore to extend the workflow to FSI simulations and assess the impact of these modeling choices through sensitivity analyses, marking an important step towards clinical decision support in aortic arch reconstruction.

5. References

1. Recco DP et al. Interdisp CardioVasc Thorac Surg. 2023;37(6):ivad210 (2023).
2. Bessems D et al. J. Fluid Mech. 2007;580:145-168 (2007).
3. Frydrychowicz A et al. Invest Radiol. 2011;46(5):317-325 (2011).

IMPACT OF WALL COMPLIANCE ON ABDOMINAL AORTIC ANEURYSM GEOMETRY-HAEMODYNAMIC RELATIONSHIP

Shravani Banagiri (1), Vijay Nandurdikar (1), Tejas Canchi (2), Alistair Revell (1), Alejandro Frangi (1,3), Ajay B. Harish (1)

1. School of Engineering, University of Manchester, UK; 2. University of Sydney, Australia; 3. School of Health Sciences, University of Manchester, UK

1. Introduction

Abdominal Aortic Aneurysm (AAA) is a localized enlargement of the abdominal aorta which poses a significant risk when the diameter of aorta exceeds 5.5cm for men and 5cm for women with 78-83% rupture fatality rate. The haemodynamic metrics like Wall Shear Stress (WSS), Time-averaged wall shear stress (TAWSS), Oscillatory Shear Index (OSI) and biomechanical metric like Peak Wall Stress (PWS) plays an important role in the growth and rupture of the aneurysm. Computational Fluid Dynamics (CFD) is employed to simulate the blood flow patterns inside the aneurysm and evaluate the overall flow behaviour inside the aorta. However, CFD studies typically assume rigid aortic wall even though it is inherently complaint and undergoes deformation due to the pulsatile flow of the blood. Fluid-Structure Interaction (FSI) enables integrated simulations of blood flow and vessel wall mechanics providing more realistic predictions of haemodynamic and biomechanical parameters. Moreover, the aneurysm morphology, wall thickness and wall properties significantly affect the structural response[1]. This study builds on a recently developed framework of generation of synthetic AAA geometries which represents the population level variations, and FSI simulations are performed to assess the impact of wall properties on the haemodynamic and biomechanical behaviour[2].

2. Materials and Methods

The 182 synthetic AAA geometries derived from gender based morphological distributions were used to setup a FSI framework[2]. Initially, the wall was modelled with a rigid outer layer and a compliant inner layer, and later both layers were considered compliant. The wall properties were modelled as nonlinear, hyperelastic neo-hookean material with a variable thickness[3]. Simvascular was used for FSI and Paraview was used for post-processing. The framework evaluates WSS, TAWSS, and OSI will be compared with the corresponding rigid wall simulations, and PWS will be computed.

3. Results

The results will present the haemodynamic metrics (WSS, TAWSS, and OSI) and compare with the corresponding rigid-wall simulations, while PWS will be computed to characterize the structural stresses in the wall. The results will help evaluate the effect of wall compliance on the relationship between the morphology and derived haemodynamic and wall stress metrics.

4. Discussion and Conclusions

The framework enables a systematic study of how incorporating aneurysm morphology, wall thickness and wall properties influence the haemodynamic and biomechanical metrics. The use of demographically stratified synthetic geometries improves the variability and predictions at the population level.

5. References

1. Scotti CM, Shkolnik AD, Muluk SC, Finol EA. Fluid-structure interaction in abdominal aortic aneurysms: effects of asymmetry and wall thickness. Biomedical engineering online. 2005 Nov 4;4(1):64.
2. Nandurdikar V, Tyagi A, Canchi T, Frangi AF, Revell A, Harish AB. Virtual Population to Re-assess AAA Risk Using Neck Geometry and Shape Compactness Alongside Maximum Diameter. bioRxiv. 2026 Mar 2:2026-02.
3. Al-Obaidi WJ. Numerical Investigation of Rupture Potential of Abdominal Aortic Aneurysm. The University of Manchester (United Kingdom); 2020.

TOWARDS A DIGITAL TWIN TO PREDICT PATIENT PROSTHESIS MISMATCH AFTER AORTIC VALVE REPLACEMENT

Jenson Jacob (1), James McLaughlin (1), Loreena Hill (2), Selim Bozkurt (1)

1. School of Engineering, Ulster University, UK; 2. School of Nursing and Paramedic Science, Ulster University, UK. Correspondence: s.bozkurt1@ulster.ac.uk

1. Introduction

Patients presenting with symptomatic severe aortic stenosis are at an increased risk of morbidity and mortality. The valvular disorder can be effectively treated with either surgical aortic valve replacement or transcatheter aortic valve implantation. The use of a prosthetic aortic valve to replace the native aortic valve, however, may result in patient-prosthesis mismatch due to inadequate blood flow through the replaced prosthetic valve. Therefore, a comprehensive characterisation of aortic valve haemodynamics and biomechanics under physiological conditions is required. Computational fluid–structure interaction (FSI) modelling enables detailed assessment of leaflet kinematics, stress distribution, and flow dynamics that are difficult to obtain experimentally. The aim of this study is to develop a Digital Twin employing FSI simulations to predict patient prosthesis mismatch after aortic valve replacement.

2. Materials and Methods

A 3D aorta geometry was obtained from the Vascular Model Repository [1] and was discretised with linear elastic shell elements (E=3.25 MPa, ν=0.45). A 3D parametric synthetic aortic valve geometry [2] was developed to assess aortic valve function. The geometric model was meshed using 10-node tetrahedral solid elements and was assigned a two-term isotropic Ogden hyperelastic model. A physiological blood velocity waveform was prescribed at the left ventricular inlet, with physiological pressure conditions at all branch outlets and initial conditions corresponding to early diastole. The simulation spanned over three cardiac cycles. FSI coupling employed the embedded shell approach. FSI simulations were performed using LS-DYNA's Incompressible Computational Fluid Dynamics (ICFD) solver coupled with an implicit structural solver. Two-way interaction between the ICFD and implicit structural solvers with mortar-based self-contact for leaflet coaptation was employed.

3. Results

The initial simulations were performed to visualise aortic valve opening and closing for a healthy condition. Results demonstrate physiological valve opening under the applied loading conditions. Aortic valve opening and closing and transvalvular pressure gradients are given in Figure 1.

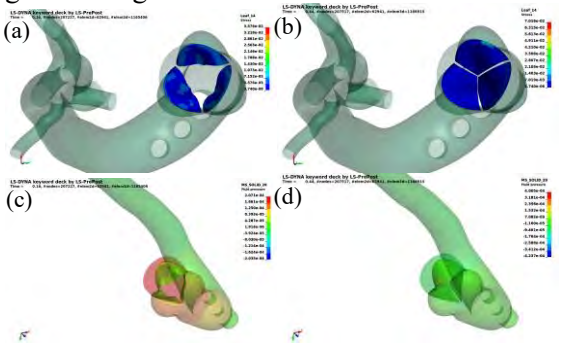


Figure 1. The aortic valve (a) opening and (b) closing and transvalvular pressure gradients for the (c) open and (d) closed valve.

4. Discussion and Conclusions

The initial results demonstrate that the developed FSI framework accurately simulates baseline aortic valve function under healthy physiological conditions, successfully capturing complex hemodynamics and leaflet kinematics. A Digital Twin predicting patient prosthesis mismatch after aortic valve replacement will be built upon the developed FSI model.

5. References

1. Wilson, N.M., Ortiz, A.K. and Johnson, A.B. (2013) 'The Vascular Model Repository: A public resource of medical imaging data and blood flow simulation results', Journal of Medical Devices, 7(4). doi:10.1115/1.4025983.
2. Thubrikar, M. (2011) The aortic valve. New York: Informa Healthcare.

Acknowledgements:

This work is funded by the Engineering and Physical Sciences Research Council (EP/Y034929/1).

FLUID–STRUCTURE INTERACTION MODELING OF PATIENT-SPECIFIC STENOTIC CAROTID ARTERIES

Márton Bence Németh (1), Zsuzsanna Mihály (2), György Paál (1), Benjamin Csippa (1)

1. Budapest University of Technology and Economics, Department of Hydrodynamic Systems, Hungary*; 2.* Semmelweis University, Department of Neurosurgery and Neurointerventions, Hungary

1. Introduction

The bifurcation of the common carotid artery is often investigated due to its susceptibility to atherosclerosis. When analyzing the resulting stenosis in computational flow simulations, a rigid arterial wall is commonly assumed. However, this approach may underestimate the effects of wall mechanics on the wall shear stress [1]. The aim of this study is to build a methodological framework on the implementation of fluid-structure interaction (FSI) models.

2. Materials and Methods

CT images of stenotic carotid bifurcations requiring carotid endarterectomy (CEA) were provided by Semmelweis University. Pre-CEA CT images were segmented to reconstruct patient-specific geometries for the simulations.

VascuCAP was used to automatically identify and determine the spatial distribution of plaque components, visible in the CT images. Following CEA, histopathological analysis was performed on the excised plaque specimens and a three-dimensional model was reconstructed to include additional plaque information. The histopathological 3D model was spatially aligned with the CT-based geometry using the simplified VascuCAP-derived plaque model as a reference.

The arterial geometry from CT segmentation was used as the basis for the fluid–structure interaction (FSI) simulations. Finite element FSI models were developed using the open-source software FEBio. The mechanical behavior of the arterial wall and plaque components was described using the Holzapfel–Gasser–Ogden (HGO) material model [2] to represent the anisotropic properties of the surrounding tissue.

3. Results

First, the FSI simulations were successfully implemented on a simplified cylindrical geometry to establish the modeling framework. The mechanical representation of the healthy artery was then created using single-layer and multilayer wall configurations. Subsequently, plaque was introduced as a wall-adhered patch with locally varying stiffness determined by its composition. Finally, patient-specific FSI simulations were performed for three carotid bifurcation cases, using the reconstructed geometries. A parameter sensitivity analysis was conducted, focusing on the material description of the plaque components.

4. Discussion and Conclusions

The HGO model is primarily intended for describing healthy, fiber-reinforced soft tissues; however, by assuming randomly oriented fibers, it can be used to approximate a broader range of material behaviors. This strategy enables a simplified and unified representation of wall mechanics, potentially applicable to complex stenotic geometries.

5. References

1. A. R. Alias, N. H. Johari, Proc. 2nd Hum. Eng. Symp. ,HUMENS 2023, 209-221
2. T. C. Gasser, R. W. Ogden, G. A. Holzapfel, J. R.Soc. Interface (2006), 3, 15-35

Acknowledgements:

The project supported by the Doctoral Excellence Fellowship Programme (DCEP) is funded by the National Research Development and Innovation of the Ministry of Culture and Innovation and the Budapest University of Technology and Economics (Németh Márton DKÖP-26-1-BME-94).

Project no. NKFI-STARTING-152593 has been implemented with the support provided by the Ministry of Culture and Innovation of Hungary from the National Research, Development and Innovation Fund, financed under the NKKP-STARTING_25 funding scheme.

NON-INVASIVE PRESSURE-VOLUME LOOP IN PATIENTS WITH AORTIC STENOSIS

Gloria Palazzo (1), Sofia Di Filippo (1), Giandomenico Disabato (1), Riccardo Gorla (1), Pietro Spagnolo (1), Massimo Lombardi (1), Francesco Bedogni (1), Francesco Sturla (1,2)

1. IRCCS Policlinico San Donato, San Donato Milanese, Italy; 2. Politecnico di Milano, Milano, Italy

1. Introduction

Left ventricular (LV) pressure–volume (PV) loops are central to the assessment of cardiac energetics but remain clinically limited due to the need for invasive measurements. Although non-invasive MRI-based methods have been proposed [1], such as elastance-based models, they rely on generalized assumptions that do not adequately account for alterations caused by valvular disease. We extend non-invasive PV loop analysis to patients with aortic stenosis (AS) and LV hypertrophy referred to transcatheter aortic valve implantation (TAVI).

2. Materials and Methods

A multimodal workflow was developed to reproduce PV loops (Fig. 1) in a cohort (n = 4) of TAVI recipients. A time-varying elastance model was fed with non-invasive brachial arterial waveform pressure acquired with Finapres® NOVA device and LV endocardial curve volume from non-contrast MRI.

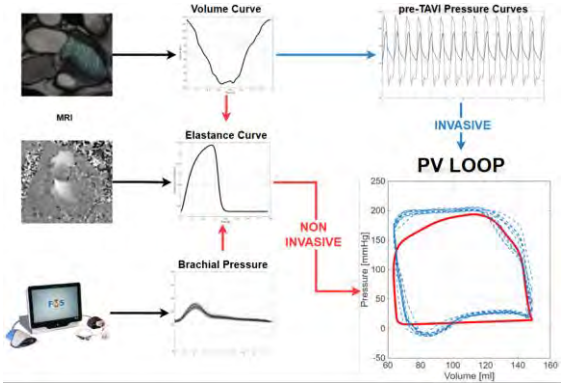


Figure 1. PV loop analysis workflow.

Phase-contrast (PC-MRI) was used to adjust AS-related systolic pressure drop; diastolic pressure was modulated using pulmonary capillary wedge pressure [2] and mitral PC-MRI. After pressure and volume synchronization, PV loop was generated, extracting stroke work (SW), potential energy (PE), and total PV area (PVA) [3]. Aortic invasive pressure curves were available from TAVI catheterization for validation.

3. Results

PV loops were successfully reproduced, reliably capturing systolic pressure peaks and end-diastolic points. LV energetics showed SW ranging 1.19 ÷ 2.14 J, PE 0.44 ÷ 1.17 J, and PVA 2.34 ÷ 3.12 J, corresponding to average percentage errors of 28.7%, 34.1%, and 31.3% versus invasive measurements.

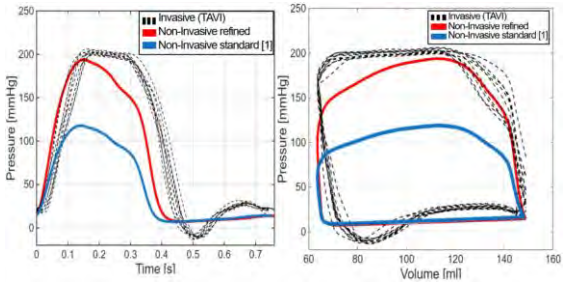


Figure 2. Refined and standard non-invasive PV loop analysis in a patient with AS.

Despite these deviations, personalized hemodynamic modulators substantially improved PV loop estimation *vs.* the standard approach. For the patient reported in Fig. 2, SW improved from 1.01 to 1.72 J (invasive: 1.83 J), PE from 0.42 J to 0.70 J (invasive: 0.71 J), and PVA from 1.43 J to 2.43 J (invasive: 2.54 J).

4. Discussion and Conclusions

By integrating hemodynamic modulators into a time-varying standard elastance model, non-invasive PV loops can effectively capture key energetic patterns of AS and LV hypertrophy, highlighting its potential as a low-risk alternative to invasive catheterization.

5. References

1. Seemann et al., Circ Cardiovasc Imaging; 12(1): e008493 (2019).
2. Kalaitzoglou M et al., ESC Heart Fail; 13(1): 1-9 (2026).
3. Klotz S et al., Am J Physiol Heart Circ Physiol; 291(1): H403-12 (2006).

Acknowledgements:
TRANSLATE project was funded by the National Plan for NRRP Complementary Investments, project n. PNC0000003.

FINITE-VOLUME IMMERSED-BOUNDARY MODELLING OF LEFT-HEART VALVE-FLOW MECHANICS FOR XENOTRANSPLANTATION

Sairam Pamulaparthi Venkata, Chanikya Valeti, Philip Cardiff

School of Mechanical & Materials Engineering, University College Dublin, Dublin, Ireland

1. Introduction

Cardiac xenotransplantation, particularly porcine-to-human heart transplantation, is being explored to address the global shortage of donor organs. However, physiological differences between porcine and human cardiovascular systems may influence haemodynamics and valve function. In this work, we present a computational framework that combines high-fidelity fluid dynamics with anatomically informed valve-motion models to study ventricular filling, systolic ejection, and valve–flow interactions, thereby enabling cross-species haemodynamic comparisons relevant to xenotransplantation.

2. Materials and Methods

Our numerical framework builds on the hybrid fictitious-domain immersed-boundary (HFDIB) methodology implemented in the openHFDIB-DEM library within OpenFOAM [1]. The solver computes incompressible left-heart flow while representing valve geometries within a non-body-fitted mesh. Ventricular motion is prescribed using an arbitrary Lagrangian–Eulerian framework, with mitral and aortic valves modelled as deforming STL surfaces with time-dependent kinematics.

The governing momentum equation with immersed-boundary forcing is

$$\frac{\partial \boldsymbol{u}}{\partial t} + \nabla \cdot (\boldsymbol{u} \otimes \boldsymbol{u}) = -\boldsymbol{\nabla} p + \nu \boldsymbol{\nabla}^2 \boldsymbol{u} + \boldsymbol{f}_{ib}, \quad (1)$$

where $\boldsymbol{u}$ denotes velocity, p the kinematic pressure, ν the kinematic viscosity, and $\boldsymbol{f}_{ib}$ the immersed-boundary forcing used to impose valve boundary conditions. Valve opening and closure are prescribed by deforming STL vertices relative to a hinge axis defined by two reference points x_A and x_B. The position of each vertex is updated according to

$$\boldsymbol{x} = \boldsymbol{x}_0 - F(\xi, t)|\boldsymbol{r}_0|\widehat{\boldsymbol{r}_0}, \quad (2)$$

where $\boldsymbol{x}_0$ is the reference vertex position, $\boldsymbol{r}_0$ the radial vector from the hinge axis, $\hat{\boldsymbol{r}}_0$ its unit direction, and $F(\xi, t)$ a spatial–temporal function prescribing valve motion.

3. Results

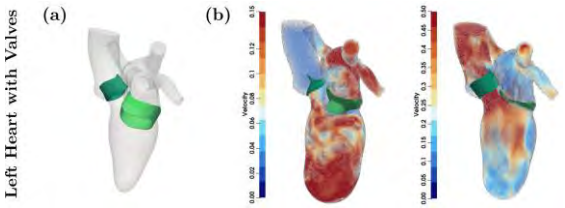


Figure 1: Human left heart (ventricle and atrium). Velocity field at t = 0.63 s (diastolic filling) and t = 0.83 s (systolic ejection) within a 1 s cardiac cycle with prescribed mitral and aortic valve states.

The immersed-boundary formulation was verified using canonical flow over steady and oscillating cylinder benchmarks, showing good agreement with body-fitted OpenFOAM simulations under mesh refinement. The framework was then applied to left-heart simulations, where velocity fields demonstrate physiologically consistent flow patterns during diastolic filling and systolic ejection.

4. Discussion and Conclusions

The presented framework enables simulation of left-heart haemodynamics with prescribed valve motion using an immersed-boundary formulation that avoids valve-fitted remeshing (Figure 1). Future work will extend the approach to anatomically detailed geometries and to fully coupled fluid–structure interaction models to enable more realistic valve biomechanics.

5. References

1. Isoz M et al., Computers & Fluids; 244:105538 (2022).

Acknowledgements:
This project has received funding from the European Research Council (ERC) under the European Union's Horizon 2020 research and innovation programme (Grant Agreement No. 101088740).

MRI-INFORMED HAEMODYNAMIC MODELLING FOR NONINVASIVELY QUANTIFYING CEREBROVASCULAR STIFFNESS

Beatrice Ghitti* (1), Sergio Dempsey (2), Finbar Argus (1), Gonzalo Maso Talou (1)

1. Auckland Bioengineering Institute, The University of Auckland, Auckland, New Zealand
2. GE HealthCare, Gisborne, New Zealand
*Corresponding author. E-mail: beatrice.ghitti@auckland.ac.nz

1. Introduction

Vascular stiffness is a developing biomarker for vascular ageing and dementia, yet it remains challenging to quantify directly. Pulse wave velocity (PWV) has emerged as a method to *indirectly* assess vascular stiffness [1]. Existing techniques for estimating spatially varying PWV in the aorta translate poorly to intracranial vessels, limiting the potentially critical interpretation of PWV measurements in relation to local neurodegeneration. While 4D flow MRI can image local pulsatility (the assumed cause of encephalopathy [2]), to date, no tools are available to noninvasively spatially characterise effective cerebrovascular stiffness (efCVS).

2. Materials and Methods

By integrating 4D flow MRI data with personalised computational haemodynamic models, here we develop a novel methodology to noninvasively quantify spatially variable efCVS. Subject-specific cerebrovascular anatomy and blood flow velocity are extracted from 4D flow MRI using QVT and QVT+ tools [3]. Blood flow is simulated using a 1D model for networks of deformable vessels [4], with automatic adaptation of network topology and boundary conditions based on the 4D flow dataset. *Local wave speed* $c(x,t)$ is defined as

$$c = \sqrt{\frac{A}{\rho}\frac{\partial p(A,K)}{\partial A}}, \qquad (1)$$

where $K(x)$ is the spatially varying stiffness parameter. We then propose a novel calibration strategy that estimates the subject-specific spatial distribution of efCVS, $K(x)$, using the extracted 4D flow velocity fields as calibration targets. This approach enables comprehensive physiological personalisation directly from noninvasive flow measurements to characterise intracranial haemodynamics.

3. Results

The baseline 1D haemodynamic model successfully demonstrated the spatial blood flow distribution and wave speed map (local PWV, Fig. 1) across the cerebrovascular network. In this contribution, we will present the results obtained by applying this workflow to a cohort of subjects that also estimate efCVS. As there is no direct measurement of efCVS for validation, model-predicted intracranial PWV will be compared against values calculated using standard PWV techniques [5] for a rigorous agreement assessment of PWV trends.

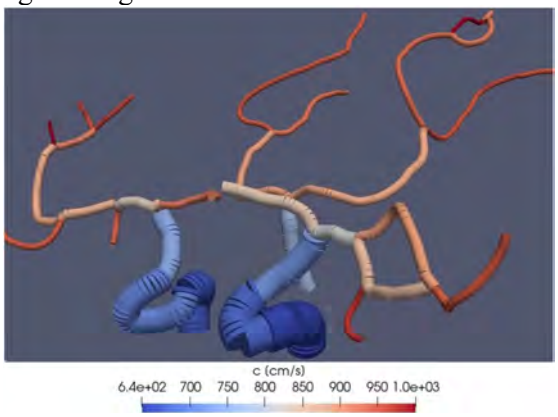


Figure 1: Spatial distribution of c (1) at selected time point predicted by the baseline (pre-calibrated) 1D haemodynamic model.

4. Discussion and Conclusions

This MRI-integrated computational workflow establishes a robust foundation for noninvasive assessment of spatially varying efCVS by personalising haemodynamic models. This approach will enable physics-consistent, whole-organ spatial characterisation of efCVS, serving as a detailed biomarker of brain vascular ageing and neurodegeneration, ultimately facilitating early diagnosis and intervention.

5. References

1. Wentland AL et al., Cardiovasc. Diagn. Ther., 4(2):193–206, 2014.
2. Bateman GA, Med. Hypotheses, 62(2):182–187, 2004.
3. Dempsey S et al., Sci Rep., 14(1):12604, 2024.
4. Ghitti B et al., Int J Numer Meth Fluids, 95(2):262-312, 2023.
5. Dempsey S et al., Interface Focus, 15(1):20240036, 2025.

TOWARD CFD-BASED ESTIMATION OF PEAK-TO-PEAK GRADIENT IN AORTIC COARCTATION

Maria Alexandra Cetățoiu (1)*, Benigno Marco Fanni (2), Chiara Bonfanti (1,2), Sara Bonfanti (1,2), Lamia Ait Ali (3), Chiara Marrone (3), Francesca Berti (1), Giancarlo Pennati (1), Simona Celi (2)

1. Laboratory of Biological Structures Mechanics (LaBS), Department of Chemistry, Materials and Chemical Engineering Giulio Natta, Politecnico di Milano, Italy;

2. BioCardioLab, Bioengineering Unit, Fondazione Toscana Gabriele Monasterio, Ospedale del Cuore, Italy;

3. Pediatric Cardiology and Adult CHD Unit , Fondazione Toscana Gabriele Monasterio, Ospedale del Cuore, Italy

maria.cetatoiu@polimi.it, Piazza Leonardo Da Vinci, 32, 20133 Milano, Italy

1. Introduction

Aortic coarctation (CoA) is a congenital narrowing of the aorta that produces a pressure gradient across the stenosis, with intervention recommended when the catheter-measured peak-to-peak gradient exceeds 20 mmHg. Patient-specific computational models based on MRI and cuff pressure data have been proposed to estimate this gradient non-invasively [1–3], but their accuracy depends strongly on outlet boundary conditions (BCs). This study compares two published BC strategies [1,3] with a new framework designed to better exploit clinical data while reducing parameter tuning.

2. Materials and Methods

Patient-specific CFD simulations of the 3D aortic arch were coupled with a 0D model using four three-element Windkessel (RCR) outlets (Fig. 1). Ascending aortic inflow Q_{AAo} was obtained from clinical 2D phase-contrast MRI, while descending aortic flow Q_{DAo}, typically measured during the same examination, informed BCs. In previous frameworks [1,2], systemic resistance is distributed among outlets according to vessel area, with Q_{DAo}mainly used for validation. In the Cetățoiu–Fanni method [3], Q_{DAo} is incorporated directly and RCR parameters are iteratively tuned to match cuff pressure. In the proposed framework, DAo resistance is determined independently by modeling coarctation pressure loss as $\Delta P = kQ^2$, where k is estimated analytically:

$$k = \frac{\rho}{2}\left(\frac{1+\left(1-\frac{A_{CoA}}{A_{AAo}}\right)^2+\left(1-\frac{A_{CoA}}{A_{DAo}}\right)^2}{A_{CoA}^2}-\frac{1}{A_{AAo}^2}\right) \quad (1)$$

with A denoting vessel cross-sectional areas and ρ fluid density. This separates stenosis losses from systemic resistance.

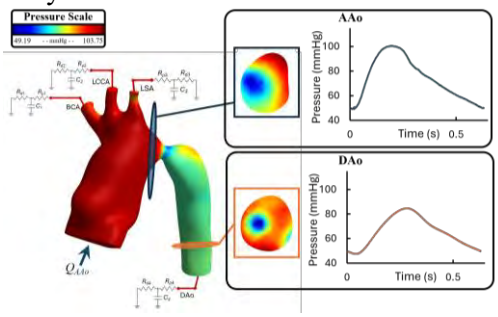


Figure 1: Patient-specific CFD model of the aorta with BCs and pressure distribution.

3. Results

Clinical and imaging data were collected for seven CoA patients (age 1–55 years). Application to an initial patient shows that the proposed framework matches pressure targets with a single iteration, whereas previous approaches require additional tuning.

4. Discussion and Conclusions

Explicitly modeling CoA pressure loss and using clinically measured Q_{DAo} improves BCs while reducing computational effort, supporting clinically applicable CFD estimation of peak-to-peak gradients. Validation on the full cohort is ongoing.

5. References

1. Antonuccio A, et al. Ann Biomed Eng. 50(5):1123-1137 (2022).
2. Nair PJ, et al. Ann Biomed Eng. 52:1335–1346 (2024).
3. Cetățoiu MA, Fanni BM, et al. J Mech Med Biol. 25(4):2154011 (2025).

CALIBRATION OF A SPHERICAL VENTRICULAR MODEL FOR CARDIAC DIGITAL TWIN APPLICATIONS

Federica Ninno (1) and Martin R. Pfaller (1)

1. Yale University, Department of Biomedical Engineering, New Haven, CT, USA

1. Introduction

Cardiac digital twins have the potential to support personalized medicine [1]. However, high-fidelity three-dimensional (3D) cardiac models remain computationally prohibitive for many-query tasks such as parameter estimation, and uncertainty quantification. Reduced-order models provide computationally efficient surrogates but require robust calibration strategies and validation against 3D simulations. Herein, we present a calibration framework in which pressure–volume (PV) data obtained from high-fidelity ventricular simulations are used to calibrate a spherical reduced-order left ventricular model [2]. We identify latent geometric, material and activation parameters and assess the predictive fidelity of the low-dimensional representation.

2. Materials and Methods

The workflow consists of three steps: (i) generation of reference PV data using a 3D ventricular model, (ii) calibration of a spherical reduced-order model through inverse optimization, and (iii) forward simulation to compare reduced-order predictions against the 3D reference. The framework was evaluated for passive inflation using an ex vivo porcine left ventricle (LV) geometry reconstructed from cine computed tomography [3], and for active contraction using 125 LV PV loops generated with a four-chamber openCARP model under varying systemic resistance, passive myocardial stiffness, and initial LV pressure.

3. Results

Fig. 1 compares representative PV loops predicted by the calibrated spherical ventricular model with the corresponding 3D simulation results for two active contraction cases under different systemic resistance, passive stiffness, and initial LV pressure. Across all 125 cases, the average root-mean-square error (RMSE) between the spherical model and the 3D reference was 0.76%.

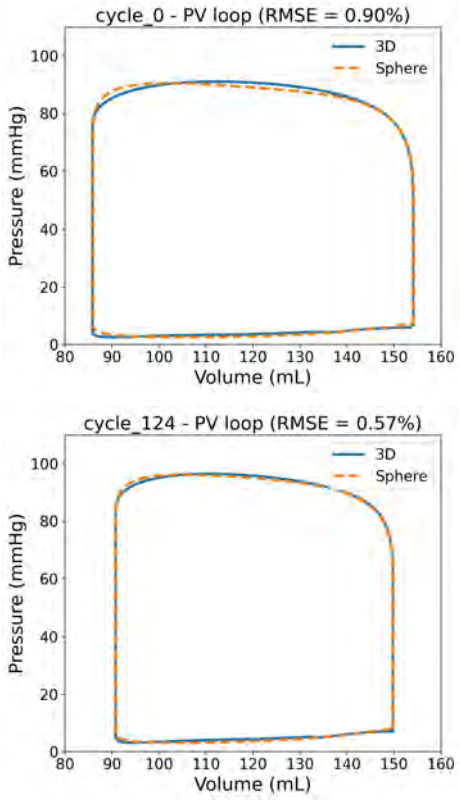


Figure 1: Comparison of 3D and calibrated reduced-order PV loops for two representative active contraction cases under different parameter settings.

4. Discussion and Conclusions

The spherical model reproduces the overall shape of the 3D PV loops with high accuracy. Future work will establish mappings between 3D geometry and reduced-order parameters.

5. References

1. Niederer S.A. et al., Nat Rev Cardiol; 16(2):100–111 (2019).
2. Caruel M. et al., Biomech Model Mechanobiol; 13(4):897–914 (2014).
3. Midgett D.E. et al., J Mol Cell Cardiol; 166:74–90 (2022).

Acknowledgements:
This work is supported by the NIH under grant R00HL161313. The authors thank A. J. Sinusas for providing the porcine LV dataset, and C. Rodero and S. A. Niederer for the active contraction PV loop dataset.

RADIOMICS-BASED IDENTIFICATION OF PATIENTS WITH CARDIOVASCULAR DISEASES FROM RETINAL IMAGES

Ilaria Bottini* (1,2,3), Anna Corti (3), Benedetta Grossi (1,2,3), Letizia M. Perri (1,3), Riccardo Tatoni (1), Mario R. Romano (1,2), Gianluigi Condorelli (1,2), Valentina D.A. Corino (3), Luca Mainardi (3)

1. Humanitas University, Italy; 2. IRCCS Humanitas, Italy; 3. Politecnico di Milano, Italy

1. Introduction

Cardiovascular diseases (CVDs) are the leading cause of death globally. While traditional risk calculators depend on standard clinical parameters, emerging evidence reveal strong associations between retinal changes and CVDs, suggesting retinal imaging as a promising, non-invasive tool for cardiovascular risk assessment [1]. Despite its potential, the application of radiomics in this domain remains under-researched. This study aims to develop a radiomics-based machine learning (ML) model to classify patients with prior CVD using retinal imaging.

2. Materials and Methods

The study utilized a publicly available dataset [2] comprising 2,440 optical coherence tomography angiography (OCTA) images from 814 eyes of 491 individuals, of whom 86 had congestive heart failure, stroke or other vascular diseases. The presence of any of the conditions was designated as the positive label for the model. The dataset included images of the superficial, deep, and choriocapillaris plexuses; only the deep plexus was analysed in this paper. Images were equalized and converted from a three-channel RGB format to a single-channel grayscale representation. The foveal avascular zone (FAZ) was segmented and excluded using a deep learning model [3], which was trained on the OCTA-500 dataset [4]. A 150-pixel frame was removed to mitigate potential noise originating from the image margins, see Fig. 1, left. A total of 465 2D radiomic features were extracted using PyRadiomics from deep plexus images (first order statistics, textural and wavelet-based). Only one image per subject was used: for subjects with bilateral images, a single eye was randomly selected. Various feature selection techniques and classification algorithms were evaluated, with model performance assessed using a five-fold cross-validation on the training set.

3. Results

From the validation set, the optimal model involved the removal of highly correlated features ($\rho \geq 0.8$), the application of Elastic Net regularization, and the use of Balanced Random Forest as the classifier. When evaluated on the test set, the model achieved a balanced accuracy of 0.74, sensitivity of 0.76, and specificity of 0.71, see Fig. 1, right.



Figure 1: Example of segmentation (left), with red regions indicating areas excluded from feature extraction. Confusion matrix on the test set (right).

4. Discussion and Conclusions

These results highlight the potential of radiomics in identifying individuals with CVD from retinal images. Future work will include the analysis of superficial and choriocapillaris plexuses images to enhance diagnostic performance. This approach may offer a novel non-invasive tool for cardiovascular risk stratification.

5. References

1. Tohà-Dalmau A et al., Opthalmology Science; 2025;5:100874.
2. Germanèse C et al., Data; 2023;8(10):147.
3. Peng L et al., OMIA 2021 conference: Springer; 2021. p. 42-51
4. Li M et al., Medical Image Analysis; 2024;93:103092.

DEFORMABLE IMAGE REGISTRATION ASSESSMENT OF THE AORTIC REMODELING IN AORTOPATHY PATIENTS.

Raphael Sivera (1), Silvia Schievano (1), Andrea Impellizzeri (3), Gian Luca Ragazzoni (2), Elena Cervi (2), Claudio Capelli (1)

1. Institute of Cardiovascular Science, University College London, United Kingdom; 2. Department of Cardiology, Great Ormond Street Hospital, United Kingdom; 3. Bart's Heart Centre, St Bartholomew's Hospital, United Kingdom.

1. Introduction

Assessing the growth of the aorta is crucial to follow-up aortopathy patients. Standard practices [1] recommend regular imaging assessment of the aortic diameters. However, manual diameter measurements can be unprecise, with ~1mm inter-op variability [2] comparable to the small longitudinal changes. Limiting the assessment to diameter variations provides an incomplete description of the three-dimensional changes neglecting local vessel bulging or changes in elongation. Image registration may be able to more accurately measure the vessel growth [3] but the practical use in a clinical setting remains challenging. In this study, we aim to assess the potential of deformable image registration to monitor longitudinal aortic changes in a patient population.

2. Materials and Methods

Patients (n=114) diagnosed with aortopathy at our Centre and who underwent at least two MR acquisitions were retrospectively included. Patients' images were roughly segmented using a 3D U-net, aligned and non-linearly registered [4] to a reference time point. Segmentations were merged and converted to surface meshes. Spacial correspondence was established between all meshes by means of a statistical shape model. Displacement fields extracted from the intra-subject registration were then interpolated at the mesh vertices. Finally, diagonal terms of the Cauchy strain tensor differential operator were computed to assess the local wall changes. These indicators were compared to the conventional clinical diameters measurements and their average spacial distribution was visualized.

3. Results

Regional averages of the circumferential local wall changes matched the diameter changes (Pearson's r=0.87 for the sinuses), see Fig (a). Higher correlation with patient growth (r=0.85 versus r=0.77) even suggests a more precise measurement of the changes.

Spatial maps, Fig (b) for the circumferential changes, highlighted the dilation and the elongation of the ascending aorta and the variability of the changes in the isthmus area.

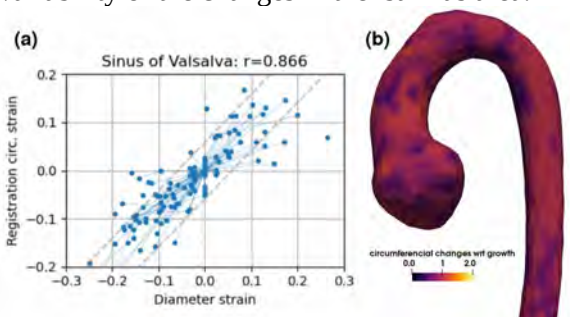


Fig. (a) Correlation between registration-based and diameter changes, each point corresponds to an individual acquisition compared to the patient's reference (b) Average circumferential changes, with slower (purple) and faster (orange) expansion areas.

4. Discussion and Conclusions

Image registration enabled a finer description of the aortic growth in a large cohort of patients with aortopathy. 3D, image-based shape analysis may provide additional reliable assessments to diameter changes in clinics. Further validation of the results using alternative methods and controlled datasets would strengthen the observations.

5. References

1. Isselbacher et al. Circulation 146(24):334, 2022.
2. Rodriguez-P et al. J.Am.S.Echo 819-826, 2016.
3. Bian et al.. Med Phys 49:2514–30, 2022.
4. Lorenzi et al. NeuroImage 81:470–483, 2013.

Acknowledgements: The authors thank the British Heart Foundation (BHF CRE) for providing financial support to this project.

A SECTOR-BASED RADIOMIC APPROACH TO CHARACTERIZE CAROTID PLAQUE EVOLUTION

M. De Santis (1), A. Tziotziou (2), D. Bos (2), L. Mainardi (1) ,V.D.A. Corino (1,3), A.C. Akyildiz (2,4), A. Corti* (1)

1. Politecnico di Milano, Italy; 2. Erasmus MC, the Netherlands; 3. Centro Cardiologico Monzino, Italy; 4. Delft University of Technology, the Netherlands

*Correspondence: anna.corti@polimi.it

1. Introduction

Carotid atherosclerosis is a leading cause of ischemic stroke, but risk stratification based mainly on stenosis severity is inadequate [1]. Plaque composition, particularly calcification, plays a critical role in plaque stability. While large calcifications may stabilize plaques, microcalcifications are linked to rupture risk. Understanding calcification dynamics is therefore key to preventing cerebrovascular events. Although radiomics has improved plaque assessment, its ability to predict longitudinal changes remains unexplored. This study introduces a sector-based radiomic approach to predict localized 2-year morphometric changes in carotid plaques.

2. Materials and Methods

The study analyzed 61 symptomatic patients [2] with carotid artery stenosis from the multicentric PARISK study, who underwent baseline and 2-year computed tomography angiography (CTA). After segmentation, each artery was partitioned into 1mm x 45° sectors, yielding 7315 plaque-containing sectors (Fig. 1). 93 baseline CTA radiomic features were extracted from each sector, using Pyradiomics. First, univariate associations with longitudinal changes in wall thickness (ΔWT), calcification thickness (ΔCT) and calcification distance (ΔCD) were assessed using odds ratios (OR). Then, machine learning models were trained to classify the positive/negative changes in the sectors by considering 80-20% training-test split with cross-validation on the training set.

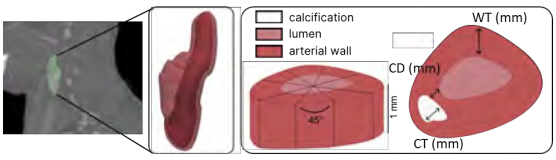


Figure 1. Carotid artery segmentation and sectorization

3. Results

Univariate analysis showed strong associations between baseline radiomic features and calcification-related outcomes (ΔCT, ΔCD; ORs 15–44), but weak associations with ΔWT (OR<2). Consistently, machine learning models achieved high sector-level performance for calcification outcomes (ΔCT, ΔCD; AUC 0.83-0.85) and limited discrimination for ΔWT (AUC 0.56), as shown in Fig. 2. Most informative features were texture-based, indicating that baseline plaque microstructure encodes information on calcification dynamics.

	ΔCD	ΔCT	ΔWT
Bal. accuracy	0.77	0.79	0.57
F1 score	0.75	0.79	0.57
Sensitivity	0.87	0.87	0.59
Specificity	0.67	0.71	0.54

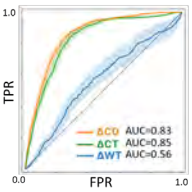


Figure 2. Machine learning results on the test set

4. Discussion and Conclusions

This study proposes a novel sector-based radiomic approach that captures local plaque heterogeneity masked by conventional whole-plaque analyses. To the best of the authors' knowledge, this is the first radiomic study to predict longitudinal plaque evolution in carotid atherosclerosis. These findings establish sector-based radiomics as a promising framework for longitudinal plaque monitoring and risk stratification.

5. References

1. Owolabi et al, Lancet. Public Heal. 7:e74–e85 (2022)
2. Tziotziou et al, Atherosclerosis, 408:120415 (2025)

Acknowledgements:
Funding by Fondazione Cariplo (2024-1126). AC is funded by the National Plan for NRRP Complementary Investments (PNC0000003).

QUANTIFYING FEATURES OF UMBILICAL CORD VASCULAR PHENOTYPES FROM ULTRASOUND IMAGING

David Hardman (1), Kathryn Hunt (2), Rosemary C. Townsend (1,3), Miguel O. Bernabeu (1), Peter Hoskins (4)

1. Centre for Medical Informatics, Usher Institute, University of Edinburgh, UK; 2. Institute for Neuroscience and Cardiovascular Research, University of Edinburgh, UK; 3. Institute for Regeneration and Repair, University of Edinburgh, UK, 4. Centre for Reproductive Health, Institute for Regeneration and Repair, University of Edinburgh, UK

1. Introduction

Abnormal coiling of the umbilical cord (UC) during pregnancy is associated with adverse maternal and neonatal outcomes, including pre-eclampsia, foetal growth restriction, and stillbirth[1]. No imaging tools exist which adequately describe UC phenotypes in vivo, and the vascular mechanisms underlying these associated adverse outcomes remain poorly understood. In this study, we extract quantitative vascular features from Doppler Ultrasound images of antenatal UCs and identify features that distinguish between qualitative differences in UC phenotypes. These features have the potential to inform clinical antenatal assessment, support predictive models of pregnancy outcomes, and create *in silico* 'digital twin' representations of vessels with which to study causal mechanisms.

2. Materials and Methods

3D Colour and Power Doppler Ultrasound images were acquired from two pregnancies exhibiting subjectively different degrees of UC coiling on sonographer assessment. UC vein and artery geometries were extracted, segmented, and vessel centrelines acquired using the *Kimimaro* skeletonizing algorithm (Fig. 1).

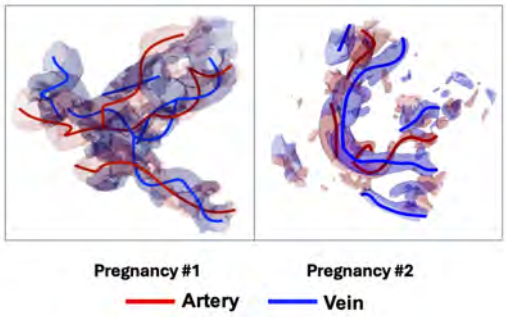


Figure 1: Vessel surfaces from ultrasound images with centrelines overlayed.

Distance- and angle-based tortuosity metrics were computed from the vessel centrelines. Vessel curvature (κ), torsion (τ) and helicity (H), based on torsion per unit length, were also measured. Curvature and torsion were used to define idealised helices representing the different geometries.

3. Results

Umbilical cords from two pregnancies exhibiting distinct UC vessel phenotypes showed significant differences in mean summed-angle tortuosity ($p<0.01$) mean helicity ($p<0.05$) and the standard deviation of helicity ($p<0.05$) (Fig. 2A-C).

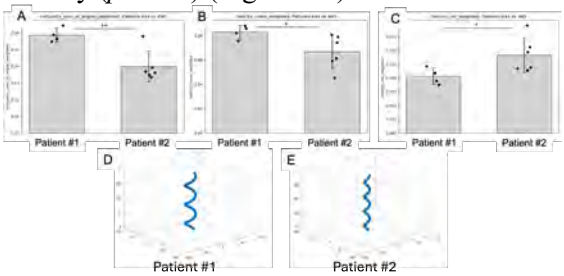


Figure 2: Differences in UC vessel features and representative idealised helices for each patient.

Average values of vessel curvature and torsion were used to describe idealised helices representing each cord (Fig. 2D-E).

4. Discussion and Conclusions

We define potential metrics for quantifying differences in UC vessel phenotypes from routine US imaging and demonstrate how these features can be used to generate synthetic vessels for computational studies of blood flow.

5. References

1. Machin GA, Ackerman J. *Pediatr Dev Pathol.* 2000;3(5): 462-471.

Acknowledgements:

DH is funded by EPSRC grant no. EP/X025705/1. KH is funded by MRC grant no. MR/Z505092/1. RCT is funded by the Chief Scientist Office (EPD/22/17)

HCM-NET: A DEEP NEURAL NETWORK FOR IMPROVED CARDIAC IMAGE SEGMENTATION OF HYPERTROPHIC CARDIOMYOPATHY

Emma McMillian (1), Abhirup Banerjee (2), Alfonso Bueno-Orovio (1)

1. Department of Computer Science, University of Oxford, Oxford OX1 3QD, United Kingdom;
2. Institute of Biomedical Engineering, University of Oxford, Oxford OX3 7DQ, United Kingdom

1. Introduction

Convolutional neural networks (CNNs) have demonstrated strong performance for automatic segmentation of cardiac magnetic resonance (CMR) images. However, their performance degrades when deployed on out-of-domain data, especially in the presence of pathological anatomy. Hypertrophic cardiomyopathy (HCM), the most common inherited cardiomyopathy affecting approximately 1 in 500 individuals worldwide, presents a significant challenge for models trained predominantly on non-HCM cohorts. Clinical deployment of deep learning models requires robustness to diseased anatomy and cross-site variability.

2. Methods

We propose HCM-Net, a lightweight finetuned U-Net-based framework from [1] for ventricular and myocardial segmentation of HCM CMR images. The model was fine-tuned on a multi-centre dataset comprised of 242 subjects (122 HCM) to enable the network to better capture HCM specific anatomical features.

To enhance robustness to out-of-domain data, the training strategy incorporates data augmentation, including motion artifacts and noise simulation. Our proposed method was evaluated on both in-distribution and out-of-distribution datasets, across both short-axis (SAX) and long-axis (LAX) views.

We systematically evaluate our method for HCM segmentation against other state-of-the-art models [1-4] and investigate strategies to improve the generalizability of CNN models across different sites and scanners.

3. Results

HCM-Net outperforms other architectures in Dice similarity coefficient by 8% on in-distribution data and 4% on out-of-distribution data. Consistent improvements were observed in 95th percentile Hausdorff distance, average surface distance, and volumetric error. Gains were larger for myocardium and right ventricle segmentation in SAX views, where HCM-related hypertrophy increases anatomical complexity.

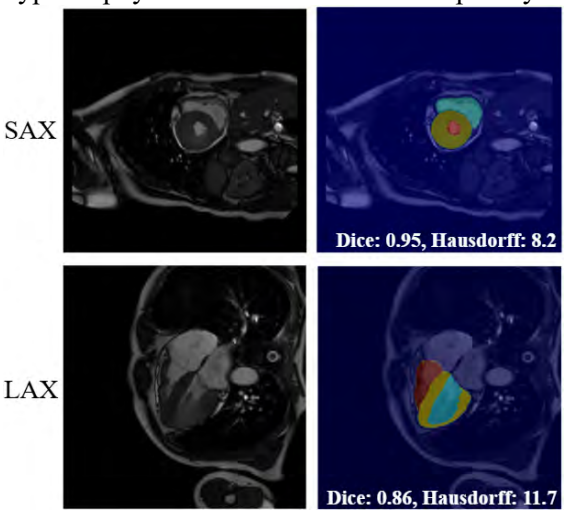


Figure 1: Qualitative assessment of SAX and LAX views for HCM subject at end-systole.

4. Discussion and Conclusions

Our findings demonstrate that pathology-specific fine-tuning and robust data augmentation improves generalization of CMR segmentation models to HCM and multi-centre data. HCM-Net offers a fully automated, data-efficient segmentation tool that improved segmentation accuracy in diseased cohorts. This approach supports future applications such as integration into 3D reconstruction pipelines, contributing to the diagnosis and treatment of HCM.

5. References

1. Chen C et al, Front Cardiovasc Med; 7:105 (2020).
2. Isensee F et al., Nat Methods; 18:203-211 (2021).
3. Baumgartner C et al., STACOM 2017, Lect Notes Comput Sci; 10663:111-119 (2018).
4. Zhou, H., et al., IEEE Trans Image Process 32:4036-4045 (2023).

Acknowledgements:

This work was supported by an EPSRC Doctoral Award (CS2425\1668004, to EM), a Royal Society University Research Fellowship (URF\R1\221314, to AB), and the SMASH-HCM project (Innovate UK Grant 10110728, to ABO).

SMARTLYF – A STRESS-INTEGRATED DIGITAL TWIN FRAMEWORK FOR FUNCTIONAL RISK STRATIFICATION IN AAA

Hendrik von Tengg-Kobligk (1), Nino L'Abate (1), Grazia-Maria Cereghetti (1), Daniel Becker (2), Mirunalini Thirugnanasambandam (4), Oliver Opatz (3), Anil Aksöz (5), Bernd Jung (1), Fabian Haupt (1)

1. Department of Radiology, Inselspital, University of Bern, Switzerland; 2. Department of Vascular Surgery, Inselspital, University of Bern, Switzerland; 3. Department of Anesthesiology and Intensive Care Medicine, Charité – Universitätsmedizin Berlin, Germany; 4. PULS/e, Department of Biomedical Engineering, Eindhoven, the Netherlands; 5 Laboratory for Rehabilitation Engineering, Bern University of Applied Sciences, Switzerland.

1. Introduction

Rupture risk assessment in abdominal aortic aneurysm (AAA) is primarily based on maximum diameter, a static surrogate that does not adequately reflect patient-specific biomechanical behaviour under physiologic load and wall stress distribution [1]. In addition, altered flow-derived parameters such as wall shear stress and relative residence time have been associated with AAA pathophysiology and progression [2,3]. Within the Virtual Physiological Human paradigm, SmartLyf aims to develop a multimodal digital framework integrating stress-based MR imaging, wearable-derived physiological signals, and computational hemodynamic modeling for individualized biomechanical risk profiling.

2. Materials and Methods

Thirty-one male participants, including 21 healthy volunteers and 10 AAA patients with aneurysm diameter below 6.0 cm, underwent MR imaging of the infrarenal abdominal aorta at rest and after controlled physical stress using a modified MR-compatible stepper. Exercise intensity was individualized based on prior bicycle spiroergometry. Two-dimensional phase-contrast and CINE MR images were acquired within 20s after exertion, followed by 4D flow MRI after recovery. Heart rate and blood pressure were recorded using MR-compatible monitoring. From synchronized imaging and physiological data, pulse wave velocity, wall stress, and stiffness parameters were derived and processed within the SmartLyf digital platform.

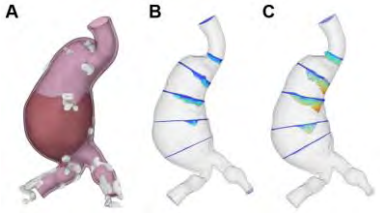


Figure 1: CT based wall modelling (**A**) with 2D and 4D MR flow modelling at rest (**B**) and stress (**C**).

3. Results

Stress MRI was technically feasible in all subjects, reaching approximately 78 percent of peak spiroergometry workload. Compared with rest, stress significantly increased heart rate (12%, $p < .001$), blood pressure (16%, $p < .001$), and peak infrarenal aortic flow (19%, $p = .006$). Post-stress 4D flow enabled volumetric flow characterisation and integration of spatial haemodynamic parameters. Stress-derived indices were associated with aneurysm diameter and structural characteristics. A fully functional digital workflow and app prototype enabled standardised acquisition, processing, and visualisation of patient-specific biomechanical data, forming the basis for future digital twin modelling.

4. Discussion and Conclusions

SmartLyf enables individualized rupture risk assessment in AAA by integrating stress-enhanced MR imaging, 4D flow analysis, biomechanical modeling, and synchronized physiological data within a unified digital framework. The feasibility data demonstrate that stress-based MR assessment captures dynamic aortic behavior beyond static diameter criteria and extend prior 4D flow–based investigations of hemodynamic markers such as wall shear stress and relative residence time in AAA [2,3], providing the methodological foundation for AI-supported digital twin approaches in predictive and precision vascular medicine.

5. References

1. Malkawi AH et al. J Vasc Surg. 52:480-488 (2010).
2. Trenti C et al. J Cardiovasc Magn Reson. 24:18 (2022).
3. Aalbregt E et al. J Magn Reson Imaging. 60:878-888 (2024).

Acknowledgements:

Innosuisse (project **39833.1 IP LS**) for providing financial project support. Thanks to A.M. Pascual and M. Rochette (Ansys, Inc.) for initial CFD results and to A. Razmi (SKAN AG) and Pascal Leimer (SIPBB) for data and study support.

AUTOMATED VMS-CFD PIPELINE FOR HEMODYNAMIC DECISION SUPPORT IN ANEURYSM SEGMENTATION

John Zarate[1], Bruno Figliuzzi[1], Philippe Meliga[1], Yves Chau[2], Elie Hachem[1]

1. PSL University, France; 2. Nice University Hospital, France

1.Introduction

Clinical management of intracranial aneurysms depends on accurate hemodynamic assessment [1]. While Deep Learning accelerates segmentation standard geometric evaluations like Dice ignore functional consequences. We present an automated end to end pipeline coupling segmentation remeshing and VMS simulation. This framework transforms medical imaging into reliable hemodynamic predictions quantifying how preprocessing strategies affect the final clinical indicators.

2. Materials and Methods

Our automated pipeline processes Computed Tomography Angiography (CTA) through distinct 3D U Nets trained with varying preprocessing strategies. Topology preserving algorithms convert masks into volumetric meshes (0.0875 mm). Finally, a Variational MultiScale (VMS) solver [2] resolves the unsteady Navier Stokes equations coupled with a Casson model. Patient specific pulsatile inflows are imposed and renormalized via Murray Law to ensure physiological consistency.

3. Results

The pipeline produced consistent clinical indicators despite anatomical variations. While local velocity probes showed sensitivity to geometry, macroscopic metrics critical for decision making such as bulge inflow and spatially averaged WSS remained robust. Figure 1 confirms that normalized WSS patterns align across all generated models demonstrating the pipeline stability for risk assessment

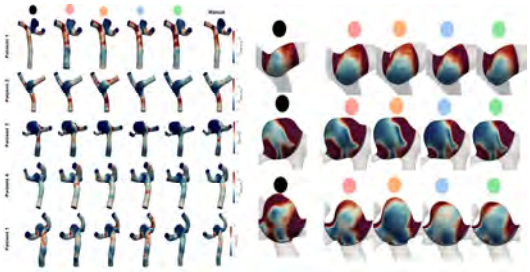


Figure 1: Left: Complete simulations across multiple AI-generated geometries. Right: Representative geometries highlighting specific pattern differences on the aneurysm bulge. Color code: Black (Ground Truth), Blue (Data Augmentation), Orange (Bilateral Filter), Green (Combined), Red (Baseline).

4. Discussion and Conclusions

We demonstrate that global clinical indicators remain stable despite local sensitivity validating the pipeline robustness against anatomical variability. This physics grounded framework ensures AI derived models are reliable beyond simple geometric overlap. Integrating this automated workflow with emerging technologies like graph neural networks [3] brings us significantly closer to a real-time decision-making tool for clinicians.

5. References

[1] Shojima M et al., Stroke; 35:2500–2505 (2004).
[2] Coupez T et al., Comput Methods Appl Mech Eng; 267:65–85 (2013).
[3] Lannelongue V et al., npj Digit. Med. (2026).

Acknowledgements:
This research was funded by the European Union's Horizon ERC grant 101045042 (Project CURE).

LEFT VENTRICULAR VORTEX DYNAMICS AS A MECHANISTIC BIOMARKER OF CARDIAC FUNCTION BASED ON CLINICAL CARDIAC DATA

Priyanshu Soni (1*), Abhra Bhattacharyya (1), Abdullah Yousuf Usmani (2), Sanjeev Kumar Vishwakarma (1), Sanjay Kumar Rai (1), Om Shankar (3), Ashish Verma (4), B.V. Rathish Kumar (5)

1. School of Biomedical Engineering, Indian Institute of Technology (BHU), Varanasi, India; 2. Department of Mechanical Engineering, Zakir Hussain College of Engineering and Technology, AMU, Aligarh, India; 3. Department of Cardiology, Institute of Medical Sciences (BHU), Varanasi, India; 4. Department of Radio-diagnosis, Institute of Medical Sciences (BHU), Varanasi, India; 5. Department of Mathematics and Statistics, Indian Institute of Technology Kanpur, India

[*Corresponding author details: priyanshusoni.rs.bme22@itbhu.ac.in]

1. Introduction

Intraventricular blood flow is three-dimensional, pulsatile, and strongly geometry-dependent. Conventional vortex-identification criteria such as the Q- and λ2-criteria do not separate rigid-body rotation from shear, a limitation most acute in the left ventricle (LV), where the transmitral jet generates shear immediately adjacent to the diastolic vortex ring [1]. This study applies the Rortex method, which isolates the rigid-body rotation component of the velocity gradient tensor, to compare vortex identification against Q and λ2 across four patient-specific LV geometries.

2. Materials and Methods

Four LV models (LV-1 to LV-4) were reconstructed from cardiac CT data and simulated under identical, physiological pulsatile inflow via transient finite-volume CFD. Post-processing included velocity, vorticity, circulation, swirling strength, WSS-based indices, and Q-, λ2-, and Rortex-based vortex identification. Thresholds were calibrated within each geometry to a common vortex volume fraction for matched-volume comparison via a rotation-purity metric; the Rortex implementation was verified against rigid-body-rotation and pure-shear benchmarks.

3. Results

Flow organisation differed markedly among the four geometries. LV-4 sustained a compact, axially stable vortex core with favourable WSS. LV-1 showed strong but diffusely distributed circulation, LV-2 fragmented end-systolic remnants, and LV-3 diffuse, weakly organised vortices with low WSS and elevated residence time, indicating stasis risk. Rortex identified more rotationally pure vortex cores than either conventional criterion in every geometry, with this advantage widening as vortex coherence decreased.

4. Discussion and Conclusions

These findings show that ventricular geometry, rather than cardiac phase, governs vortex formation and stability, and that rigid-body-rotation-based identification is most beneficial precisely where the vortex is weakest and Q- and λ2-criteria are least reliable. This positions Rortex-based analysis as a mechanistic, geometry-sensitive biomarker of LV function relevant to patient-specific and pathological studies, supporting subject-specific CFD for precision cardiology. As a complementary extension, a moving-mesh idealized-LV formulation with prescribed mitral inflow and a free aortic outlet is undergoing three-grid convergence verification (ASME V&V 20) ahead of applying this comparison to dynamically deforming domains.

5. References

1. Nagargoje MS, et al. A review on vortex dynamics in the healthy and dilated left ventricles and its application to heart health. Flow. 2025;5:E10.
2. Liu C, Gao Y, Tian S, Dong X. Rortex – a new vortex vector definition and vorticity tensor and vector decompositions. Phys Fluids. 2018;30:035103.

Acknowledgements:

The authors acknowledge financial support from the Indian Council of Medical Research (ICMR), India (GIA/2019/000607/PRCGIA IRIS cell, ID No. 2020-9527).

TOWARDS A PATIENT-STRUCTURED DATA MODEL FOR AI-DRIVEN ANALYSIS OF PHOTON-COUNTING CORONARY CTs

Andrea Arcangeli (1), Katia Capellini (1), Alberto Aimo (2), Michele Emdin (2), Mariaelena Occhipinti (3), Matilda Muca (3), Francesca Pignatelli (3), Carmelo De Gori (3), Vincenzo Positano (1), Simona Celi (1), Alberto Clemente (3)

1. Bioengineering Unit, Fondazione Monasterio, Italy; 2. Cardiology and Cardiovascular Medicine Fondazione Monasterio, Italy; 3. Department of Radiology, Fondazione Monasterio, Italy

1. Introduction

The growing use of artificial intelligence (AI) in coronary computed tomography angiography (CCTA) highlights the lack of standardized, machine-readable representations for storing patient-specific coronary information. Heterogeneous and task-specific data formats limit interoperability and the integration of multiple AI models within the radiological workflow, including radiomics-based analyses. In many AI-based coronary pipelines, centerline extraction represents a common initial step for downstream processing. The advent of photon-counting CT (PCCT) further expands these scenarios [1], enabling new AI-driven approaches for coronary modelling that offer a central and extensible framework to support reproducible AI-driven assessment and feature extraction.

2. Materials and Methods

A semi-automatic pipeline was developed for coronary lumen segmentation, centerline extraction, and patient-specific coronary modelling from ultra-high-resolution (UHR) photon-counting CT coronary CT angiography (PCCT CCTA) images (Fig. 1A). Final coronary lumen segmentation was obtained using a dedicated AI-based segmentation model trained on a dataset of 14 subjects, followed by manual refinement with 3D Slicer to ensure anatomical accuracy and consistency. The coronary centerline was extracted from the refined lumen segmentation and uniformly resampled at a fixed spatial step of 0.50 mm. When associated with the original DICOM source images and corresponding instance metadata, this representation enabled precise spatial localization of the coronary lumen within the PCCT CCTA volume (Fig. 1B).

All extracted data, including centerline coordinates, graph connectivity information, and patient-specific metadata, were stored in a structured eXtensible Markup Language (XML) file to provide a comprehensive and interoperable digital representation of the patient-specific coronary anatomy (Fig. 1C).

3. Results

The nnU-Net ResEnc M model trained on 14 UHR PCCT CCTA subjects achieved a Dice similarity coefficient = 0.74 ± 0.05 using a 5-fold cross-validation scheme

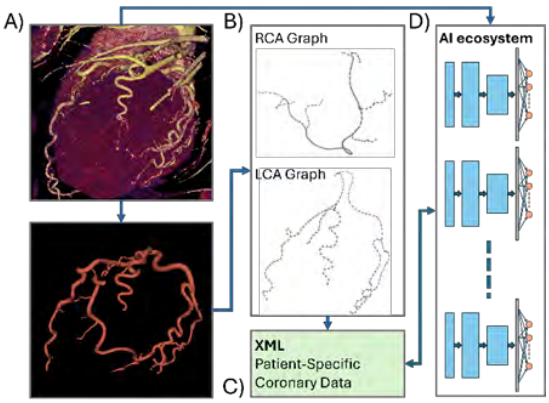


Figure 1: Pipeline from UHR CCTA coronary lumen semantic segmentation (A) to graph construction (B) and patient-specific XML data (C) enabling AI-driven downstream analysis (D).

4. Discussion and Conclusions

This work introduces a semi-automatic framework for coronary centerline extraction and structured patient-specific data modelling from UHR PCCT CCTA. The proposed XML representation enables reproducible and modular integration of AI models, supporting scalable downstream analyses within the coronary imaging workflow.

5. References

1. Meloni, A. et al, Cardiovascular diagnosis and therapy. 2024; 14(4), 698-724.
2. Isensee, F. Et al, Nature methods, 2021; 18(2), 203-211.

Acknowledgements:

This work was supported by the ACTA Study (Project 297/22 - CUP J59I24002760007) funded by Fondazione Pisa.

RECONSTRUCTION OF PLANAR BLOOD FLOW IN LEFT VENTRICLE WITH OUT-OF-PLANE MASS TRANSPORT CONSIDERED

Fumiya Yamada (1), Kenjiro Shimano (2), Suguru Shiratori (2), Hideaki Nagano (2)

1. Graduate School of Integrative Science and Engineering, Tokyo City University, Japan;
2. Department of Mechanical Systems Engineering, Faculty of Science and Engineering, Tokyo City University, Japan

g2581075@tcu.ac.jp

1. Introduction

Conventional colour-Doppler echo-cardiography with a single transducer can measure one component of the flow velocity on the inspection plane. For better understanding of haemodynamics, the second velocity component perpendicular to the measured one is calculated by a flow reconstruction method. The vector flow mapping (VFM) is one of such reconstruction methods and the most widely used for ventricular flows, being based on a two-dimensional (2D) continuity equation [1]. Therefore, mass transport in the out-of-plane direction is neglected by the VFM. This assumption is not always appropriate for three-dimensional flows [2]. Shimano et al. proposed a three-dimensional (3D) method in which mass transport in the out-of-plane direction is considered. However, the 3D method has not been fully validated in ventricular flow. In this study, using ventricular blood flow calculated by computational fluid dynamics (CFD) as reference data, Shimano's 3D method was validated.

2. Materials and Methods

Pulsatile 3D blood flow in the left ventricle was computed using CFD with the 4D left ventricular model of Grünwald et al. [3]. The 3D method was applied to a 2D flow profile on an arbitrary plane extracted from the 3D data. Noise was deliberately added to the extracted flow data so that characteristics of the 3D method could be examined. Assuming a signal-to-noise ratio of 15 to 20 dB for Colour-Doppler, a conservative estimate adds 5% Gaussian white noise to CFD data [4].

The 3D method solves the minimization problem with the following objective function:

$$f = \int_S (\alpha D^2 + \beta \omega^2)\, ds \qquad (1)$$

where D, ω and S are 2D divergence, 2D vorticity and the entire domain, respectively. The parameters α and β are positive weights. The second component is calculated by solving a discretized form of Eq. 1. Computational results of the 3D method and VFM were compared to the original 3D flow profile.

3. Results

In Fig.1, the exact 2D divergence distribution is compared to those calculated by the 3D method and VFM in the case where no noise was added.

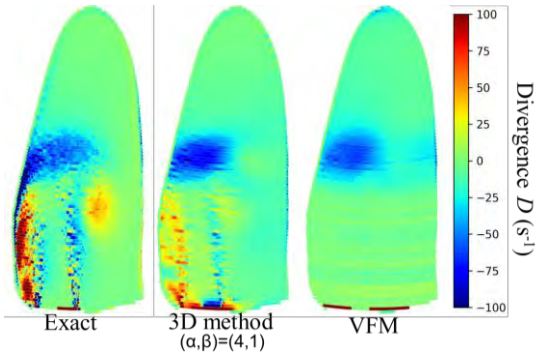


Fig.1: Comparison of 2D divergence distribution from Exact data, 3D method, and VFM

4. Discussion and Conclusions

It is clearly seen in Fig.1 that the 3D method estimated the 2D divergence more accurately than VFM. Although not shown here, the 3D method could also produce better results than VFM when noise was added to the original flow data and when different planes were chosen for the measurement plane.

5. References

1. D Garcia, et al. IEEE Trans Med Imaging.,29(10), 2010.
2. K Shimano, et al. Meccanica, 59(7), 2024.
3. A Grünwald, et al. Cardiovascular Engineering and Technology, 13(11), 2022.
4. H S Wong, et al. Comput Methods Programs Biomed, 263, 2025.

TOPOLOGICAL DEEP LEARNING ON GRAPHS FOR ARRHYTHMIA RISK PREDICTION FROM IMAGES

Evariste Njomgue Fotso (1, 2), Buntheng Ly (2), Hubert Cochet (2), Maxime Sermesant (2)

1. Inria, Université Côte d'Azur, Epione team, Sophia Antipolis, France; 2. IHU Liryc, Université de Bordeaux, Bordeaux, France

Abstract

Graph convolutional networks (GCNs) are widely used in medical image analysis on anatomical meshes and graphs, but their message passing primarily models pairwise (node-to-node) interactions, limiting higher-order anatomical representation. Topological Deep Learning (TDL) has recently enabled learning on higher-order domains (nodes, edges, faces) and has been most commonly adopted in medical imaging for segmentation tasks. In this work, we bridge TDL with clinical risk stratification by leveraging anatomical shape structure for outcome prediction. We use simplicial complex convolutional neural networks (SCCNNs) and introduce a gradient-based projection that lifts node features to edges and faces using feature gradients (compared with standard sum projection), capturing local geometric variation on cardiac surfaces.

We apply this approach to ventricular arrhythmia (VA) risk prediction from cardiac CT, where left-ventricular (LV) myocardium thinning is associated with scar and abnormal electrical activity. Our pipeline segments LV masks, computes LV myocardial thickness, and generates a mid-wall surface mesh. Myocardial thickness is used as the node feature, with higher-order information incorporated through sum or gradient-based projection.

In cross-validation, the GCN baseline achieves an AUC of 80%. SCCNN with sum projection improves AUC to 82%, and SCCNN with gradient-based projection further improves it to 84%. Beyond performance, we emphasize interpretability: qualitative Grad-CAM analysis shows that gradient-based projection produces sharper and more clinically plausible activations than sum projection, better aligned with surviving myocardium within scarred regions and providing clearer localization of re-entry channel candidates. Together, these contributions demonstrate how higher-order simplicial learning can connect anatomical shape modeling with interpretable, imaging-based VA risk stratification.

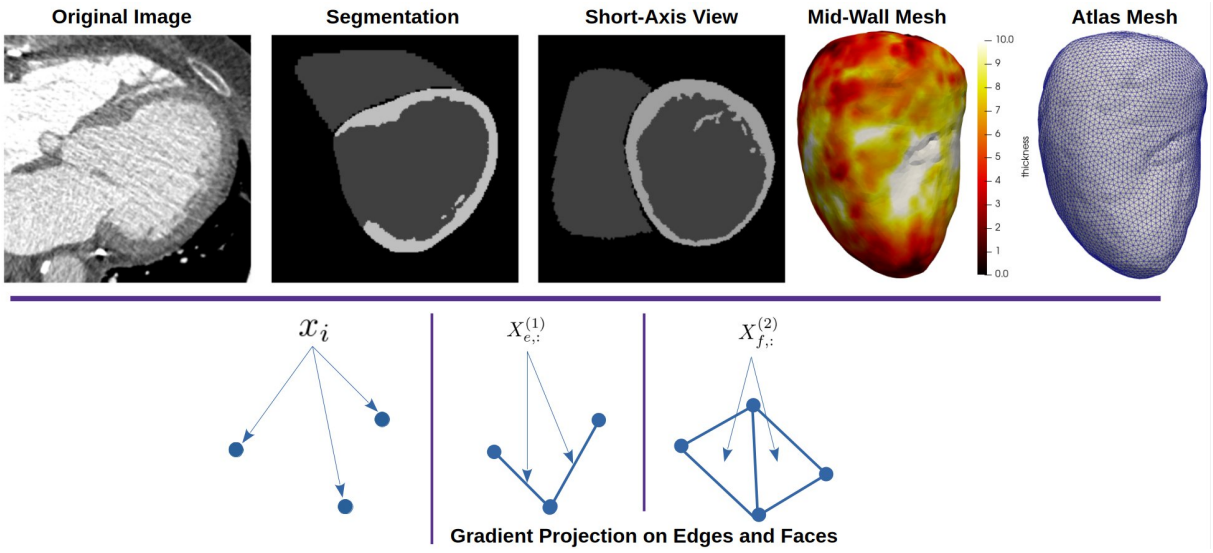


Figure 1: Data processing pipeline: from image segmentation to features projection on edges and faces.

AUTOMATED FRAMEWORK FOR CT-BASED STRAIN ESTIMATION AT THE LEFT ATRIAL APPENDAGE LANDING ZONE

Ilaria Verdirame (1, 2), Andrea Papini (1, 2), Francesca dell'Agnello (1), Rossana Buongiorno (1), Benigno Marco Fanni (1), Emanuele Vignali (1), Sergio Berti (3), Simona Celi (1)

1. BioCardioLab, Bioengineering Unit, Fondazione Monasterio, Italy; 2. Department of Information Engineering, University of Pisa, Italy; 3. Adult Cardiology Unit, Fondazione Monasterio, Italy

1. Introduction

The left atrial appendage (LAA) is the primary source of thromboembolism in patients with atrial fibrillation. While LAA occlusion (LAAO) is an established intervention, its success is closely linked to the biomechanical interaction between the device and the left atrial (LA) wall. Current clinical guidelines rely on static geometric sizing, such as maximum ostium diameters measured at a single cardiac phase [1]. However, quantifying the dynamic strain at the landing zone (LZ) provides a more accurate characterization of the mechanical environment that governs device anchoring and stability.

This study aims to quantify patient-specific strain at the LZ using multi-phase ECG-gated CT scans. To this end, an automated pipeline integrating AI-based segmentation and a mesh morphing algorithm is presented.

2. Materials and Methods

A custom-trained 3D nnU-Net [2] was employed to automatically segment the LA and the LZ of 20 patients across ten phases of the cardiac cycle (0-90%). To capture the complex wall motion, an in-house non-rigid registration algorithm was utilized to map the baseline mesh topology (0% phase) onto the target geometries segmented at the other CT phases (10-90%) [3, 4]. By preserving node count and connectivity across all segmented models, this mesh morphing approach enables the reconstruction of consistent patient-specific node trajectories, from which the infinitesimal strain tensor ε is derived:

$$\varepsilon = \frac{1}{2}(\nabla \boldsymbol{u} + (\nabla \boldsymbol{u})^T) \qquad (1)$$

where $\boldsymbol{u}$ is the displacement field.

To ensure the physical consistency required for reliable digital twins, the morphing-derived strains were validated against finite element method (FEM) simulations.

3. Results

The AI-based segmentation achieved high fidelity in identifying the LAA ostium, with a median Dice score of 0.85 and precision of 0.84. Strain mapping revealed peak maximum principal strains (ε_{max}) of 0.45–0.5 during the systolic phases (20 – 40%).

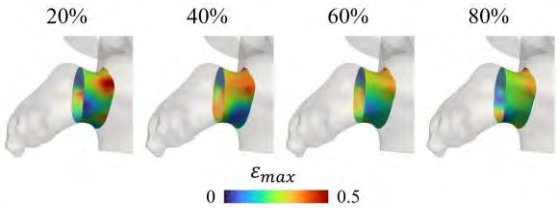


Figure 1. Distribution of the maximum principal strain (ε_{max}) at the LZ at different cardiac phases.

Validation against FEM models showed node-wise discrepancies below the CT spatial resolution of 1 mm, with no significant differences observed between the two methods ($p > 0.05$). This confirms that the automated morphing approach accurately captures the biomechanical environment of the LZ without the computational cost of full-scale simulations.

4. Discussion and Conclusions

This workflow provides an automated tool for patient-specific LZ strain assessment. By offering a user-independent characterization, it supports the development of clinical decision systems, potentially improving device sizing and reducing post-procedural complications through personalized in silico planning.

5. References

1. Glikson M et al., EIJ, 15(13):1133-1180 (2020).
2. Buongiorno R et al., CSBJ, 28:175-189 (2025).
3. Verdirame I et al., LNCS 15672 (2025).
4. Dell'Agnello F et al., CBM, 198:111202 (2025).

Acknowledgements:

This work was part of the project "PLACE - Planning LAa ClosurE" (RF-2021-12375208), funded by the Italian Ministry of Health.

MATRIX-FREE SIMULATION OF CARDIAC PERFUSION ON HIGH-PERFORMANCE COMPUTING ARCHITECTURES

Junxiang Wang[1*], Luca Dede' [1]

[1] MOX, Dipartimento di Matematica
Politecnico di Milano, Italy
e-mail: junxiang.wang@polimi.it,

1. Introduction

Cardiac perfusion is governed by fluid transport through a deformable porous myocardium and is strongly coupled with tissue mechanics [1,2]. Accurate numerical simulation of this process is essential for understanding physiological perfusion as well as pathological conditions such as ischemia and microvascular dysfunction. However, fully coupled poromechanical models of cardiac perfusion pose significant computational challenges due to nonlinear solid deformation, strong multiphysics coupling, and the large-scale three-dimensional domains required for realistic simulations.

2. Methods

This work presents a matrix-free finite element framework for poromechanical cardiac perfusion, specifically designed for large-scale high-performance computing applications [3]. The governing equations are formulated within a poromechanical framework, coupling nonlinear myocardial deformation with fluid mass conservation and permeability-driven transport in the deformable porous myocardium. All linearized operators are applied in a matrix-free manner, thereby avoiding the explicit assembly and storage of global system matrices. This formulation substantially reduces memory requirements and improves arithmetic intensity, making it well suited for modern many-core and distributed-memory architectures.

3. Results

Numerical experiments on organ-scale myocardial perfusion, representative of left ventricular flow, demonstrate the accuracy, robustness, and parallel scalability of the proposed framework. The matrix-free formulation achieves strong and weak scalability across a large number of compute cores, with memory consumption and time-to-solution that compare favourably against conventional matrix-based approaches.

4. Discussion and Conclusions

Efficient matrix-free operator evaluation, scalable solver and preconditioning strategies, and parallel implementation aspects are discussed. These findings confirm the suitability of the proposed framework for high-resolution cardiac perfusion simulations at a computational cost that would be prohibitive for conventional matrix-based methods.

5. References

[1] Barnafi Wittwer, N. A., Gregorio, S. D., Dede', L., Zunino, P., Vergara, C., & Quarteroni, A. A multiscale poromechanics model integrating myocardial perfusion and the epicardial coronary vessels., SIAM Journal on Applied Mathematics, 82(4), 1167-1193., 2022.

[2] Chapelle, D., Gerbeau, J. F., Sainte-Marie, J., & Vignon-Clementel, I. E. A poroelastic model valid in large strains with applications to perfusion in cardiac modeling., Computational Mechanics, 46(1), 91-101., 2010

[3] Kronbichler, M., & Kormann, K. A generic interface for parallel cell-based finite element operator application, Computers & Fluids, 63, 135-147., 2012.

Acknowledgment: This work was supported by the project "dealiiX: an Exascale Framework for Digital Twins of the Human Body" (project number 101172493), funded for the period 1 October 2024 – 31 December 2026.

UNCERTAINTY QUANTIFICATION IN CARDIAC MODEL PERSONALISATION FROM ULTRAFAST ULTRASOUND

Camilla Ferrario (1,2) and Maxime Sermesant (1,2)

1. Inria, Université Côte d'Azur; Sophia Antipolis, France 2. IHU Liryc, Pessec, France

1. Introduction

Reduced cardiac models enable efficient subject-specific simulations, but their personalisation requires inferring mechanical parameters that are not directly measurable *in vivo*. Ultrafast ultrasound shear wave elastography (SWE) provides non-invasive measurements of myocardial stiffness over the cardiac cycle, offering a clinically relevant target for constraining myocardial mechanics [1]. However, translating SWE-derived stiffness dynamics into model parameters remains an ill-posed inverse problem due to noisy and indirect observations, limited identifiability, and parameter non-uniqueness.

2. Materials and Methods

We formulate SWE-informed personalisation as a context-conditioned simulation-based inference (SBI) problem [2,3]. A reduced (0)D cardiovascular model is adapted for each subject using clinical context, including ventricular volumes, septal thickness, heart rate, age, sex, and body surface area. The inferred parameters are the active stiffness scale k_0 contraction rate k_{ATP}, and relaxation rate k_{SR}. For each subject, candidate parameter sets are sampled from a physiologically bounded prior and simulated with the context-adapted model. Simulated stiffness curves are summarized into interpretable SWE-derived features and concatenated with the subject context to form the conditioning vector. A neural posterior estimator, implemented using the *sbi toolbox* [4], is trained to infer posterior distributions over the active parameters from this conditioning information. Posterior samples are then propagated through the model to assess predictive agreement with the measured SWE curve, posterior contraction, and parameter dependencies.

3. Results

The framework was evaluated in 5 healthy volunteers. Posterior predictive simulations improved over the prior and reproduced the main SWE stiffness dynamics. The parameters k_0 and k_{ATP} were most consistently constrained, whereas k_{SR} showed more subject-dependent uncertainty. Pairwise posterior analysis revealed coupling between k_0 and k_{ATP}, highlighting residual non-identifiability that would not be captured by single-solution fitting

4. Discussion and Conclusions

These results support the use of context-conditioned SBI for uncertainty-aware personalisation of reduced cardiac mechanics models from non-invasive ultrasound measurements. By estimating posterior distributions rather than a single best-fit parameter set, the proposed approach provides a principled way to quantify parameter uncertainty and non-uniqueness in SWE-informed cardiac model personalisation.

5. References

1. Villalobos Lizardi JC et al. A guide for assessment of myocardial stiffness in health and disease. Nat Cardiovasc Res 2022 1:8–22. doi:10.1038/s44161-021-00007-3.

2. Cranmer K et al. The frontier of simulation-based inference. Proc Natl Acad Sci 2020 117:30055–30062. doi:10.1073/pnas.1912789117.

3. Wehenkel A et al. Simulation-based Inference for Cardiovascular Models. 2024. doi:10.48550/arXiv.2307.13918.

4. Boelts J et al. sbi reloaded: a toolkit for simulation-based inference workflows. 2025. doi:10.48550/arXiv.2411.17337.

Acknowledgements:

This work was supported by the French government through ANR funding: PEPR Digital Health ChroniCardio (22-PESN-0015) and IHU Liryc (ANR-10-IAHU-04). We acknowledge the OPAL infrastructure at Université Côte d'Azur for computational resources and technical support.

RESIDUAL GRAPH NEURAL NETWORK FOR VASCULAR RECONSTRUCTION FROM THINNING SKELETONS

Vedika Bedi, Emmeline Brown, Simon Walker-Samuel
Centre for Computational Medicine, Division of Medicine, University College London, United Kingdom

1. Introduction

Building patient-specific vascular digital twins, requires extracting vasculature network from a medical image, including, junctions, end points, and edges carrying biophysical attributes such as diameter or blood flow. Currently, extraction steps produce noisy maps and automated segmentation algorithms generate spurious branches and missing connections. Global topological reasoning on the complete network is required to resolve these errors since a spurious branch is locally indistinguishable from a real one, making this mapping a recurring bottleneck.

2. Materials and Methods

We report preliminary findings from 389 paired synthetic vascular trees, where 332 were used for training a graph neural network (GNN) and 57 for validation. Ground truth synthetic spatial graphs and their skeletonised pair, a thin centreline representation extracted from the image, from the Pymira toolkit [1] were used. A GATv2 backbone was then used to feed three head outputs: i) residual per-node coordinate prediction; ii) per-edge biophysics including a per-point radius profile; iii) candidate-pair link prediction within 10% of the field of view for broken chain reconnection. Supervision used 1-nearest-neighbour matching to ground truth edge polylines.

3. Results

The model recovered vessel positions with high accuracy ($R^2 = 0.979$, with positional errors of 1.13% of the field of view) (Fig. 1). Residual positions predictions as corrections to the skeleton rather than from scratch cut this error by 41%. Vessel radii were partially recoverable (R^2=0.2, ~16% error), and haemodynamic quantities like flow rate and branching order are effectively unrecoverable from local geometry alone ($R^2 < 0.15$), informing us that a geometry-only model cannot substitute for a physics-based simulator. Reconnecting broken vessels is architecturally capped and roughly 70% of the true vessel connections collapsed into single skeleton points during extraction, meaning the information needed to recover them was not present. This restricted recoverable topology to 30% without new node generation points. The current GNN reached 37% recall, characterising where additive link prediction saturated.

4. Discussion and Conclusions

This work demonstrated that a GNN can recover vessel positions from noisy skeletons at voxel-scale precision but that radii, haemodynamic attributes, and topological completeness remained beyond what local geometric reasoning alone can provide. The 16% radii error amplifies under Poiseuille flow to >50% per-vessel flow error, significantly exceeding clinical hemodynamic tolerance. A current limitation is the use of synthetic data only. Ongoing work targets vertex generation for the ~70% of synthetic spatial graph edges that collapse onto a single skeletonised vertex, and implementing physics-informed GNNs.

5. References

1. Brown EE, Guy AA, Holroyd NA, et al. Physics-informed deep generative learning for quantitative assessment of the retina. Nature Communications. 2024;15:6859.

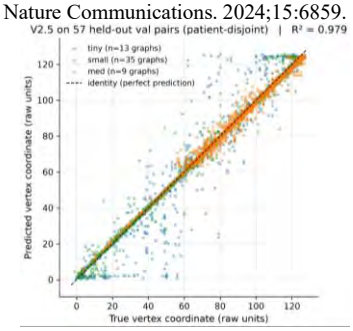


Fig. 1: Predicted vs true vertex coordinates on 57 validation pairs.

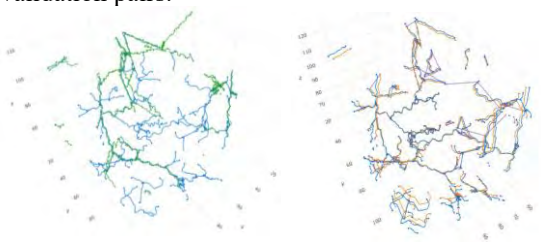


Fig. 2: **Left:** Ground Truth (green) and skeletonised (blue) spatial graph. **Right:** Corrected spatial graph (orange), and added link (purple).

Acknowledgements:
We acknowledge funding from Cancer Research UK ((28276 and C44767/A29458)) 475 and EPSRC ((EP/W007096/1)

A COMPUTATIONAL MODEL OF THE HEART TO INVESTIGATE RIGHT HEART FAILURE

Gabriel Guerin[1], Alessandro Banti[1], Claire Dupont[1], Elena Galli[2], Anne-Virginie Salsac[1], Elena Cutrì[1]

1. Université de technologie de Compiègne, CNRS, Alliance Sorbonne Université, BMBI, Compiègne, France; 2. Translational Cardiovascular Medicine, Université de Strasbourg, France;

1. Introduction

Right heart failure (RHF) is a clinical syndrome characterised by signs and symptoms of heart failure, resulting from dysfunction of the right ventricle (RV) [1]. Despite advancements in understanding RV pathophysiology over recent decades, many aspects of the condition remain unresolved due to its inherent complexity. In this context, our objective is to develop a computational model of the heart to simulate the early stages of RHF, thereby enhancing the understanding of the underlying pathology.

2. Materials and Methods

The heart geometry was created using an open patient-specific database [2]. The passive behaviour of the myocardium was characterised as an anisotropic hyperelastic material [3], whereas the active behaviour was described according to [4]. The 3D Finite Element Modelling of the heart was coupled with a 0D closed-loop model of circulation.

Simulations were performed using ANSYS LS-Dyna, with pre- and post-treatment handled using PyAnsys-Heart libraries [5]. Firstly, the physiological case was reproduced. Secondly, RHF was simulated by combining RV volume overload, RV pressure overload and RV impaired contractility.

3. Results

The pressure-volume (PV) loops of the RV in the physiological case and in the pathological conditions are shown in Fig. 1. In the case of pressure overload (green), the RV systolic peak pressure is higher, while the RV stroke volume and consequently the ejection fraction (EF) are lower than in the physiological case. The volume overload (orange) reduces the RV systolic peak pressure and increases the end-diastolic volume.

The effect of impaired contractility (red) on the PV loop is modest.

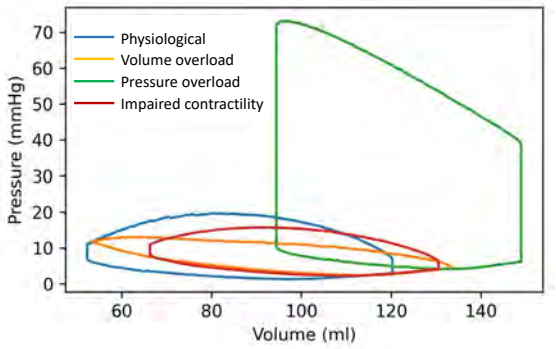


Figure 1: Right ventricular pressure-volume (PV) loops illustrating the physiological conditions (blue), volume overload (orange), pressure overload (green)and impaired contractility (red).

4. Discussion and Conclusions

The developed computational model allows us to investigate the effects of the main determinants of RHF on RV performance, namely RV volume overload, RV pressure overload and impaired contractility. The investigation of these effects will permit to gain further insights into the mechanisms occurring in the early stages of the RHF development.

5. References

1. Jogendran R. et al., Can. J. Cardiol, 41(2025), pp. 1152-1161.
2. Rodero C. et al., PLoS Comput. Biol., 2021.
3. Holzapfel G.A. and Ogden R.W., Philos Trans A Math Phys Eng Sci, 367(2009), pp. 3445-3475.
4. Guccione J.M. et al., J Biomech Eng, 115(1993), pp. 72-81.
5. Hoeijmakers et al. (2023). pyheart-lib. FIMH 2023, LNCS 13958, Springer.

Acknowledgements:

We acknowledge funding from the French Ministry of Higher Education and Research (Gabriel Guérin's PhD thesis), the Research Head Office of Université de Technologie de Compiègne, the Alliance Sorbonne Université, as well as support from ANSYS France.

IMAGE-BASED HIP FRACTURE ASSESSMENT WITH 3D CNN SURROGATES

Yijun Zhou (1), Dheeraj Jha (1), Anitha D Praveen (1), Stephen J. Ferguson (1, 2), Torsten Hoefler (1, 2), Benedikt Helgason (1, 2)

1. Singapore-ETH Centre, Singapore; 2. ETH-Zürich, Switzerland

1. Introduction

Subject-specific biofidelic finite element (FE) models can predict hip fracture risk during sideways falls by capturing femoral geometry, heterogeneous material properties, and soft-tissue cushioning [1]. However, their high computational cost limits clinical use. Here, we propose a 3D convolutional neural network (CNN) surrogate that predicts critical impact velocity for a given fall alignment, enabling estimation of fracture probability in seconds.

2. Materials and Methods

We partitioned 1591 biofidelic FE models (from Singaporean older adults) into fixed validation (n=110) and test (n=100) sets. The remaining scans formed training sets of increasing size ($N \in \{200, 500, 1000, 1381\}$) to assess data scaling. Each model underwent ~20 simulated falls at varying impact angles and speeds to determine the critical impact velocity V_{crit} - the minimum velocity at which a femur fracture occurs for a given fall angle [2]. The FE models were transformed into 3D voxel grids representing density-related material fields. We fine-tuned a pre-trained 3D ResNet encoder (MedicalNet) [3] to predict V_{crit}. The model was trained using an MSE loss, $\mathcal{L} = \|\hat{V}_{crit} - V_{crit}\|_2^2$. We then computed fracture risk as the probability $P_{Fx}(V \geq V_{crit})$ by overlaying the V_{crit} curve with fall-angle-velocity distributions derived from video data [4].

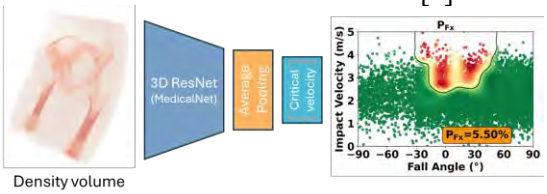


Figure 1: Density volume distribution (left) processed by a 3D ResNet encoder and global average pooling to regress a vector of critical velocities. The right panel illustrates the predicted critical velocity boundary (black curve) separating fracture (red) and non-fracture (green) simulations, which is used to compute the total fracture probability (P_{Fx}).

3. Results

Figure 2 (Left) illustrates the evolution of rMAE and R^2 as a function of training set size. Model generalization was highly sensitive to sample size. While small cohorts (N=200) showed significant overfitting, scaling to N=1,381 narrowed the generalization gap, reducing test rMAE to 0.09 (R^2=0.89) and yielding strong linear alignment with ground truth (Fig. 2, Right).

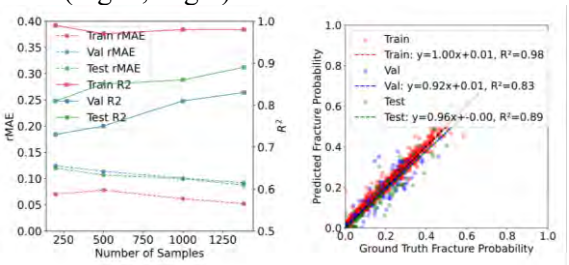


Figure 2: Figure 2: (Left) Evolution of rMAE and R^2 vs. training size. (Right) Predicted vs. Ground Truth fracture probability for the final model (N=1381).

4. Discussion and Conclusions

Model generalization proved highly sensitive to sample size. Small cohorts (N=200) resulted in overfitting and poor calibration, whereas increasing the dataset to 1,381 yielded a near-ideal regression slope (0.96). The lack of performance saturation suggests that further data scaling would likely yield continued improvements. In conclusion, the 3D-CNN model serves as a powerful tool to bypass time consuming FE Analysis producing output in seconds, thus matching time constraints of clinical practice and offering reasonable accuracy that shows clear signs of further improvement with larger datasets.

5. References

1. Fleps et al., JBMR, 34(10):1837-50 (2019)
2. Jha et al., Clin. Biomech., 106720 (2025).
3. Sihong et al., arXiv:1904.00625 (2019)
4. Jha et al., JBMR Plus, Under review (2025)

Acknowledgements:
This research was conducted at the Future Health Technologies at the Singapore-ETH Centre, which is supported by the National Research Foundation Singapore (NRF) under its Campus for Research Excellence and Technological Enterprise (CREATE) programme.

AN FPCA-BASED METHOD TO PREDICT TIBIOFEMORAL KINEMATICS FROM TWO BIPLANE RADIOGRAPHS

Elisa Jolas (1), Sacha Guitteny (1), Nolwenn Fougeron (2), Rachid Aissaoui (3), Charles Pontonnier (2), Raphaël Dumas (1)

1. Univ. Eiffel, LBMC UMR_T9406, Lyon, France; 2. Univ. Rennes, Inria, CNRS, IRISA - UMR 6074, Rennes, France; 3. ÉTS, LIO-ETS, Montréal, Canada

1. Introduction

Accurate estimation of tibiofemoral kinematics is essential for surgical planning and evaluation of medical devices such as orthoses. However, high intersubject variability and kinematic alterations in knee osteoarthritis [1] complicate individualized assessment. Partial least squares regression has previously been used to estimate healthy tibiofemoral kinematics [2]. This study aimed to predict pathological tibiofemoral kinematics from two biplane radiographs.

2. Materials and Methods

EOS biplane radiographs from 57 patients with severe knee osteoarthritis (61 ± 9 years, Kellgren-Lawrence grade 4) were analyzed. Each patient performed 2 to 5 static weight-bearing squats (from -5° to 95° knee flexion), with or without an orthosis, yielding 509 poses in total, including 339 poses with personalized valgus Evoke orthoses (Osskin, Canada, Fig. 1).

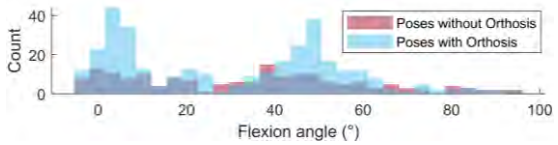


Figure 1: Distribution of knee flexion angles

Tibiofemoral kinematics were derived from 3D bone reconstructions using anatomical coordinate systems on the femur and tibia for each pose. Rotations (Euler angles, Z-X-Y sequence) and translations were analyzed as continuous functions of knee flexion using Functional Principal Component Analysis (FPCA; fdapace, RStudio [3]) to estimate mean and covariance functions and capture the main modes of variation. For prediction, images at ~0° and 45° of knee flexion, routinely acquired clinically, were used to compute principal component scores, enabling reconstruction of full-range kinematics from components explaining 95% of the variance. Prediction accuracy was evaluated on the remaining poses using leave-one-out cross-validation for patients with more than two poses, ensuring at least one pose per patient for evaluation (23 patients, 102 poses in total). Performance was assessed using the coefficient of determination (R^2) and the Root Mean Square Error (RMSE), normalized using the overall observed range across participants for each degree of freedom.

3. Results

The highest errors occurred for medial–lateral translation (Table 1: RMSE = 13.9%, $R^2 = 0.73$) and abduction–adduction rotation (RMSE = 12.4%, $R^2 = 0.66$), whereas the other degrees of freedom achieved $R^2 > 0.7$ and errors < 9%.

	Kinematics	RMSE mm or ° / %	R^2
Translation	Ant-Post	2.2 / 4.2	0.97
	Sup-Inf	2.4 / 5.9	0.94
	Med/Lat	1.9 / 13.9	0.73
Rotation	Abd-Add	1.8 / 12.4	0.66
	Int/Ext rot	4.4 / 8.3	0.73

Table 1: Prediction performance metrics for each tibiofemoral kinematic variable

4. Discussion and Conclusions

FPCA appears suitable for estimating kinematics from sparse data. Lower prediction accuracy for medial–lateral translation and abduction–adduction rotation reflects higher individual variability (osteoarthritis, orthosis). Prediction errors were within the range reported in previous studies (~3.5 mm or ° in [2]). Higher knee flexion poses showed greater errors, likely due to the limited examples at these angles in the model. Incorporating bone geometry and anthropometric characteristics could further improve prediction accuracy.

5. References

1. Zeighami A et al., J Biomech; 28(53):178-184 (2017)
2. O'Rourke D et al., J Orthop Res; 41(8):1709-1716 (2023)
3. Zhou Y et al., https://CRAN.R-project.org/package=fdapace. (2024)

Acknowledgements:
This work was funded by the Région Auvergne–Rhône–Alpes, France (PAI2021).

A VOXEL-BASED LINEAR FINITE ELEMENT MODEL TO PREDICT PROXIMAL HIP FRACTURE IN SIDE-FALLS

Jacob Wilkinson (1), Claire Brockett (1), Pinaki Bhattacharya (1)

1. Pam Liversidge Building, Mappin Street, Insigneo Institute and University of Sheffield, Sheffield S1 3JD, UK

1. Introduction

Osteoporosis (OP) is responsible for ~520,000 fractures annually in the UK, of which ~20% are hip fractures [1]. The finite element (FE) modelling based Computed Tomography to Strength (CT2S) method can classify fracture status with high accuracy [2]. Yet a barrier to its clinical use is the need to reliably mesh the irregular femur volume with tetrahedra. In contrast, the FE solver ParOSol [3] uses a voxel mesh, thus reducing operator time. The present study investigates the potential for OP hip fracture classification using ParOSol.

2. Materials and Methods

Five pairs of age-, weight- and height-matched subjects were selected from Qasim et al. [2] with similar/contrasting femoral neck aBMD T-scores and/or fracture outcomes (Table 1).

Table 1: Pairs of matched subjects with T-scores and fracture status (Fx). Data taken from [2].

Pair	T-Score	Fx	Pair	T-Score	Fx
A	-2.0	N	D	-2.5	N
	-1.0	Y		-0.2	N
B	-0.4	N	E	-0.9	Y
	-0.3	Y		-2.9	Y
C	-2.6	Y			
	-2.5	N			

Proximal femur CT scans were used to create FE models with a Cartesian axis-aligned mesh comprising 8-noded 1 mm cube (voxel) elements. Similar to [2], isotropic, linear elastic material properties, with heterogeneous (CT-derived) elastic moduli were specified; boundary and loading conditions were applied at the distal end, the centre of the femoral head and the greater trochanter simulating a neutral orientation fall loading; elements were considered to have failed if either maximum or minimum principal strains exceeded respective critical values (0.73% and -1.04% respectively). Differently to [2], fall strength was defined as the minimum force needed for all elements to fail in any contiguous region that occupies 5±1% of the proximal femur volume and is located anywhere within it, but away from boundary and loading condition application locations [4]. The FE models were analysed using ParOSol, and strength computation (post-processing) were performed using ParaView.

3. Results

Consistent with CT2S findings, ParOSol predicted failed regions in the superior aspect of the femoral neck (Figure 1A). Compared to CT2S, strength values were underestimated (by ~50%) but systematically (R^2 = 93%) such that the association with fracture status changed negligibly (Figure 1B).

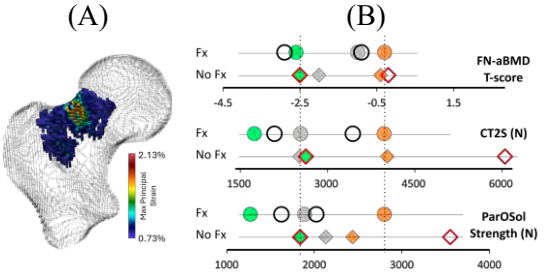


Figure 1: (A) Example predicted failed region with maximum principal strain levels. (B) Fracture status vs T-score, and CT2S- and ParOSol-predicted strengths. Dotted vertical lines mark the ambiguity zone, and identically coloured symbols indicate Table 1 pairs (A–E: grey, orange, green, red, black).

4. Discussion and Conclusions

Conclusions are limited for this preliminary analysis by the very small number of patients. The present results – consistent failed regions, systematic error, association with fracture status – do not obviate the possibility that, with further optimisation of the failure criterion, ParOSol might achieve similar accuracy as CT2S for fall strength prediction and fracture classification.

5. References

1. Borgström et al., Arch Osteoporos, 15(1):59 (2020). **2.** Qasim et al., Osteoporos Int, 27(9):2815 (2016). **3.** Flaig, PhD Thesis, ETH Zürich (2012). **4.** Majcher et al., Sci Rep, 14(1):7029 (2024).

Acknowledgements:
This project was partially supported by UKRI funding (Grant no: EP/V050346/1).

IN-SILICO INFORMED GAIT RETRAINING TO REDUCE MEDIAL COMPARTMENT LOADING IN EARLY KNEE OSTEOARTHRITIS: A PROOF-OF-CONCEPT STUDY

Miel Willems (1), Bryce A. Killen (1), Ilse Jonkers (1)

1. Human Movement Biomechanics Research group, KU Leuven, Belgium

1. Introduction

Knee osteoarthritis (KOA) is a prevalent chronic joint disorder. Conservative interventions, such as gait retraining, aim to reduce knee loading to slow structural disease progression(*1*). However, most retraining strategies are not personalized and fail to account for individual differences. Recent advances in predictive simulations enable the development of gait modifications that optimize joint loading profiles, while accounting for patient-specific alignment and habitual walking patterns(*2*). This proof-of-concept study evaluates the feasibility and implementation potential of in silico-informed gait retraining in individuals with early-KOA.

2. Materials and Methods

Seven individuals with early-stage KOA participated in personalized gait retraining. Patient-specific gait modifications were generated using a predictive simulation framework (PredSim), based on prior collected 3D motion capture and MRI-derived anatomical information. The optimisation aimed to reduce contact forces while accounting for subject-specific joint alignment. Participants practiced their modifications using real-time visual and verbal feedback. These gait modifications targeted mainly trunk and hip kinematics. Gait kinematics were monitored using an inertial measurement unit system. Contact forces were estimated using OpenSim JAM (*3*) applied to personalized musculoskeletal models.

3. Results

Substantial inter-subject variability was observed in the adopted gait strategies. Participants shifted their walking patterns towards PredSim-derived target compared to habitual gait (Figure 1A, brown bar < black bar, Friedman test, $p = 0.0021$) and most retained aspects of the modified gait seven days later (Figure 1A, yellow bar). Changes in medial compartment loading were subject-specific, with an overall trend toward reduced loading at peak contact force (Figure 1B).

4. Discussion and Conclusions

This study demonstrates the feasibility of implementing in silico-informed gait retraining in individuals with early KOA. Participants were able to approximate gait modifications derived from predictive simulations. While reductions of medial compartment loading were not uniform across patients, the observed adaptations highlight the importance of personalised intervention design. These findings support the potential of predictive modeling frameworks to inform conservative treatment for KOA. Larger-scale studies are warranted to evaluate long-term clinical efficacy and sustainability of load reductions.

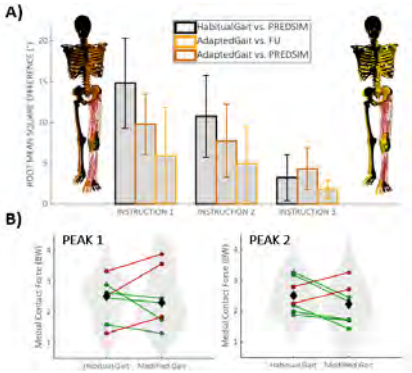


Figure 1: A) *Root Mean Square differences (group average + deviation) for the three instructions across the targeted gait phases* ***B)*** *Violin plots for contact force (in bodyweights) at first /second peak per patient, with increases shown(red) and decreases(green). The black diamonds represent the group average per condition.*

5. References

1. S. D. Uhlrich *et al.*, *Lancet Rheumatol.* **7**, e708–e718 (2025).

2. B. Killen, G. Serrancoli, F. De Groote, I. Jonkers, *Gait Posture*. **113**, 116–117 (2024).

3. C. R. Smith, S. C. E. Brandon, D. G. Thelen, *J. Biomech.* **82**, 124–133 (2019).

Acknowledgements:

The authors would like to thank the National Funds Flanders (FWO) (Grant no: G045320N and 1SC9922N) for providing financial support to this project.

SURFACE EMG-DRIVEN MODELING OF ANKLE BIOMECHANICS IN STAIR ASCENDING FOR PROSTHETIC DEVICE DEVELOPMENT

Ege Bozdag (1, 3), Beste Imamoglu Yildirim (1), Sinan Öncü (2), Can A. Yucesoy (1)

1. Institute of Biomedical Engineering, Boğaziçi University, Istanbul, Turkey; 2. Department of Mechanical Engineering, Boğaziçi University, Istanbul, Turkey; 3. Technical University of Munich, TUM School of Computation, Information and Technology, Munich, Germany

Corresponding author: Can A. Yucesoy, Email: can.yucesoy@bogazici.edu.tr

1. Introduction

The relevance of using surface electromyography (sEMG) signals and extracted features in prosthetic device control has been shown [1-3]. For powered ankle prosthesis applications, the amputation level determines the availability of residual muscles and imposes a challenge. Besides, a systematic assessment of predictive success of muscle combinations and the study of demanding motion types are needed. Consequently, (i) limiting the total number of sEMG muscle inputs, (ii) minimizing the inputs from the lower leg muscles, and (iii) completely excluding the lower leg muscles will make the control algorithm *economical*, *flexible*, and *practical*, respectively. Using healthy population data [4], our aim was to conduct a systematic analysis for ranking possible muscle combinations based on prediction success for ankle kinematics and kinetics during stair ascending motion.

2. Materials and Methods

Using a Long Short-Term Memory network, we evaluated input combinations of sEMG signals from eight lower-extremity muscles for their predictive performance of ankle angle and moment: tibialis anterior (TA), soleus (SOL), medial gastrocnemius (MG), peroneus longus (PL), vastus medialis (VM), rectus femoris (RF), biceps femoris (BF), and gluteus maximus (GMax). Time- and frequency-domain features were extracted from sEMG signals using 150-ms windows, and an optimal feature set was identified using the best-performing muscle combination from prior level-walking analysis [3]. Predictive success of muscle combinations was assessed based on Pearson's correlation coefficient ($r>0.90$ indicates successful correlation) and root-mean-square error. A score index defined as the product of the summed correlation deviations and the mean RMSE, normalized to their respective maxima for angle and moment, was used to rank them.

3. Results

210 out of 255 muscle combinations met the success criterion. The best-performing combination involved several muscles: TA + SOL + MG + PL + VM + BF + GMax ($r_{position}=0.93$, $r_{moment}=0.95$). However, a single muscle, SOL, also did meet the success criterion ($r_{position}=0.91$, $r_{moment}=0.94$). Therefore, SOL was indicated as the economical combination. No upper-leg-only muscle combination could meet the criterion, with RF+VM+GMax yielding the highest performance ($r_{angle}>0.89$, $r_{moment}>0.92$). Therefore, no practical combination could be indicated for stair ascending motion. SOL+BF ($r_{position}=0.92$, $r_{moment}=0.94$) was the flexible variation.

4. Discussion and Conclusions

Our results confirm the potential of sEMG muscle inputs in the control of powered ankle prostheses, also for a highly demanding motion. The consistent presence of the SOL in all featured muscle configurations reinforces the role of plantar flexors (MG was a part of the best-performing combination) in the predictive success of sEMG muscle inputs in ankle joint kinematics and kinetics for stair ascending motion. This was not the case in level walking. Note that testing and validation in amputee population is indicated to strengthen the clinical applicability of our method.

5. References

1. Fleming A, Stafford N, Huang S, Hu X, Ferris DP, Huang HH. J Neural Eng. 2021; 18(4):041004.
2. Keleş AD, Yucesoy CA. J Biomech. 2020; 113:110087.
3. Keleş AD, Türksoy RT, Yucesoy CA. Front Neurosci. 2023; 17:1158280.
4. Lencioni T, Carpinella I, Rabuffetti M, Marzegan A, Ferrarin M. Sci Data. 2019; 6:309.

IMPACT OF PERSONALIZED GEOMETRY ON ESTIMATIONS OF OA-RELATED BIOMARKERS IN A MULTI-SCALE FRAMEWORK

Ali Abedi [1], Seyed Ali Elahi [1], Yixuan Zhang [1], Amir Esrafilian [2], Miel Willems[1], Bryce A.Killen [1], Ilse Jonkers [1]

[1] Department of Movement Sciences, KU Leuven, Leuven, Belgium
[2] Department of Technical Physics, University of Eastern Finland, Kuopio, Finland

1. Introduction

Cartilage mechanical biomarkers (i.e., cartilage pressure, fibril strain, maximum shear stress), associated with knee osteoarthritis (OA) progression, have been identified during gait using coupled musculoskeletal (MSK)–finite element (FE) frameworks [1]. However, previous work largely relied on generic joint geometries, which omit known patient-specific anatomical characteristics that may affect the estimation of these mechanical biomarkers. Given the known association of OA risk with anatomical joint features, this work assesses the influence of personalizing articular joint contact geometries on estimated OA-related cartilage biomarkers.

2. Materials and Methods

For seven subjects (two healthy and five with medial knee OA), two models were created, one using scaled generic geometries and the second using MRI-segmented personalized geometries [2]. MSK simulations informed by motion capture data (i.e., marker trajectories and ground reaction forces) estimated medial tibial cartilage pressure distribution [3], which were then used as inputs for compartmental FE models incorporating a fibril-reinforced biphasic cartilage formulation [4]. OA-related biomarkers were calculated at the instant of the first and second knee joint loading peaks. To determine the effect of personalization, histograms of MSK contact pressures (normalized to bodyweight), maximum shear, and fibril strains were computed.

3. Results

In generic models, values were largely overlapping between cohorts, with healthy individuals occasionally showing higher values at both peaks. In contrast, the personalized model showed a trend of higher pressures, shear, and fibril strains in the OA cohort (Figure 1); however, no significant differences between cohorts or modelling approaches were confirmed (Wilcoxon tests, $\alpha = 0.05$).

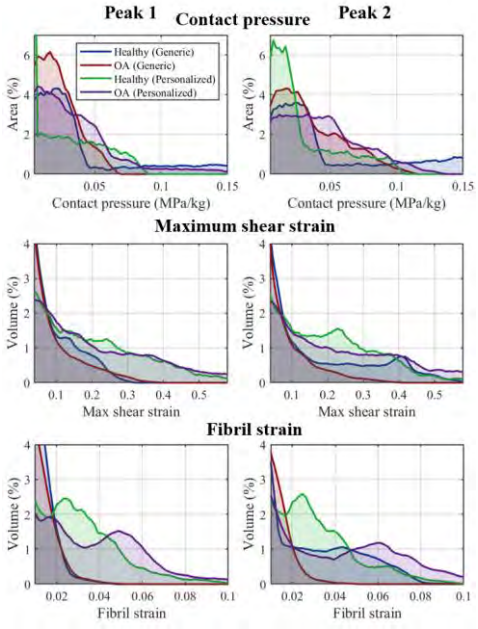


Figure 1: Histograms of average personalized and generic model outputs for healthy and knee OA subjects.

4. Discussion and Conclusions

Geometry personalization influenced OA-related functional biomarkers, although not significantly. However, the measured changes in absolute and relative values between cohorts support sensitivity to personalized anatomical modeling assumptions. These trends should be examined further in larger cohorts, along with their effect on identifying patient-specific risks of fast disease progression.

5. References

1. Esrafilian A et al. IEEE Trans Biomed Eng. 2024;72(1):56–69.
2. Killen BA et al. J Biomech. 2024;177:112387.
3. Smith CR et al. J Knee Surg. 2016;29(2):99–106.
4. Zhang Y et al. Sci Rep. 2025;15(1):35303.

Acknowledgements:
This work was supported by C14/24/117 and OA-CONNECT – 101200916.

A LOCALIZED ARTICULAR CARTILAGE TEAR INDUCES GLOBAL ADAPTATION OF BONE: A FINITE ELEMENT STUDY

Alexander Paz (1,2), Mikko Venäläinen (3), Jari Salo (4), Hanna Isaksson (5), Rami Korhonen (1), Petri Tanska (1), Mimmi Liukkonen (2)

1. Department of Technical Physics, University of Eastern Finland, Finland; 2. Imaging Center, Kuopio University Hospital, Finland; 3. Department of Medical Physics, Turku University Hospital and University of Turku, Finland; 4. Orthopaedics and Traumatology Clinic, Mehiläinen, Helsinki, Finland; 5. Department of Biomedical Engineering, Lund University, Sweden

1. Introduction

Articular cartilage lesions disrupt the habitual loading of subchondral bone. Such lesion-induced changes in cartilage mechanics may drive long-term bone remodelling toward degenerative joint disease since subchondral bone adapts to its mechanical environment. In this methodological study, we implemented a bone adaptation algorithm within a knee joint finite element (FE) model with injured femoral cartilage to simulate lesion-driven changes in subchondral bone mechanical loading and the resulting bone adaptation patterns.

2. Materials and Methods

First, we implemented a bone adaptation model [1] on a simple 3D FE geometry of a cylindrical cartilage-bone unit explant (Ø = 5 mm, h_{Bone} = 5 mm, $h_{Cartilage}$ = 1 mm) to simulate compression with a spherical indenter (Ø = 1 mm, F_{Cycle} = 3-10-3 N in 1 s) (Fig. 1). To this end, we paired MATLAB and ABAQUS. The indenter was rigid, cartilage was transversely isotropic poroelastic [2], and bone was isotropic elastic with realistic depth-dependent properties [3]. Apparent bone mineral density (BMD) was updated in each iteration proportionally to the difference between the average bone signal in the intact condition and the signal in the injured condition. The bone signal corresponds to the ratio of strain energy density to BMD.

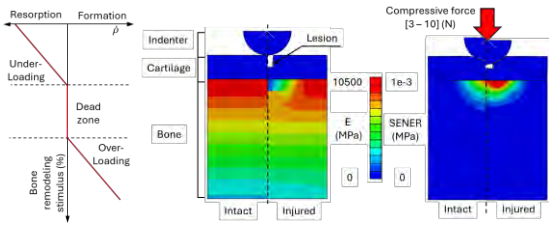


Figure 1: (Left) Bone remodelling law. (Mid) Intact vs injured elastic modulus distribution. (Right) Strain energy density (SENER) at F=10 N.

Second, the bone remodelling workflow was implemented into a personalized cone-beam CT-based knee joint FE model simulating a 0.6 s – stance phase of walking as habitual loading (Fig. 2). BMD was mapped to the bone FE mesh, and the corresponding elastic modulus was determined per element [4]. Cartilage and menisci were transversely isotropic. The uninjured cartilage geometry was obtained by manually repairing the actual injured geometry.

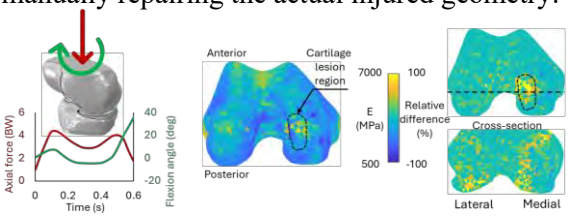


Figure 2: (Left) Knee loading. (Mid) Final elastic modulus distribution. (Right) Relative change in elastic modulus between initial and final iteration.

3. Results

Bone remodelling converges in simple (iter. = 250) and complex geometries (iter. = 150). In the knee model, changes in elastic bone modulus occurred both near and far from cartilage injury, with relative changes between initial and final iteration ranging [-88 480] %.

4. Discussion and Conclusions

Accurately predicting the severity of structural changes in injured knees would be important for better treatment planning for patients, e.g., by classifying cartilage injury sizes and shape in terms of criticality. Next, we need to calibrate and validate our predictions with clinical assessments.

5. References

1. Lerch et al., J. Orthop. Res.; 30:1822–29 (2012).
2. Klets et al., J. Biomech. 49:3891–3900 (2016).
3. Helgason et al., Clin. Biomech. 23:135–146 (2008).
4. Venäläinen et al. Sci. Rep., 29:37538 (2016).

Acknowledgements:
Funds from Finnish State Research Funding (nº 5654242, 5041833), Research Council of Finland (nº 363459, 354916), Novo Nordisk Foundation (nº NNF21OC0065373), Päivikki and Sakari Sohlberg (240074, 250070), and Sigrid Juselius (nº 250109).

DEVELOPMENT OF AN EMG-INFORMED 6-DOF MUSCULOSKELETAL KNEE MODEL FOR INJURY PREVENTION

Maria Dalle Vacche (1), Giulio Rigoni (1), Sara Chiocca (1), Fabiola Spolaor (1), Zimi Sawacha (1)

1. Dipartimento di Ingegneria dell'Informazione, Università degli Studi di Padova, Italia

1. Introduction

Anterior Cruciate Ligament (ACL) injuries affect approximately 30–78 individuals per 100,000 each year [1], highlighting the need for improved preventive strategies and a deeper understanding of knee biomechanics. Most existing musculoskeletal models (MSMs) represent the knee as a single degree-of-freedom (DOF) joint, thereby oversimplifying its complex mechanical behaviour. Although 6-DOF knee formulations have been proposed, they are often unsuitable for analysing deep squat movements [3] or do not explicitly incorporate ligament mechanics [2].

These limitations constrain the models' ability to replicate the intricate joint dynamics occurring during high-demand functional tasks, reducing their effectiveness in biomechanical assessment and injury prevention applications.

In this study, we introduce a 6-DOF knee musculoskeletal model with customizable ligament properties [4], designed to estimate muscle activations and forces, ligament forces and strains, and joint reaction forces. To incorporate subject-specific motor control strategies, two EMG-informed approaches, Computed Muscle Control (CMC) and Moco [5], were implemented in the analysis.

2. Materials and Methods

Ten healthy participants (age: 26.1 ± 1.5 years; BMI: 22.6 ± 2.0 kg/m²) and five individuals with ACL injury (age: 19 ± 2.82 years; BMI: 26.65 ± 2.04 kg/m²) performed three bipodal drop landings and squats. Kinematic and kinetic data were acquired using a stereophotogrammetric system and two force plates. Muscle activity, listed in Figure 1, was recorded at 1000 Hz with an 8-channel surface EMG (sEMG) system.

All data were processed in OpenSim using a 6-DOF knee musculoskeletal model specifically developed for deep squat tasks. The model was EMG-informed through either Moco or CMC.

Model outputs were compared across the two EMG-informed approaches and a Static Optimization method [5]. Simulated muscle activations were also validated against experimental sEMG signals by calculating the root mean square error (RMSE) and the coefficient of multiple correlation (α). Finally, Statistical Parametric Mapping (SPM) analysis [6] was conducted to evaluate differences among methods.

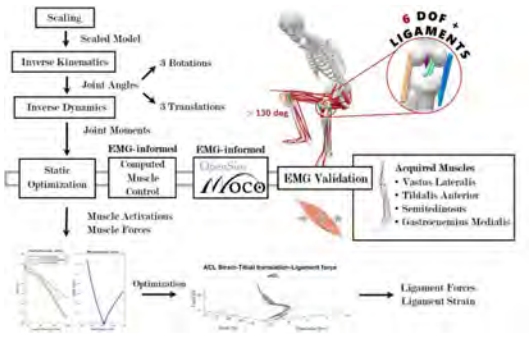


Figure 1: Schematic representation of the proposed workflow

3. Results

The EMG-informed Moco approach demonstrated the strongest agreement between simulated and experimental muscle activation patterns. In the control group, the Tibialis Anterior showed excellent correspondence, with α greater than 0.97 and a RMSE < 0.05.

4. Discussion and Conclusions

The findings support the adoption of a 6-DOF knee musculoskeletal model driven by sEMG data as a promising tool for investigating knee joint biomechanics, for applications in ACL injury screening and prevention.

5. References

1. Singh N, et al. Orthop Res Online J. 2018.
2. Catelli DS, et al. CMBBE. 2019.
3. Xu H, et al. CMBBE. 2015.
4. Blankevoort L, Huiskes R. J Biomech Eng. 1991.
5. Dembia CL, et al. PLoS Comput Biol. 2020.
6. Delp et al. IEEE Trans Biomed Eng. 2007
7. Pataky TC. CMBBE. 2012.

FRAMEWORK FOR ENDURANCE EVALUATION OF CUSTOM-MADE OSSEOINTEGRATED PROSTHESES FOR TRANSFEMORAL AMPUTEES

Giulia Galteri (1), Cristina Curreli (2), Giacomo Dozza(1), Marco Viceconti (1), Luca Cristofolini (1)

1. Department of Industrial Engineering, Alma Mater Studiorum-University of Bologna, Bologna, Italy
2. Medical Technology Lab, IRCCS Istituto Ortopedico Rizzoli, 40136 Bologna, Italy

1. Introduction

No standard defines how to evaluate the endurance behaviour of osseointegrated transfemoral prostheses, making the mechanical evaluation of such devices challenging. Validation becomes even more demanding and costly in the case of custom-made devices. This study aimed to define a reliable experimental-numerical combined framework for assessing the endurance properties of custom-made prostheses for transfemoral amputees.

2. Materials and Methods

The rationale of the endurance test was adapted from the loading and boundary conditions defined in the ISO 7206 standards for hip stems. An axial load was applied to the prosthesis tilted 10° in flexion and 10° in adduction to reproduce a 40 Nm bending moment at the osteotomy level, reproducing the heel-strike peak loading condition in accordance with ISO 7206 (±2% accuracy). In parallel, a FE model of the same experiment was developed. A mesh of ten-node tetrahedron elements (TET10) was generated. The resulting mesh consisted of 427,721 nodes and 299,070 elements for the stem, and 219,907 nodes and 155,209 elements for the embedding medium, with a minimum element edge length of 0.22 mm. The embedding medium was modelled as an elastic-plastic material, based on experimental data obtained for specific cement used [2]. A sensitivity analysis was performed to evaluate how the uncertainties in the input parameters propagate to the predictions the FE model. The test setup was used to measure strains from six rosette gauges (grid length =1mm) applied in correspondence of the minor axis of the elliptical stem cross-section and arranged at three different levels along the stem (Fig.1). The accuracy of the FE model was quantified through direct comparison with the strains experimentally measured.

3. Results

The sensitivity analysis identified the embedding level as the primary factor affecting stress in the stem (up to 6%), while alignment and friction uncertainties had a negligible impact (<1.5%). The correlation between experimental and numerical results was excellent, with $R^2 \geq 0.998$ for all gauges. The %RMSE was consistently below 2.7%, while the peak error was consistently below 3.9%.

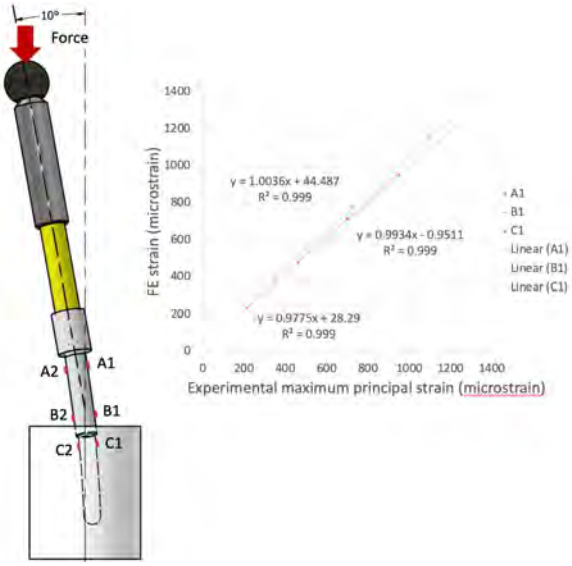


Figure 1: Left) Loading configuration and position of the strain gauges. Right) Linear regression between the maximum and minimum principal strain measured by the strain gauges and those predicted by the FE model

4. Discussion and Conclusions

FE predictions showed excellent agreement with experiments, remaining within accepted literature validation ranges [3]. Together with the sensitivity analysis, these findings support the robustness of the proposed framework. Overall, this work demonstrates the feasibility of a combined experimental-numerical approach for assessing the endurance of osseointegrated stems, with potentially great advantages for custom-made designs.

5. References

1. Overgaard S. et al (2012), EFORT Open Reviews
2. Viceconti et al. (1994), IMechE
3. Lange et al. (2021), J Engineering in Medicine

Acknowledgements:
Work funded by INAIL (PR23-CR-P5-OsteoAMI, CUP: E57G23000240005).

IMPLEMENTATION OF A MUSCULOSKELETAL PELVIC FLOOR MODEL AND SIMULATION OF PHYSIOLOGICAL SCENARIOS

Tobias Baumgartner (1), Dominika Ignasiak (2), Barbara Röhrnbauer (1),

1. IMES Institute of Mechanical Systems, School of Engineering, ZHAW Zurich University of Applied Sciences, Switzerland; 2. Institute for Biomechanics, ETH Zurich, Switzerland

1. Introduction

The levator ani muscle (LAM), an important part of the pelvic floor structure, plays a substantial role in determining pelvic organ support. If the pelvic floor muscles fail to close the pelvic floor, the connective tissue eventually gives way, leading to pelvic floor disorders (PFD) [1]. To date, the biomechanical interrelations between these structures and their respective contributions to pelvic floor function remain insufficiently understood [2]. This study presents a musculoskeletal model of the female pelvic floor integrating inverse dynamics and force-dependent kinematics to evaluate the biomechanical interplay between active (muscles) and passive (connective tissue) components under physiological conditions.

2. Materials and Methods

The musculoskeletal model comprises the LAM and connective tissue structures. Subject-specific anatomical paths are reconstructed from morphological data obtained from MRI scans using the 3D pelvic inclination correction system (PICS) [3]. The model is integrated into a spine model in the AnyBody Modelling System (AnyBody Technology A/S, Aalborg, Denmark), as visualized in Figure 1, which allows the application and control of intraabdominal pressure through recruited actuators.

The model uses inverse dynamics analysis to compute internal forces and muscle activations from specified motions, such as voluntary contraction and associated lifting of the pelvic floor. Moreover, force-dependent kinematics are applied to capture posture and tissue displacement driven by internal forces and intraabdominal pressure, such as Valsalva maneuvers.

3. Results

Preliminary simulations and sensitivity analyses of physiological scenarios demonstrate the ability to quantify and analyze individual biomechanical contributions and interactions among pelvic floor structures, based on their active and passive properties. Anatomical features, e.g. area of the urogenital hiatus and levator plate angle, known to be related to PFD [2], can be quantified and correlated to forms of PFD in future research.

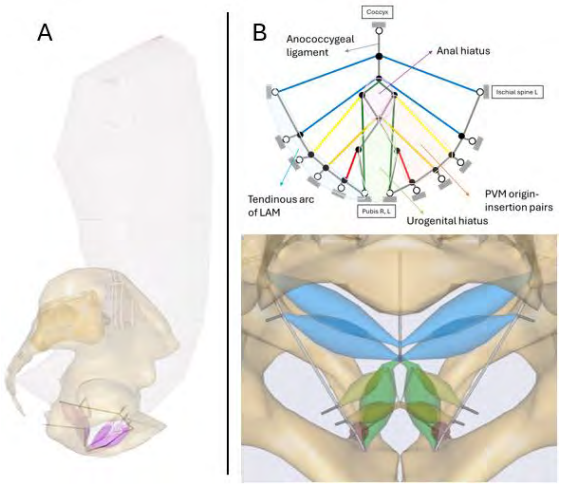


Figure 1:
A: Integration of the pelvic floor into a spine model. B: Schematic drawing and close up of the pelvic floor model within the bony pelvis (caudal view).

4. Discussion and Conclusions

This model advances the understanding of pelvic floor biomechanics. It provides a tool to study the interaction between different structures and possible effects on pathological conditions such as PFD.

5. References

1. Ashton-Miller JA, DeLancey JO. Ann N Y Acad Sci. 2007 Apr;1101:266-96.
2. J. O. DeLancey et al., Am. J. Obstet. Gynecol., vol. 230, no. 5, pp. 476-484.e2, May 2024
3. N. J. Gmür et al., Int. Urogynecology J., Mar. 2025, doi: 10.1007/s00192-025-06082-5.

Acknowledgements:
The authors would like to thank the Swiss National Science Foundation (SNSF). Part of this research has been funded by the SNSF grant PT00P2_206354 / 1.

AI-powered Digital Twin Pipeline for Skeletal Muscle Using Unified CNN-MLP-PINN Framework

Negar Mehrabi(1) and Geoffrey Handsfield (2)(3)
[1] Department of Applied Physical Sciences, University of North Carolina at Chapel Hill, Chapel Hill, NC, United States of America
2 Department of Orthopedics, School of Medicine, University of North Carolina at Chapel Hill, Chapel Hill, NC, United States of America
3 Lampe Joint Department of Biomedical Engineering, University of North Carolina at Chapel Hill and NC State University

1. Introduction

Skeletal muscle digital twins require accurate geometry, fiber architecture, and constitutive behaviour (1), but current approaches typically rely on manual steps which limits scalability and reproducibility of workflows. We proposed a unified AI powered pipeline for efficient and reliable digital twin development.

2. Materials and Methods

High-resolution lower-limb MRI was segmented to generate muscle masks and tetrahedral volumetric meshes. Muscle fiber orientations were extracted using a PINN-based method and mapped onto meshes via nearest-neighbor interpolation. Simulation outputs, including nodal displacements and element-wise stress and strain fields, were organized into a structured database for supervised and physics-informed learning. A unified CNN–MLP–PINN architecture was developed to integrate MRI-derived anatomy, automatically extracted geometric and fiber features, and finite element parameters for direct prediction of full-field stress–strain responses and optimization of material properties under physical constraints. A three-dimensional convolutional neural network (CNN) extracts hierarchical anatomical features from multi-slice MRI volumes, while a multi-layer perceptron (MLP) encodes automatically computed geometric and simulation descriptors, including muscle volume, fiber orientation statistics, element quality metrics, material constants, and loading conditions. A physics-aware attention module (2) adaptively weights correlated multimodal features according to their contribution to stress–strain responses before propagation through a physics-informed neural network enforcing constitutive laws, equilibrium, and physiological constraints.

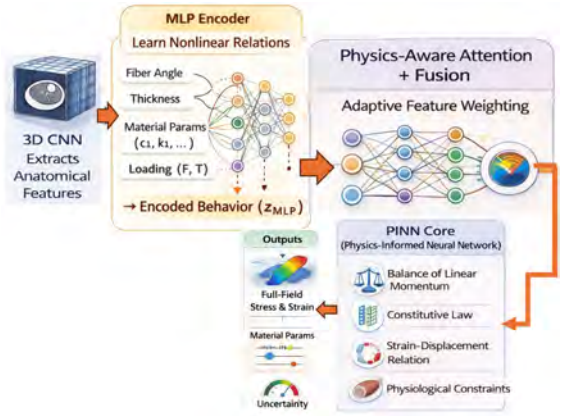


Figure.1) A hybrid CNN–MLP–PINN architecture extracts anatomical features from MRI, learns nonlinear relationships from FE-derived descriptors, geometrical and anatomical features, weights correlated multimodal features and enforces physical laws through a physics-informed module.

3. Results

Automated meshing and fiber mapping produced spatially coherent models suitable for FE analysis. The Python framework enabled efficient, fully automated simulations, and the CNN–PINN–MLP architecture showed stable training and effective physics-informed feature integration. Pipeline integration and large-scale validation are ongoing.

4. Discussion and Conclusions

This work introduces a scalable, automated, and physics-guided framework for muscle digital twin development and establishes a robust foundation for intelligent, data-driven, automated and personalized biomechanical modelling of skeletal muscle.

5. References

1-Blemker SS, Delp SL. Ann Biomed Eng. 2005;33(5):661–673 (2005).
2-Ferrón-Vivó M, Nadal E, Navarro-Jiménez JM, Gregori S, Rupérez MJ. J Mech Behav Biomed Mater. 2026;173:107225 (2026).

STATISTICAL SHAPE MODELING FOR DISTAL HUMERUS RECONSTRUCTION FROM ROUTINE CLINICAL CT SCANS

Lucy McCarthy (1), Jan Hereš (2), Stephen J. Ferguson (1), Philipp Moroder (3), Arthur Porto* (4), Eva C. Herbst* (1,4) **equal contribution*

1. Institute for Biomechanics, ETH, Zurich, Switzerland; 2. University of West Bohemia, Czech Republik; 3. Schulthess Klinik, Zurich; 4. University of Florida, U.S.A.

1. Introduction

Pre-operative shoulder imaging typically only captures the proximal third of the humerus. However, distal anatomy is important for functional assessment during surgical planning as well as for biomechanical modelling. Previous studies have explored statistical shape modelling (SSM) to infer missing humeral anatomy (1,2), but these studies used either half of the humerus or pre-aligned models which does not reflect clinical reality. This project aims to integrate SSM into a deformable registration framework to enable anatomically realistic reconstruction of complete patient-specific humeral geometry from partial CT scans without landmarks or pre-aligning targets.

2. Materials and Methods

A computational pipeline was implemented in 3D Slicer (v5.10.0) to enable distal humerus reconstruction while preserving anatomical position and scale. Healthy humeri (1,3,4) were divided into male (n=59) and female (n=46) cohorts and then split into training (70%) and testing (30%) sets. SSMs were constructed from the training set using 13 semi-automatically transferred landmarks (Fig. 1). Test set models were cropped to the proximal third and reconstructed using ATLAS, which constrains the deformation along the principal modes of variation of the SSM. Reconstruction accuracy was assessed as differences in humeral length surface error (absolute closest distance AbsD and corresponding point to point distance PtPD).

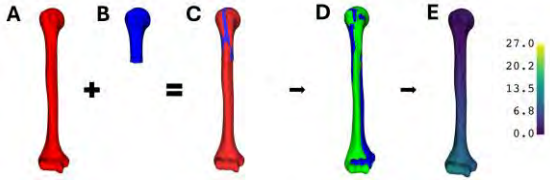


Figure 1: A) SSM template model; B) cropped target humerus; C) SSM registered to cropped target; d) reconstructed (green) versus ground truth (blue); E) surface error heatmap (AbsD).

3. Results

Table 1. Reconstruction error magnitudes.

Error Metric	Female Mean	Female Range	Male Mean	Male Range
Length (mm)	8.7 (5.8)	0.6-18.3	15.8 (11.6)	0.6-37.6
Surface AbsD (mm)	2.5 (0.8)	0-20.8	3.2 (1.4)	0-33.4
Surface PtP (mm)	7.8 (2.6)	0.03-26.4	10.7 (4.3)	0.04-38.6

* () indicates SD

4. Discussion and Conclusions

Humeral surface errors (AbsD) were similar to previous studies (1), with corresponding point surface errors demonstrating higher values (Table 1) than AbsD errors. Humeral length was generally overestimated. Future studies on larger datasets are needed to determine whether reconstruction errors are due to limited SSM sample size or to a true lack of anatomical correlation between proximal and distal morphology. Our findings highlight the potential of SSMs to support clinically relevant applications where complete humeral geometry is unavailable, offering value for surgical planning and biomechanical simulations.

5. References

1. Huang Y et al., Biomech Model Mechanobiol; 21(1):249–59 (2022).
2. Vlachopoulos L et al., JBJS; 100(8):e50 (2018).
3. Henninger, H. B. Zenodo. doi: 10.5281/zenodo.17632996, v1.2 (2025).
4. Henninger, H. B. Zenodo. doi: 10.5281/zenodo.14590062, v1 (2025).

Acknowledgements:
We thank Heath Henninger, David Ackland. Yichen Huang, Tracy Nolan and the Cancer Imaging Archive for datasets. We thank the Schwyzer-Winiker Foundation for funding.

EX VIVO EXPERIMENTAL INVESTIGATIONS AND MODELLING OF VISCO-HYPERELASTIC BEHAVIOUR OF THE HUMAN FACIAL TISSUES

Eyad Awad†,* , Noemie Briot* , Gregory Chagnon* , Djordje Peric† , Mokarram Hossain†

† Zienkiewicz Institute for Modelling, Data and AI (ZI)
Swansea University
SA1 8EN, Swansea, United Kingdom

** Univ. Grenoble Alpes*
CNRS, UMR 5525, VetAgro Sup , Grenoble INP, TIMC
38000 Grenoble, France

1. Introduction

Facial muscles play an essential role in mastication, facial expression, and speech, yet their mechanical behaviour remains insufficiently characterised, particularly regarding nonlinear and strain-rate-dependent responses. This lack of experimental data limits the reliability of biomechanical models used in surgical simulation, soft-tissue reconstruction, and computational analysis of facial mechanics. Although strain-rate effects and viscoelastic behaviour are well documented for skeletal muscle tissues, corresponding data for facial muscles remain scarce [1,2].

This study investigates the mechanical response of human facial muscle tissues under controlled ex vivo loading, with particular emphasis on strain-rate sensitivity and its implications for constitutive modelling.

2. Materials and Methods

Facial muscle tissues were obtained from several human cadavers of different sex and preservation condition, including fresh and formalin-fixed specimens. Multiple muscles were examined to capture anatomical variability, including the masseter, buccinator, and zygomatic muscles.

Following dissection, tissues were cleaned of surrounding fat and prepared as standardised specimens for uniaxial tensile testing. Preliminary tests were conducted to estimate rupture strains, which varied across tissues. Based on these measurements, a five-cycle viscoelastic loading protocol with progressively increasing stretch levels was defined.

Experiments were performed at two strain rates, 1% s^{-1} and 10% s^{-1}, while force–displacement data were continuously recorded.

3. Results

All tested tissues exhibited a clear strain-rate-dependent mechanical response. Higher strain rates consistently produced increased apparent stiffness in the stress–strain behaviour.

Although this trend was observed in all specimens, the magnitude of the rate effect varied among tissues, indicating tissue-specific viscoelastic characteristics.

4. Discussion and Conclusions

The study provides experimental insight into the visco-hyperelastic behaviour of human facial muscle tissues. The results highlight the importance of incorporating strain-rate sensitivity in constitutive models used in facial biomechanics.

The experimental dataset contributes to addressing the current lack of mechanical data for facial muscles and may support improved biomechanical models for applications such as surgical simulation and soft-tissue reconstruction.

5. References

1. Lu, Y.T., Zhu, H.X., Richmond, S., Middleton, J., A visco-hyperelastic model for skeletal muscle tissue under high strain rates, **Journal of Biomechanics**, 43(13), 2629–2632, 2010.
2. Van Loocke, M., Lyons, G.M., Hutchinson, J.R., Viscoelastic properties of passive skeletal muscle in compression**,** **Journal of Biomechanics**, 41(8), 1555–1566, 2008.

ENHANCING FALL RISK EVALUATION: A FRAMEWORK BASED ON DIGITAL HEALTH TOOLS

Paolo Riccioni (1), Roberta Fognani (1), Giuseppina Mariagrazia Farella (2), Lisa Berti (2), Alberto Leardini (3), Giuseppe Martinese (4), Marco Miceli (4), Saverio Ranciati (5), Felice Lamberti (5), Massimiliano Baleani (1), Giorgio Davico (6)

1. Laboratorio di Tecnologia Medica, IRCCS Istituto Ortopedico Rizzoli, Italy; 2. Medicina Fisica e Riabilitativa1, IRCCS Istituto Ortopedico Rizzoli, Italy; 3. Laboratorio Analisi del Movimento e Valutazione Funzionale Protesi, IRCCS Istituto Ortopedico Rizzoli, Italy; 4 Radiologia Diagnostica e Interventistica, IRCCS Istituto Ortopedico Rizzoli, Italy; 5 Dipartimento di Scienze Statistiche, Università di Bologna, Italy; 6 Dipartimento di Ingegneria Industriale, Università di Bologna, Italy.

1. Introduction

Aging is associated with a progressive loss of skeletal muscle strength and power (dynapenia), which typically results in balance impairments and reduced physical performance, ultimately increasing the risk of falling. While several biomechanical parameters are known to contribute to fall risk, it remains unclear which factor is the strongest predictor of a fall event. The present study describes an integrated and comprehensive approach aimed at investigating the mechanisms underlying fall risk. Since sarcopenia prevalence is higher in subjects affected by knee osteoarthritis (KOA), as the coexistence of KOA and sarcopenia creates a "vicious circle" in which each condition contributes to the progression of the other [1], the study is carried out on KOA patients

2. Study design

A prospective, single-arm observational study is currently being conducted at IRCCS Istituto Ortopedico Rizzoli. Subjects aged 65 to 80 years old, with KOA, are being enrolled, with a target sample size of 50 participants. Over the course of two years, and every six months following the baseline visit, all participants will be asked to perform clinical and functional evaluations (Figure 1). These include: (1) gait assessment, (2) the quantification of muscle force and power via isokinetic and isometric tests on a dynamometer, (3) measurement of real-world mobility through continuous monitoring over 5 consecutive days using a single waist-worn inertial sensor, (4) assessment of ascending and descending stairs (not at baseline), and (5) full lower-limb MRI scanning (at the first and last follow-up visits) to obtain detailed information on muscles.



Figure 1: Schematic overview of the study design.

3. Digital model for fall risk evaluation

Musculoskeletal models are being developed in OpenSim and used to perform simulations of human locomotion, eventually via an EMG-assisted approach [2]. Wearable sensor data are being processed to extract digital mobility outcomes to characterize real-world mobility. These data will be used to inform optimal-control simulations aimed at predicting real-world biomechanics and estimating muscle and joint contact forces. The muscle volumes extracted from MRIs, along with the measures of muscle strength and power, may be exploited to introduce KOA related impairments in the simulations. All data will be fed into a statistical model to identify correlations among parameters across different domains and fall events that occur during the study, with the goal of enhancing fall risk assessment.

4. References

1. Pickering ME et al., Calcif Tissue Int 2020;107:203
2. Princelle D et al., Ann Biomed Eng 2025;53:1399

Acknowledgements:

This research was co-funded by the Italian Complementary National Plan PNC-I.1 "Research initiatives for innovative technologies and pathways in the health and welfare sector" D.D.931 of 06/06/2022, "DARE - DigitAl lifelong pRevEntion" initiative, code PNC0000002, CUP: B53C2200630001"

THE IMPACT OF GAIT SPEED ON THE PREDICTED KNEE LOADS DURING LEVEL WALKING

Giorgio Davico (1)

1. Alma Mater Studiorum – University of Bologna, Italy

1. Introduction

For decades, clinical gait assessments have been largely performed in laboratory settings where the subjects were instrumented to enable the acquisition of motion capture, ground reaction force and surface electromyography data. While this still represents the gold standard, recent studies using wearables to monitor real-world mobility have highlighted that several key spatiotemporal parameters may differ substantially in the two settings [1]. In the lab, we tend to overperform, i.e., to walk faster. This is likely to affect the loads experienced by the joints [2], which can be predicted using musculoskeletal (MSK) models. Quantifying the impact of walking speed on joint loads is therefore crucial.

2. Materials and Methods

A publicly available dataset was exploited for this study [3]. Experimental motion capture and force plates data collected on 20 healthy adults (10F/10M, BMI: 23.6±3.3 kg/m^2, age: 41.2±15.0 years) walking on overground at five different speeds (metronome guided: 0-0.4 m/s, 0.4-0.8 m/s, 0.8-1.2 m/s; self-selected: normal and fast speed) were first processed in MOtoNMS. Then, a generic MSK model [4], which implemented a 6DOF knee joint and included ligaments, was linearly scaled in OpenSim [5] to approximate the size of each participant. Biomechanical simulations of gait were performed for 371 trials in OpenSim, through the MATLAB API, using the COMAK tool [6].

The resulting knee joint contact forces were interpolated to 101-point vectors, and normalized to the subjects' bodyweight.

3. Results

The preliminary results of this study showed that the loads experienced by the knee tend to increase with walking speed (differences up to 1BW, comparing fast vs normal speed). Little differences were observed between normal and metronome-based faster speed. At slower paces, the force profiles deviated from the typical M-shape, likely due to different kinematics.

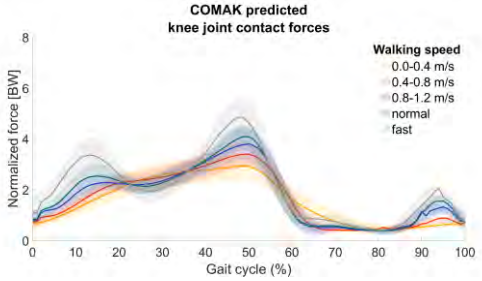


Figure 1: Knee joint contact forces predicted by the COMAK tool, for subjects walking at 5 different speeds. Data are reported as mean±sd across trials.

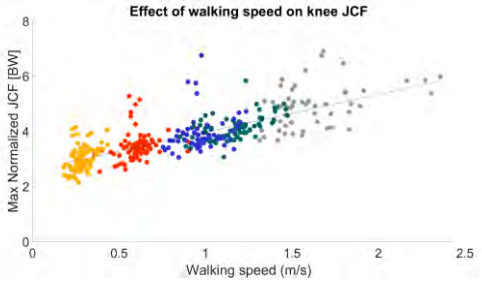


Figure 2: Effect of walking speed on the predicted knee joint contact forces (maximum peak). Colours discriminate between walking conditions.

4. Discussion and Conclusions

As gait speed appears to affect in a non-negligible way the joint loads during locomotor tasks, and people tend to walk slower in the real-world, researchers and clinicians should cautiously interpret any findings and assessments purely based on laboratory data.

5. References

1. Thi My Lien N et al., Gait Posture; 130:110254 (2026).
2. Lenton GK et al., PLoS ONE 13(11): e0206859 (2018).
3. Schreiber C, Moissenet F, Sci Data; 6(1):111 (2019).
4. Lenhart RL et al., Ann Biomed Eng; 43(11): 2675-85 (2015).
5. Delp SL et al., IEEE Trans Biomed Eng; 54(11): 1940-50 (2007).
6. Smith et al., J Knee Surg; 29(2):99-106 (2016).

FACET JOINTS COMPUTATIONAL MODELLING: DO LITERATURE-DERIVED CONTACT PARAMETERS COMPROMISE FIDELITY?

Reem Bishr, Shambo Bhattacharya, Marlène Mengoni

Corresponding author: Reem Bishr, Institute of Medical and Biological Engineering, University of Leeds, Leeds LS2 9JT, United Kingdom (Email: lbjw0434@leeds.ac.uk)

1. Introduction

Facet joints (FJ) are cartilaginous articulations located posterior to the vertebrae. They contribute to spinal motion and stability, and their degeneration has been associated with intervertebral disc (IVD) degeneration and low back pain [1]. In finite element (FE) models, FJ cartilage is commonly represented using soft-contact formulations because cartilage geometry cannot be reliably identified from CT imaging [2]. This study investigates the influence of FJ contact parameters on FE model fidelity by comparing specimen-specific parameters calibrated against experimental data, literature-derived parameters, and an imaging-based approach in which the contact clearance parameter (C0) is estimated from CT-measured facet joint space (FJS).

2. Materials and Methods

Specimen-specific FE models (N=6) of cadaveric functional spine units (FSUs) (ethics: Yorkshire and Humber REC15/YH/0096) were developed from CT images [3]. The IVDs underwent partial nucleotomy with PMMA cement to simulate lateral lumbar interbody fusion (LLIF). Bones were assigned isotropic linear elastic properties derived from CT greyscale values [4]. FJ contact was modelled using an exponential pressure-overclosure formulation defined by C0, contact closure pressure (P0), and friction coefficient (μ). Following parameters calibration [5], a linear relationship was established between minimum CT-measured FJS and calibrated C0, shown by Eq.1. Models were rerun using predicted C0, literature-based μ (0.1), and an average literature P0 (145 MPa) within the same order of magnitude as bone elastic modulus. Load-displacement curves from calibrated, image- and literature-based parameter sets were compared with experimental data.

$$Predicted\ C0 = 1.64 * FJS - 0.22 \qquad (1)$$

3. Results

The RMS error between FE and experimental curves is shown in Fig. 1. Both image-based and literature-based parameter sets significantly increased error relative to the calibrated models ($p < 0.05$), with the largest increases observed in more degenerated FSUs. This is consistent with the high variability in calibrated friction coefficients (CoV > 50%). Although less accurate than calibrated models, the image-based approach reduced inter-specimen variability, decreasing the RMS error spread by approximately 57% compared with literature-only parameters.

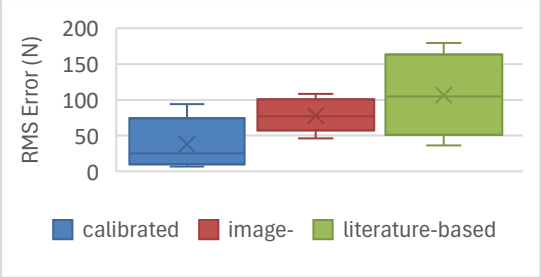


Figure 1: RMS error between FE and experimental responses across contact parameter sets.

4. Discussion and Conclusions

The widespread use of literature-derived FJ contact parameters may limit the ability of spinal FE models to represent subject-specific mechanics. Incorporating imaging information into contact definitions offers a practical route toward model personalization without the need for experimental calibration.

5. References

1. Mengoni M, BMM 20:389–401, 2021;
2. Khuyagbaatar B, et al. IHPEM 25:487–496, 2024.
3. Mengoni et al., J Biomech 49(2):259–266, 2016;
4. Day et al., JOR Spine 3(1): e1077, 2020;
5. Mengoni et al., JMBBM 48:164–172, 2015;

Acknowledgements:

We wish to thank the donor and their family for the donation of their tissue, and thanks to Dr James Warren for tissue imaging. Work is funded by EPSRC grant EP/W015617/1.

MODEL-INFORMED RADIOTHERAPY SCHEDULE SELECTION UNDER HYPOXIA: A PHENOTYPE-STRUCTURED PDE APPROACH

Francesco Albanese (1,3), Giulia Chiari (2), Marcello Delitala (1)

1. Department of Mathematical Sciences "G. L. Lagrange", Politecnico di Torino
Corso Duca degli Abruzzi 24, Torino, 10129, Italy

2. CAM – Basque Center for Applied Mathematics
Mazarredo Zumarkalea 14, Bilbo, 48009, Abando, Spain

3. Department of Mathematics, School of Science, Computing and Engineering Technologies
Swinburne University of Technology, Hawthorn, 3122, VIC, Australia

1. Introduction

Radiotherapy outcomes depend on tumor heterogeneity and microenvironmental factors. Hypoxia reduces radiosensitivity and promotes relapse, while dose per fraction and inter-fraction timing significantly affect progression. We investigate how oxygenation and continuous phenotypic adaptation shape efficient dose–interval fractionation schedules.

2. Materials and Methods

We develop a phenotype-structured PDE model coupling tumor cell density and oxygen dynamics, extending [1]. A continuous trait $u \in [0,1]$ represents resistance to hypoxia and radiation.

Radiotherapy is described through a modified linear–quadratic model in which radiosensitivity depends on the trait u and is modulated by an oxygen enhancement ratio (OER) that depends jointly on the spatial oxygen field and on the evolving phenotypic distribution. This coupling allows treatment-induced selection across the phenotypic spectrum.

Schedules are compared under a normal-tissue constraint expressed via biologically effective dose. Numerical simulations explore the admissible dose–interval space and evaluate time-to-progression (TTP).

3. Results

Under uniform oxygen supply, protocol ranking depends strongly on oxygenation. In normoxia, most schedules yield similar TTP, whereas under hypoxia selected dose–interval combinations substantially delay relapse.

Under severe hypoxia, this structure changes qualitatively: the classical dose–interval trade-off breaks down and distinct optimal regimes emerge depending on normal-tissue radiosensitivity, leading to a sharp transition between hyperfractionated and hypofractionated strategies.

When oxygen delivery is spatially heterogeneous, even at fixed total supply, identical schedules can produce markedly different TTP values. Spatial organization alone alters protocol ranking and promotes localized relapse-driving niches, indicating that average oxygen levels may be insufficient to predict treatment outcome.

4. Discussion and Conclusions

The proposed framework provides a mechanistic tool to compare fractionation strategies in oxygen-limited tumors. By integrating eco-evolutionary dynamics and oxygen modulation, the model supports schedule selection tailored to tumor oxygenation scenarios.

5. References

1. Chiari G., Fiandaca G., Delitala M. E., Hypoxia-related radiotherapy resistance in tumors: treatment efficacy investigation in an eco-evolutionary perspective, Frontiers in Applied Mathematics and Statistics, 9: 1193191, 2023.

DISCRETE-CONTINUOUS MODELLING AND CALIBRATION OF CANCER SPHEROID FORMATION

Elishan C. Braun(1), Gabriella Bretti(1), Marta Menci(2), Matteo Semplice(3), Silvia Preda(3)

1. Istituto per le Applicazioni del Calcolo "Mauro Picone (IAC-CNR), Italy ; 2. Dipartimento di Scienza e Alta Tecnologia, Universit`a dell'Insubria, Italy 3. Università Campus Bio-Medico di Roma, Italy

1. Introduction

In this work we present a 3D hybrid discrete-continuous model for spheroid formation and use data from real laboratory experiments of in-vitro cultivated spherical cell clusters in order to calibrate the mathematical model to replicate the experiments and investigate tumour formation in a more physiological relevant context.

2. Materials and Methods

We use an agent-based ODE model to describe individual cell movement and mechanics such as attraction-repulsion and chemotaxis, and reaction-diffusion PDE for oxygen and growth factor that stimulates proliferation and differentiation describes by Poisson-processes to incorporate biological variability.

$$\begin{cases} \ddot{\mathbf{X}}_i &= \displaystyle\sum_{j:\mathbf{X}_j\in B(\mathbf{X}_i,R_2)\setminus\{\mathbf{X}_i\}} K(r_{ij}) - \mu\dot{X}_i + \alpha\mathcal{F}(\nabla S(X_i)), \\ d\varphi_i &= d\mathcal{P}\left(\displaystyle\int_0^t q_i(s)\,ds\right), \\ d\phi_i &= d\mathcal{P}\left(\displaystyle\int_0^t p_i(s)\,ds\right), \\ \partial_t c &= \nabla\cdot(D_c\nabla c) - \displaystyle\sum_{i=1}^{N}\frac{\lambda(\varphi_i)c^{\gamma+1}}{k(\varphi_i)+c^{\gamma+1}}\chi_{B(\mathbf{X}_i,R_3)} \\ \partial_t S &= \nabla\cdot(D_S\nabla S) + \displaystyle\sum_{i=1}^{N}\xi(\varphi_i)\chi_{B(\mathbf{X}_i,R_3)} - \eta S, \end{cases} \tag{1}$$

We solve the equation with coupled implicit Euler method and Monte Carlo sampling for the Poisson-processes and calculate properties of forming spheroids, for instance diameter, density, roundness and diameter ratios of cell states and necrotic cells.

We apply global multigrid optimization methods with customizable cost functions to calibrate our model with available data from biological experiments that preserves its variability.

3. Results

The model reproduces key features of tumor spheroid growth observed in experimental data. The adaptive clustering approach enables the identification and tracking of spheroid structures with non-spherical geometries.

4. Discussion and Conclusions

The proposed framework provides a flexible tool for studying tumor spheroid formation by combining agent-based cellular dynamics with continuum descriptions of biochemical signals. The model can be easily customized to represent different experimental conditions and biological mechanisms, enabling the investigation of various questions related to spheroid growth and cell behavior.

5. References

1. Di Costanzo, E. et al. (2018). A discrete in continuous mathematical model of cardiac progenitor cells formation and growth as spheroid clusters (Cardiospheres). Mathematical Medicine and Biology: a Journal of the IMA 35(1):121–144.
2. Carrasco-Mantis, A. et al.(2023). A mechanobiological model for tumor spheroid evolution with application to glioblastoma: a continuum multiphysics approach. Computers in Biology and Medicine 159, 106897

3. Browning, A. et al. (2021). Quantitative analysis of tumour spheroid structure. Elife 10, e73020

Acknowledgements:

The authors would like to thank MUR for the PNRR "Digital Driven Diagnostics, prognostics and therapeutics for sustainable Healthcare" D34 Health project for providing financial support to this project.

COMPUTATIONAL MODEL OF HIGH GRADE SEROUS OVARIAN CANCER CLONAL EVOLUTION

Marilisa Cortesi (1), Emanuele D. Giordano (1)

1. ALMA MATER STUDIORUM- University of Bologna, Italy

1. Introduction

Clonal evolution, that is the ability of cancer cells of changing their features following darwinian evolution, has been shown to be a key determinant of poor survival and low treatment effectiveness in high grade serous ovarian cancer (HGSOC) [1]. Characterising this aspect in living patients is however not possible with currently available methods.

This work aims at developing a computational model of clonal evolution in HGSOC to provide insights into this process and aid the identification of potential treatment strategies.

2. Materials and Methods

Model of clonal evolution (Figure 1). The digital twin model of HGSOC that we previously developed constitutes the base for this work [2]. It includes an agent based model capable of replicating fundamental features of cell behaviour (division, death and treatment response) and a finite elements framework for the representation of the distribution of key molecules (e.g., nutrients and drugs).

Clonal evolution is implemented by allowing for the possibility of changes in the probability of each modelled cell behaviour throughout the simulation (e.g., more frequent cell doubling, reduced treatment effectiveness). The new parameter set is chosen randomly among similar configurations. This mimics the biological process where small random changes are progressively accumulated.

Sensitivity analysis. A sensitivity analysis has been conducted to characterise clonal evolution in HGSOC. It involved comparing the results obtained with different rates of clonal evolution, to quantify the importance of this phenomenon for HGSOC progression.

Validation. An initial validation of this modification has been conducted using the publicly available data from the seminal paper on clonal evolution in HGSOC [1].

Simulations of the patients included in the study have been compared with relevant patient features (e.g., intra-patient variability, treatment resistance, number of clones).

3. Results

Clonal evolution was shown to promote cell variability. This feature was shown in our previous work to be correlated with disease progression and potentially involved in the development of drug resistance [2].

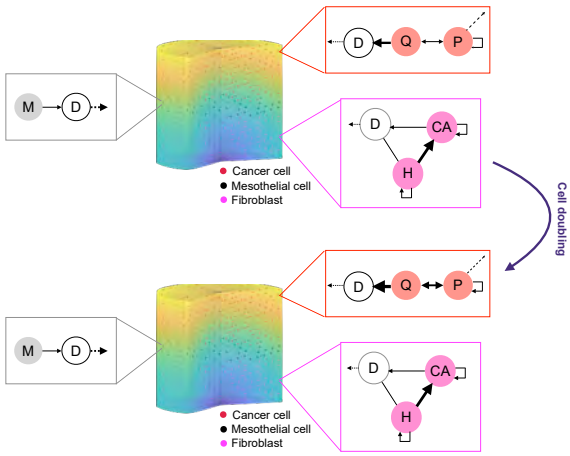


Figure 1: Model of clonal evolution. Graphs show the models of cell behaviours described in [2], where each state represents a cell status (D: dead cell, M: mesothelial cell, Q: quiescent cancer cell, P: proliferative cancer cell, H: healthy fibroblast, CA: cancer associated fibroblast). At cell division the likelihood of different behaviours can change. Notice that cancer cells have a higher rate of evolution than healthy cells (more transition rates have changed).

Coherently earlier stage diseases were better recapitulated by simulations with low clonal evolution rates, while more advanced disease models required a more rapid rate of change in the parameters.

4. Discussion and Conclusions

Clonal evolution is a fundamental feature of cancer progression that is poorly captured by currently available *in vitro* methods and clinical tools. This work sets the foundation for the use digital twins to fill this gap.

5. References

1. Burdett et al. Nat Genet **55**, 437–450 (2023)
2. Cortesi et al. Bioeng. Transl. Med. 10(6) e70082 (2025)

Acknowledgements:

The authors thank Dr. Burdett and the researchers of the CASCADE study for making available the data acquired during their 2023 work.

MECHANISTIC MODELING OF INFUSION TIME-OF-DAY EFFECT ON IMMUNE CHECKPOINT INHIBITOR ANTITUMOUR EFFICACY

Marie Haghebaert (1), Sandrine Dulong (1,2), Pasquale Innominato (3), Francis Lévi (2), Boris Duchemann (2), Annabelle Ballesta (1).

(1) Inserm U1331, Institut Curie, Mines-Paris, PSL Univ., France. (*2*) Cancer Chronotherapy unit, INSERM, Univ Paris Saclay, France. (*3) Ysbyty Gwynedd Hospital, Warwick University, UK.*

Corresponding author: Marie.Haghebaert@curie.fr

1. Introduction

Accumulated clinical evidence indicates that the antitumor efficacy of immune checkpoint inhibitors (ICIs) may depend on the time of day of administration. A recent meta-analysis reported improved survival in patients receiving ICIs earlier in the day across several advanced solid cancers [1]. These observations align with growing evidence that circadian rhythms regulate immune functions and drug responses [2]. However, the biological mechanisms underlying these time-of-day differences in ICI efficacy remain to be elucidated. To address this challenge, we develop mathematical models to investigate how circadian regulation of tumour–immune interactions may influence dosing-time dependencies of ICI efficacy and help identify personalised treatment timing strategies.

2. Materials and Methods

Our approach combines pharmacokinetic (PK) and pharmacodynamic (PD) models of ICIs based on ordinary differential equations in which selected variables or parameters are modulated by cosine functions to represent circadian rhythms. An existing compartmental PK model of nivolumab [6] was extended to evaluate the impact of parameter circadian variability or longitudinal time-dependent clearance on systemic and tissue exposure. Parameters are estimated using CMA-ES and sensitivity is assessed using Sobol indices. Next, we progressively develop three ICI PD models: (i) a circadian immune model without any tumour, (ii) a tumour–immune interaction model, and (iii) the latter including ICI treatment effects, building on an existing model [7]. Immune and circadian parameters are informed by clinical data or extrapolated from preclinical studies [3–5].

3. Results

Simulations of the PK model showed that any circadian modulation of its parameters does not translate into dosing-time dependencies of central or peripheral drug exposure. Sensitivity analyses indicated that the slow clearance of ICIs explained this behaviour. Similarly, simulations with varying clearance rates over several weeks, as documented in patients, showed no infusion timing dependency in ICI PK. We therefore focused on PD mechanisms. First, a model describing the trafficking of regulator and cytotoxic T lymphocytes was developed (16 literature-inferred parameters). Next, tumor-triggered activation of these naive T cells was modeled, further incorporating the dynamics of the antigen presenting cells. The inhibition of cytotoxic lymphocytes by cancer cells was then included, as well as its reversal by ICIs. The calibrated models were able to reproduce the clinical or preclinical data. Sensitivity analyses are currently being performed to identify parameters influencing ICI infusion time-of-day dependencies.

4. Discussion and Conclusions

This work represents an initial step toward mechanistically investigating dosing-time dependencies of ICI clinical outcomes using mathematical models designed in a stepwise manner. An ongoing prospective study investigating ICI infusion time-of-day effects on clinical outcomes of patients with lung cancer will generate circadian datasets on immunological features that will help refine, enrich, and validate such models.

5. References

1. André T etal. ESMO Open. 9:102220 (2024).
2. Lévi F et al. Annu Rev Pharmacol Toxicol (2024).
3. Fortin BM et al. Nat Immunol. 25 (2024).
4. Wang C et al. Nature. 614:136-143 (2023).
5. Druzd D et al. Immunity. 46(1):120-132 (2017).
6. Bajaj G et al. CPT Pharmacometrics Syst Pharmacol. 6(1):58–66 (2017).
7. Jafarnejad M et al. AAPS J. 21(5):79 (2019).

PREDICTING RADIOTHERAPY OUTCOMES: A MULTI-SCALE IN SILICO FRAMEWORK COUPLING VASCULAR OXYGEN DYNAMICS WITH TUMOUR PHENOTYPIC EVOLUTION

Cristina Macaluso (1), Piermario Vitullo (1), Sara Gazzoni (1), Luca Possenti (2), Tiziana Rancati (2), Paolo Zunino (1)

1. MOX, Department of Mathematics, Politecnico di Milano, Milan, Italy
2. CMON Lab, Data Science Unit, Fondazione IRCCS Istituto Nazionale dei Tumori, Milan, Italy

1. Introduction

Radiotherapy (RT) is administered to almost half of all cancer patients, yet its efficacy varies substantially due to tumour microenvironmental heterogeneity. Oxygen availability is a key determinant as well as tumour cell plasticity. The microvascular environment (MVE) thus compromises treatment through two interrelated mechanisms: creating hypoxic niches and fuelling phenotypic selection toward radioresistant stem cells. Understanding these coupled dynamics is essential for improving RT protocols.

2. Materials and Methods

We developed an integrated multi-scale computational framework comprising three coupled components. First, a phenotype-structured PDE model governs tumour cell dynamics incorporating oxygen-dependent proliferation, necrosis, phenotypic plasticity and radiobiological response [1]. Second, a 3D–1D coupled model describes oxygen transport between the vascular network and tissue [2]. A reduced-order model (ROM) based on proper orthogonal decomposition (POD) and mesh-informed neural networks (MINNs) replaces the full oxygen solver at each time step [3]. Third, patient-representative vascular networks are generated from capillary density measurements of 63 HNC patients via Voronoi tessellation and subjected to vessel pruning to simulate RT-induced MVE degradation [4]. Fractionated RT (FRT) and ultra-hypofractionated RT (UHFRT) at 50 and 60 Gy total dose were simulated on healthy and 50%-pruned networks.

3. Results

Our simulations indicate that vascular architecture acts as the primary determinant of radiotherapeutic efficacy. Under both FRT and UHFRT protocols, hypoxia-driven phenotypic de-differentiation fundamentally alters the residual tumour composition, shifting it towards radioresistant stem-like states and thereby elevating the risk of recurrence. Crucially, in scenarios where the MVE remains intact, escalating the total dose from 50 to 60 Gy yields a significant therapeutic benefit, with UHFRT outperforming conventional FRT.

4. Discussion and Conclusions

This work demonstrates the capability of our multi-scale in silico framework to dynamically disentangle the competing mechanisms dictating RT failure. The most clinically actionable insight is that vascular status—rather than dose alone—must dictate dose escalation strategies. The framework, based on patient-derived vascular data, is being used to virtually replicate clinical treatment schedules. Finally, leveraging patient-derived vascular network generation, this framework is actively being employed to replicate and optimise clinical treatment schedules, paving the way for AI-driven, patient-specific RT planning and future integration with chemoradiotherapy modelling.

5. References

1. Celora GL et al., Journal of Theoretical Biology. 2023; 556:111248.
2. Possenti L et al., Ann Biomed Eng. 2021; 49:3356–3373.
3. Vitullo P et al., Finite Elements in Analysis and Design. 2024; 229:104068.
4. Materne S. et al., Computers in Biology and Medicine. 2025; 190:110014.

Acknowledgements:
Financial support to this project is due to the EP PerMed JTC project HiROC, 2024 01/03/2025 -28/2/2028 and the HORIZON-EURATOM-2023-NRT-01-10 01/10/2024 -30/9/2027 project TETRIS.

IN SILICO MODELING OF BONE METASTASIS FOR TUMOR PROGRESSION AND THERAPY RESPONSE

Luca Marsilio (1, 2), Sergio Barrios (3), Stefan Maksimovic (3), Alice Maccarini (2, 4), Elisa Serafini (2, 5, 6), Michele Grimaldi (1,2), Thomas J. Heyman (3), Pietro Cerveri (1,4), Stefano Casarin (2,5,6), and Eleonora Dondossola (3)

1. Politecnico di Milano, Milan, Italy; 2. Houston Methodist Research Institute, Houston, Texas; 3. The University of Texas MD Anderson Cancer Center, Houston, Texas; 4. Università di Pavia, Pavia, Italy; 5. La Rochelle Université, La Rochelle, France; 6. Houston Methodist Hospital, Houston, Texas;

1. Introduction

Bone metastasis (BM) is a leading cause of morbidity and mortality in patients with advanced prostate and renal cancer [1]. The complex, dynamic interactions between tumor cells and the bone microenvironment (osteoblasts, osteoclasts, and blood vessels) drive lethal progression and therapeutic resistance. To address the limitations of traditional *in vivo* models in capturing these multifactorial dynamics, we developed A(BM)^2 – **A**gent **B**ased **M**odel of **B**one **M**etastasis - an *in vivo*-inspired, spatially explicit, multicellular agent-based model (ABM) of the bone metastatic niche to elucidate on BM onset and progression and predict the effect of anti-BM therapies [2].

2. Materials and Methods

A(BM)^2 was implemented on a 2D hexagonal grid, with each site representing a single 20 µm cell. Multiphoton microscopy (MPM) was used to map the bone matrix and initialise the model across distinct anatomical sites (tibia, femur, calvaria, and vertebra). Fluorescence imaging characterised the bone stromal niche (OBs, OCs), while intravital microscopy quantified key vascular features, including vessel size, relative distance, and the critical radius influencing cell dynamics. The model was calibrated using a random forest regressor on 12,000 simulations per tumor type to minimise the Mean Absolute Percentage Error (MAPE) against longitudinal *in vivo* growth data from prostate (PC3) and renal (RENCA) cancer models.

3. Results

A(BM)^2 successfully recapitulated tumor-specific vascular patterns and growth rates, achieving a MAPE of 4.98% for RENCA and 7.69% for PC3. The model demonstrated high predictive accuracy in simulating therapy response. Simulations of cabozantinib, a multi-kinase inhibitor specifically targeting blood vessels, predicted a greater tumor reduction in RENCA (87.7%) than in PC3 (42.6%), consistent with *in vivo* validation. Antiresorptive therapy using zoledronic acid was simulated by implementing an eightfold decrease in bone resorption speed, halting osteolysis without reducing OC numbers, consistent with *in vivo* observations.

Furthermore, simulations identified a linear relationship between drug dosage and efficacy and accurately predicted the rapid tumor regrowth and vascular rebound observed upon therapy withdrawal.

4. Discussion and Conclusions

The proposed A(BM)^2 represents a transformative tool for simulating and predicting therapeutic outcomes in BM. By bridging the gap between traditional *in vivo* research and computational modelling, this model enables the exploration of a large number of treatment regimens, alone or in combination. This approach promotes a sustainable, ethically responsible research strategy that aligns with the 3R framework for more humane research.

5. References

1. Siegel RL et al. CA Cancer J Clin. 2019;69(1):7-34.
2. Marsilio L et al. Cancer Res. 2025;85(21):4269-84

Acknowledgements:

The authors would like to thank the Cancer Prevention and Research Institute of Texas (RP230160), the NIH (R21 CA267312-01A1, P30 CA016672), the David H. Koch Center (MD Anderson), the Bookout Presidential Distinguished Chair fund, and the Italian Ministry of Research and University (FAIR PE00000013) for providing financial support to this project.

A PHYSICALLY CONSISTENT MODEL OF EXPANSILE TUMOR GROWTH

Jonathan Stollberg, Marco F.P. ten Eikelder, Dominik Schillinger

Institute for Mechanics, Computational Mechanics Group, TU Darmstadt, Germany

1. Introduction

Expansile growth leads to compression of the surrounding tissue and, during the avascular phase, to nutrient depletion in the tumor interior. This results in the formation of a necrotic core surrounded by a hypoxic rim. We develop a thermodynamically consistent modeling framework to describe the coupled evolution of tumor growth, nutrient transport, and tissue mechanics.

2. Materials and Methods

We model the tumor as a fully saturated multi-constituent mixture consisting of proliferative, hypoxic, and necrotic cells forming a solid skeleton, as well as extracellular water and dissolved nutrients. Nutrients are assumed abundant in the surrounding tissue, as for example in liver tumors.

From constituent-wise mass and momentum balances, we derive an energy–dissipation inequality that constrains admissible constitutive relations. Cell proliferation is coupled to the multiplicative decomposition of the deformation gradient following finite growth theory. Our approach yields thermodynamically admissible constitutive relations for the free energy density, growth evolution, and inter-phase mass transfer.

Appropriate choices of energy densities and source terms enable the description of cell proliferation, competition between cell species, and nutrient-dependent growth. We implement our model in a finite element framework to simulate expansile growth of an avascular tumor embedded in healthy liver tissue.

3. Results

In our model, cell phenotypes play an essential role in determining the stress state $\boldsymbol{\sigma}$ in the tumor, reflected in a new expression for the stress:

$$\boldsymbol{\sigma} = \frac{\partial \widehat{\Psi}}{\partial \boldsymbol{F}_{\mathrm{e}}} \boldsymbol{F}_{\mathrm{e}}^{\mathrm{T}} + \left[\widehat{\Psi} + \sum\nolimits_{\alpha} \phi_{\alpha} \mu_{\alpha} - p \right] \boldsymbol{I} \,. \quad (1)$$

Here, $\widehat{\Psi}$ denotes a Helmholtz free energy density, F_e the elastic part of the deformation gradient, and μ_α the chemical potential for the corresponding species volume fractions ϕ_α. The Lagrange multiplier pressure p enforces full saturation of the mixture. Consistently, the thermodynamic driving force governing the growth-rate tensor depends on the local stress state, establishing a direct coupling between mechanics and tumor growth.

Our simulations show that the proposed model captures nutrient-dependent cell-phenotype transitions and characteristic expansile growth patterns. In particular, the simulations reproduce the formation of a necrotic core surrounded by a hypoxic rim (Figure 1), consistent with theoretical predictions and clinical observations reported in the literature [1].

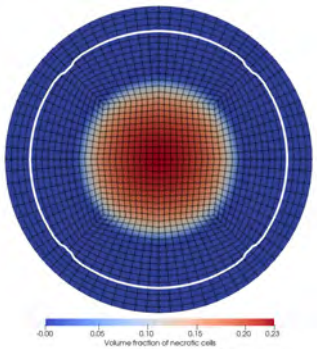


Figure 1: Formation of a necrotic core in a circular tumor. The white line indicates the boundary of the hypoxic rim.

4. Discussion and Conclusions

We present a novel thermodynamically consistent mixture framework that links stress-dependent growth with phenotype competition in avascular tumors. Our results reveal how mechanical stress regulates phenotype distribution and growth dynamics, highlighting the potential of the framework for mechanistic studies of tumor growth and tumor-tissue interaction.

5. References

1. Hanahan D, Weinberg RA, Cell; 100:57-70 (2000)

MULTISCALE RADIATION–MATTER INTERACTION SIMULATIONS IN 3D MULTICELLULAR IN SILICO TUMOR SUBSTRATES

Chiara Tinelli[1], Chiara Scotti[1], Letizia Morelli[1], Guido Baroni[1], Chiara Paganelli[1]

1. Department of Electronics, Information and Bioengineering, Politecnico di Milano, Milano, Italy

1. Introduction

Monte Carlo (MC) simulations of radiation–matter interactions through environments such as Geant4 enable the physical and chemical modeling of radiation-induced damage [1] . In this work, we present a multiscale framework for radiation–matter interaction analysis at the micrometric level, enabling cell-wise dose deposition and linear energy transfer (LET) evaluation in realistic 3D tumor cell substrates reconstructed from microscopy images. We also introduce an extension of the Geant4-DNA framework to multicellular geometries, allowing the investigation of the DNA damage at the nanometric scale [2], [3].

2. Materials and Methods

Realistic 3D multicellular substrates were reconstructed from LIVECell [4] microscopy images using an MC-based growth model, considering breast (SkBr3), ovarian (SK-OV-3), and liver (Huh7) tumor cell lines.

At the micrometric scale, MC simulations were performed using a Spread-Out Bragg Peak (SOBP) proton beams configuration delivering a total dose of 2 Gy to a 2 mm water phantom, with the multicellular substrate positioned at its center. Cell-resolved dose and LET distributions were analyzed.

For the nanometric scale, cell nuclei were approximated by best-fitting ellipsoids, and the 3D organization of the 23 human chromosome pairs was embedded within each nucleus according to published models [5]. The Geant4-DNA code was extended to operate within these realistic multicellular geometries. DNA damages were derived and cell survival probabilities estimated via Two Lesions Kinetic model [5], accounting for DNA repair kinetics.

3. Results

DNA damage was quantified at the single-cell level, accounting for both direct Double Strand Breaks (DSB) and lesions generated indirectly by reactive species. correlation (Spearman's $\rho > 0.8$) was observed between cell dose and both DSB yields (Fig 1.A) and radical-induced events. The resulting damage metrics were used as input to the TLK model to derive cell-specific survival curves, revealing cell-to-cell variability linked to differences in dose deposition and damage complexity (Fig. 1.B).

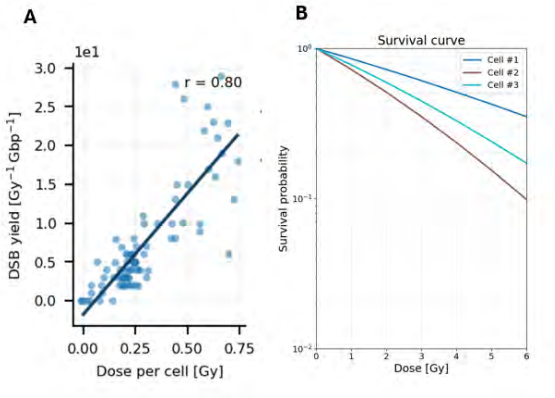


Figure 1: A: correlation between the dose deposited per cell and the number of DSB. B: example of survival curves of different cells. Both the results refer to simulations over BT474 substrate.

4. Discussion and Conclusions

This work demonstrates the feasibility of a multiscale simulation framework combining micrometric dose analysis and DNA damage quantification to retrieve radiobiological response assessment in realistic multicellular tumor substrates.

5. References

[1] S. Agostinelli *et al.*, *Nucl. Instrum. Methods Phys. Res. A*, 2003, doi: 10.1016/S0168-9002(03)01368-8.

[2] K. P. Chatzipapas *et al.*, *Precis. Radiat. Oncol.*, 2023

[3] C. Edlund *et al.*, *Nat. Methods*, 2021,

[4] K. P. Chatzipapas *et al.*, *Physica Medica*, 2024

[5] R. D. Stewart, 2001.

Acknowledgements: This work is supported by MINIONS – ERC Starting Grant n. 101116811

MACHINE LEARNING AND NETWORK MODELING REVEAL IMMUNE REGULATION IN BREAST CANCER AXILLARY METASTASIS

Alba Fischer-Carles (1,4), Gemma Piella (4), Carlos López (1,3), Tábata Sánchez-Alcántara (1), Noèlia Gallardo-Borràs (1), Esther Sauras-Colón (1), Alessio Fiorin (1,3), Marylène Lejeune (1,3), Ramon Bosch Príncep (1), Laia Adalid-Llansa (1,2), Daniel Mata Cano (1), Jérôme Noailly (4)

1. Oncological Pathology and Bioinformatics Research Group, HUTVC, IRB CatSud, URV, Spain; 2. Department of Pathology, HUJ23, ICS, Spain; 3. Department of Computer Engineering and Mathematics, URV, Spain; 4. BCN MedTech, Department of Engineering, UPF, Spain

1. Introduction

Breast cancer (BC) is the leading killing cancer in women, with a worse prognosis when metastasis occurs in axillary lymph nodes (ALN^+) [1,2]. Immune-tumor interactions are critical in metastatic progression, but mechanisms remain poorly apprehended [2]. To address this gap, we combine patient data analytics and a regulatory network model (RNM) of the tumor microenvironment (TME) to characterize ALN^+.

2. Materials and Methods

Three random forest (RF) models (1, 2, 3) were trained on clinicopathological and immune data from two luminal BC cohorts (n=83; n=344). Data analytics included feature selection, hyperparameter tuning, and SHAP interpretation. A 4th RF model used features sequentially added by SHAP values. In parallel, a high-level RNM was developed through graph projection of knowledge from 200+ publications. The RNM mapped the important features and included immune cells, cytokines, hormones, stromal components, and tumor cells, all connected by activating or inhibiting interactions. A CANCER node represented ALN^+ probability. Node activity was computed through Boolean-based ordinary differential equations [3]. Baseline attractors and main regulators were explored through 100 randomly initialized simulations.

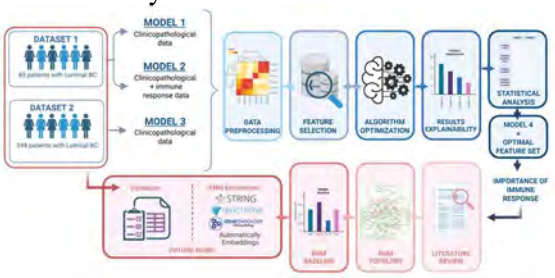


Figure 1: Outline of the study design.

3. Results

The best model, Model 4 (AUC 0.837; accuracy 0.762; recall 0.716), identified intratumoral $CD21^+$ as the strongest predictor of ALN^+ (Fig. 2A,B).

The RNM included 102 nodes and 1,001 links well distributed. Excluding the central CANCER node, endothelial cells had the highest centrality, followed by CAFs, CD8 T cells, Tregs, mDCs, MDSCs, and IL-10. CANCER node activation increased pro-tumoral and immunosuppressive components, and reduced anti-tumoral subsets; inhibition reversed this (Fig. 2C).

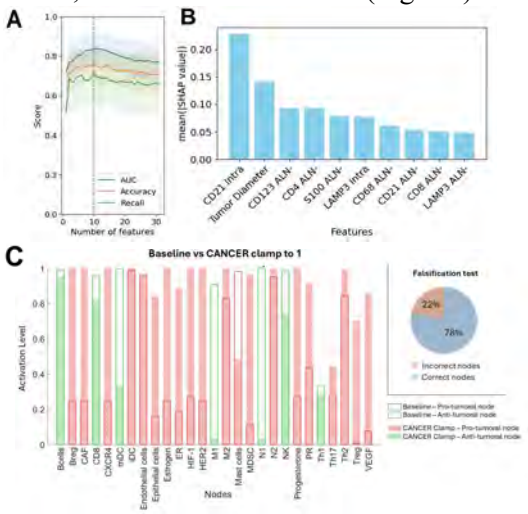


Figure 2: Results. (**A**) Performance metrics for Model 4. Solid lines: mean values; shaded areas: standard deviations. Dashed line: optimal number of features. (**B**) Mean SHAP values for each feature of Model 4. (**C**) Baseline and CANCER-clamped RNM node activation levels for the falsification test.

4. Discussion and Conclusions

RF model 4 highlighted immune features with intratumoral $CD21^+$ surpassing tumor diameter. Accordingly, the RNM was refined to focus on immune regulation, identifying key drivers of ALN^+ and reproducing ~78% of expected TME dynamics. Data analytics and graph-based biological modelling, together may guide immune-informed stratification, although further RNM refinement and validation are needed.

5. References

1. Bray F et al., CA Cancer J Clin, 74, 229–263 (2024).
2. Jana S et al., Am J Pathol, 191, 1353–1363 (2021).
3. Mendoza L et al., Theor Biol Med Model, 3, (2006).

IN SILICO PSYCHO-ONCOLOGY: AI MODELS FOR PREDICTING QUALITY OF LIFE & IDENTIFYING PREDICTORS IN WOMEN WITH EARLY BREAST CANCER

Eleni Kolokotroni (1), Paula Poikonen-Saksela (2) and Georgios S. Stamatakos (1)

1. National Technical University of Athens, School of Electrical and Computer Engineering (ICCS), Athens, Greece; 2. University of Helsinki, Faculty of Medicine, HUS Comprehensive Cancer Center, Helsinki, Finland

1. Introduction

In silico psycho-oncology, addressing problems of psychology and psychiatry in the cancer domain, is being established as a new branch of *in silico* medicine [1]. Machine learning, has proved a powerful, artificial intelligence (AI) based tool for *in silico* psycho-oncology. Within the framework of the European Commission (EC) funded project BOUNCE (www.bounce-project.eu), a prospective clinical study was conducted across four major clinical centers in Finland, Italy, Portugal and Israel. The resulting data enabled the development of multiple AI-based *in silico* models to predict resilience-related psychological and functional trajectories in women with early breast cancer. These models incorporated clinical, biological, psychological, functional & sociodemographic factors as potential predictors.

2. Materials and Methods

Our aim is to develop a binary classifier to identify patients at risk of a low decreasing quality of life (QoL) trajectory over an 18-month period following breast cancer diagnosis. The positive class corresponds to the low decreasing QoL group identified through a preliminary latent class trajectory clustering. The analysis was performed based on data from 513 newly diagnosed breast cancer patients using growth mixture modeling (GMM) on seven time points (0, 3, 6, 9, 12, 15 and 18 months) to identify groups of patients with similar longitudinal QoL trajectory patterns. A refined clustering analysis has since been conducted and is currently under review [2] (at the time of the abstract submission); the low decreasing class shows near-complete overlap with the preliminary version considered here.

Predictive modeling was formulated as a supervised classification task, with the low decreasing QoL trajectory group as the target label. The workflow included handling missing data, addressing class imbalance via downsampling and feature selection through repeated recursive feature elimination (RFE). Model performance was evaluated using (a) nested cross-validation and (b) leave-one-hospital-out cross-validation, training on three hospitals and testing on the fourth one. A random forest classifier was considered. All analyses were implemented in the R platform using the caret package. Single imputation was performed using the missForest R package. The outcome was the Global Health Status/Quality of Life (GHS/QoL) scale of the European Organisation for Research and Treatment of Cancer Quality of Life Questionnaire C30 (EORTC QLQ-C30). Predictors included baseline (M0) and 3-month (M3) psychological, sociodemographic, clinical and treatment variables.

3. Results

Acceptable to good performance was observed across validation schemes (Fig.1). RFE consistently selected the following M3 variables: C30 cognitive, physical, role and social functioning; BR23 systemic therapy side effects; C30 GHS/QoL; C30 pain; and HADS depression. Frequently selected features (selection frequency >50%) included baseline coping (CBI) and manageability (SOC), as well as M3 treatment control beliefs, fatigue (C30), anxiety (HADS) and dyspnoea (C30). The majority of the selected features generalized consistently across clinical sites.

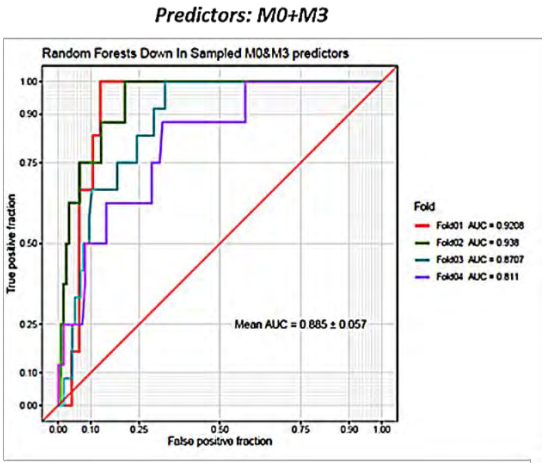


Figure 1. ROC curves for each outer fold of the nested cross validation.

4. Discussion and Conclusions

The model supports credible prediction and facilitates timely, personalized interventions aligned with expected quality-of-life patterns.

5. References

1. Stamatakos G et al. Front. Physiol. 16:1434739 (2025). https://www.frontiersin.org/journals/physiology/articles/10.3389/fphys.2025.1434739/full

2. Kolokotroni E et al, *Preprints* 2026, 2026011376 https://www.preprints.org/manuscript/202601.1376

Acknowledgements:

All BOUNCE co-authors of ref. [2] are duly acknowledged. This project has received funding from the EC under grant agreement No 777167 (BOUNCE).

MECHANISTIC MODELING OF RADIOTHERAPY-INDUCED ABSCOPAL RESPONSES IN SOLID TUMORS

Andreas G. Hadjigeorgiou (1), Yiannis Roussakis (2), Constantinos Zamboglou (2,3,4), Triantafyllos Stylianopoulos (1)

1. University of Cyprus, Cyprus; 2. German Oncology Center, Cyprus; 3. University of Freiburg Medical Center, Germany; 4. German Cancer Consortium, Germany

Corresponding author: T. S., University of Cyprus, Cyprus. Email: tstylian@ucy.ac.cy

1. Introduction

Local radiotherapy can occasionally induce regression of distant, non-irradiated tumors, known as the abscopal effect, but this phenomenon remains rare and unpredictable [1]. Its emergence depends on complex interactions among antigen release, antigen presentation, T-cell priming, trafficking, and lymphoid health. To quantitatively investigate these mechanisms, we developed a physiologically based pharmacokinetic–quantitative systems pharmacology (PBPK-QSP) model that tracks immune and tumor cells across the whole organism, including an irradiated and a distant tumor [2,3].

2. Materials and Methods

The model integrates nine immune and tumor cell types, dendritic cells, M1/M2 macrophages, Tregs, naïve and effector $CD8^+$ T cells, antigen-presenting cells, viable and dead tumor cells, across ten organ compartments plus two tumors. Radiotherapy is implemented using a linear-quadratic formulation that induces direct tumor cell death and antigen release, enabling APC formation and T-cell priming. Lymph-node irradiation is also modeled, allowing depletion of APCs and T cells. The model was calibrated to bilateral melanoma data in which only one tumor received radiotherapy, with or without irradiation of tumor-draining lymph nodes [4]. Parameter estimation used genetic algorithms and bootstrap resampling to quantify uncertainty.

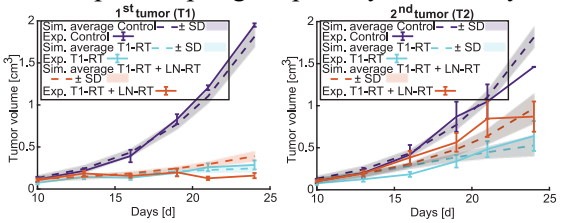


Figure 1: Model validation with experimental data.

3. Results

The model reproduced experimental tumor growth trends for irradiated and distant tumors across all treatment groups, including reduced growth of the distant tumor following local irradiation and suppression of this response when lymph nodes were co-irradiated, Fig. 1. Sensitivity analysis identified antigen capture by dendritic cells and macrophages, naïve T-cell activation, and effector T-cell cytolytic capacity as dominant determinants of abscopal responses. Variations in these parameters produced larger effects in the distant tumor than in the irradiated one, reflecting the nonlinear amplification of systemic immunity. Lymph-node irradiation shifted outcome dependence toward naïve T-cell regenerative capacity, highlighting the importance of lymphoid preservation. Variance and correlation analyses confirmed that tumor-intrinsic growth parameters dominate baseline progression, while immune-activation parameters govern systemic tumor control.

4. Discussion and Conclusions

The PBPK-QSP framework mechanistically links local radiotherapy to systemic antitumor immunity and explains why abscopal responses are rare and highly context-dependent. The model identifies three strategies to enhance abscopal probability: optimizing radiotherapy dose and fractionation to maximize immunogenic antigen release, modulating antigen processing and debris clearance, and preserving or restoring lymph-node regenerative capacity. These insights provide a quantitative basis for designing radiotherapy–immunotherapy combinations that reliably induce systemic tumor control.

5. References

1. MOLE R. H., Br. J. Radiol.; 26(305):234–241 (1953).
2. A. G. Hadjigeorgiou et al., PNAS; 122(46):e2522634122 (2025).
3. A. G. Hadjigeorgiou et al., Front. Immunol.; (In press)
4. Z. S. Buchwald et al., J. Immunother. Cancer; 8:e000867 (2020).

A GOMPERTZ-TYPE MODEL FOR SERUM PROSTATE-SPECIFIC ANTIGEN KINETICS IN PATIENTS IN ACTIVE SURVEILLANCE

Benedetta Dionisi Ferrera* (1), Fabio Badenchini (1), Cristina Marenghi (1), Alessandro Cicchetti (1), Tiziana Rancati (1), Jacopo Iacovacci (1)

1. Fondazione IRCCS Istituto Nazionale dei Tumori, Milan, Italy

**Presenting/corresponding author - benedetta.dionisiferrera@istitutotumori.mi.it*

1. Introduction

Biopsy remains the gold standard for prostate cancer (PCa) diagnosis and aggressiveness assessment; however, tumour heterogeneity may lead to sampling errors and potential misclassification.

In clinical practice, serum prostate-specific antigen (PSA) plays a key role as a biomarker for detecting prostate anomalies, including PCa. We developed a mathematical model for the dynamics of serum levels of PSA for patients in Active Surveillance (AS), a management strategy for low-risk PCa patients that aims to delay or avoid radical treatments and their associated side effects.

2. Materials and Methods

The proposed model is based on the assumption that the presence of tumour cells disrupts the architecture of the healthy prostate, thus increasing the release of PSA from the prostate into the bloodstream [1]. By additionally incorporating Gompertz-type tumour growth dynamics, the model adapts to both indolent and aggressive prostate cancer progression observed in AS [2]. In equations:

$$\begin{cases} PSA(t) = \alpha \cdot V_p \cdot F\left(GPS, V_c(t)\right) \\ V_c(t) = K\left(\frac{V_{c,0}}{K}\right)^{e^{-\gamma t}} \end{cases} \quad (1)$$

Where the production rate of PSA per unit of prostate volume α times the total prostate volume $V_p(t)$ accounts for the PSA production in the gland, and the flux function $F\left(GPS, V_c(t)\right)$ depends, in general, by the prostate cancer aggressiveness (Gleason Pattern Score) and by the volume of the tumour $V_c(t)$.

Fitted to all individual PSA dynamics from 720 patients enrolled in AS at the Fondazione IRCCS Istituto Nazionale dei Tumori di Milano between 2005 and 2022, the model estimated each patient's tumour proliferation rate γ.

3. Results

Through the parameter γ, the model seems to distinguish serum PSA dynamics likely associated with indolent cancers and dynamics likely associated with aggressive cancers.

When restricted to dynamics characterized by biologically meaningful proliferation rates ($\gamma > 0$), the Gompertzian model outperforms the predictive value of PSA density (PSAD) at diagnosis which is the biological indicator currently acknowledged as most associated with not indolent cancer, as shown in Figure 1.

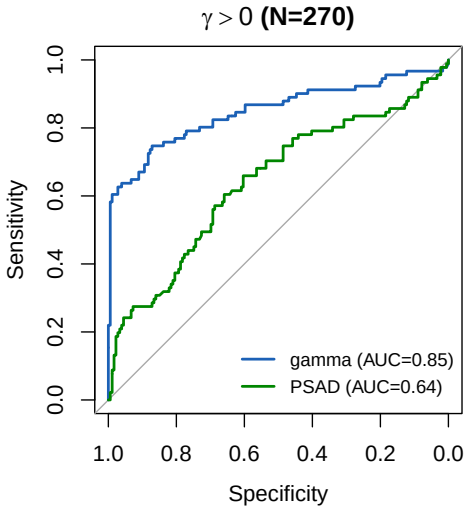


Figure 1: Comparison of the classification performance between γ and PSAD at diagnosis.

4. Discussion and Conclusions

This work aims to propose a new, reliable, and realistic model for describing PSA kinetics in AS that hopefully could be helpful in the clinical setting to understand better the process that led to the data we observed in the real world.

5. References

1. Balk SP et al. *J Clin Oncol*. 2003;21(2):383-391.
2. Tjørve KMC et al. *PLoS One*. 2017;12(6):e0178691.

A MULTISCALE MODEL OF GLIOBLASTOMA-MESENCHYMAL STROMAL CELLS TUMOR SPHEROIDS

Alzbeta Prasilova (1), Bela Charvatova (1), Tomas Bily (2)

1. Department of Cell Biology, Faculty of Science, Charles University, Prague, Czechia 2. Department of Software Engineering, Faculty of Mathematics and Physics, Charles University, Prague, Czechia

1. Introduction

Glioblastoma (GBM) is one of the most aggressive primary brain tumor in adults, characterized by rapid proliferation, invasion, therapeutic resistance, and high intratumoral heterogeneity [1]. Tumor progression and treatment response are strongly influenced by the tumor microenvironment, including interactions with mesenchymal stromal cells (MSCs) [2]. 3D spheroid models provide a physiologically relevant platform to study these interactions, yet experimental systems alone offer limited mechanistic insight and scalability. To address this, we developed a computational 3D GBM-MSC spheroid model.

2. Materials and Methods

A hybrid modeling framework was developed that combines agent-based modeling using the Cellular Potts Model with reaction–diffusion equations describing extracellular factors such as nutrients, oxygen, metabolites, and drug concentration. GBM cells and MSCs were modeled as discrete agents with rules for proliferation, apoptosis, and mechanical interactions, parameterized using experimental spheroid observations and literature data. The model reproduce tumor growth dynamics, spatial organization, cell-cell interactions and drug response predictions.

Simulations were performed for both mono-culture GBM spheroids and co-culture GBM–MSC spheroids to compare growth dynamics, spatial organization, and emergent behavior.

3. Results

The model correctly reproduces key qualitative features of experimental spheroids, including radial growth patterns, heterogeneous cell distributions, and microenvironment-driven proliferation gradients (Fig.1). In co-culture simulations, MSC presence alters spatial organization and modulates overall growth dynamics, consistent with their supportive role in the tumor microenvironment.

The drug-response extension enables simulation of concentration-dependent pathway perturbations and their downstream effects on cell fate decisions. Systematic quantitative evaluation of treatment scenarios and parameter sensitivity analyses are currently in progress.

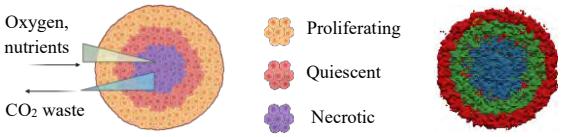


Fig. 1 Tumor spheroid and its heterogeneity. **A)** Schematics of tumor spheroid regions with different cell phenotypes and the influence of extracellular factors. **B)** Simulation of tumor spheroid regions using our model.

4. Discussion and Conclusions

We present a multi-scale computational 3D GBM-MSC spheroid model. The framework reproduces experimentally observed growth behavior and is designed to support predictive simulations of therapeutic interventions.

By coupling drug diffusion within a porous tumor-like structure to intracellular regulatory responses, the model enables mechanistic exploration of microenvironment-mediated therapy resistance. Beyond treatment response analysis, the framework provides a basis for systematic in silico exploration of therapeutic strategies and may support future drug screening or repurposing efforts.

5. References

1. Singh, S., Dey, D., Barik, D. *et al.* Glioblastoma at the crossroads: current understanding and future therapeutic horizons. *Sig Transduct Target Ther* **10**, 213 (2025).
2. Qing-mei Kang, Jun Wang, Shi-man Chen *et al.* Glioma-associated mesenchymal stem cells, *Brain* **3**, 147 (2024).

Acknowledgements:

Our thanks belong to Yuriy Petrenko, PhD and the Department of Neuroregeneration, Institute of Experimental Medicine, CAS for providing experimental data.

From Classical ML To GNNs: Accelerating Bone Stress Prediction from Hours to Milliseconds

Sikha O K[1], Abdollah Moslemivaraki[1], Elham Alizadeh[1] , Miguel A. González Ballester[1,2], Jérôme Noailly[1]

1. BCN MedTech, Department of Engineering, Pompeu Fabra University, Spain; 2. ICREA, Spain

1. Introduction

Finite Element Analysis (FEA) is the gold standard for predicting bone stress distribution but requires 5-10 hours per simulation for nonlinear models, limiting clinical applicability [1]. Machine learning metamodels offer fast alternatives [2]. This study systematically compares classical ML approaches-which treat elements independently - against Graph Neural Networks (GNNs) that leverage mesh connectivity, evaluating their performance for element-wise stress prediction in femur biomechanics.

2. Materials and Methods

Dataset: The dataset comprises 128 femur FEA simulations with 126,800 elements each (approximately 16.2 million total), tested against mesh convergence. Each element was characterized by 9 features: 3D centroid coordinates, material properties (density, stiffness), tissue type (cortical/trabecular); anatomical region (head, neck, trochanteric); boundary conditions; loading configuration. Target outputs were six independent stress tensor components (S11; S22; S33; S12; S23; S31) computed at each element. The dataset was split into 90 training (70%), 19 validation (15%), and 19 independent test (15%) cases.

Models: We implemented seven classical ML approaches: Ridge (L2, α=1.0), Lasso (L1, α=0.1), Elastic Net (L1+L2), Random Forest (50 trees), Gradient Boosting (100 trees), Cat Boost (200 iterations), and MLP (128→64 neurons). We also tested seven GNN architectures with 128/256 hidden channels: GCN, SAGE, GAT, and hybrid GCN-SAGE-Residual models. Graph edges connected face-sharing elements. All models are trained to predict six stress components per element centroid.

Training and Evaluation: Models are trained with AdamW optimizer and cosine annealing. GNNs used mixed-precision, gradient accumulation (8-16 steps), and early stopping (patience 50-100 epochs) to avoid overfitting. Hyperparameters are optimized using validation set. Model performance measured using R^2, MAE, RMSE, and MSE on test data, focusing on individual stress components. Averaged precision metrics are reported below.

3. Results and Discussions

Classical ML models achieved R^2 = 0.105–0.774, with linear models failing ($R^2 \approx 0.11$, MAE ≈ 10.2 MPa) and ensembles performing moderately (Random Forest: R^2 = 0.774, MAE = 4.33 MPa). GNN models substantially outperformed classical ML, achieving R^2 = 0.769–0.856. The hybrid GCN-SAGE-Residual (709K parameters) achieved best performance: R^2 = 0.856, MAE = 0.157 MPa, the stress prediction errors being two orders of magnitude lower than the ones with linear model. Attention mechanisms (GAT) underperformed simple aggregation, indicating graph structure, not attention, is essential for accurate stress prediction. Table 1 presents the consolidated performance metrics for all models on 6-component stress prediction (average).

5. References

1.Ruiz wills, C., et al., Bone J., 121:89-99 (2019).

2. Gulakala et al. "Graph neural network enhanced finite element modelling." *PAMM* 22.1 (2023):

6. Acknowledgments

Spanish Government (CPP2021-008574, CPP2023-010970); European Research Council (ERC-CoG-O-Health-101044828); AGAUR (2023 BP 00224).

Table 1: Performance Comparison of Classical ML and GNN Models for Element-Wise Stress Prediction

Metric	Ridge	Lasso	Elastic Net	Random Forest	Gradient Boosting	Cat Boost	MLP	GCN-128	SAGE-128	GAT-128	GCNResidual-128	GCN-256	SAGE-256	GCN-SAGE-Residual
#Params	50K	50K	50K	2M	500K	500K	200K	94K	178K	96K	128K	369K	700K	**709K**
R^2	0.111	0.109	0.105	0.774	0.771	0.707	0.759	0.804	0.803	0.769	0.795	0.821	0.816	**0.856**
MAE	10.22	10.22	10.26	4.33	4.42	5.28	4.76	0.181	0.183	0.199	0.257	0.17	0.175	**0.157**

PATIENT-SPECIFIC 3D RENAL PERFUSION MODELS IN SUPPORT OF SELECTIVE CLAMPING DURING PARTIAL NEPHRECTOMY

Saar Vermijs (1,2,3), Joris Vangeneugden (2,3,4), Kenzo Mestdagh (2,3,4), Pieter De Visschere (5), Pieter De Backer (6,7), Peter De Kuyper (8), Frederic Baekelandt (9), Christophe Ghysel (9), Yannic Raskin (10), Bernard Bynens (10), Camille Berquin (4), Nicolaas Lumen (2,4), Karel Decaestecker (2,4,8), Charles Van Praet (2,3,4), Charlotte Debbaut (1,3)

1. BioMMedA@iBME, Dept. of Electronics and Information Systems, Faculty of Engineering and Architecture, Ghent University, Belgium; 2. Dept. of Human Structure and Repair, Faculty of Medicine and Health Sciences, Ghent University, Belgium; 3. Cancer Research Institute Ghent, Belgium; 4. Dept. of Urology, ERN eUROGEN accredited center, Ghent University Hospital, Belgium; 5. Dept. of Radiology and Nuclear Medicine, Ghent University, Belgium; 6. ORSI Academy, Belgium; 7. Dept. of Urology, AZORG, Belgium; 8. Dept. of Urology, AZ Maria Middelares Hospital, Belgium; 9. Dept. of Urology, AZ Sint-Jan Brugge, Belgium; 10. Dept. of Urology, ZOL Genk, Belgium

1. Introduction

Partial nephrectomy (PN) is the recommended treatment for early-stage localized kidney cancer, but this organ-saving surgery is technically challenging. It often requires temporary clamping of the main renal artery to achieve a bloodless surgical field. However, this induces ischemia, risking damage to surrounding healthy tissue. Only clamping those arteries perfusing the tumor, i.e. selective clamping (SC), can minimize this risk, but identification of the correct arteries is often not possible on preoperative imaging. Therefore, we developed a pipeline to create patient-specific 3D renal perfusion models that facilitate preoperative planning. This pipeline is now being evaluated in a randomized controlled trial (RCT). We present the interim results here.

2. Materials and Methods

As a first step, preoperative multi-phase contrast-enhanced CT scans are converted into 3D models using AI-enabled segmentation (Medannot, Slovakia). Perfusion information is added onto these 3D models using a proprietary algorithm [1]. This information is visualized in an in-house developed web-based environment, shown in Fig. 1, allowing surgeons to plan the optimal SC strategy that minimizes bleeding risk while preserving healthy tissue.

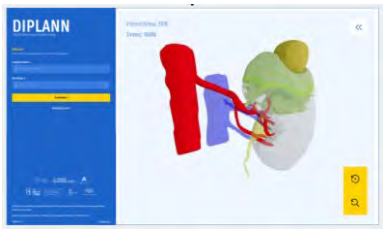


Fig 1: A 3D perfusion model with a highlighted perfusion zone in green, showing a possible SC strategy.

Regulated as Class IIa medical advice, approval was needed by the national competent authority to start 'PODRACING': a multi-centric RCT, aiming to enrol 235 adult patients undergoing robot-assisted PN [2]. In the experimental group, 3D perfusion models are used on top of CT scans to plan a clamping strategy. In the control group, only the CT scan is used. Randomization is 1:1. The primary endpoint is planning and successfully executing a SC strategy as planned. This was analyzed for the interim analysis using a χ^2-test in a subgroup of patients where SC was deemed feasible. Secondary endpoints involve perioperative and patient-reported outcomes (e.g. renal function, surgical duration, quality of life questionnaires)

3. Results

107 patients were included between Jun 2024 and Oct 2025 in four Belgian hospitals. 86% of the patients in the experimental group had a positive primary endpoint, compared to only 41.5% in the control group ($p < 0.00001$).

4. Discussion and Conclusions

Interim results of the 'PODRACING' RCT show that using our pipeline significantly increases the accuracy and frequency of SC during RAPN. Future research will analyze its effect on patient outcomes.

5. References

1. De Backer P. & Vermijs S. et al. Eur Urol (2023)
2. ClinicalTrials.gov. Identifier NCT06536439

Acknowledgements:
The PODRACING trial is supported by Stichting tegen Kanker (OST-2022-199) and FWO (1S64425N).

CIN-VIT@LLY: A REUSABLE CONCEPT FOR VIRTUAL TWINS INCUBATED WITHIN HOSPITAL INFRASTRUCTURE

Ekaterina Kutafina (1), Maike Trommer (1), Judith Wodke (2), Anna Maxion (3), Jenny Tigerholm (3), Oya Beyan (1)

1. University Hospital Cologne, Germany; 2. University Medicine Greifswald, Germany; 3. University Hospital RWTH Aachen, Germany

1. Introduction

Virtual Twins face many challenges on their way to healthcare applicability. Beyond complex modelling and validation challenges, clinical feasibility requires hospital-embedded infrastructure, interoperable data access, and standardized workflows. A major unresolved challenge is the limited integration of basic research data with clinical routine data. CIN-ViT@LLy is presented as a conceptual blueprint addressing these barriers. Focusing on cancer treatment-induced neuropathy (CIN) as a use case, we outline how hybrid Virtual Twins can be developed within existing hospital data infrastructures to bridge transdisciplinary clinical and basic research, data-driven models and physiological knowledge.

2. Materials and Methods

The concept targets early prediction and prevention of CIN as a common side effect in oncological care. The framework builds on the German Medical Informatics Initiative (MII) and the Data Integration Center (MeDIC) at the University Hospital Cologne. MeDIC is embedded in the hospital and provides secure access to routine electronic health record data structured via interoperable standards (FHIR), enabling efficient secondary use. A domain-specific knowledge graph (MeDaX-KG [1]) harmonizes routine oncology data, structured exercise-oncology cohort data, and prospective peripheral nerve excitability measurements [2]. Hybrid modelling comprises two interacting layers: an AI-driven Virtual Twin (A-ViT) for individualized risk prediction based on harmonized routine data, and a Biophysical Virtual Twin (B-ViT) integrating Threshold Tracking (TT) and Perception TT [3] measurements into mechanistic nerve fibre models. Their coupling enables cross-validation between statistical and physiological representations. All components are embedded in a Hospital Living Lab (@LLy), providing controlled development environments and regulatory-aware documentation workflows.

3. Results

As a concept, CIN-ViT@LLy demonstrates how Virtual Twin development can be structured around existing hospital infrastructures rather than isolated modelling pipelines. Integration of FHIR-based routine data with experimental neuroscience data within a shared semantic backbone illustrates a practical pathway to bridge research and care. The hybrid architecture enhances interpretability by linking AI-based prediction with mechanistic simulation. Embedding development within a hospital-based Living Lab strengthens scalability within MII networks and supports translational readiness.

4. Discussion and Conclusions

CIN-ViT@LLy serves as a reusable blueprint for clinically embedded hybrid Virtual Twins. Its key elements are: (1) leveraging Data Centers for secure use of structured routine data and research data; (2) harmonizing datasets via knowledge graphs; (3) coupling AI-driven and mechanistic models; (4) development within a regulatory-aware hospital Living Lab. While exemplified for CIN, the architecture is transferable to other clinical applications.

5. References

1. Mazein et al. MeDaX: A Knowledge Graph on FHIR. Stud Health Technol Inform 2024
2. Trommer et al. Exercise interventions for adults with cancer receiving radiation therapy alone. Cochrane Database Syst. Rev. 3, 2023
3. Mørch et al. A nociceptor excitability test for identifying alterations of the Nav1.7 channels in humans. *Pain 2025*

FROM DATA TO DIAGNOSIS: A HOSPITAL PROOF OF CONCEPT OF AI-DRIVEN ALLERGY DIAGNOSTICS

Paulina Tworek (1), Maja Szczypka (1), Marek Mikołajczyk (2), Roman Lewandowski (2, 3), Jose Sousa (1, 4)

1. Sano - Centre for Computational Personalised Medicine, Poland;
2. Voivodeship Rehabilitation Hospital for Children in Ameryka, Poland;
3. University of Warmia and Mazury, Poland;
4. Coimbra University, Multidisciplinary Institute of Ageing, Portugal

e-mail: p.tworek@sanoscience.org, j.sousa@sanoscience.org

1. Introduction

Allergic diseases affect up to 35% of children, and their diagnosis is difficult due to diverse allergens, cofactors, and inconsistent symptom-test correlations [1, 2]. Although artificial intelligence (AI) can support clinical decisions, its hospital use is challenged by incomplete, imbalanced data and the need for explainable results, which should be resolved for safe and effective diagnosis [3]. To address the challenges, we implemented designed in our team the Comprehensive Abstraction and Classification Tool for Uncovering Structures (CACTUS) in the Allergy Department of the Voivodeship Rehabilitation Hospital for Children in Ameryka to support the diagnosis of allergic diseases in children [4, 5]. The system was evaluated in a real-world clinical setting and compared with classic machine learning (ML) methods.

2. Materials and Methods

The dataset included 6757 patients diagnosed by 9 physicians at the Allergy Department of the Voivodeship Rehabilitation Hospital for Children in Ameryka, with structured clinical data (42% missing) and medical interviews. Information from unstructured data was extracted using rule-based methods and LLMs, whose performance was compared. Allergy classification was performed with CACTUS and benchmarked against classic ML models.

3. Results

Our results indicate that simple rule-based methods can effectively extract information from Polish medical unstructured data in hospitals with limited computing resources, while LLMs offer more flexible extraction with high accuracy and without manual rule creation. The extracted information was combined with tabular medical test data and used to classify patients into 5 specific allergic diseases. CACTUS achieved about 25 p.p. higher balanced accuracy than the best-performing traditional ML model. Introducing AI into medical practice requires explainable decisions. This can be achieved by identifying key features and their contribution to classification. Experiments on hospital data with different levels of missing values indicate that traditional ML models struggle to preserve feature stability, and consequently explainability, whereas CACTUS performs considerably better.

4. Discussion and Conclusions

This real-world study demonstrates the potential of CACTUS as a decision-support system for allergy diagnostics. CACTUS achieved high classification accuracy despite noisy, imbalanced and incomplete hospital data, while its stable and explainable outputs may support clinicians' trust and help optimize diagnostic workflows.

5. References

1. Chad Z, Paed. Child Health; 6(8), 555-566 (2001)
2. Bousquet PJ et al., Allergy; 60(2), 135-137 (2005)
3. Mullins CF et al., Post. Med. Journal; 99(1169) (2023)
4. Gherardini L et al., ACM TIST; 3(15) (2024)
5. Ibias A et al., Inf. Sciences; 640 (119078) (2023)

Acknowledgements:
This project was funded by the EU Horizon 2020 research and innovation programme (No 857533), the International Research Agendas Programme of the FNP (No MAB PLUS/2019/13) and the Minister of Science and Higher Education under programme No MEiN/2023/DIR/3796.

ORTHOAI: A NEUROSYMBOLIC FRAMEWORK FOR EVIDENCE-GROUNDED BIOMECHANICAL REASONING IN CLEAR ALIGNER ORTHODONTICS

Edouard Lansiaux (1,2)*, Margaux Leman (1), Mehdi Ammi (2)

1. STaR-AI, Emergency Department, Lille University Hospital, France; 2. LIASD, Paris 8 Univ., France.
**edouard1.lansiaux@chu-lille.fr*

1. Introduction

Clear aligner orthodontics lacks automated biomechanical screening tools despite documented movement predictability [1]. OrthoAI addresses this by combining geometric perception of teeth from 3D data with symbolic reasoning based on clinical constraints. The neurosymbolic pipeline tackles three key challenges: learning from landmark-only supervision, performing formal constraint-based biomechanical reasoning, and providing multi-criteria treatment quality scoring.

2. Materials and Methods

OrthoAI operates as a two-layer pipeline Pi=(P, R, phi). The perceptual module DGCNN_Seg (60,705 parameters) processes landmark-reconstructed point clouds from 3DTeethLand (MICCAI 2024, 100 scans) [2]. Since only sparse landmarks (6-8 points/tooth) are annotated, we formalize a synthesis protocol generating labeled ellipsoidal point clouds from landmark sets, with per-tooth local coordinate frames and Gaussian surface sampling (sigma=0.3 mm). Training uses a composite loss: label-smoothed cross-entropy (epsilon=0.05) combined with a batch-adaptive Dice term restricting computation to classes present in each mini-batch, avoiding gradient starvation on rare tooth classes. The reasoning module implements a Constraint Satisfaction Problem K=(V,D,C) encoding literature-derived per-stage biomechanical limits as typed hard/soft constraints with graded severity semantics [1,3,4]: bodily translation (0.25 mm/stage), extrusion (0.15-0.20 mm), axial rotation (1.5-2.0 deg). Treatment quality is scored as a Weighted Additive Value Function (WAVF) over six criteria: biomechanical compliance (w=0.30), predictability (w=0.20), staging (w=0.15), attachment planning (w=0.15), IPR indication (w=0.10), arch symmetry (w=0.10).

3. Results

DGCNN_Seg achieves 81.4% Tooth Identification Rate (TIR) on the 20-scan validation set with only 60,705 parameters, surpassing PointNet baseline (TIR=61.2%). Ablation studies confirm: removing batch-adaptive Dice reduces TIR by 7.1 pp; removing global pooling reduces TIR by 14.3 pp (resolving arch-level symmetry ambiguity). TIR and mIoU exhibit divergent optimization trajectories (TIR peak: epoch 7 at 84.1%; mIoU peak: epoch 4 at 8.25%), empirically validating the perception-reasoning decoupling principle. CSP inference across 4 patient cases detects an average of 1.5 critical and 2.0 warning violations per case, predominantly excessive rotation and anterior torque - consistent with known clear aligner limitations [1]. Mean WAVF score is 80.5 (Grade B). The complete pipeline executes in <4 s on a consumer CPU (no GPU required). WAVF sensitivity analysis shows <9% score variation under +/-50% weight perturbation, confirming grade-level robustness.

4. Discussion and Conclusions

OrthoAI formalizes a perception–reasoning decoupling: biomechanical analysis requires correct tooth identity and approximate centroids rather than precise boundaries. The framework introduces methods for landmark-only learning and imbalanced multi-class segmentation, while highlighting key limitations (synthetic training data, fixed population constraints, heuristic scoring weights). It remains a research prototype.

5. References

1. Kravitz ND et al. Am J Orthod Dentofacial Orthop. 135(1):27-35 (2009).
2. Ben Yedder H et al. 3DTeethLand Benchmark, MICCAI Challenge (2024).
3. Simon M et al. BMC Oral Health. 14(68) (2014).4. Lombardo L et al. Prog Orthod. 18(35) (2017).5. Collins GS et al. BMJ. 350:g7594 (2015).

ORTHOAI V2: FROM SINGLE-AGENT SEGMENTATION TO DUAL-AGENT TREATMENT PLANNING FOR CLEAR ALIGNERS

Edouard Lansiaux (1), Margaux Leman (1)

1. STaR-AI Research Group, Emergency Department, Lille University Hospital, France.
edouard1.lansiaux@chu-lille.fr

1. Introduction

Clear aligner treatment planning is a multi-step process. OrthoAI[1]introduced a fast open-source pipeline generating evaluated plans on a CPU in under 5 s, but had three limits: simplified tooth geometry, a single pass/fail quality score, and no movement staging. OrthoAI v2 addresses these with a dual-agent architecture, composite biomechanical scoring, and a multi-frame treatment simulator for visualizing tooth movements.

2. Materials and Methods

v2 introduces three principal contributions. (i) Dual-agent architecture: Agent 1 (DGCNN) performs point-cloud segmentation (4-layer EdgeConv, k=20, combined CE+Dice loss alpha=0.5), providing per-tooth centroids and orientation matrices. Agent 2 (CHaRM [2]) performs segmentation-free landmark detection via a lightweight PointMLP encoder (emb=128) producing per-point heatmaps for K=80 landmarks (16 teeth x 5 landmarks), conditioned on tooth presence probabilities. An orchestrator fuses both agents in three modes: parallel ensemble (confidence-weighted: w1=0.4 DGCNN, w2=0.6 CHaRM), sequential refinement (CHaRM first, DGCNN invoked only when $p_t < 0.5$), and single-agent fallback. (ii) Composite biomechanical scoring: six sub-scores replace the v1 scalar: Q = 0.30*S_bio + 0.20*S_stg + 0.15*S_att + 0.10*S_ipr + 0.10*S_occ + 0.15*S_pred, with multiplicative severity penalties (x0.85 per critical finding, x0.97 per warning). Movement limits encode four Invisalign principles: push mechanics, simultaneous movement anchorage loss, Newton reaction forces, and over-engineering factor x1.3 [3]. (iii) Multi-frame simulation: F = A x r frames (r=3/aligner) via 6-DoF SLERP interpolation, with extrusion staging deferred to t>=0.6 for anchorage establishment. Aligner count: A = max(ceil(max_j||m_j|| /0.25mm), ceil(max_j||omega_j||/2 deg), 20).

3. Results

On 200 synthetic crowding scenarios (4 arch archetypes, mild/moderate/severe crowding, 0-2 missing teeth), the parallel ensemble of v2 achieves quality score 92.8+/-4.1 vs. 76.4+/-8.3 for v1 (+21% relative gain), reduces score variance by 53%, and improves treatment feasibility from 78% to 89%, while maintaining full CPU deployability (4.2+/-0.8 s). The quality improvement decomposes as: ~+12 pts from improved composite scoring model alone (v2 DGCNN-only: 88.3 vs. v1: 76.4), and ~+4.5 pts from agent fusion reflecting genuine information gain from landmark-level geometry. Agent 2 achieves MEDE=1.38+/-0.21 mm and MSR=64.2+/-3.1% on our synthetic dataset, a ~23% reduction in effective landmark error vs. v1 centroids. Frame generation yields mean inter-frame displacement 0.25+/-0.03 mm (target: 0.25 mm) and rotation 1.8+/-0.4 deg (target: 2.0 deg). Extrusion staging correctly defers vertical movements in all 47 open-bite scenarios.

4. Discussion and Conclusions

The v1→v2 upgrade shows that most performance gains come from improved scoring, not sensing. A dual-agent architecture balances segmentation and landmark approaches, while confidence-based sequential inference reduces runtime. Next steps include validation on real IOS data, automatic movement sequencing, and attachment placement optimization.

5. References

1. Lansiaux E, Leman M, Ammi M. OrthoAI v1. arXiv:2603.00124 (2026).
2. Rodriguez-Ortega J et al. CHaRM. arXiv:2501.13073v5 (2025).
3. Glaser B. The Insider's Guide to Invisalign Treatment. (2017).4. Kravitz ND et al. Am J Orthod Dentofacial Orthop. 135(1):27-35 (2009).5. Wang Y et al. Dynamic Graph CNN. ACM Trans. Graph. 38(5):1-12 (2019).

CLINICAL EVALUATION OF A GLUCOSE–INSULIN MODEL FOR INTENSIVE CARE UNIT PATIENTS WITHOUT EXOGENOUS INSULIN

Pierre Verstraeten[1], V. Uyttendaele[1], M. Seret[1], A.-F. Rousseau[2], B. Lambermont[2], G. Minguet[2], D. Wertz[2], N. Esser[3], J. G. Chase[4], and T. Desaive[1]

[1]Model-based therapeutics, GIGA Institute, University of Liège, Belgium; [2]Department of Intensive Care, CHU Liège, Belgium; [3]Departmentof Diabetology, CHU Liège, Belgium; [4]Department of Mechanical Engineering, University of Christchurch, New Zealand

1. Introduction

Accurate glucose–insulin modelling is essential for personalised glycaemic management. The ICING physiological model has previously been validated in intensive care unit (ICU) settings [1] for patients receiving exogenous insulin as part of glycaemic control protocols.

This study evaluates ICING's ability to assess plasma insulin dynamics in ICU patients who do not receive exogenous insulin, thus relying on the estimation of endogenous insulin secretion only. Model predictions are then compared to clinical data.

2. Materials and Methods

A clinical study conducted at the University Hospital of Liège, Belgium measured plasma glucose, insulin, and C-peptide concentrations every 6 hours in adult ICU patients. Patients were included if they had a minimum ICU stay of 4 days and did not receive any exogenous insulin.

Endogenous insulin secretion is described by two different approaches: (i) the accepted gold standard Van Cauter *et al*. physiological model [2], estimating insulin secretion from plasma C-peptide concentrations, and (ii) the linear ICING secretion model based on available blood glucose levels and constant parameters set by diabetic status. The latter has the advantage not to require C-peptide lab-analysis.

These simulated insulin profiles were compared to measured insulin concentrations using the root mean square error (RMSE) and coefficient of determination (R^2) across patients.

3. Results

A total of 4 patients with complete datasets were included in the analysis. Comparing plasma insulin estimated by Van Cauter and measured insulin concentrations, RMSE was 65.49 mU/L and R^2 was -15.02. In contrast, comparing the linear ICING model with measures gave RMSE of 9,78 mU/L and R^2 of 0,64. Results are presented in *Figure 1*.

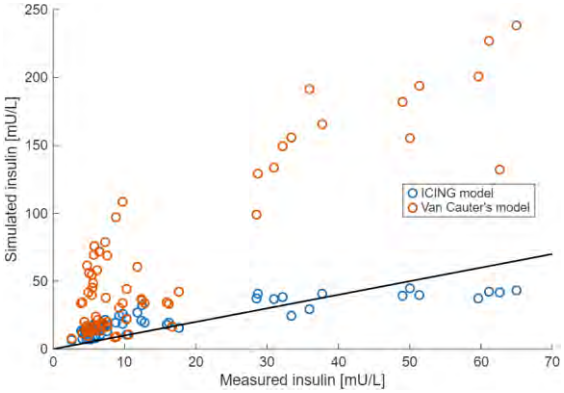


Figure 1: Simulated plasma insulin values for Van Cauter (red) and ICING (blue) methods against insulin measurements (1:1 line shown in black).

4. Discussion and Conclusions

This study provides a first evaluation of the ICING physiological model in patients who did not receive exogenous insulin administration. Comparing insulin concentrations simulated using the ICING linear endogenous secretion model showed better agreement with measured insulin values than simulations using Van Cauter's model. These results suggest the endogenous insulin secretion formulation used in ICING produces more realistic insulin dynamics than the gold standard method.

Continuation of this clinical trial will increase the patient cohort and incorporate additional confounders to refine secretion model parameterisation beyond diabetic status. This aims to improve the accuracy of endogenous insulin secretion prediction.

5. References

1. Lin J et al., Comput Methods Programs Biomed; 102(2):192-205 (2011)
2. Van Cauter E et al., Diabetes; 41(3):368-77 (1992)

Acknowledgements:

No conflict of interest. This work was supported by BOSA [Project DIGITWIN4PH]; and the Federation Wallonie-Bruxelles via the ARC project DECIPHER.

AI-CARE: A DECISION SUPPORT SYSTEM BASED ON FEDERATED AND CONTINUOUS LEARNING

Daniele Tartarini (1)(2),Manya Mittal(1), Lauren Thomas(1), Jivanthika Venkatakrishnan (1), Jonah Walton (1)

1 School of Computer Science, University of Sheffield, United Kingdom
2 INSIGNEO institute for in silico medicine, Sheffield, United Kingdom

Daniele Tartarini, d.tartarini@sheffield.ac.uk Regent Court, S14DP, Sheffield. UK

1. Introduction

Clinical decision support systems (CDSS) support clinicians in the diagnostic and prognosis by processing patient data via computational models. The effectiveness of the support depends on the reliability and accuracy of those models, which need to comply with software medical device standards (SaMD). While for mechanistic models the compliance process is consolidated and almost static, for models based on Artificial Intelligence or Machine Learning (AI/ML) the quality of the models depends on the availability of training datasets representative of the population/disease of interest. This does not correspond to the real-world scenario where data distribution changes across institutions, diagnostic devices and population demographics. Moreover patient data cannot be transferred across institutions due to privacy regulations. A model trained on at a given point in time struggles to maintain optimal performance because new data and technology become available continuously. Retraining the models on new data is impractical due to computational costs, access to sensitive data and overfitting to the latest data [1]. To solve this problem, a recent training paradigm has been developed, Continuous Learning where the AI/ML model is trained on the new datasets when they become available.

2. Materials and Methods

AI-CARE (Artificial Intelligence for Cancer Research) is a DSS framework that we developed to support clinical oncologists, which can be used by any clinician. It implements a federated learning (FL) algorithm [3] which builds an AI/ML model by combining the models trained at the institutions where patient data is available, overcoming privacy concerns. FL models are verified and validated according to SaMD regulations and become operational with the needed traceability. In this work, we expanded AI-CARE with a continuous learning algorithm, which allows each distributed institution to improve the performance of the FL model as soon as new patient data becomes available without waiting for all the participants in the FL to have enough data for a FL cycle.
The CL mechanisms face the stability-plasticity challenge, learn new information while retaining previous knowledge and avoiding catastrophic forgetting. We adopted the Deep Generative Replay CL approach using Scholar architecture with a Wasserstein GAN with Gradient Penalty (WGAN-GP)[4]

3. Results

In this work we benchmarked different configurations/approaches of CL on existing deep learning models developed for the MICCAI grand challenges. In particular, we simulated FL and CL by partitioning the dataset used for the PiCAI challenge [5] to diagnose prostate cancer and we organised the dataset to simulate different timelines for patient data availability. We identify the key factors to optimise the CL approach and comply with the SaMd requirements.

5. References

1 Qazi MA, et al. Continual Learning in Medical Imaging: A Survey and Practical Analysis DOI://10.1145/3785663. 2026
2. Cummings J, Tartarini D: AI-CARE: Digital twin platform for cancer research. VPH 2024
3. Yurdem b, et al. Federated learning: Overview, strategies, applications, tools and future directions. 2024
4. Verma T, Jin L, Zhou J, Huang J, Tan M, Chen B, et al. Front Med. 2023;10 (2023)
5 Kan H, et al. ITUnet: Integration of transformers and Unet for organs-at-risk segmentation. doi:10.1109/EMBC48229.2022.9871945

MODULAR PLUGIN TO RADIOTHERAPY TREATMENT-PLANNING SYSTEM EMPOWERS EVIDENCE-BASED TREATMENT PLANNING

Hampus Hållberg (1,2), Emmy Dalqvist (1,3), Anders Berglund (2), Eva Onjukka (1,3)

1. Department of Nuclear Medicine and Medical Physics, Karolinska University Hospital, Stockholm, Sweden; 2. Epistat AB, Uppsala, Sweden; 3. Department of Oncology-Pathology, Karolinska Institutet, Stockholm, Sweden

1. Introduction

Modern radiotherapy can exploit many degrees of freedom when individualising the dose delivery to each patient. When optimising the treatment, the 3D dose distribution in organs-of-interest (OIs) near the tumour is evaluated in terms of simple dose-volume constraints. However, the evidence regarding OI dose response is continuously evolving, now offering validated predictive models of normal tissue complication probability (NTCP).

To be able to exploit current evidence in the treatment-planning process, a plugin to a commercial treatment-planning system (TPS) has been developed, accommodating different types of prediction models. This facilitates on-the-fly NTCP estimation when evaluating treatment plans in the TPS.

2. Materials and Methods

The plugin for NTCP estimation was developed in the application programming interface of the TPS, using a modular architecture to promote flexibility, scalability and ease of maintenance. Each component of the plugin was implemented as an independent module, allowing new functionality to be added, or existing elements to be modified, without affecting the core framework.

To facilitate model definition and maintenance by users without programming experience, a user-friendly library manager was created. Currently, the plugin supports the commonly used Lyman-Kutcher-Burman model and logistic regression models, which are saved as JSON files to ensure transparency, reproducibility and transportability between systems. Developers can expand the functionality of the plugin by adding new modules or modifying existing ones through clearly defined interfaces, ensuring that the plugin remains adaptable to future methodological or clinical developments.

3. Results

Upon startup, the plugin automatically scans a designated folder containing any predefined models. From the start screen, the user can access the model library manager or the NTCP estimation screen. In the latter, dose-volume parameters for the selected model are extracted from the current patient case in the TPS; other parameter values are entered manually.

In the NTCP visualization screen, users can select one or more models to display in a trend chart and generate a report summarizing key parameters, model expressions and user-defined descriptions.

In the model library manager, components are selected successively, with available options dynamically displayed based on previous selections, such as model link function, variable type, OIs and dose-volume histogram (DVH) parameters. Preprocessing functions like conversion to equivalent dose in 2-Gy fractions (EQD2) are available. Model expressions are entered as simple text strings, supporting combinations of OIs as well as non-linear dependencies. Plugin guidelines recommend restricted access to the model library manager.

Users are responsible for evaluating the validity of added models, and traceability is facilitated through a mandatory model description field. The plugin has not been released for clinical use.

4. Discussion and Conclusions

A wide range of prediction models can be applied in the radiotherapy treatment-planning process through the developed NTCP estimation plugin. It is currently applied in an in-silico NTCP-based dose escalation study in head and neck cancer.

Acknowledgements

This project was funded by Varian, a Siemens Healthineers company.

VIBRONAV: VIBROACOUSTIC SIGNAL ANALYSIS FOR AI-ASSISTED NAVIGATION IN MINIMALLY INVASIVE PROCEDURES

Jakub Gawron(2), Artur Kos(1b), Hamza Oran(2), Szymon Rybak(1a), Dominik Rzepka(2), Katharina Steeg(3), Michael Friebe(1a), Katarzyna Heryan(1a, 2)

1: {a: The Faculty of Computer Science; b: The Faculty of Computer Science, Electronics and Telecommunications} AGH University of Krakow, Poland;
2: MedSun Labs sp. z o. o., Warsaw, Poland;
3: Justus-Liebig-University Giessen, Germany

1. Introduction

Minimally invasive procedures (MIP) are increasingly adopted across many medical disciplines due to reduced patient trauma, shorter recovery times, and lower complication rates. Despite these advantages, operators often face reduced situational awareness compared with open surgery, particularly due to limited haptic feedback during tool–tissue interaction [1, 2]. Emerging sensing technologies combined with machine learning create opportunities to extract additional information directly from physical interactions between medical instruments and biological tissues [3]. This work presents the VIBRONAV concept, which utilizes vibroacoustic signals generated during needle–tissue interaction to provide real-time navigation cues for clinicians.

2. Materials and Methods

The system integrates a miniature vibroacoustic sensor mounted on standard interventional instruments via a clip-on connector. Vibrations generated during needle insertion propagate through the instrument shaft and are captured using MEMS microphones. The acquired signals are conditioned and processed through a dedicated pipeline consisting of spectral analysis, signal characterization, and machine learning-based feature extraction.

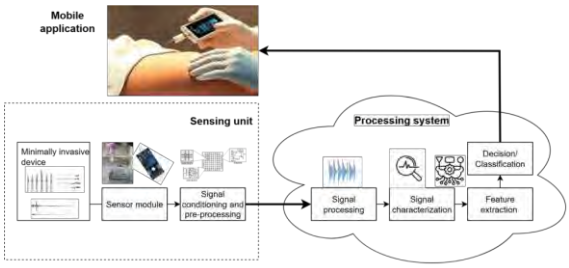


Figure 1: Conceptual architecture of the VIBRONAV system including sensing unit, signal processing pipeline, and mobile feedback interface.

3. Results

Preliminary experiments demonstrated the feasibility of detecting puncture events using ResNet-18 neural networks with an F1 score of 95.9% and tissue differentiation with approximately 80% accuracy in phantom models. The system supports multimodal acquisition (audio and synchronized video), reference data annotation, and scalable cloud-based processing for machine learning model training and inference. The compact device (<100 g) is designed to integrate seamlessly with existing surgical workflows. Experimental measurements on tissue-mimicking phantoms and biological materials demonstrate that vibroacoustic signals contain distinctive signatures associated with tissue properties and puncture events. These differences allow reliable classification of tissue interaction events and create a foundation for automated navigation feedback.

4. Discussion and Conclusions

The results demonstrate the feasibility of vibroacoustic sensing as a supplementary navigation modality in minimally invasive interventions. The combination of sensor technology, signal processing, and machine learning enables transformation of acoustic signals into clinically meaningful feedback.

5. References

[1] Illanes A. et al. Current Directions in Biomedical Engineering (2020).
[2] Sabieleish M., Heryan K. et al. Int J Comput Assist Radiol Surg (2021).
[3] Heryan K. et al. IEEE EMBS (2023).

Acknowledgements:
The research funded by the National Centre for Research and Development (NCBR) in Poland (INNOGLOBO/4/77/VIBRONAV/2024).
Research project supported/partly supported by program „Excellence initiative – research university" for the AGH University of Krakow.

DEEP MULTI-STATE MODELS FOR INDIVIDUALIZED PROGNOSIS IN MULTIPLE MYELOMA

Sebastian Schwick (1), Yasamin Salimi (1), Guillaume Azarias (3), Holger Fröhlich (1,2,4), on behalf of the CERTAINTY consortium

1. Department of Biomedical AI & Data Science, Fraunhofer Institute for Algorithms and Scientific Computing SCAI, Sankt-Augustin, Germany; 2. Bonn-Aachen International Center for Information Technology (b-IT), University of Bonn, Bonn, Germany; 3. TriNetX Oncology GmbH, Freiburg, Germany; 4. Institute for Digital Medicine, University Hospital Bonn, Bonn, Germany

1. Introduction

Multiple myeloma (MM) is a highly heterogeneous plasma cell malignancy characterized by clonal proliferation within the bone marrow. Despite advances in therapy, MM remains incurable, with patients experiencing multiple relapses across disease stages and exhibiting wide variability in overall survival. This heterogeneity necessitates personalized prognosis conditional on possible choices of therapy. However, current prediction approaches mainly focus on newly diagnosed patients and first-line therapy, leaving a significant gap in assessing risk for relapsed/refractory MM. This is particularly critical, as prior treatments substantially influence therapeutic outcomes [1].

2. Materials and Methods

CERTAINTY develops an AI-assisted digital twin to support therapeutic decisions. More specifically, we here focus on extensions of multi-state models, which allow us to predict disease progression over distinct clinical stages or lines of therapy (LoTs) [2]. They are thus particularly useful for prognosis in complex diseases such as MM [3]. We developed a novel discrete-time, multi-state deep learning framework, which allows us to appropriately represent time differences between states while encoding treatment history and other patient-specific information. Our proposed model is generative and allows to simulate possible disease outcomes for a given patient in any given state, also in a counterfactual manner. Our approach is thus compliant with the requirements of a digital twin.

3. Results

Utilizing large data of 7820 patients provided by TriNetX Oncology, we evaluated the models' prognostic performance by estimating survival within each LoT. Our model shows a favourable predictive performance compared to alternative modelling approaches as well as a good calibration. Furthermore, we extended recent XAI methods to our multi-state framework, hence providing a human-understandable interpretation of model predictions.

4. Discussion and Conclusions

CERTAINTY supports therapeutic decision-making in MM using an AI-assisted digital twin. For this purpose, our work proposes a novel method, which allows to simulate possible disease outcomes based on patient-specific data, including previous treatment history. Our approach can generally be adapted to other indication areas, where distinct diagnostic stages or LoT are of relevance.

5. References

1. Bhatt P, Kloock C, Comenzo R. Relapsed/refractory multiple myeloma: a review of available therapies and clinical scenarios encountered in myeloma relapse. Curr Oncol. 2023;30(2):2322-2347.
2. Hougaard P. Multi-state models: a review. Lifetime Data Anal. 1999;5:239-264.
3. Maura F, Rajanna AR, Zicchedu B, Poos AM, Derkach A, Maclachlan K, Durante M, Diamond B, Papadimitriou M, Davies F, et al. Genomic classification and individualized prognosis in multiple myeloma. J Clin Oncol. 2024;42(11):1229-1240.

Acknowledgements:

The CERTAINTY project is funded by the European Union (Grant Agreement 101136389). Views and opinions expressed are however those of the author(s) only and do not necessarily reflect those of the European Union or the Health and Digital Executive Agency. Neither the European Union nor the granting authority can be held responsible for them. The models were developed within the CERTAINTY project and evaluated using real-world data provided by TriNetX Oncology.

A REAL-TIME SIMULATION ENVIRONMENT FOR TAILORED BARIATRIC SURGERY

Ilaria Toniolo (1,2), Emanuele Luigi Carniel (1,2), Gianluca Mazzucco (2,3)

1. *Department of Industrial Engineering, University of Padova, Italy; 2. Centre for Mechanics of Biological Materials, University of Padova, Italy; 3. Department of Civil, Environmental and Architectural Engineering, University of Padova, Italy.*

1. Introduction

Obesity is a leading global health burden, and while bariatric surgery remains the most effective treatment, it lacks personalization [1]. While computer-assisted surgery has successfully integrated real-time digital tools in other medical fields, bariatric surgery still lacks fully integrated in silico platforms. This work presents the development of a real-time, patient-specific computational application for Endoscopic Sleeve Gastroplasty (ESG) planning and training, integrating soft-body mechanics and interactive simulation within a fully open-source workflow.

2. Materials and Methods

The workflow is based on patient-specific three-dimensional reconstructions of the stomach obtained from preoperative MRI data [2]. The geometries are imported into the Unity real-time development environment, where the simulation architecture is implemented. The model is rendered to allow visualization of both internal and external surface, reproducing the endoscopic perspective while maintaining spatial awareness. Mechanical behaviour is reproduced using a soft-body formulation based on triangular membrane elements. The internal loads of each element are derived from a hyperelastic Neo-Hookean constitutive law, enabling representation of large deformations. The governing equations are integrated dynamically through Unity's PhysX engine, which adopts a semi-implicit scheme suitable for real-time interaction. Suture placement is implemented through a raycasting-based selection of nodes on the triangulated surface mesh. Selected nodes are paired to generate stitch chains, and progressive tightening induces geometrical reconfiguration and stress redistribution within the gastric wall. Internal pressurization can be applied to simulate physiological loading conditions, allowing qualitative assessment of post-procedural mechanical functionality.

3. Results

The developed platform enables interactive, real-time manipulation of patient-specific gastric models, reproducing key procedural steps of ESG. The adopted numerical strategy achieves a balance between computational efficiency and mechanical plausibility, ensuring stable real-time performance while preserving geometrical coherence of large deformations.

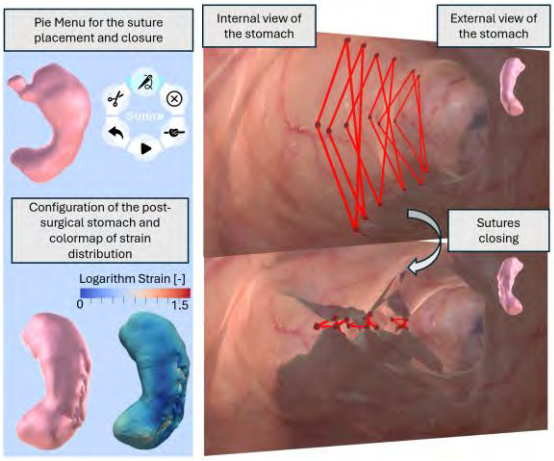


Figure 1: Overview of the real-time application.

4. Discussion and Conclusions

This study introduces a fully digital, patient-specific simulation framework for ESG planning and training. By integrating anatomical reconstruction, soft-body mechanics, and interactive visualization in a real-time environment, the platform represents a step toward computationally assisted bariatric surgery. The proposed methodology establishes a scalable foundation for future integration of validated biomechanical constitutive models and for extension to other bariatric procedures.

5. References

1. Brown WA et al., Obesity Surgery 34:1764-1777 (2024)
2. Toniolo I et al., Biocybernetics and Biomedical Engineering 46:9-18 (2026)

DATA-DRIVEN MODELLING OF EARLY KIDNEY GRAFT DYSFUNCTION CHALLENGES INJURY-CENTRIC PARADIGMS

Ana I. Morales (1,2), Marta Prieto (1,2), Alfredo G. Casanova (1,2), Óscar Pellicer (3), Javier Tascón (1,2), Annette Düwel (2), Guadalupe Tabernero (2), María A. Ramos (4), Carlos Gómez-Alamillo (4), Armando Coca (5), José D. Martín-Guerrero (3), Francisco J. López Hernández (1,2)

1. Universidad de Salamanca, Spain; 2. Instituto de Investigación Biomédica de Salamanca, Spain. 3. Universitat de Valencia, Spain; 4. Hospital de Valdecilla, Spain; 5. Hospital de Valladolid, Spain

1. Introduction

Kidney transplantation improves survival and quality of life in patients with end-stage renal disease (1). Delayed graft function (DGF) after kidney transplantation is widely attributed to acute tubular injury (ATI) due to ischemia–reperfusion (2,3), an assumption that has shaped biomarker research and early monitoring. Yet the relative contribution of structural tubular injury to early graft dysfunction has not been rigorously tested using data-driven computational models. To inform mechanistically credible *in silico* approaches, we developed a machine-learning framework integrating early clinical variables and injury biomarkers to predict DGF and short-term graft function, and to quantify the contribution of ATI markers within a multivariate setting.

2. Materials and Methods

We used clinical, procedural, and biochemical data were collected from 255 kidney transplant patients during the first days after transplantation, including serum and urinary creatinine, cold ischemia time, recipient characteristics, and urinary biomarkers associated with ATI. Supervised machine-learning models were trained to predict the occurrence of DGF and glomerular filtration rate (GFR) above or below 60 mL/min at 1 and 3 months. Model development followed a structured pipeline including feature selection and internal validation. Variable importance was quantified to assess the relative contribution of functional markers versus structural injury biomarkers. This approach enabled a direct comparison between knowledge-driven expectations (ATI as primary driver) and data-driven evidence emerging from multivariate modelling.

3. Results

A compact model primarily based on serum and urinary creatinine values at day 3, complemented by cold ischemia time and marginally by urinary N-acetyl-β-D-glucosaminidase, discriminated patients who developed DGF with high accuracy (AUC-ROC 0.895). In contrast, biomarkers reflecting tubular injury did not emerge as dominant contributors to predictive performance. Similarly, early serum creatinine combined with recipient age predicted 1- and 3-month GFR categories with AUC-ROC values of 0.810 and 0.814, respectively, again without a prominent role for tubular injury markers. These findings indicate that early graft dysfunction is better explained by functional dynamics captured by creatinine trajectories and perioperative determinants than by biochemical signatures of ATI.

4. Discussion and Conclusions

Our findings challenge an injury-centric interpretation of DGF and demonstrate how data-driven modelling can refine established mechanistic assumptions. Functional and hemodynamic variables, rather than tubular injury markers, dominated predictive performance. The resulting minimal-variable model provides a transparent framework for early risk stratification and represents a step toward credible digital twins of kidney graft function, supporting model-informed clinical decision-making and future integration of multi-scale biological determinants.

5. References

1. Wolfe RA et al. New England Journal of Medicine. 341: 1725–1730 (1999).
2. Bahl D et al. Current Opinion in Organ Transplantation. 24: 82–86 (2019).
3. Mannon RB. Nephron. 140: 94–98 (2018).

Acknowledgements:

The authors thank Instituto de Salud Carlos III (PI24/01058, PI24/01063, RD21/0005/0004, co-funded by the European Union); Fundación Senefro and Sociedad Española de Nefrología (Ayuda año 2018); and the Valencian Government (CIAICO/2024/111) for providing financial support to this project.

TOXIPRED: A WEB-BASED EXPLAINABLE AI PLATFORM FOR MULTI-ENDPOINT DERMATOXICITY PREDICTION

Marta Soltesova Prnova(1,2), Alec Rybar(2), Erik Rogansky(2), Samuel Racak(2), Anna Pylypenko(2), Dariia Sira(2), Marek Lepacek(1), Pavol Bodo(1), Lukas Soltes (2), Michal Ries (2).
1. Center of experimental medicine, Slovak Academy of Sciences, Bratislava, Slovakia 2. Faculty of Informatics and Information Technologies, Slovak University of Technology in Bratislava, Slovakia;

Corresponding author: marta.prnova@savba.sk

1. Introduction

Predictive in silico toxicology is essential for early-stage drug discovery, yet most available tools offer limited endpoint coverage, black-box predictions, and no integrated reporting.
Here we present ToxiPred (http://toxipred.fiit.stuba.sk), a freely accessible web platform developed at the Slovak University of Technology in Bratislava, covering three skin-toxicity endpoints (phototoxicity, corrosion, irritation) across eight assay-level models, with integrated SHAP and XSMILES explainability and one-click PDF reporting.

2. Materials and Methods

ToxiPred accepts SMILES, CAS numbers, trivial names, or drawn structures. Eight ML models cover three hazard categories: phototoxicity (in chemico, in vitro 3T3 NRU, in vitro 3D, in vivo), skin corrosion (in vitro 3D, in vivo), and skin irritation (in vitro 3D, in vivo rabbit), with datasets ranging from 35 to 857 compounds. Molecular descriptors and fingerprints (MACCS, Atom Pair, RDKit) were computed with RDKit; feature selection used Lasso, Boruta, RFE, or XGB Importance. Hyperparameters were tuned with Optuna or Randomized Search; class imbalance was handled by sample weighting.
Explainability operates at two levels: SHAP values attribute each prediction to individual descriptors or fingerprint bits, while XSMILES maps these contributions onto atoms of the input molecule as a colour-coded 2D depiction highlighting structural alerts. A structured PDF report — containing the structure, all predictions, SHAP charts, and XSMILES visualisation — can be exported for regulatory or publication use.

3. Results

ToxiPred delivers eight ML models across three OECD-relevant skin hazard categories. For phototoxicity, XGBoost achieved test AUROC of 0.87 (in chemico), 0.86 (in vitro 3T3 NRU), and 0.89 (in vitro 3D), while SVM reached 0.75 on the small in vivo dataset (n=35). For skin corrosion, AUROC reached 0.83 (in vitro 3D, XGBoost) and 0.80 (in vivo, GB). For skin irritation, GB achieved 0.81 (in vitro 3D) and a stacking ensemble reached 0.89–0.91 (in vivo rabbit, n=857). Test-set accuracy ranged from 0.79 to 0.86.

Model selection was endpoint-driven: XGBoost for in vitro/in chemico phototoxicity, SVM with HOMO/LUMO features for in vivo phototoxicity, Gradient Boosting for corrosion and in vitro irritation, and a stacking ensemble (XGBoost, RF, KNN, DT, SVM) for in vivo rabbit irritation.

4. Discussion and Conclusions

ToxiPred covers three skin-toxicity endpoints (phototoxicity, corrosion, irritation) across eight assay-level models, providing OECD-aligned multi-tier hazard profiling. SHAP values and XSMILES atom-level visualisation make predictions transparent, while one-click PDF export supports regulatory workflows.

Future work will extend coverage to additional dermatotoxicity endpoints (e.g. sensitisation). Platform: http://toxipred.fiit.stuba.sk

5. References

1. Halinkovič M et al., Toxicol In Vitro. 94:105701 (2024).

Acknowledgements: The authors acknowledge support from Slovak Recovery and Resilience Plan under contract no. 09I05-03-V02-00048 and VEGA 2/0137/26

COMPREHENSIVE HEMODYNAMIC PROFILING OF VAD: A MCL STUDY UNDER DYNAMIC HEART FAILURE CONDITIONS

Emanuele Vignali (1), Emanuele Gasparotti (1), Matthew Hirschhorn (2), Libera Fresiello (3), Simona Celi (1)

1. BioCardioLab, Bioengineering Unit, Fondazione Monasterio, Italy; 2. U.S. Food & Drug Administration, USA; 3. Dep. Cardiovascular and Respiratory Physiology, University of Twente, The Netherlands

1. Introduction

Ventricular assist devices (VADs) are a crucial treatment for severe heart failure. While evaluating VAD safety and performance relies on international standards [1], predicting the complex in vivo hemodynamic device-patient interactions remains challenging.

This study aims to develop a mock circulatory loop (MCL) able of subjecting a VAD to a comprehensive and wide range of physiological-pathophysiological conditions necessary to thoroughly test its functioning and cardiovascular interactions.

2. Materials and Methods

The MCL (Fig. 1a) comprises two pneumatic chambers, simulating left ventricular (LV) pressure (tunable rectangular wave) and systemic load (hardware-in-the-loop three-element Windkessel) [2], connected via an aortic branch with a mechanical aortic valve prosthesis and a VAD outflow conduit, with inflow at the LV. Thirteen tests were conducted on HeartMate 3 device to assess: the intrinsic pump hydrodynamics (IPH); the clinical support strategies (CSS), the ventricular suction (VS) phenomena and the pulse pressure (PP) function. For IPH both steady and dynamic flow tests were performed by progressively increasing the system afterload up to reverse VAD flow was reached. For the steady tests, static differential pressure steps were imposed; while for dynamic test, the distal systemic resistance was increased from a baseline heart failure (HF) condition. The baseline HF was characterised by a cardiac output (CO) of 3.8 l/min and aortic pressure 60-98 mmHg. All the IPH tests were performed at three different VAD speeds (4400, 5400 and 6400 rpm). For the CSS, the HF baseline was restored to a target healthy CO (5 l/min) by VAD activation via full (CO exclusively provided by VAD) and partial VAD support (where a shared workload was present with CO split between VAD and aortic valve). The tests for the VS caused by the LV collapse were conducted with the hardware-in-the-loop function using a virtual resistance. Finally, the PP tests evaluated the VAD's intrinsic pulsatility mode both with and without LV contractility.

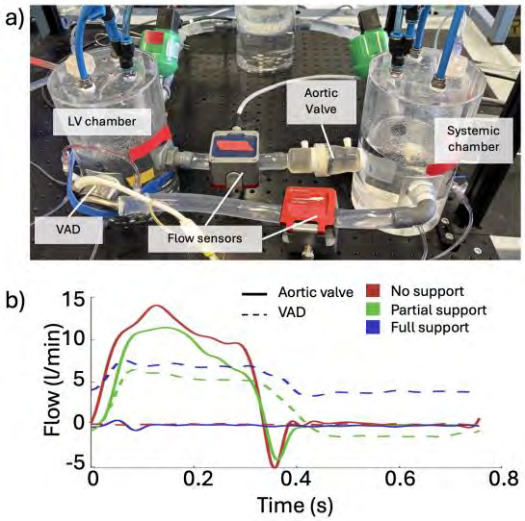


Figure 1: a) MCL setup; b) Flow results for CSS.

3. Results

Figure 1b reports the hemodynamic results in terms of VAD and aortic flow waveforms during the full and partial support tests.

4. Discussion and Conclusions

The dedicated MCL was designed to execute the diverse protocols by combining responsive hardware-in-the-loop control with a physical loop design. The proposed MCL successfully evaluated the VAD across complex physiological and pathophysiological scenarios. This provides a reliable, repeatable pre-clinical tool to assess VAD-patient interactions, supporting future regulatory advancements.

5. References

1. ISO 14708-5 - Active implantable medical devices - Part 5: Circulatory support devices.
2. Bardi F, et al, IEEE Trans Biomed Eng.;70(5):1651-1661 (2023).

From Homeostasis to Synovitis: A Regulatory Network Model of Macrophage Polarization in Knee Osteoarthritis

Yalemzerf M. Alemu (1), Zerihun Workineh (1), Laura Tio (2), Jordi Monfort (2), Jerome Noailly (1)

1. Barcelona Centre for New Medical Technologies (BCN MedTech), Department of Engineering, Pompeu Fabra University (UPF), Barcelona, Spain; 2. Cell Research on Inflammation and Cartilage, Hospital del Mar Research Institute, Barcelona, Spain

1. Introduction

Synovial macrophages (MC) regulate knee-joint homeostasis but can become dominant drivers of synovitis and tissue degeneration in osteoarthritis (OA). Their behaviour is dynamic and multistable, shifting between inflammatory (M1-like) and resolving (M2-like) states in response to local cues. Despite expanding knowledge in synovitis and OA, linking regulatory complexity to MC state transitions and measurable biomarkers remains challenging. Here, we develop a companion diagnostic (CDx) tool based on a regulatory network model (RNM) to predict MC polarization dynamics and stratify synovitis-driven OA.

2. Materials and Methods

An RNM was assembled from >100 studies to capture key signaling pathways driving MC polarization in OA synovium. It comprised >100 nodes and >300 activating/inhibitory edges across inflammatory and metabolic layers (Fig. 1). Dynamics were simulated using the Standardized Qualitative Dynamical Systems approach [2]. RNM autoregulation was evaluated through 10^4 simulations. In each simulation, node activations were randomly initialized between 0 and 1, and the system was iterated until steady-state convergence. Resulting baseline states represented the RNM attractors, further used to investigate pro-inflammatory and pro-resolving mechanisms, through node suppression (activation = 0) or persistent stimulation (activation =1) scenarios. Predictions were contrasted against synovial fluid proteomics profiles from female patients with primary knee OA (KL 2-3, n= 36).



Fig. 1: Multi-layered regulatory network topology.

3. Results

Basal dynamic simulations revealed three attractors: a dominant M2 (~71%), an M1 (~27%), and minority unsettled M1 (~2%) (Fig. 2A). Node time trajectories confirmed phenotype-specific convergence: M2 attractor was characterized by high M2 and low M1 stable markers; M1 attractor showed reciprocal pattern; unsettled state displayed intermediate oscillatory M1 with low M2 markers (Fig. 2B). Following node activation and suppression, the mixed basal state was broadly responsive. TNF-α activation or IL-10 suppression were strong drivers of M1 whereas IL-1β, INFγ, ROS or NF-kB activations shifted to unsettled (Fig. 2C). Model predictions were validated against patient-derived mean normalized synovial fluid data, showing strong cytokine concordance under the TNF-α -induced inflammatory state (Fig. 2D).

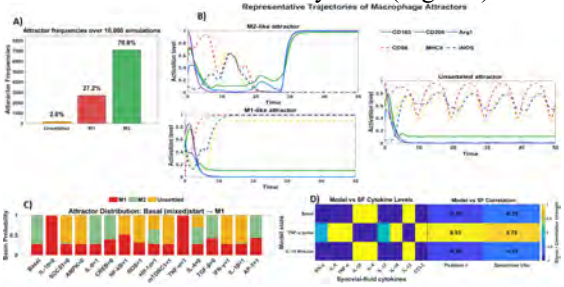


Fig. 2: MC dynamics showing attractor frequencies (A), representative trajectories (B), attractor redistribution under basal perturbations (C), and model–synovial fluid cytokine concordance (D).

4. Discussion and Conclusions

Basal simulations aligned with MC biology, revealing a homeostasis-preserving M2-dominant attractor landscape with accessible M1 state. Unsettled states supported MC polarization as a dynamic continuum [3]. Perturbation responses reflected cytokine topology: TNF-α's unconstrained access to NF-κB/AP-1 enabled M1 switching; IL-1β was tightly gated and partially redirected via CREB; IFN-γ self-limited by SOCS1; IL-10 promoted M2 repressing inflammatory hubs; IL-4 acted through STAT6 without direct repression; and TGF-β acted context-dependently via SMAD2/3 and TAK1. Overall, TNF-α and IL-10 emerged as key switch regulators of inflammatory state transitions, possibly standing for key regulators in primary knee OA.

5. References

[1] Knab K. *Front Med (Lausanne).* 2022; 9:862161
[2] Mendoza & Xenarios, Theor Biol Med Model, 3, 2006
[3] Crisóstomo et al., Results Probl Cell Differ., 2024.

Acknowledgements

European Union (ERC-2021-CoG-O-Health-101044828), Spanish Research Agency (STRATO PID2021-126469OB-C21), Catalan Agency for Business Competitiveness (PREDISARC-ACE088/23/000039).

DESIGN OF A FAST METAMODEL FOR THE GENERATION OF HD-SEMG AMPLITUDE HEATMAPS

Maroua Boubred (1), Jérémy Laforêt (1) *, Sofiane Boudaoud (1)

1. *Université de Technologie de Compiègne, CNRS, BMBI, Compiègne, France.*

Corresponding author: * Jeremy.laforet@utc.fr

1. Introduction

Electrophysiological models need to be fast and accurate for medical applications. Although analytical models accurately simulate HD-sEMG Root Mean Square Amplitude (RMSA) maps, they are computationally expensive. In this study, a deconvolutional neural network (DCNN) is proposed as a metamodel of the analytical model. The model, fed by a specific parameter configuration, reproduces spatial amplitude distributions with good accuracy and substantially lower computational cost.

2. Materials and Methods

Dataset. The training and test database includes 3,385 simulations generated with the analytical model in [1], each defined by anatomical and electrophysiological inputs and a simulated RMSA heatmap output.

Model architecture. A multilayer Transformer encoder embeds anatomical parameters, which are fused with electrophysiological features into a joint latent representation. A stack of transposed convolutional layers reconstructs the 8 × 8 RMSA heatmap.

Loss function. Mean Squared Error (MSE) combined with Maximum Mean Discrepancy (MMD) [2] ensures pixel-wise alignment and reconstruction quality.

Rejection mechanism. Out-of-distribution detection uses the Mahalanobis distance [3] in latent space, with a 95th-percentile threshold ; samples above it are labeled OOD.

3. Results

The metamodel achieved strong spatial reconstruction on unseen data (Pearson Correlation Coefficient, PCC: 82% ≥ 0.8; 48% ≥ 0.9) with low Mean Absolute Error (MAE). Computation time was reduced from 13 minutes to 29 ms per prediction. Detailed performance metrics are reported in Table 1. Representative examples of predicted and simulated RMSA maps are shown in Figure1.

Metric	Value (mean ± std)
PCC	0.862 ± 0.115
MAE	0.161 ± 0.086
Inference time	0.029 s

Table1: Model evaluation metrics.

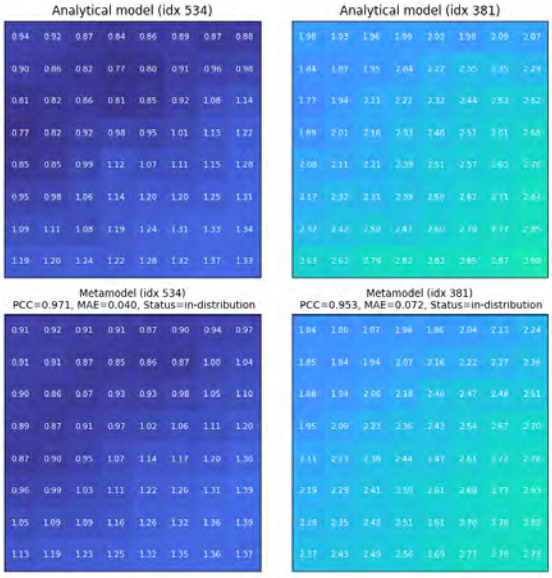


Figure1: Qualitative comparison of simulated and predicted RMSA maps.

4. Discussion and Conclusions

The proposed model preserves spatial heatmap reconstruction fidelity while markedly reducing computational cost compared to the analytical model. This metamodel enables efficient large-scale simulations and supports future medical real-time applications.

5. References

1. Carriou V, et al., *Comput. Biol. Med.*, pp. 54–68, (2016).
2. Gretton A et al., Journal of Machine Learning Research, pp. 723–773, (2012).
3. Mahalanobis P. C., Proceedings of the National Institute of Sciences of India, pp. 49–55, (1936).

Acknowledgements: The authors would like to thank the Chaire safeAI from UTC and HdF region through CNRS for providing financial support to this project.

INVESTIGATING THE DETECTION LIMITS FOR EMG-BASED CLASSIFICATION OF SPONTANEOUS MUSCLE ACTIVITY

Paul Brandenburg (1), Justus Marquetand (2), Oliver Röhrle (1), Burak Senay (2), Thomas Klotz (1)

1. University of Stuttgart, Germany; 2. University of Tübingen, Germany

1. Introduction

Pathological spontaneous muscle activity (PSA), refers to abnormal electrical activity of muscle fibres in the absence of voluntary activation. PSA can be detected using invasive needle electromyography (EMG) and its classification (e.g. fibrillations or myotonic discharges) is a key indicator for many neuromuscular disorders [1]. Currently, no validated method exists for non-invasive surface EMG-based PSA detection. Recent advances in EMG technology (i.e., high-density surface and invasive arrays), combined with computational data analysis pipelines, including in silico models linking muscle fibre activity to measured signals, provide new opportunities for surface EMG-based clinical decision making. Here, we use computer simulations to systematically study the feasibility of non-invasive PSA detection.

2. Materials and Methods

We implement a volume conductor model of skeletal muscle [2]. In short, this model links micro-scale transmembrane current sources to measurable extracellular potentials through a generalised Poisson equation. The transmembrane current is, thereby, proportional to the second spatial derivative of the transmembrane potential. Here, we use an analytical description of a single muscle fibre action potential [2, 3]. The resulting model is solved numerically using the Finite Element Method (FEM). The simulated signals allow to systematically study parameters (e.g., tissue properties) influencing non-invasive detection of PSA. The detected signal has been evaluated against a white Gaussian noise model scaled towards target amplitude (STD: 5 uV). A signal is deemed detectable, if its amplitude exceeds the standard deviation of the noise by at least a factor of three.

3. Results

Preliminary results indicate a rapid decline in signal amplitude as the fibre-to-electrode distance increases. At a given detection threshold, the signal would only be detectable within 1-2mm of the muscle fibre.

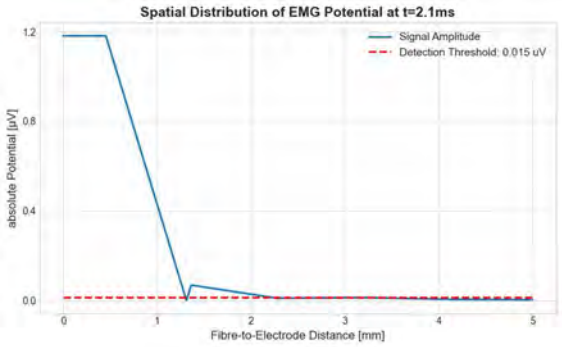


Figure 1: Simulated signal amplitude distribution, queried halfway between the neuromuscular junction and the tendon sampled at 2.1ms

4. Discussion and Conclusions

Our results provide unique insights on detectability of PSA at the skin-surface that would not be easily feasible by means of experiments. Future work will extend the model to realistic muscle architectures and enhance the biophysical realism of the bioelectrical sources. Additionally, we will use modelling to investigate alternative biomarkers for disease monitoring that ultimately can guide clinical decision making through non-invasive EMG measurements.

5. References

1. Rubin DI. Normal and abnormal spontaneous activity. Handb Clin Neurol. 2019;160:257–79.
2. Lowery MM. EMG Modeling and Simulation. 1st ed. Wiley; 2016 p. 210–46.
3. Rosenfalck P. Intra- and extracellular potential fields of active nerve and muscle fibres. A physico-mathematical analysis of different models. Acta Physiol Scand Suppl. 1969;321:1–168

Acknowledgements:

This research was funded by the German Research Foundation (Deutsche Forschungs Gemeinschaft, DFG): 548605919

AN IN-SILICO FRAMEWORK TO SIMULATE TRAINING-DRIVEN MULTISCALE SKELETAL MUSCLE ADAPTATION

Emanuele Feola (1), Nico Verdonschot (1), Massimo Sartori (1)

1. NeuBotics Lab, Chair of Neuromuscular Robotics, Department of Biomechanical Engineering, University of Twente, Enschede, Netherlands

1. Introduction

Current rehabilitation therapies following neuromuscular injuries span multiple weeks, yet scientific literature lacks a clear understanding of how skeletal muscles adapt their properties over that period. This gap in understanding how electromechanical stimuli drive chronic skeletal muscle adaptation is limiting robotic-aided rehabilitation to work on short time scales. We propose an in-silico framework of skeletal muscle adaptation able predict muscle response to training, moving toward personalized rehabilitation therapies that support recovery of impaired skeletal muscle over long time scales. As opposed to existing literature [1], our model does not rely on computationally expensive models and is able to predict multiple training regimes.

2. Materials and Methods

A Multi-Input Single-Output (MISO) Hill-type muscle model discretized in different motor units is coupled with phenomenological adaptation laws [2] defined by a system of ODE driven by training parameters (muscle length l_m, velocity $\dot{l_m}$, activation a), as represented in Fig. 1. The ODE system estimates the evolution of the model state $X(t)$ in response to training, where $X = \{l_m^{\text{opt}}, f_m^{max}, \alpha^{\text{opt}}, l_t^s, v_{max}, t_c, A_p\}$, representing muscle architectural and contractile properties.

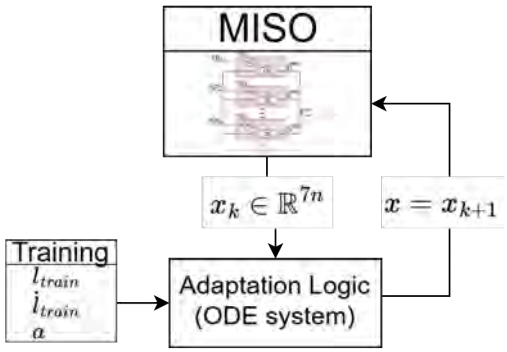


Figure 1: Discretized Hill-type muscle model coupled with phenomenological adaptation logic driven by training parameters, i.e., muscle kinematics and activation.

3. Results

Preliminary results show the framework's ability to reproduce the qualitative trends reported in the literature in response to longitudinal training regimes (Fig. 2).

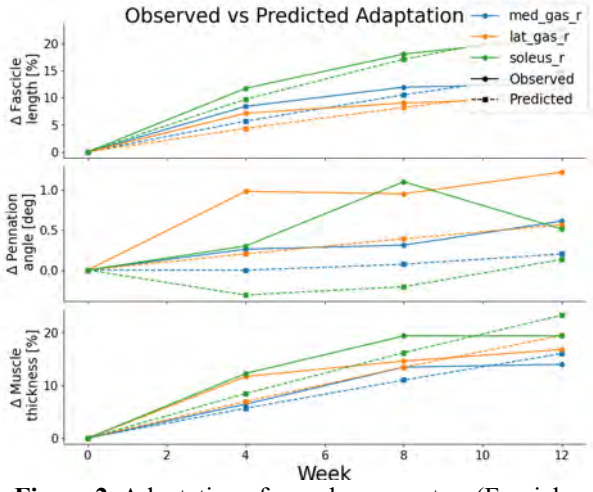


Figure 2: Adaptation of muscle parameters (Fascicle Length, Pennation Angle, Muscle Thickness) in response to 12-week eccentric training. An adaptation ODE driven by training parameters is fitted to literature data.

4. Discussion and Conclusions

We propose an in-silico framework to model skeletal muscle chronic adaptation in response to training composed of a phenomenological logic of multiscale skeletal muscle adaptation driven by training parameters. This model is coherent with literature trends of longitudinal human studies and provides a potential framework for subject-specific rehabilitation.

5. References

1. A. M. Zöllner et al., "On high heels and short muscles: A multiscale model for sarcomere loss in the gastrocnemius muscle," 2015
2. K. M. Wisdom et al., "Use it or lose it: multiscale skeletal muscle adaptation to mechanical stimuli," 2015

Acknowledgements:

This work was supported by the European Research Council with CoG grant ROBOREACTOR (no.101123866).

TOWARD DIGITAL TWINS OF OSTEOARTHRITIS: INTEGRATING GENETIC VARIANTS AND MECHANICAL SIGNALS

Anagha Gaikwad[#], Justyna Igras[#], Janine N Post

Quantitative Biology Lab, Department of BioEngineering Technologies, University of Twente, Enschede, The Netherlands. [#]Equal contribution

1. Introduction

Osteoarthritis (OA) is a heterogeneous disease in which genetic predisposition, inflammatory signalling and mechanical loading jointly determine whether cartilage is maintained or progressively degraded. However, predicting how these factors interact within individual patients remains difficult. Virtual patient approaches based on mechanistic digital twins offer a promising strategy to integrate biological knowledge and simulate disease-relevant cellular behaviour. Here we present a proof-of-principle framework toward a digital twin of cartilage signalling that can represent patient-specific regulatory states and links genetic variation, intracellular signalling and biomechanical loading across biological scales

2. Materials and Methods

Our approach builds on previously developed executable models of intracellular signalling in articular chondrocytes [1,2]. These prior-knowledge-based models capture key pathways controlling cartilage homeostasis and allow dynamic simulation of signalling activity using our ANIMO modelling tool [3]. To extend this toward virtual patient models, two complementary paths are currently being implemented. First, osteoarthritis-associated genetic variants are incorporated by mapping SNP effects onto regulatory nodes in the signalling network, allowing simulation of how patient-specific genetic backgrounds alter signalling dynamics and cartilage homeostasis. Second, mechanosensitive pathways, including YAP/TAZ signalling and mechanosensitive ion channels such as TRPV4 and PIEZO1/2, are integrated to represent cellular responses to different mechanical loading conditions. A third step focuses on clinical translation within the LoaD project, where model predictions are discussed with clinicians to guide personalised guidance on physical loading.

3. Results

The extended modelling framework enables exploration of how combinations of genetic predisposition and biomechanical stimuli influence intracellular communication in chondrocytes. Model outputs represent shifts between anabolic and catabolic cellular states, reflected by predicted production of cartilage matrix components, such as collagen type II and proteoglycans or matrix-degrading enzymes including MMPs and ADAMTS [1,2]. Ongoing work uses systematic in silico perturbation analyses to identify regulatory nodes controlling load-dependent cartilage responses and generate testable predictions on how genetic variants and mechanical loading jointly determine anabolic or catabolic chondrocyte states.

4. Discussion and Conclusions

This work represents a first step toward mechanistic virtual patients of osteoarthritis based on executable signalling networks. By integrating genetic variants and biomechanical inputs, such digital twins could support patient stratification and hypothesis generation on which loading regimes or molecular interventions are most likely to preserve cartilage homeostasis or prevent disease progression.

5. References

1. Schivo S et al. Cell Signal 2020 doi: 10.1016/j.cellsig.2019.109471
2. Khurana S et al. Front Bioeng Biotechnol 2021 doi: 10.3389/fbioe.2021.732917
3. Schivo S et al. BMC Syst Biol 2016 doi: 10.1186/s12918-016-0286-z

Acknowledgements:

The authors acknowledge financial support from the Dutch Research Council (NWO) through the NWA project 'The LoaD Project' (Grant No. NWA.1389.20.009), supporting JI, and from ZonMw for our project ROADMAPS (Project No. 09120232310042), supporting AG.

ESTIMATING EYE-HEAD-NECK MUSCLE ACTIVATIONS FOR TARGET SKULL POSITIONING

Thomas Saigre (1), Even Harsigny (1), Pablo Alvarez (1), Michel Duprez (1), Stéphane Cotin (1)

1. Université de Strasbourg, CNRS, Inria, ICube, F-67000 Strasbourg, France

1. Introduction

Muscle activation patterns during head movements are critical for understanding biomechanical function and fatigue in musculoskeletal (MSK) systems. By solving an inverse problem using a multi-scale MSK model of the eye, head, and neck, we estimate the muscle activations required to position the head at a target location. This approach integrates biomechanical principles with computational optimization, providing insights into muscle coordination and potential applications in systems biology. Furthermore, we plan to implement model order reduction by studying correlation between muscles to reduce the exploration space, thereby improving the overall process.

2. Materials and Methods

We model muscles using a Hill-type formulation[1], which decomposes each muscle into three elements: *(i)* a *contractile* element, *(ii)* a *passive element*, and *(iii)* an *elastic tendon*. The force of each muscle is computed by:

$$f = f_{\max} \times \big(\underbrace{a f_{\mathrm{a}}(\ell) f_{\mathrm{v}}(\ell)}_{(i)} + \underbrace{f_{\mathrm{p}}(\ell)}_{(ii)} + \underbrace{\beta v}_{(iii)} \big), \quad (1)$$

where the parameters $f_{\max}$, f_{a}, f_{v}, f_{p} and β are properties inherent to the muscle, ℓ its length, and v its velocity. The parameter of interest for this study is the *neuronal activation* of the muscle $a \in [0,1]$, representing how much the muscle is activated. The MSK model [2], contains 72 muscles responsible for head movement, while the eye movement [3] is modelled with the 6 extraocular muscles.

Given a target position obtained through motion capture and eye tracking, we aim at finding the activation $\boldsymbol{a}$ of all muscles to put the head and the eye in this position:

$$\min_{\mathbf{a}} \frac{1}{N} \sum_{j} \| P_j(\mathbf{a}) - T_j \|_2, \quad (2)$$

such that $0 \leqslant a_i \leqslant 1$, where T_j are target points and P_j are control points fixed to the model.

3. Results

We perform the optimization process using a gradient descent approach, aiming at minimizing the loss in Eq. 2, using the open-source software Sofa (sofa-framework.org) in which we implemented a gradient descent approach. Here, we manually generate target position by activating two specific muscles. Fig. 1 displays the evolution of the loss during the optimization process, as well as the distance between each point and its corresponding target.

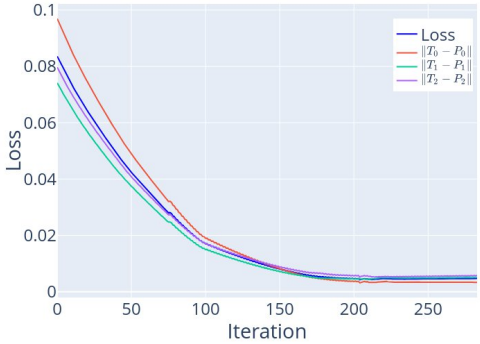


Figure 1: Evolution of the loss during optimisation process. Distance are in [m].

4. Discussion and Conclusions

The optimization process successfully positioned the head within 1 mm of the target position. While the exact muscle activation values for target generation were not retrieved, our qualitative results align well with expectations. However, the inverse problem is ill-posed yielding multiple possible muscle activation patterns. Future work will incorporate biomechanically plausible regularization, such as fatigue constraints to refine solutions. This approach has potential applications in myopia research, where altered muscle coordination may influence ocular biomechanics

5. References

1. Millard et al., Journal of Biomechanical Engineering 135.2, p021005 (2013).
2. Mortensen et al., PLoS One ; 13(6):e0199912 (2018).
3. Iskander et al., Journal of Biomechanics ; 71(4), pp. 204 - 208 (2018).

Acknowledgements:

This project was funded by the French government as part of France 2030 under the Premyom project.

KNEE JOINT VIRTUAL TWIN TO ESTIMATE MECHANO-INFLAMMATORY RESPONSES OF CARTILAGE

Anni Salo (1), Joonas Kosonen (1), Joose Peitola (1), Amir Esrafilian (1), Petri Tanska (1,2), Rami Korhonen (1), Atte Eskelinen (1,2)

1. University of Eastern Finland, Kuopio, Finland; 2. Kuopio University Hospital, Wellbeing Services County of North Savo, Kuopio, Finland

1. Introduction

Osteoarthritis is a complex, multiscale disease, which is influenced by abnormal biomechanics and joint inflammation. Previous computational models typically considered cartilage stresses and strains and inflammation as separate mechanisms for disease progression [1]. The objective of this study was to establish a knee joint virtual twin that integrates joint level computational analysis of tissue mechanical responses with exogenous pro-inflammatory cytokine diffusion, cellular responses to mechano–inflammatory stimuli, and subsequent alterations in cartilage composition.

2. Materials and Methods

Knee MRIs, motion capture, and ground reaction forces were used to generate personalized musculoskeletal (MS) and finite element (FE) models of a healthy subject using an earlier framework [2] (Fig. 1A).

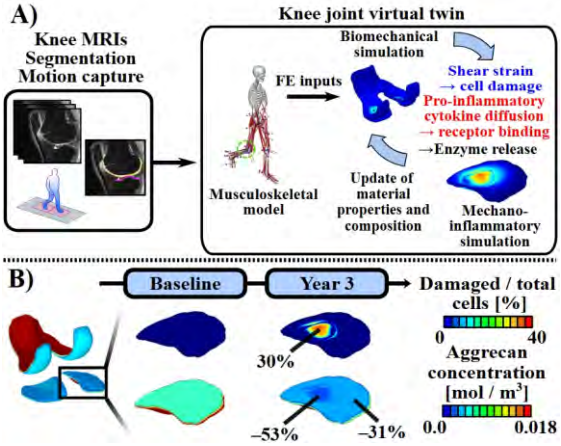


Figure 1: **(A)** The workflow of the study. **(B)** The local cell damage increased in highly sheared regions.

MS analysis outputs (knee flexion angle, joint contact forces and moments) were used as loading and boundary conditions for the FE model. Cartilage was modelled as fibril-reinforced poroviscoelastic and maximum shear strain in cartilage during stance phase of gait was simulated. Strains >15% triggered cell transition from "healthy" to "damaged". Damaged cells and cells interacting with inflammatory cytokines diffusing from synovial fluid released proteolytic enzymes causing proteoglycan loss and subsequent increase in permeability and impairment of mechanical properties. Cartilage response to 3-year mechano–inflammatory stimulus was then simulated.

3. Results

During the 3-year simulation, 30% of cells transitioned to "damaged" state. This caused a 53% reduction in localized aggrecan content (Fig. 1B). Inflammation accounted for 31% of the localized aggrecan loss.

4. Discussion and Conclusions

Cell damage distribution and aggrecan loss were consistent with experimental *ex vivo* estimates although further calibration against *in vivo* and additional *ex vivo* data is required [3]. Digital twin of mechano–inflammation provides a promising tool for designing osteoarthritis interventions such as gait retraining and anti-inflammatory drugs.

5. References

1. Orozco GA et al., J Orthop Res; 40(7):1505–1522 (2021).
2. Esrafilian A et al., IEEE Trans Biomed Eng; 72(1):56–69 (2025).
3. Amano K et al., Am J Sports Med; 46(4):890–899 (2018).

Acknowledgements:
Strategic funding of UEF, Finnish Ministry of Education and Culture (Pilot project Mathematics of Sensing, Imaging and Modelling), Novo Nordisk Foundation (NNF21OC0065373), Research Council of Finland (354916, 363459), Finnish Cultural Foundation (00230091, 00260288), European Union Horizon 2020 (Marie Skłodowska-Curie grant No. 101108335).

IMPACT OF ANISOTROPIC MUSCLE CONDUCTIVITY ON PHRENIC NERVE ACTIVATION THRESHOLDS

Laureen Wegert (1), Marek Ziolkowski (1), Alexander Hunold (1,2), Tim Kalla (1), Irene Lange (1), Jens Haueisen (1)

1. Institute of Biomedical Engineering and Informatics, TU Ilmenau, Ilmenau, Germany;
2. neuroConn GmbH, Ilmenau, Germany

1. Introduction

Prolonged mechanical ventilation can cause diaphragm atrophy due to muscle inactivity. Phrenic nerve stimulation shows potential to preserve diaphragm function [1, 2]. Computational models and digital twins support the optimization of stimulation protocols. However, most muscle models assume isotropic electrical conductivity, although muscle exhibits anisotropic conductivity depending on fiber directions. This study quantifies the impact of anisotropic muscle conductivity on phrenic nerve activation thresholds.

2. Materials and Methods

A finite element model of the neck is built with a high level of anatomical detail comprising 13 tissue types [3]. Two 1 cm by 1 cm surface electrodes are placed at the posterior border of the sternocleidomastoid muscle. Muscle fiber orientations are estimated to define local conductivity, using a flow-based approach. The anisotropy ratio, defined as the ratio of transverse to longitudinal electrical conductivity ($\sigma_t : \sigma_l$) is varied from 1:1 (isotropic) to 1:15. To isolate directional effects, the geometric mean conductivity is kept constant for all ratios [4].

The electric potential distribution is computed using a stationary solver in COMSOL Multiphysics. The scalar electric potential along the midline of the phrenic nerve is coupled to the McIntyre-Richardson-Grill axon model (10 µm fiber diameter) as extracellular potential. Nerve activation thresholds are determined for a current-controlled, cathodic monophasic pulse (150 µs).

3. Results

The nerve activation threshold for isotropic muscle conductivity is 37 mA. Increasing anisotropy leads to higher thresholds, reaching values up to 82% higher at an anisotropy ratio of 1:15, as shown in Fig. 1. A commonly assumed ratio of 1:3 results in an 18% underestimation compared to the isotropic case.

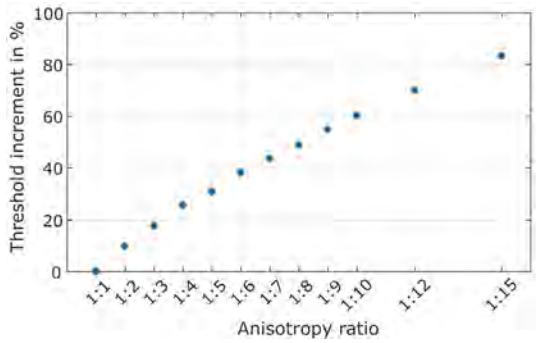


Figure 1: Relative increment of nerve activation threshold with increasing anisotropy ratio.

4. Discussion and Conclusions

Muscle anisotropy alters current pathways, directing current preferentially along muscle fibers and reducing the effective field components at the phrenic nerve.

Neglecting anisotropy leads to a systematic underestimation of activation thresholds. These findings highlight the importance of incorporating anisotropic conductivity in digital twin approaches.

5. References

[1] Geddes LA, "Electroventilation - a missed opportunity?," BI&T 32(4): 401-414, 1998.

[2] Kalla T et al., "Multimodal Measurement and Stimulation System to Investigate the Effects of Noninvasive Electrical Stimulation of the Phrenic Nerve," CDBME 11(1): 453-456, 2025.

[3] Wegert L et al., "Activation thresholds for electrical phrenic nerve stimulation at the neck: evaluation of stimulation pulse parameters in a simulation study," J. Neural Eng. 21(6), 2024.

[4] Güllmar D et al., "Influence of anisotropic electrical conductivity in white matter tissue on the EEG/MEG forward and inverse solution. A high-resolution whole head simulation study," NeuroImage 51(1): 145-163, 2010.

Acknowledgements:

This work was supported by the Federal Ministry of Research, Technology and Space (BMFTR) grant eVent (13GW0591B).

CHARACTERIZATION OF PCL SCAFFOLD MECHANICS AND THEIR SUITABILITY FOR TENDON CELL CULTURES

Ana Pérez-Ruiz (1), Miriam Corral-Barricarte (2), Elena Ruiz Robles (1), Jorge Grasa (2,3), Sabina Sanegre (1), Jirawat Iamsamang (4), Miguel Dias Castilho (4), Begoña Calvo (2,3)

1. Department of Biomedical Sciences, School of Health Sciences, Universidad CEU Cardenal Herrera, Valencia, Spain; 2 Aragón Institute of Engineering Research (I3A), Universidad de Zaragoza, Spain; 3. Centro de Investigación Biomédica en Red en Bioingeniería, Biomateriales y Nanomedicina (CIBER-BBN), Spain; 4. Biomaterial Engineering & Biofabrication, Departament of Biomedical Engineering, Eindhoven University of Technology, Eindhoven, The Netherlands

1. Introduction

Polycaprolactone (PCL) scaffolds are widely used in tendon tissue engineering due to their tunable microarchitecture and mechanical performance [1]. Here, we characterize their mechanical behaviour and evaluate tenocyte adhesion, viability, and organization to relate scaffold mechanics to tendon cell response.

2. Materials and Methods

A series of PCL scaffolds were fabricated using MEW for mechanical testing and tenocyte culture. Figure 1 shows one example with a longitudinal microfibre pattern formed by repeating wavy filaments and regular spacing.

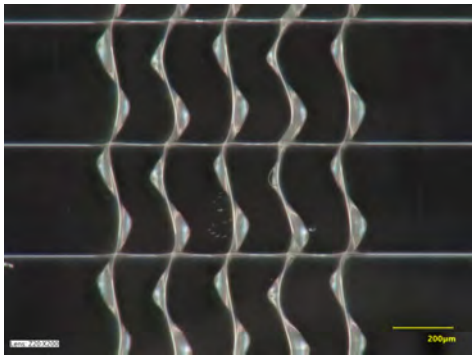


Figure 1: MEW printed PCL scaffold.

These scaffolds are used in experimental assays to characterize their elastic and viscoelastic mechanical response, while parallel tenocyte cultures allow the evaluation of cell adhesion, proliferation, and early tissue organization.

3. Results

Figure 2 shows the normalized force relaxation curves of the MEW printed PCL scaffolds, all exhibiting the expected viscoelastic decay over time. The fluorescence image of tenocytes after few weeks of culture reveals cell expansion and alignment following the scaffold architecture, indicating sustained attachment and organized growth.

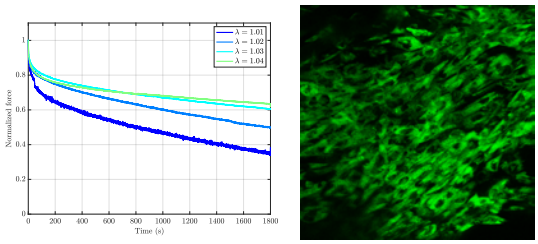


Figure 2: Relaxation tests and cell colonization.

4. Discussion and Conclusions

The stress relaxation tests show a clear viscoelastic response in the MEW printed PCL scaffolds, with an initial peak stress followed by time-dependent decay. This behaviour reflects the scaffold's anisotropic architecture and its ability to mimic tendon-like load dissipation. These results support the relevance of this design for delivering meaningful mechanical cues and motivate future work combining long-term cell culture with computational simulations [2] to further interpret and predict scaffold-cell interactions.

5. References

1. No YJ et al., Adv. Mater.; 32(18):1904511 (2020).
2. Grasa J et al., Acta Biomater.; 197:226–239 (2025).

Acknowledgements:

The authors would like to thank the support of the Spanish Ministerio de Ciencia, Innovación y Universidades.
MICIU/AEI/10.13039/501100011033 (Grants PID2023-147987OB-C31, and PID2023-147987OB-C33).

PRECLINICAL TOOL TO ESTIMATE OSTEOPOROTIC WOVEN BONE MECHANICS BASED ON EXPERIMENTAL DATA

Juan José Toscano-Angulo (1), Juan Mora-Macías (2), Pablo Blázquez-Carmona (3), Esther Reina-Romo (1)

1. University of Seville, Spain; 2. University of Huelva, Spain; 3. University of Cadiz, Spain

1. Introduction

Callus stiffness evolves over time with woven bone mineral density (BMD) and clinically determines when the fixator can be safely removed. However, callus mechanics is traditionally assessed manually or using x-ray follow-up, providing inaccurate information [1]. An accurate estimate of callus stiffness would prevent possible bone refractures and morbidity associated with excessive prolongation of fixation. This study presents a novel preclinical open-source tool based on CT finite element method (FEM) to predict the callus stiffness using experimental data.

2. Materials and Methods

Experimental callus data were derived from previous studies conducted in osteoporotic sheep model treated using distraction osteogenesis until 40 or 100 days of bone regeneration [2,3]. The FEM tool developed in MATLAB converted the callus CT voxels into finite elements. The mechanical properties of the elements were assigned using correlations between the elastic modulus and BMD derived from nanoindentation tests and µCT analysis. The porosity with respect to BMD was also considered for the woven bone. The tool was calibrated by using *in vivo* measures obtained under physiological loading conditions of 40-day calluses stiffness [3]. Subsequently, *in silico* stiffness of 100-day calluses was predicted and compared with *in vivo* stiffness measured in gait analysis [3], and also with *in silico* stiffness estimated in a previous similar study in a non-osteoporotic group [4].

3. Results

Figure 1 compares osteoporotic callus stiffness at 40 and 100 days predicted *in silico* and measured *in vivo*. The *in silico* callus stiffness estimation of a non-osteoporotic group is also shown [4]. Calibration based on the 40-day calluses yielded an *in silico* stiffness of 0.47 ± 0.41 kN/mm, compared with 0.56 ± 0.55 kN/mm measured *in vivo*. At 100 days, the predicted *in silico* callus stiffness was 5.7 ± 1.5 kN/mm, which falls within the range of the *in vivo* measurement (8.2 ± 6.1 kN/mm). The estimated *in silico* stiffness for the non-osteoporotic group was higher than that predicted for the osteoporotic group at both 40 days (2.0 ± 1.1 kN/mm) and 100 days (10.4 ± 0.3 kN/mm).

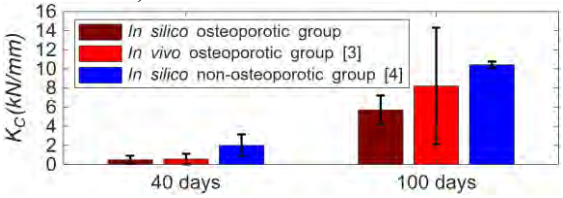


Figure 1: *In silico* and *in vivo* callus stiffness of the animals' groups at 40 and 100 days after surgery.

4. Discussion and Conclusions

An open-source preclinical tool was developed to accurately reproduce complex callus morphologies with low computational cost and without the need for mesh refinement. The predicted stiffness showed good agreement with *in vivo* experimental measurements obtained from gait analysis. In addition, applying this methodology to *in silico* comparisons of osteoporotic and non-osteoporotic calluses [4] revealed a preliminary reduction in stiffness in the osteoporotic group at both time points. These differences may be associated with osteoporosis and are consistent with *in vivo* findings [3].

5. References

1. Fisher JS et al., Skeletal Radiol; 48(3):349-361 (2017)
2. Toscano-Angulo JJ et al., PLoS One; 2;20(5):e0319910 (2025a).
3. Toscano-Angulo JJ et al., Front. Bioeng. Biotechnol; 13:1646500 (2025b).
4. Mora-Macías J et al., Int J Numer Method Biomed Eng; 35(9):e3227 (2019).

Acknowledgements:
Grant PID 2023-148828OB-I00 funded by MICIU/AEI/10.13039/501100011033 and by ERDF/EU.

MULTISCALE MODELING OF ARTICULAR CARTILAGE COLLAGEN MATRIX: MECHANICAL IMPACT OF STRUCTURAL CHANGES

Elías Núñez-Ortega (1), José A. Sanz-Herrera (1), Eamonn A. Gaffney (2), Cameron P. Brown (3), Esther Reina-Romo (1)

1. University of Seville, Spain; 2. University of Oxford, United Kingdom; 3. Queensland University of Technology, Australia

Corresponding author: Esther Reina-Romo. Escuela Técnica Superior de Ingeniería, Avenida Camino de los Descubrimientos s/n, 41092-Sevilla, Spain. Email: erreina@us.es

1. Introduction

Articular cartilage (AC) is a connective tissue covering the bone surfaces in articulating joints, whose collagen fibril network plays a key role in ensuring the tissue's mechanical integrity. Degeneration due to osteoarthritis causes structural changes in the collagen network, e.g., reorientation of collagen in the superficial zone (SZ) [1] and alterations in the interconnections between fibrils [2]. In this work, we aim to analyze *in silico* the nonlinear mechanical response of the SZ of AC in both normal and degenerate conditions. To this end, the fibril network is modeled, including their interconnections (crosslinks), and transverse tensile tests are subsequently performed.

2. Materials and Methods

A previously validated 3D multiscale fiber network model [3] is used and extended to generate fibril matrices, modeling crosslinks between fibrils for the first time (Fig. 1).

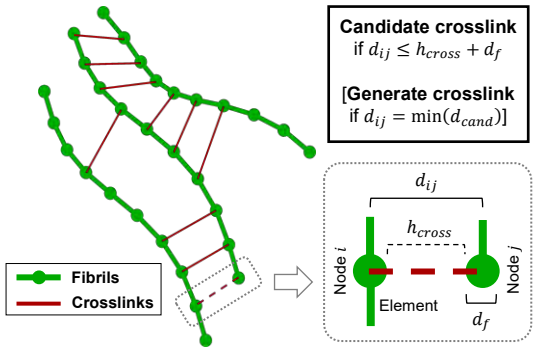


Figure 1: Schematic of crosslink generation.

A baseline case simulating normal AC is first studied, followed by systematic variations of key parameters (fibril stiffness, crosslink density, and fibril orientation) to simulate degenerative microstructural changes characteristic of osteoarthritic AC in the SZ.

3. Results

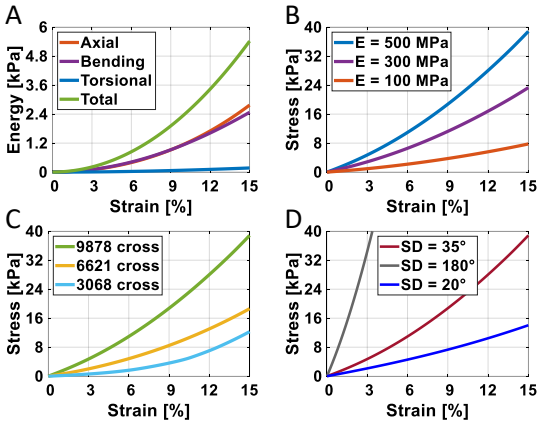


Figure 2: (A) Baseline case, strain energies. (B–D) Variation of model parameters, stress–strain curves.

4. Discussion and Conclusions

The key findings are: (i) crosslinks are predicted to linearize the macroscopic response; (ii) mechanical compensation is observed, in which a decrease in crosslinks does not reduce the network's stiffness; and (iii) some elements are found to act as stress concentrators, which may serve as critical points for damage initiation.

5. References

1. Brown CP et al., J Mech Behav Biomed Mater; 5(1):62–70 (2012).
2. Nickien M et al., WIREs Syst Biol Med; 5(4):495–509 (2013).
3. Sanz-Herrera JA et al., Comput Struct; 310:107690 (2025).

Acknowledgements:
Grant PID2023-148828OB-I00 funded by MICIU/AEI/10.13039/501100011033 and by ERDF/EU.
Grant PREP2023-001306 funded by MICIU/AEI/10.13039/501100011033 and by ESF+.

A COUPLED SIGNALING–METABOLIC MODEL OF CHONDROCYTE STATES IN OSTEOARTHRITIS

Pablo Tejero (1), Liesbet Geris (1,2,3)

1. Biomechanics Section, KU Leuven, Belgium; 2. Skeletal Biology & Engineering Research Center, KU Leuven, Belgium; 3. GIGA Research Center, U.Liège, Belgium

1. Introduction

Osteoarthritis (OA) is a chronic joint disease characterized by articular cartilage degradation, pain, and disability. In OA, chondrocytes lose homeostasis and activate inflammatory and catabolic pathways, progressively adopting a pathological state [1][2].

Protein signalling and gene regulatory pathways alone are insufficient to explain changes in chondrocyte state, as metabolic rewiring also plays a key role.

In response to stimuli such as pro-inflammatory cytokines or hypoxic conditions, glycolysis increases, oxidative phosphorylation decreases, and lactate production rises, contributing to acidosis. Lipid metabolism is also altered, and its metabolites can influence intracellular signalling pathways involved in regulating chondrocyte state [3].

To improve our understanding of these biological processes, we aim to integrate a metabolic layer into an existing gene–protein regulatory model to improve mechanistic simulations of chondrocyte states in OA.

2. Materials and Methods

Kerkhofs, Lesage and co-authors [1][2] developed a combined literature-curated and micro-array inferred mechanistic model of articular chondrocytes that captures the protein signalling and gene regulatory layers within a semi-quantitative dynamic simulation framework. This model includes 74 signalling nodes and 303 interactions between nodes, and can be used either stand-alone or as a part of a multiscale model of OA.

In this study, we established a preliminary coupling framework to extend the existing intracellular model by adding a metabolic layer based on genome-scale metabolic models (GEMs) [4]. GEMs represent cellular metabolism as a stoichiometric network and enable prediction of feasible reaction fluxes under condition-specific and nutrient-specific constraints [4].

Bidirectional coupling, between the gene/protein layers on the one hand and the metabolic layer on the other hand, was implemented through a bound-based scaling procedure. In the forward direction, normalized regulatory node activities were used as multiplicative factors on the maximum feasible bounds of mapped metabolic reactions, thereby constraining reaction capacity while preserving flux optimization within the feasible solution space. In the reverse direction, predicted fluxes were divided by their baseline reaction bounds to obtain normalized quantities that could be mapped back onto the regulatory layer.

3. Results

A context-specific metabolic model was generated from publicly available transcriptomic datasets using the XomicsToModel algorithm [4], comprising 6087 metabolic reactions and 4523 metabolites. An additional 24 literature-curated metabolism-related nodes, such as ROS, GLUT1 and lactate, and 59 new interactions between nodes were integrated into the existing regulatory network.

The preliminary coupling framework is currently being evaluated to assess the consistency of information flow between regulatory states and metabolic flux predictions.

4. Discussion and Conclusions

Despite the preliminary nature of these efforts, this development/model expansion establishes the basis for a multilevel framework linking signalling activity and metabolic fluxes in chondrocytes, with the potential to improve the mechanistic interpretation of healthy-OA transition.

5. References

1. Kerkhofs & Geris., PLOS One 2015
2. Lesage et al., BMC Biology 2022
3. Zheng et al., Ageing Research Reviews 66 2021
4. Preciat et al., Nature Protocols 2025

Acknowledgements:

The authors would like to thank the INSTant-CARMA project, funded by the European Research Council (ERC CoG, 101088919).

RULE-BASED PARTICLE SWARM OPTIMIZATION FOR PATIENT-SPECIFIC LUMPED PARAMERER CARDIOVASCULAR MODEL

Fangnan Xu[1], Emanuele Perra[2], Michael Broomé[3], Seraina A. Dual[1]

1. Department of Biomedical Engineering and Health Systems, KTH Royal Institute of Technology, Sweden;
2. Getinge, Sweden;
3. Department of Physiology and Pharmacolog, Karolinska Institute, Sweden

1. Introduction

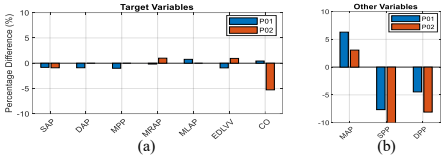
Computational cardiovascular models increasingly attract attention for the clinical insights they can provide. Among them, lumped parameter models (LPMs) provide adequate capability for estimating patient hemodynamic, high interpretability, and computational efficiency suitable for real-time use. However, clinical application requires patient-specific parameters, which are often not directly measurable. This study investigates whether optimization-based parameter identification can be achieved through a physiology-informed, rule-based approach.

2. Materials and Methods

We use a 26-segment closed loop cardiovascular LPM [1], where vessels are represented by four-element Windkessel models including systemic, pulmonary, and coronary circulations. The heart is modeled with a double-hill elastance function including septal interaction and pericardial constraint [2]. Parameter ident--ification is performed using a rule-based PSO algorithm [3] in which physiology-informed rules adjust particle velocities to promote convergence toward clinically plausible solutions. Sixteen key parameters are selected. Validation uses two patient cases, including their parameter sets, from the clinically validated Aplysia software. The corresponding model outputs generated by Aplysia also serve as target variables in the objective function.

3. Results

The patient-specific outputs reproduced the target variables with high accuracy (majority within 2% error, Figure 1A). Other variables not included in the optimization were also matched within 10% (Figure 1B), indicating some model plausibility. However, the identified parameters do not match the cases, despite good target matching. (Figure 2). Besides, the resulting pressure volume relationship also shows physiologically implausible behavior.



(a) (b)

Figure 1: Figure (a) shows target variables. The cardiac output of object P02 had -5% error. Figure (b) shows variables not involved in the optimization.

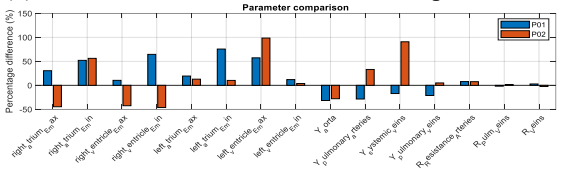


Figure 2: The chamber minimum elastances deviate substantially from their reference values, except for the left-ventricular minimum elastance. Conversely, the left-ventricular maximum elastance shows a marked deviation.

4. Discussion and Conclusions

The method accurately reproduces the target outputs; however, the recovered elastance parameters deviate from the original values, particularly the atrial and ventricular minimum elastances. This is consistent with known limitations in the identifiability of time varying elastance model parameters [4]. This indicates that the identification result is not a "local minimum," but rather a physiologically invalid solution among multiple feasible ones in the parameter space. Our study highlights the need for benchmarking tools that allow for assessement of physiologically realistic parameter matching.

5. References

1. Broomé M et al. Biomed Eng Online. 2013;12:69.
2. Rosato A, Perra E, Rullman E, Dual SA. Front Netw Physiol. 2025;5:1637551.
3. Perra E, Uribarri G, Fransén E, Dual SA. Proc 29th Eur Soc Biomech Congr; 2024; Edinburgh, UK.
4. Haghebaert M et al. J Physiol. 2025; doi:10.1113/JP287929.

Acknowledgements:
We thank and acknowledge VINNOVA (2022-00849), Digital Futures, and the Digitalisation Platform of KTH for their financial support.

AN IN SILICO FRAMEWORK FOR SPINAL CAGE DESIGN: MULTI-SCALE MODELLING OF AGENT BASED OSTEOINTEGRATION

Anneke Orlandini (1*), Chiara Carrara (2), Stefano Baraldo (1), Luca Gambardella (3), Anna Valente (1)

1. SUPSI Department of Innovative Technologies, Switzerland; 2. MCH-tronics Sagl, Switzerland; 3. USI Faculty of Informatics, Switzerland

*Corresponding author: anneke.orlandini@supsi.ch

1. Introduction

This work proposes a unified framework for spinal cage design optimization by introducing a novel Agent-Based Model (ABM) of osteointegration that accounts for implant architecture, surface functionalization, manufacturing, and patient biology integrating an AI-based surrogate model for fast inference of implant shape and manufacturing.

2. Materials and Methods

Taking as a reference a 3D-printed Ti6Al4V spinal cage case study, the ABM simulates cellular interactions and tissue formation. Table 1 maps the biological processes to their in silico models [1].

Agent/Process	In silico representation
Cells	Migration, Proliferation, Differentiation, Apoptosis
Chemotaxis	Cell-interacting diffusion models for bone-inducing chemicals
Angiogenesis	Vessel formation and nutrient release
Mineralization	Active osteoblasts forming rigid mineralized bone
Durotaxis	Local stress, strain, and Frost's Mechanostat

Table 1: Osteointegration model overview.

Micro- to nano-structured surface topographies [2] can be implemented into the ABM, after in-vitro characterization of their properties. Biological parameters are calibrated via grid search and parameter sweeps, minimizing Mean Squared Error (MSE) against micro-CT data [3]. The framework predicts osteointegration outcomes, specifically the bone volume fraction (BV/TV). To accelerate design exploration, a neural surrogate model (Figure 1) bypasses heavy ABM simulation runs. It enables fast inference across manufacturing parameters, serving as an inverse design tool to optimize implant options.

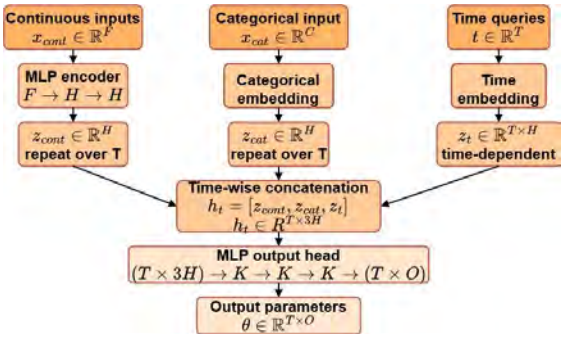


Figure 1: Neural network architecture for inverse design optimization.

3. Results

Early calibration and testing of the lattice structure show promising preliminary results, with BV/TV and bone ingrowth values falling within biologically relevant ranges.

4. Discussion and Conclusions

This *in silico* framework is a promising tool for supporting practitioners in the fast exploration of personalized implant designs and new manufacturing strategies. Further studies will include calibration and validation with in-vitro and clinical data.

5. References

1. Lafuente-Gracia L et al., (2021) Towards in silico Models of the Inflammatory Response in Bone Fracture Healing.
2. Orlandini et al., Ultrafast Laser Ablation for Scalable Surface Modification of Ti6Al4V Orthopaedic Implants (2026).
3. Kendall JJ et al., An in silico micro-multiphysics agent-based approach for simulating bone regeneration in a mouse femur defect model (2023).

Acknowledgements:

This work was supported by the European Union's Horizon Europe programme under the *WISE* project, Grant No. 101138718.

MULTISCALE IN SILICO MODELING OF CRANIOFACIAL DEFECT HEALING: FROM MECHANISMS TO VALIDATION

Laura Lafuente-Gracia (1), Lisanne Groeneveldt (1), Mojtaba Barzegari (2), Carla Geeroms (1), Aurélie Carlier (3), Liesbet Geris (1,4)

1. KU Leuven, Belgium; 2. TU Eindhoven, The Netherlands; 3. Maastricht University, The Netherlands; 4. University of Liège, Belgium

1. Introduction

Bone regeneration is a well-coordinated process involving numerous biological entities. While successful healing typically occurs within weeks, defect size, anatomical location and host factors can lead to delayed or non-healing. *In silico* models provide an interesting framework to investigate the underlying mechanisms of bone regeneration; however, their predictive capability depends on appropriate parameterization and validation against experimental data. In this work, we present a multiscale *in silico* model of bone regeneration and assess its ability to reproduce experimentally observed non-healing outcomes in craniofacial defects.

2. Materials and Methods

***In silico* model.** Building upon an established bioregulatory model of fracture healing [1], we developed a multiscale framework describing the spatiotemporal evolution of extracellular matrices, cells and biochemical factors through non-linear taxis-diffusion-reaction equations, coupled to an agent-based representation of endothelial cells. The model captures soft and hard callus formation and sprouting angiogenesis, including lateral inhibition via Dll4-Notch1 signaling, allowing for a mechanistic description of oxygen-regulated bone regeneration dynamics. The model was implemented in FreeFEM.

Domain. Computational domains were derived from critical-size mandibular and calvarial defects based on *in vivo* experiments in rodents and rabbits (Fig. 1A).

Calibration & validation. Sensitivity analyses were performed to identify the most influential parameters. Model calibration was carried out using Bayesian optimization to reproduce observed healing behavior in in-house rodent critical-size mandibular defect experiments. Model predictions were subsequently validated against independent experimental data from rabbit craniofacial defects [2].

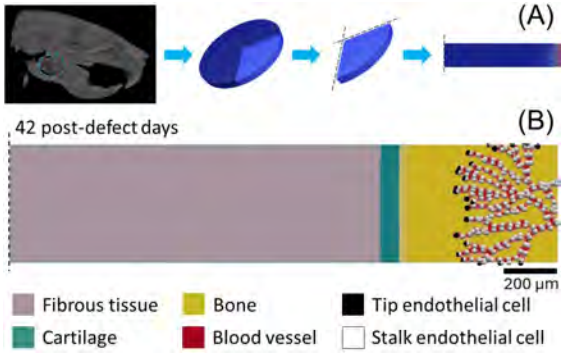


Figure 1: (A) Computational domain derived from a 5 mm rat mandibular defect. (B) Predicted non-union outcome, showing soft and hard callus distribution and vascular network with endothelial cells.

3. Results

The model reproduces key biological processes involved in bone regeneration. Simulations predict impaired healing characterized by limited bone formation and persistence of fibrous tissue, resulting in non-union outcomes (Fig. 1B). Vascular ingrowth progressively stops, limiting oxygen supply and preventing further tissue regeneration (Fig. 1B). The spatial distribution of tissues and the overall healing response are in qualitative agreement with experimental observations (not shown).

4. Discussion and Conclusions

By integrating experimental data into a mechanistic model, we developed a multiscale *in silico* model of bone regeneration able to reproduce experimentally observed non-union outcomes in craniofacial defects. The presented framework provides a basis for understanding the biological mechanisms underlying impaired regeneration and can support the *in silico* evaluation of tissue-engineered scaffold strategies to promote regeneration.

5. References

1. Carlier et al., *J Theor Biol*, 2015.
2. Kotagudda Ranganath et al., *Mater Today Bio*, 2022.

Acknowledgements:
ERC (grant no: 101088919) and RegMed XB.

KNEE OSTEOARTHRITIS MULTISCALE MODELING: INSIGHT TOWARD POPULATION LEVEL

Amin Asadi Amoli (1,2), Satanik Mukherjee (3), Liesbet Geris (1,2)

1. KU Leuven, Belgium; 2. University of Liège, Belgium; 3. Washington University at Saint Louis, USA.

1. Introduction

Knee osteoarthritis (OA) is a highly prevalent disease associated with a substantial socioeconomic burden. Digital twins of the knee are developed as a way to integrate processes playing out over different time and length scales. These digital twins can be leveraged as refinement and exploration tools to identify potential therapeutic interventions and biomarkers in complement of conventional (clinical) trials. To account for inter-patient variability and bring computational models closer to clinical applications, population-level modeling by means of virtual cohorts can be used. These virtual cohorts can also be used to study trends and uncertainty propagation across scales. In this study, a virtual cohort of OA patients was generated, focusing on the geometrical variability within the population of patients with OA severity level 2 (minimal OA) to 3 (moderate OA) on the Kellgren and Lawrence (KL) scale.

2. Materials and Methods

Large Deformation Diffeomorphic Metric Mapping (LDDMM), a specific instance of statistical shape models based on control points [1], was used to define a joint probability density function and parametrize the target shapes. Latin Hypercube Sampling [3], Gaussian copulas [2], empirical mapping, and Principle Component Analysis dimensionality reduction were then utilized for sampling a collection of synthetic geometry. Further analyses were applied to ensure the compactness, generalisation and reconstruction accuracy of developed framework. The input data for the framework was obtained from OAI database.

3. Results

The framework was able to generate 169 KL2 and 142 KL3 new geometries trained by a set of 22 and 20 KL2 and KL3 subject knee joint geometries (see selection in Fig.1). The generated synthetic samples reside within the 95% confidence interval of both the multivariate LDDMM parameter space and a multivariate space defined by conventional geometric descriptors of the knee joint. These complementary feature spaces were used to assess the plausibility and representativeness of the generated synthetic computational meshes.

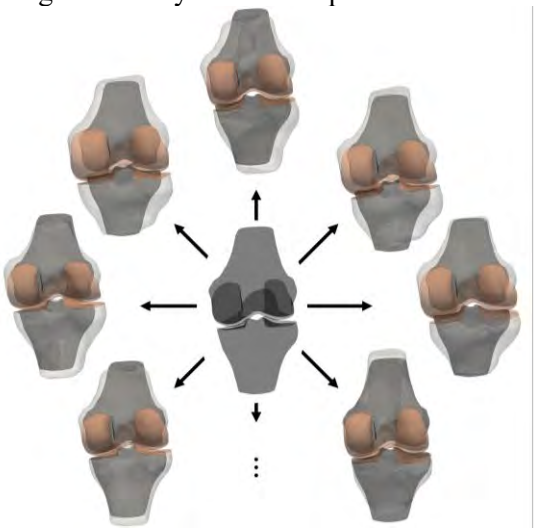


Figure 1: Schematic of statistical shape model after parameter tuning.

4. Discussion and Conclusions

In computational modeling, there are several main aspects that can be personalized, each requiring different modalities for measurement and characterization. Statistical shape modeling provides a tool to cover this personalization with the second level of correspondence for the geometry as one of the primary inputs to any computational framework. Other aspects of this in silico model, including a corresponding loading and kinematic constrains correlated with geometrical features of synthetic cohort, should be considered in the next steps.

5. References

1. Durrleman et al., *NeuroImage*, 2014.
2. Martinez et al., *Comput. Methods Appl. Mech. Engrg*, 2025
3. Verstraeten et al., *Int J Numer Meth Biomed Engng*, 2023.

Acknowledgements

ERC CoG (101088919) and BOSA (DT4PH).

IN-SILICO TRIALS FOR RENAL ANEMIA TREATMENT USING DIGITAL TWINS OF DIALYSIS PATIENTS

David J. Jörg, Doris H. Fuertinger

Renal Research Institute, New York, United States

Correspondence: david.joerg@rriny.com, doris.fuertinger@rriny.com

1. Introduction

Treatment of anemia in patients with end-stage kidney disease aims to elevate and maintain hemoglobin levels within a clinical target range through repeated administration of erythropoiesis-stimulating agents (ESAs). Adjusting ESA doses is notoriously challenging due to delayed physiological responses to treatment and external events such as bleedings or missed treatments, which may lead to hemoglobin excursions [1]. Here, we present a physiology-based in-silico trial framework for evaluating anemia treatment algorithms using thousands of digital twins derived from real-world renal anemia patients on dialysis.

2. Materials and Methods

The core of the in-silico trial framework is a physiology-based model of red blood cell formation in the bone marrow and the pharmacodynamic effects of ESAs [2]. In-silico trials simulate longitudinal hemoglobin trajectories and corresponding ESA dosing decisions over extended time horizons under predefined treatment algorithms. Stochastic components were incorporated to reflect real-world clinical processes, including laboratory measurement variability, dosing delays, and temporary interruptions of care (Fig. 1) [2].

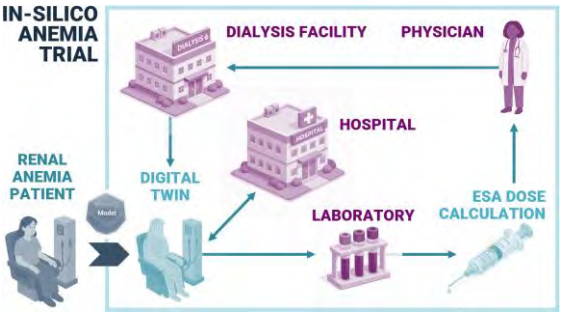


Figure 1: In-silico trial framework combining deterministic simulation modules (blue) and real-world stochastic event modules (purple). [Individual pictograms generated with ChatGPT 5.2.]

Digital twins representing 5,350 dialysis patients in Fresenius Kidney Care clinics (U.S.) were generated by calibrating the model to routinely collected clinical data [3]. Inferred patient-specific parameters included red blood cell lifespan, ESA half-life, and drug responsiveness.

3. Results

The in-silico trials quantitatively reproduced key features of real-world clinical outcomes, including the distributions of hemoglobin measurements and administered ESA doses (Fig. 2).

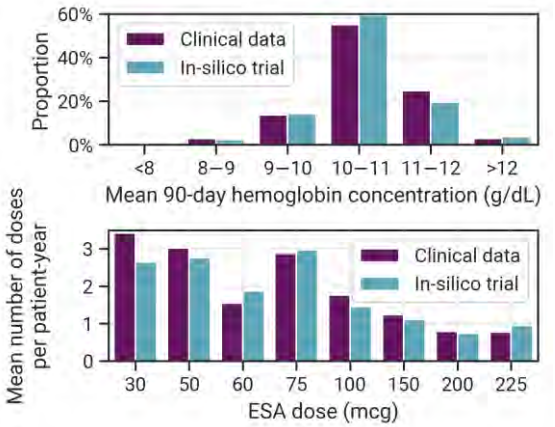


Figure 2: Comparison of in-silico trial results to real-world clinical data on hemoglobin measurements (top) and given ESA doses (bottom).

4. Discussion and Conclusions

We developed a physiology-based in-silico trial framework incorporating digital twins of real patients that captures key outcomes of real-world renal anemia treatment. The framework is routinely used to support the rational design and adaptation of anemia treatment algorithms within a large dialysis organization.

5. References

1. Jörg DJ et al., *PLOS Comput. Biol.*; 19(1): e1010850 (2023)
2. Fuertinger DH et al., *CPT: Pharmacometr. & Syst. Pharmacol.*; 7:219–227 (2018).
3. Fuertinger DH et al., *PLOS ONE*; 13(4):e0195918 (2018)

DIGITAL TWIN FRAMEWORK FOR PERSONALIZED ASSESSMENT OF HIP FRACTURE RISK REDUCTION STRATEGIES

Dheeraj Jha (1), Anita Fung (2), Yijun Zhou (1), Anitha D. Praveen (1), Enrico Schileo (3), Stephen J Ferguson (1,2), Fulvia Taddei (3), Benedikt Helgason (1,2)

1. Singapore-ETH Centre, SG; 2. ETH-Zürich, CH; 3. Istituto Ortopedico Rizzoli, Bologna, IT.

1. Introduction

Hip fractures arise from the interplay between reduced bone strength and fall-induced impact load. CT-based biofidelic finite element models (FEMs) incorporating the pelvis and surrounding soft tissues can simulate realistic sideways fall scenarios [1]. In this study, we developed subject-specific digital twin models to quantify the probability of fracture given a fall (P_{Fx}) and Relative Risk (RR) as a result of aging or risk reducing interventions.

2. Materials and Methods

An automated software pipeline [1] was used to generate CT-based biofidelic FEMs for 21 real-world post-fracture female participants (age: 78.5 ± 6.2 years) from previous study [2]. Each digital twin was subjected to simulated falls at varying impact velocity and impact alignment. P_{Fx} was calculated by overlaying the critical velocity curve onto the distribution of fall configurations derived from literature data [3] (Fig. 1). RR was calculated as the ratio between P_{Fx} before and after a simulated effect (aging, pharma intervention or use of hip protector). For pharma intervention (BMD +3.25%), RR was adjusted for 3-years of aging (BMD -1.021%).

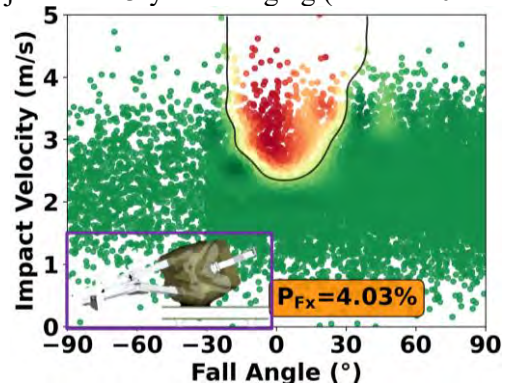


Figure 1: A sample calculation of the probability of fracture given a fall (P_{Fx}) by overlaying critical velocity curve on to fall configurations. Red dots: fractured cases. Green dots: Non-fractured cases.

3. Results

Mean P_{Fx} and RR values demonstrated distinct effects of the simulated interventions (Table 1). Ageing increased P_{Fx} and RR, indicating elevated fracture risk as expected. Pharma augmentation reduced P_{Fx} modestly. Hip protector augmentation resulted in the largest reduction in P_{Fx} and RR among the evaluated intervention strategies.

Table 1: P_{Fx} and RR for studied participants.

Models	P_{Fx} (%) (Mean ± SD)	RR [95% CI]
Unaugmented	11.53 ± 5.24	--
Ageing	12.41 ± 5.17	1.13 [1.01 - 1.25]
Pharma	10.92 ± 4.91	0.87 [0.84 - 0.90]
Hip Protector	8.07 ± 5.19	0.66 [0.55 - 0.77]

4. Discussion and Conclusions

This subject-specific digital twin framework enables direct comparison of fracture prevention strategies within the same post-fracture population. Age-related bone loss increased fracture risk, while pharma interventions, and hip protectors reduced risk. Reported relative risks for primary fracture prevention are 0.75 (95% CI: 0.48 to 1.17) [4] for alendronate treatments and 0.41, (95% CI 0.19 to 0.89) [5] for hip protectors with 100% compliance. The relative risk reductions observed in our study fall within the ranges reported in the literature, indicating consistency between the digital twin simulations and established clinical evidence. The proposed digital twin framework provides a cost-effective, and reproducible *in silico* evaluation tools may support clinical decision-making and development of novel intervention strategies.

5. References

1. Baker et al., Ann. Biomed. Eng. (2026).
2. Falcinelli et al., Bone. 67(71-80) (2014).
3. Jha et al., Under review, JBMR Plus (2025).
4. Järvinen et al. BMJ, 350:h2088 (2015).
5. Bentzen et al., Inj Prev. 14(5):306-10 (2008).

Acknowledgements:
The research was conducted at the Future Health Technologies at the Singapore-ETH Centre, which was established collaboratively between ETH Zurich and the National Research Foundation Singapore. This research is supported by NRF Singapore under its CREATE programme.

FRAILTY-AWARE *IN SILICO* TRIALS TO IMPROVE HIP FRACTURE INCIDENCE PREDICTION ACROSS COHORTS

Giacomo Savelli (1), Alessandra Aldieri (2), Marco Viceconti (2)

1. *Medical Technology Lab, IRCCS Istituto Ortopedico Rizzoli, Bologna, Italy*
2. *Department of Industrial Engineering, Alma Mater Studiorum - University of Bologna, Italy.*

Introduction

Hip fragility fractures are a major healthcare concern, associated with reduced quality of life and increased mortality [1]. More than 90% of hip fractures result from a fall, and incidence emerges from the interaction between fall exposure, impact severity, and femoral strength. *BoneStrength* is a *In Silico Trial* computational tool to predict hip fracture that combines subject-specific Finite Element (FE) models of the proximal femur with a multiscale stochastic fall-to-fracture framework [2]. Prior validations across heterogeneous cohorts showed inconsistent over/under-estimation depending on baseline risk [2], suggesting an underrepresentation of non-skeletal determinants modulating impact severity. This study integrated a frailty module into *BoneStrength* and evaluated whether it could improve prediction accuracy across cohorts with different risk profiles.

Materials and methods

Virtual cohorts were generated using a statistical morpho-densitometric atlas to sample femoral geometry and bone density distributions [2]. For each virtual subject, FE models of the proximal femur were generated with a quadratic tetrahedral mesh (average size ≈ 3 mm). Material properties were assigned based on the sampled density distribution, and failure load in different loading directions was predicted using a validated strain-based criterion [2]. Falls were stochastically sampled using a Negative Binomial distribution, to model the over-dispersion in fall frequency observed in clinical populations. Fall impact forces were obtained with a multiscale fall model, with stochastic parameters to represent fall variability and configuration-dependent force transfer [2]. If the impact force due to a simulated fall exceeded the FE-predicted failure load, the virtual patient was classified as fractured. Frailty status was operationalised using the Fried phenotype framework [3] and mapped to a modulation of postural attenuation within the multiscale fall model. The corresponding parameter (η_p) was calibrated on data from the Study of Osteoporotic Fracture [3], frailty prevalence was estimated in the validation cohorts. Fracture incidence was estimated using repeated realisations per subject in a Markov-chain simulation scheme until convergence of cohort-level incidence metrics.

Results

In the calibrated setting (Fig. 1b), observed fracture counts (red crosses) fell within the 95% prediction intervals for LIFT, FREEDOM, and ARCH; relative to the pre-calibration setting (Fig. 1a), the predicted mean retained a modest overestimation versus observations across cohorts.

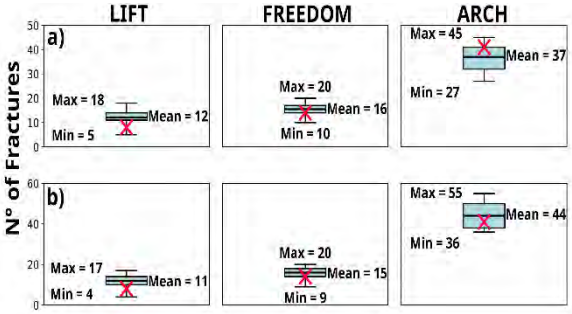


Figure 1: *Predicted fracture incidence before (a) and after (b) frailty calibration. Red crosses indicate fracture incidence observed clinical setting.*

Discussion

Integration of a frailty module into *BoneStrength* improved the consistency of hip fracture incidence predictions across heterogeneous validation cohorts. Despite modest residual overestimation, predictions showed more uniform behaviour across baseline-risk profiles than before calibration.

Frailty was implemented as a modifier of impact severity within the existing multiscale fall-to-fracture framework, enabling incorporation of functional vulnerability without introducing a separate fall-risk model.

References

1. Borgstorm et al, Arch Osteoporos. 15:59, 2020.
2. Savelli et al, Ann Biomed Eng, 53, 2025.
3. Ensrud et al, J Gerontol, 62(7):744–751, 2007.

Acknowledgements

Work supported by the Italian Complementary National Plan PNC-I.1 (D.D. 931, 06 Jun 2022), DARE – DigitAl lifelong pRevEntion (PNC0000002; CUP B53C22006450001).

IN SILICO STUDY OF POST-INTERVENTIONAL RECONSTRUCTION STRATEGIES FOR INTRACRANIAL WIDE-NECK ANEURYSMS

Anna Bernovskis (1,2), Fina Gießler (3), Franziska Gaidzik (1,4), Naomi Larsen (5), Sylvia Saalfeld (3), Philipp Berg (1,2)

1. Research Campus STIMULATE, OVGU, Germany; 2. Department of Medical Engineering, OVGU, Germany; 3. Institute for Medical Informatics and Statistics, UKSH, Germany; 4. Laboratory of Fluid Dynamics and Technical Flows, OVGU, Germany 5. Department for Radiology and Neuroradiology, UKSH, Germany

1. Introduction

Intracranial aneurysms (IAs) are pathological dilatations of cerebral arteries that often require treatment to prevent rupture. The Contour Neurovascular Device (CNS) is an intra-aneurysmal implant designed to reduce blood flow within the IA. As this treatment can induce morphological changes [1], the analysis of post-treatment hemodynamics using image-based blood flow simulations is of special interest. However, reduced blood flow after treatment limits contrast enhancement, complicating reliable reconstruction. A commonly used approach is virtual stitching, in which the pre-treatment IA is merged with the post-treatment parental vessels [2]. While enabling hemodynamic analysis, it does not reflect the actual anatomy. This study evaluates strategies for handling post-treatment data and examines the common approach.

2. Materials and Methods

Post-treatment data from five IAs treated with CNS were analyzed. Two stitching variants were generated per case to evaluate variability. As seen in Figure 1, variant 2 used a planar surface at the level of the CNS, while variant 3 placed a wall directly behind the CNS to model the endothelial layer. The final variant (4) was based on the post-treatment data without reconstruction of the IA tip.

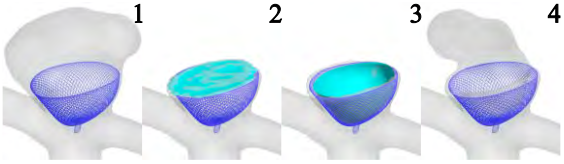


Figure 1: Post-treatment variants: (1) stitching, (2) planar surface, (3) wall, (4) post-geometry.

In total, 25 time-dependent simulations were performed to analyze velocity (velo) and wall shear stress (WSS) of the former IA and the neck region (including parental vessel).

3. Results

The analysis of velo and WSS in the IA shows only minor deviations for both stitching variants (WSS_IA: $< \pm 0.014$ Pa / Velo: $< \pm 0.0013$ m/s across all IAs). Comparable results are also observed for the planar surface and post variants, indicating strong consistency between these approaches. Only the wall variant leads to slightly larger deviations in the obtained values. This behaviour is reproduced when the analysis is restricted to the neck region, where overall differences between all variants remain small (WSS_neck: CV* ≤ 24.2 % across all IAs). In summary, the results demonstrate a high level of agreement across the investigated approaches to reconstruct the missing IA tip.

*Coefficient of Variance

4. Discussion and Conclusions

The CNS strongly attenuates IA hemodynamics, making precise IA tip reconstruction negligible. Virtual stitching is operator-robust. However, it is associated with considerable effort and results in medical inaccuracy. Alternative variants may better reflect medical anatomy, yet hemodynamic values are largely consistent across them. Rather than aiming for a highly accurate reconstruction of the IA tip, it is therefore considerably more important to correctly identify CNS position based on post-treatment data, as this factor has a greater impact on the resulting hemodynamics.

5. References

1. Larsen et al., J. Neuroradiol. 2026; 101407.
2. Korte J, Gaidzik F et al., Comput Biol Med. 2025; 197:111002.

Acknowledgements:

This study was partly funded by the German BMFTR (grant number 13GW0835A) and the German Research Foundation (grant number 548907942).

IN SILICO EVALUATION OF PATIENT DAILY ACTIVITIES ON KNEE IMPLANT WEAR USING IN VIVO DATA

Diego Barbieri (1), Lorenza Mattei (2), Marco Viceconti (3) and Cristina Curreli (1)

1. Medical Technology Lab, IRCCS Istituto Ortopedico Rizzoli, Bologna, Italy 2. Department of Civil and Industrial Engineering, University of Pisa, Italy; 3. Department of Industrial Engineering, Alma Mater Studiorum - University of Bologna, Italy

1. Introduction

The finite element (FE) method represents a promising approach for predicting wear damage in total knee replacements (TKR), providing evidence of implant safety while reducing the time and costs associated with traditional experimental testing. However, most FE studies reported in the literature have adopted standardized loading and kinematic conditions or in vivo data collected during walking trials only [1]. This may not be sufficient to accurately estimate implant surface damage, as knee prostheses are typically subjected to a variety of motor tasks throughout their lifetime. The aim of this study is to investigate how in vivo–measured daily patient activities influence the in silico wear estimation of knee implants, using the recently introduced CAMS-Knee dataset.

2. Materials and Methods

The FE wear modelling was developed in ANSYS Workbench. The model was based on the geometry of a right knee implant by Zimmer Biomet, i.e. INNEX FIXUC ultra-congruent design (Figure 1a). Numerical wear simulations employed Archard's Law to calculate surface wear. Boundary conditions were defined based on in vivo data obtained from the CAMS-Knee subject "Stan" [2], which includes synchronized in vivo implant kinematics measured using a moving fluoroscope, and tibio-femoral contact loads measured with instrumented implants during five daily activities (i.e., level walking, ramp down, squat, stairs down, and stand up–sit down) derived from six subjects. The impact of diverse kinematic and loading histories on the wear of the polyethylene insert was investigated considering the combined effect of the daily activities and estimated annual number of cycles for each motor task. That required preliminary investigations to identify a simplified combination of daily activities to limit the computational cost. A comparison was also performed with the results in terms of wear volume and wear maps obtained using ISO 14243 loading and kinematic conditions.

3. Results

The results reveal that the type of motor tasks significantly influence implant wear and the most critical task is stairs down. ISO standards conditions cause wear maps different from those obtained under in-vivo conditions and tend to notably underestimate volumetric wear by up to 70% compared to the simulated patient types (Figure 1b).

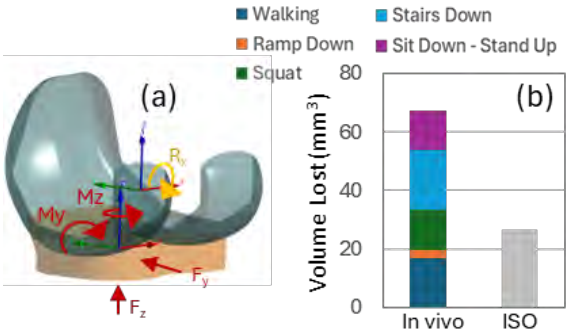


Figure 1: FE model (a); predicted wear volume under in vivo e ISO standard conditions accumulated over one year (b).

4. Discussion and Conclusions

This work represents an important step toward in silico trials for wear testing of TKR that reflect different lifestyle conditions. It also confirms the limitations of the current ISO 14243 standard, which underestimates in vivo volumetric wear and fails to accurately predict realistic wear patterns.

5. References

1. Michael J Dreyer et al., Biomed Eng Online. doi: 10.1186/s12938-024-01321-0 (2024).
2. Michael J Dreyer et al., Journal of Biomechanics; doi: 10.1016/j.jbiomech.2022.111171 (2022).

Acknowledgements:

This research is co-funded by the Italian PNC-I.1, D.D. 931 of 06/06/2022, "DARE – Digital Lifelong Prevention" initiative, code PNC0000002, CUP: B53C22006230001.

DEVELOPING A KNOWLEDGE INTEGRATION FRAMEWORK TO SUPPORT VIRTUAL PATIENT GENERATION FOR RARE DISEASES

Giulia Monchietto (1), Karen Sinclair (2), Sarah Zohar (1)

1. Inserm, Univ Paris Cité, Inria, HeKA, Paris, France; 2. Novartis Pharma AG, Basel, Switzerland;

1. Introduction

Drug development is challenging in rare and pediatric diseases, due to recruitment limitations and ethical constraints. Generation of virtual patients (VPs), through model informed drug development (MIDD[1]) approaches, is an attractive solution when low sample sizes do not allow for powered clinical trials. However, a framework is yet to be developed, which considers how much knowledge, and of which type, is required, which methods are suitable in different situations and how reliable are the generated VPs. A 2025 review found only 18/72 of in silico trials publications addressed rare or pediatric populations. Our work proposes six-steps to combine different sources of knowledge: drug (e.g. PK/PD models), disease (endpoints, progression models), clinical trials (in one or more indications) and population knowledge (clinical and demographic attributes), with available methodology to facilitate VP generation. We focus on generating VPs through stochastic simulations of concentration-time profiles via population pharmacokinetic (popPK) models to demonstrate the purpose of this workflow.

2. Materials and Methods

To generate VPs a six-steps workflow is implemented.

1. Objective statement: define the specific question of interest for the modeling activity.
2. Knowledge assessment: categorize available information into relevant domains to understand the impact of each knowledge domain on VP generation.
3. Methodological selection: identify methods and procedures applicable according to knowledge availability scenario. Initially, we focus on extrapolation of PK to a new indication, considering approaches such as direct extrapolation, integrating information from distinct indications and model ensembling methods.
4. Model evaluation: assess robustness and prediction capability. For extrapolation of PK to a new indication, prediction-based diagnostics (e.g. MDPE, MDAPE) and simulation-based tools (e.g. NPDE, CRPS) are used to ensure reproducibility of the central tendency and variability of target population.
5-6. VP generation and uncertainty quantification will be the focus of future work.

3. Results

A knowledge integration framework has been initialized proposing existing methods and procedures throughout the workflow steps, according to the knowledge available. We illustrate its application, by augmenting a psoriatic arthritis (PsA) cohort (N=50) using a Secukinumab popPK model originally built for plaque psoriasis [3], where clearance and absorption rate parameters were scaled to create a profile mismatch between populations (Step 1-2). Direct extrapolation to PsA (Step 3) failed to meet predictive performance criteria (Step 4). We then iterated through Step 3 to assess alternative approaches (investigation of sampling scheme optimisation, model re-fitting on target population and on pooled indications, etc). Model evaluation was further repeated. VP generation is performed (Step 5), but we emphasize that the uncertainty assessment (Step 6) will provide the full measure of model risk, allowing regulators to understand the total level of confidence in the evidence generated to support drug development.

4. Discussion and Conclusions

Results show an example of framework application, designed to provide a structured approach, in line with ICH M15 guidelines, to VP data generation. Future work will expand this framework to accomodate additional knowledge scenarios with more complex models and techniques, including VP generation in pediatric populations.

5. References

1. International Council for Harmonisation (ICH). ICH M15. 2026;Final:1-45
2. Chen B, et al. Ther Innov Regul Sci. 2026;60(2):423-439
3. Bruin G, et al. Br J Clin Pharmacol. 2020;86(2):338-351

Acknowledgements:

The authors would like to thank the European Union's Horizone Europe Research and Innovation program (Grant no: 101136365), Swiss State Secretariat for Education, Research and Innovation (SERI) and UKRI Innovative UK for providing financial support to this project.

PATIENT-SPECIFIC SURGICAL PLANNING OF FEMORAL FRACTURES USING DIGITAL TWINS AND MACHINE LEARNING

Oscar L. Lorente[1], Jesús Gómez[3], Antonio Bono[2], Bonifacio Martín del brio[2] , Jorge Albareda[3], Sergio Puértolas[1*]

*1. Dept. Mechanical Engineering, University of Zaragoza, I3A Institute, Spain. *email: spb@unizar.es*

2. Dept. of Electronic Engineering and Communications, University of Zaragoza, I3A Institute, Spain.

3. Orthopedic Surgery and Traumatology, University Hospital Lozano Blesa, Zaragoza, Spain

1. Introduction

The biomechanical stability of the fixation construct and the local mechanical environment at the fracture site play a key role in fracture healing and functional outcomes. However, significant inter-patient variability exists in femoral geometry, bone quality, and fracture morphology. Although treatment typically involves internal fixation using intramedullary nails or lateral plates [1], selecting the optimal surgical strategy remains challenging. Patient-specific computational models offer a promising approach for evaluating treatment options prior to surgery and supporting personalized clinical decision-making; however, their real-time application remains infeasible

2. Materials and Methods

2.1 Digital Twin Generation: Based on computed tomography (CT) scans (3 female and 3 male), reference 3D models of the complete femur were obtained. From the selected reference femur, patient-specific digital twins were generated using segmentation, transformation, and reconstruction techniques. Patient anthropometric characteristics were derived from a limited number of measurements extracted from standard clinical X-ray images. To achieve this, a methodology implemented through ad hoc programming in Rhinoceros v8 was developed. This approach enables the generation of fractured bone geometries for each case, as well as the positioning of the surgical technique to be evaluated [2], producing 3D solid models suitable for automatic FEM meshing.

2.2 Finite Element Modeling (FEM):

FEM of the fracture fixation constructs were generated from the reconstructed geometries. Physiological loads, boundary conditions, material properties, and contact interactions between bone, implant, and locking screws were incorporated. After meshing and simulation, key biomechanical indicators were evaluated, including stress and strain fields, displacement, and interfragmentary micromotion at the fracture site. These variables were analyzed to assess mechanical stability and conditions compatible with callus formation and fracture healing. Simulation outputs were processed using Python scripts to generate a structured dataset for multiple treatment scenarios.

2.3 Machine Learning: The FEM-generated dataset was used to train a Multilayer Perceptron (MLP) neural network. The trained model predicts the same healing assessment variables as FEM simulations at a fraction of the computational cost, enabling rapid evaluation of different screw configurations and supporting clinical decision-making. The resulting expert system achieves an accuracy of 98%.

3. Results

Patient-specific digital twins of the femur were successfully generated, allowing the reproducible creation of multiple fracture scenarios and surgical fixation configurations. The computational pipeline enabled the large-scale generation of structured biomechanical datasets, which are essential for training predictive machine learning models. The resulting machine learning framework demonstrated the capability to predict biomechanical indicators and recommend optimal surgical treatment strategies for individual patients in real time.

4.Discussion and conclusions

The integration of patient-specific digital twins, computational biomechanics, and machine learning provides a novel framework for personalized surgical planning in femoral fracture treatment.

5. References

[1] Ng AC, et.al. Osteoporos Int. 2012, Jun; 23(6) :1721-6.

[2] Chen, X.et.al (2016).. Biotechnology and Biotechnological Equipment, 30(3), 529–537.

Acknowledgements:

This work was supported by the Spanish Ministry of Science and Innovation and the European Union under Grant PID2022-140539OB-I00.

BREAKING THE SCALABILITY BARRIER: CLOUD-PARALLELIZED INFRASTRUCTURE FOR HIGH-THROUGHPUT IN SILICO CLINICAL TRIALS

Christine Mueri (1), Dhamodharan Pandurangan (2), Gnanaprakash Ramswami (2), Sandeep Sovani (3), Steven Levine (4), Thierry Marchal (5), Philippe Favre (1)

1. Zimmer Biomet, Switzerland; 2. Invisibl Cloud, India; 3. AWS, USA; 4. Dassault Systèmes, USA; 5. Synopsys, Belgium

1. Introduction

Traditional orthopaedic clinical trials typically enrol focused cohorts of ~100 patients, optimised for detecting primary endpoints with statistical rigour. Characterising complications that occur at low single-digit rates can, however, require case volumes that go beyond what any single study, or even registries and in silico cohorts, can readily provide. Addressing this limitation requires large-scale in silico population generation, traditionally prohibitive in computational time. This study presents the technical framework for a scalable cloud-based parallelization infrastructure to dramatically increase in silico clinical trial throughput within minimal time.

2. Materials and Methods

An existing on premises in silico trial pipeline [1] was migrated to a cloud environment. Key implementation steps included:

- **Environment setup:** Cloud environment configuration, software installation, and adaptation of pipeline dependencies
- **Population definition:** Specification of a virtual cohort with meaningful parameter variation for large-scale runs
- **Data management:** High-speed, secured transfer of large datasets with sufficient cloud and local storage provisioning
- **Job orchestration:** Implementation of queuing and monitoring interface to track progress, handle errors, and rerun failed jobs
- **Runtime optimisation:** Balancing CPU allocation against solver licenses
- **Licensing:** Securing parallel software licenses scaled to the number of concurrent models
- **Traceability:** Generation of analysis-ready summaries consistent with regulated-grade execution controls

3. Results

The cloud implementation successfully reproduced on-premises results, with approximately 1% variability attributed primarily to meshing-related differences. The orchestration layer enabled efficient queuing across pipeline steps, while the monitoring tool automated analysis-ready output generation and improved run-level traceability, including identification and management of non-converged simulations and outlier behaviour. The architecture demonstrated linear scalability, with the target of generating simulated outcomes for a 30,000 virtual patient cohort within 24 hours.

4. Discussion and Conclusions

Scaling an in silico clinical trial to the cloud requires significant technical investment that should not be underestimated; however, once deployed, the infrastructure can be reused across multiple studies, justifying the effort. Thirty thousand virtual patients correspond to roughly three times the annual total shoulder arthroplasty volume in the UK or Australia [2,3]. Delivering this volume of evidence on short timelines represents a potential step-change for implant design and pre-clinical evaluation and may support regulatory decision-making through broader sensitivity and uncertainty quantification, improved characterisation of extremes, and more robust assessment of design or surgical factors by removing bias effects due to reduced sampling.

5. References

1. Maquer G et al., EFORT 2025, Lyon.
2. UK National Joint Registry. 22nd Annual Report 2024, London.
3. Australian Orthopaedic Association National Joint Replacement Registry. Adelaide, South Australia: AOA; 2024

Acknowledgements: The authors thank Amazon Web Services for the cloud infrastructure and funding, Invisibl Cloud for the cloud pipeline implementation, ANSYS and Dassault Systèmes for software licenses.

AI-DRIVEN DECISION SUPPORT SYSTEM TO EMPOWER ENGAGEMENT IN PEDIATRIC NEUROMOTOR REHABILITATION

Simone Costantini (1,2), Fabio Alexander Storm (2), Emilia Biffi (2), Giuseppe Andreoni (2,3), Anna Maria Bianchi (1)

1. *Department of Electronics Information and Bioengineering, Politecnico di Milano, Italy; 2. Scientific Institute, IRCCS "E. Medea", Bosisio Parini, Italy; 3. Department of Design, Politecnico di Milano, Italy*

Corresponding author: Simone Costantini (simone.costantini@polimi.it)

1. Introduction

In pediatric neuromotor rehabilitation, technology-assisted, high-intensity approaches are crucial to elicit neuroplasticity and motor function recovery, though their repetitive nature can induce boredom and disengagement [1]. This is critical, as rehabilitation engagement, a co-constructed state of affective, cognitive, and behavioral involvement towards the goals of rehabilitation [2], is a prerogative for enhanced clinical outcomes. Currently, engagement assessment is done mainly using qualitative psychometric scales, which are discrete tools characterized by high inter-subject variability. Moreover, therapists rely on manual annotation of device parameters, exergames settings, and scores to ensure treatment continuity. However, this annotation process is carried out using inadequate tools lacking relational structure and standardization, increasing therapists' cognitive workload and hindering proper interactions with patients. This work aims to design, develop, and validate an e-health Decision Support System (DSS) to facilitate the therapeutic interaction, by optimizing clinical data management and providing objective, real-time engagement assessment metrics.

2. Materials and Methods

The DSS is designed using a user-centred approach, involving therapists via preliminary interviews. The DSS consists of two modules: (1) a real-time visualization dashboard to monitor patient's engagement metrics; and (2) an interactive annotation interface driven by a relational database to minimize cognitive demand through optimized data input and information retrieval. During a rehabilitation session, the DSS operates with a continuous human-in-the-loop workflow. While therapists log clinical data, heart rate variability, electrodermal activity, and inertial data are acquired via wearable sensors from the patient. Following online signal processing and feature extraction, a trustworthy Hierarchical Bayesian Model (HBM) is used to infer patients' engagement state and fluctuations, allowing therapists to consult them via the dashboard.

3. Preliminary Results

Preliminary offline validation of the HBM for engagement prediction was performed at the Scientific Institute "E. Medea" on 21 pediatric patients using Lokomat (Hokoma AG) or GRAIL (Motek Medical) systems in 58 sessions and reported promising results ($F1 = 0.79$).

4. Discussion and Conclusions

These findings justify a planned interventional pilot study involving further 10 pediatric subjects [3], in which therapists will employ the DSS throughout the sessions and then evaluate its usability with the System Usability Scale [4]. The proposed DSS is a step forward in pediatric neuromotor rehabilitation, merging real-time engagement assessment with standardized clinical data management into a single e-health system. By reducing the cognitive workload of the annotation process, the DSS allows therapists to better focus on the therapeutic relationship. Furthermore, the DSS does not override therapists in the clinical decision-making process, but provides a holistic view of the patient's engagement state, empowering therapists to tailor the rehabilitation activity to both patients' clinical and psychological needs.

5. References

1. Graffigna et al. (2017) doi:10.1701/2812.28441
2. King et al., (2014) doi:10.1111/camh.12015
3. https://clinicaltrials.gov/study/NCT06993389
4. Brooke (1996) doi:10.1201/9781498710411

Acknowledgements: This work was supported by the Italian Ministry of Health (ricerca corrente 2025-2026 to Dr. E. Biffi) and by the Italian Ministry of University and Research (doctoral scholarship to S. Costantini).

COMPARISON OF BIOMECHANICAL STABILITY OF ANKLE ARTHRODESIS TECHNIQUES USING FINITE ELEMENT ANALYSIS

Atsuki Tanaka, Noriyuki Kanzaki, Tetsuya Yamamoto, Toshiharu Takami
Ryo Okada, Shin Yoshida, Masamune Kamachi, Shohei Sano, Ryosuke Kuroda

Department of Orthopaedic Surgery, Kobe University Graduate School of Medicine, Kobe, Japan

1. Introduction

Ankle arthrodesis is an effective treatment for ankle osteoarthritis (OA). However, an optimal fixation method remains controversial. Therefore, the objective of this study is to compare the mechanical stability of multiple fixation methods in ankle arthrodesis using finite element analysis (FEA).

2. Materials and Methods

The 3-dimensional tibia and talus models were created using preoperative computed tomography (CT) images of OA patients. Three fixation models were constructed using cannulated cancellous screws (CCSs) and a minimally invasive anterior plate: (a) a double-screw model (Double), consisting of two CCSs from the medial and lateral sides of the tibia, (b) a triple-screw model (Triple), consisting of three CCSs from the medial side of the tibia, and (c) a screw-plate hybrid model (Hybrid), consisting of two CCSs from the medial and lateral sides of the tibia with an anterior plate (Figure 1). The implant material properties were assigned a titanium alloy (108.9 GPa), and the bone material properties were calculated from the CT Hounsfield units using the equation reported by Keyak et al. [1]. A vertical load of 2000 N was applied along the bone axis from the tibial shaft to simulate weight-bearing, with the distal talus fixed [2]. Linear elastic analysis was performed using FEA software (Mechanical Finder ver.13, Research Center of Computational Mechanics, Inc., Tokyo, Japan) to evaluate the 99th-percentile von Mises stress and stress distribution in the implants, as well as the contact pressure distribution at the talotibial joint.

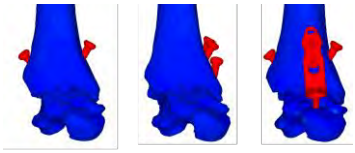


Figure 1: **Three fixation models.** (a) Two cannulated cancellous screws (CCSs) (Double). (b) three CCSs (Triple). (c) Two CCSs with an anterior plate (Hybrid).

3. Results

The 99th-percentile von Mises stress for each implant was 49.50 MPa in model (a), (b) 55.01 MPa in model (b), and 63.18 MPa in model (c) (Figure 2). Mean and peak contact pressures on the talus surface were 2.51 and 36.52 MPa in model (a), 3.28 and 32.08 MPa in model (b), and 2.06 and 26.79 MPa in model (c), respectively. (Figure 3). Contact pressure was more concentrated anterior to the talus in models (a) and (b).

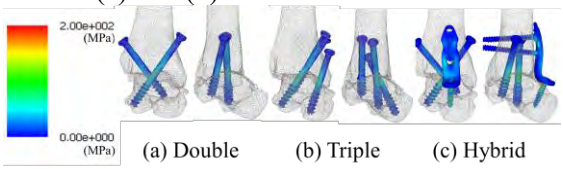


Figure 2: **The distribution of von Mises equivalent stress of implants.**

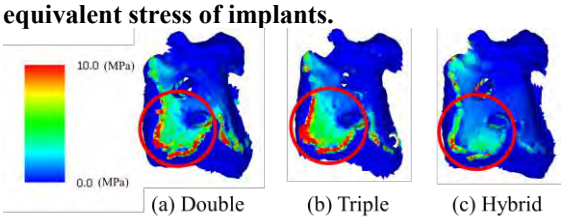


Figure 3: **The distribution of contact pressure on the talus surface.**

4. Discussion and Conclusions

The 99th-percentile von Mises stress remained below the yield strength of the titanium alloy in all models, indicating adequate structural safety under simulated weight-bearing conditions. Model (c), which included two CCSs and an anterior plate, showed lower contact pressure, particularly in the anterior talus. Because excessive contact pressure may increase the risk of non-union [3], anterior plate placement may help reduce anterior contact pressure and potentially lower the risk of non-union.

5. References

1. Keyak JH, Lee IY, Skinner HB. J Biomed Mater Res. 1994;28(11):1329-1336.
2. Feng B, Gao QB, Dai GM, et al. Eur J Med Res. 2023;28(1):574.
3. Weigert A, Kistler M, Bauer L, et al. J Orthop Surg Res. 2024;19(1):475.

ANGULATED SCREW CONFIGURATION REDUCES IMPLANT STRESS IN SUBTALAR ARTHRODESIS: A FINITE ELEMENT STUDY

Tetsuya Yamamoto, Atsuki Tanaka, Noriyuki Kanzaki, Toshiharu Takami, Ryo Okada, Masamune Kamachi, Shohei Sano, Ryosuke Kuroda

Department of Orthopaedic Surgery, Kobe University Graduate School of Medicine, Kobe, Japan

1. Introduction

Subtalar arthrodesis is widely performed for post-traumatic osteoarthritis (OA). However, the optimal screw orientation and number remain controversial. The purpose of this study was to compare the mechanical stability of three screw constructs for subtalar arthrodesis using finite element analysis (FEA).

2. Materials and Methods

Three-dimensional models of the talus and calcaneus were reconstructed from computed tomography (CT) data of a patient with subtalar OA. Three fixation constructs were evaluated: (a) posterior parallel two-screw construct (Parallel), (b) angulated two-screw construct (Angulated), and (c) three-screw construct (Triple), which included two posterior screws and an additional angulated screw (Figure 1). The implant material properties were defined as titanium alloy (Young's modulus, 108.9 GPa). Bone material properties were assigned based on CT Hounsfield units using the conversion equation [1].

A compressive preload of 100 N was applied along the longitudinal axis of each screw to simulate intraoperative tightening [2]. Subsequently, a vertical load of 2000 N was applied to the superior surface of the talus along the tibial axis to simulate physiological weight-bearing. The plantar surface of the calcaneus was fully constrained. Linear elastic finite element analysis was performed using Mechanical Finder (ver.13, Research Center of Computational Mechanics, Inc., Tokyo, Japan). Implant stress was quantified using the 99th-percentile and mean von Mises stress, and stress distribution within the implants was assessed.

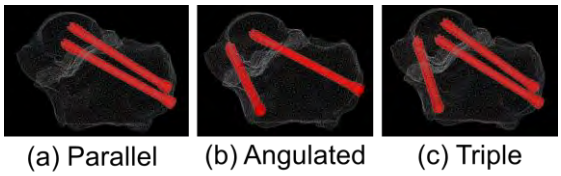


Figure 1: Three fixation constructs.

3. Results

The posterior parallel two-screw construct demonstrated the highest implant stress among all constructs, with 99th-percentile stresses of 452.5 MPa and 511.3 MPa and mean stresses of 80.4 MPa and 92.1 MPa.

The angulated two-screw construct markedly reduced implant stress compared with the parallel construct, with 99th-percentile stresses of 133.0 MPa and 157.4 MPa and mean stresses of 30.5 MPa and 40.3 MPa.

The three-screw construct showed the lowest overall stress distribution, with 99th-percentile stresses of 99.4 MPa, 118.3 MPa, and 109.0 MPa and mean stresses of 21.9 MPa, 29.4 MPa, and 33.6 MPa (Figure 2).

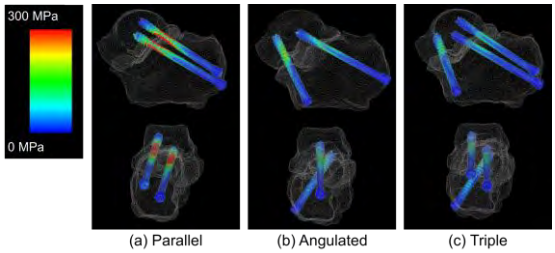


Figure 2: Distribution of von Mises equivalent stress in the implants.

4. Discussion and Conclusions

Angulated two-screw placement reduced implant stress relative to posterior parallel fixation. Although the three-screw construct yielded the lowest stress, the incremental advantage over the angulated two-screw construct was small. Therefore, the optimal construct (angulated two-screw vs three-screw) cannot be determined from these data alone; however, the findings suggest that screw orientation is a key determinant of mechanical stability in subtalar arthrodesis.

5. References

1. Keyak JH, Lee IY, Skinner HB. J Biomed Mater Res. 1994;28(11):1329-1336 (1994).
2. Lee JY, Lee YS, Knee Surg Sports Traumatol Arthrosc; 19(5):842-849 (2011).

FAST HIGH-FIDELITY NEURAL NETWORK SURROGATE FOR INFERENCE OF A CARDIOVASCULAR-BAROREFLEX MODEL

Arthur Ben-Tolila* (1), Xing Chen* (2), Joan Duprez (1), Adrien Al Wazzan (1), Erwan Donal (1), Alfredo I Hernández (1), Felix Agakov◇ (2), Virginie Le Rolle◇ (1)

1. Univ Rennes, CHU Rennes, Inserm, LTSI - U1099, Rennes, FR; 2. Pharmatics Ltd., Edinburgh, UK

** Arthur Ben-Tolila and Xing Chen are equal contributors. ◇ Felix Agakov and Virginie Le Rolle are equal contributors.*

Correspondence: Arthur Ben-Tolila (arthur.ben-tolila@univ-rennes.fr), Univ Rennes, Rennes, FR

1. Introduction

Hypertrophic cardiomyopathy (HCM) is a common inherited cardiac disease with heterogeneous phenotypes, involving left ventricular (LV) thickness, autonomic impairment, and LV outflow tract (LVOT) obstruction. Our team has recently proposed an integrated cardiovascular-baroreflex model based on [1,2] to analyse these dynamics. However, its number of parameters and the length of the simulation make it computationally expensive. We therefore developed a fast multi-output machine learning surrogate that approximates the mapping from 684 lumped-model parameters to 150 features relevant to HCM, enabling efficient exploration of the parameter space while preserving fidelity to the original simulator.

2. Materials and Methods

A lumped-parameter model of the cardiovascular system, including the cardiac electrical activity, the atria, multi-segment ventricles with myocardial strain curves, the LVOT, the circulation, and the baroreflex, was developed based on previous works [1,2] in the context of HCM. A Latin hypercube sampling of the 684 model parameters was performed in an interval of ±20% of their basal value, to derive 10000 simulations. 150 features were computed on the steady-state simulations, including LV end-diastolic and end-systolic volumes, heart rate, cardiac output, LVOT pressure gradient, peak LV strains timing and amplitude. The surrogate model was built as a 6-block residual MLP [3] with width 256, dropout 0.1, and ~1.01M parameters, trained jointly on all outputs. Performance was estimated by 5-fold cross-validation with fold-specific scaling, inner-fold validation for early stopping, and pooled out-of-fold predictions. Ordinary least squares and TabM [4] were evaluated on identical folds for comparison.

3. Results

Across outputs, the residual network achieved mean $R^2 = 0.940 \pm 0.155$ and median $R^2 = 0.979$ [IQR 0.975–0.987]; 134/150 outputs exceeded $R^2 = 0.95$ and 138 exceeded $R^2 = 0.80$. Fold-to-fold variability was low (median per-output R^2 SD = 0.0015 [IQR 0.0012–0.0026]). The model outperformed the linear baseline (median R^2 = 0.876 [IQR 0.786–0.909]) and was marginally superior to TabM (median R^2 = 0.974 [IQR 0.961–0.981]). On a laptop-class Apple M4 CPU (10-core CPU, 16 GB unified memory; PyTorch CPU backend), batched inference required 3.07 µs per sample [IQR 3.00–3.45; batch size = 256]; single-sample latency was 110 µs. Simulator PRCC and out-of-fold surrogate PRCC were highly concordant (cell-wise Pearson r = 0.996; input-importance Spearman rho = 0.997), indicating near-complete preservation of the simulator's global sensitivity structure.

4. Discussion and Conclusions

This proof of concept demonstrates the feasibility of compact surrogate modelling to predict complex physiological model outputs with high fidelity, preserved sensitivity structure, and microsecond-scale inference. Ongoing work aims to use the surrogate for parametric analyses and building digital twins.

5. References

1. Menna F et al., CinC conference, 2024, p. 1-4.
2. Ben-Tolila A et al., IEEE Trans Biomed Eng; 73(6): 2063-2073; 2026.
3. He K et al. Identity mappings in deep residual networks. ECCV; 2016.
4. Gorishniy Y et al. TabM: advancing tabular deep learning with parameter-efficient ensembling. arXiv:2410.24210; 2024.

Acknowledgements:

This work is part of the HORIZON-HLTH-2023-TOOL-05 SMASH-HCM project funded by the European Union under Grant 101137115 and UKRI 10109598.

AUTOMATED FINITE ELEMENT MODELS OF VERTEBRAE FOR PATIENT-SPECIFIC BONE FRAGILITY ASSESSMENT

Giulia Fraterrigo (1), Enrico Schileo (1), Fulvia Taddei (1), Lorenzo Grassi (2)

1. Istituto Ortopedico Rizzoli, Italy; 2. Lund University, Sweden

1. Introduction

Vertebral fractures are the most common osteoporotic fractures[1], despite up to 70% remain undiagnosed[2]. Conventional DXA-based bone mineral density (BMD) has limited predictive value due to confounding factors linked to degenerative changes[3].

Subject-specific finite element (FE) models provide more accurate strength estimates and can leverage opportunistic CT scans to improve fracture risk assessment. However, their clinical use is limited by the lack of automated pipelines. This study therefore aims to automatically generate subject-specific vertebral FE models from CT data.

2. Materials and Methods

The CT2FEM workflow uses a mesh-based statistical shape and appearance model (SSAM) of the L1 vertebra, fitted to a patient's CT scan to generate subject-specific FE models

Materials: 45 in vivo spine CT scans (voxel size 0.3x0.3x1 mm, GE BrightSpeed).

Methods: L1 vertebrae were semi-automatically segmented to extract endocortical and periosteal surfaces. A tetrahedral template mesh was morphed in MATLAB, and material properties assigned using Bonemat with cortical bone mapping[4]. The resulting 45 manually generated isotopological FE meshes were used to train a SSAM (previously proposed[5] and validated[6] for the human femur).

Automatic model generation involved fitting the SSAM to target CT scans via genetic algorithm optimization minimizing voxel-wise differences to the target CT.

Reconstruction accuracy was evaluated as mean absolute error (MAE) in shape and volumetric BMD against manually generated FE models.

3. Results

The shape of the 45 L1 vertebrae was reconstructed with a median MAE of 0.9 mm (range 0.7-1.7 mm), with peak errors of ~9 mm localized in the posterior processes (figure 1). The median MAE for the volumetric BMD was 0.06 g/cm^3 (range 0.04-0.09 g/cm^3), with the largest errors concentrated in the vertebral endplates and in the posterior processes (fig 1).

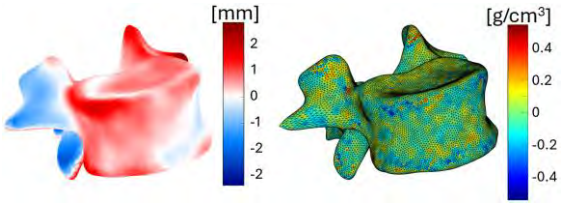


Figure 1: To the left, shape reconstruction errors for a representative vertebra. To the right, errors in volumetric BMD reconstruction.

4. Discussion and Conclusions

We presented an automatic pipeline to generate subject-specific FE models of the human vertebra from in vivo CT images, including both geometry and heterogeneous material properties for strength assessment.

The automatic models showed high agreement with manual FE models (0.9 mm, comparable to CT voxel size), and volumetric BMD was accurately reproduced (MAE 0.06 g/cm^3 vs ~1.8 g/cm^3 peak). Accuracy was highest in the vertebral body, the main contributor to strength.

Future work will apply cross-validation to the reconstructions and perform FE analyses to assess prediction of vertebral strength.

5. References

1. Kelly, M.A. et al. (2021). J. Clin. Densitom. Off. J. Int. Soc. Clin. Densitom., 24, 183–189
2. Schousboe, J.T. (2017). J. Bone Miner. Res., 32, 1783–1788
3. Jain, R.K. et al. (2017). J. Clin. Densitom. Off. J. Int. Soc. Clin. Densitom., 20, 291–303
4. Schileo, E. et al. (2020). Bone, 136, 115348
5. Väänänen, S.P. et al. (2015). Med. Image Anal., 24, 125–134
6. Grassi, L. et al. (2023). J. Bone Miner. Res., 38, 1258–1267

Acknowledgements:

We thank the C.M. Lerici Fondation for the financial support, and LUNARC (the center for scientific and technical computing at Lund University) for the computational resources.

DESIGN OPTIMISATION OF DIALYSIS CATHETERS FOR PAEDIATRIC PATIENTS USING A COMPUTATIONAL APPROACH

Claudia Bruno (1), Aila Klostermann (2), Jan Oldenburg (2), Finja Borowski (2), Michael Stiehm (2), Silvia Schievano (1), Rukshana Shroff (3), Claudio Capelli (1)

1. University College London, London, UK; 2. Institute for ImplantTechnology and Biomaterials e.V., Rostock, Germany; 3. Great Ormond Street Hospital for Children, London, UK.

1. Introduction

Central venous lines (CVLs) used for haemodialysis (HD) in children are associated with a high complication rate leading to inadequate HD and line replacement. This project aimed at: i) improving CVLs performance by combining optimisation algorithms and computational fluid dynamics (CFD) simulations and, ii) confirming these results by means of particle image velocimetry (PIV).

2. Materials and Methods

Four models of CVLs of different design and sizes (6.5Fr, 8Fr, 10Fr and 14Fr) were recreated and parametrised in SolidWorks. Steady state CFD analyses were set up in Ansys Fluent to simulate the CVLs' performance. A Design of Experiment (DOE) analysis was performed in Ansys optiSLang to assess the influence of the side holes (SHs) and shape of the tip on the performance of CVLs in terms of flow distribution, shear stress (SS) and residence time. For each CVL model, sampled designs were evaluated by the CFD solver. Metamodels of the responses were created and multi-objective optimisation algorithms were applied. Experimental testing of one specific CFD analysis was conducted using PIV. The CVL geometry was scaled five times for improved spatial resolution, while maintaining fluid mechanical comparability. The model was manufactured using two-component silicone molded in 3D-printed molds to ensure high transparency.

3. Results

Overall, the DOE showed that dimension of SHs had a predominant role over their position, and the SS was the one output that would depend more on the tip geometry. In three out of the four catheters, metamodels showed good approximation capabilities for the SHs' flow rates (CoP range: 82-99%), the tip flow rate (78-94%) and the average SS (95-97%).

The most significant reduction of average SS was seen in the 10Fr model. The Pareto-optimal solutions predicted by the metamodels ranged between 9.04-9.94 Pa in the withdrawing arterial lumen and 13.94-14.89 Pa in the infusing venous lumen. CFD simulations of the predicted designs showed good agreement (highest errors: 1.94% [arterial], 2.51% [venous]). These models showed lower values of SS (average: -26.3% [arterial], -10.4% [venous]) compared to the original design, which fell within the dominated area of the plot (Figure 1). Improvement was also seen in the 6.5Fr model. Designs showed lower average arterial SS (-16.0% in average) but increased maximum (11.6% in average) in all except three designs. PIV measurements showed good agreement between CFD and its experimental counterparts in terms of velocity distribution.

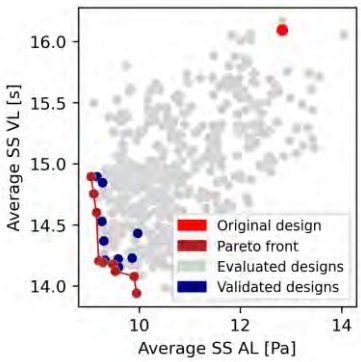


Figure 1: Multi-objective optimisation on the SS of the arterial and venous lumen of the 10Fr model.

4. Discussion and Conclusions

A workflow was developed to optimise the design and performance of CVLs for paediatric patients on HD. The optimised designs demonstrated good performance overall, in some cases outperforming the original model by reducing SS and therefore lowering the associated thrombogenic potential.

Acknowledgements:

Thanks to the NIHR (NIHR303049) and Kidney Research UK (ST_013_20220706).

STRUCTURAL DESIGN AND OPTIMIZATION OF BIODEGRADABLE ZINC ALLOY VASCULAR STENTS BASED ON MACHINE LEARNING

Zhihan Lin, Guangyin Yuan*

School of Materials Science & Engineering, Shanghai Jiao Tong University, Shanghai 200240, China

1. Introduction

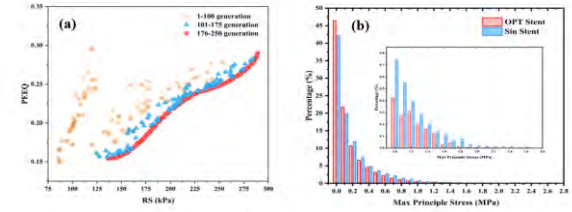
Compared to permanent stents, biodegradable zinc alloy stents exhibit inferior mechanical properties and are prone to local rapid corrosion caused by residual stress concentration during service. This study employs machine learning techniques to optimize the structural design of biodegradable zinc alloy vascular stents, developing a 100 μm thick stent with high radial strength and uniform residual stress distribution after expansion.

2. Materials and Methods

The stent material used is an annealed Zn-Cu-Mn alloy tube, previously prepared by our research group [1], with an elastic modulus of 108 GPa, a tensile strength of 361 MPa, and an elongation of 48.5%. Using the NSGA-II algorithm, stent design parameters conforming to the optimization results were obtained. The optimization objective for the stent is to maximize radial strength while minimizing equivalent plastic strain (PEEQ). After optimization, physical prototypes are fabricated and directly evaluated against existing stent designs to validate performance.

3. Results

Compared to the traditional sinusoidal-wave stent, the optimized stent exhibits a significant improvement in radial strength, along with reduced elastic recoil and axial shortening. The residual stress distribution is more uniform, resulting in better overall mechanical performance, as shown in Fig.1 and Table 1.



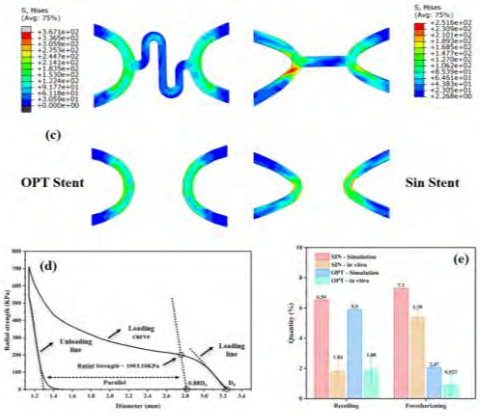


Figure 1: (a) shows the Pareto front through NSGA-II algorithm optimization; (b) shows the stress exerted on vessels by the OPT stent versus the sin stent; (c) shows contour maps of residual stress distribution for both OPT stent and sin stent; (d) shows the radial strength test diagram of the optimized stent; (e) shows simulation and experimental data comparison of radial recoil and foreshortening between the OPT stent and the sin stent.

Table 1: Result summary of the two stent types

Type	Radial strength(KPa)	Radial Recoil (%)	Foreshortening (%)
OPT	190	5.9	0.92
SIN	87	6.54	5.39

4. Discussion and Conclusions

To address the challenges of prolonged development cycles and high costs associated with traditional trial-and-error design methods, this study employs machine learning techniques to optimize the structural design of biodegradable zinc alloy vascular stents. The objective is to enhance the overall performance of the stents and meet the clinical requirements for the application of biodegradable zinc alloy vascular stents.

5. References

1. Jiang J, et al. Acta Biomater., 2022, 151: 647-660.

Acknowledgements:

This work was supported by the Science and Technology Commission of Shanghai Municipality (No. 25CL2900504).

MODELLING STENT-INDUCED REMODELLING IN ANEURYSMAL AORTAS USING HOMOGENISED CONSTRAINED MIXTURE THEORY

Sathish Kumar Marimuthu (1), **Craig Maclean** (3), **Robbie Brodie** (3), **Nicholas A. Hill** (2), **Sean McGinty** (1)

1. *James Watt School of Engineering, University of Glasgow, Glasgow, UK;* 2. *School of Mathematics and Statistics, University of Glasgow, Glasgow, UK;* 3. *R&D, TerumoAortic, Glasgow, UK*

1. Introduction

Endovascular aortic repair (EVAR) stent grafts contain metallic scaffolds covered by a fabric membrane to stop the blood from contacting the fragile aneurysmal wall. To ensure sealing and fixation, the top portion of the stent graft implanted in the healthy region above the aneurysm is designed slightly oversized and stiffer than the local aorta, which causes the aorta to expand over time [1], to relieve the excessive stresses. It is important to understand the extent of post-operative expansion in order to predict the long-term device geometry for durability assessments. The aim of this work is to develop a growth and remodelling (G&R) framework to explore and predict vascular adaptation after stenting.

2. Materials and Methods

The aorta is composed of several constituents, such as smooth muscle cells (SMC), elastic fibres, collagen fibres (CF) and elastic matrix (EM), and each constituent has its individual natural state and G&R capabilities. Humphrey and Rajagopal introduced constrained mixture theory [2], and Zhang et al. [4] used the homogenised version of it (proposed by Braeu et al. [3]) to simulate vascular adaptation after stent implantation in aortic aneurysms, but with a simplified axisymmetric cylinder and spring-based stent representation. Here, we implemented a homogenised constrained mixture theory in Abaqus Dynamics/Explicit using user material (Fortran) subroutines to model stent-induced vascular adaptation in a patient-specific aorta with the original implanted stent.

The decoupled total deformation gradient is $\boldsymbol{F} = \boldsymbol{F}_e^i\,\boldsymbol{F}_g\,\boldsymbol{F}_r^i$, which can be rewritten as $\boldsymbol{F}_e^i = \boldsymbol{F}\,\boldsymbol{F}_g^{-1}\,(\boldsymbol{F}_r^i)^{-1}$. The homogenised growth deformation gradient is $\boldsymbol{F}_g = \boldsymbol{I} + \left(\frac{\rho_R^{\text{tot}}}{\rho_{R0}^{\text{tot}}} - 1\right)(\boldsymbol{a}_0^g \otimes \boldsymbol{a}_0^g)$, where $\rho_R^{\text{tot}} = \rho_R^e + \rho_R^{c_1} + \rho_R^{c_2} + \rho_R^m$ and $\boldsymbol{a}_0^g$ is the growth direction. The constituent-specific remodelling deformation gradient is $\boldsymbol{F}_r^i = \lambda_r^i\,\boldsymbol{M}^i + \frac{1}{\sqrt{\lambda_r^i}}\left(\boldsymbol{I} - \boldsymbol{M}^i\right)$. The stress-driven mass turnover is $\dot{\rho}_R^i = \rho_R^i\,k_\sigma^i\left(\frac{\sigma^i - \sigma_h^i}{\sigma_h^i}\right) + \dot{D}^i$, and the remodelling rate is $\dot{\lambda}_r^i = \left(\frac{\dot{\rho}_R^i}{\rho_R^i} + \frac{1}{T^i}\right)\left(\frac{\lambda_e^i}{\lambda_e^i}\right)^2 \frac{\sigma^i - \sigma_h^i}{\partial\sigma^i/\partial\lambda_e^i}$. Here, k_σ^i is the stress-gain parameter and $\dot{D}^i$ is an optional degradation/loss term, often used for elastin. The scalar constituent current and homeostatic stresses are directional projections, $\sigma^i = \boldsymbol{\sigma}^i : \boldsymbol{M}^i$ and $\sigma_h^i = \boldsymbol{\sigma}_h^i : \boldsymbol{M}^i$, with $\boldsymbol{M}^i$ built from unit reference directions. Finally, the constituent Cauchy stress is computed from the elastic deformation gradient as $\boldsymbol{\sigma}^i = \boldsymbol{\sigma}^i(\boldsymbol{F}_e^i)$ and the total Cauchy stress is $\boldsymbol{\sigma} = \sum_i \boldsymbol{\sigma}^i$.

3. Results

The stress plots for the zero-stress, residual stress (axial pre-stretch and diastolic pressure), stented and G&R stages are shown below. The results show a reduction in stress from the stented stage to G&R, which supports the hypothesis of stress relaxation caused by vascular adaptations.

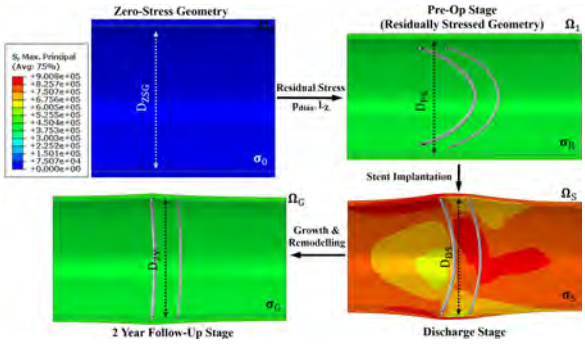


Figure 1: Stress plots for the zero-stress, residual stress, stented and G&R stages.

4. Results

A patient-specific homogenised constrained mixture theory framework was successfully implemented for preliminary AAA data. The early results support the expected stress relaxation trend after vascular adaptation and suggest that the framework can be used to investigate the influence of stent oversizing on long-term aortic response.

5. References

[1] Koenrades MA et al. J Endovasc Ther. 2018.
[2] Humphrey JD, Rajagopal KR. Math Models Methods Appl Sci. 2002.
[3] Braeu FA et al. Biomech Model Mechanobiol. 2017.
[4] Zhang S et al. Int J Numer Meth Biomed Engng. 2022.

IN-SILICO ASSESSMENT OF CONTACT FORCE EFFECTS IN CARDIAC CATHETER ABLATION

Argyrios Petras (1), Luca Pasini (1), Minha Anees (1), Zoraida Moreno Weidmann (2), David Vilades Medel (2), Aurel Neic (3), Edward J. Vigmond (4,5), Jose M. Guerra (2), Luca Gerardo-Giorda (6)

1. RICAM – Johann Radon Institute for Computational and Applied Mathematics, Austria; 2. Hospital de la Santa Creu i Sant Pau, IR SANT PAU, Universitat Autonoma de Barcelona, CIBERCV, Spain; 3. NumeriCor GmbH, Austria; 4. Liryc Heart Rhythm Disease Institute, Fondation Bordeaux University, France; 5. CNRS, Bordeaux INP, IMB, University of Bordeaux, France; 6. Johannes Kepler University (JKU), Austria

1. Introduction

Contact force between the catheter tip and cardiac tissue is a key factor in catheter ablation procedures. While its influence on lesion formation during radiofrequency ablation (RFA) is well established, its role in pulsed field ablation (PFA) remains less clear, with mixed findings reported in the literature. This work aims to assess the role of contact force in monopolar applications using an in-silico framework, enabling a direct comparison of its effects on lesion formation in RFA and PFA.

2. Materials and Methods

An in-silico framework was used to investigate the influence of catheter–tissue contact force during cardiac ablation procedures. A virtual porcine geometry was used, as described in [1], including rule-based myocardial fiber orientation at the ventricles, with the catheter positioned epicardially on the left ventricle.

RFA was simulated using an electrothermal model incorporating electric field computation and temperature evolution within the tissue [2]. PFA was modelled using the electric field–based formulation described in [1], enabling the estimation of the electric field distribution generated during pulse delivery.

In both cases, catheter–tissue interaction was accounted for by solving a contact mechanics problem to quantify tissue deformation under different applied contact forces (10 g, 20 g, and 30 g). The myocardium was modelled as a nearly incompressible orthotropic hyperelastic material using the Usyk constitutive formulation.

3. Results

The simulations show that catheter–tissue contact force significantly affects lesion formation in both ablation modalities. For RFA, lesions were quantified using the 50 °C isotherm contour. Increasing contact force resulted in a consistent enlargement of lesion dimensions. For PFA, lesions were evaluated using a lethal electric field threshold of 400 V/cm. In this case, contact force predominantly affected lesion depth, as greater tissue deformation brought deeper myocardial regions within the effective electric field. In contrast, lesion width exhibited only minor variations.

4. Discussion and Conclusions

Our results show that contact force affects lesion formation differently in the two ablation modalities. In RFA, increasing contact force enlarges lesions in both depth and width due to enhanced thermal energy transfer. In contrast, PFA is mainly affected in terms of lesion depth, while lesion width remains largely unchanged, reflecting the dominant role of the electric field distribution in determining PFA lesion extent.

5. References

1. Petras A et al., Heart Rhythm O2; 2025.
2. Petras A et al., Int J Numer Method Biomed Eng; 2019.

Acknowledgements:
A.P, L.P and L.GG acknowledge the partial support of the State of Upper Austria. A.P, L.P and A.N. acknowledge the FFG Bridge grant PFA-Mod.

DEPTH-DEPENDENT CORONARY CLEARANCE AFTER TAVI: A PATIENT-SPECIFIC IN SILICO STUDY

Sheikh Umara Zoni (1), Luis Rene Mata Quinonez (2), Sanchita Bhat (2), Lakshmi Prasad Dasi (2) and Shelly Singh-Gryzbon (1)

1. Department of Chemical Engineering & Biotechnology, University of Cambridge, Cambridge, UK; 2. Department of Biomedical Engineering, Georgia Institute of Technology, Atlanta, GA, USA

Correspondence to Sheikh Umara Zoni, Department of Chemical Engineering & Biotechnology, University of Cambridge, CB3 0AS Cambridge, UK; suz20@cam.ac.uk

1. Introduction

Transcatheter aortic valve implantation (TAVI) is an established treatment for severe calcific aortic stenosis. Despite favourable outcomes, coronary obstruction (Cob) remains a rare but life-threatening complication. Current risk stratification relies on pre-procedural CT-derived geometric measurements obtained using virtual transcatheter heart valve (THV) overlays. However, these measurements assume an idealised valve position and cannot capture deformation and displacement of THV components, calcifications, native leaflets, and the aortic root during deployment. Computational modelling can overcome this limitation by simulating valve deployment and capturing device-anatomy interactions. Therefore, this study proposes a patient-specific computational framework to simulate balloon-expandable valves (BEV) at varying implantation depths and evaluate post-deployment distances between the coronary ostia and surrounding structures as geometric indicators of potential Cob risk.

2. Materials and Methods

A patient-specific aortic root was reconstructed from CT images, while μCT data generated a 23 mm BEV model. Using Abaqus, the valve was crimped, aligned on a compliant balloon, and deployed at the *annular* level using fluid-cavity interactions. Additional simulations were performed for *sub-* and *supra-annular* implantation ($\pm$2 mm from the annulus). Post-deployment, minimum distances between surrounding structures (THV, calcification, native leaflets) and the left and right coronary ostia were measured. Tie constraints were applied between device and anatomical components, with boundary constraints at the balloon and aortic ends. Global contact with a friction coefficient of 0.26 was defined between surfaces. Material models included hyperelastic (*aorta, leaflets, skirt*), elasto-plastic (*frame, calcifications*) and elastic (*balloon*).

3. Results

Minimum distances between surrounding structures and the coronary ostia were measured across three implantation depths (Fig. 1). Supra-annular deployment produced greater leaflet clearance, whereas nominal and sub-annular cases showed smaller distances, particularly for the stent frame. The stent frame and native leaflets were more frequently closest to the coronary ostia while THV leaflets showed the greatest clearance, especially in sub-annular configurations where they remained below the ostia.



Fig. 1: Minimum distance between THV components and native leaflets to coronary arteries.

4. Discussion and Conclusions

Patient-specific simulations showed smaller clearances between surrounding structures and the LCA compared with the RCA, consistent with clinical observations that Cob following TAVI occurs more frequently in the LCA [1]. Calcifications within the LCA ostium were identified but excluded as they represented pre-existing anatomy rather than displaced structures. Aortic root calcifications near the RCA showed variable distances (1-2 mm), suggesting calcific protrusion may contribute to obstruction despite larger leaflet or frame clearances. These findings highlight the importance of evaluating both structural displacement and calcification distribution when assessing Cob risk. Future work will incorporate CFD to investigate how these geometric relationships influence coronary flow and, extend the analysis to self-expanding valves and larger patient cohorts.

5. References

1. Fan J et al. FCVM.2024;11:1432235 (2024).

HIGH FIDELITY INTRASACCULAR FLOW DISRUPTOR MODELLING FOR INTRACRANIAL ANEURYSM TREATMENT

Chiara Faitini (1), Philippe Meliga (1), Yves Chau (2), Elie Hachem (1)

1. MINES Paris, PSL University, CEMEF – Centre for material forming, rue Claude Daunesse 06904, Sophia Antipolis, France

2. Interventional Neuroradiology Department, Nice University Hospital, Nice, France

Corresponding author: Chiara Faitini, MINES Paris, PSL University, CEMEF, rue Claude Daunesse 06904, Sophia Antipolis, France. Email: chiara.faitini@minesparis.psl.eu

1. Introduction

Intrasaccular flow disruptors are endovascular devices employed in the treatment of bifurcation intracranial aneurysms, with the aim of sealing the aneurysm and restoring the physiological blood flow in the brain arteries. Given the novelty of these devices, surgical pre-planning and device size selection remain significant clinical challenges. In this work, we propose a computational framework that predicts the mechanical behaviour of flow disruptors and provides an evaluation of post-implant hemodynamics. This represents an important step towards enhancing clinical pre-planning and decision-making.

2. Materials and Methods

Intrasaccular flow disruptors are braided NiTi structures deployed within the aneurysm and conforming to its often irregular morphology. While previous literature has primarily addressed the prediction of device deployment from a purely geometrical perspective [1], we propose a high-fidelity framework that integrates experimental mechanical testing with advanced computational simulations. The experimental phase involves uniaxial compression tests on various device samples, following established protocols for stent characterization [2]. These data inform Finite Element (FE) simulations in Abaqus, which are used to develop a robust model and simulate device deployment within patient-specific scenarios. Finally, the framework is complemented by Computational Fluid Dynamics (CFD) simulations to assess the hemodynamic impact in the treated cases.

3. Results

The mechanical testing results, integrated with Digital Image Correlation (DIC) data, were leveraged to calibrate the FE solver, enabling the development of a constitutive law that ensures a robust pre-implant performance assessment. Figure 1 illustrates the real sample and its virtual reproduction, as well as the force-displacement relation under compression. Hemodynamic results will also be presented to complement the work.

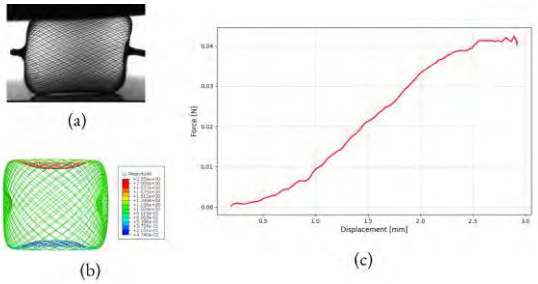


Figure 1: Experimental testing (a), Abaqus model (b) and force-displacement relation (c).

4. Discussion and Conclusions

This work introduces a robust computational framework for simulating the deployment of intrasaccular flow disruptors and analysing the resulting changes in blood flow patterns. By grounding the model on experimental mechanical data, we have achieved a high level of reliability. This methodology represents a significant advancement in reducing procedural risks and optimizing clinical outcomes through precise patient-specific device modeling.

5. References

1. R. Muñoz et al. Computers in Biology and Medicine. 2022.
2. R. Ubachs et al. Journal of the Mechanical Behavior of Biomedical Materials. 2023.

Acknowledgements:

The authors would like to thank the European Research Council (Grant no: 101045042) for providing financial support to this project.

FSI MODELLING OF SUB-CLINICAL LEAFLET THROMBOSIS FOLLOWING TRANSCATHETER AORTIC VALVE INTERVENTION

Maria Isabel Pons Vidal (1), Harriet Hurrell (2), Simon Redwood (2), Tiffany Patterson (2), Jack Lee (1)

1. School of Biomedical Engineering and Imaging Sciences, King's College London, UK; 2. St Thomas Hospital, London, UK

1. Introduction

TAVI is now the dominant form of aortic valve replacement over surgery, and its indication is expanding to include younger and lower risk patients. However, in 30% of the cases, Subclinical Leaflet Thrombosis (SLT) is reported within 1 year of the procedure [1]. Clinical investigation has yielded conflicting evidence regarding causes and mechanisms of SLT, with implications for patient management and the need for redo-TAVI procedures. We present our work-in-progress FSI modelling to assess the haemodynamic contribution to SLT in a patient-specific setting.

2. Materials and Methods

Edwards Sapien 3 and Ultra bioprosthetic transcatheter valves were imaged using a micro-CT scanner at 17um resolution. The stent geometry was unrolled flat and reconstructed in 2D, yielding a precise blueprint which was then reconstituted to a 3D structure. The leaflet attachment points were identified in the image, which allowed CAD reconstruction of the leaflets, which were validated against leaflet surface geometric measurements.

Clinical data were obtained from a patient undergoing an observational trial at St Thomas Hospital, London, and included the standard of care workup data as well as pre- and post-TAVI CT scans, and invasive pressure measurements. The anatomy spanning LVOT to proximal aorta were segmented and surface-processed in Rhino, and meshed in gmsh for simulations. The TAVI mesh was placed using the post-TAVI CT as reference, making sure to match the commissural alignment.

To compute the flow and valve motion, immersogeometric method [2] was employed which consists of a variational multiscale-stabilised Navier-Stokes solver, isogeometric shell mechanics model representing the leaflets, and immersed boundary coupling of the domains using dynamic augmented Lagrangian method. Inlet flow was taken from the pressure wire measurements while the distal BC was addressed by a 3-element windkessel model. Blood residence time in the aortic sinus region was calculated using an Eulerian advection-diffusion formulation [3].

3. Results

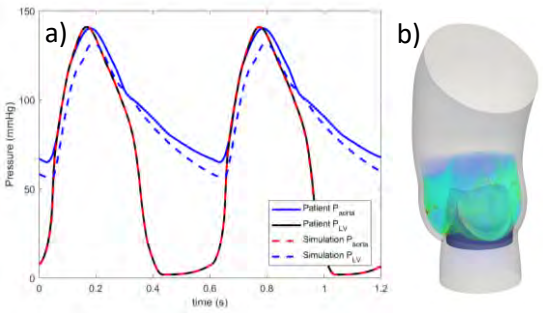


Figure 1: **a)** Aortic and LV pressures, data and simulation **b)** Residence time in sinus region

The distal pressure of the tuned model matched the invasive measurements (Fig 1a) and the cardiac outflow was within the range estimated from echocardiography (5.4 L/min, <12% error), showing a reasonable agreement of the model and clinical data. The blood residence time was elevated in the native sinus, showing a clear dependence on the individual aortic anatomy (Fig 1b).

4. Discussion and Conclusions

Mechanisms of thrombosis in TAVI is an evolving concept and involves many mediators. Though our preliminary results will need to be expanded to further patients, computational modelling provides a unique capacity to integrate structural, haemodynamic and biological risk factors to study the phenomenon.

5. References

1. Makkar RR, Blanke P, Leipsic J, et al. J Am Coll Cardiol. 2020;75(24):3003–3015.
2. Kamensky, D. Comput & Math App 2021;81:634-648.
3. Reza, MMS and Amirhossein A. J biomech 2019;88:122-129.

DESIGN, IN-VITRO AND IN SILICO EVALUATION OF TWO IDEALIZED AORTIC ENDOGRAFT CONFIGURATIONS

Luca Battaglia (1), Michele Conti (2,3), Martina Schembri (2) and Giovanni Spinella (3)

1. Department of Experimental Medicine, University of Genoa, Italy, 2. Department of Civil Engineering and Architecture, University of Pavia, Italy. 3. C3D Lab, IRCCS San Donato, Milan, Italy 4. Department of Vascular and Endovascular Surgery, Policlinico San Martino Hospital, Genoa, Italy

1. Introduction

Stent-graft performance is profoundly influenced by structural design [1]. To predict the biomechanical behavior of customizable poly(ε-caprolactone) (PCL) scaffolds prior to manufacturing, this study presents a robust Finite Element Analysis (FEA) framework. We evaluate two idealized aortic endografts, an off-the-shelf (OTS)-inspired ring-based design and a continuous S-wave lattice, simulating the highly non-linear dynamics of crimping and deployment.

2. Materials and Methods

Idealized PCL endografts (90 mm length, 10% oversized) were modeled based on averaged porcine aortic dimensions (harvested and prepared as biological testbeds-Fig 2A). Two PCL device types were 3D-printed using a pneumatic extrusion-based 3D printer (Cellink, BioX) and closed on a cylindrical mandrel (Fig 1A-B). The two devices are an OTS-inspired structure supported by an 80% infill mesh (Fig 1C), and a continuous S-wave lattice (Fig. 1D).

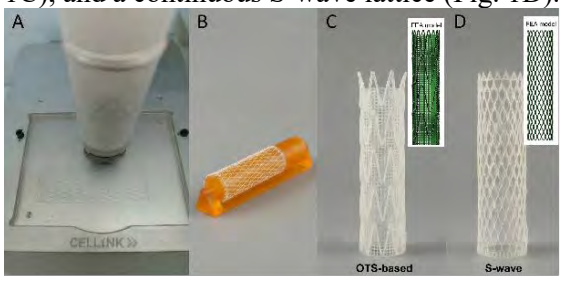


Figure 1: **Manufacturing process and final prototypes of the 3D-printed endografts**. **(A)** Flat 3D printing of the polymer mesh. **(B)** Assembly of the mesh onto a cylindrical mandrel. Final 3D-printed OTS-based **(C)** and S-wave **(D)** endografts.

Models were imported into Abaqus/Explicit, characterizing the PCL with an elastoplastic constitutive model to capture permanent deformations during compression. Simulations involved two quasi-static steps: (1) *Crimping*, applying radial displacement via a rigid surface to compress grafts into a simulated catheter, and (2) *Deployment*, progressively retracting the virtual sheath to allow self-expansion against the aortic wall (Fig 2B).

3. Results

Explicit FEA successfully captured the transient dynamics of both devices (Fig 2C). During crimping, the OTS design exhibited critical stress concentrations at ring nodes, resulting in an 8% permanent diameter reduction (D_r), incomplete wall apposition, and poor migration resistance. Conversely, the S-wave lattice showed a more uniform stress distribution and 5% D_r. However, upon deployment, the S-wave model predicted localized non-uniform expansion, forming a U-shaped segment capable of causing lumen obstruction (Fig 2D).

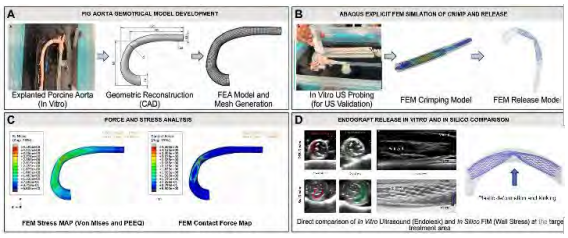


Figure 2: Multimodal validation workflow. (A) Aortic geometric modeling and mesh generation. **(B)** *In vitro* US setup and Abaqus FEA simulation of crimping/deployment. **(C)** Post-deployment FEA structural assessment. **(D)** *In vitro-silico* validation.

4. Discussion and Conclusion

Explicit FEA is a highly effective virtual testing tool for polymeric endografts. The continuous S-wave geometry offers superior stress distribution and shape recovery compared to the OTS design, despite localized incomplete activation. These numerical insights provide a critical foundation for optimizing lattice architectures before manufacturing. Future work will leverage these FEA models in an iterative design loop, followed by experimental validation via in-vitro mock loop testing.

5. References

1. B.R. Bewley, et al, "The evolution of stent grafts for endovascular repair of abdominal aortic aneurysms: how design changes affect clinical outcomes," 10.1080/17434440.2019.1684897.

Acknowledgements:

This work was funded by the European Union (ERC, EPEIUS, 101125466).

A SYSTEMATIC REVIEW OF MULTISCALE VENTRICULAR MODELS: BRIDGING CELLULAR MECHANICS AND GLOBAL HAEMODYNAMICS

Akhilesh Kamqtikar (1), Dirk Donker (1,2), Libera Fresiello (1)

1. *Cardiovascular and Respiratory Physiology, TechMed Centre, University of Twente, Enschede, The Netherlands*
2. *Intensive Care Centre, University Medical Centre Utrecht, Utrecht, The Netherlands*

a.j.kamtikar@utwente.nl , Tel.: +31 53 489 8972, P.O. Box 217, 7500 AE Enschede, The Netherlands

1. Introduction

Understanding how cellular-level myocardial dysfunction drives global pump failure is essential for diagnosing cardiomyopathies and developing targeted therapies. While computational models could support personalised haemodynamic management, the integration of detailed microscale mechanics with whole-heart haemodynamics varies significantly across the literature. This systematic review evaluates computational frameworks that explicitly couple internal cellular mechanics with whole-heart haemodynamics, assessing their capacity to translate microscale pathology into systemic clinical outputs.

2. Materials and Methods

Following PRISMA guidelines [1], Scopus, Web of Science, and PubMed were searched from inception to January 2026. Boolean queries combined terms for cellular mechanics (cardiomyocyte*, sarcomer*, stress*, *strain*) with in-silico and haemodynamic*. Eligible studies explicitly coupled cellular mechanical quantities (e.g., myofibre stress) with global haemodynamics (e.g., pressure-volume loops). Studies relying solely on phenomenological organ-level models or lacking internal mechanics/systemic links were excluded. Extracted data were categorized by multi-scale connection methods (e.g., fibre-to-ventricle scaling, lumped-parameter coupling), circulatory models, and tissue mechanics. An integration rubric evaluated bi-directional feedback strength.

3. Results

From an initial 13,367 records, screening yielded 304 studies for full-text assessment. Following 113 exclusions—primarily lacking cellular frameworks (n=24), mechanical outputs (n=23), or global haemodynamic linkage (n=12)—191 studies were included. Preliminary analysis reveals substantial variation. In terms of model architecture, coupling architectures range from one-way drivers to bi-directional feedback using diverse contraction methods (e.g., time-varying elastance, cross-bridge kinetics). Regarding application, mechanical values are currently being stratified across diverse physiological conditions. Interpreting usability, multi-scale validation depth and clinical translation vary significantly. Furthermore, initial data extraction highlights a predominant reliance on idealised ventricular geometries and a scarcity of models featuring closed-loop bi-directional feedback.

4. Discussion and Conclusions

This review maps multi-scale and reduced-order modelling strategies with systemic haemodynamics, offering trade-offs between computational cost and physiological fidelity. This analysis is also intended to guide fit-for-purpose model selection. Multi-scale computational models are well positioned to act as digital twins for clinical decision-making. Establishing a consensus on these frameworks will provide a much-needed methodological blueprint for investigating complex ventricular mechano-energetic mismatches. These standardisation efforts should also encompass credibility assessment, that is essential to upscale bench modelling to bedside applications in cardiovascular care.

5. References

1. Page et al., BMJ 372, 2021

Acknowledgements:

This work is supported by the University of Twente starter grant.

IN-SILICO CLINICAL TRIAL OF AN INVESTIGATIONAL PULMONARY VALVE DEVICE FOR TREATING PAEDIATRIC PATIENTS

Nils Götzen* (1), Tahir Turgut (1), Vincent Bouwman (1), Deniz Oztürk (2), Maria Bastron (2), Salvatore Pasta (3), Giovanni Gentile (4), Bart Meuris (5), SimInSitu Consortium (6)

1. 4RealSim Services BV, The Netherlands; 2. Capvidia BV, Belgium; 3. University of Palermo, Italy; 4. IRCCS ISMETT, Italy; 5. UZ-Leuven, Belgium; 6. SimInSitu, EU

Corresponding Author: Nils Götzen, 4RealSim Services BV, email: nils@4realsim.com

1. Introduction

Development of dedicated heart valve devices for paediatric patients with congenital heart diseases is dealing with animal models (e.g. sheep) that poorly represent the relevant cases and human clinical studies which suffer from low enrolment rates [1]. Within the SimInSitu project [2] we developed an in-silico platform to test an investigational Pulmonary Valve (PV) device among others and used the platform to conduct a in-silico clinical trial (ISCT). The trial was set up as a refinement study to inform a potential real study with regards to patient risks originating from device sizing and placement.

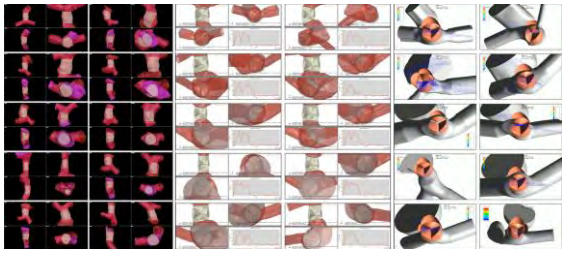


Figure 1: in-silico models and simulation results of Pulmonary Valves implanted into paediatric patient model.

2. Materials and Methods

We developed the in-silico platform comprising the device model and patient-specific model (Abaqus-FlowVision FSI co-simulation) following a hierarchical system through a bottom-up approach (Figure 1), which was also used to conduct the credibility assessment according to ASME V&V standards and the FDA guidance [3]. In summary, various in-vitro structural and haemodynamic tests, in-vivo animal data, in-vivo human data, and patient cohort data were used to validate the entire platform with respect to various Questions of Interest. The ISCT included ten paediatric patients ranging between 5-18 years of age, which were virtually treated with PV devices available in three sizes. Implantation was conducted under close clinical guidance, while clinical evaluation was conducted based on the immediate outcome of the device implantation (shaping / size mismatch) and in-silico data.

3. Results

For each patient, Regurgitation Fraction, Pressure Gradients, Geometrical /Effective Orifice Area, and general flow / leaflet kinematics were determined. From the ten cases only five reached successfully the endpoints, while two of these cases would benefit from larger devices. The investigated patient cohort was in general rather old and consequently the available devices often undersized. This is in agreement with the targeted age group of these devices / device-sizes, which is rather between 4-16 years, depending on the individual case.

4. Discussion and Conclusions

The ISCT can be used in the overall preoperative evaluation of this device. Sizing and positioning can be tested while patients can be excluded from the study purely on the basis of this test. Some patients clearly show a potential benefit of upscaling one size. To our knowledge, this is the first ISCT of a pulmonary heart valve conducted as a Refinement Study using advanced patient-specific FSI modelling. This approach seems to be a realistic first application step for ISCT in high-risk device development. Model credibility was evaluated extensively and can generally be considered as appropriate with respect to the model risk level.

5. References

1. Pammi et al. DOI: 10.1016/j.landig.2025.01.007
2. SimInSitu, GA no: 101017523
3. FDA 2023, FDA-2021-D-0980

Acknowledgements:

The authors would like to thank the European Research Council (GA no: 101017523) for providing financial support to this project.

COUPLED ANATOMICAL-PHYSIOLOGICAL CALIBRATION FOR GENERATING CARDIOVASCULAR VIRTUAL POPULATIONS

Beatrice Ghitti* (1), Jenny Lang (1), Alireza Sharifzadeh-Kermani (1), Finbar Argus (1), Melina Ragheb (1), Gonzalo Maso Talou (1)

1. Auckland Bioengineering Institute, The University of Auckland, Auckland, New Zealand
*Corresponding author. E-mail: beatrice.ghitti@auckland.ac.nz

1. Introduction

While computational cardiovascular models hold great potential for clinical application and in-silico trials (e.g., [1]), most rely on a "one-size-fits-all" approach. This neglects crucial sex-specific anatomical and functional variations, limiting the reliability and applicability of in-silico trial predictions. Here, we propose a coupled calibration framework that incorporates both anatomical and physiological variability to generate plausible cardiovascular virtual populations.

2. Materials and Methods

Sex-specific statistical atlases of vascular anatomy are generated (with adaptable complexity) based on [2] and a data-driven literature review of diameter measurements. Each vessel's joint distribution is computed via a Wasserstein distance-based weighted average of the individual lognormal probability density functions (PDFs). Sex-specific baseline blood flow fractions (BFFs) for discrete and distributed organs are identified (e.g., [3,4]) and mapped to corresponding supplying vessels. Physiological variability is introduced via artificial Gaussian noise by applying an Additive Log-Ratio transform.

Anatomical-physiological coupling. First, BFFs are sampled. Then, terminal BFF noise variables are projected and propagated upstream via a nominal flow-weighting scheme, yielding a unique effective z-score to sample each vessel's diameter. Finally, the population instances are evaluated using the ratio Q/d^3 as a local wall shear stress (WSS) proxy, pruning non-physiological models.

3. Results

This contribution demonstrates the generation of cardiovascular virtual populations incorporating coupled anatomical (Fig. 1, top) and functional (bottom) variability. By removing non-physiological instances via local WSS assessment, we will show that the subsequent simulations produce realistic haemodynamic outputs across the cohorts when compared with physiological ranges.

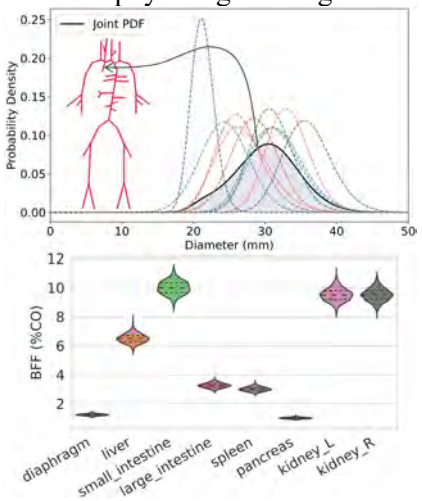


Figure 1: (Top) Consensus PDF of the ascending aorta diameter. (Bottom) Selected organs' BFF distribution for a population of 1000 samples.

4. Discussion and Conclusions

This framework lays the groundwork for generating (cardio-)vascular virtual populations by coupling sex-specific anatomical statistical atlases with physiological calibration. This methodology can be leveraged to generate haemodynamically plausible cohorts tailored to specific clinical applications. Ultimately, this scalable approach can provide a comprehensive baseline for in-silico clinical trials, offering a robust alternative to "one-size-fits-all" models by capturing human physiological variability.

5. References

1. Payne et al., Prog Biomed Eng, 5(2), 2023.
2. Uflacker's Atlas of Vascular Anatomy, 3rd Ed., 2021.
3. Williams LR, Leggett RW, Clin Phys Physiol Meas., 10(3):187-217, 1989.
4. Valentin J, Annals of the ICRP, 32(3-4): 1-277, 2002.

Acknowledgements:
The authors thank VITAL Horizon Europe (Grant 101136728) for the financial support.

GENERATIVE MODELING WITH CONDITIONAL LDDMM FLOW MATCHING FOR DOMAIN UNCERTAINTY QUANTIFICATION

Sarah Katz (1), Francesco Romor (1), Jia-Jie Zhu (2), Alfonso Caiazzo (1)

1. Weierstrass Institute for Applied Analysis and Stochastics, Germany;
2. KTH Royal Institute of Technology, Sweden

Corresponding author: Sarah Katz (katz@wias-berlin.de)

1. Abstract

In [1], a domain shape registration method using Large Deformation Diffeomorphic Metric Mappings (LDDMM) was introduced, enabling (through pullbacks/pushforwards between target and reference aorta geometries) various applications in data assimilation, pressure estimation, and solution manifold learning.

Here we will discuss an extension of this approach: conditional LDDMM flow matching used for generative modeling, with an example application in shape uncertainty quantification. An article [2] detailing this is in preparation.

2. ResNet-LDDMM

In [1], registration maps were constructed as flows of a velocity function computed using a feed-forward deep neural network:

$$d/dt\,\phi^{\theta}(t,x) = f^{\theta}(\phi^{\theta}(t,x)) \qquad (1)$$

With suitable conditions on f_θ and a loss function based on the chamfer distance, a case-specific training procedure results in a bi-Lipschitz homeomorphism between the reference geometry at $t=0$ and a close approximation of the target geometry at $t=1$.

3. Conditional LDDMM flow matching

We pair each (previously computed) velocity field f^i with a conditioning variable c_i (containing a low-dimensional representation of the domain by centerline coordinates and in-radii) and instead train a time-dependent field b^θ to match the conditional drift

$$u_{cond}(t,x,c_i) = f^i(x) + \sigma(t)\,\epsilon \qquad (2)$$

for each test case i and each time t . Here $\sigma(t)\,\epsilon$ is a diffusion term with $\epsilon \sim N(0,1)$.

For each test case, the conditioning variable is perturbed and the corresponding SDE's solution is sampled to generate variant geometries.

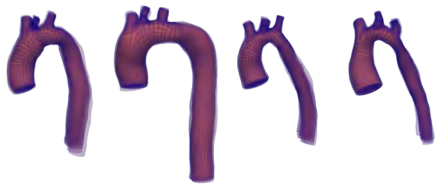


Figure 1: Variants of four base geometries.

4. Uncertainty quantification

Batches of similar geometries are generated and simulations of pulsatile flow through the aorta are run to quantify the impact of the geometric variation on various flow statistics. Samples of varying size are also compared.

5. References

1. Romor, Galarce, Brüning, Goubergrits, Caiazzo. Data assimilation performed with robust shape registration and graph neural networks: application to aortic coarctation. **10.48550/arXiv.2502.12097**
2. Katz, Romor, Zhu, Caiazzo. Generative modeling with conditional LDDMM flow matching: Application to domain uncertainty quantification in hemodynamics. *In preparation.*

Acknowledgements:
Funded by the German Research Foundation (DFG) under Germany's Excellence Strategy – The Berlin Mathematics Research Center MATH+ (EXC-2046/1, EXC-2046/2, project ID: 390685689).

An RBF-based Framework for Geometric Control of Cardiovascular Statistical Shape Models

Andrea Baldini (1, 2), Leonardo Geronzi (2), Marco Evangelos Biancolini (1, 2)
1. Univerisity of Rome Tor Vergata, Italy; 2. LivGemini srl, Italy

Corresponding author: andrea.baldini@uniroma2.it

1. Introduction

Traditional Statistical Shape Models (SSMs) provide compact representations of anatomical variability [1] but lack clinical interpretability due to abstract latent shape coefficients. In the cardiovascular field, patient-specific anatomical features directly influence clinical decisions and procedure feasibility. This study introduces a framework to control aortic SSMs through a geometry-aware mapping of tangible anatomical descriptors.

2. Materials and Methods

We analyzed 61 thoracic aortas from the TotalSegmentator [2] dataset using a 3D attention enhanced U-Net. Five geometrical descriptors (GD) were then extracted: regional maximum diameters (ascending, arch, descending), centerline length, and tortuosity. An SSM was built by applying Principal Component Analysis (PCA) to iso-topological meshes previously generated via a two-step RBF morphing procedure [3]. To map GD to the global geometry, we developed a non-linear surrogate model using RBF interpolation [4], linking the input feature space directly to the PCA modal coefficients. We evaluated the model accuracy by synthetizing 3D anatomies from predefined target parameters and computing the Relative Percentage Error (RPE) between the reconstructed morphological dimensions and the original inputs. Finally, a tool-augmented Large Language Model was adopted to translate natural language intents into deterministic model inputs. The interface's reliability was evaluated against a 15-case benchmark assessing tool selection and argument extraction accuracy.

3. Results

The constructed SSM exhibited rapid variance saturation, with the first 10 modes retaining 95% of the anatomical variance. Geometric validation across 16 distinct configurations (Figure 1) reported an overall mean RPE of 4.52% ± 4.03% (average RPEs across all validation cases: 3.6% for ascending and arch diameters, 6.08% for descending diameter, 6.7% for centerline length, and 2.5% for tortuosity).

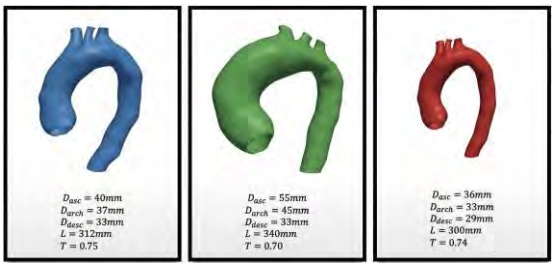


Figure 1: SSM-generated aortas (validation set)

Evaluation of the semantic natural language interface achieved a tool selection accuracy of 93.3% and an argument extraction accuracy of 86.7%.

4. Discussion and Conclusions

This study demonstrated that RBF-based mapping can successfully transform the abstract PCA latent space into an interpretable domain by anchoring statistical models to tangible clinical constraints. Furthermore, the proposed framework showed the feasibility of augmenting LLMs to intuitively and rapidly generate patient-specific virtual populations from SSMs, potentially enabling advanced in-silico trials and interactive medical digital twins.

5. References

1. Ambellan, F., et al. Biomedical Visualisation, vol. 3, pp. 67-84, Springer, 2019.
2. Wasserthal, J., et al. Radiology: Artificial Intelligence, 5(5):e230024, 2023.
3. Geronzi, L., et al. Computers in Biology and Medicine, 162:107052, 2023
4. Biancolini, M. E., et al. Springer, 2017.

Acknowledgements:
The authors acknowledge funding from the EU-PNRR Mission 4, Component 2, Investment 2.3.

THROMBECTOMY SIMULATIONS FOR AN IN-SILICO TRIAL EVALUATING THE PERFOMANCE OF TWO STENT-RETRIEVERS

Virginia Fregona (1), Giulia Luraghi (1), Luca Bontempi (2,3), Thijs Kuipers (4), Piotr Połeć (5), Martijn Hoeijmakers (6), Frank Gijsen (2,3), Henk Marquering (4), Charles Majoie (4), Francesco Migliavacca (1), Jose Felix Rodriguez Matas (1)

1. Politecnico di Milano, IT; 2. Erasmus Medical Center, NL;
3. Delft University of Technology, NL; 4. Amsterdam UMC, NL: 5. ACC Cyfronet AGH, PL; 6. Ansys

1. Introduction

Mechanical thrombectomy (MT) is a minimally invasive treatment for acute ischemic stroke aimed at removing occlusive clots from large cerebral arteries using stent-retrievers and/or aspiration catheters. A finite element (FE) model of the MT procedure has been previously developed and validated against *in vitro* data [1]. This methodology can be exploited to run *In Silico* Trials (ISTs) [2]. In this work, an IST is performed to compare the performance of two stent-retrievers, considering a variety of cerebrovascular anatomies and clot mechanical properties.

2. Materials and Methods

The virtual population consists of 100 cerebrovascular models, characterised through a morphometric analysis [3]. For each anatomy, 3 occlusion locations are considered (internal carotid artery terminus and M1 and M2 segments of the middle cerebral artery (MCA)), and for each, 3 clot mechanical properties are assigned. Two stent-retriever designs, one with an open and one with a closed structure, are being evaluated, resulting in a total of 1800 MT simulations. Simulation outcome will be classified as positive when no fragments or only fragments smaller than the median diameter of the M3 segment of the MCA are lost from the clot; negative when at least one lost fragment is larger than M3. The total volume of the lost fragments larger than M3 will be also computed and normalized by the initial clot volume.

3. Results

With each simulation lasting from 12 to 24 hours and with the computational resources provided, the results will be ready for September and will be entirely presented at the VPH conference. Preliminary simulations were run on the more tortuous anatomies using upper and lower bound mechanical properties to finalize the automated pre- and post-processing pipeline. In Figure 1 and example of post-processing for the most tortuous anatomy is shown: the simulations had different outcomes depending on the clot mechanical properties: positive with the highest clot stiffness and negative for the lowest clot stiffness (Figure 1).



Figure 1 Example of post-processing: the centre of the clot fragments is shown over the vessel centreline.

4. Discussion and Conclusions

Based on previous studies [3][4], morphometric vessel characteristics and clot mechanical properties are expected to significantly influence the MT outcomes. No a priori assumptions are made regarding the comparative performance of the investigated stent-retrievers.

The present study illustrated the potential of ISTs for systematic and controlled device comparison in patient-specific conditions.

5. References

1. Luraghi et al, *Interface Focus*, 2020
2. Viceconti et al, *Int J Clin Trials*, 2016
3. Bridio et al, *Front Med Technol*, 2021
4. Fregona et al, *J Mech Behav Biomed Mater*, 2025

Acknowledgements: This project has received funding from the European Union's Horizon Europe research and innovation programme under the grant agreement No 101136438.

We gratefully acknowledge Polish high-performance computing infrastructure PLGrid (HPC Center: ACK Cyfronet AGH) for providing computer facilities and support within computational grant no. PLG/2025/018003.

AN IN SILICO WORKFLOW FOR TAVI: SYNTHETIC COHORTS, MECHANICAL SIMULATIONS, AND DEEP LEARNING SURROGATES

Jan Oldenburg (1), Laura Supp (1), Finja Borowski (1), Matthias Leuchter (1), Marc-André Weber (2), Alper Öner (1), Klaus-Peter Schmitz (1) and Michael Stiehm (1)

1. Institute for ImplantTechnology and Biomaterials e.V., GER 2. Institute of Diagnostic and Interventional Radiology University Medical Center Rostock, GER

1. Introduction

The expansion of Transcatheter Aortic Valve Implantation (TAVI) to lower-risk patients necessitates improved prediction of long-term complications, such as aortopathy and valve thrombosis. In silico clinical trials (ISCTs) are a promising method to improve the understanding and safety of TAVI but are hampered by challenges in creating virtual cohorts and by the high computational cost of mechanistic simulations. This work introduces an *in silico* framework – from synthetic patient generation to machine learning-based, near-real-time, patient-specific outcome prediction.

2. Materials and Methods

First, a synthetic patient cohort (n = 100) was generated from CT data using a principal component analysis based shape model including the aortic root and aortic arch and a convolutional variational autoencoder for volumetric calcifications, as previously described [1,2]. Second, this cohort underwent virtual TAVI by explicit finite element (FE) simulations in Abaqus/Explicit 2023, including balloon post-dilatation (BPD). A prototype, in-house-designed TAVI device was implanted in two commissural orientations. Third, transient computational fluid dynamics (CFD) simulations were performed in OpenFOAM to analyze systolic hemodynamics, yielding 565 successful simulations across untreated, TAVI, and TAVI+BPD conditions. TAVI and TAVI+BPD were each simulated in two commissural alignments, and metrics such as wall shear stress (WSS) were computed. Finally, the resulting data were used to train deep learning surrogate models for blood flow prediction, including a DeepONet with PointNet shape encoders (DON-PN) [3] and an autoregressively trained 3D U-Net [4].

3. Results

The cohort generation method yielded realistic virtual anatomies [2]. Structural simulations showed that BPD significantly improved stent expansion and circularity, with final stent deformation correlating with calcification distribution. Hemodynamic analysis indicated that BPD yielded more centered flow jets and reduced WSS hotspots. Among the deep learning architectures, U-Net and DeepONet-based models most accurately predicted post-procedural velocity and pressure fields (see Figure 1).

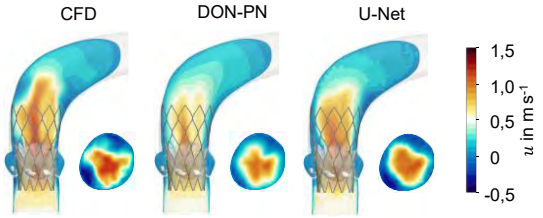


Figure 1: Systolic flow in outflow direction at time 0.2 s; from left to right: CFD result, DON-PN prediction, and U-Net prediction.

4. Discussion and Conclusions

We demonstrated a pipeline for conducting TAVI ISCTs. Our results provide mechanistic evidence that procedural choices such as BPD can improve hemodynamic outcomes. We also showed that deep learning surrogate models can predict patient-specific 3D blood flow in near real time – a key step toward personalized TAVI planning and rapid *in silico* evaluation of novel device designs, thereby enhancing procedural safety for a broader patient population.

5. References

1. Oldenburg J et al. Current Directions in Biomedical Engineering, 2024; 10(4): p. 469-472
2. Supp L et al. Biomechanics and Modeling in Mechanobiology, 2025; 24: p. 1605–1618
3. Park J, Kang N, Neural Networks, 2026; 198: 108560
4. Çiçek Ö et al. MICCAI, 2016; 9901: 424–432

Acknowledgements:

The authors thank the European Union's Horizon 2020 research and innovation program (grant agreement No 101017578) and all those who contributed to data collection, data analysis, and the discussion of the results.

VIRTUAL STROKE PATIENT GENERATION USING GENERATIVE AI FOR *IN SILICO* THROMBECTOMY TRIALS

Sabine Verstraeten (1,2), Thijs Kuipers (1,2), Erik Bekkers (3), Praneeta Konduri (1,2,4)
Charles Majoie (2), Henk Marquering (1,2)

1. Department of Biomedical Engineering and Physics, Amsterdam UMC, The Netherlands;
2. Department of Radiology and Nuclear Medicine, Amsterdam UMC, The Netherlands;
3. Informatics Institute, University of Amsterdam, The Netherlands;
4. Department of Neurology and Neurological Sciences, Stanford University, United States

1. Introduction

Mechanical thrombectomy is a minimally invasive procedure to retrieve occluding thrombi in patients with a large vessel acute ischemic stroke. To accelerate the development and clinical introduction of new thrombectomy devices, *in silico* trials are emerging as a powerful strategy [1, 2]. *In silico* thrombectomy trials require large and diverse populations of virtual patients, including representations of cerebral vessels and occluding thrombi. Kuipers et al. [3] introduced a diffusion-based generative model to generate anatomically plausible cerebral vessel trees. In a subsequent study, they developed a generative model to create synthetic thrombi and model thrombus shape and composition. In the present study we aim to integrate these two generative frameworks into one pipeline for the automated generation of virtual stroke patients, combining synthetic cerebral vessel anatomies with thrombi.

2. Materials and Methods

The synthetic vessel model outputs vessel centrelines of the internal carotid artery (ICA), middle cerebral artery M1 and M2 segments, and the anterior cerebral artery (ACA), together with corresponding local vessel radii. The synthetic thrombus model produces point cloud representations of the thrombus shape. Within the proposed pipeline, an occlusion site (ICA, M1, M2, or ACA) is first selected according to the distribution observed in a clinical trial [4]. The longitudinal axis of the thrombus is aligned with the centreline and the thrombus is scaled to match the local vessel radius. Finally, the thrombus point cloud is spatially transformed to follow the curvature of the vessel.

3. Results

In a preliminary evaluation, the pipeline successfully generated five virtual stroke patients with synthetic cerebral vessel anatomies and thrombi positioned at clinically relevant occlusion sites. In all cases, the thrombi were fully contained within the vessel lumen without large protrusion, indicating anatomical plausibility. Two examples are shown in Fig. 1.

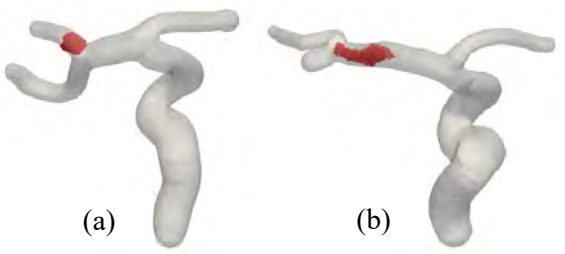


Figure 1: Examples of synthetic cerebral vessel trees (white) with synthetic thrombi (red) in M2 (a) and M1 (b).

4. Discussion and Conclusions

Our preliminary results demonstrate the feasibility of the diffusion-based virtual stroke patient pipeline. Quantitative validation against clinical cohorts, specifically comparing synthetic and real clot shape and location distributions, remains planned future work. Once validated, the pipeline will support large-scale *in silico* thrombectomy trials and accelerate stroke treatment development.

5. References

1. Konduri PR et al., Front. Neurol.; 11:558125 (2020).
2. Miller et al., Comput. Methods Programs Biomed.; 228:107244 (2023)
3. Kuipers TP et al., MIDL; nnn:1-11 (2024)
4. Berkhemer et al., N. Engl. J. Med.; 372.1: 11-20 (2025)

Acknowledgements:
This work was supported by the UvA strategic theme Responsible Digital Transformations. The authors would like to thank Gravity Medical Technology for their support during the project.

IN SILICO CLINICAL TRIAL FOR PVL EVALUATION AFTER TAVI

Laura Supp (1), Jan Oldenburg (1), Matthias Leuchter (1), Jan Brüning (2), Claudio Capelli (3), Alper Öner (1), Marc-André Weber (4), Klaus-Peter Schmitz (1), Michael Stiehm (1), Finja Borowski (1)

1. Institute for ImplantTechnology and Biomaterials e.V., Germany, 2. Institute of Computer-assisted Cardiovascular Medicine, Charité - Universitätsmedizin Berlin, Germany, 3. Institute of Cardiovascular Science, University College London, UK, 4. Institute of Diagnostic and Interventional Radiology, University Medical Center Rostock, Germany

1. Introduction

Transcatheter aortic valve implantation (TAVI) is an established minimally invasive treatment for severe aortic stenosis. Despite advances in device design, paravalvular leakage (PVL) remains a relevant complication. Clinical studies link PVL to calcification patterns and anatomical dimensions. Complementing clinical observations, numerical simulations offer insights into PVL. *In silico* clinical trials (ISCT) enable systematic and statistically supported analyses of these influencing factors, thereby contributing to design improvements.

2. Materials and Methods

For the ISCT (Fig. 1), first a virtual cohort of 243 synthetic TAVI patients was generated [1]. The calcification patterns were generated using a conditional convolutional variational autoencoder for an existing virtual cohort of the aortic root [2,3]. Finite element (FE) analyses were performed for pre-dilatation and deployment of the prosthesis, followed by computational fluid dynamics (CFD) simulations to analyse PVL. The FE simulations were conducted using Abaqus/Explicit 2023. The following steady-state CFD simulation were performed with openFOAM. The severity of PVL was determined based on volume flow. Statistical analyses were conducted to evaluate correlations between PVL, calcification distribution and anatomical parameters [1].

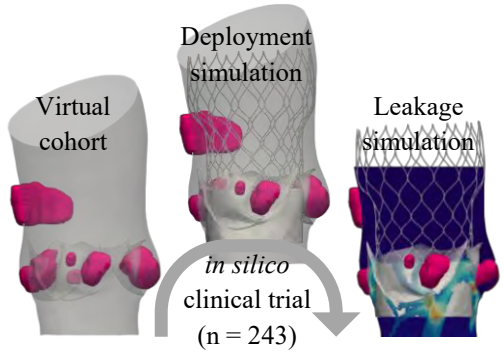


Figure 1: Workflow of the *in silico* clinical trial to determine the impact of calcification

3. Results

The PVL distribution shows a high degree of concordance with findings form clinical studies. The risk of PVL is influenced less by the total amount of calcification and more by its distribution. The eccentricity index, the diameter of the sinotubular junction, oversizing and the combination of aortic angle with the calcium volume between the right- and non-coronary leaflet also affect PVL severity [1].

4. Discussion and Conclusions

The ISCT provides insight into the factors influencing PVL. This method also allows the analysis of specific subcohorts. Owing to its numerical approach, a wide range of parameters can be determined retrospectively, and anatomical characteristics can be quantified. One such subcohort consists of functionally bicuspid TAVI patients, who can be modeled and simulated with this workflow to assess device safety for TAVI in bicuspid anatomies and to investigate advanced designs adapted for these patients.

5. References

1. Supp L et al., Biomechanics and Modeling in Mechanobiology, 2025; 24: p. 1605-1618.
2. Oldenburg J et al., Current Directions in Biomed Eng, 2024; 10(4): p. 469-47.
3. Verstraeten S et al., Int J Numer Meth Biomed Eng, 2023; e3778.

Acknowledgements:

The authors would like to thank the European Union's Horizon 2020 research and innovation program for the financial support under grant agreement No 101017578 (SIMCor) and all those who contributed to data collection, data analysis, and the discussion of the results.

Financial support by the ERDF and the ESF within the collaborative research between economy and science of the state Mecklenburg-Vorpommern is gratefully acknowledged.

DEVELOPMENT AND VALIDATION OF A VIRTUAL COHORT FOR VA ECMO AND MECHANICAL VENTILATION

Federica Colombi (1), Duarte A. M. Dias (1), Dirk W. Donker (1,2), Libera Fresiello (1)

1. *Cardiovascular and Respiratory Physiology, TechMed Centre, University of Twente, Enschede, The Netherlands*
2. *Intensive Care Center, University Medical Center Utrecht, Utrecht, The Netherlands*

*federica.colombi@utwente.nl, Tel.: +31 53 489 9758, P.O. Box 217, 7500 AE Enschede, The Netherlands

1. Introduction

Patients receiving veno-arterial extracorporeal membrane oxygenation (VA-ECMO) represent a heterogeneous population, posing significant challenges for therapy monitoring and clinical management. Virtual patient populations (VP) provide a valuable and de-risked framework to explore pathophysiological variability and optimize VA-ECMO therapy. In this study, a VP of patients undergoing concurrent VA ECMO and mechanical ventilation (MV) was generated using a validated lumped parameters cardiopulmonary simulator (CPS).

2. Materials and Methods

The CPS includes non-linear models of the heart chambers, systemic and pulmonary circulations, and lung and chest wall mechanics. The VA ECMO circuit, connected between the right atrium and descending aorta, comprises tubing, a resistive oxygenator and a quadratic pump pressure–flow relationship [1]. MV was modelled in volume-controlled mode, and the generated intrathoracic and alveolar pressures affect cardiovascular transmural pressures.

The CPS was calibrated using average data from 80 cardiogenic shock patients undergoing concomitant MV and VA ECMO [2]. MV positive end-expiratory pressure and tidal volume were set to 7 cmH_2O and 450 mL, respectively, while VA ECMO flow was varied between 2–4 L/min, as reported in the clinical study [2]. Model outputs were validated against literature values for ventricular mechanics and systemic and pulmonary pressures.

For VP generation, a global sensitivity analysis (GSA, 34816 evaluations) identified parameters driving pathophysiological variability, which were subsequently sampled using a Sobol sequence over clinical ranges. The resulting VP was filtered for physiological plausibility.

3. Results

The CPS reproduced the hemodynamic response to VA ECMO flow changes observed in the reference cohort, with simulated variables within clinical ranges (Fig. 1). GSA identified 7 parameters (heart rate, ventricular elastances, peripheral resistance, blood volume, venous tone, ECMO speed), from which 8192 virtual subjects were generated. Of these, 3000 satisfied the physiological acceptance criteria, covering a broad range of key hemodynamic variables (examples in Fig. 2).

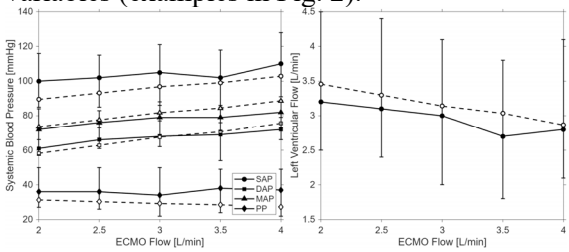


Figure 1: Simulated (dashed) vs clinical (continuous) left ventricular flow, systolic, diastolic, mean and pulse pressures (SAP, DAP, MAP, PP) [2].

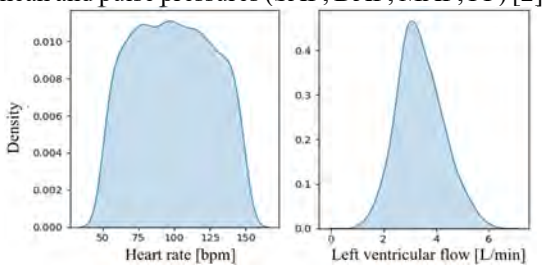


Figure 2: Distribution of heart rate and left ventricular flow in the virtual population.

4. Discussion and Conclusions

The VP approach proposed enables systematic exploration of cardiopulmonary heterogeneity under MV and VA-ECMO, offering a mechanistic *in-silico* framework for evaluating support strategies in critically ill patients. Future VP validation will be conducted against an independent VA ECMO clinical database.

5. References

1. Colasanti et al, Artif Organs., 2021.
2. Saura et al, J Am Coll Cardiol., 2025.

DEFINING RELIABILITY DOMAIN FOR PHYSICALLY REPRESENTATIVE INTERLAMELLAR FAILURE MODELLING OF ANNULUS FIBROSUS

Shambo Bhattacharya, Marlène Mengoni

Institute of Medical and Biological Engineering, University of Leeds, Leeds, United Kingdom

Corresponding author: Shambo Bhattacharya, Institute of Medical and Biological Engineering, University of Leeds, Leeds LS2 9JT, United Kingdom (Email: s.bhattacharya2@leeds.ac.uk)

1. Introduction

The Annulus Fibrosus' (AF) interlamellar matrix (ILM) is critical to intervertebral disc's structural integrity, where delamination often precedes herniation[1]. While surface-based cohesive model has been used for representing the ILM [2], its application within multi-layered idealised geometries for modelling AF's lamella-ILM assembly is highly sensitive to numerical perturbations and round-off imprecisions[3]. As these artefacts mask the underlying damage evolution physics and hinder accurate and reliable experimental correlations, establishing a reliability domain is imperative to ensure damage analysis and calibration remain physically representative and computationally stable. The present study aims to quantify how this reliability domain varies as a function of cohesive parameters and the degree of lamellar refinement, providing a benchmark for high-fidelity failure simulations.

2. Methods and Framework

An idealised parallelepiped finite element (FE) model (5×5×5 mm), previously tested *in vitro*[2], was developed to simulate the AF's multilayered lamellae-ILM structure (Fig. 1). The lamellae were modelled as an anisotropic hyperelastic Holzapfel material with a single fibre family, with ±20° in successive layers [2,4] (Fig. 1). The ILM was modelled as a surface-based cohesive contact governed by a bilinear traction-separation law (maximum traction before damage, $T_{max} = 0.1$ MPa). Displacement-controlled radial tensile tests were simulated with selective kinematic coupling that allows lateral Poisson's contraction, to prevent edge-effects. The reliability region was quantified by the variations in damage value at delamination (D_3) with respect to the number of lamellae (N_{LAM}) (L=16, 20 and 25) and to an increase in ILM-to-lamellar stiffness ratio (K_{ILM}/K_{LAM}) from 0.2 to 4.5.

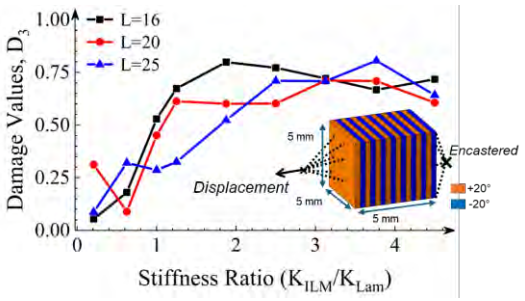


Fig. 1. FE model of Lamella-ILM assembly (right). Variations in D_3 with increase in stiffness ratio (left).

3. Results and Analyses

While the perturbations led to arbitrary delamination localisation, D_3 values showed convergent behaviour with increase in K_{ILM}/K_{LAM}. For $K_{ILM}/K_{LAM}<1$, perturbations dominated upon damage onset precluding any physically representative damage evolution study. For $K_{ILM}/K_{LAM}>1$, D_3 converged to ~0.7 for all lamellar configurations. Notably, $N_{LAM}=20$ exhibited higher stability in D_3 across the stiffness ratios exceeding 1.25 (Fig. 1).

4. Discussion and Conclusion

At $N_{LAM}\approx20$, a reliability domain exists for $K_{ILM}/K_{LAM}>1.25$ where damage progression can be analysed and calibrated up to a threshold of ~0.7. Beyond this, perturbations triggered delamination, masking the underlying physics. Further investigations into diverse loading and damage parameters will establish a comprehensive, multiaxial reliability domain for deterministic failure analysis.

5. References

1. Tavakoli et al., J Orth Res 34(8), 2016.
2. Mengoni et al., JMBBM. 48:164–172, 2015.
3. Liu et al., JCAM. 386(3):113219, 2021.
4. Mengoni et al., R. Soc. Open Sci. 4(8), 2017.

Acknowledgements:
The authors thank Engineering and Physical Sciences Research Council, UKRI (Grant reference: EP/X032183/1) for financial support.

MUSCULOSKELETAL FE MODEL OF THE LUMBAR SPINE: COMPARING HEALTHY AND PATHOLOGIC LORDOSIS

Linda Carpenedo, Luigi La Barbera

LaBS, Dept. of Chemistry, Materials and Chemical Engineering, Politecnico di Milano, Italy

1. Introduction

Lumbar lordosis typically ranges between 40 and 60°, allowing balanced load-sharing between intervertebral discs, facet joints, and surrounding musculoskeletal (MSK) structures. Curvatures exceeding 60° are generally defined as hyperlordosis and may shift loads posteriorly, increasing stress on the facet joints and requiring compensatory mechanisms such as pelvic retroversion and greater muscular activity. When these mechanisms are insufficient, abnormal load distributions can arise [1]. Directly quantifying spinal loads *in vivo* is challenging because measurements are invasive and unfeasible in clinical practice. As a result, computational modeling has become an important alternative for investigating spine biomechanics. In this study, a deformable MSK finite element (FE) model is proposed to analyze the role of soft tissues in spinal load-sharing during functional conditions. The model is used to evaluate how pathological lordotic alignment may alter physiological load distribution.

2. Materials and Methods

This study employs a validated parametric CAD geometry of the lumbar spine, where passive structures are modeled as continuous deformable bodies in Abaqus, and active muscles are included as force-generating elements whose magnitudes are determined through an optimization procedure that solves muscular redundancy [2]. Both a normolordotic (60°) and a hyperlordotic (70°) lumbar column geometries are generated by adjusting the segmental lordosis distribution across the lumbar levels and subsequently reassembling the full MSK architecture. A 20° trunk flexion is simulated. The healthy model is validated against *in vivo* muscle forces and intradiscal pressures (IDPs) [3]. The model is finally used to compare compressive (CFs) and shear forces (SFs), as well as ligament strains, between the two configurations to assess soft-tissue load-sharing.

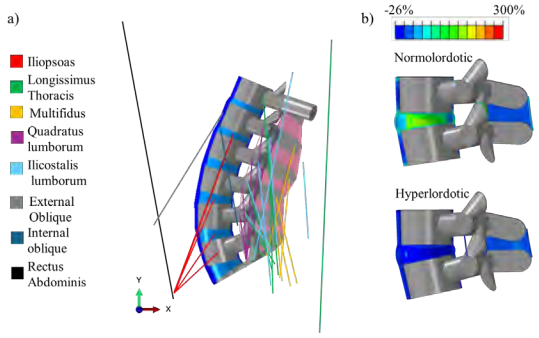


Fig. 1: a) muscular architecture (normolordotic), b) absolute max principal strains on L3-L4 for normo- (up) and hyper- (down) lordotic configurations

3. Results

Estimated muscle forces are physiologically plausible, with abdominal activation exceeding 10% of maximal voluntary contraction. IDPs are comparable between the two lordotic curvatures and within expected ranges (≈1 MPa at L3–L4) [2]. The anterior column sustains the largest CFs and SFs, with the anulus reaching CFs over 180% of BWs and SFs of 30% BW. Among posterior ligaments, the facet capsular ligaments (FCLs) contribute most to load-sharing (over -5% BW for CFs and 1% BW for SFs). Load-sharing patterns are similar between curvatures. Color maps show greater compression in the anterior column of the hyperlordotic configuration during flexion (Fig. 1b).

4. Discussion and Conclusions

Validated against *in vivo* data for a healthy condition [3], this FE model highlights the critical role of the anterior column and FCLs for spine biomechanics. The model is also used to evaluate how varying lordotic curvatures affect load-sharing, highlighting minor differences in load-sharing but different strain patterns. By providing deep insights into soft tissue contributions during daily tasks, the model sets the stage for future sensitivity analyses on muscular architecture and complex activities.

5. References

1. Jentzsch T et al., Clin Spine Surg., 2017.
2. Carpenedo L, La Barbera L, CMBBE, 2025.
3. Arjmand N et al., J Biomech, 2006.

COMPARISON OF VISCOELASTIC AND BIPHASIC MODELS OF BOVINE DISC RELAXATION, CREEP AND STIFFNESS

Basil Mathai (1), Meg Alipat (1), Shambo Bhattacharya (1), Ruth Wilcox (1), Nagitha Wijayathunga (1), Marlène Mengoni (1)

1. *Institute of Medical and Biological Engineering, University of Leeds, UK*

Correspondence: m.mengoni@leeds.ac.uk

1. Introduction

Biomechanical characterization of intervertebral disc (IVD) tissues is essential for understanding spinal biomechanics and determining how mechanical behaviour varies with anatomy and tissue health. The present study aims to compare viscoelastic and biphasic constitutive modelling approaches in their ability to simulate different loading scenarios in the intervertebral disc.

2. Materials and Methods

Three bovine IVDs experimentally subjected to 10% strain relaxation for one hour followed by cyclic compression (175 N ± 15% amplitude over 450 cycles at 1 Hz) were modelled with the Finite Element method. Specimen-specific endplates anatomies were generated from microCT images. The IVD comprised the annulus fibrosus (AF) and nucleus pulposus (NP). Boundary conditions were prescribed to constrain the distal surface while imposing axial loading at the proximal surface replicating the experimental setup.

The AF elastic behaviour was represented with an anisotropic hyperelastic model incorporating two embedded fibre families [1]. The NP elastic behaviour was represented with an isotropic hyperelastic model [1]. The tissues viscous behaviour was represented through either a linear viscoelastic formulation [2] or a biphasic formulation, implemented in FEBio.

A custom optimisation framework was developed to calibrate each FE model against the corresponding experimental relaxation data, using a global-local hybrid scheme. A differential evolution algorithm provided global exploration, and a local L-BFGS-B step provided refinement under bounds with physiological constraints. The relaxation-calibrated material parameters were then used to simulate cyclic compression with both a viscoelastic approach and a biphasic approach.

Cyclic behaviour was analysed through the change of linear stiffness with cycles as well as the change of average displacement (creep).

3. Results

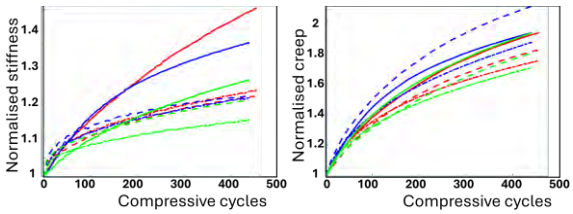


Figure 1: Normalised dynamic stiffness (left) and creep (right) during cyclic loading (plain lines viscoelastic data, dashed lines biphasic data, dotted lines experimental data; colours represent samples).

Across the three specimens, both modelling approaches were calibrated for relaxation with a mean force difference of 5.5 N. Under cyclic compression, simulated deformations showed specimen-dependent offsets in displacement. Both viscoelastic and biphasic approaches (Figure 1) were able to predict creep over 500 cycles (RMS error in displacement variation below 5%). However, the biphasic formulation was able to predict stiffness better than the viscoelastic formulation (RMS error in stiffness variation below 5% for biphasic, between 5% and 15% for viscoelastic models).

4. Discussion and Conclusions

Both constitutive formulations can accurately capture the non-linear force relaxation and yield comparable predictions of macroscopic creep deformation. However, discrepancies in predicted cyclic stiffness highlight the difference in the physics of each formulation, emphasising the need to define the intended context of use when considering a modelling approach and associated material properties.

5. References

1. Mengoni et al., Royal Society Open Science 4(8), 170807 (2017)
2. Hayward et al., Proc Inst Mech Eng H, 240(2):139–15 (2026)

Acknowledgements

The work was funded by the Engineering & Physical Sciences Research Council [EP/X032183/1]

METABOLIC RISK FOR INTERVERTEBRAL DISC STRATIFICATION, BASED ON PERSONALIZED CHEMO-MECHANICAL SIMULATIONS

Estefano Muñoz-Moya, Carlos Ruiz Wills, Gemma Piella, Jerôme Noailly

BCN MedTech, Department of Engineering, Universitat Pompeu Fabra, Barcelona, Spain

1. Introduction

While lactate has been proposed as an early in-vivo marker of intervertebral disc (IVD) degeneration (IDD)[1], intradiscal metabolic transport and morphology are suspected to control metabolic stress on IVD cells[2]. We hypothesized that a "risk axis" (x_{risk}) could be learned from patient-personalized (PP) mechano-transport finite-element (FE) simulations and stratify the metabolic risk for nucleus pulposus (NP) cell death, based on morphological markers from medical images.

2. Materials and Methods

We analyzed N=169 PP IVD models generated through a morphing process[2], with healthy tissue properties and under daily mechanical loading over three simulated days. We solved fully coupled equations of oxygen, glucose, and lactate, metabolic transport, and we determined NP cell viability[3]. At day 3, we built 32 morphophysics predictors (20 morphometrics[2] + 12 solute/pH across posterior, center of the NP, and anterior transition zone ATZ, volumes of interest[2]). A supervised x_{risk} was learned with logistic regression (higher=worse) and stratified by 1D Fisher–Jenks (K = 3: Low / Mid / High) clustering methods. Performance assessment used repeated 5-fold cross-validation (CV; 10 repeats) with majority-class downsampling to 30 controls per repeat. Feature–risk was profiled with SHAP values, Spearman trends, and effect sizes.

3. Results

Figure 1A shows the 1D strata on the x_{risk} that separated positive IVDs (13/169 discs with simulated NP cell death) with strong discrimination (full-fit RAUC 0.997; CV RAUC 0.95±0.08). Fisher–Jenks concentrated all positives IVD in the High stratum. ATZ solute/pH features dominated separation. Notably, the ATZ lactate increased approximately linearly from Low, to Mid, and then to High (Spearman ρ=+0.93; r^2=0.89, Figure 1B), while ATZ glucose and pH showed reciprocal decreases. IVD geometrical descriptors (e.g., anterior AF sagittal area, disc mid-height) that led to the largest modifications of the anterior paths of solute transport under mechanical loads, ranked among the top SHAP drivers for ATZ solutes, linking disc morphology to waste accumulation.

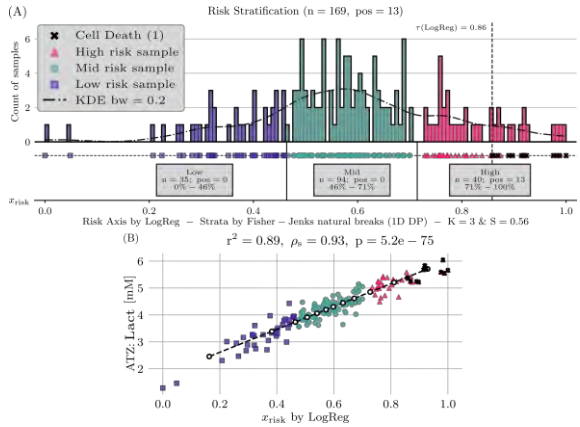


Figure 1: A) Risk-axis (x_{risk}) distribution. B) Lactate concentration across the Low, Mid, and High strata.

4. Discussion and Conclusions

Clinically, qualitative, interpretable tools are needed to flag early IDD risks before overt structural change. Hereby, a single supervised axis yielded a simple ordering with a practical readout: "higher risk points to higher ATZ lactate." This mechanistic pattern complements MR spectroscopy reports that lactate alterations precede matrix changes[1] in IDD, suggesting lactate-sensitive acquisitions (e.g., MRS) paired with IVD morphological markers could support early screening and monitoring. Near-linear lactate rise along the axis offers a straightforward visual cue (Figure 1B) that clinicians can track longitudinally. Validation with external cohorts is ongoing. Future work will pair axis scores with MRI markers, integrate PP loading and tissue property maps to test causality, and translate PP FE fields into clinic-ready biomarkers. This framework shows that morphophysics-aware, axis-based stratification can bridge image-based morphological IVD phenotypes and metabolic risk for early IDD.

5. References

1. Thippeswamy PB et al., Global Spine J. 15(5):2736–2743 (2025).
2. Muñoz-Moya E et al., Front Bioeng Biotechnol. 12:1384599 (2024).
3. Muñoz-Moya E et al., SSRN Preprint. doi:10.2139/ssrn.5364238 (2025).

Acknowledgements:
European Research Council (ERC 2021 CoG O-Health 101044828) and ICREA Acadèmia.

MECHANO-BIOLOGICAL MODELING OF SPINAL FUSION SURGERY

Davide Ninarello (1), Hanna Isaksson (2), Luigi La Barbera (1)

1. LaBS, Dept. of Chemistry, Materials and Chemical Engineering "G. Natta", Politecnico di Milano, Italy; 2. Department of Biomedical Engineering, Lund University, Lund, Sweden

1. Introduction

Lumbar interbody fusion (LIF) is widely used for the treatment of disc pathologies. However, it is still associated with a high risk of complications, such as pseudoarthrosis and implant subsidence. Mechano-biological numerical models are a powerful tool to improve our understanding and support clinical pre-operative planning. The aim of the present work is to develop a mechano-biological tissue differentiation algorithm suitable for simulation of fusion after LIF.

2. Materials and Methods

An iterative framework coupling Python and ABAQUS 2022 finite element simulations was developed, in which mechanically regulated [1] cell and tissue processes were modelled via a user-defined element [2].

First, fractional factorial analysis (FFA) was used to determine the relative influence of the parameters. A simplified axisymmetric 2D L4–L5 functional spine unit (FSU) was used with a 500 N compressive load (Figure 1a). A two-level screening (23 factors) identified the 10 most influential parameters, followed by a three-level Taguchi design. Bone concentration and FSU stiffness were evaluated up to 300 days post-surgery.

Secondly, a realistic surgical scenario of posterior lumbar interbody fusion (PLIF) was simulated on a 3D L4–L5 FSU with bilateral facetectomy, partial discectomy, bilateral cages, and posterior titanium fixation (Figure 1b). Two cage materials (Ti6Al4V, E=110GPa; PEEK, E=4.5GPa) were compared, with PEEK hydrophobicity modeled as a 25% reduction in osteoblast activity. Daily loading was represented by a 500 N follower load and 7.5 Nm pure moment in flexion. Bone concentration and spatial distribution were computed up to 1 year from surgery.

3. Results

The FFA identified bone formation and resorption rates as the dominant parameters, accounting for >75% of the total response variance. In the 3D PLIF model, higher bone concentration was predicted in the anterior (32% and 31% for Ti and PEEK, respectively) compared to the posterior disc region (5% and 10%). Bony bridging within the cage holes occurred only with PEEK cages (Figure 1c).

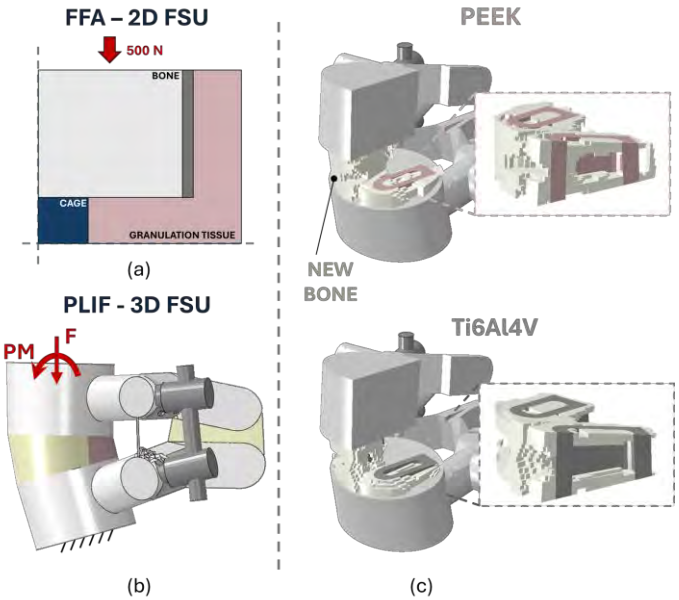


Figure 1 (a) 2D-FSU for the FFA; (b) 3D PLIF model; (c) Bone spatial distribution at 1 year follow-up (bone concentration >25%)

4. Discussion and Conclusions

The FFA identified bone formation and degradation rates as most influential parameters, consistent with literature [2]. The mechano-biological model successfully captured the influence of cage material on fusion outcomes after PLIF in a 3D model, predicting higher bone concentration in the anterior region, in agreement with clinical evidence [3]. Furthermore, the absence of bony bridging within Ti cages may be attributed to stress shielding effect, partially mitigated by the lower stiffness of PEEK cages. Overall, this study demonstrates the potential of advanced mechano-biological models to simulate lumbar interbody fusion and support pre-surgical planning. Future efforts should include more realistic patient-specific cases.

5. References

1. Claes & Heigele, J Biomech (1999);32:255–66
2. Isaksson et al., J Theor Biol (2008); 255:26–39
3. Seo et al., Medicine (2017);96:e7816

Acknowledgements:

This research work was partially funded by NextGenerationEU program, MUR, Italia domani - P.N.R.R. and GreenBone Ortho S.p.A, Italy

MECHANO-METABOLISM FINITE-ELEMENT PREDICTIONS IN EARLY LUMBAR DISC DEGENERATION AND LOW BACK PAIN STRATIFICATION

Estefano Muñoz-Moya[1], Terence McSweeney[2], Jaro Karppinen[2], Carlos Ruiz Wills[1], Mark van Gils[3], Gemma Piella[1], Jerôme Noailly[1]

1. BCN MedTech, Department of Engineering, Universitat Pompeu Fabra, Barcelona, Spain

2. Research Unit of Health Sciences and Technology, University of Oulu, Oulu, Finland

3. Faculty of Medicine and Health Technology, Tampere University, Tampere, Finland

1. Introduction

Low back pain intensity (LBPi) and intervertebral disc (IVD) degeneration (IDD) are multifactorial conditions where imaging, mechanics, and bio–psycho–social factors interact[1]. In the Northern Finland Birth Cohort (NFBC), Disease State Fingerprint (DSF) models[2] showed that LBPi is driven mainly by psychosocial and stress-related variables, whereas level-specific IDD is dominated by MRI-derived radiomics and structural flags[1]. However, these epidemiological fingerprints lack a direct mechanistic interpretation of vulnerability. Focusing on IVD metabolism, we hypothesized that a finite-element (FE)-derived risk axis (x_{risk}), originally learned from patient-personalized (PP) mechano-transport simulations[3], could be transferred to NFBC through a morphology-based surrogate and incorporated into DSF as a new mechanistic biomarker.

2. Materials and Methods

The SpineView cohort[4] (N=169 PP IVDs) was our mechanistic reference. The target was a FE-derived continuous risk score, S_{risk}, associated with nucleus pulposus cell death predictions because of metabolic stress under mechanical loads, and defined from a 32-feature morphophysics space of 20 morphological descriptors[4] and 12 mechano-transport readouts[3]. A Support Vector Regression (SVR) model was trained to predict S_{risk} from 3D IVD morphology (train / validation /test splits 60/20/20). The surrogate was then independently tested on N=516 reconstructed L4–L5 PP discs from NFBC routine MRI, generated through Pixel2Mechanics and mesh morphing[4]. The resulting surrogate score, S_{risk}^{NFBC}, was incorporated as a new Mechanical Risk leaf into DSF models of LBPi and severe IDD (Pfirrmann>3), allowing the FE-derived mechanistic axis to be merged with the existing bio–psycho–social fingerprint framework[1].

3. Results

The surrogate SVR reproduced the original FE-derived S_{risk} with high accuracy on the SpineView test set (r2=0.97). The dominant morphological drivers were annulus volume, disc middle height, and anterior sagittal area, consistent with the regions previously linked to transport and cell-viability risk[3]. Applied to NFBC discs, the surrogate yielded an approximately Gaussian distribution of the score S_{risk}^{NFBC}, with most subjects in the Mid-risk stratum. When merged into DSF, the mechanistic risk leaf showed non-negligible relevance in the L4–L5 IDD and LBPi models (Fig. 1).

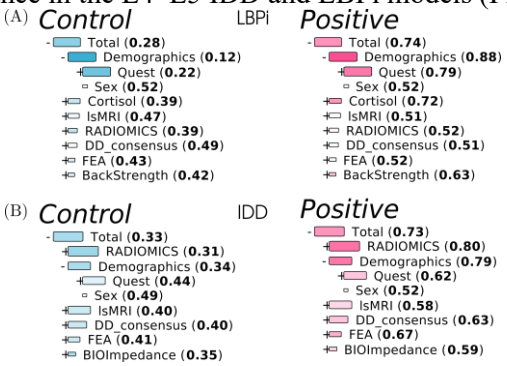


Figure 1: DSF tree including the Mechanical Risk leaf for A) LBPi and B) L4–L5 IDD.

4. Discussion and Conclusions

The new node added a disc-specific mechanistic dimension to the NFBC fingerprints, complementing the psycho-social dominance of LBPi and the imaging dominance of IDD. A morphology-only surrogate can transfer a simulation-derived mechanistic risk axis into a large epidemiological cohort and embed it into a bio–psycho–social fingerprinting framework. In NFBC, this FE-derived mechano-metabolic risk behaved as a level-specific biomarker, supporting the idea that macro-scale morphology encodes clinically relevant metabolic information that can be recovered from standard MRI. The framework connects personalized mechanistic modeling with interpretable population-health stratification, enabling mechanistic variables to coexist with psychosocial, clinical, and imaging features.

5. References

1. Tanguay-Sabourin C. et al., Nat Med. 29 (2023).
2. Cluitmans L et al., Stud Health Technol Inform. (2013).
3. Muñoz-Moya E. et al., SSRN Preprint. doi:10.2139/ssrn.5364238 (2025).
4. Muñoz-Moya E. et al., Front Bioeng Biotechnol. (2024).

Acknowledgements:
European Research Council (ERC 2021 CoG O-Health 101044828) and ICREA Acadèmia.

A MULTIPHYSICS PHASE-FIELD FRAMEWORK FOR FRACTURE RISK ASSESSMENT IN METASTATIC VERTEBRAE

Masoud Ahmadi (1), Alkaios Lamprakis (1), Nicholas Ovenden (1)
Dept of Mathematics, University College London, United Kingdom

1. Introduction

Accurately predicting vertebral fracture risk in metastatic bone disease remains challenging. Existing computational models often lack robust, clinically interpretable frameworks and fail to integrate patient-specific anatomy, lesion features, and physiological loading, leading to variable fracture and fatigue predictions [1]. This study introduces a patient-specific phase-field finite element framework to model fracture initiation, propagation, and fatigue in metastatic vertebrae. The approach combines imaging-based geometry reconstruction with spatially varying material properties representing tumour-induced degradation, alongside biomechanically informed loading conditions.

2. Materials and Methods

A continuum phase-field model for brittle fracture is combined with linear elasticity and further extended using a history-dependent degradation law to represent the accumulation of damage and the progressive loss of stiffness under cyclic loading typical of daily activities [2].

We examine common modelling assumptions, such as geometric idealisations, representations of the cortical shell, and choices of constitutive laws, and assess how these influence the predicted mechanical response and fracture behaviour. Whereas clinical tools often treat bone as a homogeneous solid, our approach couples phase-field fracture with poroelasticity to capture the interplay of solid and fluid mechanics within tumour-compromised tissues.

3. Results

Numerical simulations demonstrate a strong sensitivity of vertebral failure and fatigue response to lesion size, patient-specific geometry, and material modelling choices. The findings identify which modelling assumptions reliably capture the global mechanical response and fracture mechanisms, and which may lead to non-negligible deviations.

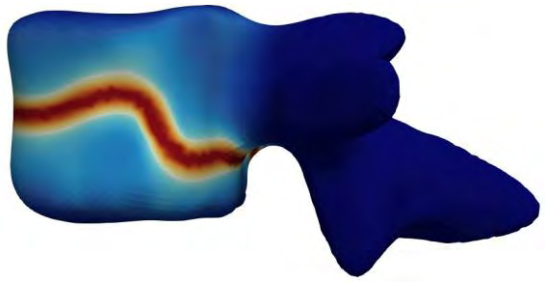


Figure 1: Predicted crack path through an anatomically accurate vertebra under compressive loading.

4. Discussion and Conclusions

By addressing key gaps between qualitative clinical assessment and quantitative mechanical prediction, this work contributes to the development of mechanically informed tools for vertebral fracture risk assessment, with potential impact on surgical decision-making and fracture prevention in spinal oncology [3, 4].

5. References

1. Bianchi D. et al (2022), Journal of Clinical Medicine, 11, 2850, 2022.
2. Carrara, P. et al. (2020) Comp Methods in App Mech and Eng, 361, 112731, 2020.
3. Damron, T. A. et al. (2020) Journal of Orthopaedic Research, 38, 1175-1190, 2020.
4.. Wewel JT, O'Toole JE. Neurooncol Pract. 2020 Nov 18;7(Suppl 1):i5-i9.

Acknowledgements:
The authors would like to thank the UK Engineering and Physical Sciences Research Council (EP/W007096/2) and the Department of Mathematics at UCL for providing financial support to this project.

REGIONAL AND AGE-RELATED MRI-DERIVED T2 MAPPING IN HUMAN INTERVERTEBRAL DISCS

Rémy Benais (2,3,4), Margherita Pasini (1), Marco Palanca (1), Luca Cristofolini (1), Fabio Baruffaldi (5), Simone Fantoni (5), Leonardo Conti (6), Cristina Bignardi (2,3), Alessandra Aldieri (1)

1. Department of Industrial Engineering, Alma Mater Studiorum, University of Bologna, Italy; 2. Department of Mechanical and Aerospace Engineering, Politecnico di Torino, Italy; 3. Polito^{BIO}MedLab, Politecnico di Torino, Italy; 4. Institute of Continuum Mechanics and Biomechanics, Friedrich-Alexander-University Erlangen-Nuremberg, Germany; 5. Medical Technology Laboratory, IRCCS Istituto Ortopedico Rizzoli, Italy; 6. Department of Physics and Astronomy, Alma Mater Studiorum, University of Bologna, Italy

1. Introduction

Magnetic resonance imaging (MRI) T2 mapping measures the decay of the transverse magnetization of water protons [1,2]. In the intervertebral disc (IVD), the measured T2 relaxation times reflect water and proteoglycan (PG) content [1,2], both of which decrease with degeneration [2]. While the link between IVD mechanical properties and T2 relaxation times is unclear, T2 mapping is a non-invasive method to detect changes in IVD composition. Accordingly, in this preliminary study, we evaluated T2 relaxation times in IVDs, hypothesizing differences in young and senior IVDs which may show signs of degeneration.

2. Materials and Methods

Six human lumbar (L1-L2) IVD specimens from three young (ages 31-36) and three senior (ages 62-63) subjects were MRI scanned (3T Discovery MR750w, GE, USA) with a sagittal 8-echo time, T2 mapping sequence (Repetition time = 2000 ms; echo time (TE) = 6.4-51.2 ms; matrix = 512x512, field of view = 180x180 mm; slice thickness = 2 mm; slice gap = 2.6 mm). T2 relaxation times were extracted from the images in the IVDs' annulus fibrosus (AF) and nucleus pulposus (NP) by fitting the following equation:

$$S(TE) = S_0 e^{-\frac{TE}{T2}} \qquad (1)$$

S: MRI signal intensity, S_0: signal (for TE=0)

Following Gaussian filtering, T2 relaxation time distributions were compared between the young and senior IVDs. Statistical significance was assessed using a Mann-Whitney U test.

3. Results

Qualitatively, young IVDs showed clearer AF-NP delineation, whereas senior IVDs exhibited reduced contrast between regions (Figure 1). Consistently, AF and NP T2 relaxation time ranges were more separated in young subjects but overlapped in the senior group (Figure 2). Statistically significant differences ($p<0.001$) were observed between young and senior subjects for the full IVD (mean T2: 50.0 vs 55.0 ms) and NP (mean T2: 55.2 vs 70.6 ms). No significant differences were found in the AF (Figure 2).

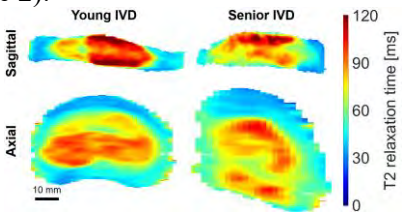


Figure 1: Cross-sectional sagittal and axial views of T2 maps of representative young and senior IVDs.

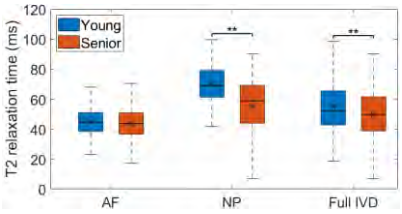


Figure 2: Box plots of T2 relaxation times in the AF, NP, and full IVD, between age groups. 'X': mean, '—': median, '**': $p<0.001$.

4. Discussion and Conclusions

The findings support the hypothesis that T2 relaxation time in the IVD varies with age and regionally. The regional differences suggest that age-related changes are not uniformly distributed across the AF and NP, reinforcing the value of T2 mapping for detecting regional IVD alterations. Future work will couple these findings with mechanical investigations to determine if T2 mapping can directly inform subject-specific local mechanical properties.

5. References

1.Marinelli N. et al., Spine; 34:520-524 (2009).
2.Ogon I et al., JOR Spine; 3:e1066 (2020).

Acknowledgements:

Funded by the Fondazione del Monte di Bologna e Ravenna (No. 2024.0053) and the European Union's Horizon Europe programme under the Marie Skłodowska Curie Grant Agreement (No. 101169278).

KNEEVIEW: AN OPEN-SOURCE REPOSITORY OF PATIENT-SPECIFIC KNEE GEOMETRIES AND STRUCTURED MESHES

Renate Janssen (1,*), Sai Natarajan (1), Francis Chemorion (1), Igor Radalov (3), Jordi Monfort Faure (4,5), Miguel A. González Ballester (1,2), Jérôme Noailly (1)

Universitat Pompeu Fabra, Spain, 2. ICREA, Spain, 3. Department of Radiology, Hospital Del Mar, Spain, 4. Rheumatology service, Hospital Del Mar, Spain, 5. Hospital del Mar Research Institute, Inflammation and Cartilage Research Group, Spain

**Corresponding author: renate.janssen@upf.edu*

1. Introduction

Finite-element (FE) modelling to investigate knee biomechanics is often limited by data availability. While the osteoarthritis initiative (OAI) [1] provides imaging data, transforming these into subject-specific FE meshes requires substantial manual and computational effort. Existing open models such as OpenKnee [2] represent important contributions but are limited to unstructured meshes and low subject count (n=8). To address this, we present a repository of 80 patient-specific bone geometries of the femur, tibia, patella and fibula that is being expanded with personalized structured FE models through mesh morphing.

2. Materials and Methods

The dataset included T2, fat saturated, knee MRI scans from 93 patients (55 female) acquired at Hospital Del Mar, Barcelona. An nnUNet trained on 36 expert annotations verified by a specialized musculoskeletal radiologist was compared with four foundation models (FMs), TotalSegmentator (TS), MEDSAM2, MRI-Core and SegmentAnyBone. A webservice, Kneeview (https://knee.view.upf.edu), hosts the repository. After excluding subjects with missing demographics, 80 segmentations were retained. We adapted the Bayesian Coherent Point Drift algorithm for tissue-specific morphing of bones, with automatic interpolation for soft tissues.

3. Results

The nnUNet achieved high segmentation performance on a hold-out test dataset of 15 volumes with an average Dice score of 0.986 ± 0.001, IOU of 0.971 ± 0.002 and Hausdorff Distance (HD95) of 14.464 ± 12.727. This HD95 variance was driven by distal tibial artefacts (Tibia HD95: 16.49 ± 14.22) while other bones gave an average HD95 of 1.46 ± 0.242. Among the FMs, TS showed the best performance (Dice 0.92 ± 0.002, IoU 0.85 ± 0.003, HD95 7.38 ± 0.20) but remained below the task-specific nnUNet. All annotated 3D models were successfully incorporated into Kneeview. The FE mesh included the complete knee joint with ligaments, bones and menisci without distorted or zero-volume elements.

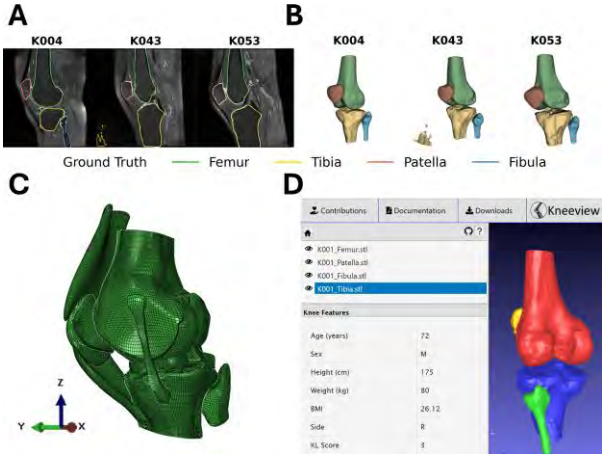


Figure 1: nnUNet segmentations and Kneeview interface. a) nnUNet segmentation against ground truth. b) 3D visualization of segmentations. c) FEM model d) Example of kneeview interface.

4. Discussion and Conclusions

A collection of 80 patient-specific models was successfully created and is accessible through our Kneeview. The high Dice scores and clear improvement over FMs confirm the pipeline's importance for simulation-ready geometries in musculoskeletal modelling. As Kneeview continues to grow, it shall address the shortage of open-source simulation-ready knee geometries. Future work will include structured FE meshes for all subjects following validation in full gait cycle simulations.

5. References

1. Lester, HSSJ, 2012
2. Chokhandre et al., Ann Biomed Eng, 20233.

Acknowledgements:

Financial funding from European Union, Horizon Europe MSCA (No.101169278), ERC (ERC-2021-CoG-O-Health-101044828), and the Spanish government (STRATO-PID2021-126469OB-C21).

PHYSIOME LINKS (PHLYNX): A WEB-BASED TOOL FOR MODULAR, MULTISCALE MODEL COUPLING AND DEVELOPMENT

Jarrah M. Dowrick (1)*, Finbar Argus (1), Hugh Sorby (1)

1. Auckland Bioengineering Institute, The University of Auckland, Auckland, New Zealand

*Correspondence: j.dowrick@auckland.ac.nz

1. Introduction

CellML facilitates the sharing and reuse of mathematical models [1], but its capability for modular model development remains largely underutilised. In the absence of rich semantic annotation, coupling existing CellML models into a larger system requires extensive, error-prone text-based edits. Physiome Links (PhLynx) is a new open-source, web-based software tool that abstracts text manipulation into a visual environment, enabling seamless modular development [2].

2. Materials and Methods

Built on the Vue 3 VueFlow library, PhLynx represents CellML components as "module nodes". Users connect these nodes with arrows to establish conduits over which variables can be coupled, replacing text-based edits with an intuitive visual interface. The core coupling mechanism creates variable equivalences via external configuration files or assignment in PhLynx. The exported CellML model can be simulated in the new OpenCOR web app [3] or in Python with Myokit [4].

3. Results

To demonstrate the capacity of PhLynx to facilitate rapid model coupling across domains, we couple a cardiac electrophysiology model with a mechanical crossbridge model [5, 6]. Coupling was achieved in less than five minutes (Fig. 1).

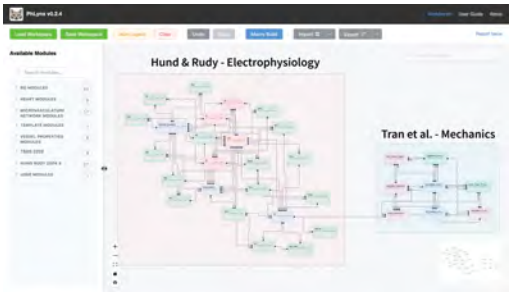


Figure 1: Node-based coupling of a cardiac electrophysiology (orange region) and mechanical crossbridge (blue region) model in PhLynx.

Simulation of the combined model was then performed in web OpenCOR (Fig. 2).

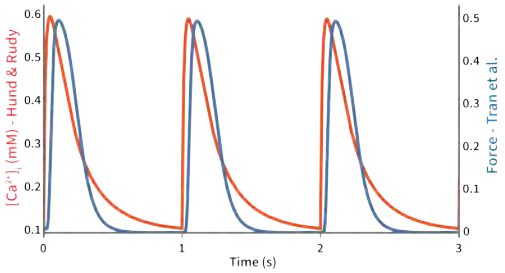


Figure 2: Coupled model simulation results in web OpenCOR. Orange – calcium, blue – force.

4. Discussion and Conclusions

PhLynx addresses barriers that have discouraged truly modular CellML development. The browser-based architecture also removes installation friction for use in teaching and collaborative settings. Future work will integrate the Physiome Model Repository [7], enabling users to import and couple published models without leaving PhLynx. We are also working to reduce barriers for model annotation and using this information to support annotation-driven coupling, alongside companion tools for efficient model calibration.

5. References

1. Clerx M et al., J Integr Bioinform, 17:2-3 (2020).
2. Dowrick JM et al.. "Physiome Links (PhLynx)." https://phlynx.com (2026).
3. Garny A et al.. "Web OpenCOR." https://opencor.ws/app (2026).
4. Clerx M et al. Prog Biophys Mol Biol; 120(1): 100-114 (2016).
5. Hund TJ, Rudy Y. Circulation 110(20):3168-3174 (2004).
6. Tran K et al., Biophys J, 98(2): 267-276 (2010).
7. T. Yu et al., Bioinformatics, 27(5): 743-774 (2011).

Acknowledgements:

The authors would like to thank the European Research Council (Grant no: 101136728) for financially supporting this project.

SEMANTIC ANNOTATION FOR COMPUTATIONAL BIOLOGICAL MODELS

Leo Willyanto Santoso, Weiwei Ai, Kenneth Tran, David P. Nickerson

Auckland Bioengineering Institute, The University of Auckland, New Zealand

1. Introduction

Computational biological models play a central role in physiological research by enabling the simulation of complex processes. Large repositories of high-quality models have been developed and shared using standards such as CellML [1]; however, their reuse and integration remain limited. A major barrier to interoperability is the lack of explicit, machine-readable semantics describing the biological meaning of model variables. This limitation becomes particularly critical in the context of the Virtual Physiological Human (VPH) vision [2], where composing models across organs, tissues, and cellular processes is essential. Semantic annotation offers a principled solution to this challenge [3], but existing annotation practices remain largely manual, time-consuming, and unscalable. This work addresses the need for automated semantic annotation to support interoperability, reuse, and model composition.

2. Materials and Methods

This research proposes an automated, evidence-driven pipeline that jointly analyses biological models encoded in CellML and their associated research publications. First, the mathematical structure of the model is extracted, capturing a structured representation of model components, variables, units, and equations. In parallel, the accompanying research paper is parsed to extract candidate sentences describing model variables and biological processes. OCR noise detection and sentence validation are applied to improve text quality, followed by LLM-guided sentence normalization to ensure consistency and clarity. In the final phase, semantic annotations are generated by selecting and ranking relevant textual evidence, identifying the semantic roles of model variables, and mapping these roles to concepts from established biological ontologies.

The resulting annotations are produced in a machine-readable format suitable for downstream computational use.

3. Results

The proposed pipeline enables the automatic generation of semantic annotations that link model variables to explicit biological meaning supported by textual evidence from the literature. By integrating structural information from the models with contextual information from research papers, the approach reduces ambiguity in variable interpretation and produces consistent ontology-based annotations. The resulting annotated models are more interpretable, interoperable, and suitable for reuse across modelling workflows. This framework explores the feasibility of scalable semantic annotation without requiring manual curation for each model.

4. Discussion and Conclusions

Automated semantic annotation addresses a fundamental obstacle to model composability at scale. By transforming implicit biological assumptions into explicit, machine-readable knowledge, the proposed approach supports FAIR principles and directly contributes to the long-term goal of integrating heterogeneous models. Automated semantic annotation represents a critical enabling technology for building interoperable model ecosystems and, ultimately, for enabling composable, interoperable multi-scale models required for robust and trustworthy human digital twins.

5. References

1. Loyd CM et al. The CellML Model Repository. Bioinformatics. 2008; 24(18):2122–2123.
2. Coveney PV et al. The Virtual Physiological Human. Interface Focus. 2011; 1(3):281–285.
3. Neal ML et al. Harmonizing semantic annotations for computational models in biology. Briefings in Bioinformatics. 2019; 20(2):540–550.

Acknowledgements:
The authors would like to thank the University of Auckland for financial support.

THE ACUTE PHASE RESPONSE TO BURN INJURY: AN IN SILICO MODELLING APPROACH

Roland V. Bumbuc (1,2,3), Vivek M. Sheraton (3), Patrick P.P.G Mulder (1,5,6, 8), Bouke K. H. L. Boekema (1,5,6), Alfons G. Hoekstra (3), Paul P. P. M. van Zuijlen (1,4,5,6,7), H. Ibrahim Korkmaz (1,2,4,6)

1. Department of Plastic, Reconstructive and Hand Surgery, Amsterdam Movement Sciences (AMS) Institute, Amsterdam University Medical Center (UMC), VUmc location, Netherlands; 2. Department of Molecular Cell Biology and Immunology, Amsterdam Infection and Immunity (AII) Institute, Amsterdam University Medical Center (UMC), VUmc location, Netherlands; 3. Computational Science Lab, Informatics Institute, faculty of Science, University of Amsterdam, Netherlands; 4. Burn Center and Department of Plastic and Reconstructive Surgery, Red Cross Hospital, Beverwijk, Netherlands; 5. Burn Research Lab, Beverwijk, Netherlands; 6. Alliance of Dutch Burn Care, Beverwijk, Netherlands; 7. Amsterdam UMC location University of Amsterdam, Pediatric Surgical Centre, Emma Children's Hospital, Netherlands; 8. Civil-Military Centre of Expertise for Trauma Care (CETC), Central Military Hospital, Ministry of Defence, Utrecht, Netherlands.

1. Introduction

Burn injuries trigger a coordinated acute phase response (APR), characterized by complement activation, immune cell recruitment, and cytokine signalling, which collectively regulate early tissue repair. These processes operate across interacting spatial and temporal scales, ranging from subcellular molecular signalling cascades to tissue-level remodelling dynamics. However, their integrated spatio-temporal dynamics remain incompletely characterised in existing computational and experimental models [1]. Existing *in silico* models of burn-associated acute inflammation are limited in mechanistic scope and are not validated against human clinical data [2]. We propose a multiscale, mechanistic computational model of the APR during the first three weeks following burn injury, within a defined context of use, and based on human clinical data, present first validation results.

2. Materials and Methods

A multiscale hybrid *in silico* model was implemented across three coupled timescales: complement kinetics (seconds to minutes), cytokine field diffusion (minutes to hours), and cell-level wound progression (days to weeks). Cell behaviour was represented using the Cellular Potts model on a three-dimensional lattice. Complement cascade dynamics were resolved via a system of ordinary differential equations (ODEs) initialised by local damage signals. Cytokine and chemokine transport was modelled by reaction-diffusion equations discretised using a finite volume method. Model parameters were based on published human burn data [3].

3. Results

Preliminary simulations explored how variations in burn severity such as different burn depth, % total body surface area burned and complement factor concentrations influence early acute inflammatory dynamics in burn wounds. Simulated concentrations for complement factors in blood and wound were compared against reference ranges reported in human burn patient data. The results are consistent with qualitative ranges in early inflammatory response in burn injuries in adults; however quantitative agreement at the general population level remains limited at this stage of model development. Interactions between complement activation and pro-/anti-inflammatory cytokines are still under development.

4. Discussion and Conclusions

This early-stage *in silico* model provides a mechanistic representation of complement-mediated acute inflammation in burn injury, capturing spatio-temporal interactions, complement factors, and subsequent cytokine signalling at the human physiological scale. The framework demonstrates potential for hypothesis generation (e.g., how inhibition of the APR effects cytokine release) and sensitivity analysis (e.g., which complement factors most influence inflammation dynamics). It is still under active development, with systematic validation against independent clinical datasets is ongoing.

References

1. Bumbuc RV et al. 2023 IEEE Int Conf Bioinform Biomed (BIBM). 2023;3676(1):3676–3683.
2. Korkmaz HI et al. Front Immunol. 2024;15(1):1303776.
3. Mulder PP et al. Front Immunol. 2026;17(1):1793945.

THE PHYSIOME MODEL REPOSITORY: CURRENT STATUS AND FUTURE PLANS

David P. Nickerson, Tommy Yu, Alan Garny, Aung Kyaw Hein, Peter J. Hunter

Auckland Bioengineering Institute, University of Auckland, Auckland, New Zealand

1. Introduction

The Physiome Model Repository (PMR; https://models.physiomeproject.org) is a public repository of open-source computational models [1]. Originally developed for use as a repository of mathematical models encoded in the CellML format, PMR now consists of a diverse array of computational models and simulation experiments. These models are, in some cases, supplemented with rich metadata.

2. Materials and Methods

The core content in PMR is the collection of workspaces. Each workspace is a version-controlled repository (using Git). Users can share their workspaces with other users (read and/or write access) and to make the publicly available (read-only). Specific versions of workspaces can be published as "exposures", like making a software release.

PMR supports the presentation of various file types as part of exposures. Comprehensive support is available for CellML models, displaying mathematics, metadata, documentation, generated procedural code, etc. Support for other data types varies and relies on users being able to correctly configure their workspace and exposure for optimal presentation. In all cases, however, exposures provide an unambiguous method to identify a very specific version of the content of a workspace.

The PMR web interface allows users to browse workspaces and exposures, as well as for users to manage their own content. Various search interfaces are available, from the basic text-based search through to the comprehensive SPARQL query engine for searching through the indexed semantic metadata. All features available via the web interface are also available via the comprehensive API for programmatic access.

3. Results

As of March 2026, PMR has 1300 publicly available workspaces and over 941 exposures. Those exposures include 1098 CellML models. Of those, 219 make use of the CellML "import" feature to reuse models. Checking with libCellML [2], 897 of these models are valid CellML and 618 appear able to be simulated as-is.

Extracting the keywords included in the CellML models from the exposures it is possible to get an overview of the types of models in the repository. A word cloud generated from those keywords is shown in Figure 1.

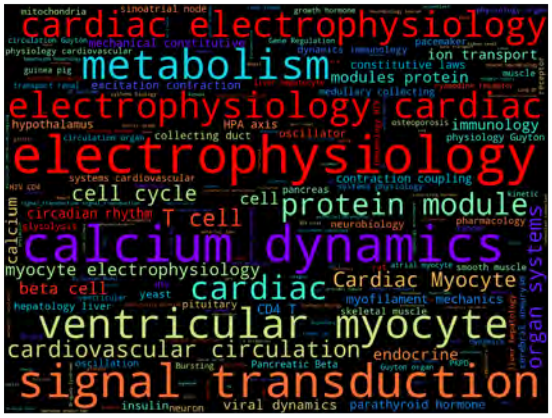


Figure 1: Word cloud showing the keywords included in CellML models across PMR exposures.

4. Discussion and Conclusions

A new version of the PMR infrastructure is about to be launched. This will be a significant modernisation of the web interface and programmatic services. Ensuring existing content remains resolvable and available for use, especially in training new AI algorithms and agents, while leveraging external services for enhanced capabilities, is critical to the continued success of the repository.

5. References

1. https://doi.org/10.1093/bioinformatics/btq723
2. https://doi.org/10.5281/zenodo.14065120

Acknowledgements:

The authors would like to thank the NIH SPARC program (Award no: OT3OD025347) for providing financial support to this project.

TOWARDS A REACTION-DIFFUSION FRAMEWORK FOR IN SILICO ASSESSMENT OF HEALING IN BREAST-CONSERVING SURGERY

Oriana De Becker (1), Jos Vander Sloten (1), Liesbet Geris (1,2)

1. KU Leuven, Belgium; 2. ULiège, Belgium

Department of Mechanical Engineering, KU Leuven, Belgium, email: oriana.debecker@kuleuven.be

1. Introduction

Breast cancer is among the most prevalent cancers in developed countries, and current treatment strategies are highly effective. Breast-Conserving Surgery (BCS) successfully removes cancerous tissue, but often leads to unsatisfactory aesthetic outcomes, negatively affecting patients' quality of life. To address this, temporary scaffold-based strategies are under development to support tissue regeneration. In this context, models of breast tissue healing provide a valuable tool for preclinical *in silico* assessment of these emerging approaches.

While computational models of tissue healing are widely developed for applications such as bone regeneration, modelling efforts focussed on breast tissue remain limited. Most existing work addresses general dermal wound healing [1,2], with few models specifically tailored to breast tissue [3], highlighting the need for a dedicated computational effort.

2. Materials and Methods

A biochemical reaction-diffusion framework is developed based on the model of Harbin *et al.* (2023) [3] and extended to include macrophages, which play a crucial role in the initial inflammatory response, and myofibroblasts, key drivers of fibrosis. These are considered alongside the originally included components: the chemical signalling agent TGF-β, fibroblasts, and collagen. Each entity is governed by a dedicated reaction–diffusion equation following the general form given in Eq. 1. The source term s_x captures the relevant biochemical and cellular interactions, including production, degradation, and inter-entity interactions.

$$\dot{x} = -\nabla \cdot (D_x \nabla x) + s_x \qquad (1)$$

The coupled reaction-diffusion framework is implemented in COMSOL Multiphysics and evaluated on a simplified two-dimensional geometry representing a post-surgical cavity surrounded by healthy breast tissue.

3. Results

Fig. 1 shows the mean concentration within the cavity for all entities over the healing period.

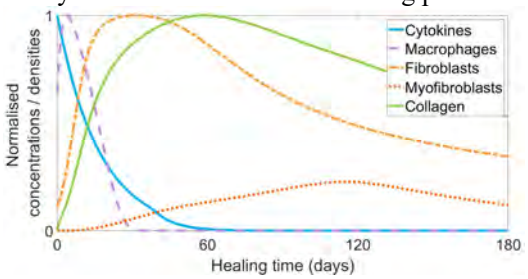


Figure 1: Mean concentration of modelled entities (TGF-β: blue, macrophages: purple, fibroblasts: light orange, myofibroblasts: dark orange, and collagen: green) as a function of healing time.

4. Discussion and Conclusions

Although the model is still undergoing calibration based on literature data, the temporal evolutions shown in Fig. 1 follow the expected healing trends, with an early peak in macrophages and rapid decline of cytokines, followed by a delayed increase in (myo-) fibroblasts and collagen deposition.

These results highlight the potential of the proposed framework and motivate its further extension to three dimensions and the explicit inclusion of mechanical cues in future modelling steps.

5. References

1. Tepole AB. *Comput Methods Appl Mech Eng. 2017*; 314:46-70.
2. Koppenol DC et al., *Biomech Model Mechanobiol.* 2017;16:15–32.
3. Harbin Z et al., *Comput Biol Med.* 2023;165:107342.

Acknowledgements:
The authors would like to thank the Endowed Materialise Chair at KU Leuven for providing financial support to this project.

DHPI: a multiscale model for drug–host–pathogen dynamics in infectious disease

Alessandro Ravoni (1), Enrico Mastrostefano (1), Davide Moretti (1), Elia Onofri (1), Francesca Pelusi (1), Paolo Tieri (1), Filippo Castiglione (1,5), Aristides Dokoumetzidis (2,3), Evangelos Karakitsios (1), Salvatore D'Agate (1,4), Alessandro Di Deo (1,4), Umberto Villani (1,4), Oscar Della Pasqua (1,4)

1. Institute for Applied Computing "Mauro Picone", CNR, Rome, Italy; 2. Department of Pharmacy, National and Kapodistrian University of Athens, Greece; 3. Pharma-Informatics Unit, Athena Research Center, Greece; 4. Clinical Pharmacology and Therapeutics Group, University College London, UK; 5. Medicine Department – Pulmonary Systems Medicine, University of Florida, Gainesville, USA

1. Introduction

Treatment outcome in infectious diseases emerges from the interplay between drug exposure, pathogen dynamics and host immunity, but pharmacological and immunological processes are typically modelled separately. We present the Drug–Host–Pathogen Integration (DHPI) model, a data-informed multiscale *in silico* framework that combines these components within a unified simulation environment, enabling calibration against clinical data, quantification of drug- and immune-mediated bacterial killing, and analysis of how therapy influences the immune response and long-term disease trajectories.

2. Materials and Methods

The DHPI model combines three independently developed mechanistic components: a physiologically based pharmacokinetic (PBPK) model [2] describing drug distribution in lung tissue, a pharmacokinetic–pharmacodynamic (PKPD) model [3] linking drug exposure to bacterial killing, and a stochastic agent-based model (ABM) [1] representing infection dynamics and host immune response.



Figure 1: Architecture of the DHPI model.

Drug concentrations from the PBPK model are mapped to bacterial phenotypes in the ABM, while the PKPD component converts local exposure into phenotype-specific killing probabilities applied to individual bacteria. Phenotype-specific efficacy parameters are inferred via Approximate Bayesian Computation from clinical data.

3. Results

As a proof of concept, the framework is applied to pulmonary tuberculosis treated with rifampicin monotherapy. Calibration reproduces bacterial load dynamics during treatment; validation against independent early bactericidal activity data confirms predictive consistency. Because drug- and immune-mediated elimination events are explicitly tracked, the model directly decomposes treatment effects: in the tuberculosis case study, 81–88% of bacterial killing is drug-mediated and 12–19% immune-mediated. Simulations further indicate that the immune configuration reached during therapy influences long-term disease trajectories, with treatment-associated immune memory correlated with favourable outcomes.

4. Discussion and Conclusions

The DHPI model demonstrates that heterogeneous mechanistic models operating at different scales can be jointly calibrated from clinical data and validated on independent observations. The modular architecture supports extension to multidrug regimens, host-directed therapies and patient-specific simulation, providing the building blocks for digital twin applications in the evaluation of treatment response in infectious diseases.

5. References

1. Rapin N., Lund O., Bernaschi M., Castiglione F. PLoS One. 2010.
2. Karakitsios E., Dokoumetzidis A. J. Antimicrob. Chemother. 2024.
3. Muliaditan M., Della Pasqua O. Br. J. Clin. Pharmacol. 2020.

Acknowledgements:
"This work has received support from the Innovative Medicines Initiatives 2 Joint Undertaking (grant No 853989 ERA4TB)."

BRIDGING PHARMACOKINETICS, PHARMACODYNAMICS AND PHARMACOGENOMICS WITH PHARMACOLIBRARY – FREE LIBRARY TO MODEL PHARMACOLOGY

Tomáš Kulhánek, Simon Denil, Gökhan Ertaylan
Flemish institute of technology and research (VITO), Belgium

...

1. Introduction

Mechanistic modeling of drug pharmacokinetics (PK), pharmacodynamics (PD), and pharmacogenomics (PGx) is essential for rational drug development and personalized therapy. Existing tools—such as Certara's SimCyp, Open Systems Pharmacology PK-Sim/MoBi, MediWare's MWPharm++, and MATLAB SimBiology®—either specialize in a single modeling aspect (e.g., physiology based pharmacokinetics (PBPK) or therapeutic drug monitoring or bundle model definition with simulation in proprietary environments, limiting reusability and interoperability.

To address this, we introduce Pharmacolibrary, a free Modelica library, unifies PK, PD, PBPK, toxicokinetics and enhanced it with PGx with acausal connectors and SI units. As it focuses on pure modeling aspect, the further simulation and analysis is left to users' preference with demonstrated export of the models to standard Functional Mockup Interface (FMI) which allows direct integration to simulation and analysis tools such as Python, Matlab, etc.

2. Materials and Methods

Pharmacolibrary implements acausal Modelica connectors and basic PK,PD,PGx components that ensure mass balance and physiological mixing of modeled compound. Integration with libraries focusing on biology, chemical and physiology modeling is demonstrated in Fig 1.

3. Results

The library contains components for PK,PD,PGx,PBPK modeling, basic PK models of all drugs that have registered ATC code 5496 corresponding to 4364 distinct chemical substances and examples of PD,PGx models. It is published at GITHUB[1].

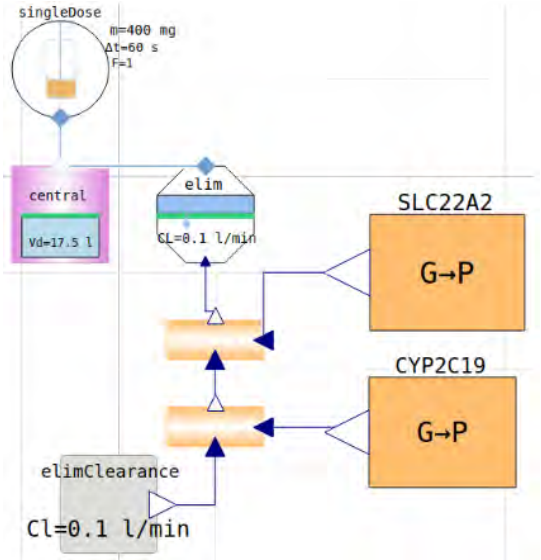


Figure 1: Example integration of 1-compartment PK model of gentamicin and PGx influence of CYP2C19 genotype and SLC22A2 genotype on clearance of it.

4. Discussion and Conclusions

Pharmacolibrary addresses key limitations in pharmacology modeling by providing reusable, acausal Modelica components for PK/PD/PBPK/TK/TD/PGx that ensure mass balance via specialized connectors, enable diagram-based construction over error-prone equations filling a Modelica ecosystem gap.

5. References

[1] Pharmacolibrary, source code, GITHUB: https://github.com/digital-biosystems/Pharmacolibrary

Acknowledgements: The authors were supported by the ONCOSCREEN, RAIDO and DVPS projects, funded by the European Union's Horizon Europe research and innovation programme under grant agreement No. 101097036, 101135800 and 101213369.

PERSONALIZED SIMULATION USING FINITE ELEMENTS OF MULTI-NEEDLE INSERTION IN PROSTATE BRACHYTHERAPY

Christos Panagiotis Papanikas (1), Evripidis Sellountos (1), Eleftherios Ioannou (1), Vasileios Vavourakis (1,2)

1. Mechanical & Manufacturing Engineering Department, University of Cyprus, Cyprus;
2. Medical Physics & Biomedical Engineering Department, UCL, United Kingdom

1. Introduction

In high dose rate (HDR) brachytherapy of prostate cancer treatment, sequential insertion of metal needles into the prostate is required so that subsequently internalized radiation is delivered to treat cancer. Typically 15 to 200 needles are inserted in the prostate during this procedure. Despite single-needle insertion biomechanics are well-documented (e.g., [1]), the cumulative mechanical interactions and organ deformations resulting from multiple insertions are less understood. However, real-time monitoring during these procedures is often limited, necessitating *in silico* models to accurately predict prostate tissue deformations. This study expands substantially from our previous work [2] and we present here a novel FEM modelling framework to simulate prostate deformation during HDR brachytherapy, thus, aiming to build a simulation tool that could assist clinicians avoiding critical structures like the urethra while maintaining optimal dose distribution in the prostate.

2. Materials and Methods

We developed an in-house scalable (CPU/GPU) FEM solver that follows a pipeline (see Fig. 1) which converts patient-derived ultrasound images –after appropriate delineation of the regions of interest using an in-house ML-based image segmentation algorithm– into 3D unstructured (tetrahedral) finite element meshes. The model embeds the prostate geometry within a cubic volume of surrounding tissue, both characterized by linear elastic material properties whereas needles are modelled as 1D deformable beams. To simulate penetration, a node-decoupling and remeshing algorithm splits elements once localized stresses exceed a predefined threshold of failure. This allows for the sequential simulation of multiple needle tracks and the quantification of displacement within the organ.

3. Results

The solver was validated against LS-DYNA through benchmarks of increasing complexity, e.g., from indentation and needle penetration into homogeneous and heterogeneous (spherical inclusion) volumes. Comparison of the FEM displacements and stresses showed strong agreement between our solver and LS-DYNA. Further validation was also conducted using retrospective clinical data, where simulations were compared to RWD anatomical morphology of the prostate (captured post-needle insertion) from TRUS imaging.

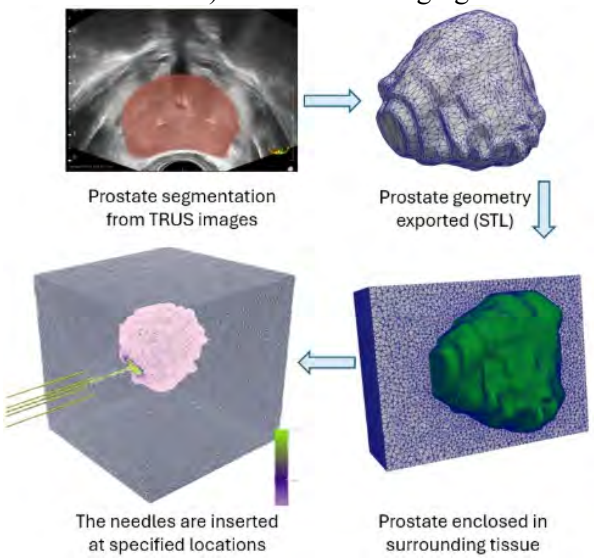


Figure 1: Modelling procedure for image segmentation of the prostate, extraction, FE mesh generation, and simulation of needle insertion.

4. Discussion and Conclusions

The proposed framework successfully captures the biomechanical response and the prostate deformations stemming from the HDR brachytherapy procedure. Accounting for the progressive organ deformation caused by sequential needle insertion, our simulator provides a robust foundation for enhanced pre-operative and intra-operative planning. This capability could enable clinicians to optimize treatment delivery and improve the accuracy of needle placement relative to sensitive anatomical structures.

5. References

1. Perrusi PHS et al., *Eurographics* 2021
2. Hadjicharalambous M et al., *Frontiers in Physiology* (2024)

MODELLING CEREBRAL AUTOREGULATION ACROSS SCALES: FROM HEALTH TO POST-STROKE DYSFUNCTION

Chryso Lambride (1,2,3), Mohamad El Amki (1,2), Susanne Wegener (1,2), Franca Schmid (3)

1. Department of Neurology, University Hospital and University of Zurich, Switzerland; 2. Neuroscience Center Zurich, University of Zurich, Switzerland; 3. ARTORG Center for Biomedical Engineering Research, University of Bern, Switzerland

1. Introduction

Cerebral autoregulation stabilizes cerebral blood flow (CBF) in response to variations in mean arterial pressure (MAP). This is primarily achieved by active changes in vessel diameter. However, the precise contributions of individual vessels and the role of impaired autoregulation for outcome after ischemic stroke remain poorly understood.

2. Materials and Methods

We present a novel computational model that describes static myogenic and endothelial regulation and computes CBF as a function of changes in MAP [1]. Autoregulation is studied in microvascular networks (MVNs) derived from realistic surface vasculatures of mice containing ~200'000 vessels each, ranging from the cortical surface to the smallest capillaries.

We evaluate autoregulatory responses at single vessel resolution for: i) healthy conditions, ii) post-occlusion reperfusion with altered vascular reactivity, and iii) chronic autoregulation dysfunction (Fig 1A). Building on our previous work [2], a specific focus is on the role of pial collateral density and arterial density, known to be decisive for stroke outcome [3].

3. Results

For healthy conditions, our model reproduces the classic static autoregulation curve (Fig. 1B) and highlights the dominant contribution of surface arteries in buffering pressure changes. Lower descending arteriole density causes more extensive arterial dilations, underlining the topological influence on autoregulation.

To mimic chronic autoregulatory dysfunction, we progressively increase the number of non-functional arteries in the territory previously affected by stroke, proving that the loss of vascular reactivity disrupts capillary perfusion (Fig 1C) and alters the autoregulation curve.

We further show that collaterals play a crucial role in maintaining residual perfusion in adjacent regions during stroke. However, they do not substantially alter reperfusion dynamics after clot removal. Instead, impaired myogenic reactivity emerged as a contributor to hyper-perfusion during and post-stroke treatment.

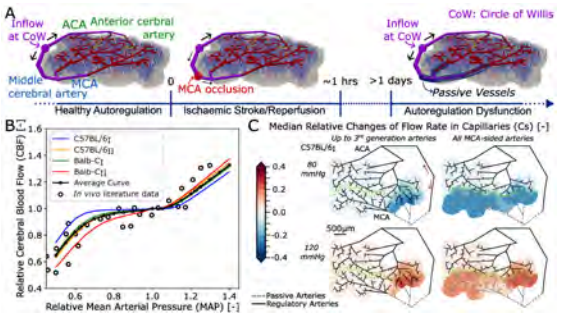


Figure 1: A) Exemplary semi-realistic MVN to study autoregulation under three different conditions. B) Healthy autoregulation curves. C) Maps of median relative changes in capillary flow for autoregulatory dysfunction of different severities for MAPs of 80 and 120 mmHg (Reference MAP: 100 mmHg)

4. Discussion and Conclusions

These findings provide mechanistic insight into how microvascular structure and vessel-level regulation shape global cerebral perfusion under both healthy and pathological conditions. Our *in silico* framework helps explain stroke-related perfusion variability and puts forward recovery of vasoreactive mechanisms as a therapeutic target to improve stroke outcomes.

5. References

1. Lambride et al., bioRxiv, 2025, doi:10.1101/2025.10.03.680208
2. Epp et al., PLoS Comput Biol, 2023, doi: 10.1371/journal.pcbi.1011496
3. El Amki et al., Int J Mol Sci, 2017, doi: 10.3390/ijms18122669

Acknowledgements:

CL, FS, and SW are receiving funding from the Swiss National (Grant No: 202192, 200703).

DIGITAL TWIN-DRIVEN MODELLING OF INTRACRANIAL ANEURYSM CARE PATHWAYS

Lea Bührer (1, 2), Abiram Sandralegar (3,4), Sandrine Morel (5), Philippe Bijlenga (3,4), Sven Hirsch (1), Georg R. Spinner (1)

1. ICLS, ZHAW, Wädenswil, Switzerland; 2. DM3L, UZH, Zürich, Switzerland; 3. Division of Neurosurgery, Geneva University Hospitals, Switzerland; 4. Faculty of Medicine, University of Geneva, Switzerland; 5. NeuroCentre, Geneva University Hospitals, Switzerland.

1. Introduction

Intracranial aneurysms (IAs) affect 3–5% [1] of the population and may remain asymptomatic until rupture, which carries high mortality and long-term disability. Preventive treatment reduces rupture risk but introduces procedural hazards, making IA care a sequential decision problem under uncertainty. Current risk stratification relies on phenotypic variables that only partially capture underlying mechanisms [1,2]. We propose a cohort-based Digital Twin framework that maps interactions across disease phases, such as detection, preventive treatment, rupture, and recovery, to support longitudinal management and reduce disease burden.

2. Materials and Methods

We use additive Bayesian networks (ABNs) to infer probabilistic dependencies among IA-related attributes. ABNs handle mixed data types, support clinically informed structure learning, and assess stability through MCMC sampling [3]. The framework is applied to a prospective cohort (HUG ASIS, n=487) of incidentally detected, asymptomatic unruptured IAs.

3. Results

Age emerged as a major determinant of one-year functional outcome (IRR 1.43, 95% CI 1.16–1.77) and interacts with the applied management strategy (Figure 1). Estimated average treatment effects show no differences between endovascular treatment, microsurgery, and observation, largely due to sample size limitations and treatment selection based on baseline condition. The ABN model captures clinically plausible temporal dependencies between baseline characteristics, management decisions, and longitudinal outcomes.

4. Discussion and Conclusions

This work establishes the first clinically grounded component of a broader Digital Twin for IA disease. The current module clarifies causal-like dependencies among unruptured IA patients and exposes the limitations of internally validated models. Future iterations will integrate genetic variables, ruptured patients, biomechanical simulations of IA growth and rupture, and computational modelling of treatment strategies. By combining mechanistic modelling and longitudinal real-world data, the Digital Twin aims to optimise sequential IA management and reduce disease burden.

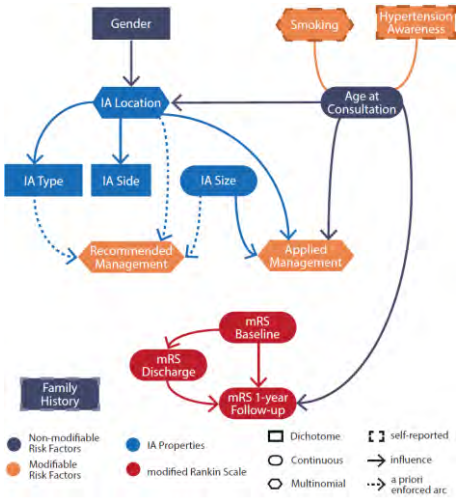


Figure 1: CPDAG of the ABN model.

5. References

1. Etminan, N. et al. The Lancet Neurology 24, 945–957 (2025).
2. Rinkel, G. J. E., et al. The Lancet Neurology 24, 958–968 (2025).
3. Delucchi, M. et al. Computers in Biology and Medicine 147, (2022).

Acknowledgements:

This work has received funding from the European Union's Horizon Europe research and innovation programme under grant agreement No 101136438 (GEMINI project). Further, it was supported by the DIZH project "Stroke DynamiX", the @neurIST project (EU FP6-IST-2004-027703), the AneuX project (Swiss SystemsX.ch initiative), the Clinical Research Centre and HUG NeuroCentre in Geneva.

TWIN MODELS OF SURVIVAL IN PATIENTS WITH GLIOBLASTOMA USING NORMATIVE NEUROIMAGING

Anna Janus (1,2), Joan Falcó-Roget (1) , Julia Rybska (1,*), Barbara Wojtarowicz (1,*), Claudio di Paola (3), Augusto Ielo (4), Sara Lillo (5,6), Letterio S. Politi (7,8), Jan K. Argasinski (1,2), Alberto Cacciola (7,8)

*1. Sano, Centre for Computational Medicine, Poland; 2. Jagiellonian University, Poland; 3. University of Messina, Italy; 4. IRCCS Centro Neurolesi "Bonino Pulejo", Italy; 5. CNAO National Center for Oncological Hadrontherapy, Italy; 6.University of Pavia, Italy; 7. Humanitas University, Italy; 8. IRCCS Humanitas Research Hospital, Italy; * Equal contributions*

1. Introduction

Driven by cancer neuron interactions [1], glioblastomas (GBMs) escape most therapeutic strategies and exhibit overall survival (OS) times rarely exceeding 2 years. Recent works have shown how in vivo models of GBM-brain scaffolds improve our understanding of disease progression and OS prognosis, both using methods from graph theory [2] and white matter imaging [3]. These findings conceptualize GBMs as network lesions rather than simple focal lesions [4]. Here, we describe a way forward to incorporate GBM-brain interactions, emphasising precision and clinical practicality.

2. Materials and Methods

We used a normative framework in a set of four independent cohorts of patients (N=367, 496, 103, 33) diagnosed with a GBM [5]. For each patient, multimodal MRI and tumor segmentation masks were normalized to a common MNI template. Then, we extracted the subset of streamlines from a normative tractogram that intersected the lesion masks to obtain patient-specific maps of GBM-brain structural scaffolds. We used survival statistics to measure the contribution of the GBM-brain structural scaffolds to patient outcomes.

To study their contribution to the OS, we proceeded in two distinct ways. We computed 1) tract density maps of these patient-specific tractograms encoding the number of streamlines intersecting the GBMs per voxel, and 2) structural connectomes by counting the number of streamlines connecting the different pairs of regions of interest [6].

3. Results

Low-dimensional embeddings of white matter density maps, derived using classical machine learning (e.g., principal component and canonical correlation analysis) and deep learning approaches (e.g., autoencoders), identified macroscale patterns of white matter involvement. These components significantly improved survival risk prediction compared to clinical covariates alone (C-index: 0.72 vs. 0.66). Network neuroscience metrics showed significant univariate associations with survival in selected cases ($p < 0.001$; C-index ≥ 0.56), while others were non-informative. Joint representations using UMAP uncovered subgroups characterized by shared connectivity profiles and distinct survival trajectories, including ranked differences in median overall survival (Kendall's τ, $p < 0.05$).

4. Discussion and Conclusions

Overall, we present a principled approach to modelling GBMs as network pathologies to enhance our understanding of the heterogeneous survival rates commonly observed in clinically homogenous samples.

5. References

1. Monje, M. Neuron; 113(17): 2734-2739 (2025).
2. Wei, Y., *et al.* Brain; 146(4); 1714–1727 (2022).
3. Falcó-Roget, J., *et al*. Neuro-Oncology; noaf234 (2025).
4. Duffau, H., and Massimo, F. The Lancet Neurology; 23(7): 655-656 (2024).
5. Louis, DN., *et al.* Neuro-Oncology; 23(8): 1231-1252 (2021).
6. Huang, CC. *et al.* Brain Struct. Funct.; 227(3): 763-778 (2022).

Acknowledgements:

National Science Centre, Poland (UMO-2024/53/N/NZ4/03513); European Union Horizon 2020 (No 857533); Foundation for Polish Science, International Research Agendas Programme (MAB PLUS/2019/13); Minister of Science and Higher Education, Poland (MEiN/2023/DIR/3796); PLGrid ACK Cyfronet (PLG/2025/018289); and National Plan for NRRP Complementary Investments, Italy (ANTHEM PNC0000003).

CEREBROSPINAL FLUID DYNAMICS AND BRAIN TISSUE POROMECHANICS FOR THE STUDY OF WASTE CLEARANCE

Ivan Fumagalli (1), Mattia Corti (1), Riccardo Petrucci (1), Nicola Parolini (1), Paola Antonietti (1)

1. MOX, Dipartimento di Matematica, Politecnico di Milano, Italy

ivan.fumagalli@polimi.it; Politecnico di Milano, piazza Leonardo da Vinci 32, 20133, Milan, Italy

1. Introduction

Neurodegenerative proteinopathies such as Alzheimer's disease are often associated with impaired clearance of metabolic waste from the brain. The Cerebrospinal Fluid (CSF) plays a key role in this process by circulating through the ventricular system and permeating the brain parenchyma, thus promoting the removal of misfolded proteins and other by-products of neural activity. Due to the strong interaction between fluid dynamics, tissue mechanics, and vascular circulation across multiple spatial scales, multiphysics models are both required to accurately represent the system and useful to investigate the contribution of different physiological and pathological processes [1].

2. Materials and Methods

We present a mathematical model combining CSF's incompressible flow in the cerebral ventricles with a poromechanics model of the parenchyma [2]. The tissue is described by a Multiple-network Poro-Elasticity (MPE) formulation accounting for interacting fluid compartments in the porous medium. The resulting interstitial filtration velocity is used to model the transport of proteins and nutrients. The coupled problem is discretized with a polytopal discontinuous Galerkin method. Simulations are performed on anatomically realistic geometries reconstructed from MRI data. To incorporate vascular effects, a one-dimensional hemodynamic model of the main cerebral arteries is also considered, allowing the investigation of scenarios including the partial obstruction of the circle of Willis [3].

3. Results

The proposed model enables the simulation of CSF flow in the ventricular system and the associated perfusion and protein transport in the brain parenchyma. Numerical experiments show physiologically consistent patterns of pressure distribution, ventricular flow, and fluid exchange between compartments. The simulations also highlight the sensitivity of fluid transport to the interface conditions between ventricles and tissue, whose calibration is often difficult due to the lack of in-vivo measurable data [4]. Such sensitivity may significantly affect waste-clearance efficiency and thus the accumulation of pathological proteins in neurodegenerative diseases. The geometric multiscale approach provides a balance between numerical accuracy in the tissue of interest and computational efficiency in the arterial network.

4. Discussion and Conclusions

The proposed framework enables the simulation of CSF circulation in the ventricles and associated filtration processes in the brain tissue. Preliminary results show physiologically consistent pressure and flow distributions and highlight the influence of modeling parameters on exchange mechanisms. This computational model provides a tool to investigate how alterations in brain fluid transport may affect waste clearance and contribute to neurodegenerative disease processes.

5. References

1. Causemann M et al., Fluid Barrers CNS; 19:84 (2022).
2. Fumagalli I et al., J Comp Phys; 513:113115 (2024).
3. Petrucci R, MSc thesis, Politecnico di Milano (2023).
4. Fumagalli I, Math in Eng; 7(2):130-161 (2025).

Acknowledgements:

This work has been supported by ICSC – Centro Nazionale di Ricerca in High Performance Computing, Big Data, and Quantum Computing, funded by the European Union – NextGenerationEU. All authors are members of INdAM-GNCS. The present research is part of the activities of "Dipartimento di Eccellenza 2023-2027", Dipartimento di Matematica, Politecnico di Milano.

AN ALLOMETRIC AND ANISOTROPIC APPROACH TO PREDICTING CRANIAL GROWTH

Mirna Potgieter (1), Dewar Finlay (1), James McLaughlin (1), Selim Bozkurt (1)

1. *School of Engineering, Ulster University, United Kingdom*

Correspondence: s.bozkurt1@ulster.ac.uk

1. Introduction

Despite significant advancements in craniosynostosis (CS) treatments [1], the condition remains associated with unpredictable morphological and functional outcomes [2]. Developing a digital twin model for skull growth patterns will enable optimisation and personalisation CS treatment.

The objective of this research is to integrate the geometric, biological and mechanical properties that describe the morphology of the skull at different phases of growth into a single tool, that can be used to guide predictive growth simulations of individual crania in healthy and CS skulls.

2. Materials and Methods

Comprehensive meta-analysis of existing literature is conducted to compile a database of normative growth metrics for bone thickness and head circumference for males and females aged 0-12 months. The data were further processed to develop percentile curves for each bone in skull and serve as the basis for individualised growth maps.

A logarithmic equation is used to calculate growth coefficients inverse to the growth curve and applied orthotropically as expansion coefficients to individual bones and sutures in Finite Element (FE) simulations on a 3D skull geometry. The mechanical properties are iteratively adjusted to represent increasing stiffening of bone and sutures over time.

3. Results

When simulating growth in a from 0-1 month, the initial head circumference of 35.16 cm increased by 12.51%, which accounts for 4.5% overprediction of growth. The frontal bone had the greatest increase in thickness, from 1.93mm to 2.14mm, resulting in a 10.78% increase, 5.82% over the target measurement.

The parietal bone thickness increased by 11.92% and the occipital bone thickness by 11.57%, which account for 1.18% and 1.23% overprediction of thickness respectively.

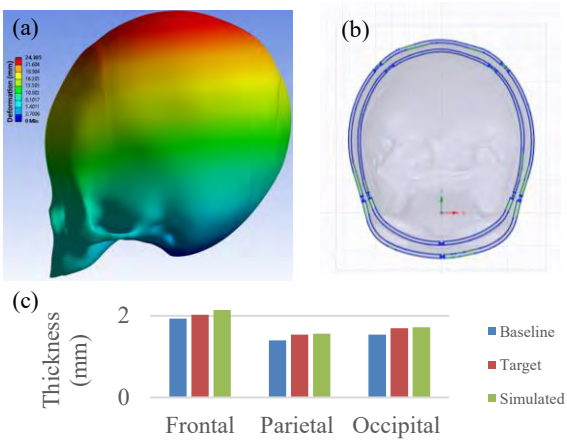


Figure 1: (a) FEA results for the skull growth, (b) comparison of the skull contours from 0 months to 1 month simulation, (c) change in bone thickness from baseline measurement at 0 months to target measurements at 1 month compared to simulated outcomes.

4. Discussion and Conclusions

Results show that applying statistical distributions to patient specific cranial measurements, enables prediction of non-uniform growth outcomes of the global and regional morphology of the skull. Notably, simulated thickness measures closely followed their respective growth percentiles, with minor deviations that mimic typical biological variation. This approach is being extended to simulate CS skulls to evaluate treatment options in a digital twin.

5. References

1. Iqbal J et al., Annals of Medicine & Surgery. 87(4):2234–42 (2025)
2. Lif H et al., Journal of Craniofacial Surgery. 36(8):3074–9 (2025)

Acknowledgements:

This work is supported by the Ulster University Vice-Chancellor's Research Scholarships scheme.

IN-SILICO MEDICINE APPLICATION OF MULTIMODAL NEUROIMAGING BIOMARKERS IN ALZHEIMER'S DISEASE

Annamaria Vernone, Carla D'Agostino, Ilaria Stura, Eleonora Ficiarà, Caterina Guiot, Fabrizio Pizzagalli, for the Alzheimer's Disease Neuroimaging Initiative

Department of Neurosciences "Rita Levi Montalcini", University of Torino, Italy.

1. Introduction

Alzheimer's disease (AD) is characterized by progressive neurodegeneration associated with structural atrophy, amyloid plaques (AP) deposition, molecular dysfunction, and iron dysregulation [1,2]. Post-mortem brain analyses have shown a close colocalization of iron and AP in AD patients in basal ganglia. T2*-weighted MRI is highly sensitive to iron deposition, which contributes to oxidative stress, while PET provides complementary functional information related to AP burden. We propose an integrated multimodal analysis based on a framework combining T1w MRI, T2*w MRI, and PET to enable unified ROI-based analyses of structural, iron-related, and functional biomarkers. As a first step, we analyzed iron- and AP–related metrics within specific brain regions known to be involved in AD pathology.

2. Materials and Methods

Data were obtained from the Alzheimer's Disease Neuroimaging Initiative (adni.loni.usc.edu). T1w, T2*w, and PET images were processed on the Leonardo HPC system at CINECA (https://www.hpc.cineca.it/systems/hardware/leonardo/) using a customized version of PetSurfer, which integrates FreeSurfer v7.4.1 and FastSurfer for segmentation and atlas-based ROI definition [3]. PET and T2*w images were co-registered to T1w space to estimate the ROI-based T2*-derived and PET-derived measures, reflecting iron content and AP deposition respectively. Statistical analyses were performed on these ROI-based measures.

3. Results

The framework enabled robust multimodal analysis and consistent ROI extraction across subjects. Integrated analyses enabled simultaneous quantification of volumetric, PET-derived, and T2*-related metrics within the same anatomical regions. High-performance computing resources ensured scalability and efficient processing of the multimodal dataset.

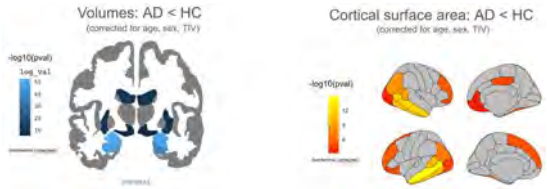


Figure: Volumes and cortical surface area reduction in AD in specific brain regions. HC=Healthy Controls (206 HC and 160 AD subjects).

Preliminary analysis showed that PET-related metrics differed between HC (N=17; age=72.0) and AD (N=13; age=72.9) patients in some of the regions involved in atrophy (e.g. putamen).

4. Discussion and Conclusions

This integrated approach provides a reproducible and scalable framework for comprehensive characterization of AD-related brain alterations.

Correlations among imaging metrics may represent a first step toward assessing the in vivo colocalization of AP and iron in specific brain regions.

By integrating imaging biomarkers, this framework advances a mechanistic understanding of disease progression.

5. References

1. Ficiarà et al. Int J Mol Sci. 2024 Feb 16;25(4):2337.
2. Vernone et al., Int. J. Mol. Sci. 2025, 26(15), 7536.
3. Guiot et al., DOI:10.5281/zenodo.17104663.

Acknowledgements:

The authors acknowledge the project 'National Centre for HPC, big data & quantum computing' PNRR MUR-M4C2. for providing financial support.

AN UNCERTAINTY-AWARE FRAMEWORK FOR SAFE EEG-BASED STROKE TRIAGE

Rosmary Blanco (1), Maritta N. van Stigt (3), Eva A. Groenendijk (3), Jan K. Argasiński (1,2), Jonathan M. Coutinho (3), Aneta Lisowska (4), Henk A. Marquering (3)

(1) Sano Centre for Computational Medicine, Poland; (2) Jagiellonian University, Poland; (3) Dept. of Neurology / Radiology and Nuclear Medicine / Biomedical Engineering and Physics, Amsterdam University Medical Center, the Netherlands;(4) Vrije Universiteit / Amsterdam University Medical Center, the Netherlands

Corresponding Author: Rosmary Blanco, Sano Centre for Computational Medicine, Czarnowiejska 36, 30-054 Kraków, Poland. Email: r.blanco@sanoscience.org

1. Introduction

Within the Virtual Physiological Human paradigm, computational models aim to describe and understand human physiology [1]. In contrast, data-driven approaches used in critical decision-making require principled uncertainty quantification to compensate for the lack of physiological constraints [2]. In safety-critical settings such as acute ischemic stroke (AIS) triage, machine learning (ML)-based electroencephalography (EEG) supports early identification of large vessel occlusion (LVO), a subtype requiring urgent endovascular treatment [3]. Conventional machine-learning models typically do not generate uncertainty estimates, making it difficult to assess when outputs should be trusted in clinical practice [4].

2. Materials and Methods

We utilised resting-state, low-density EEG data (N=718) from two prospective, multicenter studies, partitioned into a development set (80%) and an independent test set (20%), to train and validate an ensemble classifier differentiating LVO strokes (N=46) from non-LVO conditions (N=672), including no-LVO AIS (233), stroke mimics (N=308), transient ischemic attacks (N=96) and haemorrhagic strokes (N=35). Predictive uncertainty was quantified using predictive entropy and its epistemic and aleatoric components [5]. An abstention rule was defined to establish a "Safe Cohort," allowing automated classification only when uncertainty remained below a specific threshold (τ), determined through sensitivity analysis of out-of-fold predictions on the development set and evaluated on the independent test set.

3. Results

The ensemble classifier achieved an AUROC of 0.78 [95% CI 0.62-0.93] on the independent test set, with balanced accuracy of 0.74 (sensitivity 0.79, specificity 0.70). Epistemic uncertainty showed the strongest association with prediction errors (AUROC=0.83 vs 0.69 (epistemic) and 0.82 (total); $p < 0.05$). Sensitivity analysis on the development set established a safety threshold of $\tau = 0.8$. When applied to the independent test set, the safe cohort comprised 60% of the population. In this group, the residual risk was to 13%, and diagnostic accuracy increased to 86.7%. The safety-aware abstention mechanism flagged 79% of false positives as low confidence, converting misclassifications into clinical referrals.

4. Discussion and Conclusions

Integrating uncertainty quantification transforms binary classifiers into safety constrained clinical decision support systems. By flagging uncertain cases for specialist review, the risk of misclassification is reduced, and predictions can be trusted only when deemed reliable [4].

5. References

1. Viceconti M et al., Methods; 185:120-127 (2021).
2. Begoli E et al., Nat Mach Intell; 1(1):20-23 (2019).
3. Sutcliffe L et al., BMC Emerg Med; 22(1):29 (2022).
4. Kompa B et al., NPJ Digit Med; 4:72 (2021).
5. Depeweg S et al., ICML 2018 conference: PMLR; 2018. p. 1195-1204.

Acknowledgements:
The authors acknowledge financial support from EU Horizon 2020 (857533), FNP (MAB PLUS/2019/13), Polish Ministry of Education and Science (MEiN/2023/DIR/3796), the Dutch Heart Foundation, Health Holland, and Medtronic.

CT-Derived Lesion Descriptors and Computational Modelling of Intracranial Haemorrhage

Henry Kelsey (1), Professor Fiona Lecky (1), Dr Thijs Vande Vyvere (2), Dr. Alberto Marzo (1), Dr. Ning Wang (1), Dr. Xiancheng Yu (1)

1. The University of Sheffield, United Kingdom; 2. Antwerp University Hospital, Belgium

1. Introduction

Traumatic brain injury (TBI) is a major cause of mortality and disability worldwide. Intracranial haemorrhage (ICH) is a common consequence of TBI, where vascular disruption results in the formation of mass lesions that damage surrounding brain tissue. Current prognostic models, such as TBI-IMPACT [1], primarily rely on demographic and clinical variables and do not explicitly capture the biomechanical characteristics of haemorrhagic lesions.

Recent automatic segmentation tools, such as BLAST-CT [2] enable in-depth biomechanical analysis of ICH. Through the development of spatial and topological lesion descriptors, relationships between patient-specific lesions and outcomes can be explored to elucidate the role that biomechanics plays in TBI.

This study presents an automated workflow for extracting quantitative morphological and spatial descriptors of intracranial haemorrhage from clinical CT imaging.

2. Materials and Methods

Approximately 600 ICH patients were selected from the CENTER-TBI dataset based on predefined inclusion criteria. Early clinical CT scans were processed using an automated segmentation pipeline combining BLAST-CT for haemorrhage segmentation and TotalSegmentator [4] for whole-brain and skull extraction.

Binary segmentation masks were used to derive quantitative lesion descriptors. Morphological descriptors included lesion volume and shape characteristics derived from radiomics. Spatial descriptors were calculated using lesion centre-of-mass positions relative to approximate anatomical reference points, e.g. brainstem, derived from the brain segmentation. Additional metrics were normalised to account for inter-patient differences in brain volume.

3. Results

The automated pipeline successfully processed the majority of CT scans (n=597) in the selected cohort, generating structured lesion masks and associated quantitative descriptors. Preliminary analysis of the data demonstrates some relationship between lesion morphology and patient severity and outcome. These descriptors provide quantitative information beyond standard clinical practice, highlighting the potential relevance of lesion geometry and anatomical positioning in traumatic haemorrhage.

4. Discussion and Conclusions

This work presents a scalable framework for automatic segmentation and quantification of intracranial haemorrhage from clinical CT imaging. The derived descriptors provide a foundation for potential improvement to current prognostic modelling techniques and also set the groundwork for future biomechanical modelling that is consistent with the Virtual Physiological Human paradigm.

5. References

1. Steyerberg EW et al. *PLoS Med.* 2008;5:e165.
2. Monteiro M et al. *Lancet Digit Health.* 2020;2:e314–e322.
3. Steyerberg EW et al. Lancet Neurol 2019;18:923–934
4. Wasserthal J et al. *Radiol Artif Intell.* 2023;5:e230024.

Acknowledgements:
This work uses data from the CENTER-TBI study, funded by the European Union's 7th Framework Programme (FP7/2007–2013), the Hannelore Kohl Stiftung, OneMind, and Integra LifeSciences Corporation. The authors acknowledge all CENTER-TBI participants and collaborators.

GOVERNED SILENCE: AN UNCERTAINTY-GATED DIGITAL TWIN FOR PARKINSON'S DISEASE

Ahmed Hemedan (1)

1. Luxembourg Institute of Health, Strassen, Luxembourg

Correspondence: Ahmed Hemedan, Department of Transversal Translational Medicine, Luxembourg Institute of Health, 1A-B rue Thomas Edison, L-1445 Strassen, Luxembourg. Email: ahmed.hemedan.lcsb@gmail.com

1. Introduction

Parkinson's disease progresses at different rates in motor, cognitive and autonomic function [1]. Few progression models say when an individual forecast should be withheld. A confident wrong forecast may move a decision that could safely wait. We therefore treat withholding as a designed and auditable function of a digital twin [2].

2. Materials and Methods

We built SYMPHONY, a Bayesian state-space digital twin that forecasts MDS-UPDRS Part III, MoCA and SCOPA-AUT together. Latent progression is monotone, the state updates at each visit, and uncertainty propagates to every output. A confidence gate applies five structural rules in first-applicable order. They withhold an output for too few visits, an incomplete anchor assessment, high latent uncertainty, too few conditioning runs, or a boundary conditioning value. A withheld forecast returns a reason code, not a number.

We evaluated the twin in 4,628 Parkinson's Progression Markers Initiative participants, 2,799 of them prodromal, over 28,185 clinic visits [3]. Validation used five-fold participant-level cross-validation, against a linear mixed-effects model and a carry-forward rule scored on identical visits. Suppression was audited on sex, follow-up density and cohort.

3. Results

Coverage of the 95% prediction intervals was 94.2% to 95.8% of outcomes. On the matched one-step set the twin covered 93.7% to 94.1%, and the linear mixed-effects model 64.4% to 69.2% (Fig. 1). Point accuracy matched a carry-forward rule, at 6.17 against 6.22 scale points for MDS-UPDRS III, so calibration separated the methods.

The gate released a forecast at 32.7% of the 28,185 visits. Incomplete assessment accounted for 51.5% of visits, a boundary value for 11.1% and high latent uncertainty for only 0.2%. Suppression affected 65.1% of visits from men and 70.2% of visits from women (Cramér's V 0.054).

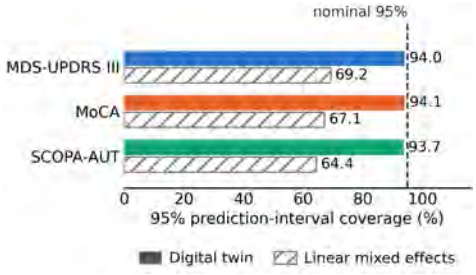


Figure 1: Coverage of the 95% prediction intervals, with the twin and the comparator scored on the same matched one-step visits.

4. Discussion and Conclusions

The twin held nominal coverage across three domains while a standard comparator did not, at similar point accuracy, so the difference is a calibration gap. The contribution is breadth across three scores with a recorded and auditable decision to withhold [4].

Silence turned on assessment completeness, not model doubt, so the release rate is cohort-specific. External validation is pre-specified and still to run. Governed silence is a candidate precondition for safe clinical deployment. A research prototype of the twin is at https://symphony-dt.com, for research use only.

5. References

1. Fereshtehnejad S-M et al., JAMA Neurol; 72(8):863-873 (2015).
2. Laubenbacher R et al., Nat Comput Sci; 4(3):184-191 (2024).
3. Marek K et al., Ann Clin Transl Neurol; 5(12):1460-1477 (2018).
4. Liu J et al., Sci Rep; 12:1762 (2022).

Acknowledgements: Supported by the National Centre of Excellence in Research on Parkinson's Disease and the Luxembourg National Research Fund.

ESTABLISHING A CLINICALLY VALIDATED PATIENT-SPECIFIC VIRTUAL PROCEDURE FOR MECHANICAL THROMBECTOMY

Renee Wu (1), Nida Ruseckaite (2*), Abhishekh H. Ashok (3*), Tomasz Matys (3*), Yogish Joshi (3*), Rohan Mudkavi (4), Georgios Toumbas (5*), Joshua Kaggie (3*), Nicholas Evans (6*), Shelly Singh-Gryzbon (2*)

*1. Dept of Chemical and Environmental Engineering, Yale University, Connecticut, US 2. Dept of Chemical Engineering and Biotechnology; 3. Dept of Radiology; 4. East & North Hertfordshire Teaching NHS Trust, Stevenage, UK; 5. School of Clinical Medicine; 6. Dept of Clinical Neurosciences; * University of Cambridge, Cambridge, UK*

Correspondence to Renee Wu, Dept of Chemical & Environmental Engineering, Yale University, New Haven, Connecticut 06520, United States; renee.wu.rsw45@yale.edu

1. Introduction

In acute ischemic stroke (AIS), the success of mechanical thrombectomy (MT) depends on complex biomechanical interactions between clot properties, vascular anatomy, and MT devices. Since these interactions cannot be measured directly *in vivo*, *in silico* models provide for mechanistic investigation. This study presents a patient-specific finite element framework for simulating single-pass stent-retriever MT and evaluates its ability to reproduce the procedural outcome observed in a corresponding clinical registry case.

2. Materials and Methods

A patient-specific MCA M1 occlusion from the Addenbrooke's Hospital registry (REC: 20/HRA/5531) was reconstructed from CTA images. Median Hounsfield Unit (HU) attenuation values classified clot composition (red blood cell-rich, fibrin-rich, or mixed) for defining *in silico* material properties [1,2]. Using Abaqus/Explicit, the Embotrap III stent-retriever was crimped, tracked, deployed, and retrieved. General contact utilized a global frictionless baseline (μ=0), with local coefficients assigned to the clot–vessel and stent–microcatheter (μ=0.4) and stent–clot (μ=0.2) interfaces. Material models included 1st order, hyperelastic Ogden (*clot*), super elastic (*stent-retriever*), and isotropic-elastic (*vessel, microcatheter*).

3. Results

The clot was classified as mixed-composition. The Abaqus model achieved full numerical stability across all procedural phases in the single-pass pipeline: pulling the stent-retriever into the microcatheter for crimping, tracking the assembly through the patient-specific vessel, deploying the device to engage the mixed-clot mesh, and retrieving the entrapped clot.

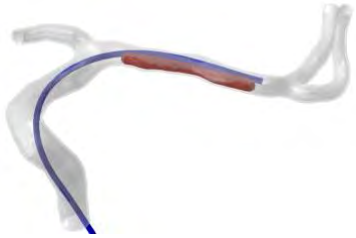


Figure 1: Tracking stage within patient-specific MCA containing the occlusive clot (red) and microcatheter (blue).

The simulated outcome from Abaqus was compared with the clinical outcome, in which successful single-pass recanalization was achieved using a combined stent-retriever and aspiration approach.

4. Discussion and Conclusions

Agreement between the simulated and clinical outcomes indicates that the current framework captures the dominant biomechanical mechanisms governing clot retrieval for this patient-specific case. Conversely, failure of the simulation to reproduce the clinical outcome indicates that additional forces, such as aspiration, are required to accurately represent the observed procedure. This validation strategy provides a systematic approach for identifying the level of biomechanical complexity required for patient-specific *in silico* models of MT. Future work will incorporate aspiration mechanics to compare isolated stent-retriever and combined-device strategies.

5. References

1. Songsaeng D et al., Asian J Neurosurg. 2019;14(3):795-800 (2019).
2. Fregona V et al., J Mech Behav Biomed Mater. 2025;163:106886 (2025).

Acknowledgements:
This project is supported by the W. D. Armstrong Trust Fund and Yale University's Alan S. Tetelman Fellowship Fund.

PHYSICS-BASED SYNTHETIC X-RAY IMAGE GENERATION FOR IMPROVING DEEP LEARNING IN MEDICAL IMAGING

Axel Allain (1), Niels Crolais (1), Clementine Hatton (1)

1. Scalian, 2 rue Antoine Becquerel, 35700, Rennes, France.

Corresponding author: Clementine Hatton, clementine.hatton@scalian.com

1. Introduction

The use of deep learning models has become increasingly common in medical image analysis, yet their performance is often constrained by the size, quality, and diversity of available training datasets. To address these challenges, we developed a physics-based simulation framework capable of generating large-scale, fully annotated synthetic X-ray datasets with controllable anatomical and pathological variability. By combining the X-ray imaging simulator gVXR [1] with virtual anthropomorphic models [2], we produced realistic radiographic projections. This framework was validated in two clinical use cases: coronary stenosis detection using synthetic coronary angiography and pulmonary nodule detection in chest X-ray and CT imaging.

2. Materials and Methods

The pipeline enables precise control over anatomical structures, pathological features, imaging angles, and acquisition parameters, while incorporating organ deformation and post-processing to replicate realistic clinical noise and artifacts. For coronary angiography, parametric 3D arterial trees with adjustable stenosis severity and location were generated. For pulmonary imaging, nodule size, density, and location were systematically varied. After simulation, post-processing was applied to simulate realistic imaging conditions. This approach enabled the creation of fully annotated datasets of 5,000–10,000 images, covering a wide range of clinical scenarios. Object detection models, including YOLOv8, NoduleNet, Faster R-CNN, RetinaNet, and Transformer-based DINO-DETR, were trained on real, synthetic, and mixed (real + synthetic) datasets to evaluate performance.

3. Results

Models trained on synthetic datasets achieved competitive performance across tasks. DINO-DETR trained on synthetic coronary angiograms demonstrated accuracy gains of 1 to 8% and recall improvements of 3 to 5%. For pulmonary imaging, on 2D-Xray, YOLOv8 demonstrated the most significant performance improvement, with sensitivity increasing up to 19% and mAP increasing up to 7%. Additionally, we observed a marked improvement in the generalization capabilities of a Retina-net model fine-tuned on synthetic data, particularly in terms of sensitivity (+14%) and mAP (+19%).

4. Discussion and Conclusions

These results demonstrate that physics-based synthetic image generation provides a scalable, privacy-preserving, and controllable solution to overcome real-world data limitations. By providing control over pathology, anatomy, and imaging parameters, this method enhances model performance, and generalization.. Future work will focus on applying this framework to additional pathologies and assessing its effectiveness in real clinical settings.

References

[1] Franck P. Vidal et al. “X-Ray Simulations with gVirtualXray in Medicine and Life Sciences”. In: *EuroVis 2025 - Dirk Bartz Prize* (2025). DOI: 10 . 2312 / EVM . 20251974.

[2] Gauthier Kervyn. “The First Open Source 3d Atlas of Human Anatomy”. In: *Acta Scientific Anatomy* 1.4 (2022), pp. 13–15.

DESIGN OF A ROBUST CNN FOR CANCER DETECTION IN MAMMOGRAPHY IMAGES

Eva Raina (1, 2), Martina Oria (1, 2), Massimo Salvi (2), Alessandra Manzin (1)

1. Istituto Nazionale di Ricerca Metrologia, Italy; 2. Politecnico di Torino, Italy

1. Introduction

Artificial intelligence (AI) systems can improve cancer detection in mammography screening, assisting radiologists in making more accurate diagnoses [1, 2]. However, prior the application in the clinics, the AI models have to be properly trained and tested on sufficiently representative data, to avoid bias and domain gap issues. In mammography, one of the factors that can impact on AI outcomes is the vendor-style, which leads to very different image features, in terms of sharpness, contrast, and gray level distribution. In this framework, we have designed and trained a Convolutional Neural Network (CNN) for classifying breast cancerous lesions, including masses, suspicious calcifications, and architectural distortions. The model is trained on mammograms acquired with scanners from different vendors.

2. Materials and Methods

A three-layer CNN, with two fully connected linear layers and alternating Max Pooling and ReLU layers, is here used for binary classification in mammography images, distinguishing between lesion and non-lesion in grayscale patches. The patches are extracted from predefined lesion masks or randomly cropped from healthy mammograms.

To test the developed CNN model on images with heterogeneous features, four mammography databases are considered, containing images acquired with scanners from different vendors, mainly Hologic and Siemens. The possible effects of domain gaps are investigated by training the CNN under three scenarios, where the training sample contains images from (i) only Hologic, (ii) only Siemens and (iii) both datasets. To limit domain generalization issues related to the use of one image type in the learning task, we also adopt a CycleGAN- based neural style transfer method, for transferring vendor style from Hologic to Siemens and vice versa. Finally, a ScoreCAM algorithm [3] is applied to the last convolutional layer of the CNN to visualize the classification results and highlight the lesion within the image patches.

3. Results

The CNN model has shown accurate results in detecting malignant lesions in mammograms with very different features. This is guaranteed if the training set contains the relative vendor style images, either real or synthetic. An example is shown in Fig.1.

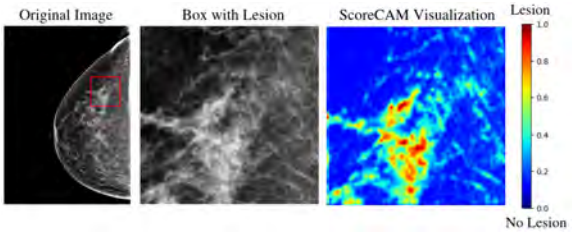


Figure 1: Visualization of the outputs of the CNN model when applied to an Hologic image with the corresponding ScoreCAM heatmap.

4. Discussion and Conclusions

The CNN model has proven to be robust, when applied to images with different vendor style and containing various types of lesions. Moreover, it has achieved high classification accuracy, even when applied to transformed images, being a promising tool for future usage in breast cancer screening.

5. References

1. Ribli D et al., Sci Rep. 2018;8:4165.
2. Zhu Z et al., Comput Model Eng Sci;136:2127–2172 (2023).
3. Rahman T et al., Comput Biol Med. 2021;132:104319.

Acknowledgements:

This work is supported by 22HLT05 MAIBAI, funded by the European Partnership on Metrology, co-financed from Horizon Europe and the Participating States.

SIMULTANEOUS 4D ULTRASOUND AND HIGH-DENSITY ELECTROMYOGRAPHY ACQUISITION OF HUMAN TIBIALIS ANTERIOR DURING DYNAMIC MUSCLE CONTRACTION

Pengfei Zhang (1), Lukas Vosse (2), Giacinto L. Cerone (3,4), Alberto Botter (3,4), Tobias Siebert (2), Oliver Röhrle (1)

1. Institute for Modelling and Simulation of Biomechanical Systems, University of Stuttgart, Germany; 2. Institute of Sport and Movement Science, University of Stuttgart, Germany; 3. the Laboratory for Engineering of the Neuromuscular System (LISiN), Department of Electronics and Telecommunications, Politecnico di Torino, Italy; 4. the PoliToBIOMed Laboratory, Politecnico di Torino, Turin, Italy

1. Introduction

Understanding the complex interplay of skeletal muscle activation, contraction/muscle deformation, and its corresponding force output requires advanced in vivo measurements. Currently, no method exists that simultaneously acquires electrical, functional, and 3D morphological data during dynamic muscle contractions. This pilot study demonstrates a novel proof-of-concept methodology for the synchronized acquisition of these three modalities on the human tibialis anterior (TA) during voluntary dynamic movement.

2. Materials and Methods

The setup integrated an isokinetic dynamometer recording joint kinematics and torque, an automated robotic 3D ultrasound system [1,2], and an ultrasound-transparent high-density surface electromyography (HD-sEMG) system (ReGrid [3]). An offline pipeline synchronized the multimodal data and reconstructed 4D (3D + time) muscle volumes at discrete joint angles. Finally, inter-volume tissue displacement was calculated via deformable 3D image registration, allowing the investigation in local tissue strains.

3. Results

The system successfully captured synchronized multimodal data, enabling 3D TA reconstruction at 1.8° joint angle steps. The ultrasound-transparent electrodes maintained a high signal-to-noise ratio, despite direct probe contact. Synchronized EMG and dynamometry data showed high inter-trial repeatability. Preliminary analysis revealed spatially heterogeneous deformation and activation patterns.

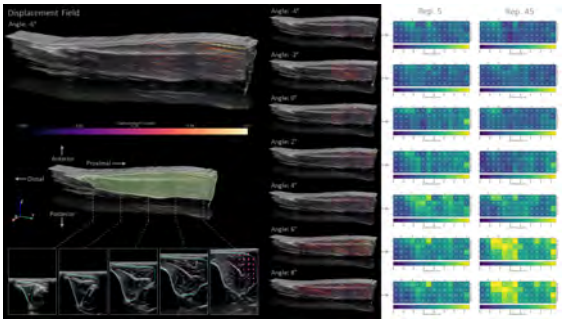


Figure 1: Reconstructed sequence of 3D ultrasound images of TA and corresponding EMG heatmaps

4. Discussion and Conclusions

This pilot study confirms the technical feasibility of in vivo acquisition of synchronized 3D ultrasound, HD-sEMG, and dynamometry data, offering a powerful tool to inform and validate subject-specific 3D continuum-mechanical models and to improve dynamic motor-unit decomposition techniques, thereby facilitating patient-specific treatment planning and prosthetic design.

5. References

1. Sahrmann, AS, et al., (2024). IEEE Transactions on Biomedical Engineering, 71(7), 2022–2032.
2. Sahrmann, AS, et al., (2024). Frontiers in Bioengineering and Biotechnology, 12.
3. Cerone GL, et al., (2026). IEEE Transactions on Neural Systems and Rehabilitation Engineering, 1–1

Acknowledgements:

This project has received funding from the German Research Foundation (DFG) as part of the Stuttgart Center for Simulation Science (SimTech, EXC2075 – 390740016) and the Major Research Instrumentation Program (INST 41/1101-1 FUGG).

AUTOMATED IN VIVO ULTRASOUND QUANTIFICATION OF THORACOLUMBAR FASCIA THICKNESS AND GLIDING

Chiara Giulia Fontanella (1,2), Lorenza Bonaldi, Carmelo Pirri (2,3), Carla Stecco (2,3), Francesca Uccheddu (1,2)

1. Department of Industrial Engineering, University of Padua; Italy; 2. Center for mechanics of Biological Materials, University of Padua; Italy; 3. Department of Neuroscience, University of Padua; Italy

1. Introduction

The thoracolumbar fascia (TLF) is a multilayered connective tissue complex comprising thoracic and lumbar components of the deep fascia [1]. Altered fascial biomechanics, including reduced inter-layer gliding and increased thickness, have been proposed as potential biomarkers of dysfunction in musculoskeletal disorders such as chronic low back pain (LBP) [2]. However, quantitative evaluation of TLF dynamics from ultrasound (US) imaging remains largely based on subjective visual assessment, limiting reproducibility and clinical translation. Objective in vivo quantification of fascial dynamics is therefore essential for biomechanical interpretation and computational modelling. We developed an automated framework for simultaneous quantification of fascial motion and thickness from dynamic US videos, integrating deep learning segmentation with dense optical flow tracking.

2. Methods

In vivo US videos of TLF were collected from 11 healthy volunteers and 10 chronic LBP patients during guided trunk extension cycles (4 s extension / 4 s flexion × 4 repetitions). A rectangular ROI on the first frame was automatically segmented into anatomical zones using a U-Net architecture with morphological refinement [3]. Dense optical flow (Farneback) was used to estimate inter-frame motion, decomposed by anatomical zones. After IQR-based outlier removal, spatial calibration, and detrending, cumulative displacements were obtained. Relative gliding was defined as displacement differences between adjacent zones, and fascial thickness was measured from the deep fascia mask on the first frame.

3. Results

The method was successfully applied to 21 in vivo videos and simultaneously identifies three anatomical zones (subcutis, deep fascia, and muscle), allowing computation of layer-specific displacement and inter-layer gliding from a single ROI. Expert clinician validation confirmed anatomical plausibility of segmentation and tracking.

Mean TLF thickness was 2.83 ± 0.64 mm in healthy volunteers and 3.61 ± 1.29 mm in LBP patients. Inter-layer displacement correlation between fascia (Middle) and muscle (Below) showed opposite trends. Healthy subjects exhibited a negative correlation ($r = -0.15 \pm 0.44$), consistent with independent layer motion, whereas LBP patients showed a positive correlation ($r = +0.16 \pm 0.52$), consistent with coupled movement (Fig. 1).

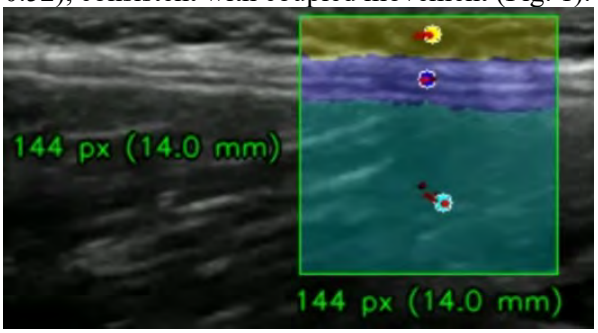


Figure 1: Automated in vivo quantification of thoracolumbar fascia from dynamic ultrasound. Representative tracking frame illustrating layer-specific displacement and inter-layer gliding from a single ROI.

4. Discussion

In this pilot cohort, LBP patients showed thicker fascia and more in-phase fascia–muscle motion, consistent with reduced gliding hypotheses. Larger cohorts are required to confirm statistical separation and define normative thresholds. These findings suggest that altered inter-layer mechanics of the thoracolumbar fascia may represent a quantifiable biomechanical marker of dysfunctional load transfer in chronic LBP. The proposed framework enables subject-specific characterization of fascial motion, supporting future integration into musculoskeletal modelling and digital human applications. The modular design allows adaptation to varying image quality and other layered anatomical regions.

References

1. Langevin et al, BMC Musculoskelet Disord, 12:203, 2011.
2. Pirri et al, Diagnostics, 13:1436, 2023.
3. Bonaldi et al, BMC Med Imaging, 25:164, 2025.

CT-BASED THROMBUS MECHANICAL PHENOTYPING IN ACUTE ISCHEMIC STROKE

L. Bontempi (1,2), J. Cruts (1), R. Cahalane (1,3), N. Boodt (1), D. Bos (1), B. Fereidoonnezhad (2), P.J. van Doormaal (1), A. van der Lugt (1), D. Dippel (1), F. Gijsen (1,2)

1. Erasmus MC, University Medical Center, Rotterdam, the Netherlands; 2. Delft University of Technology, Delft, the Netherlands; 3. University of Limerick, Limerick, Ireland

Corresponding author: Luca Bontempi, MSc – l.bontempi@erasmusmc.nl

1. Introduction

Endovascular thrombectomy (EVT) is the standard treatment for acute ischemic stroke (AIS), yet first-pass revascularization fails in up to 40% of patients [1]. *In vitro* and *in silico* evidence [2,3] indicates thrombus mechanics influence retrieval success. Imaging biomarkers reflecting thrombus mechanical properties could support thrombus-specific treatment strategies. This study investigates associations between stiffness and pre-interventional imaging features of EVT-retrieved thrombi.

2. Materials and Methods

In the prospective MR CLOT study, thrombi retrieved during EVT for AIS were collected and mechanically characterized using unconfined compression tests. Pre-interventional non-contrast CT (NCCT) and CT angiography (CTA) quantified thrombus density, perviousness, length, occlusion location, and distance from the intracranial carotid artery (ICA) terminus (*Figure 1*). Associations between thrombus stiffness and imaging features were assessed using univariable linear mixed-effects regression models, accounting for patient clustering and adjusting for age and sex.

3. Results

Median thrombus stiffness in 281 samples from 51 patients was 0.594 kPa (95% CI: 0.208; 1.115). Occlusion location and distance from the ICA terminus were significantly associated with stiffness. Thrombi from proximal M2 were significantly softer (0.236 kPa, 95% CI: 0.136; 0.409) than those from M1 (0.760 kPa, 95% CI: 0.492; 1.174) and ICA (1.106 kPa, 95% CI: 0.558; 2.192) occlusions. Increasing distance from the ICA terminus was associated with a 2% decrease in stiffness per millimetre (β = −0.009, 95% CI: −0.016; −0.002). Thrombus density, perviousness, and length were not significantly associated with thrombus stiffness.

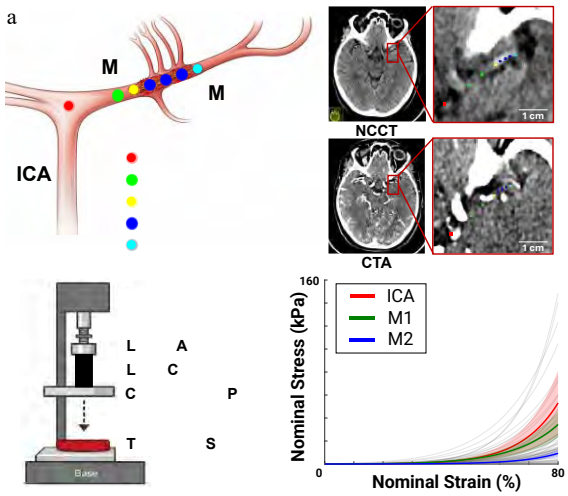


Figure 1: AIS thrombus radiological and mechanical characterization. Markers positioning on NCCT and CTA for automated quantification of thrombus imaging features (a); thrombus compression testing setup and stress-strain curves per occlusion site (b).

4. Discussion and Conclusions

Pre-interventional imaging features reflecting thrombus location are associated with *ex vivo* thrombus stiffness, particularly occlusion site and distance from the ICA terminus. These findings highlight the potential of imaging to capture biomechanically relevant thrombus characteristics and support patient-specific treatment strategies in AIS.

5. References

1. Matsukawa H, et al., J Neurointerv Surg. 17:1333-39, 2025.
2. Liu R, et al., Interv Neuroradiol. 29(6):759-767, 2023.
3. Miller C, Konduri P, Bridio S, et al. Comput Methods Programs Biomed. 228:107244, 2023.

Acknowledgements:
This study received funding from the European Union's Horizon Europe research and innovation programme under the grant agreement No. 101136438 (GEMINI).

Towards Treatment Decision Support: Validating a Personalised Collateral Digital Twin with Imaging-Derived Collateral Scores

Jen-Feng Kuo (1), Tamás István Józsa (2), Stephen John Payne (3), Wiktor Olszewski (4), Charles Majoie (4), Hemk Marquering (4) , Alfons G. Hoekstra (1)

1. University of Amsterdam, Netherlands; 2. Cranfield University, UK; 3. University of Bristol, UK; 4. Amsterdam UMC Location, University of Amsterdam, Netherlands

Corresponding author: Jen-Feng Kuo

1. Introduction

Collateral circulation governs flow redistribution after large-vessel occlusion (LVO) and influences infarct progression and outcome in ischaemic stroke. Its effectiveness depends on the functional connectivity of leptomeningeal anastomoses linking arterial territories. While population-level validation of computational stroke haemodynamics exists [1], validating personalised collateral pathway models remains challenging. We propose a personalised leptomeningeal collateral network model and validate it by mapping model parameters to automated CTA-derived collateral scores at the individual level.

2. Materials and Methods

Retrospective MR CLEAN imaging and clinical data [2] were used for validation (baseline CTA for automated vessel segmentation; baseline CTP when available). We embedded our leptomeningeal collateral network framework [3] in personalised LVO haemodynamic simulations and parameterised collateral capacity with a tunable connectivity model (e.g., probability/strength/conductance of leptomeningeal links). For each patient, we simulated flow redistribution and computed a model-derived collateral score as a function of collateral connectivity and the resulting perfusion support. Parameters were calibrated to two imaging-derived targets: (i) an MCA-territory collateral score from ipsilateral versus contralateral vessel visualisation volume on CTA [4], and (ii) an occlusion-downstream collateral score from vessel visualisation volume within the CTP Tmax-defined hypoperfused ROI (with hemispheric references where applicable) [5]. Agreement was evaluated using correlation, ICC, and Bland–Altman analysis, with subgroup analyses by occlusion site (ICA/M1/M2) and imaging availability.

3. Results

Using a tunable collateral connectivity model, we simulate patient-specific flow redistribution after LVO and compute two model-derived collateral scores that combine collateral connectivity with predicted perfusion support. These scores are compared against two automated imaging-derived collateral metrics. Model agreement and calibration are quantified using correlation, intraclass correlation coefficients (ICC), and Bland–Altman analysis, with subgroup analyses by occlusion location (ICA/M1/M2) and imaging availability. Overall, we present a validation pathway for a personalised leptomeningeal collateral network model that enables mechanistic interpretation of inter-individual collateral variability and provides a foundation for in-silico acute ischaemic stroke studies and patient-specific treatment decision support.

4. Discussion and Conclusions

We present a validation pathway for a personalised leptomeningeal collateral network model against two automated imaging-derived collateral scoring strategies. The resulting patient-specific models enable mechanistic interpretation of collateral variability and underpin in-silico acute ischaemic stroke studies and patient-specific treatment decision support. We calibrate the model to individuals using MR CLEAN imaging and clinical data.

5. References

1.Miller C. M. (2025)
2. Berkhemer O. A., New England Journal of Medicine; 372(1): 11-20 (2015).
3. Padmos R. M., Medical Engineering & Physics; 91: 1-11 (2021).
4. Boers A., American journal of neuroradiology; 39(6):1074-1082 (2018).
5. Vries L. de, European radiology; 35(10): 6127-6139 (2025).

Acknowledgements:
GEMINI has received funding from the European Union's Horizon Europe research and innovation programme under the grant agreement No 101136438.

CLASSIFICATION OF PLACENTA ACCRETA SPECTRUM USING MACHINE LEARNING AND TEXTURE ANALYSIS OF MR IMAGES

Suzie Coldman (1, 2), Guanglong Zhou (1, 2), Dengjiang Wu (1, 2), Lingzhong Guo (1, 2), Andrew Melbourne (3), Anna David (4), Nada Mufti (5), Luca Gherardini (6), Jose Sousa (6, 7), Elspeth Whitby (8), Xinshan Li (1, 2)

1. University of Sheffield, UK; 2. Insigneo Institute, UK; 3. King's College London, UK; 4. University College London, UK; 5. Imperial College Healthcare, UK; 6. Computational Intelligence, Sano Centre for Computational Personalised Medicine, Poland; 7. Multidisciplinary Institute of Ageing, MIA-Portugal, University of Coimbra, Portugal; 8. Sheffield Teaching Hospitals, UK;.

Corresponding author information: slcoldman1@sheffield.ac.uk

1. Introduction

Placenta accreta spectrum (PAS) is often diagnosed with MRI. However, only 30-66% of PAS pregnancies are identified prenatally [1-3], due to limited resources and expert radiologists. The aim of this study was to classify PAS using texture and shape features from placental MRI and machine learning (ML).

2. Materials and Methods

83 control and 41 PAS MRIs were obtained by Sheffield Teaching Hospital (STH) and 8 control and 6 PAS MRIs were obtained by University College Hospital (UCH) (Siemens 1.5T, sagittal T2 HASTE). The placenta was manually segmented with 2525 texture/shape features extracted using PyRadiomics. The STH dataset was split into training and test (80/20); UCH data was an external test. Feature selection involved intraclass correlation coefficient, zero-variance and variance inflation factor filters and logistic regression (10-fold cross-validation (CV) and 750 bootstraps). 7 ML algorithms were trained on the selected features (15-fold CV): Logistic Regression (LR), Support Vector Machine (SVM), Random Forest (RF), Gradient Boosting (GB) and CACTUS Probabilistic (PB), Degree (DG) and PageRank (PR) [4, 5]. Ensemble methods were tested with soft and hard voting; 25 repeats were used.

3. Results

Surface volume ratio, low grey level zone emphasis and total energy were frequently selected for classification; the latter two indicate the presence of dark zones on MRI. The highest mean accuracies were exhibited by CACTUS PB (0.76±0.10) on the internal and GB (0.80±0.12) on the external test set. No significant differences were observed between models on the internal test set. GB significantly outperformed SVM and all CACTUS algorithms on the external test set.

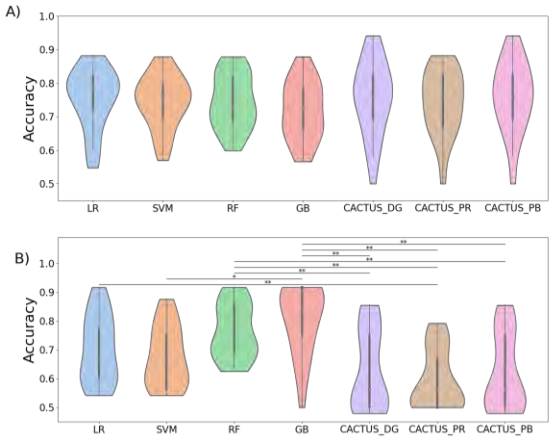


Figure 1: Violin plots of the accuracy of each ML algorithm for the A) internal and B) external test sets. * $p < 0.05$, ** $p < 0.01$

The best ensemble methods were GB-SVM and GB-LR with hard voting, both achieving mean accuracies of 0.77 and 0.81 on the internal and external test sets respectively.

4. Discussion and Conclusions

Texture and shape features selected for classification were consistent with dark bands and shape changes associated with PAS. In future, this work will be extended to include clinical features indicative of PAS, and placental position information.

5. References

1. McCall SJ et al., BJOG; 129(10): 1676-1685 (2022).
2. Fitzpatrick KE et al., BJOG; 121(1): 62-71 (2014).
3. Thurn L et al., BJOG; 123(8): 1348-1355 (2016).
4. Gherardini L et al., AIME 2025: LNCS; 2025.
5. Gherardini et al., ACM TIST, 15(3): 1-23 (2024).

BONE RESECTION PLANNING IN MIXED REALITY FOR BONE IMPLANT FITTING IN THE CALCANEUS (A CASE STUDY)

Gianni Magrini (1), Maciej Stanuch (2), Andrzej Skalski (3)

1. Politecnico di Milano, Italy, MedApp S.A., Poland 2. MedApp S.A., Poland; 3. AGH University of Krakow, Poland, MedApp S.A., Poland.

1. Introduction

Mixed reality in orthopedic procedures can be a powerful tool, especially for diagnostic assessment and preprocedural planning. It provides real-scale three-dimensional representations of diagnostic images for a better spatial understanding and depth perception, while reducing the cognitive effort to mentally reconstruct them from 2D slices [1]. Additionally, it enables hologram manipulation through voice commands and gestures, helping maintain sterility by avoiding disruption of the surgical field.

2. Materials and Methods

The case study was provided as a Computed Tomography scan showing a bone cyst in the left calcaneus. First, the calcaneus, its defect, skin, and remaining bones were manually segmented in Slicer (ver. 5.8.1). After the initial straight path for implant fitting was automatically defined, the resection plane was computed using a path-based geometric approach with optional angular adjustment via spherical linear interpolation and offset translation along the path. After the resection plane orientation was customized, the final plane could be used to divide the calcaneus mask directly into two parts: the remaining calcaneus, which will be the volume to avoid for proper implant fitting, and the calcaneus cut part. Otherwise, a more conservative approach was implemented to give the surgeon a wide range of possibilities. In this alternative approach, the resected part was intersected with the swept volume of the defect along the selected path. Then, a final shell offset was added to provide clearance between the defect and the remaining calcaneus (2 mm). The resection plane and resection areas were saved and exported to implement them in a mixed reality environment.

3. Results

The resected bone and the remaining calcaneus masks were obtained and displayed with mixed reality technology. After visual inspection, the mask is correctly overlapped with the 3D reconstruction of the left foot (Figure 1).

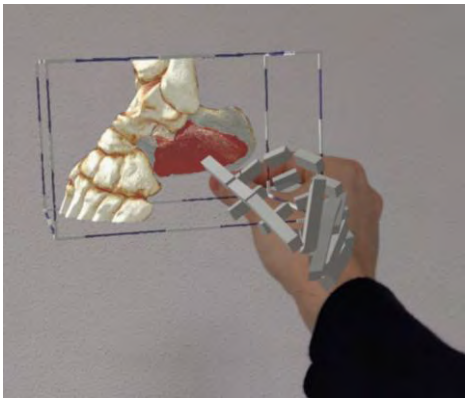


Figure 1: Virtual foot and resected bone (in red) are displayed in a mixed reality environment.

4. Discussion and Conclusions

The surgeon will have the possibility to visualize the bone resection area, and to confirm the choice or fine-tune the orientation of the cut plane and the offset for resection depth. This output represents the starting point for preprocedural planning for implant fitting.

5. References

1. Vajsbaher T., et al. Spatial cognition in minimally invasive surgery: a systematic review. BMC Surg. 2018; 18:94.

Acknowledgements:

Funded by the European Union

This study was carried out within the framework of the ReBone project (G.A. no. 101119884), funded by the European Union. Views and opinions expressed are, however, those of the author(s) only and do not necessarily reflect those of the European Union or the European Research Executive Agency (REA). Neither the European Union nor the granting authority can be held responsible for them. Dr. Rainer Mittermayr is kindly acknowledged for providing the Computed Tomography scan.

UNSUPERVISED CLUSTERING OF TRABECULAR BONE MICRO-CT RECOVERS STRUCTURAL PATTERNS MATCHING FINITE-ELEMENT STRESS

Linlin Wang (1), Junning Chen (1), Jude Meakin (2), Ion Sucala (1), Karen Knapp (3)

1. Department of Engineering, University of Exeter, Exeter, United Kingdom 2. Department of Physics and Astronomy, University of Exeter, Exeter, United Kingdom 3. Department of Health and Care Professions, University of Exeter, Exeter, United Kingdom

1. Introduction

Image-based micro-finite-element analysis (FEA) resolves fine-detailed mechanical heterogeneity within tissues [1,2], widely adopted for bone fracture risk assessment, yet the microCT volume is typically reduced to scalar morphometric descriptors [3]. Whether mechanical heterogeneity corresponds to structural patterns identifiable directly from greyscale images, without predefined morphometric categories, has not been tested. We examined this in ovine femoral trabecular bone using unsupervised voxel clustering.

2. Materials and Methods

Thirty-seven trabecular cubes from the ovine proximal femur were imaged by micro-CT at 20 µm isotropic resolution (100×100×100 voxels) [3]. Image-based FEA under uniaxial compression yielded voxel-level von Mises stress [1,2]. A 3D convolutional network clustered bone voxels on greyscale features alone, with no classification labels [4,5]. Each cluster was annotated post hoc with its mean FEA stress and ordered accordingly. Voxel-level Pearson spatial correlation quantified correspondence per cube. Robustness was tested over five random initialisations and a control with spatially randomised stress labels.

3. Results

Clusters separated into distinct stress levels that matched the FEA field spatially (Fig. 1), with median spatial correlation of 0.71, reproducible across all five initialisations. A separate label-randomisation control confirmed that the encoder requires spatially coherent supervision (Table 1).

Table 1: Effect of spatial label randomisation on stress prediction.

	Valid labels	Shuffled
AUC (5 seeds)	0.924 ± 0.003	0.629
Spatial r	0.79	−0.03

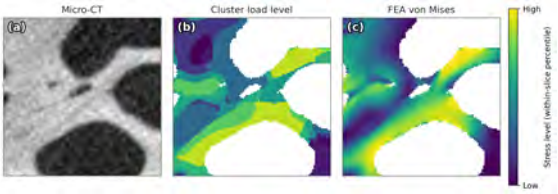


Figure 1: Representative axial slice from an ovine femoral trabecular cube. (a) Greyscale micro-CT. (b) Cluster load-level map, coloured by post hoc FEA stress annotation. (c) FEA von Mises stress. Shared colourbar indicates within-slice stress percentile.

4. Discussion and Conclusions

Greyscale micro-CT of ovine trabecular bone encodes structural organisation aligned with mechanical stress, accessible through unsupervised voxel clustering without predefined morphometric categories. The label-randomisation control confirms this alignment is mechanically grounded. This image-derived coordinate may complement conventional morphometric assessment by providing spatially resolved mechanical characterisation. Extension to other species, sites, and physiological and pathological conditions is under investigation.

5. References

1. Ulrich D et al. J Biomech. 1998;31(12):1187-1192.
2. Hambli R. Bone. 2013;56(2):363-374.
3. Bouxsein ML et al. J Bone Miner Res. 2010;25(7):1468-1486.
4. Ronneberger O et al. MICCAI 2015. Springer; p. 234-241.
5. Caron M et al. Adv Neural Inf Process Syst. 2020;33:9912-9924.

Acknowledgements:
This work was supported by a Short Industry Fellowship from the Royal Society and a Back-to-Back Research Support Award from the Oswestry Disability Index.

GEOMETRIC VERSUS CONSTITUTIVE EFFECTS OF VOCAL FOLD LESIONS: A FLUID–STRUCTURE INTERACTION STUDY

Anitha Niyingenera (1), Norah Delaney (1), Rana Zakerzadeh (1)

1. School of Science and Engineering, Duquesne University, Pittsburgh, PA, USA

1. Introduction

Human phonation arises from fluid–structure interaction (FSI) between airflow and vocal fold (VF) vibration. Benign VF lesions introduce localized geometric and material changes that disrupt vibratory symmetry and airflow. However, the relative roles of lesion size and stiffness remain unclear. This study uses parametric three-dimensional FSI simulations to determine whether phonatory disruption is primarily governed by geometric protrusion or changes in lesion elasticity.

2. Materials and Methods

A bi-layered VF model based on CT-derived geometry was embedded in a laryngeal airflow domain, with a unilateral superior-surface lesion incorporated in the cover layer (Fig.1).

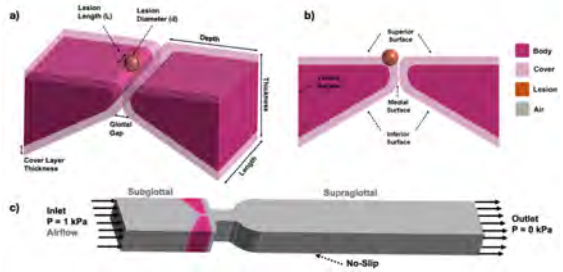


Figure 1: VF model with embedded lesion.

A parametric matrix varied three lesion lengths (L_1–L_3) and three Young's modulus values (E_1–E_3) within physiological ranges, while maintaining constant diameter. A healthy case served as baseline. Transient FSI simulations were performed in ANSYS System Coupling by solving incompressible Navier–Stokes airflow and tissue structural momentum equations with no-slip and stress continuity at the interface. Medial VF contact was included. Subglottal pressure of P_{in}=1 kPa was applied. Further implementation details are available in [1]. Maximum medial displacement (U) was quantified after periodic oscillation. Relative deviation from the healthy baseline (δ) was computed as:

$$\delta = \left| \frac{U_{lesion} - U_{healthy}}{U_{healthy}} \right| \times 100\% \qquad (1)$$

3. Results

The healthy case exhibited symmetric left–right oscillation with identical displacement amplitudes. All lesioned cases demonstrated vibratory asymmetry, with reduced displacement of the lesioned fold and increased deviation from the healthy baseline (Fig. 2). Increasing lesion length produced progressively larger displacement differences, with L_3 cases showing the greatest deviation. In contrast, elasticity variations within physiological ranges produced minimal and non-systematic changes, with displacement trends largely overlapping across stiffness cases.

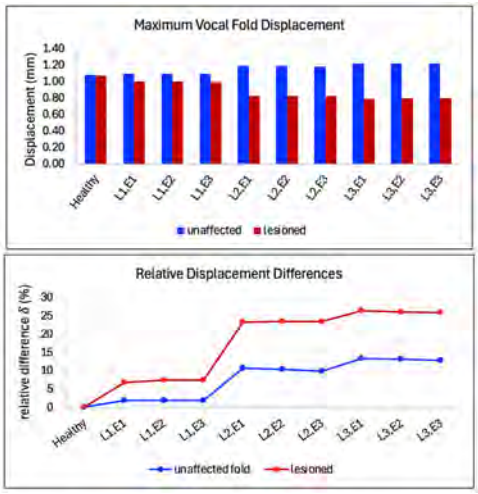


Figure 2: Effect of lesion size and elasticity.

4. Discussion and Conclusions

Lesion geometry was identified as the primary driver of vibratory disruption, while stiffness variations within physiological ranges had minimal influence. Increasing lesion size amplified displacement asymmetry relative to the healthy baseline. These findings support future patient-specific modeling and digital-twin applications in voice biomechanics.

5. References

1. Neves, M., Niyingenera, A., & Zakerzadeh, R. (2025). Bioengineering, 12(12), 1360.

Acknowledgements: This work has been supported by the NSF CMMI grant 2338676.

SURGICAL RESPONSE PREDICTION IN CTEPH FROM TWO INDEPENDENT CENTRES USING HAEMODYNAMIC MODELLING

Behdad Shaarbaf Ebrahimi (1), Ho-Fung Chan (1), Prashanna Khwaounjoo (1), Finbar Argus (1), Ge Jin (1), Xiaohui Ma (1), Martyn Nash (1), David Kaye (2), Misha Dagan (2), Atuso Doi (2), David Kiely (3), Andy Swift (3), Jim Wild (3), David McGiffin (2), Merryn Tawhai (1)

1. Auckland Bioengineering Institute, University of Auckland, New Zealand; 2. Alfred Hospital, Melbourne, Australia; 3. School of Medicine and Population Health, University of Sheffield, UK.

1. Introduction

Chronic thromboembolic pulmonary hypertension (CTEPH) is a potentially curable form of pulmonary hypertension, yet patient response to pulmonary endarterectomy (PEA) remains heterogeneous[1]. Reliable pre-operative predictors of surgical outcome are limited[2], particularly those capable of capturing patient-specific haemodynamic and vascular factors. In this study, we aim to develop and evaluate a model-based framework for predicting post-surgical haemodynamic response in CTEPH patients using data from two independent clinical centres (The Alfred Hospital, Melbourne Australia and ASPIRE registry, UK).

2. Materials and Methods

We analysed retrospective cohorts of CTEPH patients who underwent PEA in Australia (N=11) and the UK (N=11). Pre-operative assessments included right heart catheterisation (RHC), imaging-derived vascular geometry, and clinical indices of disease severity. Patient-specific computational haemodynamic models were constructed to characterise pulmonary vascular resistance (PVR) and haemodynamics pre-surgery, and to predict post-surgical PVR and haemodynamic outcomes[3]. Model-derived metrics and conventional clinical variables were integrated into a predictive framework for post-operative response, defined by changes in mean pulmonary arterial pressure (mPAP) and PVR. Cross-centre validation was performed to assess generalisability.

3. Results

Model predictions closely matched measured haemodynamic changes following PEA. Predicted reductions in mean pulmonary arterial pressure (ΔmPAP) demonstrated strong agreement with clinical measurements (R^2=0.85), while pulmonary vascular resistance (ΔPVR) predictions showed even tighter correspondence (R^2=0.96). Predictive performance remained robust across clinically relevant sub-groups, including patients with residual pulmonary hypertension and those with elevated pre-operative pulmonary capillary wedge pressure (PCWP).

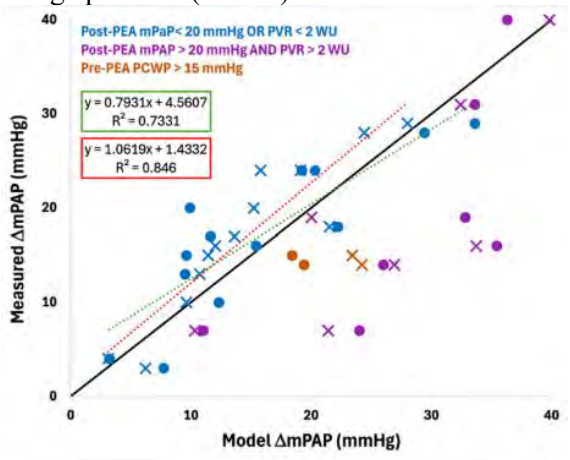


Figure 1: Model-predicted changes in mPAP demonstrate strong correspondence with measured post-PEA values across cohorts (Crosses are from one centre and circles from another one).

4. Discussion and Conclusions

We present an imaging-driven computational workflow capable of predicting patient-specific haemodynamic response to pulmonary endarterectomy in CTEPH. Beyond predictive accuracy, the workflow provides mechanistic insight into outcome variability. This approach provides personalised prognostic insight and establishes a foundation for extension to other pulmonary hypertension phenotypes.

5. References

1. D. Jenkins et al. European Respiratory Review 26, no. 143 (2017): 160111.
2. C. J. Bergin et al., American Journal of Roentgenology 174, no. 2 (2000): 509–515.
3. Ebrahimi et al. Pulm. Circ. 2025; 15 (4), e70176.

Acknowledgements:
Authors acknowledge the clinical collaborators both in UK and AU centres who provided the data that made this research possible. We would like to also acknowledge the MBIE Catalyst grant for funding this research.

A DIGITAL TWIN PIPELINE FOR AUTOMATED PULMONARY EMBOLISM BIOMARKER EXTRACTION

Morgane des Ligneris (1), Nathan Painchaud (1), Allan Serva (2,3), Laurent Bertoletti (2), Pierre Croisille (1,4), Carole Frindel (1,5), Odyssée Merveille (1)

1. Univ Lyon, INSA-Lyon, Université Claude Bernard Lyon 1, UJM-Saint Etienne, CNRS, Inserm, CREATIS UMR 5220, U1294, F-69621, Lyon, France; 2. Université Jean Monnet Saint-Étienne, CHU Saint-Étienne, Mines Saint-Étienne, INSERM, SAINBIOSE U1059, CIC 1408, Département de Médecine Vasculaire et Thérapeutique, F-CRIN INNOVTE network, all in F-42055, Saint-Étienne, France; 3. Department of Pneumology, CHU Saint-Etienne, UJM Saint-Etienne, France; 4. Department of Radiology, CHU Saint-Etienne, UJM Saint-Etienne, France; 5. IUF, Institut Universitaire de France, Paris

1. Introduction

Pulmonary embolism (PE) is the third leading cause of acute cardiovascular death [1]. Risk stratification relies on RV/LV ratio and blood biomarkers, but these are often incomplete in emergencies. Manual severity scores (Qanadli [2], Mastora [3]) are rarely used due to their complexity. We propose an automated pipeline to extract PE biomarkers from CTPA scans using a patient-specific pulmonary arterial tree (PAT) digital twin.

2. Materials and Methods

The pipeline builds a patient-specific PAT graph from AI-segmented masks (arteries, emboli, lungs, lobes). Key steps are (i) Graph modeling: Skeletonization, artifact correction, and MPA-to-distal orientation. (ii) Hierarchical labeling: Laterality, lobe, and arterial level assignment via morphological criteria. (iii) PE characterization: Clot volume, and maximum transversal obstruction. (iv) Biomarker extraction: Local (morphology, location, obstruction) and global (Qanadli/Mastora scores, TEV distribution) features.

3. Results

Automated Qanadli, Mastora scores correlated strongly with manual calculations (Spearman ρ=0.83 and 0.86). Total Embolic Volume [4] distribution distinguished proximal/distal embolic patterns (Fig. 1).

4. Discussion and Conclusions

This pipeline generates anatomically accurate digital twins and severity scores with strong agreement, supporting rapid, precise thrombotic burden and clot distribution assessment.

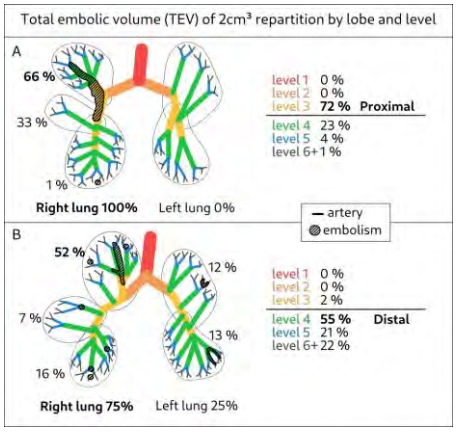


Figure 1: Total embolic volume repartition by lobes and levels.

5. References

1. S. V. Konstantinides et al., European Heart Journal, vol. 41, nº 4, p. 543-603, (2020)
2. S. D. Qanadli et al., American Journal of Roentgenology, vol. 176, no. 6, pp. 1415–1420, (2001)
3. I. Mastora et al., Eur Radiol, vol. 13, no. 1, pp. 29–35. (2003)
4. W.-M. Huang et al., Sci Rep, vol. 12, no. 1, p. 7620, May (2022)

Acknowledgements:

This work was founded by the French ANR through the PERSEVERE and PreSPIN projects (ANR-22-CE45-0018, ANR-20-CE45-0011) and within the framework of the LABEX PRIMES (ANR-11-LABX-0063). This work was also performed using HPC resources from GENCI-IDRIS (Grant 2025-AD011014039R2).

AN *IN SILICO* APPROACH TO HIGHLIGHT THE SIGNIFICANCE OF THE TIME CONSTANT OF ALVEOLAR RECRUITMENT

Ruby Dunphy (1), Sjeng Quicken (1), Jur Van Kimmenade (1), Julianna Mangold (2), Mehdi Shekarnabi (2,3), Vicente Estopier Castillo (2), Maciej Orkisz (3), Ashley De Bie Dekker (4), Igor Paulussen (4), Jean-Christophe Richard (3,5), Wouter Huberts (1), and Sam Bayat (2,6)

1. TU/e, The Netherlands; 2. Grenoble Alpes University, France; 3. Université Claude Bernard Lyon, France; 4. Catharina Hospital Eindhoven, The Netherlands; 5. Hospices Civils de Lyon, France; Grenoble University Hospital, France; 6. Grenoble University Hospital, France.

Correspondence: r.a.dunphy@tue.nl. Dept. of Biomedical Engineering, TU/e, Eindhoven, The Netherlands.

1. Introduction

Ventilator-induced lung injury (VILI) remains a major challenge associated with mechanical ventilation. To minimise the risk of VILI, ventilator settings, such as Positive End-Expiratory Pressure (PEEP), must be carefully optimised for each individual patient. Despite this need for personalisation, current bedside techniques lack the ability to continuously measure local alveolar dynamics. As a result, clinicians must rely on global lung parameters, which may not fully capture the complexities of regional lung behaviour. *In silico* modelling offers a promising solution by linking local alveolar mechanics with global lung function.

One of the primary underlying mechanisms contributing to the development of VILI is cyclic recruitment and derecruitment (R/D) or 'atelectrauma'. Bates & Irvin [1] propose that the time constant, τ, represents how quickly individual lung units will recruit/derecruit once the local airway pressure crosses its critical opening/closing pressure. They emphasise the significance of this kinetic delay in explaining the lung's dynamic mechanical behaviour, particularly in states of injury like atelectrauma.

We sought to investigate whether our *in silico* modelling framework could demonstrate this effect of the time constant on R/D behaviour.

2. Materials and Methods

This work leverages a lumped-parameter model presented in detail in [2], which estimates patient-specific regional elastance and recruitment information derived from dual-volume CT in a mechanically ventilated acute respiratory distress syndrome patient. The model was used to simulate mechanical ventilation during an incremental PEEP trial consisting of 30-second steps at 5, 10, and 15 cmH_2O. For each PEEP step, three time constants, τ = 2, 4, and 10s, were compared.

3. Results

It was observed that tidal recruitment was maximal at lower PEEP, and the rate of recruitment was greater with a lower τ (Fig.1). Increasing PEEP to 10cmH_2O resulted in the average 'static' level of recruitment to increase, while the dynamic component decreases. Above 10cmH_2O, further increases in static recruitment and tidal volume were negligible. It was consistent across all steps that an increase in the τ lead to a decrease in tidal recruitment.

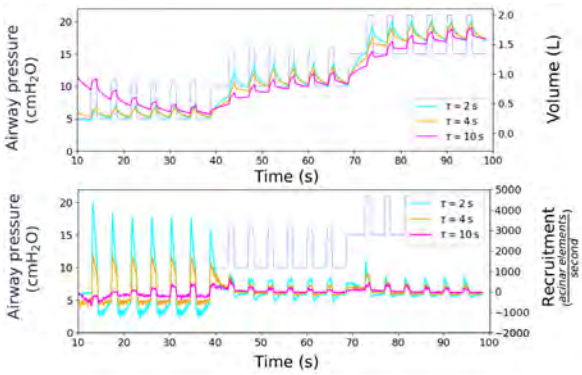


Figure 1: Volume change (top) and recruitment (bottom) during each PEEP step with varying τ.

4. Discussion and Conclusions

In this study, we utilised an *in silico* modelling framework that infers patient-specific local lung properties derived from dual-volume CT in a ventilated ARDS patient. Our model simulations suggest that a longer τ is akin to a less recruitable lung during tidal breathing, highlighting its importance on R/D behaviour, and, consequently, the onset of atelectrauma.

5. References

1. Bates JHT, Irvin CG. *J Appl Physiol*. 2002;93(2):705-713.
2. Quicken et al., ESB 2025 conference.

AI-BASED NEURAL IMPLICIT MODELLING OF THE PEDIATRIC TRACHEA FOR DATA-DRIVEN MEDICAL DEVICE DESIGN

Laith Hijazi (1), Fares Berro (2), Albraa Alaraj (2), Kevser Banu Köse (2)

1. Department of Computer Engineering, Istanbul Medipol University, Türkiye
2. Department of Biomedical Engineering, Istanbul Medipol University, Türkiye

1. Introduction

Endotracheal intubation is essential in neonatal intensive care, yet most pediatric tubes are scaled-down adult designs that poorly reflect pediatric airway variability [1]. Evidence suggests that infant tracheal morphology, particularly in premature and very young patients, differs from simplified textbook descriptions [2].

Advances in medical imaging and computational modelling now enable patient-derived anatomical analysis. In this study, we develop a computational framework combining neural implicit representations and statistical shape modelling to characterize pediatric tracheal geometry and generate a population-based anatomical reference for data-driven airway device design.

2. Materials and Methods

Retrospective computed tomography image datasets of 100 patients between the ages of 0-2 years were used to reconstruct pediatric tracheal geometries. Following image segmentation, the geometries were standardized based on the tracheal bifurcation to ensure that all geometries were aligned properly. Three-dimensional airway meshes were reconstructed and subsequently converted into neural implicit representations (INR) to obtain a compact and continuous description of tracheal geometry [3]. In this framework, each airway structure was represented as a function by learning its signed distance field through a neural network trained on spatial samples derived from the mesh surface. Correspondence optimization across the dataset enabled consistent point-wise alignment of the geometries, after which principal component analysis was applied to construct a statistical shape model, allowing extraction of the mean tracheal geometry and the principal modes of anatomical variation within the population.

3. Results

A statistical shape model was constructed, enabling estimation of the mean tracheal shape and the principal modes of anatomical variation. Neural implicit reconstruction preserved the original surface geometry with high accuracy. The analysis revealed notable variability in tracheal diameter, curvature, and bifurcation morphology, suggesting that pediatric airway anatomy differs substantially from simplified textbook representations.

4. Discussion and Conclusions

This work introduces a data-driven framework that INR with statistical shape modelling to characterize pediatric tracheal anatomy from patient-derived imaging data. The proposed approach defines a population-level anatomical space capturing both the mean airway configuration and the principal modes of morphological variability. This representation enables the generation of virtual pediatric populations that statistically reflect anatomical variability within the cohort. Such digital cohorts provide a realistic substrate for evaluating computational devices, including in silico testing. By deriving anatomical references directly from patient data, the framework supports population-informed design and preclinical evaluation of pediatric airway devices.

5. References

1. Adewale L. Anatomy and assessment of the pediatric airway. Pediatric Anesthesia. 2009;19(Suppl 1):11–23.012).
2. Deoras KS, Wolfson MR, Searls RL, Hilfer SR, Shaffer TH. Developmental changes in tracheal structure. Pediatric Research. 1991;30(2):170–175.
3. Sitzmann V, Martel JNP, Bergman AW, Lindell DB, Wetzstein G. Implicit Neural Representations with Periodic Activation Functions. Advances in Neural Information Processing Systems (NeurIPS). 2020;33:7462–7473.

THE HUMAN AIRWAYS REGISTER: A WEB DATABASE TO STANDARDISE IN SILICO LUNG GEOMETRY

Mahesh K. Ola (1), Morgan Seal (2), Raza A. Sarwar (1), Sai K. Mattireddy (1), Chris E. Brightling (3,4), Kelly Burrowes (2), Himanshu Kaul (1,3,4)

1. School of Engineering, University of Leicester, UK; 2. Auckland Bioengineering Institute, University of Auckland, New Zealand; 3. Institute for Lung Health, Leicester NIHR BRC, Leicester, UK; 4. Department of Respiratory Sciences, University of Leicester, Leicester, UK

1. Introduction

Respiratory diseases are a cause of 4 million deaths annually worldwide. *In silico* methods can predict changes in lung function due to disease or response to therapy [1-3]. These models can stratify patient-specific response *a priori*, thus forming the foundation of precision medicine strategies [2]. To deliver precision medicine at scale, however, we need sophisticated computer models that accurately recapitulate patient-specific pathophysiology and drug response [4]. The starting point of these models is the creation of precise *in silico* patient-specific lung geometries on which the relevant biophysical equations can be solved. Despite a plethora of literature on this topic, however, there is a lack of consensus on whether reported dimensions are physiologically relevant, with implications for clinical strategies that may be built using models underpinned by these estimates. Therefore, we explored how to identify physiologically relevant airway estimates and developed a database to make these available to the respiratory medicine community.

2. Materials and Methods

We conducted a systematic review of 45 published datasets including healthy individuals and (Asthma/COPD) patients. We mined airway wall thickness estimates and standardised them (for direct comparison between datasets) based on the Horsfield order airway generations (G1 to G27) [5]. We next conducted unsupervised clustering to identify the anatomically-relevant estimates and simulated a ventilation model [5] to assess their physiological relevance. We then created an online database to make all datasets available to the wider research community.

3. Results

Human airway wall thickness estimates showed high variance. For example, the tracheal thickness itself varied from *0.3–6.3mm (21x change)* and *0.52–6.99mm (13x change)* for healthy and diseased lungs, respectively. K-means clustering divided the healthy and diseased estimates into three and four clusters, respectively. Only one of the clusters in both categories yielded anatomically-relevant estimates. Simulation results in the form of pressure-volume curves and airway resistance showed these same clusters to exhibit physiologically plausible loop morphology (for both health and disease)

4. Discussion and Conclusions

Our analysis reveals that reported airway dimension estimates lack standardisation. To support future modelling efforts, we make available physiologically-relevant estimates via the *Human Airways Register*: an open-access airway-dimension database. The database will help standardise geometric inputs and quantify how measurement variability propagates to *in silico* lung function predictions. We anticipate this will enable standardisation of *in silico*, patient-specific lung geometry development and downstream simulation predictions, thereby significantly contributing to rapid development, deployment, and adoption of precision medicine approaches in respiratory healthcare.

5. References

1. R. Saunders et al., 2019, *Sci. Transl. Med.*, vol. 11, no. 479, pp. eaao6451
2. H. Kaul, 2019, *Morphologie*, vol. 103, no. 343, pp. 194–202.
3. R. Bordas et al., 2015, *PLos One*, vol. 10, no. 12, pp. e0144105
4. H. Kaul et al., 2025, *Thorax*, vol. 80, suppl. 2, pp. A335–A335.
5. A.J. Swan et al., 2012, J. Theor. Biol., vol. 300, no. 1, pp. 222–231.

Acknowledgements:

Leicester Institute for Precision Health Future 100 Scholarship; Dines Charitable Trust; Royal Society of New Zealand, James Cooke Fellowship; Royal Academy of Engineering (RF\201920\19\275); UKRI CRCRM (MR\Z505638\1); EPSRC (EP\W000490\1).

NETWORK-BASED DIGITAL TWINS REVEAL AIR POLLUTION MODIFIES GENETIC DISEASE SUSCEPTIBILITY THROUGH SHARED INFLAMMATORY PATHWAYS

A. Maertens, D. Ukaegbu, A. Kim

Johns Hopkins Bloomberg School of Public Health, United States of America

Corresponding author: Alexandra Maertens, Johns Hopkins Bloomberg School of Public Health, Environmental Health and Engineering, amaerte1@jhu.edu

1. Introduction

Understanding gene-environment interactions in complex diseases requires modeling how environmental exposures modify genetic risk at the systems level.

2. Materials and Methods

We developed network-based digital twins to simulate individual patients with varying combinations of genetic susceptibility variants and environmental epigenetic marks. Using GWAS and EWAS data for type 2 diabetes (T2D), asthma, and air pollution exposure, we modeled patients carrying disease risk variants with and without air pollution-associated epigenetic changes, then quantified disease network activation through protein interaction networks using Prize Collecting Steiner Forest.

3. Results

Our digital twin simulations revealed that genetic variants combined with air pollution epigenetic marks produced equivalent disease network activation as genetic variants alone at higher genetic load, demonstrating that environmental marks carry disease-relevant information content comparable to inherited susceptibility. Paired analysis controlling for genetic background and Steiner tree optimization showed air pollution genes connect to disease mechanisms through indirect pathways, requiring additional conserved bridging nodes—a pattern consistent across both diseases, suggesting shared systemic inflammatory mechanisms rather than disease-specific effects.

Disease-specific network topology emerged: T2D genetic architecture showed stronger network proximity to core metabolic pathways, with air pollution marks providing bridging connections, while asthma genetic variants occupied more peripheral network positions—a topology consistent with disease-specific mechanisms of environmental modification. Patient-level heterogeneity in genetic background dominated individual exposure effects, highlighting the importance of paired digital twin designs that simulate the same genetic background with and without environmental perturbation.

4. Discussion and Conclusions

More broadly, the dominance of genetic background variance over exposure effects underscores the critical importance of considering individual genetic context when interpreting exposome studies, as environmental impacts may be masked by inter-individual genetic heterogeneity.

These network-based digital twins provide a framework for quantifying gene-environment interactions at the pathway level. This approach reveals that environmental exposures can substitute for genetic load in disease network activation, suggesting that personalized environmental intervention strategies may be most effective when tailored to individual genetic architectures.

VIRTUAL POPULATIONS: GENERATING PHENOTYPE-SPECIFIC LUNG GEOMETRY USING CONDITIONAL AUTOENCODER

Joyce John (1), Kelly Burrowes (1), Justin O'Sullivan (2), Surya Bhatt (3), Eric Hoffman (4), Merryn Tawhai (1)

1. Auckland Bioengineering Institute, The University of Auckland, NZ; 2. Liggins Institute, The University of Auckland, NZ, 3. Division of Pulmonary, Allergy and Critical Care Medicine, University of Alabama at Birmingham, Birmingham, AL, USA; 4. Departments of Radiology and Biomedical Engineering, University of Iowa, Iowa, USA

1. Introduction

Accurate representation of anatomical variability is essential for building realistic virtual populations in computational physiology. In pulmonary modelling, however, most existing geometric datasets are limited in size and do not capture the full spectrum of structural phenotypes observed in chronic lung diseases. Generative models capable of producing realistic synthetic anatomies conditioned on disease characteristics could help address this limitation [1].

2. Materials and Methods

We present LobeSDFNet, a conditional deep generative framework that learns the relationship between lung lobe shape and regional tissue heterogeneity measured from computed tomography (CT). Lung lobe segmentations are represented as 3-dimensional signed distance fields (SDFs) and used to train a conditional autoencoder that encodes anatomical structure into a compact latent space while conditioning the decoder on quantitative imaging biomarkers describing tissue heterogeneity patterns.

Chest CT scans from the COPDGene Study Phase-1 were used to develop the model [2]. Lobar segmentation masks were converted to SDFs to represent lobe geometry. Tissue heterogeneity was quantified using Quadtree Decomposition (QtD), generating biomarkers describing parenchymal density variation [3]. These biomarkers were incorporated as conditioning variables in a 3D conditional autoencoder (LobeSDFNet) to learn relationships between lung shape and tissue heterogeneity.

A total of 4,141 participants were randomly partitioned at the subject level into training (n = 2,899; 70%), validation (n = 621; 15%), and test (n = 621; 15%) sets to prevent data leakage. Once trained, LobeSDFNet enables controlled generation of synthetic lung shapes conditioned on phenotype-relevant biomarker patterns. Model performance was evaluated using reconstruction accuracy of lung lobe geometry.

3. Results

Preliminary results demonstrate that conditioning on tissue heterogeneity significantly improves reconstruction fidelity and enables generation of realistic synthetic shapes that reflect disease-associated structural variation. The resulting shapes preserve key anatomical characteristics of lung lobes while exhibiting controlled phenotype-specific variability.

4. Discussion and Conclusions

This framework provides a scalable approach for generating phenotype-aware virtual lung populations, which may support downstream applications including computational simulations, machine-learning model development, and investigation of structure–function relationships in lung disease. More broadly, this work illustrates how combining imaging biomarkers with generative geometric modelling can enhance the realism and physiological relevance of synthetic anatomical datasets.

5. References

1. M. Perrone et al. *Annals of Biomedical Engineering* 53.11 (2025): 2911-2919.
2. Regan, Elizabeth A., et al. *COPD: Journal of Chronic Obstructive Pulmonary Disease* 7.1 (2011): 32-43.
3. John J, Burrowes KS, et al., *Acad Radiol*; (2025).

Acknowledgements:
This project was funded by the Dines Family Philanthropic Funding.

PHYSIOLOGICAL CLOSED-LOOP CONTROL MODEL IN SIMSCAPE FOR AUTOMATED VENTILATION STRATEGY VALIDATION

Magnus Nord (1), Visa Suomi (2)

1. MathWorks, France; 2. MathWorks, Germany;

1. Introduction

Accurate and adaptable physiological closed-loop control (PCLC) models are essential for validating advanced automated ventilation strategies and for exploring novel patient-specific respiratory support concepts. [1] The proposed Simscape-based model provides a comprehensive simulation environment with in silico models capable of representing complex cardiopulmonary interactions. It supports the evaluation of automated oxygenation and ventilation control algorithms. This includes investigations into oxygenation efficiency and into non-invasive cardiac output estimation. In addition to automation-focused applications, the model is designed for studying diaphragm-support methods, benefiting from an integrated human CO2 sensory feedback model.

2. Materials and Methods

The model was implemented in Simscape using a multi-species gas domain framework that is openly available and modifiable. Lung mechanics, airway structures, humidification systems, check valves, and modern ventilation modalities were represented using first-principles physics. Oxygenation and gas transfer behaviour follow the mathematical formulations described by Hexamer [22], enabling detailed representation of multi-component diffusion and perfusion effects. A flexible fidelity architecture allowed each subsystem to be configured according to temporal resolution requirements or the specific physiological phenomena of interest. Reduced-order models (ROMs) were generated using surrogate datasets produced by the high-fidelity model, enabling rapid simulation while preserving key dynamic characteristics.

3. Results and Discussion

The model's simulation results show that it can reproduce physiologically viable responses in a variety of ventilation settings, including titration of the set Positive End Expiratory Pressure (PEEP), changes in FiO_2, and in application of diaphragm-support modes such as Neurally Adjusted Ventilatory Assist (NAVA).

The integration of capno-dynamic methods for non-invasive cardiac output estimation enables exploration of hemodynamic safety during automated PEEP adjustments, particularly in identifying scenarios where hypoxemia is caused by impaired perfusion rather than ventilatory mismatch. The model's flexibility allows evaluation of oxygenation-efficiency algorithms for a variety of patient categories. The use of ROMs significantly reduces computation time of nonsignificant parts of the model, supporting fast iterative testing of the automation logic. The multi-species gas domain and ventilator-component models provide increased realism and fidelity when needed.

4. Conclusions

The presented Simscape model constitutes a versatile and physiologically rich simulation environment for evaluating advanced ventilation automation strategies and diaphragm-support mechanisms. By integrating high-fidelity lung mechanics, multi-species gas transport, and a configurable fidelity architecture, it enables detailed exploration of oxygenation, ventilation distribution, and cardio-respiratory coupling. The combination of first-principles modelling with ROM-based acceleration facilitates both rigorous research investigations and rapid prototyping automation concepts. This framework provides a robust foundation for future work in safe, patient-specific ventilatory control.

5. References

1. MOHAMMAD JAVAD KHODAEI , Physiological Closed-Loop Control (PCLC) Systems: Review of a Modern Frontier in Automation. IEEE Access 8:1-1 DOI: 10.1109/ACCESS.2020.2968440
2. Hexamer M et Al. "A Mathematical Model for the Gas Transfer in an Oxygenator," 2003. IFAC Proceedings Volumes 36(15):409-414

IN-VIVO EVALUATION OF A 3D-PRINTED PLA-PCL TRACHEAL STENT IN A RABBIT MODEL.

Letizia Cella (1*), Laura Vilalta (2), Mauro Malvè (3), Jorge Rosell (4), Noemi Gómez (5), Rocío Fernández-Parra (5)

Doctoral School of the Catholic University of Valencia, Spain; 2. Veterinary Hospital Canis, Spain; 3. Public University of Navarre (UPNA), Spain; 4. Valencian Institute of Pathology, Spain;5. Veterinary Referral Hospital UCV, Catholic University of Valencia San Vicente Mártir, Spain.

**Correspondence: Cella Letizia (letizia.cella@ucv.es)*

Introduction

Airway obstruction caused by stenosis, tracheomalacia, or tumors impairs respiration [1]. Conventional stents are effective but associated with long-term complications [2]. Biodegradable 3D-printed stents may overcome these limitations [3]. This study evaluated a 3D-printed PLA-PCL tracheal stent in a rabbit model.

Materials and Methods

3-D printed X-shaped biodegradable PLA-PCL tracheal stents were implanted endoscopically in New Zealand White rabbits under general anesthesia. Animals were assigned to 4-, 8-, and 12-week follow-up groups, with one sham control at each time point. Clinical examination, computed tomography (CT), bronchoscopy (Figure 1), bronchoalveolar lavage (BAL) cytology and microbiological culture, and histopathology were performed to evaluate biocompatibility. Macroscopic presence of airway stenosis, granulation tissue, re-epithelialization, inflammation, fibrosis, mucus accumulation, stent fragmentation and local tissue response was also recorded.

Results

Fifteen rabbits were included (12 with stent and 3 sham). Stent implantation was successful, with no clinical sings or mortality during follow-up period. Stent presence was 50% (2/4) at 4 weeks (Figure 1a) to 0% (0/4) at 8 weeks (Figure 1b), with one stent (25%, 1/4) at 12 weeks (Figure 1c). In animals with stents, CT showed migration, tracheal wall thickening (up to 1.2 mm), moderate granulation tissue, and luminal stenosis (up to 40%). Pulmonary CT showed mild bronchial changes and focal consolidation. BAL cytology was mainly normal or showed mild inflammation, while BAL cultures predominantly yielded presence of *Enterobacter* spp. Histopathology showed mild to moderate localized mucosal hyperplasia, inflammatory infiltrates, and fibroplasia. Focal necrosis and granulation tissue occurred only in animals with stents. Tracheal fibrocartilage and adventitia remained preserved, with no foreign material detected in the lungs.

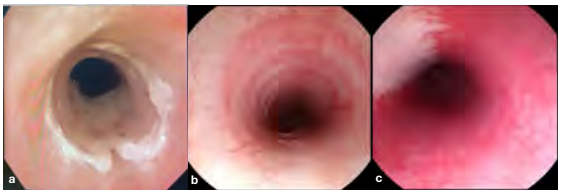


Figure 1: a. 4-, b. 8-, and c. 12-week follow-up bronchoscopy.

Discussion and Conclusions

Tissue alterations remained localized, with preservation of the tracheal fibrocartilage and adventitia. Stent loss may reflect biodegradation, fragmentation, migration, expectoration, or swallowing, although the real cause remains unclear. Oropharyngeal contamination related to the endoscopic technique, cannot be excluded. Studies optimizing sizing, geometry, radial force and degradation behavior are warrantied.

5. References

1. Sabath BF, Casal RF. Mediastinum; 7:18 (2023).
2. Ratnovsky A, et al., Med Eng Phys;37:408-415 (2015).
3. Dutau H, et al., Respiration;90(6):512-521 (2015).

Acknowledgements: Supported by grants PID2021-125731OB-C31 and PID2021-125731OB-C33 from the Spanish Ministry of Science and Innovation MCIN/AEI/10.13039/501100011033/ and AIN.

IN-SILICO ASSESSING THE RISK OF DIFFERENTIAL HYPOXIA AND O_2 DISTRIBUTION DURING PERIPHERAL VA ECMO TREATMENTS

Alessandro Ruggeri (1), Mirko Belliato (2), Michele Conti (1)

1. Department of Civil Engineering and Architecture, University of Pavia, Pavia, Italy; 2. UOC Anestesia e Rianimazione 1, Fondazione IRCCS Policlinico San Matteo, Pavia, Italy

1. Introduction

Despite the increasing use of veno-arterial extracorporeal membrane oxygenation (VA-ECMO) as temporary mechanical support for cardiopulmonary failure, survival in adults has improved only modestly [1]. Differential hypoxia remains a major fatal complication [2], driven by the competition between poorly oxygenated blood ejected by the left ventricle and highly oxygenated blood delivered by the ECMO circuit. This highlights the need to clarify how mixing zone location affects end-organ oxygenation.

Patient-specific digital twins combined with computational multiphysics simulations may help address this gap.

2. Materials and Methods

Computational fluid dynamics coupled with oxygen transport simulations were performed in COMSOL Multiphysics® v6.3 on a patient-specific model of a young female aorta [3]. Two models were generated from the healthy 3D aortic geometry: one including major abdominal branches and one excluding them.

Scenarios combining different VA-ECMO support levels with different degrees of cardiac and pulmonary dysfunction were simulated. Cardiac impairment was modeled across five severity levels by rescaling the left ventricular pulsatile waveform; ECMO flow was kept constant over time and varies depending on cardiac impairment, while maintaining a mean total aortic blood flow of 5 L/min. The resulting blood velocity field was used as the convective term in the oxygen transport simulations.

To distinguish the contributions of native cardiac output and VA-ECMO to organ oxygenation, two virtually different oxygen species were tracked. Pulmonary oxygenation dysfunction was modeled by setting cardiac blood oxygen saturation (SaO2) to 67% or 83%, while ECMO blood SaO2 was fixed at 100%. Mixing zone location was defined as the first cross-section perpendicular to the aortic centerline with at least 90% of its area showing SaO2≥93%. Several cardiac cycles were simulated until convergence.

3. Results

The simulations characterized end-organ perfusion and mixing zone location across the tested scenarios. Compared with the detailed model, the simplified model without abdominal branches predicted mixing zone positions closer to the left ventricle, with differences of up to 40.68 percentage points, and overestimated cerebral and gastric SaO2 in several cases, thereby underestimating hypoxia risk.

Intermediate scenarios also revealed complex hemodynamic behavior, including disturbed flow patterns, delayed stabilization of the SaO2 field over multiple cardiac cycles, and regions of recirculation with limited washout in the descending thoracic aorta and aortic arch. These features became apparent only when major abdominal branches were included.

4. Discussion and Conclusions

A quantitative criterion for the mixing zone location was proposed and related to end-organ perfusion during VA-ECMO. Inclusion of major abdominal branches appears important for a more appropriate assessment of differential hypoxia risk. Although mixing zone position was mainly determined by the balance between native left ventricular and ECMO flow, its clinical impact depended strongly on left ventricular SaO2; increasing ECMO support did not necessarily guarantee adequate cerebral oxygenation in the presence of severe pulmonary oxygenation deficit.

5. References

1. Tonna J E et al., ASAIO Journal 70.2 (2024): 131-143.
2. Rozencwajg S et al. *Scientific reports* 13.1 (2023): 4002.
3. Wilson N M, Ortiz A K, and Johnson A B, *Journal of medical devices* 7.4 (2013): 040923.

FROM LOCAL AIRWAY OBSTRUCTION TO GLOBAL RESPIRATORY IMPEDANCE: AN IN SILICO STUDY IN THE NEONATAL LUNG

Matteo Mentasti (1), Raffaele Dellacà (1), Chiara Veneroni (1)
Matteo Mentasti, Department of Electronics, Information and Bioengineering, Politecnico di Milano, Milan, Italy. E-mail: matteo.mentasti@polimi.it
1. Politecnico di Milano, Italy

1. Introduction

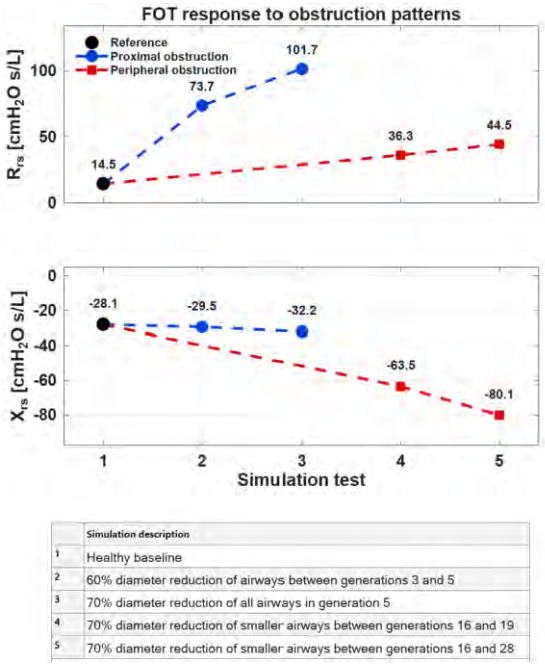
Oscillometry is a non-invasive technique that measures respiratory system input impedance. Because it requires minimal patient cooperation, it is increasingly used as a bedside tool to assess respiratory mechanics in newborns. Different oscillometric patterns have been reported in neonatal lung disease [1]; however, their interpretation is largely extrapolated from mathematical models of the adult lung and experimental studies performed in preclinical models of adult lung pathologies. How localized airway abnormalities translate into global oscillometric measurements remains poorly understood and has never been investigated in newborns. This study used an in silico model of the neonatal lung to investigate how different patterns of localized airway obstruction affect respiratory resistance (Rrs) and reactance (Xrs).

2. Materials and Methods

The computational model consists of a morphometric 3D airway tree model. The resulting model is made of 50,400 branches distributed over 28 generations. Each airway branch is represented by an equivalent mechanical model accounting for airflow resistance, gas compressibility and tissue viscoelasticity [1]. Model parameters were adapted to represent the newborn lung as in [2]. Oscillometry was simulated by applying a 5 Hz, 2 cmH_2O peak-to-peak sinusoidal pressure waveform at the airway opening. Rrs and Xrs were computed in the frequency domain by recursively solving the equivalent impedance of the airway tree. The diameter of specific airway generations of the upper or lower branches was selectively reduced.

3. Results

Simulated proximal airway obstructions produce a marked increase in Rrs, while Xrs is only minimally affected. In contrast, obstruction patterns involving the peripheral airways result in a moderate increase in Rrs accompanied by a pronounced decrease in Xrs (Figure 1). The simulated Rrs and Xrs values matched the ones reported in newborns [1].



	Simulation description
1	Healthy baseline
2	60% diameter reduction of airways between generations 3 and 5
3	70% diameter reduction of all airways in generation 5
4	70% diameter reduction of smaller airways between generations 16 and 19
5	70% diameter reduction of smaller airways between generations 16 and 28

Figure 1: Simulated changes in Rrs and Xrs for proximal and peripheral airway obstruction patterns.

4. Discussion and Conclusions

This in silico neonatal lung model successfully reproduced oscillometric measurements reported in newborns and identified distinct effects of proximal and peripheral airway obstruction on respiratory impedance. The findings are consistent with observations in adult studies and provide mechanistic insight into the interpretation of neonatal oscillometry. This computational framework offers a novel tool for investigating respiratory mechanics and may support the future clinical interpretation of oscillometry in newborns.

5. References

1. Dellacà RL et al. Intensive Care Med. 39:511-519 (2013).
2. Veneroni C et al. Comput Bio Med. 135:104582 (2021).

RADIOMICS-BASED ATRIAL FLOW PROFILE DESCRIPTION FROM 4D FLOW MRI IN ATRIAL FIBRILLATION PATIENTS

Camilla Cortesi (1,2), Giorgia Diotallevi (1), Lida Alinezhad (1), Paria Maleki (1), Matteo Falanga (1), Jonas Leite (2), Nadjia Kachenoura (2), Cristiana Corsi (1)

1. DEI, University of Bologna, Italy; *2. Sorbonne Université, CNRS, INSERM, LIB, Paris, France*

Corresponding authors: Camilla Cortesi, camilla.cortesi3@unibo.it

1. Introduction

Atrial fibrillation (AF) is the most common sustained cardiac arrhythmia and is associated with increased thromboembolic risk driven by altered hemodynamics within the left atrium (LA). Quantitative and non-invasive characterization of these flow alterations remains challenging in clinical practice. This preliminary study investigates whether radiomics can provide additional quantitative descriptors of LA blood flow patterns and their regional hemodynamic properties, to identify features that characterize AF.

2. Materials and Methods

4D Flow MRI data from 12 AF patients and 11 healthy controls were analysed to study the acquired three-dimensional velocity fields across the cardiac cycle while using time-resolved segmentation of the LA. Radiomics features were extracted using the PyRadiomics library [1] from five hemodynamic parametric maps (Through-plane flow, Wall Parallelity Degree, Normalized Vorticity, Local Normalized Helicity, and Flow Angle) [2] computed across ten anatomical planes within the LA. Feature reduction was applied based on the relevance to hemodynamic characterization reported in Huellebrand et al. [2]. Given the limited sample size, a radiomics pipeline incorporating Leave-One-Out cross-validation with nested feature selection was implemented, followed by training of a Support Vector Machine classifier. Top-ranked features were analysed at two key cardiac phases, atrial end-diastole (ED) and atrial end-systole (ES), to characterize the organization of LA flow in AF.

3. Results

Radiomics analysis of LA hemodynamic maps demonstrated good classification performance between AF patients and healthy controls. The classifier achieved 82.6% accuracy (AUC = 0.79), with a sensitivity of 0.83, and a specificity of 0.82 at atrial ED, and 86.7% accuracy (AUC = 0.93), with a sensitivity of 0.92 and a specificity of 0.82 at atrial ES. Stability analysis identified five robust features at ED and four at ES, primarily derived from Flow Angle texture patterns measuring the angle between velocity vector and the normal to the analysed plane, namely, mitral valve plane (Figure 1) and longitudinal LA plane separating the inferior from the superior pulmonary veins.

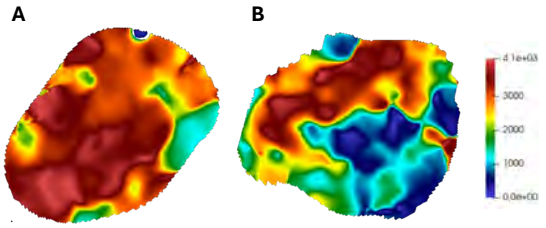


Figure 1: Flow Angle map of mitral valve plane at atrial ES. (A) AF patient, (B) healthy control. The input range [0 180]° was rescaled to standardize interval [0 4096].

4. Discussion and Conclusions

Texture features derived from Flow Angle maps revealed differences in LA flow organization between AF patients and healthy controls. AF patients showed more uniform and simplified flow, whereas controls exhibited greater spatial heterogeneity and physiological micro-vortices, particularly reflecting effective atrial contraction at ES. These findings suggest that radiomics applied to 4D Flow MRI can quantitatively capture LA flow remodelling in AF and may support the development of imaging biomarkers.

5. References

1. Van Griethuysen J et al., Cancer Research, 2017.
2. Huellebrand M et al., Frontiers in Cardiovascular Medicine, 2023.

SHUNT HEMODYNAMICS ABNORMALITIES IN SUBLINGUAL MICROCIRCULATION AS INDICATION FOR SEPSIS

Kavin Vishnu (1), Matthias P Hilty (2), Alessandro Candreva (3) and Monika Colombo* (1)
1. Department of Mechanical and Production Engineering, Aarhus University, Denmark; 2. Institute of Intensive Care, Zurich University Hospital, Switzerland; 3. Department of Cardiology, Zurich University Hospital, Switzerland
*mc@mpe.au.dk

1. Introduction

The shunting theory of sepsis [1] states that venules shunting leads to impaired oxygenation in certain microvasculature regions. Impaired recruitment of the sublingual vessels caused by shunting can provide insight into the clinical state of sepsis [1]. Here we show, through a machine learning (ML) approach, that hemodynamic abnormalities detected in the sublingual microcirculation (SM), in terms of red blood cells (RBCs) velocity and concentration, contribute to detecting and classifying shunt within capillary network.

2. Materials and Methods

Handheld vital microscopy SM images (Fig. 1-A) and related hemodynamic data are de-rived from previous works of the group [2,3] and prospective data collection of coronary microvascular disease patients, considering both controls and altered hemodynamic conditions through the application of two vasodilators (nitroglycerin and acetylcholine) to increase capillary recruitment and total vessel density (TVD). The capillary network is visualized through electronic analogue in Fig. 1-B. Hemodynamic data and RBC properties are extracted for each detected vessel. We employed labelled data to calculate hemodynamic correlations (e.g. Fig. 1-C) associated with shunts. K-means clustering is applied using unlabelled data based on features representing these known hemodynamic correlations, aiming at sorting shunts in both controls and when vasodilators were applied.

3. Results

A grading scale for identifying shunts in the three cases (Fig. 1-B) was created based on ranges of hemodynamic properties, flow properties, and clustering, with the parameters of this grading scale optimized by further application of ML algorithms. Preliminary results demonstrate notable differences in the trends and strongly significant correlations between shunts and non-shunt SM allowing for identification. Further, cases with higher TVD (following vasodilators application) additionally showed unique trends and clustering behaviour (Fig. 1-D).

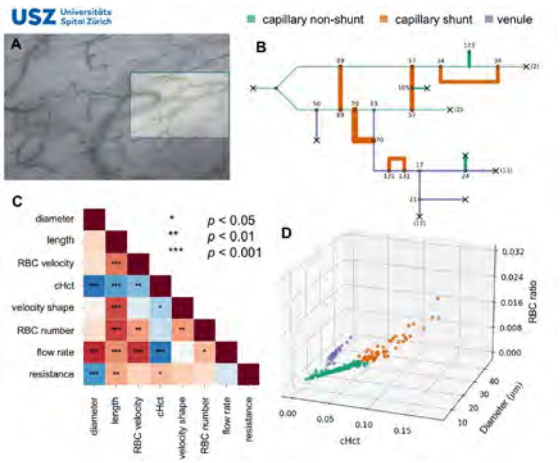


Figure 1: **A)** Handheld vital microscopy sublingual microcirculation image, with example region of interest. **B)** visualization of the electronic analogue of the sublingual microcirculation, where colours and line thicknesses are indicative for the ML-graded classes of microcirculation vessels. **C)** example of a correlation map between hemodynamic and flow derived features. **D)** clustering example of all the microcirculation vessels analysed by the ML-grading algorithm.

4. Discussion and Conclusions

The shunting grading scheme shows promising results in its ability to identify patients with sepsis. More data is expected to lead to a robust detection method for shunts in patients with different SM conditions, leading to the identification of underlying diseases such as sepsis, defining a paradigm shift in critical care management of patients.

5. References

1. Gruartmoner G et al., *Medicina Intensiva*, 2017
2. Hilty MP et *al*., *Critical Care Medicine*, 2020
3. Hilty MP et *al., Communication Biology, 2019*

BAYESIAN INFERENCE OF SEPSIS HAEMODYNAMICS FROM ARTERIAL BLOOD PRESSURE AND PHOTOPLETHYSMOGRAPHY

Hrisheekesh Vaidya (1)*, Rebecca Shipley (1), Steve Harris (1), Finneas Catling (2, 1)
1. University College London, United Kingdom, 2. Imperial College London, United Kingdom
** Correspondence to vaidya@hrish.ee*

1. Introduction

Physiological waveform data contain hidden information that could personalise therapy in critically unwell patients, aiming to reduce morbidity and improve survival. We present a Bayesian inference pipeline, based on a mechanistic 1D model, that infers latent cardiovascular state jointly from two clinically ubiquitous bedside monitoring signals: the photoplethysmography (PPG) and arterial blood pressure (ABP) waveforms.

2. Materials and Methods

Extending previous work [1], we trained a neural network surrogate of a 1D arterial tree simulator to predict distributions over ABP and PPG waveforms given a simulator parameter set. The parameter set represents the latent cardiovascular state and includes clinically relevant features such as large-vessel stiffness and vascular resistance. We used this network to define the likelihood function for Bayesian inference, using the No-U-Turn sampler [2] to explore the posterior over latent cardiovascular state parameters. We modelled known sources of noise and over-dispersed priors to encapsulate a clinically realistic range of septic individuals. We evaluated parameter identifiability in 200 simulated patients with randomised latent states to demonstrate diverse physiology.

3. Results

PPG-only inference led to poor identification of latent cardiovascular state parameters with only 54/200 PPG-only runs meeting sampling criteria (effective sample size ≥ 100 and $\hat{R} \leq 1.05$), compared with 191/200 for ABP-only waveforms, and 129/200 for joint ABP+PPG waveforms. However, for several clinically-relevant parameters, we found that the joint ABP+PPG posteriors had better coverage and reduced median absolute errors (Fig. 1).

4. Discussion and Conclusions

Although the ABP+PPG posterior was harder to explore than ABP-only inference, combining these signals led to more accurate and better-calibrated inference for clinically-relevant parameters. We hypothesise that this is because the PPG waveform as modelled contains non-redundant blood *flow* information which provides an additional constraint on the plausible cardiovascular state, beyond inference based on blood *pressure* alone. This improves accuracy and clinical utility, but also makes the posterior geometry more difficult to explore. Following human validation, these insights may guide fluid and vasoactive therapy in sepsis.

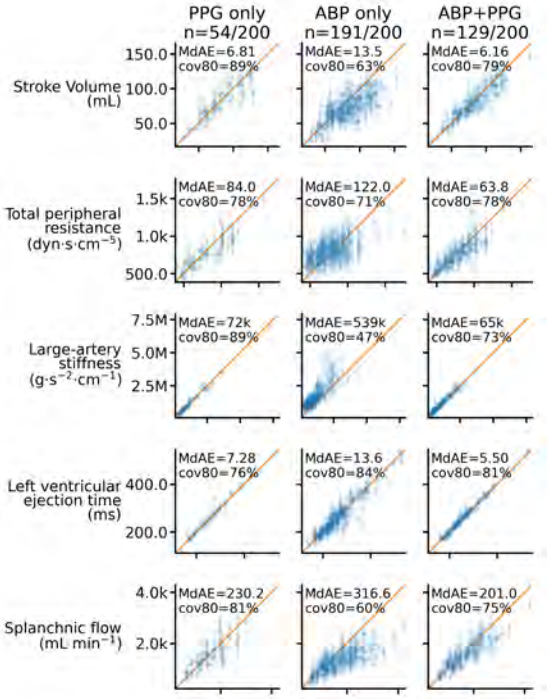


Fig. 1: Coverage/accuracy summary. Each panel plots true values (x-axis) with posterior (y-axis) median (dot) and 80% high-density intervals (HDI; vertical bar). The orange diagonal line represents perfect alignment. Text shows median absolute error (MdAE) & coverage of the 80% HDI (cov80; 80% is the target score).

5. References

1. Catling F et al; 2024; 10.1016/j.jcrc.2024.154555
2. Hoffman MD et al; 2014 (15:1593-1623); JMLR

Acknowledgements:
We are funded by the NIHR, the Wellcome Trust (222882/Z/21/Z), and the EPSRC (EP/T017791/1).

VALIDATION OF A VIRTUAL-POPULATION-BASED APPROACH FOR NON-INVASIVE CARDIOVASCULAR MONITORING IN HEALTHY VOLUNTEERS

Bianca Maria Laudenzi (1), Pavlo Yevtushenko (2), Lucas Omar Müller (1)

1. Laboratory of Mathematics for Biology and Medicine, Department of Mathematics, University of Trento, Trento, Italy; 2. Institute of Computer-assisted Cardiovascular Medicine, Deutsches Herzzentrum der Charité (DHZC), Berlin, Germany

1. Introduction

Cardiovascular and respiratory diseases remain leading causes of morbidity worldwide, and continuous remote monitoring is essential for early detection of complications in patients with chronic conditions. Wearable devices allow non-invasive tracking of vital signs but cannot directly measure clinically relevant hemodynamic indices such as stroke volume (SV) and ejection fraction (EF). In a previous in-silico study [1], we trained Gaussian Process Regression (GPR) models on a virtual population (VP) to estimate SV and EF from wearable-derived signals. This study extends that framework by validating the predictive models against real-subject data and assessing the physiological representativeness of the underlying VP.

2. Materials and Methods

Peripheral pressures and HR, alongside SV and EF measured via echocardiography, were acquired from a cohort of 30 healthy volunteers [2]. Healthy reference cutoffs were applied to these variables, yielding 20 subjects.

A lumped-parameter, closed-loop cardiorespiratory model [3], including cardiovascular, respiratory and gas exchange dynamics, was used to generate clinically relevant outputs (SV, EF) alongside wearable-acquirable signals (HR, CSBP, CDBP). The VP was generated via Sobol sampling over parameters selected through local and global sensitivity analysis. The same healthy cutoffs applied to the real cohort were also applied to the VP, then GPR models were trained on the VP to predict SV and EF. The trained GPR models were then tested on the real 20-subject dataset.

A nearest-neighbor criterion in standardized hemodynamic space (HR, CSBP, CDBP, EF, SV) was used to assess which real subjects fall within VP coverage. Moreover, a sex-specific VP extension is being developed to account for female hemodynamic characteristics reported in the literature.

3. Results

The GPR model predictions achieved good agreement with real measurements when restricted to the subjects covered by the VP (SV: MAE 5.5 mL, MAPE 5.9%; EF: MAE 0.033, MAPE 5.4%), but only 10 of 20 subjects fell within its coverage, most of whom were male. Across the full cohort, this translated into substantially larger errors (SV: MAE 16.2 mL, MAPE 23.5%), driven by the excluded, predominantly female, subjects. Preliminary results of the sex-specific VP extension show a substantially improved coverage, with 19 of 20 subjects now classified as inside the VP, and yield marked improvements across the full cohort: for SV, MAE decreased from 16.2 to 11.6 mL (MAPE from 23.5% to 16.5%), with a higher Pearson correlation ($r=0.80$ vs. $r=0.73$). EF predictions retained a low absolute error (MAE 0.033, MAPE 5.5%) but a weak, non-significant correlation with real measurements ($r=0.16$, $p=0.49$), consistent with the limited EF variability within this healthy cohort.

4. Discussion and Conclusions

These results support the feasibility of VP-trained models for non-invasive cardiovascular monitoring. Extending the VP with sex-specific parameter ranges improved both subject coverage and SV prediction accuracy across the full cohort, highlighting the importance of capturing hemodynamic heterogeneity between sexes, an aspect that will be further explored in future work.

5. References

1. Laudenzi, B. M., Cucino, A., Lassola, S., Balzani, E., & Müller, L. O. PLOS Digital Health. 4(10), e0001041. (2025)
2. Obermeier, L., Wiegand, M., Hellmeier, F., Manini, C., Kuehne, T., Goubergrits, L., & Vellguth, K. IEEE transactions on bio-medical engineering, 71(9), 2568–2579. (2024)
3. Laudenzi, B. M., Dalmaso, C., & Müller, L. O. (2025). Cardio-respiratory-model (Version v1.1.0) [Computer software]. Zenodo.

PARAMETER ESTIMATION IN CARDIOVASCULAR FLUID–SOLID INTERACTION

David Nolte, Reidmen Aróstica, Cristóbal Bertoglio

University of Groningen, The Netherlands

Corresponding author: David Nolte, d.j.nolte@rug.nl

1. Introduction

Patient-specific cardiac simulations require calibrating model parameters from physiological measurements. Previous work demonstrated parameter estimation in biventricular fluid–solid interaction (FSI) using idealized displacement and flow measurements [1]. This study assesses the feasibility of complete biventricular hemodynamic characterization during systole—jointly estimating myocardial and both systemic and pulmonary vascular parameters—from clinically realistic measurements. Robust estimation is achieved through stable semi-implicit FSI coupling.

2. Materials and Methods

Considering a patient's biventricular geometry, the dynamics of the contracting myocardium are coupled semi-implicitly [2] with a fractional step Arbitrary Lagrange–Eulerian (ALE) formulation of the Navier–Stokes equations governing the intraventricular blood flow. During systole, the atrioventricular valves are considered closed and the aortic and pulmonary valves fully open, where the distal vasculature is modeled via stable, semi-implicit resistance boundary conditions. The nonlinearly coupled FSI problem is solved with a matrix-free Newton–Krylov method.

Myocardial and vascular parameters—contractility and pericardial stiffness, systemic and pulmonary resistance—are estimated from synthetic data, mimicking realistic MRI measurements. Parameters are estimated using a reduced-order unscented Kalman filter [3], run iteratively to reduce dependence on the prior.

3. Results

Figure 1 shows the evolution of the systemic resistance and the myocardial contractility. The joint estimation of vascular and myocardial parameters reproduces accurately the ground truth from flow data or myocardial wall displacement data alone, while the former has a more pronounced bias and is slightly more susceptible to noise. Combining the data leads to accurate estimates with improved robustness. Pericardial stiffness estimation requires displacement data for accurate recovery.

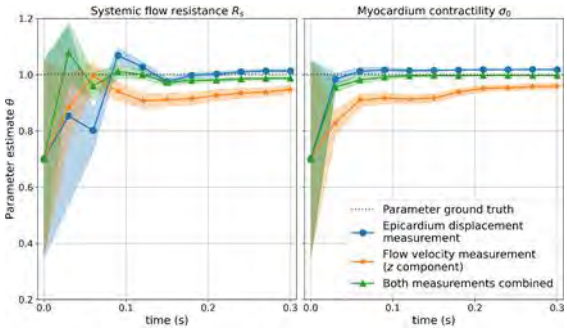


Figure 1: Parameter evolution of systemic resistance and myocardial contractility vs ground truth.

4. Discussion and Conclusions

This work extends cardiovascular FSI parameter estimation to biventricular hemodynamics through joint cardiac and vascular parameter identification. The combination of flow and displacement measurements improves estimation robustness compared to single-modality data. Stable semi-implicit coupling enables reliable estimation with resistance boundary conditions. Future work includes coupling to comprehensive circulation models and validation on clinical imaging data.

5. References

1. Aróstica R, Bertoglio C, Nolte D. FIMH 2025, LNCS 15672, Springer (2025)
2. Fernández MA, Gerbeau JF, Grandmont C. IJNME 69(4):794-821 (2007)
3. Moireau P, Chapelle D. ESAIM COCV 17(2):380-405 (2011)

Acknowledgements:
Funded by the ERC under EU Horizon 2020 (grant No 852544 - CardioZoom).

MODEL-BASED NON-INVASIVE RECONSTRUCTION OF PATIENT-SPECIFIC LEFT VENTRICLE PRESSURE-VOLUME DYNAMICS

Rahul Manoj[1], Annette Caenen[2,3], Laurine Wouters[2], Jens-Uwe Voigt[2], Jan D'hooge[2], Leif Rune Hellevik[1]

1. Division of Biomechanics, Department of Structural Engineering, Norwegian University of Science and Technology (NTNU), Trondheim, Norway;

2. Department of Cardiovascular Sciences, KU Leuven, Leuven, Belgium;

3. Institute for Biomedical Engineering and Technology, Ghent University, Ghent, Belgium.

Corresponding Author: Rahul Manoj, email: rahul.manoj@ntnu.no

1. Introduction

The left ventricular (LV) pressure–volume (PV) loop provides a mechanistically grounded representation of cardiac function, capturing preload, afterload, contractility, passive stiffness, and ventricular–arterial coupling within a single cardiac cycle [1]. Despite its diagnostic value, PV loop acquisition remains invasive, limiting routine assessment of diastolic dysfunction, where elevated LV end-diastolic pressure (LVEDP) is a key hallmark [2]. We propose a physiology-informed, closed loop lumped parameter model (LPM) that integrates multimodal clinical measurements to non-invasively reconstruct patient-specific LV PV loops and estimate LVEDP.

2. Materials and Methods

Retrospective data from 68 adults undergoing cardiac catheterization included brachial blood pressure and heart rate, echocardiographic end-diastolic and end-systolic volumes (EDV/ESV), LV geometry and valve-timing indices, Shear Wave Elastography (SWE) derived shear-wave velocity after mitral-valve closure, and invasive LVEDP as reference. A closed-loop LPM (LV elastance model + systemic arterial Windkessel + venous return) simulated LV pressure, LV volume, and aortic pressure waveforms from a 10-parameter set. The goal of the optimisation scheme was to constrain the simulated LV PV loop from all physiological directions to be patient specific. Model parameters were estimated using a two-stage optimization strategy (differential evolution followed by L-BFGS-B), minimizing a normalized loss on pressure, volume, and valve timings and SWE-based regularization.

3. Results

The framework produced stable, physiologically plausible waveforms and patient-specific PV loops. Agreement with measured targets was strong for pressures ($r = 0.80–0.95$ for SBP/DBP) and volumes ($r = 0.92–0.98$ for EDV/ESV); valve timings correlated well ($r = 0.88$). Model-derived LVEDP closely matched invasive LVEDP (mean difference 0.24 mmHg; $p = 0.641$) with correlation $r = 0.76$ ($p < 0.001$), MAE 3.22 mmHg and RMSE 4.26 mmHg. Classification of elevated LVEDP (≥16 mmHg) achieved AUC = 0.94 with sensitivity 89.2% and specificity 90.3%. In patients graded "inconclusive" by guideline echocardiography, LVEDP classification accuracy remained 89.4%.

4. Discussion and Conclusions

By combining SWE-derived myocardial stiffness with routine hemodynamics inside a mechanistic closed-loop model, we reconstruct LV PV loops non-invasively and obtain explainable PV-derived metrics. The model preserves canonical PV-loop physiology under loading changes and provides accurate LVEDP estimation against catheter reference, supporting diastolic dysfunction assessment when echocardiography is uncertain. This approach advances interpretable, patient-specific PV loop reconstruction as a practical step toward cardiovascular digital-twin for clinical decision support.

5. References

1. Burkhoff, I. Mirsky, and H. Suga, *Am. J. Physiol.-Hear. Circ. Physiol.*, vol. 289, no. 2 58-2, 2005.
2. A. Caenen *et al.*, *JACC Cardiovasc. Imaging*, vol. 17, no. 3, pp. 314–329, 2024.

DEMOGRAPHIC BIASES IN AI-ECG-BASED PREDICTION OF ATRIAL FIBRILLATION

B.G. van Willigen (1,2), M.M. Terpstra (1), C.M.A. Buck (4), H. Bleijendaal (1), T.F. Brouwer (1), R. Coronel (1), H.A. Marquering (2,3), J.R. de Groot (1)

1 Experimental cardiology, Amsterdam UMC, The Netherlands, 2 Biomedical engineering & physics, Amsterdam UMC, The Netherlands, 3 Radiology and Nuclear Medicine, Amsterdam UMC, The Netherlands, 4 Cardiovascular Biomechanics, Eindhoven University of Technology, The Netherlands

1. Introduction

Atrial fibrillation (AF) increases the risk of stroke and heart failure. Current risk scores for AF prediction perform moderately (area under receiver operating characteristic curve, AUROC 0.69–0.71) [1]. AI models using ECGs of individuals in sinus rhythm (SR) have achieved higher accuracy (AUROC 0.75–0.90) [2-4]. However, it is unclear how sex and age influence model performance. This study evaluates demographic (age and sex) biases in AI-ECG-based models to predict future AF.

2. Materials and Methods

A ResNet-based model was trained to predict AF using SR ECGs of 37 953 individuals (of whom 33% develop AF) from the Amsterdam UMC (1999–2018). The control group included all but the last recorded ECGs of individuals with only SR recordings. The AF group included all pre-AF SR ECGs of individuals with ≥1 AF event. Performance (sensitivity, specificity, precision, and accuracy) to predict AF during SR was stratified by sex and age. Bootstrapping was used to compute 95% CIs. Saliency maps (TensorFlow's GradientTape) were compared to two different models trained for sex classification and age regression to identify potential biases.

3. Results

The model achieved an AUROC of 0.83 (95% CI: 0.82–0.84), but showed higher accuracy (0.74 vs. 0.69) and specificity (0.71 vs. 0.60) but lower sensitivity (0.80 vs. 0.84) in females than in males (all, $p<0.001$). Accuracy decreased by 22% with advancing age, (from 0.79 in the 18–60 years group to 0.62 in ≥80 years). Sensitivity increased by 23% (from 0.74 to 0.91), and specificity dropped by 60% (from 0.80 to 0.32) (all, $p<0.001$). Saliency maps revealed the PR interval as the most influential segment for AF prediction (Figure 1), overlapping with age regression and sex classification models, suggesting demographic influence.

4. Discussion and Conclusions

This study demonstrates AI-models for AF prediction may capture both AF-specific and demographic-related features, given the observed performance variations across sex and the overlap in saliency maps with models trained for age regression and sex classification. Our study implies that application of these models should be demographically sensitive. This may contribute to closing the gap in diagnosis and treatment between men and women as well as between young and old.

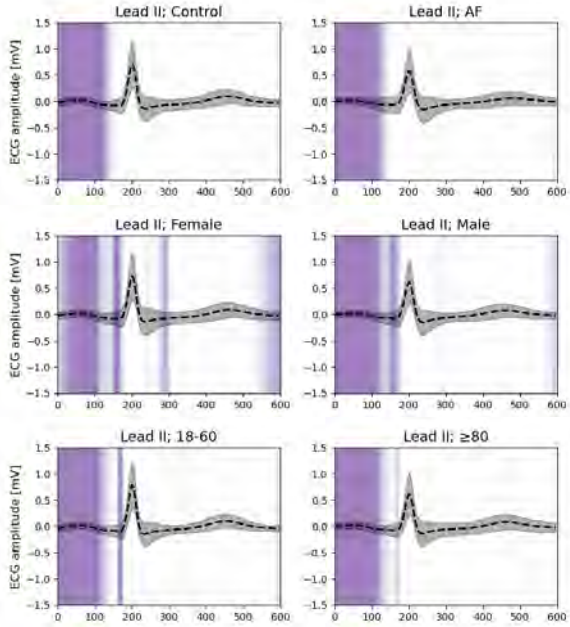


Figure 1: The mean ECG signal (dashed black line) and standard deviation (grey shading) of temporal median recordings in lead II, with saliency maps (purple gradient) for: AF prediction model (top row): control (left) vs. AF individuals (right), sex classification model (middle row): females (left) vs. males (right), and age regression model (bottom row): 18-60 years (left) vs. ≥80 years (right).

5. References

1. J. C. L. Himmelreich et al., Europace, vol. 22, no. 5, pp. 684–694, May 2020,
2. G. Jabbour et al., Eur. Heart J., vol. 45, no. 46, pp. 4920–4934, Sep. 2024
3. Z. I. Attia et al., vol. 12, no. 9, p. e007284, Sep. 2019
4. S. Khurshid et al., Circulation, vol. 145, no. 2, pp. 122–133, Jan. 2022
5. R. Wesselink et al., J. Clin. Med., vol. 12, no. 7, p. 2650, Apr. 2023

A COMBINED *IN SILICO* APPROACH FOR THE DESIGN OPTIMIZATION OF A RIGHT VENTRICULAR ASSIST DEVICE

Ilaria Guidetti (1), Canberk Yildirim (2), Elena Cutrì (3), Kadir Caliskan (4), Goksel Guven (5), Osama Soliman (2), Kerem Pekkan (6), Francesco De Gaetano (1)

1. Politecnico di Milano, Italy; 2. Royal College of Surgeons in Ireland, Ireland; 3. Université de technologie de Compiègne, France; 4. Erasmus Medical Center, Netherlands; 5. Hacettepe University, Turkey; 6. The Ohio State University, USA

1. Introduction

Right heart failure (RHF) leads to the inability of the right ventricle (RV) to support the pulmonary circulation [1]. It has high morbidity and in-hospital mortality and occurs in up to 40% of left ventricular assist device (LVAD) recipients [2]. Currently, LVADs are used off-label for RV support; therefore, there is a critical need for right ventricular assist devices (RVADs) specifically designed for RHF. Our work optimizes the design of an RVAD prototype by considering the device's performance under realistic RHF conditions. A lumped parameter model (LPM) optimization approach is combined to a computational fluid dynamics (CFD) surrogate-based optimization framework to develop a dedicated RVAD solution for RHF's patients.

2. Materials and Methods

A LPM for isolated RV infarction was established for the *in silico* implantation of the RVAD prototype. The latter was modelled using a full Euler turbomachinery equation. RVAD optimization was conducted under realistic hemodynamic conditions through objective functions aimed at restoring healthy hemodynamic parameters. The volute of the LPM-optimized RVAD was further refined performing a design optimization through a CFD surrogate model of the device. The optimized design was obtained considering three geometrical parameters and using a genetic algorithm. Two objective functions were imposed: maximization of hydraulic efficiency (η) and minimization of the modified index of hemolysis (MIH).

3. Results

The LPM demonstrated strong agreement with relevant clinical indicators for isolated RHF. The pressure drop estimated using the Euler turbomachinery equation differed by 3 mmHg from the CFD prediction at the RVAD design point. An accuracy of at least 90% was achieved comparing the CFD pressure drop predictions with the *in vitro* measurements.

The LPM-optimized RVAD allowed to restore systemic pressures and flows, right atrium pressure and RV cardiac power.

Figure 1 shows the response surfaces used in the CFD-based optimization. This produced an RVAD able to function with a η of about 32% and a MIH of 0.0066%.

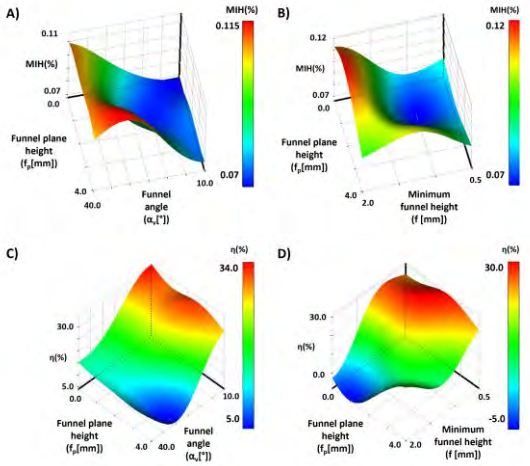


Figure 1: Response surfaces for the modified index of hemolysis (MIH) and the hydraulic efficiency (η).

4. Discussion and Conclusions

The combined *in silico* optimization approach established represents a cost-efficient tool to develop functional VADs under realistic working conditions. The optimized RVAD is able to support the RV under isolated RHF and restore healthy physiological values. Moreover, it operates with good efficiency and hemocompatibility, representing a step toward a clinically applicable solution for RHF patients.

5. References

1. Dini et al., Heart Fail Rev, 28:757-766, 2023.
2. DeFilippis et al., Card Fail Rev, vol. 8, 2022.

Acknowledgements:

We thank Kağan Uçak for his support in the experiments. The experimental validation was supported by the yESAO Travel Award 2025.

FROM RAW SEGMENTATIONS TO COMPUTATIONAL MESHES: AN AUTOMATED FRAMEWORK APPLIED TO THE HUMAN HEART

Francesco Fabbri* (1), Martino Andrea Scarpolini (1,2), Francesco Tudisco (1,3), Francesco Viola (1,2)

*1. Gran Sasso Science Institute, Italy; 2. INFN Roma Tor Vergata, Italy; 3. The University of Edinburgh, United Kingdom *Corresponding author: francesco.fabbri@gssi.it*

1. Introduction

Most computational heart models rely on single anatomies, limiting population-level representation. We present an automated pipeline that converts CT segmentations into watertight, topology-consistent meshes via template-based registration and Chamfer-distance morphing. Validated on 58 cases, the framework ensures consistent inter-subject alignment, enables statistical shape modeling, and supports synthetic geometry generation for multiphysics simulation.

2. Materials and Methods

The study includes 58 cardiac CT scans acquired in late diastole (70-80%). Segmentations were performed in 3D Slicer using AI-based chamber extraction [1], followed by manual refinement and surface reconstruction. Meshes were homogenized to a uniform resolution (30k vertices) with standardized vessel trimming.

A template-based non-rigid registration framework [2] was applied. After affine pre-alignment, a high-quality template mesh ($\mathcal{M}_{\mathcal{T}}$) was deformed toward each anatomy ($\mathcal{M}_{\mathcal{O}}^{k}$) by minimizing a chamber-wise Chamfer distance using Laplacian-regularized gradient descent (Eq. 1), with iterative template updates to refine correspondence:

$$\Phi\left(\mathcal{M}_{\mathcal{T}}, \mathcal{M}_{\mathcal{O}}^{k}\right) = \sum_{c=1}^{4} d_{\mathrm{CD}}^{c}\left(\mathcal{M}_{\mathcal{T}}^{(c)}, \mathcal{M}_{\mathcal{O}}^{k,(c)}\right) \quad (1)$$

Morphogeometric descriptors (surfaces, volumes, diameters, cross-sectional areas, inter-chamber distances) were computed for validation. PCA provided dimensionality reduction, and a Gaussian Mixture Model (GMM) modeled latent shape variability, enabling synthetic cohort generation.

3. Results

Registration performance is evaluated via Chamfer-distance convergence; registered meshes are shown in Fig. 1.

Morphogeometric descriptors indicate strong anatomical retention, with ventricular surfaces and volumes above 97-98%, atrial metrics mostly exceeding 95%, and inter-chamber distances up to 98%. PCA (15 modes, 90% CEV) and GMM clustering capture latent variability and inter-chamber correlations.

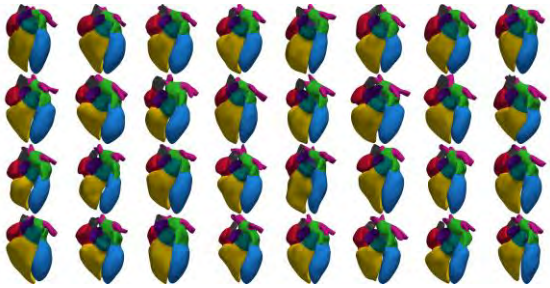


Figure 1: Cohort of 32 registered meshes preserving subject-specific variability.

4. Discussion and Conclusions

This work presents an automatic pipeline that generates simulation-ready cardiac meshes from segmented CT scans using template-based, non-rigid multi-chamber registration. The resulting isotopological geometries preserve anatomical features (≈95-99% chamber retention). PCA and GMM provide a compact statistical representation, enabling sampling and analysis of correlated population-level variability.

5. References

1. Wasserthal J et al., *Radiology: Artificial Intelligence*; 2023.
2. Scarpolini MA et al., *Frontiers in Physiology*; 2023.

Acknowledgements:
The authors would like to thank the European Research Council (Grant no: 101039657, CARDIOTRIALS) and Next Generation EU (Mission 4, Component 1, CUP D13C22001470001) for financial support.

EFFECTS OF RESPIRATORY HRV ON CARDIAC WORK

Chamal Kohombakadawala (1), Toan Pham (1,2), Kenneth Tran (1), Andrew Taberner (1,2), June-Chiew Han (1)

1. Auckland Bioengineering Institute, University of Auckland; 2. Department of Engineering Science and Biomedical Engineering, University of Auckland, New Zealand

1. Introduction

Modulation of heart rate by the autonomic nervous system is closely synchronised with respiration. Inhalation and exhalation, respectively, inhibit and restore vagal outflow, leading to increased and decreased heart rates within each breathing cycle. This cardiopulmonary phenomenon is coined 'respiratory heart rate variability' (RespHRV). Recently, it has been shown experimentally that re-instating RespHRV on diseased heart using an external pacemaker can directly improve cardiac output [1], suggesting that the pacing itself may have a direct effect on cardiac function. To test this hypothesis, we conducted an *in silico* study incorporating models of the cardiovascular system, cardiac cellular excitation-contraction coupling, and a RespHRV pacing protocol.

2. Materials and Methods

The human cardiovascular system was modelled as a six-compartment framework combining pulmonary and systemic circulations, with vasculature biophysical properties represented as resistance and capacitance in both arterial and venous compartments [2]. Within this framework, we embedded a cardiac excitation-contraction model that links ventricular electrophysiology [3] to contractile element cycling [4] through intracellular Ca^{2+} dynamics. A pacing protocol was integrated into the combined model to simulate both the presence and absence of RespHRV by varying or fixing the heart rate, respectively. RespHRV was modelled as two beats at a high rate (100.8 bpm) representing the increased heart rate during inhalation, followed by four beats at a low rate (63 bpm), representing a lower heart rate during exhalation. Absence of RespHRV was simulated with a fixed heart rate of 72 bpm. Model outputs were cardiac pressure-volume loops as functions of loading conditions, specifically vascular resistance (R_p).

3. Results

Our results show that cardiac pressure-volume work did not differ between the two pacing protocols. These results were obtained even under various loading conditions (i.e., increasing R_p) and when cardiac contractility was modelled as dependent on heart rate.

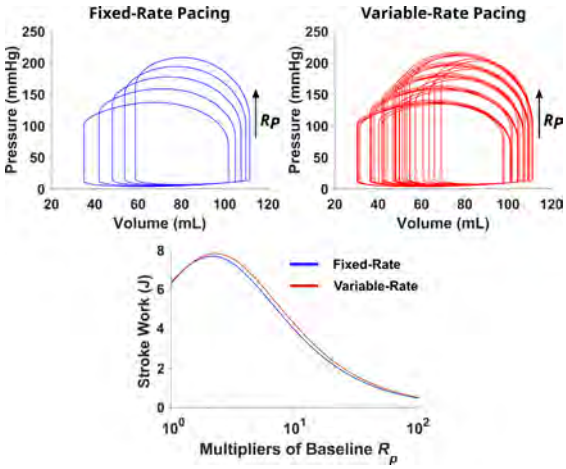


Figure 1: Pressure-volume loops and stroke work (area within the loop) between fixed-rate and variable-rate pacing.

4. Discussion and Conclusions

RespHRV alone does not directly affect cardiac work output over a range of cardiovascular loads. Our findings suggest that factors beyond RespHRV may have contributed to the improved cardiac output observed experimentally under external HRV pacing. The aforementioned 'other factors' could include cellular processes underlying changes in ionic activities, protein expressions and micro- and macro- remodelling of structures.

5. References

1. Shanks *et al.*, 10.1007/s00395-022-00911-0.
2. Burkhoff & Tyberg, 10.1152/ajpheart.1993.265.5.H1819.
3. Gattoni *et al.*, 10.1113/JP272011.
4. Musgrave *et al.*, 10.1016/j.mbs.2022.108922.

Acknowledgements:
Funding support from Marsden, HRC, and Heart Foundation of New Zealand.

GLOBAL SENSITIVITY ANALYSIS OF A LINEAR FINITE ELEMENT MODEL FOR THE PREDICTION OF FEMORAL STRENGTH

Aurélie Levillain (1), Marc Gardegaront (1), Denis Brizard (1), Cyrille B. Confavreux (2,3,4), Jean-Baptiste Pialat (2,5), Hélène Follet (3), David Mitton (1)

1. Univ Lyon, Univ Eiffel, UCBL, LBMC UMR_T9406, France; 2. HCL, Centre hospitalier Lyon Sud, France; 3. CEMOS, Service de Rhumatologie, IC-HCL, France; 4. Univ Lyon, UCBL, INSERM, LYOS UMR 1033, France; 5. INSA-Lyon, CREATIS UMR5220, UCBL, France

1. Introduction

Osteolytic bone metastases are responsible for long bone fracture leading to restricted mobility or surgery [1]. Based on quantitative computed tomography (QCT), patient-specific finite element (FE) models assessing the strength of metastasized femurs can help predict bone fracture [2]. A global sensitivity analysis (GSA) performed on a non-linear model showed the high sensitivity of the model with respect to density-based parameters [3]. Linear elastic models, defined using fewer density-dependent parameters, have been proposed in the literature [4]. The aim of this work was to assess sensitivity of the predicted failure load obtained using a linear model to various input parameters and compare with the non-linear model.

2. Materials and Methods

An *ex vivo* femur was scanned with a calibration phantom to extract bone density. After manually segmenting the femur, a linear model (adapted from [4]) was built, with a quadratic tetrahedral mesh, linear constitutive law and a failure criterion based on a volume of 0.33% contiguous failed elements. Mechanical parameters were derived from bone density. A GSA was performed using the Morris method [5], with 10 trajectories and 4 levels for each of the following parameters: femur length, orientation, segmentation, density calibration and diaphysis rotation. Ranges of variation for each parameter were chosen by repeatedly applying the nominal values and then computing two standard deviations for each measured parameters, except for the segmentation where an erosion/dilation filter was applied on a default operator segmentation (-1 to +2 voxels). The same ranges of variation as for the non-linear model were used [3].

3. Results

The mean influence of each parameter on the failure load is presented in Figure 1. For the linear model, segmentation is the most influent parameter (40%). On the contrary, density calibration is the least influent (1.6%), while it is the most influent for the non-linear model (12.5%). Other parameters have a lower influence on the failure load for both models.

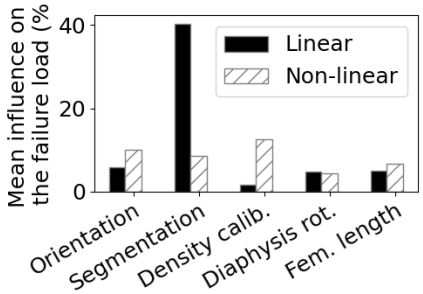


Figure 1: Mean influence of the parameters on the failure load, obtained using the Morris method, for the linear model and a non-linear model [3]. calib: calibration; rot.: rotation; Fem.: femur.

4. Discussion and Conclusions

The GSA performed on the femur revealed that the linear model is less sensitive to density than the non-linear model. Given the uncertainty regarding density estimation, especially using phantomless calibration, a linear model may be of interest in clinical practice. The linear model is more sensitive to geometry, as evidenced by the large influence of segmentation. However, the applied filters on the default segmentation (global erosion/dilation) do not reflect operator variability. Moreover, automatic segmentation allows for more reproducible results [6]. These GSA are essential for credibility assessment of the models and their clinical application.

5. References

1. Decroisette et al, J Thorac Oncol 2011.
2. Eggermont et al, Bone, 130:115101, 2020.
3. Gardegaront et al, JMBBM, 158:106676, 2024.
4. Duchemin et al, CMBBE, 11(2):105–111, 2008.
5. Saltelli et al, New York: Wiley, 1, 2004.
6. Saillard et al, Sci Rep, 14(1), 2024.

Acknowledgements:
This work was supported by MSDAvenir and Labex PRIMES (ANR-11-LABX-0063).

AI-BASED FULLY AUTOMATIC FEMUR SEGMENTATION FROM CT SCANS FOR METASTATIC PATIENT-SPECIFIC FE MODELS

Elisa Bruatto (1), Cristina Curreli (2), Barbara Dozza (3), Laura Campanacci (1), Antonino Amedeo La Mattina (2)

1. 3rd Orthopaedic and Traumatologic Clinic Prevalently Oncologic, IRCCS Istituto Ortopedico Rizzoli, Bologna (Italy); 2. Medical Technology Lab, IRCCS Istituto Ortopedico Rizzoli, Bologna (Italy); 3. Department of Biomedical and Neuromotor Sciences, University of Bologna, Bologna (Italy)

1. Introduction

Metastatic bone disease can compromise bone structure integrity and lead to pathological fractures. Patient-specific finite element (FE) models derived from computed tomography (CT) can support fracture risk assessment; however, their implementation relies on accurate femoral bone segmentation, a time-consuming and operator-dependent process. Advances in convolutional neural networks (CNNs) have demonstrated strong potential for medical image segmentation, enabling automated workflows with accuracy suitable for FE model generation [1]. This study aims to develop a fully automated pipeline for metastatic femur segmentation from CT scans by fine-tuning a pre-trained 2D U-Net model.

2. Materials and Methods

A dataset of 49 metastatic patient CT scans was divided into training (26 CTs), validation (4 CTs), and test (19 CTs) subsets. A 2D U-Net with ResNet50 encoder and PSPHead decoder was implemented in Python using the MMSegmentation framework based on PyTorch. Data augmentation was applied to limit overfitting. Model inference was performed on the test set and on an external cohort of 101 femurs from the HFValid collection [2]. Segmentation quality was assessed by evaluating the Dice Similarity Coefficient (DSC) and the Hausdorff Distance (HD) between manual and predicted geometries. To evaluate the impact of geometry-related differences arising from the introduction of the AI-based segmentation pipeline on fracture risk prediction, crack propagation simulations were performed on the 19 femurs of the test subset, adopting a recently proposed FE technique developed in Ansys [3].

3. Results

The DSC achieved on the 19 test patients was 0.977 ± 0.012, with an HD of 3.65 ± 1.44 mm. On the HFValid collection the mean DSC was 0.964 ± 0.014 and the HD was 3.94 ± 1.63 mm (Figure 1). From the comparison of the FE results obtained for the manually and the automatically segmented femurs, no significant geometry-related difference could be observed.

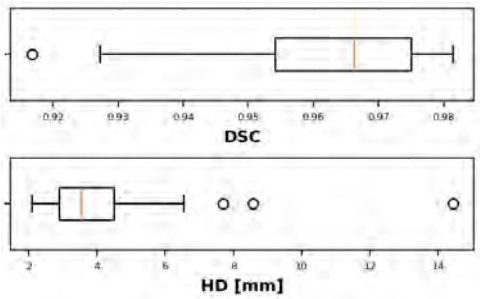


Figure 1: DSC and HD obtained for the 101 patients from the HFValid collection.

4. Discussion and Conclusions

The results showed that a pre-trained 2D U-Net can be effectively fine-tuned on a limited dataset of manually annotated CT scans for the segmentation of healthy and metastatic femurs without any requirements on the input CT characteristics. Integrating the proposed methodology into the FE pipeline would substantially reduce the time and effort required for model construction while maintaining an accuracy comparable to that of manually segmented models, thus facilitating the adoption of FE-based fracture risk prediction tools in clinical practice.

5. References

1. Bjornsson PA et al., Medical imaging 2021; vol. 11600; pp.324-330; doi:10.1117/12.2581100.
2. Aldieri A et al., University of Bologna, Jul. 2025. doi: 10.6092/unibo/amsacta/8431.
3. Bentivoglio et al., 2026. Under revision

Acknowledgements:

This research is co-funded by the Italian Complementary National Plan PNC-I.1 "Research initiatives for innovative technologies and pathways in the health and welfare sector", D.D. 931 of 06/06/2022, "DARE – Digital Lifelong Prevention" initiative, code PNC0000002, CUP: B53C22006230001.

RETHINKING BIONIC LIMBS: CAN DIGITAL TWINS ENHANCE CLINICAL DECISION-MAKING?

Laurent Frossard (1), Alireza Bavil (1), Christian Langton (1), Stefanie Feih (1,2), Sharon Latimer (3), Jayishni Maharaj (1), Claudio Pizzolato (1), Rodney Barrett (1), David Lloyd (1,2)

1 Australian Centre for Precision Health and Technology (PRECISE), Griffith University, Australia; 2 Advanced Design Prototyping Technologies Institute (ADaPT), Griffith University, Australia; 3 National Health and Medical Research Council Centre of Research Excellence in Wiser Wound Care, Griffith University, Australia

1. Introduction

The design of bone-anchored neuroprostheses (BAN) can benefit from a better understanding of the cause-and-effect relationships between rehabilitation interventions and individual's neuromusculoskeletal (NMSK) residuum limb adaptations [1]. In principle, these relationships can be modelled using a digital twin of the residuum's NMSK [1-4]. Drawing upon current knowledge and our experience in developing NMSK models for individuals fitted with BAN, this presentation will outline the essential data requirements, share key challenges, and highlight the potential advantages of future residuum digital twin technology [3].

2. Materials and Methods

Since 2020, we have applied a Biodesign approach to develop a digital twin of a residuum's NMSK system.

At this stage, computational models of the residuum's NMSK system can integrate typical medical imaging and information from portable biosensors including load cell to measure the mechanical loading applied on the residuum and ultrasound transducers to provide sonomorphometry of soft tissues and bone (Figure 1) [5].

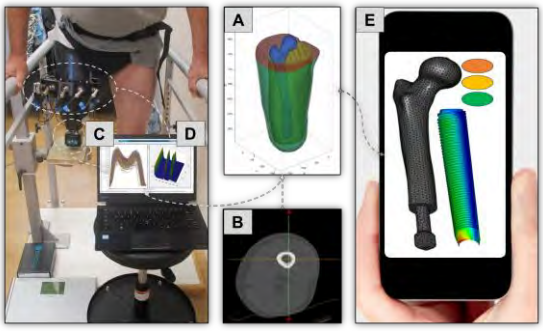


Figure 1: Development of digital twin of the residuum (A), integrating medical imaging (B) and biosensors to measure loading (C) and sonomorphometry of tissues (D) to assess strength of osseointegration using a handheld device (E).

3. Results

Some of the critical challenges faced during the development of residuum digital twin were to:

- Identify the accurate material proprieties for the soft tissues (i.e., skin, adipose, muscle),
- Provide relevant information to end-users in real-time using handheld interface (e.g., participants, clinicians).

4. Discussion and Conclusions

The potential advantages of future NMSK residuum digital twins will be to:

- Assess quality of bone around endo and/or exo skeletal implants and promote the strength of osseointegration,
- Extract residuum muscle activities and enhance the control of BAN fitted with microprocessor-controlled prostheses.

Altogether, digital twin technology of residuum's NMSK system has the potential to facilitate clinical decision-making to improve safety and efficacy of current and emerging bionic limb solutions.

5. References

1. Frossard, L. et al., Front Rehabil Sci, 2022. 3: p. 950481.
2. Frossard, L. et al., J Sci Med Sport, 2023. 26 Suppl 1: p. S22-S29.
3. Frossard, L.A. et al., Journal of Science and Medicine in Sport, 2022. 25: p. S4-S5.
4. Laubenbacher, R. et al., Nat Comput Sci, 2024. 4(3): p. 184-191.
5. Langton, C.M. et al., Journal of 3D Printing in Medicine, 2023. 7(2): p. 3DP009.

Acknowledgements:

This work was supported by research fundings from the US Department of Defense RESTORE Award W81XWH2110215-DM190659, the 2024 NHMRC Ideas grant 202963 and the 2025 Queensland Orthopaedic Research Fund (QORF) Research Grant.

BENEFITS IN TERMS OF FIT-AND-FILL AND PRIMARY STABILITY OF A OSTEOCUSTOM STEM FOR TRANSFEMORAL AMPUTEES

Giulia Galteri (1), Silvia Casadei (1), Edoardo Hirschberg (1), Domenico Alesi (2), Stefano Zaffagnini (2), Kavin Morellato (3), Emanuele Gruppioni (3) Luca Cristofolini (1)

1. Department of Industrial Engineering, Alma Mater Studiorum-University of Bologna, Bologna, Italy
2. IRCCS Istituto Ortopedico Rizzoli, Italy 3. Centro Protesi INAIL, Vigorso di Budrio, Bologna, Italy

1. Introduction

Accurate preoperative planning is crucial for transfemoral osseointegrated prostheses, as poor implant-bone matching may lead to instability or patient ineligibility. Quantitative metrics describing fit-and-fit, bone removal, and their relationship with primary stability may support surgical planning. OsteoCustom combines discrete design parameters to better match anatomical variability, yet its benefits remain unclear. This study aimed to quantify implant fit-and-fill and evaluate its relationship with primary stability to identify metrics useful for implant planning.

2. Materials and Methods

Twelve paired human cadaveric femurs were used. Pre-implant CT scans were acquired (slice-thick=0.625mm;in-plane res=0.512mm). Surgical planning and implantations were performed by orthopedic surgeons, followed by post-implant CT acquisition. Each pair was implanted with a commercial OFI-C on one femur and the OsteoCustom stem on the contralateral femur. Compression-flexion and torsion tests were performed. A 3D-DIC system was used to measure the primary stability in terms of elastic micromotions and permanent migration [2]. CT-images were upscaled fourfold (SRCNN,final in-plane-resolution=0.128) and segmented (Fiji). Stem-bone contact area was computed along the stem (Matlab). Cortical bone removal was quantified subtracting the co-registered pre- and post-implant CTs, using the Goldman eight-sector method to evaluate bone loss locally and globally. A Wilcoxon paired-test was used (Prism9.5.1, $p<0.05$). Moreover, Spearman's rank correlation was used to assess the relationship between primary stability and both cortical bone volume removal and stem–bone contact area.

3. Results

The OsteoCustom stem showed inducible micromotions more than threefold lower than those of the OFI-C stem($p<0.05$), and permanent migration more than 1.5-fold lower($p<0.05$). The OsteoCustom showed benefit compared to the commercial one, with a significant increase in stem-bone contact area($p=0.041$) and a reduction in cortical bone removal ($p=0.026$) across all twelve paired femora. Stem-bone contact area strongly and inversely correlated with micromotions (Spearman's ρ up to -0.79, $p\leq0.002$), whereas cortical bone removal showed weak or no correlation.

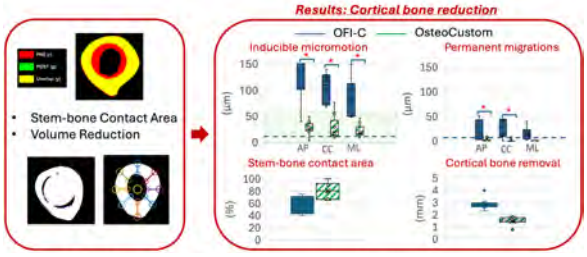


Figure 1: Left, Methods: overlay of pre and post-implant CT images used to compute stem-bone contact area and cortical bone removal. Right, Results: on the top the primary stability of both commercial and OsteoCustom stem in terms of micromotions, while on bottom the stem-bone contact area and bone removal

4. Discussion and Conclusions

Nevertheless, preserving bone stock remains clinically crucial, as it reduces fracture risk and facilitates potential revision surgery. Although larger cohorts are needed, these preliminary findings suggest that such analyses could support surgeons in implant planning, helping improve surgical decisions and potentially reducing the risk of implant failure.

5. References

1. Betti et al. 2024, JOSR
2. Galteri et al 2024, Frontiers

Acknowledgements:
Work funded by INAIL (PR23-CR-P5-OsteoAMI, CUP: E57G23000240005).

Hip Fracture Risk Assessment with a Paraboloidal Plasticity Model in Abaqus and MoFEM: Comparing Fracture Discrimination

Abdollah Moslemi (1), Elham Alizadeh (1), V V S Varaprasad Jakka (1), Callum J. Runcie (2), Andrei G. Shvarts (2), Łukasz Kaczmarczyk (2), Carlos Ruiz Wills (1), Luis del Rio 3, Silvana Di Gregorio (3), Ludovic Humbert (4), and Jérôme Noailly (1)

1. Pompeu Fabra University, Barcelona, Spain, 2. Glasgow Computational Engineering Centre (GCEC), University of Glasgow, UK; 3. CETIR Ascires, Spain, 4. 3D-Shaper Medical, Spain.

1. Introduction

Subject-specific FE analysis of 3D-DXA femur models can improve hip fracture risk assessment beyond aBMD [1]. To support translation toward scalable, license-free clinical tools, the open-source FE library MoFEM was integrated into the 3D-Shaper-based FE pipeline [2]. This study examines how adopting a common Paraboloidal plasticity model across solvers affects fracture risk prediction and discrimination.

2. Materials and Methods

A retrospective case-control cohort of 64 hip-fracture cases and 64 controls was analysed [1]. Subject-specific hexahedral FE meshes of the proximal femur were generated using 3D-Shaper® (v2.14) from hip DXA scans. Bone density was converted to element-wise Young's moduli and asymmetric tension/compression yield stresses via empirical relations [3].

A side-fall scenario was simulated by applying displacement to the femoral head through a tie constraint, enforcing rigid kinematic coupling via Lagrange multipliers:

$$L(u,\lambda,t,\theta) = {}^1\!/_2\, u^T K u - u^T f + \lambda^T\{u - t - Skew(\theta)(X - X_0)\} \quad (1)$$

where K is the stiffness matrix, f the force vector, and λ the Lagrange multiplier field. The greater trochanter and shaft were constrained. Both Abaqus and MoFEM used a perfect elastoplastic Paraboloidal yield criterion with a smooth transition between tension and compression.

Extracted descriptors for ROC analysis included bone strength (F_u), maximum displacement, and nonlinear energy. A piecewise linear model (PLM) of the force-displacement response also provided elastic quantities (F_{LE}, D_{LE}, W_{LE}), nonlinear deformation, and post-yield residual displacement (D_R) and dissipated energy (W_D).

3. Results

Solver agreement for bone strength (F_u) is shown in Figure 1. The Bland-Altman plot demonstrates a consistent systematic offset between solvers, with a relative bias of 6.28% and narrow limits of agreement (4.28-8.27%), indicating stable and predictable differences across the cohort.

Bone strength (F_u) achieved AUROC = 0.72 with both solvers, similar to 3D-DXA trabecular vBMD and exceeding DXA aBMD (0.69).

Post-yield descriptor combinations improved discrimination: the best Abaqus result was AUROC = 0.76 for (F_{LE}+W_D), while MoFEM reached 0.75 using (F_{LE}+D_R). Both combinations significantly outperformed aBMD (AUROC = 0.69; DeLong test, $P < 0.05$).

Elastic-domain descriptors yielded closely matched results across solvers (AUROC ≤ 0.75).

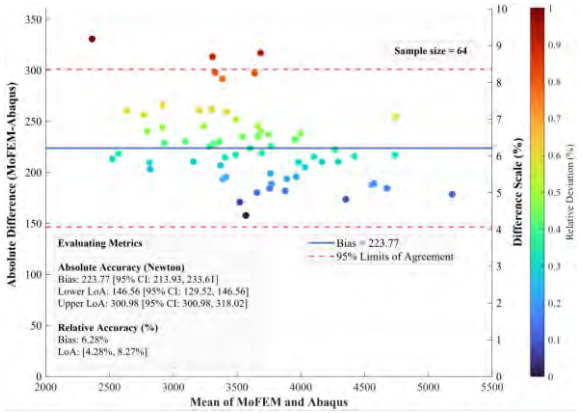


Figure 1: Inter-Solver Agreement; MoFEM vs Abaqus

4. Discussion and Conclusions

With the Paraboloidal plasticity criterion, both solvers produced closely aligned results. The Paraboloidal model provides a mechanically consistent representation of bone behaviour, characterized by a smooth tension-compression transition. Abaqus and MoFEM showed strong consistency across both elastic and post-yield descriptors, with AUROC differences remaining within 0.01–0.02 for most combinations. Together with MoFEM's open-source accessibility and its integration into the 3D-Shaper-based FE pipeline, these developments support a robust, licence-free path toward clinical fracture risk assessment.

References

1. Alizadeh et al., Front. Bioeng. Biotechnol., 2025
2. Kaczmarczyk et al., Open-Source Software, 2020
3. Ruiz Wills et al., Bone, 121:89-99, 2019

Acknowledgements:
Spanish Government (CPP2021-008574, CPP2023-010970); AGAUR (2023 BP 00224).

TOWARDS ORGAN SCALE MODELING OF THE VASCULAR MICROENVIRONMENT

Nunzio Dimola (1), Piermario Vitullo (1), Paolo Zunino (1)

1. MOX, Department of Mathematics, Politecnico di Milano, Italy

1. Introduction

The development of predictive and clinically actionable models remains a central challenge in computational oncology, due to the intrinsic multiscale and multiphysics nature of tumor growth and therapy response. In particular, the accurate description of microvascular transport processes requires the solution of computationally prohibitive simulations involving multiple scales at the organ level.

2. Materials and Methods

The methodology is motivated by coupled 3D–1D models of microcirculation, where a three-dimensional tissue domain interacts with a one-dimensional vascular network. We introduce a multiscale computational framework designed to enable scalable simulations of tissue–vasculature interactions. The approach integrates data-driven reduced order modeling (ROM) within a domain decomposition (DD) strategy to manage the computational complexity of coupled 3D–1D formulations.

The tissue domain is partitioned into smaller subregions, where the local physical behavior is approximated through surrogate models trained on high-fidelity simulations. Local reduced models are constructed using Proper Orthogonal Decomposition (POD) and neural networks [1], preserving the essential microvascular transport dynamics while drastically reducing computational cost.

An optimized Schwarz domain decomposition method [2] is then employed to iteratively couple the subdomains and reconstruct a consistent global solution over the entire tissue domain.

3. Results

Numerical experiments demonstrate accurate reconstruction of the global three-dimensional solution with significant computational savings compared to reference domain decomposition simulations. The proposed framework exhibits stable convergence and robustness across heterogeneous vascular networks, supporting its applicability to large-scale and complex geometries.

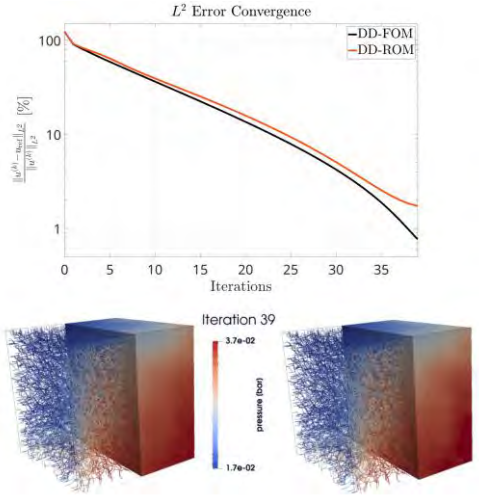


Figure 1: Convergence history of the proposed iterative algorithm.

4. Discussion and Conclusions

The presented methodology represents a step toward organ-scale modeling of the vascular microenvironment. By integrating mechanistic multiscale modeling with data-driven surrogate representations, it enables computationally efficient organ-scale simulations. Potential applications include patient-specific prediction of oxygenation and hypoxia, as well as therapy optimization, contributing to the development of digital twins in computational oncology.

5. References

1. Vitullo P et al. Finite Elements in Analysis and Design; 229, 104068, (2024)
2. Lions JL, Third International Symposium on Domain Decomposition Methods for Partial Differential Equations. SIAM; (1990).

Acknowledgements:

PV and PZ acknowledge support from the European Union's Euratom research and training programme 2021–2027 under grant agreement No. 101166699 "Radiation safety through biological extended models and digital twins" (TETRIS).

HETEROGENOUS TUMOR MICROENVIRONMENT IN NON-SMALL CELL LUNG CANCER DERIVED FROM FDG-PET DATA

Geir Nævdal (1), Ida R. Jarczyk (2), Torjan Haslerud (3,4), Steinar Evje (2)

1. *NORCE, Norway; 2. University of Stavanger, Norway; 3. Stavanger University Hospital, Norway; 4. Haukeland University Hospital, Norway*

Geir Nævdal, NORCE, Nygårdsgaten 112, 5008 Bergen, Norway, email: gena@norceresearch.no

1. Introduction

In this work, we develop and validate a digital model that captures key tumor microenvironment (TME) features, including interstitial fluid flow, chemical agent transport (e.g., FDG), and agent–cell interactions. This is a novel non-invasive approach for studying the TME for individual patients based on data that is routinely used in a clinical setting.

2. Materials and Methods

Standardized uptake values (SUVs) from an FDG-PET scan of a lung cancer patient are used. We use a multiphase modeling framework in which the tumor-host environment is treated as a mixture of three interacting continua: a stationary extracellular matrix (ECM) and two moving phases in the porous space a cellular phase of tumor cells; and an extracellular fluid phase [2]. This framework is extended to include FDG delivery and clearance. Several parameters are unknown, including the heterogenous cancer cell density, the spatial varying intratumoral vasculature and peritumoral lymphatic network, FDG kinetics, and ECM-fluid resistance which has strong impact on the underlying interstitial fluid velocity (IFV). FDG uptake rate and ECM-fluid resistance are poorly constrained by the data and are varied at three levels (low, medium, high), while remaining parameters are calibrated to SUV data using an iterative ensemble Kalman smoother (EnKS) [1, 3].

3. Results

Starting from an ensemble of 100 random parameter sets, the iterative EnKS successfully calibrates the model to achieve strong agreement with observations across all nine combinations of FDG uptake rate and fluid resistance. Figure 1 shows measured SUV data for one tumor layer (top left), the initial model output (top right), and the calibrated result after five iterations (bottom). Here we present the result for low FDG uptake rate and low ECM-fluid resistances, but similar results are achieved for all the nine combinations of these two parameters.

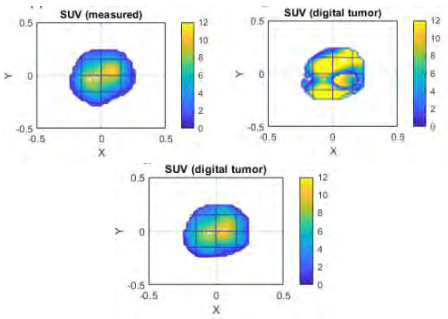


Figure 1: SUV – measured (top left) – initial model (top right) – final estimate (bottom)

4. Discussion and Conclusions

The key finding is that combining FDG uptake rate, tissue hydraulic conductivity, and late-phase SUV enables construction of a digital tumor that captures spatial heterogeneity in cancer cell density, vascular leakage, and interstitial fluid flow. Simulated FDG transport reproduces the measured heterogeneous SUV. In future work we plan to explore how TNE characteristics are changed under a treatment schedule. The aim is to obtain a tool that can be used for systematic study of treatment response, optimizing therapy schedules, and probing limits to therapeutic efficacy.

5. References

1. A. A. Emerick and A. C. Reynolds. Computers & Geosciences, 55:3–15, 2013.
2. G. Nævdal, E. K. Rofstad, K. Søreide, and S. Evje. Journal of Biomechanics, 145:111362, Dec 2022.
3. G. Nævdal and S. Evje. Journal of Computational Physics, 492:112449, Nov. 2023.

MULTISCALE THERAGNOSTIC DIGITAL TWIN FOR PREDICTING RADIOPHARMACEUTICAL UPTAKE IN RENAL CELL CARCINOMA

Lara Cavinato (1), Augustin Pottier (2)

1. MOX, Department of Mathematics, Politecnico di Milano, Milan, Italy; 2. Department of Nuclear Medicine, IRCCS Ospedale San Raffaele, Milan, Italy

1. Introduction

Clear Cell Renal Cell Carcinoma (ccRCC) exhibits pronounced spatial, vascular, and molecular heterogeneity, which critically modulates drug transport, binding kinetics, and retention. In radiopharmaceutical therapy (RPT), this heterogeneity leads to non-uniform dose deposition and variable therapeutic efficacy. Within the Virtual Physiological Human (VPH) paradigm, predictive oncology requires integrative, multiscale computational models capable of coupling systemic pharmacokinetics with tissue-scale transport phenomena and cellular-level biomarker expression [1,2].

2. Materials and Methods

We developed a patient-specific oncological Deep Learning-based Digital Twin (DT) that integrates mechanistic immuno-kinetic modeling with data-driven histopathological analysis to predict the spatiotemporal uptake of [^{89}Zr]Zr-girentuximab in ccRCC.

At the systemic level, a compartmental pharmacokinetic model describes antibody circulation, tumor extravasation, interstitial transport, receptor binding, and internalization dynamics [3]. At the tissue scale, high-resolution whole-slide histology was processed using deep learning–based segmentation to delineate vascular networks, stromal regions, and neoplastic compartments [4]. Quantitative immunohistochemistry-derived biomarker expression was incorporated as a spatially resolved parameter governing receptor-mediated binding kinetics.

The framework couples global temporal tracer dynamics with local structural and molecular heterogeneity through spatial correlation and parameter inference techniques, enabling resolution of intra-tumoral transport gradients and heterogeneous retention patterns. Model calibration and validation were performed using ex vivo microPET imaging as ground truth for radiotracer distribution.

3. Results

The DT quantitatively reproduced heterogeneous intratumoral uptake patterns and identified key physiological determinants of radiopharmaceutical retention, including vascular density, spatial proximity to perfused vessels, and local biomarker expression gradients. Multiscale coupling significantly improved predictive accuracy compared to compartmental modeling alone, demonstrating the added value of integrating structural tissue information into pharmacokinetic simulations.

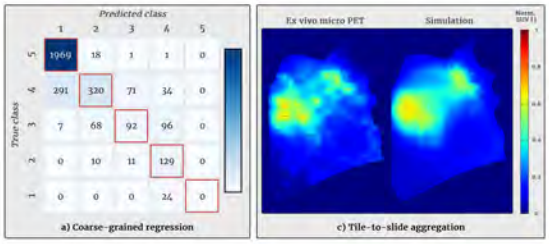


Figure 1: Simulations validation against ground-truth image: a) Confusion matrix of classification task; b) Tile-level uptake predictions aggregation against ground-truth micro PET imaging

4. Discussion and Conclusions

This VPH-aligned multiscale Digital Twin framework bridges systemic pharmacokinetics, tissue architecture, and molecular heterogeneity to enable mechanistically grounded, patient-specific prediction of RPT uptake.

5. References

1. Cavinato, Lara, et al. "A roadmap for AI-aided digital twins in computational nuclear oncology: A position paper by the EANM." The EANM Journal (2025): 100007.
2. Hong, Jimin, et al. "Deciphering the effects of radiopharmaceutical therapy in the tumor microenvironment of prostate cancer: an in-silico exploration with spatial transcriptomics." Theranostics 14.18 (2024): 7122.
3. Cavinato, Lara, et al. "Unveiling the biological side of PET-derived biomarkers: a simulation-based approach applied to PDAC assessment." European Journal of Nuclear Medicine and Molecular Imaging 52.5 (2025): 1708-1722.

DIGITAL TWINS FOR PERSONALIZED PLANNING OF LIVER CANCER TREATMENTS

Enrico Sangiorgio (1,2), Matteo Salvi (1), Selene Andreetta (3), Valentina Mazzi (1), Giuseppe De Nisco (1), Giuseppe Isu (3), Diego Gallo (1), Umberto Morbiducci (1)

1. Politecnico di Torino, Italy; 2. Università degli Studi di Palermo, Italy; 3. Medics srl, Italy

1. Introduction

Hepatocellular carcinoma (HCC) is the prevalent form of primary liver malignancy [1]. While surgical treatments are viable options for patients with early-stage HCC, more advanced stages are often managed with transarterial embolization (TAE) [1]. TAE targets tumor-feeding hepatic arteries via the intra-arterial catheter release of therapeutic microspheres [1], and its effectiveness is markedly patient-specific. Here, we propose a computational framework to generate digital twins enabling personalized TAE treatment planning.

2. Materials and Methods

A schematic overview of the framework is shown in Fig. 1. Patient-specific 3D models of the liver, tumor, and hepatic vascular networks were reconstructed from computed tomography (CT) images using an artificial intelligence (AI)-based segmentation approach built on 3D U-Net-derived architectures (Hyper Accuracy 3D technology, HA3D®, Medics srl, Turin, Italy). On the reconstructed hepatic arterial tree, TAE was virtually replicated via computational fluid dynamics (CFD) simulations. Personalized boundary conditions were derived by estimating tissue perfusion [2] using a distance-based algorithm [3]. Embolic particles were released from the tip of a catheter virtually positioned within the arterial tree and tracked over multiple cardiac cycles to predict their downstream distribution and test the tumor-targeting ability of the simulated TAE setup. Several particle transport modeling strategies were evaluated, including an Eulerian-Lagrangian formulation using inert particles and a simplified approach based on massless tracer advection.

3. Results

The presented *in silico* framework enabled the reconstruction of accurate anatomical models of HCC patients with distinct vascular anatomies and cancer scenarios. Tissue perfusion analysis facilitated the identification of hepatic segments and tumor-supplying arterial branches, allowing for the definition of perfusion-based, patient-specific boundary conditions. Finally, virtual TAE was successfully simulated across a range of heterogeneous HCC cases, characterized by varying arterial anatomies and tumor burden.

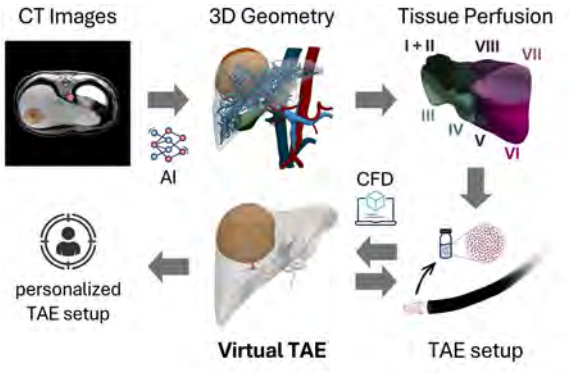


Figure 1: Overview of the *in silico* framework.

4. Discussion and Conclusions

The proposed digital twin of the TAE procedure shows potential for personalized HCC treatment planning. Virtual exploration of different TAE scenarios – varying key parameters such as catheter positioning and injection protocol – enables the identification of procedural settings enhancing tumor targeting. In addition, tissue perfusion analysis provides information on functional liver territories, supporting decision-making for prospective liver surgical resections. Overall, these findings highlight the potential of *in silico* tools in supporting more informed, patient-specific treatment decisions in liver cancer care.

References

1. Pérez-López A et al, Acta Biomaterialia; 149:1-15 (2022).
2. Aramburu J et al., Int J Numer Meth Biomed Engng; 32(11):e02764 (2016).
3. Selle D et al., IEEE Trans Med Imaging; 21(11): 1344-1357 (2002).

Acknowledgements:

This work is part of the TEPSIM project, which has received funding from cascade funding calls of NODES Program, supported by the MUR – M4C2 1.5 of PNRR, funded by the EU – NextGenerationEU (GA No. ECS00000036).

INCORPORATING ADC-DERIVED HYPOXIC SUBVOLUMES INTO PERSONALIZED TCP MODELLING IN HEAD-AND-NECK CANCER

Enrico Longhi (1), Vittoria Cortella (2), Eliana Gioscio (1) , Nicola A. Iacovelli (1), Marzia Franceschini (1), Giuseppina Calareso (1), Anna Cavallo (1), Marco Dassie (1), Luca Possenti (1), Paolo Zunino (2), Ester Orlandi (3), Tiziana Rancati (1)

1. Department of Epidemiology and Data Science/Dept of Imaging Diagnostics and Radiotherapy Fondazione IRCCS Istituto Nazionale dei Tumori, Italy
2. Department of Mathematics, Politecnico di Milano, Italy
3. Department of Clinical, Surgical, Diagnostic, and Pediatric Sciences, University of Pavia, Campus della Salute, Policlinico San Matteo, Italy

1. Introduction

Intratumoral hypoxia is a key determinant of radioresistance in head-and-neck cancer (HNC) and limits radiotherapy efficacy. Its incorporation into tumour control probability (TCP) models is limited by the lack of spatially resolved, patient-specific biomarkers. Diffusion-weighted MRI provides quantitative apparent diffusion coefficient (ADC) maps reflecting tumour microstructural heterogeneity and may serve as imaging surrogates of hypoxic burden. We propose a clinically implementable framework integrating ADC-derived hypoxia into personalised TCP modelling.

2. Materials and Methods

We retrospectively analysed 81 HNC patients treated at a single institution. All underwent pre-treatment DWI and radical radiotherapy. Gross tumour volumes were delineated on T2-weighted MRI and co-registered with ADC maps.

Following Winter et al. [1], tumour regions with restricted diffusion within a predefined ADC interval were defined as high-risk subvolumes (HRS). Their prognostic value was previously assessed using Cox modelling for progression-free survival (PFS) across 1–5 years of follow-up.

For TCP modelling, tumours were represented as two compartments: normoxic and ADC-defined hypoxic regions. Distinct dose–response relationships were implemented within a Webb–Nahum TCP framework, combining compartment-specific clonogen survival fractions to derive patient-specific TCP estimates.

3. Results

Patient-specific HRS were derived from pre-treatment ADC maps and showed prognostic relevance for PFS. Incorporation of ADC-defined hypoxic subvolumes into the TCP framework produced substantial inter-patient variability in predicted tumour control for identical prescribed doses. Variations in TCP were mainly driven by hypoxic burden rather than tumour volume, with larger hypoxic subvolumes associated with lower predicted TCP. Sensitivity analyses confirmed robustness to realistic segmentation uncertainties.

4. Discussion and Conclusions

ADC-derived hypoxic subvolumes can be integrated into mechanistic TCP modelling for HNC. Differentiating normoxic and hypoxic dose–response characteristics enables biologically informed TCP estimation and supports hypoxia-guided dose escalation and subvolume boosting in personalised radiotherapy planning.

5. References

1. Winter R. M. et al., Radiotherapy and Oncology 2025; 204:110702

Acknowledgements:
Supported by Hi-ROC, EP PerMed JTC2024, FRRB EP_PERMED2024-548

OPTIMIZATION OF A DOUBLE FLOW CANNULA FOR AN ECMO DEVICE THROUGH COMPUTATIONAL MODELLING

Pavlos Varsos (1), Martin Graffin (1), Sixtine Fleurot (2), Laure Aubrege (2), Justin Issard (2, 3), Olaf Mercier (2, 3), Irene Vignon-Clementel (1)

1. Inria Saclay, France; 2 Innovation and Preclinical Research Department, Hôpitaux Paris Saint-Joseph et Marie Lannelongue, France; 3. Department of Thoracic Surgery, Marie Lannelongue Hospital, France

1. Introduction

Extracorporeal membrane oxygenation (ECMO) provides temporary cardiopulmonary support for patients with severe respiratory or cardiac failure, particularly as a bridge to transplantation. Current systems remain bulky, limiting mobility. The BIOARTLUNG project aims to develop a portable ECMO solution through component optimization. Here, we investigate an innovative double-flow cannula by in silico modelling prior to in vivo validation.

2. Materials and Methods

The cannula is composed of three main components (Fig. 1). The inner cylindrical arterial lumen, operating in a turbulent regime, was modelled with the k–ω SST turbulence model, whereas the outer annular venous segment was solved as laminar flow. For rapid optimization, a reduced analytical model was developed. Arterial pressure losses were estimated by the Darcy–Weisbach equation with Haaland friction factors accounting for Reynolds number, hydraulic diameter, and roughness. Minor losses (bends, junctions, sudden transitions) were included based on classical fluid mechanics loss coefficients. Semi-empirical formulations with fitted parameters [1,2] on experimental data were additionally evaluated. The bare-stent venous section was approximated as a porous medium with the simplified Darcy-type relations [3], enabling efficient parametric studies. Boundary and fluid conditions were set based on in-vitro experiments with a water–glycerine blood analogue.

3. Results

CFD reproduced closely the experimental pressure–flow behaviour, and confirmed turbulent flow in the arterial cylindrical segment and predominantly laminar flow in the venous annular pathway. The arterial segment exhibited a strongly non-linear ΔP–Q relationship due to turbulence and geometric effects, whereas the venous pathway showed an approximately linear trend. The reduced analytical model captured both magnitude and trend of pressure losses with substantially lower computational cost. Preliminary parametric analysis showed that increasing the inner arterial diameter by 37% significantly reduces the required pump pressure, directly supporting the optimization objective of minimizing pumping load.

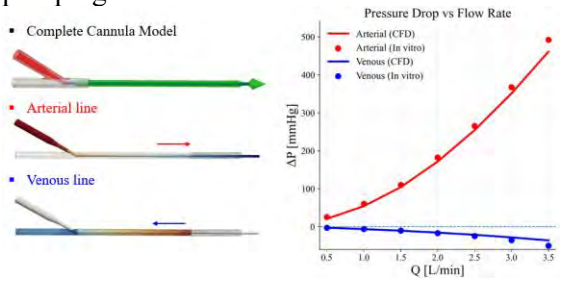


Figure 1: Cannula segments and corresponding pressure–flow CFD and in-vitro behaviour.

4. Discussion and Conclusions

The combined CFD and reduced-order analytical framework enables efficient evaluation of geometric modifications while preserving agreement with experimental observations. Optimization of the cannula geometry is ongoing and will guide future device iterations.

5. References

1. Ganushchak YM, et al. Perfusion. 35(4) (2020).
2. Montoya JP, Merz SI, Bartlett RH. ASAIO J. 37(1):4–8 (1991).
3. Ionita CN, Bednarek DR, Rudin S. Med Imaging 2012: Biomed Appl Mol Struct Funct Imaging. 8317 (2012).

Acknowledgements:

Supported by the European Research Council under the European Union's Horizon 2020 research and innovation program, project MoDeLLiver (Grant no: 864313).

GEOMETRIC ANALYSIS OF THE PULMONARY ARTERY OF HEART FAILURE PATIENTS: DEVICE LANDING ZONE ASSESSMENT

Jan Brüning (1), Natalia Solowjowa (1), Ann Laube (1), Lucie Kretzler (1), Kagithiri Srikantharajah (2), Jan Romberg (2), Cyrille Frottier (2), Leonid Goubergrits (1)

1. Deutsches Herzzentrum der Charité, Germany; 2. BIOTRONIK SE & Co. KG, Germany

1. Introduction

Implantable pulmonary artery pressure sensors (PAPS) that facilitate monitoring of blood pressure can improve clinical management of heart failure (HF) patients as well as reduce hospital readmissions due to acute decompensation [1]. To develop reliable and safe PAPS that can be implanted within the complex tree-like structure of the pulmonary artery (PA), geometric analysis this structure including identification of potential device implantation sites is necessary.

2. Materials and Methods

Computed tomography (CT) datasets of 50 HF patients, each 25 with reduced (HFrEF) and with preserved ejection fraction (HFpEF), with equal distribution between men and women were selected for this study (see table 1). The averaged spatial resolution of CT data was about 0.7 ± 0.13 mm in-plane resolution and 0.66 ± 0.15 mm slice thickness.

Table 1: *Major characterization of both HF cohorts. Ejection fraction (EF). Body mass index (BMI). Body surface area (BSA). (*) marks significantly different parameters between both cohorts.*

	HFpEF	HFrEF
Age, years (*)	69.1 ± 9.0	51.8 [14.6]
EF, % (*)	55.2 ± 5.9	25.5 ± 9.1
BMI	25.1 ± 4.6	26.9 ± 5.3
BSA	1.84 ± 0.26	1.96 ± 0.31

First, automatic segmentations of all PA was performed using a 3D nnU-Net [2] that was previously trained. Next, manual correction of segmented label fields was performed to complete partially segmented parts of the lumen, to connect interrupted vessel segments, and to separate vessel segments falsely merged due to close proximity. Figure 1 shows an example of a segmented PA. Finally, for each PA potential implantation sites according to the specific requirements elaborated for the fixation of the PAPS under development (length, diameters range and distal vessels bifurcation angles) were identified.

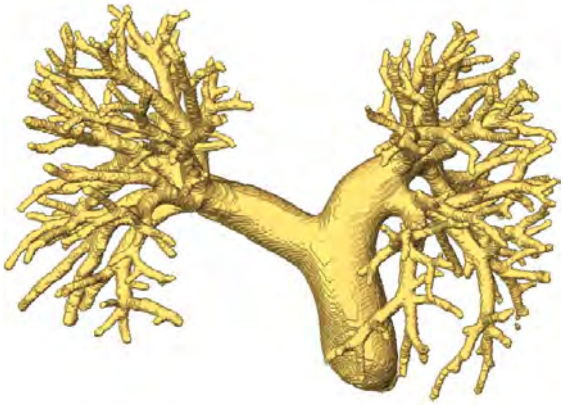


Figure 1: An exemplary pulmonary artery segmentation.

3. Results

The total length of the reconstructed PA segments was 9,011 ± 3,219 mm in the HFpEF and 8,122 ± 2,125 mm in the HFrEF cohort. On average 5.5 ± 3.2 landing zones per PA have been identified in the HFpEF and 5.0 ± 3.2 in the HFrEF cohort. No significant differences between HFrEF and HFpEF cohorts regarding PA tree morphometry were identified. Similarly, no significant difference in the number of potential landing zones between left and right PA were found. Comparison between men and women identified, however, twice as many potential landing zones in men compared to women.

4. Discussion and Conclusions

The geometric PA analysis identified a promisingly large number of potential landing sites for the PAPS of approximately five per case. Only in 4% of all cases no potential landing zone was identified. The lower number of potential implantation sites identified for women highlights the need for future device developments specifically tailored to women.

5. References

1. Shavelle DM et al. Circulation. Heart Failure. 2020;13:e006863 (2020).
2. Isensee F et al. Nature Methods. 2021;18(2):203-211 (2021).

VORTEX DURATION ASSESSMENT IN SEVERE PULMONARY ARTERIAL HYPERTENSION

Malak Sabry (1, 2), Ahmed Hassan (2, 3), Magdi Yacoub (2, 4), Pablo Lamata (1), Adelaide de Vecchi (1)

1. Dept. of Biomedical Engineering, King's College London, UK; 2. Aswan Heart Centre, Magdi Yacoub Foundation (MYF), Egypt; 3. Cardiology Dept., Cairo University, Egypt, 4. National Heart & Lung Institute, Imperial College London, UK

Corresponding author: malak.sabry@kcl.ac.uk

1. Introduction

Diagnosis and evaluation of pulmonary hypertension (PH) relies on invasive right-heart catheterisation to assess mean pulmonary artery pressure (mPAP), thus non-invasive surrogates are desirable. One possibility is to use flow patterns in the pulmonary artery (PA), which are disrupted in PH; notably, the duration of a vortex appearing in the main PA (t_{vortex}) was found to linearly correlate with mPAP [1], and was reproduced *in-silico* [2]. Also, t_{vortex} was shown to change with chronic variations in PA shape and right ventricular contraction dynamics, not with acute pressure changes, indicating that t_{vortex} is a signature of chronic PH remodelling [2]. Here, we investigate if the correlation holds in another group of patients, comparing results from the previous study (n = 25, 16 early to mild PH, and 9 controls), and 17 severe pulmonary arterial hypertension (PAH) cases, prior to vasodilator drug delivery.

2. Materials and Methods

We previously demonstrated that quantifying t_{vortex} from patient-specific rigid wall computational fluid dynamics simulations produced similar results to imaging-derived durations (mean difference of 1% across 25 cases, average age 61±11 years, average mPAP = 41±12 mmHg) [2]. Here, we applied the same workflow to quantify t_{vortex} in the 17 PAH cases (average age 30±8 years, average mPAP = 71±11 mmHg). Data from their follow-ups on vasodilator drug was available, with cases classified into responders and non-responders.

3. Results

While previous cases were close to the literature derived t_{vortex}-mPAP correlation line, cases in the current study were all positioned to the right of the line, with much larger deviations (average difference of 38% across 17 cases), indicating elevated mPAP without full haemodynamic adaptation. We also found that, at baseline, patients who would later respond to the drug deviated more from the correlation with mPAP than non-responders.

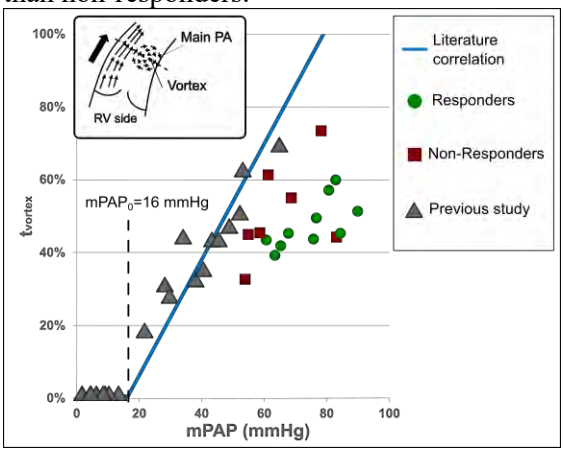


Figure 1: Points from previous and current studies, compared to literature correlation.

4. Discussion and Conclusions

Subjects in this cohort deviated more from the correlation than in the previous study. Notably, they were younger and had higher mPAP values, reflecting a less chronic state of PH. In the current cohort, responders to the drug at follow-up showed greater deviation from the correlation than non-responders, potentially reflecting an earlier disease stage before extensive remodelling. While the correlation might not hold universally, vortex duration may still provide clinical value by helping to differentiate remodelling stages in PH.

5. References

1. Reiter, G et al. Radiology 275.1 (2015): 71-79.
2. Sabry, M et al., Computers in Biology and Medicine 196 (2025): 110717.

Acknowledgements: MS is supported by MYF and Siemens Healthineers, PL & AdV are supported by Wellcome/EPSRC Centre for Medical Engineering.

COMPUTATIONAL MODELLING OF THE CARDIOVASCULAR ADAPTATION IN PULMONARY ARTERIAL HYPERTENSION

Sander Schomaker (1), Chantal Lokhorst (2), David Nolte (1), Rolf Berger (2), Tineke Willems (2), Johannes Douwes (2), Cristóbal Bertoglio (1)

1. University of Groningen; 2. University Medical Center Groningen, The Netherlands

1. Introduction

Pulmonary arterial hypertension (PAH) is a progressive cardiovascular disease currently diagnosed by a mean pulmonary artery pressure > 20 mmHg, increased pulmonary vascular resistance and normal pulmonary arterial wedge pressure [1]. Mathematical models based on biophysical principles describe the relationship between cardiovascular system properties and function. Given the limited number of paediatric PAH patients available for large-scale clinical studies, mathematical modelling offers a valuable tool to extract additional severity markers.

2. Materials and Methods

Cardiac catheterization pressure and MRI-derived flow-rate data were collected from paediatric PAH patients from 20 paediatric PAH patients representing different PAH aetiologies. A closed-loop lumped parameter model was formulated to represent the full cardiovascular system. For patients with PAH associated structural cardiac defects, the model is further adapted to reflect the resulting alterations in hemodynamics. An efficient numerical method was developed to solve the forward and parameter estimation problems, including practical identifiability analysis.

Data was rescaled, resampled, synchronized, and corrected for the expiratory motion. The model parameters were estimated for each patient. World Health Organization Functional Class (WHO-FC) was related to the estimated model parameters, such as vascular compliance and resistance, as well as cardiac chamber stiffness and contractility.

3. Results

Figure 1 illustrates the estimated RV stiffness and contractility versus WHO-FC. Increased stiffness is observed in patients within WHO-FC III and IV. Contractility increases in WHO-FC II and III but decreases in WHO-FC IV.

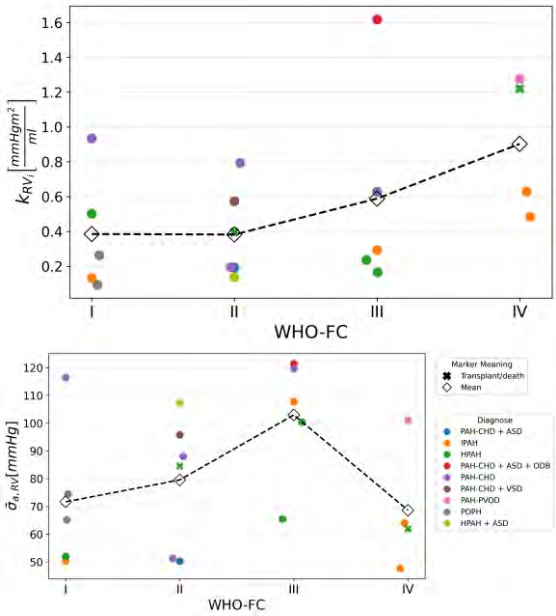


Figure 1: Estimated right ventricular stiffness (top) and contractility (bottom) versus WHO-FC.

4. Discussion and Conclusions

A computational framework was developed that operates within a clinically feasible time frame. Increased stiffness with higher WHO-FC indicates that stiffness correlate with the severity of patient symptoms, there were the contractility decreases within WHO-FC IV potentially indicating heart failure.

Estimation of patient-specific parameters provides additional insights into cardiovascular adaptation. In particular, RV stiffness emerges as a promising biomarker, which is not currently assessed in routine clinical practice.

5. References

1. Maron BA, Revised Definition of Pulmonary Hypertension and Approach to Management: A Clinical Primer; J Am Heart Assoc; 12(8):e029024 (2023).

Acknowledgements:

The authors would like to thank the European Research Council (Grant no: 852544) for providing financial support to this project.

UNVEILING CARDIOVASCULAR CHANGES AFTER LUNG RESECTION USING COMPUTATIONAL MODELS

Shiting Huang (1), Richard Good (1), Philip McCall (1), Sean McGinty (1), Benjamin Shelley (1), Ankush Aggarwal (1)

1. University of Glasgow, United Kingdom;

1. Introduction

Lung resection remains the primary treatment for lung cancer but often leads to postoperative breathlessness. Lung function impairment was traditionally considered the cause, but subsequent clinical studies indicate this symptom correlates weakly with lung function, suggesting a cardiac etiology [1,2]. However, the specific hemodynamic source, the effect of increased right ventricular (RV) afterload and impaired contractility, are still unclear due to the difficulty of clinically isolating these coupled mechanisms. Furthermore, the lack of patients' data limits the postoperative prediction and risk analysis. To address these challenges, using a computational model is a promising approach. This study qualitatively identifies the isolated mechanisms and quantitatively predicts postoperative risks using the proposed lumped parameter model.

2. Materials and Methods

A closed-loop 0D model was developed to simulate lung resection effects (Fig. 1(1)). The heart chamber is simulated using a time-varying elastance model. The valve model proposed by Mynard et al. [3] is adopted, and the circulation is represented by a three-element Windkessel model.

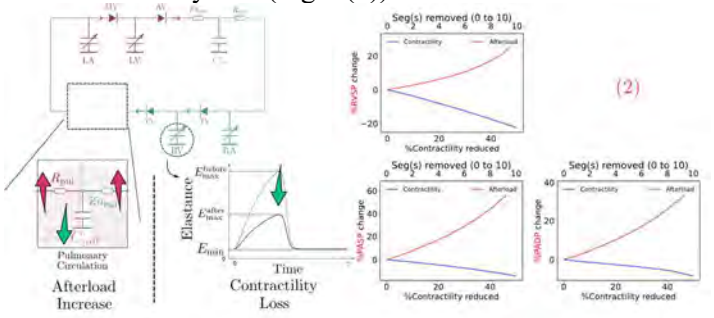
Isolate mechanisms: We simulated contractility changes by adjusting the maximum RV elastance value, and the afterload changes by the increase of the resistance/ impedance and decrease of the capacitance to simulate.

Model validation: The model was validated against clinical volume data from twenty-one lung cancer patients to ensure physiological fidelity.

Virtual Cohort Generation: We extracted the statistical distributions of the clinical cohort's volume, using Markov Chain Monte Carlo (MCMC) sampling, we generated a population size (n = 960,000) of virtual patients (VP). VP was used for preoperative risk identification for RV dysfunction.

3. Results

The results show the contractility loss and afterload increase exhibited identical volumetric trends in all volume metrics, but they displayed divergent responses in RV systolic pressure, pulmonary artery systolic and diastolic pressures. These pressures increase with afterload increase and decrease with contractility loss (Fig. 1(2)).



Input Segments	Number of Segments 3 (n=8)	4 (n=1)	5 (n=11)	9 (n=1)	Total
RVEDVI + RVESVI	62.50%	100%	72.73%	0%	66.67%
RVESVI + RVEF	62.50%	100%	63.64%	0%	61.90%
RVEDVI + RVEF	62.50%	100%	54.55%	0%	57.14%
RVESVI + LVEF	62.50%	100%	45.45%	0%	52.38%

Figure 1: (1) The schematic of two mechanisms simulation; (2) Different trend change under pressure metrics; (3) The predicting accuracy for different preop volumetric combinations

Validation results on clinical data with only afterload variation showed that our model conformed to the average trend observed in clinical practice. The results of risk prediction show RVEDV+RVESV is the superior predictor (66.7%, Fig. 1(3)) in all combinations.

4. Discussion and Conclusions

This study establishes the first computational model for postop lung resection prediction. The observed pressure divergence offers a clinically viable factor to distinguish underlying mechanisms, while the virtual cohort analysis enables potential preoperative risk stratification for surgical planning.

5. References

1. Pelletier *et al.*, Thorax, 1990; 45: 497–502
2. R. Larsen K *et al.,* Ann. Thorac. Surg. 1997, 64: 960–4
3. J. P. Mynard et al, Int. J. Numer. Methods Biomed. Eng., 2012; **28**: 626–41

COUPLED NUMERICAL–EXPERIMENTAL MODELING OF THE HUMAN SEMICIRCULAR CANAL

Manon Blaise (1), Etienne Puyoo (1), Anne-Sophie Poudrel (2), Nicolas Totaro (2), François Girardin (2), Pierre Reynard (3), Daniel Baumgartner (4), Anne Charpiot (4,5), Lucian Roiban (6), Eugen Ionescu (3)

1. INL UMR 5270, INSA Lyon (FR); 2. LVA, INSA Lyon (FR); 3. Hospices Civils de Lyon (FR); 4. ICube UMR 7357, Strasbourg (FR); 5. Hôpitaux Universitaires de Strasbourg (FR); 6. MatéIS UMR 5510, INSA Lyon (FR)

Corresponding author: manon.blaise@univ-lyon1.fr

1. Introduction

Approximately 20-30% of the global population suffers from balance disorders, most of which arise from vestibular dysfunction [1]. The semicircular canals detect angular head acceleration through endolymph displacement, cupular deflection, and hair cell activation.

We aim to develop an artificial vestibular sensor to represent the semicircular canal physiology, refine pathophysiological concepts, and enable therapeutic innovation. While several numerical models exist, they remain insufficient to capture the complex biomechanical interactions and have not been systematically validated against physical models [2].

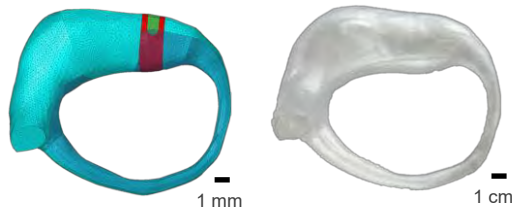


Figure 1: Lateral semicircular canal: 3D FE model with endolymph (blue), cupula (red) and crista (green) at left, and 3D-printed membranous in soft silicone at right.

2. Materials and Methods

A 3D finite element model of the human lateral semicircular canal was built under Altair HyperWorks™ (Fig. 1). Special attention was given to the geometry to reproduce the complexity of this organ. The inner membranous part of the canal was reconstructed from a previous model based on MRI slices of a patient [3]. The continuous mesh totals 61.5k hexahedral elements, including 53.5k fluid elements. As a hydrogel, the cupula, follows a viscoelastic behaviour [4]. Rotational chair protocols were simulated by applying sinusoidal angular displacements in the horizontal plane (0.01-10 Hz, peak velocity 25°/s) to replicate standard clinical testing.

Complementarily, a 10:1 scaled physical model was 3D-printed in soft silicone. An integrated piezoresistive sensor replicated the mechanotransduction of vestibular hair cells by sensing cupular deflection, thus functioning as an artificial crista ampullaris.

3. Results

Cupula transversal displacement following nodes of interest as well as Von Mises stresses are recorded. Initial numerical model validation was performed using the time constant of the cupula, defined as the time required for it to return to its resting position after rotation (T=6 s, [4]).

Bulge testing of the piezoresistive cantilever encapsulated in the artificial cupula (silicone membrane) established the relationship between applied membrane pressure and resulting cantilever deflection.

4. Discussion and Conclusions

This work presents a rare coupled numerical-experimental simulation of semicircular canal physiology. Such a physical model serves as an educational tool to illustrate physiological processes and pathologies arising from mechanical abnormalities, while the in-silico model provides insights into sensor scaling factors.

5. References

1. Paparella MM et al., Prim Care; 17(2), 299–308 (1990)
2. Gargula S et al., J Vestib Res; 36(1):15-24 (2025)
3. Chaney HV et al., J Transl Sci; 5(6):1-6 (2019)
4. Selva P et al., J Vestib Res; 19:95-110 (2009)

Acknowledgements:

This project was provided with HPC and storage resources by GENCI at TGCC thanks to the grant 2022-AD011013688, supported by IdEx Unistra (ANR-10-IDEX-0002) and SFRI (STRAT'US project, ANR-20-SFRI-0012), and the grant SHAPE-Med@Lyon (ANR-22-EXES-0012).

A COLLABORATIVE CALL TOWARDS VIRTUAL KIDNEYS AND PHYSIOLOGY-BASED MODELS OF ACUTE KIDNEY INJURY

Francisco J. López-Hernández

Instituto de Investigación Biomédica de Salamanca and Universidad de Salamanca, Spain

1. Introduction

Acute kidney injury (AKI) is currently defined and staged primarily through changes in plasma creatinine and urine output. While these criteria have improved clinical standardization, they constrain the conceptual understanding of AKI by equating renal dysfunction largely with reductions in glomerular filtration rate (GFR). However, renal excretory function emerges from a complex network of interacting processes including glomerular filtration, tubular transport, metabolic regulation, and systemic haemodynamics that are not integrated in the present AKI concept (1). Consequently, AKI can be more accurately interpreted as a dynamic continuum of disrupted renal excretory function rather than as a discrete threshold-defined condition. This perspective opens an opportunity for the development of computational models of renal functional status based on the holistic recreation of the renal homeostasis regulation network.

2. Materials and Methods

We propose a collaborative modelling framework aimed at integrating physiological knowledge, clinical data, and computational approaches to construct mechanistic models of renal excretory function. The framework is based on representing the main physiological processes governing renal homeostasis, including renal hemodynamics, glomerular filtration, tubular transport, electrolyte and water balance, and metabolic regulation. To capture these processes, the model incorporates heterogeneous inputs such as classical clinical parameters, functional ratios describing tubular performance, biomarkers reflecting structural integrity and injury, and indicators of renal functional reserve. Computational modelling and machine learning methods are used to integrate these data into a systems-level representation capable of describing complex interactions, regional heterogeneity, and multifactorial aetiologies.

3. Results

Within this framework, renal dysfunction is conceptualized as a continuous pathophysiological status defined by the configuration of the renal regulatory network. Integration of mechanistically meaningful variables allows the identification of functional states associated with different degrees of renal vulnerability and reduced functional reserve. Computational models and virtual kidneys could support predictive and personalized medicine by simulating patient-specific responses to physiological stressors such as surgery, nephrotoxic drugs, or hemodynamic instability. This approach may enable early identification of patients at risk of AKI, guide preventive strategies, and facilitate safer clinical decision making by distinguishing individuals with increased renal fragility from those with sufficient adaptive capacity.

4. Discussion and Conclusions

This proposal outlines a framework for developing physiology-based computational models of AKI integrating mechanistic knowledge with data-driven approaches. Such models could reconstruct patient-specific pathophysiological scenarios and identify individuals with increased renal vulnerability. Within the vision of the Virtual Physiological Human initiative, this strategy could enable the development of patient-specific virtual kidneys capable of simulating renal responses to clinical stressors and supporting predictive, personalized decision making. Achieving this objective will require interdisciplinary collaboration to define relevant biomarkers, characterize key regulatory mechanisms, and develop scalable modelling architectures for personalized renal physiology.

5. References

1. Docherty NG et al. Acta Physiol (Oxf); 240(8):e14181 (2024).

Acknowledgements:

The authors thank Instituto de Salud Carlos III (PI24/01058 co-funded by the European Union) for providing financial support to this project.

PERSONALISED MODELLING OF MEAL MACRONUTRIENT EFFECTS ON GLUCOSE RESPONSE

Rashmini Naranpanawa (1), Kekayan Nanthakumar (1), Jarrah M. Dowrick (1), Geoffrey Chase (2), Gonzalo D. Maso Talou (1), Merryn Tawhai (1), Finbar Argus (1)

1. Auckland Bioengineering Institute, University of Auckland, New Zealand; 2. Department of Mechanical Engineering, University of Canterbury, New Zealand

1. Introduction

Subject-specific computational models can be used to predict postprandial glucose response, enabling personalised meal guidance based on individual glycaemic profiles. There are several models to simulate glucose dynamics in humans [1, 2]; however, existing models generally do not account for the effects of meal macronutrient composition on plasma glucose appearance and are often poorly suited for home-based data, especially for personalised prediction.

2. Materials and Methods

A model for the breakdown and absorption of carbohydrates, proteins and fats in gastrointestinal tract and their respective contributions to glucose production is presented. It is integrated with a gold-standard physiological model for glucose dynamics currently used in ICU care [2]. The new model couples data from: (i) 10 days of Dexcom G7 continuous glucose monitors (CGM; Dexcom Inc, San Diego, CA, USA) at 5-minute intervals; and (ii) the meal macronutrients obtained using the DiNa App [3] to image and record the time of each meal. Subject-specific model parameters were identified using a genetic algorithm in Circulatory_Autogen [4].

3. Results

Calibration and validation results (Fig. 1) show that the overall glucose-insulin modelling framework captures subject-specific glucose dynamics for meals with different macronutrient compositions. Predictions for blood glucose level following specific meals in a preliminary cohort compare well with measured glucose levels.

4. Discussion and Conclusions

The overall approach integrates a mobile application and CGM data to predict patient-specific meal response. This pipeline enables personalised meal health guidance informed by predicted glycaemic response and more optimal control of blood glucose levels. We provide a foundation for personalised glucose prediction, which has the potential to predict whether an individual is likely to experience hyperglycaemia or hypoglycaemia following a meal. Further validation across a wider cohort will ensure robustness for use in health guidance.

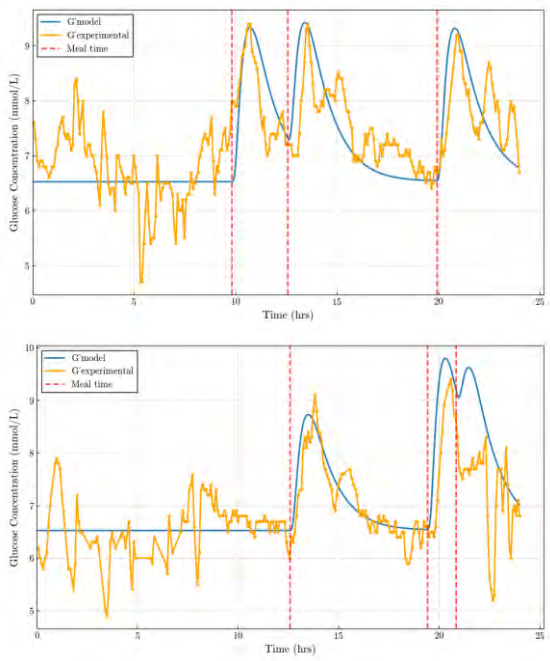


Figure 1: Model calibration (upper) and validation (lower) using one day (24-hours) of data from a subject.

5. References

1. Dalla Man, C., Rizza, R.A. and Cobelli, C. (2007). IEEE Trans Biomed Eng, 54(10), pp. 1740–1749.
2. Lin, J. et al. (2011). Comp Meth Prog Biomed, 102(2), pp. 192–205.
3. (2025). DiNa App Demo. https://dub.sh/dina-vph-demo
4. Argus, F. et al. (2022). Front Physiol, 13.

Acknowledgements:
Financial support was provided by an MBIE Catalyst (Soul Machines) grant.

PROPOSAL OF A PHYSICS INFORMED NEURAL NETWORK FRAMEWORK AS DIGITAL TWIN FOR EARLY SEPSIS DETECTION

Praveen Kumar Govarthan (1), Dheepikha Vijayarajan (2), Harini Sundaresan (2), Swathi Sudhakar (1), Ramakrishnan Swaminathan (1)

1. Department of Applied Mechanics and Biomedical Engineering, IIT Madras, Chennai, India;
2. Department of Electronics and Communication Engineering, College of Engineering, Guindy, Anna University, Chennai, India.

1. Introduction

Sepsis is a life-threatening condition that arises from a dysfunctional host response to infection. It is one of the major causes of mortality in ICUs worldwide. Early detection of sepsis is critical to improve survival rates. However, accurate diagnosis remains challenging due to indistinct clinical symptoms, inflammation from other diseases, and complex physiological changes. Recent studies using deep learning have shown that time series modelling can be effective. However, these models are completely data-driven and lack physiological interpretability, often affected by data sparsity [1]. In this work, a novel framework that integrates Long Short-term Memory (LSTM) with Physics-Informed Neural Networks (PINNs) is proposed to construct a patient-centric digital twin for sepsis detection.

2. Materials and Methods

This study uses patient-wise data from the publicly available PhysioNet/CinC Challenge 2019 dataset [2], which contains 20,336 ICU records of sepsis and non-sepsis patients. Only 8.8% of patients develop sepsis. For this study, key vital parameters - heart rate (HR), oxygen saturation (SpO_2), body temperature (Temp), respiration rate (Resp), systolic blood pressure (SBP), and diastolic blood pressure (DBP) are considered for detecting sepsis. The dataset contains substantial missing data. Fully missing columns are imputed using the global mean, while partially missing values are handled using k-nearest neighbour. Class imbalance is addressed by random undersampling, resulting in a balanced cohort of 1,790 sepsis and 1,790 non-sepsis patients. These features are then input to an LSTM model to capture temporal patterns in the physiological parameters. The integration of physics-informed constraints on vital parameters (Fig.1) introduces physiological consistency, enabling the development of a patient-specific digital twin for estimating sepsis-onset risk.

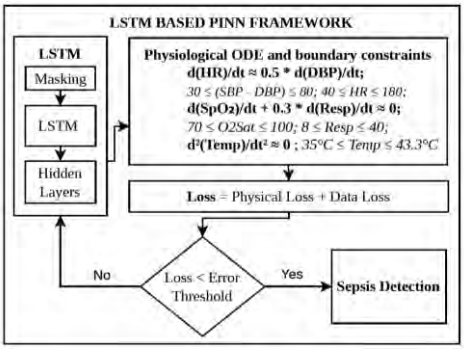


Figure 1: Block Diagram of the PINN Framework

3. Results

Results show that the preliminary experiments with the LSTM model alone achieve a balanced accuracy of 93.2%. The proposed LSTM-PINN shows improved performance, with balanced accuracy = 95.6%, recall = 88.9%, specificity = 96%, and F1 score = 91.2%. These results support integrating physiological constraints to enable more accurate sepsis prediction.

4. Discussion and Conclusions

This study presents an LSTM–PINN-based digital twin for early sepsis onset prediction by integrating temporal deep learning with physiological modeling to enhance clinical decision-making. Although the current results are based on LSTM-based training and evaluation, future work will focus on extending the framework to more advanced architectures and exploring hardware deployment for real-time sepsis detection.

5. References

1. de Araújo, A.L.V., Fonseca, F.S., Torcate, A.S. et al. Res. Biomed. Eng. 41, 55 (2025).
2. Reyna, M., Josef, C., Jeter, R., Shashikumar, S., Moody, B., Westover, M. B., Sharma, A., Nemati, S., & Clifford, G. D. PhysioNet. RRID: SCR_007345 (2019).

Acknowledgement

The authors acknowledge the support of the Department of Biotechnology, Ministry of Science and Technology, Government of India.

MODELING INCRETIN SECRETION AND EFFECTS IN RESPONSE TO VARIOUS MEAL CHALLENGES

Joshua Müller (1), Shauna D. O'Donovan (1), Lydia Afman (2), Natal A.W. van Riel (1)

1. *Dept. of Biomedical Engineering Eindhoven University of Technology, The Netherlands*
2. *Division of Human Nutrition and Health, Wageningen University, The Netherlands*

Correspondence to: j.b.muller@tue.nl

1. Introduction

Glucagon-like peptide-1 (GLP-1) is an incretin hormone secreted in two phases in response to nutrient ingestion [1]. Despite the important role of GLP-1 in regulating postprandial metabolism, through enhancing insulin secretion and inhibiting gastric emptying [2], it is poorly represented in models of postprandial metabolism. Current models either omit GLP-1 or model GLP-1 dynamics in relation to glucose alone. In this work, we developed a physiology-based mathematical model of GLP-1 dynamics by extending an existing model of glucose and lipid metabolism, to include the secretion and insulinotropic effect of GLP-1.

2. Materials and Methods

The Mixed Meal Model was chosen as it has been shown to successfully capture postprandial glucose and lipid dynamics [3]. GLP-1 secretion was modeled as a basal secretion rate plus glucose- and triglyceride-dependent components. The insulinotropic effect of GLP-1 was modeled through GLP-1-dependent modulation of a glucose-dependent insulin secretion term. This added one ODE and four parameters to the model. Parameter values were taken from literature where possible or estimated by fitting to glucose-only and mixed meal response data.

3. Results

With parameters estimated from a glucose-only meal the model exhibited the expected single early peak (Fig. 1A). With parameters estimated from a mixed meal, the model produced a similar but lower peak in response to a glucose-only meal (Fig. 1A). In response to a mixed meal the model successfully captured the expected biphasic secretion of GLP-1 (Fig. 1B). Removing the triglyceride-stimulated GLP-1 secretion led to loss of the biphasic profile. Furthermore, the model showed good quantitative agreement with the mean GLP-1 levels of the study population

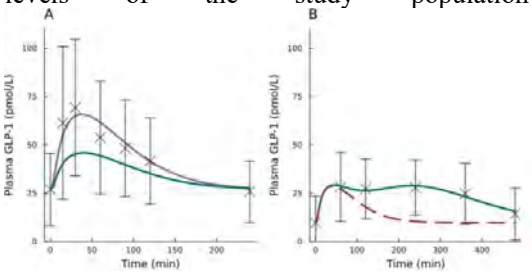


Figure 1 Simulations of the glucose-only meal (A) and the mixed meal (B) with parameters estimated from the glucose-only meal (purple) and mixed meal (green, dashed red; without contribution of triglycerides). The black crosses show the mean GLP-1 measurements, with the standard deviation indicated by the error bars.

4. Discussion and Conclusions

In the presented work we showcase the ability of the extended model to qualitatively describe GLP-1 secretion in response to two different meal compositions, in agreement with previous observations [1]. We highlight that triglyceride-stimulated GLP-1 secretion is necessary to accurately describe GLP-1 dynamics during a mixed meal. Moreover, the model captures quantitative GLP-1 trends, underscoring its ability to describe GLP-1 dynamics from meal composition instead of relying on GLP-1 measurements and a forcing function.

5. References

1. Elliott, R. M. *et al. J Endocrinol* **138**, 159–166 (1993).
2. Baggio, L. L. & Drucker, D. J. *Gastroenterology* **132**, 2131–2157 (2007).
3. O'Donovan, S. D. *et al. iScience* **25**, (2022).

Acknowledgements

The authors would like to thank TKI Agri&Food (Grant no: LWV24148) as well as the MetaboTwin consortium members for providing financial support to this project.

MODELLING THE NEUROPROTECTIVE EFFECTS OF EXERCISE ON THE CEREBRAL VASCULATURE OVER A LIFETIME

Stephen Payne (1,2)

1. University of Bristol, UK; 2. National Taiwan University, Taiwan

1. Introduction

Although ageing and hypertension are well-known to have significant negative effects on cerebral blood flow, aerobic exercise has emerged as a leading intervention that can act to improve brain health through modifications in arterial stiffness and endothelial function that both lead to short-term and long-term increases in cerebral blood flow. Mathematical models of this have been limited by the multiple, very different, time scales involved.

2. Materials and Methods

A model as recently proposed by Payne [1] that included the effects of ageing hypertension, and exercise within a simple three-state model that governed both fast and slow changes in arterial stiffness and slow changes in endothelial function. This model was calibrated against both fast and slow changes in cerebral blood flow from the experimental literature.

In this study, the model was first extended to consider a more detailed model of the arterial wall, based on the constrained mixture model [2]. This model has been widely used by other authors to mimic other conditions that govern changes in the wall properties. This combined model provides a more detailed model of the wall mechanics and enables other factors to be included in future.

Next, the model was used to consider several different exercise regimes, to explore the differences between these regimes in terms of cerebral blood flow. This is intended to start to quantify the potential improvements from different interventions.

In this study, two types of exercise were considered here: aerobic training and resistance training. In our previous work, aerobic training was assumed; however, it is known that different types of exercise have different effects on the cerebral vasculature.

The previous model uses the concept of a Representative Time Element (RTE), which is analogous to a Representative Volume Element (RVE). Short-term changes in arterial stiffness are essentially averaged over this period, applying multiple scales to separate out the slow and fast changes in cerebral physiology [1].

Different types of aerobic exercise and resistance training were applied within this RTE to compute rigorously the effect of fast changes in exercise over prolonged periods. Through comparison and calibration of the model with the experimental literature, the effects of different exercise regimes were computed.

3. Results

The results showed that the different types of exercise regime had significantly different effects on short-term cerebral physiology. By then integrating these over a whole adult lifetime (taken to be from 20-80 years of age), it was found that there can be significant cumulative differences between these two regimes.

4. Discussion and Conclusions

These results indicate that different exercise regimes can have significant differences on lifetime cerebral vasculature behaviour, indicating that different exercise regimes can be used to target the optimal intervention to maintain cerebral health.

5. References

1. Payne SJ. J Physiol. 2025;603(9):2569-82 (2025).
2. Valentin A, Humphrey JD, Holzapfel GA. Ann Biomed Eng. 2011;39(7):2027-45 (2011).

Acknowledgements:

SJP is partly funded by the Ministry of Education, Taiwan, Yushan fellowship number 113V2008-1.

BLOOD FLOW IN INTERNAL CAROTID AS A SURROGATE OF CEREBRAL BLOOD FLOW: PHANTOM AND IN-SILICO MODEL

Bruno Frackowiak, Sergei Shulepov, Marco Baragona, Andre Immink, Jens Muehlsteff

Philips Innovation and Design
High Tech Campus 37, 5656AE Eindhoven, the Nethelands

1. Introduction

Cerebral blood flow (CBF) monitoring during surgery under anaesthesia is an unmet clinical need for patient stability assessment. Brain perfusion assessment from CT/MRI lacks portability, is expensive and shows poor temporal resolution. External ultrasound is a promising alternative, considering that blood flow in internal carotid artery (ICA) serves as a reliable clinical surrogate for CBF [1]. Main objective of this study is to combine an in-silico model with an in-vitro phantom to investigate the dynamic of the cerebral regulation and the relationship between CBF and ICA blood flow.

2. Materials and Methods

Flow waveform variation in the ICA is substantially lower than in the External Carotid Artery (ECA), helping maintain a relatively constant blood supply to the brain. To reproduce this physiological characteristic, a phantom of the carotid bifurcation is incorporated into a closed loop system driven by a roller pump (Fig. 1). Adjustable flow resistances and Windkessel (WK) fluid dampers are placed at the outlets to adjust the flow waveforms. The ADAM56 1D model from [2] is adapted to mimic the phantom configuration, by including multiple tapered elements for each branch, the metal connectors and the polyurethane tubing. WK damper is represented in the model by a softer material.



Figure 1: In vitro phantom and WK fluid damper

3. Results

Ultrasound Doppler measurements on phantom in ICA and ECA are shown in Fig. 2. Simulation results (Fig. 3) on the phantom model show a reasonable agreement with measurements. At the human network level (ADAM56 original model), the waveforms become comparable to the physiological ones after a fine tuning of the impedance at the outlets.

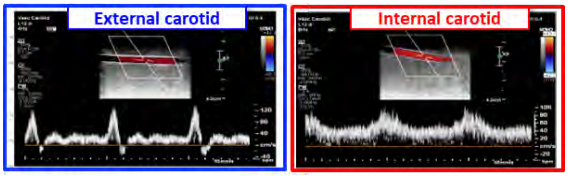


Figure 2: Ultrasound measurements on phantom

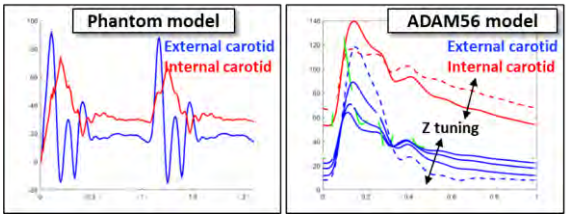


Figure 3: phantom and ADAM56 1D model results

4. Discussion and Conclusions

These results highlight a strong influence of the boundary condition at the carotid artery outlets, leading to a physiological differentiation between the ICA and ECA waveforms. The dynamics of cerebral regulation introduces time varying resistance and compliance at the carotid artery outlets, thus affecting the shape of these waveforms. Further investigation using a brain perfusion model will shed some light on the relationship between the CBF and the ICA blood flow waveform.

5. References

1. Soustiel JF et al, American Heart Association Journal 2003; 34 (8).
2. Boileau E. et al, Int. J. for Numerical Methods in Biomedical Engineering 2012; 31 (10)

Acknowledgements:

The results were achieved under the European Defence Fund project “Development of intelligent military capabilities for monitoring, medical care and evacuation for contagious, injured and contaminated personnel” (iMEDCAP, Grant Agreement Number 101121421).

MULTISCALE MAPPING OF BRAIN DEVELOPMENT BY INTEGRTING DIFFUSION MRI AND HISTOLOGY

Lanxi Xu (1)(2), Julie Albon (2), Alison Bienemann (3), Carol-Ann James (3), Marco Palombo (4), John Evans (4), Peter Theobald (1)

1. Cardiff School of Engineering, Cardiff University, United Kingdom; 2. School of Optometry, Cardiff University, United Kingdom; 3. Translational Biomedical Research Centre, University of Bristol, United Kingdom; 4. Cardiff University Brain Research Imaging Centre, Cardiff University, United Kingdom.

1. Introduction

Brain growth and remodelling involve rapid macroscopic expansion and microstructural reorganisation after birth [1]. Early postnatal development is characterised by increases in brain volume, glial proliferation, myelination, axonal reorganisation, and synaptic pruning, which shape neural connectivity [2]. Abnormal developmental trends are associated with neurological conditions such as autism spectrum disorder (ASD), attention-deficit/hyperactivity disorder (ADHD) [3], and increased vulnerability to traumatic brain injury (TBI). Characterising brain maturation therefore requires multiscale approaches linking tissue microstructure to whole-brain organisation. This study established a multiscale framework by integrating diffusion MRI (DTI/NODDI) with quantitative histology in the porcine brain model to characterise fibre architecture and cellular organisation across brain regions and developmental stages.

2. Materials and Methods

Female Welsh Large White porcine brains (1, 14, 180 days) were analysed across six brain regions. Multi-shell diffusion MRI was acquired using a 3T Connectom scanner and preprocessed with MRtrix3 and FSL to generate tractography and NODDI metrics. Histology used Luxol fast blue and Hoechst staining. LDA and Random Forest identified age- and region-related features.

3. Results

Significant regional differences in fibre architecture were observed across development. The corpus callosum showed the highest fibre amount and coherent alignment, whereas cerebral lobes exhibited greater dispersion due to complex association fibres. Brain stem fibres progressed from a loose organisation at birth to a highly aligned structure by 180 days. Nuclear density peaked at 14 days and decreased by 180 days, reflecting maturation and pruning. Random forest outperformed LDA, identifying fibre amount, orientation, and nuclei density as key age predictors, while NDI, FA, and dispersion distinguished brain regions.

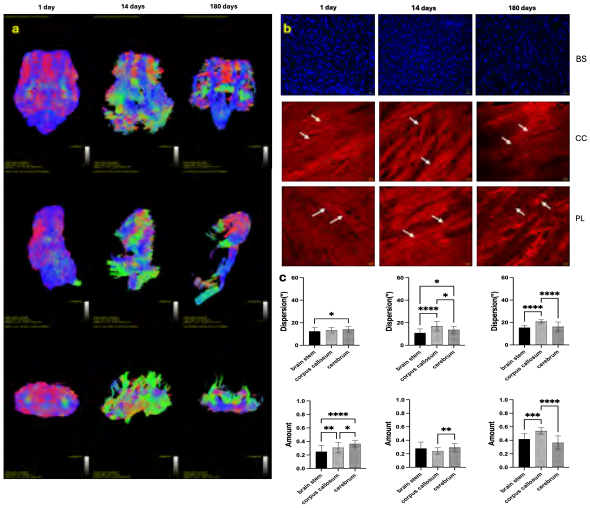


Figure 1 Multiscale characterisation of brain structure across development.

4. Discussion and Conclusions

This study established a multiscale normative dataset of porcine brain development by integrating diffusion MRI and histology. Combining DTI/NODDI metrics with quantitative fibre and cellular features enabled the identification of microstructural biomarkers of brain maturation. These findings provide a baseline framework for interpreting imaging biomarkers and modelling brain development.

5. References

1. Choe MS et al., Cereb Cortex. 2013; 23(9):2100-17.
2. Groh J, Simons M. Neuron. 2025;113(1):127-39.
3. Parenti I et al., Trends in Neurosciences. 2020;43(8):608-21.

Acknowledgements:
This study was funded by the China Scholarship Council and Cardiff University.

A SYSTEMATIC IN VITRO–IN SILICO EVALUATION OF INTRA-ARTERIAL THROMBOLYSIS EFFICACY IN MEVOS

Agnese Lucchetti (1)*, Ilona Mager (1), Charlotte S. Weyland (2), Omid Nikoubashman (3), Elephtarios Alapais (3), Johanna C. Clauser (1), Michael Neidlin (1)

1. Cardiovascular Engineering, Applied Medical Engineering, Medical Faculty, RWTH Aachen, Germany; 2. Department of Diagnostic and Interventional Neuroradiology, University Hospital Aachen, Germany; 3. Department of Diagnostic and Interventional Neuroradiology, University Hospital OWL Bielefeld, Germany

**Corresponding author: lucchetti@ame.rwth-aachen.de*

1. Introduction

Medium vessel occlusions (MeVOs) present significant challenges for standard mechanical thrombectomy due to limited vascular accessibility and risk of vessel injury associated with small-calibre arteries. Intra-arterial thrombolysis represents a promising alternative; however, no clinical consensus currently exists regarding the optimal drug dosage or the minimum catheter-to-clot distance required to achieve effective treatment. To address this gap, we propose a combined in vitro-in silico framework to systematically investigate the influence of procedural parameters (drug concentration, and catheter-to-clot distance), and biological factors (clot size, composition, and collateral circulation) on thrombolysis efficacy, with the goal of enabling patient-specific therapy optimization.

2. Materials and Methods

In vitro framework: Clot analogues were generated from human whole blood under static [1] and dynamic (Chandler loop) [2] conditions to produce fibrin-rich and erythrocyte-rich representative thrombi (Fig. 1a). Patient-specific MeVO phantoms of the anterior, middle, and posterior cerebral arteries were reconstructed from clinical imaging and integrated into a physiological flow loop using a water–glycerol blood analogue (Fig. 1b). Clots with varying composition were treated via microcatheter-delivered recombinant tissue plasminogen activator (rtPA). Recanalization time and success rate were defined as primary quantities of interest. *In silico framework:* CFD simulations (ANSYS) were performed to quantify spatial and temporal rtPA concentration profiles at the clot surface for different catheter positions, administered drug dosages, and collateral flow conditions. Boundary conditions were prescribed according to the experimental setup. Transient laminar flow and drug transport were modelled using the incompressible Navier–Stokes equations coupled with convection–diffusion equations.

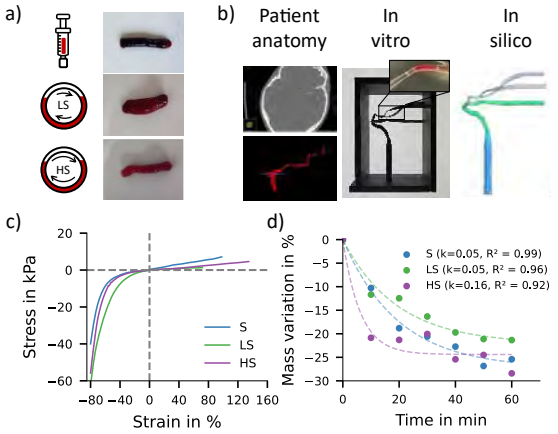


Fig. 1: a) Static (S), low-shear (LS), and high-shear (HS) clots; b) integrated in vitro–in silico framework; c) mechanical characterization of clot analogues (n_{sample} = 5 clots); d) mass variation during static thrombolysis (n_{sample} = 5 clots).

3. Results

Clot analogues prepared under different conditions showed distinct morphology, mechanics, and thrombolysis susceptibility. Static clots were stiffer and stronger in tension but weaker in compression than dynamic clots (Fig. 1c). Preliminary static thrombolysis tests indicated that static and low-shear clots exhibited similar overall degradation profiles, whereas high-shear clots underwent a more rapid initial mass loss (Fig. 1d).

4. Discussion and Conclusions

The proposed integrated approach has the potential to support evidence-based parameter selection and to contribute to patient-specific optimization of thrombolytic therapy.

5. References

1. Cahalane RME et al., Ann Biomed Eng, 51:1759–1768, 2023.
2. Zeng Z. et al., J Mater Sci Mater Med, 34:24, 2023.

MULTISCALE MODELING AND HIGH-ORDER NUMERICAL SIMULATION OF BRAIN ELECTROPHYSIOLOGY

Stefano Pagani (1), Caterina B. Leimer Saglio (1), Francesco Daniele (1), Mattia Corti (1), Niteen Kumar (1), Paola F. Antonietti (1)

1. MOX-Dipartimento di Matematica, Politecnico di Milano, Piazza Leonardo da Vinci 32, Milan, 20133, Italy

1. Introduction

Brain electrophysiology arises from complex multiscale spatial and temporal interactions linking ionic exchanges and metabolic processes to the intricate geometry and heterogeneous structure of brain tissue. Alterations in ionic homeostasis, pathological protein accumulation, or reduced metabolic supply can significantly affect neuronal excitability and promote abnormal electrical activity that propagates through neural tissue. To investigate the mechanisms of epilepsy, amyloid-β-related dysfunction, and oxygen-driven metabolic alterations, we propose a multiscale computational framework based on the monodomain equation coupled with models of neuronal ionic and metabolic dynamics.

2. Materials and Methods

We model multiscale neuronal electrical activity by coupling the monodomain equation with systems of ordinary differential equations describing ionic concentrations and gating variable dynamics. Three model formulations are considered. First, epileptic dynamics are investigated using the Barreto–Cressman ionic model [1]. The framework is then extended to account for amyloid-beta induced alterations in calcium regulation, linking neurodegeneration to neuronal hyperexcitability [2]. Finally, electrophysiology is coupled with oxygen dynamics to study metabolic impairments such as ischemia [3]. The coupled systems are discretized using a high-order discontinuous Galerkin method on polygonal and polyhedral meshes (PolyDG), which accurately resolves steep electrical wavefronts while handling structural and geometric complexities [4].

3. Results

Numerical simulations of the proposed multiscale systems reproduce complex electrophysiological dynamics across different pathological scenarios, providing insight into how functional mechanisms interact with structural substrates to regulate electrical signal propagation. The baseline formulation of the model describes seizure-like dynamics driven by extracellular potassium and the propagation of high-frequency bursting activity. Including amyloid-beta mechanisms leads to calcium dysregulation and increased neuronal excitability. Finally, an additional coupling with oxygen dynamics is introduced to investigate how oxygen deprivation impairs ionic pump activity and alters electrical wavefront propagation.

4. Discussion and Conclusions

The proposed framework provides a flexible and accurate simulation tool to investigate interactions between electrophysiology, metabolism, and neurodegeneration.

5. References

1. Leimer Saglio, C. B., Pagani, S., Corti, M. and Antonietti, P. F. (2026). *A high-order discontinuous Galerkin method for the numerical modeling of epileptic seizures,* Computers & Mathematics with Applications. 205, 112-131.
2. Leimer Saglio, C. B., Corti, M., Pagani, S. and Antonietti, P. F. *A novel mathematical and computational framework of amyloid-beta triggered seizure dynamics in Alzheimer's disease* - arXiv:2511.10369 (2025)
3. Daniele, F., Leimer Saglio, C. B., Pagani, S. and Antonietti, P. F. *Mathematical and numerical modeling of coupled oxygen dynamics and neuronal electrophysiology* - arXiv:2509.22863 (2025)
4. Leimer Saglio, C. B., Pagani, S. and Antonietti, P. F. (2025). *A p-adaptive polytopal discontinuous Galerkin method for high-order approximation of brain electrophysiology,* Computer Methods in Applied Mechanics and Engineering. 446, A, 118249.

MACHINE-LEARNING-SUPPORTED PERSONALISATION OF ZERO-DIMENSIONAL CARDIOVASCULAR MODEL WITH BAROREFLEX

Karolina Tlałka (1,2), Ian Halliday (2,3), Andrew Narracott (2,3), Maciej Malawski (1,4)

1. Sano Centre for Computational Medicine, Poland; 2. University of Sheffield, United Kingdom; 3. Insigneo Institute, United Kingdom; 4. AGH University of Kraków, Poland

1. Introduction

Incorporating a baroreflex sub-model into zero-dimensional (0D) cardiovascular (CV) models broadens the scope of applications to orthostatic stress [1]. However, the increased complexity hinders model analysis (parameter interactions) and personalisation (number of parameters, subset selection, convergence) [1]. Here we present our approach to model personalisation, in which, alongside to traditional methods we use machine learning (ML) to understand model behaviour and inform personalisation boundaries.

2. Materials and Methods

We personalised the response of a 4-chamber 0D baro-regulated model [1,2] to the Lower Body Negative Pressure relative experimental data (mean arterial pressure (MAP), stroke volume (SV) and heart rate (HR) of 10 healthy subjects [3]). We conducted global sensitivity analysis to determine the most influential parameters, and orthogonality analysis, to reveal the "parallel directions" of influence [1]. From the results, we selected a subset of 6 parameters for calibration. We utilised Differential Evolution (DE) [4] over a parameter grid [1] (to improve convergence). Our loss function is described in [1]. We repeated the calculation 100 times for each virtual subject, to assess the convergence of global optimisation. To investigate undesired oscillations present in 20% of personalised solutions, we created an artificial dataset from 10^3 simulations with different parameter sets, with a classification metric which indicated oscillations (1) or their absence (0). We used Logistic Regression with 2nd grade polynomial features (LR2) to assess which parameters, or their coupling, contribute most to this oscillatory response. Model quality was assessed using accuracy and f1 score.

3. Results

For 40% of subjects we achieved a fully convergent response within 3.5×10^3 iterations. For the rest, we selected the solution with smallest value of loss. The absolute mean errors were as follows: $\max(HR)$: 2.39%, $\min(MAP)$: 3.63%, $\min(HR)$: 5.24%. Further, we achieved an LR2 model with accuracy 0.95, f1(1) 0.95, f1(0) 0.96 (for our test set). The investigation revealed that the parameter interaction contributing most to oscillations is the product of HR sympathetic gain (G) and time constant (T). The subspace of oscillatory behaviour was identified as follows T(0;20); G(-0.6;-0.4).

4. Discussion and Conclusions

Achieving fully converged solutions is challenging because of model non-linearity and the variability in the target experimental response. Our model predicts extreme changes in MAP, SV and HR with small errors. Explainable ML can be used to improve understanding of complex non-linear behaviour and simplify the personalisation by identifying problematic parameter space to exclude from optimisation.

5. References

1. Tlałka et al., Personalization of a fully closed-loop lumped-parameter cardiovascular model with baroreflex in response to orthostatic stress. Submitted to PLOS One.
2. Ursino, doi: 10.1152/ajpheart.1998.275.5.H1733
3. Høiseth et al., 10.1097/CCM.0000000000000766
4. Storn, Price, doi: 10.1023/A:1008202821328

Acknowledgements:

Polish Ministry of Science and Higher Education: Grant MEiN/2023/DIR/3796; European Commision: H2020 Grant 85753; PLGrid: Grants PLG/2024/017108 and PLG/2025/018168 (HPC Center: ACK Cyfronet AGH). Publication supported by FNP (IRAP programme): Sano project

PARAMETER ESTIMATION OF A LUMPED-PARAMETER CARDIOVASCULAR MODEL, WITH A NOVEL UNSCENTED KALMAN FILTER

Alexander Thornton (1), Ian Halliday (1), Harry Saxton (2), Richard H Clayton (1), Xu Xu (1)
1. University of Sheffield, UK; 2. Astellas Pharma, UK

1. Introduction

Models of blood pressure and flow in the cardiovascular system have a range of potential applications in healthcare, but to be useful they need to be calibrated to represent individual patients. However, many model states and parameters are not directly observable. After successful parameter estimations of a 10 parameter, 1-chamber 0D cardiovascular model [1], this novel parameter estimation method attempts to personalise a 44-parameter model often found in the literature [2]. Larger models typically have issues around identifiability [3].

2. Materials and Methods

We introduce a "Kalman interval" between subsequent executions of the unscented Kalman filter (UKF) that allows a larger observation vector to be ingested. A detailed explanation of the new UKF method is in [1]. The modification transforms the utility of the algorithm from instantaneous state estimation for the purpose of control, to parameter estimation. The new method was used to attempt to personalise the parameters of the popular model presented by Korakianitis and Shi [2], which has known identifiability issues.

50 target parameter samples were created, sampling from a truncated, Gaussian distribution, with a standard deviation of 10% and a maximum of 45%, to test our method beyond the *prior art*. The novel filter was run for 50 cycles, and two different output sets of the model were trialled both with sampling frequencies of 100Hz, and multiplicative measurement noise of 1%. Output set 1 contains measurements of all heart chamber volumes and pressures of the non-algebraic compartments. Output set 2 contains Output set 1 with the addition of non-algebraic flows. The seed was the mean of the distribution.

3. Results

The result in figure 1 shows a subset of the 15 most identifiable parameters for the sake of brevity. The results show the average percentage of model runs which achieved ≥95% accuracy for each parameter, in effect this shows the practical identifiability with respect to this estimation method. The timing parameters, and major compliances and elastances are shown to be the most identifiable. The resistances are the least.

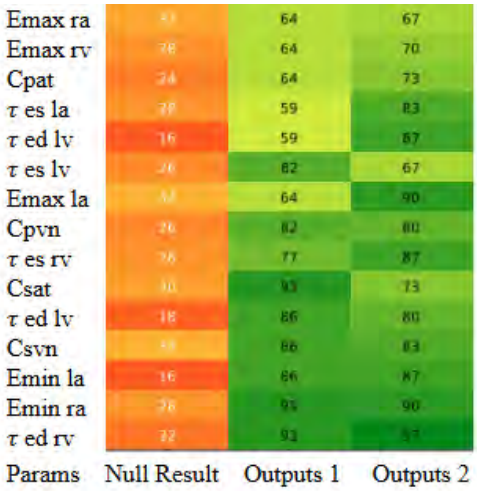


Figure 1: Average percentage of model runs which achieved ≥95% accuracy for each parameter.

4. Discussion and Conclusions

The work here demonstrates the ability of the modified UKF method to estimate higher dimensional spaces, than previously shown [1]. The format of the results also present a practical and computationally inexpensive way of understanding the practical identifiability of a model. The method is still in its embryonic stages of development but has shown promise for applications of personalising 0D cardiovascular models.

5. References

1. Thornton, A., Halliday, I., Saxton, H. and Xu, X., 2025. arXiv preprint arXiv:2601.02390.
2. Korakianitis, T. and Shi, Y., 2006. Medical engineering & physics, 28(7), pp.613-628.
3. Colunga, A.L., Colebank, M.J. and Olufsen, M.S., 2023. Journal of the Royal Society Interface, 20(200).

Acknowledgements:
The work is funded by a PhD scholarship from the University of Sheffield.

An integrated 1D-0D model of the cardiorespiratory system with short-term cardiopulmonary control mechanisms

Caterina Dalmaso (1), Pablo Javier Blanco (2), Lucas Omar Müller (1)

1. Department of Mathematics, University of Trento, Italy; 2. National Laboratory for Scientific Computing, LNCC/MCTI, Brazil

1. Introduction

Cardiovascular (CVS) and respiratory functions are strongly interconnected. The respiratory system supports cardiac function mechanically, via the respiratory muscle pump, and chemically, by providing oxygen and eliminating carbon dioxide from the blood. Notably, virtually all everyday manoeuvres (postural changes, exercise, respiratory movements) require correct coordination of these two systems.

The vast majority of modelling efforts to mathematically describe these coupled systems have considered a lumped-parameter representation of the CVS, with little or no anatomical detail. Consequently, model parameterization is limited to effective values that allow physiologically plausible responses to be obtained, but without capturing the interplay between physics and vascular topology.

As a first step toward bridging this gap, we present a model of the cardiorespiratory system that includes an anatomically detailed 1D–0D description of the cardiovascular system, a 0D description of lung mechanics, a 1D–0D description of gas transport and exchange in the systemic and pulmonary vessels, and a description of short-time scale regulatory mechanisms.

2. Materials and Methods

Simulations are performed on two 1D arterial–venous network models characterised by different degrees of anatomical detail: the anatomically detailed arterial–venous network (ADAVN) model [1] and a reduced version that includes its major arteries and veins, both coupled to a 0D lung mechanics model [2]. The models are calibrated to ensure comparable cardiac output, mean arterial pressure, and flow rates in selected arteries.

Respiratory gases are treated as passive scalars transported by blood, enabling investigation of how vascular network resolution influences tracer dynamics. Gas exchange is simulated both at the level of the lungs, assuming instantaneous diffusion across the hematoalveolar membrane, and between peripheral capillaries and tissues, assuming a homogeneous blood–tissue compartment. The gas exchange module is calibrated to account for the anatomical detail provided by the arterial network. We consider five gas consumption/production rates, defined for a baseline state using Fick's principle, and we consider twenty-five perfused tissue regions, each characterized by a specific volume.

Additionally, we include a description of local autoregulation, baroreflex, and peripheral and central chemoreflex mechanisms [3], which act on cardiovascular function and ventilation in response to acute perturbations in arterial and venous pressures and blood gas composition.

3. Results

We describe the model calibration process, show that our model reproduces cardiovascular and respiratory physiological data under normal, hypercapnic, and hypoxic conditions, and analyse the impact of each control mechanism on the response to these conditions. Finally, we employ the model to simulate the Valsalva and Müller manoeuvres.

4. Discussion and Conclusions

The presented model is a first step toward an anatomically informed, multiscale description of cardiorespiratory coupling that integrates hemodynamics, lung mechanics, and blood-gas transport and exchange with short-timescale reflex feedback mechanisms.

5. References

1. Müller LO, Watanabe SM, Toro EF, Feijóo RA, Blanco PJ. Front. Physiol. (2023)
2. Dalmaso C, Blanco PJ, Müller LO. Biomech. Model. Mechanobiol. (2025)
3. Albanese A, Cheng L, Ursino M and Chbat NW. Am. J. Physiol. Heart Circ. Physiol. (2016)

VPH2026 conference
9th International Conference on the Virtual Physiological Human
1 - 4 September 2026
Milan, Italy

PARAMETER IDENTIFICATION IN AN ECMO PHANTOM CIRCULATION MODEL

Andrés Utrera (1,2), Cristóbal Bertoglio (1), Wouter Huberts (3), Marcel Rutten (3)

1. University of Groningen, The Netherlands; 2. University of Santiago, Chile; 3. Eindhoven University of Technology, The Netherlands.

1. Introduction

Extracorporeal membrane oxygenation (ECMO) is used in many critical-care settings, like cardiac arrest and post-cardiac surgery. Its use is growing, but clinical decisions remain challenging because support strategies and operating conditions vary across centers [1, 2]. This motivates the development of computational modelling tools that are robust, easy to interpret, and estimable from available measurements. In this work, we present an ECMO-phantom model focused on practical identifiability so that parameter estimation remains interpretable and directly linked to experimental measurements.

2. Materials and Methods

We calibrated the ECMO-phantom cardiovascular lumped model using experimental phantom data and evaluated practical identifiability of its parameters. The numerical approach is based on a standard definition of a weighted least-squares cost function. Using identifiability principles, we obtained a stable estimable parameter subset while preserving physiologically coherent behavior and interpretability.

3. Results

The model showed stable and physiologically coherent behavior across representative ECMO operating conditions, including changes in support level. Practical identifiability analysis separated well-informed from weakly informed directions, defining a robust estimable subset linked to contractility, vascular loading, and ECMO hydraulic response. The optimization algorithm converged successfully and enabled estimation of approximately 25 parameters. The remainder parameters with weak local information were fixed to avoid instability and improve uncertainty handling. The resulting framework supports future protocol-oriented simulation studies, including escalation/de-escalation and support-intensity planning.

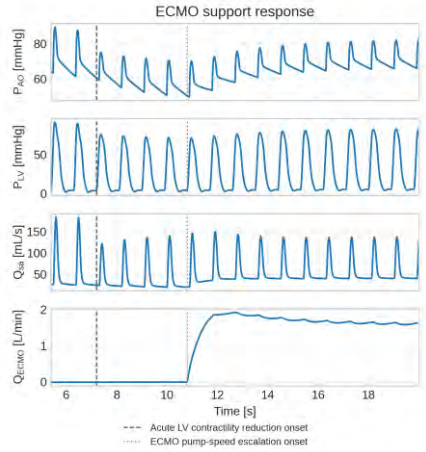


Figure 1: Forward simulation of acute left-ventricular contractility reduction followed by ECMO pump-speed escalation; vertical lines indicate both event onsets.

4. Discussion and Conclusions

This study presents an ECMO modeling framework in which robustness and practical identifiability are key aspects. The analysis yields a stable, estimable parameter subset that remains physiologically coherent under representative support changes, improving confidence in inverse estimates from experimental measurements. This work establishes a transparent preclinical basis for comparing support strategies in silico. Future work will extend the framework to broader scenarios and evaluate its value for protocol-oriented decision support.

5. References

1. Gao H et al., Healthcare; 13(12) (2025).
2. Swedzky F et al., Drugs Context; 12:2022-7 (2023).

Acknowledgements:

A.U. thanks ANID PFCHA/DOCTORADO NACIONAL BECAS CHILE 2023–21231932.

MODELING VENOUS HEMODYNAMICS: A 1D FRAMEWORK FOR INVESTIGATING VALVES AND EXTERNAL COMPRESSION

Salvatore Ferlito (1), Maha Reda (1), Ahmet Sen (2), Jordi Alastruey (2), Stéphane Avril (1)

1. Mines Saint-Étienne, INSERM, U1059 Sainbiose, F--42023 Saint-Étienne, France; 2. King's College London, Department of Digital Twins for Healthcare, School of Biomedical Engineering and Imaging Sciences, London, UK.

Correspondence to Stéphane Avril: avril@emse.fr

1. Introduction

Compression therapy is the primary treatment for chronic venous insufficiency (CVI) [1]. Despite its wide clinical use, its hemodynamic mechanisms remain unclear. In this study, we present a one-dimensional model of lower-limb venous hemodynamic to quantify the effects of venous valves and external compression on flow and pressure distribution in healthy and CVI conditions.

2. Materials and Methods

We implemented collapsible vessel mechanics, describing venous mechanical behaviour, in a one-dimensional Navier–Stokes framework [2]. Collapsible veins behaviour, modelled by the tube power law, was validated against experimental data from literature [3]. The validated framework was then applied to a representative lower-limb venous network derived from morphometric data representing the main superficial and deep veins. The model includes dynamic valve behaviour accounting for the opening and closing phases of the valve, perforator coupling and gravitational loading. The calf muscle pump activation was applied on the deep veins of the calf, with contraction and relaxation cycles changing both in time and space. External compression (EC) was added as an external pressure on veins walls to simulate compression therapy. Three configurations were analysed for flow and pressure distribution: pathological (No valves), healthy (With valves), and pathological with external compression (No valve + EC).

3. Results

Venous valves markedly reduce reflux and limit pressure elevation during the relaxation phase compared to the pathological configuration. External compression further improves hemodynamic efficiency, producing a higher net ejected volume per contraction cycle despite modest changes in reflux magnitude.

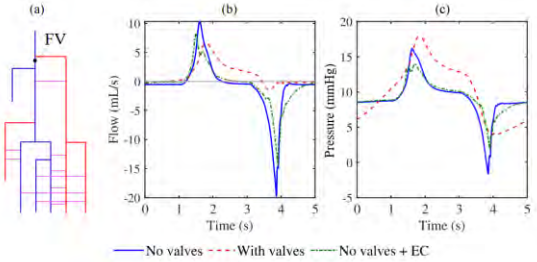


Figure 1: (a)Vascular network of the leg and point analysed. (b) Flow and (c) Pressure trends in femoral vein (FV) segment in the three configurations.

4. Discussion and Conclusions

Valve competence was the primary determinant of reflux suppression and pressure stabilization. Valve incompetence reproduced hallmark features of chronic venous insufficiency, including sustained retrograde flow and elevated residual pressures. In contrast, compression improved venous return through mechanically induced lumen reduction and increased hydraulic resistance, particularly in the superficial system. Model predictions were consistent with physiological in vivo measurements. The framework supports future system-level and patient-specific investigations to optimize compression strategies.

5. References

[1] J. Azar, A. Rao, e A. Oropallo, *J. Wound Care*, vol. 31, fasc. 6, pp. 510–519, giu. 2022.

[2] J. Alastruey *et al.*, *Am. J. Physiol.-Heart Circ. Physiol.*, vol. 325, fasc. 1, pp. H1–H29, lug. 2023.

[3] P. Flaud, P. Guesdon, e J.-M. Fullana, *Eur. Phys. J. Appl. Phys.*, vol. 57, fasc. 3, p. 31101, feb. 2012.

A 0D MODEL REPRESENTING HUMAN RESPONSE TO HYPERGRAVITY

Krzysztof Czechowicz (1, 2), Andrew Narracott (1, 2), Rodney DR Hose (1, 2), Ryan Anderton (3), Ian Halliday (1, 2), Paul D Morris (1, 2, 4)

1. The University of Sheffield, UK; 2. Insigneo Institute, UK; 3. UK Civil Aviation Authority, UK; 4. Sheffield Teaching Hospitals NHS Foundation Trust, Sheffield, UK

1. Introduction

The reducing cost of sub-orbital space flight will lead to an increase in the number of people wanting to experience it. This creates a need for health guidelines relating to health conditions which might make those trips dangerous to the individual. We propose a computational model that can simulate the behaviour of the human circulatory system during high gravitational loads exhibited during launch and landing of a space craft. [1]

2. Materials and Methods

The model consists of a cardiac model subject to a baroreflex response Rodney DR [2] and a compartmental model representing the main elements of the human circulation. The model consists of 11 nodes and 33 degrees of freedom. To improve the reliability, the model includes collapsible veins to simulate reduced venous flow from the brain. The construction of the model allowed for positioning of the model in space to respond to gravitational forces in the form of Gx and Gz accelerations. The model reports blood pressures and cardiac output.

We parametrised the model using data from tilt test experiments. The pose of the parametrised model was adapted to mimic the pose of a CSOS (Commercial Sub-Orbital Spaceflight) passenger. The model was then subjected to the hyper gravitational load as measured during space launch and return [3].

3. Results

We compared the results of the model with published experimental data from centrifuge studies. We analysed the resulting changes in the heart rate, central blood pressure and cardiac output. With the model we could also separate the influence of the Gz and Gx accelerations.

4. Discussion and Conclusions

Results from the model appear plausible. When Gz only was applied the model predicted the pressure variation well, however it did not represent the changes in cardiac output correctly. When Gx loading was added the predicted cardiac output improved.

The model can report the flow to the cerebral circulation. This information is not available from measurements however the low cerebral flow from the model coincided with the centrifuge subjects reporting changes in vision.

Successfully simulating the changes in human circulation in a healthy individual the model parameters can be modified to represent different conditions to assess their effect on the individual's ability to take part in CSOS.

Currently, we have shown that our approach can predict the average response to the changes in the gravitational load. The next step is to analyse individual's data and predict the centrifuge response based on a response to the tilt table test.

5. References

1. Morris, P.D. et al., Nat Rev Cardiol; 21, 667–681 (2024).
2. Ursino M., Am J Physiol.; 275(5):H1733-47. (1998)
3. Smith TG et al., Aerosp Med Hum Perform. 2022; 93(12):830-839.(2022)

Acknowledgements:

The authors would like to thank the UK Civil Aviation Authority for providing financial support to this project

ESTIMATION OF ARTERIAL WALL MATERIAL PARAMETERS FROM NON-INVASIVELY MEASURABLE BLOOD PRESSURE SIGNALS

Katalin Pálfalvi (1), Richárd Wéber (1)

1. Department of Hydrodynamic Systems, Faculty of Mechanical Engineering, Budapest University of Technology and Economics, Műegyetem rkp. 3., H-1111 Budapest, Hungary

1. Introduction

Cardiovascular diseases are a leading cause of mortality [1] and are strongly influenced by arterial wall mechanics, which also determines pressure amplification.

Accurate estimation of arterial wall material parameters is essential for personalized modeling, yet these parameters are usually obtained through invasive methods, their clinical use is limited. Peripheral blood pressure waveforms, however, are non-invasively measurable and contain information on arterial mechanics. This study evaluates a machine learning approach to estimate arterial wall material parameters non-invasively from radial pressure-time signals.

2. Materials and Methods

A one-dimensional hemodynamic model with nonlinear pressure–area relations and Olufsen-type wall mechanics was used to generate 34,347 virtual patients using the *first_blood* solver [2]. Parameter ranges were defined based on literature data [1].

A one-dimensional convolutional neural network (CNN) was trained to estimate arterial wall material parameters from one cardiac cycle of radial pressure–time signals of 1,000 virtual patients.

Performance was evaluated using the coefficient of determination (R^2), root mean squared error (RMSE), mean absolute error (MAE), and Bland–Altman analysis.

3. Results

The convolutional neural network successfully learned the nonlinear mapping between radial pressure waveform morphology and arterial wall material parameters. Low RMSE and MAE values were achieved for two of the three estimated parameters, indicating strong predictive capability.

However, a proportional error remained in the predictions, suggesting sensitivity of the model to parameter scaling and partial non-identifiability within the parameter space. Bland–Altman analysis revealed low mean bias but parameter-dependent dispersion.

4. Discussion and Conclusions

Arterial wall material parameters can be estimated non-invasively from radial pressure-time signals using a convolutional neural network that captures nonlinear waveform-mechanics relationships.

This simulation-based deep learning framework enables estimation of otherwise unmeasurable parameters, supporting patient-specific cardiovascular modeling and non-invasive clinical decision support.

5. References

[1] R. Wéber, M. Viharos, B. Csippa, D. Gyürki, and G. Paál, "Synthetic, Population-Based Virtual Patient Database Using a Digital Twin of the Cardiovascular System," *Cardiovasc. Eng. Technol.*, Feb. 2026, doi: 10.1007/s13239-026-00822-4.

[2] R. Wéber, M. Viharos, and D. Gyürki, https://github.com/weberrichard/first_blood

Acknowledgements:

GEMINI has received funding from the European Union's Horizon 2020 research and innovation programme under the grant agreement No 101136438.

The research was supported by the János Bolyai Research Scholarship (BO/00484/23/6) of the Hungarian Academy of Sciences and by the New National Excellence Program of the Ministry for Culture and Innovation from the source of the National Research (Wéber Richárd ÚNKP-22–5-BME-426).

The project supported by the Doctoral Excellence Fellowship Programme (DCEP) is funded by the National Research Development and Innovation Fund of the Ministry of Culture and Innovation and the Budapest University of Technology and Economics (Pálfalvi Katalin DKÖP-26-1-BME-49).

SECONDARY FLOWS INSIDE ARTIFICAL VESSEL GEOMETRIES

Péter Friedrich (1), Benjamin Csippa (1), György Paál (1)

1. Department of Hydrodynamic Systems, Budapest University of Technology and Economics, Hungary;

1. Introduction

It has been assumed that secondary flows play a role in the initiation and formation of cerebral aneurysms. [1] The relationship between the pipe topology and the developing flow-field is well understood for simpler classical engineering problems. However, for complex geometries, such as cerebral arteries it is not understood. [2] The aim of this paper is to better understand the effect of multiple bends in close proximity to the developing flow-field, using artificial geometries.

2. Materials and Methods

The artificial geometries of a circular cross-section are used, each with two 90-degree bends in the opposite direction. The geometrical parameters were the diameter of the pipe, the curvature of the bends, and the distance between them. Both bends had the same curvature. The parameters for the geometrical parameters were chosen, based on real life geometries from 27 patients. Steady-state simulations were used with 3 different physiologically relevant Reynolds-numbers totalling 990 simulations.

The post-processing was carried out by a custom-made Python code. The velocity-field was decomposed into axial and secondary components along the vessel centreline. Using the various velocity components the kinetic energy was also calculated for each velocity component. The values were averaged in slices along the centreline every 0.2mm.

3. Results

An example diagram for secondary kinetic energy is shown in Figure 1. along a dimensionless centreline. In this example, the observations indicate that increasing the distance between the bends increases the emerging kinetic energy of the secondary flow in the second bend.

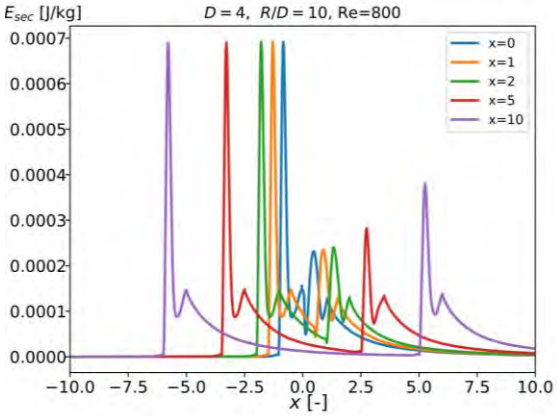


Figure 1: Kinetic energy of the secondary flow along the pipe length with varying distance (x) between the bends.

4. Discussion and Conclusions

In the paper 990 simulations were carried out on 330 different geometries. Even with only two symmetrical planar bends the results show complex interactions between the various geometrical and fluid-dynamics parameters. Another observation from the entire dataset is that, across all parameter sets, the kinetic energy of the secondary flow relative to the first bend decreases as the Reynolds (Re) number increases. Meanwhile, with increasing the Reynolds number the effect of the first bend on the second bend increased. The geometries are not fully representative of real cerebral arteries, so further investigation of non-planar and asymmetrical layouts are planned.

5. References

[1] B. Csippa, P. Friedrich, I. Szikora, and G. Paál, *Cardiovasc. Eng. Technol.*, 2025.

[2] J. Alastruey, J. H. Siggers, V. Peiffer, D. J. Doorly, and S. J. Sherwin, *Phys. Fluids (1994)*, vol. 24, no. 3, p. 031902, Mar. 2012.

Acknowledgements:

The project supported by the Doctoral Excellence Fellowship Programme (DCEP) is funded by the National Research Development and Innovation Fund of the Ministry of Culture and Innovation and the Budapest University of Technology and Economics.

MULTISCALE HEMODYNAMIC MODELING OF ECMO-INDUCED ALTERATIONS IN MICROVASCULAR FILTRATION AND THROMBOTIC RISK

Richárd Wéber (1), Márta Viharos (1), Francesco Romanò (2)

1. Department of Hydrodynamic Systems, Faculty of Mechanical Engineering, Budapest University of Technology and Economics, Műegyetem rkp. 3, Budapest, 1111, Hungary;

2. Univ. Lille, CNRS, ONERA, Arts et Métiers Institute of Technology, Centrale Lille, UMR 9014 - LMFL - Laboratoire de Mécanique des Fluides de Lille - Kampé de Fériet, F-59000 Lille, France.

1. Introduction

Extracorporeal membrane oxygenation (ECMO) profoundly alters systemic hemodynamics, gas exchange, and microvascular pressures. While its macroscopic effects are well characterized clinically, the multiscale mechanisms linking ECMO-induced flow redistribution to microvascular filtration, hemoconcentration, and potential clot formation remain incompletely understood.

2. Materials and Methods

Systemic hemodynamics were simulated using the modular 1D–0D solver first_blood [1]. ECMO was implemented as an extracorporeal circuit with flow extraction and reinfusion boundary conditions, enabling controlled variation of flow rate, cannulation site, and pump characteristics. Local outputs (pressure, flow, shear rate, residence time) were used as boundary conditions for the pulmonary microvascular model of Grotberg and Romano [2,3]. This model resolves capillary lubrication flow, Darcy interstitial transport, and Starling filtration across endothelial and epithelial membranes. Coupled simulations quantified changes in capillary pressure gradients, interstitial velocity, and wall shear stress under ECMO flow fractions ranging from 0–80% of cardiac output.

3. Results

Computed pressures are used to evaluate transmembrane velocities across the capillary–interstitium and interstitium–alveolar membranes under cardiogenic pulmonary edema conditions. In a femoral-to-carotid configuration, decreasing heart function reduces membrane velocity magnitudes across much of the domain. More negative central velocities indicate reduced edema risk due to altered hydrostatic gradients induced by extracorporeal flow redistribution. ECMO also lowers interstitial shear stress (τ_{ic}), potentially limiting fibroblast activation and matrix remodelling.

4. Discussion and Conclusions

Overall, the model highlights the complex interplay between cardiac function, extracorporeal support, pulmonary fluid transport, and biomechanical stress. These results suggest that cannulation strategy and pump management should be jointly considered to minimize both pulmonary edema risk and blood trauma during ECMO therapy.

5. References

1. Wéber, R., Gyürki, D., & Paál, G. (2023). First blood: An efficient, hybrid one- and zero-dimensional, modular hemodynamic solver. *International Journal for Numerical Methods in Biomedical Engineering*. https://doi.org/10.1002/cnm.3701
2. Grotberg, J. B., & Romanò, F. (2023). Computational pulmonary edema: A microvascular model of alveolar capillary and interstitial flow. *APL Bioengineering*, *7*(3). https://doi.org/10.1063/5.0158324
3. Grotberg, J. B., Romanò, F., & Grotberg, J. C. (2025). Flow mechanisms of the air-blood barrier. PLOS Computational Biology, 21(4), e1012917.https://doi.org/10.1371/journal.pcbi.1012917

Acknowledgements:

GEMINI has received funding from the European Union's Horizon 2020 research and innovation programme under the grant agreement No 101136438. The research was supported by the János Bolyai Research Scholarship (BO/00484/23/6) of the Hungarian Academy of Sciences and by the New National Excellence Program of the Ministry for Culture and Innovation from the source of the National Research (Wéber Richárd ÚNKP-22–5-BME-426).

TURBULENCE-INDUCED HEMOLYSIS IN A TAYLOR-COUETTE-DEVICE: DESIGN AND EXPERIMENTAL CHARACTERIZATION

Moritz Wiegand (1, 2), Aris Groh (3), Simon Bender (1, 2), Körling Pölkow (3), Christian Navid Nayeri (3), Katharina Vellguth (1, 2), Vera Froese (1, 2), Jan Brüning (1, 2), Sascha Martinke (3), Oliver Paschereit (3) and Leonid Goubergrits (1, 2)

1. Deutsches Herzzentrum der Charité, Institute of Computer-assisted Cardiovascular Medicine, Germany; 2. Charité—Universitätsmedizin Berlin, corporate member of Freie Universität Berlin and Humboldt Universität zu Berlin, Germany;3. Hermann-Föttinger Institute, Technische Universität Berlin, Gemany

Corresponding author: Moritz Wiegand, moritz.wiegand@dhzc-charite.de

1. Introduction

Blood-perfused medical devices such as ventricular assist devices operate predominantly under turbulent flow conditions. Turbulence is associated with increased flow-induced blood damage [1]. However, current blood damage models do not account for turbulent effects due to absence of reliable experimental data [2]. This study aims to establish an experimental setup capable of quantifying turbulence-induced haemolysis.

2. Materials and Methods

A flow chamber allowing to study laminar and turbulent flow under identical shear rates was developed, based on a Taylor-Couette system (TCS) with counter-rotating cylinders. Flow regimes were classified using an image-based, custom-trained neural network. Experiments were conducted with a water-dextran solution as blood-analogue fluids at physiological shear rates of 256, 396, and 537 s^{-1}. For each shear rate, one laminar and three turbulent measurement points of increasing turbulent intensity have been investigated by Laser Doppler anemometry (LDA) (Fig. 1, left). Finally, first experiments with porcine blood were performed (Fig. 1, right).

3. Results

The system reliably produced distinct laminar and turbulent flow regimes automatically identified by the neural network across all tested conditions. LDA measurements of velocity profiles, turbulent intensities, and Reynolds shear stresses were in good agreement with published data [3]. Blood measurements showed increased haemolysis in turbulent regimes.

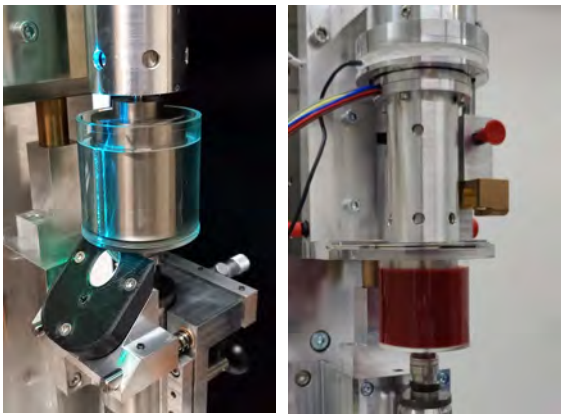


Figure 1: Two identical Taylor-Couette systems, capable of performing LDA (left) and blood measurements (right).

4. Discussion and Conclusions

The developed TCS is suitable for the study of turbulence-related blood damage. Future work will focus on reduced gap widths and two-phase blood-analogue fluids to better replicate blood behaviour.

5. References

1. Kameneva et al., ASAIO J, 2004, DOI: 10.1097/01.MAT.0000136512.36370.B5
2. Goubergrits et al., Int J Artif Organs, 2018, DOI: 10.1177/0391398818790343
3. Jiang et al., Journal of Fluid Mechanics, 2025, DOI: 10.1017/jfm.2024.1143

Acknowledgements:
This work was funded by the German Research Foundation under Grant 507267166.

ELECTROMECHANICAL SIMULATION OF LEFT VENTRICULAR CONTRACTION AFTER MYOCARDIAL INFARCTION

Adriano Schlief (1), Lukas Obermeier (1), Laura Verbeek (2), Christoph Knosalla (3), Natalia Solowjowa (3), Leonid Goubergrits (1)

1. Deutsches Herzzentrum der Charité, Institute of Computer-assisted Cardiovascular Medicine (ICM), Berlin, Germany; 2. Eindhoven University of Technology, Eindhoven, The Netherlands; 3. Deutsches Herzzentrum der Charité, Department of Cardiothoracic and Vascular Surgery, Berlin, Germany

1. Introduction

Patients with chronic heart failure resulting from myocardial infarction have a poor prognosis. The contractile ability of the heart muscle is impaired and can ultimately become life-threatening. In response to the scarred infarct region of the myocardium, the ventricle dilates, accompanied by thinning of the affected areas and a further decline in cardiac function.
Surgical ventricular reconstruction (SVR) was developed to treat this condition, often referred to as left ventricular aneurysm. The procedure aims to restore the function of the left ventricle (LV) by removing the infarcted region and recovering the physiological size and shape of the LV. To improve patient survival, determining the optimal degree of ventricular size reduction is essential. Simulation methods such as the finite element method (FEM) are promising approaches to support individualized treatment planning for SVR.

2. Materials and Methods

Pre- and postoperative CT data of two patients who underwent SVR to treat LV dilatation caused by myocardial infarction were used in this study. Patient-specific diastolic anatomies of the LV myocardium were reconstructed. Subsequently, the electromechanical simulation algorithm of PyAnsys Heart [1] was applied to simulate a cardiac cycle in Ansys LS-DYNA.
Material properties were then adjusted to match time resolved volume measurements obtained from CT images and systolic parameters such as myocardial wall thickness and longitudinal strain derived from 3D echocardiography. Furthermore, the material stiffness was increased in the infarcted region. The resulting material model was subsequently used to simulate a cardiac cycle for the postoperative condition. For this purpose, muscle fibres and Purkinje fibres were mapped onto the postoperative geometry using deformetrica [2], a diffeomorphic metric mapping algorithm.

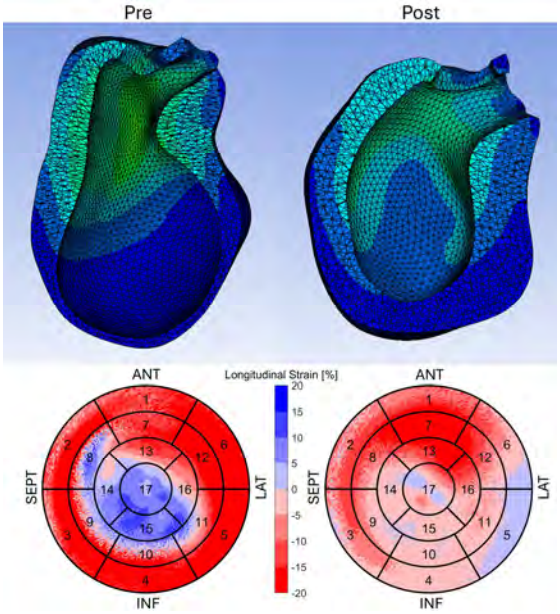


Figure 1: Pre- (left) and postoperative (right) illustration of systolic strain. Top: effective strain; bottom: bull's eye plot of longitudinal strain.

3. Results and Discussion

A postoperative recovery of myocardial contractility can be observed compared to the preoperative state. Both the temporal volume progression and the systolic ejection fraction, as well as the myocardial wall thickness, show substantial improvement. However, longitudinal strain values exhibit only local enhancements without a significant global change. Longitudinal contractility has hence not improved, which can be attributed to myocardial unloading and suture-related immobility induced by surgery.

4. References

1. Hoeijmakers, M. et al. (2023). pyheart-lib: A Python Library for LS-DYNA Multi-physics Heart Simulations. In: Bernard, O. et al. (eds) Functional Imaging and Modeling of the Heart. FIMH 2023. Lecture Notes in Computer Science, vol 13958. Springer, Cham.
2. Bône, A. et al. (2018). Deformetrica 4: An Open-Source Software for Statistical Shape Analysis. In: Reuter, M. et al. (eds) Shape in Medical Imaging. ShapeMI 2018. Lecture Notes in Computer Science, vol 11167. Springer, Cham.

THE ROLE OF LAYER-SPECIFIC COMPOSITION AND FIBER ORIENTATION ON THE MECHANICAL RESPONSE OF PORCINE PULMONARY ARTERIES

Juan Antonio Peña (1), Miguel Ángel Martínez (1,2), Estefania Peña (1,2)

1. Aragón Institute for Engineering Research (I3A), University of Zaragoza, Spain; 2 CIBER-BBN, Centro de Investigación en Red en Bioingeniería, Spain

1. Introduction

Pulmonary arteries (PA) operate under high-flow, low-pressure regimes, exhibiting unique compliance compared to systemic vessels. Understanding their layer-specific mechanics is crucial for modeling pathologies like pulmonary hypertension (PH). This study investigates the passive mechanical behavior of the media and adventitia layers in porcine PAs, correlating their structural composition with their macroscopic response to provide a robust framework for vascular constitutive modeling.

2. Materials and Methods

Proximal PAs were harvested from healthy pigs (n=6). The experimental campaign included: 1) Opening angle (OA) measurements for residual strain analysis; 2) Uniaxial tensile tests in circumferential and longitudinal directions for both intact and separated layers [1]; 3) Planar biaxial tests for validation; and 4) Confined compression tests to assess incompressibility [2]. Quantitative histology (Orcein, Masson's Trichrome, and Sirius Red) was used to determine the area fraction of elastin, collagen, and smooth muscle, alongside fiber orientation. The Gasser-Ogden-Holzapfel (GOH) [3] model was calibrated using uniaxial data and validated using biaxial data.

3. Results

Histological analysis revealed a significant structural gradient: the media is composed of 59.30±3.14% elastic lamellae, while the adventitia is predominantly collagenous (71.91±4.21%). Mean fiber angles were identified at α=44.86±4.27° for the media and a more dispersed α=49.33±10.33° for the adventitia.

Mechanically, the adventitia showed a marked "strain-stiffening" effect, being significantly stiffer than the media at high stretches ($\lambda \geq 1.3$, $p<0.05$). For instance, at λ=1.4, the adventitia's stress was nearly double that of the media in the circumferential direction. Confined compression tests confirmed the assumption of nearly perfect incompressibility.

Regarding constitutive modeling, both GOH and FFF models achieved excellent fits for uniaxial data ($R^2>0.98$). However, when these parameters were used to predict multiaxial behavior, the error increased. Specifically, the models tended to underestimate the stress in biaxial 1:1 protocols, suggesting that uniaxial calibration fails to capture the complex fiber-matrix interactions and kinematic locking that occur under multi-axial physiological loading.

4. Discussion and Conclusions

This work demonstrates that the mechanical response of the PA is a synergistic result of its layers' distinct compositions. The adventitia plays a critical role in preventing over-distension, whereas the media governs the physiological compliance. The discrepancy in multiaxial predictions suggests that current models may need to incorporate inter-fiber interactions or kinematic locking to better capture the complex 3D behavior of pulmonary tissues..

5. References

1. Peña, J. A., Martínez, M. A., Peña, E., 2015. Layer-specific residual deformations and uniaxial and biaxial mechanical properties of thoracic porcine aorta. J Mech Behav Biomed 50, 55–69.
2. Ríos-Ruiz, I., Maríınez, M., Peña, E., 2025. What about the mechanical behaviour and modelling of arteries in radial direction? J Biomech 182, 112500 (1–8).
3. Gasser, T. C., Ogden, R. W., Holzapfel, G. A., 2006. Hyperelastic modelling of arterial layers with distributed collagen fibre orientations. J R Soc Interface 3, 15–35.

Acknowledgements:

Support was obtained from the Spanish Ministry of Science and Technology through the research project PID2022-140219OB-I00, and the regional Government of Aragón support for the funding of the research project T24-20R.). The authors thank the research support from the CIBER initiative, whose actions are financed by the Instituto de Salud Carlos III with assistance from the European Regional Development Fund.

LATENT DYNAMICS NEURAL NETWORK MODELS OF CARDIAC ELECTROPHYSIOLOGY IN A PATIENT-SPECIFIC LEFT ATRIUM

Marta Di Ridolfi (1,4), Stefano Pagani (2), Federica Caforio (1,3,4), Francesco Regazzoni (2), Luca Dede' (2), Luigi Preziosi (5).

1. Dept. of Mathematics and Scientific Computing, NAWI Graz, University of Graz, Austria; 2. MOX, Dept. of Mathematics, Politecnico di Milano, Italy; 3. Gottfried Schatz Research Center, Medical University of Graz, Austria; 4. BioTechMed-Graz, Austria; *5. Dept. of Mathematical Sciences, Politecnico di Torino, Italy.*

1. Introduction

Simulating left atrial electrophysiology (EP) is crucial for advancing the diagnosis and treatment of heart diseases. Traditional modeling and simulation approaches demand substantial computational resources. To reach an efficient solution in predicting atrial EP under both physiological and pathological conditions, we employ a data-driven reduced-order model called Latent Dynamic Network (LDNet) [1], to improve computational efficiency with minimal accuracy loss.

2. Materials and Methods

Atrial EP is described by the Courtemanche-Ramirez-Nattel (CRN) ionic model [2] coupled with a monodomain equation. The high-fidelity solutions of the model are numerically obtained using a Finite Element discretization and a first-order Backward Difference scheme, using the lifeX-ep software [3].

High-fidelity solutions resulting from varying impulse localizations and timings are used to train the LDNets. By leveraging a neural ODE, the system's evolution is mapped into a low-dimensional space using a few latent variables. Then, through a second neural network, the transmembrane potential is predicted at query points in the left atrium. The optimal configuration is identified with the Optuna optimization framework [4]. LDNet performance is evaluated using Normalized Root Mean Square Error (NRMSE) and Pearson Dissimilarity (PD) metrics, with speed-up (SU) quantifying computational time reduction.

3. Results

We investigate LDNet performance in predicting left atrial EP under physiological and pathological conditions. Under physiological conditions (varying impulse localizations), the LDNet achieves $NRMSE = 2 \cdot 10^{-2}$, $PD = 5 \cdot 10^{-3}$ and $SU = 2 \cdot 10^{2}$.

In the pathological case, the left atrium is triggered by a train of impulses with varying time intervals applied at a fixed point, and the LDNet achieves $NRMSE = 5 \cdot 10^{-2}$, $PD = 6 \cdot 10^{-2}$ and $SU = 3 \cdot 10^{2}$.

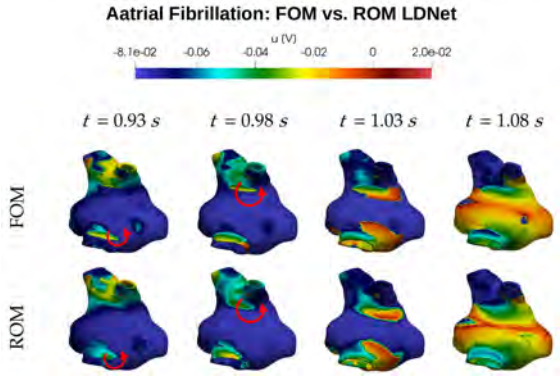


Figure 1: LDNet prediction of reentry circuits timing and localization in a pathological left atrium.

4. Discussion and Conclusions

The LDNets provide accurate approximations in both scenarios in remarkably short computational time. Specifically, the LDNets correctly predict the formation and self-sustainment of localized reentries characteristic of atrial fibrillation.

5. References

1. Regazzoni, F., et al., Nat. Commun., 15(1), 1834 (2024).
2. Courtemanche, M., et al., Am J Physiol Heart Circ Physiol. 275(1), H301-H321 (1998).
3. Africa, P. C., et al., BMC bioinformatics, 24(1), 389 (2023).
4. Akiba, T., et al. , KDD 2019. pp. 2623-2631 (2019).

HIGH SPEED ACUTE CARDIAC INFARCTION SIMULATIONS USING THE NEURAL NETWORK FINITE ELEMENT METHOD

Benjamin J. Thomas (1), Michael S. Sacks (1)

1. James T. Willerson Center for Cardiovascular Modeling and Simulation at The University of Texas at Austin, United States

1. Introduction

Simulations of cardiac disease remains a cornerstone of discovery and treatment development, yet current cardiac simulations remain unsuitable for near real-time clinical decision making due to time-intensive methods. To address this, simulations need to execute in a tractable clinical timeframe (execution times on the order of minutes). Scientific Machine Learning (SciML) exploits recent advances in machine learning to solve physics-based models. We utilized our neural network finite element SciML approach to perform realistic high-speed simulations of the normal and infarcted heart using a comprehensive heart model dataset. We demonstrate the ability to generate high fidelity pressure-volume (PV) and wall stress responses in a matter of 2-4 seconds.

2. Materials and Methods

We utilized a high-fidelity ovine heart dataset, including geometry, fiber structure, surface action potentials, and pressure-volume from a single heart. We extended our SciML "Neural Network Finite Element (NNFE)" method that utilized a finite elements mesh for problem geometry and directly solves the parameter-to-solution map by learning the displacement solution over the physiological range.

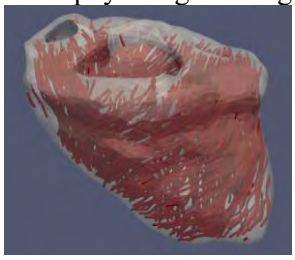


Figure 1: Realistic ovine heart Geometry contracting at end systole.

To simulate myocardial infarction, the training regime was extended to include a range of infarct sizes and anatomical locations. The final JAX-based software platform, termed 'CARDIAX,' required no data as the NNFE method solves the same governing equations by minimizing the same residual that is used in the traditional finite element method.

3. Results

The NNFE neural networks for healthy and infarcted models were trained until the errors over the physiological range were within 0.1% error of the standard FE simulation displacements. This is checked after training and is not used during training. Once trained was completed, the time to evaluate the NNFE cardiac model was approximately 0.15 seconds, with a complete pressure-volume loop in about 1 second. In additional accurate displacement, stress, and strain tensors, the NNFE method was able to accurately predict the effects of randomly size/placed infarcts.

4. Discussion and Conclusions

We demonstrated the ability to learn the normal and acutely infarcted PV loop using a high-fidelity heart model using the 'CARDIAX' NNFE method. We are currently incorporating B-spline geometries allowing patient specific geometries and reduce the problem size to reduce training and execution times.

5. References

1. Motiwale, Shurti, et al. CMAME; 427 (2024): 117060.
2. Sacks, Michael S., et al. J Biomech Engr; 144.12 (2022): 121010
3. Thomas, Benjamin J., et al. Engrxiv preprint; (2025) https://doi.org/10.31224/4923

Acknowledgements:

The authors would like to thank the National Institutes of Health (NIH R01HL184128) for providing financial support to this project.

PATIENT-SPECIFIC 1D–3D SIMULATIONS OF BLOOD AND CONTRAST FLOW IN STENTED VENOUS SEGMENTS

Marco Baragona (2), Waïl Mhaouch (1), Pauline Haulez (1)
Arjen van der Horst (2), Sergei Shulepov (2), Josep-Maria Armengol Collado (2)

1. Eindhoven University of Technology, The Netherlands; 2. Royal Philips, The Netherlands

* Correspondence: *marco.baragona@philips.com*, HTC33 Eindhoven, The Netherlands

1. Introduction

Annually, approximately 1 in 1000 adults are affected by deep vein thrombosis (DVT), a condition that can lead to severe disability or even death if left untreated [1]. While several treatment options exist, the recurrence rate of DVT is high, with 1 out of 10 iliac veins stents reoccluding within the first year [2]. In this work we aim at developing numerical tools to support the identification of hemodynamic and anatomical predictors of venous stent failure.

For this purpose, accurate prediction of blood flow and contrast agent propagation requires patient-specific and high-fidelity local models of the stented section. At the same time, the prescription of realistic boundary conditions is essential to retain the complexity of venous circulation distal and proximal to the stented section. Therefore, a multi-scale, coupled framework is needed.

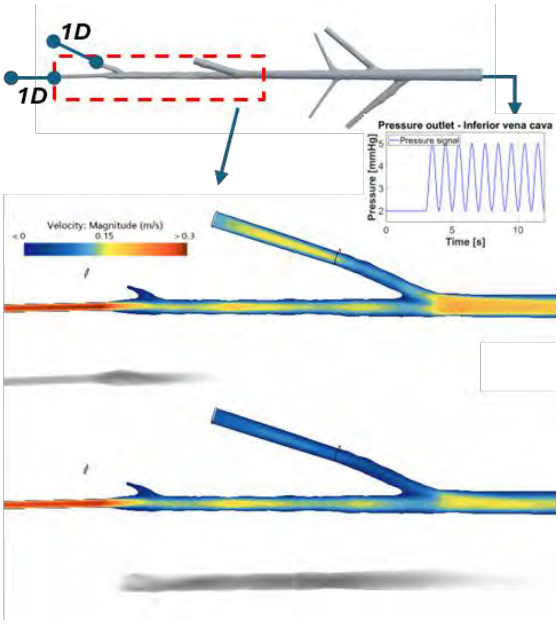


Figure 1: Sketch of the patient- specific model and example of blood velocity and contrast propagation in the local 3D ROI, roughly at the start and at the end of contrast injection (t_1~4s, t_2~6s) for one computed case.

2. Materials and Methods

The local geometry of the stented section is reconstructed using IVUS pullback data and subtraction venography and is used to build a 3D computational fluid dynamics model of venous flow and contrast injection. This local model is coupled at inflow with a simplified 1D tree representing the distal venous tree. For the 3D part, STAR-CCM+ is used. For the 1D part, an in-house code is employed.

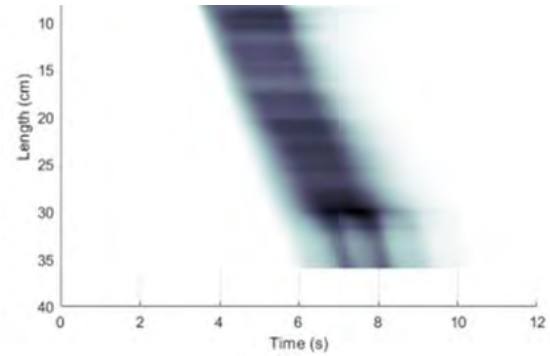


Figure 2: Example of derived numerical contrast transport space-time map from one computed case.

3. Results

Examples of results are shown in Fig 1 and 2 for one exemplary case. The derived contrast map compares well with the map reconstructed from the corresponding patient's digital subtraction venography footage (clinical data not shown).

4. Discussion and Conclusions

The focus of this work is the development of an initial 1D-3D coupling framework. Next steps will improve the efficiency of this coupling thereby allowing more accurate distal and proximal boundary conditions and enabling the generation of clinically actionable insights.

5. References

1. Cushman M, Seminars in Hematology, 44(2):62–69, (2007).
2. Rodrigues, L. D. S. et al., J. Vasc. Surg. Venous Lymphat. Disord., 9(1):275–284, (2021).

COUPLING BAYESIAN INFERENCE AND SENSITIVITY ANALYSIS FOR IN-SILICO THERAPY GUIDANCE OF HYPOTENSION DURING SURGERY

J.-N. Thiel (1), M. Zlicar (2), U. Steinseifer (1), B. Kirn (3), and M. Neidlin (1)

1. Cardiovascular Engineering, Applied Medical Engineering, Medical Faculty, RWTH Aachen University, Aachen, Germany; 2. Clinical Department of Anaesthesiology and Intensive Therapy, University Medical Centre Ljubljana, Ljubljana, Slovenia; 3. Institute of Physiology, Medical Faculty, University of Ljubljana, Ljubljana, Slovenia

1. Introduction

Computational cardiovascular models are promising tools for clinical decision support, particularly in complex conditions, such as intraoperative hypotension (IOH). IOH is characterised by a significant decrease in mean arterial pressure (MAP) and may result from vasodilation, hypovolaemia, or reduced ventricular contractility. Treatment options include vasopressors, inotropes, and fluid boluses, making selection non-trivial [1]. Although much research has focused on algorithms to predict IOH, a tool to guide decision-making regarding the most promising intervention strategy is still lacking [2]. Patient-specific predictions require calibration, typically performed using classical optimisation prone to parameter non-identifiability and lacking uncertainty quantification, hindering clinical translation. Bayesian approaches can address these limitations by facilitating parameter inference, sensitivity analysis, and uncertainty quantification in cardiovascular models. This study aims to combine Bayesian inference and sensitivity analysis using derived parameter posteriors to quantify uncertain-ties and assess their impact on patients' systemic pressure and cardiac output (CO) in response to various IOH treatments in different pathological scenarios.

2. Materials and Methods

The cardiovascular lumped parameter model (LPM) describes the heart and systemic and pulmonary circulation, with inputs representing ventricular contractility (Emaxlv), vascular resistance (Rmc), blood volume change (TBV) and heart rate, and outputs including MAP and CO. We utilize Bayesian Markov chain Monte Carlo (MCMC) to estimate parameter distributions of the LPM across different IOH scenarios. To this end, a reduced-order model was trained to enable efficient MCMC sampling. We improve parameter reliability by incorporating clinical knowledge and measurement uncertainties. Continual learning of the model is achieved by sequential parameter updating as new patient data become available. We introduce an uncertainty-aware sensitivity analysis and compare it with a classical optimisation. Figure 1 shows an overview of the implemented pipeline.

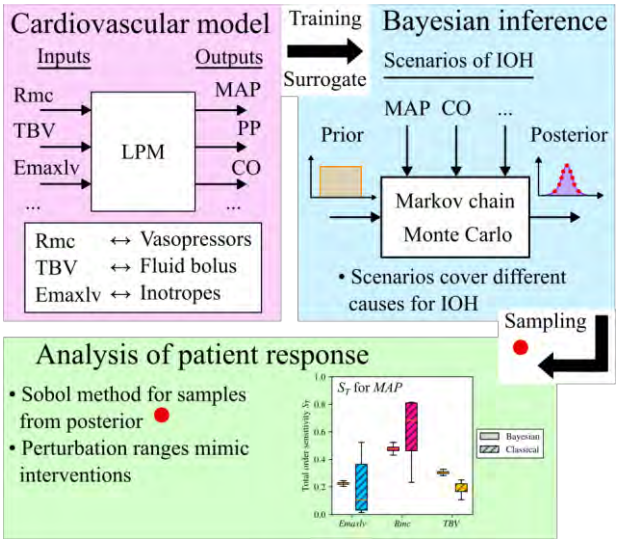


Figure 1: Overview of methods used to obtain uncertainty-aware sensitivities for hypotension therapy guidance.

3. Results

Classical optimisation yielded 28 local solutions for IOH, with notably different sensitivities, confirming unreliable therapy guidance from single-point estimates. MCMC identified physiologically meaningful parameter shifts across IOH scenarios, including impaired contractility and hypovolaemia. Parameter uncertainty decreased by about 70% with additional measurement data, and by up to 94% with sequential updating. Propagating uncertainties from MCMC through sensitivity analysis provided tighter credible intervals, resulting in more stable parameter rankings than the classical optimisation.

4. Discussion and Conclusions

Combining Bayesian inference with sequential updateing and sensitivity analysis enhances the reliability of parameter estimates and reveals scenario-dependent treatment suggestions, highlighting the potential for therapy planning. As this study uses synthetic data, the next step is validation with real patient data.

5. References

1. Kouz K. et al. Indian J Anaesth. http://dx.doi.org/10.4103/ija.IJA_939_19. 2020.
2. Hatib F. et al. Anesthesiology. http://dx.doi.org/10.1097/aln.0000000000002300. 2018.

REDUCED ORDER MODELS FOR REAL-TIME PATIENT-SPECIFIC CARDIOVASCULAR SIMULATIONS VIA WEBSERVER

Gianluigi Rozza (1)

1. SISSA Mathlab, Trieste-Italy

1. Introduction

Cardiovascular diseases are among the leading causes of death worldwide, motivating ongoing research efforts toward the development of patient-specific computational tools. Numerical simulations of blood flow have shown great potential to support clinical decision and surgical planning. However, the complexity of cardiovascular systems often results in prohibitive computational costs, limiting their applicability in clinical settings.

To this aim, we focus our attention on the study of Reduced Order Models (ROMs) [1, 2], which are designed to reduce the computational cost of complex dynamics associated with real-world applications. The ATLAS [3] web platform reflects the integration of models and data, facilitating the use of ROMs into clinical practice.

2. Materials and Methods

This contribution explores the application of advanced computational methodologies for cardiovascular modelling. Full order models are employed to describe blood flow dynamics, accounting for patient-specific geometries and physiological parameters. To overcome the associated computational burden, intrusive and non-intrusive ROMs are introduced as an efficient surrogate modelling approach.

The procedure is divided into two stages:

• the **offline** stage performs computationally expensive tasks only once. These include the computation of the reduced basis space and the definition of a mapping between the parameter space and the modal coefficients. It is noteworthy to point out that the modal coefficients depend only on the parameter while the reduced basis space does not depend on it.

• The **online** stage enables rapid evaluations as the linear combination between the modal coefficients corresponding to a new parameter and the reduced basis space.

To enhance the accessibility of these computational tools within the medical community, we introduce ATLAS. By simplifying the interaction with complex numerical models, the platform would allow clinicians to perform patient-specific evaluations on standard hardware, potentially integrating ROMs into the daily hospital routine.

3. Results

ROM-based strategies enable reductions in computational time while maintaining accuracy for patient-specific applications. Several cardiovascular applications are shown on the computational interface ATLAS, including the simulation of blood flows in coronary/carotid arteries, left atrium and aorta [4, 5].

4. Discussion and Conclusions

The approaches presented demonstrate that the integration of ROMs and data significantly enhances the efficiency of cardiovascular simulations. The platform developed aims at spreading the use of ROMs in the medical community. The final goal is to build a tool that can be used in the medical routine as a decision support.

5. References

1. Hesthaven JS, G. Rozza G, Stamm B. Certified reduced basis methods for parametrized partial differential equations. Vol.590. Springer (2016).
2. Benner P, Grivet-Talocia S, Quarteroni A. Model order reduction. Vol 1-2-3, De Gruyter (2021).
3. ATLAS web page: https://atlas.sissa.it/
4. Siena P, Girfoglio M, Ballarin F, Rozza G. Data-driven reduced order modelling for patient-specific hemodynamics of coronary artery bypass grafts with physical and geometrical parameters. Journal of Scientific Computing, 94(2):38 (2023).
5. Girfoglio M, Scandurra L, Ballarin F, Infantino G, Nicolo F, Montalto A, Musumeci F, Rozza G. Non-intrusive data-driven ROM framework for hemodynamics problems. Acta mechanica sinica, 37(7):1183-1191 (2021).

Acknowledgements:

The authors would like to thank the European Research Council (Grant no: 681447) for providing financial support to this project and PoC ATLAS (Life Science FVG Cluster).

EVALUATION OF A DIGITAL TWIN FOR REAL-TIME CARDIAC CONTRACTILITY ESTIMATION USING SYNTHETIC AND *IN VIVO* DATA

S.C. Snijders (1,2), M.C.M. Rutten (1), J.E.M. Sels (3,4), W.A.L. Tonino (1,5), W. Huberts (1,6).

1. Eindhoven University of Technology, NLD; 2. Laurentius Hospital, NLD; 3. Maastricht UMC+, NLD; 4. CARIM, NLD; 5. Catharina Hospital, NLD; 6. University of Amsterdam, NLD.

1. Introduction

Digital twin (DT) technology is revolutionizing various industries and has immense potential in healthcare as well. A human DT is a virtual representation of an individual patient, capable of mimicking the current (patho) physiological state and predicting future states, making it ideal for supporting clinical decision-making. However, its development remains challenging; it must provide real-time estimations, identify unique parameter values, while preserving model stability. The goal of this study was to develop a DT for real-time estimation of left ventricular (LV) contractility based on a reduced-order unscented Kalman filter (ROUKF) [1]. This study is the first to apply a real-time cardiac DT on *in vivo* data.

2. Materials and Methods

The DT is schematically illustrated in Figure 1. It uses a lumped-parameter model of the systemic circulation [2] to provide a model prediction, which is iteratively updated based on the discrepancy between the measurement and prediction itself (recursive algorithm). Every time new data becomes available (after Δt), the output is processed, resulting in an estimated parameter and uncertainty. This DT uses LV pressure p_{LV} as input measurement to estimate the LV contractility c_{LV}, a measure for maximum cardiac muscle strength.

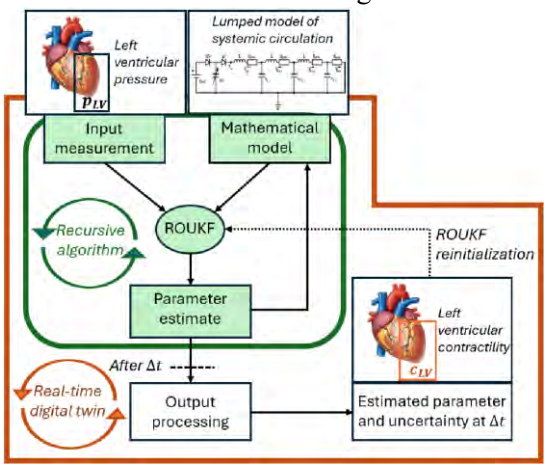


Figure 1: The real-time cardiac digital twin.

The DT was evaluated using both synthetic and *in vivo* p_{LV} measurement data, the latter collected by Johnson et al. (2018) [3]. These data were appropriate for the current study since they contained inotropic state changes leading to variations in c_{LV}. Synthetic data were used to evaluate the DTs performance, and for local sensitivity, identifiability, and stability analysis. *In vivo* data were used to evaluate the DTs applicability to this type of data, which assesses the potential for future clinical application.

3. Results

The DT estimated the true parameter c_{LV} in real-time, remained robust to measurement noise, and tracked parameter changes independent of initial conditions. The parameter estimate was identifiable despite measurement noise, and the mathematical model proved stable within a physiologically realistic range. The DT proved applicable to i*n vivo* data and was able to track inotropic state changes. The estimated parameter c_{LV} followed a similar trajectory as the clinically used contractility proxy ($\frac{dp}{dt}|_{max}$) in multiple patients, while it diverged in others.

4. Discussion and Conclusions

Application to synthetic data illustrates the algorithm's performance and contributes to delivering proof of principle. Applicability to *in vivo* data and ability to track cardiovascular state demonstrated the algorithm's potential for future clinical application. Still, future research is needed in some areas. The ROUKF proved a promising method for the development of a real-time cardiac DT, with the results highlighting its potential for real-time monitoring and personalized medicine.

5. References

1. Moireau P et al., J Comput Phys; 2011; 17(2):380–405
2. Meiburg R et al., Int J Numer Method Biomed Eng 2020; 36(10):1–21
3. Johnson N et al., Eur Heart J; 2018; 39(28):2646–55

INVESTIGATING THE TRANSLATION GAP TO UNLOCK THE POTENTIAL OF DIGITAL TWINS IN HEALTHCARE

Sara Bridio* (1), Giulia Luraghi (2), Jose Felix Rodriguez Matas (2), Gabriele Dubini (2), Francesco Migliavacca (2,3), Maurice Whelan (1)

1. European Commission, Joint Research Centre (JRC), Ispra, Italy; 2. Department of Chemistry, Materials and Chemical Engineering "Giulio Natta", Politecnico di Milano, Italy; 3. Fondazione IRCCS Cà Granda Ospedale Maggiore Policlinico, Milan, Italy

**correspondence: sara.bridio@ec.europa.eu*

1. Introduction

Digital Twins (DTs) have emerged as an innovative technology with the potential to revolutionize healthcare by providing personalized prevention plans, improved diagnosis, and tailored medical treatments. Despite significant investments and promising research outcomes, the adoption of DTs in European clinical settings remains limited [1]. This project aims to investigate the root causes of this misalignment, focusing on cardiovascular health applications, a priority area for the European Union [2] and the health sector where most promising DT solutions have been developed [1]. By examining successful case studies of DT integration in clinical workflows, we aim to identify the key factors that facilitate or hinder the translation of DTs into clinical practice.

2. Materials and Methods

The ongoing analysis involves identifying and interviewing successful startups or spinoffs that have commercialized cardiovascular DT software, as well as their primary buyers, including hospitals and medical professionals. Each interview will gather scientific information about the DT model and insights into the translation process from research to commercial use. Additionally, interviews with medical doctors using the DTs and hospitals' Value Analysis Committees will be conducted to understand the considerations that lead to a positive evaluation of DT products/services in hospital settings. The case studies will cover different stages of pathology management, including prevention, early detection and screening, and treatment and care, and healthcare facilities across various EU geographical areas.

3. Results

Collection and analysis of results are ongoing: the work is currently in the process of identifying and contacting successful case studies. Examples include AI-based ECG monitoring for preventive screening of cardiovascular risks, and patient-specific simulations for planning of vascular surgeries. Previous findings have highlighted that factors such as lack of standardization, regulatory uncertainty, limited clinical validation and uncertain economic impact have hindered the integration of DTs in clinical settings [1]. We anticipate that the analysis of successful case studies will provide valuable concrete insights into effective translation strategies.

4. Discussion and Conclusions

The successful integration of DTs in clinical practice has the potential to transform cardiovascular healthcare by providing personalized and effective prevention schemes, diagnosis and treatments. This project aims to contribute to the development of strategies that can overcome the current translation gap and facilitate the widespread adoption of DTs in European clinical settings. Results of the study will inform policymakers, healthcare professionals, and industry stakeholders about the opportunities and challenges associated with this innovative technology. Ultimately, the project aims to contribute to accelerating the translation of DTs into clinical practice, thereby improving patient outcomes in cardiovascular diseases.

5. References

1. Bridio S et al. Science Progress. 2025; 108(3).
2. https://health.ec.europa.eu/publications/communication-eu-cardiovascular-health-plan-safe-hearts-plan_en

AN INTEGRATED DECISION SUPPORT SYSTEM FOR HYPERTROPHIC CARDIOMYOPATHY DISEASE MANAGEMENT

Nabid Faiem (1), Antti Kallonen (1), Mark van Gils (1)

1. Faculty of Medicine and Health Technology, Tampere University, Tampere, Finland

1. Introduction

Hypertrophic cardiomyopathy (HCM) is a multifactorial disease with a wide range of manifestations. Management of HCM requires decision support for individual stratification, risk assessment, and treatment planning, based on a wide scope of measures. Existing clinical tools lack integration and intuitive visualization of HCM status, limiting possibilities for personalized disease management. There is need for decision support systems that provide actionable insights based on multi-modal data (imaging, -omics, signals and health records) and modern data analysis and modelling approaches.

2. Materials and Methods

A decision support system (DSS) was developed in the EU project SMASH-HCM [1] through an iterative process informed by healthcare professionals from three countries. Initial requirements were collected during the project's first year, followed by development of a prototype. Updated requirements then led to the current system version, which forms the basis of a pilot study evaluating technical performance and clinical value.

From a software perspective, the goal was to create a reproducible and scalable human digital-twin platform integrating data with mechanistic and data-driven models. The architecture follows a separation-of-concerns approach, with distinct data analysis and visualization layers supporting advanced risk stratification and patient-specific disease-progression modelling. Another design philosophy is that it supports seamless combinations of models developed with different programming languages. The delivered system employs a Flask [2] backend and Plotly Dash [3] frontend in separate Docker [4] containers, communicating via REST protocols. This design allows models developed in different programming languages to run locally within containers, or remotely through an API (MEDAI API [5]).

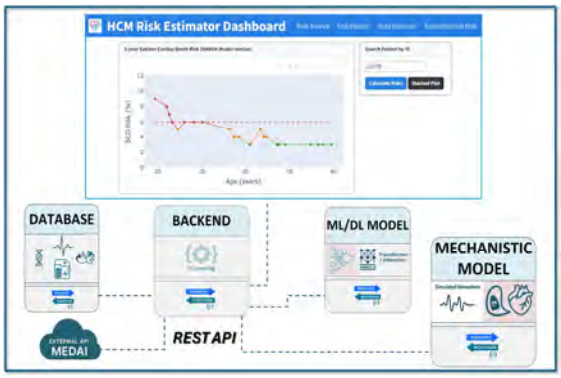


Figure 1: HCM Decision Support System.

3. Results

A decision support system (Figure 1) was co-created with clinical end-users. It has an interface that allows exploration of signal and imaging data together with health record data and visualizes risk model outputs with uncertainty estimates, feature importances, and HCM management recommendations.

The current implementation supports multiple models (e.g., European Society of Cardiology (ESC) sudden cardiac death (SCD) risk score and survival probability models), providing model-based insights for decision-making.

4. Discussion and Conclusions

Before clinical validation, further development will extend functionality with genetic data integration, patient similarity exploration, clustering visualization, and explainable AI. The work establishes a modular, extensible DSS for broader clinical and patient-facing application HCM management.

5. References

1. "SMASH-HCM project" smash-hcm.eu
2. "User Guide Flask." flask.palletsprojects.com
3. "Dash Python User Guide," dash.plotly.com.
4. "Docker Documentation" docs.docker.com/guides/
5. "Pharmatics Ltd." pharmaticsltd.com.

Acknowledgements:

This research study is funded by European Union via the project SMASH-HCM (GA 101137115).

DIGITAL TWIN INTEGRATING MULTISCALE DATA AND MODELS FOR STRATIFICATION OF HYPERTROPIC CARDIOMYOPATHY

Jari Hyttinen[1)], Katriina Aalto-Setälä[1)], Antreas Afantitis[2)] , Felix Agakov[3)] , Alfonso Bueno-Orovio[4)], Torsten Crist[5)], Kathleen Curran[6)], Virginie Le Rolle[7)], Luca Mainardi[8)], Iacopo Olivotto[9)], Stefano Severi[10)], Mark van Gils[1)], Malte vonTotleben [11)]

1)Tampere University.2)NovoMechanisc Ltd, 3) Pharmatics Ltd 4) University of Oxford, 5) University College Dublin, 6)University Klinikum Eppendorf 7) University of Rennes, 8) Politecnico di Milano, 9) University of Florence 10) University of Bologna, 11) Empirica Ltd

1. Introduction

Hypertrophic cardiomyopathy (HCM) is the most common inherited cardiac disorder. It is a multifactorial and multiorgan disease giving rise to a range of symptoms and complications including sudden cardiac death. It has various comorbidities impacting also the circulatory system, which may lead to stroke or many neurological and psychological complications. It affects all age groups, and it is a leading cause of death among young athletes. Multiple causal mutations and variations in cellular processes lead to highly diverse phenotypes and disease progression. HCM is still diagnosed as one single disease, leading to suboptimal care. Better tools for deep phenotyping of patients are needed to produce better assessments of risk and care options. [1] [2]

2. Materials and Methods

The SMASH-HCM EU HORIZON-HLTH-2023-TOOL-05-03 project develops and validates a digital twin platform to support clinicians in better stratification and patient management strategies tailored to individual patient pathophysiology, genotype and phenotype with 8 research partners, 3 hospitals, 4 SMEs, and a global health-technology corporation in collaboration with patients to advance the state of the art in human digital-twins. We integrate data from different scales from human cellular and tissue in-vitro models, in-silico models from molecular manifestation of the disease to patient cellular, tissue, whole heart and finally cardiovascular systemic level models. The in-vitro and in-silico model insight on the disease and drug mechanisms form the foundation on which we build structured clinical and unstructured data-based models with emphasis on explainable artificial intelligence towards better disease

3. Results

New models in all levels of the work was developed, from in-vitro engineered heart tissue with simulated sport challenge to in-silico single cell cardiac and smooth muscle cell models and patient tailored integrated whole heart and cardiovascular system models Further, new data-based models have been developed based on e.g., ECG, genetic data, and nonstructured data. All these are being integrated into a three-level decision support solution with deep phenotyping and risk stratification tools to support clinical workflows and decision making enabling the development of effective personalized treatment and for the patients for their self-management [2].

4. Discussion and Conclusions

SMASH-HCM will provide tools for detailed personalized assessment of the need, risks, and benefits involved, making the identification of the need for ICDs substantially easier. In addition, we will present a well-defined pathophysiology and servers as a paradigm to understand the broader spectrum of hypertrophy, translating to other myopathies and cardiac diseases and beyond. In reaching its goals, SMASH-HCM has potential to serve as a basis for future digital-twin platforms for other cardiac diseases integrating models and data from various scales and sources.

5. References

1. Maron, Barry J., et al. "Diagnosis and evaluation of hypertrophic cardiomyopathy: JACC state-of-the-art review." Journal of the American College of Cardiology 79.4 (2022): 372-389.
2. Panichella, Giorgia, et al. "Artificial intelligence applications in hypertrophic cardiomyopathy: turns and loopholes." *European Heart Journal-Digital Health* 6.5 (2025): 853-867.

Acknowledgements: The author would like to thank the HORIZON-HLTH-2023-TOOL-05-03 – SMASH-HCM (Grant agreement ID: 101137115) for providing financial support to this project and entire project team for their contributions.

CAN MAKING CARDIOVASCULAR SYSTEM MODELS EASY TO CALIBRATE BRIDGE THE GAP TO THE INTENSIVE CARE UNIT?

Finbar Argus(1), Beatrice Ghitti (1), Mohammad Shafieizadegan(1), Alireza Sharifzadeh-Kermani(1), Michelle Gee(2), Stephen Creamer (1), Behdad Ebrahimi(1), Ella Guy(4) James Fisher(3), J. Geoffrey Chase(4), Merryn Tawhai(1), Gonzalo Maso Talou(1)

1. Auckland Bioengineering Institute, The University of Auckland, NZL;
2. University of Delaware, USA; 3. FMHS, University of Auckland, NZL
4. Department of Mechanical Engineering, University of Canterbury, NZL

1. Introduction

Patient care in the intensive care unit (ICU) is often suboptimal due to inter-clinician variability. A personalised model of the cardiovascular (CVS) and respiratory systems could be used to guide care if it responded accurately to dynamic changes due to therapy inputs, such as fluid administration, mechanical ventilator settings, and inotropic drugs.

Many models of autonomic control of the CVS use various forms of Ursino and Albanese model [1]. However, calibration of these models to clinical data has yet to show utility in the ICU. Redesigning and recalibrating complex models that have parameters with unknown physiological ranges, as in Albanese et al., is very difficult. Modules (sub-models for specific physiological mechanisms or anatomical locations) that are easier to calibrate (and couple) would enable creation of CVS models tailored towards specific use-cases that give reliable, patient-specific predictions in the ICU.

2. Materials and Methods

We created autonomic control modules in CellML using PhLynx [2] (GUI for easy coupling of CellML modules) to couple with CVS modules developed in prior work [3]. Modules include non-dimensionalised control parameters that can be related to measurable quantities, so choosing their physiological ranges is more interpretable. Lung module development was guided by models used in the ICU [4].

We developed open source tools in Circulatory Autogen [3] to perform 1. global (Sobol) sensitivity analysis to reduce the parameter set for calibration, 2. identifiability analysis to ensure reliable predictions, and 3. two-stage Bayesian calibration to incorporate both population and individual data. We calibrated to ventilator pressure and flows for varying positive end expiratory pressure (PEEP), CVS response to fluid withdrawal, and CVS/respiratory response to changes in inspired oxygen fraction (FiO2).

3. Results

We demonstrate accurate population response to FiO2 (Figure 1), PEEP, and fluid withdrawal. The second stage of Bayesian calibration for personalisation is underway.

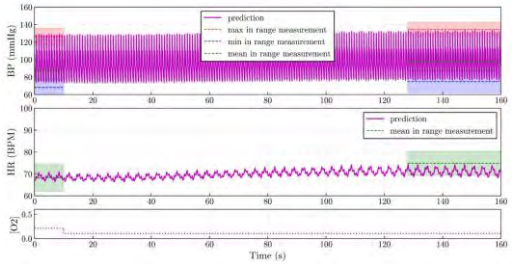


Figure 1: Population calibration to reduced FiO2.

4. Discussion and Conclusions

We developed modules for autonomic control of the CVS, enabling easy calibration to clinical data. These modules were combined and calibrated to create a CVS-respiratory model that dynamically responds to changes in FiO2, PEEP, and fluid volume changes. These developments could enable robust calibration of CVS models to individual patient data, allowing for response prediction and care optimisation.

5. References

[1]Albanese, A. et al. (2016) American Journal of Physiology-Heart and Circulatory Physiology
[2]https://phlynx.com/
[3]Argus, F. et al. (2022). *Frontiers in Physiology*.
[4]Chiew, Y. S., et al. *Ifac-Papersonline* (2018).

Acknowledgements:
UGENT - Vital: Virtual Twins as tools for Personalised Clinical Care (European Commission FP6, Grant no: 101136728)

TOWARDS REAL-TIME TAVR DIGITAL TWINS: 2D NAVIER-STOKES PINN IN STENOTIC FLOWS AND CORONARY ASSESSMENT

Jérôme Gosselin[1], Richard Leask[1], Renzo Cecere[1], Frédéric Couët[2], Sébastien Lalancette[2], Rosaire Mongrain[1]

1. McGill University, Montreal, QC, Canada; 2. Haemonetics Quebec, Quebec, QC, Canada

1. Introduction

During TAVR (Transcatheter Aortic Valve Replacement), clinicians must make rapid decisions using changing pressure data. As TAVR shifts to catheter-based, minimally invasive procedures, real-time blood flow feedback is crucial. AI-powered Digital Twins can assist[1], but traditional computational fluid dynamics (CFD) is too slow for immediate use[2]. Physics-Informed Neural Networks (PINNs), which blend fluid dynamics with deep learning, deliver results much faster[3]. This paper develops a two-dimensional PINN to model stenotic flow, demonstrating the integration of physics principles and CFD data for real-time applications in TAVR and coronary care as a first step.

2. Materials and Methods

To generate a CFD reference dataset, we solved the Navier-Stokes equations for blood-like fluid flow in a 2D axisymmetric domain with a cosine-shaped constriction and variable diameter. We trained a neural network (deep MLP) to predict velocity and pressure fields using (r, z) coordinates, Reynolds number and diameter profile as inputs. As proof of concept, the network was trained using a data-driven loss function derived from 750 CFD simulations, as well as incorporating explicit PDE residual constraints (Momentum and Continuity) enabling assessment of its ability to learn pressure-velocity relationships.

3. Results

The PINN successfully reconstructed the complex 2D axisymmetric velocity fields and pressure gradients across the stenotic domain. Compared to the CFD ground truth, the model demonstrated robust predictive accuracy on a test set of 113 simulations, yielding a mean Root Mean Square Error (RMSE) for pressure of 8.29×10^{-1}Pa (~0.0064 mmHg) and 5.55×10^{-3} m/s for the axial velocity. Figure 1 displays one typical example of the pressure and axial velocity contour plots.

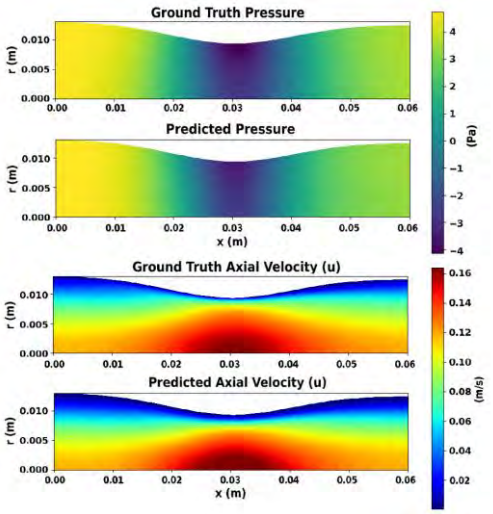


Figure 1: Typical result of a flow through a 20-30% severity stenosis (Re = 413)

4. Discussion and Conclusions

Accurate hemodynamic reconstruction shows AI's promise to generate real-time pressure metrics, essential for TAVR Digital Twins (DT). Although aimed at TAVR, this 2D stenosis model also applies to coronary circulation. By quickly estimating the pressure drop (ΔP), the PINN acts as a modern surrogate for classic models like the Gould equation[4]. This work establishes a computational foundation for coronary DTs[5], allowing rapid, non-invasive assessments such as virtual FFR, and paves the way for advanced TAVR DTs.

5. References

1. Asciak L. et al., Digit Med. 2025; 8(1):32 (2025)
2. Tahir A. M. et al., J. Clin. Med. 2023, 12(14), 4774 (2023)
3. Arzani A. et al., Phys Fluids. 2021; 33(7): 071905 (2021)
4. Gould KL, Lipscomb K, Am J Cardiol. 1974; 34(1): 48-55 (1974)
5. Kissas G. et al., Comput Methods Appl Mech Engrg. 2020; 358: 112623 (2020)

Acknowledgements:
The authors would like to thank Haemonetics Quebec for providing financial support to this project.

AN OPTIMIZATION FRAMEWORK FOR DESIGNING MECHANICALLY INFORMATIVE SOFT TISSUE EXPERIMENTS

Uzair Manack (1, 2), Benjamin Alheit (1), Nele Famaey (2), Mathias Peirlinck (1)

1. TU Delft, Department of Biomechanical Engineering, The Netherlands; 2. KU Leuven, Department of Mechanical Engineering, Belgium

Correspondence to: Uzair Manack, TU Delft, 2628 CD Delft, The Netherlands. Email: u.manack@tudelft.nl

1. Introduction

"Material Testing 2.0" (MT2.0) [1] combines the use of full-field measurement techniques and inverse material model calibration methods [2] to design experiments which produce more mechanically informative deformation gradient fields [1]. Ideally, a material model for a soft, biological tissue would be calibrated on a dataset that covers an expected physiological loading range, to accurately represent material behavior when used in a digital twin. Here, we develop an optimization framework which identifies experiments that maximize the coverage of a chosen strain-invariant space, while remaining physically feasible. We apply our framework to bulge inflation experiments with parameterized clamping geometries.

2. Materials and Methods

We quantified the strain-invariant space coverage of an experiment by discretizing a chosen strain-invariant space into a set of cells, and counting the fraction of cells covered by at least one deformation gradient measured during the experiment, which we reproduce using a finite-element model. Considering isotropic, hyperelastic materials, we defined the strain-invariant space as all mathematically admissible combinations of the first (I_1) and second (I_2) invariants of the right Cauchy-Green tensor. We optimize the clamping geometry of the bulge inflation test to maximize the coverage metric over this space. As a preliminary investigation, we parameterized and varied a circle, an ellipse, an oval, and an "*n*-foil". Any geometry which exceeded a maximum allowable strain energy was rejected.

3. Results

Figure 1 illustrates the strain-invariant space coverage for five representative clamping geometries, as well as an idealized dataset that completely covers the admissible region.

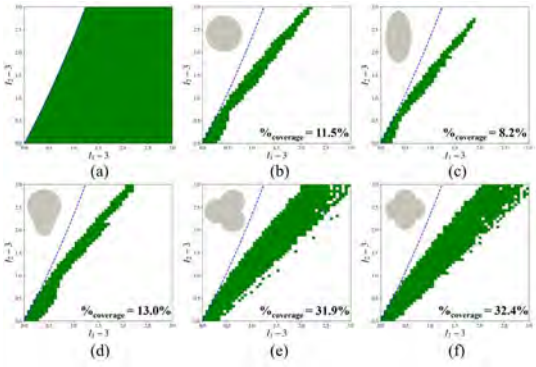


Figure 1: Strain-invariant space coverage maps for the idealized dataset (a), circle (b), ellipse (c), oval (d) and an *n*-foil with $n = 3$ (e) and $n = 4$ (f). The blue lines represent the boundary of the admissible region.

Numerical results showed that strain-field coverage depends on the chosen clamping geometry. Non-circular geometries resulted in larger coverage of the chosen strain-invariant space. In particular, an *n*-foil with $n = 4$ produced a 20.9% increase in strain-field coverage compared to the circular geometry.

4. Discussion and Conclusions

Soft tissue experiments can be systematically designed to produce deformation gradient fields with increased coverage of a prescribed strain-invariant space. Although demonstrated here for bulge inflation tests, the framework can be applied generally to design more mechanically informative soft tissue experiments under MT2.0, which may improve the reliability of inverse material model calibration methods using full-field measurements.

5. References

1. Pierron F, Grédiac M. *Strain*. 2020;57(1):e12370
2. Avril S et al. *Exp Mech.* 2008;48(4):381-402

Acknowledgements:
This project received funding from the European Union's Horizon Europe programme under Marie Curie Grant Agreement No. 101169278.

SINO-ATRIAL NODE MODEL FOR INFERRING AUTONOMIC ACTIVITY FROM HEART RATE VARIABILITY

Changqing Dong (1), Gonzalo Maso Talou (1), Kenneth Tran (1), Finbar Argus (1)

1. Auckland Bioengineering Institution, University of Auckland, New Zealand

1. Introduction

Current methods for inferring sympathetic nervous system (SNS) activity and parasympathetic nervous system (PNS) activity use heart rate variability (HRV) but assume that it is linearly related with SNS and PNS. These approaches cannot reliably separate SNS and PNS activities across physiological states [1]. We present a nonlinear SAN model that predicts norepinephrine (NE) and acetylcholine (ACh) effects on SAN dynamics through to HRV, together with an inverse problem framework for estimating NE and ACh.

2. Materials and Methods

We extend Fabbri's SAN model [2] to accurately simulate NE and ACh effects on human heart rate (HR). The bond graph framework was used to derive the biochemical equations of neurotransmitter stimulation to SAN membrane potential.

This model was implemented in CellML, while calibration (14 parameters, genetic algorithm) and identifiability (profile likelihood) analysis were performed with Circulatory Autogen. We used data from Behar et al. [3] to calibrate and validate SAN response to neurotransmitters.

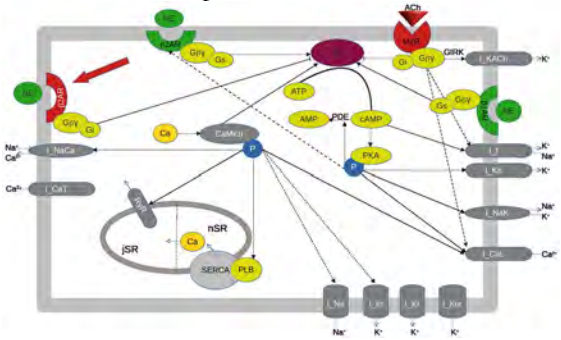


Figure 1: Improved biochemical pathways in SAN cells

After calibration, a virtual trial was performed, in which variability (Gaussian ~5% std) was added to the model parameters to create 10 virtual subjects. Then, synthetic HRV traces were generated for each subject with prescribed NE and ACh concentration traces through time. We then tested our inference problem pipeline using the baseline SAN model and each virtual subject's HRV trace to infer NE and ACh concentration traces and compared against the ground truth.

3. Results

PKA responses to neurotransmitters were predicted with an average 4% error, and HR with 7%, both matching the experimental variability reported in prior studies [3].

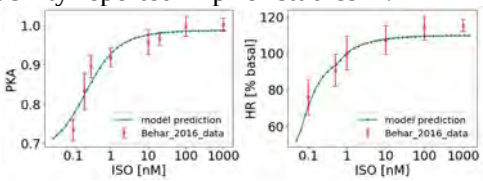


Figure 2: Left: PKA level response to ISO (fitting results); Right: HR firing rate response to ISO (validation results)

4. Discussion and Conclusions

We have demonstrated accurate calibration and validation of a SAN model that responds to NE and ACh. This model will be used in an inverse problem pipeline for inferring NE and ACh from HRV measurements. Future work will investigate the identifiability of this problem and whether including additional wearable measurements (blood pressure, ECG) can reduce uncertainties on estimated NE and ACh.

In addition, each parameter in the proposed model is directly linked to a specific biochemical process, making the framework more physiologically grounded than existing approaches [2][3] for inferring NE and ACh, enhancing interpretability.

5. References

1. Billman GE. Front Physiol. 2011; 2:86 (2011).
2. Fabbri A et al., J Physiol. 2017; 595(7): 2365-2396 (2017).
3. Behar J et al., Front Physiol. 2016; 7:419 (2016).

Acknowledgements:

The authors acknowledge support from the MBIE Catalyst Soul Machines grant and UGENT - Vital: Virtual Twins as tools for Personalised Clinical Care (European Commission FP6, Grant no: 101136728).

A COMPARATIVE INVESTIGATION ON DIFFERENT SOLUTIONS OF 1D MODEL OF BLOOD FLOW

Erfan Vaezi (1), Joaquin A.Hernández (2), Eduardo Soudah (1,2)

1.International Center for Numerical Methods in Engineering(CIMNE), Barcelona, Spain, 2.Universitat Politècnica de Catalunya (UPC), Barcelona, Spain.

1. Theoretical Background

One-dimensional (1D) models have been a primary tool for computational cardiovascular frameworks thanks to their efficiency [1]. These models capture not only pulse wave dynamics, i.e. area, pressure, and volume flow rate, but also systemic responses in complex geometries [2]. Their application includes analysis of wave form propagation through the human arterial network [3] and cardiovascular diseases such as hypertension and stenosis [4]. The vessel domain is defined via cylindrical coordinate (fig.1) as eq. 1 with r, θ, and z as radial, circumferential, and axial directions

$$\Omega_c = \begin{Bmatrix} (r,\Theta,z): 0 \le r \le R(z,t); \\ \theta \in [0,2\pi); z \in (0,L); \Delta t > 0 \end{Bmatrix} \quad (1)$$

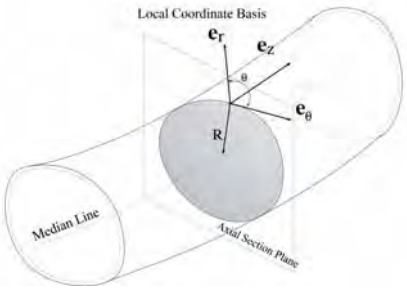


Figure 1: Cylindrical coordinate of the vessel

The model is developed based upon on the following assumptions: (1) The wall displaces along the radial direction; (2) the flow features are independent from the angular coordinate; (3) the velocity components orthogonal to the axial direction are negligible; (4) the pressure is constant on each section; (5) no body force is applied. The conservative form of the 1D model is shown in eq. 2.

$$\frac{\partial \boldsymbol{U}}{\partial t} + \frac{\partial \boldsymbol{F}(\boldsymbol{U})}{\partial z} = \boldsymbol{S}(\boldsymbol{U}),\ z \in (0,\ L),\ t > 0 \quad (2)$$

where $\boldsymbol{U}$, $\boldsymbol{F}$, and $\boldsymbol{S}$ are conservative variables, corresponding fluxes, and source terms as:

$$U = \begin{bmatrix} A \\ Q \end{bmatrix}, S = \begin{bmatrix} 0 \\ -K_R \dfrac{Q}{A} \end{bmatrix}, F = \begin{bmatrix} Q \\ \alpha \dfrac{Q^2}{A} + \dfrac{\beta}{3\rho A_0} A^{3/2} \end{bmatrix}$$

Where A and Q are area and volume flow rate. α, β, ρ, A_0, and K_r are physical parameters.

2. Research Methodology

Considering the importance of computational cost, accuracy, stability, and implementation complexity in numerical simulations, this work presents a comparative study of different approaches for solving the 1D blood flow model. In particular, both knowledge-driven and data-driven paradigms are investigated. Classical physics-based numerical methods, including Discontinuous Galerkin and Taylor-Galerkin (FEM), are compared with a data-driven approach based on Physics-Informed Neural Networks (PINNs) to solve the governing system of equations. To provide a detailed assessment, the following aspects will be discussed:

Table 1: Classification of assessment criteria

Theoretical Foundation	Overall performance
Order of accuracy Stability analysis	Wall-clock time Memory usage PINN-specific analysis
Convergence	Stability Analysis
Spatial convergence Temporal convergence Error distribution	Parameter sensitivity Long-term integration

3. Benchmark Selection

In order to provide a detailed analysis, the following benchmarks will be investigated:

1. Single uniform vessel: Assess accuracy and speed for simple wave propagation
2. Vessel with sniff sources: check stability in small arteries (high K_R)
3. Tapered vessel: Test adaptability in spatially varying A_0 and β.

Different benchmarks provide a full understanding on limitations and strength of each numerical method.

4. References

1. Soudah E et al., Comput Mech. 2014; 56: p. 1013-1022.
2. Kim D, Tithof J, 2025, arXiv:2508.18484v1
3. Wang X, PhD thesis, Universit´e Pierre et Marie Curie-Paris VI (2014)
4. Pfaller, M.R. et al., Int. J. Numer. Meth. Bio. 38(10), 3639 (2022)ICCS 2009 conference: Springer; 2009. p. 705-14

Acknowledgements: Proyecto PID2024-157828OB-I00 financiado por MICIU/AEI/10.13039/501100011033MICIU/AEI/10.13039/501100011033 y por FEDER.

PREDICTING POST-TEER HEMODYNAMICS IN MITRAL REGURGITATION USING PATIENT-SPECIFIC MODELLING

Juliana Franz[1,2], , Fabian Barbieri[2,3], Vasileios Exarchos[2,3], Katharina Vellguth[1,2], Jan Brüning[1,2], Arina Borzistaia[1,2], Markus Reinthaler[2,3], Titus Kühne[1,2], Leonid Goubergrits[1,2]

1. Deutsches Herzzentrum der Charité, Institute of Computer-assisted Cardiovascular Medicine, Berlin, Germany; 2. Charité - Universitätsmedizin Berlin, Berlin, Germany; 3. Deutsches Herzzentrum der Charité, Department of Cardiology, Angiology and Intensive Care Medicine, Berlin, Germany

1. Introduction

Transcatheter edge-to-edge repair (TEER) is a minimally invasive treatment option for patients with mitral regurgitation (MR) who are at high surgical risk. Currently, there are only limited pre-procedural planning tools available, such that decision-making for optimal device placement often occurs intra-procedurally. This can prolong intervention times and increase the risk of suboptimal outcomes. The aim of this study is to develop and evaluate a patient-specific computational model for fast, scenario-based prediction of post-TEER hemodynamics to support treatment planning and risk assessment prior to device placement.

2. Materials and Methods

A lumped parameter model of the cardiovascular system was implemented that simulates clinically relevant hemodynamics, including MR volume, left ventricular stroke volume, left atrial pressure and mitral valve pressure gradients. We personalized the model parameters to the pre-TEER state of 20 patients using intra-procedural data from transoesophageal echocardiography and invasive pressure recordings. A post-TEER model scenario was created for each patient, where mitral valve model parameters were adjusted to reflect the clinically observed changes in geometry, while arterial model parameters were modified to maintain arterial pressures at pre-TEER levels. Model predictions of post-TEER hemodynamics were compared to intra-procedural measurements following device implantation. A proof-of-concept risk assessment for post-interventional mitral valve stenosis was conducted for each patient by simulating 16 different post-TEER scenarios with varying degrees of remaining mitral valve area and MR reduction, and evaluating their impact on mitral valve pressure gradients.

3. Results

The developed model reproduced key pre-TEER hemodynamic features across all patients. Post-TEER model predictions reflected typical hemodynamic trends reported after TEER, such as reduced left atrial v-wave pressure and increased mitral valve pressure gradients. However, a direct comparison with individual patient measurements was limited by the physiological variability in the patients' cardiovascular state at the time of measurement. The 16 post-TEER simulations per patient conducted for the stenosis risk assessment were completed in a matter of minutes, demonstrating the model's potential for a fast exploration of different treatment scenarios. Mean mitral valve pressure gradients reached values >5mmHg in scenarios with severe reduction in mitral valve area, highlighting the potential use for identifying stenosis risk.

4. Discussion and Conclusions

The proposed patient-specific modelling approach enables the rapid simulation of post-TEER hemodynamic trends and may support identification of high-risk configurations prior to device placement. With further development – such as enabling predictions based solely on non-invasive data and integration of virtual device placement models – this approach holds promise as a decision-support tool for TEER planning.

Acknowledgements:
Part of this study was funded by Philips.

INFLUENCE OF AORTIC ARCH MORPHOLOGY ON CARDIOGENIC EMBOLIC STROKE RISK: A CFD-BASED FRAMEWORK

Carlo Bettinelli (1), Ione Ianniruberto (1), Fabio Morelli (1,2), Younes Tatari (3), Amirhossein Arzani (3), Daniela Mazzaccaro (2,4), Emiliano Votta (1), Francesco Sturla (2,1)

1. Politecnico di Milano, Milan, Italy; 2. IRCCS Policlinico San Donato, San Donato Milanese; 3. University of Utah, Salt Lake City, USA; 4. Università degli Studi di Milano, Milan, Italy

1. Introduction

Transcatheter aortic valve implantation (TAVI) is associated with the risk of ischaemic cerebrovascular events, e.g., stroke, caused by embolic debris transport through the aorta up to the brain [1], with aortic arch morphology potentially playing a key role. Herein, a CFD-based computational framework was developed to investigate the influence of aortic arch anatomy on the embolic transport to the brain.

2. Materials and Methods

Geometrical models of different arch types (2 Type I, 1 Type II, 2 Type III) were reconstructed from CT imaging in Mimics Medical (Materialise) and discretized into tetrahedral elements in ANSA (BETA CAE Systems). Transient CFD simulations were run in SimVascular assuming rigid aortic wall and Newtonian, incompressible blood. Pulsatile flow-rate waveforms from 4D Flow were imposed at the inlet, through the *in vivo* 3D velocity profile and through a plug-shaped one. A three-element Windkessel model was coupled to the 3D domain at each outlet and tuned using a lumped-parameter approach in svZeroDSolver to reproduce physiological aortic flow split [2].

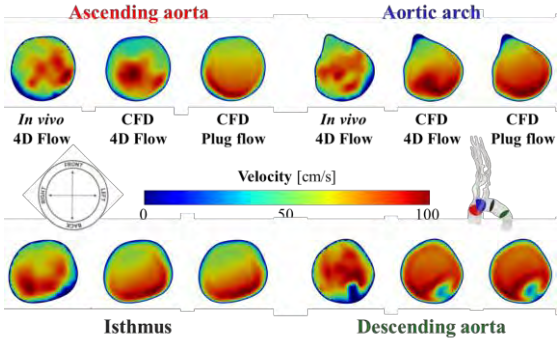


Figure 1: Comparison of CFD results with 4D Flow MRI data in a patient.

Debris embolic pathways were predicted through Maxey-Riley particle tracking using FlowVC [3] seeding spherical particles (diameter 0.325 - 1.25 mm; density 0.8 - 1.45 g/cm^3) at the aortic inlet during the systolic acceleration phase.

3. Results

CFD reliability, evaluated *vs.* 4D Flow MRI ground-truth data and target flow-split percentages, showed good agreement with patient-specific velocity fields and properly reproduced the physiological flow distribution across the aortic arch (**Fig. 1**). Particle tracking showed that heavier particles predominantly remained within the aortic arch, whereas lighter particles were more likely to enter the supra-aortic branches.



Figure 2: Terminal position of small thrombotic particles (diameter, 325 µm; density, 1.06 g/cm^3).

Debris distribution was similar in Type I and Type II arches, while Type III arches showed preferential embolization toward the left subclavian artery. The plug-flow inlet profile produced particle distributions comparable to those produced by the in vivo velocity profile.

4. Discussion and Conclusions

Although requiring further validation, CFD-based particle tracking shows promise for assessing cerebral embolic risk and clarifying the role of aortic arch morphology.

5. References

1. Postolache et al., JCM, 2023;12(17): 5645
2. Ruggeri et al., Comput. Biol. Med, 2025;194: 110493
3. Shadden et al., Ann Biomed Eng, 2014; 43, 41-58

Acknowledgements: IRCCS Policlinico San Donato is a clinical research hospital partially funded by the Italian Ministry of Health.

SEMI-AUTOMATED GENERATION OF SURGICAL BAFFLE GEOMETRY FOR BIVENTRICULAR REPAIR

Elena S. Martinez (1), Alexander D. Kaiser (1), Alexander K. Reed (1), Sascha W. Stocker (1), Amit Sharir (1), Perry S. Choi (1), Shiraz A. Maskatia (1), Michael R. Ma (1), Alison L. Marsden (1)

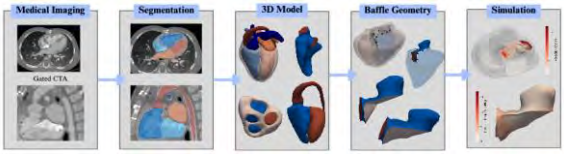
1. Stanford University, United States

1. Introduction

Congenital heart disease is a leading cause of infant mortality and long-term morbidity worldwide, with substantial impacts on quality of life and healthcare systems. Double outlet right ventricle (DORV) is a complex congenital heart defect in which biventricular repair often requires construction of an intraventricular baffle connecting the ventricular septal defect to the aorta to restore physiologic left ventricle-to-aorta outflow. Because of substantial anatomical variability, baffle design is typically performed intraoperatively, and preoperative planning remains largely qualitative.

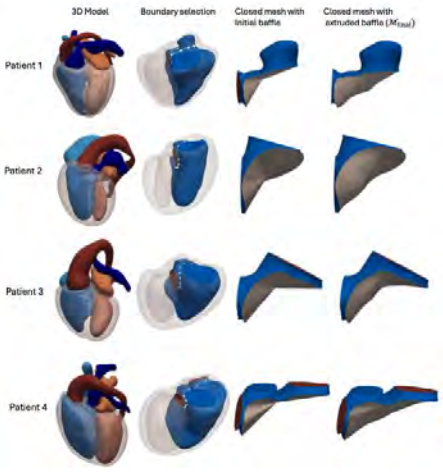
2. Materials and Methods

We present a semi-automated computational framework for patient-specific design and evaluation of intraventricular baffles in DORV. Clinical imaging is processed using machine learning-assisted segmentation to generate patient-specific three-dimensional anatomical models. The framework constructs a ventricular septal defect-to-aorta flow pathway while preserving native ventricular geometry and modifying only the baffle region using physiologically guided geometric constraints. The reconstructed anatomy is integrated into a closed computational domain for computational fluid dynamics (CFD) analysis.



3. Results

We retrospectively applied this pipeline to a cohort of DORV patients who previously underwent biventricular repair. For each case, patient-specific baffle geometries were generated and assessed using CFD to evaluate flow patterns and pressure gradients across the reconstructed outflow tract. Predicted pressure drops were within clinically acceptable ranges and consistent with available postoperative measurements.



4. Discussion and Conclusions

By combining machine learning-based anatomical reconstruction with physics-based hemodynamic simulation, this framework enables quantitative preoperative evaluation of candidate repair strategies. The approach represents a step toward patient-specific decision support for biventricular repair planning in DORV.

5. References

1. Kong F et al., Medical Image Analysis, 97, 2024.
2. Vigil C et al., The annals of Thoracic Surgery; 111(6): 2078 – 2082, 2021.
3. Kaiser, A. et al. JTCVS Open, 28: 434-443, 2025.

Acknowledgements:

The authors would like to thank the National Science Foundation (DGE-2146755 and 2310909), NIH/NHLBI (R01HL173845, K25HL175208, and R38HL143615), the American Heart Association (24CDA1272816), the Stanford Maternal and Child Health Research Institute, and the Stanford Cardiovascular Institute.

MACHINE LEARNING SURROGATE MODEL FOR HIPSC CARDIOMYOCYTE ELECTROMECHANICS

Olli Ylinen, Antti Ahola, Ossi Noita, Jussi Koivumäki, Jari Hyttinen

Computational Biophysics and Imaging Group, Faculty of Medicine and Health Technology, Tampere University, Finland

1. Introduction

Computational modelling of human induced pluripotent stem cell–derived cardiomyocytes (hiPSC-CM) enables fast and affordable experiments compared to in vitro. Experiments such as reviewing of drugs and specific drug effects, modelling of diseases and unique patients can be explored with computational models.

In computational models of cardiac electrophysiology and mechanics often the interest is in the state where the beats are identical over time, the steady state. Achieving this steady state with the current differential equation-based models can take tens of seconds in real time for a single model. However, in situations with numerous evaluations, this can be computationally exhausting. While computation time can be shortened by parallelization, solving differential equations is impractical to parallelize for large number of calculations. One solution to this is the use of surrogate models, an alternative way to calculate the equations, that specifically estimate the steady state, skipping most of the calculations [1]. Here we developed a surrogate model that estimates a hiPSC-CM model [2] response traces for accurate estimation of the steady state and be fast to run.

2. Materials and Methods

The convolutional neural network based surrogate model responds to 22 different parameter multipliers which include parameters for conductance and time dependencies of ion channels. The model outputs 1.5 second traces of the steady state of the action potential, Ca^{2+} transients, active tension, L-type Ca^{2+} current and rapid delayed rectifier K^{+} current. The data for training, validation and testing was generated with population of models approach [3] with Forouzandehmehr hiPSC-CM model [2].

3. Results

We achieved average absolute errors for each of the model outputs of less than 1% of average amplitudes. The model runtime using a modern laptop CPU decreased around 1000 times compared to the differential equation model. Utilizing a GPU the surrogate model runtime decreased an additional 10 times compared to CPU.

4. Discussion and Conclusions

This shows the potential of machine learning based surrogate modelling for models in hiPSC-CM in silico studies for considerable runtime decreases with the cost of small errors in the estimates of cardiomyocyte electrophysiology and contraction. The surrogate models can leverage fast calculation times even in cases with numerous input and output variables - as an example here with 22 input variables and main electrophysiology, Ca^{2+} and contractility output.

These types of surrogate models could be used in any situation where the model needs to be ran a lot of times. This is essential in optimizing parameters with multiple input variables such as in population modelling like in drug or disease models, sensitivity analysis or construction of larger structures of cells.

5. References

1. Thomas Grandits, et al. (2024) eLife 12:RP91911
2. Forouzandehmehr M, et al. Dis Model Mech. 2014;17(4):dmm050365
3. Ossi Noita, et al (2025) POM tool. https://github.com/TAU-CBIG/POMtool

Acknowledgements:

The study is part of SMASH-HCM project, and receives funding from the European Commissions Horizon Europe Programme under grant agreement number 101137115

AI-DRIVEN HEART FAILURE RISK PREDICTION FROM ECG VERSUS TRADITIONAL CLINICAL RISK MEASURES: WHICH PERFORMS BETTER?

Xuelong An (1)*, Weijie Sun (2), Sunil V Kalmady (2), James A White (3), Andy J Swift (1), Russell Greiner (2), Padma Kaul (2), Chen (Cherise) Chen (1)*

1. University of Sheffield, UK; 2. University of Alberta, Canada; 3. University of Calgary, Canada

**Corresponding authors: {xan4, chen.chen2}@sheffield.ac.uk*

1. Introduction

Heart failure (HF) remains a major public health challenge, affecting an estimated 64 million people worldwide. Accurate risk stratification among patients with prior cardiovascular disease is therefore critical for early intervention. Recent advances in artificial intelligence (AI) have shown its potential to capture subtle patterns from electrocardiograms (ECG) to predict the risk for future heart failure (HF), benefiting from the availability of large-scale datasets and computing power. However, it remains unclear how well such a data-driven approach performs compared with traditional clinical risk scores based on clinical, medication, and laboratory measurements, especially on unseen populations.

2. Materials and Methods

Our study focuses on patients with prevalent myocardial infarction and/or hypertension, a clinically important group for potential HF. We first developed an AI-ECG-HF model, which takes the 12-lead ECG median waves, age and sex as input, and predicts the risk score for future HF events. To train the AI model, we used the public Harvard–Emory dataset [1], where the model was trained on 168,925 subjects and validated on 18,769 subjects. We then compared our model against 3 established clinical risk scores which rely on clinical, medication, and blood biomarker variables: Health ABC [2], WATCH-DM [3], and the modified PCP-HF [4] on an external cohort (N=18,292) from the UK Biobank (UKB) to assess its clinical value on unseen population. We report model performance for 5-year HF onset using Harrell's C-index.

3. Results

Our model achieved a C-index of 0.765 [95% confidence interval (CI) 0.756-0.773] on the Harvard-Emory dataset and 0.762 [95% CI 0.732-0.792] on the external UKB dataset, which significantly outperformed the three clinical risk scores by a large margin, see detailed scores in the below Figure 1.

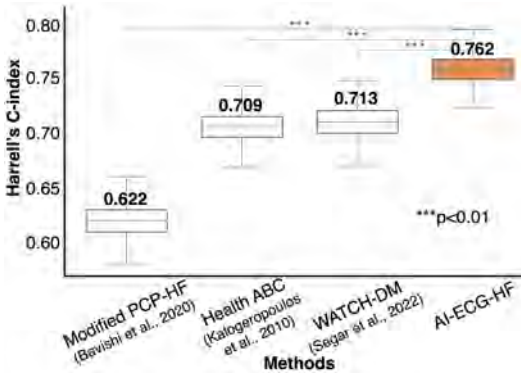


Figure 1: HF Risk Prediction Results. Performance evaluated on the UKB cohort using the three traditional approaches and our AI approach.

4. Discussion and Conclusions

Surprisingly, our AI-ECG-HF model demonstrated strong performance for HF risk stratification on the unseen UK biobank population, even though the model was purely trained from the US population (Harvard-Emory). Our study shows that the AI model can outperform conventional risk scores with more accurate risk stratification. These findings suggest that AI can unlock the prognostic value of ECG to achieve improved HF risk stratification, which could serve as a scalable and cost-efficient tool for early prevention and intervention of HF.

5. References

1. Koscova, Z. et al., Sci Data 2026
2. Kalogeropoulos, A. et al., Circ Heart Fail 2019; 3(4).
3. Segar, M. W. et al., J Am Heart As 2022; 11(11)
4. Bavishi, A. et al., Circ Heart Fail 2020; 13(11)

Acknowledgements:

This research is supported by University of Alberta and University of Sheffield Seed Grant (X/016279-1). A.J. is supported by the British Heart Foundation grant (SP/F/23/150050).

A METHODOLOGY FOR DESIGNING OPTIMIZED PATIENT-SPECIFIC BONE SCAFFOLD FROM ROUTINE CLINICAL IMAGES

Nerea Olivera Jurjo (1), Luca D'Andrea (1), Elisa Zamengo (2), Pasquale Vena (1)
1. Politecnico di Milano, Italy; 2. Ludwig Boltzmann Institute of Osteology and AUVA, Austria

1. Introduction

The number of patients suffering from bone pathologies is steadily increasing. These conditions can lead to critical bone defects that may ultimately result in fracture of the affected bone. As a common diagnostic approach, clinical imaging techniques such as Computed Tomography (CT) are routinely performed to assess the affected area. In this study, a methodology is presented that allows the mechanical characterization of the affected bone region and the evaluation of the morphology and dimensions of the defect based on routine clinical images. The objective is to design a patient-specific bone scaffold that best fits the defect and optimize the mechanical performances. The proposed methodology is applied to a specific clinical case: a calcaneus presenting a 6 cm defect caused by a bone cyst.

2. Materials and Methods

The methodology developed to address the present problem is the following. First, DICOM images form a CT are used as input. The images are segmented distinguishing trabecular bone, cortical bone, and the defect region. The segmented data were then converted from a gray-scale pixel to hexahedral mesh. Each element was assigned linear elastic material properties based on the Hounsfield Unit (HU) of the corresponding pixel using micromechanical models, specifically the Hellmich and Zhu [1,2] models for cortical and trabecular bone, respectively. Subsequently, several scaffold designs were generated by varying different design parameters. Finally, the mesh volumes were imported into finite element solvers ParOSol and Abaqus, where boundary conditions were applied based on a prior literature review. In this study, the three gait phases were considered and compared in the pathological case, the physiological case, and the pathological case with the scaffold implanted.

3. Results

The mechanical properties were successfully assigned to the studied bone (Figure 1). The resulting Young's modulus values ranged from 19.4 MPa for cortical bone to a minimum of 0.5 MPa for trabecular bone. A biomechanical model of the bone-scaffold system was successfully developed, incorporating boundary conditions corresponding to specific gait phases. Among the analyzed phases, the push-off phase showed the highest mechanical demand due to the tensile force exerted by the Achilles tendon. The results obtained from the simulations of the defect with the implanted scaffold show that the maximum and minimum principal stresses are reduced, approaching physiological values. Finally, preliminary simulation results for TPMS scaffolds with porosities from 50% to 80% indicate that the scaffold with 70% porosity provides the best mechanical performance.

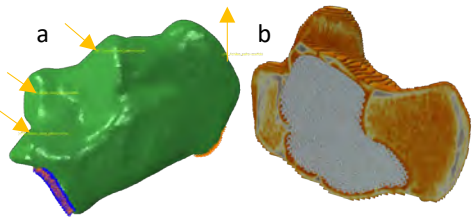


Figure 1: a) Boundary conditions applied to the calcaneus. b) Mechanical properties of the bone calculated based on the literature models [1,2].

4. Discussion and Conclusions

In the present study, a methodology is presented that enables the design of a patient-specific scaffold from routine clinical images, as well as its mechanical evaluation under different boundary conditions. The proposed approach allows the design of different scaffold geometries and their evaluation through *in silico* models in order to identify an optimal configuration that promotes mechanical stability and bone regeneration within an acceptable time frame and without significant additional costs.

5. References

1. Zysset PK, Curnier A. J Biomech. 1996;29(12):1549–1558 (1996).
2. Hellmich C, Ulm FJ. Eng Fract Mech. 2002;69(16–17):1909–1933 (2002).

Acknowledgements:
This study was carried out within the project "End-to-end multidisciplinary optimal design for improved personalized bioactive glass/ceramic bone substitute implants ReBone" funded by the European Union's Horizon Europe research and innovation programme under the Grant Agreement no.101119884.

GENERATING AN ATLAS OF PAEDIATRIC SKELETAL MODELS FOR MORPHOLOGICAL ASSESSMENT

Harriet Talbott (1,2), George Allison (1,2), Atousa Moayedi (1,2), Marta Cohen (1,2,3), Enrico Dall'Ara (1,2), Amaka Offiah (1,2,4), Xinshan Li (1,2)

1. *University of Sheffield, United Kingdom; 2. Insigneo Institute, United Kingdom; 3. Sheffield Teaching Hospitals NHS Foundation Trust, United Kingdom; 4. Sheffield Children's Hospital, United Kingdom*

Corresponding author: Dr Harriet Talbott, Pam Liversage Building, Broad Lane, Sheffield, United Kingdom. Email: h.g.talbott@sheffield.ac.uk

1. Introduction

Infants are children below 1 year of age. Understanding of morphological development of the infant skeleton is limited, due to the scarcity of data. This study aimed to develop the first 3D dataset of infant bones to enable morphological assessment for improved understanding of early bone development.

2. Materials and Methods

Following ethical approval (IRAS: 181203), postmortem CT scans of 79 (32F, 47M) infants and toddlers below the age of 3 years were retrospectively collected. A maximum of 43 bones were semi-automatically segmented from each CT scan in Simpleware ScanIP; including the long bones, pelvis, scapula, clavicles, sternum and ribs.

Of the original cohort, 67 (56 infants) included the long bones of the lower limbs (26F) which were used for the initial morphological assessment, adapted from a study carried out on older children [1]. The morphological measures were carried out on the 3D models in ScanIP.

Four measures were taken from each femur: diaphysis length, trochanter width [2], and epicondyle width and depth. Three measures were taken from each tibia: diaphysis length, condyle width, and malleolar width (Figure 1).

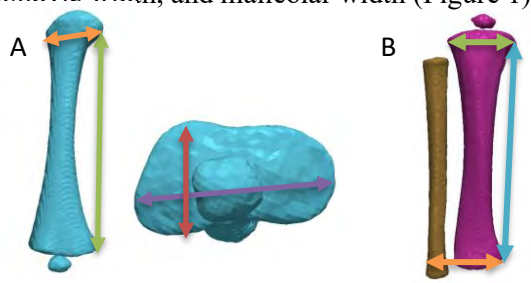


Figure 1: Measurements taken from (A) Femur (distal measures on left) and (B) Tibia

Each measure was assessed for its correlation to age (weeks), and crown to heel length (cm) using Pearson's correlation coefficient in IBM SPSS Statistics ($\alpha = 0.01$).

3. Results

The relationship between age and crown to heel length in infants had a significant positive correlation for both sexes (M: $r = 0.74$; F: $r = 0.601$; $p < 0.001$).

All measures had significant positive correlations with age ($p < 0.001$), although these were even stronger when correlated against crown to heel length. When comparing with age, the strongest correlation was seen in the femoral diaphysis length ($r = 0.86$), and the weakest with epicondyle depth ($r = 0.73$). In contrast, all seven measures had strong positive correlations with the crown to heel length ($0.91 < r < 0.94$). The strongest inter-measures relationship was found between tibial condylar and malleolar widths ($r = 0.99$).

4. Discussion and Conclusions

This study has generated a unique insight into the development of tibiae and femora in infants using morphological measurements obtained from a unique atlas of infant bones, encompassing up to 43 bones. Morphological parameters and representative 3D models of this complete atlas will be made openly available in the future.

5. References

1. Carman et al. (2023) *Sci Rep* **13**, 11733
2. Bertocci et al. (2022) *Clinical Anatomy*, 35(3), 305–315.

Acknowledgements:

The authors would like to thank the radiographers at Sheffield Children's NHS Foundation Trust for providing the CT images, and the EPSRC (Grant number: EP/Z536118/1) for providing financial support to this project.

CHARACTERIZING HEALTHY HIP DEVELOPMENT IN KIDS USING A STATISTICAL SHAPE AND APPEARANCE MODEL

Shoaib Attar (1), Hanna Isaksson (1), Magnus K. Karlsson (2), Carl Johan Tiderius (2) , Lorenzo Grassi (1)

1. Department of Biomedical Engineering, Lund University, Lund, Sweden; 2. Division of Orthopaedics, Department of Clinical Sciences, Lund University, Lund, Sweden.

1. Introduction

Hip dysplasia is characterized by an insufficient acetabular coverage of the femoral head and increases the risk of early osteoarthritis [1]. Hip dysplasia develops sometime during growth, but it is not known at what age it occurs. The aim of this study was to characterize the development of the hip in a healthy paediatric population in 3D using a statistical shape and appearance model (SSAM).

2. Materials and Methods

Bilateral CT scans from 133 children (61 girls and 62 boys, age 6-20 years) were obtained. Each CT was segmented [2], and cortical thickness was mapped (Stradview 7.3). A template volume mesh (~26K nodes, ~140K elements) was warped to the femoral anatomies to create a set of isotopological meshes. Bone mineral density (BMD) was calibrated from Hounsfield units [3] and material properties were mapped (Bonemat V3). Finally, a SSAM was built [4], and subjects were divided into age groups of 6-10, 11-15 and 16-20 years. Caput-Collum-Diaphyseal (CCD) angles were measured for all femurs. Wilcoxon rank sum test was used to identify statistically significant differences between age groups and sex.

3. Results

All first 4 principal components (PCs) of variation and CCD angle changed significantly ($p<0.05$) between youngest and oldest age groups (Figure 1, Table 1). Significant anatomical differences were observed between male and female subjects (Table 1), also when considering each age group separately for both PC scores and CCD angle. Mean CCD angles decreased with age from 131° for the youngest, to 126° for intermediate and oldest age groups.

4. Discussion and Conclusions

The SSAM showed that femoral anatomy changes significantly across age and sex (Figure 1 and Table 1).

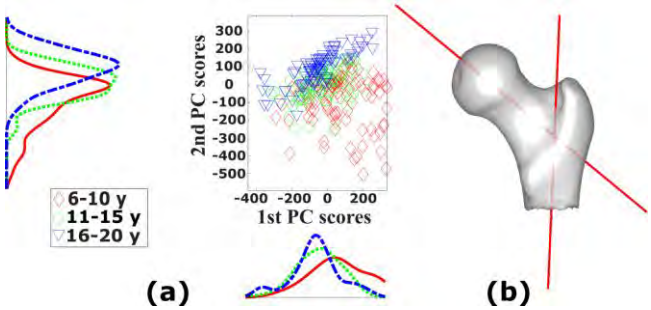


Figure 1: Principal component score plot with distribution for PC1 and PC2 (a), and mean CCD angle (b)

	PC1	PC2	PC3	PC4	CCD
(6-10) vs (11-15)	*	*	-	*	*
(11-15) vs (16-20)	-	*	*	-	-
(16-20) vs (6-10)	*	*	*	*	*
Male vs Female	*	-	-	*	*

Table 1: Statistically significant differences (*) between age groups and sex based on first four principal components (PCs) and CCD angles.

These results highlight the need to characterize healthy and pathological hip development across age and sex. While our SSAM captures the combined variation of shape and BMD, CCD angle measurements showed that shape alone changes significantly as a function of age and sex. Additional work is ongoing to add the pelvis to the current analysis. This will characterize the full hip joint development from an anatomical and biomechanical perspective.

5. References

1. Riedstra, et al., (2023) Seminars in Arthritis and Rheumatism vol. 60 0049-0172
2. Wasserthal et al. (2022) Radiology: Artificial Intelligence 5(5) 2638-6100
3. Szyszko et al., 2024 PLOS ONE 19(6): e0305474
4. Väänänen, S.P., et al., (2015) Med Image Anal 24(1) p125-134

Acknowledgements:
"Swedish Research Council [2022-03474] and Mats Paulsson Foundation".

UNCERTAINTY EVALUATION OF AN ARTIFICIAL INTELLIGENCE MODEL FOR LEG-LENGTH ESTIMATION IN A CLINICAL SETTING.

Margot Ronat (1-2), Sara Beddiaf (1), Rémi Philippot (2), Laurence Cheze (3)
1. ISTP, France; 2. LIBM, France; 3. LBMC, France

1. Introduction

Nowadays, the deployment of AI in the clinical setting has progressively become an everyday reality. A variety of algorithms are explored and applied to datasets, with efforts to select the most appropriate methods for specific contexts, yet questions remain regarding the validation of results and the degree of confidence that can be ascribed to the analyses. The issue of uncertainty quantification has emerged as a major scientific challenge, attracting considerable attention from researchers. In [1], the study highlights the reasons why medical AI models, despite their high performance, remain underutilised in clinical practice. Other investigations [2] emphasise the need to employ metrics more refined to rigorously evaluate model performance in this domain. Several scientific contributions also address classical model limitations and propose more robust approaches [3]; [4] recommends using confidence intervals to improve algorithm reliability in clinical contexts.

In the specific context of sports rehabilitation following Anterior Cruciate Ligament rupture, precise leg-length estimation is essential to complete a dataset (ex: legs stiffness) for assessing the decision to return to sport or not, complemented by quantified uncertainty to support informed and reliable clinical decisions.

2. Materials and Methods

In clinical practice, it can be difficult to measure leg length directly. To overcome this, a dataset from an anthropometric study of adults [5], initially consisting of 25 measurements, was used. After filtering out individuals without leg length measurements and removing irrelevant variables, a simplified table including height, sex, age, body weight, and leg length for 4172 men and 3379 women was obtained. According to [6], the length of body segments varies according to morphology, gender and ethnicity. A common method for estimating leg length uses a fixed percentage of height (0.53×height), but this does not take individual variations into account. To improve this estimate, a Multilayer Perceptron Regression Model, capable of modelling non-linear relationships and integrating factors such as gender, age, and weight, was used in this paper. The model's performance was evaluated using mean bias, Mean Square Error (MSE), and coefficient of determination (R^2), providing a comprehensive view of its accuracy and robustness [7].

3. Results

The MLPRegressor clearly outperforms the 0.53×Stature method on all metrics. However, this model's performance remains modest.

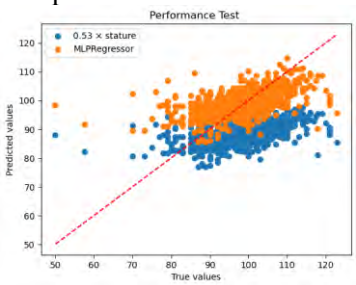


Figure 1: Leg length predicted values.

Measures of performance	MLPRegressor	0.53 * Stature
MSE	6.41	12.50
MAE	4.53	11.30
R^2	0.30	-1.66
Mean bias	0.06	-10.70

Table 1: Performance assessment metrics.

4. Discussion and Conclusions

Although MLPRegressor offers better performance, it has major drawbacks, particularly in terms of complexity, interpretability and sensitivity to noisy data. The use of this AI method in clinical settings offers great potential, but requires rigorous dataset calibration, uncertainty quantification and external validation to ensure reliable and generalisable predictions. Integrating specific clinical biomarkers (as ethnicity) can improve the accuracy and personalisation of models. Furthermore, the use of alternative machine learning models remains an important question to explore.

5. References

1. Lambert B et al., Artificial Intelligence In Medicine, 150 (2024).
2. Cabitza F., Artificial Intelligence in Medicine, Vol. 174, 2026.
3. Lindenmeyer A et al., J Pers Med. 2025 Jan 31;15(2):58.
4. Vazquez J and Facelli J-C., Journal of Healthcare Informatics Research, Vol. 6, 2022. p. 241–252.
5. Hitka M et al., Data in Brief, 55, 110536, 2024.
6. Winter, JOHN WILEY & SONS, INC, 2009.
7. Efthimiou O et al., BMJ, pp. 386, e078276, 2024.

STATISTICAL SHAPE MODELING TO ASSESS THE MORPHOLOGICAL VARIABILITY OF TIBIAL MEDULLARY CANAL

Francesca Montigiani (1), Giulia Galteri (1), Luca Cristofolini (1)

1. Dept of Industrial Engineering, Alma Mater Studiorum - University of Bologna, Italy

1. Introduction

The morphology of the tibial medullary canal is critical for basic science, and implantable device design. Its interpatient variability remains poorly characterized, mainly due to the challenges in acquiring and generating large cohorts of bone models. Statistical Shape Modeling (SSM) represents a powerful tool to capture the mean morphology and its population-wise variation. This study aims to investigate the 3D morphology of the tibial medullary canal using SSM, with the objective of quantifying inter-subject variability and determining how such variability is influenced by the length of the segment considered. Furthermore, the correlation between the subject's heigh and geometry was investigated.

2. Materials and Methods

The CT scans of 98 unpaired human tibiae were used [1,2]. Each scan was segmented (Mimics) to isolate the medullary canal between 20% and 80% of the biomechanical length (BL). A registration was performed to align all medullary canals using a MATLAB script. Twelve segment lengths were simulated. The most proximal cut was at 25% BL, with subsequent levels increased by 5% up to 80% BL (Fig. 1).

For each segment length, a SSM was developed to characterize morphological variation across the population. SSM exploits Principal Component Analysis (PCA) to extract the principal modes of geometric variation relative to the mean shape [3]. The extreme shapes ($\pm 2\sigma$ for each Principal Component, PC) were calculated to describe approximately 95% of the total morphological variation. Subsequently, the following geometric parameters were calculated by reconstructing the medullary canal at 5 mm intervals for each segment length: segment length, maximum distal variation, maximum proximal variation ($Var_{max\ prox}$), mean diameter, radius of curvature (ROC), and ellipticity (Fig. 1). Finally, the relationship between geometric parameters and subject height was assessed through the Spearman's rank correlation coefficient.

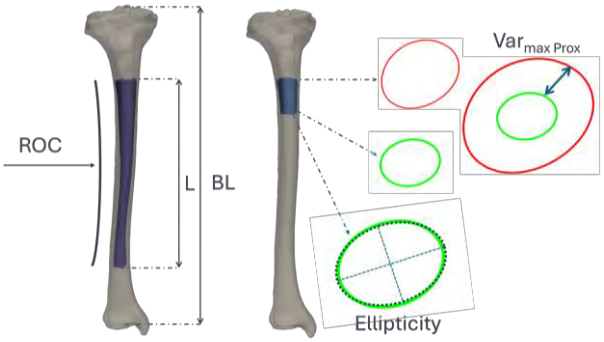


Figure 1: Left: segment of 80% BL. Right: segment of 30% BL. Geometric parameters are also indicated.

3. Results

Six PCs captured 90% of cumulative variance across all segment lengths. The geometric parameters associated with each PCs were identified for each of twelve segment lengths. For instance, in the proximal regions (30% BL) the PCs were primarily associated with geometric parameters such as mean diameter, ellipticity and $Var_{maxProx}$. Conversely, the ROC and the length did not have a major influence. In the distal regions (80% BL), length and $Var_{maxProx}$ showed greater relevance, while ellipticity and ROC had negligible relevance. The Spearman's analysis showed a significant correlation between the subject's height and $Var_{maxProx}$, mean diameter, and segment length ($\rho = 0.88$, p-value = 3.5e-27; $\rho = 0.56$, p-value = 3.4e-08; $\rho = 0.51$, p-value = 7.5e-07).

4. Discussion and Conclusions

The SSM allowed to quantitatively describe how the shape of the tibial medullary canal varies across the population. This analysis showed that the variability can be effectively captured for all lengths of the medullary canal, highlighting which parameters are most relevant at each level.

5. References

1. Edgar, HJH et al (2020). NMDID, Uni of New Mexico.
2. Kistler, M. (2013). VSDFullBody CT Collection.
3. Zhang et al. (2014), *CMBBE: Imaging & Visualization*

Acknowledgements:

Work funded by INAIL (PR23-CR-P5 – OsteoAMI, *CUP: E57G23000240005*).

PHYSICS-INFORMED MACHINE LEARNING FOR ESTIMATING CONSTITUENT-SPECIFIC PROPERTIES OF CARTILAGE

Petri Tanska (1,2), Anni Salo (1), Mika E. Mononen (1)

1. University of Eastern Finland, Finland; 2. Kuopio University Hospital, Wellbeing Services County of North Savo, Finland

1. Introduction

Osteoarthritis degrades cartilage, impairing constituent-specific mechanical properties and leading to joint pain and dysfunction. Characterizing these properties typically requires laborious inverse finite element (FE) analysis to fit a constituent-specific material model to mechanical testing data. This study explores whether a physics-informed machine learning (ML) model, trained on mechanistic FE simulation data, can directly estimate constituent-specific, fibril-reinforced poroelastic (FRPE) mechanical parameters [1,2] from mechanical testing data.

2. Materials and Methods

Synthetic data were generated by simulating indentation tests on 8 mm diameter cartilage samples using an axisymmetric FE model. Each test consisted of three consecutive stress-relaxation steps with 5% compressive strain applied at 100%/s using a 0.728 mm diameter indenter, followed by 900 s relaxation periods. Cartilage was modelled as a FRPE material characterized by five constituent-linked parameters: non-fibrillar matrix elastic modulus (E_{nf}; proteoglycans), initial and strain-dependent collagen moduli (E_0, E_ε; collagen fibrils), and initial permeability and its deformation-dependence coefficient (k_0, M; fluid phase/flow) [1,2]. Sample thickness was included as an additional input feature. Latin hypercube sampling produced 10 000 parameter sets based on reported values for human cartilage [1,2] and parameter sets were used to generate stress-relaxation curves via FE analysis. 18 ML algorithms were trained and evaluated on this physics-based simulation data, with Gaussian process regression (GPR) achieving the smallest root mean squared error (RMSE) and greatest R^2. Prediction performance was tested using nine stress-relaxation curves randomly generated via FE simulations within human cartilage parameter ranges. The trained GPR model predicted FRPE material parameters from these curves, and prediction accuracy was assessed by Pearson's correlation (r) against known FE parameters.

3. Results

GPR accurately predicted force-time curves (median R^2=0.98). E_{nf} was estimated with high accuracy (r=0.94, Fig. 1). E_0, k_0, and M were estimated moderately well (r=0.73, 0.75, and 0.82). E_ε was poorly estimated (r=0.47).

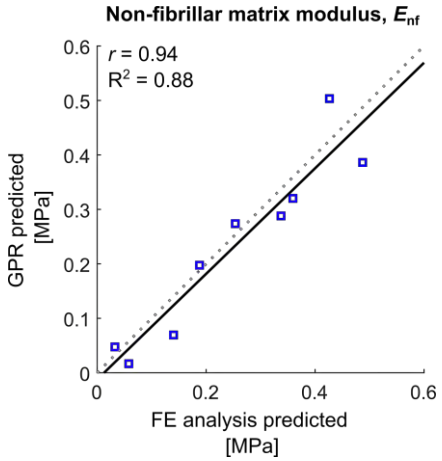


Figure 1: Non-fibrillar matrix modulus estimation accuracy. Dotted line shows line of equality.

4. Discussion and Conclusions

Based on this proof-of-concept analysis, the physics-informed GPR model trained on mechanistic FE simulations can estimate constituent-specific cartilage properties from indentation data, potentially removing the need of laborious inverse FE analysis. Future work will focus on validating this physics-informed ML approach with more diverse dataset and real-world indentation data, aiming to develop more accessible, physics informed tools for assessing tissue properties and health.

5. References

1. Ebrahimi et al., Ann Biomed Eng. 17(4):953-966 (2019)
2. Ebrahimi et al., Ann Biomed Eng. 49(9):2622-2634 (2021).

Acknowledgements: Research Council of Finland (354916), Päivikki and Sakari Sohlberg Foundation (240074, 250070), and Maire Lisko Foundation.

UISS-BMR: A MECHANISTIC AGENT-BASED MODEL OF IMMUNE–BONE CROSSTALK DURING FRACTURE HEALING

Federica Cernuto (1), Vincenzo Russo (2)

1. Department of Mathematics and Computer Science, University of Catania, Catania, Italy;
2. University of Catania, Catania, Italy.

1. Introduction

Bone fracture healing emerges from tightly coordinated immune-skeletal interactions spanning inflammatory signaling, cellular recruitment, and tissue remodelling [1]. Although bone possesses intrinsic regenerative capacity, dysregulated inflammation can impair the transition from the inflammatory to the reparative phase, leading to delayed union or non-union [2]. Capturing this immune–bone crosstalk quantitatively remains challenging due to its multi-scale and dynamically regulated nature. To address this, we developed UISS-BMR, a mechanistic extension of the Universal Immune System Simulator (UISS), an established agent-based framework for modelling immune system dynamics [3]. UISS-BMR explicitly encodes fracture-triggered immune activation and its regulatory impact on bone remodelling processes within a unified virtual physiological environment.

2. Materials and Methods

UISS is structured into physiology, disease, and treatment layers. In UISS-BMR, we extended the physiology layer by introducing a dedicated bone compartment and encoded fracture as a localized osteocyte death event initiating a damage-driven inflammatory cascade within the disease layer. Agent-based rules governing osteoblasts, osteoclasts, osteocytes, macrophages, and cytokine mediators were implemented based on literature-derived mechanistic interactions. In silico experiments were designed to simulate *(i)* baseline bone homeostasis and *(ii)* fracture-triggered immune activation, enabling comparative analysis of macrophage polarization dynamics, cytokine shifts, and osteoid deposition over time.

3. Results

Fracture was modelled as an acute osteocyte death event with release of damage-associated molecular patterns (DAMPs), initiating a rapid pro-inflammatory phase dominated by M1 macrophages (Figure 1A). The model reproduces a time-dependent shift from M1 to M2 polarization as DAMP levels decline and anti-inflammatory cytokines accumulate. This transition precedes osteoid deposition, reflected by transient provisional matrix accumulation (Figure 1B).

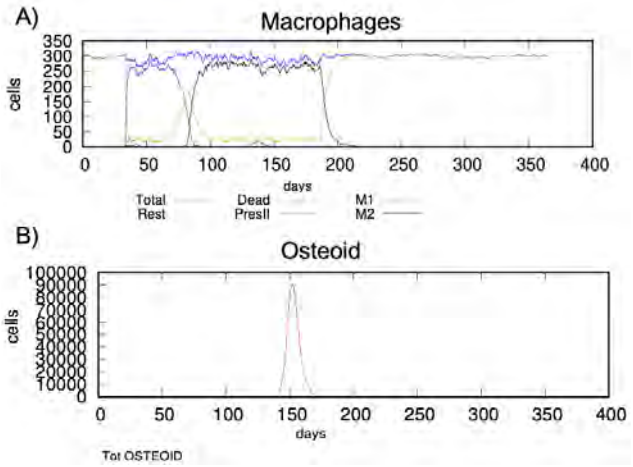


Figure 1: UISS-BMR fracture healing. (A) Macrophage polarization (M1→M2). (B) Osteoid accumulation.

4. Discussion and Conclusions

UISS-BMR provides a mechanistic, agent-based representation of immune-bone coupling during fracture healing within a unified virtual physiology environment. By explicitly linking inflammatory dynamics to bone matrix deposition, the model supports hypothesis testing on inflammation-driven healing impairments and establishes a computational foundation for future integration of therapeutic or patient-specific modules.

5. References

1. Molitoris KH et al. Curr Osteoporos Rep. 2024;22(3):330–9.
2. Wildemann B et al. Nat Rev Dis Primers. 2021;7(1):57.
3. Russo G et al. BMC Bioinformatics. 2020;21(S17):458.

Acknowledgements:
The authors gratefully acknowledge Susana G. Santos (i3S – University of Porto) for having contributed to the model conceptualization.

THE MECHANICAL INTERPLAY BETWEEN BONE AND SCAFFOLD - A COMPUTATIONAL ANALYSIS

Hajar Souhail (1), Luca D'Andrea (2*), Elisa Zamengo (3*), Stéphane Blouin (3), Andrea Berzlanovich (4), Markus A. Hartmann (3), Pasquale Vena (2), Davide Ruffoni (1)

1. University of Liège, Liège, Belgium; 2. Politecnico di Milano, Milan, Italy; 3. Ludwig Boltzmann Institute of Osteology, Vienna, Austria. 4. Center of Forensics Medicine, Vienna, Austria.

(*) equal contribution

1. Introduction

Treating bone defects is considered a major challenge in orthopaedic surgery. While autografts remain the gold standard, donor-site morbidity and limited availability restrict their use. Synthetic 3D printed scaffolds, including ceramic-like materials, offer a promising alternative, allowing to tune scaffold micro-architecture and mechanical properties. Given the inherent microstructural heterogeneity of both bone and scaffold, this study investigates the bone-scaffold system by performing virtual implantation into a human radius and by analysing the mechanical environment.

2. Materials and Methods

Micro-computed tomography images of distal radius and iliac crest from a 53-year-old donor were used to create a virtual radial defect and to reconstruct it with the iliac crest autograft. The defect was also reconstructed using two gyroid scaffolds with Triply Periodic Minimal Surface (TPMS) matching the autograft porosity: one bone-like (Young's modulus E=16 GPa) and one ceramic-like (E=100 GPa) (Fig. 1). The proximal radius was fixed, and compressive forces were applied at the lunate and scaphoid surfaces. Image-based micro-finite element analysis [1] was used to quantify bone apparent stiffness, normalized to that of the healthy bone. A local analysis of peri-scaffold region (dashed area in Fig. 1) was performed to investigate strain redistribution, distinguishing between cortical and trabecular bone.

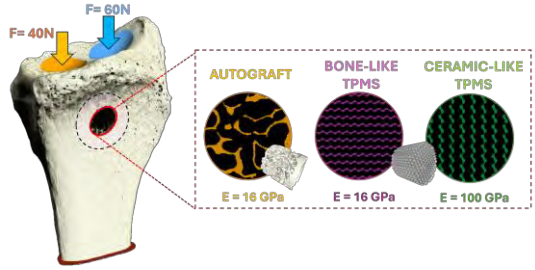


Figure 1: Radius with defect reconstructed with different scaffolds, highlighted on the right.

3. Results

Despite similar strain frequency distributions between the autograft and the bone-like TPMS scaffold (Fig. 2A), the latter is less effective at restoring bone stiffness, probably because of a reduced contact area with surrounding bone. The ceramic-like TPMS scaffold deformed minimally resulting in an apparent stiffness higher than that of the intact bone. Within all peri-implant regions, cortical bone exhibited strain shielding while trabecular bone was more prone to strain intensification (Fig. 2B).

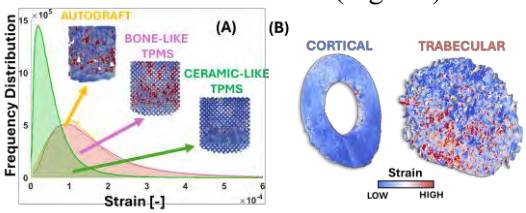


Figure 2: (A) Strain frequency distributions in the scaffolds. (B) Peri-implant strain in cortical and trabecular compartment.

4. Discussion and Conclusions

In-silico modelling of virtual scaffold implantation into a human radius revealed alterations in the apparent bone-implant stiffness and reshaping of local strain patterns in the heterogeneous peri-implant region. These mechanical cues, which influence bone remodelling around the scaffold, can be guided in a patient- and location-specific manner by tuning scaffold microstructure and material properties [2,3].

5. References

1. Flaig et al., Parallel Comput, 37: 846-854; 2011.
2.Wirth et al., J. Biomech, 45:1060-1067; 2012.
3. Ruffoni et al., Bone, 50:733-738; 2012.

Acknowledgements:

This work was supported by the EU Horizon Europe MSCA Doctoral Network "ReBone" (grant no. 101119884), with computational resources provided by the Consortium des Équipements de Calcul Intensif (CÉCI).

DESIGN, MANUFACTURING, AND TESTING OF A SYSTEM FOR *IN VITRO* SKELETAL MUSCLE TISSUE MECHANICAL STIMULATION.

Niek Klein Hofmeijer(1), Cintia Rivares Benitez (1), Jeroen Rouwkema (2), Massimo Sartori (1)

1. Neuromuscular robotics University of Twente, The Netherlands; 2. Engineering Organ Support Technologies University of Twente, The Netherlands

Corresponding author Niek Klein Hofmeijer, n.e.m.kleinhofmeijer@utwente.nl

1.Introduction

Learning how skeletal muscles structurally remodel is essential for improving personalized physical training and rehabilitation interventions. However, assessing remodelling in human subjects is challenging and often invasive. So, an *in vitro* platform which can assess this can be of great value, which led to the objective of this study; to design, manufacture and test an *in vitro* platform capable of applying mechanical stimulation to tissue engineered skeletal muscles (TESMs). The system should allow for studying remodelling across multiple (n=12) TESMs over multi-week time scales. Although TESM fabrication systems have been established [1-3], none incorporate automated mechanical stimulation, highlighting the novelty of our approach.

2. Materials and Methods

Based on a previously designed system [3] we designed and manufactured a platform that applies mechanical stimulation to TESMs by altering the distance between a flexible polydimethylsiloxane (PDMS) pillar and a stiff/ movable Polyamide 2200 (Nylon) pillar which act as attachment points for the tissue. Six wells are used, each with two mechanically stimulable and one control tissue. The twelve movable pillars are driven by one micro linear stepper actuator via a camshaft-based mechanism Fig. 1. The setup is compatible with standard inverted microscopes, enabling imaging and estimation of both passive and active forces based on PDMS pillar deflection. Mechanical performance will be evaluated in terms of accuracy, hysteresis, repeatability and long-term stability. Biological experiments with TESMs were performed to assess the practicality of the system and the effects of mechanical stimulation.

3. Results

Results show that TESMs can successfully form between the bendable and the movable pillar, remain viable for at least three weeks, and withstand mechanical stimulation Fig. 2. The tissue shown underwent two interventions by moving the polyamide pillar (88 and 44 µm), thereby stretching the tissue and deflecting the PDMS pillar to increase passive force on the tissue and influence the rate of tissue lengthening i.e., the tissue lengthened by 12.3% between day 13 and 21 after formation.



Figure 1: Custom-designed platform developed to provide controlled mechanical stimulation to TESMs.

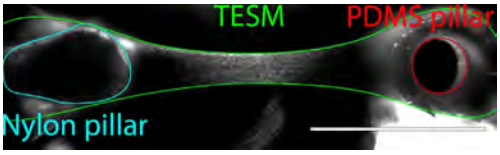


Figure 2: TESM 21 days after formation Scalebar: 1.8 mm

4. Discussion and Conclusions

In conclusion, the designed platform supports TESM formation, controlled mechanical stimulation, as well as force quantification, offering a potential system for advancing engineered muscle research, and gathering data for modelling purposes.

5. References

[1]Smith, A.S.T. et al.(2022). J. Tissue Eng **13**

[2]Iuliano A et al.(2020). *Adv. Mater. Technol.* **5**(9), .2000344.

[3]Ribeiro MC et al.(2022). *J. Pers. Med.*, **12**(2), 214.

Acknowledgements

This work was supported by the European Research Council with CoG grant ROBOREACTOR (no.101123866).

SOFT TISSUE DRIVEN BONE REMODELLING – A FRAMEWORK FOR PATIENT-SPECIFIC DENTAL PROTHESIS DESIGN

Junning Chen (1, 2), Jingxiao Zhong (2, 3), Michael V. Swain (2), Qing Li (2)

1. University of Exeter, United Kingdom; 2. The University of Sydney, Australia; 3. The Max Planck Institute of Colloids and Interfaces, Germany

1. Introduction

Several soft tissues in the oral system, particularly the oral mucosa and periodontal ligament, are situated adjacent to load-bearing bone. These tissues exhibit nonlinear mechanical behaviour due to their collagen-rich microstructure and interstitial fluid content [1]. In dental procedures that transmit loads through soft tissues to bone, such as denture placement and orthodontic tooth movement, the biomechanical environment within these tissues can influence the remodelling response of the adjacent bone [2,3]. However, the role of oral soft tissues in mediating bone adaptation remains insufficiently understood and is often underrepresented in prosthesis design and treatment planning. This gap often led to adverse clinical outcomes, e.g. progressive bone loss following denture insertion (residual ridge resorption) and pathological root resorption. These complications highlight the importance of understanding soft tissue–bone mechanical interactions. From a clinical perspective, there is therefore a need for a quantitative framework capable of evaluating treatment-induced mechanical environments and predicting bone remodelling responses [4].

2. Materials and Methods

Edentulous patients undergoing complete and implant-retained (over)denture insertion were followed for up to five years to evaluate treatment-related changes in the mandibular residual ridge. Patient-specific models were reconstructed from cone-beam computed tomography (CBCT) scans acquired at baseline and follow-ups (1, 2, and 5 years), including the mandible, oral mucosa, and denture structures, to allow virtual evaluation of different treatment options within the same patient profile.

Finite element (FE) analysis was used to quantify mechanical stimuli in both soft and hard tissues. An iterative bone remodelling algorithm simulated time-dependent ridge adaptation, driven by interstitial fluid pressure–related stimuli within the oral mucosa. The framework also enabled optimisation of denture load distribution to reduce localised mechanical concentrations and minimise the predicted risk of residual ridge resorption.

3. Results and Conclusions

Four key outcomes emerged from these studies. First, mechanical stimuli within the oral soft tissues showed stronger correlations with adjacent bone remodelling than stimuli within the bone itself, highlighting the regulatory role of soft tissue biomechanics in skeletal adaptation. Second, the virtual treatment framework effectively distinguished the mechanical environments generated by the three prosthetic treatment options considered. Third, the model successfully predicted clinically observed patterns of prosthesis-induced bone resorption, although systemic bone loss associated with ageing was not explicitly captured and requires further investigation. Finally, integrating topology optimisation demonstrated the potential to redistribute loads more favourably at the denture–mucosa interface, thereby reducing localised mechanical concentrations and minimising the risk of excessive residual ridge resorption.

5. References

1. Chen J et al., J R Soc Interface. 12(109): 20150325 (2015).
2. Zhong J et al., Acta Biomater. 170: 240-249 (2023).
3. Zhong J et al., Adv Healthc Mater. 13: 2400091 (2024).
4. Chen J et al., J Biomech. 47(7):1689–1695 (2014).

Acknowledgements:

The authors would like to thank the Australian Research Council (Grant no: DP160104602) and the UKRI Engineering and Physical Sciences Research Council (Grant no: EP/T008059/1) for providing financial support to these projects.

DECOUPLING INTER- FROM INTRA-CELLULAR STRESSES

R. Aparicio-Yuste (1,2), L. Hundsdorfer (1), E. Bastounis (1), M.J. Gómez-Benito (3)

1. Interfaculty Institute of Microbiology and Infection Medicine, Cluster of Excellence "Controlling Microbes to Fight Infections" (CMFI, EXC 2124), University of Tübingen, Germany; 2. Friedrich Miescher Laboratory of the Max Planck Society, Tübingen, Germany. 3. Engineering Research Institute of Aragon (I3A), University of Zaragoza, Spain.

1. Introduction

Cell-generated forces are guiding processes such as cell proliferation, development and are implicated in pathologies like cancer and bacterial infections [1]. However, there are still limitations in directly measuring intercellular forces, i.e. decoupling inter- from intra-cellular stresses, in cell monolayers. Addressing this question is important since the ability of cells to propagate forces in the tissue impact their cytoskeletal organization, migration, and apoptosis, and can modify the outcome of infection spread or cancer progression [1]. We introduce a novel technique, single cell Monolayer Stress Microscopy (scMSM)—a method that uses live-cell segmentation to reconstruct cell shapes and junctions, enabling stress computation in monolayers at the single-cell level.

2. Materials and Methods

The scMSM computational approach decouples intracellular forces (arising mainly from actomyosin contractility) from intercellular forces (across cell-cell junctions). Cellpose and Trackmate are used as AI-based network to automatically track and segment cells within monolayers over time (Figure 1, step 1) [2].

The segmentation of cells is then imported into MATLAB to extract cell geometry, apply image filtering, and generate finite element meshes for stress analysis (Figure 1, step 2). The monolayer is modelled as a thin, homogeneous, linear elastic structure of constant thickness, allowing for a plane-stress approximation where only in-plane stresses are considered. Moreover, traction forces are computed via traction force microscopy—representing how cells pull on their matrix—and are applied as external loads on the monolayer (Figure 1, step 3).

3. Results

The automatic segmentation of cells within a monolayer, which we previously applied to static images of cells [3], is here extended to live-cell microscopy data. Building on the resulting separate mesh definitions for cells and their junctions, intracellular and intercellular stresses can be computed independently across the monolayer. We observe that the cell division plane correlates with the direction of the cell's principal stress, suggesting that cells divide along the direction of maximal stress.

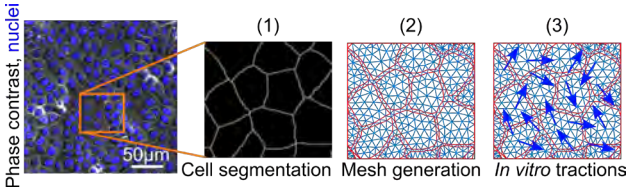


Figure 1: scMSM applied on MDCK cells

4. Discussion and Conclusions

In this work, we quantitatively analyse live-cell microscopy images of uninfected and bacterially-infected epithelial monolayers to infer intercellular stresses, filling a critical gap in current biomechanical analysis. scMSM allows the mechanical state of individual cells in a monolayer to be assessed and the relative roles of internal and junctional forces to be quantified, e.g., in bacterial spread. Clarifying these mechanisms could inform the development of anti-infectives that block bacterial dissemination by targeting key pathways.

5. References

1. Keshavanarayana et al. Trends Cell Biol (2025)
2. Pachitariu et al., Nature Methods, 1-8, (2022)
3. Aparicio-Yuste et al. Comput. Biol. Med. (2025)

Acknowledgements:

This work is part of the project PID2024-155426OB-I0, funded by the Spanish Agency of Research and ERDF, UE. The authors would like to thank the Alexander von Humboldt Foundation for the support through the Postdoctoral Fellowship Program (RAY), and the Deutsche Forschungsgemeinschaft (DFG, German Research Foundation) under Germany's Excellence Strategy – EXC 2124 – 390838134 and the DFG grant 490839690 for providing financial support to this project.

TOWARDS AN IN SILICO MODEL OF THE GUT-BRAIN AXIS: FROM GASTROINTESTINAL STIMULATION TO COGNITIVE PERCEPTION

Emanuele Luigi Carniel (1), Ilaria Toniolo (1), Alice Berardo (1), Chiara Giulia Fontanella (1), Beatrice Pomaro (1), Gianluca Mazzucco (1), Lino Polese (1), Silvana Perretta (2)

1. Centre for Mechanics of Biological Materials, University of Padova, Italy
2. Department of General Surgery, CHRU Strasbourg, IHU Strasbourg, France

1. Introduction

The gastrointestinal (GI) tract and the nervous system form a tightly coupled, bidirectionally interacting system whose function emerges from the integration of chemo-mechanical, hormonal, neural, and cognitive processes. Physical and psychological well-being critically depend on the coordinated operation of this multi-scale system. In silico methods have already proven to be reliable and effective tools for gastrointestinal diagnosis [1] and surgical planning [2]. However, despite extensive research on the gut-brain axis, current computational descriptions remain fragmented across disciplines: GI chemo-mechanics, receptor-level transduction, neural signaling, and higher-level outcomes (satiety and feeding decisions) are often modeled in isolation. This perspective outlines a roadmap toward an integrated in silico physio-chemo-mechanical framework that explicitly couples GI chemo-mechanics with neuro-sensory signaling and central processing, enabling system-level predictive analyses of how peripheral stimuli shape satiety and feeding decision-making.

2. Conceptual framework

A modular pipeline is proposed, spanning: (i) bolus transport through the esophagus, where phenomenological models have been developed [1], but electro-mechanical wall models coupled with fluid-structure interaction must be defined to capture bolus-tissue interaction; (ii) gastric processing, where multi-physics models quantify chemo-mechanical stimulation of the GI wall [3]; (iii) chemo-mechano-transduction modules linking bolus chemistry and tissue mechanics to gastro-receptor activation and downstream hormonal/neural signals; (iv) central nervous system integration, leveraging neurological modeling to map afferent inputs to region-specific activation patterns [4]; and (v) outcome layers translating central patterns into quantitative proxies of satiety and feeding decision-making [5].

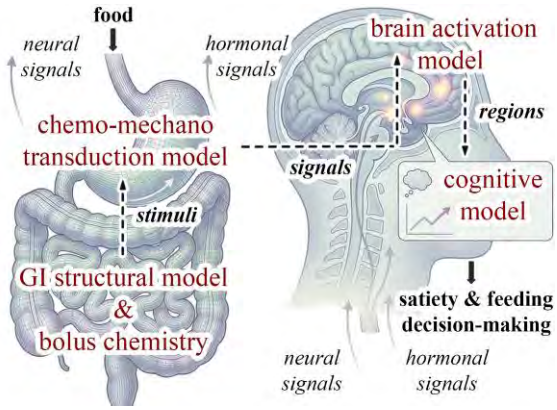


Figure 1: Mechanistic in silico modelling of the gut-brain axis: from food ingestion to satiety and feeding decision-making.

3. Expected impact

An integrated gut-brain digital framework would support mechanistic hypothesis testing, stratification of physiological versus pathological responses, and in silico exploration of diagnostic, surgical, and therapeutic strategies. By enabling predictive analyses of the interplay between GI chemo-mechanical stimuli, neuro-sensory responses, and central processing, such a framework would provide a mechanistic basis to interpret the cascade of events from food ingestion to satiety and feeding decision-making. Coupled with inverse modeling and calibration on clinical data, the framework would enable patient-specific digital twins to guide personalized behavioral, psychological, pharmacological, and/or interventional strategies [6].

4. References

1. Frigo et al, IEEE Trans Biomed Eng; 65:1476-1485 (2018).
2. Carniel et al, Bioengineering; 7:48 (2020).
3. Toniolo et al, Comput Methods Programs Biomed; 243:107889 (2024).
4. Kim et al, Nat Rev Neurosci; 23:135-156 (2022).
5. Al-Zubaidi et al, Neuroimage; 217:116931 (2020).
6. Toniolo et al, Surg Endosc; 36:7998-8011 (2022).

THE ECOSYSTEM WITHIN US: SIMULATING MICROBIOME DYNAMICS TOWARDS A DIGITAL TWIN OF THE HUMAN GUT

Shahad Qathan (1), Denny Popp (2), Florian Centler (1)

1. University of Siegen, Germany; 2. University of Leipzig Medical Center, Germany

1. Introduction

The human microbiome has been recognised as an important factor for human health and wellbeing in recent years. Harbouring hundreds of different microbial species, a typical human gut microbiome is a complex ecosystem in itself, and we are only at the beginning of understanding how the manyfold internal interactions and interactions between microbiome and the host impact human health. Computational tools are emerging capable of simulating and predicting microbiome dynamics at natural diversity [1]. Combining these with patients' gut microbiome data, now routinely obtained by amplicon or shotgun metagenome sequencing of stool samples, opens up novel ways for early disease detection, monitoring of disease progression, and exploring strategies to modulate a patient's individual gut microbiome towards a desired state.

2. Materials and Methods

We have developed a computational simulation model able to simulate the metabolic uptake and growth of a microbiome consisting of hundreds of microbial species [2]. Employing the dynamic Flux-Balance-Analysis approach [3], each member species is simulated individually, detailing how nutrients are taken up and processed by the species' metabolic network to produce biomass for growth. Compounds secreted during this process enter a common compound pool which is accessible to other species, enabling microbial cross-feeding. The simulation approach is based on genome-scale metabolic models built upon the collection of enzymes encoded on each species' genome. Simulations hence provide not only trajectories of pool compound concentrations and biomass concentrations of all microbiome member species, but also trajectories of flux activities for each individual enzyme. Such detailed data are helpful in deriving a mechanistic understanding of observed global dynamics, and is furthermore compatible with multi-OMICS data able to refine the model.

3. Results

The computational simulator enables the creation of synthetic or patient-derived *in silico* microbiomes which resemble their natural counterpart in diversity. Systematic scenario simulations can be used to explore their dynamic repertoire, assess stability and resilience, and identify key drivers of observed dynamics. As a tool for basic research, this enables novel insights in microbial ecology, and can establish the potential and limits for modulating microbiomes towards healthy states. Simulations based on patients' data can be used to predict the impact of, for example, a change in nutrition, or the use of antibiotics, helping in choosing the best treatment strategy.

4. Discussion and Conclusions

Human microbiome science is an evolving field. A definition of a "healthy" gut microbiome is still missing, and reported associations between the gut microbiome and many diseases are often still lacking a mechanistic link. Computational modelling of this complex system can help in gaining a better mechanistic understanding and establishing a link to host health. With more knowledge accumulating, a digital twin of the human gut will become evermore informative and helpful in the early detection of diseases and in planning treatment strategies tailored to a patient's individual microbiome. As the gut also interacts with many other organ systems, the digital twin of the gut must likewise ultimately be linked to other organ models.

5. References

1. W. T. Scott Jr *et al.*, *PLOS Comput. Biol.*, vol. 19, no. 8, p. e1011363, 2023
2. D. Popp and F. Centler, *Front. Bioeng. Biotechnol.*, vol. 8:574, 2020
3. R. Mahadevan, J. S. Edwards, and F. J. Doyle, *Biophys. J.*, vol. 83, no. 3, pp.1331–1340, 2002

Acknowledgements:

The authors would like to thank the German Federal Ministry of Education and Research for providing financial support (FKZ 031A317).

[LIB]OPENCOR: MOVING COMPUTATIONAL BIOLOGY TO THE WEB

Alan Garny, David P. Nickerson, Peter J. Hunter

Auckland Bioengineering Institute, University of Auckland, Auckland, New Zealand

1. Introduction

Computational biology has benefited from standards and formats such as CellML [1], SED-ML [2], and COMBINE archives [3]. OpenCOR [4] allows researchers to reproduce and reuse CellML-based models, but it is a pure cross-platform desktop application while the software industry has been moving towards Web-based applications (i.e. accessible from any device with a Web browser without the need for installing anything), facilitating colla–boration. Therefore, to make computational biology more accessible, we decided to create a Web-based version of OpenCOR.

2. Materials and Methods

(Legacy) OpenCOR is both a frontend and a backend application, an approach that proved to have limitations (e.g., with its Python bindings). Moving to the Web, we decided to separate the frontend and backend components, allowing for greater flexibility and scalability.

libOpenCOR is the new backend component of OpenCOR. It is a cross-platform C++ library for CellML manipulation and simulation with Python and JavaScript bindings. The frontend component of OpenCOR is now a Web-based application that relies on libOpenCOR to provide a user-friendly interface for model editing, simulation, and visualisation. It is being developed using modern Web technologies and frameworks. It can be packaged as a Web app, as well as a traditional desktop application.

3. Results

The desktop version of OpenCOR is available on Windows, Linux, and macOS, on both Intel and ARM architectures. It can be downloaded from https://opencor.ws while the Web version can be accessed at https://opencor.ws/app. Both versions provide the same user experience, with the desktop version leveraging the performance benefits of C++ while the Web version offers the added benefit of being accessible from any device with a Web browser without compromi–sing on performance or features.

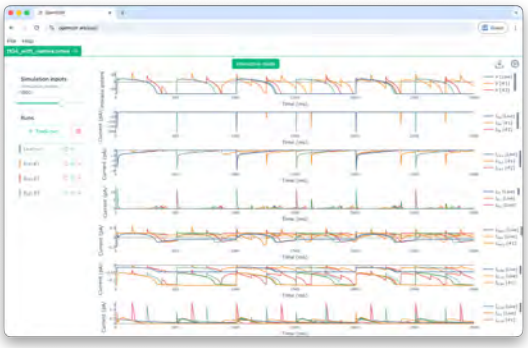


Figure 1: Web version of OpenCOR.

Figure 1 shows Web OpenCOR. The left panel allows the user to customise the simulation pa–rameters and to keep track of simulations of interest while the right panel displays the simu–lation results, which are updated in real-time as the simulation parameters are changed.

Interactive simulations let modellers set up and share simulation protocols that showcase model behaviour. Others can then edit and re-share to add their own perspective, improving reprodu–cibility and making workflows more FAIR.

4. Discussion and Conclusions

Our Web-based OpenCOR has already shown promising results, as demonstrated at a recent VITAL workshop attended by 75 participants. However, we are still in the early stages of development, and there are many features and improvements that are being worked on.

5. References

1. Clerx M et al., J Integr Bioinform. 2020; 17(2-3): 20200021 (2020).
2. Smith LP et al., J Integr Bioinform. 2024; 21(1): 20240008 (2024).
3. Bergmann FT et al., J Integr Bioinform. 2015; 12(2): 261 (2015).
4. Garny A, Hunter PJ, Front Physiol. 2015; 6: 26 (2015).

Acknowledgements:

The authors would like to thank the NIH SPARC program (Award no: OT3OD025347) for providing financial support to this project.

From Neural Dynamics to Precision Therapy for Parkinson's Disease: A Multiscale In Silico Model of Cortical Excitability and Network Imbalance

Jiyoun Jung (1,3), Hong-Yuan Chu (2,3), William W. Lytton (1,3)

1. Department of Physiology and Pharmacology, SUNY Downstate Health Sciences University, Brooklyn, NY, USA ; 2. Department of Pharmacology and Physiology, Georgetown University Medical Center, Washington, DC, USA ; 3. Aligning Science Across Parkinson's (ASAP) Collaborative Research Network, Chevy Chase, MD, USA

1. Introduction

Parkinson's disease (PD) is traditionally considered a basal ganglia disorder, yet increasing evidence implicates pathological cortical beta synchronization in motor impairment [1]. The cellular mechanisms underlying this hypersynchrony remain unclear.

2. Materials and Methods

We adapted a previously developed multiscale M1 model in NEURON/NetPyNE [2], comprising ~10,000 neurons and ~30 million synapses across excitatory (IT, PT, CT) and inhibitory (PV, SOM) populations. Parkinsonian perturbations included PT hypoexcitability and reduced thalamocortical input based on MitoPark data.

3. Results

The PD model generated excessive beta synchronization in layer 5 inhibitory circuits and IT5B populations while suppressing PT5B recruitment. Beta-locked inhibitory synchrony rigidified temporal gating, disrupted dendritic coincidence detection in PT neurons, and suppressed corticospinal output. These changes produced prolonged beta bursts, exaggerated beta–gamma coupling, impaired movement recruitment, and subcritical avalanche dynamics. Increased IT synchrony and reduced PT firing were observed across layer 5 circuits. Power spectral analysis showed elevated beta-band activity and reduced gamma-band engagement relative to control conditions. Modulation index measurements further confirmed enhanced pathological beta–gamma coupling in the PD state. Therapeutic control points emerged: theta stimulation of layer 5 interneurons desynchronized beta activity and restored PT output, while norepinephrine restoration increased PT gain, reduced IT hypersynchrony, and normalized network dynamics.

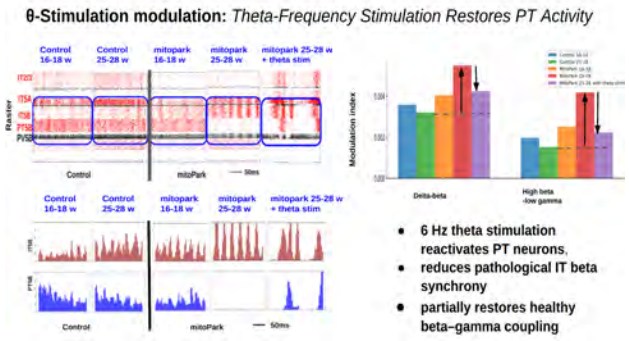


Figure 1. 6 Hz theta stimulation restores PT activity and normalizes cortical dynamics in the Parkinsonian model.

4. Discussion and Conclusions

These results suggest that intrinsic excitability deficits and inhibitory timing rigidity drive cortical dysfunction in PD. Targeted neuromodulation or neuromodulatory restoration can normalize network dynamics, demonstrating the predictive value of multiscale mechanistic modeling within the Virtual Physiological Human (VPH) framework.

5. References

1. de Hemptinne C et al. Exaggerated phase–amplitude coupling in Parkinson's disease. PNAS. 110(12):4780–4785 (2013).
2. Dura-Bernal S et al. NetPyNE: A tool for data-driven multiscale modeling of brain circuits. eLife. 8:e44494 (2019).

Acknowledgements:

Supported by the Aligning Science Across Parkinson's (ASAP) Collaborative Research Network. Computational resources were provided by SUNY Downstate Health Sciences University.

A SYSTEMS APPROACH TO REELIN-NOTCH SIGNALING TO DECIPHER REGULATORY DYNAMICS IN LYMPHANGIOGENESIS

Sophie Bekisz (1), Yanisse Graïne (1), Agnès Noël (2), Liesbet Geris (1,3), Luiz Ladeira (1)

1. Biomechanics Research Unit, University of Liège, Belgium; 2. Laboratory of Biology of Tumor and Development, University of Liège, Belgium; 3. Skeletal Biology and Engineering Research Center, KU Leuven, Belgium.

Correspondence: Luiz Ladeira, lcladeira@uliege.be

1. Introduction

Vascular patterning is governed by complex signalling crosstalk, with the Notch pathway serving as a widely recognized regulator of endothelial cell (EC) fate. While Reelin-Notch interactions are well-documented in neural development, their role in the lymphatic system remains largely unexplored. This study investigates whether Reelin modulates Notch signalling during lymphangiogenesis[1], providing a regulatory mechanism for lymphatic endothelial cell (LEC) fate.

2. Materials and Methods

We developed a knowledge-driven signalling map of Reelin and Notch pathway's crosstalk by integrating Reactome entries (R-HSA-8866376, R-HSA-157118) and a systematic review of the literature to identify crosstalk components. LEC-specific transcriptomic datasets were used for cell specificity contextualization. The map was converted into a probabilistic Boolean model, and simulations were performed using MaBoSS [1], enabling the simulation of pharmacological perturbations targeting the Reelin and Notch pathways. Key regulatory interactions between both pathways and predicted model outputs were tested through complementary *in vitro* approaches, including gene expression by RT-qPCR and drug perturbation assays.

3. Results

We identified and mapped Reelin and Notch pathway's crosstalk. Data integration and RT-qPCR analyses identified that the canonical neuronal adaptor DAB1 is replaced by DAB2 in LECs, where we demonstrated that key components of the Reelin pathway are expressed basally and modulated upon stimulation. Boolean simulations revealed that Reelin signalling can sustain Notch activation over time. The model predicted that inhibition of upstream ADAMs proteases showed greater effect on reducing Notch signalling than γ-secretase inhibition alone (both enzymes being Notch pathway bottleneck proteases). Also, dual inhibition of FYN (a Reelin regulator) and γ-secretase resulted in superior suppression of Notch signalling in a stimulated condition. These results are now being confirmed *in vitro*.

4. Discussion and Conclusions

The finding that DAB2 can replace DAB1 in the LECs suggests a cell-type-specific version of the Reelin pathway. This supports the observation that Reelin signalling is a conserved regulatory module with context-dependent adaptors [2]. The model's prediction that Reelin sustains Notch signal indicates that Reelin serves as an amplifier, a role consistent with its function in neuronal migration [3]. The higher efficacy of inhibiting ADAMs over γ-secretase alone highlights the importance of upstream proteolytic enzymes in maintaining network stability. Crucially, the synergistic effect of targeting FYN and γ-secretase, as highlighted by the combined application of *in silico* and *in vitro* approaches, suggests that the Reelin pathway can be exploited to sensitize LECs to Notch-targeted therapies.

5. References

1. Stoll et al., Bioinf., 33(14), 2226 (2017). **2**. Calvier et al., Arterioscler. Thromb. Vasc. Biol., 41(4), 1309–1318 (2021). **3**. Hashimoto-Torii et al., Neuron, 60, 273 (2008).

Acknowledgements:

The authors would like to thank the ERC (101088919, INSTant CARMA), the Fondation Hospital Universitaire Léon Fredericq (FHULF), and ULiège A.R.C. 19/23-21 («INovLYMPHATIC»). Sophie Bekisz is a F.R.S.-FNRS postdoctoral fellow.

[1] Formation of new lymphatic vessels from pre-existing ones.

A PBK-TD GUT MICROBIOME MODEL OF THE FIRST 1000 DAYS OF LIFE: TOWARDS A PREVENTIVE HEALTHCARE DIGITAL TWIN

Tu-Ky Ly (1), Alfons G. Hoekstra (1), Vivek M. Sheraton (1)

1. Computational Science Lab, Informatics Institute, Faculty of Science, University of Amsterdam, The Netherlands.

Corresponding author: Tu-Ky Ly, t.n.ly@uva.nl

1. Introduction

The Developmental Origins of Health and Disease (DOHaD) framework establishes that the first 1000 days of life constitute a critical window related to long-term disease risk [1]. The gut microbiome, shaped by birth mode, environmental exposure, and diet [2], is a key mediator: disruption of early bacterial colonizers is linked to adult metabolic disorders, including diabetes and obesity. A Digital Twin in Healthcare framework, combined with mechanistic modelling, offers a powerful paradigm for personalized preventive intervention. Physiologically based kinetic-toxicodynamic (PBK-TD) modelling provides the mechanistic foundation, spanning from the molecular scale of microbial metabolism to the whole-body physiology of a growing child [3]. We propose a human PBK-TD model of gut microbiome from birth to 1000 days, as a preventive digital twin to further assess food intake.

2. Materials and Methods

A multi-scale mechanistic PBK-TD model was developed, based on a human lifetime PBK model [5], including gut microbiome growth and metabolic activity of *Bifidobacterium longum* (*BL) subsp. longum* and *BL infantis* [2]. Within the gut, glucose and lactose are metabolized into succinate by *BL longum*, and into acetate and lactate by *BL infantis*, with all substrates and metabolites distributed across gut and blood compartments. Key inputs include: (i) initial bacterial *inoculum* determined by birth mode and maternal microbiome status [2], (ii) oral food intake, and (iii) oral antibiotic exposure. All data were sourced from MetaHealth and UK Biobank [2,4].

3. Results

The model reproduces infant growth trajectories and gut microbial colonization dynamics, capturing the influence of birth mode, maternal microbiome, and food intake, consistent with existing data [2,3]. Simulations of different feeding schemes further demonstrated that breastfed infants had higher levels of protective strain *BL infantis*. Simulations of the impact of the environment, such as antibiotic exposure, led to a modulation of gut microbiome composition. Bacterial growth was reduced and metabolite balance altered in the gut lumen, consistent with existing data [2,4]. Based on these model outputs, reflecting the gut microbiome dynamics, the model can operate bidirectionally, comparing individual food intake against reference data to generate personalized dietary recommendations.

4. Discussion and Conclusions

We present a multi-scale mechanistic PBK-TD model for early-life gut microbiome development. The model captures birth conditions, environmental exposures, and dietary inputs across the first 1000 days. The model can be further extended to adulthood simulations - calibrated against UK Biobank data - to estimate metabolic disease onset probability. Coupled with a patient data feedback loop, this architecture is designed to evolve into a fully operational digital twin for personalized preventive healthcare and future *in silico* nutritional intervention trials.

5. References

1. Charles MA et al. 2016. Médecine/sciences.
2. Pucci N et al. 2025. PeerJ.
3. Stevanoska M et al. 2024.Toxicology Letters.
4. MetaHealth Consortium. https://nwo-metahealth.nl/ (2024).
5. Beaudouin R et al. 2010. Regul Toxicol Pharmacol.

Acknowledgements:

This work is part of the MetaHealth project, funded by NWO (NWA.1389.20.080). The authors acknowledge the use of UK Biobank data.

PERSONALIZED MODELS TO UNVEIL MECHANISMS OF ENGINEERED T-CELL THERAPY IN MULTIPLE MYELOMA

Sophia Orozco-Ruiz[1,2,3], Vincent Noël[1,2,3], Gautier Stoll[1,2,3], Saran Pankaew[1,2,3], Laia Gasull-Celades[4], Esmee van Vliet[4], Patricia Hernández-López[4], Peter Brazda[4], Farid Keramati[4], Christina Kuhn[5], Michael Rade[5], David Fandrei[5,7,9], Miriam Alb[6], Zsolt Sebestyén[4,10], Maximilan Merz[5,7,8,9], Jürgen Kuball[4,10], Kristin Reiche[5,11,9,12], Emmanuel Barillot[1,2,3], Laurence Calzone[1,2,3]

1. Institut Curie, Université PSL, F-75005, Paris, France; 2. INSERM, U1331, F-75005, Paris, France; 3. Mines ParisTech, Université PSL, F-75005, Paris, France; 4.Center for Translational Immunology, University Medical Center Utrecht, Utrecht University, Utrecht, the Netherlands; 5. Fraunhofer Institute for Cell Therapy and Immunology IZI, Leipzig, Germany; 6. Department of Internal Medicine II, Chair of Cellular Immunotherapy, University Hospital Würzburg; 7. Department of Hematology, Hemostaseology and Cellular Therapy, University Hospital of Leipzig; 8. Myeloma and Cellular Therapy Services, Memorial Sloan Kettering Cancer Center, New York, NY, USA; 9. Cancer Center Central Germany (CCCG) Leipzig-Jena, University Hospital of Leipzig, Leipzig, Germany; 10. Department of Hematology, University Medical Center Utrecht, Utrecht University, Utrecht, the Netherlands; 11. Institute of Clinical Immunology, Medical Faculty, University of Leipzig, Leipzig, Germany; 12. Center for Scalable Data Analytics and Artificial Intelligence (ScaDS.AI), Dresden, Leipzig, Germany

1. Introduction

Engineered T cells are showing great promise in the treatment of hematologic malignancies. In this therapy, patients' own T lymphocytes are engineered to express synthetic receptors that recognize specific tumour-associated antigens, thus leading to an improved tumour control. Despite its success, toxicity and therapeutic resistance represent challenging aspects and the mechanisms that determine treatment success remain to be elucidated. Here, we propose a modelling approach to explain mechanistic differences in engineered T cells that shed light into Multiple Myeloma (MM) patients' response to therapy.

2. Materials and Methods

We developed a knowledge-based T cell Boolean model. We parameterised the model with single cell RNAseq data from two different studies: (1) a longitudinal study of MM patients receiving chimeric antigen receptor (CAR)-T cell therapy [1] and (2) an in vitro study of T cells engineered with defined gamma delta TCRs (TEGs) co-cultured with tumour cells [2]. We obtained patient and cell-personalised models on which we performed stochastic simulations and perturbation analysis [3].

3. Results

The personalised models were able to reproduce experimentally observed phenotypic differences in T cells with distinct engineered receptors and in patients with different responses. Our results show variability between cells expressing the same engineered receptor, providing mechanistic insight onto these differences. Further, through perturbation analysis, we propose ways to redirect the models towards phenotypes associated with an improved therapeutic outcome.

4. Discussion and Conclusions

Our personalized in-silico models serve as a representation of T cells coming from patients and healthy donors. The models can be used to generate and test hypotheses and then implemented as virtual twins to assist patients and clinicians in treatment selection.

5. References

1.Rade et al. Cancer Cell; 10.1016/j.ccell.2025.10.014
2.Hernández-López et al. Nat Immunol; 10.1038/s41590-023-01665-0;
3.Calzone et al. Computational and Structural Biotechnology Journal; 10.1016/j.csbj.2022.10.003

Acknowledgements:

This project was funded by the European Union under Grant Agreement number 101136379. Views and opinions expressed are however those of the author(s) only and do not necessarily reflect those of the European Union or the Health and Digital Executive Agency. Neither the European Union nor the granting authority can be held responsible for them.

TOWARDS A DIGITAL TWIN OF THE HUMAN GUT: A MULTISCALE COUPLED PDE MODEL OF HOST-MICROBIOTA INTERACTION

Eleonora Pastremoli (1,2), Beatrice Laroche (1,2), Lorenzo Sala (1,2)
1 Univ. Paris-Saclay, INRAE, MaIAGE, France; 2. Univ. Paris-Saclay, Inria, MUSCA, France.

1. Introduction

The gut microbiota plays a vital role in human health, yet its complexity limits the feasibility of *in vivo* studies. To bridge this gap, we present a multiscale computational framework that lays the groundwork for a Digital Twin of the human colon. By coupling microscopic cellular interactions with tissue-level dynamics, this approach provides a predictive platform for simulating host-microbiota interactions in healthy and diseased states, supporting progress towards personalized precision medicine.

2. Materials and Methods

The mathematical framework dynamically couples a 2D axisymmetric colon model [1] with a 1D crypt model [2] through bidirectional mass exchange at the mucosal interface. The macroscopic domain captures the complex dynamics of the intestinal lumen through a strongly coupled system of partial differential equations (PDEs), including non-Newtonian fluid dynamics (Stokes flow) and the transport and metabolism of bacteria (Advection-Diffusion-Reaction). Simultaneously, the microscopic model tracks host cell dynamics along the crypt axis and regulates the vital exchanges across the mucosal wall. The system is discretized and solved in Python using the FEniCSx finite element library for the colon domain, coupled with an in-house solver for the crypt model. A triangular mesh with three-level local refinement at the mucosal interface is employed for the colon to capture cross-scale fluxes and ensure numerical stability, while a regular discretization is used for the crypt model [2]. The numerical scheme involves a multi-step approach solving the crypt model, followed by the colon's Stokes and ADR equations. To address computational costs and move towards real-time applications, we developed a non-intrusive Model Order Reduction strategy combining Proper Orthogonal Decomposition with Neural Networks [3].

3. Results

The model successfully replicates the healthy steady-state dual-layer mucus structure, showing a protective hard mucus barrier that excludes bacteria from the epithelium, while a soft mucus layer promotes stable microbial colonization [4, 5].

Numerical simulations provide key insights into host-microbiota interactions under localized perturbations, demonstrating the framework's potential for predictive modelling. Specifically, the model revealed how a compromised mucus barrier leads to bacterial infiltration into the inner mucus, triggering an immune response as a dynamic feedback mechanism to restore equilibrium [6].

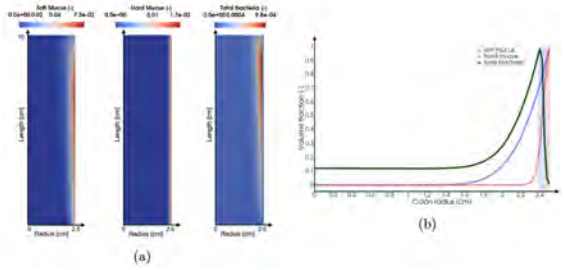


Figure 1: (a) Spatial distribution of soft, hard mucus, and total bacteria population within the colon domain; (b) overlay of their normalized profiles.

4. Discussion and Conclusions

We present a validated multiscale computational framework describing host–microbiota interactions in the colon, coupling structural, transport, and biochemical processes across scales. The modular architecture enables scalable simulations and provides a flexible basis for future incorporation of individualized data, such as microbiota composition and dietary inputs. This perspective opens the way toward real-time computational platforms for in silico experimentation, with potential applications in personalized intervention design and decision support in gastrointestinal health.

5. References

1. Labarthe S et al., J Theor Biol; (2019).
2. Haghebaert M et al., J R Soc Interface; (2024).
3. Balzotti C et al., arXiv:2206.15384 (2022).
4. Jakobsson HE et al., EMBO Rep; (2015).
5. Nyström EE et al., Science; 372(6539): (2021).
6. Pastremoli E et al., HAL Open Science; hal-05524422 (2026)

REAL-TIME PREDICTION OF EARLY LIVER ALLOGRAFT DYSFUNCTION USING AN IMAGE-BASED MULTISCALE BIOMECHANICAL MODEL

Luis Mandl (1,2), Steffen Gerhäusser (1), Anton Schnurpel (2), Anna-Lena Hoh (2), Uta Dahmen (3), Matthias König (4), Tim Ricken (1), Hans-Michael Tautenhahn (2)

1. University of Stuttgart, Germany; 2. University of Leipzig Medical Center, Germany; 3. Humboldt University of Berlin, Germany; 4. Jena University Hospital, Germany

1. Introduction

Liver transplantation remains the only curative therapy for patients with end-stage liver disease. However, the demand for transplantable organs substantially exceeds their availability. Surgeons are therefore frequently required to decide whether marginal grafts, such as steatotic livers, are suitable for transplantation based on limited information and a small set of static parameters. This uncertainty contributes significantly to the risk of early graft dysfunction and highlights the need for quantitative decision-support tools.

2. Materials and Methods

We present a multiscale biomechanical framework designed to predict organ perfusion (portal perfusion, e.g. ml/min/g liver tissue) and the metabolic resilience of marginal steatotic grafts in real time. At the lobular scale, blood flow is modeled as anisotropic transport through a homogenized porous medium following the approach described in [1]. At the cellular scale, hepatocyte dynamics are represented by systems of ordinary differential equations capturing key biological processes including cellular energy balance (ATP concentration in liver tissue), ischemic injury (% HMGB1 staining), and hepatocellular death (% single-cell necrosis).

Model parameterization is achieved through an automated histology and imaging pipeline that generates spatially resolved tissue maps with quantified morphological features. The pipeline integrates automated vessel detection and steatosis quantification, enabling extraction of structural parameters such as vascular diameter and steatosis fraction for model initialization. Physics-informed deep learning is employed both for histological image segmentation and as a surrogate model to accelerate the underlying biomechanical simulations.

3. Results

The multiscale model generates quantitative predictions of post-reperfusion graft function (e.g. peak ALT) from image-derived structural parameters such as vascular diameter [2]. Initial validation experiments demonstrate that the framework reproduces characteristic perfusion patterns observed in steatotic compared with non-steatotic liver lobules. These results indicate that histology-derived morphological features can be translated into physiologically meaningful parameters for multiscale biomechanical simulations and provide a quantitative basis for predicting early graft dysfunction.

4. Discussion and Conclusions

Computational decision support in transplant medicine remains an emerging field. We present a novel image-based multiscale biomechanical framework for the assessment of marginal steatotic liver grafts. By integrating porous-media theory [3], systems biology models, automated quantitative histology, and physics-informed deep learning [4], this approach establishes a foundation for transparent and patient-specific modelling of graft function and may support future data-driven decision-making in liver transplantation.

5. References

1. Ricken T et al.; Biomechanics and Modeling in Mechanobiology, 2014, 14(3), 515-536.
2. Tautenhahn, H.-M, et al.; GAMM-Mitteilungen, 2024, 47(2).
3. Ehlers, W.; Porous media, 2002, (pp. 3-86)
4. Mandl, L et al.; Computer Methods in Applied Mechanics and Engineering, 2025, 434, 117586.

Acknowledgements:
We would like to thank the DFG for providing financial support to this project under Grant No. 465194077.

SMOOTH MUSCLE CELL POPULATION VARIATION

Nicole Anderton (1), Ossi Noita (1), Francesca Menna (2), Jose Suihkonen (1), Arthur Ben-Tolila (2), Jussi Koivumäki (1), Joan Duprez (2), Virginie Le Rolle (2), Jari Hyttinen (1)

1. Faculty of Medicine and Health Technology, Tampere University, Tampere, Finland; 2. University of Rennes, CHU Rennes, Inserm, LTSI-UMR, Rennes, France

Correspondence: Nicole Anderton (nicole.anderton@tuni.fi), Tampere University, Tampere, 33520, Finland

1. Introduction

The mechanisms of the smooth muscle cell (SMC) contraction, vessel mechanics and cardiovascular haemodynamics are tightly coupled and complex. Owing to the reciprocal interdependence of these systems, their cascade of functionality has neither been completely understood nor computationally integrated. Closing this gap would prove invaluable in elucidating the mechanisms of cardiovascular disease onset and progression. This is particularly relevant to hypertrophic cardiomyopathy (HCM) where compromised cardiovascular function has been observed, without evidence that it is owing to a HCM mutation [1]. We address this by developing a multiscale vascular model coupling SMC models, with vessel and cardiovascular system level models enabling bidirectional coupling between cellular contractile dynamics, vessel mechanics and haemodynamics. SMC activation modulates vessel diameter and blood flow while mechanical loading feeds back to the cellular level. Central to this work is addressing the biological variability with the development, and extensive validation, of a population of SMC models. SMC populations are highly relevant for HCM stratification, as vascular tone regulation, coronary perfusion, and afterload are determinants of myocardial oxygen supply–demand balance and drug response and are modulated by inter-individual variability in SMC electrophysiology and contractility.

2. Materials and Methods

A well-established base SMC model was selected [2]. Additional stretch, shear and calcium driven contractile elements were integrated into the electrochemical model [3,4]. Parameters were selected and varied to create a population of models, using the POM Tool (https://github.com/TAU-CBIG/POMtool). The population was subjected to a comprehensive set of physiological challenges (Rest, Stretch, norepinephrine and nitric oxide stimulation-NENO and V-Clamp) to determine each individual model's ability to reproduce expected qualitative behaviours across a range of conditions.

3. Results

Of the population of 10000; 1897 cells passed both the Rest and Stretch challenges. Once the NENO challenge was considered only 557 of those cells met all conditions. Of those,only 222 cells passed the challenge with the lowest acceptance rate, V-Clamp.

4. Discussion and Conclusions

This work lays the foundation for incorporating biological variability into vascular system simulations. Integrating this into vessel wall passive biomechanics and systemic cardiovascular models allows for population-based drug and disease modelling.

5. References

1. Anderton N *et al*., EMBC 2025conference: IEEE; 2025. p. 1-6.
2. Kapela A et al., Theor Biol. 253(2):238–260 (2008).
3. Yang J et al., Med Eng Phys. 25(8):691–709 (2003).
4. Murtada S C et al., *J. Theor. Biol,* 297: 176–186 (2012).

Acknowledgements:
This work is part of the HORIZON-HLTH-2023-TOOL-05 SMASH-HCM project funded by the European Union under Grant 101137115.

A REPRODUCIBLE FRAMEWORK FOR COUPLING TISSUE LEVEL AND INTRACELLULAR KINETIC MODELS OF HEPATOCYTES

Matteo Pedrazzi (1), Peter Kottman (1), Marta Cascante de Serratosa (2), Dirk Drasdo (1)
1. Inria Saclay Research Center, France; 2. Department of Biochemistry and Molecular Biomedicine – University of Barceolna, Spain

1. Introduction

The aim of this work is to establish a multi-level tissue model that implements intracellular kinetic models, incorporating the pathways considered crucial for liver function at the level of individual cells to permit studying how liver function is impacted by microarchitectural alterations in acute and chronic liver injury. The models are implemented in the modular open-source software CompuTiX, for which a prototype focussing on in vitro multicellular simulations has recently been made available.

2. Materials and Methods

The CompuTiX software, developed in-house and open-source, follows FAIR principles (Findable, Accessible, Interoperable and Reusable). It is a high-performance library for agent-based simulations, with a particular focus on computational tissue modelling. It can internally call solvers for ODE systems coded as SBML files, the standard data format for describing biological models.

The intracellular model developed integrates and refines already existing models for ammonia detoxification pathways [1] and underlying mechanisms and dynamics of lipid droplets [2]. In addition, further reactions have been added to compute the concentrations of common bio-markers used in the clinics to assess liver function.

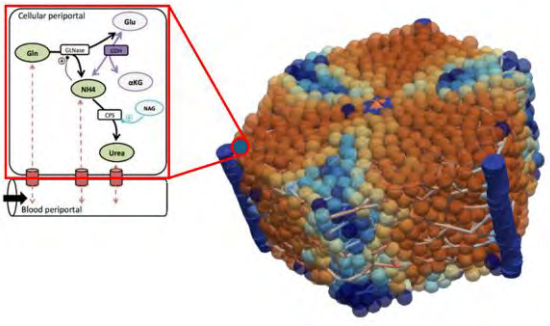


Figure 1: A screenshot from a simulation of flow and transport in the liver lobule using CompuTiX. Intracellular reactions, ammonia detoxification model [1] here, are solved inside each cell.

The model is parameterized using available data provided by project partners and / or published references. It considers liver zonation i.e., the execution of different reactions in different liver lobule zones (periportal, mid-lobular, and pericentral, e.g. [3]), as well as variations of microarchitecture, zonation and intracellular parameters as they occur in different disease states.

3. Results

Using the developed intracellular zonated model together with the SBML simulator integrated in the CompuTiX software, this work enables the exploration of entanglement intracellular dynamics with tissue-level mechanisms including cell growth, division, death, cell-cell crosstalk, mechanical and chemical interactions as well as flow and transport in sinusoids inside a freely accessible and modifiable digital liver twin prototype extension of CompuTiX.

4. Discussion and Conclusions

This work introduces a multiscale framework that links intracellular and multicellular models to provide insights into hepatocyte behaviour across different biological scales. The modular and open-source design facilitates reproducibility and enables straightforward integration of additional intracellular models or tissue-level mechanisms, making the framework a flexible platform for exploring liver tissue dynamics and disease processes.

5. References

1. A. Ghallab, *Journal of Hepatology*, vol. 64, no. 4, pp. 860–871, Apr. 2016.
2. C. Wallstab, *The FEBS Journal*, vol. 284, no. 19, pp. 3245–3261, 2017.
3. J. Dichamp, *Front. Bioeng. Biotechnol.*, vol. 11, 1049564, 2023.

Acknowledgements:
The work is conducted in collaborations with clinical partners within the ARTEMIs (Grant no: 101136299) and LySyM Cancer (Grant no: PTJ-031L0257A to SD) European projects.

A COMPUTATIONAL MODEL OF OXYGEN SENSING IN THE RODENT CAROTID BODY GLOMUS CELL.

Pragalath Neethirajan (1), Dale Sasis (2), Mohammad Shafiezadegan (2), Gonzalo Maso Talou (2), Finbar Argus (2)

(1) Faculty of Medical and Health Sciences, University of Auckland, Auckland, New Zealand
(2) Auckland Bioengineering Institute, University of Auckland, Auckland, New Zealand

1. Introduction

The carotid body detects changes in oxygen tension through type 1 glomus cells. In acute hypoxia, inhibition of oxygen-sensitive potassium currents trigger membrane depolarisation, calcium influx, catecholamine release, and activation of afferent nerve fibres [1]. However, which potassium currents are responsible for initiating this response remains uncertain. Candidate mechanisms include TASK-1/-3 background leak channels, voltage-gated potassium channels, and calcium-dependent potassium channels [2]. Due to experimental studies having typically examined these currents in isolation, their findings have remained inconsistent. Here, we developed an experimentally informed computational model of the type 1 glomus cell to enable holistic hypothesis testing of candidate oxygen-sensing mechanisms within an integrated cellular model informed by experiments.

2. Materials and Methods

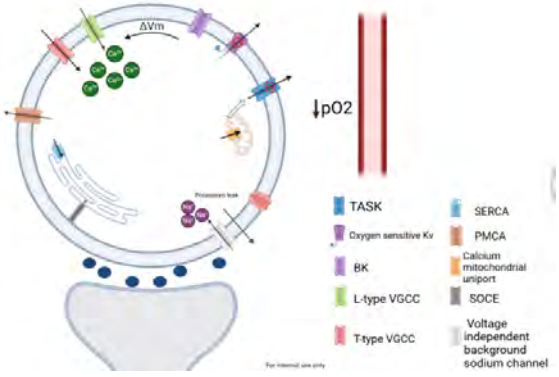


Figure 1: Type 1 Glomus cell schematic. TASK, represents heteromeric Twik -1/-3 related acid sensitive K^+ channel; Kv, Voltage gated K^+ channel; BK, big calcium dependant K^+ channel; L-Type VGCC, L-type voltage dependent Ca^{2+} channel; T-type VGCC, T-type voltage gated calcium channel; SERCA, Sarcoplasmic/Endoplasmic Reticulum Ca^{2+}-ATPase; PMCA, Plasma Membrane Ca^{2+}-ATPase; SOCE, Store-Operated Calcium Entry

A lumped compartment model of the glomus cell was developed incorporating potassium, sodium and calcium currents, with multicompartmental handling of intracellular calcium processes (Fig.1). Ion currents were represented with Hodgkin-Huxley formulations with the kinetics calibrated to experimental data from patch-clamp experiments, while intracellular calcium dynamics were modelled using michelis-menten fluxes. Channel conductances will be calibrated and validated with experimental whole-cell patch-clamp recordings.

3. Results

The model will be calibrated to reproduce key features of hypoxic glomus-cell activation. Oxygen-dependent modulation of candidate potassium currents will generate distinct electrophysiological signatures, allowing a probabilistic framework to identify which current/s most plausibly account for the initial hypoxia-induced depolarisation.

4. Discussion and Conclusions

We investigate the electrophysiological basis of oxygen sensing in carotid body type-1 glomus cells. By embedding alternative candidate currents within a cell model, this approach enables discrimination between hypotheses' and improves understanding of whole-cell ionic perturbations under physiological hypoxia.

5. References

1. Ureña, J. et al. (1994) Hypoxia Induces Voltage-Dependent Ca2+Entry and Quantal Dopamine Secretion in Carotid Body Glomus Cells. *Proceedings of the National Academy of Sciences - PNAS*. [Online] 91 (21), 10208–10211.
2. Asuncion Rocher & Philip I. Aaronson (2024) The Thirty-Fifth Anniversary of K+ Channels in O2 Sensing: What We Know and What We Don't Know. *Oxygen (Basel, Switzerland)*. [Online] 4 (1), 53–89.

Acknowledgements: n/a

BONE REMODELING MULTISCALE COMPUTATIONAL MODEL: COUPLING CELLULAR AND TISSUE DYNAMICS

Ana Clara Verly (1), Pedro M Amaral (2), Lahis S de Assis (3), Flávia de S Bastos (1), Bárbara Quintela (1)

1. Computational Modeling Graduate Program, Federal University of Juiz de Fora (UFJF), Brazil; 2. Computational Engineering (UFJF), Brazil; 3. Applied and Computational Mechanics (UFJF), Brazil;

1. Introduction

Computational models have become valuable tools for studying complex biological processes, such as bone remodeling [1]. Multiscale approaches integrate cellular dynamics with tissue-level biomechanics, combining mathematical models and finite element simulations [2]. This study aims to develop a coupled multiscale computational framework that couples an inflammation model with a biomechanical model to represent bone remodeling across cellular and tissue levels to investigate the interaction between hormonal regulation and bone mechanics.

2. Materials and Methods

At the cellular scale, the biological component is formulated as a system of nonlinear ordinary differential equations (Fig. 1) describing the interactions between innate immune system cells and bone cells during the bone repair process, including macrophages, cytokines, mesenchymal stem cells, and osteoblasts. Hormonal regulation is incorporated through estradiol-dependent parameters, enabling simulation of physiological variations in bone remodeling. At the tissue scale, the mechanical behavior is represented using a Finite Element Model implemented in Abaqus with a UMAT subroutine describing tensile damage evolution based on a damage formulation previously proposed in the literature [3].

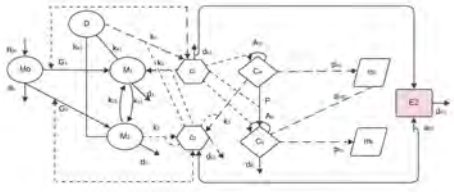


Figure 1: ODE-based model representing cellular interactions, model parameters, and estradiol (E2).

The coupling strategy enables bidirectional interaction between scales: biological variables influence tissue mechanical properties, while mechanical stimuli affect cellular responses.

3. Results

A bone fracture-healing scenario was simulated, with the central region representing the fracture gap, where damage evolution is evaluated during healing, driven by the ODE-based biological model (Fig. 2).

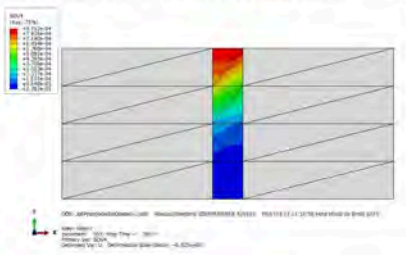


Figure 2: Bone healing scenario simulated using a finite element model.

4. Discussion and Conclusions

This work represents preliminary results for a multiscale computational framework for bone remodeling. Future developments will incorporate realistic 3D bone geometries to enable more accurate biomechanical simulations and support applications in fracture analysis and personalized bone health assessment.

5. References

1. Ji B, Zhang et al. Mathematical modelling of bone remodelling cycles including the NFκB signalling pathway. Comput Biol Med. 2019;107:257–264 (2019).
2. Coelho PG, Fernandes PR, Rodrigues HC. Multiscale modeling of bone tissue with surface and permeability control. J Biomech. 2011;44(2):321–329 (2011).
3. Assis LS et al. Influence of temperature on the mechanical behavior of a reinforced concrete beam. J Eng Exact Sci. 2023;9:15215-01a (2023).

Acknowledgements:

The authors would like to thank CAPES and FAPEMIG for financial support.

IN SILICO DESIGN OF MG-BASED DEGRADABLE POROUS SCAFFOLDS FOR THE REPAIR OF CRITICAL-SIZE DEFECTS

Sophie Nguyen (1 *), Mojtaba Barzegari (2), Liesbet Geris (1,3)

1. Biomechanics Section, Department of Mechanical Engineering, KU Leuven, Belgium; 2. Electrochemical Materials and Systems, Department of Chemical Engineering and Chemistry, TU Eindhoven, The Netherlands; 3. Biomechanics Research Unit, GIGA In Silico Medicine, University of Liège, Belgium

** Corresponding author: Sophie Nguyen, sophie.nguyen@kuleuven.be*

1. Introduction

Critical-size bone defects arising from trauma, disease, or surgery remain difficult to treat because the intrinsic regenerative capacity of bone is limited. Biodegradable porous scaffolds have emerged as a promising alternative to grafting strategies for bridging such defects, yet the mechanisms governing bone regeneration within scaffolds are still not fully understood. Most large-animal studies rely on endpoint analyses, providing little insight into the dynamic interplay between bone formation and material degradation. In silico modeling could help provide longitudinal data of these coupled processes, supporting the design and development of more effective regenerative therapies. Here we developed a multi-factorial in silico model to study the balance between the kinetics of porous scaffold degradation and the rate of bone formation.

2. Materials and Methods

A set of partial differential equations (PDEs) was established describing the chemistry of corrosion of a magnesium scaffold, as well as bone ingrowth through the spatiotemporal concentration of bone cells. The model implicitly tracks the degradation and bone formation fronts in a phase-field framework, including curvature-based effects. The PDEs are solved numerically using the finite element method and implemented in FreeFEM. The interface between the scaffold and bone is refined over time through a mesh adaptation procedure, allowing accurate tracking of the moving interfaces. The model outputs are the concentration of bone cells and magnesium ions, the geometry of the degrading scaffold, and the density of new bone over time. The model will be informed by unpublished large animal data at various time points.

3. Results

The model is applied to a gyroid scaffold, investigating various differences in speed between the bone formation and implant degradation. Figure 1 shows the results of the simulation where both processes occur at comparable speed, showing scaffold degradation while new bone is forming at the scaffold surface and filling the pores.

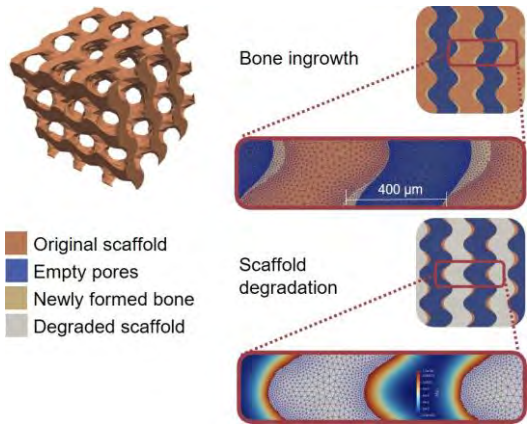


Figure 1: Bone ingrowth (yellow) into pores (blue) of a degrading (grey) gyroid scaffold. Orange regions are the initial scaffold geometry.

4. Discussion and Conclusions

This work introduces an in silico model that quantitatively captures the spatiotemporal evolution of scaffold degradation and bone ingrowth, addressing the current lack of in vivo longitudinal data. Once validated, the model is intended to serve as a design tool to optimize scaffold geometry and support the development of treatments to repair critical-size bone defects.

Acknowledgements:

The research was financially supported by the PRosPERoS-II project, funded by the Interreg VA Flanders - the Netherlands program, CCI grant no. 2021TC16RFCB041.

MECHANICS OF DIFFUSIVE CROSSLINKERS IN BIOPOLYMER NETWORKS: A CONTINUUM APPROACH

Luís Pacheco (1,2), Marco Parente (1,2), João Ferreira (1)

1. Faculty of Engineering - University of Porto, Portugal;
2. INEGI – Institute of Science and Innovation in Mechanical and Industrial Engineering, Portugal;

1. Introduction

The mechanical phenotype of cells has emerged as a key biomarker of disease progression. Cellular structural behavior is governed by the actin cortex, a dynamic biopolymer network exhibiting viscoelastic properties due to the transient binding of crosslinker proteins. While current continuum models capture network hyperelasticity, they often neglect the mechanochemical feedback governing crosslinker diffusion and stress-driven unbinding. To address this, we propose a coupled diffusion-deformation continuum framework to predict cytoskeletal remodelling.

2. Materials and Methods

The total crosslinker concentration is decomposed into bound and free phases. To capture the mechanical response at finite strains, we employ a micro-sphere homogenization of extensible actin filaments [1], where their contour length and density dynamically adapt to the local concentration of bound crosslinkers. The evolution between the bound and free states is governed by reversible reaction kinetics [2], featuring a slip-bond mechanochemical coupling where increased filament force accelerates crosslinker detachment. Finally, the spatial transport of free crosslinkers is driven by the gradient of the chemical potential, derived from Flory-Huggins polymer thermodynamics. The resulting coupled system is implemented numerically through a user-defined element in *Abaqus* [3].

3. Results

Evaluation of the constitutive model at the material point level suggests that the stretch-induced unbinding of crosslinkers governs both macroscopic stress relaxation and frequency-dependent hysteresis under cyclic loading. To evaluate macroscopic behavior and replicate experimental cell probing techniques, a 3D finite element cube indentation test was performed. Indentation results indicate that higher strains under the spherical probe trigger local crosslinker detachment, leading to sharp chemical potential gradients (Fig. 1). By driving a spatial flux of free crosslinkers toward less stressed regions, the mass transport mechanism is expected to dictate the force-relaxation response of the network.

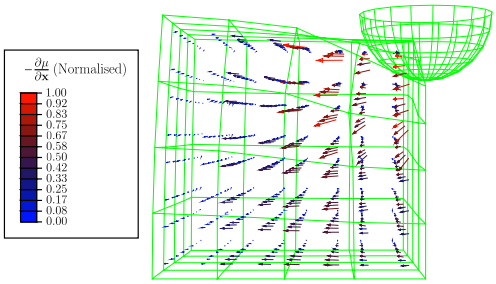


Figure 1: Chemical potential gradients driving free crosslinker diffusion during spherical indentation.

4. Discussion and Conclusions

By treating crosslinkers as a diffusing phase rather than static parameters, this coupled framework captures the transient viscoelasticity of the cytoskeleton. The integration of mechanochemical coupling allows the model to predict complex spatial behavior, such as local relaxation and dynamic mass transport, under complex boundary conditions. This framework provides a microstructurally-informed foundation to investigate how transient cytoskeletal changes influence cell mechanics in disease states, with future work focusing on calibration against experimental results.

5. References

1. G. A. Holzapfel et al., J Mech Behav Biomed Mater. 38, 78–90 (2014).
2. M. Arricca et al., J Mech Phys Solids. 181, 105425 (2023).
3. S. A. Chester et al., Int J Solids Struct. 52, 1–18 (2015).

Acknowledgements:
The authors would like to acknowledge financial support from Fundação para a Ciência e a Tecnologia (FCT) through grant 2024.00670.BD.

ESTIMATION OF ACTIVE MYOCARDIAL CONTRACTILITY VIA PHYSICS-INFORMED NEURAL NETWORKS FOR SCAR DETECTION

Matthias Höfler (1,4), Francesco Regazzoni (2), Stefano Pagani (2), Elias Karabelas (1,4), Christoph Augustin (3,4), Gundolf Haase (1,4), Gernot Plank (3,4), Federica Caforio (1,3,4)

1. Dept. of Mathematics and Scientific Computing, NAWI Graz, University of Graz, Austria; 2. MOX, Dept. of Mathematics, Politecnico di Milano, Italy; 3. Gottfried Schatz Research Center, Medical University of Graz, Austria; 4. BioTechMed-Graz, Austria

Corresponding author: Federica Caforio, Dept. of Mathematics and Scientific Computing, Heinrichstrasse 36, 8010 Graz, Austria, federica.caforio@uni-graz.at

1. Introduction

The estimation of active myocardial properties from displacement or strain data is a major challenge in cardiac imaging. In myocardial infarction, fibrotic tissue loses contractile function, and non-invasive detection of these regions is clinically important for scar identification. We present a physics-informed neural network (PINN) framework [1] that estimates spatially varying active contractility parameters from displacement and strain data.

2. Materials and Methods

Two neural networks are trained simultaneously: NN_u approximates the displacement field, and NN_{S_a} approximates the active contractility field S_a. The loss combines a data fidelity term on observed displacements, a PDE residual enforcing momentum balance, and a Neumann boundary residual. Training data are FEM-generated displacement and strain fields corrupted with additive Gaussian white noise, characterised by limiting dispersion LD $= 3\sigma/\max(\mathrm{u})$.

Several enhancements address limitations of vanilla PINNs [2], including Residual-Based Attention, exact Dirichlet boundary enforcement; random Fourier features on NN_{S_a}; a boundary-weighted gradient penalty on NN_{S_a}. For the time-dependent case, a decoupled space-time formulation substantially reduces computational cost. Full details are in [2].

3. Results

We illustrate the method on a 10 mm cubic domain containing a spherical scar (S_a= 7.87 kPa) with a grey zone (S_a= 37.79 kPa) embedded in healthy tissue (S_a= 118.08 kPa). The PINN accurately reconstructs the contractility field and correctly identifies scar contours without any prior assumption on scar shape, size, or number (Fig. 1).

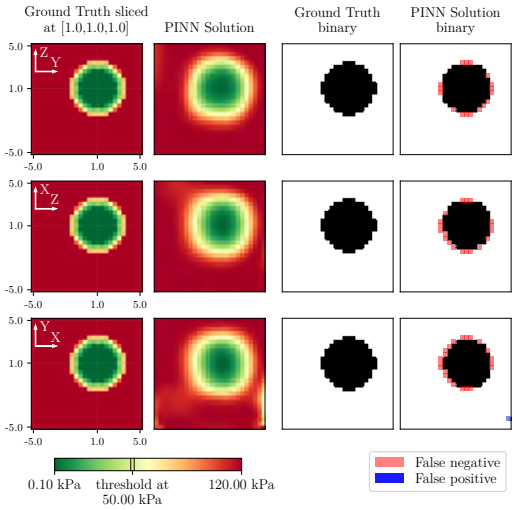


*Fig. 1: S_a field reconstruction for a scar with grey zone (*LD *= 0.05). Three orthogonal slices shown.*

4. Discussion and Conclusions

PINNs can reliably identify fibrotic myocardial regions from displacement and strain data alone, without requiring stress measurements. The physics-based formulation constrains the solution space, enabling accurate parameter estimation even from sparse, noisy data. This hybrid approach leverages the complementary strengths of mechanistic cardiac models and neural network flexibility. Future work will extend the framework to patient-specific geometries and physiological fibre architectures, towards non-invasive scar characterisation in clinical workflows.

5. References

1. Höfler M et al. arXiv:2505.03382 (2025).
2. Raissi M et al. JCP. 2019;378:686–707.
3. Guccione JM et al. JBE 1991;113(1):42–55.
4. Bestel J, Clément F, Sorine M. MICCAI 2001. LNCS 2208:1159–1161.

PERSONALIZED TRACKING OF CORE TEMPERATURE FROM WEARABLES VIA A PHYSICS-GUIDED BAYESIAN ODE

(1), Yamo Cao (2), Yawen Cao

1. Nanyang Technological University, Singapore

1. Introduction

Heat stress during exercise and hot environments can elevate heat-illness risk. Core body temperature (T_{core}) is a key marker, yet direct sensing (rectal/ingestible) is intrusive. Mechanistic thermoregulation models are physiologically grounded but often require many parameters/inputs and may degrade when simplified or non-personalized across workloads and environments [1]. Wearable-driven estimators, including heart-rate-based algorithms such as ECTemp, are practical but can be condition- and subject-dependent under varying metabolic demand and heat exposure [2], [3]. We therefore pursue a structure-preserving approach that personalizes thermoregulatory dynamics from sparse history while yielding uncertainty for safety-critical use. In this work, we develop a physics-guided Bayesian ODE model for wearable-based T_{core} tracking that personalizes dynamics from sparse history and provides uncertainty for safety-critical use. In leave-one-subject-out testing, it achieves 0.15°C MAE and 0.97 Pearson correlation.

2. Methods

We estimate T_{core} from wearable signals using a physics-guided model (Fig. 1). A GRU encodes prior-session history and an MLP encodes static context; their concatenation forms a subject/session representation. Conditioned on this representation, Bayesian heads infer ODE parameters governing Tcore dynamics, enabling lightweight personalization with posterior uncertainty.

$$\frac{d\hat{T}_t}{dt} = \alpha(\widetilde{HR}_t - HR_{\text{base}}) - \beta(\hat{T}_t - T_a) \qquad (1)$$

where HR_{eff} is a learned effective drive from normalized heart rate and smoothed workload, and T_{amb} is de-normalized ambient temperature acting as an exogenous boundary condition. Tcore is propagated by forward Euler integration and initialized by the first measured T_{core} sample.

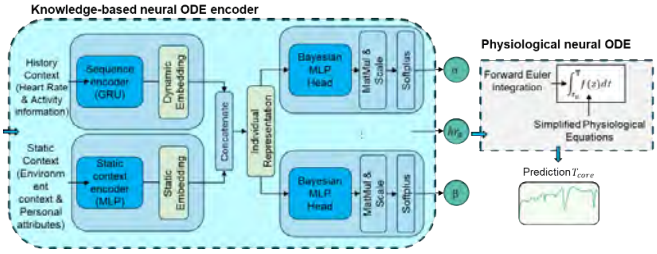


Figure 1: Model overview: personal history and context encoders → Bayesian ODE parameters → Euler-integrated T_{core}

3. Results

In leave-one-subject-out testing on the controlled protocol dataset, the model achieves 0.15 °C MAE and 0.97 Pearson correlation, tracking both absolute level and temporal trends. Inferred parameters are stable and interpretable at the session level: α modulates HR-driven heating, while β captures ambient-gradient cooling. Parameter posteriors provide confidence signals that can flag low-support regimes (e.g., sparse history).

4. Discussion and Conclusions

A personalized, physiology-structured ODE decoder can estimate T_{core} accurately while retaining interpretable parameters (α, β) and uncertainty information. By combining mechanistic constraints with learned personalization, the framework supports explainable, confidence-aware thermoregulation tracking and serves as a building block for digital-twin-oriented heat-stress monitoring.

5. References

1. Brodland GW, Veldhuis JH. PLoS One. 2012;7(9):e44281 (2012).
2. Maška M et al., IEEE Trans Med Imaging; 32(6):995-1006 (2013a).
3. Caiazzo A et al., ICCS 2009 conference: Springer; 2009. p. 705-14

Acknowledgements:
Research supported by the Ministry of Education, Singapore Academic Research Fund (AcRF) Tier 1 under Grant RG146/23.

PRE-OPERATIVE, DIAGNOSIS-ADJUSTED RISK PREDICTION OF PROLONGED HOSPITALISATION AFTER PAEDIATRIC CARDIAC SURGERY WITH CARDIOPULMONARY BYPASS

Francesca Kessler (1), Alexandros Zenonos (1,2), Richard Issitt (1, 2), Vivek Muthurangu (1)

1. UCL Institute of Cardiovascular Science, UK; 2. Great Ormond Street Hospital for Children, UK

Correspondence: Francesca Kessler, UCL Institute of Cardiovascular Science, francesca.kessler.21@ucl.ac.uk

1. Introduction

Foreseeing prolonged length of stay (PLOS) after paediatric cardiac surgery with cardiopulmonary bypass (CPB) is crucial for delivering safe, equitable, and efficient care, especially if the prediction can be made before the start of surgery [1,2]. Major differences in post-operative LOS exist between different diagnoses groups [3]. Diagnosis-adjusted PLOS (DAPLOS) prediction would substantially increase granularity and achieve more individualised predictions, especially when clinical adoption of the prediction models is also tackled [4].

2. Materials and Methods

Two machine learning (ML) models, a logistic regression (LR) and XGBoost, were compared for DAPLOS prediction, defined as a binary variable where LOS exceeds the 75th percentile for its diagnosis group. For facilitation of the models' clinical application, low and high-risk cutoffs were identified to enable clinical risk stratification, using a sensitivity and specificity cutoff of 95%. Finally, the risk scoring models were implemented in a user-friendly webpage application.

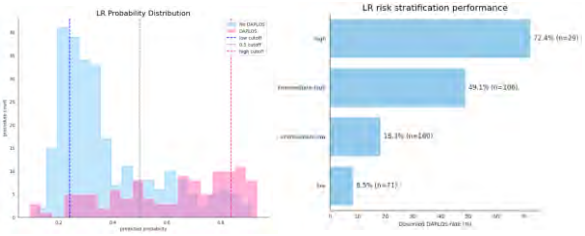


Figure 1: Probability distribution and risk stratification cutoffs (left) and risk stratification performance for the observed DAPLOS rate (right) for the LR prediction model.

3. Results

The LR and XGBoost were able to predict DAPLOS with an ROCAUC of 0.79 and 0.84, an accuracy of 0.74 and 0.79, and a PRAUC of 0.76 and 0.76 respectively. A high-risk group could be identified for both models, with a PPV of 72% for the LR and 90% for XGBoost. For both models, the number of procedures with DAPLOS in each risk group accurately resembled the stratification, as visible in their probability distributions and risk stratification (Figures 1 for LR, Figure 2 for XGBoost). Furthermore, the models were successfully implemented in an openly accessible web-based application.

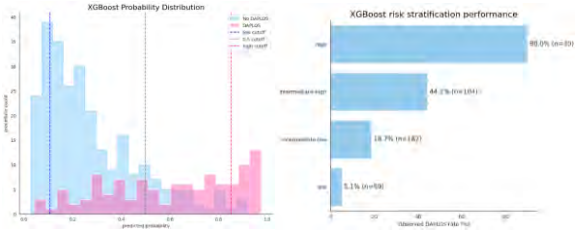


Figure 2: Probability distribution and risk stratification cutoffs (left) and risk stratification performance for the observed DAPLOS rate (right) for the XGBoost prediction model.

4. Discussion and Conclusions

This study demonstrates that prolonged hospitalisation relative to diagnosis group can be accurately predicted, including classification into four risk groups, using routine EHR data and simple ML algorithms. To the best of our knowledge, this is the first study to perform this prediction preoperatively and implement the models in an openly accessible web-based application. Building further on this research, understanding the effect of incorporating intraoperative data could benefit future prediction models, as well as prediction of the exact LOS days, for an even more granular prediction.

5. References

1. Garg L. et al. Systems and Humans. 2012;42; 1332:1345.
2. Pasquali, S. et al. Ann Thorac Surg. 2014; 98(5); 1660:1666.
3. Rogers L. et al. Ann Thorac Surg. 2017;104:211-9.
4. Mohammadi, I. et al. BMC Cardiovasc. Disord.; 2024; 24;718

Acknowledgements:

The authors would like to thank Great Ormond Street Charity for providing financial support to this project.

UNSUPERVISED MATERIAL MODEL DISCOVERY OF MYOCARDIAL TISSUE BEHAVIOR

Mathias Peirlinck
Delft University of Technology, Delft, the Netherlands

Accurately characterizing myocardial tissue mechanics is critical for improving patient-specific diagnoses and therapies in cardiac disease. Because of the tissue's complex, anisotropic, and nonlinear properties, researchers often rely on multiple mechanical tests, e.g. biaxial tensile and triaxial shear, to capture its orthotropic behavior. These methods typically assume minimal variability among samples and rely on homogeneous deformation patterns that do not reflect the natural heterogeneity of myocardial tissue. Additionally, the dissection and gluing steps required for triaxial shear testing can introduce artifacts that alter the mechanical response. In this work, we propose a single-shot framework that leverages a single specimen's microstructural and geometrical complexity and resulting heterogeneous deformation to infer its orthotropic mechanical behavior. This offers a more direct and integrated analysis of the anisotropic and nonlinear mechanical envelope while negating the impact of sample variability and invasive preparations.

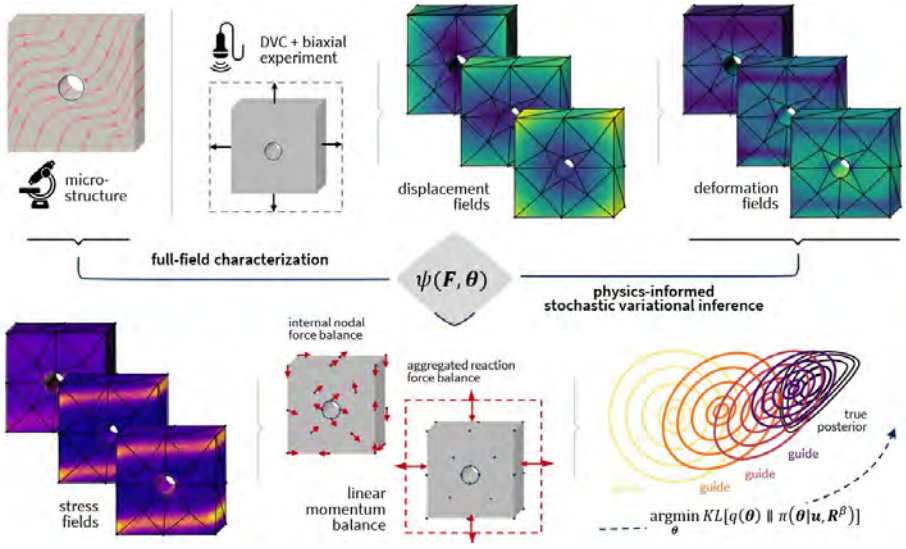
Methods. We generate synthetic tissue slabs with varying fiber heterogeneity and two geometries (rectangular and perforated) to reflect realistic myocardial tissue behavior. The slabs followed the Holzapfel–Ogden hyperelastic model, capturing the nonlinear, orthotropic nature of heart muscle tissue. Leveraging the finite element approach, we simulate biaxial tensile tests, generating displacement fields and aggregated reaction forces that serve as our observed data.

To infer the unknown constitutive parameters, we utilize the generated displacement fields as boundary conditions while reformulating the static mechanical equilibrium problem in its variational form. Through this formulation, we define a likelihood function that compares the aggregated force measurements with the model-predicted reaction forces, which depend on both the measured displacements and the unknown material parameters. Combined with uninformative priors on the parameters, we leverage Bayes' rule to compute the posterior distribution for the unknown constitutive parameters. Lacking a closed-form solution, we employ stochastic variational inference, an iterative, optimization-based technique, to efficiently approximate our posterior distribution. Minimizing the Kullback-Leibler divergence between the posterior and its mean-field approximation, we converge toward constitutive parameter estimates that best reproduce the synthetic data. Finally, we validate our inferred constitutive parameters using an unseen synthetic tissue slab with different fiber heterogeneity and geometry.

Results & Discussion. We recover nearly all constitutive parameters to high precision, with relative errors averaging around 1e-7. Even the most challenging $\boldsymbol{a_{fs}}$ and $\boldsymbol{b_{fs}}$ parameters were identified within 1% of their true values. Validation on a highly nonlinear mechanical equilibrium problem further demonstrated that the inferred parameter set reproduced displacement profiles with 99.9% accuracy and reaction forces to machine precision.

These findings highlight the effectiveness of our unsupervised, full-field stochastic variational inference in capturing the orthotropic and nonlinear nature of complex tissues using only displacement and reaction force measurements. By eliminating the need for multiple specialized tests, this method has the potential to simplify current biomechanical characterization protocols. In doing so, it also paves the way for deeper insights into the evolving mechanical behavior of highly anisotropic tissues, a critical step toward enhancing patient-specific diagnostics and treatments.

Reference: Krijnen, R. P., Joshi, A., Kumar, S., & Peirlinck, M. (2025). *arXiv preprint arXiv:2510.09498*.



SCALABLE INFERENCE OF GUT MICROBIOTA LOTKA–VOLTERRA MODELS WITH PHYSICS-INFORMED NEURAL NETWORKS

Lorenzo Sala[1,2], Yanis Jouanaud[1], Nicolas Jouvin[3], Hugo Gangloff[3], Beatrice Laroche[1,2]

[1]Univ. Paris-Saclay, INRAE, MaIAGE, France; [2]Inria, MUSCA, France;
[3] Univ. Paris-Saclay, AgroParisTech, INRAE, MIA Paris-Saclay, France

1. Introduction

Longitudinal microbiome sequencing provides time-resolved abundance profiles of microbial communities, yet translating these measurements into mechanistic insight remains challenging. Ecological interaction models such as the Generalized Lotka–Volterra (GLV) system offer an interpretable description of microbial competition and cooperation, but classical parameter estimation methods often fail due to nonlinear coupling, instability regions, and poor identifiability. Generalized smoothing approaches (GSA) [1] provide a principled framework for handling sparse data by relaxing strict ODE constraints, yet they become computationally prohibitive when scaling to high-dimensional systems.

2. Materials and Methods

We describe microbial dynamics through the GLV system:

$$\frac{dx_i}{dt} = \mu_i x_i(t) + \sum_{j=1}^{N} a_{ij}\, x_i(t)\, x_j(t) \quad \forall i = 1, \dots N,$$

where $x_i(t)$ denotes species abundance, μ_i intrinsic growth rates, and a_{ij} interaction coefficients. To address the associated inverse problem, we embed the GLV equations within a Physics-Informed Neural Network (PINN) [2]. The neural network represents latent trajectories, while automatic differentiation enforces consistency with the governing ODEs. We introduce a novel alternating inference strategy, iteratively updating (i) neural trajectory representations under fixed parameters and (ii) ecological parameters under fixed trajectories. This approach balances data fidelity and dynamical regularization, acting as a physics-based smoothing method for sparse time-series data. It can be interpreted as a scalable, neural reformulation of generalized smoothing, avoiding repeated numerical integration and large basis expansions typical of classical GSA.

3. Results

On a simplified synthetic three-species oscillatory GLV system under sparse and noisy observations, classical GSA and the proposed PINN-based GSA achieve comparable trajectory reconstruction (profiled solution error 0.059 vs 0.045). However, the computational cost is significantly lower for the PINN framework (5.116 s vs 30.357 s), supporting its scalability toward higher-dimensional microbiome models. Figure 1 illustrates the comparative reconstructions.

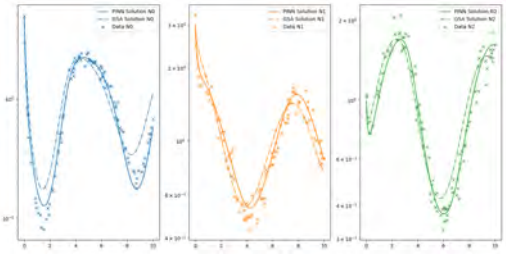


Figure 1: Synthetic three-species GLV data reconstruction using classical GSA and the alternating PINN approach.

4. Discussion and Conclusions

The proposed alternating PINN framework preserves reconstruction accuracy while substantially reducing computational cost compared to classical generalized smoothing. By embedding mechanistic GLV equations within a neural architecture, the method balances data fidelity and dynamical regularization, stabilizing inference from sparse microbiome time-series data. Overall, this work demonstrates how knowledge-driven ecological modelling can be effectively integrated with data-driven learning, enhancing scalability and robustness without sacrificing mechanistic interpretability in nonlinear biological systems.

5. References

1. Ramsay JO et al., J R Stat Soc Series B; 69(5):741–796 (2007)
2. Hossie PJ et al., ESAIM Proc Surv; 81:104–122 (2025)

A FEASIBILITY PIPELINE: STRUCTURING MULTIMODAL REAL-WORLD DATA FOR DIGITAL TWIN DEVELOPMENT

Abiram Sandralegar (1,2), Ekaterina Golubeva (3), Lea Bührer (3,4), Sandrine Morel (5), Philippe Bijlenga (1,2)

1. Division of Neurosurgery, Geneva University Hospitals, Switzerland; 2. Faculty of Medicine, University of Geneva, Switzerland; 3. Centre for Computational Health, Institute of Computational Life Sciences, Zurich University of Applied Sciences, Switzerland; 4. Department of Mathematical Modeling and Machine Learning, University of Zurich, Switzerland; 5. NeuroCentre, Geneva University Hospitals, Switzerland.

1. Introduction

Digital twin deployment in healthcare requires longitudinal, structured, and semantically interoperable real-world data embedded in routine care. Yet hospital information systems remain fragmented across free-text narratives, imaging archives, structured forms, and administrative coding systems. This fragmentation —not modelling capacity— constitutes a major bottleneck for scalable digital twin development. We hypothesised that a hospital-embedded, disease-oriented structuring pipeline integrating clinical standardisation, structured reporting, administrative code reuse, automated Large Language Model (LLM)-based text extraction, imaging categorisation, and ontology-driven semantic harmonisation could transform heterogeneous documentation into digital twin–ready datasets without disrupting workflows. We further hypothesise that meaningful interaction with validated decision-support tools could incentivise higher-quality data capture; however, such tools have not yet been available at clinical grade for prospective evaluation.

2. Materials and Methods

We implemented a modular structuring framework within a tertiary academic centre and applied it to a longitudinal intracranial aneurysm cohort (n = 3,154; 2007–present). Clinical pathways were standardised within the electronic health record. Disease-specific structured forms defined variables for prospective capture. Diagnostic (ICD) and procedural billing codes supported case identification and intervention recovery.

Free-text documents were processed using an LLM-based extraction pipeline. Radiological examinations were retrieved programmatically and curated via a high-throughput clinician validation interface. All variables were mapped to SNOMED-CT within a unified semantic framework.

3. Results

The pipeline enabled identification and consolidation of all 3,154 patients diagnosed over 18 years. Age at diagnosis and sex were available for 100% of cases. Among 1,125 prospectively documented patients, baseline condition was captured in >90%. Structured forms alone yielded <10% completeness for discharge interventions and outcomes. Integration of administrative codes substantially improved recovery of procedural data. Follow-up outcomes at 1 and 5 years reached ~70% completeness.

Infrastructure development required sustained investment, including research nurse support, master-level abstraction, and development of an LLM-based structuring system enabling generation of a minimal digital twin–ready dataset.

4. Discussion and Conclusions

Constructing a digital twin–ready cohort from routine hospital data is feasible but resource-intensive. Structured forms alone are insufficient for sustainable large-scale capture. A layered strategy—combining clinical standardisation, administrative code reuse, automated text extraction, imaging curation, and semantic harmonisation—is required to reconcile clinical reality with modelling needs. Over two decades, the absence of clinically validated decision-support tools prevented testing whether prediction-driven clinician interaction could improve structured data quality. Digital twin deployment may therefore depend not only on infrastructure, but on integrating clinically useful decision-support systems that create feedback loops within care processes.

ADAPTIVE MODEL REDUCTION FOR EFFICIENT DATA AUGMENTATION FOR MACHINE LEARNING CLASSIFICATION

M. Stefanati (1), S. Gahima (2), J. F. Rodríguez Matas (1), A. García-González (2,3), P. Díez (2,3)

1. DCMC, Politecnico di Milano, Italy; 2. Universitat Politècnica de Catalunya, Spain; 3. CIMNE, Spain

Corresponding author: Marco Stefanati, marco.stefanati@polimi.it

1. Introduction

Peak von Mises stress (pVMS) is a key biomechanical marker of atherosclerotic plaque vulnerability [1]. High-fidelity full order models (FOMs) estimate pVMS accurately but remain too computationally expensive for large-scale studies or near real-time clinical use. Reduced-order models (ROMs) based on Proper Orthogonal Decomposition (POD) offer a promising alternative, yet their performance deteriorates when arterial geometry and material composition vary significantly. This work introduces an adaptive model reduction (AMR) strategy designed to preserve accuracy in heterogeneous arterial sections while drastically reducing computational cost.

2. Materials and Methods

We build an unfitted FOM framework where arterial sections are represented on a fixed background mesh [2]. Displacement snapshots for a large set of arterial geometries are used to construct a POD basis explaining 99.9% of the variance. AMR approximates the displacement field, $\tilde{\boldsymbol{y}}$, as:

$$\tilde{\boldsymbol{y}}(\boldsymbol{\mu}) \approx \boldsymbol{y}^{\star} := D_z(\bar{\boldsymbol{y}} + \boldsymbol{U}^{\star}\boldsymbol{z}) + D_w\boldsymbol{w}, \qquad (1)$$

where $\boldsymbol{\mu}$ is a vector of geometric features, $\bar{\boldsymbol{y}}$ is the average displacement of the section, $\boldsymbol{U}^{*}$ is the left singular matrix of the POD, $\mathbf{z}$ and $\mathbf{w}$ are the modal and nodal descriptions respectively, and D_z and D_w are Boolean matrices to arrange DOF. AMR locally enriches the reduced system by applying the ROM where the basis is reliable, while FOM is retained near the lumen and calcifications, where pVMS concentrates. The method is validated on realistic arterial sections and used to generate a large pVMS dataset for machine-learning (ML) classification.

3. Results

Compared to the classic ROM, AMR reduces pVMS errors sixfold while reducing computational cost. Using extended snapshots further improves accuracy and computational efficiency. In a large-scale case study of 159K simulations, AMR reproduces the statistical behavior of high-fidelity FOMs and reduces computational cost by approximately 70%. ML models trained on AMR-generated data achieve the predictive performance of those trained on FOM datasets [3].

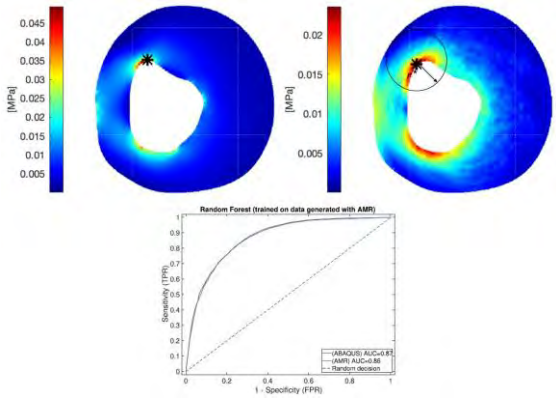


Figure 1: VMS field in an arterial section for FOM (left top panel) and AMR (right top panel); and ROC of classifier model (bottom panel) for FOM (red curve) and AMR (blue curve) data.

4. Discussion and Conclusions

The proposed AMR framework balances accuracy and efficiency by preserving high-fidelity resolution only where needed. Its compatibility with voxelized imaging and fixed-mesh workflows supports integration into clinical pipelines. By enabling fast generation of large, high-quality biomechanical datasets, AMR facilitates interpretable ML tools for plaque vulnerability assessment. Future work will extend the method to nonlinear anisotropic materials and three-dimensional geometries.

5. References

1. Corti A et al., CMPB, 260: 1-12 (2025).
2. Gahima S et al., Comput Mech, 1-14 (2025).
3. Stefanati M et al., CMPB, 254: 1-9 (2024).

ROBUST LEARNING DOMAIN FORMULATION FOR DEEP LEARNING MODELS IN A SMALL DATA REGIME

Kevin Zhao* (1), Beatrice Ghitti (1), Martyn P. Nash (1,2), Gonzalo Maso Talou (1)

1. Auckland Bioengineering Institute, University of Auckland, New Zealand
2. Dept. of Engineering Science and Biomedical Engineering, University of Auckland, New Zealand

*Corresponding Author, Email: kzha559@aucklanduni.ac.nz

1. Introduction

Traditional methods for modelling biophysical processes within the human body (e.g., the finite element method) are often computationally intensive. Deep learning models are a suitable alternative due to their ability as a universal approximator [1].

However, data-driven deep learning models require large amounts of data to train, with such data often being sparse, noisy or requiring invasive procedures to acquire. Training deep learning models in this small data regime can be difficult, impractical and/or infeasible.

2. Materials and Methods

Neural networks (NNs) inherently learn low-frequency contributions of biophysical fields more efficiently than higher-frequency contributions, a phenomenon named spectral bias [2]. Consequently, NNs tend to underperform in inferring function associated with higher-frequency contributions.

The goal of this work is to define a convenient reference configuration, where biophysical fields are characterised by a lower spectral response. By mapping the fields to such a reference configuration, spectral bias is leveraged to accelerate the learning process and increase the accuracy of network predictions.

To find the optimal reference configuration for a field, we solve an optimisation problem where the spectral response is minimised over the set of all permissible mappings.

3. Results

This methodology was applied to a simple analytical 1D chirp function with an exponentially increasing frequency. The space of permissible mappings was defined using monotonic cubic spline deformations with a fixed number of control points.

A feedforward NN was trained separately on the original spatial configuration and the optimal reference configuration. Multiple random initialisations were used to generate a confidence interval of output predictions.

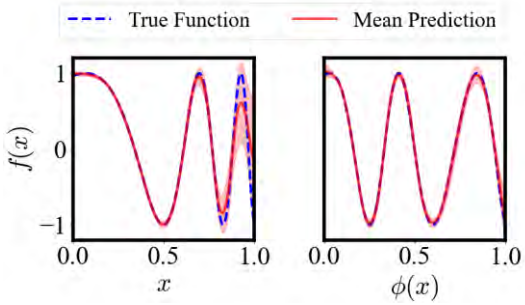


Figure 1: Mean predictions from the NN with confidence intervals (±SD; shaded) on the original (left) and optimal reference (right) configuration.

Preliminary results (Fig. 1) show that training a NN on the optimal reference configuration results in more accurate predictions with lower variance in the regions corresponding to higher frequencies in the original function.

4. Discussion and Conclusions

By mapping a higher frequency field to a lower frequency representation, the performance of a neural network can be improved without the need for additional data.

This methodology will be applied to multi-dimensional biophysical fields, demonstrating precise learning of complex and high-frequency behaviour even in small data regimes.

5. References

1. Hornik, et al. Neural networks 2:359-66, 1989.
2. Nasim, et al., International conference on machine learning. PMLR, 2019.

Acknowledgements:
The authors thank the VITAL Consortium (Horizon Europe Grant no: 101136728) for funding this project.

PATIENT-SPECIFIC 0D CIRCULATION MODELING WITH REGRESSION-BASED PARAMETER UPDATES TO PREDICT POST-HEPATECTOMY OUTCOMES

Francesco Songia (1), Kevin Hakkakian (2), Stephanie Roullet (2,3), Audrey Coilly (2,4), Nicolas Golse (2,4), Irene Vignon-Clementel (1)

1. Inria Saclay, France; 2. AP-HP Hôpital Paul-Brousse; 3. Inserm U1176, Université Paris-Saclay; 4. Inserm U1193, Université Paris-Saclay

1. Introduction

Post-hepatectomy liver failure remains the leading cause of death following surgery to treat liver cancer. Digital twins have emerged as a way to anticipate surgical risk. This work aims to predict post-resection hemodynamic changes and support the evaluation of portal hypertension risk.

2. Materials and Methods

We employ a patient-specific whole-body 0D (lumped-parameter) circulation model [1][2] calibrated on preoperative measurements. We then simulate liver resection and the resulting changes in hemodynamic, and compare model predictions with postoperative measurements. In addition, we propose a novel approach based on a regression model to account for further patient-specific differences in response to resection by updating a small set of lumped parameters during the simulation. The regression incorporates clinical data including patient history, perioperative events (e.g., bleeding, fluid administration, anesthesia), and specific procedures such as portal vein embolization. Finally, we perform uncertainty quantification on both the 0D model and the regression-based parameter updates, propagating measurement and parameter uncertainty to obtain predictive intervals for postoperative hemodynamic outcomes.

3. Results

The proposed hybrid framework provides patient-specific postoperative hemodynamic predictions that can be directly compared to postoperative measurements and complemented with predictive intervals to support risk-oriented interpretation.

4. Discussion and Conclusions

We propose a hybrid mechanistic–learning modeling approach that combines a patient-specific 0D blood circulation model with a data-driven regression to capture additional patient-specific responses to resection. This enhances the predictability of post-surgery hemodynamic outcomes and the evaluation of portal hypertension risk. This framework can be readily applied to a range of hemodynamics surgical interventions.

5. References

[1] Golse N, Joly F, Combari P, Lewin M, Nicolas Q, Audebert C, Samuel D, Allard MA, Sa Cunha A, Castaing D, Cherqui D, Adam R, Vibert E, Vignon-Clementel IE. Predicting the risk of post-hepatectomy portal hypertension using a digital twin: A clinical proof of concept. J Hepatol. 2021 Mar;doi: 10.1016/j.jhep.2020.10.036.

[2] Sala L, Golse N, Joosten A, Vibert E, Vignon-Clementel I. Sensitivity Analysis of a Mathematical Model Simulating the Post-Hepatectomy Hemodynamics Response. Ann Biomed Eng. 2023 Jan; doi: 10.1007/s10439-022-03098-6.

LLM + MULTISCALE MODELING FOR NEUROLOGY

W. Lytton (1), J. Lee (3), A. Newton (1), C. Kelley (2), R. McDougal (3), J. Jung (1), M. DiStasio (3), G. Cedersund (4)

1. DHSU Brooklyn NY USA; 2. McGill Montreal Canada; 3. Yale New Haven CT USA; 4. Linkoping Sweden

1. Introduction

Neurology is a clinical field primarily built on top of neuroscience but also drawing extensively from other areas. Consideration of ischemic disease must also consider cardiology, cardiac science, as well as the field of hypertension in endocrinology and affiliated sciences. As such, a digital twin (DT) can be particularly valuable in bridging the gaps across clinical and scientific specialties to extend the scope of care. DT must incorporate various types of artificial intelligence (AI) and data integrator (DI: gathering and updating values from a variety of body sensors). In the context of ischemia DI would consolidate EKG, echocardiogram, Swann-Ganz cardiac measures, carotid echo, MRI, MRV, CT, fMRI, blood pressure, coagulation profile and times, with future possibility of including MR-NMR spectroscopy across brain areas.

2. Materials and Methods

Cohering large language model (LLM) and mechanistic multiscale modelling (MSM) 1. Prior work with LLM to query and summarize patient input. (1;2) 2. Prior work with MSM to combine vascular models, metabolic neuronal networks with explicit capillary distribution and spreading depression. (3) 3. MSM simulates & constrains detailed reaction–diffusion, electrophysiology, circuit models. (4) 4. LLM correlates literature and simulation details to identify boundaries for simulation.

3. Results

1.LLMto structure patient information Trialbased assessment of 3 trials on 46 cases (138 trials) (1) used GPT-4 with rate limit of 200 requests/minute and 100000 tokens/min (4 tokens/3words)) and produced excellent results for hemisphere stroke (F1 0.9), cord (0.94); fair for brainstem (0.8); poor for cerebellar stroke (0.37) 2. LLM presents preventive health alternatives 3. Micro-to-tissue-scale imulations produce clinically interpretable signatures of spreading depression propagation with degree of hypoxia Established reaction–diffusion + electrophysiology models demonstrate that: (4). 4. Immediate post-lesion functional changes can be reproduced by altered activation network dynamics alone (5). 5. Macroscale data assimilation uses “functional avatar” principles (6): a. MRIderived structural and diffusion features, b. perfusion proxies and oxygenation-related signals, c. electrophysiology d. pathology/autopsy findings for capillary densities.

4. Discussion and Conclusions

DT personalization can narrow degeneracy in multiscale parameters, enabling patient-specific predictions and therapy advanced testing (e.g., preserving ECS volume could inhibit SD propagation). LLMs excel at ingesting large corpora of text and converting them into structured knowledge. Mechanistic models excel at enforcing conservation laws, causal structure, and multiscale coupling. Spreading depolarization is a VPH “bridge disease” spanning 1. microscale: channel and pump kinetics, ion gradients; 2. mesoscale/tissue: reaction–diffusion, ECS geometry, oxygen perfusion; 3. clinical imaging correlates, injury progression. This makes SD an ideal proving ground for integrated VPH-style workflows that move beyond electrophysiology-only modelling (4;7).

5. References

1. Lee JH, Choi E, McDougal R, LyttonWW. GPT-4 performance for neurologic localization. Neurol Clin Pract, 14(3): e200293. 2024.

2. Lee JH, Choi E, Angulo SL, McDougal RA, Lytton WW. Neurological history both twinned and queried by generative artificial intelligence. Front Med (Lausanne), 11: 1496866. 2024.

3. Newton A,Kelley C, Guo A,Wang J, Zink S, Distasio M, Mcdougal RA, LyttonW. Subcellular to tissue scale modeling of ischemia and spreading depolarization. IBRO Neurosci Rep, 15: S792.2023.

4. Kelley C, Newton AJH, Hrabetova S, McDougal RA, Lytton WW. Multiscale computer modeling of spreading depolarization in brain slices. eNeuro, 9(4): ENEURO.0082–22.2022. 2022.

5. Sober SJ, Stark JM, Yamasaki DS, Lytton WW. Receptive field changes after strokelike cortical ablation: a role for activation dynamics. J Neurophysiol, 78(6): 3438–3443. 1997.

6. Casas Bn, Lantz J, Viola F, Cedersund G, Bolger AF, Carlh ll CJ, Karlsson M, Ebbers T. Bridging the gap between measurements and modelling: a cardiovascular functional avatar. Sci Rep, 7(1):6214. 2017.

7. Newton AJH, McDougal RA, Hines ML, Lytton WW. Using NEURON for reaction-diffusion modeling of extracellular dynamics. Front Neuroinform, 12: 41. 2018.

GLUCODIFFSURV: TREATMENT-AWARE CONTINUOUS-TIME DIFFUSION FORECASTING WITH TIME-TO-HYPOGLYCEMIA RISK

Sarmad Maqsood (1), Eglė Belousovienė (2), Tomas Tamošuitis (2), Rytis Maskeliūnas (1)

1. Department of Applied Informatics, Vytautas Magnus University, 44404 Kaunas, Lithuania;
2. Department of Intensive Care, University of Health Sciences, Kaunas, Lithuania

1. Introduction

ICU glucose is irregularly measured and strongly treatment-driven, making short-horizon forecasting and hypoglycemia anticipation challenging [1,2]. Measurement timing is often informative (checks become more frequent during instability), and fixed-grid resampling can blur treatment–response dynamics and understate uncertainty near safety thresholds [3]. We introduce GlucoDiffSurv, a treatment-aware continuous-time model that learns directly from event streams and outputs probabilistic forecasts with aligned hypoglycemia risk within 30 and 60 minutes.

2. Materials and Methods

From MIMIC-IV v3.1 ICU stays [4], we construct per-stay continuous-time event streams comprising glucose observations and intervention events (insulin bolus/infusion rate changes, dextrose). Each event is represented as (t_i, c_i, m_i), where t_i is the timestamp, c_i the event type, and m_i the mark (e.g., glucose value, dose, or rate). A causal event encoder with time-gap embeddings (Δt) aggregates the history up to each glucose anchor t_k into a latent state h_k. Forecasting is formulated as next-observation prediction, where the diffusion head models the conditional distribution of the next glucose given h_k and the observation gap Δt_k; K diffusion samples yield a median forecast and prediction intervals. In parallel, a hazard-based head estimates hypoglycemia risk (glucose < 70 mg/dL) within 30 and 60 minutes. We use patient-level splits (subject_id) and report metrics in gap bins: Bin A ($\Delta t \leq 30$ min) and Bin B ($30 < \Delta t \leq 60$ min).

$$y_k = g(t_{k+1}),\ \Delta t_k = t_{k+1} - t_k,\ p_\theta(y_k | h_k, \Delta t_k) \quad (1)$$

3. Results

In Bin A, GlucoDiffSurv achieved R^2 = 0.93 with MAE = 4.5 mg/dL and RMSE = 11.3 mg/dL and in Bin B, R^2 = 0.91 with MAE = 5.2 mg/dL and RMSE = 12.1 mg/dL. Hypoglycemia prediction reached AUPRC@30 = 0.55 and AUROC@30 = 0.89; AUPRC@60 = 0.65 and AUROC@60 = 0.91, with 90% PI coverage of 0.92 (Bin A) and 0.94 (Bin B).

4. Discussion and Conclusions

GlucoDiffSurv demonstrates that treatment-aware continuous-time modeling with diffusion uncertainty can support accurate short-gap prediction and calibrated near-term risk in ICU data without fixed-grid resampling. By conditioning on interventions and Δt, the model better matches ICU measurement processes, while diffusion sampling provides prediction intervals that remain informative near hypoglycemia thresholds. These outputs are intended for decision support (not treatment recommendation). Limitations include retrospective measurement bias and site-specific practice patterns; future work will broaden interventions and assess generalization.

5. References

1. Mehdizavareh, Hadi, Arijit Khan, and Simon Lebech Cichosz. "Enhancing glucose level prediction of ICU patients through hierarchical modeling of irregular time-series." *Computational and Structural Biotechnology Journal* 27 (2025): 2898-2914.
2. Maqsood, Sarmad, et al. "GlucoNet-MM: A multimodal attention-based multi-task learning framework with decision transformer for personalised and explainable blood glucose forecasting." *Diabetes, Obesity and Metabolism* 27.12 (2025): 7416-7430.
3. Rodriguez-Almeida, Antonio J., et al. "Incorporating uncertainty estimation and interpretability in personalized glucose prediction using the temporal fusion transformer." *Sensors* 25.15 (2025): 4647.
4. Johnson, Alistair EW, et al. "MIMIC-IV, a freely accessible electronic health record dataset." *Scientific data* 10.1 (2023): 1.

Acknowledgements:
The study is funded by the Lithuanian Research Council (LMT) under project grant number P-PD-24–169.

GNN-BASED SURROGATE MODEL FOR OBSTETRIC INJURY PREDICTION

Rita Moura (1,2), Dulce Oliveira (1), Diana Antunes (2), Daniel Fidalgo (1), Marco Parente (2)
1. INEGI, Portugal; 2. Faculty of Engineering of the University of Porto, Portugal

1. Introduction

Childbirth-related complications remain a major global health challenge, with over 40 million women experiencing long-term complications each year [1]. Biomechanical models of childbirth, particularly finite element models (FEM), enable quantitative and physiologically meaningful predictions of maternal tissue response [2]. However, their high computational cost limits clinical applicability. To address this gap, we integrate artificial intelligence (AI) with biomechanical simulations to support personalized decision-making. Specifically, a Graph Neural Network (GNN) surrogate model was trained on synthetic data generated from FEM simulations. By representing the pelvic floor mesh as a graph, the model preserves spatial topology while enabling near real-time prediction of biomechanical responses during labor, maintaining both accuracy and biomechanical consistency.

2. Materials and Methods

Childbirth simulations were conducted to generate diverse pelvic floor (PF) muscle responses across varying maternal geometries and material properties.

A Graph Convolutional Network (GCN) was trained to map biomechanical inputs to resulting tissue stress distributions. The PF finite element meshes were represented as graphs, with nodes corresponding to mesh vertices and edges encoding element connectivity and mechanical interactions. Node features included spatial coordinates, boundary conditions, and displacement constraints, while edge features captured element properties and topological relationships.

For this proof of concept, only one-tenth of the dataset was used. The model was trained on 80% of the data, with the remaining 20% reserved for testing. Performance was evaluated using quantitative metrics, including the mean squared error (MSE).

3. Results

The implemented GCN successfully learned the mapping between biomechanical input parameters and nodal stress distributions. Preliminary results demonstrate convergence during training and stable generalization behavior on unseen test data.

Predicted stress fields closely matched FEM simulations, particularly in high-stress regions critical for injury risk assessment. Quantitative evaluation yielded a test MSE of 0.63, with high spatial correlation between predicted and reference stress fields.

These results support the feasibility of GNN-based surrogate modeling for accelerating childbirth biomechanical simulations.

4. Discussion and Conclusions

This study highlights the potential of using GNNs as surrogate models for childbirth simulations. By exploiting the inherent graph structure of finite element meshes, the framework captures complex spatial relationships while markedly reducing computational cost compared to conventional FEM approaches.

Although current results serve as a proof of concept, they demonstrate the potential of GNN-based surrogates for real-time biomechanical prediction and personalized childbirth risk assessment.

Future work will focus on hyperparameter tuning to improve quantitative performance, expanding the dataset to capture anatomical variability, and incorporating additional structures, such as the fetus, into the analysis. The ultimate goal is to embed this surrogate model into a digital twin framework for real-time, personalized obstetric risk assessment.

5. References

1. Vogel JP et al., The Lancet Global Health, 12(2), e317–e330 (2024).
2. Hoyte LPJ and Damaser M. Academic Press (2016).

Information classification: Internal

IDENTIFIABILITY OF LATENT TRAJECTORIES WITH NEURAL ODES IN SMALL DATA REGIMES

Timo Rachel (1), Hanning Yang (1), Tim Litwin (1), Meropi Karakioulaki (2), Moritz Hess (1)

1. Institute of Medical Biometry and Statistics, Faculty of Medicine and Medical Center, University of Freiburg, Freiburg, Germany; 2. Department of Dermatology, Medical Faculty and Medical Center, University of Freiburg, Freiburg, Germany

1. Introduction

In many inflammatory diseases where biomarkers such as CRP and IL-6 play a central role, clinical routine typically involves dense measurements at baseline, while subsequent follow-up assessments – particularly in rare diseases such as EB – are sparse and irregularly spaced. These distorted observation processes complicate the reconstruction of latent patient trajectories, even when the underlying inflammatory dynamics are conceptually well understood. In this work, we investigate to what extent a Neural ODE model can still identify distinct trajectory patterns under such conditions, assuming a simplified ODE system for inflammatory markers as the correct ground truth.

2. Materials and Methods

We define a simple, analytically solvable ODE system that serves as the reference model for biomarker trajectories for multiple patient subgroups with varying baseline values and dynamics. From this system, we generate synthetic time series and superimpose various distorted observation processes, including dense baseline measurements and strongly thinned, irregular follow-up measurements as typically seen in routine care. A Neural ODE-based model is trained on these partially observed trajectories; we then evaluate its ability to reconstruct the latent continuous-time trajectories and separate the predefined subgroups in the learned latent space.

3. Results

We demonstrate under which conditions of the observation process Neural ODEs can still reliably reconstruct latent patient trajectories and separate subgroups in the latent space. The results systematically show how reconstruction error, separability, and trajectory stability degrade with increasing sparsity and irregularity of measurements. Furthermore, we identify critical thresholds for sampling density and missingness patterns beyond which identifiability of the underlying dynamics breaks down.

4. Discussion and Conclusions

By assuming the ODE-based generative model as the true dynamics, we isolate the pure impact of distorted observation processes on Neural ODE performance. Our investigation reveals in which regimes of measurement density and missingness patterns these models can deliver robust latent trajectories. The findings provide concrete guidelines for applying such methods to real clinical data like EB and other rare inflammatory diseases.

5. References

1. Chen RTQ, Rubanova Y, Bettencourt J, Duvenaud D. Neural Ordinary Differential Equations. arXiv:1806.07366 (2019)
2. Rubanova M et al., Latent ODEs for Irregularly-Sampled Time Series; NeurIPS; 2019.
3. Iakovlev V et al., Latent Neural ODEs with Sparse Bayesian Multiple Shooting; ICLR; 2023.
4. Chen RTQ et al., Neural Ordinary Differential Equations; NeurIPS; 2018.
5. Kidger J et al., Neural Controlled Differential Equations for Irregular Time Series; NeurIPS; 2020.

Acknowledgements:

The authors would like to thank the Deutsche Forschungsgemeinschaft (DFG, German Research Foundation) – Project-ID 499552394 – SFB 1597" for funding the project.

HUMAN-LEVEL MRS SCORING FROM NEUROSURGICAL LETTERS USING A LARGE LANGUAGE MODEL

Abiram Sandralegar (1,2), Alban Bornet (3), Elias Benguettat (1), Feres Ravarelli (1), Paul E. Constanthin (1,2), Alexandre Lavé (1), Julien Haemmerli (1,4), Insa Janssen (1), Jelia Issa (2), Elham Qaderdan (2), Ethan G. Godin (2), Karl Schaller (1,2), Douglas Teodoro (3), Philippe Bijlenga (1,2)

1. Division of Neurosurgery, Geneva University Hospitals, Switzerland; 2. Faculty of Medicine, University of Geneva, Switzerland; 3. Data Science for Digital Health (DS4DH), Department of Radiology and Medical Informatics, Faculty of Medicine, University of Geneva, Switzerland, 4. Department of Neurosurgery, Winterthur Kantonsspital, Switzerland.

1. Introduction

Functional outcome assessment using the Modified Rankin Scale (mRS) underpins clinical decision-making, quality monitoring, and research in cerebrovascular neurosurgery. Yet, decades of outcome information remain locked in unstructured clinical letters, requiring time-intensive manual review and limiting large-scale retrospective analyses. Large language models (LLMs) may offer a transformative solution by converting narrative documentation into structured outcome data.

2. Materials and Methods

We conducted a validation study within the ongoing @neurIST research program at a tertiary academic neurosurgical center. A total of 103 authentic clinical letters (2007–2025) from patients treated for intracranial aneurysms were randomly selected from the institutional electronic health record.

mRS scores were assigned by a consensus of two attending neurosurgeons (reference standard), three neurosurgical residents, and three medical students. A general-purpose open-source Large Language Model (Qwen3-32B) extracted mRS scores from the same letters without task-specific fine-tuning or preprocessing. Agreement was evaluated using quadratic weighted kappa (QWK), intraclass correlation coefficient (ICC), mean absolute error (MAE), exact and ±1 agreement rates, and grouped outcome classification metrics. Statistical equivalence was assessed using Wilcoxon signed-rank tests and Bayesian analysis.

3. Results

The LLM demonstrated excellent agreement with the attending consensus (QWK 0.95; ICC 0.95; MAE 0.34), comparable to students (QWK 0.95; MAE 0.33) and residents (QWK 0.93; MAE 0.35). Exact agreement reached 70.9%, while accuracy within ± 1 point exceeded 95%. No statistically significant differences were observed between the model and human raters ($p>0.7$), and a separate Bayesian inferential analysis favored equivalence, indicating a high probability of no clinically meaningful difference between groups. Performance remained stable across clinically meaningful outcome categories (mRS 0–1: no or minimal disability; 2–5: moderate to severe disability; 6: death).

4. Discussion and Conclusions

We demonstrated here that a general-purpose LLM achieved human-level reliability in extracting functional outcomes from authentic neurosurgical documentation under real-world conditions. Secure on-premise deployment without preprocessing demonstrates feasibility of governance-compliant AI integration within institutional infrastructures. Automated outcome extraction may enable scalable, FAIR-aligned (Findable, Accessible, Interoperable, and Reusable) structuring of real-world clinical data and support the development of learning cerebrovascular care systems.

SYNTHETIC PATIENTS TO ENHANCE MULTIPLE SCLEROSIS TRIAL DESIGN VIA COVARIATE ADJUSTMENT: A PROOF OF CONCEPT.

Monica Franzese (1)*, Ettore Dolcetti (2)*, Raimondo Reggio (3)*, Andrea Colacino (1), Marco Aiello (1), Diego Centonze (2), Roberto Gomeni (4), Emilio Merlo Pich (3) # Marco Salvatore (1)#.

*(1) IRCSS Synlab SDN, Napoli, Italy; (2) IRCSS Neuromed, Pozzilli, Italy; (3) Gelf Health, Milano, Italy; (4) Pharmacometrica, France. *First author equal contribution; # Co-last corresponding authors.*

1. Introduction

The advancement of algorithms for synthetic patient generation is changing the evidence-supporting landscape for in silico trials to optimise Phase II clinical studies in line with current Regulatory requirements in Europe and USA. Here we present a proof-of-concept study *for* a virtual patient framework applied to an *in silico* trial aimed to produce a simulated control arm based on a covariate adjustment optimization in patients with relapsing–remitting multiple sclerosis (RRMS).

2. Materials and Methods

A pre-selected RRMS cohort of 155 patients from Central Italy (IRCSS Neuromed) with 3-year follow up and key longitudinal endpoints (MRI gadolinium-enhancing lesions, NEDA, EDSS) was used to train a Bayesian non-linear mixed-effects model implementing a Riemannian manifold for aligning individual trajectories to a common reference (1). The resulting ***synthetic population*** was assessed for Fidelity using marginal distributions and meta-correlation matrices aimed to closely matching real longitudinal data. Privacy vs. the original dataset was kept, according to DCR and IMS test. Utility was assessed by attempting to enhance trial efficiency, training an artificial neural network on a 75%/25% split to predict 3-year EDSS-worsening (ΔEDSS > 1) in patient under low efficacy treatment defined '*level-1'* (e.g. β-interferon) using several baseline covariates. Relevant covariates were assessed using a Artificial Neural Network algorithm (ANN), and simulation of *level-2* drug effects (i.e., ocrelizumab) was carried out on a synthetic patient population selected according to propensity scores based on key predictors (2).

3. Results

After variable-importance filtering (>5%)with ANN, gender, basal covariate included a) disease duration, b) disease activity, and c) three CSF cytokines (MIP-1α, IL-17, IL-6), that emerged as relevant predictors. These predictors were used to create an enriched "high-risk" virtual control arms via propensity score-based filtering of a 5,500 synthetic RRMS population. Simulated trials of *level-2* ocrelizumab effect treatment demonstrated that covariate-adjusted virtual arm (A) would improve signal-to-noise ratio and the Effect Size compared to unselected conventional virtual arm (B) (i.e., Effect Size A: r = 0.1252, vs. Effect Size B: r = 0.0930).

4. Discussion and Conclusions

Covariate-adjusted virtual arms could be successfully obtained and implemented *in silico* clinical trials via a propensity score enrichment based on predictive variables derived form a synthetic patient dataset, that was amplified from a smaller size, single-centre, regional RRMS population', improving signal-to-noise ratio and effect size compared to unselected virtual arms. Further studies of various synthetic and real datasets must be run to support the possible generalization relevance of this Proof of Concept.

5. References

(1) Schiratti et al. Journal of Machine Learning Research, 18: 1-33. ⟨hal-01540367v3⟩ (2017).
(2) Gomeni et al. Psychiatry Res. Sep; 327:115367. doi: 10.1016/j.psychres 2023.115367 (2023).

Acknowledgements:
The authors would like to thank the *Spoke 8 - Centro Nazionale per AI e Big Data (Missione 4, PNRR, Italy)* for providing financial support.

FEMUR FRACTURE PREDICTION IN POSTMENOPAUSAL WOMEN: MULTI-COHORT CLINICAL VALIDATION OF BBCT-HIP PIPELINE

Julia A. Szyszko (1), Antonino A La Mattina (2), Marilina Amabile (2), Claudio Ripamonti (3), Lucia Lisi (3), Pinaki Bhattacharya (4), Fabio Baruffaldi (2), Alessandra Aldieri (1) & Marco Viceconti (1)

1. Department of Industrial Engineering, University of Bologna 2. Medical Technology Laboratory, IRCCS Istituto Ortopedico Rizzoli, Bologna 3. SSD Medicina e Reumatologia, IRCCS Istituto Ortopedico Rizzoli, Bologna 4. Mechanical, Aerospace and Civil Engineering & INSIGNEO Institute for In Silico Medicine, University of Sheffield

1. Introduction

Hip fragility fractures represent one of the most severe manifestations of osteoporosis, associated with increased morbidity, mortality, and significant healthcare burden [1]. Although DXA-derived T-score is the clinical gold standard for diagnosing osteoporosis, nearly half of patients classified as non-osteoporotic experience fragility fractures [2]. Finite Element (FE) models have emerged as promising tools for improving fracture risk assessment. Within this context, the Bologna Biomechanical Computed Tomography (BBCT)-hip model was developed [3], which calculates an absolute risk of hip fracture (ARF0) for a subject coupling a mathematical-stochastic model of a fall with a subject-specific FE model of the femur (Fig. 1).

2. Materials and Methods

A multi-cohort [4,5] population of postmenopausal women with both CT scans and T-score available and comprising 65 fractured and 293 non-fractured subjects was considered. Thanks to the availability of the CT scans, weight and height information for each subject, BBCT-hip pipeline could be implemented and the subject-specific ARF0 values computed.

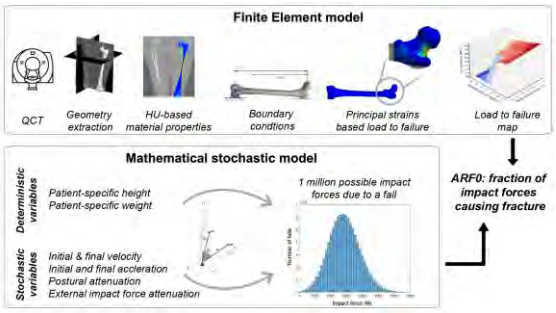


Figure 1: Overview of BBCT-hip pipeline.

BBCT-hip stratification accuracy was then assessed through a ROC analysis and compared to the stratification accuracy of T-score.

3. Results

BBCT-hip showed an AUC of 0.78, which turned out to be statistically significantly higher ($p<0.05$) than the AUC of aBMD, equal to 0.64 (Fig. 2).

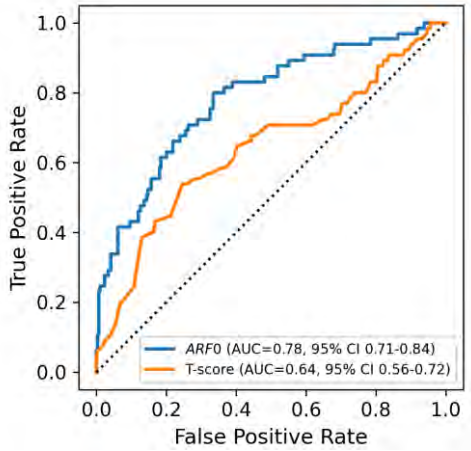


Figure 2: ROC curves obtained from ARF0 (blue) and T-score (orange).

4. Discussion and Conclusions

This study demonstrated an improved accuracy of BBCT-hip in separating fractured from non-fractured subjects compared to T-score in a clinical population. Such result provides evidence supporting the clinical implementation of BBCT-hip and similar *in silico* methodologies.

5. References

1. Kanis et al., Osteoporos Int; 30(1):3-44 (2019) **2.** Mai et al., J Clin Endocrinol Metab; 104(8): 3514-3520 (2019) **3.** Aldieri et al., Comput Methods Programs Biomed; 240:107727 (2023) **4.** Yang et al., Osteoporos Int; 25(1):251-63 (2014) **5.** Aldieri et al., 10.6092/unibo/amsacta/8431 (2025)

Acknowledgements:

This research was co-funded by the Italian Complementary National Plan PNC-I.1 'Research initiatives for innovative technologies and pathways in the health and welfare sector' D.D. 931 of 06/06/2022, 'DARE - DigitAl lifelong pRevEntion' initiative, code PNC0000002, CUP: B53C22006230001.

PHANTOMLESS CALIBRATION FOR THE ESTIMATION OF BONE STRENGTH IN PAEDIATRIC FEMORA

George Allison (1)(2), Salman Almutairi (3), Amaka C Offiah (2)(3), Xinshan Li (1)(2)

1. School of Mechanical, Aerospace & Civil Engineering, University of Sheffield, UK; 2. Insigneo Institute, University of Sheffield, UK; 3. School of Medicine and Population Health, University of Sheffield, UK

1. Introduction

Finite element (FE) analysis of paediatric bone based on retrospective computed tomography (CT) scans is restricted by the need for a density calibration phantom, limiting the amount of CT scans available for an under-researched population as clinical scans often use variable currents. This study aims to develop and validate a phantomless calibration technique to overcome this limitation and to demonstrate its application in one child with rickets and 10 clinical CT scans with variable current.

2. Materials and Methods

Sixty-three anonymised post-mortem CT scans were obtained from Sheffield Children's Hospital. All scans were acquired using a GE Lightspeed VCT 64, comprising **S-C**: 55 children (0-1 year old) with no known skeletal pathologies scanned with two constant currents (59mA and 100mA), **S-V**: 7 (0-1 year old) with variable current scans, and **S-R**: one 10-month-old child with rickets (variable current). Offline European Spine Phantom (ESP) calibration scans were available for **S-C** and **S-R**. Material properties were determined based on Hounsfield units through two methodologies: (a) ESP calibration (**MOD1**) and (b) phantomless calibration using air, fat, and muscle peaks (**MOD2**) [1]. Using the PyPeCT2S pipeline, four-point bending was simulated with equidistant diaphyseal forces and partially fixed ends.

3. Results

MOD2 calibration generally performed well against the MOD1 calibration when comparing predicted FE strengths in the **S-C** cohort in Figure 1. There was negligible bias and consistent agreement at the lower predicted critical moments, while there were more pronounced differences in higher values. Outliers trended in the negative region of the plot indicating that MOD2 generally predicted lower bone strength than MOD1. For the same age range, the predicted critical moments using MOD2 in variable current scans (**S-V**) showed strong agreement with the trend of MOD1 critical moment against age (Figure 2). When both calibration methods were applied to **S-R**, they resulted in a 40% difference with an over prediction using MOD2, in contrast to general trend observed in Figure 1.

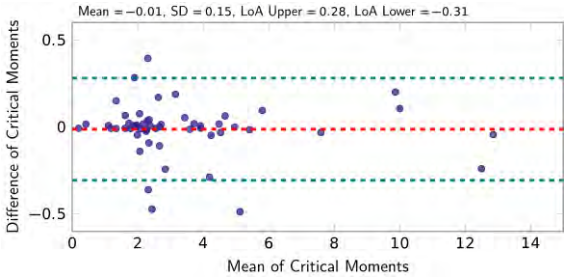


Figure 1: Difference in predicted critical moment (Nm) between **MOD1** and **MOD2** calibrations in group **S-C** children up to 1-year-old (n=55).

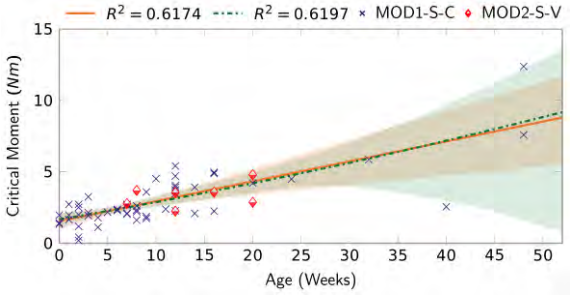


Figure 2: Critical moment against age (0-1 year) comparison for **S-C (MOD1)** and **S-V (MOD2)** (n=62).

4. Discussion and Conclusions

Phantomless calibrations were comparable to phantom-based calibration, especially for infants with no skeletal pathology scanned at a constant current. The **S-V** cohort of variable current cases predicted well while **S-R** showed a large deviation from MOD1 results. The preliminary results for constant current cases suggest that phantomless calibration could be used when ESP calibration is unavailable, however the inconsistencies need to be investigated further.

5. References

1. Eggermont et al. 10.1371/journal.pone.0220564

FROM ASTM F543 PHYSICAL TESTING TO IN SILICO EVIDENCE: CREDIBILITY ASSESSMENT OF A DEVICE-AGNOSTIC FE MODEL

David Benoit (1,2), Franck Le Navéaux (1), Loïc Degueldre (1), Marie-Hélène Beauséjour (2), Yvan Petit (2), Éric Wagnac (2), Julien Clin (1)

1. Numalogics, Canada; 2. École de Technologie Supérieure, Canada
Corresponding author: David Benoit, dbenoit@numalogics.com

1. Introduction

Computational modeling and simulation (CM&S) is increasingly used to complement or in some cases replace traditional bench testing during orthopedic device development and regulatory assessment. For metallic orthopedic bone screws, axial pullout performance is commonly evaluated using ASTM F543 testing in polyurethane foam blocks. However, iterative testing across design variants can be costly and time-consuming. To support the use of CM&S as a surrogate for physical testing, a thorough credibility assessment is essential to demonstrate that the model reliably represents the physical phenomena of interest for its defined context of use (COU).

2. Materials and Methods

This work presents an end-to-end methodology to establish the credibility of a finite element (FE) model that simulates screw pullout according to ASTM F543-A3. The credibility assessment was conducted based on the ASME V&V 40 framework and the recent FDA guidance on CM&S credibility assessment and was specifically structured to demonstrate the model's device-agnostic capabilities, enabling its use as a surrogate for physical testing across diverse screw types and designs.

The credibility assessment covered verification, calibration, validation, and applicability evidence categories, evaluating a total of 25 credibility factors. Verification aimed to identify potential errors in the source code, assess discretization and solver accuracy, and implement a methodology to eliminate use errors. Material calibration involved characterizing the polyurethane foam under compressive, shear, and tensile stress states to accurately capture its complex mechanical properties. Validation was performed by comparing simulation results with experimental pullout tests on 18 commercially sourced orthopedic screw designs, spanning a broad range of applications and design variations. The FE model's predictive performance was further benchmarked against the Chapman analytical formula, an FDA-recognized method for estimating screw pullout force.

3. Results

The FE model achieved a mean absolute percentage error of 8.0% versus 15.9% for the Chapman analytical formula, with excellent agreement (ICC = 0.979) and strong ranking capability (Spearman = 0.985). Applicability evidence showed that validation points were fully encompassed by the model's COU and covered representative ranges of critical design parameters to ensure the model's validation aligned with its intended use.

4. Discussion and Conclusions

The device-agnostic nature of the model enables its use across a broad range of orthopedic screw designs, demonstrating how CM&S can be leveraged beyond individual device assessments. This credibility assessment also served as the evidentiary basis for FDA Medical Device Development Tools qualification of the model, which can now support regulatory applications through comparison of new designs to predicates, assessment of performance equivalence, and identification of worst-case configurations. The methodology may serve as a reference for the credibility assessment of models in other standardized medical device evaluations.

TOWARDS THE VIRTUAL MOUSE TWIN FOR PRE-CLICNICAL TESTING OF NEW TREATMENTS FOR OSTEOPOROSIS

Enrico Dall'Ara (1), Thomas Valerio (1), Sanjay Singh (1), Silvia Dirstaru (1), Saira Farage-O'Reilly (1), Vee San Cheong (1), Peter Pivonka (2)

1. University of Sheffield, United Kingdom; 2. Queensland University of Technology, Australia

1. Introduction

Combined biomechanical and pharmacological treatments for Osteoporosis (OP) can improve bone mineral density and reduce the risk of fracture. Mechano-regulation laws predicted well bone apposition in a mouse model of OP treated with bone anabolics, but prediction of bone resorption was poor [1]. The goal of this study was to move towards the development of the virtual mouse twin for skeletal applications (VMT:SK), a multiscale computational model that predicts bone adaptation over time associated with treatments for OP.

2. Materials and Methods

The approach combines three types of models (Figure1): 1) Musculoskeletal (MSK) models of the mouse hindlimb informed from gait, muscle and ground reaction force (GRF) data, to evaluate the joint/muscle forces; 2) Validated micro-computed tomography (microCT) based micro-Finite Element (microFE) models of the mouse tibia to calculate the local mechanical stimuli [2]; 3) Bone cell population models (BCPM) to predict bone adaptation based on local biomechanical and biochemical stimuli.

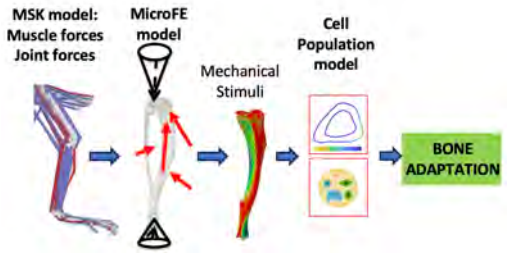


Figure 1: Multiscale model for predicting bone adaptation in the mouse tibia.

For this work we have: performed sensitivity analyses to identify the most important muscle forces in the MSK models and the effect of muscle insertion surface on the predicted strain energy density (SED); coupled MSK and micro-FE models based on inertia relief and evaluated its effect against simplified uniaxial loading; coupled micro-FE and BCPM to evaluate the bone adaptation in the tibial midshaft and compared against bone adaptation measurements from *in vivo* microCT of five C57Bl/6 ovariectomised female mice subjected to external controlled mechanical loaded [3].

3. Results

The main outcomes of these sub-studies were:

- 13 important muscle forces and GRF components affect knee and ankle forces;
- Modelling realistic muscle insertion areas is important for obtaining realistic SED values;
- Inertia relief can reduce the impact of boundary conditions in the microFE models but may overestimate local strains;
- Coupled microFE and BCPM predict between 75 and 100% of the periosteal bone adaptation in most slices for most mice (Figure2).

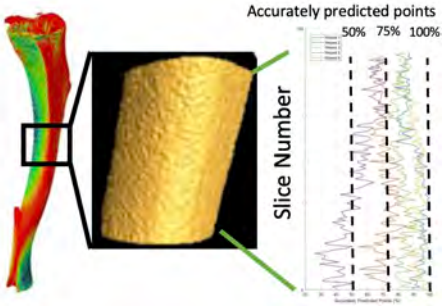


Figure 2: Prediction of the coupled microFE and BCPM for the midshaft of the tibia for 5 different mice (different colours).

4. Discussion and Conclusions

While promising results from the multiscale VMT:SK have been obtained, current developments aim to improve the accuracy of the model: informing MSK models by mouse specific mouse gait analysis; considering heterogeneous mechano-sensation and mechano-regulation informed by the distribution of osteocytes; informing the BCPM from population 3D histology and immunohistochemistry.

5. References

1. Cheong VS et al; ActaBiomat; 136:291 (2021)
2. Oliviero S et al; JMBBM; 113:104190 (2021).
3. Roberts B et al,; SciRep; 10(1):8889 (2020)

Acknowledgements:
We thank the EPSRC (EP/Z000203/1) for providing financial support to this project.

A DYNAMIC MUSCULAR-ARTICULAR DATASET FOR LOWER LIMB DIGITAL TWINS: FIRST APPLICATION AND IN VIVO VALIDATION

Michele Conconi (1), Manuel Romeo (1), Nicola Sancisi (1), Raphaël Dumas (2)

1. Department of Industrial Engineering, University of Bologna, Italy; 2. LBMC UMR_T 9406, University Eiffel - University Lyon 1, France

1. Introduction

In personalised medicine, a scalable, comprehensive, and accurate digital twin of the lower-limb musculoskeletal structure is essential for advancing orthopaedic preoperative planning, prosthetic design, and functional status analysis. Historically, available templates have served primarily as anatomical atlases. While they may offer detailed definitions of muscular geometry, they often lack biofidelity in their articular geometry, violate consistency between articular structures, and provide insufficient kinematic data. This study seeks to bridge that gap by developing a dynamic dataset that integrates detailed muscular and articular geometries with a wide range of articular poses.

2. Materials and Methods

The TLEM 2.0 (a comprehensive musculoskeletal model [1]) served as the foundational template. To overcome its original limitation of simplified hinge joints, the articular modelling was significantly refined based on bone morphology. 3D articular kinematics for the tibiofemoral, patellofemoral, talotibial, and calcaneotalar joints were reconstructed using a joint congruence maximisation algorithm [2]. With these reconstructed reference motions, the most isometric fibres for the primary ligaments of the knee and ankle were identified, and the contact points and normals were defined to characterise the articular interfaces. As an application, parallel mechanisms were synthesised for the ankle and knee joints. These mechanisms were integrated into the full lower-limb musculoskeletal model to perform scaling, inverse kinematics and static optimisation. The framework was validated against in vivo experimental data. Joint angles and joint reaction forces were compared with bone-pin kinematics during running in 3 volunteers [3] and with instrumented implant measurements during walking in 4 patients [4], respectively.

3. Results

Joint angle patterns were generally reproduced, although mechanisms showed increased knee internal-external rotation ($R^2 = 0.45$), likely due to anatomical differences and kinematic changes associated with demanding tasks such as running, consistent with experimental reports of differences between running and walking [5]. Medial and lateral knee contact forces were predicted with mean errors of 0.28 and 0.29 body weight, respectively, an accuracy level that has so far required a high level of model personalisation [6].

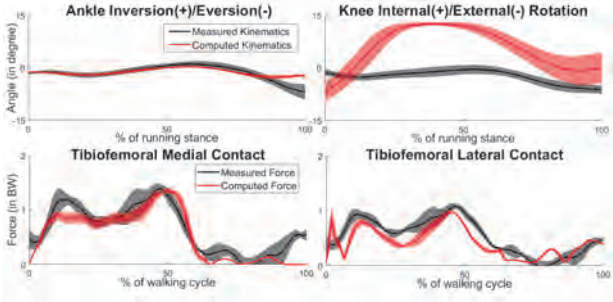


Figure 1: Measured and computed ankle and knee kinematics (top) and tibiofemoral contact forces (bottom) of one volunteer (SP) or patient (SC) from each dataset.

4. Discussion and Conclusions

Integrating morphology-based articular geometry into a musculoskeletal model provides biofidelity and reliable kinematics and dynamics, despite not being subject-specific. This comprehensive dynamic dataset offers a robust, scalable template for enhancing orthopaedic planning and prosthetic design.

5. References

1. Carbone, V. et al., J. Biomech.;734-741, 2015
2. Conconi, M. et al., IEEE Trans. Biomed. Eng.; 1084-92, 2021
3. Reinschmidt, C. et al., J. Biomech.; 729-732, 1997
4. Fregly, B.J. et al., J. Orthop. Res.; 503-513, 2012
5. Wang, W. et al., Gait Posture; 231-237, 2021
6. Marra, M.A. et al., J. Biomech. Eng.; 020904, 2015

Acknowledgements

Supported by a Franco-Italian University grant (Partenariat Hubert Curien, Galileo 48932SG).

PHANTOM TYPE MATTERS: A BENCHTOP VALIDATION OF FEMUR STRENGTH DETERMINATION WITH FINITE ELEMENT MODELS

Ellie Galliker (1), Alexander Dams (1), Dheeraj Jha (2), Giulia Galteri (3), Alexander Baker (1), Sami Väänänen (4), Lorenzo Grassi (5), Vee San Cheong (2,6), Hanna Isaksson (5), Luca Cristofolini (3), Stephen J Ferguson (1, 2), Benedikt Helgason (1, 2)

1. ETH Zürich, Switzerland; 2. Singapore-ETH Center, Singapore; 3. University of Bologna, Italy; 4. Kuopio University Hospital, Finland; 5. Lund University, Sweden; 6. University of Sheffield, UK

Corr. author: E. Galliker: ellie.galliker@hest.ethz.ch

1. Introduction

Hip fractures in older adults are associated with high mortality, long-term disability, and substantial economic burden [1]. Current clinical fracture risk assessment relies strongly on bone mineral density assessments [1]. Femoral strength (S_F) estimated from quantitative CT–based finite element models (FEMs) has demonstrated superior fracture discrimination in large cohort studies [2]. Nevertheless, FEMs are sensitive to various parameters linked to imaging protocols and sample selection. Therefore, the aim of this study was to investigate the sensitivity of material calibration in a benchtop setting.

2. Materials and Methods

Experimentally matched FEMs from two cadaveric studies were analysed: 12 unpaired femurs from Finland [3] (mean age 70 ±18) and 14 paired femurs from Italy (mean age 72 ±14). Specimens were CT-scanned with two different calibration phantoms: a QRM hydroxyapatite phantom (P_{HA}) and a Mindways dipotassium phosphate phantom (P_{K2}). All bones were mechanically tested with the same sideways fall configuration (10° adduction, 15° internal rotation, Fig. 1) of Zani et al. [4]. Specimen-specific FEMs were built using the material conversion equations described in [2, 5] for P_{HA} and [6] for P_{K2}, and experimental boundary conditions were implemented, adjusting methods described in [2].



Figure 1: CT scan, experimental setup [4], and FEM.

3. Results

Linear regressions between experimental S_F and FEM-predicted S_F for both calibrations are shown in Fig. 2. Mean absolute error was 0.98 kN (30.6%) for P_{HA} and 0.37 kN (9.6%) for P_{K2}, RMSE 1.17 kN and 0.59 kN, respectively.

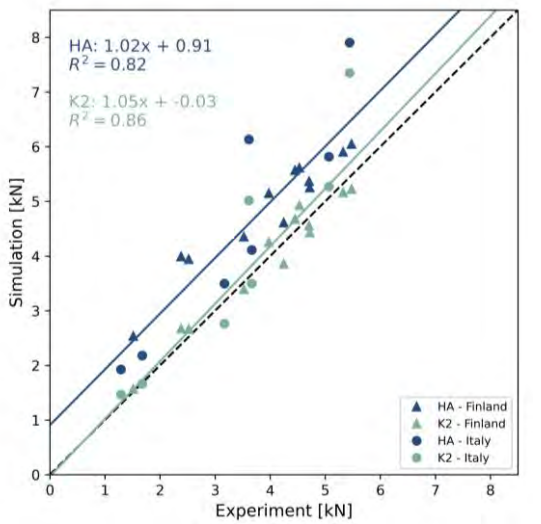


Figure 2: Simulation vs. experimental femur strength, pooled from both sites. For contralateral pairs, left and right S_F was averaged (N=19).

4. Discussion and Conclusions

Both phantom calibrations yielded strong linear agreement with experimental S_F. However, P_{K2} demonstrated substantially lower prediction error and improved quantitative agreement. These findings highlight that phantom type and chosen material conversion equations can meaningfully influence FEM prediction for benchtop validation and when applied in a clinical setting.

5. References

1. Veronese N et al., Injury; 49(8):1458–60 (2018).
2. Fleps I et al., Bone; 154:116219 (2022).
3. Kok J et al., J Biomech; 122:110445 (2021).
4. Zani L et al., J Mech Med Biol; 14(1) (2014).
5. Enns-Bray W et al., J MBBM; 78:196-205 (2018).
6. Jha D et al., Arch Osteoporos; 20:139 (2025).

Acknowledgements:
Funding: Korean-Swiss Science & Technology Programme, ETH Zürich Foundation & Doc.Mobility Fellowship Programme, AO Foundation, NRF Singapore (FHT programme), Swedish Research Council.

INTER-RATER VARIABILITY OF BONE FRAGMENT SEGMENTATION AND SURGICAL REDUCTION IN COMPLEX TIBIA FRACTURES

Simon Comtesse (1,2), Lea Sommerhalder (2), Lara Zamboni (2), Alexander Crotta (2), Thomas Zumbrunn (2), Benedikt Helgason (1), Stephen J. Ferguson (1)

1. Institute for Biomechanics, ETH Zurich, Zurich, Switzerland; 2. CustomSurg AG, Switzerland

1. Introduction

Patient-specific preoperative planning with finite element (FE) may improve trauma surgery and clinical outcomes [1], but their credibility requires rigorous verification and validation [2]. Manual steps in patient-specific models introduce subjectivity, necessitating assessment of inter-rater variability [3], which is assessed for bone segmentation and surgical reduction in complex proximal tibia fractures.

2. Materials and Methods

Inter-rater segmentation variability was assessed from three independent segmentations of two proximal tibia fractures, a cadaveric tibia (female, 84y, BMI 28 kg/m^2) and a clinical tibia (female, 72y, BMI 21 kg/m^2), using a consistent surgical reduction (**Figure 1**). Inter-rater reduction variability was evaluated from three independent virtual reductions based on a common baseline segmentation (**Figure 2**).

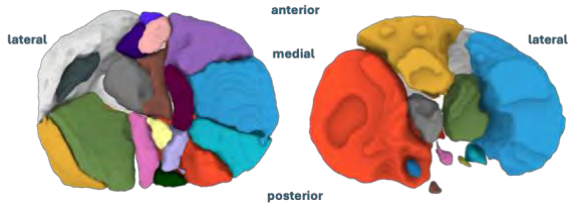


Figure 1: Baseline segmentation of a left cadaveric tibia (left) and a right clinical tibia (right).

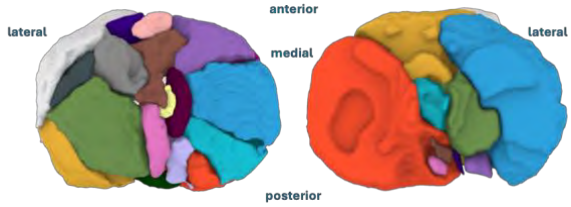


Figure 2: Default surgical reduction based on the baseline segmentation of a left cadaveric tibia (left) and a right clinical tibia (right).

FE models incorporated Hounsfield Units-derived bone properties and walking loads from instrumented total knee replacements [4]. Plates and screws were placed consistently across segmentations and reductions. Fragment displacements and screw von Mises stresses were evaluated as comparative outcomes.

3. Results

For the clinical tibia fracture, inter-rater segmentation and surgical reduction resulted in a small difference of 7% and 4% for maximum fragment displacement, and 4% and 13% for screw von Mises stresses, respectively. In contrast, substantially larger variations were observed for the cadaveric fracture (**Figure 3**).

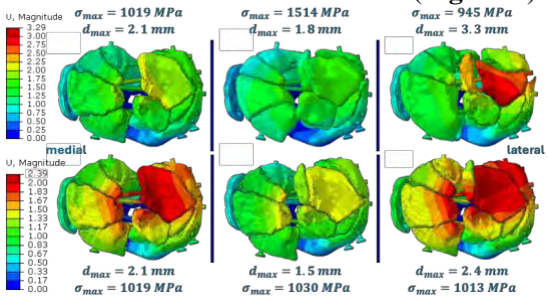


Figure 3: Inter-rater variability for segmentation (top row) and surgical reduction (bottom row) for the cadaveric tibia fracture (d_{max} = max. fragment displacement, σ_{max} = max. screw von Mises stresses).

4. Discussion and Conclusions

In systematic investigations of segmentations in whole bones, Wysocki et al. [5] demonstrated large variations in the FE model output. Our study showed that inter-rater variability in segmentation and surgical reduction may be case-dependent. A stable construct with good bone quality showed minimal sensitivity to segmentation and surgical reduction, whereas a less stable cadaveric construct with poorer bone quality exhibited greater variability.

5. References

1. Pätzold P et al., J Orthop Surg Res. 21, 155 (2026)
2. FDA, Silver Spring, MD, USA (2023)
3. Galappaththige S et al., PLoS comp bio, 18(10) (2022)
4. Bergmann G et al., PLoS one 9.1 (2014)
5. Wysocki M and Doyle S, Scientific reports, 21.1 (2022)

Corresp.: Simon Comtesse, Gloriastrasse 39, 8006 Zurich, Switzerland, simon.comtesse@hest.ethz.ch

CLINICAL METRIC ERRORS INDUCED BY THE PROPAGATION OF LANDMARKING UNCERTAINTY IN AUTOMATED TKA PLANNING

Ysé Roch (1, 3), Dorian Lozano (3), Nolwenn Fougeron (5), Benoît Gaulin (1,2), Clément Horteur (1,2), Yohan Payan (1), Marek Bucki (3), Antoine Perrier (1,3,4)

1. TIMC, Univ. Grenoble Alpes, CNRS, France; 2. Grenoble-Alpes CHU, France; 3. Twinsight, France; 4. GH Diaconesses Croix St-Simon, France; 5. Univ. Rennes, Inria, CNRS, France

Correspondence: yse.roch@univ-grenoble-alpes.fr

1. Introduction

Automated total knee arthroplasty (TKA) planning relies on anatomical landmarks to compute surgical metrics. These algorithms are typically evaluated on localization accuracy alone, yet a small positioning error can have very different clinical consequences depending on the metric considered. We present a Monte Carlo framework quantifying how landmark errors propagate into TKA planning metrics, illustrated by two contrasting cases: the mechanical hip-knee-ankle angle (mHKA) and the external tibial torsion angle (ETT).

2. Materials and Methods

Thirty osteoarthritic TKA subjects (67.1 ± 8.8 years) underwent preoperative full-leg CT imaging. Landmarks were manually annotated twice by two surgeons on segmented lower-limb meshes, characterizing landmark positioning variability [1]. These distributions were propagated through 14 TKA planning metrics via atlas-based inverse morphing and Monte Carlo simulation (50,000 iterations/metric/patient). Sensitivity was quantified by the 90% confidence interval of metric deviation (CI_{90}) and the Chatterjee coefficient (ξ), which measures statistical dependency between landmark displacement and metric deviation [2]. An automatic landmarking procedure, custom-made, was also applied to the same subjects.

3. Results

Automatic landmarking achieved a mean error of 2.4 mm, comparable to manual inter-operator variability (2.3 mm). Error propagation revealed a 146-fold range in angular variance across metrics. The mHKA was robust ($CI_{90} < 2°$), with heterogeneous but predominantly low landmark-metric dependency (ξ ranging 0–0.29), driven primarily by tibial plateau landmarks along the X-axis. In contrast, the ETT was highly sensitive ($CI_{90} = 16.9°$), with strong statistical dependency at malleolar landmarks (Fig 1, medial malleolus: $\xi = 0.231$), reflecting four landmarks defining two short transverse axes where in-plane errors compound without geometric averaging.

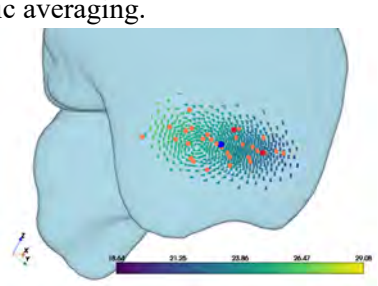


***Fig 1: ETT sensitivity to medial malleolus displacement**, subject 11 (lateral view). Arrow color encodes the induced angular error magnitude (°); orange dots show manual annotation variability; blue dot indicates the reference position.*

4. Discussion and Conclusions

Standard landmarking accuracy is an insufficient predictor of clinical metric reliability. The ETT/mHKA contrast shows that geometric configuration, not error magnitude, determines sensitivity: short transverse axes amplify errors multiplicatively, while a long mechanical axis absorbs them. Patient morphology further modulates this effect, making landmark criticality both metric-specific and patient-dependent. This framework directly supports risk-stratified verification and validation of automated TKA planning systems.

5. References

1. Horteur C, et al. Eur J Radiol. 2025 Oct;191:112292. PMID: 40652606.
2. Roch Y et al. How do lower-limb landmarking errors impact morphometrics in total knee arthroplasty planning? (under review), 2025.

Acknowledgements:
Funded by FRM (DIC20161236448), Région AuRA (PIT), and GENCI/IDRIS (grant 2023-A0160313879). IRMaGe facility: ANR-11-INSB-0006. CIFRE thesis (Twinsight/UGA). Clinical data: CHU Grenoble Alpes.

SIMULATION OF THE ABDOMINAL WALL FOR PERSONALIZED HERNIA ASSESSMENT

Evangelia Antoniadi (1), Maria Pia Ferraz (2), Marco Parente (1), Elisabete Silva (1)

1. LAETA/INEGI, Faculty of Engineering, University of Porto, Portugal
2. Ii3S, Faculty of Engineering, University of Porto, Portugal

1. Introduction

The abdominal wall is a dynamic, mechanically active structure that undergoes significant deformation due to breathing, movement, and intra-abdominal pressure. Numerical models play a crucial role in understanding the biomechanics of hernia repair by accounting for variations in patient profiles, surgical techniques, and device characteristics. These methods have the potential to guide future device designs, enhance surgical procedure simulations, and support the personalization of surgeries, aiming to reduce recurrence rates [1,2]. In this work, a three-dimensional finite element model of the abdominal wall was developed from MRI data of a healthy individual to enable the biomechanical investigation of hernia formation and abdominal wall mechanics.

2. Materials and Methods

A 3D model of the abdominal wall was developed from manually segmented MRI data of a healthy subject using MIMICS software. The model incorporates a multilayer anatomical representation, including the rectus abdominis muscles, linea alba, lateral abdominal muscles, and connective tissue. Intra-abdominal pressure was applied to characterize the mechanical response of the abdominal wall. Specifically, intra-abdominal pressure (IAP) was simulated at 2.67 kPa in the standing position, 2.23 kPa in the sitting position, 10.85 kPa during coughing, and 5.29 kPa during the Valsalva maneuver [3]. Hernia formation was then simulated by applying a localized anatomical modification along the midline, corresponding to the linea alba, enabling analysis of stress concentrations and deformation patterns associated with herniation.

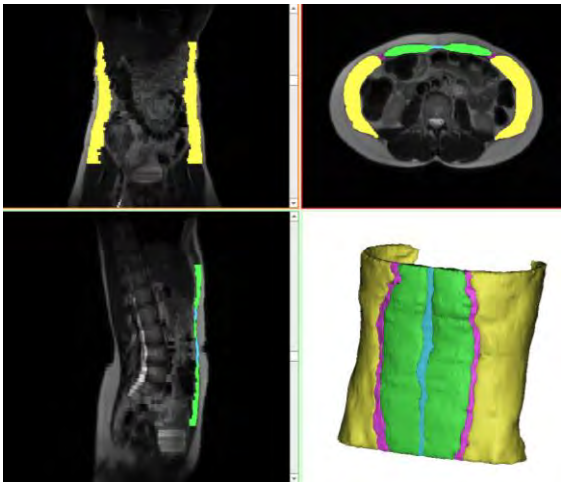


Figure 1: MRI image with manual segmentation of the abdominal wall.

3. Results

A localized discontinuity will be introduced in the central region of the abdominal wall, corresponding to the linea alba, to simulate hernia formation and enable the future simulation of surgical mesh implantation.

4. Discussion and Conclusions

This modeling framework provides a predictive, patient-specific tool for investigating hernia mechanics, supporting surgical planning, and contributing to the design of personalized repair strategies that may reduce recurrence and postoperative complications.

5. References

1. A. Jourdan et al., Comput. Methods Programs Biomed., vol. 244, Feb. 2024.
2. E. Antoniadi et al., Materials, vol. 18, no. 15, pp. 1–28, 2025.
3. W. S. Cobb et al., Journ. of Med. Research vol. 129, no. 2, pp. 231–235, 2005

Acknowledgements:
The authors gratefully acknowledge funding from LAETA via the project UID/50022/2025.

GEMINI: DIGITAL TWIN FOR PERSONALIZED ISCHEMIC STROKE TREATMENT DEVICE SELECTION: A STUDY PROTOCOL

Thomas Brouwer (1)(2), Bart Emmer (1), Jonathan Couthinho (3), Bob Roozenbeek (4), Sandra Cornelissen (5), Hester Lingsma (6), Luca Bontempi (7), Giulia Luraghi (8) Charles Majoie (1) Henk Marquering (2)

1. Department of Radiology and Nuclear Medicine, Amsterdam UMC, The Netherlands; 2. Department of Biomedical Engineering and Physics, Amsterdam UMC, The Netherlands; 3. Department of Neurology, Amsterdam UMC, The Netherlands; 4. Department of Neurology, Erasmus MC, The Netherlands; 5. Department of Radiology and Nuclear Medicine, Erasmus MC, The Netherlands; 6. ; 7. Department of Biomedical Engineering, Erasmus MC, The Netherlands; 8. Laboratory of Biological Structure Mechanics (LaBS), Department of Chemistry, Materials, and Chemical Engineering, Politecnico di Milano, Italy

1. Introduction

Although endovascular treatment has improved ischemic stroke outcomes, treatment success varies substantially, reflecting the complex and patient-specific nature of stroke.[1] Endovascular treatment device selection relies largely on population-based evidence and clinician experience. Digital twins – patient-specific, data-driven computational models – offer a novel approach to support technical treatment decisions. The GEMINI (Generation of Multiscale digital twINs In acute stroke) consortium was established to develop and clinically evaluate digital twins to support technical approach selection for acute ischemic stroke.[3]

2. Methods

The GEMINI Trial is a multicenter, randomized, stepped-wedge cluster design trial. Outcome assessment is blinded. Patients with computed tomography angiography – confirmed anterior circulation intracranial vessel occlusion, who are eligible for endovascular treatment, are included. The intervention group receives standard-of-care with the addition of a patient-specific digital twin to support technical approach (stent retriever or aspiration catheter or combination) choice. The digital twin visualizes the technical approaches, calculates percentage-chance of first-pass success, and calculates percentage-chance of thrombus fragmentation for each technical approach. Control group receives standard-of-care without the addition of a digital twin for technical approach choice. Primary outcome is first-pass success. Secondary outcomes include hemorrhage presence, infarct growth, and NIHSS at 24 hours, and mRS at 3 months. A total of 300 patients will be enrolled in two centers, based on an anticipated 25% relative increase of first-pass success.

3. Discussion and Conclusions

The GEMINI Trial is the first randomized clinical evaluation of digital twin technology in stroke care.

4. References

1. Goyal M et al. Lancet. 2016 Apr 23;387(10029):1723-31. Doi: 10.1016/S0140-6736(16)00163-X. PMID: 26898852.
2. https://dth-gemini.eu

Acknowledgements:

This abstract received funding from the European Union's Horizon Europe research and innovation programme under grant agreement No 101136438 (GEMINI project)

Disclaimer:

This publication reflects only the author's view, and the European Commission is not responsible for any use that may be made of the information it contains.

CALIBRATION OF A BIOCHEMO-MECHANO MULTI-SCALE COMPUTATIONAL MODEL TO PREDICT BONE ADAPTATION

Silvia Dirstaru[1], Saira Farage-O'Reilly[1], Vee San Cheong[1], Sanjay Singh[1], Ilaria Bellantuono[1], Peter Pivonka[2], Enrico Dall'Ara[1]

1. University of Sheffield, United Kingdom; 2. Queensland University of Technology, Australia

1. Introduction

Computational models capable of predicting bone adaptation over space and time may reduce the need for animals in pre-clinical trials for new treatments against osteoporosis. Multi-scale models combining micro finite element (micro-FE) models and bone cell population models (BCPM) can be used to predict bone adaptation based on both biomechanical and biochemical stimuli. This project aims to calibrate a multi-scale model to predict bone adaptation in the mouse tibia.

2. Materials and Methods

In a previous study, six female C57Bl/6 mice were used, in which micro-computed tomography (micro-CT) images of the tibia were obtained at weeks 18 and 20 of age [1]. At week 19, the right tibia was subjected to external mechanical loading. Local biomechanical stimuli were evaluated using micro-FE models based on micro-CT [2]. The biochemical cues that induce bone remodelling have been incorporated by coupling the micro-FE model with a BCPM based on ordinary differential equations [3]. Three parameters, associated with maximum amount of deformation, the threshold value that produces 50% of response and response steepness for mechano-regulation in the model were calibrated by site-specific optimisation to minimise the difference between the measured and predicted bone remodelling. Separate sets of optimal parameters were found for seven tibial sections, each corresponding to 10% of the tibial length.

3. Results

Different optimal parameters were found across mice and sections. Section-specific optimisation improved the prediction of bone formation by 5-12%. The accuracy of the model in predicting periosteal apposition was highest in the tibia midshaft (80% ± 11%; Range: 60-97%) and lowest closest to the tibiofibular junction (66% ± 15%; Range: 29-89%) (Figure 1).

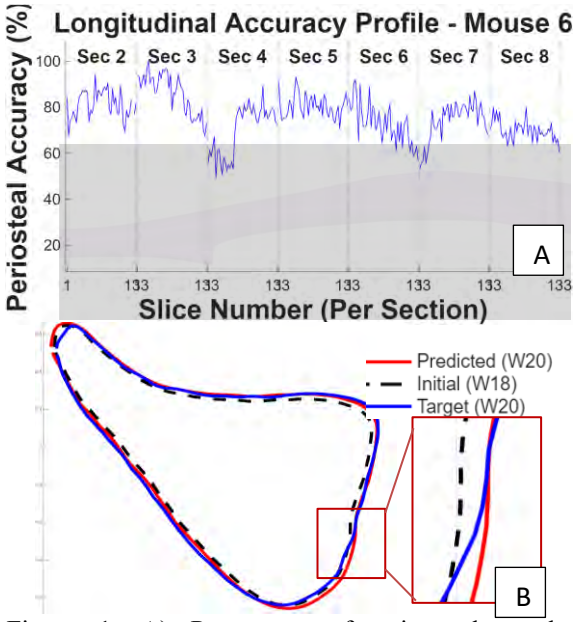


Figure 1: A) Percentage of points along the periosteum, predicted within one voxel of the experimental data. B) Visual representation of the apposition at the end of simulation period (red solid line) in contrast to the experimental data for week 18 (black dashed line) and week 20 experimental data (blue solid line).

4. Discussion and Conclusions

These findings indicate that tuning the mechano-regulation parameters alone in the bone adaptation models may not be sufficient to achieve optimal predictions across the whole tibia length. This might be the result of variations in bone cell distributions and localised stresses. Future work will explore the sensitivity of the model to biochemical inputs.

5. References

[1] B. C. Roberts et al, Bone, vol. 127, Oct. 2019, doi: 10.1016/j.bone.2019.06.024.
[2] S. Oliviero et al, J. Mech. Behav. Biomed. Mater., vol. 113, Jan. 2021, doi: 10.1016/j.jmbbm.2020.104190.
[3] C. Miller et al, Nov. 2023, doi: 10.5204/thesis.eprints.244742.

Acknowledgements:
The project was funded by the EPSRC (EP/Z000203/1).

CREDIBILITY ASSESSMENT APPROACH FOR VIRTUAL IMPLANT TESTING OF CUSTOM-MADE CRANIOMAXILLOFACIAL DEVICES

Sven Herrmann (1), Thomas Koett (1), Laura Alarcon Rueda (1), Steffen Aberle (1), Agnes Beckmann (1)

1. *Engineering inSilico, KLS Martin SE & Co. KG, Germany*

Corresponding Author: Sven Herrmann, KLS Martin SE & Co. KG, Kolbinger Str. 10, 78570 Mühlheim, Germany, E-Mail: Sven.Herrmann@klsmartin.com

1. Introduction

Custom-made implants are increasingly important in craniomaxillofacial (CMF) surgery, yet their uniqueness makes conventional physical testing per patient infeasible. Patient-specific finite element analysis (PS-FEA) offers a promising alternative for virtual implant testing of these devices [1], but decision relevant use requires credible models. A hierarchical verification and validation (V&V) strategy appears well suited for this purpose. Although prior works provide key elements in this regard [2], no existing framework fully implements a comprehensive, standards-based credibility assessment for PS-FEA of custom-made implants (IPS®, KLS Martin, Germany). Therefore, we introduce a hierarchical credibility assessment approach for virtual testing of IPS® CMF devices, structuring V&V activities across system tiers, and aligning it with risk-informed credibility frameworks [3].

2. Materials and Methods

In this approach, the PS-FE model is decomposed top down into 4 inherent tiers of complexity (system, sub-systems, components, materials) (Fig. 1). Context of use (COU) and model risk are defined once at the system level [3]. Phenomena identification and ranking table analysis identifies the elements most critical to the quantities of interests (QOIs), forming the basis for the V&V hierarchy. Each identified element along this hierarchy is assigned a role for the next higher tier, with corresponding V&V activities, comparators, credibility factors and goals selected according to evidence categories [3] and model risk. The model aspects of lower tier elements are implemented in the higher tiers after demonstrating applicability for their role along the hierarchy. Overall applicability remains to be demonstrated on the system level with respect to the COU with a final adequacy assessment confirming the overall credibility.

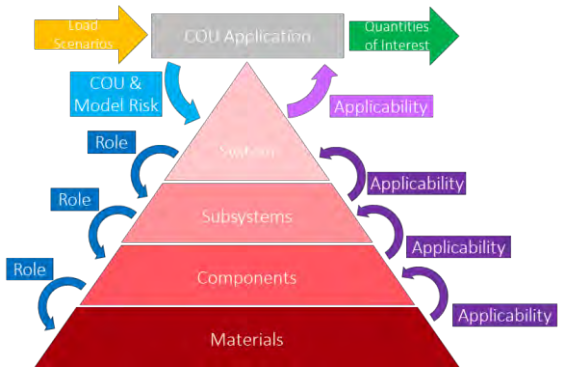


Figure 1: V&V hierarchy of a PS-FE model.

3. Results

The hierarchical credibility assessment approach is performed for the virtual testing application of IPS® implants as COU with stress-based QOIs. Using benchtop tests, this comprises characterization of Ti-6Al-4V material, validation of the mechanical behaviour of involved components, and validation of an entire CMF subsystem in interaction with adjacent bones. On the system level, retrospective analysis of clinical data including patient cases with CMF implants are used as comparator.

4. Discussion and Conclusions

The approach presented here demonstrates that credibility of PS-FEA can be managed across an entire V&V hierarchy in line with established risk-informed credibility frameworks. Mapping crucial tier elements to established evidence categories and credibility factors ensures alignment with regulatory expectations. Although applied here to virtual testing of IPS® CMF implants, the approach is generalizable and can be applied to other custom-made devices where physical testing per patient is infeasible.

5. References

1. Andres A et al.; Bioengineering; 12, 545 (2025).
2. Pathmanathan P et al., PLoS Comput Biol 20(8):e1012289 (2024).
3. Food and Drug Administration (FDA), Docket No. FDA-2021-D-0980 (2023).

FROM STANDARDS TO PRACTICE: SCALABLE CREDIBILITY ASSESSMENT OF VIRTUAL PHYSIOLOGICAL HUMAN MODELS

Karol Zając (1), Marek Kasztelnik (2), Piotr Połeć (2), Piotr Nowakowski (1,2)

1. Sano – Centre for Computational Medicine, Poland; 2. ACC Cyfronet AGH, Poland;

1. Introduction

The credibility and clinical translation of Virtual Physiological Human (VPH) models critically depend on systematic Verification, Validation and Uncertainty Quantification (VVUQ). While standards such as ASME VV40 provide methodological guidance, their practical adoption remains limited due to the computational cost and engineering complexity of executing large-scale VVUQ campaigns [1].

2. Materials and Methods

Within the GEMINI project [2], we contribute methodological and computational expertise aimed at enabling rigorous, large-scale VVUQ studies for complex physiological models.

Our methodology emphasizes the systematic design of numerical experiments, reproducibility of results, and clear separation between model development and VVUQ execution.

The approach is grounded in ASME V&V40 principles and good programming practices, translating abstract credibility assessment concepts into executable computational campaigns. Large ensembles of simulations are executed on HPC infrastructures using hybrid parallelism, combining tightly coupled solvers with ensemble-based and task-parallel execution patterns [3]. Automation is used to manage parameter sampling, job submission, monitoring, and post-processing, allowing VVUQ studies to scale to thousands or more simulations without manual intervention.

3. Results

Applying this approach within GEMINI use cases demonstrates that comprehensive VVUQ analyses can be performed at scales that are otherwise impractical in typical VPH research settings. The methodology enables efficient global sensitivity analyses and uncertainty quantification while maintaining full traceability of model versions, parameters, and computational environments. Strong scaling and throughput-oriented execution strategies significantly reduce time-to-insight, supporting iterative credibility assessment during model development.

4. Discussion and Conclusions

By framing VVUQ as a scalable, automated process aligned with established standards, our approach supports broader adoption of rigorous credibility assessment across the VPH community. In this work, VVUQ is not considered an afterthought nor a collection of several additional simulations, but a carefully designed and systematic computational process.

5. References

1. D. Suleimenova, et. Al., Journal of Computational Science, 53, (2021). Tutorial applications for Verification, Validation and Uncertainty Quantification using VECMA toolkit. doi:10.1016/j.jocs.2021.101402
2. A Generation of Multi-scale Digital Twins of Ischaemic and Haemorrhagic Stroke Patients: https://dth-gemini.eu/
3. M. Kasztelnik, et. Al., ICCS 2023, Digital twin simulation development and execution on hpc infrastructures. doi:10.1007/978-3-031-36021-3_2

Acknowledgements:

This project has received funding from the European Union's Horizon 2020 research and innovation programme under grant agreement No 101136438 (GEMINI).

We gratefully acknowledge Polish high-performance computing infrastructure PLGrid (HPC Center: ACK Cyfronet AGH) for providing computer facilities and support within computational grant no. PLG/2025/018003 and PLG/2026/019160.

VERIFICATION AND VALIDATION OF MDSIM'S ATLAS SPINE MODEL: APPLICATION TO A PATIENT-SPECIFIC DEFORMITY CASE

Matteo Tarquini (1), Morteza Rasouligandomani (1), Siril Teja Dukkipati (1), Deniz Kaçar (1), Roger Assaker (1), Laurent Adam (1)

1. MDsim S.A., Luxembourg

Correspondence: Matteo Tarquini, MDsim S.A., 9 avenue des Hauts-Fourneaux, L-4362 Esch-sur-Alzette, Luxembourg.

1. Introduction

Patient-specific finite element (FE) spine models can support surgical planning only if their modelling methods are verified and their biomechanical predictions are validated against independent data. This work summarizes ASME V&V 40 based verification and multi-level validation of The MDsim biomechanical atlas model of the spine and illustrates its first retrospective application to a deformity case with bilateral rod fracture.

2. Materials and Methods

The biomechanical model spans T1 to the sacrum and includes cortical and cancellous bone, vertebral processes, facet cartilage, nonlinear intervertebral discs (IVDs) with annulus fibres, and nonlinear ligaments. Verification comprised mesh-refinement and material-sensitivity analyses. Validation was performed under three loading configurations: pure moments, follower-load compression, and preload-plus-bending, against published cadaveric and FE benchmarks [1-4]. To assess the use of 1D ligament elements, a 3D-printed sacrum–L1 phantom was tested under the same loading modes, both intact and after one-level instrumented fusion. Finally, a patient-specific post-operative model of a pelvis-T9 fusion was reconstructed from the CT scan and loaded with gravity preload and bending moments (flexion, extension, lateral bending, axial rotation), to compare predicted rod stresses with a clinically observed bilateral rod failure.

3. Results

The selected mesh showed convergence of key outputs (vertebral stresses and rotations, IVD strains), and material perturbations of ±20% produced changes in the order of ±15% in kinematics and intradiscal pressure. Under pure moments, total lumbar range of motion at 7.5 Nm remained within experimental variability and the published FE envelope [1], with a mean deviation of 1.12°. Segmental flexion rotations were also reproduced with a mean error of 0.50° [2]. Under follower load, the predicted L4-L5 intradiscal pressure matched the reported trend with a 0.25 MPa deviation at 1000 N [1,3,4]. In the preload-plus-bending configuration, flexion-related pressure changes were captured with less than 0.1 MPa average error. Phantom validation showed range of motion (ROM) errors below 10% in the intact model and about 3.2% on average after instrumentation, supporting the adequacy of 1D ligaments for global kinematics. In the patient specific analysis, right lateral bending produced peak rod stresses above the 2-year endurance limit in the same regions where failure was later observed; when residual rod pre-stress was added, the contralateral failure pattern was also illustrated by the model.

4. Discussion and Conclusions

The biomechanical model of MDsim combines numerical verification, literature-based validation, physical phantom testing, and first-case clinical back-analysis within a single framework. The agreement obtained for ROM and IVD pressure supports its use as biomechanically validated and reproducible platform for physiologically relevant spine simulations. The retrospective clinical result suggests potential for pre-operative risk assessment of instrumentation failure, although broader retrospective and prospective studies are still required before routine clinical deployment.

5. References

1. Dreischarf M, Zander T, Shirazi-Adl A, et al. J Biomech. 2014;47(8):1757-1766.
2. Bellina E, Laurino ME, Perego A, et al. J Biomech. 2024;164:111951.
3. Naserkhaki S, Arjmand N, Shirazi-Adl A, et al. J Biomech. 2016;49(7):1255-1263.
4. Schultz A, Andersson G, Ortengren R, et al. J Bone Joint Surg Am. 1982;64(5):713-720.

GAIT AND MRI-DERIVED DISC MORPHOLOGY ALTERATIONS IN PATIENTS WITH LUMBAR HERNIATION

Inês Mendes (1), Nuno Cristino (2,3), Rita Fernandes (4, 5, 6), André Castro (1, 7)

1. ESTSetúbal, Instituto Politécnico de Setúbal, Portugal; 2. Neurosurgery Department, Hospital da Luz Setúbal, Portugal; 3. iNOVA4Health, NOVA Medical School, Universidade Nova de Lisboa, Portugal; 4. ESS, Instituto Politécnico de Setúbal, Portugal; 5 Comprehensive Health Research Center, NOVA Medical School, Universidade Nova de Lisboa, Portugal; 6. LBMF, CIPER, Faculdade de Motricidade Humana, Universidade de Lisboa, Portugal; 7. IDMEC, Instituto Superior Técnico, Universidade de Lisboa, Portugal

1. Introduction

Lumbar disc herniation (LDH) is a common cause of low back pain and functional disability. Although gait adaptations in LDH patients are well documented, the relationship between intervertebral disc (IVD) morphology and locomotor alterations is still unclear. Magnetic resonance imaging (MRI) enables quantitative assessment of IVD structure and may provide relevant imaging biomarkers associated with LDH [1-3]. This study investigates MRI-derived morphometric descriptors of lumbar IVD and their relationship with gait alterations.

2. Materials and Methods

An exploratory cross-sectional study was conducted at Hospital da Luz Setúbal, including 8 LDH patients and 8 matched healthy controls. Spatiotemporal gait parameters were collected during overground walking to characterize locomotor performance. Lumbar MRI scans (T2-weighted images) were analysed to extract morphometric descriptors of the IVD spaces based on vertebral geometry, enabling estimation of IVD height and structural configuration. Statistical analyses (Mann-Whitney U test) were performed to identify functional and structural characteristics associated with LDH.

3. Results

LDH patients showed altered gait patterns compared with healthy controls, with changes in spatiotemporal parameters consistent with compensatory locomotor strategies. These differences suggest modifications in gait timing and spatial organization, indicative of functional adaptation.

MRI analysis revealed structural alterations in LDH patients, including reduced IVD height and changes in vertebral-derived geometric descriptors at affected lumbar levels. Demographic characteristics are presented in Table 1, confirming matching between groups.

Table 1: Characteristics of LDH patients and healthy individuals. Data are reported as median (IQR).

Variable	Healthy	LDH	p-value
Age (years)	52.0 (11.0)	55.0 (20.5)	0.792
BMI (kg/m^2)	26.6 (6.1)	28.0 (7.1)	0.728

4. Discussion and Conclusions

LDH is associated with concurrent structural and functional alterations, with MRI-derived IVD changes aligning with gait adaptations observed in affected patients. Findings suggest that localized IVD degeneration may contribute to altered spinal biomechanics and compensatory locomotor strategies. Overall, results support the value of combining imaging and gait analysis, providing complementary insights into both structural degeneration and functional impairment in LDH, and reinforcing the importance of a multimodal assessment approach.

5. References

1. Mendes I et al., Ann. Biomed. Eng.;2026; 54(4): 1-15
2. Lee K et al., J. Int. Med. Res.; 2021; 136(7): 1-9
3. Bonab M et al., Neurospine; 2023; 20(3): 947-958

Acknowledgements:

The authors acknowledge funding from Fundação para a Ciência e a Tecnologia (FCT), for its financial support via LAETA (project UID/50022/2025), and COST Action EuroCurvoBioNet CA22153, supported by COST (European Cooperation in Science and Technology).

DIGITAL TWINS IN HEALTHCARE: AN ANALYSIS WITHIN THE EU REGULATORY FRAMEWORK

Martina Baltuzzi (1)

1. *University of Torino, Italy; University of Bologna, Italy; KU Leuven, Belgium*

1. Introduction

Through the implementation of technologies capable of simulating and predicting clinical conditions, the European Union is shifting from a reactive model of care to a preventive one. Digital twins (DTs) represent one of the most advanced expressions of this transition [1]. While they promise improvements in personalized and predictive medicine, their deployment also raises legal questions within European health law. This research analyses the applicability and pertinence of the current European regulatory framework to medical digital twins.

2. Materials and Methods

The research adopts a doctrinal legal analysis combined with policy review. It examines European initiatives promoting digital twins in healthcare and the interaction between key EU regulations relevant to digital twins, addressing their applicability. The following regulations are considered: General Data Protection Regulation; Artificial Intelligence Act; Medical Device Regulation; In Vitro Diagnostic Regulation; Data Governance Act; European Health Data Space Regulation.

3. Results

The concept of "digital patient" has been explored in several EU-funded projects, such as DISCIPULUS and the European Virtual Human Twins Initiative, reflecting EU's interest towards the development of digital twin models in healthcare. DTs are currently not governed by any specific provisions under European law; once implemented, however, they could fall within the scope of the key regulations examined in this study. As digital twins process large volumes of data, often classified as special categories of personal data, specific legal bases would be required under the GDPR. Under the AI Act, DTs may qualify as AI systems and be categorized as high-risk, triggering strict requirements regarding risk management, transparency and human oversight. They may then be classified as medical devices under the MDR or as in-vitro diagnostic devices under the IVDR according to their intended use and application, entailing conformity assessment procedures and risk-based classification. Finally, they may benefit from both the data altruism mechanism introduced by the DGA [2] and the harmonized framework for primary and secondary use of electronic health data defined by the EHDS, as facilitated access to diverse data sources and increased interoperability would better DT's accuracy in modelling [3].

4. Discussion and Conclusions

Despite the EU's growing interest in medical digital twins, current European normative framework does not directly address them. While it aims at balancing innovation with the protection of fundamental rights, specifically privacy, regulatory challenges however remain. For instance, tensions may arise between data minimization requirements and the need for large datasets in the development of DTs, or AI models may not align within traditional conformity assessment procedures. Thus, further initiatives may soon prove necessary to ensure that digital twins are adequately regulated within the EU.

5. References

1. Sun, T., et al. (2022). The Digital Twin in Medicine: A Key to the Future of Healthcare? *Frontiers in Medicine*, 9, 907066
2. Paseri, L. (2025). *Il governo dei dati: Interesse pubblico, altruismo e partecipazione*. Università degli Studi di Torino; G. Giappichelli Editore.
3. Cristofaro, L. (2024). *Towards a Code of Conduct for the re-use and integration of Virtual Human Twins: Analysis of the legal landscape and identification of legal and ethical challenges*.

Acknowledgements:

This research was supported by a PhD scholarship awarded to Martina Baltuzzi by the Universities of Torino and Bologna.

ETHICAL AND TECHNICAL FRONTIERS IN VIRTUAL HUMAN TWINS FOR HEALTHCARE

Michele Barbier, Inria, France

This presentation is not merely technical — it is a moral and philosophical call to ensure that the power of Virtual Human Twins serves humanity, not the other way around. As technology advances, so must our ethical frameworks — to preserve what makes medicine truly human.
This summary reflects the full scope, depth, and urgency of my ethical analysis of Virtual Human Twins — grounded in both scientific rigor and humanistic values

Introduction
The integration of Virtual Human Twins (VHTs) into clinical practice represents a transformative leap in personalized, predictive, and preventive medicine. These patient-specific digital replicas — built on hybrid data- and knowledge-driven models — enable dynamic simulation of physiological systems, supporting diagnosis, therapy planning, drug development, and medical training. However, their deployment raises profound ethical, technical, and governance challenges that must be addressed to ensure responsible innovation.

Ethical key considerations
This presentation outlines key considerations for the VPH2026 conference, emphasizing the urgent need to align technological advancement with core ethical principles: autonomy, beneficence, non-maleficence, and justice. VHTs demand robust frameworks for privacy, consent, and data governance, particularly as they evolve into adaptive, lifelong digital companions. The GDPR-compliant data handling is essential to protect individuals from surveillance, exclusion, or algorithmic determinism. Moreover, Verification, Validation, and Uncertainty Quantification (VVUQ) are critical to ensure algorithmic credibility, and clinical reliability — without which trust in AI-assisted medicine erodes.

Human agency
A central tension lies in balancing human agency with algorithmic insight. Over-reliance on predictive models risks diminishing clinical judgment and patient autonomy, fostering "algorithmic heteronomy." Medicine must remain a practice of discernment, responsibility, and human encounter — not merely data optimization. Ethical guardrails must also address social justice: ensuring equitable access, avoiding techno-eugenics, and prioritizing frugality to align with ecological sustainability goals. Energy-intensive infrastructures contradict the imperative of green digital health.

AI regulatory pathways and guidelines
The presentation will explore regulatory pathways, including the EU AI Act, Ethics guidelines for Trustworthy AI (2) and JRC's AI Evidence Pathway, alongside practical toolkits like ALTAI and the Ethics & Algorithms Toolkit. It will also examine the STANDING Together consensus on mitigating bias in health datasets (1). Interdisciplinary collaboration — between clinicians, engineers, ethicists, and policymakers — is essential to navigate these challenges.

Conclusion
We invite researchers and practitioners to co-create governance models that preserve human dignity while harnessing the immense potential of VHTs. As Hannah Arendt warned, we must not fall into "doing without understanding." The question is no longer merely how systems work, but how we use them to serve humanity — responsibly, equitably, and sustainably.

5. References
1. Alderman JE, et al. *Tackling algorithmic bias and promoting transparency in health datasets: the STANDING Together consensus recommendations*. The Lancet Digital Health, 2025;7(1):e64–e88.
2. European Commission. *Ethics Guidelines for Trustworthy AI*. Publications Office of the EU, 2019. https://op.europa.eu/en/publication-detail/-/publication/62c24e61-6129-11f0-a9d0-01aa75ed71a1

FROM ALGORITHMS TO HEADLINES: MEDIA COVERAGE OF IN SILICO MEDICINE

Davide Montesarchio (1,2), Zita Van Horenbeeck (1,2), Mona Del Piero (2)
1. VPH Society, Belgium; 2. KU Leuven, Belgium

1. Introduction

In silico medicine, encompassing virtual human twins, computational modeling, and Artificial Intelligence (AI), is rapidly advancing toward widespread adoption [1]. Understanding how it is portrayed in the media becomes crucial as news coverage shapes public perception, policy priorities and funding agendas through reciprocal dynamics [2,5]. This mixed-method study analyses how newspapers across countries report on in silico medicine in the last decade, examining temporal trends, terminology, and dominant narratives to inform more effective science communication strategies.

2. Materials and Methods

This study consists of a longitudinal media analysis of newspaper articles published between 01/01/2014 and 31/12/2025. Twelve major newspapers from six countries were included in the study: USA (*The New York Times*, *The Washington Post*), UK (*The Times*, *The Guardian*), Belgium (*De Standaard*, *Le Soir*), France (*Le Figaro*, *Libération*), Italy (*Il Corriere della Sera*, *Il Resto del Carlino*), and Australia (*Herald Sun*, *The Australian*). Science magazines for lay audiences (*New Scientist*, *Popular Mechanics*, *Wired*) were also analyzed. Articles were retrieved via *ProQuest* and *Nexis Uni* databases [3, 4]. Search queries comprised 27 terms from five domains: AI and data-driven approaches; digital/virtual/in silico medicine; computational infrastructure; modeling and simulation; precision/ personalized medicine. Retrieved articles were deduplicated and screened for relevance before undergoing mixed-methods analysis [3,4]. Quantitative analyses assessed reporting frequency, keyword usage in headlines, and temporal trends, while qualitative thematic coding through software Atlas.ti analysed the narratives and recurring frames used to portray in silico medicine, revealing how particular promises, risks and governance approaches are stabilised in news media.

3. Results

Coverage of in silico medicine increased steadily across all countries, markedly accelerating after 2018. Keyword analysis revealed that since 2016 newspapers converged around AI-related terms while covering in silico medicine. Since then, AI-related terms are present in more than 50% of the headlines, getting close to 90% in 2024 (Fig. 1). Qualitative analysis is ongoing and results will be presented at the conference.

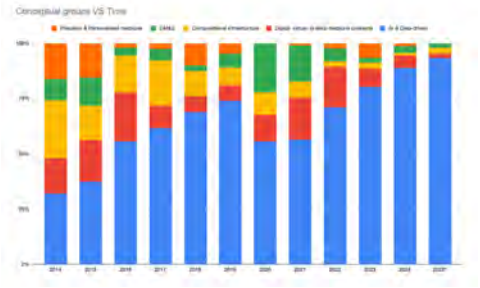


Fig.1: Conceptual groups VS Time.

4. Discussion and Conclusions

Media attention to in silico medicine has been rapidly growing in the past decade. At the same time, the public discourse has been increasingly framed around AI-related terms, mirroring a broader attention to AI. This trend is double-edged. On one hand it boosts visibility, allowing in silico technologies to benefit from AI's media spotlight. On the other, it risks oversimplifying the field's multidisciplinary nature by overshadowing elements like mechanistic modeling and virtual human twins. Understanding these trends can help researchers, institutions, and policymakers design effective communication strategies, foster informed public debate and better align policy with realities of digital health innovation.

5. References

1. The future of in silico trials and digital twins in medicine. PNAS nexus, 4(5), pgaf123.
2. Wlezien, C., & Soroka, S. (2024). Media reflect! Policy, the public, and the news. American Political Science Review, 118(3), 1563-1569.
3. Mach, K. J., Salas Reyes, R., Pentz, B., Taylor, J., Costa, C. A., Cruz, S. G., ... & Klenk, N. (2021). News media coverage of COVID-19 public health and policy information. Humanities and Social Sciences Communications, 8(1).
4. Sun, S., Zhai, Y., Shen, B., & Chen, Y. (2020). Newspaper coverage of artificial intelligence: A perspective of emerging technologies. Telematics and Informatics, 53, 101433.
5. Mechanic, D. (2005). The mass media's influence on health law and policy. Houston Journal of Health Law & Policy, 5(2), 187–211.

THE ZERO-ENTROPY ENVIRONMENT: WHY REGULATION OF DIGITAL TWINS MUST ADDRESS HUMAN AGENCY

Valerio Prosseda (1), Marta Bertolaso (1)

1. Università Campus Bio-Medico, Research Unit of Philosophy of Science and Human Development, Italy

1. Introduction

Digital twins in rehabilitation and assistive robotics promise personalized optimization of human-machine interaction, however a fundamental paradox undermines their clinical safety: highly autonomous systems designed to maximize therapeutic performance systematically degrade the very agency they aim to restore. When a robotic twin corrects every movement error before the patient can attempt it, the patient becomes a passenger in their own recovery. Current regulatory frameworks and emerging standards lack the conceptual tools to address this, whether a system preserves conditions for human authorship.

2. Materials and Methods

A systematic review of shared agency in human-robot interaction was conducted following PRISMA guidelines. Disciplinary perspectives (cognitive neuroscience, embodiment research, control engineering) were analysed for how they conceptualize, measure, and design for agency. Implicit measures (Intentional Binding, sensory attenuation) were compared against explicit self-report measures to identify epistemological contradictions.

3. Results

Three findings carry direct regulatory implications. (1) The *autonomy-agency paradox*: engineering perspectives treat agency as a zero-sum trade-off with automation [1], while interaction-based studies show agency can be preserved when assistance aligns with user goals. Current regulations assess the machine in isolation, not the human-machine system. (2) *Measurement divergence*: implicit measures capture pre-reflexive sensorimotor coupling; explicit measures capture retrospective narrative judgments. These systematically dissociate—users can report agency while their motor systems register loss of control [2]. Frameworks relying on user self-reports may miss this entirely. (3) *The zero-entropy environment*: eliminating all performance friction—perfect assistance, zero delay—collapses the conditions for agency, producing learned helplessness, a structural consequence of treating friction as a problem.

4. Discussion and Conclusions

These findings share a common cause: regulatory frameworks operate by treating agency as a fixed property to divide between human and machine, binary, measurable by physical metrics, and aligned with optimized performance by default. The zero-entropy environment is the logical consequence: a system passing every regulatory test while failing the patient phenomenologically. The AI Act defines oversight as technical intervention capacity, not experienced control; the MDR interprets harm as physical, not existential. Current frameworks cannot diagnose this because their ontology renders it invisible. Regulation of digital twins must expand from physical to *agentic safety*: the maintenance of conditions under which human authorship can emerge. This requires conformity assessments of human-machine coupling, operational definitions of oversight accounting for phenomenological experience, and recognition that no friction is a potential harm. The zero-entropy environment offers a diagnostic lens: optimizing all friction away, it is a way current frameworks cannot measure.

5. References

1. Collier MA, Narayan R, Admoni H. The Sense of Agency in Assistive Robotics Using Shared Autonomy. HRI 2025; 880–888.
2. Grynszpan O, et al. The sense of agency in human-human vs human-robot joint action. Consciousness and Cognition. 2019;75:102820.
3. Regulation (EU) 2024/1689 — Artificial Intelligence Act.
4. Regulation (EU) 2017/745 — Medical Device Regulation (MDR).

IN SILICO METHODOLOGIES IN HIGH-RISK MEDICAL DEVICE DEVELOPMENT: IMPLICATIONS FOR HEALTHCARE SYSTEMS

David Rösler (1) (2), Thomas Czypionka (1), Jan Brüning (3), Siegfried Eisenberg (1), Markus Kraus (1), Miriam Reiss (1), Clemens Zech (1)

1. Institute for Advanced Studies Vienna, Department of Health Systems and Health Policy, Austria;
2. University of Vienna, Department of Science and Technology Studies, Austria;
3. Charité Berlin, Institute of Computer-assisted Cardiovascular Medicine, Germany

1. Introduction

The development of high-risk medical devices is increasingly shaped by in silico methodologies (ISMs), including computational modelling, digital twins, and virtual cohorts. While these approaches are gaining traction in early-stage device development, their broader implications for healthcare systems remain insufficiently understood. Beyond potential efficiency gains in research and development, ISMs may affect patient safety, regulatory processes, healthcare costs, and equitable access to medical technologies. This study examines how ISMs are currently applied across the medical device life cycle and explores their anticipated impacts on healthcare systems from the perspectives of key stakeholders across multiple regulatory contexts.

2. Methods

We conducted a qualitative study using semi-structured expert interviews and patient focus groups to capture stakeholder perspectives on the adoption and system-level implications of ISMs. In total, 48 interviews were conducted with stakeholders from academia, industry, regulatory authorities, and healthcare professionals across Europe, North America, South America, and Asia. Additionally, two focus groups with patients diagnosed with cardiovascular disease were held in Austria and the United Kingdom. Interviews and focus groups were audio-recorded where possible, transcribed verbatim, and analysed using qualitative content analysis with a combined deductive–inductive coding approach. Data collection and analysis proceeded iteratively until theoretical saturation was reached.

3. Results

Stakeholders consistently identified three cross-cutting domains through which ISMs may affect healthcare systems: safety, costs and expenditures, and access and equity. ISMs were perceived to enhance patient safety by enabling earlier identification of adverse effects, expanding effective sample sizes through virtual cohorts, and improving the inclusion of underrepresented populations such as children. Cost-related impacts were viewed as ambivalent: while ISMs may reduce development costs and accelerate time to market, downstream effects on prices and healthcare expenditure depend on regulatory acceptance, market competition, and reimbursement frameworks. Regarding access, stakeholders anticipated faster availability of incremental device innovations and improved evidence generation for reimbursement decisions, potentially facilitating earlier and broader patient access. However, concerns were raised about data availability, model validation, and unequal concentration of modelling expertise.

4. Discussion and Conclusions

This study highlights the potential of ISMs to reshape high-risk medical device development with significant implications for healthcare systems. While stakeholders expect gains in safety, efficiency, and inclusivity, these benefits are contingent on robust validation frameworks, regulatory clarity, and transparent governance of data and modelling expertise. Without such safeguards, ISMs may introduce new risks and exacerbate existing inequalities. From a health system perspective, the findings underscore the importance of aligning regulatory, reimbursement, and innovation policies to ensure that efficiency gains translate into tangible benefits for patients and payers. By systematically mapping stakeholder expectations and concerns, this study contributes to a better understanding of how digital innovation in medical device development can support sustainable, safe, and equitable healthcare systems.

Acknowledgements:

The authors of this study have received funding from the European Union's Horizon 2020 research and innovation programme under grant agreement No. 101017578 (SIMCor).

PRIVACY BY DESIGN IN MEDICAL AI: MITIGATING LIFECYCLE RISKS

Mohamed Maouche (1), Paolo Soda (2), Michele Barbier (1)

1. National Institute for Research in Digital Science and Technology - Inria, France; 2. Research Unit of Artificial Intelligence and Computer Systems, Department of Engineering, Università Campus Bio-Medico di Roma, Italy and Department of Diagnostics and Intervention, Umeå University, Sweeden

1. Introduction

In medical AI, privacy is not an add-on but a foundational requirement. Medical images, while indispensable for diagnosis and research, frequently contain embedded personal data: patient identifiers in metadata, anatomical features that enable recognition, or model parameters that inadvertently memorize sensitive patterns. These risks span the entire AI lifecycle (from acquisition to deployment) and can enable re-identification even in ostensibly "anonymized" datasets. As emphasized by the European Commission's High-Level Expert Group on AI, "privacy by design must be embedded at every stage of the AI system's development," particularly in high-risk domains such as healthcare (1).

2. Case study: MRI brain images and lifecycle risks

Brain MRI images, though invaluable, pose significant privacy threats at each lifecycle stage. During acquisition, identifiers may persist in metadata or facial features; in preprocessing and storage, scans can be re-identified when linked with clinical records, requiring strict access controls and on-premise or federated storage. During model training, AI systems may memorize unique anatomical patterns, calling for approaches such as federated learning and configurable differential privacy to limit data leakage. At deployment and inference, outputs like attention maps or predictions may disclose sensitive traits, necessitating output sanitization and uncertainty calibration. In reuse and retention, models may continue to encode personal data even after consent withdrawal, making verifiable unlearning and comprehensive traceability logs critical to compliance with GDPR and the EU AI Act. These risks further underscore the need for systematic privacy auditing of both datasets and trained models, including re-identification risk testing, memorization audits, and regular vulnerability assessments across the AI lifecycle.

A 2023 study in *npj Digital Medicine* showed that even "de-identified" MRI datasets can be re-identified using deep learning models trained on public benchmarks, underscoring the urgency of lifecycle-wide safeguards (2).

3. Technical safeguards and governance

Each stage demands a combination of technical safeguards and robust governance mechanisms (dynamic consent, audit trails, privacy impact assessments, and data minimization) to ensure privacy is not an afterthought but the core pillar of trustworthy, patient-centred medical AI. Federated learning, for example, enables training across distributed sites without centralizing raw data, aligning with GDPR's data minimization principle and reducing exposure risks. In particular, privacy auditing should extend beyond data handling practices to include systematic testing of trained models for unintended memorization, leakage risks, and adversarial exploitability.

4. Recommendations and contribution

This presentation seeks to alert and sensitize developers, clinicians, radiologists, and medical AI practitioners to often-overlooked privacy risks in medical imaging (from metadata leakage to model memorization) by systematically mapping them across the AI lifecycle. We argue that privacy should be treated not as a mere regulatory hurdle but as a prerequisite for trustworthy, ethical, and legally compliant medical AI. We will outline concrete design and governance strategies drawn from the privacy literature to operationalize privacy by design in high-risk medical imaging workflows. Neglecting these safeguards risks eroding patient trust, violating fundamental rights, and ultimately undermining the very systems intended to improve care.

5. References

1. European Commission. HLEG AI (2019). *Ethics Guidelines for Trustworthy AI.* Ethics guidelines for trustworthy AI | Shaping Europe's digital future

2. Kaissis, G., Ziller, A., Passerat-Palmbach, J., Ryffel, T., Usynin, D., Trask, A., ... & Braren, R. (2021). End-to-end privacy preserving deep learning on multi-institutional medical imaging. *Nature Machine Intelligence*, *3*(6), 473-484.

MORE THAN A DATA SUBJECT: RETHINKING PATIENTHOOD IN THE DEVELOPMENT OF MEDICAL DIGITAL TWINS

Zita Van Horenbeeck (1,2), Elisa Elhadj (2), Elisa Lievevrouw (3), Ine Van Hoyweghen (2)
1. VPH Institute, Belgium; 2. TRANSFORM, KU Leuven, Belgium; 3. Meaningful Interactions Lab KU Leuven, Belgium

1. Introduction

As medical digital twins are nearing clinical adoption, this paper examines observed contradictions between anticipated future patienthood and patient roles in current research practices. The envisioned patienthood that becomes thinkable in discussions on the future of medical digital twins starkly contrasts their roles and the extent to which patients are currently able to contribute meaningfully to ongoing research. A socio-technical approach to understanding these tensions is proposed, revealing how not only economic and technical challenges, but also underlying assumptions and values co-shape the future of digital patienthood. Bridging this observed gap calls for reflexivity across research fields, a conversation that this paper seeks to introduce.

2. Methods

This research is informed by multiple qualitative data collection moments in the context of different projects[1]. Five focus groups were held across different geographical locations (Belgium, Italy, Hungary, France, the UK) to explore potential social implications of in silico medicine. Under the ISW project, these implications were further discussed with the consortium in an extensive reflection workshop. Two additional focus groups took place during an EDITH-CSA public meeting in Paris in January 2024. The setup for the latter differed; the guiding scenarios were written more future-oriented, yet still realistic and situated in a clinical context. This deliberate future-oriented setup rendered visible tensions between current research practices and envisioned future possibilities for patient involvement in research. The extensive empirical dataset was qualitatively analysed through software Atlas.ti by means of thematic coding, an iterative process of assigning codes to identify recurring and analytically relevant patterns and themes.

3. Results and conclusion

Drawing on future-oriented anticipatory discussions with modelers, medical digital twins are associated with remarkable promises for future patient involvement. Their applications, such as personal forecasting or VR tools, are expected to enhance inter-stakeholder communication and realize more equal collaborations, promising a transformation for the future of digital patienthood. However, in discussions of current research practices, which we note vary significantly, the patient narrative differs. Patients are seen as a uniform, yet fallible group, with their roles in technical research limited to data contribution, with limited agency in shaping research agendas or model design. This reveals a gap between an envisioned 'empowered patienthood' with the emergence of medical digital twins and the constrained involvement in current practice. Building on Science and Technology Studies (STS) scholarship, this paper proposes a socio-technical perspective to make visible living institutional assumptions and values that contribute to this observed gap. As medical digital twins are nearing clinical adoption, addressing and overcoming this gap requires a reflexive stance from researchers across fields, to which this paper aims to contribute from the side of Social Science and Humanities (SSH).

Acknowledgements:
The authors would like to thank the Belgian Digital Twins for Personalised Healthcare (DT4PH) project for financial support to conduct this research and the EU's Horizon 2020 research and innovation programme for funding the different projects (Grant agreements: 101016503; 101016496; 101017578).

[1]DT4PH, In Silico World, SIMCor, SimCardioTest

REAL-TIME PERSONALIZED HEART MODELS FOR HARDWARE IN THE LOOP INTERACTION WITH DEVICES

Nelushi Adhikari (1), Benjamin Allen (1), Rory Fenwick-Rose (1), Visa Suomi (2), Pourash Patel (3), David P Nickerson (1), Mark L Trew (1), Weiwei Ai (1)

1. Auckland Bioengineering Institute, New Zealand; 2. MathWorks, Germany; 3. MathWorks, USA

Correspondence: weiwei.ai@auckland.ac.nz

1. Introduction

Biophysical computer models of cardiac electrophysiology (EP) are valuable for mechanistic analysis and procedure planning[1]. However, most are unsuitable for analyzing cardiovascular implantable electronic devices (CIED) in closed loop. There are few models encoding EP dynamics for interactive device studies. We present a real-time model with EP dynamics, disease states, such as AFib substrates, and drug effects of dose-dependent amiodarone[2]. The model interacts through hardware interfaces with physical CIED.

2. Materials and Methods

Robust hybrid-automata (HA) models capture cardiac EP and conduction dynamics[2]. They deploy to conduction networks[1] derived from CT (Fig 1). The EP verified models include nodal tissues, Purkinje networks and ventricular fiber rotation. They run in Simulink® and seamlessly deploy to a Speedgoat real-time machine for hardware-in-the-loop interaction with CIED. Published data are used to modify biophysical membrane EP models for AFib and amiodarone effects, and these drive HA parameterizations (Fig 2).

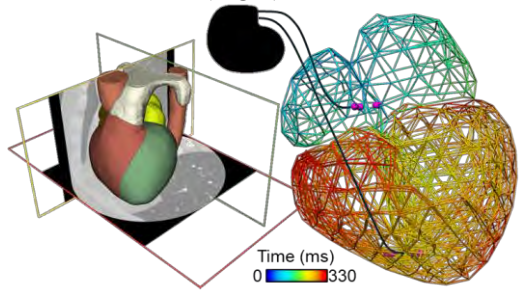


Figure 1: Human CT images are segmented and processed to generate model networks[1]. Normal heart activation sequence.

3. Results

Patient-derived network models run in predictable real-time. The Figure 1 model has 943 points and 2820 edges requiring 20.8±0.5s to simulate 30s of EP in normal and abnormal rhythms. Sinoatrial and atrio-ventricular EP exhibits autorhythmic properties, dynamic overdrive suppression and vagal activity. Myocardial EP has dynamics and conduction velocity restitution. Electrograms at atrial and ventricular probe locations are passed to pacemakers and they pace the model with a hardware/model latency of 5.5 ms. AFib and AFib+Amiodarone EP models (Fig 2) alter electrograms for testing pacemaker settings.

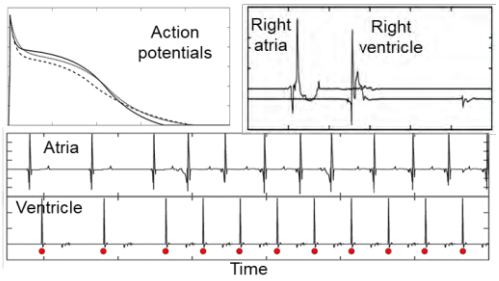


Figure 2: Action potential and electrograms. Lower trace: closed-loop CIED ventricular pacing (red dot).

4. Discussion and Conclusions

This new model provides unprecedented capabilities for generating healthy and disease state electrograms and responding in closed loop to CIED such as pacemakers. Clinical scenarios can be replayed and alternative timing parameters explored. The interactive paradigm can be deployed to assess interventions altering EP circuits, such as ablation. The combination of AFib, amiodarone and pacemakers present known clinical complication[3].

5. References

1. Rutherford SL et al., Circ Res;111:301 (2012).
2. Ai W et al., IEEE J Biomed Health Info; 24:1579 (2019).
3. Essebag V et al., Arch Int Med;167:1648 (2007).

Acknowledgements:

The Health Research Council of New Zealand (24/1308) and MathWorks Inc. provided financial support to this project.

CFD REDUCED-ORDER MODELS FOR INTERACTIVE ASSESSMENT OF CARDIAC HEMODYNAMICS FOR PEDIATRIC SURGERY

Benigno Marco Fanni (1), Emanuele Vignali (1), Emiliano Costa (2), Emanuele Di Meo (3), Marco Camponeschi (3), Vincenzo Carbone (4), Marco Evangelos Biancolini (3), Simona Celi (1)

1. BioCardioLab, Bioengineering Unit, Fondazione Monasterio, Italy; 2. ENGYS, Italy; 3. RBF Morph, Italy; 4. InSilicoTrials Technologies, Italy

1. Introduction

Computational modeling is increasingly used to support pre-operative planning in congenital heart disease, where surgical outcomes are strongly influenced by patient-specific anatomy and hemodynamics. Among palliative procedures, the modified Blalock–Taussig shunt (mBTS) plays a critical role in regulating pulmonary blood flow [1]. The present study introduces an integrated computational pipeline aimed at enabling rapid, reproducible, and interactive hemodynamic assessment of mBTS configurations in a patient-specific context.

2. Materials and Methods

A patient-specific model including the aortic, pulmonary circulation and the mBTS was segmented from medical imaging data.

High-quality volumetric meshes were generated and used for CFD simulations performed under physiologically consistent boundary conditions derived from literature and patient data. The proposed CFD and Radial Basis Function (RBF) morphing framework builds upon previous methodological developments [2,3] and was implemented using open-source tools to ensure reproducibility and computational efficiency. Parametric RBF-based geometry deformation was employed to generate multiple mBTS configurations, which were used to construct Reduced-Order Models (ROMs) based on Proper Orthogonal Decomposition (POD). The resulting ROMs were integrated into a Virtual Reality (VR) environment, enabling real-time interaction with anatomical variations and corresponding hemodynamic parameters within an immersive environment.

3. Results

The proposed framework is shown in Figure 1. The interactive VR-based platform was evaluated through exploratory sessions involving technicians and pediatric cardiac surgeons. Participants were asked to analyze different mBTS configurations and associated hemodynamic patterns using the proposed system. Structured questionnaires were administered to assess usability, clarity of hemodynamic information, and perceived clinical relevance. Feedback indicated that the immersive and interactive visualization facilitated understanding of flow distribution and supported intuitive comparison between alternative surgical configurations.

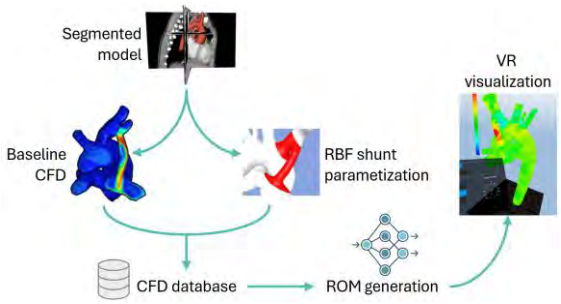


Figure 1: Scheme of the proposed framework, from medical imaging segmentation to VR visualization.

4. Discussion and Conclusions

The proposed framework demonstrates the potential of combining CFD model reduction with immersive visualization technologies to support rapid, patient-specific evaluation of mBTS hemodynamics. Such an approach may facilitate informed surgical decision-making within clinically viable timeframes.

5. References

1. Alsaghier et al, JTCVS;161(2):379-390 (2021).
2. Kardampiki et al, Electronics;11(3):1930 (2022).
3. Capellini et al., MEP; 91(1):68 (2020).

Acknowledgements:

This work was supported by the European Union–NextGenerationEU, through the Italian Ministry of University and Research (MUR) under the National Plan for Recovery and Resilience (PNRR) programme, Ecosystem of Innovation iNEST (Interconnected Nord-Est Innovation Ecosystem), project ECS00000043–CUP G93C22000610007.

DIGITAL TWINS AS A "THIRD PARTY" IN CARE: ETHICAL IMPLICATIONS FOR THE PATIENT–DOCTOR RELATIONSHIP

Noémie Dié (1) and Michèle Barbier (2)

1. Dassault Systèmes, France; 2. Inria, France

Introduction

AI-enabled "virtual twins" such as those developed in the national project Meditwin promise to transform medical care by creating dynamic, data-driven simulations of individual patients to guide prevention, diagnosis, and treatment. For patients, these systems offer the prospect of more tailored decisions, earlier warning of risks, and clearer explanations of proposed interventions, but they also change how it feels to be represented, to give consent, and to share responsibility for what happens in care (1).

As part of MediTwin, a round table discussion was organised with patient associations, developers and doctors to discuss ethical issues related to virtual twins in healthcare.
This presentation focuses on the **patient's perspective** on digital twins as a continuously updated "third party" in the consultation room.

Patients-doctors relationships

Patients might benefit from twin-based platforms that act as verified "wikis" before consultations, and triage tools where AI or nurses handle routine questions so that in-person time with their usual doctor can concentrate on what matters most. At the same time, patients are concerned about how constant digital access will affect their doctor's availability, the confidentiality of their data, and whether they can still rely on a familiar, accountable human interlocutor.

Risk of reducing patients to data

The workshop further highlighted patient worries that digital twins might reduce them to data profiles, exacerbate inequities in access, or enable commercial exploitation of their "black-gold" health data. Predictive uses are particularly ambivalent: patients may want early warnings and simulations of treatment options, but fear receiving non-actionable or alarming predictions without adequate human framing, timing, and support. Participants stress that patients should decide what they want to know, when, and through which channel—including the right not to be constantly immersed in "disease time"—and that cognitively vulnerable patients require special safeguards.

The family, the relatives

Finally, the discussion situates patients within a broader care ecosystem of relatives and multidisciplinary teams. Many patients come accompanied to serious consultations, record explanations, and rely on others to help interpret information. Digital twins must therefore be designed not only for one-to-one doctor–patient interactions but also to support collective understanding without replacing lived experience or undermining trust.
The session argues that, from the patient's viewpoint, ethically robust digital twins are those that enhance autonomy, equity, and relational care, rather than merely optimizing technical decision support (2).

This presentation will share the patient's perspective on digital twins in the context of the MediTwin project.

References

1. Bruynseels K, Santoni de Sio F, van den oven J. Digital Twins in Health Care: Ethical Implications of an Emerging Engineering Paradigm. *Frontiers in Genetics*. 2018.
2. Vallée A. Envisioning the Future of Personalized Medicine: Role and Realities of Digital Twins. *Journal of Medical Internet Research*. 2024

Acknowledgment

"*This work received funding from the MEDITWIN Bpifrance i-Demo project as part of the France 2030 program."*

MODEL-BASED DESIGN OF PHYSIOLOGICAL CLOSED-LOOP CONTROL SYSTEMS FOR MEDICAL DEVICES

Visa Suomi (1), Magnus Nord (2)

1. MathWorks, Germany; 2. MathWorks, France

1. Introduction

Physiological Closed-Loop Control (PCLC) systems enable automated medical therapies that adapt continuously to a patient's physiological state and are increasingly used in applications such as mechanical ventilation, dialysis, and drug infusion [1]. These systems require close integration between physiological models, control algorithms, and embedded device software. While the field has made substantial progress in physiological modeling, translating these models into executable, validated, and deployable closed-loop systems remains challenging [2].

This work presents a Model-Based Design workflow using Simulink that unifies physiological modeling, closed-loop simulation, real-time validation, and deployment-oriented code generation. The approach supports both exploratory research and medical device software development, while addressing regulatory expectations for safety-critical systems through traceable, model-driven implementation.

2. Materials and Methods

Closed-loop system models were constructed *in silico* by integrating physiological representations, medical device dynamics, and feedback control algorithms within a modular modeling framework in Simulink. Lumped-parameter physiological models were used to represent key patient responses relevant to ventilation, dialysis, and infusion therapy, allowing rapid adaptation to different clinical scenarios and patient variability.

To evaluate closed-loop behavior under realistic execution constraints, the models were deployed to Speedgoat rapid-prototyping hardware for real-time and hardware-in-the-loop (HIL) simulation. This enabled deterministic interaction between devices and virtual patients, supporting early assessment of robustness, timing behavior, and fault conditions with system-level testing.

The same models were used as the basis for automatic generation of embedded software, enabling a direct transition from validated simulation models to deployable code. This workflow supports development practices aligned with IEC 62304 standard by promoting traceability between requirements, models, tests, and generated code, and by reducing manual implementation steps that are common sources of error in safety-critical software.

3. Results

The unified workflow enabled rapid iteration of PCLC designs and consistent reuse of models across *in silico* simulation, real-time HIL testing, and embedded deployment. Real-time simulations demonstrated stable closed-loop performance across varying physiological conditions and disturbances. Model reuse across development stages improved consistency, reduced development effort, and enhanced transparency for testing, verification and validation activities.

4. Discussion and Conclusions

This work highlights the value of an integrated Model-Based Design approach for physiological closed-loop medical devices. By combining executable physiological models, real-time HIL simulation, and deployment-ready code generation within a single environment, Model-Based Design with Simulink supports both fast innovation and regulatory readiness. The ability to align model development with IEC 62304-oriented workflows positions this approach as a practical and scalable foundation for translating PCLC research into safe, robust, and effective medical devices.

5. References

1. Khodaei, MJ, et al. "Physiological closed-loop control (PCLC) systems: Review of a modern frontier in automation." *IEEE Access* 8 (2020): 23965-24005.
2. Hahn, JO, and Omer TI. "Physiological closed-loop control in critical care: opportunities for innovations." Progress in Biomedical Engineering 4.3 (2022): 033001.

EMBEDDING ETHICS IN INSILICO HEALTH: AN EMPIRICAL ETHICS APPROACH TO VIRTUAL HUMAN TWIN DEVELOPMENT

Kiara Scheunpflug (1)

1. Vrije Universiteit Amsterdam, The Netherlands; 2.KTH Royal Institute of Technology, Sweden

1. Introduction

Virtual Human Twins (VHTs), within the broader InSilico Medicine, are emerging as transformative tools for biomedical research, precision medicine, and clinical trial innovation. While technical development is advancing rapidly, the social, ethical and legal dimensions, how responsibility is allocated, how data governance is enacted, and how innovation aligns with societal and regulatory expectations, remain underexplored (Elhadj et al., 2023, Viceconti et al., 2023).Existing frameworks, including Ethical, Legal, and Social Implications (ELSI), Responsible Research and Innovation (RRI), and Technology Assessment (TA), provide normative guidance, but their practical integration within VHT development and regulatory practice is not well understood. This project examines these gaps, focusing on how interdisciplinary research teams navigate the complex interplay between innovation, ethics, and governance.

2. Materials and Methods

This research employs an empirical ethics approach to investigate how ethical and regulatory considerations are interpreted, negotiated, and operationalized in InSilico research environments. Data are drawn from a combination of regulatory mapping, document analysis, semi-structured interviews with key stakeholders, and ethnographic observations in VHT research labs (STIR method) (Fisher & Schuurbiers,2013). This multi-method design allows for an in-depth understanding of how actors engage with European governance frameworks, data standards and own practices while simultaneously interpreting and applying ethical principles, navigating moral responsibilities, and integrating normative considerations into everyday VHT research practice.

3. Results

Preliminary findings are expected to shed light on how researchers and developers navigate ethical and regulatory challenges.

4. Discussion and Conclusions

By empirically examining the intersection of ethics, regulation, and technological development, this project aims to provide actionable insights to support responsible innovation in VHTs. It emphasizes the need for governance structures that consider both societal values and practical research realities and seeks to inform the development of approaches to VHT research and deployment that are ethically sound, socially responsive, and aligned with regulatory frameworks.

5. References

Elhadj, E., Van Horenbeeck, Z., Lievevrouw, E., Geris, L., & Van Hoyweghen, I. (2023). In Silico World WP5 Stakeholder Engagement-Responsible Research and Innovation Workshop Report.

Fisher, E., & Schuurbiers, D. (2013). Socio-technical integration research: Collaborative inquiry at the midstream of research and development. In Early engagement and new technologies: Opening up the laboratory (pp. 97-110). Dordrecht: Springer Netherlands.

Viceconti, M., De Vos, M., Mellone, S., & Geris, L. (2023). Position paper from the digital twins in healthcare to the virtual human twin: a moon-shot project for digital health research. IEEE Journal of Biomedical and Health Informatics, 28(1), 491-501.

Acknowledgements:

This PhD research is conducted within the InSilicoHealth Network, funded by the Marie Skłodowska-Curie Actions (MSCA) under Horizon Europe (HORIZON-MSCA-2023-DN-01).

The author would like to thank the European Commission (Grant no: 101169278) for providing financial support to this project.

UNSUPERVISED FAIRNESS ASSESSMENT TO ADDRESS INTERSECTIONALITY AND PROXY FEATURES

Emma Beauxis-Aussalet
Vrije Universiteit Amsterdam, The Netherlands

1. Introduction

If AI errors occur more often for specific populations,it creates bias and discrimination (e.g., against an ethnicity, gender, or age) [1]. The impacted populations can be unknown beforehand: their characteristic sensitive features may not be available (e.g., ethnicity, religion, sexual orientation), and they may be defined by several features (e.g., intersectionality) or by proxy features that are not considered as sensitive [2]. Unsupervised methods can explore the combinations of all available features to identify clusters for which errors are significantly higher, i.e., discriminated populations [3,4]. Our work develops such unsupervised methodology applied to medical data. We provide a reusable model-agnostic tool (python package) including data visualization and feature engineering methods. The tool integrates state-of-the-art clustering methods (e.g., density-based), distance metrics (e.g., Gower's), hyperparameter tuning, feature weighing (e.g., giving more importance to specific sensitive features). The tool currently addresses binary classification and regression problems, and can assess error types independently (e.g., identifying FN in all data points classified as positive). Our future work will extend the tool to multiclass and ranking problems (e.g., for recommender systems).

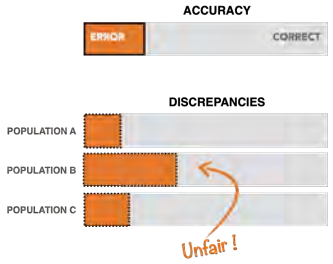


Figure 1: Illustration of fairness problem: a population impacted by higher error magnitudes than other populations.

2. Materials and Methods

Existing methods [3,4] use hierarchical clustering and bisecting K-means. Our tool introduces density-based clustering (e.g., HDBSCAN, Mean-Shift) with or without iterative hierarchical clustering (e.g., bisecting approaches). For the latter, our tool includes data rescaling and hyperparameter tuning at each iteration. For further feature engineering, our tool can compare clustering results obtained with specific sets of features, e.g., to include potential proxy features in the fairness assessment. Notably, the feature engineering can also include XAI feature importance (e.g., SHAP values, Figure 2).

The tool provides cluster quality metrics that assess (1) the general cluster separability (i.e., silhouette score), (2) the differences in error magnitudes among clusters (i.e., level of bias), and (3) the specificity of sensitive feature values for each cluster (i.e., identifying which clusters represent specific social groups).

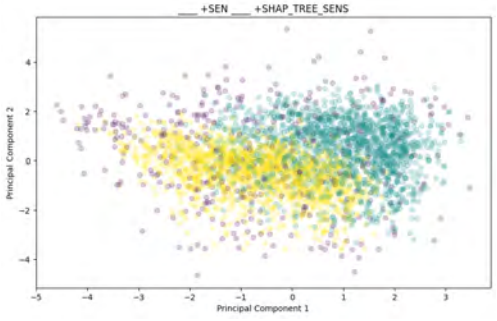


Figure 2: Results for UCI diabetes dataset, using sensitive features and their SHAP values.

4. Discussion and Conclusions

Initial results are promising, and the tool is largely applicable to a variety of health applications. For computer vision or text analysis, clustering can be done at the embedding level.

5. References

1. Obermeyer et al. "Dissecting racial bias in an algorithm used to manage the health of populations." Science (2019).
2. Gupta et al. "Proxy fairness." arXiv preprint arXiv:1806.11212 (2018).
3. Nasiriani et al. "Hierarchical clustering for discrimination discovery: A top-down approach." IEEE Conference on Artificial Intelligence & Knowledge Engineering (2019).
4. Misztal-Radecka et al. "Bias-Aware Hierarchical Clustering for detecting the discriminated groups of users in recommendation systems." Information Processing & Management (2021).

DIGITAL TWINS IN HEALTHCARE. NORMS, EPISTEMOLOGY AND ETHICS IN EUROPE

Martina Baltuzzi (1)

1. University of Torino, Italy; University of Bologna, Italy; KU Leuven, Belgium

1. Introduction

Digital Twins (DTs) – virtual models that mirror physical entities through bidirectional data exchange – are increasingly recognised as a transformative tool for healthcare, with the potential to enhance personalized and precision medicine. Originating in industrial and aerospace applications, DTs have recently entered the medical domain, exemplified by the European Commission's Virtual Human Twins Initiative (2023). While DTs promise improved diagnostic accuracy and real-time monitoring, their adoption in such a sensitive sector raises significant normative questions. This work investigates the implementation of DTs in European healthcare from an interdisciplinary perspective, integrating legal, epistemological, and ethical analysis.

2. Materials and Methods

The research adopts an interdisciplinary methodology, combining legal analysis with epistemological and ethical reasoning. It begins with a systematic review of EU legal sources (GDPR, Data Governance Act, AI Act, Regulation 2021/694), policy documents, and interdisciplinary literature on DTs. The analysis is enriched through engagement with computer scientists, engineers, and external stakeholders, ensuring that findings remain both legally sound and practically applicable to real-world healthcare settings.

3. Results

Three major areas of criticality emerge. Legal challenges concern liability in medical malpractice, informed consent, and data governance; current EU law (notably the GDPR) lacks DT-specific provisions, and fragmented national approaches risk inefficient regulation or AI underuse in medicine. A further concern is algorithmic discrimination, as predictions based on historical data may reinforce existing inequalities (the "fossilization problem"). Epistemological implications relate to the limits of virtually modelling complex biological entities and the risk that algorithmic predictions may not only anticipate but actively shape future outcomes (unfalsifiability, preemptive intervention and self-fulfilling prophecy problems). Ethical considerations concern algorithmic bias in training data and the impact of DTs on patient autonomy, which may shift toward either paternalistic or empowering models of care.

4. Discussion and Conclusions

The integration of DTs into European healthcare holds significant promise for personalized medicine but requires a coordinated normative response. Current EU legislation does not adequately address DT-specific risks regarding liability, discrimination, and data governance. Epistemological and ethical concerns, particularly regarding predictive reliability and patient autonomy, cannot be resolved through legal regulation alone. The research argues for a harmonized, interdisciplinary regulatory framework that balances technological innovation with human-centric values, ensuring DTs support, rather than undermine, patient trust and autonomy in clinical decision-making.

5. References

1. Grieves, M., Origins of the Digital Twin Concept, Florida Institute of Technology 8, 3-20, (2016).
2. Matsumi, H., Solove, D. J., The Prediction Society: AI and the Problems of Forecasting the Future. *GWU Legal Studies,* (2024).
3. Pagallo, U., *Il dovere alla salute. Sul rischio di sottoutilizzo dell'intelligenza artificiale in ambito sanitario*, Mimesis, Milano, (2022).

Acknowledgements:

This research was supported by a PhD scholarship awarded to Martina Baltuzzi by the Universities of Torino and Bologna.

REGIONAL ASSESSMENT OF BRAIN MECHANICAL PROPERTIES DURING AGEING

Sahar Zolghadr (1), Nina Reiter (1), Jan Hinrichsen (1), Lucas Hoffmann (2), Stefan Rampp (3), Lars Bräuer (4), Friedrich Paulsen (4), Silvia Budday (1)

1. Institute of Continuum Mechanics and Biomechanics, Friedrich-Alexander-University Erlangen-Nuremberg, Germany; 2. Department of Neuropathology, Universitätsklinikum Erlangen, Friedrich-Alexander-University Erlangen-Nuremberg, Germany; 3.Department of Neuroradiology, Universitätsklinikum Erlangen, Friedrich-Alexander-University Erlangen-Nuremberg, Germany; 4. Institute of Functional and Clinical Anatomy, Friedrich-Alexander-University Erlangen-Nuremberg, Germany.

Correspondence: Sahar Zolghadr, Institute of Continuum Mechanics and Biomechanics, Friedrich-Alexander-University Erlangen-Nuremberg, Germany, Email: Sahar.zolghadr@fau.de

1. Introduction

Aging is an intricate process in the brain that affects tissue at the cellular to organ levels, ultimately resulting in brain atrophy. Neurodegenerative diseases like Alzheimer's disease (AD) and Parkinson's disease change both the mechanical properties and structural morphology of brain tissue [1]. In our work, we assess whether the mechanical properties of brain tissue, including the shear modulus and nonlinearity parameter, change during aging.

2. Materials and Methods

Eighteen human brains from body donors were previously obtained and mechanically tested for different brain regions under three different modes: compression, tension, and torsion using a rheometer. Some of the donors had suffered from neurological diseases like Alzheimer's. To calculate the shear modulus and nonlinearity parameter of the modified one-term Ogden model,

$$\Psi_{iso} = \frac{2\mu}{\alpha^2}\left(\bar{\lambda}_1^{\alpha} + \bar{\lambda}_2^{\alpha} + \bar{\lambda}_3^{\alpha}\right) \qquad (1)$$

Where $\bar{\lambda}_a$ are isochoric principal stretches, an inverse parameter identification framework was employed [1], in which material parameters were iteratively adjusted to match the experimental results. This approach was implemented in Python, coupled with the finite element simulation library of deal.ii.

3. Results

In this study, the tested brains were divided into normal aging and diseased aging groups. The estimated parameters α and μ exhibited substantial region-dependent properties but no clear trends with age. Fig. 1 reports the average values of μ and α as a function of age. The diseased group has been divided into two groups based on their specific pathologies.

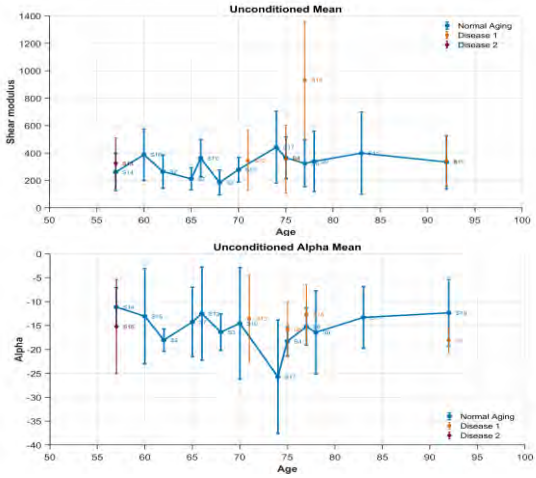


Figure 1. Brain tissue shear modulus and non-linearity parameter as a function of age.

4. Discussion and Conclusions

Our results suggest that the nonlinear large-strain mechanical properties of human brain tissue do not change as a function of chronological age. Rather, other factors, such as lifestyle and local changes in the tissue's microstructure, may affect the measured properties.

5. References

1. Olsson ch et al.2025. "Effects of Parkinson's disease on mechanical and microstructural properties of the brain." NeuroImage: Clinical 48.
2. Hinrichsen J et al. 2023. "Inverse identification of region-specific hyperelastic material parameters for human brain tissue." Biomechanics and Modeling in Mechanobiology 22: 1729–1749

Acknowledgements:
This project has received funding from MSCA (Grant No. 101169128). We thank our research group for their valuable support.

"INSILICOHEALTH MSCA JOINT DOCTORAL NETWORK: TRAINING VIRTUAL TWIN PROFESSIONALS TO SUPPORT HEALTHY AGEING"

Erica Beaucage-Gauvreau (1), Rocío Castro Viñuelas (1), Laura Vangeel (1), Ilse Jonkers (1,2)

1. iSi Health, KU Leuven, Belgium; 2. Department of Movement Sciences, KU Leuven, Belgium

1. Introduction

Population ageing is one of the major societal challenges of the coming decades, increasing the prevalence of chronic diseases and multimorbidity while placing growing pressure on healthcare systems. Virtual Human Twins offer promising approaches for understanding age-related physiological changes, predicting disease progression, and supporting personalised prevention and treatment. However, advancing these technologies requires researchers who can integrate expertise from engineering, biomedical sciences, clinical practice, and social sciences.

The InSilicoHealth Marie Skłodowska-Curie Joint Doctoral Network addresses this need by training a new generation of interdisciplinary researchers capable of developing and implementing virtual twin technologies to support healthy ageing.

2. Materials and Methods

InSilicoHealth is an international doctoral network funded under the Marie Skłodowska-Curie Actions. The programme brings together European universities, research institutes, industrial partners, and associated organisations to provide an integrated research and transferable skills training.

The research programme focuses on developing innovative in silico health solutions targeting age-related functional decline in three interconnected physiological systems: the brain, the cardiovascular system, and the musculoskeletal system, while also integrating the ethical, legal societal implications (ELSI).

The training programme combines scientific research, network-wide events, secondments in academia and industry, and activities designed to strengthen communication and collaboration across disciplines.

3. Results

The project has established a collaborative European network involving beneficiary universities and associated partners from academia, healthcare, and industry. The doctoral projects collectively address key challenges in developing clinically relevant virtual twin technologies while fostering knowledge exchange across disciplines.

Beyond scientific research, the programme delivers structured training in digital health innovation, ethics, responsible research, and stakeholder engagement. This integrated approach prepares doctoral candidates to translate computational models into future healthcare applications.

4. Discussion and Conclusions

InSilicoHealth represents an innovative model for doctoral education in Virtual Human Twin research by combining excellence in computational modelling with interdisciplinary collaboration and clinical relevance. The programme contributes to building the next generation of scientists capable of advancing virtual twin technologies for healthy ageing and accelerating their translation into clinical practice.

Through its collaborative European network, interdisciplinary curriculum, and strong engagement with industrial and healthcare partners, InSilicoHealth is expected to strengthen research capacity in in silico medicine and support the development of innovative digital health solutions addressing the challenges of an ageing population.

Acknowledgements:

Funded by the European Union (Grant Agreement No. 101169127). Views and opinions expressed are however those of the author(s) only and do not necessarily reflect those of the European Union. Neither the European Union nor the granting authority can be held responsible for them.

PREDICTING ADVERSE EVENTS AFTER FROZEN ELEPHANT TRUNK REPAIR USING PATIENT-SPECIFIC FLUID-STRUCTURE INTERACTION SIMULATIONS

Yu Zhu (1), Kaihong Wang (1), Amir Awwad (2) Aung Ye Oo (2) Mark Field (3) Monika Radike (3) Ulrich Rosendahl (4) Saeed Mirsadraee (4) Xiao Yun Xu (1)

1. Imperial College London, UK; 2. Barts Health NHS Trust, UK; 3. Liverpool Heart and Chest Hospital, UK; 4. Royal Brompton and Harefield Hospitals, UK

1. Introduction

Predicting adverse events following frozen elephant trunk (FET) repair for type A aortic dissection (TAAD) remains challenging. This study aimed to identify biomechanical predictors of post-operative complications based on patient-specific fluid–structure interaction (FSI) simulations. In addition, a combined haemodynamic–structural index (HSI) was evaluated to examine whether integration of flow-derived and wall-mechanical metrics improves predictive performance compared to individual parameters.

2. Materials and Methods

Thirty-nine TAAD patients undergoing FET repair were included for FSI simulations, of whom 15 developed adverse outcomes. Post-operative geometries were reconstructed from baseline CTA imaging. The detailed model setup is shown in Figure 1.

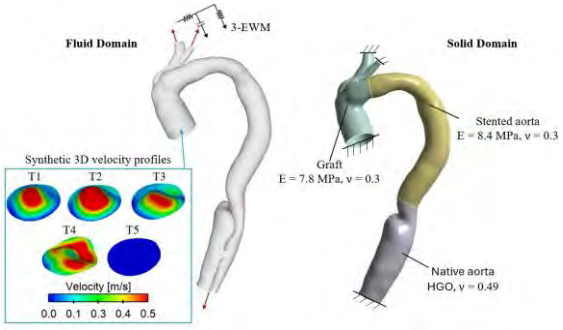


Figure 1: Schematic of FSI simulation setup. The synthetic velocity profiles were generated based on patient's heart rate and stroke volume [1].

Haemodynamic and biomechanical metrics were extracted from graft, stented-aorta, and native-aorta regions. Initial variable screening was based on Mann–Whitney U test, followed by forward likelihood-ratio multivariable logistic regression after z-standardisation. Receiver operating characteristic (ROC) analysis was used to predict probabilities, and DeLong testing was performed to compare ROC curves.

3. Results

Multivariable logistic regression retained spatial-mean time-averaged wall shear stress (TAWSS) within the stented segment (OR 4.882, p = 0.006) and peak systolic wall stress (WS) in the native aorta (OR 3.102, p = 0.019). ROC analysis showed moderate discrimination for TAWSS alone (AUC = 0.701) and weaker performance for WS alone (AUC = 0.678). HSI was defined using the multivariable logistic regression coefficients ($HSI = 1.586 * Z(\overline{TAWSS}_{SG}) + 1.132 * Z(WS^{max}_{Aorta})$), which achieved higher discrimination (AUC = 0.815), although differences compared with single predictors were not statistically significant by DeLong testing.

4. Discussion and Conclusions

FSI simulations identified high spatial-mean TAWSS within the stented segment as the primary haemodynamic marker associated with adverse outcomes after FET repair for TAAD, while peak systolic WS in the native aorta provided complementary structural information when integrated into a multivariable model. The combined HSI showed improved discrimination compared with single predictors, although DeLong testing did not demonstrate statistically significant differences between ROC curves, likely reflecting limited sample size. These findings suggest that adverse events after FET are influenced by coupled flow and structural mechanics, supporting the use of integrated biomechanical metrics for patient-specific risk assessment and motivating validation in larger cohorts.

5. References

1. Wang K, et al., Comput. Biol. Med. 191, p.110158 (2025).

Acknowledgements:

Yu Zhu would like to thank the British Heart Foundation (FS/IPBSRF/23/27098) for providing financial support to this project.

ADVANCING ABDOMINAL AORTIC ANEURYSM RISK ASSESSMENT THROUGH ANEURYSM MORPHOLOGICAL CHARACTERIZATION

Maria Lavinia Alfarano (1, 2), Eduardo Soudah (1, 2), Miquel Aguirre (1, 2)

1. Universitat Politècnica de Catalunya (UPC), Barcelona, Spain; 2. CIMNE-International Center for Numerical Methods in Engineering, Barcelona, Spain

1. Introduction

Abdominal aortic aneurysm (AAA) rupture causes thousands of deaths worldwide annually, with a higher rupture rate in women [1]. Therefore, beyond the usually adopted maximum diameter criterion, more reliable methods to estimate AAA rupture risk are needed [1]. Towards this ultimate goal, this work aims to develop a user-friendly, fully automatic algorithm, which, starting from the aneurysmal sac (AS) isolation, extracts relevant morphological features to improve aneurysm characterization.

2. Materials and Methods

From the 3D surface of the infrarenal abdominal aorta affected by the aneurysm, the vessel centreline is obtained. The aorta is sliced by planes orthogonal to the centreline at equally spaced intervals. For each slice, the diameter is computed as the maximum point-to-point distance. Then, the corresponding radii are represented as parallel segments in the 2D radius-position plane, where the vertical coordinate represents the radius length and the horizontal coordinate represents the position (i) along the centreline, i.e., the first position is the closest to the renal arteries and the last position is the closest to the iliac arteries (see figure 1). The interpolation of the segments endpoints yields a function, $R(x) \in C^2$, describing radius variation along the centreline. The AS is identified as follows:

$$AS = \{i : x_{Left} \leq I < x_{Rigth}\},$$

where, x_{Left} is the location of the local minimum of $R(x)$ that preceds the location of the local maximum of $R'(x)$ before the peak of $R(x)$ and x_{Rigth} is the location of the local minimum of $R(x)$ after the location of the local negative minimum of $R'(x)$ beyond the peak.

3. Results

Figure 1 illustrates the AS detection in a representative case.

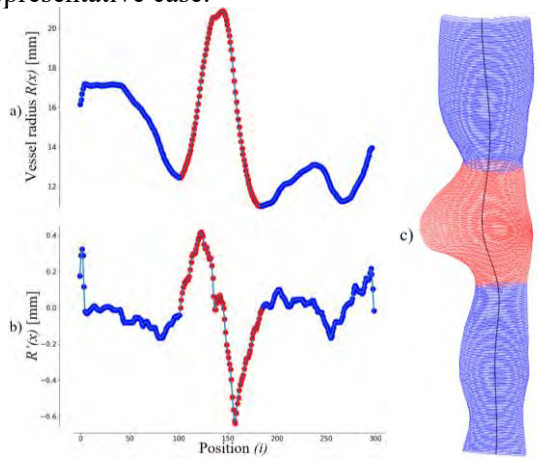


Figure 1: a) Variation of the aorta radius $R(x)$ along the vessel's positions; b) Radius derivative $R'(x)$; c) Sliced surface of the representative case, and the centreline. AS is displayed in red, the remaining aorta in blue.

4. Discussion and Conclusions

The results show that the AS isolation technique implemented in the algorithm successfully detects the aneurysm from the proximal to the distal neck [2]. Once fully validated, the method will enable the automated extraction of relevant morphological characteristics [2, 3]. These features could then be incorporated into machine learning models along with clinical variables and biomechanical properties, with the aim of improving AAA outcome prediction [1].

5. References

1. Kerr et al. Biol Sex Differ; 16, 96 (2025).
2. Soudah et al. Comput Math Methods Med (2013).
3. Brummer et al. IEEE Trans Med Imaging; 40, 297–309 (2021).

IS THE THIRD BRANCH OPTIMAL? A PATIENT-SPECIFIC FSI ANALYSIS OF TRIPLE-BRANCHED TEVAR

Binghuan Li[1], Yu Zhu[1,2], Simona Sica[3], Mario D'Oria[4], Giovanni Tinelli[3], Sandro Lepidi[4], Xiao Yun Xu[1]

1. Department of Chemical Engineering, Imperial College London, UK;

2. National Heart and Lung Institute, Imperial College London, UK;

3. Fondazione Policlinico Universitario Agostino Gemelli IRCCS, Rome, Italy;

4. Department of Medical Surgical and Health Sciences, University of Trieste, Italy.

1. Introduction

Triple-branched endografts allow complete supra-aortic revascularisation during thoracic endovascular aortic repair (TEVAR), avoiding surgical debranching. However, optimal branch configuration remains unclear due to complex haemodynamic effects and potential complications such as flow imbalance or thrombus formation. Previous computational studies demonstrate that branch orientation and design significantly influence cervical perfusion, shear stress, and platelet activation [1-3]. This work evaluates whether inclusion of a third branch is haemodynamically favourable using patient-specific fluid-structure interaction (FSI).

2. Materials and Methods

A patient-specific triple-branched TEVAR geometry was reconstructed, including antegrade IA and LCCA branches and a retrograde LSCA branch. Blood was modelled as an incompressible, non-Newtonian fluid and the native aorta as anisotropic hyperelastic tissue within a strongly coupled FSI framework [4]. In addition to the baseline triple-branch case, three virtual configurations were generated: (1) shortened LSCA branch, (2) fenestrated LSCA branch, and (3) LSCA-LCCA bypass (Figure 1).

3. Results

The percentage outlet flow split across four cases are reported in Table 1. Shortening the retrograde LSCA branch (Case 1) modestly redistributed flow from the descending aorta (DA) toward supra-aortic vessels, increasing IA, LCCA and LSCA perfusion. The fenestrated configuration (Case 2) further shifted flow away from DA with the largest increase in LSCA perfusion. In contrast, the LSCA-LCCA bypass (Case 3) slightly reduced IA perfusion while markedly increasing LCCA flow, indicating strong sensitivity of cervical perfusion to branch design and revascularisation strategy.

	DA	IA	LCCA	LSCA
Base	70.0	13.8	6.3	10.2
1	65.7↓	15.8↑	7.0 ↑	11.4↑
2	58.2↓	18.1↑	7.1 ↑	15.9↑
3	71.2↑	11.0↓	17.8↑	

Table 1: Outlet flow split (%) across four cases.

On the other hand, LSCA protrusion length is associated with increased flow disturbance, as reflected by the extent of low time-averaged wall shear stress (TAWSS < 0.4 Pa) regions (Figure. 1). The base configuration exhibited the largest low-TAWSS area (118.5 cm^2), compared to 105.2 cm^2, 99.3 cm^2 and 89.8 cm^2 in Case 1, 2, 3, respectively. Spatially, extended low-shear regions were localised near the LSCA branch, particularly at the site of graft kinking.



Figure 1: Iso-volume plots showing regions of low TAWSS (<0.4 Pa) of four configurations.

4. Discussion and Conclusions

The third branch supports preservation of physiological perfusion but introduces local haemodynamic challenges depending on configuration. Results suggest that shortening the retrograde LSCA branch improved cervical flow perfusion while reducing low-TAWSS regions, suggesting a potential reduction in thrombotic risk compared with the base configuration. However, alternative strategies produced greater redistribution of global flow, highlighting a trade-off between maintaining balanced perfusion and minimising adverse local haemodynamics.

5. References

1. van Bakel et al., Eur J Cardiothorac Surg (2018).
2. Tricarico et al., Eur J Vasc Endovasc Surg (2020).
3. Chiu et al., Informatics in Medicine Unlocked (2018).
4. Li et al., J Biomechanics (2026).

CORRELATING PATIENT-SPECIFIC RUPTURE RISK WITH NON-INVASIVE DESCRIPTORS IN ASCENDING AORTIC ANEURYSMS

João Moutinho Gonçalves (1), Lauranne Maes (1), Nele Famaey (1),(2)

1. KU Leuven, Belgium; 2. FIBEr KU Leuven, Belgium

1. Introduction

Ascending thoracic aortic aneurysms (ATAAs) are a vascular condition with mortality rates exceeding 90% after rupture. They are defined by a permanent dilation of the ascending aorta to at least 1.5 times its normal diameter. Current guidelines for prophylactic surgery rely on maximum diameter thresholds, although this criterion is an imperfect predictor of rupture risk. Previous studies have proposed biomechanics-based indices as alternative predictors of rupture risk [1]. In this work, a patient-specific numerical framework is developed to compute a biomechanical rupture index and correlate it with non-invasive imaging-derived descriptors in a retrospective patient cohort.

2. Materials and Methods

As part of an ongoing study conducted at UZ/KU Leuven, ATAA patients underwent 4D CT imaging prior to surgical intervention, during which aneurysmal tissue samples were resected. CT scans were segmented and the excised tissues mechanically tested at FIBEr KU Leuven to determine patient-specific material properties and tissue strength. Details of the experimental data acquisition are described in [1].

Table 1: Values of the Spearman coefficient, ρ, and its p-value for the correlations between the non-invasive descriptors and the BRR in the circumferential direction (n=15)

	DCA	*DCV*	*K*	*T*	*D*
ρ	-0.521	-0.693	-0.046	0.525	0.25
p	**0.046**	**0.004**	0.869	**0.044**	0.369

A finite-difference solid mechanics model was developed to compute the in vivo stress state of the ATAA. Patient-specific geometries were reconstructed from spline-fitted centerlines and aneurysm shapes, while tissue behavior was described as a mixture of Neo-Hookean elastin and disperse collagen fibers ([2]) with constituent specific pre-stretches. Loading was represented by patient-specific diastolic and systolic pressures. Deformation and stress fields at systole were computed thereafter.

To assess rupture risk, a biomechanical rupture risk index (*BRR*) was defined as the ratio between the peak stress at the inner wall and tissue strength in each direction (circumferential and axial). Spearman's rank correlation was computed between *BRR* values and non-invasive descriptors derived from imaging data, including area distensibility (*DCA*), volume distensibility (*DCV*), maximum centreline curvature (*K*) and torsion (*T*), and the aneurysmal diameter at systole (*D*).

3. Results

Provisional results (Table 1.) indicate an improved correlation between *BRR* and *DCV* for failure in the circumferential direction compared to the previous study [1] (from p=0.01 to p=0.004) in which geometry was assumed as an axisymmetric cylinder for all patients. In contrast, the correlation significance in the axial direction weakened (from p=0.003 to p=0.11). Torsion showed a very modest but statistically significant correlation with *BRR* (p=0.044).

4. Discussion and Conclusions

By using patient-specific geometry, this study confirms the findings of [1] that volumetric distensibility may be a relevant non-invasive indicator of rupture risk in ATAAs. In addition, torsion of the aortic centreline might also provide information on rupture risk, although further work is still required to confirm such finding.

5. References

1. Vander Linden, Klaas, et al. JTCVS open 16 (2023): 66-83.
2. Gasser, T. Christian, et al. Journal of the royal society interface 3.6 (2006): 15-35.

Acknowledgements:

This work has received funding from the Horizon Europe programme (Marie Curie Grant Agreement No. 101169278).

CAN IN SILICO GROWTH AND REMODELLING MODELS PREDICT ATAA EVOLUTION?

Dario Tarantino (1), Salvatore Pasta (1,2), Benedetta Fantaci (3)

1. Department of Engineering, Università degli Studi di Palermo, Italy; 2. Department of Research, IRCCS ISMETT, Italy; 3. Aragon Institute of Research Engineering, Universidad de Zaragoza, Spain.

1. Introduction

Ascending thoracic aortic aneurysms (ATAAs) are termed "silent killers" due to their asymptomatic nature and high pre-hospital mortality rate. The pathology is driven by a complex interplay of altered hemodynamics and extracellular matrix disruption, leading to a progressive weakening of the aortic wall. Currently, clinical intervention relies on a maximal diameter threshold (e.g., $\geq$ 5.5 cm) [1]; however, nearly 40% of dissections occur below this limit. Therefore, there is an urgent need for personalized strategies. In this work, we propose an in silico growth and remodelling (G&R) framework for ATAA prediction.

2. Materials and Methods

A patient-specific finite-element (FE) model of an ATAA was reconstructed from CT imaging, with the vascular wall characterized by an anisotropic hyperelastic HGO constitutive law. To simulate physiological constraints, inlet and outlets of the aorta were restricted to rotational degrees of freedom. A two-step multiphysics approach was employed: first, a CFD simulation was performed to map the pressure profile across the aorta; this profile then served as the mechanical load for the structural G&R simulation. G&R was modelled through a multiplicative decomposition of the deformation gradient, $\mathbf{F} = \mathbf{F}_e\mathbf{F}_g$, using a local coordinate system to enforce anisotropic growth directions [2]. Remodelling was localized to regions of peak intraluminal pressure, where the tangential components of $\mathbf{F}_g$ increased while the radial component decreased, effectively capturing the characteristic bulging and wall thinning of the pathology. The temporal evolution of the stretch ratio $\vartheta(t)$ was modelled with the following relaxation law:

$$\partial\vartheta/\partial t = k(\vartheta_{max} - \vartheta(t)),$$

where ϑ_{max} and k were calibrated to replicate the patient-specific longitudinal evolution of the aneurysm diameter.

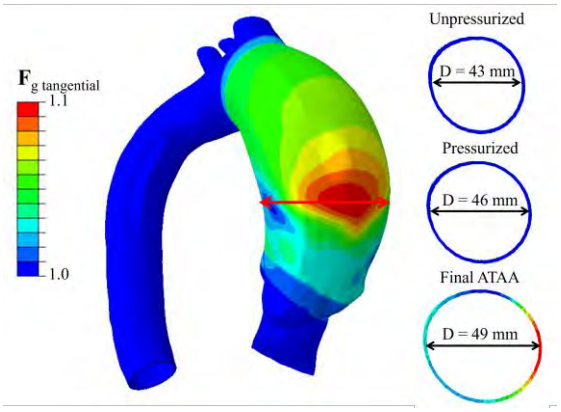


Figure 1. Contour plot of the tangential components of **F**g and corresponding cross-sections at the site of maximum remodelling.

3. Results

The simulation successfully replicated the morphological evolution of the patient-specific ATAA (Figure 1). Peak remodelling values were localized to the mid-ascending aorta, coinciding with the regions of maximum intraluminal pressure. Cross-sectional analysis at the site of maximum remodelling demonstrated a progressive expansion of the aortic diameter: the pressurized baseline diameter of 46 mm evolved to a final pathological state of 49 mm, matching the 3 mm increase observed in the patient.

4. Discussion and Conclusions

This study demonstrates that a pressure-mediated G&R framework can effectively reproduce patient-specific ATAA progression. This approach represents a step toward personalized risk assessment, offering a quantitative basis for clinical decision-making.

5. References

1. Isselbacher EM. Circulation; 111:816–28 (2005).
2. Fantaci, B et al.,. Comp Bio Med, 180, 108976 (2024).

Acknowledgements:

This work was supported by the ASSOCIATE (2022L7KK7L) research project grant by "Progetti di Ricerca di Rilevante Interesse Nazionale" (PRIN) of the "Ministero dell'Università e della Ricerca".

MODELING THE ROLE OF OBESITY IN KIDNEY DISEASE TREATMENT WITH GLP-1 AGONIST

Jordan H. Mallette(1), Robert L. Hester(1), John S. Clemmer(1)

1. Department of Physiology, University of Mississippi Medical Center, Jackson, MS, USA

1. Introduction

Chronic kidney disease (CKD), or a persistent reduction in eGFR (<60 mL/min/1.73m^2), remains a leading cause of morbidity and mortality [1]. Glucagon-like peptide-1 receptor agonists (GLP1RA) have shown to improve cardiometabolic and renal outcomes [2], but the mechanisms remain unclear. Long-term effects of GLP1RA on renal hemodynamics during CKD have not been well-characterized.

2. Materials and Methods

All simulations were performed using HumMod, a large mathematical model of human physiology [3]. Quantitative effects of semaglutide on appetite, insulin secretion, renal sodium handling, and afferent renal tone were incorporated into HumMod based off of animal data. The model was validated using GAMM models of clinical EHR data from patients with obesity and CKD treated with semaglutide [4]. Obese CKD was modelled by increasing fat mass (55 kg) and reducing renal mass (75%), which was associated with increased sympathetic outflow, blood pressure (BP), and cardiac output. 12-month responses to GLP1RA were determined under the following conditions:

1) Control: CKD alone
2) GLP1RA: CKD + GLP1RA
3) GLP1RA (Renal): CKD + GLP1RA direct renal effects (w/o weight loss)
4) GLP1RA (Diet): CKD + GLP1RA direct dietary effects (w/o weight loss)

3. Results

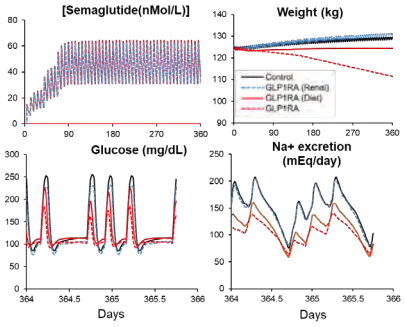


Figure 1: Simulated changes in drug concentration, weight, glucose, and sodium excretion (NaE).

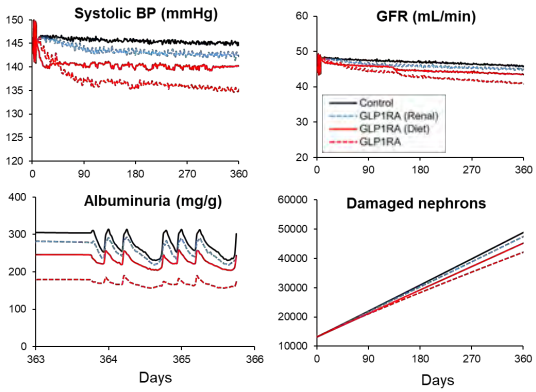


Figure 2: GLP1RA effects on BP, GFR, albuminuria, and damaged nephrons during CKD.

4. Discussion and Conclusions

Clinical trials suggest GLP1RA may have renal benefit in CKD patients [2,5]. Our model of CKD at baseline was associated with decreased eGFR, elevated albuminuria, hypertension, and CKD progression (damaged nephrons) that were improved with GLP1RA (Figures 1-2). However, our model showed that direct actions of GLP1RA on the kidney were minor in comparison with the benefit from weight loss, which played a key role in reducing glomerular pressure and albuminuria, although dietary effects of GLP1RA (reduced salt and carbohydrates) also played a renoprotective role. Our results suggest that GLP1RA has renal protective effects, even in the absence of diabetes, primarily through reducing body weight and cardiometabolic demand.

5. References

1.Writing Group for the CKDPC, et al., JAMA. 2023;330(13):1266-77.
2.Perkovic V, et al., NEJM. 2024;391(2):109-21.
3.Clemmer JS, et al., AJP Heart.2025;329(4):H825
4.Mallette JH, et al., Obesity. *In press*. 2026.
5.Colhoun HM, et al., Nat Med. 2024;30(7):2058-66

Acknowledgements:

This work was supported by the National Heart, Lunch, and Blood Institute (T32HL105324) and the National Institute of General Medical Sciences (U54GM115428).

IN SILICO COMPARISON OF SUBSTRATE-BASED ABLATION STRATEGIES IN STRUCTURAL VENTRICULAR TACHYCARDIA

Niccolò Biasi (1), Matteo Parollo (2), Davide Vultaggio (3), Giulio Zucchelli (2), Alessandro Tognetti (1,3)

1. Research Center E. Piaggio, University of Pisa, Italy; 2. Second Division of Cardiology, Cardio-Thoracic and Vascular Department, Pisa University Hospital, Italy; 3. Information Engineering Department, University of Pisa, Italy

Correspondence to Niccolò Biasi; email: niccolo.biasi@ing.unipi.it; address: L. Lazzarino, 1, 56122 Pisa, Italy

1. Introduction

Catheter ablation has emerged as a cornerstone treatment for scar-related ventricular tachycardia (VT) in patients affected by structural heart disease (SHD). Substrate-based approaches for the identification of ablation targets have recently gained attention, as they avoid the drawbacks associated with arrhythmia induction [1,2]. This work aims to exploit computational simulations to compare different substrate-based ablation strategies in SHD: scar homogenization (SH), primary and secondary DZ ablation, and CMR-guided scar dechanneling (SD).

2. Materials and Methods

Fifteen consecutive patients prospectively enrolled in the VOYAGE clinical trial [3] for late-gadolinium enhancement cardiac magnetic resonance (LGE-CMR) aided/guided VT ablation were retrospectively analysed. LGE-CMR was segmented with ADAS3D software for scar characterization. LGE-CMR derived normalized-pixel-intensity maps were processed with the CardioMat toolbox [4] for generating cardiac electrophysiology models of the left ventricle of each subject, including fiber orientation and Purkinje network. A virtual ablation platform (AblateTool) was developed and integrated into the CardioMat pipeline. AblateTool allows virtual ablation by simple mouse clicks with tunable ablation lesion size. All the virtual ablations for the 3 different strategies were executed endo-epicardially by an expert cardiac electrophysiologist. Finally, a virtual induction protocol was performed in each model pre- and post-ablation. For VT induction, we used a standardized protocol (S1 600 ms x 6, S2 350 ms, S3 300 ms, S4 280 ms) pacing from all 17 segments of the left ventricle separately in a monodomain model.

3. Results

A total of 63 distinct sustained VTs were induced in 12 patients (mean 5.25 VTs per patient); 3 patients were non-inducible. All three ablation strategies significantly reduced the number of inducible VTs compared with baseline (residual VTs per patient: 1.2 [−82%], P=0.005; 2.41 [−62%], P=0.005; 2.9 [−52%], P=0.01, respectively), with no significant difference among the strategies (P = ns). Scar homogenization required a significantly greater ablation volume (17.41±7.22 mL) than both corridor (9.17±4.4 mL, P=0.003) and DZ ablation (10.62±5.7 mL, P=0.01), while ablation volume did not differ between corridor and DZ ablation (P=ns).

4. Discussion and Conclusions

Our in-silico study showed that that both corridor and DZ ablation effectively reduce VT inducibility with greater efficiency than conventional scar homogenization.

5. References

1. Aziz Z et al., Circulation; 140.17 (2019): 1383-1397.
2. Berruezo A et al., Pacing and Clinical Electrophysiology; 44.6 (2021): 1115-1125.
3. Lilli A et al., BMC Cardiovascular Disorders; 22.1 (2022): 169.
4. Biasi N et al., Computers in Biology and Medicine; 185 (2025): 109529

Acknowledgements:

This work was supported by the Regione Toscana under the program FSE+ 2021-2027 (SICARDIO) and the program PRS 2016-2020 (Bando ricerca salute 2018), and by the Next Generation EU project ECS00000017 Tuscany Health Ecosystem (THE, PNRR, Spoke 9: Robotics and Automation for Health).

IN SILICO EVALUATION OF TRANSCATHETER TRICUSPID VALVE REPLACEMENT WITH THE EVOQUE SYSTEM

Marta Pillitteri (1), Alessandra Zerillo (2), Giuseppe Sausa (2), Salvatore Pasta (1,2)
Stefano Cannata (2), Caterina Gandolfo (2)

1. University of Palermo, Italy; 2. IRCCS ISMETT, Italy

1. Introduction

Tricuspid regurgitation (TR) is a progressive condition of the tricuspid valve (TV) associated with advanced heart failure, affecting 1.6 million people every year. Although surgical repair of the diseased valve is the preferred treatment option, transcatheter interventions based on edge-to-edge repair, device implantation, or leaflet approximation have recently been proposed [1]. Among transcatheter tricuspid valve replacement (TTVR) therapies, the Evoque system (Edwards Lifesciences, USA) has shown superior clinical benefit compared to medical therapy alone in the TRISCEND II trial. This study aims to simulate TTVR with the Evoque device in a patient treated for severe TR at the organ transplant institute ISMETT.

2. Materials and Methods

Reverse engineering of the Evoque stent frame was performed using CT scans of the device, followed by CAD modelling. The device is equipped with an inner Nitinol stent frame with sutured valve leaflets, while a second outer frame is designed to conform to the native valve anatomy. Nine anchors engage the native TV leaflets. Segmentation of the patient's right heart and native TV was carried out using Slicer medical imaging software.

The stent frame was modelled using a superelastic constitutive model implemented in ABAQUS/Explicit (Dassault Systèmes, USA). A structured mesh with 0.2 mm brick elements was used. The right heart and TV models were meshed with tetrahedral elements and assigned anisotropic constitutive behaviour [2].

Simulations consisted of the simultaneous crimping of the two stent frames using distinct cylindrical surfaces, followed by engagement of the TV with the anchors. Later, deployment was simulated by moving a rigid sleeve, followed by mapping of the device skirt and valve leaflets. Computational flow analysis was also performed in Fluent (Ansys, USA), under physiological pressure conditions.

3. Results

Figure 1 shows the final deformed shape of the patient model after TTVR. The nine anchors properly engaged the TV leaflets, ensuring stable fixation of the device. Flow analysis revealed slight leakage occurring in the region where the valve leaflets are shortest.

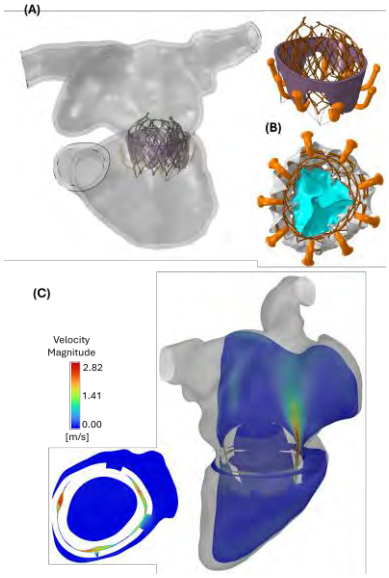


Figure 1: (A) structural simulation of stent frame; (B) final Evoque simulation; (C) flow velocity.

4. Discussion and Conclusions

This study represents the first in silico investigation of TTVR with the Evoque system. The simulations provided insight into the conformability of the Evoque device within the TV and identified regions at risk of paravalvular flow. Future studies are needed to extend the model to a larger cohort and to validate device deployment using post-TTVR imaging.

5. References

1. Otto CM et al., JACC. 77:1276 (2021).
2. Stevanella et al. Med Eng Phy. 32:1213 (2010)

Acknowledgements:
We thank Edwards Lifesciences for providing a demo sample of Evoque system.

EFFICIENT TRANSIENT 0D MICROVASCULAR HEMODYNAMIC MODEL TO INVESTIGATE PERICYTE-INDUCED STALLS.

Shiyu Liu (1), Gonzalo Maso Talou (1), Beatrice Ghitti (1), Harvey Davis (2), Finbar Argus (1)

1 Auckland Bioengineering Institute, University of Auckland, New Zealand;
2 University College London, United Kingdom.

1. Introduction

Pericyte contraction can markedly narrow capillary diameter, mechanically obstructing neutrophils, resulting in capillary flow stalls [1]. Unpublished data show that skeletal muscle exhibits distinct stall profiles characterized by high frequency and long durations (tens of minutes). However, the functional significance of these stall patterns remains unclear.

Modelling large microvascular networks is computationally expensive, partly due to the nonlinear coupling between blood flow, hematocrit, resistance, and viscosity, which typically requires iterative solvers [2].

2. Materials and Methods

We used the bond graph framework to derive ordinary differential equation CellML modules for capillary hemodynamics, incorporating vessel geometry, hematocrit-dependent viscosity, and flow-dependent red blood cell (RBC) bifurcation partitioning.

To address the nonlinear coupling and the computational cost associated with iterative solving for algebraic loops, we introduced time dynamics for hematocrit partitioning at bifurcations, representing non-instantaneous inertial effects:

$$\frac{dH_\alpha}{dt} = -\mathrm{k}\varepsilon_\alpha,$$

$$\varepsilon_\alpha = H_\alpha - \frac{H_{parent} FQE_\alpha}{FQB_\alpha}, \quad (1)$$

where k controls the speed of convergence between the current and the target hematocrit in the α daughter vessel (H_α) captured in ε_α, while *FQB* and *FQE* represent fractional flow and red blood cell distribution, respectively.

3. Results

Implementation of Eq.1. enabled transient simulation of hemodynamics in a simple *in-vivo* image-derived microvascular network without requiring iterative solvers. This formulation allows dynamic changes in vessel hematocrit to propagate through the network in time, enabling efficient simulation of microvascular responses to local pericyte modulation (Figure 1).

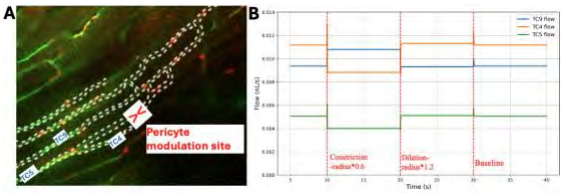


Figure 1: image-derived network (A) simulation of the transient response of TC flow to upstream pericyte modulation (B).

Preliminary simulations showed that extreme constriction (10% of the original radius) of low-branch-order pericytes does not substantially impair flow to TCs. Instead, targeted constriction was more effective at redistributing flow toward specific TCs than direct dilation.

Future work will quantify Eq.1.'s transient solving efficiency relative to iterative solving and validate the predicted flow dynamics using experimental RBC velocity measurements before and after pericyte modulation.

4. Discussion and Conclusions

We present a microvascular model for simulating transient microvascular hemodynamics without iterative solvers.

Results show that local pericyte modulation primarily redistributes flow rather than completely blocking downstream flow.

5. References

1. Davis H, Attwell D. J Physiol. 2023;601(12):2263–2272.
2. Rasmussen, P. M., et al., Microcirculation, 2018, 25(3), e12445.

Acknowledgements:
The authors would like to thank the VITAL Horizon Project (Grant no: 101136728) for providing financial support to this project.

AI-BASED GEOMETRIC AND HEMODYNAMIC BIOMARKERS FOR ABDOMINAL AORTIC ANEURYSM PREDICTION

M. Benovoy(1), A. Satriano(1), A. Guest (1), A. Forneris(1), M. Biglioli (2), B.B. Ghoshhajra(3), G. Soulez(4), S.C. Muluk(5), B.W. Starnes(6), R.D. Moore(1,7), E.S. Di Martino(1,2)

1 ViTAA Medical Solutions Inc., Montréal, Québec, Canada; 2 Department of Biomedical Engineering, University of Calgary, Alberta; 3 Department of Radiology, Harvard Medical School, Boston, Massachusetts, US; 4 Centre Hospitalier de l'Université de Montréal, Québec, Canada; 5 Division of Vascular Surgery, AHN Allegheny General Hospital, Pittsburgh, Pennsylvania, US 6 Division of Vascular Surgery, University of Washington, Seattle, Washington, US; 7 Division of Vascular Surgery, University of Calgary, Alberta, Canada

1. Introduction

Abdominal aortic aneurysm (AAA) rupture carries a mortality exceeding 80%, yet the only clinically adopted risk marker remains maximum diameter (5.5 cm men, 5.0 cm women), despite up to 60% of aneurysms above this threshold never rupturing while 13% below it do [1]. Reports that women rupture at smaller diameters [2] motivate physics-based methods that directly capture patient-specific wall weakness, regardless of sex. The same gap also limits surveillance planning before repair and outcome prediction after endovascular repair (EVAR), where type-I endoleak and failed sac shrinkage are followed qualitatively rather than predicted beforehand. We evaluated a common biomarker framework across four decision points: 12-month rupture risk, 1-year growth, and post-EVAR type-I endoleak and sac reduction.

2. Materials and Methods

For each patient, 3D reconstructions of the aortic wall, lumen, and intraluminal thrombus (ILT) were built from CT angiography, with blood flow simulated by computational fluid dynamics and wall strain derived from multiphase CT (when available), yielding geometry-based parameters and the three biomarkers that comprise the Regional Aortic Weakness (RAW) map [3]: ILT thickness/volume, time-averaged wall shear stress (TAWSS), and peak wall strain. Rupture risk used a LightGBM model trained on a matched population, benchmarked against diameter on external cohort (n=88). Growth (≥2.5 mm at 12 mos) used an Extra Trees classifier with Boruta feature selection (n=36) [6]. Post-EVAR type-I endoleak and sac reduction used linear discriminant models trained on pre-operative imaging (n=17 and 23).

3. Results

Across the four use cases, the same biomarker platform showed consistent discrimination (Table 1). For rupture risk, sensitivity was 90% versus 29% on a withheld external cohort (n=88); diameter missed 15 of 21 ruptures (71%), all below the surgical size threshold, versus 2 (9%) for the AI model. Across models, RAW biomarkers were ranked highly, while diameter ranked low or was absent.

Use case	AUC	N
Rupture risk (12-mo)*	0.88	88
Growth (≥2.5mm, 12-mo)	0.92	36
Type-I endoleak**	0.80	17
Sac reduction**	0.84	23

Table 1: AUC by use case (*single-phase CT; **pre-operative scan before EVAR).

4. Discussion and Conclusions

These results suggest RAW's biomarkers can support decision-making across the AAA care pathway: flagging elevated rupture risk below the surgical threshold, informing surveillance via growth prediction, and, from pre-operative imaging alone, identifying patients at risk of type-I endoleak or poor sac remodeling after EVAR. Directly measured strain avoided FEA assumptions and together with TAWSS was a strong predictor of 1-year growth despite a small cohort (n=36) [4]; strain was similarly influential for post-EVAR endoleak and sac-reduction prediction. Single phase only was available for the rupture cohort. Since diameter incompletely captures sex-related risk, and women fare worse after repair [5], this approach may help clarify sex-specific risk. Larger, prevalence-representative cohorts are needed before adoption.

5. References

1. Chaikof EL, Dalman RL, Eskandari MK, et al. J Vasc Surg. 2018;67(1):2-77.
2. Lo RC, Lu B, Fokkema MT, et al. J Vasc Surg. 2014;59(5):1209-1216.
3. Forneris A, Kennard J., et al. Front. Cardiovasc. Med., 2021; vol. 8.
4. Forneris A, et al. JVS Vasc Sci. 2023;4:100119.
5. Pace G, et al. R. Ann Vasc Surg. 2026 (in press).

DEVELOPMENT AND VALIDATION OF AN *IN SILICO* FRAMEWORK TO PREDICT FRACTURE OF METASTATIC VERTEBRAE

Luca Cristofolini[1], G. Barbanti-Bròdano[2], V. Carbone[3], E. Dall'Ara[4], R. Ferenc[5], S.J. Ferguson[6], J.M. Garcia Aznar[7], N. Germscheid[8], A. Lazary[9], M. Palanca[1], S. Sale[10], P. Vajkoczy[11], JJ Verlaan[12], L. Vidacs[13], E. Voisin[14]

1. University of Bologna, IT; 2. Rizzoli Orthopaedic Institute, IT; 3. InSilicoTrials Technologies, IT; 4. Univ. of Sheffield, UK; 5. FrontEndART, HU; 6. ETH Zurich, CH; 7. Univ. of Zaragoza, ES; 8. AO Foundation, CH; 9. Buda Health Center, HU; 10. Eurice, DE; 11. Charité Berlin, DE; 12. Univ. Medical Center Utrecht, NL; 13. Univ. of Szeged, HU; 14. Voisin Consulting Life Sciences, FR

1. Introduction

Metastases can significantly compromise the strength of the affected vertebrae, exposing patients to a critical risk of suffering a vertebral fracture in their remaining lifetime. Fracture can be prevented by stabilization, a very invasive surgery. Current clinical decision tools (e.g. the Spine Instability Neoplastic Score, SINS) are pretty crude and provide unclear indications for ≈60% patients. Consequently, about 30% metastatic patients suffer fractures, and another 30% undergo unnecessary surgeries. The METASTRA project aims to develop and validate a combination of credible AI and VPH models, to improve the evaluation of the risk of fracture.

2. Materials and Methods

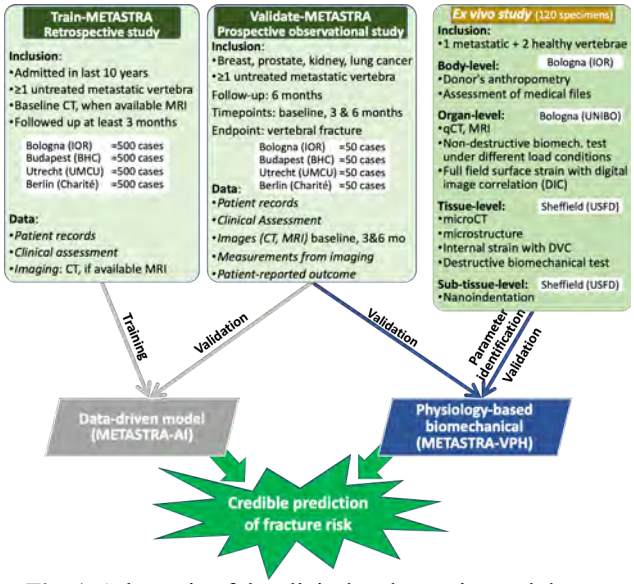


Fig. 1: Schematic of the clinical and experimental data used to develop, train and validate the models.

Three unprecedentedly large datasets of cases with vertebral metastases are collected (Fig. 1). A multicentric retrospective dataset (Train-METASTRA) includes clinical images and medical records of 2000+ patients with vertebral metastases. A smaller but more detailed prospective study (Validate-METASTRA) will collect observational data from 200+ patients with metastases followed up for 6 months. Finally, an *ex vivo* test campaign is providing morphological and mechanical properties from different modalities at different scales (from body-level down to the sub-tissue level) from 120+ cadaveric spine segments.

3. Results

We are developing two families of models which will be deployed in cascade. The first step relies on Explainable AI, combining parameters semi-automatically extracted from medical records and images. The AI models are trained on the multicentric retrospective dataset. The AI model outcomes are validated using the prospective dataset. The AI models also provide an indication of confidence. Those cases which are not reliably assessed according to the AI, are analyzed with detailed VPH models, capturing the subject-specific anatomy, material properties etc. The VPH models are intrinsically multiscale and incorporate sub-models for the healthy bone, metastasis, intervertebral disc, and interfaces. The data from the *ex vivo* study are used to initiate the model parameters. The model predictions will be validated against the *ex vivo* tests, and the prospective study.

4. Discussion and Conclusions

These models will be embedded in the METASTRA decision support system. We aim to reduce the indeterminate diagnoses from the current 60% down to 20% cases, with significant benefits for the patients in terms of quality of life and surgical risk reduction, and for healthcare providers.

Acknowledgements: METASTRA project funded by the European Union, HEU topic HLTH-2022-12-01, grant 101080135

CIRCADIAN RHYTHMS WITHIN THE INTERVERTEBRAL DISC

Laura Baumgartner (1), Jérôme Noailly (1)

1. BCN MedTech, Pompeu Fabra University, Spain

Correspondence: Laura Baumgartner (laura.baumgartner@upf.edu), Department of Engineering, UPF, Barcelona

1. Introduction

Intervertebral disc (IVD) degeneration is a major risk factor for low back pain. Articulating and stabilizing the spine, the IVD is exposed to high loads. Due to organ avascularity, IVD cells live within a hostile nutritional environment. While the impact of mechanical loads and nutrition have been widely studied, daily oscillations caused by circadian rhythms (CR), are largely unknown, despite a recognised importance thereof [1]. This work introduces a mathematical framework to approximate the effect of CR on the mRNA expression (exp) of the main structural proteins (Aggrecan (Agg), collagen types I, II (Col-I, Col-II) of the IVD's central tissue, the Nucleus Pulposus (NP).

2. Materials and Methods

A previously developed parallel networks (PN) methodology for NP cell activity predictions [2], was extended to accept CR dynamics. It interprets mRNA exp as interconnected small, directed parallel networks. PN are fed with *in vitro* measurements of cell responses to varying exposure to stimuli. Each link is determined by two normalised variables, θ and x, respectively reflecting the importance, and the concentration, of a stimulus for an mRNA exp. CR were represented as sine functions with a period of 24h, where phase shift and amplitude were modulated (Fig.1), based on experimental information [1] (Fig.2). Decline of amplitude without stimulus was directly derived from [1]. Col-I was assumed to oscillate in antiphase to Agg/Col-II, because of its opposite function to Col-II in the NP.

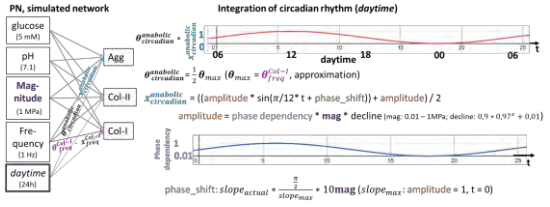


Figure 1: Simulated network (input conditions in brackets) with approximations of CR dynamics

3. Results

Simulations predicted phase advance/delay for stimulation at mid descending/mid ascending phase. Stimulation at peak resulted in highest amplitude, and no phase shift, stimulation at trough disrupted the CR of Agg, Col-II (Fig.2).

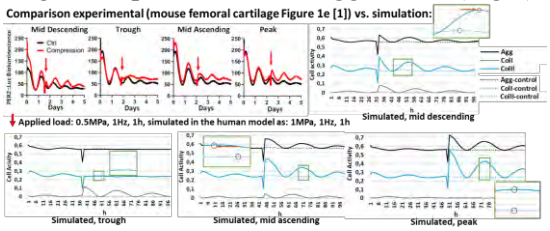


Figure 2: Experimental (top left) [1] vs. simulations. Phase shift visualized in zoom.

4. Discussion and Conclusions

The model largely reproduced CR impact dynamics seen in experimental research (Fig.2). Interestingly, the initial antiphase of Col-I is dynamically shifted depending on impact conditions, which might explain high CR-related variability of gene exp [3]. mRNA downregulation at impact could only be reproduced using 1MPa of impact load in the human model, vs. 0.5MPa in [1]. Hence, simulations suggest 0.5MPa to be a high load for mouse cartilage. Per2 and Agg/Col-II are activated trough the SMAD2/3 pathway, based on which similar Per2-Agg/Col-II dynamics were assumed; and high similarity between cartilage and IVD cell responses [1] proposes cartilage to be a good model to approximate IVD dynamics. This is the first model that allows to investigate highly dynamic CR-based IVD regulations. Future work shall allow to simulate multiple impacts to approximate human activities along days and weeks. This would allow (e.g.) to shed light on gene exp dynamics of shift workers.

5. References

1. Dudek M et al., Nat Commun 14,7237 (2023)
2. Baumgartner L et al., bioRxiv (2024)
3. Zhang et al. PNAS 111(45) (2014)

Acknowledgements:
ERC-2021-CoG-O-Health-101044828

LESION SIZE AND LOCATION AFFECT THE COMPRESSIVE FAILURE LOAD OF HUMAN METASTATIC VERTEBRAE

Robert Roger (1), Rajdeep Ghosh (1), Áron Lazáry (2), Lingzhong Guo (1), Damien Lacroix (1), Enrico Dall'Ara (1)

1. The University of Sheffield, UK; 2. National Center for Spinal Disorders, Budapest, Hungary

Corresponding Author: Robert Roger, rvroger1@sheffield.ac.uk

1. Introduction

Approximately 16% of cancer patients are clinically diagnosed with vertebral metastases [1], which present in different types of lesions depending on the primary tumour. Lytic lesions reduce bone mineral density and increase fracture risk. Lytic lesions form in a variety of locations and volumes, yet the biomechanical impact of these factors remains poorly quantified and is not considered in current clinical stability scores. Computed tomography (CT)-images based finite element (FE) modelling can mechanistically evaluate these effects. This study aimed to assess how location and volume of simulated lytic lesions affect vertebral failure.

2. Materials and Methods

Six radiologically healthy lumbar vertebrae from six cancer patients with spine metastases were semi-automatically segmented from densitometrically calibrated CT-images. Heterogeneous isotropic elasto-plastic homogenised FE (hFE) models were created. Spheroidal lesions with volume of 10%, 20%, or 30% of the vertebral body volume (VBV) were simulated by assigning linear elastic material properties (E=0.01MPa, ν=0.4995). Lesion's location was defined by the distance from the centre of the VB (r), the cross-sectional angle (θ), and their axial position (h) (Figure-1).

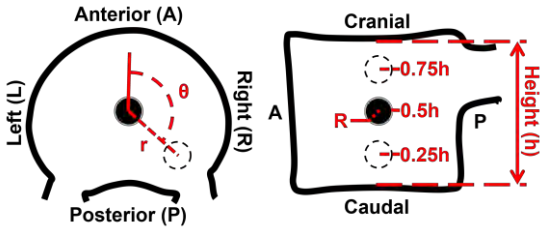


Figure 1: Schematic of the transverse (left) and sagittal (right) planes of the VB displaying the location of the centre of virtual lesion.

Compressive ultimate force (F_U) was calculated for each hFE model at 1.9% of apparent axial deformation. Normalised F_U was calculated with respect to intact control vertebra.

3. Results

The range of normalised F_U was 6.7±4.0%-25.2±2.9%, 13.0±4.4%-38.9±7.7%, and 17.7±5.7%-49.9±4.3% for lesions occupying respectively 10%, 20%, and 30% of the VBV (Figure-2). The largest effects were found for lesions involving the cortical shell or endplates.

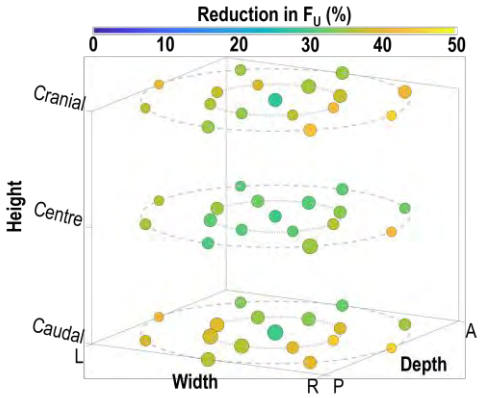


Figure 2: Mean reduction in F_U due to the single simulated lesion with a volume of 30% VBV. Markers indicate the location of the centre of the lesion. Marker colour represents the mean F_U reduction across the six investigated vertebrae, and marker radius represents the corresponding standard deviation.

4. Discussion and Conclusions

Both lesion size and location influenced the F_U of the vertebra and should be considered in scoring systems to estimate vertebral stability. Larger lesions produced greater F_U reduction. Substantial variability across locations indicates position is equally important for assessing vertebral stability, in function of the original density distribution. Lateral regions located close to the cortex were most detrimental, suggesting these areas represent biomechanically vulnerable regions. Current work is focusing on increasing the sample size, and investigating the effect of the shape and orientation of the lesions.

5. References

1. Van Den Brande et al., J Bone Oncol., 2022

Acknowledgements:

Supported by the METASTRA project (EU H2022 grant ID:101080135; UK Horizon Europe Guarantee Extension ID:10075325).

A BIOMECHANICS-BASED DECISION SUPPORT SYSTEM FOR PREDICTING METASTATIC VERTEBRAL FAILURE RISK

Rajdeep Ghosh (1), Eddie Shearman (1), Robert Roger (1), Marco Palanca (2), Enrico Dall'Ara (1), Damien Lacroix (1)

1. The University of Sheffield, United Kingdom; 2. Department of Industrial Engineering, Alma Mater Studiorum - University of Bologna, Italy

Corresponding Author: Rajdeep Ghosh, rajdeep.ghosh@sheffield.ac.uk

1. Introduction

Spinal metastases often cause pathological vertebral fractures, yet clinical tools like the Spinal Instability Neoplastic Scale (SINS) score cannot quantify the mechanical effects of a lesion on the vertebral strength. In this study a reproducible, densitometrically calibrated qCT to Finite Element (FE) modelling pipeline was developed to compare metastatic and radiological control vertebrae within the same segment to enable subject-specific mechanical risk assessment beyond radiology.

2. Materials and Methods

Twelve human spine segments were scanned using qCT, each including at least one metastatic vertebra and an adjacent lesion-free control. Lesions were classified as lytic (n=6), blastic (n=1), or mixed (n=5). Subject-specific geometries (Fig 1) were segmented, aligned, and meshed with 10-noded tetrahedral elements. Density-dependent nonlinear isotropic properties were assigned using Bonemat based on qCT-calibrated BMD. Axial compression to 1.9% apparent strain was applied to compute failure load and ultimate strength. A normalised intra-segment failure load (F^*), as shown in Eq. 1, quantified lesion-specific biomechanical effects independent of inter-patient variability.

$$F^* = \frac{F_{met}}{F_{control}} \qquad (1)$$

3. Results

Predicted failure loads ranged from 0.2–6.2 kN (controls: 1.7±1.5 kN; metastatic: 1.8±1.6 kN) with no significant group difference (p>0.05). F^* reflected lesion-specific effects: lytic lesions mostly reduced strength (F^*<1 in 5/6 cases), mixed lesions showed variable response, and the blastic case increased strength (Fig 2). Ultimate strength ranged from 0.3–10.4 MPa (controls: 2.4±2.3 MPa; metastatic: 2.6±2.8MPa).

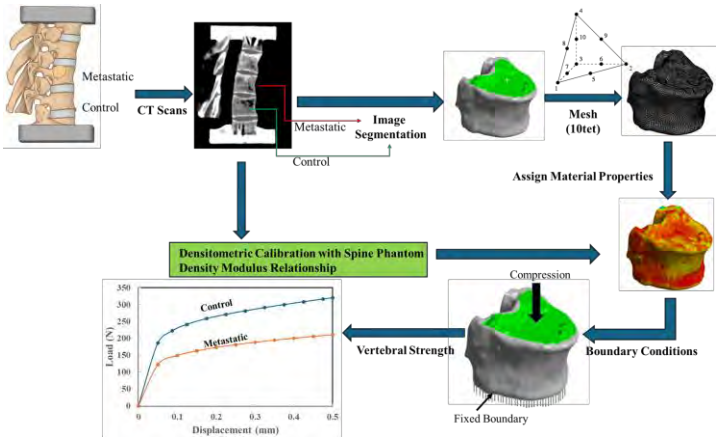


Figure 1: *In silico* framework to predict vertebral failure

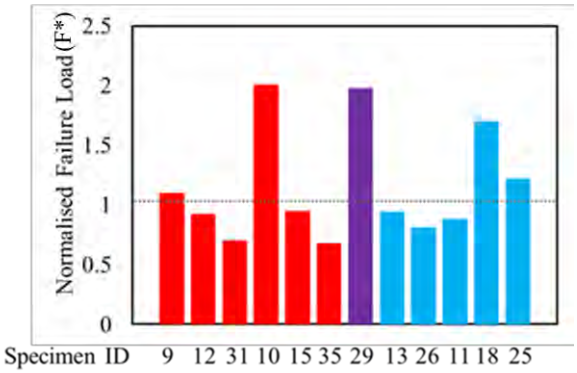


Figure 2: Normalised intra-segment failure load for all the tested specimens (Lytic; Blastic; Mixed).

4. Discussion and Conclusions

This study systematically compares metastatic vertebrae with paired controls across major lesion types using a calibrated nonlinear qCT-based FE framework. The study shows that vertebral strength depends on lesion-induced load redistribution, revealing risks difficult to assess using clinical imaging alone. The findings highlight SINS limitations and support subject-specific FE modelling for personalised fracture-risk assessment.

Acknowledgements:

METASTRA (EU H2022 grant ID 101080135; UK Horizon Europe Guarantee Extension ID: 10075325), Metaspine (MSCA-IF-EF-ST, 832430/2018).

INVERSE OPTIMIZATION OF BONE-TUMOUR INTERFACE AND MATERIAL MAPPING IN METASTATIC VERTEBRAE

Jaime Muñoz-Allué (1), Enrico Dall'Ara (2), Marco Palanca (3), María Ángeles Pérez (1), José Manuel García-Aznar (1)

1. *Aragon Institute of Engineering Research (I3A), University of Zaragoza, Spain*
2. *Division of clinical medicine and Insigneo institute, Univ. of Sheffield, United Kingdom*
3. *Dept of Industrial Engineering, University of Bologna, Italy*

1. Introduction

Vertebral metastases significantly alter the mechanical integrity of the spine, increasing fracture risk. While patient-specific Finite Element (FE) models have become a powerful tool for clinical assessment, the mechanical properties of the bone-lesion interface and the metastatic tissue remain largely unknown. Hounsfield Unit (HU) to elastic modulus (E) conversions are normally used to assign material properties in bone [1]; however, their direct application to metastatic lesions may not fully capture the mechanical behaviour of blastic or lytic lesions. This study presents an inverse optimization framework to estimate lesion and interface properties by comparing FE simulations with *ex vivo* experimental Digital Volume Correlation (DVC) data [2].

2. Materials and Methods

From CT scans of spine segments with two-vertebrae (one metastatic and one control) and the respective intervertebral discs (Fig. 1a), a subject-specific FE model is generated (Fig. 1c). The metastatic vertebra is divided into three domains: the bone, the metastatic lesion, and a cohesive interface layer. Heterogeneous bone properties are assigned using Bonemat (Fig. 1b). To determine the optimal mechanical parameters, an optimization algorithm was integrated into the pipeline (Fig. 1e). The algorithm iteratively modifies: (i) the parameters of the cohesive bone–tumour interface (K, δ), which govern the traction–separation relation and its damage evolution, and (ii) a stiffness scaling factor (α) that uniformly scales the heterogeneous elastic modulus assigned to the metastatic lesion. The objective function minimizes the difference between FE-predicted strains and the experimentally measured DVC strains.

3. Results

The inverse model successfully identified parameter values that reduced the relative error compared to baseline models by 3.4−6.5% (Fig. 1e). These results suggest that correcting the material mapping of metastatic tissue through the optimized stiffness scaling factor (α) improves the accuracy of the FE predictions and that the bone–tumour interface may influence the local mechanical interaction.

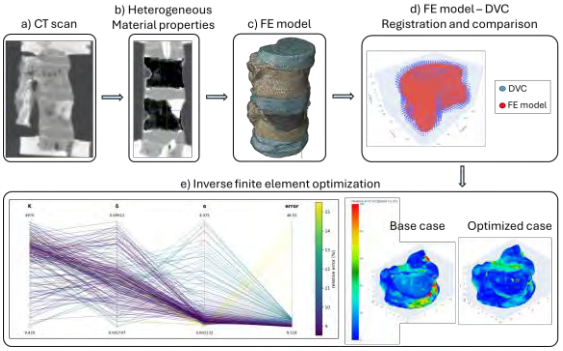


Figure 1: Workflow of the inverse optimization framework: (a) CT scan, (b) bone and lesion material mapping, (c) FE model, (d) FE–DVC strain comparison, (e) parameter optimization and relative error.

4. Discussion and Conclusions

By solving the inverse problem, this optimization pipeline provides a robust validation tool that enables the characterization of mechanical properties that are inaccessible *in vivo*. This framework serves as a foundation for developing credible digital twins, directly supporting clinical fracture risk assessment and decision-making.

5. References

1. Molinari L, Falcinelli C, Meccanica, 57, 2022.
2. Palanca et al., Bone, 173, 2023.

Acknowledgements:
This work was supported by the European Union through Horizon Europe programme (METASTRA grant 101080135).

INTEGRATING IMAGING BIOMARKERS AND RADIOTHERAPY DOSE INTO CARDIOVASCULAR DIGITAL TWINS FOR LONGITUDINAL RISK MODELING

Alessandra Catalano (1), Eliana Gioscio (1), Francesco Pisani (1), Chiara Veronese (1), Paola Vallerio (1), Luca Dedè (2), Paolo Zunino (2), Alessandro Cicchetti (1)*

1. Fondazione IRCCS Istituto Nazionale dei Tumori, Milan, Italy;

2. MOX, Department of Mathematics, Politecnico di Milano, Italy

**Presenter/Corresponding Author alessandro.cicchetti@istitutotumori.mi.it*

1. Introduction

Radiotherapy (RT) is a key treatment for lung cancer, but it often results in unavoidable irradiation of the heart and major vessels. Digital twins represent a promising paradigm for personalized, longitudinal modeling of cardiovascular function, enabling investigation of treatment-related alterations and supporting future simulation-informed risk stratification in cardio-oncology.

2. Materials and Methods

LOCATION MATTERS is a prospective observational study enrolling patients undergoing thoracic RT for lung cancer. The study includes baseline cardiovascular assessment (ECG, TSA, Echocardiography, blood samples) before treatment, and follow-up evaluations at 3-12 months post-RT. To date, 17 of 25 patients have been enrolled. For each patient, clinical history, imaging-derived biomarkers, functional cardiovascular measurements, and radiotherapy treatment descriptors are collected.

Moreover, *patient-specific cardiovascular features are extracted from CT imaging and functional examinations.* The available information includes:

- cardiac structure and function derived from echocardiography;
- pulse wave velocity and wall thickness for large vessels;
- imaging-based risk biomarkers, including vessel diameters, aortic plaque burden, coronary calcifications, and estimates of epicardial, visceral, and perivascular fat.

*Digital Twin (DT) Modeling Workflow: t*he cardiovascular DT is built around a modular modeling framework [1] that enables:

-Patient-specific representation through calibration of key physiological parameters from clinical data [2] (e.g. anatomical geometry, resistances, compliances, elastance-related descriptors);

-Personalized simulations providing individualized trajectories and functional outputs not directly accessible in routine clinical practice;

-Physiological interpretability, supported by the modular structure and parameter-based personalization;

-Treatment-effect modeling, where thoracic radiotherapy is introduced as a time-dependent perturbation of selected parameters (e.g., compliance, resistance, contractility proxies).

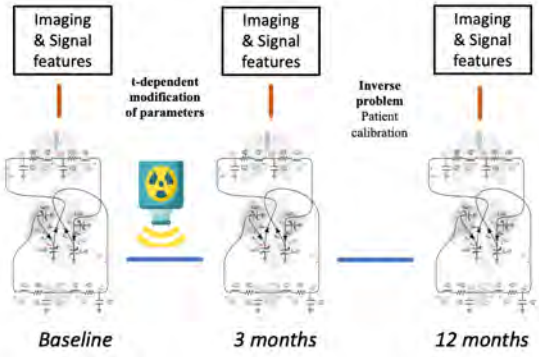


Fig 1: Digital Twin Modeling Workflow [1].

3. Discussion and Conclusions

This work proposes a modular DT workflow for cardiovascular risk assessment in thoracic RT patients that combines longitudinal patient data with mechanistic 0D cardiovascular modeling. The framework enables patient-specific simulations and supports the study of treatment-induced perturbations over time. In the long term, this approach may contribute to simulation-informed risk stratification and decision support in cardio-oncology.

4. References

1. Dedè L, Regazzoni F, Math Biosci Eng. 2021 Apr 15;18(4):3364-3383 (2021).
2. Alimohammadi M, Pichardo-Almarza C, Front Physiol. 2016 Jun 21;7:238 (2016).

Acknowledgements: Funded by AIRC 27480.

PATIENT-SPECIFIC FINITE ELEMENT ANALYSIS OF STENTING FOR SINUS VENOSUS ATRIAL SEPTAL DEFECTS

Muhammad Chatoo (1), Nerea Romate Alonso (1), Fabrizio Crasci (2), Silvia Schievano (1), Giuliano Giusti (3), Claudio Capelli (1)

1. University College London & Great Ormond Street Hospital for Children, UCL, London, UK; 2. Universita' degli studi di Palermo, Palermo, Italy; 3. Niguarda Hospital, Milan, Italy

Corresponding Author: Claudio Capelli, Email: c.capelli@ucl.ac.uk

1. Introduction

Sinus venosus atrial septal defects (SVASDs) represent a complex subset of congenital heart disease. While covered stent correction (CSC) offers a minimally invasive surgical alternative, its efficacy is often limited by stent migration, pulmonary vein (PV) compression, or residual shunting [1]. Predicting the device–tissue interactions is crucial to planning a successful intervention. This study aims to optimise the decision-making process by means of a patient-specific finite element (FE) framework to assess how procedural practices and variables influence biomechanical outcomes.

2. Materials and Methods

A patient-specific SVASD geometry was reconstructed from ECG-gated CT and discretised using shell elements. Venous walls were modelled as linear elastic (E = 0.4 MPa, ν = 0.48) and a 10-Zig Cheatham-Platinum (CP) stent as elasto-plastic, discretised with beam elements. FE simulations were run with a commercial software (Abaqus/Explicit). The main simulations steps for in situ deployment included the following phases: stent crimping, balloon-driven expansion, deflation, and subsequent device recoil. Additional scenarios incorporated the presence of an anchoring stent or caudal flaring, replicating procedural practices. The framework was established to evaluate the effects of various deployment strategies, stent positioning, and oversizing. For each simulation, the following parameters were assessed: i) anchorage in the superior vena cava (SVC); ii) PV compression; and iii) defect coverage. Anchorage was measured by nodal contact pressure (CPRESS), compression through logarithmic minimum principal strain (LE_{min}), and coverage via direct inspection.

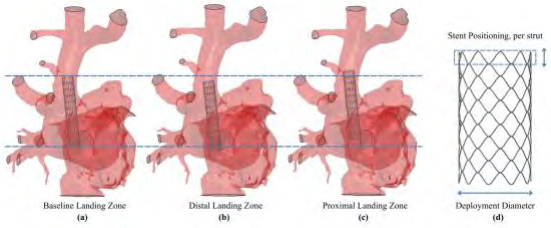


Figure 1: (a-c) Stent positioning within the patient-specific anatomy. (d) Schematic of the CP stent.

3. Results

Results of the FE simulations (n=36) revealed that anchorage and coverage were strongly dependent on stent positioning and deployment strategy. Proximal positioning with anchoring stents generated the highest CPRESS values, indicating mechanical stability within the SVC. Caudal flaring provided the most complete defect coverage, effectively mitigating residual shunting. Oversizing reduced contact in single-stent configurations at baseline and distal zones, suggesting that overexpansion in non-cylindrical regions may induce stent malapposition. PV compression remained within a 10% LE_{min} threshold in all scenarios, indicating a low risk of clinically significant obstruction for the specific patient's model.

4. Discussion and Conclusions

A patient-specific in silico framework can assess the mechanical performance of CSC for SVASD, highlighting the potential FEA holds as a pre-procedural planning tool. Future work should include personalized tissue properties [2], fluid-structure interactions [3], and a validation study on a large cohort of patients.

5. References

1. Hansen JH et al., J Am Coll Cardiol; 75(11):1266-1278 (2020).
2. Nolan DR et al., J Mech Behav Biomed Mater; 39:48-60 (2014).
3. Chiastra C et al., J Mech Behav Biomed Mater; 34:217-230 (2014).

FINITE ELEMENT MODELLING OF PERCUTANEOUS PULMONARY VALVE IMPLANTATION IN PAEDIATRIC ANATOMIES

Maria Lecuona (1), Liam Swanson (1), Abdul Salam (2), Sachin Khambadkone (2), Giuliano Giusti (3), Silvia Schievano (1,2), Claudio Capelli (1,2)

1. Institute of Cardiovascular Science, University College London, London; (2) Great Ormond Street Hospital for Children, London; (3) Niguarda Hospital, Milan, Italy

1. Introduction

Percutaneous pulmonary valve implantation (PPVI) is a minimally invasive and effective treatment for severe pulmonary regurgitation and stenosis [1]. Self-expandable PPVI devices have recently been introduced to treat patients with too large or dynamic right ventricular outflow tract (RVOT), expanding the cohort of patients who can benefit from the procedure. However, predicting device behaviour remains challenging, as detailed information on its interaction with the RVOT and surrounding structures is limited [2]. This study aims to develop a physics-based predictive framework of the Harmony Transcatheter Pulmonary Valve (Medtronic Inc, US), providing clinicians with enriched pre-procedural information.

2. Materials and Methods

Patients referred for Harmony TPV25 implantation from two clinical centres were included in this study. Pre-procedural computed tomography (CT) images were post-processed to reconstruct the implantation site, aortic root and coronary arteries. A finite element model (FEM) was set up using the commercial software Abaqus 2024 (Dassault Systèmes), with the device discretized using beam elements and the anatomy using shell elements. For each patient, different device positions (varying from proximal – close to the right ventricle – to distal – close to the pulmonary artery bifurcation) and implantation site compliances (varying from rigid walls to high compliance) were tested.

Simulations evaluated implantation feasibility and optimal placement based on: i) safe anchoring; and ii) reduced risk of pulmonary bifurcation obstruction, paravalvular leakage, and coronary artery compression. Results were assessed quantitatively (reaction forces and contact pressures) and qualitatively via immersive virtual reality (VheaRts). The feasibility of TPV implantation was then compared to the standard protocol based on diameters measured from images.

3. Results

A total of 7 patients were modelled to assess the feasibility of implantation. Numerical analysis allowed to predict the final configuration of the device within the implantation site (Examples in Figure 1).

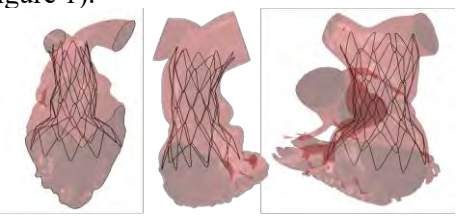


Figure 1: Examples of simulated PPVI of TPV25 in patient-specific cases

The analysis of the RFs, contact nodes and visual inspection in VR allowed to identify a preferred placement strategy (e.g. distal for patient in Figure 2). For 6 of the cases the FEM analysis confirmed the implantability of the TPV25. For one patient, the risk of compressing coronary was highlighted. The results were in accordance with the pre-procedural assessment in 6 cases out of seven.

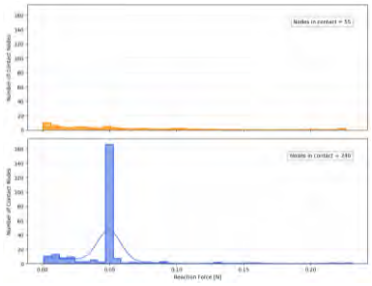


Figure 2: Distribution of RF and contact nodes in (A) proximal and (B) distal scenarios

4. Discussion and Conclusions

The proposed framework enabled simulations to be successfully performed for all patient-specific anatomies, providing individualized predictions of stent deployment and providing support pre-procedural planning for self-expandable devices used in PPVI.

5. References

1. Khalil, M et al. Trans Pediatrics, 2019.
2. Benson, L. N. *et al. Circ. Cardiovasc. Interv.* 2020.

PATIENT-SPECIFIC MECHANICAL THROMBECTOMY SIMULATION: A CONVERSATION BETWEEN CLINICIANS AND ENGINEERS

Thomas Brouwer (1), Virginia Fregona (2), Thijs Kuipers (1), Luca Bontempi (3,4), Frank Gijsen (3,4), Henk Marquering (1), Jose Felix Rodriguez Matas (2), Francesco Migliavacca (2), Giulia Luraghi (2), Charles Majoie (1)

1. Amsterdam UMC, NL; 2. Politecnico di Milano, IT; 3. TU Delft, NL, 4. Erasmus MC, NL

1. Introduction

The introduction of mechanical thrombectomy (MT) has improved clinical outcomes in patients with acute ischemic stroke; however, treatment success varies substantially, reflecting the complex nature of stroke [1]. The primary goal of MT is to achieve successful recanalization. Currently, a wide range of MT devices is available, making it increasingly difficult for interventionists to decide which device or combination of devices to use in a specific patient. Validated computational models offer an innovative approach to support these device-selection decisions. In this work, we present a clinician-modeler collaborative workflow to build patient-specific MT simulations.

2. Materials and Methods

To build the simulations of four MT cases from the MR CLEAN NO IV trial, several patient-specific characteristics were collected: *i*) patient vasculature, ideally from post-operative images (Fig 1a), *ii*) clot length, location, (Fig 1a) and composition *iii*) device used and its position within the vessels at the moment of clot engagement (Fig 1b), and *iv*) procedural outcome, assessed with the expanded treatment in cerebral infarction (eTICI) score. The pre-procedural anatomy, with the occluding clot, was reproduced *in silico* [2]. Then, the whole procedure was replicated with the methodology developed by [3]. Finally, the *in silico* outcome was compared with the technical outcome.

3. Results

Figure 1b-c shows the comparison between *in vivo* and *in silico* aspiration catheter position at the moment of clot engagement. Figure 1d shows some frames of clot retrieval simulation. The *in silico* outcome was compatible with the positive first pass effect obtained in the clinical case.

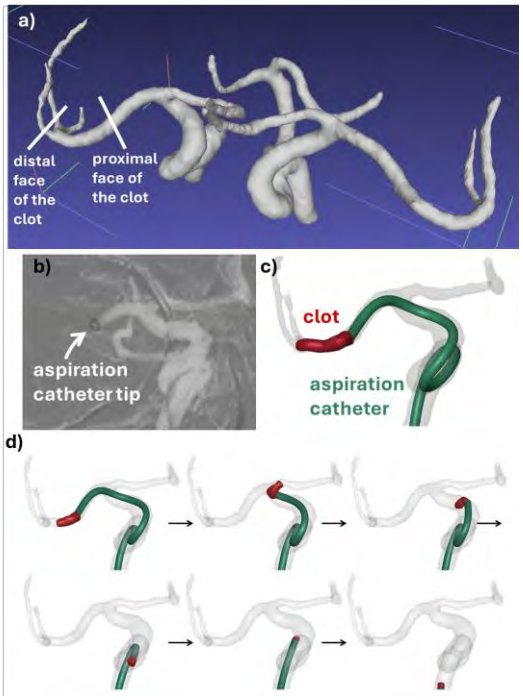


Figure 1 Example of a patient-specific case.

4. Discussion and Conclusions

Even if simulations proved able to reproduce clinical cases, the requirement of a complete vascular model and the long computational time (around 24 hours) limits clinical applicability. For this reason, the methodology will be extended to a virtual population to develop a tool capable of real-time prediction of EVT outcome. This work is an example of how much the collaboration between engineers and clinicians is vital for the development of these models.

5. References

1. Goyal M et al., Lancet, 2016
2. Fregona V et al, Phys Eng Sci Med, 2025
3. Luraghi G et al, Interface Focus, 2020

Acknowledgements:
This project has received funding from the European Union's Horizon Europe research and innovation programme under the grant agreement No 101136438).

ENGINEERING DESIGN CHOICES - A DIRECT PATIENT COMPLICATION RISK

Lisa Prahl Wittberg (1), Lars Mikael Broman (2,3)

1. Dept. Engineering Mechanics, KTH, Sweden; 2. ECMO Centre Karolinska, Karolinska University Hospital, Sweden; 4. Dept. Physiology and Pharmacology, Karolinska Institute, Sweden

1. Introduction

Extracorporeal membrane oxygenation (ECMO) is a life-saving intervention for respiratory and/or circulatory support. Patient's blood is pumped through a circuit composed of cannulae, a blood pump, membrane lung, and tubing with connectors, exposing the blood to highly unsteady flow fields. Despite technological and medical advancements, thrombosis in the ECMO circuit remains a challenge. To reduce flow-induced coagulation activation and hemolysis stresses exerted on the red blood cells (RBC), platelets and von Willebrand factor (vWf) need to remain at near physiological levels (<12 Pa) [1]. This work focuses on flow-induced coagulation activation, combining clinical and engineering expertise to expose and understand these events for transfer back to the clinical setting.

2. Materials and Methods

To illustrate our approach, we use our work regarding the outlet of a membrane lung (ML; Quadrox iD, Getinge, Rastatt, Germany) [2]. 3D surface scanning and caliper measurements were used to reconstruct ML geometry. The outlet was characterized by "pins" protruding into the blood flow path. Thirty-three percent of the cross-section area was obstructed by a temperature sensor socket, male purge-line cap, and a Luer-lock port. Large eddy simulations with WALE sub-grid model were performed for blood flows at 1 and 4 L/min. Blood was considered Newtonian (viscosity of 3.5 mPa s). Moreover, a thrombus was extracted in the geometry after ECMO support and analyzed using scanning electron microscopy (SEM).

3. Results

The geometrical features of this ML outlet resulted in development of recirculation bubbles and strong vortical structures similar to characteristics of bluff bodies. Based on the protruding components diameters, the Reynolds number indicated a subcritical flow regime with transition to turbulence. A turbulent vortex street developed for both flow rates, along with counter-rotating vortex pairs extending to the outlet of the computational domain. Fluid strain rates >10,000/s were observed along with areas of elongational flow characterized with shear rates >2,000/s. This corresponded to levels where both vWf may unfold and platelet activation may occur if entrapped in these flow structures. SEM showed the thrombus mainly composed of fibrin and RBCs covered in cell fragments. The RBCs of regular, echinocytes, and polyhedrocyte types were identified.

4. Discussion and Conclusions

This work illustrates undesirable flow structures developing in geometries found in several medical device with protruding objects obstructing the flow path and Luer-lock port, where stable recirculation zones develop. In the studied device, a change of polymer and adding a coating material approved it for long-term use. However, none of the outlet adjuncts are necessary for ECMO. The work motivates design improvements but also discussion on how to enhance the cross-disciplinary interaction between clinic, basic engineering and industrial application development. Moreover, our work also show how basic fluid mechanical knowledge is relevant in a clinical context influencing factors, e.g. which components to use for reduced potential of coagulation/platelet activation, vWf unfolding, hemolysis, etc., and consequent risk reduction of emboli entering the patient.

5. References

1. Chan C et al. J Biomech 130 (2022)
2. Nilsson F et al. ASAIO J. Aug 26 (2025).

Acknowledgements:
The research was funded by the Swedish Research Council (2019-04800) and the European Research Council (ERC CoG 2021: Project 101045453—fitsCAN)

BREAKING SILOS WITH DYNAMIC DATA GOVERNANCE

Maria Quaranta (1), Andreas Kremer (1), Kristin Reiche (2), Anne Funck Hansen (3) on behalf of the CERTAINTY consortium

1. Information Technology for Translational Medicine, Esch-sur-Alzette, Luxembourg; 2. Fraunhofer Institute for Cell Therapy and Immunology IZI, Leipzig, Germany; Interdisciplinary Transformation University (IT:U), Linz, Austria & Center for Scalable Data Analytics and Artificial Intelligence (ScaDS.AI), Dresden, Leipzig, Germany; 3. Fraunhofer Society for the Advancement of Applied Research, Munich, Germany

1. Introduction

In interdisciplinary data science projects, innovation is often hindered by lack of timely access to essential, high-quality datasets. Overcoming this barrier is crucial for advancing data-driven research and achieving translational breakthroughs. This issue is exacerbated by the need to integrate diverse sources such as real-world data, OMICs, imaging, and genetics on a continued basis, while navigating compliance requirements and administrative barriers.

2. Materials and Methods

To address this challenge, CERTAINTY showcases a novel governance framework, based on a living Data Management Plan (DMP) and a lean Joint Controller Agreement (JCA) under Art.26 of the General Data Protection Regulation (GDPR), originating from IDERHA (joint publication in preparation). DMP and JCA are tightly linked to the Grant and Consortium Agreements, aligning consortium responsibilities with daily data processing and model development. The JCA distributes GDPR data controller responsibilities and governs DMP evolution with clear procedures, thereby ensuring legal and ethical compliance. The DMP acts as the operational backbone for CERTAINTY's Virtual Twin, documenting data lifecycles, mapping flows, defining security and integrity measures, integrating FAIR (Findable, Accessible, Interoperable, and Reusable) principles, and supporting versioned updates. The interrelation between the DMP and JCA allows for smooth adaptation to new circumstances (Figure 1).

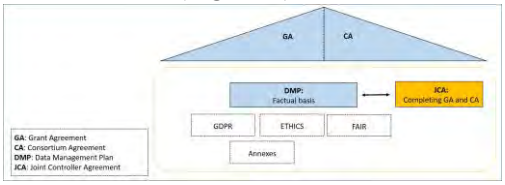


Figure 1: High level overview of the JCA/DMP data governance framework

3. Results

The framework demonstrates that an integrated legal and operational governance can actively enable innovation by breaking downs silos linked to static data sharing agreements drafted in isolation from data management [1]. By utilizing synergies between scientific and legal accountability requirements, CERTAINTY demonstrates that compliance and innovation do not just coexist but moreover fuel each other, shattering old boundaries and driving scientific breakthroughs.

4. Discussion and Conclusions

Whereas the European regulatory law is often pointed out as a primary explanatory factor for innovative deficiency [2], the integrated governance framework highlights the potential improvements available to research initiatives already today. The integrated governance framework provides a transferable blueprint for data-driven development of virtual patient twins.

5. References

1. Bontridder, N et al. Journal of AI Law and Regulation Volume 1, Issue 2 (2024) pp. 249 – 253 (2024)
2. Fröhlich H et al., J Med Internet Res 2025;27:e76491 (2025)

Acknowledgements:

The Authors thank fellow Researchers and Lawyers of IHI IDERHA and CERTAINY. The IDERHA project is supported by the Innovative Health Initiative Joint Undertaking and its members, under grant agreement No 101112135. Funded by the European Union, the private members, and those contributing partners of the IHI JU. Views and opinions expressed are however those of the author(s) only and do not necessarily reflect those of the aforementioned parties. Neither of the aforementioned parties can be held responsible

for them. CERTAINTY was funded by the European Union under Grant Agreement number 101136379. Views and opinions expressed are however those of the authors only and do not necessarily reflect those of the European Union or the Health and Digital Executive Agency. Neither the European Union nor the granting authority can be held responsible for them.

TRANSLATING DIGITAL TWIN GLUCOSE PREDICTIONS INTO PATIENT ACTION THROUGH AI BEHAVIOURAL COACHING

Kekayan Nanthakumar (1), Rashmini Naranpanawa (1), Finbar Argus (1), Elizabeth Broadbent (2), Merryn Tawhai (1) Gonzalo Maso Talou (1)

1. Auckland Bioengineering Institute, University of Auckland, New Zealand. 2. Faculty of Medical and Health Sciences, University of Auckland, New Zealand

1. Introduction

Type 2 Diabetes management demands continuous monitoring over multiple domains, including diet, exercise, medication and glucose monitoring [1], yet most people receive support only during clinic visits. Glucose prediction models can forecast glycaemic trajectories from continuous glucose monitoring (CGM) data [2], offering potential to inform these daily decisions in real-time. However, these models remain confined to ICU settings using intermittent blood glucose measurements [3] or research environments inaccessible to patients. The missing component is a patient-facing layer that translates glucose forecasts into contextualised, actionable and continuous coaching in between clinic visits.

2. Materials and Methods

We developed the Digital Health Navigator (DiNa), an AI-powered digital human coaching system (Figure 1) that serves as the patient-facing interface for digital twin glucose prediction. DiNa integrates: (i) a multimodal data pipeline capturing CGM, smart watch bio-signals, meals, medications, and activity; (ii) integration with a glucose dynamics predictor; and (iii) an LLM-powered coaching engine delivering adaptive behavioural coaching to address self-care dimensions [1]. Formative evaluation included focus groups (N=11; age 30–70 years) with prototype interaction, and moderated usability testing (n=10, SUS, NASA-TLX). A prototype demo is available at: https://dub.sh/dina-vph-demo

3. Results

The platform achieved good usability (SUS=76.1, SD=15.0) with low cognitive load (NASA-TLX=26.7, SD=14.05). Focus groups identified that participants valued data-informed feedback but described self-management as cognitively demanding work under fatigue and time pressure, indicating that prediction-based coaching must reduce effort rather than add to it. Existing tools failed to recognise culturally specific foods or translate information into actionable daily guidance, reinforcing the need for contextualised coaching over raw prediction output.



Figure 1: Close-looped architecture coupling glucose digital twin predictions with AI coaching.

4. Discussion and Conclusions

This work addresses a critical translational gap: the absence of a patient-facing layer that converts physiological predictions into behavioural action offering continuous coaching. Formative findings demonstrate this coupling is technically feasible and acceptable to diverse users. A future 12-week clinical trial will generate linked coaching, prediction, and outcome data, enabling adaptive policy development via reinforcement learning, positioning patient-facing coaching as a necessary component of the virtual physiological human vision.

5. References

1. Kolb L. The Science of Diabetes Self-Management and Care (2021): 47(1):30–53.
2. Lutsker, G., et al. *Nature* (2026): 1-9.
3. Seret, M., et al. *J Diabetes Sci Tech* (2026): 19322968251412857.

Acknowledgements:

Financial support was provided by MBIE Catalyst Strategic (Soul Machines) grant #3726194.

REGULATORY GAPS AND A LIFECYCLE-BASED FRAMEWORK FOR GENERAL DIGITAL TWINS UNDER THE EU MDR AND AI ACT

Cindy Welzel (1), Stephen Gilbert (1)
1. Else Kröner Fresenius Center for Digital Health, TUD Dresden University of Technology, Germany

1. Introduction

Digital twins (DTs) in healthcare are increasingly proposed for personalized risk prediction, therapy optimization, and prevention (1). While narrow DT applications resemble task-specific decision-support tools, general DTs aim to represent adaptive, multi-scale physiological systems integrating heterogeneous clinical and molecular data. Despite technological progress, regulatory pathways for clinical DTs remain unclear (2). Existing frameworks such as the EU Medical Device Regulation (MDR) and the AI Act were not designed for such general, continuously adaptive models, potentially hindering clinical translation. We identify key regulatory gaps and propose a lifecycle-based framework to support regulatory readiness of clinical DTs.

2. Materials and Methods

A structured conceptual analysis of relevant regulatory frameworks was conducted, focusing on their applicability to continuously learning DTs. Regulatory challenges were mapped and based on identified gaps, a framework was developed and applied to a hypothetical metabolic DT.

3. Results

General DTs differ from conventional medical devices in three respects:
(i) they generate patient-specific model instances based on continuously integrated, potentially multi-modal data;
(ii) they combine mechanistic simulation with data-driven components; and
(iii) they may include self-learning through recalibration or adaptive updating.
They therefore function as dynamic simulation systems embedded in clinical workflows rather than static products. Current EU conformity assessment procedures are designed for fixed product versions, creating ambiguity regarding oversight of individualized model instances and accountability for adaptive behaviour. Although the AI Act introduces Predetermined Change Control Plans (PCCPs) to manage anticipated modifications, their practical operationalization remains unclear, and the MDR concept of "significant modification" does not clearly define boundaries for permissible adaptive updates. To address these gaps, we propose a lifecycle-based framework comprising three elements:
(1) dual-level oversight, separating assessment of the core DT architecture from oversight of patient-specific calibration and updating;
(2) an adaptive change envelope, aligned with the AI Act's concept of PCCPs;
(3) a continuous validation process integrating real-world performance monitoring with automated safety surveillance and predefined intervention triggers.

4. Discussion and Conclusions

General DTs challenge conventional medical product evaluation, which assumes static products with narrow intended purposes. By contrast, they require oversight of dynamic, patient-specific simulation systems. While MDR and the AI Act provide a risk-based foundation, guidance for adaptive updates and individualized calibration remains limited. Our proposed framework translates these challenges into structured regulatory adaptations, supporting controlled model evolution and continuous validation, thereby facilitating responsible clinical translation of general DTs.

5. References

1. Gilbert S, Drummond D, Cotte F, Ziemssen T. Editorial: Digital twins in medicine—transition from theoretical concept to tool used in everyday care. Front Digit Health. 2025 Feb 27;7. doi:10.3389/fdgth.2025.1573727
2. Derraz B, Breda G, Kaempf C, Baenke F, Cotte F, Reiche K, et al. New regulatory thinking is needed for AI-based personalised drug and cell therapies in precision oncology. npj Precis Onc. 2024 Jan 30;8(1):1–11. doi:10.1038/s41698-024-00517-w

Acknowledgements:
This study was supported by the BMBF-funded project LiSyM-Cancer II initiative, consortium DEEP-HCC (grant number: 031L0315A).

SPINESIM: A BIOMECHANICAL DIGITAL TWIN FOR SURGERY PLANNING AND BIOMECHANICAL ANALYSIS

Matteo Tarquini (1), Morteza Rasouligandomani (1), Siril Teja Dukkipati (1), Deniz Kaçar (1), Roger Assaker (1), Laurent Adam (1)

1. MDsim S.A., Luxembourg

Correspondence: Matteo Tarquini, MDsim S.A., 9 avenue des Hauts-Fourneaux, L-4362 Esch-sur-Alzette, Luxembourg.

1. Introduction

SPINEsim is a software in which patient-specific biomechanical digital twin is developed to support planning of spine surgery. In this case study, a short-segment fusion for degenerative L4-L5 spondylolisthesis was used to compare an optimal alignment scenario, with restoration of local lordosis, against a hypo-lordotic scenario, with insufficient segmental correction.

2. Materials and Methods

A patient-specific spinal model was built from imaging to simulate a single-position fusion with anterior-to-psoas access and anterior cage placement under gravity preload and daily loading conditions (bending in all direction, up to 7.5Nm) [1-3]. Two postoperative alignments were compared: an optimal alignment, with a 12° cage restoring L4-L5 lordosis to 17° and preserving a higher distal lumbar contribution, and a hypo-lordotic alignment, with L4-L5 reduced to 2.5° and lower L(L4-S1) contribution despite similar PI and LL. Biomechanical outcome included annulus fiber and annulus shear strain, bone compressive stress, and L3-L4 relative displacement.

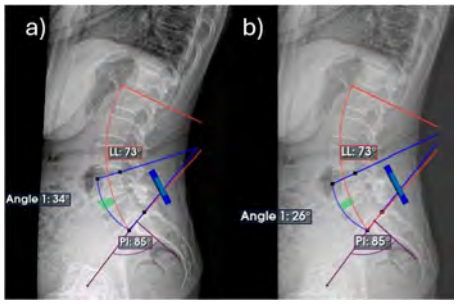


Figure 1 a) optimal lordosis alignment; b) hypolordotic alignment. Both surgery plans were developped in SPINEsim.

3. Results

Optimal alignment: Restoring local lordosis preserved a more physiological distal lumbar contribution to global lordosis and improved adjacent-segment biomechanics, with lower strain, loading, and displacement above the fusion.

Hypo-lordotic alignment: Despite similar global LL, insufficient segmental correction altered distal lordosis distribution and worsened adjacent-level mechanics. Compared with the optimal alignment, annulus shear strain increased by about +8% and +12% (for flexion and extension respectively) with respect to optimal alignment, and relative displacement between L3 and L4 was also increased. This suggests that acceptable global alignment may still mask a mechanically unfavorable local undercorrection.

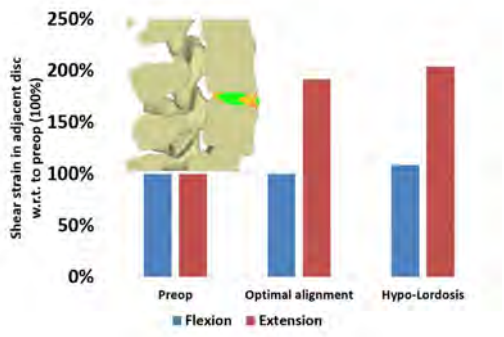


Figure 2: Annulus shear strain: preop and two postop differences

4. Discussion and Conclusions

This case shows that patient-specific biomechanical digital twins can reveal clinically relevant effects not captured by static spinopelvic parameters alone. In particular, the degree of L4-L5 segmental correction influenced adjacent-segment loading, supporting a more personalized and mechanics-informed approach to fusion planning.

5. References

1. Bernier E., Driscoll M. J Biomech. 2023;161:111863.
2. Naserkhaki S. et al. J Biomech. 2016;49(7):1255-1263.
3. Dreischarf M. et al. J Biomech. 2014;47(8):1757-1766.

TOWARDS QUALIFICATION AND REGULATORY ACCEPTANCE OF VIRTUAL CONTROL GROUPS (VCGs) - THE IHI VICT3R PROJECT

Thomas Steger-Hartmann (1), Karolina Kopańska (2,3), Ferran Sanz (4), Frank Bringezu (5), Inari Soininen (6)

1. Bayer AG, Pharmaceuticals, Berlin, Germany; 2. John Hopkins University, Center for Alternatives to Animal Testing (CAAT), Baltimore, USA; 3. CAATevents gGmbH, Solingen, Germany; 4. Universitat Pompeu Fabra, Hospital del Mar Research Institute, Barcelona, Spain; 5. Merck Healthcare KGaA, Chemical & Preclinical Safety, Darmstadt, Germany; 6. SYNAPSE Research Management Partners SL, Madrid, Spain

1. Introduction

The use of virtual control groups (VCGs) in animal toxicity studies has the potential to save 25% of the animals used in preclinical toxicity studies. Generating these VCGs requires standardized procedures to select appropriate data sets from a large repository of high-quality historical control data (HCD) originating from previous animal safety studies. The collected data is curated and stored using standardized terminologies.

The publication of the VCG concept [1] led to the formation of a new European consortium within the Innovative Health Initiative with the title "Developing and Implementing Virtual Control Groups to Reduce Animal Use in Toxicology Research" (VICT3R) [2].

2. Objectives & Methods

VICT3R aims to reduce animal use in studies for safety assessments through the implementation of the VCG concept. Key to regulatory acceptance will be that VCGs do not compromise study outcomes or endanger patient and consumer safety. To this end, VICT3R has initiated a request for scientific advice on qualification of the VCG concept to the European Medicines Agency (EMA).

For this procedure, the consortium submitted the results of 28 animal studies across 5 species, where the concurrent controls (CCGs) have been replaced by adequately selected VCGs and subsequently compared regarding original study outcome as proposed in [3].

VCGs hereby represent a valuable transitional initiative in the field of NAMs [4].

3. Results

In all cases evaluated the replacement of CCGs with VCGs with predefined selection criteria resulted in similar overall study conclusions and in the same NOAEL as determined for the studies using CCG.

4. Discussion and Conclusions

Based on the evidence derived from the reanalysed study it can be considered that VCGs can be used to substitute for CCGs. A qualification for at least in non-clinical non-GLP rat dose range finding (DRF) studies to inform on dose selection for subsequent pivotal rat GLP-compliant repeat- dose studies seems realistic.

Further regulatory approaches to extend VICT3R's regulatory outreach will be presented.

5. References

1. Steger-Hartmann T et al., ALTEX 2020; 37(3):343-349
2. Steger-Hartmann T et al., Toxicol Pathol 2025; 53(2):230-233 .
3. Golden et al., Altex 2024; 41(2):282-301.
4. Sanz et al., NAM Journal 2025; 1, 100065.

Acknowledgements:

This project is supported by the Innovative Health Initiative Joint Undertaking (IHI JU) under grant agreement No 101172693.

The JU receives support from the European Union's Horizon Europe research and innovation programme and COCIR, EFPIA, Europa Bío, MedTech Europe, and Vaccines Europe and Instem Scientific Limited.

Funded by the European Union, the private members, and those contributing partners of the IHI JU. Views and opinions expressed are however those of the author(s) only and do not necessarily reflect those of the aforementioned parties. Neither of the aforementioned parties can be held responsible for them.

PORTAL THROMBOSIS FOLLOWING MAJOR LIVER SURGERY: THE IMPACT OF HEMODYNAMIC SHEAR

Morgane Garreau (1), Ana Vlasceanu (1,2,3), Amaury Facque (3), Giulia Cardillo (4), Abdul I. Barakat (4), Nicolas Golse (2), Irene Vignon-Clementel (1)

1. INRIA Saclay, France; 2. Centre Hépato-Biliaire - Hôpital Paul Brousse, AP-HP, France; 3. CHRU Tours, France; 4. LadHyX, CNRS, Ecole Polytechnique, IP Paris, France

1. Introduction

Cholangiocarcinoma is the most common biliary tract cancer. Its main curative treatment is surgical resection. One of the main complications of this surgery (so-called major hepatectomy) is portal vein thrombosis. Its incidence rate is around 10%, and it can be fatal [1]. Hemodynamic shear appears to play a role in the development of thrombosis.

2. Materials and Methods

The cohort is composed of 17 patients who underwent hepatectomy with portal vein resection. 7 *cases* developed thrombosis following surgery, while 10 *controls* did not. All patient geometries are segmented from post-operative scans. A third group is created based on *virtual surgeries* performed on pre-operative CT scans of the cases, with a vascular graft inserted instead of simple anastomosis. Computational fluid dynamics (CFD) simulations are conducted with the finite-element code FELiScE [2]. Blood is modeled as a Newtonian fluid. The inlet boundary condition is based on an averaged inflow and distributed with the ratio Splenic Vein:Superior Mesenteric Vein = 1:2. The imposed inlet velocity is a parabolic profile. 3-element Windkessel models are implemented at the outlets based on the subtending liver volume distribution. The simulations are post-processed with in-house Python scripts to delineate flow features that are different among the groups. A specific focus is set on shear and the following marker is proposed:

$$SRG_{proj} = \overrightarrow{\nabla\dot{\gamma}} \cdot \frac{\vec{u}}{||\vec{u}||} \qquad (1)$$

It represents the projection of the shear rate ($\dot{\gamma}$ [s^{-1}]) gradient in the direction of the velocity vector ($\vec{u}$ [cm/s]). It comes from the observation of Nesbitt et al. who described regions of negative shear gradients as being prothrombotic [3].

3. Results

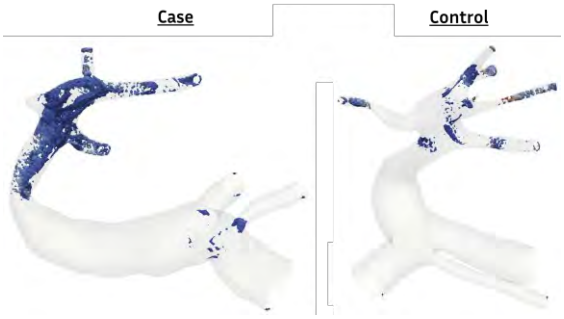


Figure 1: Regions where SRG_{proj} < -250 $(cm.s)^{-1}$ for one case of thrombosis and one control.

Thresholds to highlight the regions associated with SRG_{proj} values below -250, -500, -750 and -1000 $(cm.s)^{-1}$ were investigated as illustrated in Figure 1 for one *case* and one *control*. The volumes meeting each of these thresholds were computed for each patient. With the exception of one control, a clear separation between the *cases* and *controls* groups was observed.

4. Discussion and Conclusions

This study presents preliminary results focused on determining relevant hemodynamic markers for prediction of thrombosis following major liver surgery. Shear gradients appear to play an essential role in the onset of the pathology. Current effort aims at modeling thrombus formation in the portal vein geometries through the extension of a recently developed model [4].

5. References

1. Yoshiya S et al., World Journal of Surgery; 38:1491–1497 (2014).
2. https://gitlab.inria.fr/felisce/felisce
3. Nestbitt WS et al., Nature Medicine; 15(6):665-673 (2009).
4. Cardillo G, Barakat AI. Biomechanics and Modeling in Mechanobiology; 24:1465–1484 (2025).

AGEING AS A SCAR: REDEFINING AGEING AS AN ACCUMULATION OF SMALL DAMAGES DURING LIFETIME

Pierre-Alexandre Grott (1), Marielle Ousset (1), Anne Lorsignol (1), Paul Monsarrat (1), Louis Casteilla (1), Diane Peurichard (2)*, Jenny Paupert (1)*

*1. RESTORE Research Center, Université de Toulouse. INSERM 1301, CNRS 5070, EFS, ENVT, France ; 2. Inria Paris, team MUSCLEES, Sorbonne Université, CNRS, Université de Paris, Laboratoire Jacques-Louis Lions UMR7598, France ; *Contributed equally*

1. Introduction

With age, tissues lose their function in association with structural alterations. We propose that this decline results from the lifelong accumulation of small damages events. In this framework, a single damage would not induce tissue-scale destructuring but could locally introduce small architectural errors during the repair process, ultimately leading to a long-term destructuring [1]. To test this hypothesis we used a 2D agent-based mathematical model [2] previously calibrated biologically and temporally [3] on adipose tissues.

2. Materials and Methods

The model enables emergence of *in-silico* tissues composed of two agents, cells and dynamically cross-linked fibers, interacting via simple physical principles like repulsive forces, fibers alignment and cell-cell volume exclusion. From these generated tissues, we simulate damage by removing agents within a defined region and letting the tissue evolve toward a new equilibrium following under controlled repair processes. These include fibers insemination at the damage edges with speed v_f, crosslinking of the newly created fibers with probability P_f and inflammatory signals delaying cell insemination. We evaluate tissue-scale disorganization using a Global Repair Index (GRI), which quantifies the distance between the initial tissue architecture and the repaired state. Based on the GRI, we discriminate three different outcomes: *regeneration* (<0.7), *unstructured* (0.7<GRI>2) or *scarring* (>2).

3. Results

Using the GRI on different lesion sizes, we identify a range of "small damages" that do not induce tissue-scale destructuring. However, depending on the parameter values governing the repair process, these small damages can generate local structural modifications, as measured by local quantifiers in Fig.1.

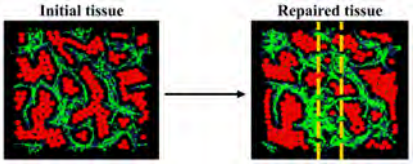


Figure 1: Example of a tissue simulation before (left) and after (right) a single small damage. Dotted lines indicate the previous damage boundary.

We then investigate the impact of repeated small damages on the tissue architecture evolution. We analyze the repair outcome after six small damages for highly crosslinked reconstructed networks, and examined the influence of damage locations and frequencies. We show that, within a given timeframe, varying the frequency of damage does not significantly modify the repair outcome. In contrast, the spatial location of repeated lesions utterly changes tissue structure.

4. Discussion and Conclusions

Our results show that while a single small damage does not affect structure at the tissue scale, the repetition of such small damages progressively alters global tissue architecture. Depending on the characteristics of the perturbations, this cumulative effect can drive the tissue toward unstructured or scarred state, as observed in aged tissue. These findings reveal the destructive nature of repetitive small damages over time. Finally, we report a fourth tissue behavior emerging *in-silico* under repeated perturbations, characterized by unresolved inflammation; investigations into this phenomenon are ongoing.

5. References

1. Kemoun Ph et al., Ageing Research Reviews. 2022 Jan;73:101537.
2. Peurichard D et al., Journal of theoretical biology. 2017 Spring;429:61–81.
3. Pacary A et al., npj Regenerative Medicine. 2024

DISRUPTED BRAIN DYNAMICS IN EARLY PARKINSON'S DISEASE: TOWARD DIGITAL BIOMARKERS AND BRAIN DIGITAL TWINS

Doris Pischedda (1), Matteo Vitacca (1), Fulvia Palesi (1,2), Alessandro Tessitore (3), Rosa De Micco (3), Mattia Siciliano (3), Fabrizio Esposito (3), Claudia A.M. Gandini Wheeler-Kingshott (1,2,4), Egidio D'Angelo (1,2)

1. Department of Brain and Behavioral Sciences, University of Pavia, Pavia, Italy; 2. Digital Neuroscience Centre, IRCCS Mondino Foundation, Pavia, Italy; 3. Department of Advanced Medical and Surgical Sciences, University of Campania "Luigi Vanvitelli", Naples, Italy; 4. Department of Neuroinflammation, UCL Queen Square Institute of Neurology, Queen Square Multiple Sclerosis Centre, NMR Research Unit, London, UK

Corresponding author: Doris Pischedda, doris.pischedda@unipv.it

1. Introduction

Parkinson's disease (PD) is a progressive neurodegenerative disorder characterized by motor (e.g. tremor) and non-motor (e.g. decline of cognition, affective alterations) symptoms arising from dopaminergic degeneration. Increasing evidence suggests that PD reflects distributed neural circuit dysfunction and altered excitation/inhibition (E/I) balance. Brain Digital Twins (BDT) [1] provide a framework to link macroscale neuroimaging findings to mechanistic circuit alterations by estimating biophysiologically interpretable parameters useful to unravel the complexity of PD and optimize therapeutic treatments.

2. Materials and Methods

We used The Virtual Brain (TVB) framework [2] with (f)MRI data to generate subject-specific multiscale brain models of early-stage PD patients (N=48) and healthy controls (HC, N=18) to extract parameters reflecting long-range connectivity and local E/I synaptic dynamics, both at the whole-brain and resting-state network (RSN) levels.

First, we compared model parameters between PD patients and HCs to identify disease-related alterations. Second, we examined whether these parameters predicted motor, cognitive, and affective clinical measures. Finally, we assessed whether TVB parameters could discriminate PD patients from HCs better or beyond clinical and cognitive scores.

3. Results

PD patients exhibited increased long-range connectivity within ventral attention network. Network-specific parameters reflecting global connectivity or local E/I balance within the frontoparietal, visual, and attention networks predicted motor severity, affective symptoms, cognitive performance, and quality of life. Notably, TVB model parameters reliably discriminated PD patients from HCs, whereas cognitive and clinical measures alone did not.

4. Discussion and Conclusions

These findings demonstrate that personalized brain modeling can capture mechanistically interpretable alterations in E/I balance and large-scale connectivity appearing in early PD which are prodromal to cognitive impairment. By linking neuroimaging data to circuit-level parameters this approach provides candidate digital biomarkers of distributed network dysfunction and establishes a foundation for BDTs aimed at clinical stratification and personalized therapeutic optimization.

5. References

1. E. D'Angelo and V. Jirsa, "The quest for multiscale brain modeling," *Trends Neurosci.*, vol. 45, no. 10, pp. 777–790, Oct. 2022.
2. M. Schirner *et al.*, "Brain simulation as a cloud service: The Virtual Brain on EBRAINS," *NeuroImage*, vol. 251, p. 118973, May 2022.

Acknowledgements:

This work was supported by #NEXTGENERATIONEU (NGEU) and funded by the Ministry of University and Research (MUR); National Recovery and Resilience Plan (NRRP) project; MNESYS (PE0000006) – A Multiscale integrated approach to the study of the nervous system in health and disease (DN. 1553 11.10.2022)

CARDIACFOAM: TOWARDS A FRAMEWORK FOR *IN-SILICO* INSIGHTS INTO PIG-TO-HUMAN HEART XENOTRANSPLANTATION

Simão Nieto de Castro (1), Pablo Castrillo (1,2), Claire Conway (3), Philip Cardiff (1)

1 School of Mechanical & Materials Engineering, University College Dublin, Ireland.
2. Instituto de Estructuras y Transporte, Universidad de la República, Uruguay.
3. Department of Anatomy and Regenerative Medicine, Royal College of Surgeons in Ireland (RCSI), Ireland

1. Introduction

Cardiac computational modelling is transitioning from a research-driven methodology to a clinically integrated and regulator-recognized technology. The clinical importance of these tools is highlighted by recent and pivotal advances in cardiac xenotransplantation, specifically pig-to-human procedures. Reports from the American Heart Association [1] on the first porcine transplants showed graft growth and altered electrical conduction. Similar outcomes were observed in pig-to-baboon transplants, which provided evidence for clinical translation but did not achieve long-term survival [2]. Current studies are primarily focused on immunology, while limited work has addressed interspecies mechanical and electrical mismatch, which requires an integrated electromechano-haemodynamic modelling framework. In settings where clinical datasets are limited, *in-silico* data is essential.

2. Materials and Methods

The current work is developing `cardiacFoam` – an open-source, large-scale electromechanical solver built in OpenFOAM –to simulate whole-heart porcine and human hearts under human loading. Designed to operate modularly with the solids4foam [3] library, this framework establishes the basis for *in-silico* cardiac xenotransplantation studies. It incorporates state-of-the-art anatomical and physiological porcine and human models (Figure 1), including ionic models of electrophysiology, Purkinje network, fibre generators, mechanical myocyte models, and the governing electromechanical equations [4].

3. Discussion and Conclusions

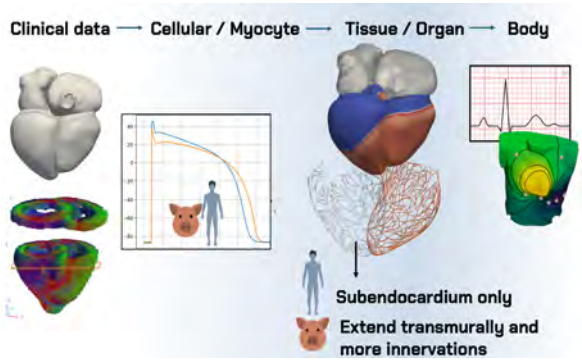


Figure 1. `cardiacFoam` framework: clinical data input and interspecies and myocyte electrophysiology differences

`cardiacFoam` aims to enable systematic cross-species comparison of porcine and human cardiac electromechanics, including pig hearts in human recipients. By allowing controlled *in-silico* investigation of these scenarios before *in vivo* studies, the framework can also help improve the interpretation of preclinical pig studies and support the development and evaluation of cardiac therapies and electromechanical devices more efficiently and cost-effectively. With continued clinical input and interdisciplinary collaboration, this work aims to improve care and life support systems.

4. References

1. M.M Mohiuddin, et al., The Lancet, 402(10399): 397 – 410, 2023.
2. M.M. Mohiuddin, et al., American Journal of Transplantation, 2026.
3. P. Cardiff et al., Journal of Open Source Software, 10(108): 7407, 2025.
4. A. Quarteroni et al., Cambridge University Press, 2019.

Acknowledgements:
This project has received funding from the European Research Council (ERC) under the European Union's Horizon 2020 research and innovation programme (Grant Agreement No. 101088740).

A NOVEL ELECTROMECHANICAL MODEL OF THE MEDIAN NERVE WITH APPLICATION TO CARPAL TUNNEL SYNDROME

Rittelmann, Jana (1); Röhrle, Oliver (1); Bleiler, Christian (1)

1. Institute for Modelling and Simulation of Biomechanical Systems, University of Stuttgart, Germany

Corresponding author: jana.rittelmann@imsb.uni-stuttgart.de

1. Introduction

Carpal tunnel syndrome (CTS) is the most common entrapment neuropathy in peripheral nerves and is therefore of great importance in everyday clinical practice. CTS refers to damage to the median nerve and impairment of its function due to compression within the carpal tunnel in the wrist [1]. However, it is difficult to measure parameters of diagnostic value such as pressure and tissue stiffness non-invasively [2]. Their correlations to CTS symptoms are not fully understood, highlighting the relevance of developing a novel model of median nerve biomechanics and electrophysiology.

2. Materials and Methods

Based on the anatomy and physiology of a healthy individual, a novel in-silico framework was created to investigate the mechanical behavior of the human median nerve under load. The 3D geometrical FE model (Fig. 1) includes the nerve's detailed microstructure considering the different collagenous layers and the axons. Individual material models based on hyperelastic strain-energy functions were formulated to account for the distinct mechanical properties of the microstructural components, including strain-stiffening behavior which is relevant in CTS diagnostics. To the authors' knowledge, a model including all these aspects at once does not presently exist.

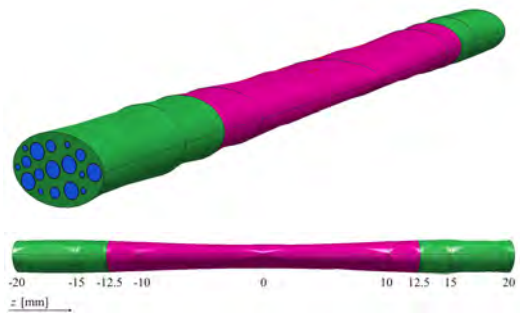


Figure 1: 3D nerve model based on anatomical data of the human median nerve under physiological conditions including the tissue microstructure.

Two FE-based case studies were carried out, analyzing the mechanical response to longitudinal stretch (λ_{max} = 1.1) and transverse compression (p_{max} = 150 mmHg). In addition, the signal conduction in a human myelinated axon was investigated by employing an adapted Hodgkin-Huxley model [3,4]. The load-induced deformation from the FE studies was used to assess the effects of mechanical load on signal propagation.

3. Results

The FE-based studies show median nerve behavior consistent with literature, while providing new insights to stress and stiffness distributions within the nerve tissue. The tissue stiffness increases with applied load, implying strain-stiffening behavior, while the nerve cross-sectional area decreases. The electrophysiological model achieves conduction velocities within the physiological range, while fascicle deformation results in a slower signal propagation.

4. Discussion and Conclusions

The presented model is the first of its kind considering the level of detail for both anatomy and biomechanics, successfully reflecting the behavior of a healthy human median nerve. Moreover, it integrates mechanical and electrophysiological aspects, with particular relevance for CTS research in a clinical context.

5. References

1. Antoniadis G et al., S3-Leitlinie Karpaltunnelsyndrom, DGH/DGNC (2022).
2. Schrier V et al., Muscle Nerve 61(6):826-33 (2020).
3. Hodgkin AL, Huxley AF, J Physiol 117(4):500-44 (1952).
4. Goldman L, Albus JS, Biophys J 8(5):596-607 (1968).

Acknowledgements:

The authors would like to thank the European Research Council (Grant no: 101055186) for providing financial support to this project.

NEUROANATOMY ATLAS AS A CORE FOR VIRTUAL BRAIN TWIN: SHARING THREE-DECADE-LONG EXPERIENCE

Wieslaw L. Nowinski

Sano Centre for Computational Personalised Medicine, Krakow, Poland

Email: w.nowinski@sanoscience.org; URL: www.wieslawnowinski.com

1. Introduction

The Virtual Human Twin (VHT) is a ground-breaking initiative, and one of the key barriers in its deployment is the lack of advanced models [1]. To facilitate overcoming it, I propose a concept of a core knowledge-based model or atlas and illustrate it with working examples.

2. Materials and Methods

Three types of atlases can be distinguished: core, comprehensive, and specialized. A core atlas is a basic, generic, and standard reference from which comprehensive and specialized atlases as well as clinical applications can be developed. It should be as small as possible and as large as necessary: compact and simple enough to be developed efficiently, yet sufficiently rich to capture the field's core knowledge and remain easily extendable. Extension can occur through internal growth of core content or via "mergers and acquisitions." Key features of a core atlas include being normal, accurate, parcellated, labeled, of high quality, stereotactic, composable, and modular. Here, we focus on brain applications, which were preselected as one of five use cases for the VHT. Because neuroanatomy is the foundation of neuroscience, neurosurgery, neuroradiology, and neurology, a neuroanatomic atlas is chosen as the core brain atlas (CBA). The CBA concept is illustrated through our long-term development of brain atlases and atlas-enabled applications.

3. Results

The atlas [2] is taken as the CBA. It includes 3D models of the cerebrum, cerebellum, brainstem, white matter, tracts, deep structures, and intracranial vasculature. This CBA has been extended towards a comprehensive atlas by growing from the central nervous system to the peripheral nervous system, and from the brain to the head and neck with 3,000 components [3]. Another example is a repository with over 8,600 3D neuroimages [4]. Specialized atlases derived from the CBA are an atlas of arterial variants [5] and an atlas of neurologic disorders [6].

4. Discussion and Conclusions

Clinical applications benefit from mapping 2D brain atlases onto tomographic scans. Accordingly, the CBA is merged with a 2D highly parcellated anatomic brain multi-atlas. Furthermore, this extended CBA is merged with a probabilistic functional atlas, unifying neuroanatomy and neuro-electrophysiology. Beyond medical education, clinical applications of such an extended CBA will be presented for neurosurgery [7], neuroradiology [8], neurology, brain mapping, and stroke [9].

5. References

1. Viceconti M et al., IEEE Journal of Biomedical and Health Informatics, 28(1):491-501 (2024).
2. Nowinski WL et al., Journal of Neuroscience Methods; 204(1):44-60 (2012).
3. Nowinski WL et al., Thieme, New York (2015).
4. Nowinski WL, Neuroinformatics;23(3),42 (2025).
5. Nowinski WL et al., Neuroinformatics; 7(4):255-264 (2009).
6. Nowinski WL et al., Thieme, New York (2014).
7. Nowinski WL et al., Journal of Neurosurgery; 113(6):1234-41 (2010).
8. Nowinski WL, The Neuroradiology Journal; 29(4):260-8; (2016).
9. Nowinski WL, Neuroinformatics; 18(4):549-567 (2020).

Acknowledgements:

This publication is supported by: the European Union's Horizon 2020 research and innovation programme under grant agreement Sano No. 857533; the International Research Agendas programme of the Foundation for Polish Science, co-financed by the European Union under the European Regional Development Fund; and the Ministry of Science and Higher Education "Support for the activity of Centers of Excellence established in Poland under Horizon 2020" on the basis of the contract number MEiN/2023/DIR/3796.

CERTAINTY: A CELLULAR IMMUNOTHERAPY VIRTUAL TWIN FOR PERSONALISED CANCER TREATMENT

Markus Kreuz (1), Ulrike Weirauch (1), Maria Quaranta (2), Andreas Kremer (2), Stefan Franke (3), Holger Fröhlich (4), Yasamin Salimi (4), Sebastian Schwick (4), Maximilian Merz (5), Regina Demlova (6), Carl Steinbeisser (7), Kristin Reiche (1,8) on behalf of the CERTAINTY consortium

1. Fraunhofer IZI, Leipzig, Germany; 2. Information Technology for Translational Medicine, Esch-sur-Alzette, Luxembourg; 3. ICCAS, Universität Leipzig, Leipzig, Germany; 4. Fraunhofer SCAI, Sankt Augustin, Germany; 5. Myeloma Service, Memorial Sloan Kettering Cancer Center, New York, USA; 6. Faculty of Medicine, Masaryk University, Brno, Czechia; 7. Collaborate Project Management, Munich, Germany; 8. Interdisciplinary Transformation University (IT:U), Linz, Austria

1. Introduction

Adoptive cellular immunotherapy (ACI) is a novel therapy with the potential to revolutionize the treatment of cancer and other diseases but substantial challenges persist: complex manufacturing, significant toxicities, resistance mechanisms, and high costs. Virtual twins, digital patient representations integrating real-world data with computational models, enable groundbreaking personalized medicine approaches. The CERTAINTY project [1] pioneers a virtual twin (VT) ecosystem to support individualized CAR T-cell treatment strategies for relapsed/refractory multiple myeloma throughout the entire patient journey.

2. Materials and Methods

In CERTAINTY, we have assembled an interdisciplinary team of data managers, legal experts, clinicians, computer scientists, biologists, and AI specialists dedicated to the development of the ACI-VT.

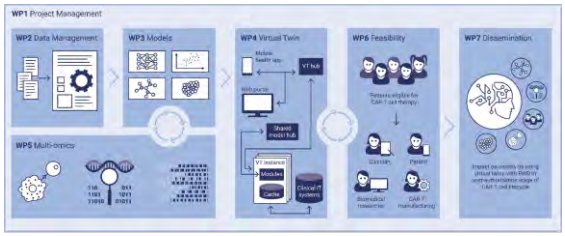


Figure 1: Schematic overview of work package organization and dependencies in CERTAINTY.

3. Results

We defined minimum design specifications for adapting VTs to "living drugs" like CAR T cell therapy, pioneering a foundational framework for ACI-VTs that simulate individual patient pathophysiology [2]. As a foundation for both VT development and predictive modelling, we are compiling patient-level data encompassing ~10,000 multiple myloma (MM) patients, with over 1,000 receiving anti-B-cell maturation antigen (BCMA) CAR T therapy in real-world settings. Analysis of 61 patients revealed superior complete response rates with cilta-cel (78% vs. 38%) and longer progression-free survival. A longitudinal single-cell multi-omics atlas of 135 samples demonstrated CD4+ cytotoxic T cell expansion associated with response and toxicity, while non-responder CD8+ T cells exhibited impaired effector function. Soluble BCMA reduction correlated with CAR T expansion and systemic inflammation, revealing mechanisms driving differential therapeutic outcomes [3]. Furthermore, we developed a model predicting individual MM progression events from routine blood work, trained on CoMMpass (N = 1,186) and externally validated in GMMG-MM5 (N = 504) [4].

4. Discussion and Conclusions

Within CERTAINTY, we curated extensive MM datasets to develop initial predictive models for clinical progression and side effects using clinical annotations and molecular data. Currently, we are advancing multi-scale mechanistic models and implementing the VT prototype. As ACI therapy expands, we envision ACI-VTs evolving in parallel to enable true precision health.

5. References

1. Reiche K, et al., Lancet Haematol. 2025 Jul;12(7):e490-e491.
2. Weirauch U, et al., NPJ Digit Med. 2025 Aug 1;8(1):493.
3. Rade M, et al., Cancer Cell. 2025 Dec 4:S1535-6108(25)00490-8
4. Ferle M, et al., NPJ Digit Med. 2025 Apr 30;8(1):231

Acknowledgements:
The CERTAINTY project is funded by the European Union (Grant Agreement 101136379).

INTEGRATION OF SINGLE-CELL RNA-SEQ DATA INTO VIRTUAL TWINS FOR MULTIPLE MYELOMA CAR-T CELL THERAPY

Christoph Kämpf* (1), Georg Popp* (1), Johannes Keller (2), Alexander Scholz (1,3), Natalja Seeger (1), Maria Quaranta (4), Romain Tching (4), Maximilian Merz (1,5,6), Stefan Franke (2), Kristin Reiche (1,3,7,8,9) on behalf of the CERTAINTY consortium

*(1) Fraunhofer Institute for Cell Therapy and Immunology IZI, Leipzig, Germany; (2) Innovation Center Computer Assisted Surgery (ICCAS), Leipzig, Germany; (3) Institute of Clinical Immunology, Medical Faculty, University of Leipzig, Leipzig, Germany; (4) Information Technology for Translational Medicine, Esch-sur-Alzette, Luxembourg; (5) Myeloma and Cellular Therapy Services, Memorial Sloan Kettering Cancer Center, New York, NY, USA; (6) Department of Hematology, Hemostaseology and Cellular Therapy, University Hospital Leipzig, Leipzig, Germany; (7) Interdisciplinary Transformation University (IT:U), Linz, Austria; (8) Center for Scalable Data Analytics and Artificial Intelligence (ScaDS.AI), Dresden, Leipzig, Germany; (9) Zuse School of Embedded and Composite AI (SECAI) Dresden-Leipzig, Germany. *Authors contributed equally.*

1. Introduction

BCMA-directed CAR-T cell therapy, an engineered adoptive cellular immunotherapy (eACI) improves outcome for relapsed/refractory multiple myeloma (MM), but patient-specific response and toxicity remain difficult to predict [1]. Virtual patient twins (VTs) are *in silico* counterparts of individual patients suitable to support treatment planning and monitoring in eACIs [1,2]. As eACIs involve living cells, it is advantageous to integrate longitudinal multi-omics data in VTs. Single-cell RNA-seq (scRNA-seq) provides per-cell gene expression data of the tumour, its microenvironment, and the CAR-T cells [1]. However, existing VT infrastructures (VTIs) lack concepts for integrating scRNA-seq datasets. We present a prototype implementation that links scRNA-seq data to a CAR-T VTI for MM.

2. Materials and Methods

The VTI includes an Observational Medical Outcomes Partnership (OMOP) Common Data Model (CDM), data-access services, and model services. Physical biosamples are presented in the OMOP-CDM `SPECIMEN` table to ensure OMOP-consistent linkage according to v5.4. ScRNA-seq datasets are integrated as custom concepts within the `OBSERVATION` table. Both tables are linked and the identifier of the external scRNA-seq object is stored. Using patient-derived PBMC scRNA-seq datasets [3], we benchmarked the data integration by processing subsets across increasing cell counts and compared different high-level container objects for scRNA-seq data matrices.

3. Results

The implementation links pseudonymized clinical patient IDs to specific scRNA-seq datasets via the `PERSON`, `SPECIMEN`, and `OBSERVATION` tables in a secure infrastructure. Benchmarks of the request handler quantify runtime and memory scaling of different high-level container objects for sparse subsetting, establishing operational thresholds for the VTI. To validate end-to-end utility, the implementation successfully extracts features from the scRNA-seq subsets. As an example, we computed the proportion of CAR^+ T cells and fed this parameter directly into a test CAR-T model within the VTI.

4. Discussion and Conclusions

We provide an OMOP-based, VT-ready implementation that integrates scRNA-seq data into a CAR-T VTI with end-to-end tests. By linking `OBSERVATION` and `SPECIMEN`, our architecture separates scRNA-seq and clinical data, while ensuring strict traceability. To support the broader community efforts, we publish our minimal vocabulary extension as an open reference implementation. Future work will align with ongoing OHDSI genomics efforts, encode features derived from scRNA-Seq in `MEASUREMENT`, and extend to single-cell multiomics assays.

5. References

1. Weirauch U et al. NPJ Digit Med. 2025.
2. Aghamiri SS, Amin R. Curr Issues Mol Biol. 2025;47:321.
3. Rade M, et al. Cancer Cell. 2025 Dec 4:S1535-6108(25)00490-8.

Acknowledgements:

The Authors thank fellow Researchers of CERTAINY. CERTAINTY was funded by the European Union under Grant Agreement number 101136379. Views and opinions expressed are those of the authors only and do not necessarily reflect those of the European Union or the Health and Digital Executive Agency.

I-OPADE: A MULTIMODAL BIOMARKER PLATFORM ENABLING DIGITAL TWIN-BASED PRECISION PSYCHIATRY

Alexandru Floares (1), Lampros Androutsos (1), Adrian Zetty (1), Sheraz Naseer (1), Maaz Mohsin (1), OPADE Group

1. Artificial Intelligence Expert SRL (AIE), Romania

Correspondence: Alexandru Floares, Artificial Intelligence Expert SRL (AIE), Romania

1. Introduction

Current antidepressant prescribing relies on trial-and-error, with remission rates below 30% after initial treatment. Digital twin approaches — integrating patient-specific multimodal data with predictive AI — offer a path toward in silico treatment optimisation. We developed i-OPADE, a cloud-based platform developed within the European OPADE project, that constructs computational patient representations from multimodal biomarkers to predict antidepressant response in Major Depressive Disorder (MDD).

2. Materials and Methods

The platform processes six data modalities through standardised pipelines: genomics, methylation, microbiome, peptide immunoprofiles, electroencephalography (EEG), and clinical parameters. Each modality contributes a distinct layer to the patient's computational representation. We adopted a unimodal-first strategy to evaluate each modality's independent predictive power before multimodal fusion. Treatment response was defined as ≥50% Hamilton Depression Rating Scale (HAM-D17) reduction at 8 weeks. Data from 150 patients across five European clinical sites were harmonised and partitioned using a 75/25% train-test split. Advanced dimensionality reduction filtered high-dimensional inputs (e.g., 789,626 methylation sites to 200 features). SHapley Additive exPlanations (SHAP) provided global feature rankings and patient-level interpretability, supporting EU AI Act transparency requirements.

3. Results

Five unimodal models demonstrated strong predictive performance. The genomic model achieved 85.7% accuracy (AUC: 85.4%), which compares favourably with published MDD prediction benchmarks (typically 70–77%). The immunoprofile model achieved 81% accuracy (AUC: 85.5%), representing, to our knowledge, the first model using peptide-based immune signatures to predict antidepressant response. Additional models — clinical (80%), methylation (78.3%), and microbiome (77%) — revealed complementary biological signals including gut-brain axis markers. SHAP analysis identified interpretable features spanning synaptic plasticity genes (CBLN1), glycosylation enzymes (CRPPA), and microbial taxa. Each validated unimodal model serves as a building block for a more comprehensive patient digital twin.

4. Discussion and Conclusions

i-OPADE demonstrates that multimodal computational patient representations can achieve clinically meaningful prediction accuracy while maintaining interpretability. The unimodal-first approach ensures each component of the patient's digital twin is independently validated before integration, avoiding black-box fusion. By establishing the predictive ceiling of each biomarker modality, this strategy enables principled construction of digital twins where every layer carries validated clinical signal. This platform provides foundational infrastructure for digital twin-based treatment selection in psychiatry, with multimodal fusion and external validation ongoing.

Acknowledgements:

This work was supported by the European OPADE (grant No. 101095436) and DTRIP4H (grant No. 101188432) projects, funded by the European Union's Horizon Europe research and innovation programme.

A DATA INTEGRATION PIPELINE COMBINING FUNCTIONAL DATA ANALYSIS WITH MULTI-LAYER CORRELATION NETWORK

Riccardo Asnaghi (1), Aurelia Morabito (1), Marta Carrara (1), Manuela Ferrario (1)
1. Department of Electronics, Information, and Bioengineering, Politecnico di Milano, Milano, Italy

1. Introduction

High-throughput technologies enable comprehensive multi-omics profiling, offering insights into complex biological systems. Modeling temporal dynamics and cross-layer interactions in multimodal longitudinal data is challenging due to sparsity, irregular sampling, and limited sample sizes. Functional data analysis (FDA) [1] converts discrete longitudinal measurements into smooth functional trajectories, while multi-layer correlation networks [2] capture system-wide interactions across biological strata. Here, we present a computational pipeline that integrates longitudinal multi-omics and clinical data by combining FDA with multi-layer networks, enabling dynamic systems-level inference despite data heterogeneity.

2. Materials and Methods

We applied the pipeline to a five-day experimental septic shock dataset of twenty anesthetized, mechanically ventilated domestic pigs randomized to sepsis or sham groups. Metabolic, clinical and cardiovascular parameters were measured up to 72 hours post-resuscitation [3,4]. Longitudinal measurements were transformed into smooth functional representations using B-spline basis expansions. Dynamic correlation in FDA assesses how the relationship between two functional processes changes across the time, capturing time-varying associations. This analysis identified variables with similar temporal patterns within each group, with significance controlled via Benjamini–Hochberg false discovery rate (FDR, $\alpha = 0.05$). Significant associations were used to construct group-specific multi-layer networks, which were analyzed using centrality measures (e.g., betweenness, closeness, degree, strength, clustering coefficient) and network similarity metrics (e.g., Euclidean, weighted Jaccard, DeltaCON).

3. Results

The sham network exhibited a densely clustered topology (218 edges), whereas the sepsis network had only 112 edges, reflecting connectivity loss, especially in metabolic interactions and intra-layer links. Centrality measures were significantly reduced in sepsis ($p<0.05$), except for betweenness centrality, indicating diminished network integration. Low similarity scores (Euclidean distance = 16, w. Jaccard similarity = 0.1, DeltaCON = 0.341) confirmed topological reorganization under septic conditions.

4. Discussion and Conclusions

Node-level analysis highlighted proline and asymmetric dimethylarginine (ADMA) as key contributors to network restructuring. Edge-level disruptions involved fluid balance versus urine output and metabolic ratios (citrulline/glutamate and glycine/glutamate). These changes indicate shifts in energy metabolism, protein mobilization, endothelial function, and renal/hemodynamic stress during systemic inflammation. The results obtained in this study are consistent with those from previous studies that analyzed metabolomic and hemodynamic data separately [4].

The pipeline successfully integrates heterogeneous longitudinal datasets, providing a robust framework to identify dynamic biomarkers of systemic dysregulation.

5. References

1. J. A. Dubin and H.-G. Müller, J. Am. Stat. Assoc., vol. 100, no. 471, pp. 872–881, Sep. 2005.
2. Z. Hammoud, and F. Kramer, Big Data Anal., vol. 5, no. 2, 2020.
3. M. Carrara et al., Sci. Rep., vol. 12, no. 1, p. 19279, Nov. 2022.
4. M. Ferrario et al., Sci. Rep., vol. 11, no. 1, p. 18430, Sep. 2021.

BIOMECHANICAL EFFECT OF PERCUTANEOUS PULMONARY VALVE POSITIONING IN PATIENT-SPECIFIC MODELS

Mariachiara Arminio (1), Diego Gallo (1), Dario Carbonaro (1,2), Rodrigo Paz (3,4), Facundo Del Pin (3), Umberto Morbiducci (1), Silvia Schievano (5), Claudio Chiastra (1), Claudio Capelli (5)

1. Politecnico di Torino, Turin, Italy; 2. University of Calabria, Rende (CS), Italy; 3. Ansys/Synopsys, Inc., Livermore, California, USA; 4. CONICET, National Council for Scientific and Technical Research, Argentina; 5. University College London & Great Ormond Street Hospital for Children, London, UK

1. Introduction

Percutaneous pulmonary valves (PPVs) are implanted to restore pulmonary valve functionality in patients with congenital heart disease [1]. The effect of PPV positioning on the long-term functioning of the device remains an open clinical question [2]. Fluid-structure interaction (FSI) simulations enable the investigation of PPV mechanics, blood flow patterns, and their interaction. In this study, FSI simulations are employed to assess the impact of valve orientation and implantation height on device biomechanics in patient-specific scenarios.

2. Materials and Methods

Data from four patients who underwent PPV implantation at our Centre were retrospectively collected. Geometric models of the right ventricular outflow tract and pulmonary arteries (PAs) were reconstructed from computed tomography images. A geometric model of the Melody (Medtronic) PPV was created in SolidWorks (Dassault Systèmes). Valve leaflets were positioned within the patient-specific models to match the image-derived implantation height and native valve leaflet orientation (scenario N), as shown for a representative case in Fig. 1A. Additional simulation scenarios were generated by introducing a 90° (R_{90}) and 180° (R_{180}) leaflet rotation, and lowered implantation height (H), Fig. 1B. The models were meshed in HyperMesh (Altair). FSI simulations were performed by coupling the LS-DYNA (Ansys/Synopsys Inc.) ICFD and implicit structural solvers. Patient-specific flow-rate waveforms (Q) and resistances (R) were imposed at the inflow and outflow sections, respectively, Fig. 1A. The PA wall was assumed as rigid, whereas the PPV leaflets were modelled as linear elastic.

3. Results

PPV orientation and implantation height did not qualitatively alter PA flow patterns. However, non-native leaflet orientations led to a more intense vortex production compared to the native orientation, with a 19% average increase in vorticity stretching in the representative patient. Moreover, a lower implantation height, preventing PPV stent protrusion into the pulmonary bifurcation, resulted in less complex local flow patterns and higher projected orifice area (with a 30% peak systolic increase in the representative patient), Fig. 1C.

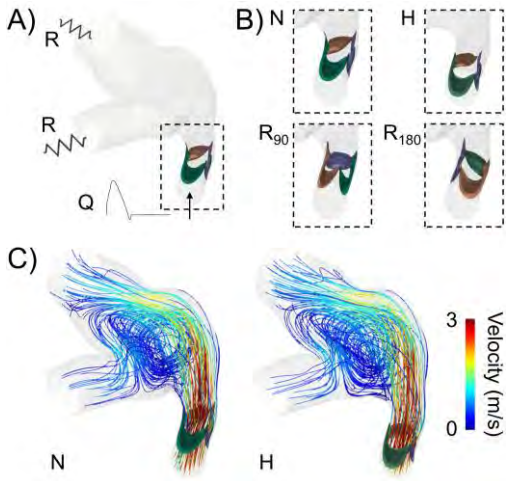


Figure 1: A) Set up for the FSI simulations, B) leaflet position in the considered scenarios, C) peak-systolic velocity streamlines for scenarios N and H.

4. Discussion and Conclusions

The proposed FSI approach enables patient-specific investigation of PPV biomechanics under operating conditions characterized by different PPV positions. As such, it represents a powerful tool for optimizing device implantation and, ultimately, improving procedural outcomes.

5. References

1. Chau AK, Pediatr Investig; 6(4):280-290 (2022).
2. Schiavone NK et al., Cardiovasc Eng Tech; 16: 138-153 (2025).

PATIENT-SPECIFIC COMPUTATIONAL FLUID DYNAMICS BEFORE AND AFTER TRANSCATHETER AORTIC VALVE IMPLANTATION

Laura Bevis (1), Yousaf Bhatti (2), Elisa Rauseo (1,2), Elias Karabelas (3,4), Xu Chen (1), Richard Burns (1), Abbas Khan (1), Steffen E Petersen (1), Christoph M Augustin (4), Aurel Neic (3), Gernot Plank (3,4), Caroline H Roney* (1), Gregory Slabaugh* (1), Anthony Mathur* (1,2)

*1. Queen Mary University of London, UK; 2. Barts Health NHS Trust, UK; 3. Numericor Gmbh, Austria; 4. BioTechMed-Graz, Austria; 5. Medical University of Graz, Austria. *Joint senior author.*

Corresponding author: Laura Bevis, l.bevis@qmul.ac.uk

1. Introduction

Aortic stenosis (AS), a restriction of the aortic valve, reduces blood flow to the body and is fatal if left untreated. Transcatheter Aortic Valve Implantation (TAVI) has become a standard, minimally invasive treatment for select patients with AS. As its use expands to lower-risk patients with longer life expectancies, TAVI durability holds increasing importance [1]. Digital twins using Computational Fluid Dynamics (CFD) can provide insights into turbulent blood flow patterns in the aortic root, which can impact long-term performance, thrombus formation, and device longevity. Co-development with the Heart Team ensures clinical relevance, alignment with clinical workflows, and optimisation of existing rich clinical datasets.

2. Materials and Methods

A previously developed pipeline [2], co-designed with the clinical team, was used to generate standardised patient-specific CFD models and boundary conditions from routine pre-TAVI computed tomography (CT) and pre- and day one post-TAVI transthoracic echocardiography (TTE) data. Using strict exclusion criteria to ensure data standardisation, minimisation of uncertainty, and adherence with model assumptions, 8 retrospective clinical cases with consistent data quality, availability, and imaging timeframes, were selected. Blood flow was simulated before and one day after TAVI using a residual-based variational multiscale solver, and the resultant flow patterns analysed [3].

3. Results

A clean, high-quality dataset of retrospective TAVI cases was designed and curated, providing a critical resource for CFD modelling. Patient-specific models of the 8 cases were generated and high-resolution blood flow simulations successfully conducted in line with established TAVI workflows and clinical guidelines (Figure 1). Post-TAVI conditions led to reduced vorticity and helicity downstream of the valve, matching clinical experience (30% and 50% on average, respectively).

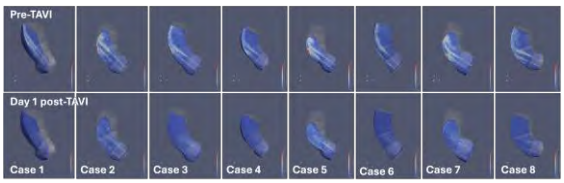


Figure 1: Phase-averaged helicity in 8 patients before and after TAVI.

4. Discussion and Conclusions

Overall, we collaboratively: i) developed a pipeline to simulate turbulent aortic flow in patients undergoing TAVI, ii) curated a high-quality retrospective dataset for CFD modelling, and iii) analysed blood flow pre- and post-TAVI in 8 patient-specific cases. Further analysis against clinical outcomes will enable detailed assessment of the impact of turbulent flow patterns on real-world events.

5. References

1. Praz F et al. (2025), EJCTS; 67:ezaf276.
2. Bevis L et al. (2026), CinC 2025, 52.
3. Fuchsberger J et al. (2022), J Comput Sci; 57:101506.

Acknowledgements:

The authors acknowledge the ARCHER2 UK National Supercomputing Service, and support from UKRI Future Leaders Fellowship (MR/W004720/1). This work forms part of the research portfolio of the National Institute for Health Research Barts Biomedical Research Centre (NIHR203330).

TOWARDS PATIENT-SPECIFIC VENTRICLE-TAVI INTERACTION: A VALIDATED ELECTROMECHANICAL MODEL OF LEFT VENTRICLE

Benedetta Grossi (1,2,3), Ludovica Cestariolo (3), Carlo Boccaperta Schiavetti (3), Tommaso Casini (3), Letizia Maria Perri (1,3), Giulio Stefanini (1,2), Gianluigi Condorelli (1,2), Giulia Luraghi (3), Francesco Migliavacca (3,4), José Félix Rodriguez Matas (3)

1. Humanitas University, Italy; 2. Humanitas Research Hospital, Italy; 3. Politecnico di Milano, Italy; 4. Fondazione IRCCS Cà Granda Ospedale Maggiore Policlinico, Italy

Corresponding author: Benedetta Grossi (benedetta.grossi@humanitasresearch.it), Humanitas University, Italy.

1. Introduction

Transcatheter Aortic Valve Implantation (TAVI) is a minimally invasive treatment for aortic stenosis. Despite its growing adoption, the onset of conduction disturbances remains a major clinical concern [1]. These complications arise from the mechanical interaction between the implanted device and the patient's conduction system, with reported incidence up to 35% [1]. However, their occurrence remains largely unpredictable, highlighting the need for patient-specific (PS) models to provide mechanistic understanding and predictive insights. In this context, this study presents the development and clinical validation of a PS electromechanical (EM) model of the left ventricle (LV), with the ultimate goal of paving the way for integration with finite element TAVI simulations for PS risk prediction.

2. Materials and Methods

Left ventricular geometry of a patient who underwent ventricular electroanatomical mapping (EAM) was reconstructed from CT images, and discretized into a high-resolution hexahedral mesh (HM, Δx=0.4mm) and a coarser tetrahedral mesh (TM, Δx=1.5mm), to assess the influence of mesh resolution on simulated electrical propagation. Myocardial fibre architecture was assigned using the Laplace–Dirichlet rule-based method [2], and the Purkinje network was generated using a fractal growth algorithm implemented within the LsDyna software [3]. Electrophysiological (EP) simulations were conducted on both meshes using a monodomain formulation, while EM simulations were performed on the TM only, using a hyperelastic constitutive law including calcium-driven active stress. EP validation compared simulated activation patterns, conduction velocity (CV), and activation times (AT) with clinical EAM data. Mechanical validation was conducted by comparing computed functional indicators with echocardiographic data.

3. Results

Endocardial activation patterns showed good overall agreement with clinical EAM data. CV was 0.663 ± 0.020 mm/ms for the TM and 0.590 ± 0.030 mm/ms for the HM, compared to 0.605 ± 0.020 mm/ms measured clinically. Global AT was accurately reproduced, with values of 156.1 ms (TM) and 163.8 ms (HM) versus 160 ms from EAM (2.4% error). Local AT comparison showed root mean square error values of 14.3 ms and 11.6 ms for TM and HM, respectively, confirming reliable electrical propagation. EM simulations yielded functional parameters consistent with the patient's systolic condition: simulated end-diastolic volume (163 mL) and ejection fraction (35%) closely matched echocardiographic data (150 mL; 33%).

4. Discussion and Conclusions

The proposed framework successfully integrates electrophysiology and mechanics into a fully PS EM model of the LV, achieving good quantitative agreement with clinical EAM and functional measurements. This approach provides a robust platform for personalized cardiac modelling and represents a promising tool to investigate post-TAVI conduction disturbances, with potential implications for PS risk prediction and procedural planning.

5. References

1. Winter et al., Sci Rep, 10:15568, 2020.
2. Bayer et al., Ann Biomed Eng, 40:2243–54, 2012.
3. Sahli Costabal et al.,J Biomech, 49:2455–65,2015.

Acknowledgements:
B.G., L.M.P., G.L. and F.M. are supported by the European Research Council (ERC, project PROTEGO, G.A. 101162753).

IN-SILICO HEMODYNAMIC MODEL FOR THE ASSESSMENT OF MITRAL REGURGITATION QUANTIFICATION METHODS

Irea Vervaeke (1), Joris Degroote (2, 3), Annette Caenen (1, 4), Patrick Segers (1)

1. IBITECH-BioMMedA, Department of Electronics and Information Systems, Ghent University, Belgium
2. Department of Electromechanical, Systems and Metal Engineering, Ghent University, Belgium
3. Flanders Make-MIRO, Ghent, Belgium
4. Department of Cardiovascular Sciences, KU Leuven, Belgium

Corresponding author: Irea.Vervaeke@UGent.be

1. Introduction

Mitral valve regurgitation (MR) is the most common valvular disease, characterised by incomplete closure of the mitral valve. Leak severity can be quantified by the effective regurgitant orifice area (EROA) and regurgitant volume (RVol), which can be assessed using echocardiographic methods. However, current guidelines recommend confirming these findings using an integrative approach. The aim of our work is to develop an in-silico framework to enhance ultrasound-based MR quantification.

2. Materials and Methods

A geometrically idealized 3D computational fluid dynamics (CFD) model of the left heart was created, based on average adult dimensions (Fig 1A). A constant pressure inlet of 10 mmHg was applied at the pulmonary veins; for the aorta, an outlet pressure of 100 mmHg was assumed in systole, and a wall was imposed at the aortic valve in diastole. The mitral valve was modelled as a time-varying truncated cone; with opening and closing times set to 50ms. To simulate a mild and severe MR case, the leakage area was set to 20 and 43 mm², respectively. Blood flow was actuated by prescribed left ventricular (LV) wall motion, reducing end-diastolic volume (126 mL) by a stroke volume (SV) of 81 ml (ejection fraction of 55%).
The mesh consisted of about 500k tetrahedral elements and was remeshed when the skewness of elements exceeded 0.95 and the orthogonality dropped below 0.1. Four cardiac cycles of 1s were simulated in ANSYS Fluent, assuming laminar incompressible flow.

3. Results

Fig 1A shows a large central jet forming in the left atrium during systole, reaching peak velocities of about 4.70 m/s for both cases. Additionally, flow reversal occurs in the pulmonary veins. The RVol reached 24.79 mL and 34.53 mL for mild and severe MR, respectively (Fig 1B).

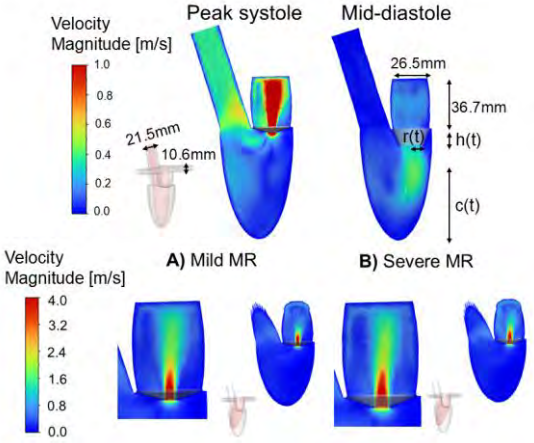


Fig 1: Velocity fields for (top) the fourth cardiac cycle in mild MR, (bottom) peak systole in mild (A) and severe (B) MR.

4. Discussion and Conclusions

Under the imposed boundary conditions, mild and severe MR show similar flow fields and velocities, but a larger leakage area increases backward flow into the left atrium. However, the simulated RVol remains below the severe threshold reported in recent guidelines, likely reflecting model simplifications and unmodeled compensatory changes in LV volume and SV with MR. Future work will incorporate more realistic anatomy and boundary conditions to better represent severe MR. Nevertheless, the moving-boundary approach enables physiologically realistic simulations of left ventricular fluid dynamics and regurgitant jet formation throughout the cardiac cycle.

Acknowledgements:
This work was supported by the Research Foundation Flanders (FWO) under the Strategic Basic Research program S009226N.

AN IN-SILICO STUDY ON THE IMPACT OF INDIVIDUAL GEOMETRICAL FEATURES FOR PREDICTING HEART VALVE FUNCTION

Pavlo Yevtushenko (1), Katharina Vellguth (1), Leonid Goubergrits (1), Marie Schafstedde (1,2)

1. Charité-Universitätsmedizin Berlin, Germany; 2. Berlin Institute of Health, Germany

1. Introduction

Abnormalities in heart valve shape and size, either being congenital or acquired through disease, naturally compromise the heart's function and can ultimately lead to heart failure if left untreated. Several approaches exist to relate valve shape to valve function in order to aid diagnosis and treatment planning, ranging from simple planar measurements to complex three-dimensional hemodynamic simulations. The latter, however, are rather unfeasible for a clinical application given their complex nature and simpler methods for assessing valve function are desirable. To this end, this study evaluates the impact of various geometric parameters on aortic and mitral valve function for patients with heart valve diseases.

2. Materials and Methods

Utilizing statistical shape models (SSM) of diseased mitral (MV) and aortic valves [1] (AV), a large set of geometries covering a wide range of anatomical features was created. These geometries were then used to perform hemodynamic simulations, producing valve-specific flow-pressure curves which characterize the hemodynamic function of each valve. 500 MV and 1100 AV simulations were performed in total, characterizing approx. 200 mitral and 300 aortic valves.

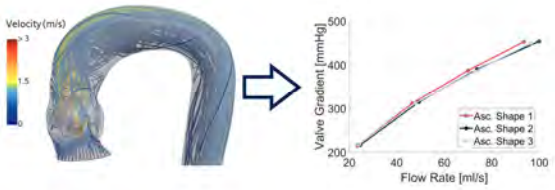


Figure 1: Exemplary fluid dynamic simulation result (left) and valve characteristic curves for different ascending aorta shapes (right).

Using this geometric and hemodynamic data, a feed-forward network (FFN) was trained to predict valve function from a set of basic geometry features, such as annulus diameter, opening area and valve plane orientation.
After achieving sufficient accuracy on the base-line network, ablation studies were performed to identify the most impactful features, hypothesizing that omitting features which are not important for valve function would not negatively impact the FFN's performance. In addition, random errors were added to input features to test feature sensitivity.

3. Results

For both valves, orifice area had the highest impact on the FFN's accuracy, whereas annulus sizes and leaflet areas contributed little to the predictive capability. For most AV cases, the shape and size of the ascending aorta had a negligible effect on AV function, although some cases exhibited a pronounced dependence on ascendens geometry.

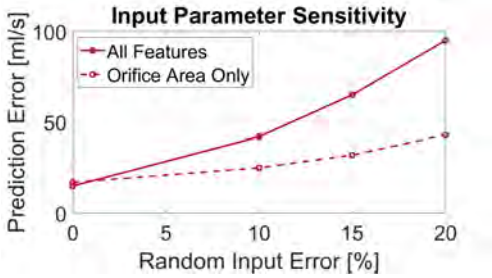


Figure 2: Error sensitivity for MV regurgitation

Random errors in the input data degraded prediction performance as expected, however, the relationship between input uncertainty and output error was found to be non-linear. Moreover, FFN's using large sets of input features degraded quicker than those only using a few features (Fig. 2).

4. Discussion and Conclusions

The results identified key geometrical features which could aid the development of computationally manageable valve function modelling with e.g. machine learning methods. More work is ongoing to assess the importance of aortic shape as well as to identify interaction effects.

5. References

1. Verstraeten S, et al. Generation of synthetic aortic valve stenosis geometries for in silico trials. Int J Numer Method Biomed Eng. 2024 Jan, doi: 10.1002/cnm.3778

PATIENT-SPECIFIC HAEMODYNAMIC DIGITAL TWIN WITH PATHOLOGICAL VALVE DYNAMICS

Antonio José Escobar (1), Omar Chehab (1,2), Tiffany Patterson (1,2), Jack Lee (1)

1. School of Biomedical Engineering & Imaging Sciences, King's College London, United Kingdom; 2. St Thomas' Hospital, United Kingdom

1. Introduction

In valvular heart disease, stenosis and regurgitation reshape pressure–volume relationships, so capturing pathological valve behaviour is central to creating a faithful model. Many lumped parameter model implementations represent valves as simple diode-like elements, enforcing idealised flow and failing to reproduce these pathological dependencies. As a step towards a patient-specific haemodynamic digital twin, we investigated whether patient-specific lumped parameter models can reproduce invasive haemodynamics in mitral regurgitation, and whether a pathology-capable dynamic valve formulation improves agreement over traditional diode-like valves.

2. Materials and Methods

We developed a closed-loop lumped parameter model representing a four-chamber heart driven by time-varying elastance coupled to systemic and pulmonary circulations. To isolate the impact of valve physiology, two valve representations were implemented: (i) a conventional diode valve enforcing idealised one-way flow, and (ii) a pathology-capable dynamic valve model[1], in which effective orifice area varies as a state variable between parameterised open and closed valve areas, enabling representation of both stenotic restriction and regurgitant leakage. Patient-specific parameter estimation was performed by fitting the model to invasive pressure and volume waveforms from mitral regurgitation patients, providing a strong validation for haemodynamic modelling. To define the estimable parameter set, sensitivity analysis was used to identify parameters that should be fixed, while structural identifiability analysis was used to determine how many parameters could be reliably left free without making the model underdetermined. The resulting reduced parameter subset and priors were then used for Markov chain Monte Carlo fitting (random-walk Metropolis).

3. Results

The dynamic model achieved a lower PV-shape NRMSE than the diode baseline (0.077 vs 0.095). Visually, it also reproduced the observed pressure–volume trajectory more closely, whereas the diode model produced a more rectangular loop. Agreement with echo-derived regurgitant fraction and outflow metrics was also improved across the cohort (n=13). The model reduced percentage error in key haemodynamic indices, including LV ejection fraction (4.9% vs 20.4%), stroke volume (2.5% vs 24.6%), and LV dP/dt_max (12.4% vs 39.0%) relative to the diode baseline.

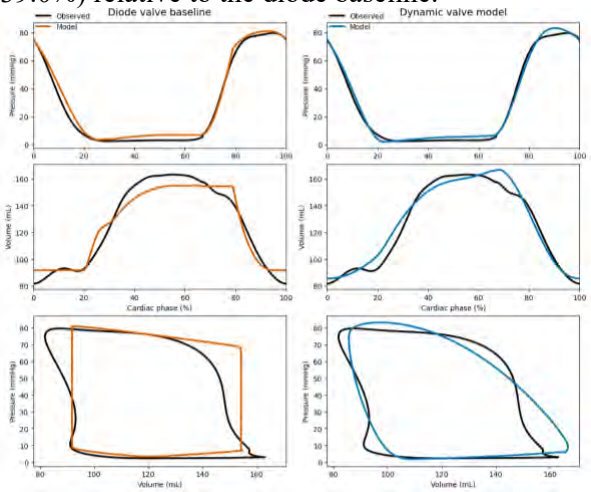


Figure 1: Patient-specific fit for a mitral regurgitation case.

4. Discussion and Conclusions

The results show that, in mitral regurgitation patients, a pathology-capable valve formulation improves patient-specific agreement with invasive waveforms and key haemodynamic indices compared with a diode-valve baseline. Because valve disease is represented modularly through parameterised open and closed valve areas, the formulation also provides a flexible basis for future work investigating predictive capabilities in patient-specific digital twin applications.

5. References

1. Mynard JP, Davidson MR, Penny DJ, Smolich JJ. Int J Numer Methods Biomed Eng. 2012;28(6-7):626-641

A MITRAL VALVE DIGITAL TWIN FOR SURGICAL PLANNING

Michael Sacks

Willerson Center for Computational Cardiology

Oden Institute for Computational Engineering and Sciences, Department of Biomedical Engineering
University of Texas at Austin, USA

1. Introduction

Mitral regurgitation (MR) is the most common valvular disease in the United States affecting over 2% of the population and is expected to double by 2030 due to population aging. MR is a major prognostic factor of mortality: the risk of mortality with severe MR at five years is 36% and even moderate MR nearly doubles the risk of mortality in patients with multiple cardiac comorbidities [1]. MV repair has been popular as the techniques are safe and improves patient outcomes. However, its efficacy has been unclear, with the outcomes largely dependent on MR etiology, MR severity, and existing comorbidities. These critical limitations coupled with contradictory clinical trial findings strongly emphasize the need for a patient-specific approaches.

A critical component of patient-specific predictive MV simulations is the implementation of patient-specific mechanical properties. However, these properties are impossible to discern directly from standard-of-care transesophageal echocardiographic imaging, so we have developed a method to calibrate the functionally equivalent properties such that we are ultimately able to accurately *predict* the post-repair state.

2. Materials and Methods

First, we developed a finite-element model of the full, patient-specific MV apparatus [4]. As the MV chordae tendineae (MVCT) are not typically visible on standard-of-care transesophageal echocardiography (TEE), we quantified the MVCT insertions and origins from 5 CT-imaged excised human hearts. Then, we segmented the MV leaflet geometries and papillary muscle (PM) positions for 5 patients from their *preoperative* TEE images. By mapping the population-averaged MVCT insertion density map onto the patient leaflet geometries, we were able to generate patient-specific full MV apparatus models that incorporated both the leaflets and MVCT network.

For preoperative leaflet closure, we defined the segmented end-diastolic (ED) to end-systolic (ES) annular and PM displacements as boundary conditions and applied a ventricular pressurization. Given that patient-specific material properties are impossible to obtain from TEE imaging, we calibrated the tissue material model by iteratively adjusting MV leaflet and MVCT prestrains such that the change in l^2-norm between the simulated and segmented preoperative ES geometries was less than 5%.

3. Results

With the fully calibrated preoperative MV apparatus model, we were able to *predict* the post-TEER ES geometry to within a millimeter and closely match the leaflet strain patterns when compared to simulations that directly applied postoperative boundary conditions, which validates our calibration protocol for the mechanical properties.

4. Discussion and Conclusions

Herein, we have presented an approach for *predicting* the postoperative state of the MV apparatus both immediately after repair and at 3 months post-repair using standard-of-care, preoperative clinical imaging alone. This pipeline allows us to quantitatively interrogate the impact of the repair procedure on MV behavior, such as shifts in deformation and nonphysiological stress concentrations. Once such methods are integrated into the clinical pipeline, the altered post-repair MV state can be routinely predicted and we can elucidate mechanistic drivers of repair failure, which constitute key targets for optimized treatment durability and efficacy. Such approaches will define the elements of a full MV digital twin for each patient.

5. References

[1] Enriquez-Sarano, M, et al., New Engl J Med, 352(9):875-83, 2005.
[2] Rego, BV, et al., Ann Biomed Eng, 51(1):71-87, 2023.
[3] Ayoub, S, et al. J Roy Soc Interface, 14(135):21070580, 2017.

Acknowledgements: NIH R01HL184128

UNCERTAINTY AND SENSITIVITY IN VENOUS MODELLING ACROSS 0D, 3D AND STATISTICAL SHAPE FRAMEWORKS

Magdalena Otta (1,2), Karol Zając (1), Ian Halliday (2), Chung Lim (3), Janice Tsui (3,4), Maciej Malawski (1,5), Andrew Narracott (2)

1. Sano Centre for Computational Medicine, Poland; 2. University of Sheffield, UK; 3. Royal Free Hospital, UK; 4. University College London, UK; 5. AGH University of Kraków, Poland

1. Introduction

The reliability of predictive simulations in vascular medicine depends critically on quantification of uncertainty, yet this remains insufficiently addressed, particularly in patient-specific workflows where data limitations, anatomical variability and modelling assumptions interact. This work synthesises four studies spanning 0D modelling, 3D patient-specific CFD, inflow variability and statistical shape modelling (SSM) in the context of deep vein thrombosis (DVT), targetted at translation within the existing clinical patient pathway.

2. Materials and Methods

Sensitivity of a 0D model [1] of lower limb circulation was quantified using local derivatives, Sobol indices and orthogonal measures to assess influence of anatomical perturbations on key flow metrics. For 3D CFD, we evaluated how geometric variability from segmentation choices influences wall shear stress localisation [2] and inflow perturbations were used to characterise downstream flow variability. Anatomical uncertainty was further assessed using a statistical shape modelling (SSM) framework constructed from venous geometries of 12 patients, with principal modes in 2D and 3D examined for their haemodynamic impact [3].

3. Results

Across scales, uncertainty quantification revealed substantial, nonlinear effects on haemodynamic predictions. In the 0D network, flows in the iliofemoral segment were dominated by the common, external and internal iliac radii with Sobol indices capturing nonlinear interactions. With patient-specific 3D CFD, geometric variability from segmentation produced larger changes in the size and location of lowWSS and highOSI regions than inflow perturbations. Inflow perturbations of ±20% and controlled changes in junction angle and curvature systematically altered lowWSS and highOSI distributions. Use of an SSM approach demonstrated flow metrics were consistently affected by shape perturbation, although anatomies produced assuming only angiography data was available estimated larger lowWSS areas than anatomies produced using volumetric MRI imaging data. and the choice of shape alignment influenced interpretation of shape modes in 2D and 3D.

4. Discussion and Conclusions

Without uncertainty bounds, deterministic simulations can overestimate the clinical utility and reliability of predictions; differences arising from segmentation limit the accuracy of patient-specific results while statistical shape analysis captures anatomical variability in a structured way. Overall, modelling workflows which aspire to clinical reliability can productively evolve by leveraging the range of uncertainty and sensitivity checks considered in this work.

5. References

1. Otta et al. *Sensitivity analysis of a model of lower limb haemodynamics* (doi: 10.1007/978-3-031-08757-8_7)
2. Otta et al. *Towards sensitivity analysis: 3D venous modelling in the lower limb* (doi: 10.1007/978-3-031-97557-8_8)
3. Otta et al. *Iliac vein morphology and wall shear stress* (doi: 10.64898/2026.02.17.706277) **preprint**

Acknowledgements:

This project has received funding from the European Union's Horizon 2020 research and innovation programme under grant agreement No 857533 and was conducted within the project of the Minister of Science and Higher Education "Support for the activity of Centers of Excellence established in Poland under Horizon 2020" on the basis of the contract number MEiN/2023/DIR/3796 and is supported by Sano project carried out within the International Research Agendas programme of the Foundation for Polish Science, co-financed by the European Union under the European Regional Development Fund. A part of this work was supported by the National Science Centre (NCN) under Preludium'22 grant agreement UMO-2023/49/N/ST6/04252. We acknowledge the Polish high-performance computing infrastructure PLGrid (HPC Center: ACK Cyfronet AGH) for providing computer facilities and support within computational grant no. PLG/2024/017108 and PLG/2025/018168.

TOWARDS HEPATIC DIGITAL TWINS: MULTISCALE-MULTIPHYSICS MODELING AND VALIDATION OF LIVER REGENERATION

Jannes Hohl, Adnan Ebrahem, Etienne Jessen, Dominik Schillinger

Institute for Mechanics, Computational Mechanics Group, Technical University of Darmstadt, Germany

1. Introduction

Liver regeneration after partial hepatectomy (PHx) restores organ mass and function through hemodynamic adaptation, vascular remodeling, and hepatocyte proliferation. Computational models of this process are increasingly explored as components of digital twins for hepatic surgery, but require rigorous verification and validation. Here, we present a multiscale-multiphysics model of liver regeneration and assess its predictive capability using longitudinal µCT data from murine partial hepatectomy.

2. Materials and Methods

The proposed framework integrates vascular architecture, tissue perfusion, and mechanobiological growth within a multiscale computational model of liver regeneration. A multiscale perfusion model combines optimization-based synthetic vascular tree generation with a multicompartment homogenized flow formulation [1,2]. Tissue deformation and growth are described using a finite-growth formulation acting on both the liver parenchyma and the embedded vascular network. The local volumetric growth factor evolves according to hyperperfusion-driven growth stimuli [3].

Model calibration and validation are performed using longitudinal µCT-based three-dimensional reconstructions of male C57BL/6J mice (n = 5) undergoing 70% partial hepatectomy, with imaging acquired before surgery and at days 4, 8, 14, and 21 [4]. Predictive capability is assessed using leave-one-out cross-validation. Quantitative comparisons assess organ-scale volume recovery, spatial growth patterns, and major vessel remodeling.

3. Results

Quantitative comparisons with µCT reconstructions show good agreement in total liver volume recovery and the spatial distribution of growth, resulting in realistic predictions of organ shape evolution during regeneration, see Fig. 1. Cross-validation demonstrates predictive capability for regeneration dynamics and liver morphology in unseen subjects.

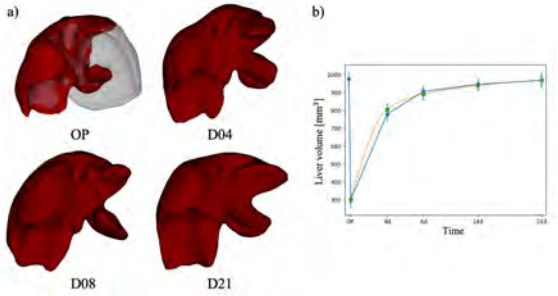


Figure 1: a) 3D reconstructions of the regenerating mouse liver at selected time points after PHx and b) quantitative liver volume recovery over time.

4. Discussion and Conclusions

The presented approach provides a multi-scale model of liver regeneration that links vascular hemodynamics to tissue growth. Validation against longitudinal µCT data demonstrates the capability of the model to predict organ-scale regrowth and shape evolution after PHx. These results support the credibility of the framework and represent a step toward a digital twin in hepatic surgery. However, several developments remain necessary before such models can serve as digital twins, including the integration of metabolic liver function, biochemical regulation, and pathological processes such as fibrosis, steatosis or tumor growth.

5. References

1. Jessen E, Steinbach MC, Schillinger D, IEEE Trans. Biomed. Eng.; 72:2871-2881 (2025).
2. Hohl J et al., Biomech. Model. Mechanobiol.; 25:10 (2026).
3. Ebrahem A et al., J. Mech. Phys. Solids; 200:106113 (2025).
4. Zafarnia S et al., Front. Physiol.; 10:904 (2019).

Acknowledgements:

This work was supported by the European Research Council (ERC) through the European Union's Horizon 2020 Research and Innovation Programme under Grant 759001, achieved as part of the ERC Starting grant Project 'ImageToSim'.

CORONARY DIGITAL TWIN GENERATION FROM ULTRA HIGH-RESOLUTION PHOTON-COUNTING CT: AN ITERATIVE APPROACH

Andrea Arcangeli (1), Katia Capellini (1), Alberto Aimo (2), Michele Emdin (2), Mariaelena Occhipinti (3), Matilda Muca (3), Francesca Pignatelli (3), Alberto Clemente (3), Vincenzo Positano (1), Simona Celi (1), Carmelo De Gori (3)

1. Bioengineering Unit, Fondazione Monasterio, Italy; 2. Cardiology and Cardiovascular Medicine Fondazione Monasterio, Italy; 3. Department of Radiology, Fondazione Monasterio, Italy

1. Introduction

Ultra high-resolution (UHR) photon-counting CT (PCCT) provides unprecedented spatial detail for coronary imaging [1], enabling patient-specific digital twin modelling. However, lumen segmentation from UHR coronary CT angiography (CCTA) remains challenging and time-consuming. We propose an iterative segmentation framework that progressively expands the dataset while reducing operator workload, enabling high-fidelity coronary lumen modelling.

2. Materials and Methods

A semi-automatic pipeline was developed for coronary lumen segmentation and patient-specific coronary modelling from 14 UHR PCCT CCTA image datasets (matrix 1024x1024, 1000-1300 slices, slice thickness 0.10 mm). The pipeline followed an iterative strategy. At each iteration, labeled data (LD) were used to train a model, while unlabeled data (UD) were segmented. Each iteration consisted of the following steps:

1. A nnU-Net ResEnc model was trained using LD.
2. Initial lumen masks for UD were generated using the trained model.
3. Systematic refinement was performed through a multi-step Geodesic Active Contour (GAC) procedure (shrinking, plaque thresholding, skeleton-based re-expansion), requiring empirical parameter tuning.
4. Final manual correction was performed in 3D Slicer.

In the first iteration, LD were obtained from the public ImageCAS dataset [2], while in subsequent iterations LD produced by the previous iteration were used.

3. Results

Seven PCCT UD were processed in the first iteration, obtaining 7 LD used as LD input for the second iteration. The processing time was about 5 hours. In the second iteration (task 1), the nnU-Net ResEnc model trained using leave-one-out (LOO) cross-validation (CV) achieved a mean Dice coefficient of 0.70 ± 0.07 for lumen segmentation. GAC was not needed thanks to the quality of the model segmentation. The processing time was ~30 minutes. A total of 14 LD (7 from the first iteration and 7 from the second) were used as input for the third iteration. In the third iteration, the nnU-Net ResEnc model achieved a Dice of 0.74 ± 0.04 (Fig. 1B), using the same LOO CV scheme on the 7 subjects from the second iteration and preserving the same validation patient. The processing time was comparable to the second iteration, resulting in a ~90% reduction in operator time at the second and third iterations (Fig. 1A-C).

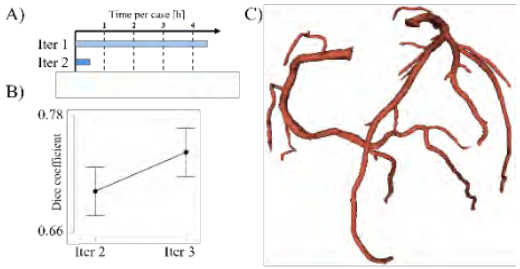


Figure 1: Processing time (A), nnU-Net performance (B), UHR lumen segmentation (C).

4. Discussion and Conclusions

The iterative framework reduced manual workload by ~90% while preserving accurate lumen segmentation, enabling quantitative analysis and computational simulations.

5. Reference

1. Meloni, A., et al., Cardiovascular diagnosis and therapy. 2024; 14(4), 698-724.
2. Zeng, A. et al., Computerized Medical Imaging and Graphics; 109(2023).

Acknowledgements:

This work was supported by the ACTA Study (Project 297/22 - CUP J59I24002760007) funded by Fondazione Pisa.

MICROSTRUCTURE-DRIVEN IN SILICO MACHINE LEARNING MODEL FOR PHOTOACOUSTIC THROMBUS CHARACTERIZATION

Hamed Ghodsi (1), Sid Kumar (2), Behrooz Fereidoonnezhad (3), Sophinese Iskander-Rizk (1)

1. Department of Precision and Microsystems Engineering, Faculty of Mechanical Engineering, Delft University of Technology, Delft, The Netherlands;
2. Department of Materials Science and Engineering, Delft University of Technology, The Netherlands;
3. Department of BioMechanical Engineering , Faculty of Mechanical Engineering, Delft University of Technology, The Netherlands;

1. Introduction

Mechanical thrombectomy, the gold standard treatment for acute ischemic stroke, still faces procedural failures due to limited pre-operative knowledge of thrombus characteristics [1]. Improved clot characterization could enhance treatment planning and device selection. Photoacoustic microscopy offers a promising label-free approach for intravascular thrombus assessment. We present a multiscale, microstructure-driven in silico pipeline for 3D thrombus modelling that generates heterogeneous clot models with varying compositions and porosities to train machine learning models for predicting red blood cell (RBC) content, porosity, and structural heterogeneity.

2. Materials and Methods

Clinically relevant thrombi were generated using an optimized REFINE algorithm [2] combined with AI-derived geometries trained on patient non-contrast computed tomography (NCCT) images A total of 1300 unique thrombi with fully defined fibrin–platelet–RBC networks were generated. 1000 of samples used for training and the rest were used for testing. Photoacoustic responses were simulated at 30 µm resolution using our multiscale framework, preserving microstructural information in the output signal.

From the simulated data, we extract multi-domain input features of the in-silico thrombi and corresponding ground-truth output parameters from the multi-scale photoacoustic simulation. These include time to frequency domain spectral descriptors (representative spectra and spectral clustering), as well as image features such as speckle statistics and contrast. A nonlinear regression model based on Gradient Boosted Decision Trees is used for prediction. To reduce redundancy and prevent overfitting, we incorporate a feature compression step using Partial Least Squares (PLS) prior to training.

3. Results

Preliminary results on 491 simulated samples demonstrate accurate prediction of RBC content, porosity, and heterogeneity (Figure 1A). The trained model shows strong agreement with ground truth parameters. A representative 3D thrombus microstructure used for training is shown in Figure 1B.

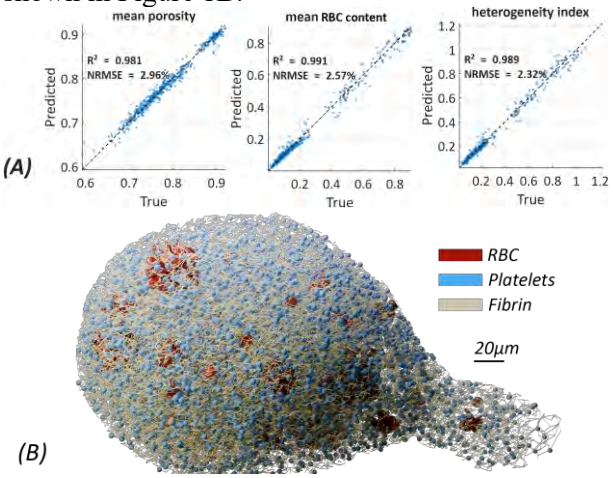


Figure 1: A. preliminary prediction RMSE for 491 samples. B. Sample generated microstructure

4. Discussion and Conclusions

Our microstructure-driven in silico framework enables prediction of thrombus composition and structural properties from simulated photoacoustic data.

5. References

1. Jolugbo P, Ariëns RA. Stroke. 2021;52(3):1131–1142 (2021).
2. Ghodsi H, Cardona S, Fereidoonnezhad B, Iskander-Rizk S. J. Phys.: Photonics. 2025;8(1):015017 (2025).

Acknowledgements:

This work was partly supported by the Dutch Research Council (NWO) under the Grant OCENW.XS24.2.210 awarded to SIR and the Delft University of Technology, Cohesion Grant awarded to SIR and BF and SK.

A COMPUTATIONAL MODEL OF CHEMICALLY- AND MECHANICALLY-INDUCED THROMBUS FORMATION IN CEREBRAL ANEURYSMS

Giulia Cardillo (1), Pierre Pouponneau (2), Abdul I. Barakat (1)

1. LadHyX, CNRS, Ecole Polytechnique, Institut Polytechnique de Paris, Palaiseau, France; 2. Artedrone Microrobots Cerebral Vascular, Paris, France

1. Introduction

Thrombosis, the process of blood clot formation, is one of the leading causes of death worldwide. It is governed by both biochemical and mechanical factors. Experimental evidence [1] suggests that local spatial variations in blood shear rate—i.e. spatial shear gradients—drive thrombogenesis by promoting platelet aggregation. Given this, developing a computational model capable of reliably predicting thrombus formation in the presence of shear gradients is essential. They occur in various scenarios, including vascular stenoses, bifurcations, aneurysms, and the vicinity of implantable endovascular devices.

The aim of this study is to develop a predictive computational model of thrombus formation that, for the first time, integrates thrombogenetic biochemical aspects and shear-induced platelet activation with the crucial role of spatial shear gradients on platelet aggregation.

2. Materials and Methods

A two-dimensional computational model of platelet plug formation was developed using the commercial multi-physics finite element solver COMSOL 6. The biochemical component of the model can be described by a set of coupled convection-diffusion-reaction equations including resting and activated platelets and different pro- and anti-thrombotic chemical species. Thrombus growth is represented as a large increase in blood viscosity, and its impact on the blood flow field is incorporated into the analysis. A simplified model of the coagulation cascade allows accounting for the role of fibrin fibers. The mechanical component of the model includes both the shear-induced platelet activation and platelet aggregation induced by spatial shear gradients.

3. Results and discussion

The proposed thrombosis model was firstly validated against different series of experimental data. Then thrombus formation in different idealized aneurysms of different sizes was investigated.

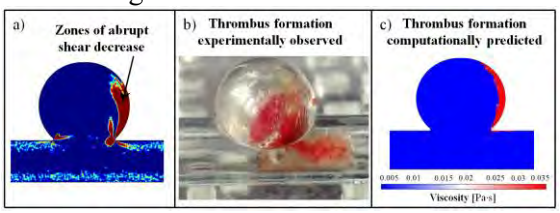


Figure 1: Thrombus formation in an aneurysm after 2 hours: a) Zones of abrupt shear decrease correlate closely with the localization of the thrombus. b) Experimentally observed thrombus formation. c) Computational predictions.

Figure 1a)&b) confirms that the experimentally observed localization of the thrombus correlates with zones of abrupt shear rate decrease, while Figure 1b)&c) depicts a qualitative comparison between the experimentally observed and computationally predicted thrombus formation in an idealized aneurysm geometry. Sensitivity analyses were performed to identify the role of different patient specific parameters in thrombogenesis.

The developed computational model constitutes a tool for thrombogenesis evaluation and for the optimization of the design of the endovascular device flow path.

4. References

1. Nesbitt WS et al. Nature Medicine 15: 665-673, 2009.

Acknowledgements:

The authors gratefully acknowledge the financial support provided by the Lefoulon-Delalande Foundation and the AXA Research Fund.

WITHIN LIVER VASCULAR NETWORKS: QUANTIFYING THE INTERPLAY BETWEEN GEOMETRY AND TRANSPORT

Jérôme Kowalski *(1), Lorenzo Sala (2), Dirk Drasdo (1), Charlotte Debbaut (3), Irene Vignon-Clementel (1)

1. Inria Saclay, France; 2. INRAE, France; 3. Ghent University, Belgium

* Mail : 1, rue Honoré d'Estienne d'Orves, 91120 Palaiseau, France. Email : jerome.kowalski@inria.fr

1. Introduction

Evaluating transport dynamics in the vascular network of the liver is key for patient-specific medical imaging and function assessment in health and disease. Using the concept of structured trees [1], we aim to reproduce key hemodynamics and transport dynamics features of real vascular trees and better understand how sensitive these are to the vascular geometry.

2. Materials and Methods

We leveraged the vascular corrosion cast of a healthy human liver in [2]. By extending VMTK's [3] centerline extraction method, we automatically extracted the centerline of the hepatic artery, portal vein and hepatic vein trees at macro and mesoscale. From the obtained geometry, we extracted the vessel length and radii, as well as key bifurcation quantities such as bifurcation asymmetry and power index defined in [4].

We developed a simulation pipeline that adopts Poiseuille flow in each branch of the trees, and advection-driven transport. To replicate the behavior under blood flow of the real liver trees, we employed the concept of structured trees [1] that assumes a self-similar geometry of blood vessels at each level of the tree.

In addition, we studied the transport dynamics of a complex vascular structure through two reduced models characterizing the tree in-out transport relationship. To do so, we sought for the parameters of the reduced model, such that its output fit best the observed transformation induced by the tree on a concentration bolus injected at the inlet. The reduced models are:

1. Advection-diffusion transport within a cylindrical pipe
2. Gamma probability distribution of the transit times.

3. Results

The theoretical framework showcased correlations between tree-level measures of geometry, blood flow and chemical species transport (such as the equivalent resistance, the variation in path length and the transit time distribution, see Fig. 1). Through the same simulation pipeline, it enabled to reproduce key hemodynamics and transport properties of the healthy human liver cast and highlight major differences between the three liver vascular networks.

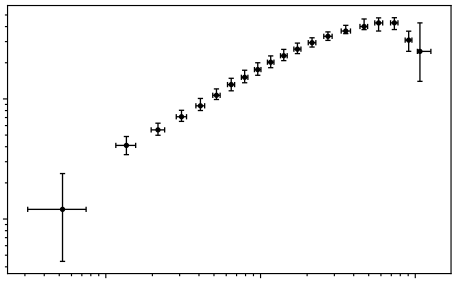


Figure 1: Correlation between the variance of transit times and the standard deviation of all path lengths within structured trees. ρ: Spearman correlation

4. Discussion and Conclusions

This study quantifies the strong entanglement between geometry, hemodynamics and transport both in synthetic and real vascular trees. Evaluating these quantities in an organ and comparing to measured baseline values may enable diagnosis various vascular trees pathophysiological conditions.

5. References

1. M. S. Olufsen, *AJP-Heart and Circulatory Physiology,* vol. 276, no. 1, pp. H257–H268, Jan. 1999
2. C. Debbaut *et al, J. Anat.*, vol. 224, no. 4, pp. 509–517, Apr. 2014
3. R. Izzo, D. Steinman, S. Manini, and L. Antiga, *JOSS*, vol. 3, no. 25, p. 745, May 2018
4 M. Zamir, Journal of Theoretical Biology, vol. 197, no. 4, pp. 517–526, Apr. 1999

Acknowledgements:

Financial support from the European Research Council under the European Union's Horizon 2020 research and innovation program (Grant no: 864313) are gratefully acknowledged.

MODELLING HAEMORRHAGE AND PHYSIOLOGICAL RESPONSE IN PENETRATING TRAUMA

Aaloka Jayakody (1), Brian Shaw (3), Amy Pullen (3), Rashmini Naranpanawa (1), Mohammad Shafieizadegan (1), Vinod Suresh (1, 2), Finbar Argus (1)

1. Auckland Bioengineering Institute, University of Auckland, New Zealand; 2. Department of Engineering Science and Biomedical Engineering, University of Auckland, New Zealand; 3. Defence Science and Technology, New Zealand Defence Force, New Zealand

1. Introduction

Traumatic haemorrhage is a leading cause of preventable death following penetrating injuries, as rapid physiological deterioration often limits the effectiveness of treatment. Ethical and practical constraints restrict the use of controlled clinical studies, making computational modelling an essential alternative for evaluating therapeutic strategies under reproducible conditions. However, existing cardiovascular models lack integration of real-time haemorrhage, wound-specific parameters, physiological compensation, and coagulation dynamics.

2. Materials and Methods

This study introduces a closed-loop computational model of the human circulatory system using Circulatory Autogen [1]. Baroreflex control was incorporated to simulate autonomic regulation of blood pressure, and a trauma module was implemented to model vascular rupture, blood loss, and clot formation. Wound parameters, including diameter, anatomical location, and penetration depth, were configurable to represent various injury conditions.

Baseline model parameters were defined (heart rate = 60 bpm, total blood volume = 5 L, stressed volume = 1.72 L) or calibrated to physiological targets (mean arterial pressure = 90 mmHg, stroke volume = 112 mL, mean aortic flow = 112 mL/s) corresponding to a healthy adult male.

To ensure that the model responds realistically to autonomic compensation mechanisms, the model was further calibrated against published Lower Body Negative Pressure (LBNP) data [2] representing graded central hypovolaemia.

3. Results

Simulations at -30 mmHg and -50 mmHg reproduced experimentally reported trends, tachycardic responses (77.7 and 97.7 bpm), and progressive reductions in stroke volume (93.9 and 73.5 mL), consistent with baroreflex-mediated compensation. Simulation of an uncontrolled haemorrhage in the kidney with a 1 cm wound diameter and 3 cm penetration depth resulted in 1.7 L of blood loss within 2 minutes and a reduction in mean arterial pressure to 50 mmHg, which closely corresponds to published data [3] reporting mean arterial pressure reductions to 40-50 mmHg within 1-2 minutes following injury.

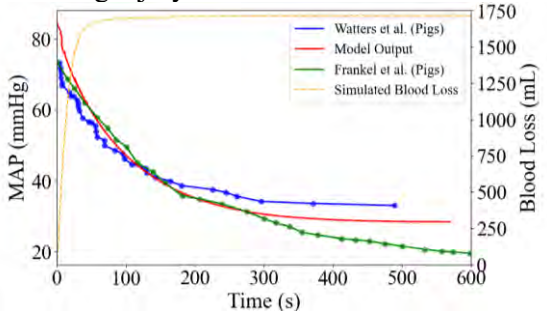


Figure 1: Model-predicted MAP compared with pig literature data during haemorrhage, with simulated blood loss over time [3].

4. Discussion and Conclusions

These findings demonstrate the model's ability to reproduce critical haemodynamic responses to trauma, supporting its application to optimise haemorrhage treatment strategies, guide advancements in battlefield medical interventions, and design personal protective equipment.

5. References

1. Argus F et al., Front Physiol; 13:1018134 (2022)
2. Cooke WH et al., J Appl Phy; 96(4):1249-61 (2004).
3. Frankel DAZ et al., J Surg Res; 143(2):276-280 (2007).

Acknowledgements:

Financial support was provided by Defence Science and Technology, New Zealand Defence Force.

LINKING CORONARY MORPHOLOGY TO CARDIAC ALLOGRAFT VASCULOPATHY THROUGH STATISTICAL SHAPE MODELLING

Bianca Griffo (1), Csenge Fogarasi (2), Maurizio Lodi Rizzini (1), Alessandra Aldieri (3), Diego Gallo (1), Marco Laudato (4), Hedvig Bille Andersson (2), Juliane Jurga (2), Michael Melin (2), Jannike Nickander (2), David Marlevi (2), Umberto Morbiducci (1)

1. Politecnico di Torino, Turin, Italy; 2. Karolinska Institute, Solna, Sweden; 3. Alma Mater Studiorum - University of Bologna, Bologna, Italy; 4. KTH Royal Institute of Technology, Stockholm, Sweden

1. Introduction

Cardiac allograft vasculopathy (CAV), a progressive vascular disease observed in heart transplant recipients, represents a main factor limiting long-term graft function and patient survival. CAV is characterized by a diffuse thickening of the arterial wall that distinguishes it from coronary atherosclerosis [1], with other anatomical attributes that remain largely unmapped. Here, we aim at identifying coronary anatomical attributes linked to CAV using statistical shape modelling (SSM), which has been recently used to capture coronary shape features associated with future myocardial infarction [2].

2. Materials and Methods

Seventy-four (33 healthy, 41 with CAV) left anterior descending (LAD) coronary arteries were reconstructed from coronary angiography acquired in heart transplant patients recruited at Karolinska University Hospital (Stockholm, Sweden). LAD anatomical three-dimensional (3D) reconstructions were then employed to build a principal component analysis (PCA)-based statistical shape model (Fig. 1). In detail, a non-parametric approach based on the open-source code *Deformetrica* was employed to compute a template (*i.e.*, the average shape of the population) and moment vectors located at a control points grid, which drive the template deformation towards each vessel-specific shape [3,4]. An approach combining PCA applied on moment vectors and linear discriminant analysis (LDA) was adopted within a leave-one-out cross-validation (LOOCV) scenario [2]. PCA scores with the greatest ability to discriminate between healthy subjects and CAV were selected according to Kruskal-Wallis statistical test (Fig. 1).

3. Results

Three PCA scores had significant discriminative capacity in separating CAV and healthy vessels and were considered and used as input for LDA. The LOOCV performed on LDA, evaluated through the receiver-operating characteristic (ROC) curve (Fig. 1), yielded an area under the curve (AUC) equal to 0.83 (95% CI 0.73–0.93, p<0.0001).

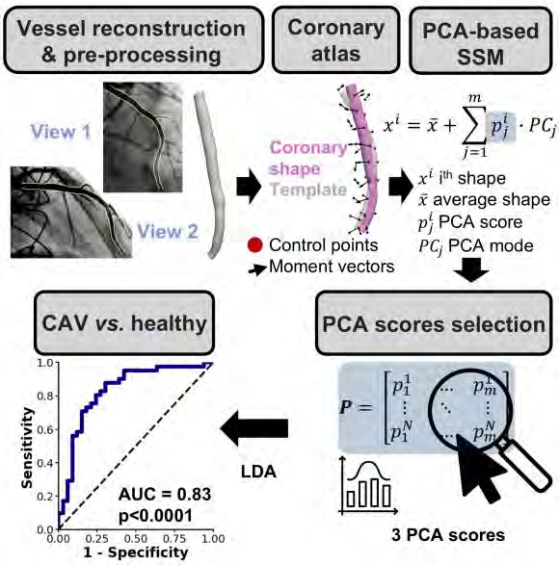


Figure 1: Workflow of the study.

4. Discussion and Conclusions

This study identified distinct coronary anatomical attributes associated with CAV adopting SSM-based shape features. The proposed approach, identifying distinct anatomical signatures, can enrich our knowledge on the processes leading to CAV in transplanted patients.

5. References

1. Pober JS et al., Cardiovasc Res;117:2624–2638 (2021).
2. Griffo B et al., J Biomech;189:112829 (2025).
3. Durrleman S et al., Neuroimage;101:35-49 (2014).
4. Aldieri A et al., Comput Biol Med;127:104093 (2020).

HEMODYNAMIC CHARACTERIZATION OF ATHEROSCLEROTIC CAROTID BIFURCATION

Valentina Quartieri (1), Ferris Harte (4), Alessandro Mastrofini (3), Eva Karlöf (2), Ulf Hedin (2), Michele Marino (3), Thomas Christian Gasser (1)

1. Department of Engineering Mechanics, KTH Royal Institute of Technology, Sweden; 2. Department of Molecular Medicine and Surgery, Karolinska Institute, Sweden; 3. Department of Civil Engineering and Computer Science Engineering, University of Rome Tor Vergata, Italy; 4. Department of Biomedical Engineering, Eindhoven University of Technology, Netherlands

1. Introduction

Cardiovascular diseases remain the leading cause of mortality worldwide, accounting for approximately 32% of global deaths [1]. Atherosclerosis, a major contributor to stroke and cardiovascular events, is characterized by plaque formation within the arterial wall initiated by endothelial dysfunction and lipid infiltration. Hemodynamic forces play a key role in disease progression, as local flow patterns and wall shear stress (WSS) influence endothelial permeability and lipid transport [2]. Computational fluid dynamics (CFD) enables the investigation of patient-specific hemodynamic environments; however, linking hemodynamic indicators to clinically observed plaque phenotypes remains challenging, particularly in carotid bifurcations.

2. Materials and Methods

Patient-specific carotid artery geometries were obtained from subjects treated at Karolinska University Hospital (Solna, Sweden). Plaque components (LRNC, IPH, CALC and matrix tissue) were segmented from computed tomography angiography (CTA) images using clinically validated software. Hemodynamic simulations were performed in COMSOL Multiphysics to analyse blood flow within carotid bifurcations. Idealized geometries were additionally considered to assess model robustness, while Doppler ultrasound measurements were used to define physiologically realistic inflow conditions.

3. Results

Simulations revealed heterogeneous WSS distributions associated with complex carotid geometry. Regions of disturbed flow were observed near the bifurcation and stenotic areas, consistent with locations of advanced plaque morphology identified from imaging data (Fig. 1).

4. Discussion and Conclusions

Combining imaging-based plaque characterization with patient-specific CFD simulations enables identification of hemodynamic environments associated with plaque development and vulnerability. The proposed framework supports clinically relevant in silico models for personalized risk assessment and provides physiologically consistent inputs that can be integrated with previously developed biomechanical structural modelling approaches accounting for vascular adaptation and stress redistribution mechanisms [3], established on the same clinical dataset.

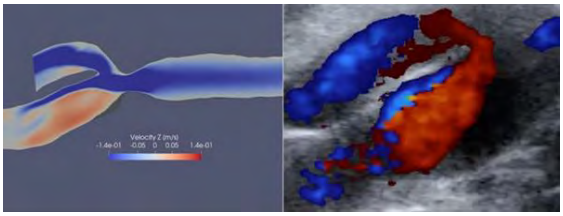


Figure 1: Simulated blood flow in stenotic carotid bifurcation (Direct Numerical simulation calibrated to patient-specific 3D Doppler ultrasound).

5. References

1. World Health Organization. Cardiovascular diseases (CVDs) fact sheet. Available at: https://www.who.int/news-room/fact-sheets/detail/cardiovascular-diseases-(cvds) (accessed October 2025).
2. Soulis JV, Fytanidis DK, Papaioannou VC, Giannoglou GD. Wall shear stress on LDL accumulation in human RCAs. Med Eng Phys. 32:867–877 (2010).
3. Mastrofini A, Karlöf E, Hedin U, Gasser CT, Marino M. Modulating vascular stresses through homeostatic remodelling: a multi-patient analysis of atherosclerotic carotid biomechanics. J R Soc Interface. 22:20250313 (2025).

Acknowledgements:
This work was supported by the MedTechLabs project MTL-UH-CG 2025.

THE POTENTIAL OF SOUND ANALYSIS FOR THE SURVEILLANCE OF HEMODIALYSIS ARTEROVENOUS FISTULAE

Sofia Poloni (1), Simona Zerbi (2), Chiara Ghilardini (2), Luca Soliveri (3), Carmela Giuseppina Condemi (2), Anna Caroli (1), Andrea Remuzzi (3), Michela Bozzetto (1)

1. Department of Biomedical Engineering, Istituto di Ricerche Farmacologiche Mario Negri IRCCS, Bergamo, Italy; 2. Unit of Nephrology and Dialysis, ASST Papa Giovanni XXIII, Bergamo, Italy; 3. Department of Management, Information and Production Engineering, University of Bergamo, Dalmine, Italy

1. Introduction

The arteriovenous fistula (AVF) remains the cornerstone of hemodialysis treatment [1]; however, its long-term function is frequently compromised by stenosis formation and consequent vascular access failure [2].

The aim of this investigation was to characterize the divergent evolution of two AVFs, comparing one that developed stenosis with another that maintained long-term patency.

2. Materials and Methods

Two distal radiocephalic AVFs from the ongoing clinical study *VASOUND* were evaluated, showing markedly divergent clinical trajectories. AVF1 developed progressive juxta-anastomotic venous stenosis starting from 40 days post-surgery and underwent angioplasty at 6 months, whereas AVF2 matured and remained patent over 18 months. Follow-up visits were performed at day 1, 7, 14, 28, 42 and 60 after surgery, and every 3 months thereafter. At each visit, brachial blood flow volume (BFV) was measured by Doppler Ultrasound, systemic blood pressure was recorded, and AVF sounds were collected at the anastomosis using the electronic stethoscope Littman 3200.

Brachial artery resistance (R) was calculated as mean arterial pressure over BFV. Sounds' peak amplitudes in low (100–250 Hz) and high (500–750 Hz) frequency bands were extracted, and their ratio defined as the High-to-Low Peak Ratio (HLPR) [3]. Longitudinal trends of HLPR and R were analysed, and their association after maturation was assessed using a linear mixed-effects model using RStudio.

3. Results

This preliminary analysis showed that after the maturation phase, characterized by hemodynamic and acoustic fluctuations, AVF1 was characterized by a progressive increase in HLPR over time accompanied by an increase in brachial artery resistance. In contrast, AVF2 exhibited lower and stable values of both R and HLPR over time. A significant positive association between HLPR and brachial R was observed after maturation (0.146 ± 0.025, $p = 0.0004$).

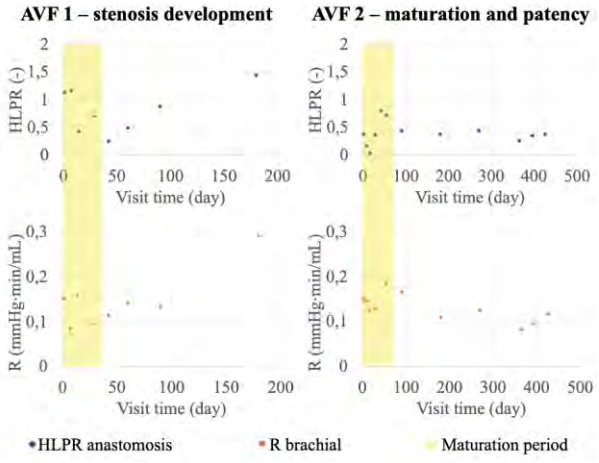


Figure 1: Time evolution of HLPR and brachial R of AVF 1 and AVF 2.

4. Discussion and Conclusions

These preliminary findings in two AVFs suggest that the progressive increase of HLPR over time reflects the evolution of stenosis formation and the consequent increase in brachial artery resistance. Therefore, AVF sound analysis may offer a fast, non-invasive, simple and cost-effective method for AVF monitoring.

5. References

1. Drew DA et al., J Am Soc Nephrol. 26(1):183-91 (2015).
2. Alonso A et al., Ann. Vasc. Surg.; 121:469-476 (2025).
3. Poloni S et al., Ann Biomed Eng.; 53(1):230-240 (2025).

Acknowledgements

Authors would like to thank GeneralCasa Spa for providing financial support.

IMPROVING ONE-YEAR SURVIVAL FORECASTING IN PULMONARY ARTERIAL HYPERTENSION USING MACHINE LEARNING MODELS

Ning Wang (1), Ze Ming Goh (1,2), Harry Saxton (6), Marcelle Paula-Ribeiro (1,2), Joe Longbottom (1), Maximilian Balmus (3,4), Alexander Rothman (1,2), Martin Wilkins (4), Richard Wilkinson (5), Keith Worden (1,2), David Wagg (1), Steven Niederer (3,4), Xu Xu (1), Richard Clayton (1)

1. University of Sheffield, UK; 2. Sheffield Pulmonary Vascular Disease Unit, Royal Hallamshire Hospital, Sheffield Teaching Hospitals NHS Foundation Trust, UK; 3. The Alan Turing Institute, UK; 4. Imperial College London, UK; 5. School of Mathematical Sciences, University of Nottingham, UK; 6. Astellas Pharma, UK

1. Introduction

Between 1980 and 2021, 1 to 33% of pulmonary arterial hypertension (PAH) patients worldwide died within one year of diagnosis [1]. Current prognostic assessment relies on REVEAL score, which aggregates predefined clinical variables but may not fully capture individual disease heterogeneity [2]. This study aims to develop and compare machine learning models incorporating demographics, laboratory features, and measurements from right heart catheterization (RHC) or cardiac magnetic resonance (CMR).

2. Materials and Methods

This study analyses 416 newly diagnosed PAH patients from the ASPIRE dataset [3]. Three feature groups are defined: RHC-based, CMR-based, and combined. These groups are used to train LASSO-logistic regression and support vector machine (SVM) models, followed by a 10-fold cross-validation strategy. Predictive performance is then compared against the REVEAL score alone using area under the ROC curve (AUC) by receiver operator characteristic (ROC) curve. Finally, SHapley Additive exPlanations (SHAP) is applied to quantify individual feature contributions [4].

3. Results

Both LASSO and SVM models present comparable improvements over the REVEAL score when predicting one-year using RHC- or CMR-based features. Specifically, CMR-based model achieves the highest AUC of 0.7522, compared to 0.7211 for the RHC-based model and 0.7122 for the REVEAL score, while the combined features perform worse than REVEAL score. Key predictive CMR-based features included left ventricular ejection fraction (LVEF, %, mean |SHAP| = 0.5282), maximum septal angle (mean |SHAP| = 0.5083), and ventricular mass index (VMI, %, mean |SHAP| = 0.1961). Higher values of these features were associated with reduced one-year survival forecast accuracy. In contrast, minimum septal angle and right ventricular cardiac output (RVCO) exhibited the opposite association.

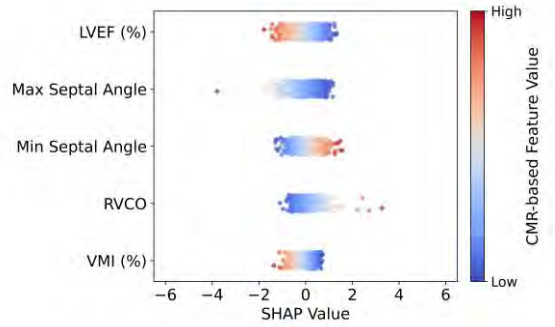


Figure 1: SHAP values of the top five CMR-based features ranked by mean |SHAP| in SVM model.

4. Discussion and Conclusions

Machine learning models incorporating CMR imaging and clinical data can improve one-year survival forecast in PAH compared with the REVEAL score. CMR-derived features offered superior prognostic value over RHC-based features. These models may enhance risk stratification and support personalised clinical decision-making.

5. References

1. Emmons-Bell S et al., Pulm Circ; 12(1):e12020 (2022).
2. Benza RL et al., Chest; 156(2):323–337 (2019).
3. Alabed S et al., Eur Heart J Digit Health; 3(2):265–275 (2022).
4. Mersha M et al., Neurocomputing; 599:128111 (2024).

Acknowledgements:
The authors would like to thank the UK EPSRC (Grant no: EP/Z531297/1) for providing financial support to this project.

FAST COMPUTATIONAL FRAMEWORK FOR PATIENT-SPECIFIC TEVAR PLANNING

Sara Barati (1), Asia Stellino (1), Giulia De Campo (1), Anna Ramella (1), Giulia Luraghi (1), Jose Felix Rodriguez Matas (1), Irene Fulgheri (2), Santi Trimarchi (2,3), Francesco Migliavacca (1,2)

1. Politecnico di Milano; 2. IRCCS Policlinico di Milano; 3. Università degli Studi di Milano, Italy

1. Introduction

Finite element (FE) simulations are increasingly used to predict the outcomes of endovascular interventions and support pre-operative planning. However, their broader clinical adoption is limited by high computational cost. In this study, we have developed a fast computational framework that significantly reduces the process time. The proposed method was applied to five real clinical cases of Thoracic Endovascular Aortic Repair (TEVAR), demonstrating its potential to provide reliable results.

2. Materials and Methods

Aortic anatomies of five TEVAR patients were reconstructed. All cases were suitable for device sizes 34 and 36 and included arch types I, II, and III with Penetrating Atherosclerotic Ulcer (PAU) pathology (Figure 1).



Figure 1: A) The reconstructed 5 patient-specific anatomies. B) The process of shape deformation from the template to the target geometry applied to patient 2. C) Overlay of the patient-specific anatomy and the deformed geometry.

Non-parametric statistical shape modelling [1] was used to define the deformation from an ideal aortic geometry (template) to the patient-specific geometry (target) using Eq. 1

$$S_i \approx \phi_i(B_{0,i})T + \varepsilon^i \qquad (1)$$

where S_i is the target shape, ϕ_i the shape function, $B_{0,i}$ the momenta, T the template and ε^i the residuals. The deformation parameters (resolution $\boldsymbol{\lambda_w}$ and the stiffness $\boldsymbol{\lambda_v}$) were optimized to obtain the best configuration for each case. The resulting deformation function was then applied to the device deployed in the template geometry to provide its final configuration in the patient-specific anatomy. Finally, the fast simulation results were compared with the previously validated approach based on explicit finite element simulation of the procedure. [2].

3. Results

The proposed method showed a good agreement with the validated simulation results. The average cross-sectional area error was less than 10% in all cases. The difference in the prosthesis length was less than 3%, with fast simulation predicting a slightly shorter device in four of five cases (Figure 2). The total process time for the fast simulation is about 1 hour which improves that of the validated simulation (about 10 hours) significantly.

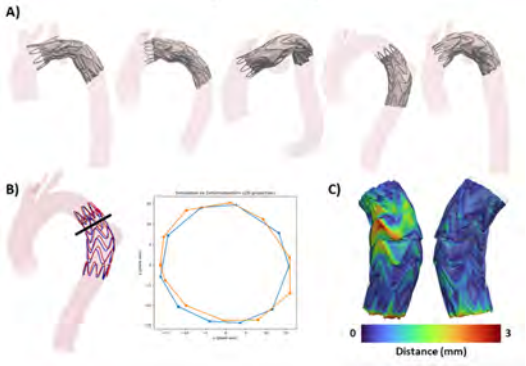


Figure 2: A) Deployed configuration in patient-specific anatomies. B) The overlap of the high-fidelity (red) and fast simulation (blue) results and a cross-sectional area. C) Distance contour between the simulation and deformation graft models.

4. Discussion and Conclusions

The proposed approach provided accurate results. Further developments enable a plug-and-play platform for surgeons to test different scenarios of treatment strategy, in a clinically relevant timeframe.

5. References

1. Pajaziti E, et al., PLoS Computational Biology: 2023.
2. Ramella A et al., Eur J Vasc Endovasc Surg; 2026.

SYNCHROTRON PHASE-CONTRAST TOMOGRAPHY REVEALS MYOCARDIAL ORGANISATION IN FETAL AORTIC STENOSIS

Lisa Chestnutt (1, 2), Joseph Brunet (1, 3), Hector Dejea (3, 4), Vaishnavi Sabarigirivasan (2), Kan Yan Chloe Li (2), Anne Bonnin (5), Margie Olbinado (4, 5), Bart Bijnens (6), Monique Jongbloed (7), Lucile Houyel (8), Adrian Crucean (9), Peter D Lee (1), Andrew Cook (2)

1. UCL Mechanical Engineering, UK; 2. UCL Institute of Cardiovascular Science, UK; 3. The European Synchrotron, France; 4. Anaxam, Switzerland; 5. Paul Scherrer Institute, Switzerland; 6. ICREA-Universitat Pompeu Fabra, Spain; 7. Leiden University Medical Center, The Netherlands; 8. Necker–Enfants Malades Hospital, France; 9. Birmingham Women's and Children's Hospital NHS Trust, UK

Correspondence details: Lisa Chestnutt, UCL Mechanical Engineering, lisa.chestnutt.24@ucl.ac.uk

1. Introduction

Fetal aortic stenosis (AoS) with intact ventricular septum is associated with left-ventricular (LV) dysfunction and can represent an early stage of 'single ventricle disease' (SVD) [1]. It is a clinical challenge to determine whether the LV myocardium retains sufficient functional capacity to support pre-natal intervention or post-natal biventricular repair. Comparing myocardial microstructure across healthy hearts, those with potentially treatable obstruction (AoS), and those beyond the window for intervention (aortic atresia, AA) may help support clinical decisions.

2. Materials and Methods

This study employs synchrotron-based phase-contrast tomography to characterise myocardial architecture followed by structure tensor analysis. Second-trimester human fetal hearts were imaged at 5.8 µm effective voxel size at the TOMCAT beamline of the Swiss Light Source at Paul Scherrer Institute. The dataset comprised AoS (n=5, 22.8 ± 2.3 weeks' gestational age (WGA), mean ± std), AA (n=12, 23.7 ± 2.0 WGA), and healthy controls (n=18, 20.3 ± 2.4 WGA). Cardiotensor was used for structure tensor analysis of myocyte aggregates, calculating helical angles (HA, representing the dominant angle of myocardial aggregates) within a cylindrical LV coordinate system [2,3].

3. Results

Healthy hearts showed a transmural HA transition of 81 ± 20° to –33 ± 23° (mean ± std) from trabecular myocardium to epicardium at mid-ventricular level, indicating a preserved transmural architectural gradient. In AA, this range was reduced (45 ± 29° to –38 ± 18°), indicating altered architecture. AoS showed the greatest variability, with some displaying near-normal organisation and others similar to AA, with fewer positive HA values (68 ± 40° to –31 ± 32°) (Figure 1). Endocardial fibroelastosis (EFE) was present in both AoS and AA.

4. Discussion and Conclusions

AoS spans a continuum between normal myocardial architecture and the greater disorganisation seen in AA. Alongside EFE, altered HA in the trabecular region likely contributes to impaired ventricular filling, contractility, and capacity to respond to intervention. These findings advance our understanding of myocardial structural variability, specifically in fetal SVD, providing a foundation for future computational modelling linking structure with function.

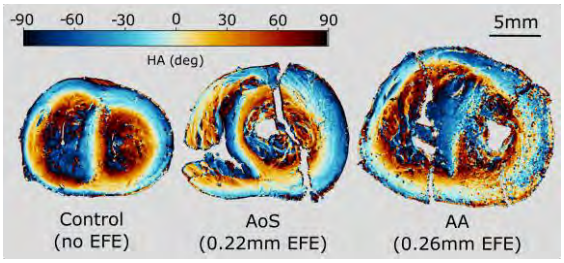


Figure 1. Representative short axis slices showing HA and mean LV EFE thickness in control (20 WGA), AoS (22 WGA) and AA (20 WGA) hearts.

5. References

1. Sharland, G.K. et al., 1991; Br Heart J:66(419-24)
2. Brunet, J. et al., 2025; arXiv:2508.07476
3. Garcia-Canadilla, P. et al., 2018; Circ Card Img: 11(10)

Acknowledgements:

The authors would like to thank EPSRC (EP/Y034929/1), Additional Ventures (SVRF 1019894), and CZI Foundation (CZIF2022-316777) for providing financial support.

SIMSCAPE-BASED CARDIOVASCULAR MODELS FOR NEXT-GENERATION ECMO SYSTEM DEVELOPMENT

Magnus Nord (1), Visa Suomi (2)

1. MathWorks, France; 2. MathWorks, Germany;

1. Introduction

Extracorporeal membrane oxygenation (ECMO) systems increasingly rely on high-fidelity computational models to support design, control, and clinical innovation. Traditional lumped-parameter cardiovascular models available in Simscape™ Electrical provide pressure-flow dynamics of the closed-loop circulation [1]. However, next-generation ECMO development requires explicit tracking of gas-exchange behavior, oxygenation efficiency, and patient-pathology interactions. To address this need, we extend established cardiovascular models by incorporating O_2 and CO_2 mass-fraction dynamics directly into the Simscape environment.

2. Materials and Methods

Building on the model published in [1] and the cardiovascular library available on MATLAB File Exchange [2], we introduce new state variables representing oxygen and carbon-dioxide fractions across the cardiovascular and extracorporeal circuits. These additions enable a physiologically meaningful representation of blood-gas transport, oxygenator behavior, and pathological conditions under ECMO support.

The new in silico model can be used for development of adaptive control strategies such as closed loop sweep-gas control, and for physiology-aware control of oxygenation, CO2 removal, and hemodynamics. Model Predictive Control (MPC) and Multi-input Multi-Output (MIMO) controllers can be used based on simulated state. When developing adaptive oxygenator control based on metabolic state, the new Simscape model can be used to simulate fluctuating metabolic rates.

The new in silico model was in part generated by Claude from Anthropic This was enabled by MathWorks Model Context Protocol (MCP), which standardizes communication between MATLAB and agentic AI systems Using this MCP-enhanced environment, biomedical engineers can rapidly prototype, refine, and validate complex first-principle models. This significantly accelerating the creation of coupled cardiovascular gas-exchange systems.

3. Results and Discussion

The resulting model family augments existing pressure-flow cardiovascular representations with gas-fraction transport for O_2 and CO_2. Early results show benefits across multiple ECMO-related engineering domains such as physiology-informed model behavior; control system design for ECMO flow, sweep gas, and oxygenation; gas-exchange optimization studies; virtual testing of oxygenator designs, patient-pathology interaction simulation and support for clinical decision-making algorithms

These models are being used throughout the ECMO development pipeline, from initial algorithm prototyping to subsystem verification and full system testing.

4. Conclusions

The integration of blood-gas fractions into existing Simscape cardiovascular models enables more realistic physiological behavior and more representative ECMO system simulations. The new Simscape model can be used in development of several control strategies such as Metabolic-adaptive sweep control and MIMO full-ECMO controllers.

5. References

1. J. Fernandez de Canete et al. “Object-oriented modeling and simulation of the closed-loop cardiovascular system by using Simscape”. Computers in Biology and Medicine, Volume 43, Issue 4, 1 May 2013, Pages 323-333
2. Cardiovascular System in Simscape™ with ECMO Machine. https://www.mathworks.com/matlabcentral/fileexchange/125310-cardiovascular-system-in-simscape-with-ecmo-machine

TOWARDS A DIGITAL TWIN FOR PERSONALIZED PREDICTION OF RADIOTHERAPY RESPONSE OF PROSTATE CANCER

Beatriz Blanco (1), Miguel Anxo Vicente-Pardal (2), Hector Gomez (3), Guillermo Lorenzo (2)

1. Universidade de Santiago de Compostela, Spain; 2. Universidade da Coruña, Spain; 3. Purdue University, United States of America

1. Introduction

The analysis of prostate-specific antigen (PSA) dynamics following external beam radiotherapy (EBRT) is crucial for monitoring prostate cancer (PCa) recurrence. A sustained increase in PSA levels is indicative of biochemical relapse, although this progression may occur slowly and remain undetected for several years using standard clinical criteria based on fixed population-derived thresholds. However, such criteria do not account for patient-specific PCa dynamics and may therefore delay relapse identification. Mechanistic modeling of PSA kinetics provides a quantitative framework to characterize post-treatment tumor dynamics and extract predictive information from longitudinal PSA trajectories [1-2]. Here, we apply a previously validated mechanistic model [1] to an independent clinical dataset to evaluate its predictive potential for constructing digital twins to guide clinical decision-making.

2. Materials and Methods

Longitudinal PSA measurements from 885 PCa patients treated with EBRT were analyzed using a mechanistic model of PSA dynamics [1]. Patient-specific parameters were estimated by nonlinear least-squares regression using both global fitting and a data assimilation framework, in which model parameters were sequentially updated by progressively incorporating additional PSA measurements. Model-derived quantities were evaluated as predictive biomarkers of biochemical relapse using receiver operating characteristic (ROC) curve analysis. Clinical benefits were quantified using the Days Gained to Biochemical Relapse Diagnosis (DGBRD) metric, defined as the time gained by model-based relapse detection relative to standard PSA-based criteria. Model robustness was assessed using 10-fold cross-validation, and suboptimal ROC thresholds were explored to evaluate sensitivity–specificity trade-offs that improve DGBRD, and thus contribute to early detection of biochemical relapse.

3. Results

Global model fitting enabled accurate reconstruction of patient-specific PSA trajectories, with median (IQR) RMSE values of 0.25 (0.11–0.32) ng/mL for non-relapsing patients and 0.85 (0.46–0.99) ng/mL for relapsing patients. ROC curve analysis identified time to progression (T_p) and tumor proliferation rate (ρ_s) as strong predictors of biochemical relapse (AUC>0.98). Using a suboptimal ROC threshold corresponding to 80% of the maximum Youden index, these biomarkers increased the DGBRD while maintaining high sensitivity (>98%), at the expense of reduced specificity (>75%). Hence, relapse detection was anticipated relative to standard PSA criteria with median (IQR) DGBRD of 315 (11.25–710.75) days for T_p and 410 (0–574) days for ρ_s.

4. Discussion and Conclusions

These results support the potential of mechanistic modeling of PSA dynamics as a tool for early identification of biochemical relapse after EBRT and provide independent validation of the mechanistic framework previously proposed in [1]. This study may support the development of digital twins and virtual clinical trial frameworks to evaluate personalized treatment and monitoring strategies that aim at optimizing clinical care.

5. References

[1] Lorenzo G, Di Muzio N, Deantoni CL, Cozzarini C, Fodor A, et al. iScience. 2022;25(11):105430.

[2] Phan T, Crook SM, Bryce AH, Maley CC, Kostelich EJ, Kuang Y. Appl. Sci. 2020;10(8):2721.

Acknowledgements:

The authors acknowledge grant PID2023-146347OA-I00 funded by MICIU/AEI/10.13039/501100011033 and ERDF/EU. GL acknowledges grant RYC2022-036010-I funded by MICIU/AEI/10.13039/501100011033 and ESF+.

A CAUSAL COMPUTATIONAL FRAMEWORK FOR DIGITAL TWINS IN BREAST CANCER RADIOTHERAPY

Francesca Arceci (1), Benedetta Dionisi Ferrera (2), Tiziana Rancati (2), Marzo Tezzele (3), Piermario Vitullo (1), Paolo Zunino (1)

1. Politecnico di Milano, Milano; 2. Fondazione IRCCS Istituto Nazionale dei Tumori, Milano; 3. Emory University, Atlanta.

1. Introduction

Computational oncology aims to provide patient-specific models integrating clinical, biological, and treatment data to support prediction, decision-making, and long-term risk monitoring. In breast cancer radiotherapy, predicting severe late toxicity remains challenging due to the complex interplay between dosimetric exposure, individual susceptibility, and biological response. A key challenge in oncology digital twins (DTs) is establishing a rigorous framework that links heterogeneous observational data to clinically meaningful predictions while ensuring interpretability, causal coherence, and computational scalability.

2. Materials and Methods

We propose a multi-layer probabilistic framework connecting three levels: a *data level* collecting multimodal clinical, dosimetric, and molecular variables [1]; a *causal level* formalizing cause–effect relationships [2]; and a *computational level* embedding these relationships into predictive and decision-support models. At the causal level, directed acyclic graphs (DAGs) are employed to disentangle exposures variables, outcomes and confounders, allowing the investigation of mechanisms underlying treatment-related adverse events beyond purely predictive correlations. To bridge the causal and computational levels, we introduce an algorithm grounded in causal adjustment theory: admissible adjustment sets satisfying the back-door criterion are identified, the minimal structural sufficient set is selected via a Random Walk with Restart ranking strategy, and a Bayesian Network is constructed from the resulting causally valid subgraph. The resulting computational model is indeed built upon probabilistic graphical models [3], whereas its structure is explicitly constrained by DAG-based causal principles. This yields a unified framework for predictive and causal inference within digital twin systems, reducing the dimensionality while preserving the identifiability of direct effects.

3. Results

The methodology is demonstrated in breast cancer radiotherapy for severe late toxicity prediction. Retrospective dosimetric, genomic, and clinical data are used to model risk components. The resulting causally informed Bayesian Networks support individualized risk stratification and quantification of direct exposure effects on toxicity.

4. Discussion and Conclusions

We present a causally coherent and computationally efficient pathway from observational oncology data to interpretable predictive models. By integrating causal inference into Bayesian Network construction through optimal adjustment set identification, the framework ensures predictive performance while preserving clinical interpretability. In breast cancer radiotherapy, such models may enhance toxicity prediction, support personalized treatment planning, and enable adaptive long-term monitoring.

5. References

1. Seibold, P. et al., *Radiotherapy and Oncology*, 138, 59–67 (2019).
2. van Amsterdam W.A.C. et al., Clininical Oncology, Volume 38 (2025)
3. Willcox, K.E. et al., *Nature Computational Science*, 1(5), 337–347 (2021).

Acknowledgements:

This work is part of the TETRIS project: “Risk assessment tools for severe side effects after breast radiotherapy: radiation safety through biologically extended models and digital twins”. This project has received funding from the Euratom Research and Training Programme (Grant No. 101166699).

ENABLING CLINICAL PROGNOSIS OF BREAST CANCER DURING NEOADJUVANT THERAPIES

Francesca Lovallo (1), Maria Valeria De Bonis (2), Gianpaolo Ruocco (1,2)

1. Department of Engineering 2. iBMB Srls - University of Basilicata, Italy

Corresponding author: Gianpaolo Ruocco, ibmb4info@gmail.com

1. Introduction

There is a definite need for quantitative tools that support personalized treatment and prognosis for Breast cancer (BC). Numerical simulation can describe tumor dynamics by integrating diffusion-reaction PDEs for cellular diffusion and proliferation, depending on the administered therapy. But most existing models poorly integrate imaging-derived spatial information and cannot directly lead to discrimination between lesion and surrounding tissue. We propose a spatially resolved workflow starting from diagnostic CE-MRI up to simulation, describing explicitly such binary information.

2. Materials and Methods

Preoperative CE-MRI scans identifying a few cubic cm nodular lesion in a sample patient's breast were sent to pre-processing for high signal-to-noise ratio using 3D Slicer [1]. Segmentation was based on seed-guided region growing, corresponding to breast and its background. Post-processing to obtain geometrically proper surfaces was based on sequential smoothing, with selected filters to achieve an optimal compromise between geometric fidelity and numerical regularity. A STL file keeping the two binary structure as separate domains was sent into a FEM workflow (Fig.1).

Thereafter, the tumor was modeled as a single-phase tissue composed of a cell population, which progressively grows and invades the ROI by a Gompertzian growth; likewise, drug species were applied reflecting the therapeutic regimen by using the same diffusive-reactive PDE framework [2]. Numerical post-processing then employed a Level-Set method to isolate the interface letting the binary tissue information emerge.

3. Results

This workflow was employed to obtain patient-specific lesion evolution, preserving tumor morphology, localization, and tissue heterogeneity in early stage BC treated with neoadjuvant therapies (NAT) (Fig.2).

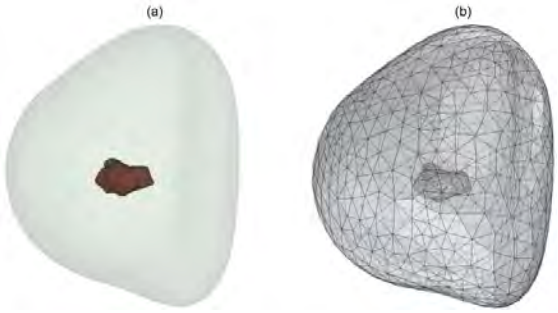


Figure 1: (a) Isolated 3D rendering of the segmented ROI, showing healthy tissue (green, semi-transparent) and lesion (dark red). (b) Volumetric mesh at the ROI.

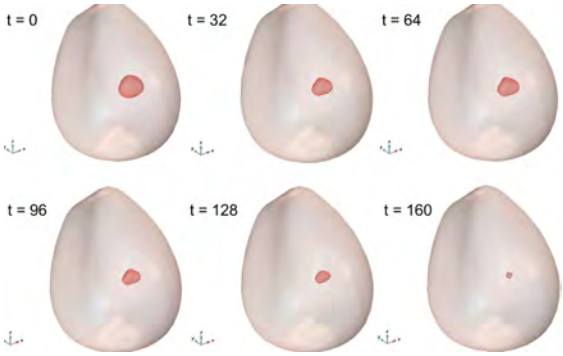


Figure 2: Evolution of the lesion under NAT at different days using an isosurface with a nominal tumor concentration of 2000 mol/m^3. Lesion volumes were validated clinically.

4. Discussion and Conclusions

This operational virtual twin is directly usable in clinical environments to support response assessment, as well as personalized therapeutic and surgical planning, addressing the paradigm of precision oncology.

5. References

1. 3D Slicer Community. 3D Slicer v. 4.1: Software documentation. 2020.
2. Ruocco G. International Journal of Heat and Mass Transfer. 2026;261:1286060 (2026).

PBPK-DRIVEN OPTIMIZATION OF CAR-T DELIVERY AND EFFICACY

Andreas G. Hadjigeorgiou (1), Lance L. Munn (2), Triantafyllos Stylianopoulos (1), Rakesh K. Jain (2)

1. University of Cyprus, Cyprus; 2. Massachusetts General Hospital / Harvard Medical School, USA
Corresponding author: T. S., University of Cyprus, Cyprus. Email: tstylian@ucy.ac.cy

1. Introduction

CAR-T cell therapy has transformed the treatment of hematological malignancies, yet its efficacy in solid tumors remains limited due to poor infiltration, immunosuppression, and abnormal tumor vasculature. Vascular normalization through anti-VEGF therapy has recently emerged as a promising strategy to enhance immune cell trafficking and reprogram the tumor microenvironment (TME) [1]. Building on these findings, we developed a physiologically based pharmacokinetic (PBPK) model to simulate the dynamics of CAR-T cells and endogenous immune populations in solid tumors under normalization , Fig. 1 A-B [2].

2. Materials and Methods

A whole-body PBPK framework was constructed, incorporating vascular and extravascular compartments across major organs, lymphatic drainage, and a mechanistic tumor module describing immune–tumor interactions. The model tracks CAR-T cells, $CD8^+$ T cells, dendritic cells, macrophage subtypes, and regulatory T cells. Transport kinetics, immune activation, exhaustion, and suppression were represented through population-balance equations. Model parameters were calibrated using in vivo data from murine GBM models treated with anti-VEGF, CAR-T, or combination therapy, and validated against tumor growth and immune profiling datasets. Simulations explored systemic and local CAR-T delivery, dose thresholds, dual-dose scheduling, and the timing of pretreatment normalization.

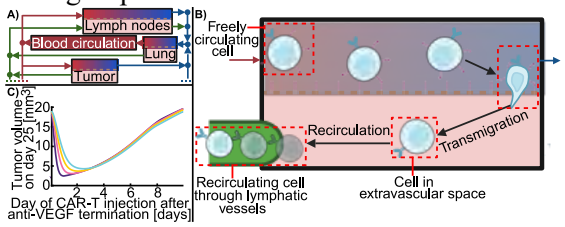


Figure 1: PBPK model and key outcomes. A) Model compartments linked by blood and lymph flow. B) Immune-cell transport from vascular to extravascular space. C) Tumor volume on day 25 vs. CAR-T injection day after anti-VEGF termination.

3. Results

The model reproduced experimental tumor growth and immune infiltration patterns across two GBM models. Vascular normalization increased CAR-T and $CD8^+$ T-cell infiltration, reduced M2 macrophages and Tregs, and lowered the CAR-T therapeutic dose threshold by approximately fivefold. Optimal scheduling analyses revealed that early CAR-T administration after normalization maximizes efficacy, and that a second CAR-T dose is most effective when delivered near the peak proliferative phase of the first dose. Anti-VEGF-producing CAR-T cells benefited from prior vascular normalization when higher intratumoral CAR-T densities were required to maintain normalization, Fig 1C. In desmoplastic tumors, combining vascular and stroma normalization before administering anti-VEGF-producing FAP-CAR-T cells further reduced tumor burden and expanded the therapeutic window. Local CAR-T delivery outperformed systemic injection by achieving similar tumor control with substantially fewer cells and improved $CD8^+$ T-cell recruitment.

4. Discussion and Conclusions

The PBPK model provides a quantitative framework for optimizing CAR-T therapy in solid tumors by integrating vascular and stromal normalization strategies. Simulations highlight the importance of normalization-induced immune reprogramming, dose thresholds, and precise timing of CAR-T administration. The results support the design of optimized dosing regimens, combination therapies, and delivery routes to enhance CAR-T efficacy while reducing toxicity. This modeling approach can guide preclinical study design and accelerate translation to clinical protocols.

5. References

1. X. Dong et al., J. Immunother. Cancer; 11:e005583 (2023).
2. A. G. Hadjigeorgiou et al., PNAS; 122(46):e2522634122 (2025)

TRI-PHASIC REPROGRAMMING OF THE SPHINGOSINE-1-PHOSPHATE AXIS DRIVES OVARIAN CANCER PROGRESSION AND ANOIKIS RESISTANCE

Aharon Shmuel Baskin (1), Ben Davidson (2,3), Reuven Reich (4), Tali Tavor Re'em (1)

1. *Dept. of Pharmaceutical Engineering, Azrieli College of Engineering, Jerusalem, Israel; 2. Dept. of Pathology, The Norwegian Radium Hospital, Oslo University Hospital, Oslo, Norway;3. The Medical Faculty, University of Oslo, Oslo, Norway; 4. Institute of Drug Research, School of Pharmacy, The Hebrew University, Jerusalem, Israel;*

Corresponding author: Aharon Shmuel Baskin, aharonshmuelba@jce.ac.il; Dept. of Pharmaceutical Engineering, Azrieli College of Engineering, 26 Ya'akov Shribom St, Jerusalem 9103501, Israel.

1. Introduction

Tubo-ovarian high-grade serous carcinoma (HGSC) mortality is heavily driven by metastatic dissemination and malignant effusions. Tumor cells within effusions must survive in detached conditions (anoikis resistance) [1]. The Sphingosine-1-Phosphate (S1P) signaling axis regulates these survival mechanisms [2]. However, the dynamic, stage-specific evolution of this pathway across anatomical compartments remains poorly understood. In the context of *in silico* oncology, computational modeling of pathway rewiring is critical for identifying site-specific therapeutic vulnerabilities [3]. Here, we utilize clinical expression data to computationally map the compartment-specific signaling architecture of the S1P axis in HGSC.

2. Materials and Methods

We obtained patient-derived specimens representing distinct HGSC compartments: ovarian tumors (n=37), peritoneal/omental metastases (n=41), and malignant effusions (n=132). We established mRNA and protein expression profiles for S1P-metabolizing enzymes (SPHK1/2, SGPL1, SGPP1) and S1P receptors (S1PR1-3). To decode the pathway's structural rewiring, we employed in silico network mapping using nonparametric Spearman rank correlation matrices. This computational approach integrated the receptor-enzyme profiles with downstream survival and cytoskeletal effectors to reconstruct the site-specific signaling architectures [4].

3. Results

Computational mapping revealed distinct compartment-associated remodeling of the S1P axis. Ovarian tumors exhibited a tightly coupled SPHK2/S1PR1/PI3K/Akt survival module. In peritoneal metastases, this receptor-Akt network was decoupled, showing metabolic instability driven by high SGPL1 expression. Effusions displayed profound systems-level rewiring: elevated SGPP1 and a unique S1PR2/S1PR3-p85 correlation structure. The *in silico* model identified an effusion-exclusive cytoskeletal survival complex (p130Cas, p-Akt, p-Ezrin) that promotes anoikis resistance. Clinically, elevated S1PR2 in effusions correlated with poorer overall survival (p=0.011).

4. Discussion and Conclusions

This in silico reconstruction uncovers fundamental, compartment-dependent rewiring of the HGSC S1P network. Identifying the effusion-specific S1PR2-driven survival complex demonstrates how computational mapping decodes microenvironmental adaptations. These insights emphasize that S1P-targeted therapeutic interventions must be strictly compartment-aware to effectively disrupt disease progression.

5. References

1. Ford CE et al. Br J Cancer. 2020;123:9-16.
2. Pyne NJ, Pyne S. FEBS Lett. 2020;594:3583-601.
3. Rostami N et al. Mol Diagn Ther. 2019;23:467-87.
4. Taha TA et al. Biochim Biophys Acta. 2004;1682:48-55.
5. Luo D et al. J Med Chem. 2022;65:14553-77.

REALISTIC *IN SILICO* TUMOUR SUBSTRATES FOR DW-MRI SIMULATIONS

Chiara Scotti[1], Chiara Tinelli[1], Fabio Casaccio[1], Paolo Fenech[1], Guido Baroni[1], Letizia Morelli[1], Chiara Paganelli[1]

[1]Dipartimento di Elettronica, Informazione e Bioingegneria, Politecnico di Milano, Italy

1. Introduction

Diffusion Weighted Magnetic Resonance Imaging (DW-MRI) is a valuable tool for tumour microstructural characterisation and outcome prediction, as demonstrated by [1] and [2], whose frameworks match cancer patients DW-MRI signals, with ones simulated in virtual tumour substrates. However, such substrates are simple geometrical packings of spheres and ellipsoids, that fail to capture complex cell interactions and membrane irregularities that affect the diffusion. To better characterise intra- and inter-patient tumour heterogeneity, more complex tumour substrates should be included in such studies. To generate more realistic and complex packings, Monte Carlo simulations of virtual cell cultures based on the Glazier-Graner-Hogeweg (GGH) method [3] can be used.

2. Materials and Methods

The LIVECell dataset [4] contains phase-contrast images of cell cultures at different growth stages, from which five cell lines were selected: *BT474*, *Huh7*, *MCF7*, *SkBr3*, *SKOV3*. The microscopy images were extruded in 3D exploiting custom reconstruction algorithms and were then used for initialisation and parameter tuning for virtual cell culture simulations based on the GGH Monte Carlo framework [3]. A Kruskal-Wallis test and subsequent Dunn's post-hoc were performed on cell volumes to verify if the substrates were significantly different. Moreover, a statistic similarity test [5] was carried out, comparing simulated cell volumes and those coming from a test set of microscopy images that were not included in the simulations. The substrates were then converted into meshes compatible with DW-MRI simulations. Particularly, the DW-MRI simulations were carried out with the same parameters chosen by [1] and [2], but with an in-house GPU-accelerated framework to reduce computational times.

3. Results

A total of 25 virtual cell culture simulations were set up. The generated substrates were available at multiple steps of the simulations, characterised by different cell counts, volume fractions and cell volumes. The Kruskal-Wallis and post-hoc performed showed that there was a statistically significant difference in cell volumes between cell lines (p-value<0.05). Statistic similarity scores on cell volumes showed good agreement between real and simulated data, with an average of 0.88, 0.89 and 0.80 for mean, median and standard deviation respectively. An example of the simulated DW-MRI signals at different values of volume fraction and cell count is available in Figure 1.

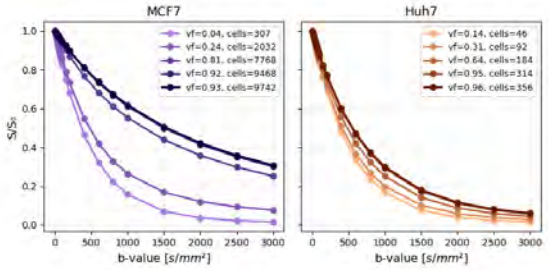


Figure 1: examples of DW-MRI signals for two cell lines at different values of volume fraction and cell count.

4. Discussion and Conclusions

This framework allows for the generation of biologically-informed *in silico* tumour substrates. These substrates can be used to extend the works of [1] and [2], providing more realistic data and vaster arrays of DW-MRI signals.

5. References

[1] G. Buizza *et al.*, *Med. Phys,* Mar. 2021.
[2] L. Morelli *et al.*, *Med. Phys,* May 2023.
[3] M. H. Swat *et al.*, *Methods in Cell Biology*, Academic Press Inc., 2012.
[4] C. Edlund *et al.*, *Nat. Methods*, Sep. 2021.
[5] Inc. DataCebo, "Synthetic Data Metrics," May 2024, 0.14.1.

Acknowledgements:
This work is supported by MINIONS – ERC Starting Grant n. 101116811.

PATIENT-SPECIFIC IN SILICO 3D MODEL OF BRAIN METASTASIS TREATMENT IN RESPONSE TO STEREOTACTIC RADIOSURGERY

Eleftherios Ioannou (1), Christos Panagiotis Papanikas (1), Dimitra Flouri (1), Loizos Siakallis (1), Georgia Karaoli (2), Elisavet Papageorgiou (2), Marilena Theodorou (2), Vasileios Vavourakis (1,3)

1. Mechanical & Manuf. Engineering Department, University of Cyprus, Cyprus;
2. Bank of Cyprus Oncology Centre, Cyprus; 3. Medical Physics & Biomedical Engineering Dept., UCL, UK

1. Introduction

Brain metastases (BMs) affect an estimated 20% of cancer patients [1]. Current treatment typically involves surgery, radiation therapy or both. Stereotactic radiotherapy (SRT) is a local therapy that can offer improved survival and reduced morbidity for cancer patients while avoiding whole-brain radiotherapy, which causes cognitive impairment [2]. However, predicting patient response to treatment on an individual basis remains elusive, due to the lack of reliable digital tools for clinical decision-making for patients diagnosed with brain metastases.

2. Materials and Methods

We present an organ-scale *in silico* modelling procedure (Fig. 1) that simulates the dynamics of secondary brain tumours in response to radiation treatment (i.e., SRT) by incorporating key biological processes such as tumour growth, necrosis, and oedema development. The model is formulated as a system of PDEs representing the spatiotemporal dynamics of each component and their interactions. It also integrates patient-specific data such as brain geometry, radiation dose distribution and the tumour region, to provide a personalized framework for predicting disease progression and treatment efficacy.

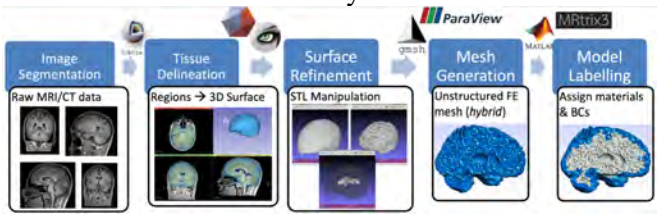


Figure 1: Pipeline for image segmentation and registration; DL for feature extraction and radiomics; model to fuse MRI and SRT data and personalised *in silico* prediction in response to radiotherapy.

3. Results

The model is applied to a recently published set of 40 BM patients [3], calibrated based on segmented regions of tumour/necrosis/oedema derived from 2 to 5 time points per patient. Results demonstrate the model's capability to replicate the spatiotemporal evolution of BM, including tumour regression (Fig. 2), necrosis and oedema development. Further, a data assimilation technique was applied to predict tumour evolution using input from only 1 or 2 follow-ups and was able to predict evolution in the remaining follow-ups for most cases.

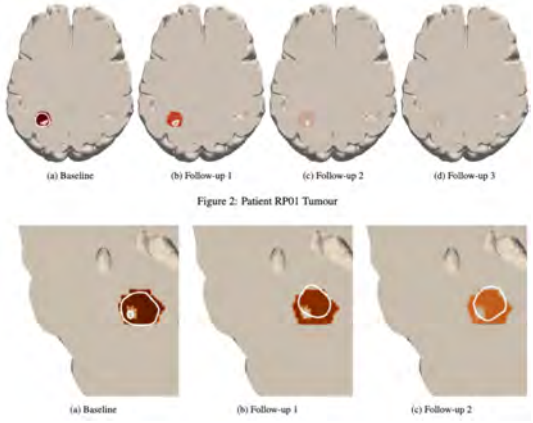


Figure 2: BM evolution of patient P29 after SRT.

4. Discussion and Conclusions

This study demonstrates the ability of the *in silico* model to predict BM progression and SRT outcome. By incorporating patient-specific data, the model provides a personalised framework that accounts for tumour heterogeneity and individual anatomical differences. The demonstrated capability of the data assimilation technique shows great potential for clinical application. Generating accurate predictions of tumour evolution utilizing data from the 1st follow-up after initial treatment can inform clinical decision-making by providing an early indication of treatment trajectory.

5. References

1. Achrol A. et al., Nat Rev Dis Primers (2019)
2. Kuntz L et al., Radiation Oncol (2023)
3. Flouri D et al., Sci Data (2025)

Acknowledgements

This work was financially supported by the Cyprus Cancer Research Institute (Project: PROTEAS; Grant: CCRI_2021_FA_LE_105).

UNRESOLVED CFD-DEM MODELING OF PLATELETS DYNAMICS ACCOUNTING FOR ACCURATE PARTICLE SHAPE

Francesca Zucchelli (1), Jonas Latt (1), Bastien Chopard (1)

1. Computer Science Department, University of Geneva, 1227 Carouge, Switzerland.

1. Introduction

Platelets (PLTs) play a key role in haemostasis and their dysfunction could result in the onset of severe cardiovascular disorders. Prevention and early diagnosis is possible but challenging, as current *in vitro* tests lack high predictive power due to the difficulty of characterising PLTs dynamics *in vivo*. Thus, *in silico* blood models prove to be essential and Unresolved CFD-DEM simulations, which are based on a fluid mesh coarser than the particle diameter, allow for large-scale microfluidic modelling of hundreds of thousands of particles. This approach provides an effective compromise between computationally heavy particle-resolved simulations and single-phase models, that neglect particle-scale dynamics. In this unresolved framework already effective for RBCs [1], we integrated oblate drag, lift and torque models [2] to drive PLTs motion in plasma. Finally, to include the inherently interactive nature of PLTs dynamics, we performed fully resolved bi-dispersed first-principles simulations and validated the unresolved model within a physiologically relevant context.

2. Materials and Methods

Blood is modelled as a suspension of RBCs and PLTs in Newtonian incompressible plasma. The Unresolved CFD-DEM method requires specific force models for fluid-particle interaction: RBCs were treated as deformable particles and their dynamic was implemented as in [1], while PLTs were considered rigid oblates with drag, lift and torque implemented based on [2]. The fully resolved simulations were realized using LEDDS [3] a Lattice Boltzmann solver. Both RBCs and PLTs were modelled as rigid oblate particles in Couette flow.

3. Results

PLTs trajectories and MSDs were extracted to quantify particle radial diffusion, cell free layer thickness and margination ability at different shear rates, Ht% and channel dimeters. The obtained results agree with the literature [4].

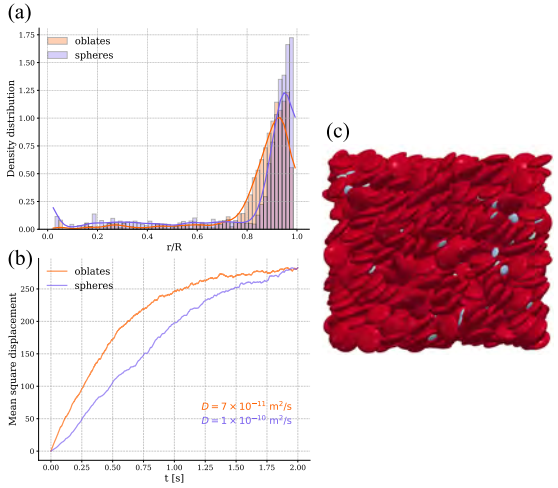


Figure 1: Comparisons of (a) final density distribution of PLTs across channel normalised radius (b) MSDs and correlated diffusion coefficients: oblates (orange) and spheres (lilac). (c) Illustration of fully resolved setup.

4. Discussion and Conclusions

This study clearly shows how considering the true geometrical nature of PLTs leads to effective and reliable unresolved blood flow models, displaying a behaviour much more physiologically accurate than previous models based on spheres. Lastly, the fully resolved simulations revealed how particle–particle interactions modify drag, lift and torque experienced by individual particles, leading to force models that differ from those derived under single-oblate shear flow assumptions.

5. References

1. Porcaro C, Saeedipour M., (2024) Comput. Biol. Med. 181, 109081.
2. Ouchene R., Phys. Fluids, 32 (2020), 073303.
3. Maggio-Aprile R. et al., arXiv:2512.04997, 2025.
4. H. Ye et al, Eng. Mech, 2019, 145(4), 04019021.

VIRTUAL PATIENTS FOR MECHANISTIC MODEL DISCOVERY IN VASCULAR MECHANOBIOLOGY

Alessandro Mastrofini (1), Michele Marino (1)

1. M2M Group, University of Rome Tor Vergata, Italy

1. Introduction

Understanding how molecular cues, cellular dynamics, and biomechanical forces collectively drive vascular inflammation remains a major challenge in atherosclerosis research. Growing evidence indicates that disruptions in lipid handling, immune responses, and mechanical stresses create interconnected feedback loops whose relative influence differs among individuals and does not adhere to a single causal pathway [1]. This complexity demands modeling approaches that can accommodate competing mechanistic explanations. We introduce a graph-informed mechanochemical framework that converts biological interaction knowledge into computationally testable models, supporting virtual patient generation and systematic investigation of vascular inflammation mechanisms [2].

2. Materials and Methods

A curated multiscale interaction graph describing lipid species, cytokines, macrophage and SMC phenotypes, oxidative and osteogenic cues, extracellular matrix turnover, and mechanical drivers was encoded through semantic rules [3,4]. Nodes denote biomechanical (hemodynamics indexes and/or vessel stresses measures) and biological (cells and molecules) entities; edges capture activating, inhibiting, or modulatory influences. Edges connecting biomechanical entities allow to select modules from a library of computational models of vessel fluid and structural mechanics. Edges connecting biological entities are converted into operators with different functional form (e.g., linear, weighted Hill-type, bell, soft-max) that define system couplings and specifies phenotype controller ODEs. Edges between biological and biomechanical entities define the architecture of the final chemo-mechano-biological model.

To maintain interpretability, each interaction is assigned a low/medium/high influence mapped to normalized coefficients. This supports automated construction of baseline virtual patients from a modular chemo-mechano-biological library, while mechanism-specific variants arise through adjustments in graph structure or pathway selection.

Competing hypotheses—e.g., inflammation-first, lipid-first, or mechanically amplified routes—are tested using Bayesian simulation-based inference, with posterior evidence indicating which mechanisms best explain observed patterns. Gaussian Process Regression supports parameter identification from datasets obtained in a clinically-relevant environment.

3. Results

The graph-based rationale generated compact ODE–PDE mechanochemical models capturing biochemical transport, phenotype transitions, and structural mechanics. Perturbing graph connectivity produced diverse virtual-patient families with distinct mechanistic behaviors. Initial inference analyses showed separable signatures for inflammation- and lipid-driven scenarios.

4. Discussion and Conclusions

This framework offers a scalable and interpretable workflow for mechanistic discovery in vascular inflammation. By combining automated model assembly, parsimony-oriented design, and Bayesian discrimination, it supports next-generation virtual-patient studies and personalized mechanochemical modeling.

5. References

1. Libby, P. (2021). *Nature* 592, 524–533.
2. Buehler, M. J. (2024). *MLST* 5(3), 035083.
3. Gierig, M., Gaziano, P., Wriggers, P., and Marino, M. (2024). *J Biomech* 166, 112058
4. Marino, M., Sauty, B., and Vairo, G. (2024). *Biomech Mod Mech* 23, 1091-1120

Acknowledgements:

The authors would like to thank the European Research Council (ERC-CoG-2025, Acronym: VISTA, Grant no: 101230891) for providing financial support to this project.

GRAPH-DERIVED MECHANOCHEMICAL SIMULATIONS CAPTURE VARIABILITY IN ATHEROSCLEROSIS PROGRESSION

Alessandro Mastrofini (1), Aikaterini Tziotziou (2), Daniel Bos (2,3), Ali C. Akyildiz (3,4), Michele Marino (1)

1. Multiscale and Multiphysics Mechanics Group (M2M), Department of Civil Engineering and Computer Science Engineering, University of Rome Tor Vergata, Italy; 2. Department of Cardiology, Biomedical Engineering, Cardiovascular Institute, Thorax Center, Erasmus MC, Netherlands; 3 Department of Radiology & Nuclear Medicine, Erasmus Medical Center, Netherlands; 4 Department of Biomechanical Engineering, Delft University of Technology, Netherlands

1. Introduction

Atherosclerosis progression results from nonlinear interactions among lipid metabolism, inflammatory signaling, cellular phenotype transitions, and arterial wall biomechanics. Most computational models rely on simplified pathways or weakly constrained parameter sets, limiting their ability to capture clinical heterogeneity [1,2]. We present a graph-derived mechanochemical framework that couples ODE-based phenotype regulation with transport–reaction PDEs and finite-element biomechanics to simulate plaque evolution in idealized and patient-specific geometries.

2. Materials and Methods

A curated biological interaction network, covering lipids, cytokines, macrophage and smooth muscle cell (SMC) phenotypes, matrix remodeling, oxidative cues, and mechanical drivers (strain, shear stress), was translated into a coupled mechanochemical model using standardized operators. A parameter estimation strategy was applied to define active pathways while preserving biological interpretability. Phenotype transitions (e.g., contractile vs synthetic SMCs and M1/M2 macrophages) were modeled with bistable controller ODEs, while biochemical and cellular processes were described by diffusion–reaction PDEs coupled structural mechanics. Patient-specific blood biomarkers informed initial and boundary conditions. Simulations were performed on (i) reduced-order synthetic geometries derived from PARISK population descriptors and (ii) two patient-specific carotid bifurcations from the PARISK longitudinal study [3].

3. Results

In synthetic geometries, selective activation of specific graph pathways generated a broad spectrum of progression, including lipid-dominated plaques, self stimulating inflammatory loops, and divergent calcification-resorption trajectories.

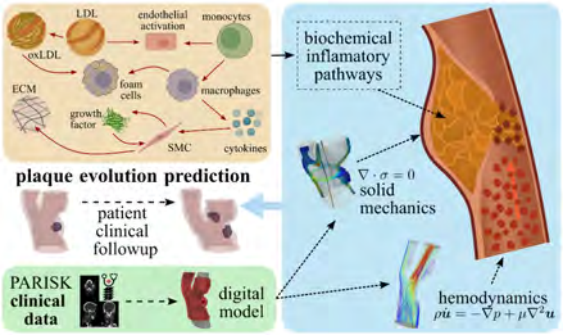


Figure 1: Integration of the patient-specific clinical data into a multiphysics model of plaque evolution.

These simulations qualitatively recapitulated the variability patterns observed in PARISK. In patient-specific models, simulations remained numerically stable while preserving biological interpretability. Variations in LDL levels, monocyte counts, and inflammatory markers led to distinct spatial patterns of lipid deposition, macrophage phenotype transitions, and calcification dynamics. Local predictions of calcification growth or regression were consistent with two-year follow-up imaging, supporting the framework's capacity to capture inter-patient variability.

4. Discussion and Conclusions

The graph-derived mechanochemical model successfully produced clinically consistent progression patterns at both population and individual scales. By integrating blood-derived biomarkers, reproducing diverse plaque evolution trajectories, and preserving biological interpretability, the approach demonstrates strong potential as a tool for future risk stratification and personalized modeling of vascular disease progression.

5. References

1. Ajoolabady A. et. al. Cell Cell Death Dis, 2024
2. Abou-Jaoudé W. et al. Front. Genet, 2016
3. Truijman MTB et al. International Journal of Stroke. 2013

Acknowledgements:
This work is supported by the ERC Consolidator Grant VISTA, n. 101230891.

MODELLING THE TRANSPORT OF OXYGEN AND CARBON DIOXIDE IN THE HUMAN VASCULAR SYSTEM

Márta Viharos (1), Richárd Wéber (1)

1. Department of Hydrodynamic Systems, Faculty of Mechanical Engineering, Budapest University of Technology and Economics, Műegyetem rkp. 3, Budapest, 1111, Hungary

1. Introduction

Blood flow in the human vascular system is a complex and physiologically essential process responsible for transporting respiratory gases, nutrients, and metabolic waste. Oxygen (O2) delivery and carbon dioxide (CO2) removal are fundamental for cellular metabolism and play a key role in maintaining homeostasis and vascular regulation. Figure 1 illustrates the process of carbon dioxide transport in the systemic capillaries. This work develops a mathematical model describing the coupled transport of O2 and CO2 within systemic and pulmonary capillaries and integrates the main physiological transport mechanisms into a computational hemodynamic framework, called first blood [1].

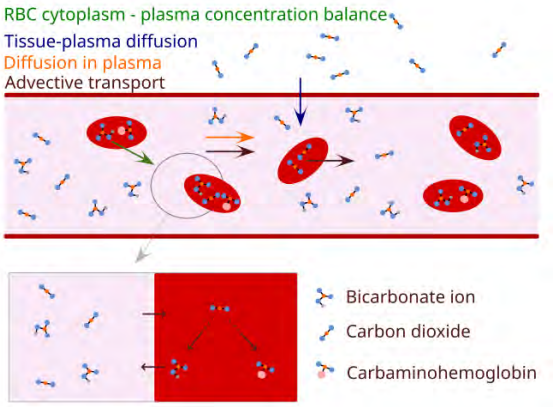


Figure 1: Transport of carbon dioxide in the systemic capillaries.

2. Materials and Methods

The model is derived from the law of mass conservation and incorporates the primary physiological transport mechanisms of O2 and CO2. Oxygen transport is modeled through hemoglobin binding and dissolution in plasma [2], while carbon dioxide transport includes bicarbonate formation in red blood cells, carbaminohemoglobin binding, and dissolution in plasma. The resulting coupled differential equations describing gas exchange and transport dynamics are discretized using the finite difference method and implemented in the open-source hemodynamic solver first_blood.

3. Results

The developed model enables numerical simulation of coupled O2 and CO2 transport within systemic capillaries and reproduces the relative physiological contributions of the different transport pathways. The implementation remains computationally efficient and suitable for integration into larger circulation models.

4. Discussion and Conclusions

The proposed framework provides a basis for simulating gas-dependent autoregulatory mechanisms and contributes to comprehensive modeling of human circulation and its control processes. Plans include using the model for stroke research.

5. References

[1] Wéber, R., Gyürki, D., & Paál, G. (2023). First blood: An efficient, hybrid one- and zero-dimensional, modular hemodynamic solver. *International Journal for Numerical Methods in Biomedical Engineering*. https://doi.org/10.1002/cnm.3701

[2] Y. Bing, 'Multi-Scale, Multi-Compartment Coupled Flow-Oxygen Models of Ischaemic Stroke'. PhD thesis, University of Oxford, 2022

Acknowledgements:

GEMINI has received funding from the European Union's Horizon 2020 research and innovation programme under the grant agreement No 101136438. The research was supported by the János Bolyai Research Scholarship (BO/00484/23/6) of the Hungarian Academy of Sciences and by the New National Excellence Program of the Ministry for Culture and Innovation from the source of the National Research (Wéber Richárd ÚNKP-22–5-BME-426).

FROM GLOBAL HAEMODYNAMICS TO SARCOMERE MECHANICS: AN IN-SILICO MODEL APPLIED TO DILATED CARDIOMYOPATHY

Akhilesh Kamtikar (1), Dirk Donker (1,2), Libera Fresiello (1)

1. *Cardiovascular and Respiratory Physiology, TechMed Centre, University of Twente, Enschede, The Netherlands*
2. *Intensive Care Centre, University Medical Centre Utrecht, Utrecht, The Netherlands*

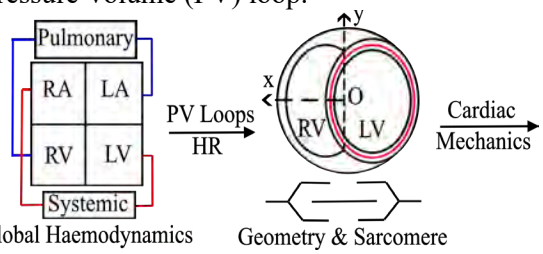
a.j.kamtikar@utwente.nl , Tel.: +31 53 489 8972, P.O. Box 217, 7500 AE Enschede, The Netherlands

1. Introduction

Translating system level, clinically accessible haemodynamics to cellular-level mechanics remains challenging in remodelled hearts. We address this with a multiscale in-silico model linking global haemodynamics to sarcomere mechanics, and applying it to the normal and dilated cardiomyopathy (DCM) phenotypes to investigate cardiac dysfunction mechanisms.

2. Materials and Methods

The in-silico framework couples a validated lumped parameter closed-loop cardiovascular simulator (CVS) [1] to a Geometric–Sarcomere Module (GSM) of biventricular mechanics. Adapted from the TriSeg model [2], the GSM solves midwall ventricular geometry, and links the predicted sarcomere mechanics to the CVS pressure-volume (PV) loop.



CVS haemodynamics (heart rate, PV loops, systemic and pulmonary pressures) and GSM geometry (cardiac wall volumes and reference geometry) were tuned to healthy and DCM phenotypes using literature data. The GSM predicted cardiac midwall stress-strain (SS) loops, wall thickness, sarcomere length and stresses, were validated against literature data.

3. Results

The simulated DCM left ventricular PV loop shows a rightward shift compared to the healthy phenotype (end-diastolic volume: 260 vs. 130 mL). Corresponding SS loop shows lower peak strain magnitude in DCM (-10% vs. -26%), whilst peak myofibre stress is markedly higher (150 vs. 95 kPa). This creates a mechano-energetic mismatch: DCM ventricular stroke work is lower (0.9 vs. 1.3 J), but the myofibres work remains comparable (1.3 vs. 1.4 J). Consequently, mechanical efficiency (ratio of ventricular stroke work to myofibre work) drops from 93% to 69%, indicating the dilated heart is structurally inefficient and requires higher stress to maintain comparable pressure and cardiac output.

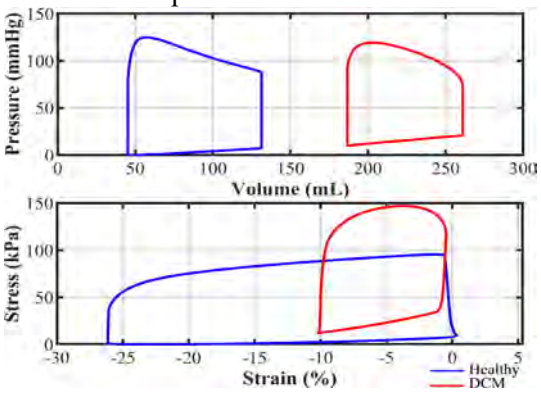


Fig. 1: Healthy and DCM and SS and PV loops.

4. Discussion and Conclusions

The model shows that maintaining systolic pressure in a geometrically enlarged, thin walled and dilated ventricle, requires a compensatory surge in active and passive myofibre stress. The model can support the investigation of DCM profiles, with different ventricular haemodynamics and underlying geometric characteristics, to unmask inefficient pump mechanics and define tailored therapeutic strategies.

5. References

1. Fresiello et al, Front. Physiol. 13, 2022
2. Lumens et al, Ann Biomed Eng. 37, 2009

Acknowledgements:
This work is supported by the University of Twente starter grant.

A MULTI-SCALE APPROACH TO MODELING SWIRLING BLOOD FLOW IN THE LEFT HEART AND AORTA

Gorodkov A.[1], Zharkov Ya.[1], Talyguin E.[1], Beglov I.[2], Agafonov A.[1], Chernykh N.[1]

[1] *Bakulev National Medical Research Center for Cardiovascular Surgery, Moscow, Russia*

[2] *MIREA – Russian Technological University, Moscow, Russia*

Corresponding author: Alexandre Gorodkov, agorodkov@bk.ru

1. Introduction

To date, four main methodological approaches have been developed for studying blood flow in the central circulatory system: analytical modeling based on hydrodynamic equations, experimental flow visualization and measurement methods (primarily 4D flow MRI and PIV), geometric approximations of flow channels, and computational fluid dynamics (CFD). Each of these approaches has its own advantages, but none alone is self-sufficient for the full range of clinical tasks. The aim of this study was to integrate these approaches for modeling the processes occurring in the heart and aorta during the generation of pulsatile swirling blood flow.

2. Materials and Methods

Modified exact Bürgers vortex solutions [1,2], supplemented by an external variable force created by left ventricular contraction, were used as the hydrodynamic model. Analysis of the streamlines of the resulting flow allowed formulation of boundary conditions that maintain the swirling flow structure throughout the entire cardiac cycle. Construction of a parameterized geometric model of the flow channel based on CT data showed that the streamlined surfaces from the left atrium to the aortic bifurcation satisfy the condition zr^2 = const at the moment of maximum flow velocity, with the power exponent p close to 2 in all three consecutive segments studied [3]. Cross-sectional radii were approximated by cyclic surfaces whose axes followed rational Bézier spline curves [3].

Experimental investigation of the flow in bench experiments and MRI 4D Flow data showed that the flow structure generally corresponds to the analytical expressions used [4]. Numerical modeling in COMSOL Multiphysics with the k–ω turbulence model was validated against physical experiments by comparing flow rates and streamline helix turn counts [4]. A parametric study varying the convergence index N from 1.25 to 2.75 and dome height from 0 to 15 mm was conducted to identify optimal channel geometry [5].

3. Results

Multi-scale modeling showed that swirling blood flow in the left ventricle and aorta provides a reproducible vortex oriented along the channel axis, characterized by uniformly low shear stresses and absence of boundary layer thickening and separation, with sufficient pressure–flow characteristics. Geometric parameterization confirmed that the condition $(z_0+z)\cdot r^2=B$ holds across all three segments with exponents p=1.94, 2.09, and 2.05 [3]. Numerical modeling demonstrated that among channels of the form zR^N=const, only N=2 maintains a stable vortex structure along its entire length, with 82% lower viscous losses compared to N=1 and 15% lower than N=3 [4]. A spherical dome of optimal height (7 mm) at the jet origin further reduced losses and provided a twofold reduction in peak shear stresses [4,5]. The flow reproduced by CFD in parameterized boundaries was consistent with 4D flow MRI patterns.

4. Discussion and Conclusions

The proposed approach allows reproducing and analyzing blood flow generation and maintenance at the level of mechanisms ensuring homeostasis. Such modeling will enable predicting circulatory changes due to alterations in dynamic geometry of the vascular bed and cardiodynamic disturbances, planning cardiac surgical interventions, and designing implantable devices in contact with blood flow.

5. References

1. Kiknadze GI, Krasnov YK. Sov Phys Dokl. 1986;31:799–801.
2. Burgers JM. Adv Appl Mech. 1948;1:171–199.
3. Beglov I et al. Appl Sci. 2025;15:5291.
4. Zharkov YE et al. Dokl Biochem Biophys. 2024;513(Suppl 1):S36–S52.
5. Zharkov YE et al. Dokl Biochem Biophys. 2025;520(1):6–19.

CFD-ABM FRAMEWORK QUANTIFIES MONOCYTE NLRP3 INFLAMMASOME ACTIVATION HOTSPOTS DRIVEN BY ARTERIAL LOW-SHEAR HEMODYNAMICS

V V S Varaprasad Jakka (1), Mané Sarkissian (1), Yalemzerf Motbaynor Alemu (1), Jérôme Noailly (1)

1. BCN MedTech, Universitat Pompeu Fabra (UPF), Barcelona, Spain

1. Introduction

Atherosclerotic plaques develop preferentially in arterial regions with disturbed flow and low wall shear stress [1]. The NLRP3 inflammasome responds to shear stress [2], hypoxia [3], and oxidized lipids [4], yet whether spatial inflammasome clustering emerges from hemodynamic forces alone or requires monocyte-endothelial interactions remains unresolved. We developed a coupled CFD-ABM framework tracking 4,000 monocyte trajectories through realistic hemodynamic fields over 10 hours, with state-dependent NFκB and NLRP3 activation, to reveal whether spatial clustering arises from first principles.

2. Materials and Methods

A curved iliac artery (184.5 mm; diameters 12.2/12.5 mm) was meshed in OpenFOAM v10 (~150,000 cells). simpleFoam computed steady-state flow (U = 0.35 m/s, Re = 1295) for time-averaged wall shear stress [1]. particleFoam tracked 4,000 monocyte particles (9 µm, stick-on-contact adhesion [5]) over 10 hours. Trajectories were exported to BioDynaMo (v1.05) for agent-based modeling, with hemodynamic fields interpolated to agent positions each timestep. NFκB activation was modeled as state-dependent following the monocyte adhesion cascade [5], with fold-change multipliers iteratively verified against physiologically plausible outputs; NLRP3 required NFκB-dependent transcriptional priming [6] plus environmental second signals shear stress [2], hypoxia [3], and oxLDL [4] derived from mass-transfer coupling, not prescribed a priori. Monocytes were assigned classical (85%), intermediate (5%), or non-classical (10%) phenotypes across six independent runs (CV = 2.7%).

3. Results

After 10 hours, 8.0% of monocytes (321 ± 9 / 4,000) achieved firm adhesion. NFκB showed strong state-dependence: rolling cells had basal activity (0.155 ± 0.089), adhered cells showed a 5.2-fold increase (0.800 ± 0.124), and transmigrating cells reached peak levels (0.876 ± 0.098). Only the adhered 8% activated NLRP3 (population average: 0.066), yet these cells reached near-maximal levels (0.83-0.99). The middle vessel region showed 2.26-fold NLRP3 activation (0.103 ± 0.142 vs. 0.046 ± 0.078 at inlet), coinciding with the lowest velocity (245 vs. 350 mm/s) and highest cell accumulation (143 ± 4 vs. 61 ± 2).

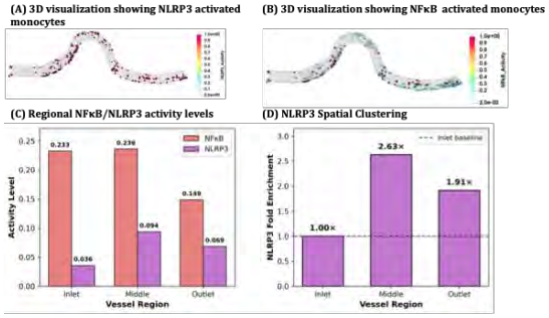


Figure 1. (A–B) 3D visualizations of NLRP3 and NFκB monocyte activation. (C) Regional activity levels. (D) NLRP3 spatial clustering.

4. Discussion and Conclusions

This is the first CFD-ABM framework linking arterial hemodynamics to single-cell inflammatory signaling over 10-hour timescales. Notably, NLRP3 spatial enrichment arose from coinciding hemodynamic and biochemical conditions reduced velocity prolonging monocyte residence, promoting hypoxia, and amplifying adhesion-triggered NFκB priming rather than any assumed inflammatory predisposition. The 5.2-fold NFκB amplification upon adhesion suggests that monocyte capture precedes NFκB priming, followed by NLRP3 activation in hypoxic low-shear zones, mechanistically explaining preferential plaque localization at arterial curvatures [1]. Scaling to 350 × 10^6 agents targets whole-body inflammation mapping, though validation against patient lesion histology remains future work.

References

[1] Chiu & Chien. Physiol Rev. 2011; 91:327-387.
[2] Xiao H, et al. Circulation. 2013; 128:632-642.
[3] Wang X, et al. FASEB J. 2024;38: e23854.
[4] Jiang Y, et al. Biochem Biophys Res Commun.
[5] Ley K, et al. Nat Rev Immunol. 2007; 7:678-689.
[6] Bauernfeind FG, et al. J Immunol. 2009; 183.

Acknowledgements: ERC Consolidator Grant O-Health (No. 101044828).

PATIENT-SPECIFIC ATRIAL MODELS CALIBRATED WITH CLINICAL LOCAL ACTIVATION MAPS FROM TRIPLE-EXTRA PACING

Duna de Luis-Moura[1], Chiara Celotto[2], Saman Golmaryamii[3], María Termenón-Rivas[1], Giada S Romitti[1], Etel Silva[3], Juan Fernandez-Armentia[3], José F Rodriguez[2], Alejandro Liberos[1], Miguel Rodrigo[1]

[1]CoMMLab, Universitat de València,València, Spain. [2]Department of Chemistry Giulio Natta, Politecnico di Milano, Milano. [3]Department of Cardiology, Hospital Universitario Puerta del Mar, Cádiz, Spain

1. Introduction

Advanced pacing protocols such as triple extrastimuli (3-Extra) can uncover conduction abnormalities involved in Atrial Fibrillation (AF) maintenance [1]. This study develops personalized left atrial (LA) computational models capable of reproducing local activation time (LAT) maps in 3-Extra pacing protocol.

2. Materials and Methods

Twenty patient-specific volumetric LA meshes (~0.3mm) were generated from CT segmentations. Fiber orientation and tissue differentiation was included from an atrial atlas, and patient-specific fibrosis was inferred from peak-to-peak voltage maps (fig 1A).

The electrophysiological model was calibrated in three phases: 1) by global diffusion (25 to 650%) (fig 2B); 2) by local diffusion based on LAT errors (fig 2C); and 3) by ionic remodeling (25%/healthy to 125%/chronic AF) [2] (fig 2D). Calibration was performed against LAT maps from the third 3-Extra (fig 1B) by minimizing the mean absolute error (MAE) (fig 1C).

3. Results

Across the 20 patients, the median percentage of fibrosis was 9.6 [6.5 - 16.7]%, obtaining a baseline simulation with MAE of 34 [28 - 45] ms. Global diffusion adjustment required a median increase of 250 [175 - 425]%, reducing the MAE to 14 [13 - 18] ms. The local diffusion correction resulted in a MAE of 14 [13 - 17] ms. And finally, ionic remodeling was set to a median of 63 [50 - 88]%, achieving a final MAE of 13 [12 - 16] ms (fig 3).

4. Discussion and Conclusions

Personalized volumetric atrial models integrating CT-based anatomy and clinical electrophysiological data can accurately reproduce patient-specific activation times during 3-Extra pacing. These results support the use of this framework for future *in silico* evaluation of personalized therapeutic strategies in AF.

5. References

1. Silva Garcia E, et al. EP Europace, 25(11) (2023).
2. Barrios-Álvarez de Arcaya J, et al. Annals of Biomedical Engineering, pp. 1–14, (2025).

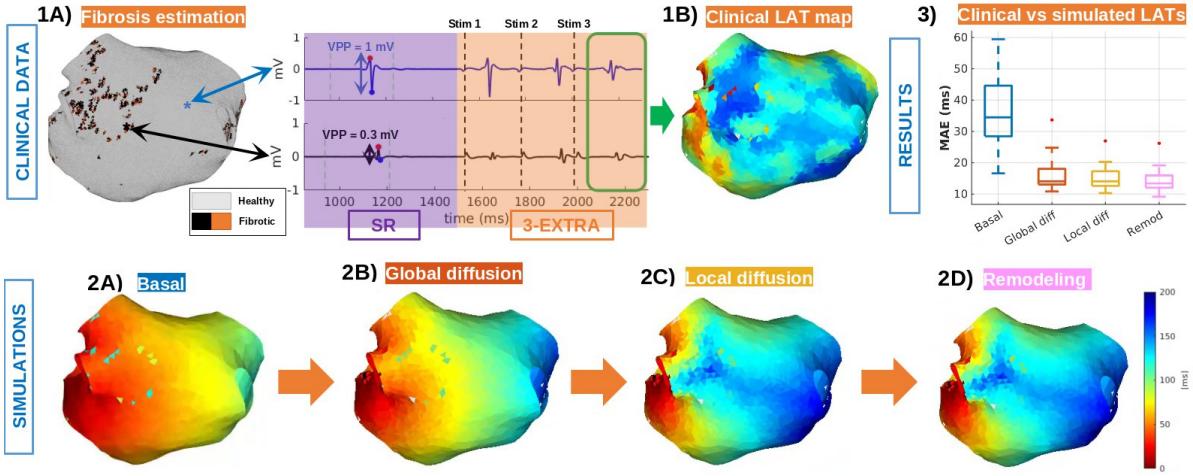


Figure 1: Summary of the methodology followed in the study and its main results.

9th International Conference on the Virtual Physiological Human
1 - 4 September 2026
Milan, Italy

A GRAPH NEURAL FRAMEWORK FOR FULL-CYCLE VENTRICULAR MYOCARDIAL FINITE ELEMENT BIOMECHANICS SIMULATIONS

Siyu Mu (1), Wei Xuan Chan (1), Choon Hwai Yap (1)

1. Department of Bioengineering, Imperial College London, UK

1. Introduction

Finite element modelling (FEM) is a powerful computational tool for investigating cardiac biomechanics and predicting function, but traditional FEM is very slow, discoursing clinical adoption [1]. Deep learning (DL) offers a faster alternative. However, PINN-FEM require reduced-order modelling that reduces accuracy, and still need many minutes for inference, while existing one-shot networks succeeded in modelling only passive diastolic mechanics without systolic contractions [2]. Here, we introduce CardioGraphFENet, a DL graph-based FEM surrogate for real-time full-cycle left ventricle (LV) modelling generalized across any arbitrary LV 3D mesh input.

2. Materials and Methods

Our method, CardioGraphFENet (CGFENet), functions as a unified surrogate for both forward FEM (predicting pressure and displacement fields) and inverse FEM (predicting the zero-pressure load-free configuration). The architecture integrates a graph fusion encoder to extract mesh features and uses GRUs to encode time-dependent mechanics. It is trained with a self-supervised cycle-consistent strategy, where the predicted forward FEM step is enforced to match the predicted reversal of the step. The framework was trained on a synthetic dataset of over 1.8 million LV states, generated from a range of LV shapes from a statistical shape model [3] and varying physiological conditions.

3. Results

CGFENet was benchmarked against GraphUNet and MeshGraphNet and demonstrated the best performance. For loading displacement prediction, the model achieved an accuracy of 90% of nodes having <1mm error, and RMSE<2 mmHg for pressure prediction. When combined with a lumped parameter model, the predicted P–V loop closely matched the FEM ground truths. For a full cycle simulation of 50 time points, CGFENet reduced computation time from several hours to under one minute, a 70-fold acceleration.

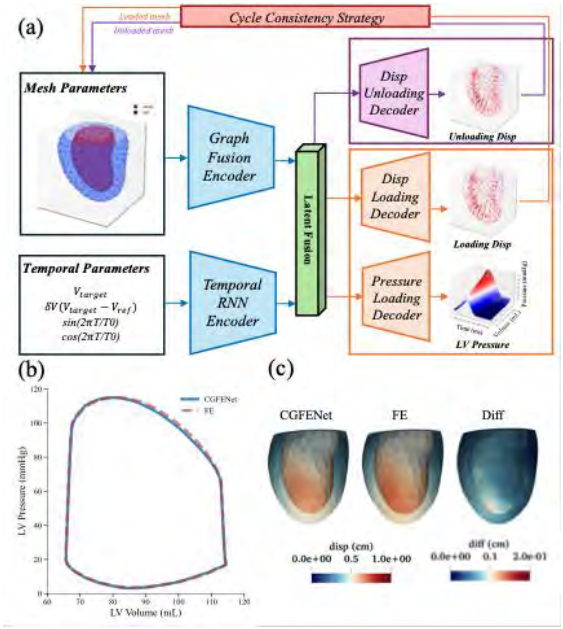


Figure 1: (a) Overview of the CardioGraphFENet architecture for bidirectional LV mechanics prediction. (b) Comparison of predicted and FEM P-V curves. (c) Displacement prediction compared with FE simulation and the corresponding error map.

Model	Vertex Acc <1mm ↑	Pressure RMSE (mmHg) ↓
GraphUNet	0.85 ± 0.01	5.83 ± 0.22
MeshGraphNet	0.81 ± 0.03	3.63 ± 0.10
Ours	**0.90 ± 0.01**	**1.70 ± 0.17**

Table 1: Baseline comparison of displacement accuracy and pressure prediction.

4. Discussion and Conclusions

CGFENet is the first DL FEM graph-based surrogate with very fast predictions outputs, and is faster and more accurate than PINN. It also allows anyone without FEM skills to perform FEM very quickly. By addressing speed and skill issues, it can encourage clinical adoption and enabling large clinical trials. Being robust, fast and flexible, it can be used in various secondary optimization loops.

5. References

1. C. Rodero et al., Front. Phys., 2023.
2. D. Dalton et al., CMAME., 2023.
3. P. Medrano-Gracia et al., JCMR, 2014.

VALIDATION OF A COMPUTATIONAL MODEL FOR CARDIAC PERFUSION IN MYOCARDIAL ISCHEMIA DETECTION

Viola Cusumano (1,2), Riccardo Maragna (1), Ettore Ventura (1), Guido Nannini (3), Gianluca Pontone (1), Christian Vegara (2)

1.Centro Cardiologico Monzino, IRCCS, Milano; 2.LaBS, Dipartimento di Chimica, Materiali e Ingegneria Chimica "Giulio Natta", Politecnico di Milano, Milan, Italy; 3. Dipartimento di Elettronica Informazione e Bioingeneria, Politecnico di Milano, Milano, Italy;

1. Introduction

Quantitative myocardial blood flow (MBF) assessment is essential for diagnosing coronary artery disease (CAD). Stress computed tomography perfusion (stress-CTP) enables MBF quantification but requires pharmacological stress and additional radiation beyond routine coronary CT angiography (CCTA). Computational perfusion models offer a non-invasive alternative for estimating MBF from resting CCTA but remain limited by patient-specific parameter calibration and small validation cohorts. This study proposes a stenosis-guided calibration strategy for cardiac perfusion modeling validated in 100 patients.

2. Materials and Methods

We retrieved CCTA and stress-CTP scans from 109 PERFECTION study patients (Centro Cardiologico Monzino, Milan). Patient-specific coronary arteries and left ventricular myocardium were reconstructed from CCTA and coupled by mapping myocardial perfusion regions to coronary outlets [2]. A coupled mathematical model combining Navier–Stokes equations for epicardial coronary flow with a three-compartment Darcy model for intramyocardial hemodynamics, accounting for vessel distensibility, was employed [2]. Simulations were performed using the finite element library LifeX. Model calibration stratified patients by maximum stenosis degree (SD) and assigned region-specific SD. Validation was performed on 100 patients by mapping simulated and stress-CTP MBF maps onto the 17-segment AHA model and evaluated ischemia classification agreement using a simplified 7-segment representation (Figure 1).

3. Results

Global performance in the 100-patient validation cohort yielded an area under the ROC curve (AUC) of 0.78, indicating good discrimination between ischemic and healthy segments. Performance was evaluated across three stenosis severity groups, and validation metrics are summarized in Table 1. These results indicate good discriminative ability for ischemia detection while maintaining a conservative classification strategy.

SD group	Sensitivity	Specificity
< 50 %	-	0.91
50 – 70%	0.61	0.76
≥ 70%	0.83	0.41

Table 1: Segment-level diagnostic performance across stenosis severity groups in the 100-patient validation cohort.

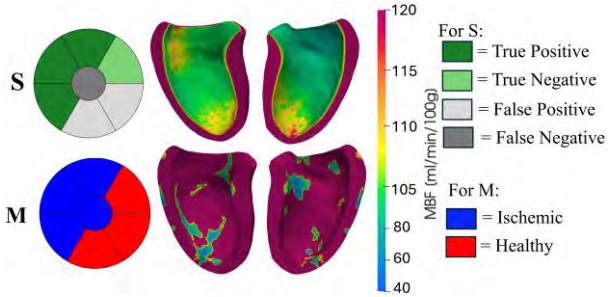


Figure 1: Simulated (S) and measured (M) MBF maps shown as bull's-eye representations and corresponding 3D endocardial views.

4. Discussion and Conclusions

This study provides a large-scale validation, on 100 patients, of a calibration strategy for computational cardiac perfusion modeling. Results show promising agreement with stress-CTP and support the feasibility of computational perfusion modeling for ischemia detection from resting CCTA.

5. References

1. Pontone, G. et al. JACC: Cardiovascular Imaging, 2019.
2. Montino Pelagi, G. et al. Biomechanics and Modeling in Mechanobiology, 2024.

TOWARDS THE VALIDATION OF PATIENT-SPECIFIC LEFT ATRIAL CFD SIMULATIONS: A COMPARATIVE PIV STUDY

Ilaria Verdirame (1, 2), Emanuele Gasparotti (1), Emanuele Vignali (1), Benigno Marco Fanni (1), Simona Celi (1)

1. BioCardioLab, Bioengineering Unit, Fondazione Monasterio, Italy; 2. Department of Information Engineering, University of Pisa, Italy

1. Introduction

The left atrial appendage (LAA) is the main site of thrombus formation in non-valvular atrial fibrillation (AF) due to its complex anatomy and local blood stasis. While LAA occlusion (LAAO) is an established procedure to mitigate this risk, it induces significant hemodynamic shifts within the left atrium (LA) that require precise characterization [1]. In this context, computational fluid dynamics (CFD) provides a powerful tool for patient-specific hemodynamic assessment; however, its clinical reliability depends on the rigorous validation of predicted flow patterns [2]. In accordance with ASME V&V40 standards, this work aims to validate patient-specific CFD simulations through direct comparison with high-resolution particle image velocimetry (PIV) data in both pre- and post-LAAO configurations.

2. Materials and Methods

The LA of a patient with AF was reconstructed from pre-procedural CT images and used to fabricate a transparent PDMS phantom via brush-spin-coating. The model was integrated into a pulsatile mock circulatory loop for in vitro investigation. To ensure optical access for PIV measurements, a refractive-index-matched blood analog (water-glycerol-urea) was employed [3]. The post-LAAO scenario was reproduced by incorporating a PDMS model of the occlusion device into the LA phantom. Planar velocity fields were acquired in longitudinal and transverse planes using a LED-based PIV system.

In parallel, transient CFD simulations were conducted using ANSYS Fluent. To enable a consistent comparison with the in vitro data, identical inflow and outflow boundary conditions were imposed.

Finally, PIV images were processed via double-frame cross-correlation and compared with corresponding CFD slices to quantify the agreement between numerical and experimental approaches.

3. Results

The comparison of velocity fields in Figure 1 shows a strong correspondence between the CFD and PIV data in both longitudinal (Fig. 1a) and transverse (Fig. 1b) planes. Both approaches captured the main flow structures within the LA and reproduced the changes in velocity distribution observed after LAAO.

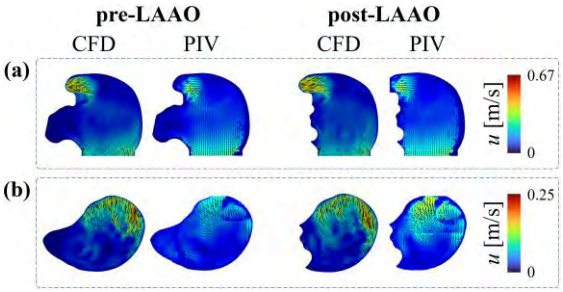


Figure 1. CFD and PIV velocity magnitude (u) distributions for pre- and post-LAAO scenarios in longitudinal (a) and transverse (b) planes.

4. Discussion and Conclusions

The observed agreement between CFD and PIV suggests that patient-specific simulations can reproduce the main hemodynamic features of both pre- and post-LAAO configurations. While further validation on a larger cohort is warranted, these results represent a step toward strengthening the credibility of CFD models for procedural planning applications.

5. References

1. Alkhouli M et al., JACC Adv., 1(5):100136 (2022)
2. Morrison TM et al., ASAIO J., 65(4):349-360, (2019)
3. Gasparotti E et al., BioSysRob (2025)

Acknowledgements:

This work was part of the project “PLACE - Planning LAa ClosurE” (RF-2021-12375208), funded by the Italian Ministry of Health.

A V&V40-ALIGNED CREDIBILITY FRAMEWORK FOR REGULATORY-GRADE LEFT ATRIAL APPENDAGE OCCLUDER IN-SILICO TRIALS

Oscar Camara (1)

1. *Universitat Pompeu Fabra, Department of Engineering, Barcelona, Spain*

1. Introduction

Left atrial appendage occlusion (LAAO) is a non-pharmacological alternative for stroke prevention in atrial fibrillation (AF) patients, yet device-related thrombus (DRT) affects 2–3% of cases. While patient-specific computational fluid dynamics (CFD) provide a platform to evaluate haemodynamics, the lack of standardized verification, validation, and uncertainty quantification (VVUQ) practices remains a major barrier to clinical and regulatory adoption. This work presents a structured roadmap to assess the credibility of LAAO-specific fluid simulations, aligned with the ASME V&V40-2018 standard [1].

2. Materials and Methods

The framework defines a Context of Use (CoU) focused on the preclinical evaluation of device designs and implantation strategies. The Question of Interest (QoI) asks whether the coverage of the pulmonary ridge (PR) by a device (plug or pacifier) increases the likelihood of low blood flow velocities (< 0.2 m/s), thereby promoting DRT [2]. Following V&V40, we implemented a VVUQ plan:

1. Numerical Verification: Mesh and time-step refinement studies were performed in ANSYS Fluent to ensure solution convergence.
2. Sensitivity Analysis (SA): The influence of boundary conditions (BCs), wall motion, and device positioning was assessed using sensitivity metrics.
3. Uncertainty Quantification (UQ): Variability propagation was planned across more than 1,400 simulations to prioritize dominant inputs.
4. Experimental Validation: A hierarchy of in-vitro phantoms was used, ranging from rigid-wall silicone models for high-resolution PIV to dynamic-wall models using soft robotic actuators to reproduce impaired atrial contraction [3].
5. Credibility Assessment: Evidence was integrated to evaluate if the model is fit for purpose

3. Results

Verification activities confirmed that numerical errors were small relative to physiological variability. The sensitivity analysis identified boundary conditions and device positioning as the modelling choices with the highest impact on peri-device velocity metrics [4], whereas blood rheology and wall motion had secondary effects. Large-scale UQ propagated these uncertainties to establish confidence intervals for low-flow zones. Validation results showed high qualitative and quantitative agreement between CFD-predicted velocity patterns and measurements in rigid and dynamic phantoms.

4. Discussion and Conclusions

This framework demonstrates "how good is good enough" for using in-silico models in LAAO assessment. By identifying that pulmonary ridge coverage and distal positioning are critical hemodynamic determinants for DRT, the model provides actionable mechanistic insights. This roadmap, developed under the H2020 EU SimCardioTest and GEMINI projects, bridges the gap toward regulatory-grade digital twins for complex cardiovascular interventions.

5. References

1. ASME V&V 40-2018, ASME (2018).
2. Freixa X et al., EuroIntervention; 16(15):e1288-e1294 (2021).
3. Mendez K et al., CVET; 16(3):279-295 (2025).
4. Albors C et al., PLOS Computational Biology; 20(9):e1011546 (2024).

Acknowledgements:

This work was supported by the European Union's Horizon 2020 programme (GEMINI, Grant No. 101136438), the Spanish Ministry of Science (GENERALITAAT, Grant No. PIT2022-143239OB-I00).

TOWARDS CREDIBLE ECG-BASED VENTRICULAR DIGITAL TWINS: UNCERTAINTY-AWARE LIMITS OF CONDUCTION-SUBSTRATE DETECTABILITY

Julia Camps (1), Oscar Camara (1)

1. Universitat Pompeu Fabra, Barcelona, Spain

Corresponding author: Julia Camps, Universitat Pompeu Fabra, Barcelona, Spain; julia.camps@upf.edu

1. Introduction

Digital twins are increasingly proposed as tools for mechanistic interpretation and decision support in cardiovascular medicine, but their clinical adoption depends not only on physiological realism, but also on credible assessment of what model-based outputs can and cannot be inferred under realistic uncertainty. In electrocardiography, this issue is particularly important because multiple sources of variability may alter the apparent visibility of underlying substrates. Here, we present an uncertainty-aware credibility assessment of ECG-based ventricular digital twins, using regional conduction abnormalities as a representative case study.

2. Materials and Methods

We considered a population of representative biventricular anatomies under sinus rhythm and simulated ventricular activation using a pure Eikonal model. QRS-only 12-lead pseudo-electrocardiograms were computed with an infinite-volume forward formulation. To reflect realistic use conditions, we incorporated three key uncertainty sources: anatomical variability, lead-placement variability through an electrode ensemble, and measurement uncertainty through noise-aware ECG biomarkers. Regional conduction slowing was introduced as the perturbation of interest on otherwise healthy baselines. Detectability was assessed primarily from QRS duration, with supporting morphology-based biomarkers used for secondary interpretation, and interpreted relative to uncertainty-aware thresholds.

3. Results

Preliminary analyses indicate that the detectability of conduction abnormalities is strongly context dependent. The same perturbation can produce clearly distinguishable ECG changes in some settings and remain practically indistinguishable in others once realistic uncertainty is included. Detectability varies with anatomical background, region, perturbation severity, and lead configuration, showing that apparent signal changes in idealised simulations may overestimate what can be robustly interpreted in practice.

4. Discussion and Conclusions

These results support a shift from asking whether a digital twin can reproduce a given ECG pattern to asking whether the inferred substrate is credible under the relevant uncertainty sources. In this framework, ECG-based ventricular digital twins become not only simulation tools, but testbeds for defining the practical information limits of mechanistic ECG interpretation. This credibility-oriented perspective is essential for responsible translation of cardiac digital twins towards healthcare use.

Acknowledgements:

The project that gave rise to these results received the support of a fellowship from ‘la Caixa’ Foundation (ID 100010434) to JC (LCF/BQ/PI25/12100029).

AUTOMATED CREDIBILITY ASSESSMENT: A MODEL-AGNOSTIC PIPELINE APPLIED TO CARDIAC DIGITAL TWINS

Stephen A. Creamer (1), Alireza Sharifzadeh-Kermani (1,2), Finbar J. Argus (1), Debbie Zhao (1), Martyn P. Nash (1,3), David P. Nickerson (1)

1. Auckland Bioengineering Institute, University of Auckland, NZ; 2. Mātai Medical Research Institute, NZ; 3. Department of Engineering Science and Biomedical Engineering, University of Auckland, NZ

1. Introduction

Verification, validation, and uncertainty quantification are critical considerations when translating computational models, particularly digital twins, for clinical application. Despite common use in other fields, most published biomedical digital models lack credibility assessment due to a paucity of suitable tools [1]. Therefore, a reproducible, automated, and accessible way to perform this assessment is required.

2. Materials and Methods

This study developed an automated and modular open-source codebase, which enables arbitrary execution of a model characterisation framework. This framework enables the creation of modelling workflows for evaluating specific aspects of a model's credibility.

The codebase allows the use of commonly used scientific programming libraries (e.g., *SciPy*, *scikit-learn*) to enable interchangeable systems with plug-and-play model workflows. To ensure reproducibility, the workflow automates the creation of a standardised archive, which enables exchange and recreation of the workflow on other devices to validate existing results. Furthermore, the same credibility workflow can be used across a research domain, allowing standardised and reproducible comparisons of similar models.

3. Results

To demonstrate the workflow, a simple cardiomyocyte model was assessed with common credibility assessment use-cases (global sensitivity analysis (GSA), a Gaussian process emulator (GPE), correlation analysis and numerical testing). To further illustrate the workflow, GSA is undertaken on a previously used highly-parameterised 0D-cardiovascular system model, and a GPE is demonstrated on a 3D-heart biomechanics model (due to its traditional high computational cost restraints).

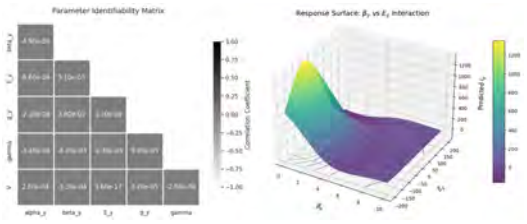


Figure 1: Subset of cardiomyocyte model credibility assessment results generated by executing the workflow using the pipeline.

The framework successfully executed automated GSA and building of a GPE of the cardiomyocyte model, demonstrating an accessible method for credibility analysis. Within the statistical bounds provided, GSA found significant differences between first-order (0.09) and total-order (0.91) sensitivities suggesting strong non-linear interactions, which are confirmed in the GPE plot. Furthermore, the model was determined to be identifiable, with the correlation matrix showing high structural identifiability and near-zero correlations between parameters, allowing robust parameter recovery.

4. Discussion and Conclusions

The framework demonstrated how different methods of credibility assessment can be undertaken in a standardised way. This enables FAIR principles to be achieved through increased accessibility and generation of common methodologies and templates for conducting credibility assessment on digital twins.

5. References

1. NASEM. (2024). *Foundational Research Gaps and Future Directions for Digital Twins*.

TRANSITION-LIKELIHOOD SURROGATES FOR CALIBRATING ORGAN-ON-CHIP AND TUMOUR-ON-CHIP CELL TRAJECTORIES

Fabian Spill (1), Zipeng Wang (1), James Andrews (1), Ben Cardoen (1), Huanbo Lyo (2), Shuo Wang (2)

1. *School of Mathematics, University of Birmingham, UK*
2. *School of Computer Science, University of Birmingham, UK*

Correspondence: Fabian Spill (f.spill@bham.ac.uk)

1. Introduction

Organ-on-chip platforms yield high-content time-lapse trajectories of cells and multicellular aggregates. Building digital twins for these microphysiological systems requires calibrating mechanistic, stochastic movement models to trajectories, a setting where simulation-based inference (SBI) is natural [1]. However, many movement ABMs are non-differentiable and their step-to-step transitions can be *singular* (e.g. constant-speed projection), making likelihood-based scoring ill defined. We propose a reusable transition-likelihood surrogate that enables calibrated, differentiable inference from trajectory data and is directly applicable to tumour-on-chip migration and invasion assays.

2. Materials and Methods

We define an observation-space likelihood via an explicit measurement model: observed velocities equal latent simulator velocities plus small Gaussian localisation noise. This **likelihood contract** turns singular latent transitions into proper densities and fixes the measurement scale used for training, evaluation and inference. We learn the one-step conditional density with a conditional mixture density network (MDN) [2] trained on simulator transitions, optionally conditioned on parameters and microenvironment covariates. Composing one-step densities yields an explicit trajectory likelihood and enables gradient-based calibration without simulator calls at inference time.

3. Results

Across a synthetic benchmark of heterogeneous bias-field geometries, the surrogate achieves low held-out log loss with near-nominal predictive coverage, supporting calibrated probabilistic forecasting. Parameter-conditioned surrogates enable fast maximum-likelihood or MAP inference from short trajectory windows. On real cell tracks, calibration reproduces observed changes in speed and turning statistics under posterior predictive checks.

4. Discussion and Conclusions

Transition-likelihood surrogates provide a lightweight, reusable likelihood layer that can sit inside organ-on-chip digital-twin pipelines, bridging high-throughput imaging readouts and mechanistic ABMs. For tumour-on-chip assays, the approach enables hypothesis testing about how microenvironmental cues alter cell-scale motility, while keeping the measurement model explicit and auditable.

5. References

1. Cranmer K, Brehmer J, Louppe G. The frontier of simulation-based inference. Proc Natl Acad Sci U S A. 2020;117(48):30055-30062. https://doi.org/10.1073/pnas.1912789117
2. Bishop CM. Mixture density networks. Aston University, Neural Computing Research Group Technical Report NCRG/94/004. 1994. https://publications.aston.ac.uk/id/eprint/373/1/NCRG_94_004.pdf

Acknowledgements:

FS is supported by a UKRI Future Leaders Fellowship, grant no. (MR/T043571/1).

COMPUTATIONAL MODELING OF TUMOR-ON-CHIP ORGANOIDS: LINKING MECHANICS AND METABOLISM

Pedro Garcia-Gomez (1), Paula Guerrero-Lopez (1), Silvia Hervas-Raluy (2), José Manuel Garcia-Aznar (1)

1. Multiscale in Mechanical & Biological Engineering (M2BE), Aragon Institute of Engineering Research (I3A), University of Zaragoza, Zaragoza, Spain;

2. Institute for Computational Mechanics, Technical University of Munich, Germany;

1. Introduction

Tumor-on-chip organoids are based on 3D cell cultures in microscale devices to mimic the functions and complexity of human tumours *in vitro*. Thanks to the precise control offered by microfluidic technology, it is possible to recreate key tumour microenvironment factors , such as, the biochemical and landscape.

Mathematical modelling of tumour organoids uses various numerical approaches to simulate their growth, which range from continuum approaches (1) to agent-based modelling (2). Using them, we explored how biophysical properties of the surrounding matrix exert a determinant regulatory role in the 3D architectural organization of these organoids (1,2). In this work, we go a step further to investigate how mechanical microenvironment regulates the metabolism of tumour cells determining the dynamics of their proliferation.

2. Materials and Methods

Here, we present an agent-based model that integrates tumour metabolism and mechanics to simulate 3D tumour spheroid growth. Our framework uses ordinary differential equations to simulate metabolic reactions and couples them with an already validated mechanical model (3), in which the interactions between cells and the extracellular matrix are governed by different forces. The ATP cell levels, derived from metabolic pathways, regulate the different cell states: proliferating, quiescent, and apoptotic. These states directly control the mechanical forces exerted by and on each cell. To gain more insight on the undergoing mechanisms of this study, 3D microfluidic experiments were carried out in the lab. A549 lung adenocarcinoma cells were seeded in microfluidic devices and the growth of the spheroids was measured. From these experiments, we obtained growth curves that we later used for the calibration and validation of our model using Bayesian techniques.

3. Results

In order to quantify the growth of the experimental and computational spheroids, we measured their 2D projected area at day 7. The computational results agree with the data experiments, as shown in Figure 1.

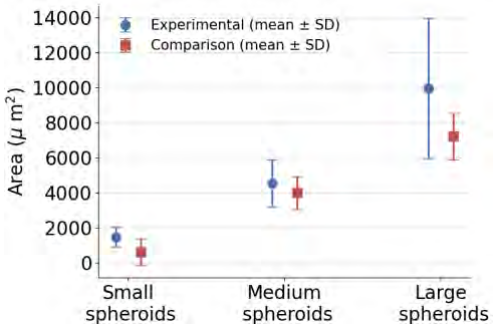


Figure 1: Experimental and computational spheroid 2D projected area for small, medium and large spheroids.

4. Discussion and Conclusions

Our model accurately reproduces the experimental measurements of tumour organoid growth obtained in our laboratory. It also allowed us to discern different dynamics that cancer cells exhibit under the same conditions, providing insight into the potential factors contributing to variability in organoid size.

5. References

1. Hervas-Raluy S., et al. Computers in Biology and Medicine, 159, 106895 (2023).
2. Camacho-Gómez D, García-Aznar JM, & Gómez-Benito MJ. Engineering with Computers. 38(5), 4135-4149 (2022).
3. Gonçalves IG, Garcia-Aznar JM. PLoS computational biology, 17(2), e1008764 (2021).

Acknowledgements:

This work has received funding from the European Research Council (ERC) under the European Union's Horizon 2020 research and innovation programme (ICoMICS grant agreement No 101018587).

SYNCHRONIZING EXPERIMENTAL AND COMPUTATIONAL MODELS OF ENDOTHELIAL BARRIER FAILURE

Óscar Paseta (1), Alejandro Martín-Contreras (1), Alejandra González-Loyola (2,3), José Manuel García-Aznar (1), María José Gómez-Benito (1)

1. Multiscale in Mechanical and Biological Engineering (M2BE), Aragon Institute of Engineering Research (I3A), University of Zaragoza, Zaragoza, Spain. E-mail address: gomezmj@unizar.es; 2. Aragon Health Research Institute (IIS Aragón), Zaragoza, Spain; 3. Aragonese Agency Foundation for Research and Development (ARAID)

1. Introduction

Gap formation in endothelial monolayers (EM) is a critical driver of both physiological processes, such as normal immune cell function, and pathological conditions like cancer metastasis. The emergence of these gaps is governed by a complex interplay of biochemical and mechanical factors, including active actomyosin-generated forces, passive cellular stiffness, the inherent dynamics of cell-cell junctions and the extracellular matrix mechanical (ECM) properties [1].

In this work, we focus on gap formation within small microvessels, specifically examining how the mechanical stiffness of the surrounding tissue modulates this process.

2. Materials and Methods

We present an integrated *in silico* and *in vitro* study investigating the barrier integrity of EM. Initially, we conducted *in vitro* experiments following the methodology established by Polacheck et al. [2] (Fig. 1, left). We generated a cylindrical endothelial monolayer (160µm in diameter) within two distinct collagen matrices [3]. These experiments were then modelled using a finite element (FE) framework encompassing both the EM and its surrounding ECM (Fig. 1, right). Our model accounts for cell-cell adhesion dynamics via a stochastic catch-bond law [4], allowing for a direct comparison between experimental and numerical results.

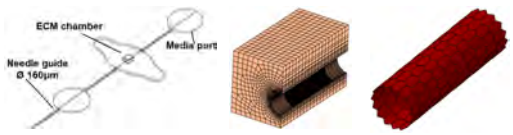


Figure 1: *Microfluidic Device and Modeling. (left) Schematic design of the microfluidic device highlighting the main parts, the central region of the chamber identifies the simulated domain; (right) FE model of half-ECM and EM.*

3. Results

We observed, both *in silico* and *in vitro*, that barrier integrity is significantly modulated by the mechanical properties of the surrounding ECM. Specifically, increased matrix stiffness correlates with a higher frequency of gap formation and elevated permeability. We quantified this loss of functional integrity *in vitro* via vessel permeability assays with FITC-Dextran and *in silico* by tracking the temporal dynamics of gap formation.

4. Discussion and Conclusions

Our results demonstrate the phenomenon of vascular disruption within stiffened tumour matrices. Through *in vitro* assays, we successfully measured vessel permeability as an indirect indicator of gap formation within a 3D environment. Whereas, the *in silico* simulations allowed us to quantify the underlying mechanical environment, which is a critical driver of these disruption events.

This study highlights a synergistic framework, leveraging experimental data for biological validation and computational modeling for the mechanistic depth necessary to understand barrier dynamics of EM.

5. References

1. McEvoy, E et al. Nat Commun, 13(1), 7089. (2022)
2. Polacheck, WJ, et al. Nat Protoc 14(5), 1425–1454. (2019).
3. Martín-Contreras, A, et al. Acta Biomater 212, 413–427 (2026).
4. Nieto, A et al. Eng Fract Mech, 224, 106718. (2020)

Acknowledgements:

The authors would like to thank MCIN/AEI /10.13039/501100011033 and ERDF A way of making Europe (Grant no: PID2024-155426OB-I00).

SIMULATING THE FOREIGN BODY RESPONSE WITH AN AGENT-BASED MODELING APPROACH

Jennifer Riccio* (1), Luca Presotto (1), Giuseppe Chirico (1)

1. *Department of Physics, University of Milano-Bicocca, Milan, Italy*

*Corresponding author: jennifer.riccio@unimib.it

1. Introduction

The foreign body response (FBR) is an inflammatory process triggered by implanted materials or other exogenous bodies in living tissues [1]. It emerges from the interplay of immune cells (including macrophages), signaling molecules, and tissue remodeling mechanisms (involving fibrocytes and fibroblasts), making its quantitative characterization challenging. In this context, *in silico* approaches are valuable for describing the progression of FBR, with agent-based (AB) models being effective in capturing the intercellular interactions. In this work we proposed an AB model, built upon the framework introduced in [2], to reproduce the key mechanisms of the FBR and to simulate the roles of cells in the response induced by biomaterial implantation.

2. Materials and Methods

In [2], macrophages are stimulated on a 2D grid by a pathological pro-inflammatory mediator (PIM). We improved this framework introducing a mechanical PIM to represent the implanted biomaterial. It promotes the secretion of chemical PIM and anti-inflammatory mediators (AIM), both representing cytokine signals. These diffuse and drive cellular chemotaxis and fibroblast recruitment, leading to fibrotic capsule formation around the implant. Macrophages, fibrocytes and fibroblasts can be recruited or locally resident in the tissue. We are now extending the model, by introducing recruitment of cells from blood vessels and the effect of excluded volume to prevent cells from overlapping with the biomaterial region.

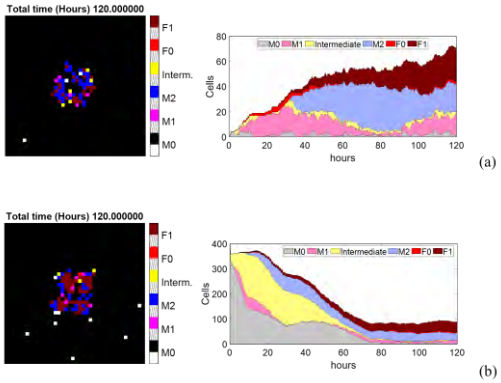


Figure 1: Cell distribution at the last frame (left) and overall number of cells counted at each time of the simulation (right) lasting 120 h, without (a) and with (b) resident macrophages. F1: fibroblasts; F0: fibrocytes; Interm.: intermediate macrophages; M0: non-activated macrophages.

3. Results

Simulations lasted 120 h to simulate chronic inflammation. Results were quantified in terms of spatial distributions and number of cells at each time of the simulation. The model was validated on experimental data.

4. Discussion and Conclusions

Preliminary results indicate that the proposed AB model can reproduce most of the key phenomena underlying the FBR. Future developments will aim at building a digital twin of the FBR.

5. References

1. Rahaman SG et al., Am J Physiol. Cell Physiol; 329(5):C1468–C1486 (2025).
2. Minucci SB et al., PLoS ONE. 2024;19:e0270779 (2024).

Acknowledgements:

The authors thank NextGenerationEU, through the Italian Ministry of University and Research under the PNRR-M4C2-I1.3 Project PE_00000019 “HEAL ITALIA,” for providing financial support to this project, and the EU through the FET-OPEN project IN2SIGHT (Grant Agreement No. 964481) for funding provided to Giuseppe Chirico.

COMPUTATIONAL MODELING OF PROTEIN ACCUMULATION AND MIGRATION IN THE CNS IN THE CONTEXT OF EPILEPSY

Leticia Ribeiro (1), Eliana Toscano (2), Marcelo Lobosco (1,3), Barbara Quintela (1,3,*)

1. Computer Science Department, Federal University of Juiz de Fora (UFJF), Brazil; 2. Pathology Department (UFJF), Brazil; 3. Computational Modeling Graduate Program (UFJF), Brazil;

**Corresponding author: barbara.quintela@ufjf.br*

1. Introduction

An integrated understanding of the molecular and cellular dynamics involved in disease progression for epilepsy remains limited. *In vivo* studies face ethical and methodological constraints, while *in vitro* experiments or histopathological analyses provide only static snapshots of a highly dynamic and multifactorial process.

In the context of epilepsy, several *in silico* models have been proposed to study seizures [1], predict surgical outcomes [2], or focus on brain state classification [3]. However, as recent studies indicate that epilepsy presents protein deposits similar to other neurodegenerative diseases [4], the present work aims to propose a new *in silico* model to study protein accumulation and migration in the context of epilepsy.

2. Materials and Methods

The proposed model considers migration from the Entorhinal Cortex (EC) to the Dentate Gyrus (DG). In each region, three variables are considered: concentration of p-Tau (P), population of microglia with phagocytic efficiency (M+), and microglia with reduced efficiency (M-). Microglia are activated by the presence of p-tau (β) and slowly reduce their phagocytosis ability (α) (Fig. 1).

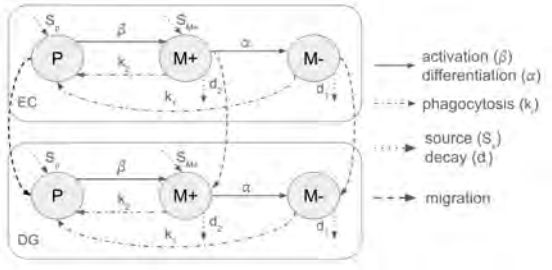


Figure 1: Model visual representation.

3. Results

The proposed model represents the migration of protein from EC to DG and shows that, over time, as microglial phagocytic efficiency declines, p-tau accumulates mainly in DG (Fig. 2).

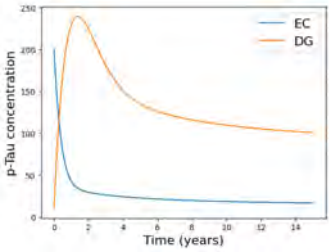


Figure 2: p-Tau concentration over time.

4. Discussion and Conclusions

The proposed model allows for a qualitative understanding of the protein accumulation dynamics associated with epilepsy and other neurodegenerative diseases over the years. In Alzheimer's Disease (AD) a late accumulation of protein is observed in DG region and in epilepsy there is evidence indicating earlier deposit in this region. Future work proposes model VV&UQ considering *in vivo* and *in vitro* experiments.

5. References

1. Zavaleta-Viveros, J. A., et al. (2023). A modification to the Kuramoto model to simulate epileptic seizures as synchronization. J. Math. Biol., 87(1):9.
2. Rigney, G., Lennon, M., and Holderrieth, P. (2021). The use of computational models in the management and prognosis of refractory epilepsy: A critical evaluation. Seizure, 91:132–140.
3. Dallmer-Zerbe, I. et al. (2023). Computational modeling allows unsupervised classification of epileptic brain states across species. Sci. Rep., 13(1):13436
4. Toscano, E., et al. (2023). Hyperphosphorylated tau in mesial temporal lobe epilepsy: a neuropathological and cognitive study. Mol. Neurobiol., 60(4):2174–2185.

Acknowledgements:

The authors would like to thank FAPEMIG (TEC BIS 00702-25) for financial support.

MECHANICAL LOADING ORGANIZES DISTINCT REGULATORY ATTRACTOR STATES IN NUCLEUS PULPOSUS CELLS

Zerihun G. Workineh (1), *Jérôme Noailly (1)*

1. *Department of Engineering, Universitat Pompeu Fabra, Barcelona, Spain*

1. Introduction

Intervertebral disc nucleus pulposus cells (NPC) continuously convert mechanical loads into biochemical signals through mechanotransduction (MT). Normal loads maintain homeostasis and excessive loads trigger pro-catabolic responses [1]. Yet, the biological cross-talks subjacent to MT pathways remain poorly understood**.** Hence, we integrated a regulatory network model (RNM) to capture NPC biological functions across mechanical regimes.

2. Materials and Methods

A systematic review of 130+ studies was conducted to classify mechanical loadings relevant to NPC. Literature and curated pathway databases (Reactome and KEGG) knowledge was mapped into a directed RNM with 140 nodes and 353 edges, connecting mechanoreceptors, intracellular mediators, transcription factors (TF), and effectors (Fig. 1). The RNM was solved as a semi-quantitative ODE system consistent with Boolean logic [2]. Baseline attractors were identified from 100 simulations iterated until steady-state convergence, after random node initialization between 0 and 1.

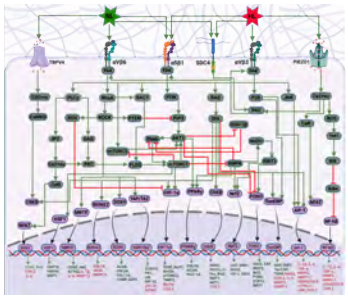


Fig. 1. Schematic of integrated NPC MT signalling pathways

Mechanical input nodes were: normal load (NL), activating $\alpha_5\beta_1$ and $\alpha_V\beta_6$ integrins, and TRPV4; hyperphysiological load (HL), activating $\alpha_5\beta_1$ and $\alpha_V\beta_3$ integrins, and PIEZO. They defined the load regimes: Hypo (NL $\leq$ 0.1; HL $\leq$ 0.1); Normal (NL > 0.1; HL $\leq$ 0.1); Hyper (NL $\leq$ 0.1, HL > 0.1), initiating cytoskeletal, kinase, redox, inflammatory, and transcriptional pathways (Fig.1).

Results

Hypo-loading globally dampened the RNM response across various biological functions. Normal loading coordinated anabolic signalling, increasing matrix proteins (ACAN, COL2A1), growth factors (TGFβ, IGF1, GDF5), and transcription factors (e.g., SOX9, PPARγ). Hyperloading redirected the network, elevating pro-inflammatory cytokines, proteases (MMPs, ADAMTS), oxidative stress and apoptotic (ROS, BAX, CASP3/9), and degeneration-associated TF (NF-κB, AP-1), nodes (Fig. 2). Out of 45 RNM falsification tests against independent NPC load response reports, ~95% agreed with experimental observations.

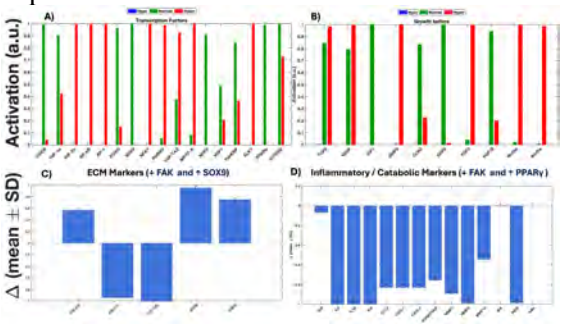


Fig. 2: Activation levels of transcription (A) and growth (B) factors (A); *in silico* rescue strategy, starting from the hyperphysiological loading attractor (C, D).

4. Discussion and Conclusions

The RNM integrated dispersed MT knowledge into a systems-level regulatory model of NPC biological functions. NL stabilized anabolism through FAK-ROCK-SOX9, AMPK-SIRT1-NRF2, Ca^{2+}-CREB, FAK-AKT1-HIF-1α, FAK-ERK-PPARγ, FAK-ERK-TonEBP. HL attractor was characterized by NF-κB/ AP-1, FAK/ Ca^{2+}-ROCK-ROS, PI3K-AKT1-mTOR, and FAK-ROCK-YAP/ TAZ/ MRTF activations. Centrality and sensitivity analyses identified FAK signalling, redox regulators, and anabolic TF as key regulators of load-dependent state transitions. Indeed, rescue simulations showed that coordinated suppression of FAK signalling together with activation of SOX9, NRF2, and PPARγ destabilized hyperloading-induced pro-catabolism (Fig. 2C, D)., supporting multi-axis therapies in disc degeneration

5. References

1. Shi S. et al., *Arthritis Res Ther* 24, 119 (2022).
2. Mendoza et al., Theor Biol Med Model. 2006, 3(13)

Acknowledgements:
European Research Council (ERC-CoG O-Health-101044828).

AUTOMATED IMAGE-BASED RECONSTRUCTION OF 3D SUBCELLULAR STRUCTURES FOR FINITE ELEMENT MODELING

Weisheng Li (1), Chengyuan Wang (1), Feihu Zhao (1)

1. Zienkiewicz Institute for Modelling, Data & AI, Faculty of Science & Engineering, Swansea University, UK

1. Introduction

Understanding how structure governs cellular mechanics is critical for mechanobiology and disease modeling [1]. Currently most of the computational models have simplified the internal structures / cytoskeletal organization of cells, which however have high complexity according to the cell images. To facilitate the development of realistic cell mechanics model, we developed an automated image-based workflow that converts confocal z-stacks into realistic 3D finite element models, reconstructing actin fibers, microtubules, nucleus, cortex, and cytoplasm. Furthermore, it is applied in cell biomechanics (e.g., vibriation) simulations.

2. Materials and Methods

In this framework, single-cell confocal z-stack images were used to construct a three-dimensional finite element (FE) model of the cytoskeleton and major organelles. Raw fluorescence volumes were exported in TIFF format and processed in ImageJ for segmentation and 3D skeletonization of the actin network. The binary skeleton was imported into Python, where voxel indices were converted to physical dimensions and mapped to the Abaqus coordinate system. Sparse sampling (15-pixel stride) and connectivity filtering were applied to remove noise and retain only fiber segments ≥0.1 μm. Valid segments were discretized as 1D truss elements and assigned prestress using a UMAT (24% tensile strain). Additional structures were reconstructed using image-derived geometry: the nucleus was modeled as an ellipsoid, the cytoplasm using a 3D convex hull, microtubules as beam elements grown from the centrosome with reflection around the nucleus, and the cortex extracted as the outer actin envelope and meshed using shell elements. All components were integrated into an automated FE workflow for downstream biomechanical simulations.

3. Results

A full image-based finite element cell model was analyzed using modal analysis to assess multiscale mechanics. The ten modes ranged from 10.857–19.388 kHz (Fig. 1), aligning with reported cellular vibration measurements [2]. Lower modes reflected whole-cell bending and torsion, while higher modes localized along cytoskeletal structures, demonstrating that realistic cytoskeletal architecture strongly shapes cellular mechanical response (Fig. 1).

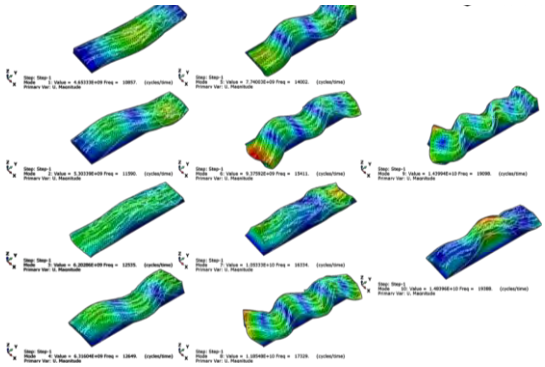


Fig 1: Cell displacements under the vibration frequency of 10.857–19.388 kHz.

4. Discussion and Conclusions

The vibration patterns obtained demonstrate that image-based cytoskeletal architecture strongly governs cellular mechanical response, supporting its relevance for mechanophenotyping [1]. Model fidelity remains limited by imaging resolution and incomplete structural input. With higher-resolution multimodal imaging, this framework could provide an important tool for modelling the realistic disease-specific cell, e.g., to simulate cytoskeletal degradation in cancer progression and diagnosis.

5. References

1. Geltmeier, A et al. , PloS one, 2015.
2. Puerto-Belda, V et al. , PRX Life, 2024

AI-DRIVEN CAUSAL COUNTERFACTUAL DIGITAL TWIN OF THE LEFT ATRIAL APPENDAGE

Hector J. Hortua (1,2), Sandra Ortega-Martorell (1,2), Timothy Fairbairn (2), Gregory Y.H. Lip (2), Ivan Olier (1,2)

1. AI and Digital Technologies Research Institute, Liverpool John Moores University, UK;

2. Liverpool Centre for Cardiovascular Sciences, Liverpool John Moores University, University of Liverpool, and Liverpool Heart and Chest Hospital, UK

1. Introduction

Digital twins in cardiology aim to build patient-specific, continuously updated 3-dimensional representations of cardiac anatomy to predict outcomes under alternative clinical scenarios. Here, we introduce an AI-driven 3D digital twin of the left atrial appendage (LAA) that could support "what-if" scenarios. For instance, how LAA morphology might be influenced by clinical interventions while remaining causally plausible and anatomically consistent. This frames the problem as counterfactual 3D generation, where modifications follow an assumed causal graph rather than relying on unconstrained 3D editing, which can produce unrealistic and clinically misleading anatomies.

2. Materials and Methods

We model the 3D LAA morphology as an endogenous variable within a Structural Causal Model (SCM) [1] whose parents represent patient's cardiovascular history. Counterfactual inference follows Pearl's Abduction-Action-Prediction paradigm: i) abduct exogenous noise compatible with the observed data, ii) apply an intervention at the clinical node, and iii) predict the counterfactual LAA morphology while holding the abducted noise fixed. The LAA mechanism is implemented as an amortized, explicit generative model based on a 3D Hierarchical Variational Autoencoder (HVAE), fine-tuned with soft model-based interventions to prevent conditioning collapse [2,3].

3. Results

Figure 1 illustrates one example of our 3D-HVAE counterfactual generation.

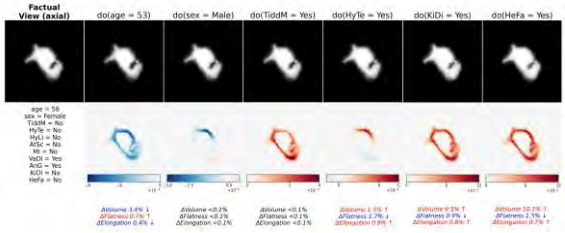


Figure 1: LAA counterfactuals from our deep SCM. Direct causal effect (red: increase; blue: decrease).

The first column shows the factual LAA in an axial view (a randomly selected slice). The following columns show the counterfactual samples generated after applying different model-based interventions (i.e., $do(\cdot)$ on each parent variable in the SCM). The bottom row reports how key geometrical variables of the LAA change with respect to the factual case, highlighting that the interventions lead to controlled and interpretable morphological variations. Across the benchmarked settings, HVAE is consistently strongest on composition [3], with SSIM of 0.992 ± 0.001 (1 cycle) and 0.991 ± 0.002 (10 cycles), indicating superior anatomy preservation, an essential requirement for patient-specific 3D LAA digital twins. In terms of realism, HVAE achieves a low FID of 0.305 ± 0.072, reflecting counterfactuals that remain close to the data distribution. Finally, HVAE shows strong reversibility, with scores of 0.882 ± 0.044 (1 cycle) and 0.843 ± 0.045 (3 cycles), supporting its use when LAA counterfactuals must remain anatomically believable and minimally perturbed outside the intervened factor.

4. Discussion and Conclusions

We report a 3D-HVAE that produces counterfactual LAA shapes that remain patient-consistent, as reflected by strong composition, realism, and reversibility even after multiple cycles. This suggests that interventions are well controlled, rather than causing drift or irreversible artifacts. Overall, these results open a path to incorporate causality into digital twins and generate more plausible clinical LAA "what-if" scenarios.

5. References

1. Pearl, J. Causality. Cambridge UP (2009)
2. Pawlowski N et al, NeurIPS 2020
3. Melistas T et al, NeurIPS 2024

Acknowledgements:

Funded by the European Union's Horizon Europe under Grant Agreement No. 101136244 (TARGET, https://target-horizon.eu/).

IMPACT OF FIBROSIS ON BLOOD FLOW IN THE LEFT ATRIUM

Yvonne Stöcker (1), Christoph Augustin (2), Alejandro Gonzalo (3), Åshild Telle (3), Manuel Guerrero-Hurtado (4,5), Oscar Flores (5), Nazem Akoum (3), Patrick Boyle (3), Juan Carlos del Alamo (3), Manuel García-Villalba (1)

1. TU Wien, Austria; 2. Medical University of Graz, Austria; 3. University of Washington, USA; 4. Hospital General Universitario Gregorio Marañón, Spain; 5. Universidad Carlos III de Madrid, Spain

yvonne.stoecker@tuwien.ac.at

1. Introduction

The left atrial appendage (LAA), a small pouch connected to the left atrium (LA), is widely recognized as the predominant location of thrombus formation in the atrium. Its complex geometry promotes regions of slow or recirculating flow, particularly when atrial wall kinetics are impaired by fibrotic remodeling, with or without sinus rhythm. In these situations, blood stagnation increases the likelihood of clot formation and subsequent ischemic stroke.

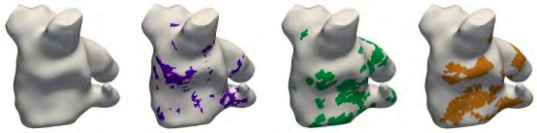
Although coagulation and thrombogenesis involve complex biochemical pathways, blood residence time (RT) within the LA is widely used as a practical hemodynamic surrogate for thrombosis risk.

Computational fluid dynamics (CFD) studies have previously examined how abnormal atrial motion alters intracardiac flow and promotes stasis in the LAA. However, most of these investigations neglect the effects of hypocontractile stiffened fibrotic tissue on atrial wall motion, leaving an incomplete understanding of how different fibrosis distributions affect flow patterns and clot risk.

2. Materials and Methods

We performed high-resolution, patient-specific electro-mechanical (EM) simulations of atrial tissue [1]. With this framework it is possible to apply multiple fibrosis distributions to the same baseline LA anatomy while independently adjusting the overall portion of fibrotic tissue.

Examples of the baseline anatomy with different fibrosis configurations are illustrated in Fig. 1.



a b c d

Figure 1: Baseline geometry without fibrosis (a) and the same anatomy with varying fibrosis amounts and distributions (b–d).

The resulting motion fields produced by the EM simulations were then used to drive CFD analyses [2]. This workflow allowed us to isolate how fibrosis amount and spatial distribution influence atrial flow behavior, focusing on RT within the LA and LAA.

3. Results

The results indicate that RT within the LA body is primarily determined by the overall amount of fibrotic tissue with only minor sensitivity to its spatial distribution. In contrast, RT within the LAA responds to more complex changes in global atrial flow and is influenced by both fibrosis amount and pattern.

4. Discussion and Conclusions

These findings highlight the importance of realistic atrial mechanics when evaluating LAA thrombotic risk. While fibrosis burden alone appears sufficient to explain changes in RT within the main LA cavity, the LAA exhibits stronger sensitivity to how fibrotic tissue is distributed.

From a clinical perspective, incorporating patient-specific fibrosis mapping into hemodynamic modeling may improve risk stratification for stroke, particularly in patients with impaired atrial function in sinus rhythm.

5. References

1. Augustin CM et al., Comput Meth Appl Mech Eng; 368, 114092, (2021).
2. Stöcker Y et al., bioRxiv; 2025.10.24.684343.

FUNCTIONAL LAGRANGIAN TRACKING: QUANTIFYING THE INFLUENCE OF WALL MOTION ON LEFT ATRIAL HEMODYNAMICS

Paula Casademunt (1), Xabier Morales Ferez (1), Manal Barrouhou (1), Pedro Cepas (2), Ada Doltra (2), Xavier Freixa (2), Oscar Camara (1)

1. Universitat Pompeu Fabra, Department of Engineering, Barcelona, Spain; 2. Hospital Clínic, Universitat de Barcelona, Cardiovascular Institute, Barcelona, Spain

1. Introduction

Personalized left atrial (LA) computational fluid dynamics (CFD) offer a non-invasive platform for patient-specific thromboembolic risk assessment [1]. While quantitative CFD validation is standard, existing metrics often lack the depth to characterize complex transport mechanics. This study implements a Lagrangian tracking scheme that assigns functional value to blood trajectories based on their temporal entry and exit phases. This approach enables the quantification of how simplifying atrial wall motion to longitudinal mitral valve (MV) displacement impacts simulated flow trajectories compared to 4D flow magnetic resonance imaging (MRI).

2. Materials and Methods

Patient-specific CFD models (n=2 sinus rhythm (SR); n=2 atrial fibrillation (AF)) were developed from 4D flow MRI [2]. MV outlet conditions were prescribed using MRI-derived velocity curves, while wall motion was simplified to longitudinal displacement. Adapting Bäck et al. [3], Lagrangian particles representing discrete blood volumes were injected from the pulmonary vein inlets and categorized by entry phase (reservoir, conduit, or booster) to quantify the contribution of each phase to the total inflow. These volumes were tracked to determine their hemodynamic outcome, categorized as ejection during E- or A-waves or retention. CFD-derived results were compared against 4D flow MRI measurements.

3. Results

Flow-timing discrepancies were observed between modalities. In SR, 4D flow MRI showed 96% reservoir inflow, whereas CFD shifted the majority to conduit (53%) and booster (42%) phases. This shift in inflow timing induced premature ejection and negligible retention (2%) in the SR CFD models, in contrast to 23% retention in MRI. Conversely, AF results showed consistent retention fractions: 85% for CFD and 86% for MRI. This alignment in AF occurred despite a persistent inflow timing shift – 89% conduit inflow in CFD versus 90% reservoir inflow in MRI.

4. Discussion and Conclusions

Disregarding radial LA wall motion treats the atrium as a compliance-limited conduit rather than a distensible reservoir. This lack of compliance prevents physiological LA wall relaxation during ventricular systole, inhibiting passive reservoir filling. Consequently, inflow is delayed until MV opening, creating a "pass-through" effect where inlet flow is coupled to, and driven by, simultaneous outlet ejection. In AF, the absence of the atrial booster pump reduced modality discrepancies. In this context, omitting radial motion is a more congruent assumption, as dyssynchronous contractions reduce volumetric variation. However, the persistent shift in inflow timing confirms that the underlying transport kinetics remain non-physiological. This phase-resolved Lagrangian framework identifies these discrepancies, proving that longitudinal MV motion alone cannot replicate atrial pressure-suction mechanics.

5. References

1. Albors C et al., PLOS Computational Biology; 20(9): e1011546 (2024).
2. Morales-Ferez X et al., Cardiovascular interventions; 17(15):1840-1842 (2024).
3. Bäck S et al., American Journal of Physiology; 326(3): H511-H521 (2024).

Acknowledgements:

This work was supported by the European Union's Horizon 2020 programme (GEMINI, Grant No. 101136438), the Spanish Ministry of Science (GENERALITAAT, Grant No. PIT2022-143239OB-I00), the Agència de Gestió d'Ajuts Universitaris de Recerca (Grant No. 2024FI-100419). This work is part of Maria de Maeztu Units of Excellence Programme CEX2021-001195-M, funded by MICIU/AEI/10.13039/501100011033.

MODELLING THROMBUS FORMATION IN THE LEFT ATRIAL APPENDAGES BY SMOOTHED PARTICLE HYDRODYNAMICS

Sumanta Laha (1), Vladimir Ivannikov (2), Katarzyna Polak-Kraśna (1)

1. Institute of Active Polymers, Helmholtz-Zentrum Hereon, Germany.
2 Institute of Material Systems Modeling, Helmholtz-Zentrum Hereon, Germany

1. Introduction

Atrial fibrillation (AF) is strongly associated with thrombus formation in the left atrial appendage (LAA), primarily due to impaired atrial contraction and reduced washout. The LAA acts as a flow stagnation cavity under AF conditions, promoting platelet activation and making it the dominant source of cardioembolic stroke in AF patients. LAA occluders are widely used to mechanically isolate the appendage from the left atrium (LA). However, device implantation and incomplete sealing can generate complex flow structures that may sustain thrombus formation near the device surface [1]. A predictive in silico framework that captures both haemodynamics and biochemical clotting processes is therefore essential. This study proposes a particle-based multiphysics model of thrombus formation in a patient-specific LA–LAA geometry, integrating blood flow dynamics, platelet activation, and fibrin deposition using smoothed particle hydrodynamics (SPH).

2. Materials and Methods

A patient-specific LA–LAA geometry was reconstructed and used as the computational domain. Pulsatile inflow conditions representative of atrial fibrillation were prescribed. Blood flow was modelled using a particle-based SPH formulation. A SPH based multiphysics thrombosis model [2] was coupled to the flow field, incorporating platelet activation, aggregation, and fibrin formation. Thrombus growth was represented through particle deposition, allowing dynamic interaction between clot formation and the evolving flow field. The framework was applied to investigate how variations in LAA morphology influence flow stagnation and thrombus initiation.

3. Results

Simulations under atrial fibrillation–like inflow conditions revealed persistent recirculation zones within the distal regions of the LAA. These areas were characterised by low wall shear stress and prolonged residence time, creating favourable conditions for platelet activation. The coupled multiphysics model predicted progressive thrombus accumulation within these stagnant regions. Clot initiation was typically observed near the distal trabeculated regions of the appendage, where flow velocities were minimal. As thrombus volume increased, local flow structures were further altered, reinforcing stagnation and promoting continued clot growth. Comparative analysis indicated that LAA morphology plays a significant role in thrombogenic potential. Geometries with deeper cavities and narrow neck regions exhibited stronger flow confinement and larger stagnant zones, leading to enhanced platelet activation and accelerated thrombus development.

4. Discussion and Conclusions

The proposed framework captures the interplay between atrial haemodynamics and biochemical clotting mechanisms in a unified particle-based environment. The multiphysics coupling reveals how leakage, shear gradients, and residence time collectively regulate thrombus initiation and progression. Understanding the haemodynamic behaviour of different LAA anatomies is essential for identifying morphologies with elevated thrombogenic risk. Such insights may contribute to improved clinical stratification of patients and help guide indications for left atrial appendage occlusion procedures.

5. References

1. Alkhouli M, De Backer O, Ellis C et al. J Am Coll Cardiol Intv. 2023;16(6):627–642 (2023).
2. S. Laha, G. Fourtakas, P. K. Das, A. Keshmiri. Phys. Fluids. 2025;:1–35 (2025).

Acknowledgements:
This work was supported by the German Federal Ministry of Education and Research (Go-Bio) grant number 16LW0642K.

PREDICTIVE MODELLING OF ANTICOAGULANT EFFICACY AND FIBRINOLYTIC DYNAMICS IN ATRIAL FIBRILLATION

Anna Maria Lo Presti (1,2), Alessandro Tamburini (2), Enrico Napoli (2), Gaetano Burriesci✉ (1,2,3) and Alessandra Monteleone✉(1)

1. Ri.MED Foundation, Palermo, Italy; 2. Engineering Department, University of Palermo, Italy; 3. UCL Mechanical Engineering, University College London, UK

✉ Corresponding authors (gburriesci@fondazionerimed.com, amonteleone@fondazionerimed.com)

1. Introduction

Atrial fibrillation (AF) is a common arrhythmia [1] and a major cause of thromboembolic events [2]. In non-valvular AF, thrombi form predominantly in the left atrial appendage (LAA) [3] due to blood stasis and coagulation dysregulation. Although current clinical guidelines recommend long-term anticoagulant therapy [4], the patient-specific haemodynamic response, optimal dosing, and overall therapeutic efficacy remain difficult to quantify. This study presents a new computational approach to model the effect of common anticoagulants. In particular, the effect of Rivaroxaban (one of the most prescribed direct oral anticoagulants [5]) on thrombus formation is simulated, evaluating stabilisation and potential fibrinolysis-driven clot dissolution in treated and untreated patient specific cases.

2. Materials and Methods

A mono-physics fluid–structure interaction model based on smoothed particle hydrodynamics (SPH) is employed on a patient-specific LAA geometry under AF [6].

Rivaroxaban is explicitly modelled as a transported and reacting specie within a framework integrating the coagulation cascade, including both extrinsic and intrinsic pathways, together with the fibrinolytic system. This approach allows for a dose-dependent assessment of factor X_a inhibition and its effect on thrombus dynamics.

Thrombus formation and stabilisation are represented through the biochemically driven conversion of fluid particles into a solid phase when local concentration and haemodynamic thresholds are reached, allowing dynamic thrombus growth, structural remodelling, and lysis [6].

3. Results

Factor Xa inhibition by rivaroxaban significantly attenuates thrombin generation and thrombogenesis. However, simulations indicate that recommended therapeutic dosing prevents thrombus formation only during the early phase.

Residual thrombi persist, despite therapeutic Rivaroxaban levels and the presence of the fibrinolytic system.

4. Discussion and Conclusions

The integration of the coagulation cascade with anticoagulants pharmacodynamics and fibrinolytic regulation in a patient-specific LAA geometry provides predictive insight into treatment efficacy. This framework enables quantitative assessment of the dynamic balance between thrombin generation, pharmacological inhibition, and endogenous fibrinolysis, supporting personalised thromboembolic risk stratification in AF.

5. References

1. Linz D, Gawalko M, Betz K, Hendriks JM, Lip GYH, Vinter N, Guo Y, Johnsen S. Lancet Reg Health Eur. 37:100786 (2024).
2. Watson T, Shantsila E, Lip GY. Lancet. 373(9658):155–166 (2009).
3. Cresti A *et al.* EuroIntervention. 15(3):E225–E230 (2019).
4. Hindricks G *et al.* Eur Heart J. 42(5):373–498 (2021).
5. Yan VKC, Li HL, Wei L, Knapp MRJ, Wong ICK, Chan EW. Drugs. 83(4):315–340 (2023).
6. Lo Presti AM, Monteleone A, Musotto G, Tamburini A, Napoli E, Burriesci G. Comput Biol Med. 191:110134 (2025).

Acknowledgements:

This work was supported by PNRR Project 39-033-20-DOT204NJ79-9840 (DM 117/2023) via industry-focused doctoral programs.

EVALUATING DEVICE-DEPENDENT HEMODYNAMICS AFTER LEFT ATRIAL APPENDAGE OCCLUSION: A NUMERICAL WORKFLOW

Benigno Marco Fanni (1), Chiara Bonfanti (1,2), Alma Brambilla (3), Ilaria Verdirame (1,4), Rossana Buongiorno (1), Emanuele Gasparotti (1), Francesca Berti (2), Sergio Berti (5), Giancarlo Pennati (2), Lorenza Petrini (3), Simona Celi (1)

1. BioCardioLab, Bioengineering Unit, Fondazione Monasterio, Italy; 2. LaBS, Department of Chemistry, Materials and Chemical Engineering, Politecnico di Milano, Italy; 3. Department of Civil and Environmental Engineering, Politecnico di Milano, Italy; 4. Department of Information Engineering, University of Pisa, Italy; 5. Adult Cardiology Unit, Fondazione Monasterio, Italy

1. Introduction

Left atrial appendage occlusion (LAAO) has become an established alternative for stroke prevention in patients with non-valvular atrial fibrillation who cannot tolerate long-term anticoagulation [1]. Despite demonstrated clinical efficacy, complications such as incomplete sealing and device-related thrombus formation remain important concerns [2]. Patient-specific computational modelling can offer mechanistic understanding of these phenomena; however, a comprehensive numerical framework capable of reproducing the complete LAAO workflow across different device types is still lacking. This study presents a numerical approach to investigate pre- and post-procedural atrial hemodynamics for multiple LAAO devices.

2. Materials and Methods

A multi-step computational framework combining finite element (FE) analysis and computational fluid dynamics (CFD) was developed. The workflow includes: CFD simulation of baseline left atrial blood flow [3]; FE deployment of LAAO devices; and CFD analysis of post-implant hemodynamics. Patient-specific left atrial geometries were reconstructed from pre-operative CT images and used consistently across all simulation stages. Two occlusion systems, the Watchman FLX and the Amplatzer Amulet, were virtually implanted in two patient anatomies. Device sizing and positioning were determined from anatomical measurements, while deployment simulations accounted for realistic catheter constraints and atrial wall mechanical properties [4]. Post-implant CFD domains were generated from FE-deformed geometries to evaluate flow patterns under identical boundary conditions.

3. Results

In Figure 1 we reported a patient anatomy simulated with both the Watchman FLX (Figure 1a) and the Amplatzer Amulet (Figure 1b) devices. While both devices successfully isolated the LAA, local hemodynamics at the device–blood interface differed notably between the two devices.

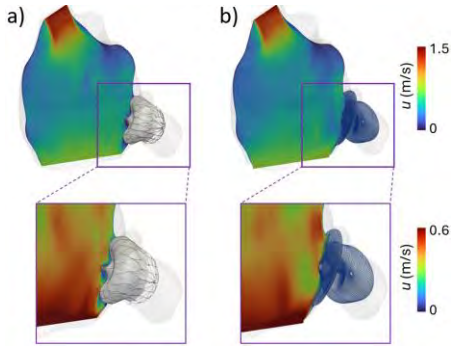


Figure 1: Velocity (u) map for the same anatomy simulated with Watchman FLX (a) and Amulet Amplatzer (b).

4. Discussion and Conclusions

The proposed framework enables a detailed, patient-specific comparison of LAAO devices and their hemodynamic impact. By integrating realistic deployment mechanics with post-implant flow analysis, this approach may support device selection, procedural planning, and risk stratification, ultimately contributing to improved outcomes in LAAO interventions.

5. References

1. Alkhouli et al., JACC; 1(5):100136 (2022).
2. Friedman et al., JACC; 9(1):108-110 (2023).
3. Fanni et al., Applied Sciences; 10(4):1148 (2020)
4. Danielli et al, Int J Num Meth Bio; e3814 (2024)

Acknowledgements:
This work is part of the project "PLACE – Planning LAa ClosurE" (RF-2021-12375208), funded by the Italian Ministry of Health.

MULTISCALE FRAMEWORK FOR THROMBUS RISK ASSESSMENT AND ANTITHROMBOTIC MANAGEMENT AFTER LEFT ATRIAL APPENDAGE OCCLUSION

Marc Molla (1), Maria Segarra-Queralt (1), Manal Barrouhou (1), Carlos Albors (3), Andy L. Olivares (3), Pedro Cepas (2), Jordi Mill (3), Gabriel Bernardino (1), Xavier Freixa (2), Oscar Camara (1)

1. Department of Engineering, Universitat Pompeu Fabra, Spain; 2. Department of Cardiology, Hospital Clinic de Barcelona, Spain; 3. Virtest Technologies SL, Spain

1. Introduction

Direct oral anticoagulants (DOACs) are prescribed to reduce stroke risk in atrial fibrillation (AF) patients [1], but left atrial appendage occlusion (LAAO) appears as an alternative for those with bleeding risk [2]. Nonetheless, device related thrombosis (DRT) still poses a challenge, and a short period of anticoagulation is needed after LAAO [3]. To assist clinicians in balancing thrombus formation against bleeding risk when prescribing antithrombotic therapies, we propose a personalized multiscale computational framework. This approach couples 0D biochemical models of the coagulation cascade and drug effects with high-fidelity computational fluid dynamics (CFD) simulations.

2. Materials and Methods

The model was tested on two cases from Hospital Clínic (Barcelona, Spain). Patient 1 showed no signs of DRT and was treated with a 2.5 mg dose of Apixaban (DOAC) after LAAO intervention. In contrast, Patient 2 showed DRT that persisted under the administration of 100 mg of Aspirin and disappeared with the transition to 2.5 mg dosage of Apixaban. The effects of the two antithrombotic therapies were modelled with an 11-species system of the coagulation cascade. This system was coupled with computational fluid dynamics (CFD) and implemented in the Ansys Fluent 2021R2 solver (ANSYS Inc., USA), following the pipeline described in [4]. Validation data of DRT presence was collected from post-intervention follow-up computed tomography (CT) scans.

3. Results

Simulations for Patient 2 reveal that fibrin accumulates around the device surface both in the absence of anticoagulants and under the administration of Aspirin, indicating a high probability of thrombus formation in both scenarios. Conversely, lower concentration levels were observed in Patient 1 (Fig.1). In parallel, hemodynamic indices computed from CFD alone were able to predict the low DRT risk for Patient 1, but incorrectly indicated a high DRT risk for Patient 2. In contrast, fibrin accumulation is significantly reduced for both patients when the effects of Apixaban are incorporated into the system, aligning with the absence of DRT in the follow-up CT scans.

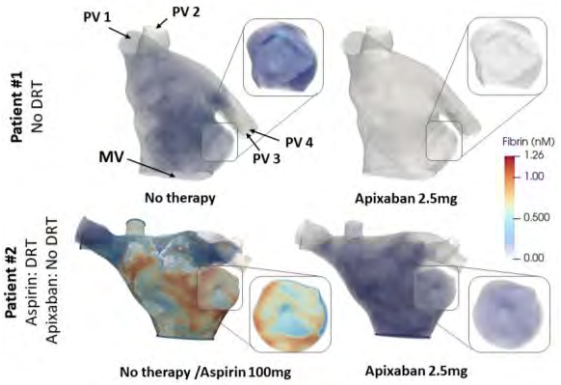


Figure 1: Fibrin accumulation after 2 cardiac cycles for the two patients in the left atrium. The four pulmonary veins (PVs) and mitral valve (MV) are labelled for Patient 1. DRT: Device-related thrombosis.

4. Discussion and Conclusions

Combining the effects of anticoagulant therapy with CFD simulations could help explain the absence of DRT in Patient 2's follow-up, which could not be captured by the CFD-only simulations described in [4]. Moreover, the model stays consistent with the low predicted DRT risk for Patient 1 by CFD alone. Thus, our coupled multiscale model may support planning for post-LAAO anticoagulant therapy.

5. References

1.Altiok, E. et al. Dtsch Arztebl Int 115,776 (2018).
2.Boersma, L. V. et al. Heart Rhythm 14, (2017).
3.Simard, T. J. et al. EIJ 18, 224–232 (2022)
4.Mill, et al. REC Interv Cardiol 3, 4 (2021).

Acknowledgements:
Funded by the Spanish Ministry of Science (PID2022-143239OB-I00 and RYC2022-035960-I) and the European Union (GA 101136438-GEMINI).

COMPARISON OF ANGIOGRAPHY- AND CCTA-BASED CORONARY RECONSTRUCTIONS FOR WALL SHEAR STRESS ESTIMATION

Vittorio Lissoni[1], Andrea Marrone[1], Mariano Pellicano[1], Alfonso Ielasi[1], Giulio Guagliumi[1], Francesco Migliavacca[2], Dario Pellegrini[1]

1. IRCCS Ospedale Galeazzi-Sant'Ambrogio, Milan, Italy; 2. Deparment of Chemistry, Materials and Chemical Engineering "Giulio Natta", Politecnico di Milano, Italy

1. Introduction

Wall shear stress (WSS)–related indices, estimated through computational fluid dynamics (CFD), are associated with coronary plaque progression and instability [1-3]. The FORECAST project integrates optical coherence tomography (OCT) and CFD to improve major adverse cardiovascular events (MACE) prediction, through plaque vulnerability assessment (OCT) and CFD analysis derived from angiography-based coronary models. In the present study we compare CFD results obtained from CCTA, the current standard methodology for coronary segmentation, and angiography to assess reliability of our methodology.

2. Materials and Methods

Coronary geometries were independently reconstructed from CCTA, using Medis (Medical Imaging, Leiden, The Netherlands), and invasive angiography using QangioPlus (Pulse Medical, Shanghai). Mean blood velocity was derived with angiographic frame count method and used to scale average flow curves retrieved from literature [4], split at bifurcations according to Murray's law and used as outlet boundary conditions.

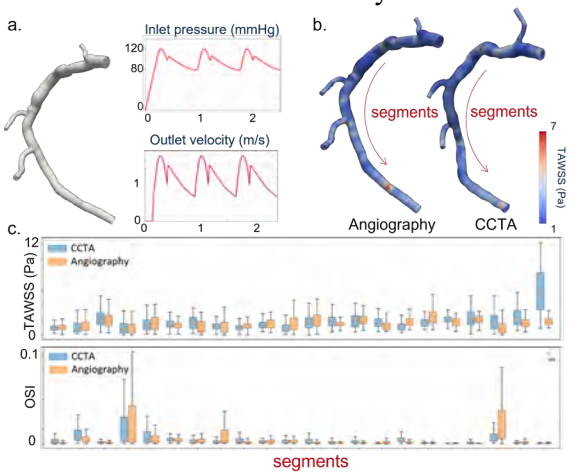


Figure 1. Angiographic reconstruction of vessel with applied boundary condition (a), TAWSS in the Angiography and CCTA-reconstructed vessels (b), TAWSS and OSI comparison along the vessels (c)

Simulations were run using the ICFD module of LS-Dyna (Ansys, Canonsburg, PA, USA). For paired comparison, vessels were divided in consecutive 5 mm centerline segments. Statistical analysis on WSS-related indexes followed a paired design: (i) descriptive visualization; (ii) non-parametric paired testing; and (iii) equivalence testing (TOST).

3. Results

First analysis was performed on a right coronary artery. Time averaged WSS (TAWSS) plots in the two reconstructed models are reported in figure 1b along with TAWSS and Oscillatory shear index (OSI) distribution along the centerlines (fig 1c). Spearman results above 0.69 were found for all WSS-indexes except transverse (TRANSWSS). Other statistical analysis results are reported in table 1.

	Wilcoxon test	TOST equivalence test		
	p-value	Reference value	Delta min	Delta min %
TAWSS	0.95	1.8 (median)	0.19	11%
OSI	0.43	0.5 (full scale)	0.0010	0.2%
RRT	0.75	0.69 (median)	0.097	14%
TRANSWSS	0.17	0.013 (median)	0.0068	49%

Table 1. Statistical analysis results

4. Discussion and Conclusions

Results demonstrate good agreement between CCTA- and angiography-based reconstructions. Statistical analysis showed consistent trends in WSS-derived indices, no systematic bias and small differences between the two methods. Overall, angiographic reconstruction provides results comparable to the gold standard CCTA. Future work will expand sample size and include OCT-based geometries.

5. References

1. F. Gijsen et al., Eur Heart J., 40(41):3421-3433, 2019
2. N. Okamoto, PLoS One, 15(12):e0244015, 2020
3. A. Kumar, J Am Coll Cardiol. 72(16):1926-1935, 2018
4. A. Pappano et al, *Cardiovascular physiology*, 10th ed. 2013

Acknowledgements:

The FORECAST study was supported by an Early Carrer grant from the Fondazione Regionale per la Ricerca Biomedica (FRRB).

ON THE VARIABILITY OF THE INTRAMURAL RIGHT CORONARY ARTERY: A STATISTICAL SHAPE ANALYSIS

Chiara Catalano (1), Adele Chiavetta (2), Michele Conti (2,3), Salvatore Pasta (1,4), Antonio Rosato (2), Mauro Lo Rito (5)

1. Department of Research, IRCCS ISMETT, via Tricomi, 5, Palermo, Italy; 2. 3D and Computer Simulation Laboratory, IRCCS Policlinico San Donato, 20097 San Donato Milanese, Italy; 3. Department of Civil Engineering and Architecture, University of Pavia, Pavia 27100, Italy; 4. Department of Engineering, Università degli Studi di Palermo, Viale Delle Scienze Ed.8, Palermo, Italy; 5. Department of Congenital Cardiac Surgery, IRCCS Policlinico San Donato, 20097 San Donato Milanese, Italy

1. Introduction

Right anomalous aortic origin of coronary artery (R-AAOCA) is a rare congenital anomaly. Significant concern arises when the RCA has an intramural course (i.e., within the tunica media of aortic wall) and an interarterial trajectory (i.e., between aorta and pulmonary artery), due to its reported association with sudden cardiac death (SCD) [1]. Though anatomical features, as ostial morphology, take-off angle, and intramural segment length, have been related to adverse cardiac events [2], their relative contribution to risk remains unclear. By employing statistical shape modelling (SSM), this study seeks to provide a quantitative framework to capture the complex morphology of R-AAOCA at population level, overcoming the limitations of isolated geometric metrics.

2. Materials and Methods

R-AAOCA shape variability was analysed in 63 patients presenting an interarterial and intramural course. Aortic and coronary anatomies were reconstructed by segmenting diastolic CTA scans via the medical imaging software Mimics (Mimics v24, Materialise, Leuven, Belgium). The segmented surfaces were resampled at adequate resolution to ensure consistent quantification of geometric features. An iterative closest point (ICP) algorithm was then applied to establish point-to-point correspondence across subjects. Alignment was achieved through rigid transformations minimizing inter-surface distances. Principal Component Analysis (PCA) was subsequently performed to extract the dominant modes of shape variation within the cohort. For each principal component (PC), ± 1–3 standard deviation reconstructions were generated to facilitate morphological interpretation. Individual PC scores were then correlated with available clinical parameters.

3. Results

The main shape modes are illustrated in Figure 1. The first principal mode accounted for 38.9% of total shape variability, primarily reflecting a global dimensional scaling of the aortic root–coronary complex. Mode 2 described the positional variability of the intramural segment relative to the aortic wall. Mode 3 and 4 were mainly associated with variations in coronary curvature.

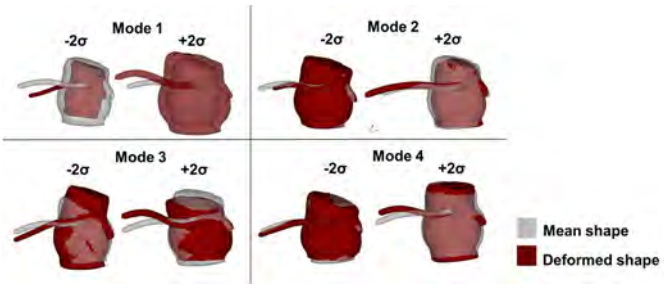


Figure 1: Dominant shape modes as deformations of the mean template from −2σ to +2σ along each principal component.

4. Discussion and Conclusions

SSM enabled decomposition of R-AAOCA morphology into interpretable geometric domains. Notably, it demonstrated a coordinated deformation pattern involving both coronary tract and aortic root, suggesting that aortic geometry may influence the spatial configuration of the RCA. The understanding of the mechanistic link between shape and morphological risk predictors can reveal important insight not only on the R-AAOCA condition, but also for the development of novel risk metrics.

5. References

1. Basso, C., & Thiene, G. (2016). *IOC Manual of Sports Cardiology*, 275-285.
2. Cong, M., et al. (2021). *Quantitative Imaging in Medicine and Surgery*, *11*(5), 2062.

Acknowledgements:

This work was supported by the SMART project funded by the European Commission N*extGenerationEU*- PNRR M6-C2- Investimento: 2.1 "Rafforzamento e potenziamento della ricerca biomedica del SSN", PNRR-MCNT2-2023-12378301, CUP: I73C24000400001.

DEVELOPMENT OF A PATIENT-SPECIFIC DIGITAL-TWIN FOR HCM RISK STRATIFICATION USING EXPLAINABLE AI

Marion Taconné (1), Nabid Faiem (2), Antti Kallonen (2), Miriana C. Torquati (2), Valentina D.A. Corino (1,3), Pietro Cerveri (1,4), Luca Mainardi (1), Mark van Gils (2)

1. Politecnico di Milano (DEIB), Italy; 2. Tampere University, Faculty of Medicine and Health Technology, Finland; 3. IRCCS Centro Cardiologico Monzino, Italy; 4. University of Pavia, Italy

1. Introduction

Hypertrophic cardiomyopathy (HCM) is a primary cause of sudden cardiac death [1], requiring precise risk stratification to guide clinical interventions. While current tools like the ESC score [2] show limited discriminative power, this study introduces an explainable AI (XAI) decision support system (DSS). By integrating multimodal data, the system provides transparent, actionable insights designed to bridge the gap between machine learning research and routine clinical practice.

2. Materials and Methods

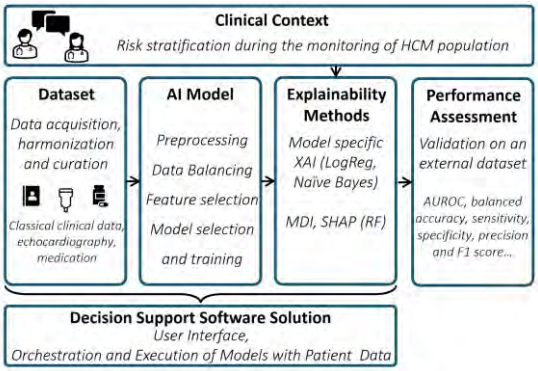


Figure 1: Overview of the methodological steps.

The DSS was developed using data from 1,201 patients from the Sarcomeric Human Cardiomyopathy Registry (SHARE) and externally validated on 382 patients from Rennes Hospital. The predictor space encompasses 82 features, including echocardiographic, clinical, and medication data. A Random Forest (RF) ensemble was selected for the core engine due to its balance of high performance with clinical interpretability provided by SHapley Additive exPlanations (SHAP). The DSS solution was developed based on iterative definition of user requirements using questionnaires and workshops with clinicians from 3 different countries. The system integrates a Flask-based backend and a Plotly Dash frontend in a fully dockerized environment, providing a modular platform. The backend handles data retrieval, model execution, and API communication, while the frontend enables clinicians to explore a patient's information, and risk predictions through interactive dashboards. The architecture follows a containerized microservice approach, which simplifies development and extension of new models. As personalized models originate from different researchers, we developed a language-agnostic framework to orchestrate models built in Python, MATLAB, R, and C++. This transparent approach allows clinicians to verify model logic against clinical reasoning.

3. Results

The RF ensemble achieved an internal AUC of 0.85±0.02, significantly outperforming the ESC score (0.56±0.03). External validation (AUC 0.72) confirmed superior risk separation ($p < 0.001$). Longitudinal analysis demonstrated that the software could track risk trajectories over time; patients experiencing events showed a clear upward trend in their XAI-generated risk scores (mean slope 0.145), while event-free patients remained stable (mean slope 0.003).

4. Discussion and Conclusions

The DSS addresses the "black box" challenge of AI in healthcare by providing dual-layered interpretability. By visualizing both global trends and patient-specific factors, the system fosters clinical trust and supports shared decision-making. While external performance reached an AUC of 0.723, the high specificity of 0.877 ensures the tool remains robust in identifying low-risk patients across different healthcare settings. This study presents a structured XAI pipeline for HCM risk prediction, implemented within a clinical decision support framework. By combining high-fidelity ML models with transparent visualization, the system enhances the applicability and personalized nature of cardiovascular risk assessments.

5. References

1. Maron B.J. et al., Circulation 102(8) :858–864 (2000).
2. O'Mahony C et al., European Heart Journal 35(30):2010–2020 (2014).

Acknowledgements: This study is funded by EU with the projects INSIGHT-LV and SMASH-HCM (GA 101198472, 101137115).

PERSONALISATION OF CORONARY BLOOD FLOW IN HEALTHY VOLUNTEERS DURING EXERCISE

Grace Faulkner (1,2), Xu Xu (1,2), Julian Gunn (1,2,3), Rebecca Gosling (1,2,3), Paul Morris (1,2,3), Ian Halliday (1,2)

1. University of Sheffield, UK; 2. INSIGNEO, UK; 3. Sheffield Teaching Hospitals, UK

1. Introduction

In ischemic heart disease, surrogates of coronary flow (e.g. FFR) and left ventricular function (e.g. EF) are used to assess disease severity. Such haemodynamic metrics are taken at rest or during a pharmacological stress - an approximation of the symptomatic state. Here, a non-invasive personalisation of a 0D model including coronary flow and cardiac function is subject to initial evaluations.

2. Materials and Methods

Data. Healthy volunteers (IRAS:240185) completed an incremental supine ergometry test during an MRI scan (Signa Artist 1.5T, GE). Exercise levels were defined as:

$$RHR + x\,(maxHR - RHR) \quad (1)$$

where RHR is resting heart rate, maxHR = (220–age) [BPM] and x = 0.15, 0.3, 0.45 identifies target exercise levels. Brachial pressure was recorded every 2 mins. Cardiac energetics were analysed [1]. *Model*. A four-chamber model with CRCR systemic and pulmonary circulations, and RCR coronaries (x3) was used [2]. Local sensitivity analysis informed parameter subset selection for optimal personalisation [3] to patient data using a Nelder-Meade algorithm [4]. The loss function was a L2 norm of key cardiac energetics outputs, ESV, EDV, coronary blood flow (CBF) and systolic-diastolic velocity ratios. CBF was estimated from PVA, Emax and HR [5, 6].

3. Results

Our personalisation was able to recapture synthetic pressure and volume data well with the addition of CBF constraints, but the flow distribution across the three coronary arteries was deemed insufficiently informed (Figure 1).

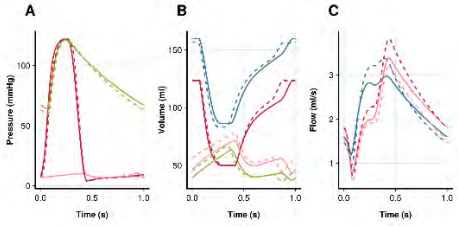


Figure 1: Model outputs personalised to synthetic data. (a) pressures, (b) chamber volumes (c) CBFs. Solid (dashed) lines: ground truth (personalisation).

12 healthy volunteers completed the exercise protocol. Key metrics are presented in Table 1.

Table 1: Mean derived metrics from exercise testing for rest and three levels of exercise.

	Rest	1	2	3
ESV [ml]	55±14	53±18	45±17	33±11
EDV [ml]	140±22	150±36	142±43	126±39
SW [J]	0.94±0.22	1.16±0.29	1.19±0.41	1.18±0.43
PVA[J]	1.26±0.29	1.49±0.35	1.46±0.46	1.39±0.46
CBF [ml/s]	**2.16±0.41**	**3.01±0.61**	**3.27±0.94**	**3.49±1.09**
5% CO [ml/s]	**4.65±0.81**	**6.49±1.20**	**7.21±2.25**	**7.76±2.57**

4. Discussion and Conclusion

Calculated CBF was underestimated compared to literature flows and the expected 5% cardiac output [7] suggesting better informed targets are needed for our non-invasive personalisation.

5. References

1. Seemann et al., Circ Cardiovasc Imaging;12:e008493 (2019)
2. Baraikan et al., Fluids;8(159) :fluid8050159 (2023)
3. Li et al., IEEE Trans. Control Syst. Technol.; 12(3) (2004)
4. Mogensen et al., J. Open Source Softw.; 3(24) (2018)
5. Harasawa et al., Circ. Res.; 71(2) (1992)
6. Arthurs et al., Am J Physiol Heart Circ Physiol; 310:H1242-H1258 (2018)
7. Fournier et al., EuroIntervention; 17(4):e309-e316 (2021)

Acknowledgements:
This project was funded by the NIHR Sheffield BRC. The authors would also like to thank the UoS MRI team for their support.

TOWARDS A PATIENT-SPECIFIC FRAMEWORK FOR THE PREDICTION OF CORONARY IN-STENT RESTENOSIS

Anna Ranno (1), Kevin Linka (1), Felix Vogt (1), Marek Behr (1)

1. RWTH Aachen University, Germany.

1. Introduction

The treatment of cardiovascular diseases often involves percutaneous coronary intervention (PCI). Even with drug-eluting stents (DES), implantation can give rise to in-stent restenosis (ISR), i.e., uncontrolled tissue growth and obstruction to the blood flow, due to endothelial denudation and overstretch injuries [1]. This work is aimed at coupling hemodynamics, tissue modeling, and pharmacokinetics to predict coronary ISR growth.

2. Materials and Methods

The coupling scheme in Fig. 1 summarizes all physics and the corresponding interactions [2].

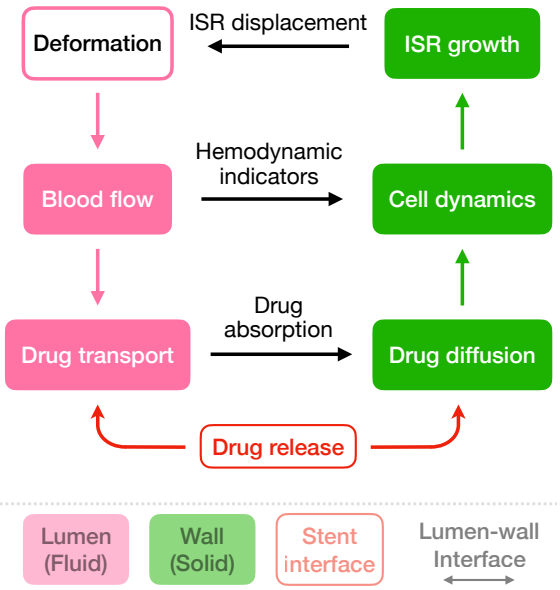


Figure 1: Coupling scheme (adapted from [2]).

The stented artery lumen constitutes the fluid domain. Navier-Stokes equations are used to simulate blood flow. Hemodynamic indicators, such as wall shear stress (WSS) and oscillatory shear index (OSI) are extrapolated and coupled to certain cell dynamics. Drug transport from the DES into the lumen is modeled by means of an advection-diffusion equation and tailored boundary conditions. We identify the solid domain with the arterial wall. Advection-diffusion-reaction equations form the basis of cell dynamics and pharmacokinetics in the vessel wall. The cell dynamics are coupled to a continuum mechanical description of ISR growth [3]. The drug concentration is coupled at the lumen-wall interface to account for downstream uptake of the drug. To account for the lumen deformation due to ISR, we employ an elastic mesh update method. Since the healing process and drug elution span a time frame of weeks, a staggered approach is derived to couple the fluid and the solid models. All model components are discretized by means of finite element method.

3. Results

The method is first tested on an idealized artery with a ring stent, to verify the quasi-steady assumption, which proves to be reasonable and efficient. The lumen deformation impacts WSS but not drug distribution or uptake [2]. We then apply this framework on a patient-specific case. We reconstruct the lumen of a stenosed coronary artery and perform a virtual stent implantation. We simulate 50 days after virtual PCI. We compare the effects of drug and hemodynamics coupling on the cell dynamics and ISR growth prediction, and vice versa.

4. Discussion and Conclusions

Minimal drug uptake from the fluid has negligible effects on cell dynamics and ISR. Thus, if drug release is predominantly abluminal, the fluid contribution can be neglected. Hemodynamic indicators have a substantially stronger influence on ISR prediction. ISR intensifies in areas of low WSS and higher OSI. Future work should include more patient-specific simulations and validation, as well as explore the effects of heart pulsation and blood pressure on the artery wall.

5. References

1. Cornelissen A et al., Int J Cardiol; 388: 131151 (2023).
2. Ranno A et al., Sci Rep; 15: 39229 (2025).
3. Manjunatha K et al., Comput Biol Med; 167: 107686 (2023).

IMPACT OF SEGMENTATION UNCERTAINTY ON CORONARY ARTERY HEMODYNAMICS: A CFD SENSITIVITY ANALYSIS

Giulia Frigerio (1), Luca Mariani (1), Fabio Morelli (1), Alberto Redaelli (1)

1. *Department of Electronics Information and Bioengineering, Politecnico di Milano, Italy;*

Corresponding author: Giulia Frigerio, giulia.frigerio@polimi.it, Via Giuseppe Ponzio 34 Milano (MI), Italy

1. Introduction

Coronary artery disease (CAD) remains a leading cause of mortality worldwide. Coronary Computed Tomography Angiography (CCTA)-based computational fluid dynamic (CFD) is increasingly used to derive hemodynamic indices such as wall shear stress (WSS) and wall pressure gradient (WPG) for evaluating lesion severity [1]. However, these indices are highly sensitive to lumen geometry accuracy. Given the nonlinear dependence of WSS ($\propto r^{-3}$) on vessel radius, even sub-millimetre segmentation errors may translate into clinically relevant index variations. The impact of residual geometric uncertainty on CFD-derived indices remains poorly quantified. This work addresses this gap by introducing radius perturbations representing plausible segmentation uncertainty.

2. Materials and Methods

Four patients with CAD who underwent CCTA acquisition at 0.4 mm resolution were included. For each patient, a baseline geometry was obtained from semi-automatic lumen segmentation, and four perturbed geometries were generated by uniformly scaling the vessel radius by ±10% and ±20%, simulating segmentation uncertainty of approximately 1–2 pixels. Steady-state CFD simulations were performed under patient-specific boundary conditions, imposing to each perturbation the same inlet flow rate and tuning outlet Windkessel elements to match the baseline mean aortic pressure at the inlet. Time-averaged WSS (TAWSS) and WPG were computed.

3. Results

All four patients showed a consistent and monotonic relationship between vessel radius and hemodynamic indices. TAWSS increased markedly with decreasing radius (Table 1), consistent with the theoretical WSS $\propto r^{-3}$ dependence. WPG median values were not significantly different across geometries, while IQR decreased systematically with increasing radius (e.g. IQR_{max}(-20%) = 4.12, IQR_{min}(+20%) = 1.10 for P005), indicating a more homogeneous pressure gradient distribution in dilated vessels. As shown in Fig. 1, WSS magnitude varied substantially across geometries, whereas the spatial distribution of high and low WPG regions remained consistent.

Table 1: Median and IQR of TAWSS [Pa] across all five geometries for 2 patients.

geometry	**P001**	**P004**
-20 %	2.81 (1.48-5.46)	7.06 (3.62-12.43)
-10%	1.91 (1.03-3.69)	4.84 (2.44-8.65)
base	1.38 (0.76-2.63)	3.47 (1.73-6.14)
+10%	1.04 (0.57-1.96)	2.56 (1.27-4.55)
+20%	0.81 (0.45-1.51)	1.95 (0.97-3.45)

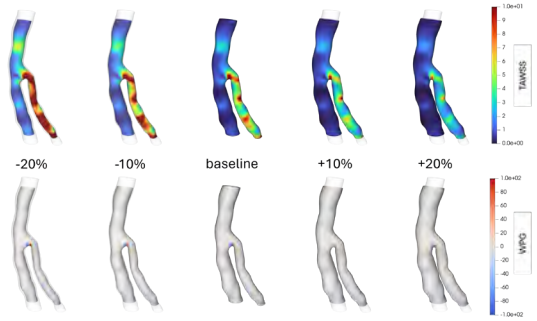


Figure 1: Example of sensitivity plot of TAWSS [Pa] and WPG [x10^3 Pa/m] vs. radius perturbation.

4. Discussion and Conclusions

These results confirm that coronary CFD indices are highly sensitive to segmentation-induced geometric variability, with TAWSS being the most vulnerable due to its non-linear dependence on radius, an error potentially significant for lesion risk stratification. The adoption of photon-counting CT [2], with its higher spatial resolution, could mitigate these effects. Overall, these findings highlight the need for uncertainty quantification workflows in clinical CFD pipelines.

5. References

1.Pandey et al., *Computer Methods and Programs in Biomedicine*, 187:105243, 2020.
2. Sharma et al., *Cureus*, 16:e73119, 2024.

TOWARD A PHYSIOLOGY-INFORMED DIGITAL TWIN FOR STRESS-INDUCED CORONARY DYNAMICS IN AAOCA

Antonio Rosato (1), Mauro Lo Rito (2), Mauro L. Agnifili (3), Francesco Bedogni (3), Michele Conti (1,4)

1. 3D and Computer Simulation Laboratory (C3Dlab), IRCCS Policlinico San Donato, Italy; 2. Congenital Cardiac Surgery Department, IRCCS Policlinico San Donato, Italy; 3. Department of Clinical and Interventional Cardiology, IRCCS Policlinico San Donato, Italy. 4. DICAr, Compmech, Università degli Studi di Pavia, Italy.

1. Introduction

Fluid-structure interaction (FSI) simulations can reproduce the interplay between coronary compression and flow limitation, believed to underlie ischemia in the anomalous aortic origin of a coronary artery (AAOCA) with intramural segment [1]. Here we propose a physiology-informed patient-specific FSI framework incorporating invasively measured coronary microvascular resistance (CMVR) to simulate coronary hemodynamics and estimate fractional flow reserve (FFR), under resting and effort conditions.

2. Materials and Methods

Subjects with AAOCA underwent invasive physiological assessment using continuous thermodilution to measure coronary blood flow, pressure ratio (Pd/Pa), and CMVR. Patient-specific geometries of the aortic root and proximal coronary arteries were reconstructed from CT images and discretized into conformal tetrahedral meshes. Blood was modeled as an incompressible Newtonian fluid and vessel walls with a hyperelastic constitutive model. The distal coronary circulation was represented using lumped-parameter networks informed by measured CMVR [2]. FSI simulations were performed using the *SimVascular svFSI* solver, at rest and under two exercise scenarios defined by increasing rate-pressure product values. Agreement between simulated and invasive measurements at rest was assessed using linear regression and Bland-Altman analysis.

3. Results

Twenty-two patients with AAOCA were included. Simulated coronary blood flow showed strong agreement with invasive measurements ($r=0.87$, $p<0.001$), with minimal bias in Bland-Altman analysis. Resting Pd/Pa was reproduced with negligible bias (-0.003), although inter-patient variability was only partially captured. Simulated FFR at rest remained within the non-pathological range in all coronary arteries. Under effort conditions, FFR in healthy coronary arteries remained stable with no pathological values, whereas anomalous right intramural coronaries showed a marked reduction (mid-effort: median 0.83, IQR 0.67-0.94; maximal effort: median 0.82, IQR 0.66-0.93) (Figure 1). FFR≤0.80 was observed in 47% of patients with intramural right coronaries during simulated effort.

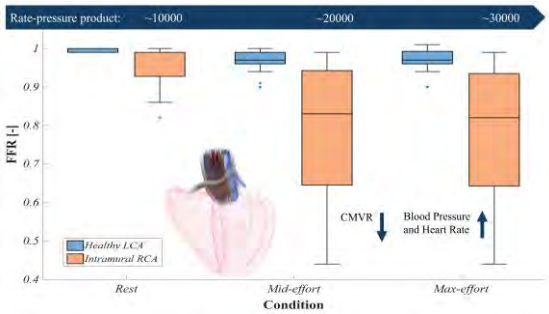


Figure 1: Simulated FFR response to increasing effort conditions in healthy left coronary arteries (LCA) and intramural right coronary arteries (RCA).

4. Discussion and Conclusions

This study demonstrates the feasibility of a physiology-informed digital twin framework for patient-specific simulation of AAOCA using invasively measured CMVR to define distal boundary conditions. Although the framework relies on literature-based vessel wall properties and lacks formal uncertainty quantification, the results indicate that exercise-like conditions are required to uncover functional impairment not apparent at rest, and simulated FFR under effort may reveal otherwise undetected coronary compromise.

5. References

1. Jiang MX et al., JTCVS Tech. 2022 Feb 25;13:144-162.
2. Ceserani V et al., Sci Rep 13, 17448 (2023).

Acknowledgements:

This study was partially supported by Ricerca Corrente funding from Italian Ministry of Health to IRCCS Policlinico San Donato.

IN SILICO DESIGN AND ASSESSMENT OF A NOVEL ARTIFICIAL SPHINCTER FOR INTESTINAL STOMA CONTINENCE

Veronica Bosco (1), Giacomo Properzi (1), Ilaria Toniolo (1,2), Fabrizio Vittadello (3), Giacomo Sarzo (3), Emanuele Luigi Carniel (1,2), Chiara Giulia Fontanella (1,2)

1. Department of Industrial Engineering, University of Padova, Italy
2. Centre for Mechanics of Biological Materials, University of Padova, Italy
3. Padova University Hospital, Italy

1. Introduction

Ostomy procedures for colorectal cancer and inflammatory bowel disease affect over 700,000 people in Europe (70,000 in Italy) and about 1 million in the United States [1]. Although life-saving, stomas reduce quality of life due to continuous reliance on external collection bags. There is currently no clinically alternative to replace the stoma bag temporarily. Artificial Intestinal Sphincters (AISs) are promising, but current devices are unsatisfactory. Still, their success depends on balanced tissue-device interaction to prevent inflammation and erosion. Here, an in silico tool for AIS design was developed, with the goal of supporting both functionality and safety.

2. Materials and Methods

A finite element model including colon and AIS was developed (Fig. 1a). The colon was represented as a collapsed cylindrical tube, while intestinal tissue was described with Ogden hyperelastic model, whose parameters were identified via inverse analysis of ad hoc mechanical tests. The AIS was modelled as a pneumatically driven hyperelastic cuff, and elastomers with different hardness (70, 80, 90, 95 Shore A) were assigned to assess their effect on lumen sealing and tissue loading. Simulations were performed with an explicit solver (Abaqus Explicit 2025, Dassault Systèmes) in two steps: a linear cuff pressure ramp, followed by a linear ramp of intraluminal pressure. Pressure levels were chosen consistently with physiological colon ranges (5, 10, 12 kPa).

3. Results

AIS functionality was assessed in terms of performance and reliability [2]. Performance was defined as the ability to maintain continence under increasing intraluminal pressure and was quantified as the area under the curve relating the intraluminal pressure required to reopen the lumen to the applied cuff pressure (Fig. 1b). Reliability was defined as the ability of the AIS to achieve sealing without inducing adverse tissue effects due to excessive compression and vasoconstriction. Hydrostatic pressure distribution within the tissue was used as a reliability indicator. Performance (Fig. 1c) and reliability (Fig. 1d) were reported depending on material hardness.

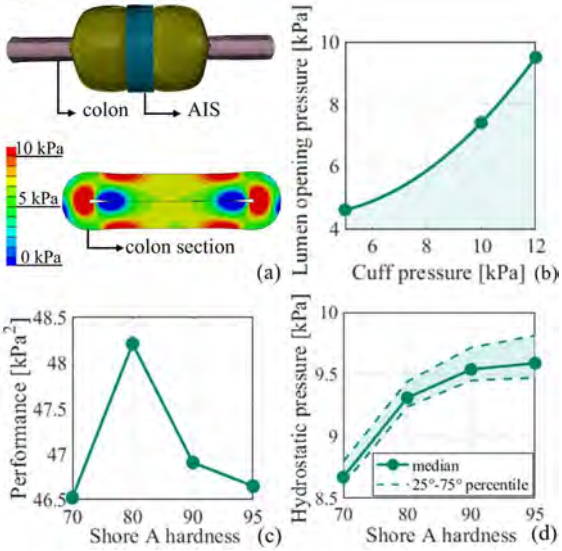


Figure 1: Finite element model of the colon-AIS interaction and distribution of hydrostatic pressure on colon section (a). Definition of the AIS performance metric (b). AIS performance (c) and reliability (d) as a function of device material properties.

4. Discussion and Conclusions

The proposed in silico approach supports efficient and cost-effective AIS design by jointly addressing performance and reliability, and by quantifying the impact of material properties. Similar analyses were conducted to optimize the device geometry. Further work is needed to fully define the AIS system, including ancillary components such as the cuff pressure regulation and control unit.

5. References

1. Maculotti D et al, MethodsX; 13:102986 (2024)
2. Mascolini MV, Carniel EL, Artif Organs; 48:1112-1125 (2024)

ROUGHNESS-INDUCED LIFTING OF PLATELET-LIKE PARTICLES: A NUMERICAL STUDY

Giulia Malaguzzi[1], Barthelemy Thibaud[1], Corentin Raveleau[1], Simon Mendez[1] and Franck Nicoud[1,2]

1. IMAG, University of Montpellier, CNRS, Montpellier, France; 2. Institute Universitaire de France, Paris, France

1. Introduction

Ensuring hemocompatibility in blood-contacting devices remains challenging, as surface-induced platelet adhesion triggers thrombosis. While various microstructured surfaces have been investigated to reduce blood material contact area [1], this study explores if microstructures can repel platelet-like particles. We demonstrate that well-chosen roughness can drift particles away from the wall, potentially preventing adhesion and subsequent activation.

2. Materials and Methods

Platelets are first modelled as spherical particles of radius a moving in a linear shear flow under Stokes conditions, generated by a translating top flat wall located at $x_3 = 15a$. The bottom surface features various geometries, such as the asymmetric sawtooth pattern shown in Fig. 1.

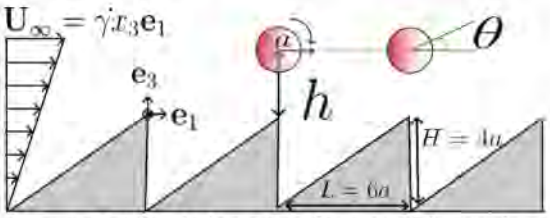


Figure 1: Simulation setup for a particle moving over an upward-facing pattern. Top wall not shown.

Stokes equations are solved via an in-house quadratic 3D Boundary Element Method library, with fluid viscosity matching blood plasma ($\mu = 1.2$ mPa · s). Exploiting linearity of flow equations, the 6-components translational/rotational velocity vector of a force-free particle is computed as $\boldsymbol{U_0} = -\boldsymbol{M}\boldsymbol{F_0}$. Here, $\boldsymbol{F_0}$ denotes the force/torque on a stationary particle and $\mathbf{M}$ the mobility matrix, defined as the inverse of the resistance matrix $\boldsymbol{R}$. The latter is numerically constructed via six unit-velocity simulations. Further details are available in [2].

For any (x_1, x_3) position, the local drift angle is defined as the ratio of normal u_3 to longitudinal u_1 velocity components: $\theta = u_3/u_1$. Then, the mean drift angle $\bar{\theta}$ at altitude x_3 is estimated over a period L of the structure:

$$\bar{\theta}(x_3) = \frac{1}{\mathrm{L}} \int_0^{\mathrm{L}} \theta(x_1, x_3) \mathrm{d}x_1 \qquad (1)$$

3. Results

Table 1 shows results for different patterns and two tip-to-particle distances, $h = 2.5a$ and $h = 3a$ (see Fig. 1).

Pattern	h/a	$\bar{\theta}$
Upward facing sawtooth pattern	3	1.6×10^{-4}
	2.5	4.6×10^{-4}
Downward facing sawtooth pattern	3	-1.6×10^{-4}
	2.5	-4.6×10^{-4}
Squared pattern	3	≈ 0

Table 1: Mean drift angles $\bar{\theta}$ of a spherical particle at distances h along various wall patterns.

4. Discussion and Conclusions

This analysis demonstrates that upward facing sawtooth microgrooves generate non-inertial repulsion of platelet-like particles, while downward facing patterns induce an opposite drift, and squared roughness has no net effect. These results agree with Stokes flows reversibility. Further results presented at the conference will include drift angles scaling laws with respect to the shear rate, surface distance, and the effect of the particle shape on the lifting mechanism.

5. References

1. Movafaghi S et al., Mater. Horizons; 6(8):1596-1610 (2019).
2. Raveleau C, PhD thesis, University of Montpellier, 2025.

Acknowledgements: This work was publicly funded through ANR (the French National Research Agency) under the "Investissements d'avenir" program with the reference ANR-16-IDEX-0006.

UNCERTAINTY ANALYSIS OF IN SILICO BIOHEAT TRANSFER MODELING IN THE HUMAN HEAD EXPOSED TO BLUETOOTH RADIATION

Ivan D. Horvat (1), Jana Wedel (2), Klementina Vidjak (3), Dragan Poljak (3), Jure Ravnik (1)

1. University of Maribor, Faculty of Mechanical Engineering, Slovenia; 2. Friedrich-Alexander-Universität Erlangen-Nürnberg, Germany; 3. University of Split, Faculty of Electrical Engineering, Croatia

1. Introduction

Bioheat modeling of human head exposure to Bluetooth radiation has become increasingly important with the widespread use of 5G and Bluetooth technologies. Accurate prediction of EM-induced thermal effects, particularly at higher frequencies, is essential. This work presents an in silico bioheat framework with associated uncertainty analysis.

2. Materials and Methods

A custom OpenFOAM implementation was developed to solve the bioheat equation in human tissue [1] and coupled with electromagnetic (EM) field results obtained with the time domain solver from the CST Studio 2021. A Stochastic Collocation Method [2] is employed to quantify uncertainties arising from unknown and spatially varying antenna positions, as well as from variability in the thermophysical and EM properties of the tissues.

3. Results

A human head model consisting of 10 distinct tisuses is analyzed together with a Bluetooth earbud operating under typical conditions. The predicted thermal response includes metabolic heat generation, device self-heating, and electromagnetic power absorption. Figure 1 illustrates the pointwise specific absorption rate (SAR) distribution, and Figure 2 presents the corresponding EM-induced temperature rise with the head.

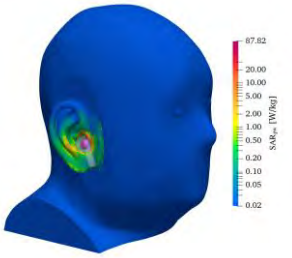


Figure 1: Pointwise SAR distribution in the head model, SAR = $\sigma \mid E \mid^2 / (2\ \rho)$.

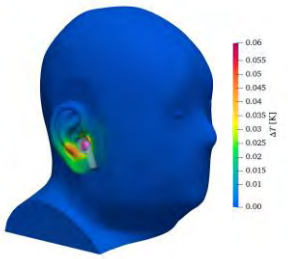


Figure 2: EM-induced temperature rise in the head model.

4. Discussion and Conclusions

Parametric simulations incorporating uncertanties in antenna placement and tissue material properties enable the identification of the dominant contributors to variability in the predicted temperature fields. The results emphasize the critical role of accurate parameter characterization in ensuring the robustness and crediblity of in silico bioheat simulations.

5. References

1. Horvat et al., “Towards Implementation of Advanced Bioheat Models in Human Head Exposed to 5G Radiation.” (2025), SoftCOM 2025, Split.
2. A. Šušnjara et al., “Stochastic-deterministic boundary element modelling of transcranial electric stimulation using a three layer head model.” (2021), EABE, Vol 123, pp 70-83, doi:10.1016/j.enganabound.2020.11.010.

Acknowledgements:

The authors thank the Slovenian Research and Innovation Agency project J7-60118, and the Croatian Science Foundation (IPS-2024-02-7779).

CLINICALLY-BASED FE FOOT MODELING FOR OA PATIENTS

Benoît Viguie, Baptiste Pierrat, Woo-Suck Han, Jérôme Molimard

Mines Saint-Etienne, Univ Jean Monnet, INSERM, U 1059 Sainbiose, Saint-Etienne, France

1. Introduction

Rheumatoid arthritis (RA) affects 0.77% of the population [1], causing erosion of the joints and surrounding tissues and resulting in intense pain, toe deformities, and loss of functionality [2]. Custom orthotic insoles allow for offloading pressure under the metatarsal heads while walking and standing and help alleviating pain. While the effects of insoles on foot segment movements, plantar pressure, and pain reduction have been demonstrated [3], the impact of insole design on biomechanical behavior inside the foot remains poorly characterized. Studying the mechanical behavior inside the foot in a patient-specific way requires numerical simplifications, e.g. using generic bone geometries [4], or focusing on the effect of the insole on the metatarsophalangeal joint only [5]. Few authors investigated a general foot-shot interaction under movement [6].

This study aims to develop a complete workflow, adapted from the patient data (CT scan, gait parameters) to the internal load of the foot during a gait cycle with insole.

2. Materials and Methods

In the clinical trial (Montpellier IRB decision 2025-A02220-49), we are collecting CT scans, leg position and vertical load under walking conditions for a cohort of RA patients. As it is still on-going, we present here preliminary results on cadaveric data. A generic model of the foot was constructed by manually segmenting images of the Visible Human Project. This model included the geometry of each bone and the location of ligament insertions. A mesh-morphing technique was employed between generic model and patient specific CT scan [6]. First, the two feet were aligned bone by bone using Sequential Least Squares Programming (SLSQP) minimization. Then, the source geometry was approximated to the target through a normal projection and smoothing routine. Subsequently, RBF mesh-morphing was carried out using inverse multiquadratic functions.

The geometry was imported into the Abaqus FE software. The bone were considered as rigid bodies. Cartilages were obtained by dilating the surfaces in the joint regions. The ligaments and muscles were incorporated as linear spring elements under tension. Soft tissues were modeled as homogeneous hyperelastic materials. Two types of contact were considered: contact between the bones and contact between the plantar surface and the ground. The constructed model was subjected to a complete gait cycle by simultaneously applying a vertical force to the tibia and moving it in a sagittal plane.

3. Results

The average Hausdorff distance between the mesh-morphed bone and the target bone geometry is 0.06 mm [S.D. 0.09 mm]. The pressure applied to the fat pads beneath the metatarsal heads was computed throughout the gait cycle and exhibited two distinct peaks, one associated to initial forefoot loading and the other one to the propulsion phase. Larger shears stress on the fat pads appeared under the medial sesamoid bones. Last, ligament strain was maximum on the tibiotalar part of the deltoid ligament.

4. Conclusions

A complete patient-specific workflow was validated. First results suggest that describing the whole gait model is necessary to identify the critical loading conditions for the soft tissues of the foot. Further work will explore the correlation between insole features and joint unloading for RA patients of this study.

5. References

1. Stolt, M., et al. (2017). Rheum. Int.
2. Weiss, R., et al. (2008). Gait Posture.
3. Tenten-Diepenmaat, M. et al. (2019). J. Foot Ankle Res.
4. Chen, W. et al. (2010). Med. Eng. Phys.
5. Spirka, T. et al. (2014). J. Biomech.
6. Kroupa, N. et al. (2020). Front. Bioeng. Biotechnol.

Acknowledgements:

This work was supported by ANR under grant ANR-22-CE19-0004-01.

A COMPUTATIONAL FRAMEWORK OF SHEAR WAVE ELASTOGRAPHY TO ASSESS PRETERM BIRTH RISK

Camilo A. Duarte (1), Eden Katz (1), Ivan M. Rosado-Mendez (2, 3), Kristin M. Myers (1)
1. Department of Mechanical Engineering, Columbia University, United States; 2. Departments of Medical Physics and Radiology, University of Wisconsin-Madison, United States

1. Introduction

Shear wave elastography (SWE) is a cost-effective, minimally invasive ultrasound technology with potential for *in vivo* assessment of spontaneous preterm birth (sPTB) risk [1] (delivery < 37 weeks of gestation). By measuring shear wave speed (SWS) induced by a transvaginal ultrasound probe (Fig. 1a), SWE provides a biomarker of cervical stiffness, as shear waves propagate faster in stiffer tissues. Since premature cervical softening often precedes sPTB[2], SWE could detect biomechanical changes in the cervix missed during examination. However, the high variability of SWS values, driven by the cervix's complex anisotropic and time-dependent mechanical behavior, hinders its clinical utility. *In silico* testing using finite element (FE) simulations of shear wave propagation can help identify and quantify sources of variability and ultimately minimize them, thereby establishing SWE as a robust diagnostic tool for sPTB.

2. Materials and Methods

A SWE-FE platform was implemented in the software FEBio to simulate shear wave propagation due to the application of an acoustic radiation force (ARF) field modeled a transient Gaussian body force. Simulations of shear wave propagation were performed using low and high-fidelity CAD 3D geometries of the cervix (Fig. 1b) with mesh and boundary conditions shown in (Fig. 1c). Each geometry uses a constitutive material model calibrated from *ex vivo* human tissue, capturing nonlinear elasticity, anisotropy, and collagen organization at non-pregnant (NP) and late-pregnant (PG) states. Finally, SWS was estimated as group velocity using a time-to-peak displacement algorithm applied to the FE node-displacement field [3].

3. Results

A representative FE transient simulation is shown in Fig. 1d. Our results indicate that SWS is highly sensitive to material properties, such as the tissue's bulk modulus, fiber initial stiffness, and the preferential orientation of the collagen fibers, and their degree of disorganization. Consequently, from NP to PG, SWS decreased as tissue stiffness decreases and collagen fibers become more dispersed in the cervix (Fig. 1e). Additionally, SWS is sensitive to the anatomical location at which it is measured, and was found to be greater at the internal os (IO) compared to the external os (EO)(Fig. 1e).

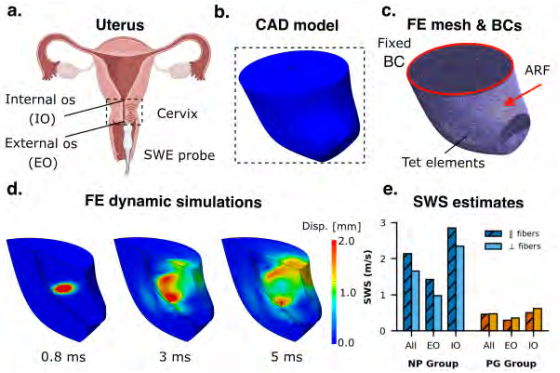


Figure 1: Computational FE framework implemented to simulate ultrasonic shear waves propagating in the cervix.

4. Discussion and Conclusions

This work emphasizes the importance of accounting for tissue anisotropy and nonlinear tissue stiffness when measuring SWS. Future efforts should focus on developing SWE protocols that account for biological sources of variability and maximize sensitivity to cervical remodeling pathways that are early predictors of sPTB.

5. References

[1] H. Feltovich, et al., Am. J. Obstet. Gynecol.2012, vol. 207, no. 5, pp. 345–354. [2] Vink and H. Feltovich, Seminars in Fetal and Neonatal Medicine, 2016, vol. 21, no. 2, pp. 106–112, 2016. [3] M. L. Palmeri et al., IEEE Trans. Ultrason. Ferroelectr. Freq. Control, 2017, vol. 64, no. 1, pp. 78–92.

Acknowledgements:
We thank GE HealthCare and the Iris Fund for providing financial support to this project.

SEX-SPECIFIC COMPUTATIONAL MODELLING FOR AMS 800 ARTIFICIAL URINARY SPHINCTER

Maria Vittoria Mascolini (1,2), Conall Quinn (1,2), Eoghan Cunnane (3), Brian Watschke (4), Thomas Sinnott (5), Noel Smith (5), Caitríona Lally (1,2)*

1.Trinity Centre for Biomedical Engineering, Trinity College Dublin, Ireland; 2.Advanced Materials and BioEngineering Research Centre (AMBER) & School of Engineering, Trinity College Dublin, Ireland; 3.Bernal Institute and School of Engineering, University of Limerick, Ireland; 4.Urology, Boston Scientific Corp, Inc, Minnetonka, USA; 5. Urology, Boston Scientific Corp, Inc, Clonmel Co, Ireland.

**Corresponding author: Caitríona Lally (lallyca@tcd.ie)*

1. Introduction

Stress urinary incontinence affects around 10% of males and 40% of females [1]. Severe cases require surgical treatments in both sexes. The AMS 800 artificial urinary sphincter (AUS) is the gold standard in males, while its use in females remains somewhat limited by surgical complexity, despite growing clinical interest [2]. AUS complications are well documented in males and have also been reported in females, with high rates of revision and explantation, mainly related to device mechanical failure and urethral degenerative phenomena [2,3]. To improve outcomes with AUS, understanding device–urethra interactions across different anatomies is crucial. This study aims to develop an in silico platform to analyse sex-specific differences in biomechanical interactions between the AMS 800 device and urethral tissue.

2. Materials and Methods

Finite element (FE) models of female and male urethras (Fig. 1) were developed in Abaqus (2020, Dassault Systèmes Simulia Inc.), based on histological images [4,5], while a FE device model was created from geometry provided by Boston Scientific. A hyperelastic formulation was used for the device [3], male urethra [4], and female urethra [6].

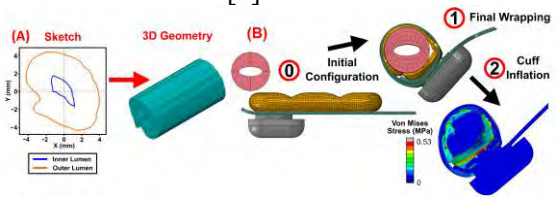


Figure 1 (A) Definition of urethra geometry. (B) Simulation of AMS 800 functioning.

The FE analysis simulated the AUS functioning (Fig. 1) including the wrapping of the AUS cuff around the urethra and the inflation according to clinical practice, at rest and under voiding conditions.

3. Results

The simulation of the AMS 800 inflation enabled lumen occlusion in both male and female urethra models. Resting-condition simulations allowed evaluation of the sex-specific tissue mechanical response. Increasing AUS pressure up to 80 cmH_2O resulted in higher compressive stress and strain. The most loaded regions were identified in both female and male anatomies, with differences in stress distribution between the two models. Under voiding condition, the simulations showed the AMS 800 performance by quantifying the maximum intraluminal pressure at which continence was maintained for both sexes.

4. Discussion and Conclusions

The in silico platform simulated the key operational aspects of the AMS 800 in interaction with male and female urethras. Future work will focus on mechanical testing of female urethra to fill the literature gap and refine the tissue model. Sex-specific comparative analyses across different device sizes will support reducing AUS complications and facilitating AUS implantation in females.

5. References

1. Lugo T et al., StatPearls [Internet] (2025) https://www.ncbi.nlm.nih.gov/books/NBK539769/
2. Estaphanous P et al., Cureus. 16(11):e73136 (2024)
3. Natali AN et al., Math Biosci Eng. 17: 3894-3908 (2020).
4. Cunnane EM et al., Biomaterials. 269:120651 (2021)
5. Attari A et al., Ann Biomed Eng. 49(8): 1848–1860 (2021)
6. Zhang Y et al., Ann Biomed Eng. 37(7):1425-33 (2009)

BIOMECHANICAL BENEFIT OF CERVICAL CERCLAGE DURING PREGNANCY: A COMPUTATIONAL STUDY

Abigail Laughlin (1), Erin Louwagie (1), Adriana Delagarza (1), Hannah Haider (1), Mirella Mourad (2), Michael House (3), Kristin Myers (1)

1. Columbia University, USA; 2. Columbia University Irving Medical Center, USA; 3. Tufts Medical Center, USA

1. Introduction

Cervical insufficiency is defined as the inability of the cervix to retain a pregnancy in the second trimester and is a major risk factor for preterm birth (PTB). Patients with cervical insufficiency are often treated with a cervical cerclage - a suture placed around the cervix to prevent it from dilating prematurely [1,2]. In the United States, 15,000 cerclage procedures are performed annually [3]. While effective, cerclage placement carries risks such as tissue laceration, and optimal placement strategies to maximize clinical benefit remain unclear. In this work, we developed a patient-specific computational model to evaluate how cerclage location affects cervical deformation under physiological loading.

2. Materials and Methods

The cervical and uterine anatomy of a pregnant individual with threatened PTB in the second trimester was built in SolidWorks (Dassault Systèmes, Vélizy-Villacoublay, France) using established methods [4]. This individual later received a cervical cerclage, and cerclage location along the cervical length was identified on transvaginal ultrasound. Four models were generated for this individual: baseline (no cerclage), ultrasound (clinical location), +20% (above the clinical location), and -20% (below the clinical location). Solid models were discretized in Hypermesh (Altair Inc., Troy, MI), and finite element analysis (FEA) was performed in FEBio Studio [5]. A prescribed displacement was used to simulate the reduction in cervical diameter at these locations imposed by the cerclage. Tissue material properties were assigned based on prior mechanical testing data, and each configuration was simulated with both a soft and stiff cervix [4]. Physiological boundary and loading conditions were applied [4].

3. Results

Stretch in the internal cervical face was reduced at all cerclage locations compared to the baseline model (Fig. 1). In both the soft and stiff cervix cases, the deformation at the internal cervical face reduced with higher cerclage placement (Fig. 1). The cervix lengthened in all cases with cerclage placement, with the largest increase (4.5 mm) observed for the highest placement in the soft cervix. Across all locations, lengthening was greater in the soft cervix model than in the stiff cervix model.

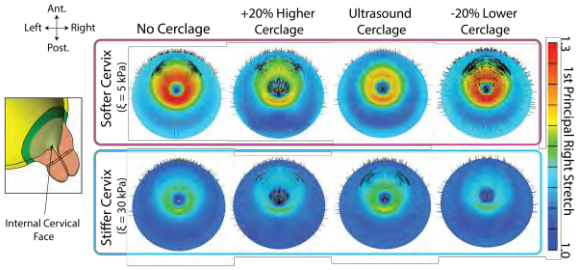


Figure 1: First principal stretch on the internal cervical surface for all cerclage configurations. Vectors denote the local direction of maximum stretch, illustrating reduced circumferential stretch at the internal os following cerclage placement.

4. Discussion and Conclusions

Cerclage placement affects the deformation of the internal cervical face under applied intrauterine load, with decreased deformation found with higher cerclage placements. This work provides a mechanical rationale for optimizing cerclage location and a framework for future patient-specific surgical planning.

5. References

1. ACOG, Obstet Gynecol; 138(2):320-3 (2021).
2. ACOG, Obstet Gynecol: 123(2):273-9 (2014).
3. Friedman A et al., Obstet Gynecol; 126(2):243-9 (2015).
4. Louwagie E, Doctoral Thesis (2024).
5. Maas S et al., J Biomech, 134(1):011005 (2012).

Acknowledgements:

This work is supported by the National Institutes of Health under award number 5R44HD116620-02. The content is solely the responsibility of the authors and does not necessarily represent the official views of the National Institutes of Health.

RADIOMICS AND *IN SILICO* ASSESSMENT OF TUMOUR ENVIRONMENT FOR PREDICTING RECURRENCE AFTER RT

Valentin Septiers (1,2), Hilda Chourak (1), Carlos Sosa-Marrero (1), Aurélien Briens (1), Jennifer le Guévelou (1), Renaud De Crevoisier (1), Maria A. Zuluaga (2), Oscar Acosta (1)

1. Univ Rennes – CLCC Eugène Marquis – INSERM – LTSI – UMR 1099, Rennes, France;

2. EURECOM, Data Science Department, Biot, France;

Corresponding author: Valentin Septiers, valentin.septiers@univ-rennes.fr

1. Introduction

Current radiomics approaches for predicting recurrence after prostate cancer (Pca) radiotherapy (RT) mainly focus on imaging features extracted within the tumour segmentation [1], often neglecting the tumour environment (TE). Furthermore, while recent studies have employed explainability techniques, such as SHapley Additive exPlanations (SHAP) [2], the resulting explanations are often difficult to interpret, lacking biological or clinical interpretability.

2. Materials and Methods

This study investigates the role of TE in predicting recurrence using data from 315 PCa patients treated with conventional RT. Based on the Phoenix criteria, 59 patients experienced biochemical recurrence [3]. To assess the role of TE, dilation and erosion of tumour margins (segmented by expert radiation oncologists) were performed on pre-treatment 3T MRI T2-weighted (T2w) images and Apparent Diffusion Coefficient (ADC) maps. IBSI-compliant [4] radiomic features were extracted from both modalities for each delineation created. After non-supervised feature selection, the prediction of recurrence was made, comparing classical machine learning algorithms (stratified 5-fold cross-validation, 100 repetitions). Then, a global SHAP explainability analysis was used on the best-performing delineations to assess feature contributions.

3. Results

Best performing delineations, with a logistic regression, were the 1.5mm dilation in the x, y and z directions (Accuracy: 0.73 and F1w: 0.74), and the crown associated to this dilation (dilation of 1.5mm - tumour, acc: 0.69 and F1w: 0.72), yelding better results than tumor mask baseline (Acc: 0.67 and F1w: 0.7).

Thus, prediction of recurrence highlighted the significance of TE and the relevance of both intra- and peri-tumoural information. SHAP analsyis revealed that homogeneity features from ADC (related to cellularity) were the most influencial in predictions. To further explore the impact of tissue homogeneity,a multiscale computational model [5] simulated the response to irradiation on heterogeneous digital twins, demonstrating that dense and poorly vascularised tumours were more prone to recurrence (**Figure 1**).

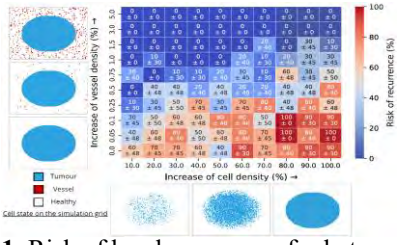


Figure 1: Risk of local recurrence for heterogeneous digital twins. On the Y axis, the vessel density in the peritumoural area, and on the X axis, the cell density in the intra-tumoural zone.

4. Discussion and Conclusions

Tumour and surrounding tissues homogeneity were found important in predicting recurrence, and simulation based on heterogeneous digital tissues showed that tumour density and vasculature had an impact on recurrence. This research supports personalised treatment for PCa by identifying key imaging features and explaining their predictive value in relation to biology.

5. References

1. Dutta A. et al., Phys. Imaging Radiat. Oncol.; 2024.
2. Lundberg S.M. et al., Advances in Neural Information Processing Systems; 2017.
3. Abramowitz M.C. et al., Cancer; 2008.
4. Zwanenburg A. et al., Radiobiology; 2020.
5. Sosa-Marrero C. et al. IEEE TBME; 2021.

Acknowledgements:

With financial support from ITMO Cancer of Aviesan within the framework of the 2021-2030 Cancer Control Strategy, on funds administered by Inserm (PredTwin project).

MODELLING AND SENSITIVITY ANALYSIS OF HYPOXIA-ACTIVATED DRUGS IN SOLID TUMORS

Alessandro Coclite (1), Riccardo Montanelli Eccher (2), Luca Possenti (3), Piermario Vitullo (2), Paolo Zunino (2)

1. Department of Electrical and Information Engineering, Politecnico di Bari; 2. MOX, Department of Mathematics, Politecnico di Milano; 3. Data Science Unit, Fondazione IRCCS Istituto Nazionale dei Tumori, Milano

1. Introduction

The efficacy of hypoxia-activated prodrugs (HAPs) in solid tumors is governed by tightly coupled transport-metabolism interactions, making predictive modelling and parameter exploration computationally expensive. Here, a multiscale model of oxygen and tirapazamine (TPZ) is combined with global sensitivity analysis to identify the key drivers of tissue exposure and surviving fraction (SF).

2. Materials and Methods

The framework in [1] couples a three-dimensional porous tissue model with a one-dimensional vascular network. Blood flow and intravascular transport are computed along the network; oxygen and TPZ diffusion and consumption are solved in the tissue, with transvascular exchange linking them. TPZ activation depends on local oxygen, and cell loss feeds back on oxygen consumption. A spatially averaged surrogate (0D) captures key nonlinearities in drug metabolism and SF, with surrogate functions used one-way in the spatial formulation. [1] Global sensitivity is assessed using the Morris elementary-effects method, first screening parameters on the 0D model and then restricting the 3D-1D-0D analysis to the most influential subset. Elementary effects are summarized through each input mean absolute effect and its standard deviation.

3. Results

The 0D screening identifies vascular TPZ concentration as the primary driver of spatially averaged tissue exposure, with a mean absolute effect approximately two orders of magnitude larger than other parameters and low variability across elementary effects, indicating limited interaction dependence. For SF, vascular TPZ concentration remains dominant, but TPZ metabolism and oxygen availability parameters become prominent, with higher variability consistent with nonlinear effects and interactions. SF sensitivity also increases at later observation times as differences in exposure and metabolism accumulate over the treatment window. Guided by these results, the spatial analysis focuses on seven influential parameters spanning vascular drug input, metabolic activation, and oxygen transport and consumption. The 3D-1D-0D model reveals heterogeneous TPZ distribution shaped by vascularization, with the SF field reflecting the local balance between delivery and activation. Spatial-average sensitivity indices for SF are about one order of magnitude smaller than in the 0D model, with larger relative dispersion, indicating that spatial heterogeneity reduces direct single-parameter control and amplifies coupled interaction effects. Oxygen-related parameters exhibit non-monotonic behaviour; changes in oxygenation affect SF through competing mechanisms. These non-monotonic trends emerge from the coupled transport/metabolism dynamics and are difficult to anticipate a priori. [1]

4. Discussion and Conclusions

The framework is physiologically grounded yet computationally efficient for predicting spatio-temporal oxygen/drug fields and cytotoxic response for HAP therapy. Sensitivity analysis identifies vascular TPZ concentration and metabolic activation parameters as the primary levers governing efficacy, with oxygen-related parameters playing a secondary but nonlinearly coupled role. Limitations include the exploratory nature of the setting and the absence of patient-specific calibration. Future work will integrate experimental/clinical data, incorporate vascular dynamics and tumor growth, and extend the biology to additional mechanisms relevant to HAP response.

5. References

1. Coclite A., Montanelli Eccher R., Possenti L., Vitullo P., Zunino P. AIMS Mathematics. 2025;10(11): 25504-25544.

DIGITAL TWINS FOR THE OPTIMISATION OF INTRA-ARTERIAL THERAPY IN LIVER CANCER

Elena Cutrì (1,2), Pierre-Antoine Eliat (3), Francesco de Gaetano (4), Antoine Petit (5), Michel Rochette (6), Yan Rolland (2), Hervé Saint-Jalmes (2), Johanne Bezy Wendling (2)

1. Université de technologie de Compiègne, CNRS, Alliance Sorbonne Université, BMBI, Compiègne, France; 2 Univ Rennes, CLCC Eugène Marquis, Inserm, LTSI - UMR 1099, F-35000, Rennes, France; 3 INRAE, INSERM, Univ Rennes, Nutrition Metabolisms and Cancer, NuMeCan, St Gilles,Rennes, France; 4 Department of Chemistry, Materials and Chemical Engineering "Giulio Natta", Politecnico di Milano, 20133, Milano, Italy; 5 Therenva, F-35000, France; 6 ANSYS, Villeurbanne, France

Corresponding author: elena.cutri@utc.fr

1. Introduction

Selective internal radiation therapy (SIRT), which involves the intra-arterial administration of radioactive microspheres into the hepatic artery, has gained recognition as an effective treatment for patients with advanced Hepatocellular carcinoma (HCC) [1]. Although a work-up is performed prior to treatment, suboptimal outcomes may still occur [2]. Consequently, optimising the treatment is of utmost importance. To address this, a digital twin of the hepatic vasculature was developed to simulate SIRT and coupled with an optimisation strategy to determine the most effective injection configuration.

2. Materials and Methods

The geometry was segmented from patient-specific images using a purpose-designed multiscale algorithm. The computational fluid dynamics (CFD) problem was configured to incorporate microsphere injection through a multiphase formulation. The optimisation process was conducted using the Response Surface Optimization package available within the ANSYS Workbench™. Initially, the input parameters (i.e., catheter position and inclination) and the output parameters (i.e., the microspheres' mass flow rate to the tumour) to be optimised were defined, and the design space was constructed. Subsequently, response surface models were generated to interpolate the entire design space. Finally, the optimisation procedure was carried out.

3. Results

Among the investigated input parameters, the response surface for the microspheres' mass flow rate at the tumour is shown as a function of catheter inclination (Figure 1). The optimisation strategy enabled us to identify three catheter tip positions that maximised the microspheres' flow rate to the tumour, thereby ensuring the administration of nearly 80% of the microspheres to the tumour.

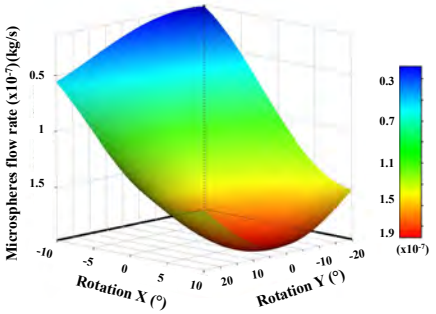


Figure 1: Response surface of microspheres mass flow rate at the tumour varying the catheter tip inclination.

4. Discussion and Conclusions

A digital twin of a patient-specific hepatic vasculature was developed and integrated with an optimisation strategy to optimise the SIRT. This digital twin holds the potential to assist clinicians in identifying the optimal injection site and performing dosimetry assessments, thereby facilitating the personalisation of treatment.

5. References

1. Sangro B et al., Int. J. Radiat. Oncol. Biol. Phys. 66 (2006) 792–800.
2. Chiesa C et al., EJNMMI Phys. (2021) 77.

Acknowledgements:

This study was supported by a grant from the European Community and the Region of Brittany for the project 'Assistance à la RtMi par un Outil temps Réel en routine clinIQUE - ARMORIQUE' (2019-2022).

PATIENT-SPECIFIC PREDICTION OF GLIOBLASTOMA GROWTH VIA REDUCED ORDER MODELING AND NEURAL NETWORKS

Sara Gazzoni (1), Donato Cerrone (1), Davide Riccobelli (2), Piermario Vitullo (1), Francesco Ballarin (3), Jacopo Falco (4), Francesco Acerbi (4), Andrea Manzoni (1), Paolo Zunino (1), Pasuqale Ciarletta (1)

Enter the affiliation information here ("Affiliation" style)
1. Politecnico di Milano, Italy; 2. SISSA, Italy; 3. Università Cattolica del Sacro Cuore, Italy; 4. Fondazione I.R.C.C.S. Istituto Neurologico Carlo Besta, Italy

1. Introduction

Glioblastoma (GBL) is among the most aggressive brain tumors in adults, characterized by patient-specific invasion patterns driven by the brain microstructure [1]. In this work, we present a proof-of-concept mechanistic learning framework for patient-specific prediction of GBL growth.

2. Materials and Methods

The approach integrates a diffuse-interface mathematical model to describe the tumor evolution [2,3] with machine learning techniques to enable real-time prediction and parameter identification from longitudinal neuroimaging data. A reduced-order modeling strategy, based on proper orthogonal decomposition (POD), is trained on synthetic data generated from patient-specific brain anatomies reconstructed from magnetic resonance imaging (MRI) and diffusion tensor imaging (DTI), following a strategy similar to [4]. A neural network surrogate learns the direct and inverse mapping from the model parameters and the tumor distribution projected onto the reduced space, a method usually referred to as the POD-NN approach.

3. Results

Once trained, the POD-NN achieves a computational speed-up of 99% in the prediction of tumor evolution (see Table 1).

Method	Elapsed Time
FOM	780 s
POD-Galerkin	475 s
POD-NN	5 s

Table 1: Comparison of computational times.

Regarding the inverse problem, small discrepancies may arise between parameters predicted by the surrogate model and true patient-specific ones. However, simulations performed using the predicted parameter set accurately reproduce the observed tumor dynamics. In particular, the tumor volume evolution obtained with the predicted parameters closely matches that generated with the true parameters, as shown in Figure 1.

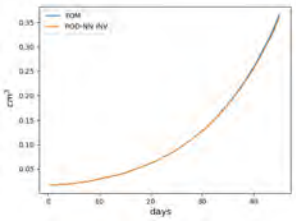


Figure 1: Volume fraction of tumor over time with true and predicted set of parameters.

4. Discussion and Conclusions

This hybrid methodology bridges mechanistic modeling and data-driven learning, addressing both the direct and inverse problems of GBL evolution and in time-sensitive clinical scenarios.

The current contribution focuses on methodological innovation, providing a rigorous computational foundation for the future clinical deployment of patient-specific digital twins in neuro-oncology.

In conclusion, our approach represents a significant step toward the development of interpretable, scalable, and efficient computational tools for precision medicine in the management of Glioblastoma.

5. References

1. Deisboeck, T. S. et al., Cell proliferation, 34(2), 115–134 (2001).
2. Colombo, M. C. Et al. PLOS ONE 10(7): e0132887 (2015).
3. Wise, S. M. et al., Journal of theoretical biology, 253(3), 524–543 (2008).
4. Agosti, A. et al., Math Meth Appl Sci. 2020; 43: 8945–8979 (2020).

Acknowledgements:
This work was partly supported by MUR through the grants PRIN 2020 Research Project MATH4I4 and Dipartimento di Eccellenza.

A 3D–1D OPTIMIZATION FRAMEWORK FOR THE SIMULATION OF ANGIOGENESIS AND TUMOR PROGRESSION

Denise Grappein (1), Chiara Giverso (2), Stefano Scialò (2)

1. MOX, Department of Mathematics, Politecnico di Milano;
2. Department of Mathematical Sciences G. L. Lagrange, Politecnico di Torino

1. Introduction

Tumor growth beyond a limited size depends on the formation of a functional vascular network to ensure oxygen and nutrient supply. This process, known as tumor-induced angiogenesis, is driven by tumor-secreted factors that stimulate new capillary formation from existing vessels. To capture the resulting multiscale interaction between vascular growth and tumor progression, we propose an optimization-based 3D–1D coupling strategy [1, 2] for simulating the perfusion of tumoral tissue in the presence of a growing capillary network.

2. Materials and Methods

The tumor is described as a multiphase cell aggregate composed of tumor cells, extracellular matrix, and interstitial fluid [3]. The model consists of a nonlinear PDE system for tumor cell volume fraction, fluid pressure, oxygen, and VEGF concentration, and it is discretized by Finite Elements. Capillary growth is modeled by a discrete hybrid tip-tracking approach, where the vascular geometry is updated at each time step according to angiogenic stimuli, and the PDE system is solved on the updated configuration. Coupling between the 3D tissue and the 1D vascular network is achieved through an optimization-based formulation. Interface fluid and nutrient exchange are enforced via auxiliary variables, leading to an equivalent constrained minimization problem.

3. Results

Numerical simulations are performed to analyze the coupled tumor–vessel dynamics.
The optimization framework enables flexible and independent mesh choices for tissue and vessels, while interface variables provide direct access to exchange quantities without post-processing.
A sensitivity analysis based on the Morris elementary effects method is conducted to identify the most influential parameters and assess their impact on the model outputs. The results confirm the key role of the capillary network in tumor progression, showing that vascular development strongly influences tissue perfusion and growth dynamics.

4. Discussion and Conclusions

The proposed framework provides a consistent and flexible approach for modeling tumor–vascular interactions. The results highlight the role of angiogenesis in sustaining tissue perfusion and driving tumor evolution.
The sensitivity analysis further supports parameter relevance assessment and provides insight for parameter calibration. Overall, the framework offers a solid basis for future investigations and therapeutic studies targeting vascular growth.

5. References

1. Berrone S., Grappein D., Scialò S., Num. Alg. 95: 499-526, (2024)
2. Berrone S., Giverso G., Grappein D., Preziosi L., Scialò S., CAMWA 151:252-270, (2023)
3. Giverso C., Scianna M., Grillo A., Mech. Res. Commun. 68:31-39, (2015)

Acknowledgements:
Author D.G. acknowledges that part of this work was carried out while holding a post-doctoral fellowship financed by INdAM.

ESTIMATING PROSTATE CANCER RADIOSENSITIVITY THROUGH A DIGITAL TWIN (VHT) OF TUMOUR RESPONSE TO RADIOTHERAPY

Eleni Kolokotroni (1), Simon Spohn (2), Anca-Ligia Grosu (2), Dimos Baltas (2), Constantinos Zamboglou (2), Ilias Sachpazidis (2) and Georgios Stamatakos (1)

1. National Technical University of Athens, School of Electrical and Computer Engineering (ICCS), Athens, Greece; 2.University of Freiburg, Department of Radiation Oncology, Freiburg, Germany

1. Introduction

Current radiotherapy (RT) approaches for prostate cancer (PCa) are moving towards extreme precision and schedules tailored to a patient's specific tumor response. In this context, the Oncosimulator (OS) [1,2], being an *in silico* medicine mechanistic multiscale digital twin (virtual human twin or VHT), has been employed in order to simulate the clinical prostate tumor response to externally delivered radiotherapy regimens.

2. Materials and Methods

The OS is grounded in a discrete entity–discrete event modeling framework, enabling the representation of tumor dynamics across multiple biological scales. At the initial time point, tomographic imaging data are integrated with histopathological and molecular information to generate a virtual 3D reconstruction of the anatomical region of interest.

A sampling-based approach, the Latin Hypercube Sampling (LHS) method, has been applied for the study of our multi-parametric model. The LHS is used to generate a plausible collection of model parameter values that correspond to virtual tumors having a common proliferation pattern in terms of volume doubling time, Td, and growth fraction (GF).

Subsequently, radiosensitivity estimates for real PCa tumors were calculated based on the observed radiation-induced tumor shrinkage, quantified from medical imaging data, and corresponding simulation studies performed using the OS. Data has been provided by the University of Freiburg, within the framework of the European Commission (EC) supported project PersoRad (ERAPERMED2019-299).

3. Results

Multiparametric analyses of the OS revealed that the tumor regression pattern observed during and after radiotherapy is not only influenced by sensitivity to irradiation but also depends significantly on the proliferation profile of the tumor.

Fig. 1 shows the boxplot of the estimated parameter α of the Linear Quadratic (LQ) model for a patient, for three different proliferation profiles: (a) low proliferation: Td=1100 days, GF=6%, (b) moderate proliferation: Td=500 days, GF=10%, (c) high proliferation: Td=200 days, GF=30%. It is noted that the proliferation profile characterized here as low corresponds to the median of the values found in literature for patients referred to radiotherapy.

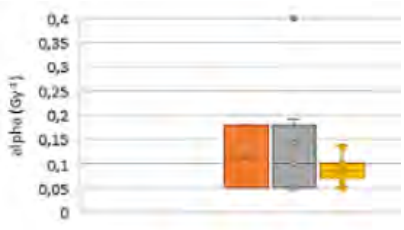


Figure 1. Estimated radiosensitivity parameter alpha (α) (in Gy^{-1}) of the LQ model for a low (orange color), a moderate (grey color) and a high (yellow color) proliferation profiles

4. Discussion and Conclusions

Correlating *in vivo* radiosensitivity estimates with a patient's molecular profile offers significant potential for identifying distinct resistance and sensitivity phenotypes. By leveraging machine learning to analyze whole-genome data, gene expression profiles, and transcriptomic or proteomic signatures, tumor cell response to treatment can be precisely quantified in the context of *in silico* oncology.

5. References

1. Stamatakos G et al., Front. Physiol. 16:1434739, 2025, https://www.frontiersin.org/journals/physiology/articles/10.3389/fphys.2025.1434739/full
2. Kolokotroni E, et al., J. Pers. Med. 2024, 14(5), 475. https://doi.org/10.3390/jpm14050475

Acknowledgements:

This study has been supported by the Greek Secretariat of Research and Innovation ("PersoRad" project (T11EPA4-00021) and the EC (PersoRad (ERAPERMED2019-299)).

A PARALLEL-DISTRIBUTED FINITE ELEMENT FRAMEWORK FOR 3D/2D CHEMO-MECHANICAL COUPLING IN CELL MOTILITY

Mattia Serpelloni (1), Paolo Tesini (2), Alberto Salvadori (1)

1. *Department of Mechanical and Industrial Engineering, Università di Brescia, Brescia, Italy;*
2. *Department of Civil, Environmental, Architectural Engineering and Mathematics, Università di Brescia, Brescia, Italy*

mattia.serpelloni@unibs.it; paolo.tesini@unibs.it; alberto.salvadori@unibs.it;

1. Introduction

Cellular locomotion governs fundamental biological phenomena, ranging from embryonic tissue formation to oncological dissemination. Replicating these dynamics computationally entails coupling the internal mechanical response of the cell with the chemical transport of adhesion molecules along the cell membrane. Expanding upon the foundational principles established in [1], this work introduces a robust numerical simulator engineered via the open-source deal.II library (https://dealii.org). Our solver is specifically tailored to track the spatio-temporal evolution of transmembrane proteins across continuously deforming lipid bilayers.

2. Materials and Methods

To capture this complex behaviour, we implement a parallel-distributed, one-way coupled algorithm defined by three primary features. Firstly, we deploy a dual-triangulation topology: a 3D volumetric grid for the large-deformation mechanics of the cytoplasm and nucleus, paired with a 2D surface manifold for membrane activities. This allows for independent, localized mesh refinement. Secondly, we utilize a hierarchical time-stepping strategy to resolve the biological timescale mismatch: 3D bulk deformations are advanced at macroscopic intervals, whereas rapid biochemical reactions on the cell membrane are captured through fine-scale temporal increments. Finally, we introduce customized algorithmic stabilizations [2] to mitigate non-physical oscillations. By integrating a lumped-mass approach to enforce strictly positive solutions and, where necessary, an adaptive, residual-driven shock-capturing technique, we apply artificial viscosity strictly around abrupt concentration shifts.

3. Results

The resulting architecture accurately recreates fundamental motility stages, such as initial rolling, adhesion, and mechanical spreading.

Furthermore, it successfully captures spatial patterns, including the well-known "coffee-ring" aggregation of receptor proteins at the cell-substrate contact area.

These results demonstrate the solver's ability to maintain stability even under sharp concentration gradients and significant geometric deformations.

4. Discussion and Conclusions

The developed framework aims to provide a scalable tool for investigating the chemo-diffusive activities of receptors during cell motility. The dual-triangulation approach and hierarchical time-stepping seek to reduce the computational cost compared to monolithic schemes. Further developments aim to optimize communication-intensive tasks during either bulk or manifold re-meshing to leverage the full capacity of massive High-Performance Computing (HPC) resources.

5. References

1. Serpelloni, M., Arricca, M., Ravelli, C., Grillo, E., Mitola, S., Salvadori, A., “Mechanobiology of the relocation of proteins in advecting cells: in vitro experiments, multi-physics modeling, and simulations”, Biomech. Model. Mechanobiol., 22, 1267–1287 (2023)

2. Hinton, E., Rock, T., and Zienkiewicz, O. C., “A note on mass lumping and related processes in the finite element method”, Earthq. Eng. Struct. Dyn., 4.3, 245-249 (1976)

Acknowledgements:

This research is funded by: the European Union’s Horizon 2020 research and innovation programme HORIZON-EUROHPC project ‘dealii-X: an Exascale Framework for Digital Twins of the Human Body’ (topic HORIZON-EUROHPC-JU-2023-COE-03-01).

Project grant no. 101172493.

ILLUMINATING CARDIAC MECHANISMS: FROM FLUORESCENT SARCOMERES TO IDENTIFIABLE MODELS OF ARRHYTHMIAS

Moritz Bauer (1), Frédéric Sonak (1), Jens Timmer (1), Viviane Timmermann (1,2)

1. Institute of Physics, University of Freiburg, Germany; 2. Institute of Molecular Medicine and Cell Research, University of Freiburg, Germany

1. Introduction

Cardiac arrhythmias emerge from coupled cellular mechanics and electrophysiology, yet translating high-resolution mechanical experiments into structurally identifiable mathematical models remains challenging. We present an integrated workflow that extracts sarcomere-length metrics from fluorescent imaging and feeds these measurements into quantitative mechanistic models of arrhythmia dynamics [1].

2. Materials and Methods

In α-actinin-tagged cardiomyocytes derived from mouse-induced pluripotent stem cells and carrying human mutations, we trace Z-lines using dynamic-programming seam carving and estimate sarcomere spacing with a sliding fast Fourier transform and quality controls to reduce bias during nonlinear contractions. These time-resolved sarcomere-length estimates provide model limits and observables for fitting and identifiability analysis. We estimate the parameter vector θ by maximum likelihood

$$\hat{\theta} = argmax_{\theta}\, \mathcal{L}(\theta|y) \qquad (1)$$

where $\mathcal{L}$ denotes the likelihood of the observed sarcomere-length data y. For each parameter θ_i, we calculate the profile likelihood by re-optimising all remaining parameters

$$PL(\theta_i) = max_{\theta, j\neq i}\, \mathcal{L}(\theta|y) \qquad (2)$$

We prioritise minimal, well-structured models and assess structural identifiability, i.e., the requirement that different parameter values produce distinguishable outputs, to avoid non-identifiability that confounds sensitivity analyses and prediction [2].

3. Results

In practically identifiable settings, maximum-likelihood estimation (Eq. 1) provides parameter estimates with finite confidence intervals and model predictions that can be compared with the measured data [3].

4. Discussion and Conclusions

The integration of automated sarcomere imaging analysis with identifiability-aware modelling addresses a key barrier to linking cellular mechanics with quantitative models of arrhythmia dynamics. By explicitly linking automated imaging analysis and identifiability-aware modelling, our pipeline supports reproducible parameter estimation and mechanistic interpretability of arrhythmia pathways, with a route towards patient-specific simulations to inform therapy.

5. References

1. Freytag J, Beyer S, Timmer J, Timmermann V. 2025;52. doi:10.22489/CinC.2025.314.
2. Wieland F-G, Hauber AL, Rosenblatt M, Tönsing C, Timmer J. Current Opinion in Systems Biology. 2021; 25:60–69. doi:10.1016/j.coisb.2021.03.005.
3. Raue A, Kreutz C, Maiwald T, Bachmann J, Schilling M, Klingmüller U, Timmer J. Bioinformatics. 2009;25(15):1923–1929. doi:10.1093/bioinformatics/btp358.

Acknowledgements:

The authors thank Prof. Dieter Fürst for providing the microscopy images. The authors acknowledge funding from the Deutsche Forschungsgemeinschaft (DFG, German Research Foundation) – Project-ID 403222702 – SFB 1381, the Cluster of Excellence 'Centre for Integrative Biological Signalling Studies' (CIBSS) by the DFG under Germany's Excellence Strategy – EXC-2189 – 390939984, the Hans A. Krebs Medical Scientist Program, Faculty of Medicine, University of Freiburg, and the Baden-Württemberg Stiftung ('ArrhythMEC').

A CAUSAL AI-DRIVEN DIGITAL TWIN OF CARDIAC ELECTROPHYSIOLOGY

Dharmesh Mistry (1,2), Sandra Ortega-Martorell (1,2), Zainab Mahmood (1,2), Hector J. Hortua (1,2), Robyn Lotto (1,2), Ellen Dawson (1,2), Gregory Y.H. Lip (2), Ivan Olier (1,2)

1. AI and Digital Technologies Research Institute, Liverpool John Moores University, UK.
2. Liverpool Centre for Cardiovascular Sciences, Liverpool John Moores University, University of Liverpool, and Liverpool Heart and Chest Hospital, UK.

1. Introduction

This study introduces a counterfactual, causal AI-driven digital twin linking upstream clinical and demographic determinants to cardiac electrophysiology. These determinants represent upstream factors that may influence cardiac electrical phenotypes. By explicitly modelling their structural relationships, we aim to simulate how interventions on this upstream state propagate to alter ECG phenotypes.

Developed within the EU TARGET project on digital twins for atrial fibrillation (AF) [1], we introduce a deep structural causal model (DSCM; [2]) that generates observational and interventional upstream states under explicit do-operations. A conditional generative model then synthesises ECG signals from this causally consistent state, enabling interventionally grounded in-silico experimentation.

2. Materials and Methods

Our framework comprises the DSCM and a conditional ECG generator. The DSCM learns causal graph-guided structural relationships to generate causally consistent upstream clinical and demographic states under observational and interventional regimes. ECGs are synthesised exclusively from these upstream states.

In the absence of real interventional data, the DSCM was first evaluated on a synthetic dataset defined by a known non-linear causal graph to verify behaviour under explicit do-operations. Distributional fidelity was assessed using the mean Kolmogorov-Smirnov (KS) statistic for continuous variables and Jensen-Shannon (JS) divergence for categorical variables.

The framework was applied to PTB-XL [3] and MIMIC-IV [4]. Causal graphs were derived through data-driven discovery with structural constraints and clinician review. Generated ECGs were evaluated through clinician inspection and downstream task performance.

3. Results

On the ground-truth data, the DSCM yielded high-fidelity observational and interventional distributions (KS_{obs}=0.04, JS_{obs}=0.03, KS_{int}=0.05, JS_{int}=0.04). Interventions generated the expected downstream distributional shifts (Fig. 1), supporting structural consistency under do-operations. Applied to PTB-XL, conditioning ECG synthesis on the generated upstream states produced physiologically coherent signals. Counterfactual interventions induced corresponding changes in ECG morphology (Fig. 2). Clinician review indicated consistency between the intervened upstream states and resulting electrical patterns.

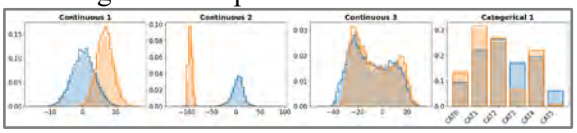


Fig. 1: True observational and interventional distributions (blue and orange lines) vs generated distributions (blue and orange semi-transparent fill).

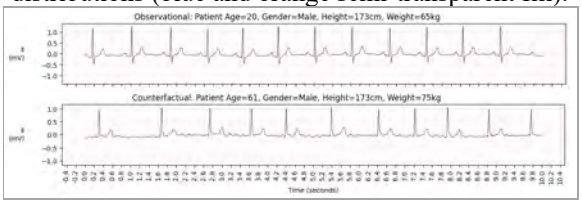


Fig. 2: ECGs generated before and after age intervention (do[age=61]) illustrating a shift from sinus rhythm to AF (irregular RR intervals, absence of organised P-waves).

4. Discussion and Conclusions

Our causal framework generates structurally consistent upstream states and corresponding ECG signals under intervention. By preserving dependencies between clinical-demographic determinants and cardiac electrophysiology, it allows controlled counterfactual simulation within a data-driven digital twin, supporting more rigorous in-silico experimentation in AF modelling.

5. References

1. Ortega-Martorell et al., Eur Heart J. 2025;46(3)
2. Poinsot A et al., IJCAI 2024 Proc; p. 8207-15
3. Wagner P et al., Sci Data. 2020;7(1):154
4. Johnson A.E.W. et al., Sci Data. 2023;10(1)

Acknowledgements:
Funded by the EU Horizon Europe under Grant Agreement No. 101136244 (TARGET, https://target-horizon.eu/).

MULTIMODAL OPTIMISATION OF CARDIAC ELECTROPHYSIOLOGY MODELS USING 12-LEAD ECG AND CT IMAGING

Buntheng LY (1), Nicolas Cedilnik (2), Mihaela Pop (2), Josselin Duchateau (1, 3), Fréderic Sacher (1, 3), Pierre Jaïs (1, 3), Hubert Cochet (1, 3), Maxime Sermesant (1, 2)

1. Institut Hospitalo-Universitaire Liryc, France; 2. Centre Inria Université Nice Côte d'Azur, France; 3. Bordeaux University Hospital, France

1. Introduction

We present a multimodal personalisation framework for the electrophysiological model that integrate cardiac CT imaging with sinus rhythm ECG recordings.

2. Materials and Methods

We developed a two-stage optimisation framework that extends previous work [1] in which in silico ventricular tachycardia (VT) induction was performed using electrophysiological models personalised from CT-derived myocardial wall thickness. In both stages, we adopted the Covariance Matrix Adaptation Evolution Strategy (CMA-ES) as the optimisation method.

In the first stage, 34 candidate early-activation sites were selected on the left and right ventricular endocardium. The objective function (Eq. 1) comprises a primary term that optimises the accuracy of QRS complex peaks and amplitudes, and a secondary term, defined as the mean absolute error over discretised QRS complexes, which acts as a regularisation component.

$$L_{onset} = \frac{1}{3}\left[\sum \left(|p_{qrs} - p^*_{qrs}| + |v_{qrs} - v^*_{qrs^*}|\right)\right] + \alpha\frac{1}{n}\left[\sum |\Psi_{qrs}[n] - \Psi^*_{qrs}[n]|\right] \quad (1)$$

In the second stage, we optimised the myocardial electrical conductivity parameter. The objective function (Eq. 2) seeks parameter values that minimise the discrepancy in QRS peak times between the simulated and recorded ECG signals.

$$L_{params} = \frac{1}{3}\left[\sum |t_{qrs} + t_{qrs^*}|\right] + \alpha\frac{1}{n}\left[\sum |\Psi_{qrs}[n] - \Psi^*_{qrs}[n]|\right] \quad (2)$$

3. Results

We evaluated the optimisation framework using data from six patients referred for catheter ablation of recurrent post-infarct ventricular tachycardia. The optimised parameters yielded a mean QRS peak accuracy of 91.20% and a QRS width error of 3.94 ms, markedly superior to the 37.42 ms error obtained with baseline parameters.

The full VT induction protocol of Cedilnik et al. [1] was applied to four patients with sufficient VT recordings. Optimised parameters produced induced VT cycle lengths closer to those observed clinically; notably, VT induction succeeded in patient 003, which had failed with baseline parameters (Table 1).

Table 1. Comparison of VT cycle lengths obtained using optimised and baseline parameters with recorded VT.

Patient	Opt.(ms)	Base.(ms)	Recorded (ms)
001	525 ($\epsilon = 18$)	560 ($\epsilon = 53$)	507
003	350 ($\epsilon = 168$)	n/a	518
004	330 ($\epsilon = 40$)	380 ($\epsilon = 10$)	370
005	395 ($\epsilon = 51$)	580 ($\epsilon = 134$)	446

4. Discussion and Conclusions

We propose a fully automated multimodal optimisation pipeline for electrophysiological models, integrating ECG signals and CT scans. This optimisation not only corrects discrepancies in VT cycle length but also enables VT induction in one test subject that could not be induced using baseline parameters.

5. References

1. Cedilnik N et al. Efficient patient-specific simulations of ventricular tachycardia based on computed tomography-defined wall thickness heterogeneity. JACC Clin Electrophysiol 2023.
2. Hansen N, et al. CMA-ES/pycma: r4.0.0, 2024.

Acknowledgements:
This work has been supported by the French government through the National Research Agency (ANR) 3IA Côte d'Azur, IA Cluster project and IHU LIRYC [ANR-19-3IA-0002, ANR-23-IACL-0001, ANR-10-IAHU-04]; and through the France 2030 and the European Union (Next Generation EU) MediTwin project.

OPTIMIZATION STRATEGIES FOR VENTRICULAR ACTIVATION PERSONALIZATION FROM SURFACE ECG

Guadalupe García-Isla (1), Jorge Sánchez (1), Sandra Perez-Herrero (1), Javier Saiz (1), Gernot Plank (2), Elena Zappon (2)

1. Center for Research and Innovation in Bioengineering (Ci2B), Universitat Politècnica de València, Spain; 2. Division of Biophysics and Medical Physics, Gottfried Schatz Research Center Medical University of Graz, Austria

1. Introduction

Non-invasive personalization of ventricular activation models from surface ECG is a key challenge in cardiac digital twin generation. Most existing approaches focus on optimization of His–Purkinje (HP) root node locations and activation times [1]. However, little attention has been paid to how structuring of the optimization problem influences computational efficiency and solution robustness. This work investigates how different optimization strategies affect the final solution.

2. Materials and Methods

Three global optimization methods (tree-structured Parzen estimator, genetic algorithm (GA), particle swarm optimization (PSO)) and a local finite-difference (FD) refinement strategy were compared for the optimization of the spatial positions and activation times of seven HP root nodes. These methods were assessed both in joint spatio-temporal inference and in sequential pipelines, separating spatial root node localization from final spatio-temporal refinement. Performance was evaluated using RMSE, Pearson's correlation coefficient (CC), and number of forward simulations required to reach best fit across five inference runs per configuration. Simulations were carried out using eikonal-based model coupled to a lead-field ECG formulation [1, 2].

3. Results

Sequential optimization improved convergence efficiency across all optimizers with comparable IQR (Figure 1). Standalone GA (0.161±0.002 RMSE, 96.27±0.56 CC) and hybrid GA+FD strategy (0.168±0.005 RMSE, 94.61±0.41 CC) achieved the highest performance. GA+FD significantly reduced simulation cost compared to fully joint global search, lowering from >2000 to 390±19 simulations to best fit.

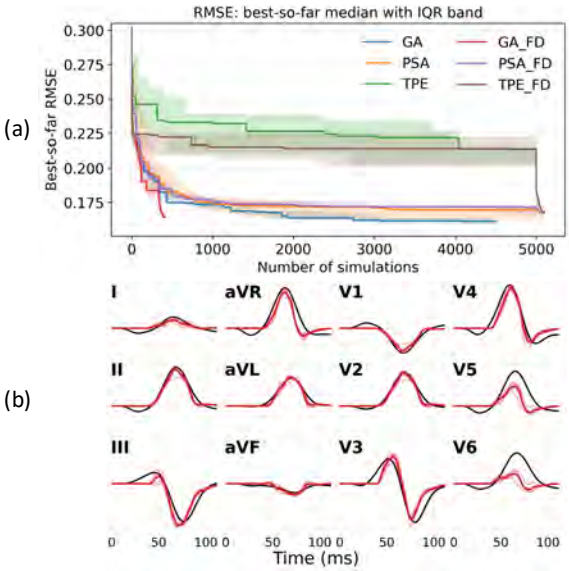


Figure 1: (a) Median and IQR RMSE for five runs for each optimization pipeline. (b) Mean best inference (GA+FD) (red) vs clinical (black) ECG.

4. Discussion and Conclusions

These findings suggest that a hierarchical optimization strategy may aid in cardiac digital twin generation. Beyond optimizer choice, the way the inference problem is structured may influence computational tractability and robustness, with implications for large-cohort studies and in silico clinical trials.

5. References

1. K. Gillette et al., "A Framework for the generation of digital twins of cardiac electrophysiology from clinical 12-leads ECGs," Med. Image Anal., vol. 71, Jul. 2021, 2doi: 10.1016/j.media.2021.102080.
2. S. Pezzuto, et al., "Evaluation of a rapid anisotropic model for ECG simulation," Front. Physiol., vol. 8, no. MAY, May 2017, doi: 10.3389/fphys.2017.00265.

Acknowledgements:
Funded by CIAPOS/2024/033 and co-funded by the European Social Fund Plus (ESF+).

PHYSIOBLOCKS: AN OPENSOURCE PYTHON LIBRARY FOR SIMULATING BLOCK DIAGRAMS OF PHYSIOLOGICAL SYSTEMS

Dominique Chapelle (1,2), Colin Drieu (1,2), François Kimmig (1,2)

1. Inria, France; 2. CMAP, Ecole Polytechnique, CNRS, Institut Polytechnique de Paris, France

1. Introduction

The PhysioBlocks Python library is designed to simulate the dynamics of physiological systems (in particular cardiovascular systems) represented by block diagrams, in order to provide built-in modularity. The library is distributed on GitHub under the LGPL license, and the initial distribution focuses on providing building blocks associated with lumped-parameter models of the cardiovascular system, including the simplified heart model that has been developed at Inria for over a decade [1].

2. Major Principles

The main objects defined and manipulated in the library are the following:

- **Block**: individual modeling module
- **Node**: physical locations where **Blocks** are interconnected and share various physical quantities named **DOFs** (degrees of freedom), and where fluxes coming from connected modules satisfy balance equations (a.k.a. Kirchhoff laws), with one such equation per type of flux present at the node
- **Net**: overall specific system consisting of a set of **Blocks** connected via a set of **Nodes**

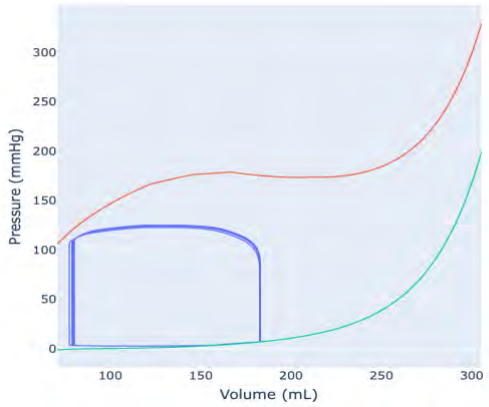
In the cardiovascular system example, **Blocks** represent individual organs or compartments within the system, **DOFs** borne by the nodes are typically blood pressures, and the associated fluxes exchanged are blood flows.

There are three typical user levels:

1. **Configure and run physiological systems simulations.** Here, the user takes a pre-existing **Net**, and has the ability to adjust various parameters before running simulations. The specificity of PhysioBlocks in this regard lies in the concept of *configuration aliases*, by which only the subset of parameters relevant to the user is being directly exposed
2. **Create new systems with existing Blocks.** This is where the modularity paradigm of the library is paramount. Here, the user has the ability to build a new **Net** *without writing any code*, by simply connecting existing **Blocks** via a set of **Nodes**
3. **Write and add new Blocks to the library.** At this advanced level, the user has the ability to devise a new **Block** when needed

3. Typical Results

For a simple cardiovascular system consisting of a single cardiac cavity as modelled in [1] and an arterial tree represented by a double *R-C* Windkessel model, and for time steps of 1ms (with one nonlinear system solved by Newton iterations at each time step) we obtain results in roughly real time on a standard computer (M3 Max MacBook Pro), see simulated P-V loops and generated End-Diastolic / Systolic P-V Relationships in figure.



4. Perspectives

Future distributions will incorporate new blocks, including for models other than that of the cardiovascular system (external contributions are strongly encouraged), and data assimilation features to directly enable digital twin applications.

5. References

1. Caruel M et al., BMMB 13(4):897–914, 12 2013.

Acknowledgements:

The PhysioBlocks library is being developed as part of the MEDITWIN project, funded by the French government (France 2030) and by the European Union (France Relance plan).

MATRIX-FREE ALGORITHMS FOR CARDIAC ELECTROMECHANICAL SIMULATIONS

Andrea Tonini (1), Luca Dede' (1)

1. MOX, Dipartimento di Matematica, Politecnico di Milano, Italy

1. Introduction

Mathematical cardiocirculatory models play a crucial role in cardiology by providing valuable insights into diagnostics and into the effects of cardiovascular diseases. High-fidelity 3D cardiac models require substantial computational resources, as they involve complex interactions among blood flow, tissue mechanics and biochemistry. These resources are typically available in high-performance parallel computing environments. Consequently, effective cardiac simulations require not only physically accurate mathematical models, but also efficient and scalable algorithms and software capable of exploiting modern computing hardware.

2. Materials and Methods

We consider a 3D-0D cardiac electromechanical model composed of several coupled submodels representing the different physical processes occurring in the heart: electrophysiology, active force generation and mechanics [1]. These processes are characterized by distinct spatial and temporal scales, which necessitate a multiscale modeling approach. Accurately capturing the contribution of each physical component requires a sufficiently fine computational mesh, which, together with the model complexity, leads to high computational costs, even when simulations are performed in parallel.

In matrix-based implementations, processors store and communicate portions of the system matrices during the simulation. However, during communication phases, the hardware computational resources are not fully utilized, resulting in increased computational costs. In contrast, matrix-free algorithms avoid explicit matrix assembly by recomputing matrix entries at each iteration, thereby enabling more efficient use of hardware resources and reducing computational time, especially for higher polynomial degrees of the finite element space [2].

3. Results

We investigated the impact of matrix-free algorithms on electromechanical simulations, focusing on their effects on computational efficiency, resource utilization and accuracy. By quantifying these aspects, we provide insights into the advantages and limitations of matrix-free approaches in multiscale and multiphysics cardiac simulations. Strong scalability of the matrix-free approach is observed for a high number of processors, whereas the performance of matrix-based algorithms is hindered by excessive communication overhead.

4. Discussion and Conclusions

Matrix-free algorithms represent a valid alternative to matrix-based approaches in communication-dominated regimes. Thanks to their efficiency in handling high order finite elements, matrix-free algorithms enable accurate solutions on coarser meshes compared to matrix-based implementations.

5. References

1. Fedele M., Piersanti R., Regazzoni F. et al. A comprehensive and biophysically detailed computational model of the whole human heart electromechanics, Computer Methods in Applied Mechanics and Engineering, 410, 115983, 2023.

2. Kronbichler M., Kormann K. A generic interface for parallel cell-based finite element operator application, Computer and Fluids, 63, 135-147, 2012.

Acknowledgements:

The authors acknowledge the project Horizon Europe-JU-RIA dealii-X, 2024-2026, "Dealii-X: an Exascale Framework for Digital Twins of the Human Body" (CORDIS ID: 101172493) for providing financial support to this project.

BINARY OUTPERFORMS MULTI-CLASSIFICATION NEURAL NETWORK MODELS FOR PREDICTION OF OUTCOMES IN PPCM

Juliet Nagawa (1), Kevin L. Sack (1,2), Sarah Kraus (1), Mazin Sirry (3), Ntobeko A.B. Ntusi (1,4), Neil H. Davies (1), Karen Sliwa (1), and Thomas Franz (1,5)

1. University of Cape Town, South Africa; 2. Medtronic Inc., USA; 3. International University Kuwait, Kuwait; 4. SAMRC, South Africa; 5. University of Southampton, United Kingdom.

Corresponding author: Juliet Nagawa, Juliet.Nagawa@uct.ac.za

1. Introduction

While most patients with peripartum cardiomyopathy (PPCM) recover with standard medical therapy, the identification of patients who will not recover remains a challenge [1]. This study aimed to compare the performance of multi-classification and binary classification artificial neural networks (ANN) in predicting PPCM outcomes at 6 months after diagnosis, without and with the left ventricular assist device (LVAD) therapy, which is given to critically ill patients.

2. Materials and Methods

A multi-classification ANN model was developed to predict three PPCM outcomes: recovery, poor outcomes, and mortality. The synthetic minority over-sampling technique was implemented to account for the imbalanced classes in the dataset. Three binary classification ANNs, namely ANN1, ANN2, and ANN3, were developed to predict recovery, poor outcomes, and mortality in PPCM, respectively. All the ANNs were trained with an augmented demographic and cardiac function dataset of 2,502 patients and tested with a dataset of 62 patients with data at diagnosis and 6 months thereafter. Results from patient-specific finite element models for six PPCM patients at diagnosis, without and with LVAD, served as inputs in the ANN models to predict patient outcomes at 6 months. The LVAD support was varied at 8,000, 10,000, and 12,000 revolutions per minute (rpm).

3. Results

The multi-classification model performed poorly (accuracy: 42% and F1 score: 41%) while the binary classification ANN1, ANN2, and ANN3 exhibited high accuracy (91%, 100% and 100%) and F1 scores (89%, 100% and 100%) for predicting recovery, poor outcomes, and mortality, respectively. No mortality was predicted by either the multi-classification or the ANN3 models. The multi-classification ANN predicted recovery for one patient with the 8,000 and 10,000 rpm LVAD and poor outcomes for the other patients for all LVAD conditions.

Without LVAD, ANN1 predicted recovery at 6 months for two patients known to have recovered and two patients known not to have recovered. ANN2 correctly predicted poor outcomes for two patients known not to have recovered. ANN1 predicted recovery for five patients with the 8,000 rpm LVAD and for all patients with the 10,000 and 12,000 rpm LVAD. ANN2 predicted poor outcomes for one patient with the 10,000 rpm LVAD and for none of the patients with the 8,000 and 12,000 rpm LVAD.

4. Discussion and Conclusions

The binary classification ANNs outperformed the multi-classification ANN in predicting outcomes at 6 months in PPCM patients. Multi-collinearity between the outcome variables could have impeded the performance of the multi-classification ANN [2]. Hence, the binary classification ANNs have greater potential to predict PPCM outcomes at 6 months post-diagnosis. Future work will target using larger PPCM datasets for validation and extension of the prognostic period.

5. References

1. Viljoen C, et al. Current Opin. Cardiol. 2023; 38(3): 223-232.
2. Chan, JY et al. Mathematics, 2022. 10(8): 1283.

Acknowledgements:
The authors thank Dassault Systèmes Simulia Living Heart Project, Dr. Leopold und Carmen Ellinger Stiftung, and DAAD-AIMS for financial support.

TOWARD REAL-TIME HEMODYNAMIC EVALUATION OF STENTED INTRACRANIAL ANEURYSMS USING GRAPH NEURAL NETWORKS

V. Lannelongue (1), U. Pelissier (1), P. Garnier (1), C. Faitini (1), P. Meliga (1), E. Hachem (1)

1. Mines Paris, PSL University, Centre for material forming (CEMEF), Sophia Antipolis, France.

vincent.lannelongue@minesparis.psl.eu

1. Introduction

Intracranial aneurysms (IAs) are life-threatening vascular pathologies whose rupture causes subarachnoid hemorrhage with a fatality rate of about 35%. When an aneurysm is deemed at risk, endovascular treatments such as coils or flow-diverter stents are deployed to reduce rupture risk and promote thrombosis and vascular remodeling. Clinical studies report that treatment strategies may change in up to 60% of cases when patient-specific blood-flow simulations support clinical decision making [1]. However, high-fidelity hemodynamic simulations based on computational fluid dynamics (CFD) remain impractical for routine clinical use due to their high computational cost. To address this limitation, fast and reliable prediction of blood-flow dynamics and derived hemodynamic indicators is required. Building on our previous work on physically constrained graph neural networks (GNNs) for aneurysm hemodynamics [2], we propose a transformer-based GNN capable of predicting pulsatile blood-flow dynamics in both untreated and stented aneurysms within clinically compatible time frames.

2. Materials and Methods

We generated a realistic IA dataset by combining patient-specific internal carotid artery geometries with parametrized aneurysm morphologies. High-fidelity blood-flow simulations were computed by solving the three-dimensional incompressible Navier–Stokes equations. A variational multiscale (VMS) formulation ensured accurate flow resolution, while the Carreau–Yasuda model captured the shear-thinning non-Newtonian behavior of blood. Flow-diverter stents were deployed using a clinically validated virtual deployment strategy [3], enabling both treated and untreated configurations for each vascular geometry. This dataset was used to train a transformer-based GNN architecture [4], designed to capture spatial interactions on vascular meshes and model the temporal evolution of pulsatile blood flow.

3. Results

The proposed model achieves near real-time predictions for both treated and untreated aneurysm geometries, reducing computational time from more than 20 hours required by traditional CFD simulations to approximately one minute using our framework. Model accuracy is evaluated on velocity fields and clinically relevant hemodynamic indicators such as wall shear stress (WSS). In addition, the model is tested on patient-specific geometries outside the distribution of the training dataset to assess its generalization capabilities.

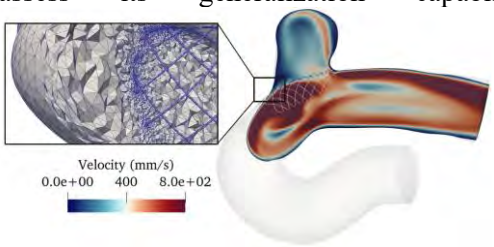


Figure 1: GNN blood flow prediction in stented intracranial aneurysm.

4. Discussion and Conclusions

Pre-operative evaluation of flow-diverter treatment strategies is a critical component of personalized intracranial aneurysm care. Our results demonstrate that data-driven surrogate modelling can provide high-fidelity hemodynamic predictions in clinically compatible time frames, opening the possibility of integrating patient-specific blood-flow analysis directly into clinical workflows. This work therefore represents a step toward real-time digital twins for treatment planning in intracranial aneurysms.

5. References

1. Chong, B. W. et al., AJNR; 2019, 40(10)
3. Lannelongue, V. et al., NPJ Digital Medicine; 2026.
3. Jeken-Rico, P. et al., Computer in Biology and Medicine; 2024.
4. Garnier, P et al., NCAA; 2026.

Acknowledgements:

The authors would like to thank the European Research Council for providing financial support to this project (CURE, 101045042).

AN IN SILICO PLATFORM FOR OPTIMIZING STROKE TREATMENT DEVICES

Janneke Cruts (1), Thijs Kuipers (1,2), Kenia Lopez (1), Mahsa Mojtahedi (1), Martijn Oetelmans (1), Henk Marquering (1,2), Thomas Kerbusch (1)

1. inSteps B.V., the Netherlands; 2. Amsterdam UMC, the Netherlands

1. Introduction

Acute ischemic stroke (AIS), a leading cause of death worldwide, results from occlusion of a cerebral artery by a lodged blood clot. Mechanical thrombectomy, a clot removal procedure, is the standard of care for large-vessel occlusions. Although clinical trials remain the gold standard for validating new therapies, they are costly and time-consuming. We aim to accelerate device development and improve trial efficiency for AIS with the use of in silico modeling.

2. Materials and Methods

We present a novel in silico modeling platform that automatically integrates finite element method (FEM) simulations with AI-based geometric generation. Cerebral vascular anatomies and thrombus morphologies, capturing realistic patient-specific variability, are generated using state-of-the-art generative models [1]. The resulting geometries are incorporated into a FEM simulation of the complete thrombectomy procedure, performed in Abaqus/Explicit 2025. The clot is modeled as a hyper-elastic material with stress-based damage (failure threshold: 0.23 MPa), the stent-retriever as superelastic nitinol, the catheter as deformable linear elastic, and the vessel as rigid linear elastic [2]. A friction coefficient of 0.2 is applied for clot-vessel and clot-stent interfaces. A key novelty of the FEM model is the physiologic simulation of clot lodging prior to thrombectomy, by applying a proximal pressure of 30 mmHg to the clot.

3. Results

Figure 1 presents a set of AI-generated synthetic vessels (Fig. 1A) and a representative FEM thrombectomy simulation in one of the synthetic vessels (Fig. 1B-C), demonstrating successful clot retrieval. The approach was applied across multiple geometries, ranging from simplified tubes to a cohort of synthetic vessels. The FEM simulations required approximately 12 hours of computational time on an AMD Ryzen 9 16-core Processor.

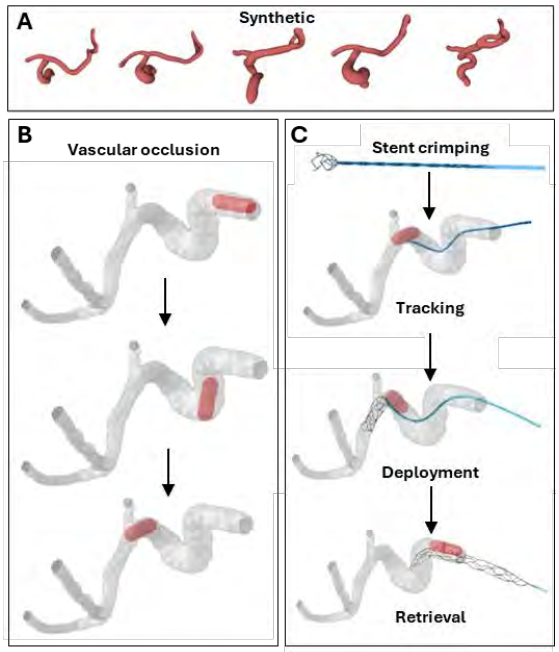


Figure 1: In silico platform results: (A) generated synthetic vessels, (B) FEM clot lodging, and (C) FEM thrombectomy in a synthetic vessel.

4. Discussion and Conclusions

The platform successfully integrates automated synthetic vessel and clot generation with thrombectomy simulations, incorporating physiological clot pressure, and realistic clot-catheter interaction and stent-retrieval forces. This framework enables rapid stent design evaluation and could accelerate clinical translation of stroke therapies. Future work will focus on incorporating clinically relevant clot phenotypes, model validation, and acceleration of the FEM simulations.

5. References

1. Kuipers TP et al. Medical Imaging with Deep Learning. (2024)
2. Fregona V et al. J. Mech. Behav. Biomed. Mater, 163, 106886 (2025).

ON THE INFLUENCE OF THE LARYNX IN THE ADMINISTRATION OF INHALED MEDICATIONS

Mauro Malvè (1,*), Carmen Sánchez-Matás (2), José Luis López-Villalobos (3), Rocío Fernández-Parra (4)

1. Universidad Pública de Navarra (Instituto INAMAT²), Spain; 2. Hospital Universitario 'Virgen de la Arrixaca', Spain; 3. Hospital Universitario 'Virgen del Rocío', Spain; 4. Hospital Veterinario UCV, Universidad Católica de Valencia San Vicente Mártir, Spain

** Corresponding author: Mauro Malvè, Universidad Pública de Navarra, mauro.malve@unavarra.es*

1. Introduction

The interaction between flow conditions and anatomical configuration is critical for effective drug deposition, as even small geometric variations can markedly affect aerosol trajectories [1]. Previous studies emphasize the influence of anatomical realism, including patient-specific features, on flow behavior [2]. In this context, interindividual variability in laryngotracheal morphology, particularly the larynx–trachea angle, can significantly alter flow structures and aerosol transport. The present work aims to evaluate the impact of geometric variations on inspiratory flow and inhaled drug deposition.

2. Materials and Methods

Figure 1 shows the three geometries considered: (A) a planar, symmetric Weibel airway; (B) a planar, asymmetric 'typical-path lung model' [3]; and (C) a realistic, non-planar, asymmetric airway. Airflow (60 L/min) was modelled as turbulent, and the transport of aerosols was simulated using particles with diameters ranging from 1 to 10 µm, using Ansys CFX.

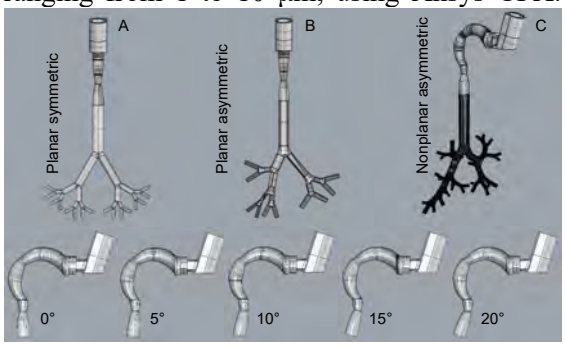


Figure 1: Geometrical models and variations in the laryngotracheal angle considered in the study.

3. Results

Variations in the laryngotracheal angle induce changes in flow structure, which enhances inertial particle deposition. For 1 µm particles, planar models show low deposition, whereas nonplanar geometry yields near-total deposition for zero angle geometry (see Figure 2). In contrast, 10 µm particles exhibit substantially higher deposition, reaching up to 85%, particularly in distal branches.

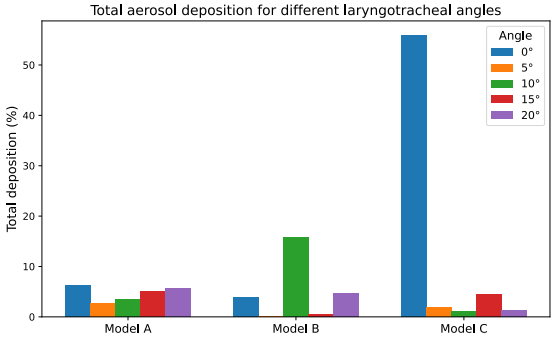


Figure 2: Total deposition fraction for different laryngotracheal angles and particle of 1 µm.

4. Discussion and Conclusions

Variations in the larynx–trachea angle alter jet orientation, pressure losses, and inertial impaction, leading to significant differences in particle transport. Fine-particle deposition depends on geometric complexity and inlet conditions, whereas larger particles are mainly governed by inertial mechanisms [1]. These results highlight the limitations of simplified models and the importance of realistic geometries when evaluating inhaled drug delivery.

5. References

1. Zhang Z, Kleinstreuer C, J. Comput. Phys; 198(1):178-210 (2004).
2. Van Ertbruggen C et al., J. Appl. Physiol.; 98(3):970-980 (2005).
3. Huang J et al., Particuology; 9:39-43 (2011).

Acknowledgements:

This study was funded by grants PID2021-125731OB-C31 and PID2021-125731OB-C33 from the Ministry of Science and Innovation (MCIN/AEI/10.13039/501100011033) and FEDER ("A way to build Europe").

AI–MECHANISTIC FRAMEWORK FOR SYNERGISTIC DRUG REPURPOSING AND PRECLINICAL DOSE-RATIO OPTIMIZATION

G. Brachet[1], A. Alioui[1], G. Arbia[1], N. Mackenzie[1], D. Baron[1], M. Murray[1]
[1]CXS Therapeutics, 16B rue de la République, 37230 Fondettes, France.
The order of authors does not reflect the relative contribution to this work.

1. Introduction

Repurposed drug combinations offer a pragmatic route to multi-target intervention in neurodegeneration, but preclinical decision is hindered by limited model translatability and by AI (artifical intelligence) methods that are often black-box and weakly grounded in physiology. We present a hybrid, traceable framework that couples knowledge graphs, explainable AI and mechanistic modelling to identify synergistic combinations and optimise dose/ratio selection for preclinical studies[1,2].

2. Materials and Methods

We have developed a hybrid computational framework combining mechanistic physiological modeling and explainable AI to support the preclinical optimization of drug combinations. This approach integrates structured biomedical literature, annotations related to drugs, targets, and metabolic pathways, as well as experimental preclinical datasets into disease-specific biological networks. We formulate combination selection as an inverse problem. For candidate molecules A and B, the synergy in modelled as S = nA + mB with n,m > 0. We then estimate (A,B,n,m) by minimising, accross targets k, the distance between predicted response y'_k(S) and a desired target y_k^{target}, using weighted multi-marker optimisation.

The mechanistic components rely on mathematical representations of key biological processes and exposure-response relationships, while machine learning modules are used to evaluate drug combinations, explore dose-ratio spaces, and prioritize experimental conditions. This hybrid architecture preserves biological traceability by explicitly linking model parameters to measurable pathways, targets, and experimental endpoints. Mechanistic modules implement ODE-based to simulate exposure–response and pathway modulation, enabling sensitivity/uncertainty analysis [1,3,4].

3. Results

This framework was applied to a neuro-degenerative disease use case and supported the identification of synergistic drug combinations. Using integrated biological networks and AI–based scoring, the approach enabled the identification of a candidate combination (CXS003) targeting complementary pathways involved in neurodegeneration. Proof-of-concept studies performed *in vitro* and *in vivo* confirmed the candidate efficacy. In Parkinson cellular models, CXS003 demonstrated neuroprotective effects, while *in vivo* experiments in parkinsonian models showed both preservation of neuronal function behavioral outcomes.

4. Discussion and Conclusions

This work illustrates how a hybrid AI–mechanistic framework can support model-informed decision-making in preclinical neuroscience. The approach enabled the rational identification of a synergistic drug combination, subsequently supported by *in vitro* and *in vivo* proof-of-concept studies demonstrating neuroprotective and behavioral effects in parkinsonian models. Ongoing developments focus on *in silico* dose optimization to refine subsequent *in vivo* experiments, improve translational robustness, and reduce experimental uncertainty[5].

5. References

1. Viceconti M, Hunter P. The Virtual Physiological Human:. Annu Rev Biomed Eng. 2016/
2.Qadri YA et al. Explainable AI: A Perspective on Drug Discovery. Pharmaceutics. 2025.
3.Roberts P et al. A humanized clinically calibrated quantitative systems pharmacology model for hypokinetic motor symptoms in Parkinson's disease. Front Pharmacol. 2016.
4. Ivanova O, Karelina T. Quantitative systems pharmacology model of α-synuclein pathology in Parkinson's disease-like mouse for investigation of passive immunotherapy mechanisms. CPT Pharmacometrics Syst Pharmacol. 2024.
5.Marshall LJ et al. Poor Translatability of Biomedical Research Using Animals - A Narrative Review. Altern Lab Anim. 2023;51(2):102-135.

Acknowledgements:
The authors thank France Parkinson and France 2030 for their financial/scientific contributions.

GRAPH NEURAL NETWORKS FOR MULTIPHYSICS LEARNING OF THROMBOSIS FORMATION IN INTRACRANIAL ANEURYSMS

Ugo Pelissier (1), Valentine Sterlin (1), Philippe Meliga (1), Elie Hachem (1)

1. Computing and Fluids Research Group (CFL), Center for Material Forming (CEMEF), Mines Paris

1. Introduction

Intracranial Aneurysms (IAs) are pathological dilations of cerebral arteries that affect 3-5\% of the population [1]. Their rupture can lead to a subarachnoid haemorrhage. Computational Fluid Dynamics (CFD) can provide detailed insights into the complex flow patterns within IAs, helping clinicians to better understand the nature of the risk. Coupled with a thrombus formation model, CFD could assess the likelihood of complete aneurysm occlusion following endovascular treatment.

Reducing the computational cost of CFD simulations is an active area of research. Adaptive mesh refinement techniques can significantly reduce the number of mesh elements required to accurately capture the flow dynamics and thrombus formation within IAs [2]. Even with these advancements, the computational demands of CFD remain a barrier to their widespread clinical adoption.

2. Materials and Methods

Graph Neural Networks (GNNs) have emerged as a powerful framework for learning on unstructured meshes used in CFD simulations. With a Message Passing (MPS) architecture, GNNs can operate directly on mesh-based simulations, making them well-suited for applications in fluid dynamics. At the same time, Transformers have shown remarkable results in various domains, including natural language processing and computer vision and have been applied for learning on physical simulations as well. State-of-the-art (SOTA) Transformer-based GNN architecture proposed by Garnier et al. [3] has proven to outperform traditional MPS architecture by 20% with a similar number of parameters and being four times faster to train.

3. Results

In this study, we investigate the potential of this Transformer-based GNN architecture to predict thrombus formation within IAs. The challenge relies on the multi physics nature of the problem, which involves coupling between fluid dynamics, platelet transport, and biochemical reactions. To the best of our knowledge, previous works on learning multi physics simulations with GNNs have been limited to MPS architectures, working either with a limited number of nodes on standard datasets or with greater number of nodes but with a single graph. Here, we demonstrate the ability of the Transformer-based GNN to learn on a complex dataset of patient-specific IA geometries, performing SOTA results in terms of accuracy and computational cost. We provide valuable information on the training process and the impact of predicting multiple physical fields simultaneously.

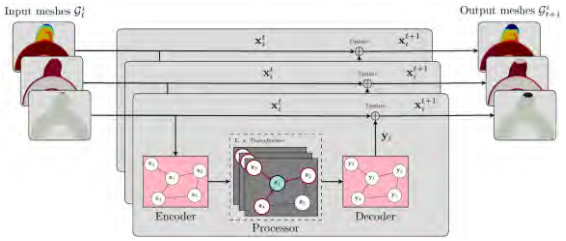


Figure 1. General workflow of the proposed approach for a single-step prediction. A GNN encoder processes the mesh features, followed by multiple Transformer blocks as a processor, before decoding to physical outputs and updating the previous mesh.

4. Discussion and Conclusions

The model exhibited a robust behaviour to variations of inflow boundary conditions and was able to generalize to a greater number of cardiac cycles than those seen during training. This robustness is crucial for clinical applications, where patient-specific conditions can vary significantly.

5. References

1. M. Vlak et al. Prevalence of unruptured intracranial aneurysms, with emphasis on sex, age, comorbidity, country, and time period : a systematic review and meta-analysis. The Lancet Neurology, 10(7) :626–636, July 2011.

2. U. Pelissieret al. A Continuum Approach with Adaptive Mesh Refinement for Platelet Plug Formation. International Journal for Numerical Methods in Biomedical Engineering, 41 (7). July 2025.

3. P. Garnier,et al. MeshMask: Physics-Based Simulations with Masked Graph Neural Networks. International Conference on Learning Representations. 2025.

Acknowledgements:

This project has received funding from the European Union (ERC, CURE, 101045042).

BAYESIAN OPTIMIZATION FOR COMPUTATIONAL DESIGN OF OCULAR DRUG DELIVERY SYSTEMS

Eduardo A. Chacin Ruiz (1), Katelyn E. Swindle-Reilly (2), Ashlee N. Ford Versypt (1)

1. University at Buffalo, The State University of New York, United States of America; 2. The Ohio State University, United States of America

1. Introduction

Chronic retinal diseases rely on intravitreal therapeutic delivery. Implantable controlled release drug delivery systems (DDSs) have been developed to reduce the frequency of dosing. We have previously developed a mechanistic computational model [1] for ocular drug delivery systems based on experimental data [2]. This mechanistic model uses the finite element method in COMSOL Multiphysics to solve partial differential equations for ocular therapeutic drug diffusion through two annular polymer layers surrounding a drug-loaded core in cylindrical DDSs. Here, we focus on a Bayesian optimization (BO) approach to optimize the design of such DDSs in tandem with a Gaussian process (GP) surrogate of the mechanistic model.

2. Materials and Methods

The two design variables of the DDSs are the thickness of the polymeric annulus and the fraction of polymer 1 (polycaprolactone, PCL). We used Latin hypercube sampling (LHS) to run the mechanistic model for 10 combinations of the design variables. This yielded the cumulative release percentage and the drug release rate over time. The optimization objective is to maximize the time the release rate is above a therapeutic threshold. We call the time that the release rate crosses the threshold (and thus the maximum value for a given design) as "t_cross_days''. Using the values of t_cross_days that resulted from LHS, we trained a surrogate model using GP regression. For BO, we used an acquisition function (expected improvement) to identify the next combination of design variables to sample that would either explore the design space where there was substantial uncertainty in the GP surrogate model or exploit the design space to suggest the most likely optimal design based on the current surrogate model. Then the selected sample of design variables was passed to the mechanistic model. The resulting t_cross_days value used to update the GP surrogate model for the first BO iteration. The process was repeated.

3. Results

BO took 10 iterations to converge to a device design (not on the design space boundaries) that varied within a tolerance of 5 days, yielding an optimal release time of 225 days from an implant smaller than a grain of rice.

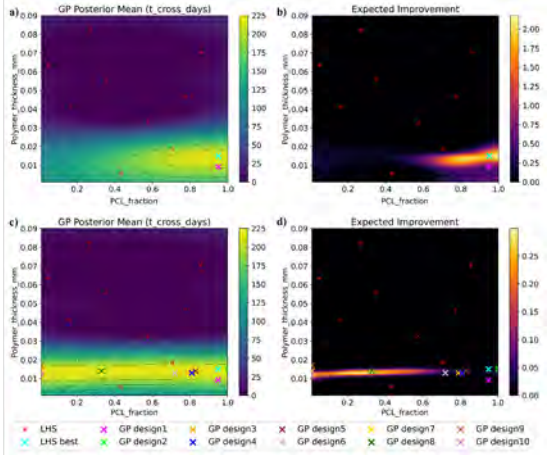


Figure 1: BO for the polymer thickness and PCL fraction to maximize the time that a drug delivery system maintains the release rate over a threshold (t_cross_days). a,b) first iteration and c,d) after 10 iterations. a,c) GP posterior mean and b,d) expected improvement contour maps across the design space of polymer thickness and PCL fraction.

4. Discussion and Conclusions

BO was more efficient than our naïve implementation of user-selected combinations of design variables via the mechanistic model alone. BO is outside the scope of optimization tools currently packaged with COMSOL software for the mechanistic model.

5. References

1. Chacin Ruiz EA, et al., bioRxiv; 2025.12.29.696951 (2025).
2. Jiang P, et al., J Controlled Release; 320: 442-456 (2020).

Acknowledgements:
This work was supported by National Institutes of Health grant R01EB032870 to KESR and ANFV.

CREDIBILITY ASSESSMENT OF DATA-DRIVEN PREDICTORS: APPLICATION TO SURROGATE MODELLING

Antonino Amedeo La Mattina (1), Alessandra Aldieri (2), Serena Moscato (3), Valerio Antonio Arcobelli (3), Sabato Mellone (3), Marco Viceconti (2)

1. Medical Technology Lab, IRCCS Istituto Ortopedico Rizzoli, Italy; 2. Department of Industrial Engineering, Alma Mater Studiorum – University of Bologna, Italy; 3. Department of Electrical, Electronic and Information Engineering, Alma Mater Studiorum – University of Bologna, Italy

1. Introduction

The recent advances in machine learning are pushing the adoption of data-driven models into clinical practice. Unlike biophysical models, for which a risk-based verification, validation and uncertainty quantification (VV&UQ) strategy has been clearly codified [1], such guidelines are still missing for data-driven models. The aim of this work is to present a practical example of the adaptation of the VV&UQ process to a data-driven predictor [2]; in particular, we will focus on a deterministic surrogate model with multiple scalar inputs and a single scalar output.

2. Formalization

Such predictor can be formalised as a function that links an n-dimensional input space $\mathcal{I}$ to a 1-dimensional output space $\mathcal{O}$.

Having no assumptions about the model function regularity, it must be explicitly tested that the model behaves consistently across its entire input space $\mathcal{I}$. Specifically, existence, uniqueness, and smoothness must be checked.

3. Validation

For a data-driven model, the validation is intrinsically entangled with the training process, as this is an optimization of the model (hyper)parameters so that a chosen error metric (*e.g.*, root mean square error on the test dataset) is minimised. The best-fitting model defines the optimal model form (*e.g.*, random forest) and hyperparameter values (*e.g.*, tree number, depth).

4. Verification

To limit biases and to adopt a more conservative approach, verification is conducted on a new dataset D created by uniform sampling of the input space $\mathcal{I}$.

Existence is tested by checking that all the outputs of the model on the dataset D are inside the admissible output space $\mathcal{O}$.

Uniqueness for deterministic models should be checked by software quality assurance.

Lipschitz continuity is checked as a proxy for smoothness [3]: the model is required to have limited sensitivity to each of the input parameters in the neighbourhood of the sample points in the dataset D.

Convergence of the parameter values is tested by repeated trainings of the optimal formal model (*e.g.*, random forest with a certain tree number and depth) with an increasing number of rows of the training dataset and checking the outputs of this "reduced model" on the dataset D. When these outputs are stably close to the corresponding outputs of the optimal model, convergence is achieved; the number of rows needed for convergence (K) is recorded.

Numerical error is then evaluated by repeatedly training the optimal formal model with different sets of K rows from the training set and collecting its outputs on the dataset D. The standard deviation of the output for each sample point is the numerical error.

5. Current work and future development

We are currently working on a Python library for the automation of the VV&UQ process of data-driven predictors, given a simple YAML configuration file. The library will be uploaded on PyPI and integrated in an automated MLOps workflow.

6. References

1. ASME V&V 40-2018 (2018).
2. Viceconti *et al.*, IEEE J Biomed Health Inform; 29(7):5284-5290 (2025).
3. Curreli *et al.*, Int J Numer Methods Biomed Eng; 37(7):e3470 (2021).

Acknowledgements

This work was partially supported by grants METASTRA (HORIZON, number 101080135) from the European Commission, and by the Italian Complementary National Plan PNC-I.1, "DARE - DigitAl lifelong pRevEntion" initiative, code PNC0000002.

A MORPHING-BASED FRAMEWORK FOR PERSONALIZED UTERINE ANATOMICAL MODELING

Nuno Miguel Ferreira (1), António Ramos Silva (1), Marco Parente (1), Sofia Brandão (2), Elisabete Silva (1)

1. *LAETA/INEGI, Faculty of Engineering of the University of Porto, Portugal*
2. *CESPU, H2M Polytechnic University of Health, CESPU, Vila nova de Famalicão*

1. Introduction

Accurate representation of anatomical variability is a fundamental requirement in computational biomechanics of the female pelvic cavity. Finite element analysis has been widely used to investigate load transfer mechanisms and organ support; however, most computational studies rely on generic anatomical geometries [1]. The generation of patient-specific models remains limited by the time-consuming and labor-intensive processes. Morphing techniques offer a promising alternative by enabling controlled geometric adaptation of validated baseline models while preserving mesh topology and numerical stability. When driven by quantitative anatomical measurements derived from magnetic resonance imaging (MRI), such approaches can provide an efficient pathway toward individualized modeling [2]. This study aims to develop and validate a morphing-based framework driven by MRI-derived anatomical measurements to generate patient-specific uterine geometries.

2. Materials and Methods

A previously validated 3D pelvic finite element model served as the framework. The uterus geometry was reconstructed from anatomical literature data and used as the baseline for comparison with morphed uterus models. Physiological loading was simulated by applying a 4 kPa intra-abdominal pressure (Valsalva maneuver).

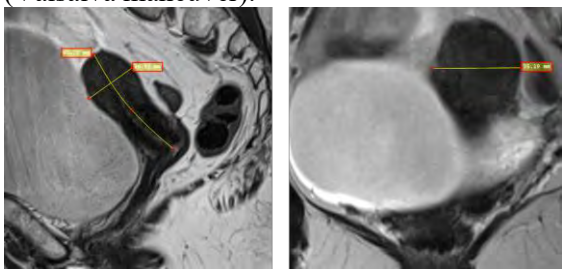


Figure 1: MRI image with the anatomical measurements of uterus.

A parameterized CAD model of the non-pregnant uterus and cervix was defined from MRI-derived anatomical measurements, Figure 1. Volumetric morphing was implemented using Radial Basis Function interpolation with a Thin-Plate Spline kernel, enabling controlled geometric adaptation while preserving mesh.

3. Results

The morphing framework successfully reproduced the global uterine morphology derived from MRI segmentation while preserving mesh topology and connectivity. No mesh distortion or numerical instability was observed, Figure 2.

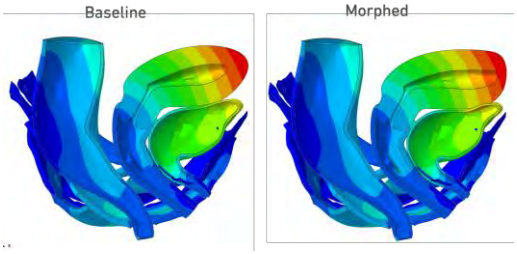


Figure 2: Comparation of displacement magnitude across baseline and morphed uterine geometries.

4. Discussion and Conclusions

The proposed validation strategy demonstrates that RBF-based morphing can accurately reproduce MRI-derived uterine anatomy while maintaining mechanical fidelity under physiological loading. By avoiding complete remeshing and repeated segmentation workflows, the method significantly reduces preprocessing effort while preserving biomechanical reliability.

5. References

1. N. M. Ferreira et al., Int. J. Numer. Method. Biomed. Eng., vol. 41, no. 11, Nov. 2025.
2. Y. Bazilevs et al., Comput. Methods Appl. Mech. Eng., vol. 199, no. 5–8, pp. 229–263, Jan. 2010.

Acknowledgements: The authors gratefully acknowledge funding from FCT PhD grant 2024.00925.BD, and to LAETA via the project UID/50022/2025.

TOWARDS A CORNEAL DIGITAL TWIN: EXPERIMENTAL VALIDATION OF A BIOMECHANICAL MODEL OF CORNEAL DEFORMATION

Elena Redaelli (1), Judith Birkenfeld (1)

1. The Spanish National Research Council, Madrid, Spain

1. Introduction

Understanding corneal biomechanics is essential for improving the diagnosis of ectatic disorders [1], optimizing refractive surgery, and refining intraocular pressure (IOP) assessment [2]. Air-puff tonometry provides rich spatio-temporal deformation data, yet translating these measurements into predictive biomechanical models remains challenging. Despite numerous models of corneal air-puff deformation reported in the literature [3], comprehensive validation against experimental or clinical data remains lacking, limiting their credibility and translational relevance. This study proposes a validation framework for a comptational model serving as as a base for the development of a corneal digital twin.

2. Materials and Methods

Air-puff-induced corneal deformation was reproduced ex vivo in porcine globes within 48h postmortem following the experimental setup described in [4]. A collimated air puff was applied to the corneal apex while the dynamic deformation of the anterior corneal surface was recorded using optical coherence tomography. The IOP was set to 15 mmHg by adjusting the height of a saline column connected via a syringe. Uniaxial tensile tests were conducted on corneal strips immediately following the air-puff measurements to characterize the tissue's mechanical response. A 3D finite element model of the cornea was developed, incorporating the physiological pre-stress induced by IOP. The corneal tissue was modeled using the Holzapfel–Gasser–Ogden model. The experimentally applied air-puff loading conditions were reproduced in the simulation to generate the predicted corneal deformation response.

3. Results

Model validation focused on the temporal evolution of the apex vertical displacement. The RMSE between simulated and experimental displacement signals was 0.11 mm (8.8%), indicating a strong overall correspondence between the two curves. The maximum displacement error was 0.018 mm, demonstrating the model's ability to accurately reproduce the peak deformation amplitude. Global deformation behavior was further evaluated through the area under the displacement–time curve, which yielded to a relative difference of -1.71%.

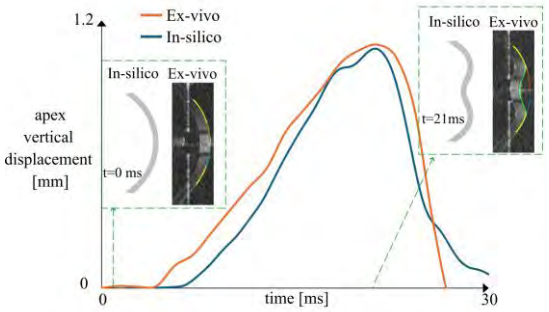


Figure 1: Temporal displacement of the corneal apex during the air puff in the ex-vivo case (in orange) and in the in silico case (in blue).

4. Discussion and Conclusions

The agreement observed in apex displacement dynamics and quantitative validation metrics supports the ability of the model to reproduce the essential features of air-puff–induced deformation. This validation strategy represents a step toward the development of a corneal digital twin.

References:

1. Rahmati SM et al., J. Mech. Behav. Biomed. Mater. 113; 104155 (2020).
2. Simonini I et al., J. Mech. Behav. Biomed. Mater. 58; 75-89 (2015).
3. Redaelli E et al., Front. Bioeng. Biotechnol. 10, 1-12 (2022).
4. Bronte Ciriza D et al., Biomed. Opt. Express. 12 (10), 6341 (2021).

Acknowledgements:

This project has received funding from from the Spanish "Ministerio de Ciencia, Innovación y Universidades" (Grant RYC2022-037910-I, 202445AT005, FULBR24029, ILINK25057).

ISO RECOMMENDATIONS AND REQUIREMENTS FOR PREDICTIVE COMPUTATIONAL MODELS IN PERSONALISED MEDICINE

Martin Golebiewski* (1), Laura Lopez-Perez (2), Elena Martinelli (3), Tito Poli (3)

1. HITS gGmbH, Heidelberg, Germany; 2. Universidad Politécnica de Madrid, Spain; 3. Department of Medicine and Surgery, University Hospital of Parma, Italy.

* martin.golebiewski@h-its.org; HITS gGmbH, Schloss-Wolfsbrunnenweg 35, 69118 Heidelberg, Germany

1. Introduction

Many different types of human data are used to set up computational models and Virtual Human Twins (VHTs) for simulations and predictions, e.g. for in silico clinical trials, disease prognosis, treatment predictions or patient stratification. These data need to be interoperable to integrate them into the models or use them for model validation. To achieve this, standards are crucial for structuring, describing, and associating models and data, as well as their respective parts, graphical visualization, and applied methods. Such standards also assist with describing how components interact together, or are linked, and how they are embedded in their context.

2. Materials and Methods

The ISO committee ISO/TC 276/WG 5 Data Processing and Integration has released several standards that provide recommendations and requirements for in silico modelling in the field of personalized medicine.

3. Results

ISO 20691:2022 [1] provides a framework for the development and application of domain-specific and interoperable (meta-)data standards in the life sciences. It defines requirements and rules for the application of standards for formatting, description, and documentation of data, as well as for the design of data formats for many different life science domains and of terminologies for semantic description.

The standard series ISO 9491 provides a guideline with specific recommendations and requirements for predictive computational models in personalized medicine research. It has two parts, the first ISO 9491-1 "Guidelines for constructing, verifying, and validating models" [2] has been published as ISO technical specification in 2023 and recently revised and transformed into an ISO international standard. It gives recommendations and requirements for data preparation, integrating data into models, model formatting, validation, simulation, storing, sharing and application in clinical trials as well as ethical requirements for modelling. The annex lists specific community standards and widely used modelling approaches for in silico approaches in personalized medicine. The second part of ISO 9491 provides guidelines for implementing computational models in clinical integrated decision support systems (ISO/TS 9491-2) and contains recommendations for computational models and their application in the clinical research context [3].

To complement these activities, a new joint working group is currently formed between the ISO/TC 276 Biotechnology and IEC/TC 62, the IEC technical committee developing standards for medical equipment, software, and systems, to address the standardization of the credibility of computational modelling used in medical devices. The group addresses the verification, validation, and uncertainty quantification of models. This work will build on the national US standard ASME V&V 40:2018 for assessing the quality and model credibility of medical devices [4] and extend it to an international standard.

4. Discussion and Conclusions

These ISO standards will support the modelling and data integration processes, rendering the models and their results more reliable.

5. References

1. https://www.iso.org/standard/68848.html
2. https://www.iso.org/standard/83516.html
3. https://www.iso.org/standard/87403.html
4. ISBN: 9780791872048

Acknowledgements:

We gratefully acknowledge funding from the European Commission under grant agreements no. 825843 and no. 101083771, as well as from the Klaus Tschira Foundation (KTS).

ASSESSING THE ROBUSTNESS OF RETINAL VASCULAR GRAPH COMPLETION FOR DIGITAL TWIN HAEMODYNAMIC MODELLING

Emmeline Brown (1,2), Vedika Bedi (1), Pradeep Keshavanarayana (1), Ranjan Rajendram (2,3), Simon Walker-Samuel (1)

1. Centre for Computational Medicine, UCL United Kingdom; 2. Moorfields Eye Hospital, United Kingdom; 3. Institute of Ophthalmology, UCL, United Kingdom

Emmeline.brown@ucl.ac.uk

1. Introduction

Retinal blood flow modelling requires complete vascular networks, yet segmentations often contain discontinuities. We present a semi-automated pipeline to refine artery–vein retinal spatial graphs, incorporating a graph neural network to infer vessel connectivity and support scalable digital twin modelling.

2. Materials and Methods

85 retinal photographs with artery–vein segmentations were converted to spatial graphs using the Pymira toolkit [1]. Networks were semi-automatically edited to create single-inlet, single-outlet topologies, with connectivity interpolated where gaps existed. Although retinal vascular networks are physiologically fully connected and required for flow modelling, this is not always reflected in segmentation datasets. A graph autoencoder was trained to reconstruct connectivity from synthetically degraded graphs with edge dropout levels of p = 0.1–0.5 over 50 epochs.

3. Results

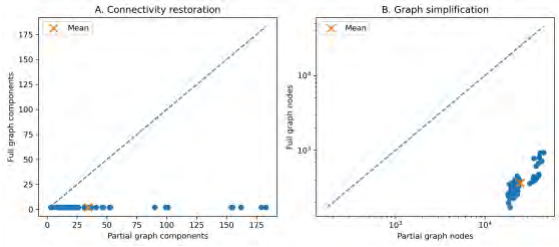


Figure 1: Manual correction of vascular graphs restores connectivity and reduces graph complexity

Segmentation-derived graphs were highly fragmented, with a mean of 34.4 connected components and ~25,051 nodes per image. After manual correction, graphs were simplified and topologically consistent, with ~365 nodes and two connected components representing arterial and venous trees (~98.5% reduction) (Figure 1).

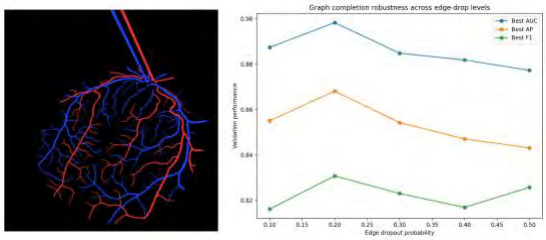


Figure 2: Left: Spatial graph derived from vessel segmentation. **Right:** Reconstruction performance across edge dropout levels

A graph neural network trained to reconstruct connectivity from synthetically degraded graphs (edge dropout 0.1–0.5) showed stable performance across conditions (recall 0.98–0.99, precision 0.69–0.72, F1 ≈ 0.81–0.83, AUC ≈ 0.88–0.90) (Figure 2). Performance was comparable between arterial and venuous graphs, indicating robustness of the approach across vessel types.

4. Discussion and Conclusions

The resulting artery–vein spatial graphs provide a basis for vascular flow modelling. The graph neural network learned structural and geometric features, facilitating downstream modelling.

5. References

1. Brown EE, Guy AA, Holroyd NA, *et al.* Physics-informed deep generative learning for quantitative assessment of the retina. Nature Communications. 2024;15:6859.

Acknowledgements:
SWS would like to acknowledge funding from Cancer Research UK ((28276 and C44767/A29458)) 475 and EPSRC ((EP/W007096/1)).

12 LABOURS DIGITAL-TWINS PLATFORM: ENABLING VALIDATION AND CLINICAL TRANSLATION OF VIRTUAL HUMAN TWINS

Thiranja Babarenda Gamage (1), Chinchien Lin (1), Linkun Gao (1), Ayah Elsayed (1), Jiali Xu (1), Gregory Sands (1), Koray Atalag (1), Martin Golebiewski (2), Xiaoming Hu (2), Jun Huh (1), Claire Rye, (1), Carvin (Rui) Chen (1), Matt Pestle (1), Nick Jones (1), Cheng-kai Jin (3), Robyn Whittaker (3), Anthony Doyle (1,3), Martyn Nash (1), Peter Hunter (1), Merryn Tawhai (1), David Nickerson (1)

1. University of Auckland, New Zealand, 2. Heidelberg Institute of Theoretical Studies, Germany; 3. Health New Zealand – Te Whatu Ora, New Zealand

1. Introduction

Personalised, physics-driven "digital twin" models of human anatomy and physiology can revolutionise healthcare, especially with continuous home-based monitoring from wearable or implantable devices. Integrating global advancements in computational modelling at various biological levels can create a "Virtual Human Twin" (VHT) to enhance our understanding of human physiology and diseases. The DigitalTWINS platform developed by the Auckland Bioengineering Institute's 12 Labours project aims to provide infrastructure for creating personalised digital twins and supporting clinical studies to validate their application in research and clinical environments.

2. Materials and Methods

The platform (Figure 1) leverages current international tools and best practices in ethics, safety, and FAIR data management, including from EDITH, SPARC, SEEK, and NFDI4Health. To support traceability and reproducibility, all data is stored using the FAIR-compliant SPARC Dataset Structure (SDS), with computational tools and workflows standardised using the Common Workflow Language (CWL) and executed via Apache AirFlow. Access is provided through both a user portal and an API. The platform's FHIR-based data model provides complete provenance for all models, measurements, and tools, with results accessible via GUI tools in workflows that can be dynamically integrated with the platform's portal. Furthermore, the Investigation-Study-Assay (ISA) standard is adopted to describe research or clinical studies, which can be managed and executed via a dashboard on the portal, further accelerating the path from research to clinical application.



Figure 1: Platform overview (see pdf version).

3. Results

We present our latest efforts in using this platform within: 1) research environments for verifying & validating workflows in accordance with ASME V&V40 principles (including applications in pulmonary hypertension [1], upper limb rehabilitation, and monitoring of uterine function); and 2) clinical environments for demonstrating efficacy and gathering evidence for regulatory approval (including a 900-patient multi-centre trial in the New Zealand public health system for breast cancer diagnosis).

4. Discussion and Conclusions

The adoption and support of this platform has significant potential to foster an ecosystem that enables FAIR and reproducible research outcomes and provide a foundation for integrating and translating international research efforts for assembling multi-scale, -physics, -organ VHTs.

5. References

1. T. Babarenda Gamage, Cassyni Seminar doi.org/10.52843/cassyni.3st2d2 (2024).
2. Ebrahimi B et al., Pulmonary Circulation. 2025; 15:e70176 (2025)

Acknowledgements:

NZ Ministry of Business, Innovation and Employment (UOAX2013), and University of Auckland Foundation..

VIVARIA: VIRTUAL LABORATORY FOR 3RS-ALIGNED ANIMAL PROCEDURE TRAINING.

Massimo Verzeni(1), Federica Riva(2), Benedetta Grossi(1), Francesco Migliavacca(1), Luca Mainardi(1), and Pietro Cerveri(1,4)

1 Department of Electronics, Information and Bioengineering, Politecnico di Milano, Milan, Italy,
2 Department of Veterinary Medicine and Animal Science, Università degli Studi di Milano, Milan, Italy
3 Department of Chemistry, Material and Chemical Engineering, Politecnico di Milano, Milan, Italy
4 Department of Industrial and Information Engineering, Università degli Studi di Pavia, Pave, Italy

1. Introduction

This study develops a desktop-based virtual environment (VE), called VIVARIA, using Ultraleap optical hand tracking [1] to support the training of laboratory animal science (LAS) procedures [2]. VIVARIA enacts simulations identifying precision-critical phases, and step-level usability validation combining interaction metrics with subjective questionnaire.

2. Materials and Methods

Unity was used to implement a modular task/step/condition framework, with automatic logging of interaction metrics. The architecture ensured controlled execution and consistent recovery after critical errors. By recording metrics at the step level, it enabled the detection of precision-critical phases. 26 M.Sc. students in Veterinary and Biotechnology performed three simulated procedures, mouse cage transfer (MCT), jaw blood sampling (JBS), and intraperitoneal injection (IPI), and the resulting logs were analysed together with post-session questionnaire data.

3. Results

First, participants familiarized with hand controls and tool manipulation (Fig. 1). Then, they performed the three tasks. On average, the completion times differed substantially: 28, 124 and 86 s for MCT, JBS and IPI, respectively. Critical errors were found, with 19 errors recorded in the JBS (Fig. 2) and 10 errors in the IPI, while no errors occurred during MCT. Step-level analysis further highlighted the difficulty of JBS, showing a success rate of 46.15%, compared with 76.92% for IPI. Negative correlation ($\rho=-0.40$) was found between total number of grasp attempts and lower interaction controllability.

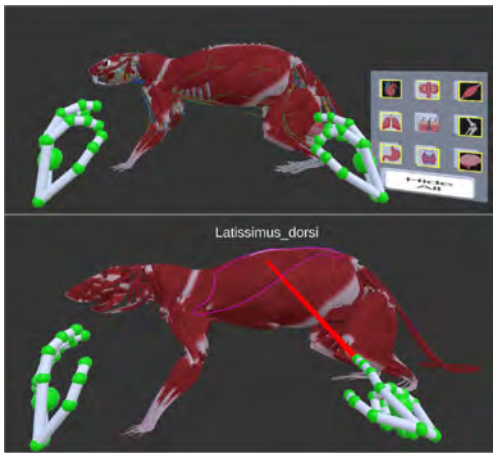


Figure 1: Two example of VE practice.



Figure 2: Jaw blood sampling task.

4. Discussion and Conclusions

The results revealed challenges in precision-demanding phases. From questionnaire, users confirmed usability and the educational value of VIVARIA. Overall, this work can be intended for the early-stage training of LAS procedures.

5. References

1. Steed A and Lai J. Virtual Reality, 29(3), (2025).
2. Franco NH et al., Laboratory Animals. 57(2):109–111, (2023).

Acknowledgements:
This research was supported by Regione Lombardia, Italy.

DIGITAL TWINS FOR POSTOPERATIVE OUTCOME PREDICTION IN TEVAR: A PROOF-OF-CONCEPT STUDY

Anna Ramella (1,2), Giulia De Campo (1), Sara Barati (1,2), Giulia Luraghi (1), Irene Fulgheri (3), Gabriele Piffaretti (4), Robin Heijmen (5), Francesco Migliavacca (1,3), Santi Trimarchi (3)
1. Politecnico di Milano, Italy; 2. AllStent srl, Italy; 3. Policlinico di Milano, Italy; 4. ASST Sette Laghi, Italy; 5. Radboud University Medical Centre, Netherlands.

1. Introduction

Thoracic endovascular aortic repair (TEVAR) has become the preferred treatment for thoracic aortic pathologies and consists of inserting a self-expandable stent-graft (SG) to restore the vessel lumen. The current procedural planning is based on geometric assessment, though it neglects device–aorta interaction [1].
This study reports the use of a validated high-fidelity finite element (FE) methodology to replicate the TEVAR procedure in patient-specific anatomies [2]. The aim is to establish the credibility of the TEVAR digital twin for clinical use, by validating numerical results with post-operative data.

2. Materials and Methods

Pre-operative and post-operative computed tomography angiography (CTA) images of *twenty* patients, who underwent TEVAR using the Valiant Captivia stent-graft, were retrospectively collected under ethical committee approval. The patient-specific anatomy was segmented in VMTK (Orobix) from pre-operative CTA images, and a digital twin of the corresponding SG model was generated in ANSA (BETA CAE) [2,3]. Explicit FE numerical simulations were conducted using LS-DYNA (Ansys) to replicate the stent-graft implantation (Fig.1).

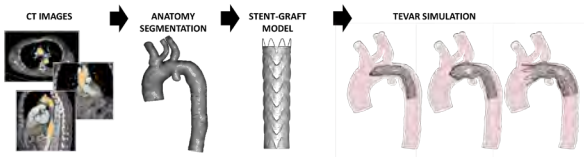


***Figure 1**: Example of TEVAR simulation workflow for a patient-specific case.*

To ensure the accuracy of the TEVAR digital twin, the simulated stent configuration was compared with the stent reconstructed from post-operative images, using the stent ring opening area (OA) percentage errors as a quantitative metric.

3. Results

As reported in the plot in Fig.2, the simulations accurately replicated stent-graft implantation in patient-specific anatomies, with eOA% consistently below 10% per stent ring, averaging 4%. Notably low errors were observed in the proximal and distal stent rings, critical for ensuring sealing (<3.7% average) (results not shown). Simulations ran in about 10 hours, compatible with the current planning practice and showed improved accuracy compared to values reported in the literature [4].

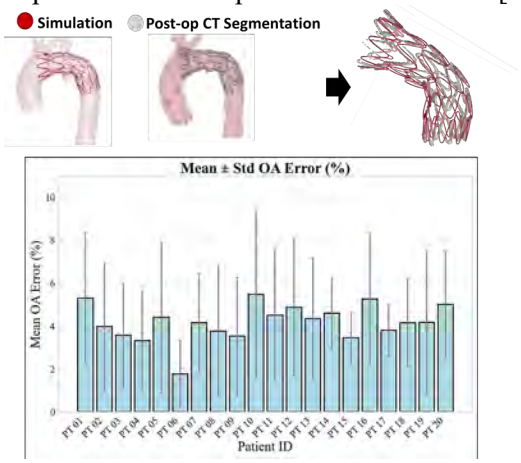


***Figure 2**: Simulation validation process and Mean ± Std OA Errors (%) for the 20 patients.*

4. Discussion and Conclusions

The credibility of a TEVAR digital twin is essential for its trustworthiness and integration into clinical practice. The findings of the proposed study validate the use of numerical simulations for predicting stent-graft post-operative configuration paving the way for a reliable tool for pre-procedural planning. This methodology can be applied to different commercial stent-graft designs to select the best devices for the specific patient.

5. References

1. Upchurch et al., *J Vasc Surg*, 2021;73:55S-83S
2. Ramella et al., *Ann Biom Eng*, 2022;50:1941-53
3. De Campo et al., *J Biomech*, 2025;190:112875
4. Kan et al., *Comp Meth Biomed*, 2024; 244:107994

Acknowledgements PRIN 2022 Mission 4, Component 1: 2022L3JC5T", European Union – NextGenerationEU, National Recovery and Resilience Plan (NRRP) (CUP D53D23014380006).

A VIRTUAL PATIENT PLATFORM FOR PREDICTING ATRIAL FIBRILLATION BURDEN AFTER CATHETER ABLATION

Albert Dasí (1), Haseeb Valli (2), Iain Sim (2), Tom Wong (2), Shouvik Haldar (2), Caroline H Roney (1)

1. Queen Mary University of London, UK; 2. Royal Brompton & Harefield NHS Foundation Trust, UK

1. Introduction

Atrial fibrillation (AF) burden is a promising biomarker for disease stratification and therapy guidance. Cardiac digital twins may offer a scalable approach to predict future AF burden pre-procedurally, improving patient selection and optimising ablation strategy. This work aimed to develop and validate a digital twin framework for predicting 12-month AF burden at the time of index catheter ablation.

2. Materials and Methods

Bi-atrial digital twins were constructed for 60 AF patients enrolled in the CASA-AF multi-centre randomized controlled trial (NCT02755688). The trial randomized patients with long-standing persistent AF to catheter ablation (CA) or thoracoscopic surgical ablation (SA). AF burden was recorded over 12-months using implantable loop recorders. Late gadolinium enhancement cardiac magnetic resonance (LGE-CMR) images were acquired before ablation and at 6 months follow-up. For each patient, two complementary digital twins were developed: a pre-ablation digital twin, derived from baseline LGE-CMR to predict future AF burden, and a post-ablation digital twin, derived from follow-up data to mechanistically interrogate clinical outcomes (**Figure**). First, the atrial anatomy was automatically segmented from the CMR scans using an ensemble of 3D residual encoder UNet models. Then, atlas-derived fibres were mapped onto the resulting atrial surfaces using Universal Atrial Coordinates. Native fibrosis and ablation scar were derived from the image intensity ratios (IIR) of baseline and follow-up LGE-CMR scans, respectively, and included in the corresponding digital twins. To predict 12-month AF burden at the time of index ablation, the planned ablation set was imposed on the pre-ablation digital twin. Conversely, the post-ablation digital twin incorporated the actual ablation scar (**Figure**: planned vs actual ablation scar). Burst stimulation was delivered from 10 atrial sites and AF simulations were continued for 60 seconds. A vulnerability index was defined as the product of the number of induced AF episodes and their duration.

3. Results

The simulated vulnerability index closely matched clinical AF burden, supporting its validity as a quantitative surrogate. Notably, discrepancies between clinical outcomes and the vulnerability index derived from the pre-ablation digital twin were interrogated using the post-ablation digital twin. This comparison enabled identification of mechanistic drivers of recurrent AF, such as conduction gaps within ablation lines or residual fibrotic substrate not targeted by ablation.

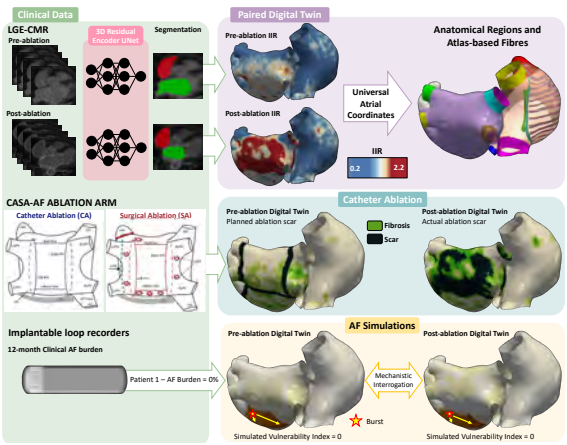


Figure. Digital platform for predicting AF burden.

4. Conclusions

This is the first computational framework using cardiac digital twins to predict future AF burden in a large patient cohort and validated against 12-month clinical data. In addition to offering mechanistic insights into the factors driving AF recurrence, this framework can be used to guide therapy and optimize ablation strategies.

5. Acknowledgments

This work received funding from the UK Research and Innovation Future Leaders Fellowship (Grant No. MR/W004720/1).

IN SILICO EVALUATION OF ARRHYTHMIA IN PRESENCE OF CARDIOMYOPATHY-RELATED ELECTRICAL REMODELING

Alessandra Corda (1), Massimiliano Maines (2), Stefano Pagani (3), Maxime Sermesant (4), Domenico Catanzariti (2), Maurizio Del Greco (2), Christian Vergara (1)

1. LaBS, Dip. di Chimica, Materiali e Ingegneria Chimica, Politecnico di Milano, Italy; 2. Dept. of Cardiology, S.M. del Carmine Hospital, Rovereto, Italy; 3. MOX, Dip. di Matematica, Politecnico di Milano, Italy; 4. Inria, Université Côte d'Azur, IHU Liryc, 3IA Côte d'Azur, France.

Correspondence: alessandra.corda@polimi.it

1. Introduction

Cardiomyopathies can trigger arrhythmias by altering the electrophysiological properties at cellular and macroscopic scales. Computational modelling offers a non-invasive tool to quantify these changes and assess the associated arrhythmogenic risk. In this work, we identify the arrhythmogenic substrate by analysing the functional and anatomical drivers of the following conditions: acute myocardial ischemia (*Test 1*), non-ischemic fibrosis (*Test 2*) and dilated myocardium (*Test 3*).

2. Methods

The Ten Tusscher-Panfilov and monodomain models were used to simulate cellular behaviour and macroscopic propagation, respectively.

In Test 1, in collaboration with Centro Cardiologico Monzino, we integrated *stress-Computed Tomography Perfusion* data to identify low myocardial blood flow regions, incorporating both regional and transmural ionic heterogeneity [1].

In Test 2, in collaboration with S.M. del Carmine Hospital, we exploited *Magnetic Resonance Imaging* for ventricular and fibrosis segmentation and electro-anatomical mapping to calibrate macroscopic conductivities. To assess simulated arrhythmic events, we exploited follow-up data from *Cardiac Resynchronization Therapy* devices.

Finally, in Test 3, in collaboration with Inria, we employed an optimization framework to fit the simulated action potential curves against experimental optical mapping data.

3. Results and Discussion

Test 1 showed that the spatial distribution and heterogeneity of ischemic regions, rather than total volume, are the primary determinants of arrhythmogenesis, with confined zones exhibiting higher arrhythmic propensity [2].

In Test 2, ectopic simulations at fibrosis borders correctly identified the clinical status of three patients: P6 and P10 were classified as arrhythmic due to high reentry incidence (6/10 sites), while P11 was non-arrhythmic (3/10 sites) [3]. An example of progression of a reentry is reported in Fig. 1. These results align with Test 1, linking arrhythmogenic risk to substrate heterogeneity.

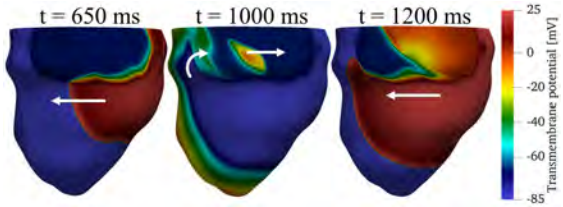


Fig. 1: Evolution of a reentry (Test 2). The arrows indicate the direction of the wavefront.

For Test 3, the optimization framework successfully fitted the simulated action potential to the optical mapping data, enabling the replication of experimental traces from dilated hearts. The results of this calibration are shown in Fig. 2.

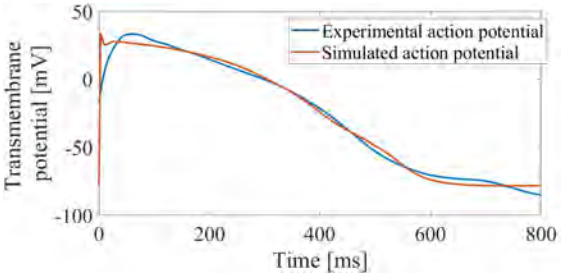


Fig. 2: Output from the calibration process (Test 3).

4. Conclusions

Our framework shows that electrophysiology simulations can non-invasively identify arrhythmic vulnerability, providing a clinically relevant tool for personalized risk stratification and patient-specific treatment criteria.

5. References

1. Dutta S. et al., Prog. Biophys. Mol. Biol. (2017)
2. Corda A. et al., Comput. Biol. Med. (2025)
3. Corda A. et al., medRxiv 2025.12.15.25342270

Acknowledgements:
Funded by Italian Ministry of Health (PNC-E3-2022-23683266), PROGETTO "INNOVA".

A PATIENT SPECIFIC HYDRODYNAMIC– SOFT ROBOTIC CARDIOPULMONARY SIMULATOR TO INVESTIGATE COMBINED VA ECMO AND MECHANICAL VENTILATION THERAPIES

Fresiello, Libera (1); Trapman, Tom (1); Colombi, Federica (1); Donker, Dirk W. (1,2)

1: Cardiovascular and Respiratory Physiology group, TechMed Centre, University of Twente, Enschede, The Netherlands;
2: Intensive Care Center, University Medical Center Utrecht, Utrecht, The Netherlands

1. Introduction

Venoarterial exatracorporeal membrane oxygenation (VA ECMO) is used in combination with mechanical ventilation (MV) to support patients with cardiovascular and/or respiratory failure. At present there are no simulators that can test the interaction of both devices in a high fidelity patient specific setup.

2. Materials and Methods

A 60 years old patient from UMC Utrecht undergoing peripheral VA ECMO was considered as a case study. Hemodybnamic data, cardiac ultrasound, computer tomography (CT) scans, VA ECMO and MV settings were collected. The simulator backbone is a closed loop lumped parameter model, whose 4 heart chambers, pulmonary and systemic circulation [1] were tuned to patient hemodynamics.

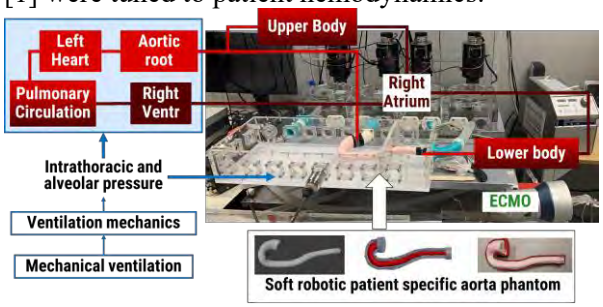


Figure. 1:Overview of the simulator.

The computational model was connected to a hydrodynamic system using the *hardware in the loop* technique: the right atrium and the aorta were represented in vitro - to enable the connection of a real VA ECMO device – and functionally connected to the remainder in silico circulation. For the aorta, an echogenic silicone phantom was produced via mould casting. The phantom replicated patient anatomy (retrieved from CT), and realistic mechanical properties. The in silico MV model reproduced pressure control mode with same settings used in the clinics. Airways resistance, chest and lungs compliance were tuned to clinical data. The simulated intrathoracic and alveolar pressures were transmitted to the heart and thoracic vessels in silico and to the aorta phantom in vitro through a dedicated hydraulic chamber. Model tuning was performed at VA ECMO flow 2.2 L/min, then the support was increased to 2.4 and 2.6 L/min and the simulator prediction was compared to patient data.

3. Results

The simulator predicts patient hemodynanics in combination with the VA ECMO and the MV therapies (Figure. 2).

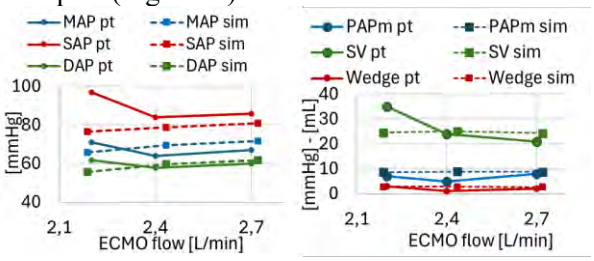


Figure. 2:Patient (pt) and simulated (sim) mean/ systolic /diastolic pressure (MAP /SAP/DAP), pulmonary arterial pressure (PAPm), left ventricular stroke volume (SV) and wedge pressure (Wedge).

The aorta phantom has a compliance of 1.29 mL/mmHg in line with patient data. Simulated tidal volume is 373±0 mL vs 364±4 mL measured on patient, for clinically comparable ventilation pressures. The main effects of heart-lung interaction are observed on cardiac output, pulmonary and systemic hemodynamics, modulated by the inspiration-expiration phases.

4. Discussion and Conclusions

The simulator offers a high fidelity and personalizable representation of cardiovascular and respiratory pathophysiological status. The soft robotic aorta phantom enhances the applicability of the setup toward evaluation of medical devices in intensive case scenarios, with multiple concomitant therapies and complex multiorgan pathological conditions.

5. References

1. Fresiello L. Front Physiol. 2022 Oct 13;13:967449.

PATIENT-SPECIFIC COMPUTATIONAL ANALYSIS OF ASCENDING TEVAR: ASSESSING DEVICE DEPLOYMENT AND HEMODYNAMICS

Giulia De Campo (1), Jasper de Kort (2,6) Anna Ramella (1), Giulia Luraghi (1), Sara Barati (1), Irene Fulgheri (2), Santi Trimarchi (2,3), Gabriele Piffaretti (4,5), Francesco Migliavacca (1,2)

1. Politecnico di Milano, Italy; 2. IRCCS Policlinico di Milano, Italy; 3. Università degli Studi di Milano, Italy 4. Department of Medicine and Surgery, University of Insubria School of Medicine, Varese, Italy 5.ASST Settelaghi, University Teaching Hospital, Varese, Italy 6. Department of Vascular Surgery, University Medical Centre Utrecht, Utrecht, The Netherlands

1. Introduction

Ascending TEVAR (aTEVAR) has emerged as an alternative for patients unsuitable for open surgical repair for pathologies of the ascending aorta [1]. This region of the aorta presents unique challenges, including short landing zones, proximity to the coronary ostia and supra-aortic branches, high haemodynamic forces, and the absence of dedicated endografts [1]. Numerical simulations offer a valuable tool to predict stent-graft placement and haemodynamic performance in patient-specific anatomy. This study presents a case report evaluating device deployment and fluid dynamics in ascending TEVAR, with the novel inclusion of aortic valve proximity.

2. Materials and Methods

A custom-made device was selected for this patient. The device was designed, meshed, and prestressed, before performing an FE simulation of the TEVAR procedure following the "tracking method" [3,4]. The device material properties are taken from literature [5]. The model incorporates the aortic valve to accurately describe the complex environment where the device has been placed. The simulation was validated comparing the opening area (OA) of each ring of the simulated stent-graft with the one of the CT-post of the patient.

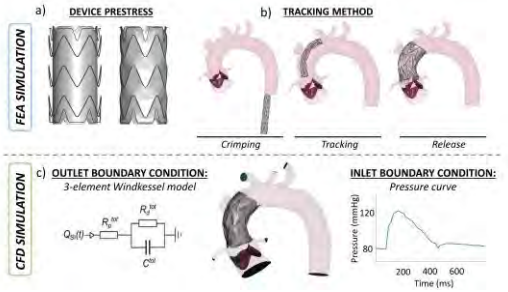


Figure 1: a) device prestress; b) representation of the "tracking method"; c) CFD boundary conditions.

After validation, CFD and FSI simulations were performed. A pressure curve taken from a database of patient-specific pressure measurements was set at the inlet of the domain, while Windkessel models were applied to all the outlets.

3. Results

Starting from the validation of the FE structural simulation, the error in the opening area comparison is lower than 8% for all the stent struts, evidencing a very good agreement between the simulated and the CT segmented device. From the haemodynamic point of view, preliminary results demonstrate how the presence of the valve impacts the velocity profile.

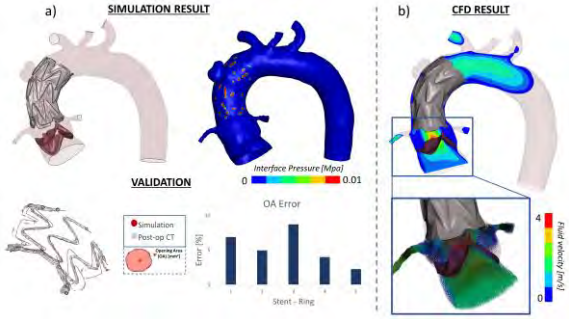


Figure 2: a) FEA simulation result and validation; b) velocity results from CFD simulation

4. Discussion and Conclusions

Investigating the complexity of the ascending aortic environment through numerical simulations can help predict potential complications and support procedural planning. Information on contact pressures and haemodynamic indices may further assist the decision-making process for ascending TEVAR, which remains a high-risk intervention.

5. References

1. de Kort JF, et al. EJVES. 2025.
2. Romarowski, Conti. Comput Biol Med. 2018.
3. De Campo, Barati. J Biomech; 2025;190.
4. Ramella, De Campo. EJVES; 2026.
5. Ramella, Barati. Ann Biomed Eng. 2025

A TOPOLOGY OPTIMIZATION COMPUTATIONAL FRAMEWORK FOR FEMORAL STENT DESIGN: EXPERIMENTAL ASSESSMENT

Dario Carbonaro (1,2), Nicola Ferro (3), Francesco Mezzadri (4), Elena Torta (1), Erika Temellini (5), Sara Zambon (1), Diego Gallo (1), Simona Perotto (5), Umberto Morbiducci (1), Claudio Chiastra (1)

1. Politecnico di Torino, Italy; 2. Università della Calabria, Italy; 3. Università Ca' Foscari Venezia, Italy; 4. Università di Modena e Reggio Emilia, Italy; 5. Politecnico di Milano, Italy

1. Introduction

The development of laser-cut vascular stents is largely incremental, relying on minor geometric adjustments to rings and connectors. Topology optimization (TO) is a mathematical approach that identifies optimal material distributions under prescribed objectives and constraints, enabling the exploration of unconventional stent designs beyond traditional refinement strategies. This study presents a TO-based computational framework for the design of innovative stents with clinically relevant mechanical properties. The framework was applied to femoral artery stents, which continue to exhibit high restenosis rates (>30% at two years post-implantation). Physical prototypes were manufactured to assess the feasibility and robustness of the approach.

2. Materials and Methods

The proposed framework models the stent as a periodically repeated unit cell, and consists of three steps. First, a novel 2D stent unit cell is generated using inverse homogenization TO with the microSIMPATY algorithm [1], targeting key mechanical properties, including volume fraction (i.e., contact area), radial stiffness, and foreshortening [2], while enforcing laser-cut manufacturability through a density filter that ensures a minimum strut width [3]. Second, the optimized unit cell is periodically repeated in the axial and circumferential directions to form a planar stent pattern, and an automated routine generates a CAD file suitable for laser cutting, removing contour irregularities. Finally, stent prototypes are fabricated by laser cutting from the generated CAD file. The framework was evaluated by generating three optimized unit cells with different prescribed mechanical requirements (i.e., Designs 1, 2, and 3). For each design, three stent prototypes were manufactured and assessed through radial crimping tests and foreshortening evaluation.

3. Results

Figure 1 presents the three optimized unit cells and the corresponding stent prototypes. All designs were successfully manufactured without structural failure. Radial stiffness measured from crimping tests showed reasonable agreement with the TO targets, with relative errors of 0.2%, 31.0%, and 2.8% for Designs 1-3, respectively. The foreshortening error was 30.9% for Design 1. Foreshortening could not be adequately assessed for Designs 2 and 3 due to structural instability during testing.

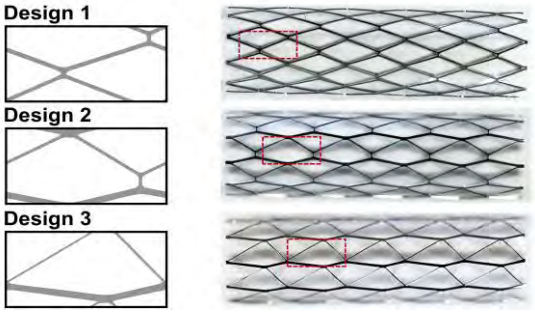


Figure 1: Novel optimized femoral stent designs.

4. Discussion and Conclusions

The framework enables unconventional, laser-cut femoral stent designs and represents a device-level digital twin supported by experimental validation. Experimental results show that the fabricated prototypes meet the prescribed mechanical targets, at least in terms of radial stiffness, highlighting the potential of TO to explore novel stent concepts beyond incremental refinements of existing designs.

5. References

1. Carbonaro D et al., Comput Methods Appl Mech Engrg; 416:116288 (2023).
2. Carbonaro D et al., Comput Methods Programs Biomed; 257:108467 (2024).
3. Ferro N et al., Finite Elem Anal Des; 244 (2025).

Acknowledgements:
This study was conducted within the RESET project, funded by the EU – NextGenerationEU and the Italian MUR (PRIN 2022 PNRR, D.D.1409 of 14/09/2022).

STRUCTURAL AND HEMODYNAMIC ANALYSIS OF A SMART STENT DESIGN TOWARDS A DIGITAL TWIN PLATFORM

Mahtab Vafaeefar (1), Marcin Jan Kraśny (2), Muhammad Farooq (2), Icaro Soares (2), Derek O'Keeffe (3), Adnan Elahi (2), Monika Colombo (4), Ted Vaughan (1)

1. Biomechanics Research Centre, University of Galway, Ireland; 2. Translational Medical Devices (TMD) Lab and Electrical & Electronic Engineering, University of Galway, Ireland; 3. Health Innovation Via Engineering (HIVE) Laboratory, University of Galway, Ireland; 4. University of Aarhus, Denmark.

1. Introduction

Abdominal Aortic Aneurysm (AAA), defined as an aortic diameter exceeding 3.0 cm, is a silent condition with a fatal rupture rate of 80%, if left untreated. Endovascular Aneurysm Repair (EVAR) has become the preferred treatment due to its minimally invasive approach and strong short-term outcomes[1]. However, EVAR devices are frequently complicated by endoleaks, where blood re-enters the aneurysm sac and restores the risk of rupture. While current imaging-based surveillance is effective, it is often restricted by high costs and lack of real-time data. This project investigates the structural and hemodynamic performance of a smart implantable stent designed to wirelessly monitor pressure[2] and provide continuous, post-EVAR detection of endoleaks.

2. Materials and Methods

The structural integrity of a commercial stent-graft (Medtronic Endurant II) was evaluated using multi-physics computational and experimental frameworks. Finite element (FE) analysis was used to characterize the radial force-displacement behaviour of single-ring and full-stent device [Fig. 1a] under crimping loading. The stent and graft materials were considered as superelastic Nitinol and lamina material properties, respectively. The device was deployed into an idealised AAA geometry [Fig. 1a]. Tissue material was considered linear elastic, adopted from a 3D-printed resin prototype for benchtop testing. Computational fluid dynamics (CFD) was used to evaluate the pressure changes and hemodynamic of endoleaks. Blood was modelled as a Newtonian laminar flow, was first simulated in untreated AAA geometry, validated against pressure data using experimental setup [Fig. 1b], following convergence studies. Based on the deformed aorta post-EVAR, representative endoleak geometry was generated, to allow blood flow to enter aneurysm sac region. Pressure change in the sac region was calculated, compared to the AAA via validated CFD model [Fig. 1b].

3. Results

The radial force-diameter curve of the stent ring is captured [Fig. 1c] for material calibration. The artery deformation and mechanical stress due to the deployment of the stent-graft was calculated using the FE model [Fig. 1d, e]. The CFD simulations show large negative pressure within the sac region at low velocities and experienced delayed peak pressure compared to the AAA model [Fig. 1f, g].

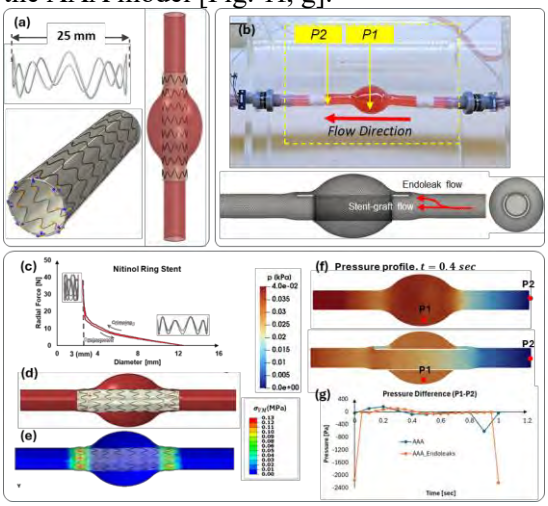


Figure 1: (a) single ring M-shaped, stent-grant, and deployment in AAA geometry; (b) anatomical benchtop setup for AAA blood flow, and CFD model for endoleaks; (c) radial force vs diameter for single nitinol ring; (d) stent-graft deployment, and (e) stress distribution on aorta walls post-EVAR; (f, g) pressure profile, and pressure difference in sac calculated in AAA, and endoleaks post-EVAR.

4. Discussion and Conclusions

This research uses validated FE and CFD models to examine integrated biosensors effect stent mechanics and to identify pressure-based indicators of endoleaks. Collectively, these multi-physics models establish the framework for a digital twin, aimed at enhancing the long-term monitoring of EVAR stent functionality.

5. References

1. England A, (et al.), Ulster Med J.82:3-10. 2013.
2. Silva, N. P. (et al.), Sensors, 24, 3526, 2024.
3. Demanget, N. (et al.), JMBBM, 5, 272–282, 2012

Acknowledgements:

Project funded by Disruptive Technologies Innovation Fund (DTIF) Programme 2022.

CONSTITUTIVE FRAMEWORK FOR COUPLED MULLINS-TYPE SOFTENING AND FINITE VISCOELASTICITY IN ARTERIES

Juan Antonio Peña (1), Miguel Ángel Martínez (1,2), Estefania Peña (1,2)

1. Aragón Institute for Engineering Research (I3A), University of Zaragoza, Spain; 2 CIBER-BBN, Centro de Investigación en Red en Bioingeniería, Spain

1. Introduction

Soft fibrous tissues, such as ligaments and arteries, exhibit strongly nonlinear, anisotropic, and time-dependent mechanical behavior due to their heterogeneous microstructure. These tissues consist of collagen fibers embedded in a compliant ground matrix, producing both directional stiffness and viscous dissipation. This work proposes a unified constitutive model that combines finite-strain anisotropic viscoelasticity with directional pseudoelastic softening to capture both rate-dependent and history-dependent effects.

2. Materials and Methods

To motivate the coupled viscoelastic-damage model, we consider the finite-strain anisotropic viscoelastic constitutive behaviour proposed by Peña et al [1] and the directional pseudo-elastic softening model proposed by Peña & Doblaré [2]. Softening and viscoelastic phenomena are here assumed to affect only the isochoric elastic part of the deformation, as proposed by Simo [3]. The model decomposes the stress into equilibrium and non-equilibrium parts, with internal variables controlling the evolution of viscous deformation and pseudoelastic softening. It is implemented in a three-dimensional finite element framework and tested under cyclic loading conditions representative of arteries and other fibered tissues.

3. Results

The developed constitutive model was first validated using experimental data from cyclic uniaxial and biaxial tests on pulmonary arteries. The results show that the formulation successfully captures the Mullins effect, showing a clear reduction in stiffness after the first loading cycle. This softening is particularly visible in the fiber directions, demonstrating that the directional pseudo-elastic approach is consistent with the physical behavior of the tissue.

Additionally, the model accurately predicts the time-dependent response of the arterial wall. It shows a significant increase in the hysteresis area when the strain rate changes from 0.01 s^{-1} to 1 s^{-1}, as well as a realistic stress relaxation over time. The explicit separation of fiber and matrix contributions allows for a better representation of anisotropic softening, where the energy dissipation is correctly distributed between the different components of the tissue.

4. Discussion and Conclusions

Results demonstrate that the model can accurately predict viscoelastic relaxation and stress softening simultaneously. The explicit separation of fiber and matrix contributions allows realistic representation of strain-rate dependence and directional softening. This approach provides a thermodynamically consistent and computationally efficient tool for simulating the mechanical response of fibrous soft tissues under complex loading, offering a strong basis for biomechanical and clinical applications.

5. References

1. Peña, E., Calvo, B., Martínez, M.A., Doblaré, M., 2007. An anisotropic visco-hyperelastic model for ligaments at finite strains: Formulation and computational aspects. Int J Solids Struct 44, 760–77.
2. Peña, E., Doblaré, M., 2009. An anisotropic pseudo-elastic approach for modelling Mullins effect in fibrous biological materials. Mech Res Commun 36, 784–790
3. Simo, J.C., 1987. On a fully three-dimensional finite-strain viscoelastic damage model: Formulation and computational aspects. Comput Methods Appl Mech Engrg 60, 153–173

Acknowledgements:

Support was obtained from the Spanish Ministry of Science and Technology through the research project PID2022-140219OB-I00, and the regional Government of Aragón support for the funding of the research project T24-20R.). The authors thank the research support from the CIBER initiative, whose actions are financed by the Instituto de Salud Carlos III with assistance from the European Regional Development Fund.

INFLUENCE OF INTER-FIBRE CONTACTS ON THE MECHANICS OF BIOPOLYMER NETWORKS

Pritesh Ramya (1), Frank J. H. Gijsen (1,2), Behrooz Fereidoonnezhad (1)

1. Delft University of Technology, Delft, The Netherlands; 2.Erasmus University Medical Center, Rotterdam, The Netherlands

Corresponding author: Pritesh Ramya, P.Ramya@tudelft.nl

1. Introduction

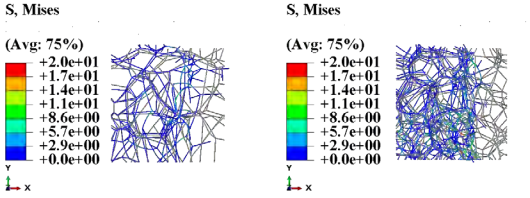
Mechanical behaviour of cardiovascular tissues, such as artery, is strongly governed by their underlying fibrous microstructure [1]. A reliable representation of the fibre deformation under physiologically relevant loading modes becomes crucial to understand the mechanical behaviour of such tissues. In this work, a topologically aware Discrete Fiber Network (DFN) model representing mesoscale microstructural volume element is developed and its response under tensile and compressive loading are simulated. Particularly, the role of inter-fibre contact in the bulk mechanical response as a function of fibre concentration is investigated.

2. Materials and Methods

A topologically aware in-house DFN generator [2] was used to generate 3D fibre networks with prescribed topology at concentrations of 0.6 and 1.2 mg/ml in a 40x40x40 μm^3 cubic domain, with all other fibre-level properties kept identical (Fig.1). The networks were discretized with Timoshenko beam elements and simulated in ABAQUS/Explicit under uniaxial tension and compression up to 30% deformation. Inter-fibre contact was incorporated under quasi-static conditions. Simulations with and without inter-fibre contact were compared.

3. Results

Figure 1 shows the deformed network at $\lambda = 0.7$ in compression, overlaid on the undeformed configuration, together with the fibre von Mises stress distribution. Figure 2 shows that inter-fibre contact has negligible effect in tension, consistent with [3], but produces a small divergence in compression, with relative differences at $\lambda = 0.7$ of 3.4% for 0.6 mg/ml and 0.26% for 1.2 mg/ml.



(a) 0.6 mg/ml (b) 1.2 mg/ml

Figure 1: Von mises stress (MPa) distribution in compressed network (coloured) at stretch ratio, λ =0.7 against undeformed configurations (grey).

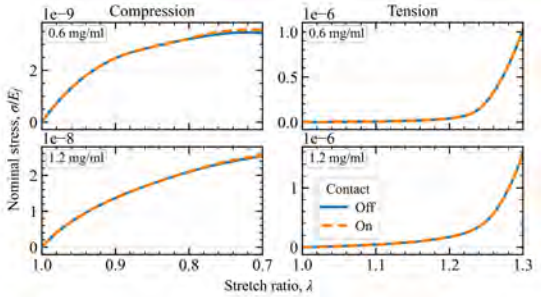


Figure 2: Bulk mechanical response under uniaxial tension and compression with contact enabled (dashed) and disabled (solid).

4. Discussion and Conclusions

The results of compression test simulations suggests that inter-fibre contact may introduce additional internal resistance as the network densifies, leading to increased load carrying capacity with increased compression. However, within the current modelling framework this effect appears weaker at higher concentration. Although the size of the volume element may be one of the plausible contributors to this observation, these preliminary results indicate a nontrivial interaction between inter-fibre contact and network topology in compression, motivating further systematic investigations.

5. References

1. Jansen I et al., Basic Res Cardiol. 119(2):193-213 (2024).
2. Cardona S et al., J Mech Phys Solids. 106257 (2025).
3. Islam MR, Picu RC. J Appl Mech. 85(8):081011 (2018).

THE IMPORTANCE OF INELASTICITY WHEN SIMULATING BALLOON DEPLOYMENT IN DISEASED ARTERIES

Silvia Renon (1), Richard Good (2), Ankush Aggarwal (1), Sean McGinty (1)

1. James Watt School of Engineering, University of Glasgow, UK; 2. School of Cardiovascular & Metabolic Health, University of Glasgow, UK.

1. Introduction

Elastic recoil after drug-eluting stent (DES) or drug-coated balloon (DCB) deployment is a key measure of procedural success but involves inelastic arterial behaviour as the arterial lumen only undergoes a partial rather than complete restoration to its original shape. This phenomenon is particularly noteworthy in Drug-Coated Balloon usage [1]. While studies have modelled inelastic plaques, most focus on stents [2], and existing balloon models oversimplify plaque mechanics [3]. To our knowledge, no study has used a realistic inelastic plaque model for lesion preparation and drug elution. This computational analysis aims to accurately predict the state of the diseased artery after device deployment, therefore taking into account inelasticity in patient specific plaque geometries and lesion preparation techniques.

2. Materials and Methods

Finite element analysis was used to model balloon deployment in patient-specific plaques, incorporating plasticity. Clinically relevant parameters like plaque composition, balloon-to-artery ratio (BAR), and balloon type were tested. Elastic recoil ratio (ERR), residual stenosis (RS), and stress-strain distributions were computed and compared to clinical values and plaque rupture thresholds.

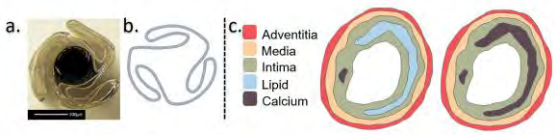


Figure 1: Tri folded balloon is modelled based on real-life props (a, b); Plaque models composition (c): wall - hyper elastic Yeoh material model, plaque - perfect plasticity and linear hardening.

3. Results

Plastic strain and stress distributions after balloon expansion were visualized in cross-sections of patient-specific geometries. Plaque compositions, including lipidic, calcified, and mixed plaques (Fig. 2, right), were tested as well as lesion preparation balloon types, with varying BAR for each plaque type (Fig. 2, left).

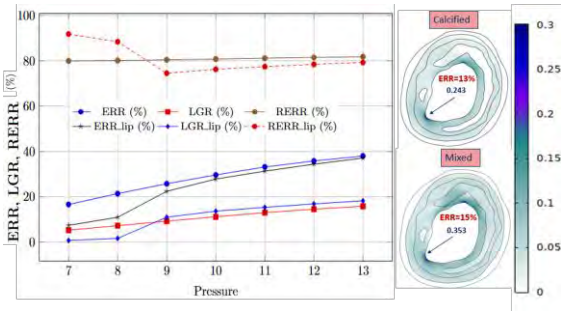


Figure 1: (left) ERR, LGR, RERR plotted over increasing pressure for mixed and lipidic plaque. (right) Equivalent plastic strain distribution plotted in calcified and mixed plaque.

4. Discussion and Conclusions

Perfect plasticity and linear hardening models produced ERR and LGR values consistent with clinical data. Plaque composition influenced plastic strain distribution and residual stresses, impacting plaque damage and morphology. BAR and plaque composition significantly affected deployment outcomes, with higher balloon pressure increasing plastic deformations. Understanding lesion preparation's effect on plaque morphology is essential for optimizing drug transport and improving DCB efficacy

5. References

1. Jeger et al, JACC: cardiovascular interventions, 13(12):1391-1402, 2020.
2. Gastaldi et al, Biomech Model Mechanobiol, 9:551-5561, 2010.
3. Helou et al, int J Numer Meth Biomed Engng, 37:e3499, 2021.

Acknowledgements:

This work was supported by grant Mary Gibb Dunlop Scholarship from the University of Glasgow

BIO-DIGITAL TWIN OF THE FIRST TRIMESTER PLACENTA FOR DRUG RISKS ASSESSMENT

Michael Gasik* (1); Alessandra Manzin (2); Jessica Petiti (2); Carla DiVieto (2); Ricardo Ferrero (2); Volodymyr Kuzmenko (3); Chrsitian Silva (3); Ines Mendes Pinto (4); Miguel Neves (4); Beatriz Pais (4); Regina Grillari (5); Matthias Wieser (5); Lisa Muiznieks (6); Olivier Fournier (6); Rashmi Ramakrishnan (7); Andrew Daly (7); Carla Baldasso (8); Novella Saccenti (8); Francesco Franchini (8); Andrea Cruz (9); Hugo Olivera (9)

1. Seqvera Ltd. Oy, Finland; 2. INRIM, Italy; 3. CellInk Bioprinting AB, Sweden; 4. I3S, Portugal; 5. Evercyte GmbH, Austria; 6. Microfluidic Innovation Center, France; 7. National University of Ireland Galway, Ireland; 8. Enginsoft s.p.a., Italy; 9. INL, Portugal

1. Introduction

Pregnant women suffer from a range of conditions that require either ongoing or acute treatment: 40–80% of pregnant women take at least one medication during their pregnancy, most frequently during the first trimester. Many medicines are administered in pregnancy 'off label', and >90% of clinically approved drugs lack appropriate information on efficacy, safety, and pharmacokinetics in pregnancy.
there is a pressing need for novel and powerful investigative techniques that can uncover the aetiology of pregnancy complications caused by medicinal substances.

2. Materials and Methods

Innovative solution integrating digital *in silico/in vitro* (biodigital twin) system (Fig. 1), has been achieved in LIFESAVER project [1] for an effective screening of chemicals and pharmaceuticals for pregnant women, excluding animal testing, which is not possible with other approaches to the same level of confidence.

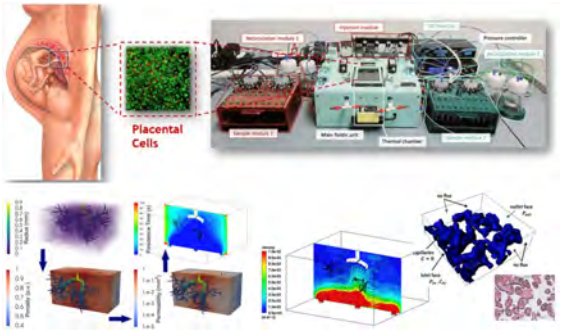


Figure 1: The concept and the system of the LIFESAVER bio-digital twin.

The essential parts of the biodigital twin comprise an integrated MPS with a proprietary chip with human immortalized cells on a core bioprinted membrane, with combined multiplexed biosensors as smart edge devices, linked with tandem *in silico* models built-up and tailored to the *in vitro* part and to real-size 1st trimester 3D placenta.

3. Results

The recent proof-of-concept was achieved with experiments using doxycycline, bisphenol A and their mixtures demonstrating a stable dual-flow operation, reproducible transport kinetics (<7%CV) and maintained barrier integrity under physiological conditions [2]. The *in silico* tandem allows both validation of the MPS chip flows and concentrations in time and space and connection of these transport parameters into a 3D model, able to perform virtual experiments.

4. Discussion and Conclusions

This biodigital twin is a reliable method to identify the risk of foetal exposure to medicines or their metabolic products/derivatives that could potentially harm, providing independent Risk of Exposure Assessment Data (iREAD) in ethical and cost-effective way. It addresses a crucial evidence gap as there is a lack of evidence on which substances transfer across the placenta and in which quantity. In regulatory aspect, the method is going to replace substantial part of DART related to testing of the drugs and chemicals transport through the placenta (especially in the first trimester), compliant to ICH E21.

5. References

1. https://lifesaverproject.eu/
2. Fournier O. et al., Adv. Sensor Res. 5:e00166 (2026).

Acknowledgements:
This research has received funding from the European Union under Horizon2020 programme through LIFESAVER project (GA 101036702).

FINITE ELEMENT MODEL OF BONE INFLAMMATION-ON-CHIP TO CALIBRATE MACROPHAGE MECHANOBIOLOGY

Edoardo Borgiani (1,2), Gabriele Nasello (1,2), Ayse Kose (1,2), and Liesbet Geris (1,2)

1. Prometheus, Division of Skeletal Tissue Engineering, KU Leuven, Leuven, Belgium; 2. Division of Biomechanics, Department of Mechanical Engineering, KU Leuven, Leuven, Belgium.

1. Introduction

Long bones can autonomously restore their structure and load-bearing function after fracture. While multiscale computational models have advanced our understanding of bone healing mechanisms [1], the inflammatory phase, critical for successful regeneration [2], remains poorly represented *in silico* [3]. We introduce a new computer model that integrates hematoma mechanics and the mechanosensitive behaviour of bone marrow derived macrophages (BMDMs). To define their mechano-regulatory rules, we developed an inflammation-on-chip pipeline that mimics the heterogeneous mechanical environment of the hematoma, allowing cellular-level analysis of early inflammatory responses.

2. Materials and Methods

Mechanobiology was implemented using a finite element model (FEM) to simulate fracture mechanics, complementing a previously developed multiscale agent-based model of the immune response within the hematoma [4]. The mechanobiological rules were calibrated *in vitro* through an inflammation-on-chip setup using uBeat microfluidic devices (BiomimX). Primary mouse bone marrow monocytes were differentiated into BMDMs, maintained as naïve (M0) or polarized into pro- (M1) and anti-inflammatory (M2) phenotypes. Cells were seeded in a 3.0 mg/ml collagen type I hydrogel, mimicking hematoma mechanical properties and embedded in the microfluidic chip. User-defined compression or stretch was applied for 24 or 72 hours, together with non-stimulated control cases. 3D immunofluorescent images were acquired by spinning-disk confocal microscopy after phenotype-specific staining. A FEM of the microfluidic device was created to predict strain distribution sensed by the BMDM population. Spatiotemporal comparison between FEM-predicted fracture mechanics and *in vitro* BMDM behaviour provided rules for *in silico* calibration.

3. Results

The BMDM population within the microfluidic chip showed a predominantly pro-inflammatory profile when mechanical stimulation was applied *in vitro*. When BMDM were seeded and subjected to 10% stretch, expression of the pro-inflammatory marker iNOS increased, when compared with controls. Marker intensity was highest along the channel sides, where the FEM predicted greater strain magnitudes (Fig. 1).

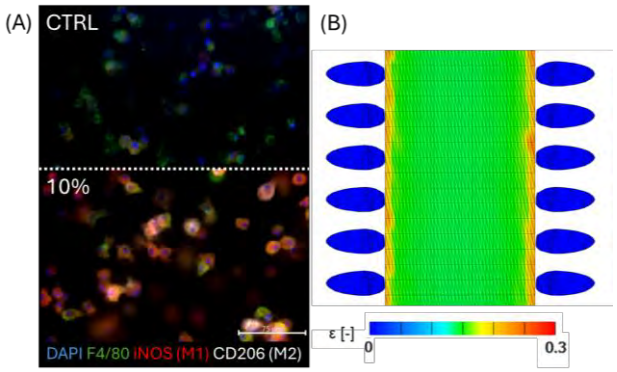


Figure 1: A. Comparison in marker intensity between control (CTRL) and 10% stretch microfluidic device. B. FEM of the microfluidic device when stretch is simulated.

4. Discussion and Conclusions

Inflammation-on-chip is a game-changing approach to calibrate models of the immune response in bone healing. The heterogeneous mechanical environment replicated *in vitro* provides mechanobiological insights into BMDM regulation within the hematoma. The calibrated *in silico* model will offer essential support for predicting the role of mechanical regulation in enhancing fracture regeneration from the initial immune response onward.

5. References

1. Borgiani et al., Front. Physiol.; 8:287 (2017).
2. Duda et al., Nat Rev Rheum.; 19:78-95 (2023).
3. Lafuente-Gracia et al., Front. Bioeng. Biotech.; 9:703725 (2021).
4. Borgiani et al., Front. Imm., 14:1231329 (2023).

MULTI-PHYSICS COMPUTATIONAL MODEL OF METASTATIC BONE REMODELLING

Claire C. Villette (1,2), Liesbet Geris (2,3)

1. QMUL, UK; 2. KU Leuven, Belgium; 3. ULiege, Belgium

1. Introduction

Bone metastases (BMs) severely disrupt bone remodelling by shifting the balance between osteoclast mediated resorption and osteogenic bone formation toward excessive osteolysis. Mechanical loading induces opposing, anabolic effects [1]. To support the investigation of loading regimens with therapeutic potential, this study developed a computational model of load induced bone remodelling in the presence of metastatic breast cancer cells.

2. Materials and Methods

A hybrid cellular automaton (HCA) model was implemented in Python, integrating three interconnected modules:

(i) The cell module used a cellular automaton [2] to describe migration, proliferation, death, and functional activity of osteogenic cells, osteoclasts, and cancer cells. Logistic functions defined the influence of mechanical stimulation and receptor occupancy on ECM-modifying behaviour and biochemical signalling.

(ii) The biochemical module used partial differential equations (PDE) describing diffusion and binding kinetics of RANKL, OPG and PTHrP (key drivers of bone remodelling and cancer modulation).

(iii) The mechanics module solved a quasi static equilibrium problem using a hyperelastic neohookean constitutive law. Tetrahedral meshes with ~4.5 µm resolution were used, and von Mises stress served as the mechanical stimulus regulating cellular responses.

All PDE problems were solved alongside the cellular automaton using the FEniCSx solver.

3. Results

As proof of concept, predicted RANKL and OPG concentrations, integrated across the model volume, were compared with gene-expression data from in-vitro layered hydrogel cultures of osteogenic cells, osteoclasts, and breast cancer cells [3]. Both static and dynamic loading (0.5% uniaxial compression) were evaluated. The model captured the experimentally observed order of magnitude increase in RANKL/OPG ratio in the presence of cancer cells, and its strong reduction under dynamic loading (Figure 1).

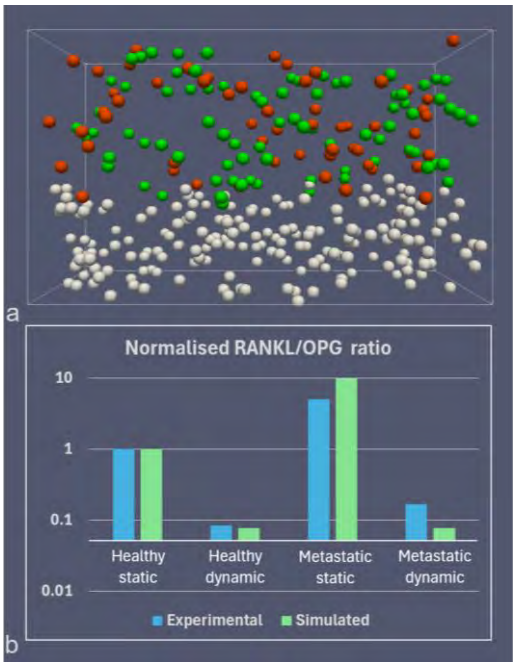


Figure 1: (a) Model slice showing layered osteogenic cells (white), osteoclasts (red), and cancer (green) (b) Simulated RANKL/OPG concentration ratio compared to experiments.

4. Discussion and Conclusions

An HCA framework was implemented which reproduces key cancer-induced perturbations of bone remodelling signals and their modulation by mechanical stimulation. Further work involves investigation of loading regimens with therapeutic potential.

5. References

1. Lynch et al., 2013. Journal of Bone and Mineral Research, 28(11), pp.2357-2367
2. Lai et al., 2022. International Journal for Numerical Methods in Biomedical Engineering 38.1, e3542
3. Kumar et al., 2024. Cell Reports 43.5

Acknowledgements:

The authors would like to thank **FWO** for providing financial support to this project.

COMPUTATIONAL EVALUATION OF PDAC-ON-CHIP RELEVANCE FOR RADIOBIOLOGICAL AND CHEMO-RADIATION STUDIES

Sofia Tartaro(1)*, Alessia Beretta(2), Marianne Aznar(3), Paolo Zunino (4), Tiziana Rancati(1),Sandro Pasquali(2), Luca Possenti(1)

1.Fondazione IRCCS Istituto Nazionale dei Tumori, Data Science Unit, Milan, Italy; 2. Fondazione IRCCS Istituto Nazionale dei Tumori, Molecular Pharmacology Unit, Milan, Italy; 3. Division of Cancer Sciences, The University of Manchester, Manchester, United Kindom; (4) Politecnico di Milano, Department of Mathematics, Milan, Italy.

** Corresponding author, sofia.tartaro@istitutotumori.mi.it.*

1. Introduction

Pancreatic ductal adenocarcinoma (PDAC) is frequently associated with a hypoxic, poorly vascularized, desmoplastic microenvironment, rich in dense fibrotic stroma, which can constitute up to 90% of the tumor mass. Such a peculiar micro-environment impairs drug and oxygen diffusion, thereby affecting PDAC radio- and chemoresistance. A microfluidic chip model was proposed to mimic the PDAC microenvironment *in vitro (PDAC-on-chip; Figure 1a*). Here, we propose a computational evaluation of the relevance of the PDAC-on-chip as a preclinical model for chemo-radiotherapy (CRT) applications.

2. Materials and Methods

The computational framework integrates: (i) a vascularized Multiscale Model (MM) and (ii) an avascular agent-based model (ABM), implemented in GetFem++ [1], and in PhysiCell [2], respectively. The ABM simulates the growth rate of PANC-1 tumor spheroids over 20 days, accounting for oxygen diffusion and hypoxia-induced necrosis by integrating experimental and literature data. The MM extends this framework by introducing Gemcitabine (GEM) diffusion towards a vascular domain, simulating the PDAC-on-chip vascular compartment. Transport dynamics were evaluated under no-desmoplasia, moderate desmoplasia, and extreme desmoplasia conditions. The last two conditions were modeled using oxygen diffusion coefficient reductions of 30 and 50%, and drug diffusion coefficient reductions of 90 and 97%, relative to free diffusion in water.

3. Results

The ABM reproduced the experimental spheroids' growth rate. Increasing levels of desmoplasia led to the expansion of the spheroids' necrotic core. The Oxygen Enhancement Ratio (OER), according to the Wenzl–Possenti relationship, indicates higher doses are needed in the spheroid core to achieve the same treatment response observed under normoxic conditions (Figure 1d). In the MM, reduced drug diffusivity led to a diffusion-limited transport (Figure 1c-d).

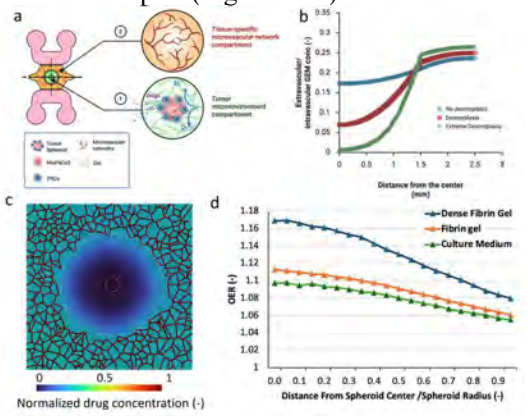


Figure1:a)Schematic representation of the PDAC-on-chip; b-c)GEM concentration in the MM and representative image of extreme desmoplastic condition; d)OER distribution along spheroid radius.

4. Discussion and Conclusions

This computational evaluation demonstrates the feasibility of the PDAC-on-chip as a relevant model for CRT applications and enables mechanistic investigations of how vascular architecture and desmoplasia influence PDAC radio- and chemoresistance.

5. References

1. Possenti L. et al., Comput. Biol. Med. 2024; doi:10.1016/j.compbiomed.2024.108334.
2. Ghaffarizadeh A. et al., PLoS Comput. Biol. 2018; doi: 10.1371/journal.pcbi.1005991

Acknowledgements

This work was funded by 5xmille funds for healthcare research (Ministry of Health)

A POROELASTIC MIXED FINITE ELEMENT FORMULATION FOR MODELLING THE INTERVERTEBRAL DISC

Liliana Sierra Fisher (1), Callum J. Runcie (1), Andrei G. Shvarts (1), Lukasz Kaczmarczyk (1) and Jérôme Noailly (2)

1. Glasgow Computational Engineering Centre, University of Glasgow, United Kingdom;
2. BCN MedTech, Universitat Pompeu Fabra, Spain.

1. Introduction

This work presents a hybridised mixed finite element formulation for modelling solid–fluid interaction within a fully saturated porous media, motivated by the numerical challenges encountered when simulating biological tissues such as the intervertebral disc (IVD) [1]. Non-physical pressure oscillations and numerical instabilities caused by transient loading limit the reliability of standard low-order formulations. By leveraging the open-source parallel finite element library MoFEM [2], this research aims to develop a robust IVD model establishing the foundation for large-scale biomedical simulations capable of bridging mechanical and inflammatory dimensions [3].

2. Materials and Methods

A linear poroelastic framework is adopted in which displacement, fluid pressure, and fluid flux are treated as independent fields. In contrast to the standard formulation, fluid flux is approximated as an independent field in the $H(\mathrm{div})$ (Raviart-Thomas) space. Pressure is approximated in the discontinuous L^2 Lebesgue space (instead of the continuous H^1 Sobolev space). This mixed approach effectively eliminates non-physical pressure and flux oscillations typically caused by instantaneous loading and abrupt material property changes, improving the accuracy of the solution. Through hybridisation – approximating the flux field in a 'broken' $H(\mathrm{div})$ space - continuity of normal flux is imposed through the introduction of Lagrange multipliers on element interfaces [4]. This method decouples the flux and pressure fields such that the "locking" effect (pressure instability) observed in simulations involving nearly incompressible constituents or low permeability is mitigated, resulting in a more robust and stable solution.

3. Results

The proposed formulation is validated against classical analytical benchmarks alongside biomechanical simulations of hydrated tissues replicating the experimental and numerical results of Chandran and Barocas [5] and Castro [6], respectively. Alongside mitigating the locking phenomenon commonly observed in poroelastic problems [7], this hybridised approach enables static condensation, resulting in a better-conditioned, faster solution which is optimised for parallel architectures and GPU acceleration. Current research is focused on applying this solver to patient-specific meshes of the IVD, establishing the framework's utility for clinical modelling.

4. Discussion and Conclusions

This numerical foundation is an essential step towards a scalable poro-hyperelastic solver capable of computing large-scale, patient-specific simulations of the full spine. The current framework provides the necessary stability and scalability to incorporate non-linear constitutive laws, fibre induced anisotropy, Donnan osmotic pressure, and strain-dependent permeability in the future.

5. References

1. Vignollet, J., Kaczmarczyk, L., and Pearce, C. J. (2013). Computers & Structures, vol. 118, pp. 109–114. doi: 10.1016/j.compstruc.2012.10.010.
2. Kaczmarczyk, Ł., et al. (2020). Journal of Open Source Software, vol. 5, no. 45, p. 1441. doi: 10.21105/joss.01441.
3. Malandrino, A., et al. (2015). Frontiers in Bioengineering and Biotechnology, vol. 3. doi: 10.3389/fbioe.2015.00005.
4. Dobrev, V., et al. (2017). LLNL-JRNL-732140, SIAM.
5. Chandran, P. L., and Barocas, V. H. (2004). Journal of Biomechanical Engineering, vol. 126, no. 2, pp. 152–166. doi: 10.1115/1.1688774.
6. Castro, A. P. G., Yao, J., Battisti, T., and Lacroix, D. (2018). Frontiers in Bioengineering and Biotechnology, vol. 6, p. 142. doi: 10.3389/fbioe.2018.00142.
7. Phillips, P. J. (2005). PhD dissertation, The University of Texas at Austin, Austin, Texas.

SYNTHETIC POPULATION OF ALZHEIMER'S DISEASE TO TRAIN MACHINE LEARNING PREDICTIVE ALGORITHMS

Chiara Pollicini (1)*, Raimondo Reggio (1)*, Benedetta Baldini (1)*, Vito Ivano D'Alessandro (2)*, Luisa De Palma (2), Attilio De Nisio (2), Anna Lanzolla (2), Tiziana Basileo (2), Filippo Attivissimo (2), Emilio Merlo Pich (1).

(1) IFAB, International Foundation for Artificial Intelligence and Big Data for Human Development, Bologna, Italy; (2) Department of Electric and Information Engineering, Polytechnic University, Bary, Italy. *The first 3 authors equally contributed to this project.

1. Introduction

Alzheimer's Disease (AD) exhibits slow, nonlinear progression of brain structure neuropathology starting 10-15 years before cognitive impairments become clinically measurable. Longitudinal studies showed a substantial inter-individual variability but a common trend starting from a Prodromal AD (PrAD) condition characterized by biomarkers and neuroimaging changes progressing then to the stage of Minimal Cognitive Impairment (MCI) and eventually to dementia (AD). The observation that novel therapeutics work better when given at the very early stages of the disease progression is calling for reliable methodologies to estimate the individual risk of cognitively normal (CN) subjects. While large cohorts of participants progressing in AD are current available, missing data and other allocation errors are importantly often reducing the reliability of datasets needed for machine learning training or LLM modelling. For this reason, we set to develop synthetic patients from a selected datasets of real participants to the ADNI database and explore their capability to individual risk assessment at the CN stage for developing dementia in the 5-10 years window.

2. Materials and Methods

We generated a synthetic cohort of 1,500 AD-spectrum patients using a modified AD Course Map algorithm, nonlinear mixed-effects model that accounts for individual differences through temporal warping and phenotypic variations. The model integrated 32 multimodal variables common to a real patient population. Form the ADNI database. Individualised predictions were obtained via a pipeline that included CoxPH, Random Survival Forrest and Gradient boosting survival analysis to obtain AUC, NPV and PPV

3. Results

Validation across three dimensions Fidelity, Utility, and Privacy showed that synthetic data preserved statistical properties of real patients. Distributional similarity (KS<0.15) and correlation structure analysis showed minimal absolute difference ≤ 0.05. Temporal dynamics validation revealed matching proportions of non-stationary trajectories (72.1% vs 67.3%) between real and synthetic cohorts. Train-on-Synthetic and Test-on-Real methodology yielded minimal performance degradation (4.67% accuracy decline). Privacy was confirmed using DRC ratio$\leq$0.50 and IMS=0. This validated synthetic cohort was used to assess individualized risk of transition CN-to-MCI and CN-to-AD, obtaining significant NPVs (range 0.87-0.98), but non-significant PPVs at both 5 and 10 years. SHAP analysis identified tau-related biomarkers and episodic memory as primary parameters driving the risk.

4. Discussion and Conclusions

This validated synthetic dataset enables robust fidelity, utility and privacy preservation, and proven useful in exploring key parameters relevant for excluding the progression of CN individual towards dementia within 5-10 years.

5. References

Maheux E, Koval I et al. Nat Commun. 2023 Feb 10;14(1):761.

Acknowledgements:

The project was financially supported by an Innovation Grant 'CN for AI & Big Data', Missione 4, PNRR (Grant no: 0013)

IN SILICO MUSCULOSKELETAL ANALYSIS OF WEAR IN HIP RESURFACING: COMPARISON OF WALKING AND RUNNING

Alican Tuncay Alpkaya (1), Zainab Altai (2)(3), Ajay Kumar (2), Leiming Gao (4), Ahmed Soliman (5), Stephen McDonnell (6), Wenxing Guo (7), Stefan Maas (5), Nelson Cortes (2), Bernard X.W. Liew (2)

(1) Kırklareli University, Kırklareli, Turkey (2) School of Sport, Rehabilitation and Exercise Sciences, University of Essex, Colchester, Essex, United Kingdom (3) Institute of Public Health and Wellbeing, University of Essex, United Kingdom (4) Department of Engineering, Nottingham Trent University, United Kingdom (5) Department of Engineering, Faculty of Science, Technology and Medicine, University of Luxembourg, Luxembourg (6) Division of Trauma and Orthopaedic Surgery, University of Cambridge, Addenbrooke's Hospital (7) School of Mathematics, Statistics and Actuarial Science, University of Essex, Colchester, Essex, United Kingdom

1. Introduction

Hip resurfacing arthroplasty (HRA) is commonly used in young, and active patients considering better joint stability and bone preservation [1], yet implant longevity faces wear-related complications [2]. Although HRA wear has been investigated under walking-representative loading conditions [2], to our knowledge, no study to date has examined its wear performance under high-impact activities such as running. This study investigates wear in hip resurfacing during running compared to walking to better understand implant performance and longevity under high impact loading scenarios.

2. Materials and Methods

Wear in Alumina (Al_2O_3) femoral cap that articulates on an Alumina acetabular socket (Al_2O_3-on-Al_2O_3) was analysed for a HRA patient (Male, 65Years) under walking and running. Personalised hip Joint reaction forces for walking and running were measured and derived using 3D optical motion capture (Vicon) with in-ground force plates (Kister) and musculoskeletal simulations. Resultant reaction force during walking and running is shown in Fig. 1. Finite element (FE) simulations were performed for 5 million cycles (5Mc) using explicit analysis in LS-DYNA.

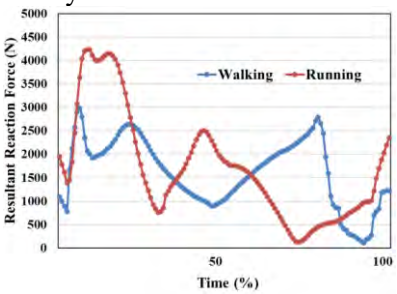


Fig. 1. Resultant joint reaction force profiles under walking and running conditions.

Outer surface of acetabular cup was fixed, and loads were applied through the internal surface of the femoral cap. The Archard wear law applied to compute sliding wear. Geometry was updated after each simulation with a scaling factor of 250,000 cycles.

3. Results

The total linear wear depth was approximately $0.1015mm$ in walking (Fig. 2a), and $0.1117mm$ in running (Fig. 2b), indicating a 10% increase in running. Likewise, mean contact area was approximately $152.9mm^2$ in running and $119.5mm^2$ in walking, corresponds to a 28% increase. Based on linear wear depth and contact area, the estimated volumetric wear was approximately $17.08mm^3$ for running and $12.13mm^3$ in walking, suggesting that running produced about 40.8% greater volumetric wear than walking.

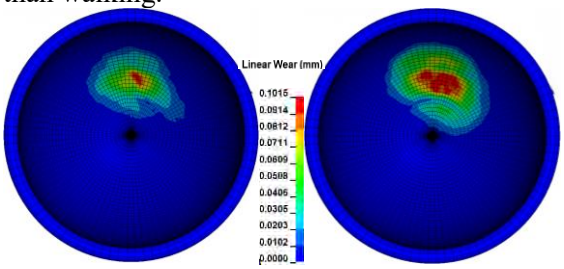


Fig. 2. Predicted wear depth after 5 million cycles: (a) walking, and (b) running condition.

4. Discussion and Conclusions

Despite a modest increase in linear wear depth, the enlarged contact area during running led to substantially higher volumetric wear. Results of this analysis indicated that the joint loading associated with running may accelerate material loss compared to walking. Therefore, activity can be considered as an important factor in the tribological evaluation of implant performance and longevity.

5. References

1.Al-Jabri T., et al., Orthopedic Reviews. 2023;15.
2.Liu F, et al., Journal of Biomechanics, 2008; 41(3):686-694.

Acknowledgements: This work was funded by the Medical Research Council (MR/Y013557/1).

A NETWORK-BASED PHYSIOLOGY-INFORMED RISK SCORE FOR POSTOPERATIVE PULMONARY COMPLICATIONS

D Vijay Anand* (1), Nicholas Tetlow (2), John Whittle (2), Vanessa Diaz (3) Nicholas Ovenden (1) Rebecca Shipley (3)

1) Department of Mathematics, University College London, UK
2) Department of Targeted Intervention, University College London, UK
3) Department of Mechanical Engineering, University College London, UK
*Corresponding author: v.dharmalingam@ucl.ac.uk

1. Introduction

Postoperative pulmonary complications (PPCs) occur in ~10–20% of patients after major surgery and are associated with increased mortality and excess healthcare costs. Existing risk stratification tools are largely based on population-derived scores and provide limited insight into individual physiology. In this study, we use preoperative cardiopulmonary exercise testing (CPET) data within a network physiology[1] framework to quantify coordinated system-level interactions and identify physiological patterns associated with PPCs.

2. Materials and Methods

We collected preoperative CPET data from 92 patients undergoing radical cystectomy surgery. PPCs were defined using the Postoperative Morbidity Survey (POMS) for the pulmonary domain on postoperative days 3, 5, and 7 (PPC: score=1 on all three days; no PPC: score=0 on all three days; n=20 vs n=72). Spearman correlation networks were constructed using the CPET variables, viz. oxygen uptake (VO_2), carbon dioxide production (VCO_2), ventilatory equivalents (VE/VO_2, VE/VCO_2), end-tidal carbon dioxide ($PetCO_2$), and dead-space fraction (V_D/V_T). To ensure network stability, we applied Benjamini–Hochberg false discovery rate control and bootstrap resampling ($q \leq 0.05$, $|\rho| \geq 0.5$), retaining only stable and reproducible edges. A mechanistic cardiorespiratory model [2] was simulated with varied dead-space fraction and ventilatory drive to interpret patient group network differences.

3. Results

The networks showed a ventilatory-efficiency cluster with an inverse VE/VCO_2–$PetCO_2$ relationship, consistent with alveolar ventilation equation $PaCO_2 \propto VCO_2/V_A$, and with effective alveolar ventilation (V_A) reduced at higher V_D/V_T. Patients with PPCs showed stronger coupling of V_D/V_T within this cluster, consistent with a system-level loss of ventilatory efficiency. Elevated VE/VCO_2 and increased V_D/V_T are established predictors of PPCs. Simulations reproduced these dynamics: increasing dead space and ventilatory drive increased VE/VCO_2 and decreased $PetCO_2$, informing a z-score standardised risk score:

$Z = z(VE/VCO_2) + z(V_D/V_T) - z(PetCO_2)$.

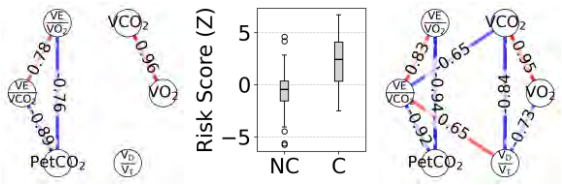


Figure 1: Correlation networks at peak exercise for patients without (left) and with PPCs (right). The risk score shows statistically significant difference.

4. Discussion and Conclusions

CPET correlation networks capture phase-specific differences in coordinated ventilatory-efficiency behaviour associated with PPCs in a radical cystectomy surgical cohort. Mechanistic modelling links these associations to physiological determinants of effective alveolar ventilation and supports an interpretable biomarker construction beyond categorical scoring systems. Prospective validation in larger, independent surgical cohorts is required.

5. References

1. Morandotti, Cecilia, et al. The Journal of Physiology (2025).
2. Timischl S. (Thesis) University of Graz; (1998).

Acknowledgements:
This research/study/project was funded by CHIMERA (EP/T017791/1) and supported by the National Institute for Health and Care Research University College London Hospitals Biomedical Research Centre.

CLINICIAN ENGAGEMENT: TURNING SURVEY RESULTS INTO ACTIONABLE BEST PRACTICES

Janaki Raman Rangarajan[1,2], Finneas J.R. Catling[3,4], Claudio Capelli[4], Zita Vanhorenbeeck[1,2], Erica Beaucage-Gauvreau[2], Irene E Vignon-Clemente[5], Liesbet Geris[1,2,6]

1. *VPH Society, Belgium; 2. KU Leuven, Belgium; 3. Imperial College London, UK; 4. University College London, UK; 5. INRIA, Centre de Recherche de Paris, France; 6. U Liege, Belgium*

Janaki@vph-society.org

1. Introduction

Over the past five years, the adoption of digital solutions such as computational modelling and simulation (CM&S) appears to have increased in clinical settings. However, there is a lack of data to periodically assess and monitor this trend. This study aims to collect such relevant data and use them to support the analysis of a dedicated clinical working group, with the goal of translating the findings into actionable best practices and identifying necessary cautions for the VPH community.

2. Materials and Methods

Two surveys were conducted three years apart (2021, n=161 [1]; 2024, n=279 [2]) to evaluate clinician awareness, trust, and barriers regarding use of *in silico* tools in clinics. Both iterations utilized ~25 questions. Quantitative measures tracked awareness and usage, while qualitative metrics assessed trust, barriers, and opportunities. Based on the responses, our working group synthesized successful and unsuccessful engagement strategies into learnings and best practices.

3. Results

The answers to the two surveys showed an increase in familiarity with the concept of in silico medicine (rising from 38.8% to 51.4%) and usage of computational mechanics (increasing from about 27% to 51%) and Artificial Intelligence (rising from 23.3% to 53.3%). The application of modelling continues to grow for intervention planning (22.8% to 55.9%) and enriching diagnosis (29.1% to 43.1%), alongside an increase in usage frequency (exceeding 20 times/year for 37% of respondents, up from 21%).

In addition, discussions within the Clinical WG underscored the importance of nuanced, relatable terminology, such as framing the mechanistic models be explained as capturing the mechanistic principles known from physiology and biology, and ideally also resonating with the clinician's bedside reasoning applied when treating patients. Subsequent testimonials from community members including both modellers and clinicians, highlighted the need for educational initiatives at clinical conferences as well as interdisciplinary training & doctoral programs. They also emphasized the importance of recognizing constraints on time and resources within clinical routines, alongside disparities across healthcare systems and policies.

4. Discussion and Conclusions

The survey results provided quantitative measures on the use of modelling in clinics, while highlighting critical gaps and concerns regarding the applicability and comprehensibility of the models. Deliberations with community members identified several best practices, including the strategic engagement of early-career physicians and the necessity of interdisciplinary cross-fertilization. Furthermore, the analysis also acknowledged a significant mismatch in expectations.

In conclusion, in this study, we present clinical survey results alongside actionable best practices designed to help young researchers foster effective engagement with healthcare professionals.

5. References

1. Lesage R, et al., (2023) *Front. Med.Technol.* 5:1125524.
2. Vanhorenbeeck Z. et al., *VPH 2004 conference*: VPH 2024. p. 202

Acknowledgements:

This work was supported by EU-funded projects, REALM (GN. 101016496) and contributions of VPH Clinical WG members.

IN SILICO MODELS TO SUPPORT THE OFF-LABEL USAGE OF POLYESTER BANDS FOR LUMBAR ISTHMIC RECONSTRUCTION

Chiara Milani (1), Danilo Maritato (1), Laura Scaramuzzo (2,3), Fabrizio Giudici (2), Luigi La Barbera (1)*

1. LaBS, Dept. of Chemistry Materials and Chemical Engineering "G.Natta", Politecnico di Milano, Italy
2. IRCCS Galeazzi-Sant'Ambrogio Hospital, Milan, Italy
3. IRCCS Agostino Gemelli University Policlinic, Rome, Italy

1. Introduction

Lumbar isthmic reconstruction using titanium cables is a standard surgical technique in the treatment of lumbar spondylolysis in young and active patients with a fractured vertebral arch (Fig.1a). This technique preserves spinal mobility, it ensures primary stability and a solid long-term fusion [1], but titanium cables have been recently discontinued by the manufacturer leaving no other option. Thereby, it is urgent to find an alternative effective and safe option.

This *in silico* biomechanical study aims to explore the biomechanical performance of a polyester sublaminar band – today cleared for cervical spine treatments – as an off-label device for isthmic reconstruction (Fig.1b).



(a) standard titanium cable *(b) new polyester band.*

Figure 1: *Isthmic reconstructions using cables/band around the pedicle screws' and below the posterior spinal process of L5.*

2. Materials and Methods

A validated finite element model of the L4-S1 segment of a healthy adult was modified to reproduce a bilateral fracture of the vertebral arch and bilateral pedicle screw implantation [2]. A retrospective database of 12 adolescents with spondylolysis was used to assess model's morphology and its suitability to represent younger patients.

The titanium cable and the polyester band were mechanically tested to characterize their non-linear force-displacement curve up to failure. Each device was virtually implanted on a dedicated spine segments and modelled using 1D elements. Functional loadings combining compressive force (400N) and bending moment (±10.6Nm) were applied [3]. The RoM (range of motion) and the displacements of the fracture gap served to compare primary stability.

3. Results

The adult spine model well matched the anatomical characteristics of the targeted adolescent cohort.

Lateral bending and axial torsion were the movements leading to the highest forces on both devices, but loads never exceeded 15% of the experimental failure. The polyester band proved to be equivalent or even superior to the titanium cable in effectively reducing the RoM, particularly in flexion, extension, and axial torsion. Additionally, the polyester band was more effective than the titanium cable in reducing the displacements of the fracture gap (-87% vs. -73%).

4. Discussion and Conclusions

Model predictions were positively evaluated in both the intact and bilaterally fractured conditions [2]. Although a direct model validation was not possible, the biomechanical model demonstrated good agreement with the successful clinical outcomes previously reported in the literature [1].

The findings indicate that the polyester band represents a promising and safe alternative to the standard titanium cable for isthmic reconstructions, providing adequate primary stability in terms of both RoM and displacements at the fracture gaps.

Based on the *in silico* evidence presented here, polyester bands have now been systematically adopted at IRCCS Galeazzi–Sant'Ambrogio Hospital for lumbar isthmic reconstruction in young and active patients.

Updated clinical follow-ups will be soon presented and discussed, with the goal of further refining and validating the computational models learning from new clinical evidence.

5. References

1. Giudici et al, Eur Spine J, 20 Suppl 1:S115-20, 2011.
2. Haj-Ali et al, Clin Biomech, 68:37-44, 2019.
3. Sairyo et al, Am J Sports Med, 33(4):583-90, 2005.

DEVELOPMENT AND VALIDATION OF DIGITAL TWINS FOR CHD: ENDOVASCULAR PULMONARY FLOW RESTRICTION PROCEDURE

Sara Bonfanti (1,2), Martina Severi (1), Paola Di Vincenzo (1), Maria Alexandra Cetatoiu (1), Emanuele Gasparotti (2), Benigno Marco Fanni (2) Simona Celi (2), Giancarlo Pennati (1), Francesca Berti (1)

1. LaBS – Dept of Chemistry, Materials and Chemical Engineering, Politecnico di Milano, Italy; 2. BioCardioLab – Bioengineering Unit, Fondazione Toscana "Gabriele Monasterio", Massa, Italy

1. Introduction

Pulmonary artery (PA) banding is a palliative surgical strategy to control pulmonary overcirculation in neonates with complex congenital heart disease (CHD). A fully percutaneous alternative, based on off-label use as pulmonary flow restrictor (PFR) of a modified Micro Vascular Plug™ (MVP, Medtronic), has recently emerged to reduce invasiveness [1]. However, device migration, peri-device leakage, and unpredictable post-implant behavior remain major concerns [2, 3].
This study aims to develop and validate a high-fidelity digital twin of an MVP and to integrate it within simplified PA models, based on pre&post implant patient-specific angiographic measurements to investigate device–artery interaction towards a predictive biomechanical framework.

2. Materials and Methods

A geometrically accurate digital twin of the MVP-7Q was reconstructed from high-resolution optical images (Fig. 1a and b). The Nitinol frame was discretized using linear beam elements in Abaqus/CAE 2022, following mesh sensitivity analysis. The parameters describing the superelastic behavior were calibrated and validated through indentation and crush tests [4] (Fig. 1c and d).
Patient-specific deployment simulations (finite element analysis, FEA) were performed using simplified PA models with pre-implant diameters (13 arteries from 7 patients), represented as cylindrical Neo-Hookean hyperelastic shell conduits. The wall mechanical parameters were calibrated to reproduce post-implant angiographic diameters.
To further experimentally validate the computational framework, two mock-up vessels were fabricated using Ecoflex 00-31 silicone (described as a first-order Ogden material), to allow in vitro deployments. First, compliance tests were conducted and compared with corresponding FE simulations to validate the FE replica of mock vessels.
Finally, in vitro and in silico deployment procedures were performed on the mock-vessels, and post-implantation diameters were quantitatively compared.

3. Results

The digital twin accurately reproduced the superelastic response of the Nitinol frame, showing strong agreement between experimental and numerical force–displacement curves in both local and global tests (Fig.1e). During deployment validation (Fig. 1f), the discrepancy between experimental and numerical post-implantation diameters was below 2% in both proximal and distal regions, confirming the predictive capability of the model.

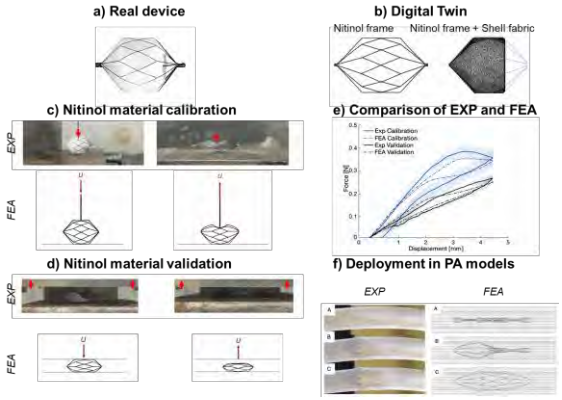


Figure 1: Workflow of the study

4. Discussion and Conclusions

This study presents a validated experimental–computational pipeline for the biomechanical assessment of endovascular PFR. The validated digital twin provides a solid foundation for future simulations and in vitro testing.

5. References

1. Khan AH et al. Cath Cardiov Interv; 93 (2019).
2. Agasthi P et al. PAB. StatPearls (2023).
3. Kizilski SB et al. Cardiov Eng Tech; 14 (2023).
4. Berti F et al. Ann Biomed Eng; 50 (2022).

PERSONALIZATION OF PATIENT-SPECIFIC CARDIAC ELECTROPHYSIOLOGY MODELS IN CONGENITAL HEART DISEASE

Javiera Jilberto (1), Elena Martinez-Sabdy (2), Henry Chubb (1), Alison Marsden (1,2,3,4)

1. Pediatric Cardiology; 2. Institute for Computational and Mathematical Engineering; 3. Cardiovascular Institute; 4. Department of Bioengineering; Stanford University, USA

1. Introduction

Congenital heart defects (CHDs) are structural cardiac abnormalities that often require surgical intervention. Many patients with CHD also develop electrophysiological (EP) abnormalities, further impairing cardiac function. Cardiac resynchronization therapy (CRT) has been shown to restore EP function, but its design and optimization in CHD patients are challenging due to patient heterogeneity [1]. Patient-specific computational models offer a promising framework to optimize CRT by enabling individualized mechanistic investigations. However, personalizing EP simulations requires estimating model parameters from limited clinical data, a process hindered by parameter identifiability issues [2]. In this work, we aim to use body surface potentials (BSPs) recorded during sinus rhythm and CRT pacing in CHD patients to estimate simulation parameters under varying data-availability scenarios and assess estimation accuracy.

2. Materials and Methods

Heart geometries were reconstructed from computed tomography images. Figure 1A shows the geometry and the BSPs leads' position for a CHD patient with congenitally corrected transposition of the great arteries. A Purkinje network with an initial length l_i was generated using the method described in [4]. Simulations were performed by solving the monodomain equation [3]. The conductivity tensor was defined as $\boldsymbol{D} = D_{purk}\boldsymbol{I}$ in the Purkinje network and $\boldsymbol{D} = D_{iso}\boldsymbol{I} + D_{ani}\boldsymbol{f} \otimes \boldsymbol{f}$ in the myocardium, where $\boldsymbol{f}$ denotes the fiber direction. BSPs from 150 simulations with different combinations of $D_{purk}, D_{iso}, D_{ani}, l_i$ were generated using Latin hypercube sampling and used to train branched latent neural maps (BLNMs), to construct a surrogate model [3]. Parameter estimation was performed by minimizing the mean squared error between observed data and BLNM predictions.

3. Results

Figure 1B shows an example of the BLNM estimate fit to the ECG data using synthetic data. The testing MSE for the BSP fit was 5.3 ± 9.3 and 1.2 ± 4.0 mV^2 when using only the 12-lead or the full set, respectively. The parameter estimation errors were 25% and 27% when using the 12-lead or full BSP set, respectively.

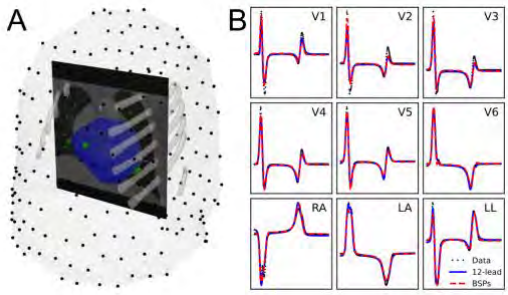


Figure 1: (A) CT heart reconstruction (blue), CRT leads (green), and BSPs (black dots). (B) 12-lead ECG fit using 12-lead or a full set of BSP.

4. Discussion and Conclusions

The flexibility of BLNMs enabled us to generate surrogate models that depend on both EP and geometrical parameters and easily perform uncertainty quantification (UQ) analysis [3]. In the future, to improve parameter estimation, we intend to leverage the full dataset, which includes sinus rhythm and pacing, to perform broader parameter estimation and UQ in a cohort of CHD patients. This study is crucial for understanding and guiding the clinical data collection needed to generate CHD cardiac digital twins.

5. References

1. Chubb H et al., Circ Arrhythm Electrophysiol, (2020); 2. Li et al., IEEE Rev. Biomed. Eng, 18, 316–336. (2024); 3. Salvador M, & Marsden A, Comput. Method. Appl. M., 418, 116499 (2024); 4. Sahli Costabal F et al, J. Biomech., 49(12), 2455–2465. (2016)

Acknowledgements:

The authors would like to thank the American Heart Association (Grant no: 25TPA1481491) for providing financial support to this project.

MULTISCALE SIMULATION FRAMEWORK TO INVESTIGATE ARRHYTHMIA MECHANISMS IN PAEDIATRIC-LIKE VENTRICLES

Leto L Riebel[1], Z Jenny Wang[1], Hector Martinez-Navarro[1], Mark Levin[2], Blanca Rodriguez[1]

[1]University of Oxford, United Kingdom, [2]Departments of Medicine, Pediatrics, and ACE-WS, University of Pennsylvania School of Medicine, USA.

1. Introduction

Congenital diseases underlying vascular dysfunction, such as Williams-Beuren Syndrome, often manifest during childhood where, whilst rare, resulting ischemia may cause devastating ventricular arrhythmias [1].

Modelling and simulation offers a unique tool to systematically investigate arrhythmia mechanisms and identify and test new treatments. Human-based simulations are especially powerful where clinical studies are limited due to ethical concerns or small patient numbers, such as in paediatric diseases.

2. Materials and Methods

Here, we created a human-based multiscale electrophysiological modelling and simulation framework to investigate arrhythmia mechanisms during ischemia in small, paediatric-like ventricles with Purkinje. For this, we scaled an adult human MRI-derived biventricular geometry and corresponding ECG electrodes to produce three further models, corresponding to biventricular masses of an approximately 5-, 9-, and 13-year-old [2].

To demonstrate trust, we considered verification, validation, and uncertainty quantification principles. Particularly, we compared simulated ECGs against clinical ECG biomarkers of children at the corresponding age groups [3]. Finally, to demonstrate the capabilities of our framework, we simulated anteroseptal ischemia in the paediatric-like model to investigate mechanisms of ventricular fibrillation in rare congenital diseases, like Williams-Beuren Syndrome.

3. Results

Our simulations firstly show that lower ventricular mass is responsible for crucial paediatric ECG biomarkers, such as reduced QRS and QT-interval duration.

Furthermore, through 1,200 simulations in the small, paediatric-like ventricles, we show that the maximum action potential shortening (modulated by ischemia-induced ionic remodelling) and the underlying action potential restitution is more determinant of ventricular fibrillation risk than the size of the ischemic area.

Accordingly, we identified wide and flat T-wave peaks, caused by severe ischemia, as well as longer QT duration, caused by patient variability in action potential duration, as ECG markers that may be indicative of elevated arrhythmic burden.

4. Discussion and Conclusions

Our work builds on rigorous validation and knowledge integration in modelling and simulation of ventricular arrhythmias in adults [4], to create a paediatric-specific framework. Whilst further development and validation is required to wholly reproduce paediatric electrophysiology on a multiscale level, our framework demonstrates human modelling and simulation as a powerful tool to identify arrhythmia mechanisms, contribute to risk stratification, and enable virtual therapy testing in vulnerable cohorts, such as children with rare congenital diseases.

5. References

[1] Bird et al., The Journal of Pediatrics (1996).
[2] Khoury et al., Journal of the American Society of Echocardiography (2009).
[3] Saarel et al., Circulation: Arrhythmia and Electrophysiology (2018).
[4] Martinez-Navarro et al., Frontiers in Cardiovascular Medicine (2024).

Acknowledgements:
This project was funded by a Wellcome Trust Senior Research Fellowship in Basic Biomedical Sciences to B.R. (214290/Z/18/Z), the Oxford BHF Centre of Research Excellence (RE/24/130024), and the EPSRC project CompBioMed X (EP/X019446/1).

STUDY OF ELECTROMECHANICAL SIMULATIONS OF RIGHT BUNDLE BRANCH BLOCK IN PAEDIATRIC PATIENTS

Ana Montañés (1), Jorge Sánchez (1), Sandra Pérez (1), Isabel Hernández (1), Jonathan Krauß (3), Ferran Prats (2), Ferran Roses (2), Javier Saiz (1), Beatriz Trénor (1)

1. Research Center for Biomedical Engineering and Innovation (Ci2B), Universitat Politècnica de València, Spain; 2. Department of Paediatric Cardiology, Vall d'Hebron University Hospital, Barcelona, Spain; 3. Institute of Biomedical Engineering, Karlsruhe Institute of Technology, Karlsruhe, Germany

1. Introduction

Incomplete right bundle branch block (IRBBB) is a common finding in paediatric electrocardiograms, particularly in children aged 5-12 years [1]. Although often considered a benign physiological variant, delayed right ventricular activation may alter ventricular contraction timing, with consequences for cardiac mechanics and haemodynamics. This project addresses the limited understanding of these biomechanical effects by developing personalized 3D whole-heart computational model of the paediatric heart to investigate different right bundle branch block (RBBB) scenarios through electromechanical simulations.

2. Materials and Methods

A 9 year-old patient-specific three-dimensional whole-heart paediatric model was reconstructed from clinical imaging, including fibre orientation and a His-Purkinje conduction system. Electrical propagation was simulated using an eikonal model with detailed human cellular models. Myocardial mechanics incorporated active [2] and passive properties [3] and fully coupled to a 0D circulatory model [4]. Complete right bundle branch block (CRBBB) and different IRBBB scenarios were simulated to assess the electrical dyssynchrony and its consequences on ventricular contraction dynamics.

3. Results

RBBB increases the filling pressure of the right ventricle (RV). The magnitude of this alteration varies across simulated RBBB scenarios, as shown in Figure 1. Due to IRBBB or CRBBB, an electrical delay in the activation shifted the volume curves in time, as shown in Figure 2. However, that shift did not alter the total volume of the RV cavity. The same phenomena were observed for the mean deformation along the longitudinal fibre direction.

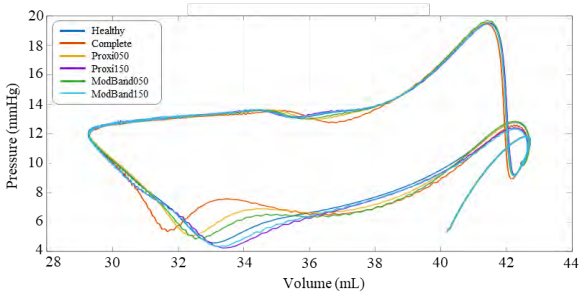


Figure 1: PV-Loops right ventricle.

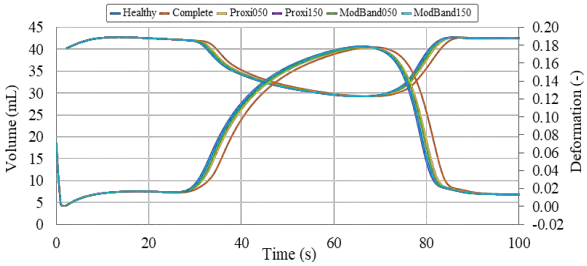


Figure 2: Time course of volume and deformation.

4. Discussion and Conclusions

In our whole-heart simulations, without structural remodelling, RBBB, altered electrical behaviour preserving global mechanical function, although delayed ventricular activation and contraction were observed.

5. References

1. Meziab O et al., Congenital Heart Disease; 13(3):419–427 (2018).
2. Land S et al., Journal of Molecular and Cellular Cardiology; 106:68–83 (2017).
3. Usyk TP et al., in Cardiovascular Soft Tissue Mechanics (Cowin SC, Humphrey JD, eds.); Kluwer Academic Publishers:143–164 (2004).
4. Gerach T et al., Mathematics; 9(11):1247 (2021).

Acknowledgements:

This work was partially funded by the Generalitat Valenciana (CIPROM/2023/2014) and by grant PID2022-140553OB-C41 funded by MICIU/AEI/10.13039/501100011033 and FEDER/UE. The authors also acknowledge the support of the TecnoVitae Foundation.

QUANTIFYING THE ENERGETIC BURDEN OF FONTAN STENOSES: A PATIENT-SPECIFIC CFD STUDY

Jan Brüning[1,2], Adriano Schlief[1,2], Marie Schafstedde[1,2,3], Anastasia Schleiger[2,3], Peter Kramer[2,3]

Deutsches Herzzentrum der Charité, Institute of Computer-assisted Cardiovascular Medicine, Berlin, Germany; 2. Charité - Universitätsmedizin Berlin, Berlin, Germany; 3. Deutsches Herzzentrum der Charité, Department of Congenital Heart Disease, Berlin, Germany

1. Introduction

Patients with univentricular heart defects who have undergone Fontan palliation face long-term complications due to the lack of a sub-pulmonary ventricle, leading to elevated central venous pressure and limited cardiac output. While stenoses in the pulmonary arteries or the Fontan conduit are common, identifying which lesions require intervention remains challenging; morphological findings often do not clearly correlate with clinical symptoms or invasive pressure gradients. This study aims to utilize patient-specific *computational fluid dynamics* (CFD) to objectify the hemodynamic burden of such stenoses and evaluate the potential benefit of virtual stenting to support clinical decision-making.

2. Materials and Methods

A cohort of 30 Fontan patients, categorized into three groups, was identified:

- **Group 1**: 10 patients with pulmonary artery stenosis (either left or right) treated via stenting.
- **Group 2**: 10 patients with Fontan conduit stenosis treated via stenting.
- **Group 3**: 10 control patients without hemodynamically relevant stenosis.

Patient-specific 3D anatomies are reconstructed from pre-interventional MRI or CT data. For Groups 1 and 2, the post-interventional vascular geometry is created by geometrically implanting a virtual stent mimicking the exact device used for the intervention. These anatomical models are validated against planar measurements obtained via angiography during the intervention. Steady-state CFD simulations are performed for the pre- and post-interventional states. Inflow and outflow boundary conditions are set using 4D velocity-encoded MRI data when available. Otherwise, literature-based flow splits for the venae cavae and pulmonary arteries are applied alongside echocardiography-based cardiac output measurements. Key functional parameters, specifically power loss and circulatory efficiency, are calculated to quantify the energetic burden. Finally, these hemodynamic markers are compared against patient-reported quality-of-life questionnaires to establish clinical relevance [1].

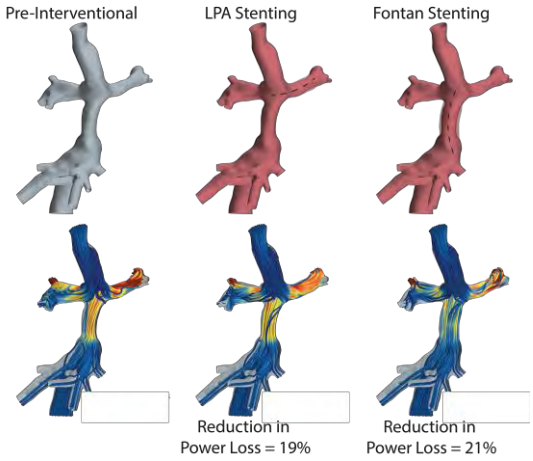


Figure 1: Change in power loss due to different stenting strategies respectively.

3. Anticipated Results and Discussion

This study is designed to demonstrate that CFD can provide objective criteria, such as a threshold for power loss, that justify interventional therapy even in asymptomatic patients. By comparing pre- and post-stenting simulations, we expect to quantify the "hemodynamic gain" achieved by the intervention. It is hypothesized that standardizing these simulations will allow for a reproducible assessment of whether a stenosis significantly compromises the Fontan circulation. Ultimately, this virtual treatment planning approach aims to reduce unnecessary radiation exposure from heart catheterizations and improve long-term outcomes by optimizing patient-specific therapy.

4. References

1. Mercer-Rosa L et al. *The Annals of thoracic surgery* vol. 114,3 (2022): 841-847.

Acknowledgements:

Supported by the Deutsche Herzstiftung e.V. (Project: “Computergestützte individuelle Therapieplanung bei Patienten mit univentrikulären Herzfehlern”)

QUANTIFYING THE BIOLOGICAL SIGNIFICANCE OF UNCERTAINTY IN HAEMODYNAMIC MODELS OF INTRACRANIAL ANEURYSMS

Natalie Benson (1, 2), Jovana Serbanovic-Canic (3), Melika Gul (1, 2), Alberto Marzo (1, 2)

1. School of Mechanical, Aerospace and Civil Engineering, The University of Sheffield, UK; 2. INSIGNEO Institute for in silico medicine, The University of Sheffield, UK; 3. School of Medicine and Population Heath, The University of Sheffield, UK

1. Introduction

Haemodynamics are a primary driver of intracranial aneurysm (IA) development and rupture risk. While computational fluid dynamics (CFD) is increasingly used to predict clinical outcomes, results are highly sensitive to modelling choices - such as anatomy reconstruction, solver type, and boundary conditions - leading to often "acceptable" discrepancies in flow predictions. Specifically, Benemerito and McCollough [1] identified wall shear stress (WSS) variability of up to 2.5 Pa, alongside significant uncertainty ranges in the Oscillatory Shear Index (OSI) (0.25-0.5) between different numerical methods (finite volume and lattice Boltzmann) and parameter variability. This study evaluates the biological significance of these uncertainties, demonstrating how minor variations in flow parameters can trigger vast differences in endothelial cell (EC) response.

2. Materials and Methods

Human aortic endothelial cells (HAECs) from four distinct donors were used across four experimental repeats (n=4) to evaluate biological responses to haemodynamic variability. Cells were exposed to flow conditions for 72 hours, with WSS magnitudes of 0.4, 1.5, and 3 Pa applied under both steady unidirectional laminar flow and oscillatory (1 Hz) regimes. Immunofluorescence was employed to quantify the expression and localisation of eNOS and VE-cadherin. Statistical significance was determined via two-way ANOVA followed by Tukey's multiple comparisons test using GraphPad Prism v10.6.1, with an alpha value of $p < 0.05$.

3. Results

Exposure to physiological and disturbed flow regimes induced distinct changes in endothelial phenotype and function (Figure 1).

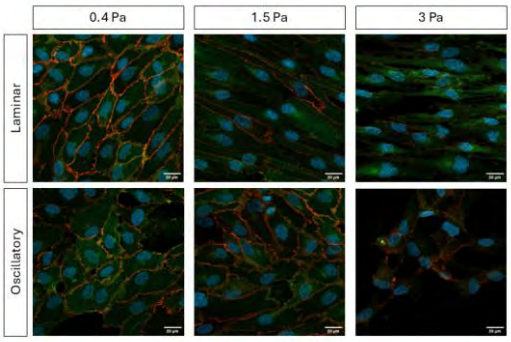


Figure 1: Immunofluorescence images of HAECs.

eNOS expression was significantly upregulated in HAECs exposed to steady unidirectional 1.5 and 3 Pa WSS compared to those under oscillatory and 0.4 Pa shear stress ($p < 0.0001$). Flow-induced alterations in VE-cadherin expression and organisation were observed ($p < 0.0001$). Specifically, disturbed flow disrupted VE-cadherin dynamics at cell-cell junctions, resulting in discontinuous VE-cadherin junctional staining, indicating impaired barrier integrity.

4. Discussion and Conclusions

This study demonstrates that "accepted" numerical discrepancies in CFD models carry profound biological significance. Our results prove that shifting haemodynamics within specific ranges fundamentally alters endothelial phenotypes. Specifically, variations in WSS magnitude and direction triggered significant changes in eNOS expression and VE-cadherin junctional integrity. These findings bridge the gap between fluid dynamics and cellular mechanobiology , emphasizing that even minor model uncertainties can lead to divergent biological predictions. For CFD to reliably inform clinical decisions regarding IA progression, models must achieve a level of precision that respects these biological thresholds.

5. References

1. Benemerito I, McCullough J, Narracott A, Coveney PV, Marzo A. Comput Biol Med. 2025;197(PtB):111050. (2025)

CALCIFICATION MORPHOLOGY AND HEMODYNAMICS IN THE INTRACRANIAL CAROTID ARTERY: A 3D AND 1D FSI FRAMEWORK

Federica Fontana (1,2), Pritesh Ramya (1), Mathieu J. B. M. Pourquie (1), Frank J. H. Gijsen (1,2), Daniel Bos (2), Ali C. Akyildiz (1,2), Selene Pirola (1)

1. Delft University of Technology, The Netherlands; 2. Erasmus Medical Center, The Netherlands

Corresponding Author: Federica Fontana, f.fontana@tudelft.nl

1. Introduction

Intracranial Carotid Artery (ICA) calcifications are established risk factors for cerebrovascular diseases, such as dementia and stroke. Current studies on intracranial arteriosclerosis have focused on calcium volume as a marker of disease burden, neglecting the role of calcification morphology and its impact on ICA hemodynamics. This study addresses this gap through a framework combining morphometric analysis with 3D and 1D Fluid-Structure Interaction (FSI) modelling.

2. Materials and Methods

From CTA images of 100 stroke patients, lumen and calcifications of 200 ICAs were reconstructed, and morphometric features automatically extracted [1]. 3D FSI models of a subgroup of 4 arteries were developed in FEBio (Fig. 1). A sensitivity study on key modelling choices – inclusion of surrounding tissues, wall thickness, and initial wall stresses – informed 3D FSI simulations comparing calcified and non-calcified models. In parallel, parametric 3D FSI models of vessels with varying calcification degree were used to derive constitutive relations for a 1D FSI model, via polynomial regression on transmural pressure and lumen radius data.

3. Results

The morphometric analysis revealed a prevalent calcium location in the C4 segment (56.0%), with anteroinferior orientation (38.5%), a mean circumferential width of 43.5°, and a mean thickness of 1.2 mm. The sensitivity study showed that surrounding bone tissue significantly alters all biomechanical factors (+42% in 1st Principal Stresses, +18% in Pulsatility Index and Pressure drop, +5% in TAWSS). In the four-patient comparison, calcifications consistently induced stress concentrations near the inclusion (max principal stress +50%) with a limited pressure drop increase (+5%). The 1D model reproduced 3D transmural pressure results within 1% maximum deviation (Fig. 2).

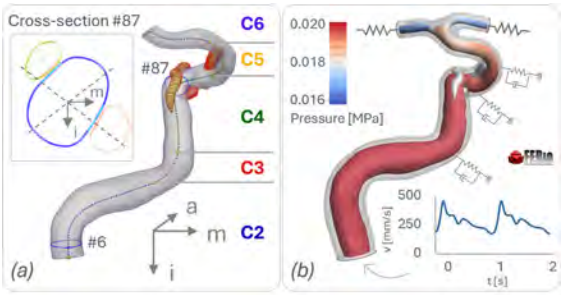


Figure 1: ICA division in the C2 to C6 segments. The anterior, inferior, and medial orientations are indicated (a). 3D FSI model of a patient-specific left ICA, with a representation of the main BCs (b).

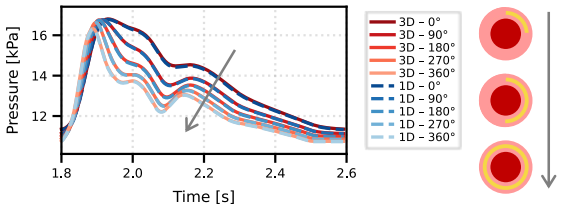


Figure 2: Comparison of transmural pressure between 3D and 1D models, for varying circumferential calcification extents (°).

4. Discussion and Conclusions

This study provides a morphometric characterisation of ICA calcifications. The developed 3D FSI models represent a verified tool to study the hemodynamic impact of calcifications across their wide morphological variability. The 3D and 1D frameworks can offer complementary perspectives on local flow alterations and propagation of pressure disturbances in downstream vascular networks, respectively. Future work will extend both approaches to larger patient cohorts, accounting for calcification morphology.

5. References

1. Berghout BP & Fontana F et al., J Clin Med, 14(10) 3274, (2025)

EXPLORATION OF FLOW DIVERSION FOR BIFURCATION ANEURYSMS

Benjamin Csippa (1), Levente Sándor (1), György Paál (1), Isvtán Szikora (2)

1. Budapest University of Technology and Economics, Department of Hydrodynamic Systems, Hungary; 2. Semmelweis University, Department of Neurosurgery and Neurointerventions, Hungary

1. Introduction

Recently, due to high rates of complete occlusion in sidewall cases, flow diverters (FDs) are increasingly used for bifurcation aneurysms. However, more distal bifurcation aneurysms present a new challenge: jailing a main side branch. This warrants a deeper understanding of necessary flow modification and the risks of branch compromise; a task suited for in silico hemodynamics analysis.

2. Materials and Methods

We used our in-house computational framework for the deployment of flow diverters and subsequent hemodynamic analysis, detailed in [1]. Six bifurcation aneurysms were selected, comprising two each of the ACA, MCA, and basilar tip locations. Two flow diverters were selected—one with higher and one with lower hydrodynamic resistance—to reflect nominal and oversized scenarios. Both branches were stented individually, and two ICA waveforms were selected from the literature to represent male and female phenotypes [2].

First, the aneurysmal mean velocity reduction (AMVR) [1] was used to evaluate post-interventional hemodynamics with 35% threshold [3] for adequate surrogate metric. Additionally, the cycle-averaged branch flow rate reductions were computed to analyse the jailing effect.

3. Results

In all cases and virtual treatment scenarios considered, AMVR was higher using the male waveform, still case-to-case variability was significant as anatomies respond differently to different FD scenarios. In four of the six cases AMVR > 35% were achieved regardless of the waveform or the branch selection. After quantifying the side-branch flow reductions a strong geometry and branch selection dependence was observed with high degree of complexity whether a "jailed" artery will behave due the rerouting of the flow splitting.

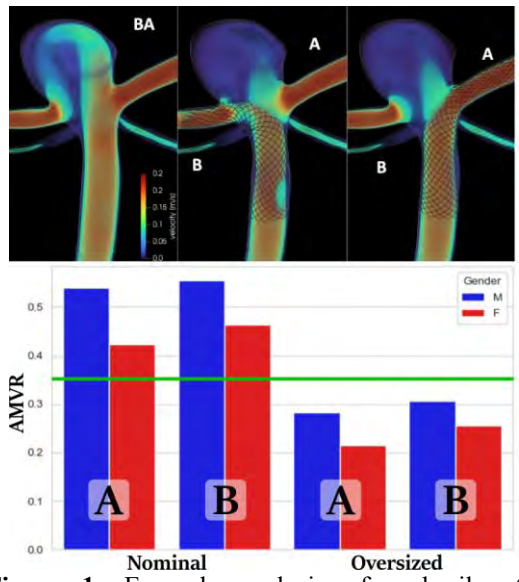


Figure 1: Example analysis of a basilar tip aneurysm. Top: flow field before and after the treatment into one or the other side branche. Bottom: AMVR for all cases considered. Green line shows the literature threshold of 35% AMVR.

4. Discussion and Conclusions

FD efficacy for bifurcation aneurysms appears to be less consistent than for sidewall cases, notably, two of six cases failed to reach the AMVR > 35% surrogate threshold despite varying the inlet waveforms or branch selection. These findings, validate clinical intuition that FD treatment for bifurcation aneurysms are inherently more challenging, necessitating further investigation.

5. References

1. Csippa B et al., Clin Neuroradiol; 2024:9 (2024).
2. Kim M O et al., J Hypertens; 35(11):2245-2256 (2017).
3. Ouared R et al., J Neurointerv Surg; 8(12):1288-1293 (2016).

Acknowledgements:

GEMINI has received funding from the European Union's Horizon Europe research and innovation program under the grant agreement No 101136438. We acknowledge the Digital Government Development and Project Management Ltd. for awarding us access to the Komondor HPC facility based in Hungary.

PATIENT-SPECIFIC HAEMODYNAMIC MODELLING OF THROMBECTOMY EXTRACTION FORCE

Nida Ruseckaite (1*), Abhishekh H. Ashok (2*), Tomasz Matys (2*), Yogish Joshi (2*), Rohan Mudkavi (3), Georgios Toumbas (4*), Joshua Kaggie (2*), Nicholas Evans (5*), Shelly Singh-Gryzbon (1*)

*1. Dept of Chemical Engineering & Biotechnology; 2. Dept of Radiology; 3. East & North Hertfordshire Teaching NHS Trust, Stevenage, UK; 4. School of Clinical Medicine; 5. Dept of Clinical Neurosciences; * University of Cambridge, Cambridge, UK*

Correspondence to Nida Ruseckaite, Dept of Chemical Engineering & Biotechnology, University of Cambridge, CB3 0AS Cambridge, UK; nr577@cam.ac.uk

1. Introduction

A Direct Aspiration first-Pass Technique for mechanical thrombectomy (MT) achieves high recanalisation rates and is cost-effective when used alone; however, the mechanical forces required to dislodge a clot of varying size and composition remain poorly quantified. Therefore, this study analyses the relative contribution of wall-clot friction and haemodynamic loading to extraction resistance.

2. Materials and Methods

Seven MT cases with MCA M1/M2 occlusions were selected from the Addenbrooke's Hospital registry (REC: 20/HRA/5531). Patient-specific vascular models were reconstructed from CTA images, and clot location and length identified. Clot type (white [W], mixed [M], red [R]) and corresponding friction coefficients ($\mu_W = 0.258$, $\mu_M = 0.209$, $\mu_R = 0.247$) were estimated from median Hounsfield unit values and literature correlations [1,2]. CFD simulations were performed using non-Newtonian (Bird-Carreau) laminar flow with pulsatile inlet conditions, three-parameter Windkessel outlets, and no-slip boundaries at vessel walls and the proximal clot surface to approximate stagnation pressure. The required pull force F_{Req} was calculated using Eq. 1., where F_{Drag} is peak systolic hemodynamic force, P_{Sys} is systolic blood pressure, D is vessel diameter, and L is clot length.

$$F_{Req} = \left(\mu \cdot P_{Sys} \cdot \pi \cdot D \cdot L\right) - F_{Drag} \qquad (1)$$

3. Results

Wall-clot friction was the dominant resistive force, while hemodynamic loading assisted dislodgement, offsetting frictional resistance by ~22% at peak systole. White thrombi required higher pull force (F_{Req}>0.45 N) than red or mixed types (Fig. 1.). However, predicted extraction force did not directly correspond to procedural outcome. The case requiring the most passes (n = 5) had the lowest predicted pull (0.1 N), whereas the highest resistance (0.58 N) achieved single-pass success with aspiration alone. Combined techniques were mainly used for red and mixed thrombi.

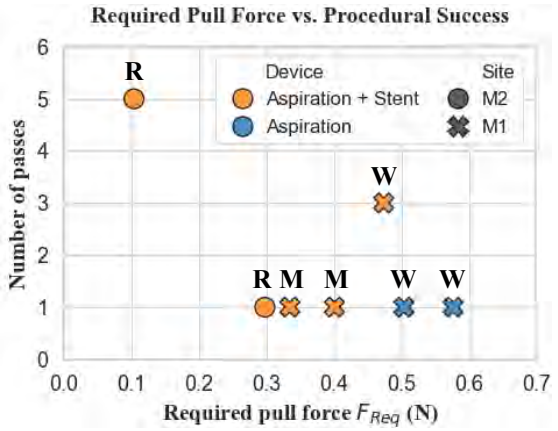


Figure 1: Number of passes vs estimated extraction force [W-white, M-mixed, R-red].

4. Discussion and Conclusions

This preliminary patient-specific framework isolates the roles of frictional and haemodynamic forces in MT. While white thrombi present higher frictional burdens, their stiffness may facilitate a more stable clot-catheter interface, enabling single-pass clot retrieval in larger M1 vessels. Conversely, higher pass rates in distal M2 segments despite lower resistance suggest procedural failure is governed by anatomical accessibility and engagement efficiency rather than friction. Future work will expand these findings in a bigger patient cohort.

5. References

1. Gunning GM et al., J NeuroIntervent Surg 2018;10(1):34–38 (2017).
2. Songsaeng D et al., Asian J Neurosurg. 2019;14(3):795-800 (2019).

Acknowledgements:
This project is supported by the W. D. Armstrong Trust Fund.

CFD-BASED IDENTIFICATION OF VASOSPASM PREDICTORS IN ANEURYSMAL SUBARACHNOID HEMORRHAGE

Elisabetta Criseo (1), Marianna Di Feliciantonio (2), Katerina Negri (2), Luca Caschera (3), Luca Mariani (1), Tommaso Zoerle (2), Giorgio Conte (3), and Alberto Redaelli (1)

1. Department of Electronics Information and Bioengineering, Politecnico di Milano, Milan, Italy; 2. Neuroscience Intensive Care Unit, Department of Anesthesia and Critical Care, Fondazione IRCCS Ca' Granda Ospedale Maggiore Policlinico, Milan, Italy; 3. Neuroradiology Unit, Fondazione IRCCS Ca' Granda Ospedale Maggiore Policlinico, Milan, Italy

Corresponding author: Elisabetta Criseo; email: elisabetta.criseo@polimi.it

1. Introduction

Aneurysmal subarachnoid hemorrhage (aSAH) is a life-threatening condition caused by the rupture of an intracranial aneurysm [1]. Vasospasm is a major complication of aSAH; developed 4 to 14 days after aSAH, it is a diffused narrowing of cerebral arteries that can cause cerebral infarction [2]. Vasospasm risk stratification is performed in clinical practice using grading scales with poor predictive accuracy. This work investigates the possibility of using complementary information extracted from personalized 3D CFD simulations of the cerebral vasculature, performed on admission imaging, for vasospasm risk assessment.

2. Materials and Methods

To develop the patient-specific models of four aSAH patients (two vasospasm-free patients, P1 and P2, and two pathologic, P3 and P4), only routinely acquired clinical data were used. The geometries of the carotid, vertebral and cerebral arteries are reconstructed from the patients' admission angio-CTs. The inlet flow rate is estimated from the patients' hemodynamic information, while outlet boundary conditions are imposed using resistances. These are calibrated with a 0D model generated from the centreline of the patient-specific geometry; the calibration aims to match the computed flow rate to the TCCD-measured one at the middle cerebral arteries (MCA). The steady-state CFD simulations with calibrated outlet resistances are performed using Simvascular.

3. Results

In the 3D CFD simulations analysis, a comparison between pathologic and vasospasm free patients is performed, revealing marked underperfusion in some Circle of Willis (CoW) branches of the two vasospasm patients. P3 presents a flow difference of 370% (26 ml/min) between the two least perfused branches, which are the anterior cerebral artery (ACA) and the posterior communicating artery (Pcom), while for P4 the difference is 58% (18 ml/min) between the two anterior cerebral arteries. In vasospasm-free patients, a much less marked difference is observed, as in the two least perfused branches the flow differs of 2 ml/min and 12 ml/min in P1 and P2, respectively, involving in both cases, the Pcom. Additionally, the helicity of the flow is analysed and the descriptors defined in [3] are computed. Patients that will develop vasospasm show higher propensity to develop vortical flow in the ACA than vasospasm-free patients. Markers of disturbed shear are identified in P3 both in the anterior cerebral artery and in the anterior communicating artery. Note that P2, P3 and P4 share the aneurysm position, in the anterior communicating artery.

4. Discussion and Conclusions

These findings suggest that the presence of certain hemodynamic features could influence vasospasm pathogenesis. Underperfusion of some pathways in the CoW could be an indicator of a poor ability to exploit collateral pathways, and in case of arterial narrowing, determine a worse outcome. Nevertheless, determining whether hemodynamics contribute to risk requires validation in a larger population with adequate statistical power, which is currently an ongoing activity.

5. References

1. J. Claassen and S. Park. *The Lancet*, 400(10355):846–862 (2022).
2. C. A. Luisi, et al. Scientific Reports, 14(1):8194, (2024).
3. D. Gallo, et al. Journal of biomechanics 45.14 (2012): 2398-2404.

ELECTRICAL IMPEDANCE-BASED ORAL CANCER DIAGNOSIS USING COMPUTATIONAL AND IN VITRO MODELS

Malwina Matella (1), Rachel Furmidge (2), Mary Paterson (3), Craig Murdoch (2), Helen Colley (2), Zi-Qiang Lang (3), Dawn Walker (1)

1. School of Computer Science, University of Sheffield, UK; 2. School of Clinical Dentistry, University of Sheffield, UK; 3. School of Electrical and Electronic Engineering, University of Sheffield, UK

1. Introduction

According to WHO [1], in 2022 there were almost 400,000 new cases and 200,000 deaths related to oral cancer worldwide. Oral cancer diagnosis involves scalpel biopsy followed by histopathological assessment, which is a painful, invasive procedure, with long waiting times. Electrical impedance spectroscopy (EIS) is a non-invasive technique that allows real-time detection of pathological and cancerous tissue changes based on the influence of cellular level tissue structure on the opposition to the flow of alternating current. In this pilot study, we aim to explore the feasibility of EIS in detecting oral cancer and dysplasia using tissue engineering and computational models.

2. Materials and Methods

Tissue-engineered (TE) models of healthy, dysplastic and cancerous oral epithelium were grown in an in vitro environment, and their impedance was measured using a tetrapolar EIS device. Histology images of these tissues provided data to inform 'Virtual Oral Tissues' (VoTs). Due to the structural complexity of biological tissues, we developed a multiscale computational finite element (FE) model which consists of cellular and tissue scale levels, where the transfer impedance results from lower scale are assigned as material properties on the higher level. Initially, the FE models were used to investigate the impact of tissue characteristics that relate to the WHO list of features characterising dysplasia [2] on computed EIS spectra. Secondly, the FE model was used to simulate a virtual spectra dataset to augment the TE measurements. Simulated EIS spectra were used to build neural networks (NN) to classify TE healthy, dysplastic and cancerous oral epithelium.

3. Results

Comparison of the EIS spectra from in vitro TE models and computational models revealed a promising agreement for all types of tissues. Assessment of the simulated morphological features of oral dysplasia features suggested that extracellular space thickening, surface keratin and loss of stratification had the highest impact on the EIS signal. A NN classifier was trained on the FE and fine tunned on a subset of the TE spectra (unused for testing), this achieved a balanced accuracy of 77.4% in discriminating dysplasia, cancer and healthy tissues, and 85.8% in classifying cancer and dysplasia.

4. Discussion and Conclusions

In summary, our preliminary investigation showed the utility of FE and ML models in predicting and classifying the EIS spectra of healthy and pathological oral epithelium in vitro models. Moreover, the FE-based computational modelling permitted the identification of influential dysplastic tissue characteristics which impact the EIS signal, suggesting this technology might be suitable for dysplasia detection that could help us improve and speed up the current suspected cancer patient's pathways. In the future, we plan to translate this research to a clinical investigation with patient cohorts to further test the effectiveness of EIS technology in the in vivo environment.

5. References

1. Global Cancer Observatory, WHO International agency for research on cancer (online: https://gco.iarc.who.int/media/globocan/factsheets/populations/900-world-fact-sheet.pdf)
2. WHO Classification of Tumours Editorial Board. Head and Neck Tumours. Lyon: IARC, 2023.

Acknowledgements:
The work was funded by Yorkshire Cancer Research Sheffield Pioneer Award (YCRSPF/2023/172).

Correspondence:
Dawn Walker: d.c.walker@sheffield.ac.uk

ATLAS: INTEGRATING AI, KNOWLEDGE GRAPHS, AND COMPUTATIONAL LIVER MODELS FOR CLINICAL TUMOR BOARD DECISION SUPPORT IN LIVER ONCOLOGY

Anton Schnurpel (1), Mojtaba Nayyeri (2), Mariia Myshkina (3), Luis Mandl (1,2), Sandra Nickel (1), Matthias König (3), Steffen Staab (2), Tim Ricken (2), Hans-Michael Tautenhahn (1)

1. University of Leipzig Medical Center, Germany; 2. University of Stuttgart, Germany; 3. Humboldt University of Berlin, Germany

1. Introduction

Treatment decisions in liver oncology are complex and commonly discussed in multidisciplinary tumor boards. For major entities such as hepatocellular carcinoma (HCC) and cholangiocarcinoma (CCC), therapeutic strategies depend on numerous clinical, imaging, and pathological parameters. Despite the availability of clinical guidelines, tumor board decisions often remain experience-driven and lack systematic integration of heterogeneous patient data and prior clinical outcomes.

2. Materials and Methods

ATLAS (AI and Simulation for Tumor Liver Assessment) is a computational framework designed to integrate heterogeneous clinical and modelling data for structured analysis of liver tumor board decisions. The system combines machine learning methods with computational liver models and links them through a dynamic, time-resolved knowledge graph representing structured clinical information. The framework is applied to a retrospective cohort from the University Hospital Leipzig including clinical tumor board data. A large language model provides an intuitive interface for exploring the integrated data and model outputs.

3. Results

A functional demonstrator for visualizing individualized treatment strategies was implemented and evaluated. The framework integrates heterogeneous data sources including clinical guidelines (e.g., S3), HCC-related literature, retrospective clinical data, patient-specific in silico models, and computational simulations. The underlying dataset comprises more than 10,000 patients, of which over 2,000 cases with approximately 200 variables per patient have currently been structured and analysed, with about 400 new cases added annually. The system enables structured exploration of therapy pathways and similarity-based analysis of patient trajectories. Clustering approaches (e.g., k-nearest neighbour and t-SNE) identify patients with comparable clinical characteristics, enabling similarity-based patient matching and visualization of treatment patterns (Figure 1).

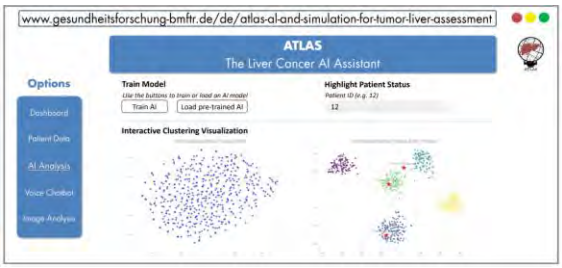


Figure 1: Schema of the functional demonstrator for visualizing treatment decisions.

4. Discussion and Conclusions

Computational frameworks that integrate heterogeneous clinical data with modelling approaches represent an important step toward more transparent and data-informed decision processes in liver oncology. The ATLAS framework demonstrates how retrospective tumor board data, clinical guidelines, and computational modelling can be combined within a unified analytical environment. Such integrative approaches may support clinicians in exploring complex treatment strategies, facilitate comparison with similar patient trajectories, and contribute to more structured and reproducible tumor board discussions.

5. References

1. Myshkina M, et al.; Preprint. 2025.
2. Fathauer L, Meek J.; Applied Clinical Informatics. 2012;3(3):337–348.

Acknowledgements:
Supported by the Federal Ministry of Research, Technology and Space (Grant No. 031L0304).

UTERINE DEFORMATION TRAJECTORIES ACROSS GESTATION REVEAL THE EVOLVING MECHANICAL STATE OF PREGNANCY

Echo Xu (1), Erin Louwagie (1), Teseo Schneider (2), Denis Zorin (3), Daniele Panozzo (3), Kristin Myers (1)

1. Columbia University, USA; 2. University of Victoria, CAN, 3. New York University, USA

1. Introduction

The uterus undergoes dramatic morphological changes during pregnancy as it grows and stretches with the developing fetus [1]. Aberrant mechanical responses to this process can precipitate uterine rupture, dysregulated contractility, and preterm birth [2]. Yet quantifying uterine mechanics across normal gestation remains limited by sparse anatomical data and insufficient characterization of organ-level kinematics. Here, we present a computational framework to capture the deformation trajectory and mechanical state of the uterus throughout normal pregnancy.

2. Materials and Methods

Inner and outer uterine wall surface meshes were derived from existing ultrasound-based solid models of 47 participants across four visits in the late first (L1), middle second (M2), late second (L2), and middle third (M3) trimesters [1]. For each consecutive visit pair, the current-visit (CV) geometry was remeshed to establish a template surface mesh. The reference-visit (RV, visit prior to CV), rigidly aligned by center of gravity to the CV, was then conformed to this template via iterative closest-point projection with Taubin smoothing and feature-angle-based vertex pinning, ensuring consistent vertex connectivity while accommodating morphological variability across gestation. Matched RV-CV surface meshes were repositioned to a shared anatomical landmark *in-vivo*, and vertex-level deformation trajectories were computed by interpolating between configurations (Fig. 1a). Volumetric tetrahedral meshes were generated from RV surfaces with original boundary vertices preserved, and Dirichlet boundary conditions were assigned by fitting a linear displacement function to precomputed trajectories on matched boundary facets. Quasistatic finite element analysis (FEA) of uterine deformation was performed in PolyFEM with compressible Neo-Hookean properties from experiments [3] (Fig. 1b). Intrauterine pressure (IUP) was recovered from the weak-form equilibrium equations applied to FEA results. Element-averaged principal stretches were computed to characterize spatial distribution.

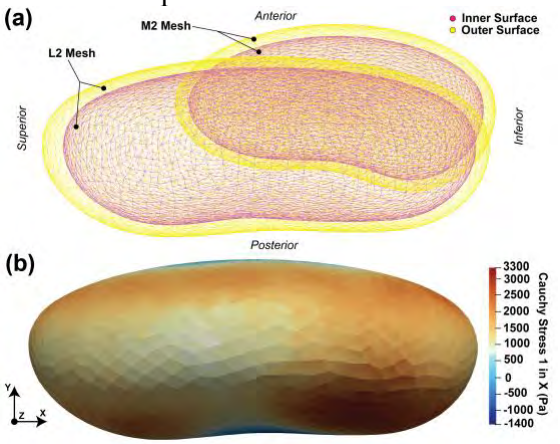


Figure 1: Representative model showing (a) repositioned RV (M2) and CV (L2) surface meshes with consistent surface connectivity and (b) resulting Cauchy stress map after deformation.

3. Results

Preliminary simulations (M2 to L2, n=18) demonstrated that the framework successfully resolves large gestational deformations while preserving patient-specific anatomy. At L2, the cohort yielded a mean IUP of 384.4 ± 290.9 Pa, a maximum principal stretch of 2.00 ± 0.45 with corresponding through-thickness thinning of 0.79 ± 0.18, and peak stretch concentrated in the inferior-posterior quadrant (9/18 patients).

4. Discussion and Conclusions

This computational framework quantifies *in-vivo* uterine deformation trajectories across pregnancy and establishes quantitative reference of boundary conditions for computational analysis. Our ongoing FEA incorporates postpartum models from the same cohort and a continuum growth formulation to decompose elastic and growth contributions to total uterine deformation. With PolyFEM's differentiability, we will perform large-scale sensitivity studies to identify biomechanical determinants of peak tissue stress and stretch.

5. References

1. Louwagie EM et al. npj Womens Health.2024;2:33. 2. Arrowsmith S. Curr Res Physiol. 2023;6:100105. 3. Fang S et al. Ann Biomed Eng. 2021;49(8):1923-1942.

PATIENT-SPECIFIC CERVICAL MATERIAL STIFFNESS QUANTIFIED FROM IN-VIVO ASPIRATION AND ULTRASOUND-DERIVED PREGNANCY IN-SILICO MODEL

Abigail Laughlin (1), Erin Louwagie (1), Adriana Delagarza (1), Lei Shi (2), Michael House (3), Mirella Mourad (4), Kristin Myers (1)

1. Columbia University, USA; 2. Kennesaw State University, USA; 3. Tufts Medical Center, USA; 4. Columbia University Irving Medical Center, USA

1. Introduction

Preterm birth (PTB, delivery before 37 weeks of gestation), affects 10% of births worldwide and is the leading cause of death in children under 5 [1]. Cervical length (CL) measured by transvaginal ultrasound (TVUS) is used to clinically assess PTB risk, but has limited predictive value [2]. The cervix is a three-dimensional structure with tissue material properties that evolve with extracellular matrix remodeling in pregnancy. Its shape, stiffness, and remodeling rate vary among individuals [3]. Cervical tissue aspiration is an *in-vivo* method to mechanically test the cervix [4]. In this work, a computational model of the cervical aspiration procedure was developed to incorporate cervical boundary conditions derived from clinical TVUS. Inverse finite element analysis (IFEA) was then used to quantify computed cervical material stiffness (cCs) during clinical cervical length screening in 30 pregnancies at risk for PTB.

2. Materials and Methods

TVUS and aspirated cervical stiffness (aCs) measurements from 30 second-trimester pregnancies with a short CL (<20mm) and no prior PTB were included in this study [5]. Cervical length and diameter were measured from TVUS images and used to generate patient-specific cervical models with an aspirator probe for IFEA. The measured aCs pressure was applied beneath the probe, and cervical material stiffness bounds were defined from existing mechanical data. The probe was modeled as a rigid body [6]. The computed cervical material stiffness (cCs) was varied until the simulated deformation matched *in-vivo* deformation within 1%. All simulations were performed in FEBio Studio [7]. Wilcoxon tests compared CL, aCs, and cCs between term and preterm deliveries.

3. Results

CL and cCs differed significantly between individuals who delivered preterm and at term, with greater significance for cCs than for CL (p=0.029 and p=0.019, respectively). aCs was not significantly different between the two outcome groups (p=0.111). Both CL and cCs were larger in term deliveries.

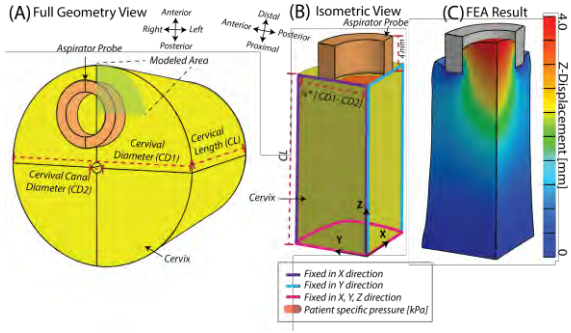


Figure 1: Schematic of cervical geometry (A) and boundary conditions for IFEA (B). Representative displacement field from simulation results (C).

4. Discussion and Conclusions

cCs showed a greater difference between outcome groups than CL and aCs, indicating that patient-specific tissue material properties may improve PTB risk assessment and understanding of cervical remodeling during pregnancy.

5. References

1. WHO, Preterm Birth (2023).
2. ACOG, Obstet Gynecol; 138(2):320-3 (2021).
3. Louwagie E et al., npj Women's Health; 2, 33 (2024).
4. Badir S et al., BMC Preg & Childbirth, 20:391 (2020).
5. Mourad M et al., Am. J Obstet Gynecol; 230 (1) S150-S151 (2024)
6. Louwagie E, Doctoral Thesis (2024).
7. Maas S et al., J Biomech, 134(1):011005 (2012).

Acknowledgements:

This work is supported by the National Institutes of Health under award number 1R01HD091153-01.

EVOLUTIONARY DIGITAL TWIN FRAMEWORK FOR OPTIMAL AMINOGLYCOSIDE DOSING IN NEONATES WITH SUSPECTED SEPSIS

Michela Prunella (1*), Chiara Romano (2,3*), Alessandro Borri (2,3), Nicola Altini (1), Maria Domenica Di Benedetto (2), Pieter Annaert (4), Karel Allegaert (5,6,7), Anne Smits (6,8), Vitoantonio Bevilacqua (1)

1. Department of Electrical and Information Engineering (DEI), Polytechnic University of Bari, Bari, Italy; 2. Center of Excellence for Research DEWS (Design Methodologies of Embedded Controllers, Wireless Interconnect and Systems-on-chip), Department of Information Engineering, Computer Science and Mathematics (DISIM), Università degli Studi dell'Aquila, L'Aquila, Italy; 3. CNR-IASI Biomathematics Laboratory, National Research Council of Italy, Rome, Italy.; 4. Laboratory for Pharmacotechnology and Biopharmacy, KU Leuven, Leuven, Belgium.; 5 Department of Pharmaceutical and Pharmacological Sciences, KU Leuven, 3000 Leuven, Belgium; 6 Department of Development and Regeneration, KU Leuven, 3000 Leuven, Belgium; 7 Department of Hospital Pharmacy, Erasmus MC, 3015 GD Rotterdam, The Netherlands; 8 Neonatal intensive care unit, University Hospitals Leuven, 3000 Leuven, Belgium

**Corresponding authors: michela.prunella@poliba.it, chiara.romano1@graduate.univaq.it*

1. Introduction

Accurate prediction of amikacin concentration and of underlying bacteria selection and evolution when treating suspected sepsis in vulnerable neonatal population, provides the foundation for adaptive dose and scheduling.

2. Materials and Methods

A four compartments ODE-based PBPK model (*hearth*, *kidney*, *serum blood* and *remainder*) for renally-cleared amikacin dynamics is integrated with an eco-evolutionary PD module, relating antibiotic exposure to sensitive and resistant bacterial dynamics. Glomerular filtration rate is continuously updated using a recurrent neural network. The framework is informed and cross-validated using three neonatal cohorts comprising 1,634 extremely preterm-to-term neonates, encompassing cases with acute kidney injury, perinatal asphyxia treated with therapeutic hypothermia, and inotrope and/or ibuprofen co-administration. Subsequently, an iterative single-cycle optimizer was compared to an MPC-based approach in balancing efficacy and safety while accounting for resistance-driven changes in the minimum inhibitory concentration (MIC).

3. Results

PBPK model prediction accuracy showed robust results in heterogeneous neonatal subgroups. Nonlinear optimal control achieved bacteriostatic exposure across all digital-twin neonates, with safety preserved in most cases at higher MICs, while MPC further reduced bacterial rebound during late therapy [1].

4. Discussion and Conclusions

The predictive capability of the framework was confirmed through extensive simulations demonstrating consistent improvements in joint PK-PD indices of therapeutic success either on real or virtual digital twin neonatal cohorts, by allowing anticipatory treatment adjustments and optimal control of bacteria resistance patterns.

5. References

1. Matcha, S., *et al. Pediatr Res* **98**, 936–941 2025.

Acknowledgements:

The work was funded by: Italian Ministry of University and Research, under the National Plan for Complementary Investments to the NRRP, project ``D34H—Digital Driven Diagnostics, prognostics and therapeutics for sustainable Health care" (project code: PNC0000001), Spoke 2: ``Multilayer platform to support the generation of the Patients' Digital Twin", CUP: B53C22006170001, and Spoke 3: ``Wearable technologies, sensors and biomarkers for care through Digital Twin approaches", CUP: B53C22006100001; Senior research grant from the Research Scientific Foundation-Flanders (FWO) - G0D0520N, I-PREDICT: Innovative Physiology-based pharmacokinetic model to pREdict Drug exposure In neonates undergoing Cooling Therapy; KU CELSA research project (Central Europe Leuven Strategic Alliance, CELSA/24/022); Senior Clinical Investigatorship of the Research Foundation – Flanders (FWO) (18E2H24N).

INTRAVENTRICULAR TRANSPORT ORGANIZATION AND WASHOUT EFFICIENCY UNDER GRADED LEFT VENTRICULAR WALL MOTION INSUFFICIENCY

Oleksandr Barannyk (1), Dhanush Suresh (1), Matteo Bianchi (1), Aysan Rangchian(1), Vutheara Phath (1)

1. 1 Edwards Lifesciences, USA; Correspondence: oleksandr_barannyk@edwards.com

1. Introduction

Left ventricular (LV) contraction organizes intraventricular blood transport and enables efficient washout. Clinical imaging shows that ventricular dysfunction disrupts these flow structures, producing abnormal vortex dynamics, prolonged residence times, and flow stagnation linked to thrombus formation and heart failure progression [1-3]. Because the role of wall motion abnormalities is difficult to isolate in vivo, controlled experiments are needed to determine how transport changes as contraction becomes asymmetric.

This study quantifies LV washout dynamics under graded lateral wall contraction insufficiency.

2. Materials and Methods

An anatomically representative silicone LV model was tested in a cardiac pulse duplicator under physiologic conditions. LV geometry and valves were held constant while wall motion simulated four contraction states: symmetric (LV-HLTH), mild (LV-MLCR), moderate (LV-MDCR), and severe contraction reduction (LV-SVCR, ~half of the wall non-contracting). Ten cardiac cycles were recorded per condition. Time-resolved flow fields were measured using 4D particle tracking velocimetry (4D-PTV). First-pass trajectory analysis quantified three washout metrics averaged across cycles:

- Fresh clearance (Wfresh) – mitral inflow exiting within the same cycle.
- Resident washout (Wresident) – pre-existing ventricular blood ejected.
- Net renewal (Wnet) – fraction of ventricular blood replaced per heartbeat.

3. Results

Transport efficiency decreased as contraction asymmetry increased.

Under symmetric contraction (LV-HLTH), washout was efficient (Wfresh ≈ 0.69, Wresident ≈ 0.18, Wnet ≈ 0.50). Mild reduction (LV-MLCR) preserved transport (Wnet ≈ 0.48). A transition occurred at LV-MDCR, where Wfresh ~0.38, Wresident ~0.12, and Wnet ~0.26. Under LV-SVCR, flow compartmentalized into an actively pumped region and a slowly exchanging lateral reservoir. Fresh clearance partially recovered (~0.43), but resident washout (~0.13) and net renewal (~0.30) remained reduced.

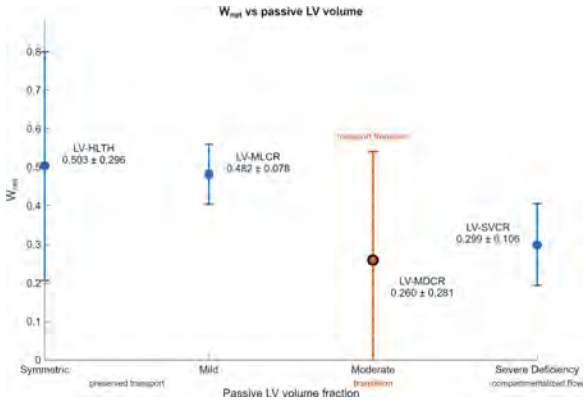


Figure 1. Net ventricular renewal fraction (Wnet) versus passive LV volume fraction.

4. Discussion and Conclusions

Regional contraction deficiency shifts transport from efficient jet-mediated washout to a two-compartment system consisting of an actively pumped region and a passive reservoir. The transition between mild and moderate deficiency indicates a threshold where ventricular mechanics generate stagnation zones, consistent with clinical 4D-flow MRI observations in cardiomyopathy.

5. References

1. Eriksson J et al. Four-dimensional blood flow–specific markers of LV dysfunction. Circulation. 2010.
2. Töger J et al. Vortex ring formation in the human left ventricle. JACC Cardiovascular Imaging. 2012.
3. Elbaz MSM et al. Vortex flow and viscous energy loss in cardiomyopathy using 4D flow MRI. J Magn Reson Imaging. 2014

Acknowledgements:

The authors would like to thank Edwards Lifesciences, for providing financial support to this project.

IN SILICO MODELLING OF LEFT VENTRICULAR PHYSIOLOGY: A FRAMEWORK FOR STUDYING AGE- AND SEX-RELATED CHANGES

Marta Zattoni (1, 2), Patrick Segers (1), Annette Caenen (1, 3), Mathias Peirlinck (2)

1. Ghent University, Belgium; 2. TU Delft, The Netherlands; 3. KU Leuven, Belgium

1. Introduction

Cardiovascular aging induces alterations in the left ventricle (LV), including increased wall thickness and reduced cavity volume, which influence chamber stiffness and function. Quantifying the isolated impact of geometrical and functional stiffness variations is important for interpreting age- and sex-specific cardiac pathophysiology. We developed hybrid 3D-0D *in silico* models of the healthy LV with an automated parameter calibration workflow to evaluate how LV changes at the macroscale shift global pressure-volume (PV) behavior.

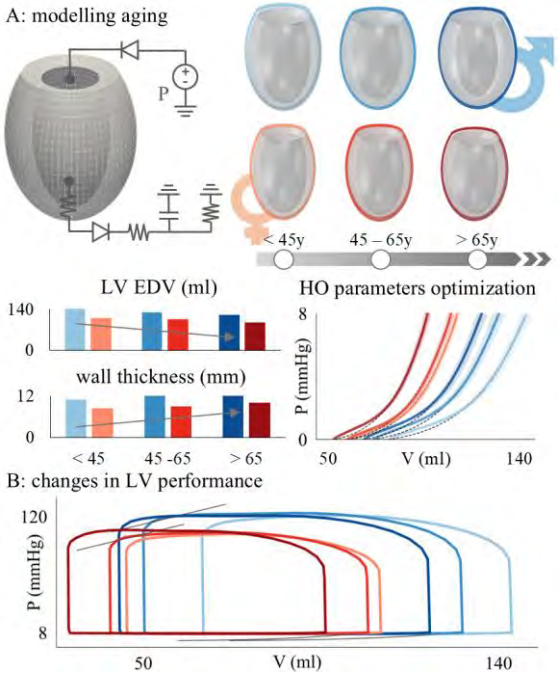
2. Materials and Methods

We generated 6 3D-0D models in Abaqus (v2024) representing three age groups (<45y, 45-65y, >65y) for both sexes (M, W). Passive myocardial mechanics were implemented with Holzapfel-Ogden (HO) (2009) constitutive law, whose parameters were defined with an optimization algorithm to match target end-diastolic volume (EDV) and wall thickness at 8 mmHg according to echocardiographic reference values for each case (Fig. 1A) [1]. Active contraction followed Guccione *et al.* (1993). The LV was coupled to a three-element Windkessel (WK). WK and active parameters were calibrated to reproduce a 45-65y baseline PV loop [2], and then held constant across all cases to isolate the effects of geometrical and stiffness changes. EDPV relationship was derived using the Klotz method [3], and end-systolic (ES) PV relationship was obtained from PV loops at incrementally increasing preload.

3. Results

HO scale factors (a_f, a_s, a_{fs}) increased in men (4.4% at 45-65y; 2.7% at >65y) and decreased in women (-3.0% and -2.4%), whereas HO exponential rates (b_f, b_s, b_{fs}) remained relatively constant (<1% variation). PV loops stabilized after 5 cardiac cycles, and the last was analysed (Fig. 1B). ED operational stiffness increased by 19.0% (M) and 14.7% (W); ES elastance increased by 83.1% (M) and 222% (W).

Figure 1. A: 3D-0D model scheme, 6 LV geometries and age- and -sex related changes implemented. B: PV loops with ESPVR and EDPVR shown for age 45-65y in M (blue) and W (red).



4. Discussion and Conclusions

The proposed 3D-0D modelling framework captures key features of healthy LV physiology, yielding global PV behavior that reflects the increases in chamber stiffness and ES elastance that have been seen with healthy aging in men and women. The approach provides a controlled and physiologically realistic platform for future investigations of age- and sex-specific mechanisms.

5. References

1. Addetia K et al., J Am Soc Echocardiog; 35(5):449-459 (2021).
2. van Osta N et al., Phil. Trans. R. Soc. A; 383:20240208 (2025).
3. Klotz S et al., Am J Physiol Heart Circ Physiol; 291:H403-H412 (2006).

Acknowledgements

MZ: EU project 101169278 – InSilicoHealth – HORIZON–MSCA–2023. AC: Research Foundation Flanders, under grant 12B3124N.

Image-Driven Computational Modelling of Right-Heart Hemodynamics

Erika Xhelo (1), Francesca Renzi (2), Giovanni Puppini (3), Stiljan Hoxha (4), Giovanni B. Luciani (1), Christian Vergara (2)

1. Department of Surgery, Dentistry, Pediatrics, and Obstetrics/Gynecology, University of Verona, Verona, Italy; 2. LaBS, Dipartimento di Chimica, Materiali e Ingegneria Chimica "Giulio Natta", Politecnico di Milano, Milan, Italy; 3. Department of Diagnostic and Public Health, University of Verona, Verona, Italy; 4. U.O.C. Cardiochirurgia, Azienda Ospedaliera Universitaria Integrata di Verona, Verona, Italy

Corresponding author: Erika Xhelo, Piazzale L. Scuro, 10 - 37134 Verona, Italy. e-mail**:** erika.xhelo@univr.it

1. Introduction

Pulmonary Valve Replacement (PVR) is a key intervention for patients with repaired right-heart congenital defects, yet quantitative criteria to compare surgical strategies remain limited. Image-driven Computational Fluid Dynamics (CFD) offers a patient-specific framework to integrate anatomy, motion and flow dynamics for treatment planning. This work presents an image-based pipeline to reconstruct right-heart anatomy and motion and to quantitatively assess the hemodynamic impact of different PVR strategies in congenital heart disease patients from the University Hospital of Verona.

2. Materials and Methods

We reconstruct 3D geometries and time-resolved cardiac displacements from multi-stack cine-MRI. Manual endocardial segmentation on a single time frame is propagated to the full cardiac cycle using Optical Flow algorithm [1]. Valves are explicitly delineated across all frames. We employ the Multi-Series Morphing technique [2] to obtain motion-consistent anatomical models. CFD simulations allow to discretize Navier–Stokes equations in an Arbitrary Lagrangian–Eulerian using the Finite Elements library *life*^{x} [3]. Valve behaviour is represented through physiological opening patterns and turbulence is modelled via a Large Eddy Simulation approach [4].

3. Results

We apply the framework to a healthy control and to patients with Tetralogy of Fallot and Pulmonary Atresia with Intact Ventricular Septum, before and after three PVR procedures: i) homograft surgery; ii) bioprosthetic valve implantation; iii) transcatheter valve procedure. Pre-operative cases exhibit disturbed flow, elevated peak velocities, and increased wall shear stress (WSS) compared to the healthy control (Figure 1). All PVR strategies improve global hemodynamics, though with distinct flow signatures: velocity profiles are smoother after homograft, bioprostheses show more collimated jets and moderate reductions in Kinetic Energy, and transcatheter valve implantation is characterized by localized vortices and increased peak velocities.

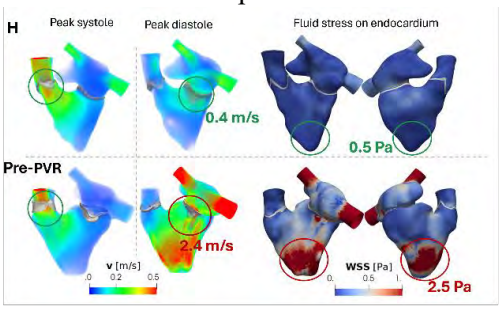


Figure 1: Comparison of velocity magnitude and WSS between a healthy control (H) and the ToF patient in the pre-operative state (Pre-PVR).

4. Discussion and Conclusions

This study provides a unified image-driven framework to systematically compare PVR strategies in a patient-specific setting. This approach has the potential to support treatment selection and longitudinal follow-up in congenital heart disease, highlighting the relevance of computational modelling as a clinical decision-support tool.

5. References

1. Liu C., PhD thesis, Massachusetts Institute of Technology, 2009.
2. Renzi F. et al., Int J Numer Method Biomed Eng, 41(1), 2025.
3. Africa P.C., SoftwareX, 101252, 2022.
4. Renzi F. et al., Biomech Model Mechanobiol, 24(4), 2025.

ARTIFICIAL INTELLIGENCE-BASED DECISION SUPPORT SYSTEM FOR RISK STRATIFICATION AND EARLY DETECTION OF HEART FAILURE

Nenad Filipovic (1,2), Djordje Jakovljevic (3), Zoran Bosnic (4), Dimitrios Boucharas (5)

1. BioIRC doo Kragujevac, Andre Marinkovica 26, 34000 Kragujevac, Serbia; 2. Faculty of Engineering, University of Kragujevac, Sestre Janjic 6, 34000 Kragujevac, Serbia; 3. University Hospitals Coventry and Warwickshire NHS Trust, Coventry, UK; 4. University of Ljubljana, Faculty of Computer and Information Science, Ljubljana, Slovenia; 5. Department of Biomedical Research, Foundation for Research and Technology Hellas, Greece

Corresponding author: Nenad Filipovic, BioIRC doo Kragujevac, Serbia; e-mail: fica@kg.ac.rs

1. Introduction

Heart failure (HF) affects up to 15 million people in Europe and remains a leading cause of hospitalization, mortality and healthcare expenditure. HF is a complex, heterogeneous syndrome typically accompanied by a heavy burden of comorbidities (Figure 1), which complicates early detection and individualized risk stratification [1]. The STRATIFYHF project [2] addresses this need by developing an artificial intelligence (AI)-based Decision Support System (DSS) that integrates multiscale computational modeling with large-scale clinical data for earlier diagnosis and personalized HF management across primary and specialist care.

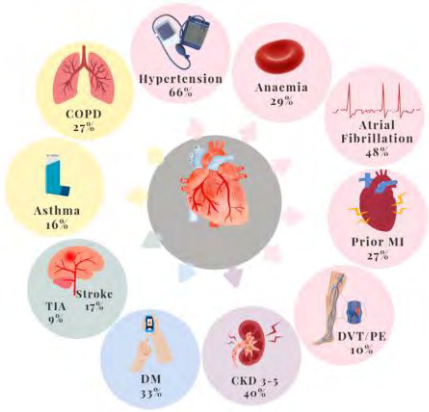


Figure 1: Prevalence of major comorbidities in the heart failure population, illustrating the multimorbid clinical context integrated by the STRATIFYHF Decision Support System for individualized risk stratification.

2. Materials and Methods

The DSS couples machine-learning risk and early-diagnosis modules with patient-specific 3D biomechanical heart simulations, orchestrated by a Workflow Manager Module that schedules high-computation tasks. Retrospective data were collected from 5,624 confirmed HF patients and 4,465 suspected cases, complemented by access to more than 11 million primary-care records and 680,000 confirmed HF cases through national databases. Patient-specific cardiac models were reconstructed from imaging to derive functional biomarkers supporting the risk and diagnostic modules.

3. Results

The integrated platform delivers machine-learning risk and early-diagnosis modules, patient-specific 3D cardiac simulations and intuitive clinician-facing interfaces. The retrospective cohort and linked national records established the reference dataset for model development and validation, and the high comorbidity burden of the target population (Figure 1) confirms the need to combine data-driven prediction with mechanistic cardiac modeling.

4. Discussion and Conclusions

By enabling earlier intervention and personalized treatment strategies, the STRATIFYHF DSS aims to reduce hospital admissions, prevent disease progression and contribute to more efficient and sustainable healthcare systems. Prospective clinical validation is ongoing to confirm the added value of integrating AI-based risk prediction with patient-specific biomechanical modeling.

5. References

1. McDonagh TA, Metra M, Adamo M, et al. 2021 ESC Guidelines for the diagnosis and treatment of acute and chronic heart failure. Eur Heart J. 2021;42(36):3599-3726.
2. www.stratifyhf.eu

Acknowledgements: This work received funding from the European Union's Horizon Europe programme (STRATIFYHF project); the authors thank all consortium partners.

TOWARDS DIGITAL TWIN FRAMEWORKS FOR MONITORING VENTRICULAR SEPTAL DEFECT

Mitchel Colebank (1), Ethan Mahan (1), Hamilton Baker (2)

1. University of South Carolina, USA; 2. Medical University of South Carolina, USA

1. Introduction

Ventricular septal defect (VSD) is the most common congenital heart defect. Defined by a hole between the left and right ventricle (LV and RV, respectively), a VSD can close naturally when small, but may remain open when the VSD is medium in size and hemodynamic conditions favor a left-to-right shunt. Computational models, rigorously analyzed via sensitivity and identifiability methods, can provide an uncertainty-aware forecasting tool for additional clinical insight. This requires multiscale models that can predict trajectories of cardiovascular function.

2. Materials and Methods

The model is a lumped parameter system of the four heart chambers, systemic circulation, and pulmonary circulation [1]. Parameters are scaled using a maturation and adaptation approach[2] to simulate pediatric hemodynamics from birth to two years of age. The VSD is simulated as a Bernoulli-like resistance, where $R_{VSD} \propto 1/r_{VSD}^2$ is inversely proportional to the VSD radius. The pediatric circulation is adapted such that pulmonary vascular resistance is high in the first hours to days after birth, stabilizing towards adult values. We simulated hemodynamics across the first two years of life without a VSD and validated to literature data [2] to ensure model trajectories are consistent. Then, we simulated small ($r = 0.1$ cm), medium ($r = 0.3$ cm), and large ($r = 0.6$ cm) VSDs and their hemodynamic effects over the first two years of age. We used variance-based global sensitivity analysis [3] to determine which parameters were most influential over the simulated lifespan.

3. Results

Validated predictions of mean arterial pressure (MAP) and mean pulmonary arterial pressure (mPAP) are shown in Figure 1 (a,b). These results show that mPAP rapidly decays during the first years of life consistent with data. Pressure-volume loops in the LV and RV are shown in Figure 1 (c,d) show volume overload in both chambers, which is stiffer RV. Sensitivity analyses (not shown) reflect changes in model sensitivity with age suggesting more importance of compliance at later ages. This suggests that inferred parameters be identified based on age group.

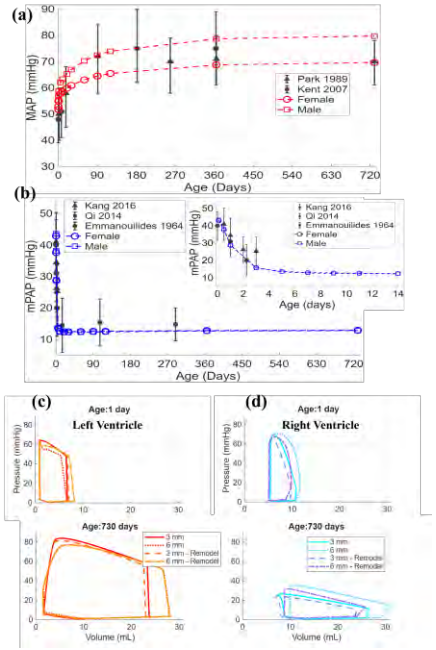


Figure 1: Changes in (a) MAP and (b) mPAP over two years of life. Data are as previously reported [2]. Simulated pressure-volume loops (LV, (c); RV, (d)) show the effects of a VSD without remodeling versus with RV stiffening at later ages.

4. Discussion and Conclusions

We provide an initial design for simulating hemodynamics with a VSD. With additional sensitivity and identifiability analyses, our approach can provide a digital twin framework for VSD management. This will use routine echocardiography data (e.g., cardiac sizes) for hemodynamic forecasting that reduces uncertainty in VSD decision making.

5. References

1. Colebank et al. arXiv:2602.04008 (2026).
2. Hiebing et al. J Biomech Eng, 145(10): 101007 (2023).
3. Colunga et al. J R Soc Interface, 20 (200): 20220735 (2023).

IN VIVO DEFORMATION OF THE HUMAN SINGLE VENTRICLE

Benjamin J. Thomas (1), Radomir Chabiniok (2), Michael S. Sacks (1)

1. James T. Willerson Center for Cardiovascular Modeling and Simulation at The University of Texas at Austin, United States; 2. Division of Pediatric Cardiology, Department of Pediatrics at University of Texas Southwestern Medical Center, United States

1. Introduction

Single ventricle (SV) disease is a congenital condition where the ventricles fuse during in utero development. The abnormal shape of the SV directly influences the underlying biomechanics of the patient's heart and can lead to increased mortality. We determined the local in vivo SV deformations over a single cardiac cycle to obtain regional strains fields and area changes. By determining the in vivo deformation, we can better understand this disease and develop better metrics to characterize the severity of the disease.

2. Materials and Methods

3D in vivo images of 3 patients with SV were segmented over the cardiac cycle, with 15-20 frames total per heart. To compute the 3D wall strains, we use truncated hierarchical B-splines (THB-spline) to encapsulate the SV endocardial and epicardial surfaces. Cubic order was used for the in-surface directions and linear order for the transmural direction. As in previous surface-based studies, we exploited the local support nature of B-splines to compute local deformations. Use of THB-splines further allowed local mesh refinement for regions of more complex geometry and deformation that are common to the SV. The resulting personalized mesh convects with the SV over the cardiac cycle, allowing 3D shape and strains to be directly computed.

3. Results

Use of THB splines resulted in high fidelity fits with far fewer control points than our previous NURBS based method, with no loss of accuracy. Results from all three patients demonstrated very complex, asymmetric, and generally very abnormal deformations patterns. These included focal regions of high deformation (>30% strain), irregular shape, and pronounced irregular end-diastole to end-systolic deformations. Some transmural shearing was also observed, especially mid-ventricle.



Figure 1: End diastolic state is shown in gray and the end systolic is in red.

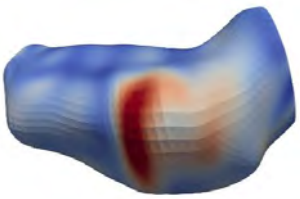


Figure 2: The strains determined by the spline fit.

4. Discussion and Conclusions

We have shown the unique ability to compute the in vivo deformations of the single ventricle. This gives key insights into the local strain patterns that the ventricle undergoes. An improvement to this method would be to also take into account the biomechanics of the tissue when tracking over time to fill in the 3D volume and give more accurate estimates throughout the ventricle. Use of THB-splines will facilitate direct translation to efficient computational modeling already in progress.

5. References

1. Kim, Jaemin, et al. Ann Biomed Engr; 53.1 (2025): 83-98
2. Hiremath, Gurumurthy, et al. JSCAI; 2.3 (2023): 100599

Acknowledgements:

The authors would like to thank the National Institutes of Health (NIH R01HL184128) for providing financial support to this project.

A PROBABILISTIC MULTIPHYSICS COMPUTATIONAL MODEL FOR VENTRICULAR DYSSYNCHRONY AND CRT

Ester Bergantin (1), Federica Caforio (2,3,4), Christoph Augustin (3,4) Simone Pezzuto (1)

1. University of Trento, Italy; 2. University of Graz, Austria; 3. Medical University of Graz, Austria; 4. BioTechMed-Graz, Austria

1. Introduction

Cardiac electrical dyssynchrony due to left bundle-branch block (LBBB) leads to heterogeneous myocardial contraction and impaired pump function. Cardiac resynchronization therapy (CRT) improves cardiac performance by restoring ventricular electrical synchrony through pacing. This work aims to model the effects of dyssynchrony on cardiac mechanics and pump function and to investigate different pacing strategies.

2. Materials and Methods

We present a personalized modeling pipeline, based on the work of [1], for simulating the interaction between electrophysiology (EP) and cardiac pump function that can be used to investigate LBBB and its treatment. Patient-specific geometries, reconstructed from cardiac magnetic resonance (CMR), were used to compute activation maps with a 3D Eikonal model. The Purkinje network was identified using a probabilistic approach to reproduce patient-specific ECG signals. Following [2], we recovered a distribution of Purkinje networks compatible with the observed ECG using Bayesian Optimization (BO) combined with Approximate Bayesian Computation. The resulting activation maps were used to simulate different pacing strategies by introducing protocol-specific initiation sites. Activation times were then averaged and used as input in CircAdapt, a cardiovascular model capable of describing heterogeneous mechanical activation [3]. CircAdapt parameters were calibrated using a BO-based approach to match CMR-derived clinical variables. A numerical assessment including local identifiability analysis and synthetic recovery tests was performed to evaluate calibration robustness.

3. Results

EP simulations accurately captured the delayed LV free wall activation and dyssynchrony characteristic of LBBB. Among the pacing strategies investigated, conduction system pacing and biventricular pacing achieved the most synchronous electrical activation. However, results revealed a strong patient-specific response: in one patient, extensive LV endocardial scar tissue limited the benefit of all pacing modalities. Hemodynamic biomarkers also revealed a heterogeneous and strongly patient-specific response to the different pacing strategies. Notably, variability across activation samples had negligible impact on global mechanical outcomes.

4. Discussion and Conclusions

No single pacing strategy consistently optimized all EP and hemodynamic metrics, underscoring the multifactorial nature of CRT response and the inadequacy of single-biomarker optimization. The one-way coupling between electrical and mechanical models proved effective in capturing pacing-induced changes at affordable computational cost. The systematic use of Bayesian Optimization at both the EP and circulation stages enabled patient-specific calibration and explicit uncertainty quantification across the modeling pipeline. The proposed framework, relying exclusively on non-invasive clinical data, bridges 3D electrophysiological simulations with regional cardiovascular modeling, enabling investigation of CRT effects from local activation patterns to global hemodynamic response. These characteristics make it well-suited for exploring multiple pacing strategies and supporting personalized CRT planning within clinically feasible time frames.

5. References

1. Meiburg et al., Europace 25 (6) (2023) euad144
2. Alvarez-Barrientos et al., MedIA; (2025) 103460
3. Walmsley et al., PLoS Comput. Biol. 11 (7) (2015) e1004284

Acknowledgements:

This contribution was produced with the support of a scholarship financed by the Ministerial Decree no. 118 of 2nd March 2023, based on the NRRP - funded by the European Union - NextGenerationEU - Mission 4, Investment 4.1.

IN SILICO MODEL OF THE STRUCTURAL RESPONSE OF FLOW DIVERTERS FOR ENDOVASCULAR CEREBRAL TREATMENTS

Gabriele Boezi[1], Alessandro Mastrofini[1], Michele Marino[1]

1.Multiscale and Multiphysics Mechanics Group (M2M), Department of Civil Engineering and Computer Science Engineering, University of Rome "Tor Vergata", Via del Politecnico, 1, 00133, Rome, Italy

1. Introduction

Despite their use, the biomechanical behaviour of flow diverters (FDs) remains insufficiently studied [1].

In this work we present the verification and validation of a computational model of the mechanical response of two FD devices, Pipeline™ Vantage and Pipeline™ Flex, both under controlled *in vitro* settings and thanks to *in vivo* imaging-based measurements.

The aim is first to reduce the number of costly experimental tests for future characterizations, and then to investigate *in silico* the behaviour of FD in patient-specific geometries.

2. Materials and Methods

A finite element model was developed, representing each filament as a helical curve discretized with large-strain Timoshenko beam elements.

Wire–wire interaction at crossover points was modelled enforcing translational continuity while preserving independent rotation.

The constitutive parameters were derived from a SEM-based analysis [2].

Multiple experimental tests, including bending conditions beyond the traditional standard settings, were numerically reproduced evaluating vertical displacement at the extremities and braid angle distributions as output quantities of interest. Uncertainties in the initial configuration were explicitly considered and quantified. The validated model was then applied to simulate deployment in patient-specific vascular geometries.

3. Results

The hinge-like formulation avoids explicit contact algorithms, reducing computational expense. The numerical results were consistent with the experiments, confirming the reliability of the model in capturing the global behaviour of the braided structure (Figs. 1 and 2)



Figure 1: Bending test of the Pipeline™ Vantage FD. Comparison between experimental deformed configuration with vertical displacement at the extremities (top) and corresponding finite element simulation (bottom).

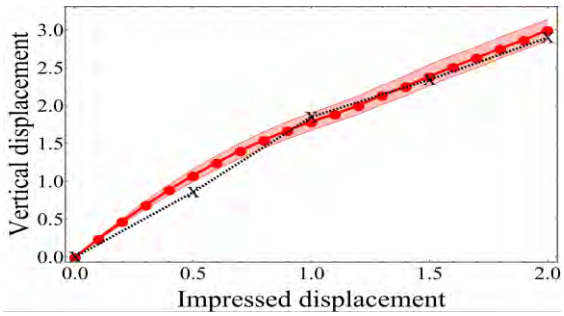


Figure 2: Vertical displacement of the proximal face versus imposed displacement: experiments (black) vs computational results (red, mean ± s.d.). The red region represents the variation of numerical results due to the exp. uncertainties in the measurement of the initial braid angle in the open configuration.

4. Discussion and Conclusions

Future developments will focus on implementing an explicit wire-wire contact formulation as well as including more advanced constitutive models. Quantitative validation will be performed by comparing simulated deployments with CT-scan images of stents expanded in patient-specific vessels.

5. References

1. Zaccaria A, Pennati G, Petrini L J Mech Behav Biomed Mater 119 (2001).
2. Di Cosmo et al, Proceedings EMMS 2026, Mechan. Machine Science Series, Springer (2026).

Acknowledgements: This work is supported by the ERC Consolidator Grant VISTA, n. 101230891.

ESTABLISHING CREDIBILITY OF A CALIBRATED DROPLET MODEL TO CAPTURE RED BLOOD CELL DEFORMATION *IN SILICO*

Hannah Palahnuk (1), Nicolas Tobin (1), Keefe B. Manning (1,2)

1. The Pennsylvania State University, Department of Biomedical Engineering, USA;
2. Penn State Hershey Medical Center, Department of Surgery, USA

1. Introduction

Hemolysis occurs in mechanical circulatory support devices (MCSDs) at a rate of 5-18%[1]. Validated strain-based hemolysis models, those governed by red blood cell (RBC) deformation, may aid in the design of MCSDs to decrease the hemolytic rate. In this study, we test the credibility of a calibrated droplet deformation model at predicting human RBC deformation in canonical flows accurately. This study is the first step toward developing an improved hemolysis modelling framework that would aid in clinical decision-making with computational modelling and/or novel MCSD design.

2. Materials and Methods

In Silico: Numerical experiments were completed in OpenFOAM. The laminar, incompressible Navier Stokes equations were solved numerically in shear and extensional microfluidic channels. Flow was coupled to the Maffettone-Minale droplet deformation model which assumes the RBCs are neutrally buoyant liquid droplets that deform to ellipsoids under flow [2]. Constitutive deformation and relaxation parameters were altered to best reflect experimental deformation data [3].

In Vitro: Human blood was collected from healthy human volunteers. Isolated RBCs were resuspended in physiologic salt solution at 0.5% hematocrit with Dextran-40kDa for varied viscosity ratios (λ, λ = RBC cytosol viscosity/suspending solution viscosity). The RBC cytosol viscosity is ~6 cP, and the suspending solutions had viscosities of 2.0 cP and 4.17 cP for λ = 3 and 1.44, respectively. Solutions were flowed in shear and extensional microfluidic channels (**Figure 1A**) on an inverted microscope stage and cells were imaged with a high-speed camera. RBC deformation was captured in shear flow from 5,000–200,000 s^{-1} and in extensional flow from 330–1,330 s^{-1}. Images were processed in ImageJ to quantify cell deformation.

3. Results

The calibrated model reproduces the flow-induced deformation behavior of *in vitro* human RBCs in multiple conditions (**Figure 2B, C**). The mean absolute error (MAE) remained ≤ 0.15 in all shear flow conditions tested and ≤ 0.11 for extensional strain rates ≥ 660 s^{-1}.

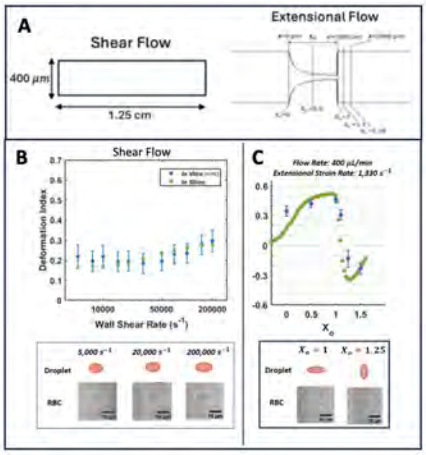


Figure 1. A: Shear and extensional flow microchannel geometries. **B:** Shear flow data for *in silico* droplets and *in vitro* RBCs at λ = 3. Representative droplets and RBCs are shown for three shear rates. **C:** Extensional flow data at 1,330 s^{-1} for *in silico* droplets and *in vitro* RBCs λ = 3. Representative droplets and RBCs are shown for two locations in the channel. The channel location is plotted as normalized axial position (Xo).

4. Discussion and Conclusions

The model adaptations successfully produce accurate RBC deformation results at MCSD relevant strain rates for two flow types and two suspension viscosities. Further model development and *in vitro* work are needed to extend the approach to cell rupture.

5. References

1. Papanastasiou, C. A. *et al. World J. Cardiol.* **12**, 334–341 (2020).
2. Maffettone, P. L., Minale, M. *J. Non-Newt. Fluid. Mech.* **78**(2), 227-241 (1998).
3. Palahnuk, H., *et al. Annals BME* (2026).

CREDIBILITY ASSESSMENT OF A COMPUTATIONAL PHYSIOLOGICAL SIMULATOR FOR HEART-LUNG INTERACTION

Federica Colombi (1)*, Marijn P. Mulder (1), Magnus Hallbäck (2), Kenny Rumindo (2), Fredrik Jalde (2), Elira Maksuti (2), Dirk W. Donker (1,3), Libera Fresiello (1)

1. Cardiovascular and Respiratory Physiology, TechMed Centre, University of Twente, Enschede, The Netherlands

2. Getinge, Acute Care Therapies, Maquet Critical Care AB, Solna, Sweden

3. Intensive Care Center, University Medical Center Utrecht, Utrecht, The Netherlands

*federica.colombi@utwente.nl, Tel.: +31 53 489 9758, P.O. Box 217, 7500 AE Enschede, The Netherlands

1. Introduction

Heart–lung interaction (HLI) arises from heart, thoracic vessels and lungs mechanical coupling. Although monitoring HLI in the intensive care unit (ICU) aids patient management, its analysis is complicated by mechanical ventilation and cardiopulmonary status heterogeneity. *In-silico* models can untangle this complexity, offering a mechanistic representation of HLI phenomena. We present the credibility assessment of a cardiopulmonary simulator (CPS) designed to: *"simulate mechanical ventilation effects on hemodynamics to investigate novel HLI-based monitoring and therapeutic strategies*".

2. Materials and Methods

The CPS builds upon a pre-existing closed-loop lumped-parameter model [1], enriched with respiratory mechanics, collapsible pulmonary vessels and vena cava, pericardium and interventricular septum. CPS risk was scored as medium-low and credibility was assessed according to FDA guidance [2]. Following code verification and parameter optimization, 23 validation tests were conducted on 5 ICU profiles, under various controlled mechanical ventilation settings (tidal volume 4-10 mL, controlled mode, inspiratory/expiratory ratio 1:2-3:1, positive end expiratory pressure (PEEP) 0-20 cmH_2O) and fluid infusion (+625 mL). Simulated cardiac, pulmonary and systemic hemodynamic data was compared with clinical literature and deemed satisfactory for errors $<\pm10\%$ for pressures, $<\pm20\%$ for cardiac volumes, or when falling within the clinical standard deviation.

3. Results

For all the 23 tests, CPS output matched clinical data. Examples of validation are in Fig. 1 for beat-to-beat hemodynamics over a ventilation cycle, and in Table 1 for steady-state hemodynamics for PEEP and fluid infusion tests.

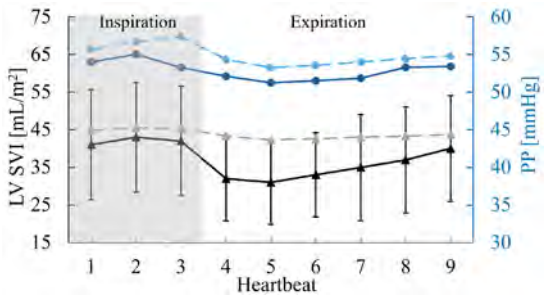


Figure 1: Simulated (dashed line) vs clinical pulse pressure and left ventricular stroke volume index [3].

PEEP cmH_2O	**CI** $L/min \cdot m^2$	**LVEDVI** mL/m^2	**RVEDVI** mL/m^2
0	**4.6** - 4.5	**61** – 61	**100** - 98
10	**4.3** - 4.2	**58** – 54	**95** - 88
20	**4.1** - 3.4	**55** – 44	**95** - 75
20+fluid	**4.9** - 4.5	**66** – 60	**110** - 100

Table 1: Simulated (bold) vs clinical (plain) cardiac index and left and right ventricular end-diastolic volume index [4].

4. Discussion and Conclusions

The CPS captures ventilatory induced changes in hemodynamics, indicating high fidelity when reproducing HLI (patho)physiology. These findings support its application as *in-silico* framework to investigate HLI-based monitoring and treatment strategies across ICU cohorts.

5. References

1. Fresiello L et al, Front. Physiol., 2016.
2. U.S. Food and Drug Administration (2023).
3. Jardin et al, Circulation, 1983.
4. Dhainaut et al, Chest, 1986.

Acknowledgements:
The work was conducted in collaboration with and received funding from Maquet Critical Care AB, part of Getinge.

UNCERTAINTY QUANTIFICATION OF TAVI SIMULATIONS

Letizia Maria Perri (1,2), Benedetta Grossi (2,3,1), Carlotta Bramante (1), Francesco Migliavacca (1,4), Gianluigi Condorelli (2,3), Giulia Luraghi (1)

1. Politecnico di Milano, Italy; 2. Humanitas University, Italy; 3. Humanitas Research Hospital, Italy; 4. Fondazione IRCCS Cà Granda Ospedale Maggiore Policlinico, Italy

Corresponding author: Letizia Maria Perri (letiziamaria.perri@polimi.it), Politecnico di Milano, Italy.

1. Introduction

Transcatheter Aortic Valve Implantation (TAVI) is an established minimally invasive treatment for aortic stenosis, yet post-procedural complications remain a major clinical challenge [1]. Patient-specific Finite Element analysis (FEA) is a powerful tool for predicting procedural outcomes, but its accuracy is limited by uncertainties in key inputs. Quantifying how wall thickness and mechanical properties propagate into simulation outputs is therefore relevant, motivating the use of Uncertainty Quantification (UQ) and Sensitivity Analysis. This study implements a design of experiments (DOE)-based UQ framework for TAVI simulations to address this issue.

2. Materials and Methods

FEA was performed on a single patient following the workflow proposed by Grossi et al. [2], with all modeling assumptions kept constant except for the parameters investigated. A full-factorial DOE was performed to assess uncertainty, varying aortic wall thickness (1.98-3 mm) and aorta material properties defined by seven third-order Yeoh models, for a total of 49 simulations. Outcomes were evaluated globally and in a region of interest (ROI) below the membranous septum using two predictors of conduction disturbances, a known post-TAVI complication [1]: variation of von Mises stress (ΔVM) and Contact Pressure Index (CPI). Regression analyses were conducted to quantify the influence of model parameters, with statistical significance defined at $p < 0.01$.

3. Results

Out of 49 simulations, 6, with the thinnest walls and softest materials, failed due to numerical instability. Across the aortic root, ΔVM showed variability, with a normalized standard deviation (SD) of 0.48. Wall thickness was the dominant contributor, with thinner walls producing a ≈60% increase in ΔVM (Figure 1a). Material properties had minimal impact in the ROI but influenced regions with larger deformation. Regression analysis confirmed wall thickness as the only statistically significant parameter (Figure 1b). CPI remained stable across physiological configurations, with an average of 27.6%, SD 8.2%, and normalized SD 0.30, further reinforcing the dominant influence of the aortic wall thickness.

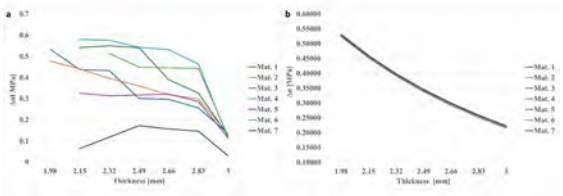


Figure 1: (a) ΔVM in the ROI versus wall thickness for different material sets. (b) Multivariate fit of ΔVM as a function of wall thickness; each curve corresponds to a fixed material set.

4. Discussion and Conclusions

This study provides the first UQ assessment of TAVI simulations focused on aortic wall thickness and material properties. Results show that wall thickness is the primary driver of mechanical response during device-tissue interaction. This emphasizes that accurate wall thickness characterization is more critical than detailed material refinement for reliable patient-specific TAVI simulations.

5. References

1. Grossi, Perri, Prog Biomed Eng, 8:012001, 2026.
2. Grossi, Comput Biol Med, 182:109159, 2024.

Acknowledgements:
L.M.P., B.G., F.M. and G.L. are supported by the European Research Council (ERC, project PROTEGO, G.A. 101162753).

ROBUST HEMODYNAMIC DESCRIPTORS FOR DIGITAL TWIN-BASED ASSESSMENT OF AORTIC FLOW RESTORATION

Tianai Wang (1), Teresa Lemainque (2), Christine Quast (3), Tobias Zeus (3), Michael Neidlin (1)

1. Cardiovascular Engineering, Applied Medical Engineering, RWTH Aachen University, Germany; 2. Dept of Diagnostic and Interventional Radiology, RWTH Aachen University, Germany; 3. Dept of Cardiology, Pulmonary Diseases and Vascular Medicine, Heinrich-Heine University, Germany

1. Introduction

Aortic valve diseases such as aortic stenosis (AS) significantly alter physiological blood flow patterns, inducing clinical complications. Thus, restoring physiological flow after interventions such as transcatheter aortic valve implantation (TAVI), is emerging as a central therapeutic objective [1]. Volumetric imaging techniques such as 4D Flow MRI enable in-vivo visualization of blood flow but limited spatial and temporal resolution restrict the reliable estimation of hemodynamic quantities. Similarly, complementary high-resolution CFD introduces modelling assumptions and uncertainties. These uncertainties challenge the use of patient-specific models as clinical digital twins. This work investigated which hemodynamic descriptors remain robust across imaging and modeling regimes and are therefore suitable for digital twin-based assessment of aortic flow restoration post-TAVI.

2. Materials and Methods

We developed a multimodal framework combining 4D Flow MRI and patient-specific CFD simulations to analyze aortic hemodynamics. The framework enables systematic investigation of uncertainties arising from imaging parameters and model assumptions. To quantify imaging-related uncertainties, systematic in-vivo scans with varying scanning parameters and synthetic CFD-derived MRI datasets were used to evaluate impact on hemodynamic parameters.
Modeling uncertainties were assessed by systematically varying inlet and outlet boundary conditions and wall motion modeling. A range of hemodynamic markers were evaluated for robustness across modeling regimes. Finally, a data-driven methodology for holistic flow comparison based on dimensionality reduction (DR) was developed, enabling comprehensive, quantitative comparison of spatiotemporal flow fields and their link to clinical outcomes.

3. Results

Imaging variations and modeling choices substantially affected commonly used hemodynamic quantities characterizing volumetric flow structures, while descriptors derived directly from the velocity field showed higher robustness across imaging and modeling settings, as shown for a subset in Fig. 1a as an example. The proposed DR-based framework enabled comprehensive comparison of pre- and post-TAVI flow fields and detected structural differences in flow patterns that were not captured by conventional scalar metrics, but directly linked to procedural outcome (Fig 1b)

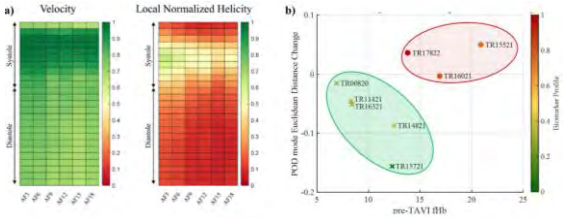


Figure 1 a) Sensitivity comparison of hemodynamic parameter sub-selection to MRI acquisition induced uncertainties. **b)** DR-based flow restoration assessment and k-means clustering, subsequent comparison to clinical outcomes.

4. Discussion and Conclusions

This work demonstrates that reliable digital twin-based hemodynamic assessment requires careful selection of flow descriptors that remain stable across imaging and modeling regimes. Velocity-field-based metrics and data-driven, DR-based flow comparison methods provide a promising basis for clinically transferable analysis. The proposed framework supports holistic evaluation of flow restoration following cardiovascular interventions and contributes to improving the credibility and clinical applicability of patient-specific cardiovascular digital twins.

5. References

[1] Garg P et al, Nat Rev Cardiol (2024) 21, 264–273

DEEP LEARNING RAPID ESTIMATION OF PULSATILE INTRACRANIAL ANEURYSM WALL SHEAR STRESS

Wenhao Ding (1), Yiying Sheng (2), Dylan Roi (3), Hwa Liang Leo (2), and Choon Hwai Yap (1)

1. Imperial College London, United Kingdom; 2. National University of Singapore, Singapore; 3. Imperial College Healthcare NHS Trust, United Kingdom

1. Introduction

Intracranial aneurysm (IA) involves a weakness in the cerebral arterial wall that bulges and carries a potentially lethal risk of rupture. Despite extensive biomechanics studies and meta-analysis suggesting a correlation between fluid mechanics markers and aneurysm instability [1], these markers have yet to be adopted by physicians, who continue to rely on simple morphological markers to assess risks [2], even though this is inaccurate (false-positive rates up to 56%) [3]. key reasons for this are that computational fluid dynamics (CFD) simulations are time-consuming and require specialized expertise, and thus physicians are unable to obtain sufficiently large sample sizes of fluid dynamics data to evaluate their clinical utility.

We developed a deep learning (DL) framework to address this. We first developed a DL aneurysm shape generator to circumvent the issue of small clinical samples available. We used it to create a large dataset of IA fluid dynamics, which trained a DL pulsatile wall shear stress (WSS) predictor. This WSS predictor can be used without CFD skills for real-time, high-throughput predictions.

2. Materials and Methods

Our DL IA shape generator is a two-part conditional VAE trained with 109 patient-specific IA morphologies [4], which produces both the aneurysm pouch and its parent vessels suitable for CFD simulations. Next, mass shape generation and CFD simulations produced a large dataset with 16,000 steady and 730 transient simulations on diverse morphologies [5]. Finally, we utilized a graph Transformer to predict WSS over a full cardiac cycle, using cotangent Laplacian eigenvectors as positional encoding and incorporating time and mass-flow waveform features. Steady-flow cases were added as augmentation during training to enhance accuracy. Codes and datasets are publicly shared (figure's QR codes)

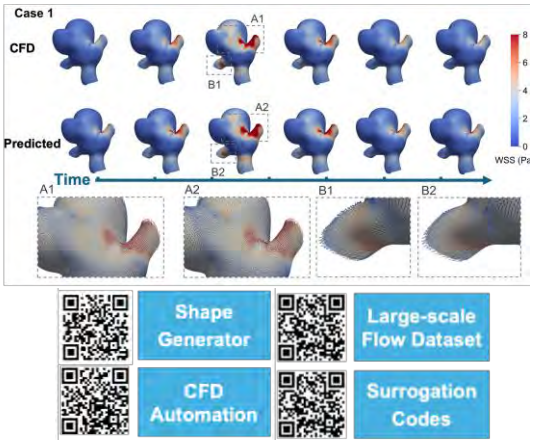


Figure 1: Hemodynamics surrogation

3. Results

Our model captures WSS pattern evolution across diverse geometries, achieving excellent spatial pattern and WSS magnitude accuracy (maximum-normalized relative L2 error). The augmentation with steady flow CFD data substantially improves generalization and fewer transient data is needed for high accuracy.

Table 1: Ablation experiments

Backbone	cases	†	SSIM	rL2*(%)
Graph U-Net	520		0.967	4.05
	520	✓	0.981	3.20
	100		0.913	6.56
	100	✓	0.967	3.85
Graph Transformer	520		0.973	3.45
	520	✓	**0.982**	**2.84**

†: Augmentation with steady flow CFD data

4. Discussion and Conclusions

We present the first DL model for pulsatile IA WSS prediction, and also works well for other parameters (OSI, pressures). The approach is exportable to other biomedical flows problems.

5. References

1. Brodland. PLoS One. 2012;7(9):e44281.
2. Maška. IEEE TMI; 2013;32(6):995-1006.
1. Zhou. Sci Rep. 2017;7(1):5331.
2. Etminan. Neurology. 2015;85(10):881–889.
3. Mocco. Neurosurgery. 2018;82(4):491–496.
4. Ding. MICCAI, 2025;15969:595–604.
5. Ding. NeurIPS 2025 (Poster #121403).

COMPARISON OF UNCERTAINTY QUANTIFICATION METHODS FOR ANEURYSM HEMODYNAMICS

Damján Miklós (1), Karol Zając (2), Levente Sándor (1), Benjamin Csippa (1), György Paál (1)

1. Budapest University of Technology and Economics, Faculty of Mechanical Engineering, Department of Hydrodynamic Systems, Hungary, 2. Sano - Centre for Computational Medicine, Poland

1. Introduction

Future digital twins in healthcare (DTH) can serve as decision-making tools and eventually for *in silico* trials. However, trusting these methodologies requires standardised certification by notified bodies like the EMA and FDA, including verification, validation, and uncertainty quantification (UQ). In this study, we developed UQ frameworks for hemodynamic simulations of flow diverter treatments in brain aneurysms.

2. Materials and Methods

A 2D aneurysm model was used to evaluate different UQ methods. The simulation output was the Aneurysm Mean Velocity Reduction (AMVR), as an AMVR greater than 35% can be a simplified clinical endpoint for successful occlusions [1]. The AMVR is influenced by multiple sources of uncertainty, including geometry, boundary conditions, and stent resistance. However, our study focused on the latter two. The aim of this study was to develop a detailed UQ framework that addresses the specific challenges of DTH.

The framework consists of four steps. First, a multivariate distribution of the correlating input parameters was constructed. These parameter distributions were truncated to positive values. The second step involved point selection to efficiently sample the input space, thereby reducing its size. Two methods were compared: tensor grid-based (Gauss-Hermite quadrature) and space-filling (quasi-Monte Carlo). Third, the AMVR was calculated using an in-house hemodynamic solver, and a surrogate model (SM) was fitted to the results. Two approaches were compared: Gaussian process (GP) [2] and polynomial chaos expansion (PCE) [3]. A new method was developed to efficiently construct a PCE basis for truncated, highly correlated normal distributions. The study was repeated for a wide range of sample sizes. Finally, Latin Hypercube sampling was used on the SM to estimate the probability density function of the AMVR.

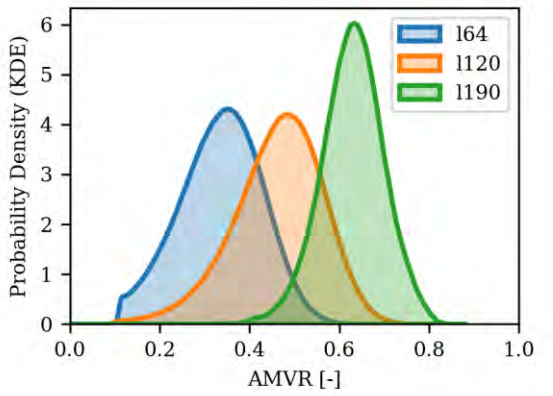


Figure 1: Probability density function of the AMVR using stents with different resistance characteristics.

3. Results

For a sample size of around 100, the statistical measures have a relative error of only 0.1% compared to the largest sample size, representing a thousand-fold computational gain over Monte Carlo based direct evaluation. The probability density function of the AMVR (Figure 1) was calculated using the Gaussian process surrogate model.

4. Discussion and Conclusions

Both models performed similarly. The application-specific parameter constraints made the sampling and the surrogate modelling challenging. As the results of our study will be used for further analysis and require detailed information about the distribution, the Gaussian process was chosen as the preferred model.

5. References

1. Ouared R et al., J Neurointerv Surg; 8(12):1288-1293 2016.
2. Forrester A et al., Engineering design via surrogate modelling: Wiley; 2008.
3. Najm HN. Annu Rev Fluid Mech; 41:35-52 2009.

Acknowledgements:

GEMINI has received funding from the European Union's Horizon Europe research and innovation program under the grant agreement No 101136438.

DIGITAL TWIN CALIBRATION, VALIDATION, AND PREDICTION: A TISSUE-ENGINEERED SCAFFOLD-MANDIBLE SYSTEM

Ben M. Ferguson (1), Ali Kiapour (2), Jeffrey Hajibandeh (3), Jonathan R. Clark (4), Qing Li (1)

1 School of Aerospace, Mechanical and Mechatronic Engineering, The University of Sydney, NSW, Australia, 2 Department of Neurosurgery Massachusetts General Hospital, Harvard Medical School, Boston MA, USA 3 Department of Oral & Maxillofacial Surgery, Massachusetts General Hospital, Harvard Medical School, Boston MA, USA 4 Department of Head & Neck Surgery, Chris O'Brien Lifehouse, Royal Prince Alfred Hospital, Sydney NSW Australia

1. Introduction

Digital twins (DT) have the potential to transform medical device design and testing; however, robust methods for their development and validation remain an open challenge. Here, a DT is developed for a mandible reconstruction scenario, as part of the preparatory phase for a preclinical trial. The DT is realised through a series of studies encompassing inverse analysis, validation, design optimisation, and biomechanical evaluation, forming an interconnected *in silico–ex vivo–in vivo* pipeline (see Fig. 1). Crucially, the DT features bidirectional data exchange between a virtual representation and its physical counterpart.

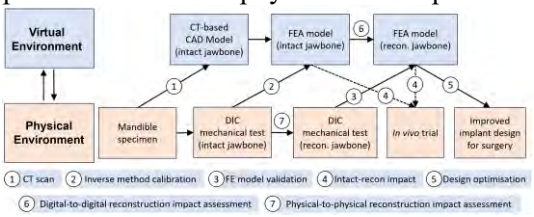


Fig. 1: The digital twin ecosystem.

2. Materials and Methods

Initial calibration of the DT uses an inverse methodology with response surface error-term minimisation to estimate the effective Young's modulus of the intact mandible, based on full-field deformation measurements captured using digital image correlation (DIC) cameras. The CT-image-based finite element (FE) model of the reconstructed version of the mandible, implanted with 3D-printed scaffolds, is then validated under the same experimental conditions.

Using the validated CT-FE model, the scaffold unit cell geometry is optimised to enhance mechanobiological stimulus and permeability, thereby improving the rate of neo-tissue ingrowth. Also, the model is used to predict the biomechanical performance of the implant before its implantation *in vivo*. Thirteen weeks after implantation, µCT analysis is used to visualise the extent of neo-tissue ingrowth.

3. Results

Qualitative and quantitative analysis determined the bone modulus to be 9.5 ± 0.5 GPa (Fig. 2).

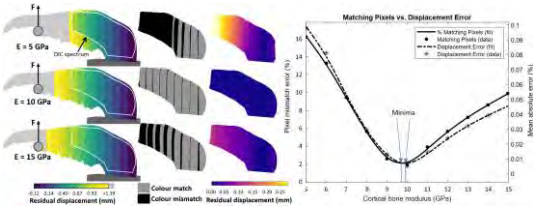


Fig. 2: Comparisons of FEA-predicted displacements with the experimental DIC measurements.

Fig. 3 shows that varying the scaffold microstructure significantly affects its biomechanical response and permeability properties. The microstructural geometry of the scaffold was optimised for mechanobiological stimulus and permeability, and the most optimal trade-off between these competing design objectives resulted in a scaffold porosity of 77% [1]. The CT-FE model predicted that the size and location of the partial defects along the lower border of the ramus posed minimal risk of mechanical failure for the implant under physiological load. This prediction was confirmed in practice, as none of the implants fractured during the 13-week observation period. µCT analysis showed neo-tissue ingrowth within the scaffold pores [2].

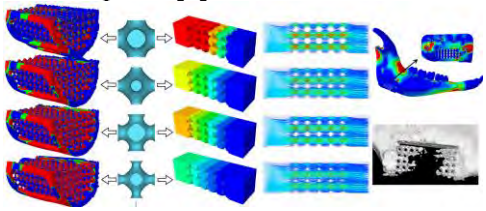


Fig. 3: Multiobjective optimisation of scaffold unit cell with FE, CFD, and surrogate modelling, as well as FE predictions and µCT images of neo-tissue ingrowth within the 3D-printed scaffold implant.

4. Discussion and Conclusions

This research demonstrates the feasibility of integrating pre-operative data, post-implantation changes, and mechanical feedback within a single coherent DT.

5. References

1. Ferguson BM et al., *J. Mech. Behavior Biomed. Mater.*; (2024), 164 , 10.1016/j.jmbbm.2024.106883

2. Xin, H., Ferguson BM., et al. *ACS Biomater. Sci. Eng.*; (2024),10(5):2863-2879 10.1021/acsbiomaterials.4c00262

EXPERIMENTALLY INFORMED IN SILICO MODEL OF FOOT-INSOLE INTERACTION

Sofia Pettenuzzo (1), Roccangelo Nuzzolese (1), Alice Berardo (1), Elisa Belluzzi (2), Assunta Pozzuoli (2), Pietro Ruggieri (2), Emanuele Luigi Carniel (1), Chiara Giulia Fontanella (1)

1. Department of Industrial Engineering, University of Padova, Italy; 2. Orthopedics and Orthopedic Oncology, Department of Surgery, Oncology and Gastroenterology, University-Hospital of Padova, Italy

1. Introduction

The human foot is exposed to repetitive mechanical loading and multiple pathologies that can impair its function, with significant socioeconomic impact [1]. Orthopaedic insoles are routinely prescribed to relieve pain and redistribute plantar loads, but their effectiveness depends on patient-specific tissue-device interaction. This limitation stems from the scarcity of robust, experimentally derived constitutive descriptions of plantar soft tissues for computational models. Therefore, this study aims to develop an experimentally informed in silico foot-insole model interaction, combining imaging-based anatomy with constitutive laws whose parameters are identified from dedicated mechanical testing of human tissues, enabling stress/strain estimation for insole design.

2. Materials and Methods

The *in silico* foot model was developed from CT/MRI segmentations and combined with mechanical properties derived from experimental tests and constitutive laws. Soft tissues were harvested from the feet of patients (4 M; 56±18 yrs; BMI: 26±2 kg/m²) who underwent amputation for leg cancer (CESC Code: AOP2649). After preconditioning, compression tests at different strain rates were conducted to assess the non-linear behaviour of the tissues, while tensile tests up to failure were performed to characterise the anisotropic response; viscoelasticity was assessed through stress-relaxation tests. The 3D finite element model was developed in Abaqus CAE 2025. After defining a constitutive formulation for each tissue, model parameters were identified by inverse analysis of the experimental tests [2]. Finally, contact between foot and insoles during different physiological activities was analysed.

3. Results

The adipose tissue exhibited incompressible, isotropic, and visco-hyperelastic behaviour, with regional variability (Fig. 1a); while the skin, plantar fascia, and tendons showed anisotropic visco-hyperelastic behaviour (Fig. 1b-d). Foot-insole simulations provided stress and strain distribution inside the tissues (Fig. 2).

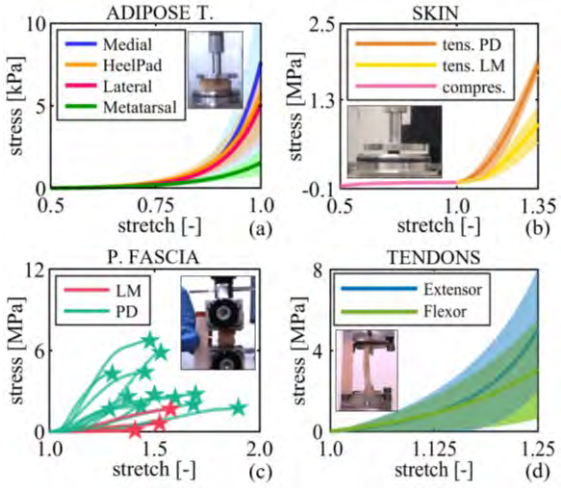


Figure 1: Stress-stretch curves: adipose tissue (a), skin (b), plantar fascia (c) and tendons (d).

4. Discussion and Conclusions

The results offer a refined mechanical characterisation of human foot tissues, including constitutive parameters in the foot model. This highlights its utility in simulating tissue-orthopaedic device interactions and in developing strategies to prevent foot pathology.

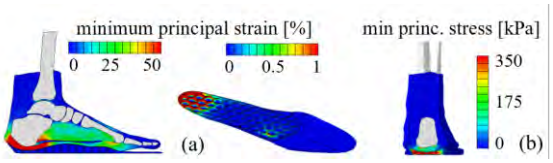


Figure 2: Foot-insole interaction FE simulation: min principal strain (a) and min principal stress (b).

5. References

1. Wafai et al, Sensors, 15: 20392–20408, 2015.
2. Pettenuzzo et al, Bioengineering 11: 42, 2024.

Acknowledgements:
This work was supported by PR Veneto FESR 2021-2027, Project n. D19J24000820007, titled RELIABLE.

FATIGUE-DRIVEN TOPOLOGY OPTIMIZATION OF POROUS HIP IMPLANTS FOR STRESS-SHIELDING MITIGATION

Roberta Cromi[1], Michela Miuccio[1,2], Mattia Concari[1,2], Francesca Berti[1], Stefano Foletti[2], Tomaso Villa[1]

1. *Department of Chemistry, Materials and Chemical Engineering "Giulio Natta" (LaBS) – Politecnico di Milano*
2. *Department of Mechanical Engineering (MetaMAT Laboratory) – Politecnico di Milano*

1. Introduction

Over 35% of femoral stems fail consequently to the stress-shielding phenomenon [1]. Although anatomically shaped femoral stems improve physiological load transfer, only architected materials –especially triply periodic minimal surface structures (TPMS)– enable the modulation of mechanical properties [2], thereby limiting bone resorption. Thus, this work proposes a methodology to design a mechanically reliable femoral implant, capable of withstanding ISO fatigue requirements while mitigating stress-shielding through the optimization of TPMS density distribution.

2. Materials and Methods

CT scans of an adult female patient were used for femoral geometric reconstruction and Young's modulus (E) mapping. A titanium anatomical stem was design: both neck and distal end were kept solid; whereas the core consisted of a porous architecture. Diamond, Gyroids and Schwarz sheet-based TPMS were computationally tension-tested and compared. Based on [3], a density-driven topological optimization (DTO) algorithm was developed to distribute the cells' relative density (ρ). The DTO constraints included: (i) the feasible range of ρ; (ii) the maximum acceptable material fraction, limited by the target value; (iii) the maximum allowable *von Mises stress* scaled by a safety factor (η=2). For each material fraction, uniform and optimized TPMS distributions were compared with the bulk stem. To ensure computational efficiency, a homogenization approach was adopted. Stress-shielding reduction and fatigue resistance were assessed under a 70kg physiological gait [4] and the ISO 7206-4 loading configuration, respectively.

3. Results

The CT-based mapping resulted in an E range of 0.5-22GPa. Designs A and B, characterized by an overall ρ of 60% and 65% respectively, are obtained from the DTO (Figure 1).

The bulk stem exhibits a bone resorption of 22%; stress-shielding and fatigue results for designs A and B are summarized in Table 1.

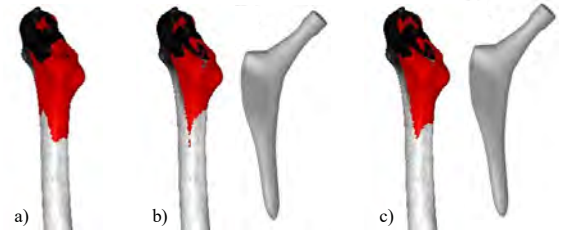


Figure 1: a) Bulk; (b) Design A; (c) Design B. The TPMS optimized implants are shown together with the bone resorbed elements, highlighted in red.

Configuration		BR	Failure	η_T
Design A	U	10.6%	5.2%	0.95
ρ=60%	O	11.4%	5.2%	1.14
Design B	U	11.8%	3.9%	1.04
ρ=65%	O	15.5%	2.4%	1.32

Table 1: Bone resorption (BR), failed elements percentage and minimum safety factor in tension (η_T) for the uniform (U) and optimized (O) designs.

4. Discussion and Conclusions

The porous implants achieve up to 50% stress-shielding reduction compared to the bulk stem. The optimized designs worsen bone resorption but improve fatigue performance. Although up to 5% of the total elements are classified as failed under the fatigue constraint (η=2), all the optimized TPMS distributions exhibit a minimum η greater than 1, indicating that no actual yielding occurs. Thus, DTO enable a tunable balance between mechanical reliability and bone preservation, potentially customizable to patient-specific clinical needs through the ρ.

References

1. W-dahl A *et al.*, AIMS Materials Sci, 2024
2. Ma J *et al.*, J. Tissue Eng, 2024
3. Fernandes P *et al.*, Appl Sci, 2023
4. Behrens BA *et al.*, Proc Inst MECH Eng H, 2008

Acknowledgements

Thanks are due to Dr. Massimo Franceschini, orthopaedic surgeon, for his clinical support.

MULTISCALE BONE MORPHOLOGY AS PREDICTOR FOR MULTIAXIAL OSTEOSYNTHESIS SCREW FAILURE

Anna De Cet (1), Juan D. Silva-Henao (2,3), Andreas Reisinger (1,2)

1. Department of Biomechanics, Faculty of Medicine, Karl Landsteiner University, Krems, Austria; 2. Institute of Lightweight Design and Structural Biomechanics, TU Wien, Wien, Austria; 3. CADS GmbH, Perg, Austria

1. Introduction

Osteosynthesis screw failure due to mechanical overloading remains a major clinical concern in fracture fixation. Previous studies correlated peri-implant bone morphology and loading conditions with screw holding capacity using µCT-derived parameters [1]. However, reliance on µ-CTs limit the applicability of these approaches in clinics, where high resolution images are not available. This study evaluates whether screw holding capacity can be predicted using clinical-resolution CT data.

2. Materials and Methods

Locking screws (2.5 mm) were implanted in porcine bone specimens (n = 94) and tested under cyclic overloading in ten loading scenarios, including axial, shear, mixed loading, and simulated plate elevations, (Figure 1), [2]. Failure force (F_{fail}) was defined as the maximum force prior to screw–bone interface failure.

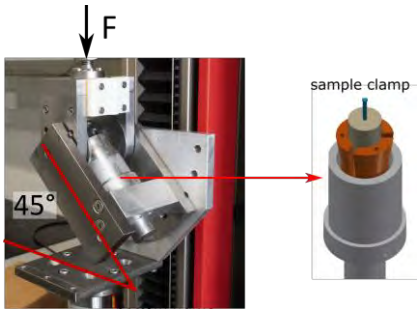


Figure 1: (left) test-setup in 45° inclination (mixed loading) and (right) cylindrical sample with screw in sample clamp.

The peri-implant morphology (BV/TV, trabecular thickness [Tb.Th.], cortical thickness [Ct.Th.]) was quantified from pre-implantation µCT scans. To simulate clinical CT resolution, datasets were coarsened and morphology was characterized by mean grey values (GV) of the full volume and predefined subregions (Figure 2). Correlation analyses identified parameters best predicting F_{fail} for both high- and low-resolution datasets.

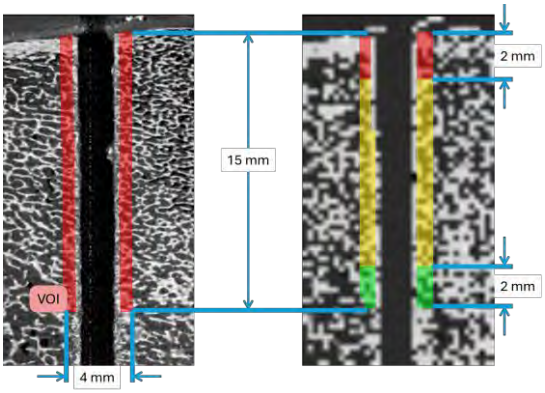


Figure 2: (left) µ-CT scanned bone sample, highlighting the VOI utilized for analysis, and (right) the simulated clinical resolution CT, the relevant sections of the VOI highlighted in different colours.

3. Results

Mean GV was the strongest predictor of F_{fail} across load cases (average $R^2 = 0.62 \pm 0.17$) and demonstrated predictive performance comparable to BV/TV derived from µCT scans (average $R^2 = 0.79 \pm 0.04$, [1]). Restricting the analysis to one of the subregions reduced robustness.

4. Discussion and Conclusions

It was shown that clinical resolution CTs could be utilized to predict screw-bone interface failure as well, although structural detail is reduced compared to µCT. A significant study limitation includes the artificial nature of the clinical resolution CTs; direct comparison of multiscale imaging should be considered to ensure the applicability of this approach.

5. References

1. Silva-Henao et al., J Mech Behav Biomed Mater, 2025; 168: 107043.
2. Silva-Henao et al., Med Eng Phys, 2024; 126: 104143.

3D PRINTED HYDROXYAPATITE INTERVETREBRAL FUSION CAGES FOR PATIENT SPECIFIC APPLICATIONS

Anna De Cet (1,2), Martina Colombo (1), Luca D'Andrea (1), Ilaria Rota (1), Luigi La Barbera (1), Pasquale Vena (1), Dario Gastaldi (1)

1. Department of Chemistry, Materials and Chemical Engineering "Giulio Natta", Laboratory of Biological Structure Mechanics (LaBS), Politecnico di Milano, Piazza Leonardo da Vinci 32, Milan, 20133, Italy; 2. Department of Biomechanics, Faculty of Medicine, Karl Landsteiner University, Dr. Karl-Dorrek-Straße 30, Krems, 3500, Austria

1. Introduction

Intervertebral fusion surgeries aim to replace degenerated discs with artificial implants made of titanium alloys or PEEK, both requiring grafts to ensure bone growth, which is required for the stability of the implant. Synthetic hydroxyapatite (HAp) has been proposed as an alternative material for these implants, due to its ability to support bone regeneration [1]. HAp's intrinsic fragility requires an accurate balance between porosity, necessary for bone ingrowth, and mechanical performance [2], which can be achieved through the accurate and patient-tailored design and computational testing of the implanted device. This study aims to evaluate the effect of different design and modelling choices on an implanted patient-specific cage for the L1-L2 vertebral segment.

2. Materials and Methods

A multidetector CT dataset, characterized by standard clinical resolution (0.326 x 0.326 x 0.6 mm) was chosen from the open-source repository of the VerSe 2020 Challenge [3]; the L1 and L2 vertebrae were isolated and segmented. Anisotropic site-specific mechanical properties were assigned based on local Houndsfield Unit (HU) values. A porous intervertebral fusion cage was designed, and a titanium alloy-based posterior fixation system was included in the model (Figure 1, right). First, the effect of homogenized properties as a modelling strategy was compared to the results obtained from microstructured devices. Then, four microstructural choices were tested, leveraging different inner geometries (FCC, Kelvin and Voronoi) and a porosity gradient (90% at the inner core, 60% externally).

3. Results

The macroscopic behaviour of the homogenized and microstructured scaffolds proved comparable, while localized damage was significantly overestimated in the first cases (Figure 1, left). All damage reported in the microstructured devices was low and mostly associated with tension stresses, and the introduction of a porosity gradient did lead to a significant reduction of damage inside the device.

4. Discussion and Conclusions

Based on relevant mechanical parameters, both the uniform FCC and graded Voronoi microstructures were able to achieve a sufficient compromise between mechanical performance and a positive interaction with the surrounding tissue. The necessity of microstructural representation of the devices, when the aim is to evaluate damage-related performance, was highlighted.

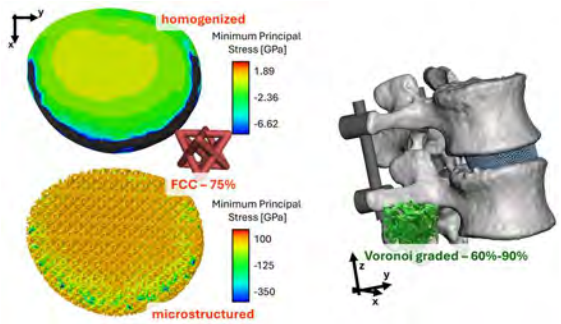


Figure 1: Comparison of homogenized and microstructured devices (left) and complete computational model simulated (right).

5. References

1. Fiume E. et al., Acta Biomat.; 119:405-418 (2021).
2. Ibrahimi S. et al., Comput. Methods Appl. Mech. Eng.; 423:116842 (2024).
3. Liebl H. et al., arXiv; 2021

Acknowledgements:
The authors kindly thank Elisa Salcioli for her contributions to the development of the project.

A MICROSTRUCTURE AND GRAIN ORIENTATION BASED FRAMEWORK FOR PREDICTING CORROSION IN MG WE43

KARAMIFARD, F.[1], VAUGHAN, TJ. [1], MCHUGH, PE.[1]

[1]*Biomedical Engineering, School of Engineering and Institute for Health Discovery and Innovation, University of Galway, Ireland*

1. Introduction

Magnesium (Mg) alloys are promising bioresorbable implant materials, but their rapid corrosion in physiological environments limits performance. Corrosion behaviour depends strongly on the polycrystalline microstructure, particularly crystallographic orientation [1]. In this study, Mg WE43 is modelled using a polycrystalline framework.

2. Materials and Methods

An orientation resolved surface-based corrosion model was implemented in Abaqus via a USDFLD subroutine with scalar damage and element removal [2]. Orientation dependent damage weighting enabled preferential basal plane corrosion (as per observation [1]). Pit initiated (Fig.1(a)) degradation propagated via an active surface criterion, with layer-by-layer corrosion observed in grains with horizontally oriented basal planes. Diffraction Contrast Tomography (DCT) characterised Mg WE43 microstructures were compared with idealised grain models (Fig.1(b, c)), and simulations were performed for varying grain sizes.

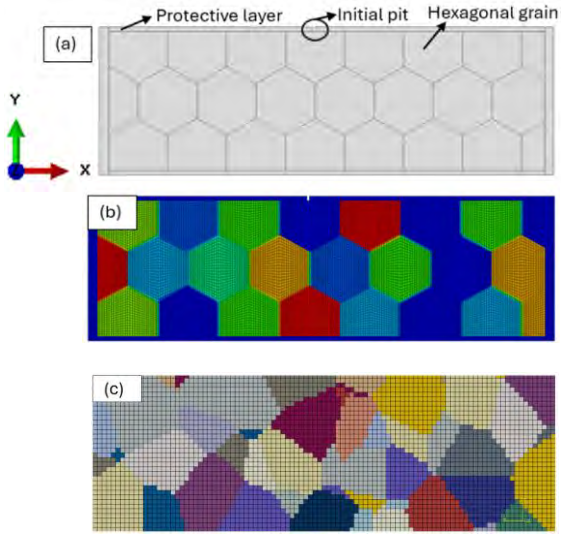


Figure 1: (a) Idealized model geometry, (b) Grain orientations, (c) DCT-based model.

3. Results

Figure 2(a) compares irregular (DCT-based) and idealised regular grain geometries. Both show similar overall damage evolution; therefore, the remaining models were generated using regular grain shapes.

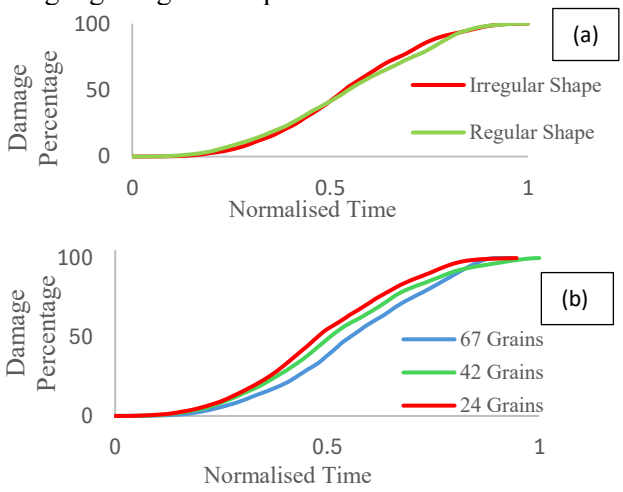


Figure 2: (a) Irregular vs. regular grain geometries, (b) Effect of grain number on damage.

Figure 2(b) shows the influence of grain size (24, 42, and 67 grains). Although all cases follow similar trends, finer grain structures exhibit slightly delayed damage progression.

4. Discussion and Conclusions

This study presents a framework that incorporates crystallographic orientation into corrosion modelling of Mg WE43, improving prediction of pitting behaviour. The model evaluates the influence of grains on corrosion progression, supporting microstructural design strategies. Future work will extend the approach to a full 3D DCT informed model.

5. References

1. Wang L et al., S. Corros Sci; 201:110273 (2022).
2. Quinn C et al., J Mech Behav Biomed Mater; 138:105637 (2023).

Acknowledgements:

This research was conducted with the support of the Hardiman Research Scholarship awarded by the University of Galway.

IN SILICO MODEL TO PREDICT THE MECHANICAL STABILITY OF TIBIAL PLATEAU FIXATION STRATEGIES

Marta Spataro [a,b], Maike Reul[c,1], Piyush Uniyal [b], Dario Milone [a], Giacomo Risitano [a], Harm Hoekstra [d], Thierry Scheerlinck[c], G.Harry van Lenthe [b]

[a] *Department of Engineering, University of Messina, Contrada di Dio, 98166 Messina, Italy*
[b] *Department of Mechanical Engineering, Biomechanics Section, KU Leuven, Leuven, Belgium*
[c] *Department of Orthopaedic and Trauma Surgery, UZ Brussels, Brussels, Belgium*
[d] *Traumatology, UZ Leuven, Leuven, Belgium*

1. Introduction

Tibial plateau fractures represent a major challenge in orthopaedic surgery. Although cadaveric testing remains the gold standard for evaluating implant stability, it is limited by specimen availability and cost. Finite element (FE) models have emerged as valuable tools to predict fracture risk and evaluate fixation devices using patient-specific approaches [1]. The aim of this study was to develop and validate a nonlinear *in silico* method to predict structural stability and failure behaviour of the proximal tibia after fixation.

2. Materials and Methods

Ten pairs of human cadaveric tibiae were used for experimental validation. Pre-test CT scans were acquired for all specimens. Mechanical tests were performed to failure using an Instron 3367 machine under a 6° valgus load. CT images were segmented to reconstruct the bone-implant models, including the fixation plates. FE models were generated with bone properties assigned element-wise from CT Hounsfield Units according to Keyak et al. [2]. A nonlinear iterative routine in Abaqus allowed elements to transition from linear elasticity to a softening regime through damage evolution, capturing post-yield behavior. Bone–implant interactions were modeled as frictional contact [3]. The main outcomes were failure load and total absorbed energy prior to fracture.

3. Results

The comparison between experimental data and FE predictions is shown in Figure 1. For bone strength, FE results were slightly lower than experimental measurements, with overlapping variability. For stiffness, the FE model showed a consistent overestimation compared to experimental values. Despite this difference, the model captured the broad range of mechanical responses observed in the cadaveric specimens. Overall, the FE simulations reproduced the experimental trend for bone strength ($R^2 = 0.8$), while stiffness was generally overestimated.

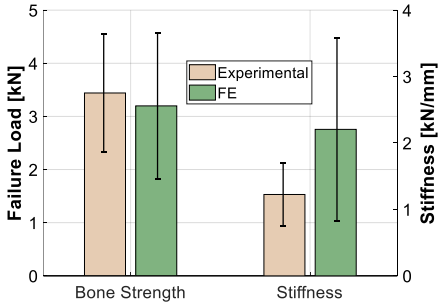


Figure 1: Comparison of experimental and in silico results for failure load [kN] and stiffness [kN/mm]

4. Discussion and Conclusions

The results demonstrate that the proposed In The proposed in silico workflow effectively reproduced the mechanical behaviour of tibial plateau fixation constructs. The agreement in failure load and the strong correlation suggest that the nonlinear routine captured the transition from elastic behaviour to structural collapse. Future work will investigate contact conditions in greater detail, including screw pretension and friction effects, and extend the validated pipeline to evaluate different fixation strategies for patient-specific simulations.

5. References

1. Munckhof et al., Clinical Biomechanics, 2014 Jan. Volume 29, Issue 4.
2. Keyak et al., Clin Orthop Relat Res. 2005 Aug;NA;(437):219–28.
3. Ferre al., JMBBM, 2022 Aug; Volume 134,105392.

Acknowledgements:
The authors thank the ARTE group (Vrije Universiteit Brussel) for specimen preparation, Gert Van Gompel (UZ Brussel) for CT imaging, and Wouter Willekens (FIBEr, KU Leuven) for conducting the experimental tests.

DEVELOPMENT OF A COMPUTATIONAL MODEL FOR THE IN SILICO PREDICTION OF SPATIOTEMPORAL EVOLUTION, METASTATIC DISSEMINATION AND THERAPEUTIC RESPONSE IN BREAST CANCER

Nikolaos Th. Papadopoulos (1), Iro Sotiriadou (1), Melina Tzika (1), Markos G. Tsipouras (1)

1. *Department of Electrical and Computer Engineering, University of Western Macedonia, 50100 Kozani, Greece*

1. Introduction

While Machine Learning (ML) increasingly dominates oncology, its "black-box" nature lacks biophysical grounding and clinical interpretability. To address this, we introduce a deterministic, coupled non-linear "white-box" PDE–ODE framework for solid tumors.

2. Materials and Methods

We developed a novel, coupled non-linear PDE–ODE system to accurately model the complex dynamics of the Tumor Microenvironment (TME). The mathematical framework captures the continuous interaction between normoxic, hypoxic, apoptotic, and healthy cell populations. Furthermore, the system holistically incorporates the extracellular matrix (ECM) as well as the spatiotemporal evolution of oxygen and drug concentrations.

Patient-specific parameter calibration utilizes clinical data from the Wisconsin Breast Cancer dataset [1]. Following strict data normalization, we construct explicit linear relationships mapping clinical features to biophysical parameters: normoxic baseline proliferation rate is scaled by tumor Area; baseline diffusion is modulated by Fractal Dimension; spatial distribution of blood vessels correlates with Texture; and the metastatic escape rate is driven by Compactness. To capture realistic biological heterogeneity, the effective computational radius is formulated as a linear combination of the dataset's original Radius and Fractal Dimension, augmented by a stochastic noise function. Similar spatial noise is applied to the blood vessel distribution to simulate realistic, chaotic angiogenesis.

We simulate 4D tumor spatiotemporal evolution within a 3D computational cube. Initially, total cancer cell density follows a sigmoid spatial distribution based on each node's Euclidean distance from the center and the effective radius. Enforcing a strict carrying capacity K per node, healthy cells occupy the remaining volume up to a physiological baseline, preserving realistic free space for tumor invasion.

Dynamically, the phenotypic "Go-or-Grow" dichotomy updates cellular diffusion and proliferation rates at each time step via a non-linear feedback loop tied to the metastatic escape rate. For numerical stability and computational efficiency, the continuous system is rigorously nondimensionalized and discretized via an implicit Finite Difference Method (FDM), utilizing vectorized array operations for parallelized in silico execution.

3. Results

Pending full implementation, the digital twin simulates 6-month spatiotemporal tumor evolution, explicitly quantifying population distributions, tumor shrinkage, and metastatic escape under varying *in silico* drug schedules. Comparative analyses will be presented.

4. Discussion and Conclusions

This deterministic "white-box" framework effectively bridges mathematical biology and clinical oncology. By comparatively evaluating multiple simulated treatment regimens over time, the oncologist can proactively identify the absolute optimal, personalized therapeutic strategy for each individual patient. Ultimately, this computational tool empowers clinicians to move decisively beyond generalized protocols towards true precision medicine.

5. References

1. Wolberg, W. *Breast Cancer Wisconsin (Original)* [Dataset]. 1990.
2. Flandoli, F. *Elements of Mathematical Oncology*. [Unpublished Manuscript].

A GENETICALLY ADJUSTED RADIATION DOSE PER THE PREDICTION OF LATE BREAST FIBROSIS AFTER RADIOTHERAPY

Benedetta Dionisi Ferrera* (1), Eliana Gioscio (1), Wouter Van Amsterdam (2), Petra Seibold (3), Maria Carmen De Santis (1), Eliana La Rocca (1), Alessandro Cicchetti (1), Christopher J Talbot (4), Catharine West (5), Tiziana Rancati (1), REQUITE consortium

1. Fondazione IRCCS Istituto Nazionale dei Tumori, Milan, Italy; 2. University Medical Center Utrecht, Netherlands; 3. Cancer Research Center, Germany; 4. Department of Genetics & Cancer Sciences, University of Leicester, United Kingdom; 5. Division of Cancer Sciences, University of Manchester, United Kingdom

**Presenting/corresponding author - benedetta.dionisiferrera@istitutotumori.mi.it*

1. Introduction

Radiotherapy (RT) after minimal surgery is a standard treatment for breast cancer. Despite advances in RT delivery techniques, some doses unavoidably reach breast-surrounding healthy tissues, which can cause RT-induced side effects.

The risk of developing side effects varies substantially among individuals, reflecting its multifactorial origin.

To account for inter-individual variability, we defined a normal tissue genetically adjusted radiation dose (NT_GARD) combining the patient-specific maximum dose to the breast [1] (corrected to 2Gy-fractionation, α/β=3Gy, EQD2MaxD) with individual genetic susceptibility.

2. Materials and Methods

Using data from the REQUITE breast cancer cohort (n=1823), we modelled genetic susceptibility through a polygenic risk score (PRS). Specifically, 127 single-nucleotide polymorphisms (SNPs) previously associated with late side effects were evaluated for association with fibrosis using a backward stepwise Cox proportional hazards model combined with 1,000 bootstrap resampling iterations.

The contribution of each SNP was assessed based on its selection frequency and ranking position across bootstrap samples, through a definition of a Normalized Area as in [2].

The 20 SNPs with the largest Normalized Area values were selected for inclusion in the PRS.

The PRS was defined through standardisation of Cox-multivariable prediction, while NT_GARD was derived from a two-variable Cox-model including PRS and EQD2MaxD, according to the formula:

$$NT_{GARD} = EQD2MaxD + \left(\frac{\beta_{PRS}}{\beta_{EQD2MaxD}} \cdot PRS\right) \quad (1)$$

Where $[(\beta_{PRS}/\beta_{EQD2MaxD}) \cdot PRS]$ represents the individualised genetic contribution that increases/decreases the effectiveness of the physical dose exposure [3].

3. Results

Employing a multiple-exposure Directed Acyclic Graph for variables selection, a multivariable Cox model identified NTGARD as significantly associated with risk of late fibrosis (CTCAE grade≥2 fibrosis in tumour bed or outside tumour bed, HR=1.032 per 1 genetically adjusted Gy).

4. Discussion and Conclusions

By explicitly incorporating genetic susceptibility into dose modelling, NT_GARD provides a biologically grounded, patient-specific measure of effective radiation dose.

We can use the NT_GARD tool to evaluate in-silico the effect/gain of different dose distributions (variation in technique, radiation type, dose-constraint goals) intersected with the specific patient genetic background, reaching biologically-driven RT choices.

5. References

1. Mukesh MB et al. *Radiother Oncol*. 2013;108(2):293-298.
2. Avanzo M et al. *Phys Med*. 2012;28(4):296-306.
3. Palorini F et al. *Radiother Oncol*. 2016;118(1):92-98.

Acknowledgements:

EU-FP7 grant 601826 (REQUITE Project). Horizon-EURATOM grant 101166699 (TETRIS).

OPEN-SOURCE CYTOARCHITECTONIC MAPPING OF GLIOBLASTOMA FOR SURGICAL PLANNING

Paola Papaleo (1), Marco Freddi (1), Giovanni Pignoni (1), Leonardo Frizziero (1)

1. Alma Mater Studiorum - University of Bologna, Viale del Risorgimento 2, 40136 BO (Italy).

1. Introduction

Anatomically informed identification of tumour subregions is crucial for patient-specific modelling and clinical interpretation. Glioblastoma shows significant spatial heterogeneity and infiltrative growth. Atlas-based anatomical frameworks have been proposed as a support for presurgical planning in neuro-oncological patients [1]. This work presents an open-source, patient-specific workflow for locating glioblastoma subregions within the Julich cytoarchitectonic Brain Atlas, which is freely accessible through the EBRAINS research infrastructure after atlas-to-patient registration.

2. Materials and Methods

Multiparametric MRIs were uploaded to 3D Slicer [2]. Four series were selected: pre- and post-contrast T1, T2 FLAIR, and T2-weighted. Pre-contrast T1 was used as a reference for resampling and registration. MONAI was used to automatically segment tumour components "Neoplasm" and "Necrosis". To avoid skull influence on atlas registration, 3D brain extraction was performed using the AI-based HD Brain Extraction software module.

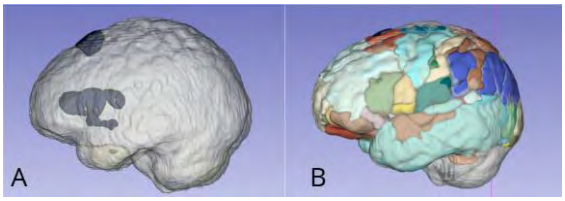


Figure 1: A) Glioblastoma segmentation in 3D skull-stripped patient brain; B) registration of Julich Brain Atlas on patient brain.

The Julich Brain Atlas, openly available through EBRAINS, was used as the anatomical reference [3]. Since the atlas is defined in standard space, a compatible MNI template was introduced as an intermediate reference and affinely registered to the patient's skull-stripped brain (Fig.1). The resulting transformation was then applied to the Julich atlas to bring the parcellation into patient space for overlap analysis. Results were automatically exported in spreadsheet format.

3. Results

Overlap analysis showed that the neoplastic subregion mainly involved insular and frontal opercular regions, with the highest overlap in Area Id7 (Insula), followed by Areas Op8 and Op9 (frontal operculum). Smaller overlap was observed in the anterior cingulate and mesial frontal regions, including Area 33, Area p24b, and Area 6ma (preSMA). The necrotic subregion showed a more limited extent, mainly affecting the same insular-opercular district, with predominant involvement of Area Id7 and minor overlap in Areas Op8 and Op9.

4. Discussion and Conclusions

This study presents a fully open-source, patient-specific workflow integrating MRI preprocessing, AI-based tumour segmentation, atlas registration, and voxel-wise overlap analysis. The approach supports 3D anatomical visualisation for preoperative interpretation, surgical access assessment, and the didactic training of young clinicians. Although demonstrated on a single proof-of-concept case, it provides a scalable basis for future oncological digital twin applications.

5. References

1. Sarubbo S. et al., *Oper Neurosurg (Hagerstown)*; 20(1): E6-E14 (2021).
2. Fedorov A. et al., *Magn Reson Imaging*; 30(9):1323-1341 (2012).
3. Amunts K. et al., *Science*; 369(6506):988-992 (2020)

Acknowledgements:

The authors thank the German Oncology Center in Cyprus for providing the anonymised patient imaging data used in this study. This work was supported by the European Union through the DTRIP4H project under Grant Agreement n° 101188432.

A PROTOCOL FOR IN-SILICO RADIOTHERAPY DOSE-ESCALATION OF HIGH-RISK HEAD AND NECK CANCER

Emmy Dalqvist (1,2), Hampus Hållberg (1,3), Tiziana Rancati (4), Anna Embring (2,5), Gabriella Alexandersson von Döbeln (5,6), Eva Onjukka (1,2),

1. Department of Nuclear Medicine and Medical Physics, Karolinska University Hospital, Stockholm, Sweden; 2. Department of Oncology Pathology, Karolinska Institutet, Stockholm, Sweden; 3. Epistat AB, Uppsala, Sweden; 4. Data Science Unit, Fondazione IRCCS Istituto Nazionale dei Tumori, Milan, Italy; 5. Department of Radiotherapy, Karolinska University Hospital, Stockholm, Sweden; 6. Department of Clinical Science, Intervention and Technology, Karolinska Institutet, Stockholm, Sweden;

1. Introduction

With a 'one-treatment-fits-all' approach as state of the art in head and neck (H&N) cancer radiotherapy, opportunities for dose escalation remain unexplored, despite loco-regional recurrence rates of approximately 40% after radiotherapy. Over the past decade, numerous radiotherapy prediction models have been developed [1, 2]. The risk of side effects may depend on the dose to multiple anatomical structures simultaneously; in the H&N region these are often close to the tumour and demonstrate a functional interplay among each other. A subset of patients with more favourable anatomy may tolerate a higher tumour dose without substantially increasing their overall risk of side effects. This highlights the potential for individualised, model-guided dose escalation aimed at improving tumour control and survival; this will be addressed by developing an in-silico study protocol.

2. Materials and Methods

Since 2014, the Karolinska University Hospital quality registry for H&N cancer has collected clinician-reported follow-up data alongside patient- and treatment-specific parameters (concomitant chemotherapy, smoking status, TNM stage, HPV status, etc). As of July 2024, the registry includes 2243 patients with a compliance rate of approximately 70%. This constitutes a real-world dataset suitable for validating prediction models [3] and providing subjects for in-silico studies. Further, a locally developed plugin to a radiotherapy treatment planning system (TPS) will support the study.

3. Results

The protocol for the in-silico dose escalation study includes the individualisation of the prescription dose, based on the risk of side effects estimated by prediction models in the literature [1, 2], integrated in the TPS plugin. Model selection is guided by local validation [3] and TRIPOD reporting quality. Model-guided dose-escalation will be performed in silico, for a local retrospective cohort of high-risk H&N cancer patients, considering multiple scenarios preserving an acceptable risk of side effects.

4. Discussion and Conclusions

The proposed in-silico study protocol explores a paradigm shift towards model-guided individualised dose prescription in radiotherapy. It paves the way for an intensified, evidence-based treatment for high-risk H&N cancer patients, associated with higher cure rates and longer survival.

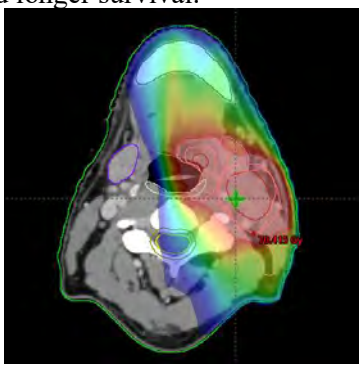


Figure 1: H&N cancer radiotherapy example illustrating a patient's unique exposure to radiation dose, depending on tumour location, tumour size etc.

5. References

1. Van den Bosch L, et al. Comprehensive toxicity risk profiling in radiation therapy for head and neck cancer: A new concept for individually optimised treatment. *Radiother Oncol*. 2021; 157:147-154.
2. Stieb S, et al. NTCP Modeling of Late Effects for Head and Neck Cancer: A Systematic Review. Int J Part Ther. 2021;8(1):95-107.
3. Dalqvist E, et al. Validated prediction of xerostomia in a real-world population: a step toward model-guided radiotherapy. *Acta Oncol*. 2025;64:1087-1094.

Funding

Varian, a Siemens Healthineers company

A TRANSLATIONAL POROMECHANICS MODEL: APPLICATIONS TO SKIN CANCER AND LOW-GRADE GLIOMA

Davide Baroli (1), Argyrios Petras (1), Luca Gerardo-Giorda (1)

1. Johann Radon Institute for Computational and Applied Mathematics of the Austrian Academy of Science, Austria

1. Introduction

The mechanical and transport properties of tumour tissue are central to cancer progression, treatment delivery, and therapeutic response. Computational oncology has increasingly embraced mechanistic modelling as a tool for patient-specific decision making, with predictive digital twins emerging as a promising paradigm for integrating imaging data with biophysical models of disease progression [1]. In this work, we present a translational coupled (thermo)-poro-elastic computational framework designed to bridge continuum mechanics and clinical oncology.

2. Materials and Methods

Grounded in mixture theory, the model accounts for solid deformation, interstitial fluid transport, and heat transfer through a system of fully coupled partial differential equations. Spatial discretisation is performed via finite elements on patient-representative geometry. All simulations are implemented in the open-source platform FEniCSx [1,2].

3. Pilot Application I: Skin Cancer

The first pilot exploits the naturally stratified architecture of soft tissue — epidermis, dermis, and subcutaneous layer — each characterised by distinct poromechanical and thermal properties. This pilot is directly motivated by recent advances in hierarchical poromechanical modelling of human skin, which demonstrated the critical role of interstitial fluid dynamics and microcirculation in governing tissue mechanical and biological response [2]. In the oncological context, the pilot targets localised irreversible electroporation, where the spatial distribution of interstitial pressure, vasculature, tissue deformation, and heat deposition critically determines therapeutic efficacy and damage localisation.

4. Pilot Application II: Low-Grade Glioma

The second pilot translates the framework to low-grade glioma (LGG), a diffusely infiltrating primary brain tumour associated with progressive alteration of the cerebral poromechanical environment. The model captures the coupling between tumour-induced mechanical stress, modified interstitial fluid dynamics, and thermal loading, providing a computational basis for evaluating emerging hyperthermal and electroporation-based neurosurgical strategies. Both pilots share a common mathematical and numerical infrastructure, with translational adaptation achieved solely through geometry, material parameters, and boundary conditions. This modularity positions the framework as a versatile in silico platform for multi-site oncological applications, with prospective use in personalised treatment planning, dosimetry optimisation, and hypothesis-driven preclinical investigation.

5. References

1. Pash G et al. Predictive Digital Twins with Quantified Uncertainty for Patient-Specific Decision Making in Oncology. arXiv:2505.08927 [Preprint]. 2025. PMID: 40463701.
2. Lavigne T et al. Hierarchical Poromechanical Approach to Investigate the Impact of Mechanical Loading on Human Skin Micro-Circulation. Int J Numer Method Biomed Eng. 2025;41(7):e70066. https://doi.org/10.1002/cnm.70066

ORAL MICROBIOTA-CONDITIONED TREATMENT EFFECT ON PROGRESSION-FREE SURVIVAL IN HEAD AND NECK CANCER

Michele Salerno (1)*, Salvatore Alfieri (1), Yunsheng Dong (1), Nicola Alessandro Iacovelli (1), Marzia Franceschini (1), Tiziana Rancati (1), Loris De Cecco (1) Ruth Keogh (2), Jacopo Iacovacci (1)

1. Fondazione IRCCS Istituto Nazionale dei Tumori di Milano, Milan, Italy;
2. Department of Medical Statistics, London School of Hygiene & Tropical Medicine, United Kingdom
**Presenting/Corresponding Author: michele.salerno@istitutotumori.mi.it*

1. Introduction

Variability in treatment response among head and neck cancer (HNC) patients receiving radiotherapy (RT) or chemoradiotherapy (CRT) suggests a role for patient-specific biological factors.[1] Evidence indicates that the oral microbiota influences treatment response and prognosis in HNC.[2] Here, we estimated the effect of the baseline oral microbiota on HNC treatment efficacy measured by progression free survival (PFS).

2. Materials and Methods

Data from 158 HNC patients with non-metastatic tumours of the Larynx, Oral Cavity, Oropharynx and Nasopharynx of the MicroLearner cohort (NCT03294122) were analysed, including pre-RT salivary microbiota and follow-up to 36 months. Shotgun metagenomics was used to obtain genus-level microbiota salivary profiles. A core microbiota of 17 genera (rel. ab. ≥2% in ≥10% of subjects) was identified. After clr-transformation and normalisation [3], hierarchical clustering with "correlation" distance and "average" agglomerative linkage was performed on the core profiles to cluster patients into three groups (n=53, n=47, n=48) based on their characteristic microbiota pattern. The treatment effect of CRT versus RT was estimated within each cluster using G-computation.[4] A discrete-time hazard model was fitted to predict counterfactual survival under both treatment levels, and marginal survival curves and cluster-specific survival ratios were derived (Figure 1). [5] The conditional average treatment effect (CATE) was expressed as survival ratio (1), with 95% confidence intervals obtained via bootstrapping.

$$CATE_{SR}(m,t) = \frac{E[S^1(t)|M_0 = m]}{E[S^0(t)|M_0 = m]} \qquad (1)$$

3. Results

The analysis showed that at 12 months patients in microbiota cluster 3 receiving CRT had higher PFS compared to patients receiving CRT alone (SR=1.23, 95%CI=0.75-2.60), differently from patients in cluster 1 (SR=0.96, 95%CI=0.78-1.30) and cluster 2 (SR=0.52, 95%CI=0.51-0.87). These trends persisted at 36 months (Figure 1).

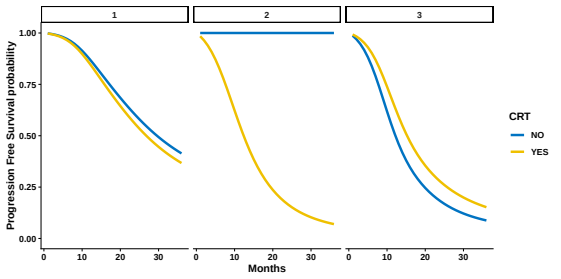


Figure 1: PFS marginal curves stratified by treatment within baseline-microbiota clusters.

4. Discussion and Conclusions

These findings suggest that the baseline salivary microbiota could be exploited to guide treatment strategies in HNC.
Establishing whether the oral microbiota acts as an effect modifier for the radiation dose will require further investigation through the analysis of treatment-associated confounders.

5. References

1. Belgioia L, et al. Focus on Main Hot Topics in Research" Frontiers in oncology 10:604965 (2021).
2. Bagheri Z, et al. Journal of Oncology 2022:3845104 (2022).
3. Aitchison J, Biometrical Journal. 30(7):794 (1986).
4. Robins J, Latent Variable Modeling and Applications to Causality (pp. 69-117) (1997).
5. Hernán MA, Epidemiology. 21(1):13-5 (2010).

Acknowledgements: J.I. acknowledges funding from AIRC grant MFAG 31114.

COMPUTATIONAL ESTIMATES OF THE PERITUMORAL HYPOXIA LEVERAGING MICROVASCULATURE PATIENT SPECIFIC DATA

Luca Possenti (1), Enrico Longhi (1), Eliana Gioscio (1) , Nicola A. Iacovelli (1), Marzia Franceschini (1), Giuseppina Calareso (1), Anna Cavallo (1), Ester Orlandi (2), Paolo Zunino (3), Tiziana Rancati (1)

1. Department of Epidemiology and Data Science/Dept of Imaging Diagnostics and Radiotherapy Fondazione IRCCS Istituto Nazionale dei Tumori, Italy
2. Department of Clinical, Surgical, Diagnostic, and Pediatric Sciences, University of Pavia, Campus della Salute, Policlinico San Matteo, Italy
3. Department of Mathematics, Politecnico di Milano, Italy

1. Introduction

Hypoxia is recognized as a key factor in cancer radioresistance, directly impacting the effectiveness of radiotherapy. Besides the method to estimate intra-tumoral hypoxia, also hypoxic pockets in the peri-tumoral regions might have a role. We introduce a computational workflow to simulate oxygen delivery in the microenvironment of head and neck cancer patients and evaluate the presence of hypoxia in peritumoral regions. These computational estimates for hypoxia at the microscale were derived from the transport equation and microvascular description. Such computational information might provide computational data that can be included into treatment prediction models.

2. Materials and Methods

We adapted the workflow proposed in a previous work [1] by including a direct reference to the full set of patient-specific data. Briefly, the workflow leverages microvascular data collected with a sublingual microscope to determine capillary density, vascular radius distribution, and red blood cell velocity in the microvasculature. Using this data, we created a synthetic description of the microvasculature that reproduces these patient characteristics. This digital microvasculature is then used to estimate the presence of hypoxia within the microenvironment by employing a multiscale 3d1d computational model specifically designed to describe oxygen delivery at the microscale [2].
We analyzed data from 8 patients providing information on microenvironment oxygenation.

3. Results

Three computational replicates of each patient-specific microvasculature were computed. Data were extracted as descriptors of the oxygen partial pressure distribution (minimum, average, maximum; Figure 1) and as quantification of hypoxic subvolumes using three different thresholds (5, 2, and 1 mmHg).

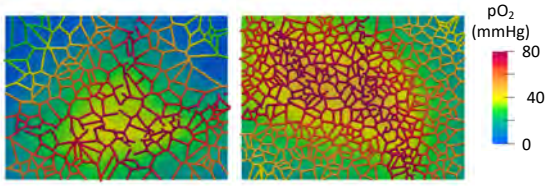


Figure 1: Computational oxygen distribution in the microenvironment for two of the eight patients considered.

4. Discussion and Conclusions

The obtained computational descriptors provide a patient-specific estimate of the possible hypoxia present in the peri-tumoral region. Such data can be used in conjunction with other descriptors (e.g., hypoxia scores describing tumoral hypoxia from imaging), to provide a more comprehensive description of the tumoral and peritumoral regions. This description can support predictive models for radiotherapy treatment, including hypoxia as a modifier of outcome.

5. References

1. Materne, Possenti, et al. Comput Biol Med. 2025
2. Possenti, Vitullo et al. Comput Biol Med. 2024

Acknowledgements:
This work is supported by Hi-ROC, EP PerMed JTC2024, FRRB EP_PERMED2024-548

FROM PATHWAY PERTURBATION TO MORPHOGENETIC FAILURE: VIRTUAL TISSUE NAMS FOR TOXICOLOGY

James A. Glazier (a), Job H. Berkhout (b,c), Thomas B. Knudsen (a), Harm J. Heusinkveld (b)

a. Biocomplexity Institute and Dept. of Intelligent Systems Engineering, Indiana University, Bloomington, USA
b. Centre for Health Protection, National Institute for Public Health and the Environment (RIVM), the Netherlands
c. Institute for Risk Assessment Sciences, Utrecht University, the Netherlands

Correspondence: James A. Glazier, Biocomplexity Institute & Dept. of Intelligent Systems Engineering, Indiana University, Bloomington, IN 47408, USA. Email: jaglazier@gmail.com

1. Introduction

Mechanistic, multicellular Virtual-Tissue simulations are increasingly useful New Approach Methodologies (NAMs) for connecting molecular perturbations to emergent tissue-level adverse outcomes in in silico toxicology. In the broader push toward adoption of digital twins in healthcare, these models provide digital-twin-enabling building blocks: mechanistic multiscale coupling, interpretable intermediate readouts, and uncertainty-aware scenario testing, without requiring patient-specific digital twins.

2. Materials and Methods

I will describe a CompuCell3D-based workflow that links exposure- and dose-dependent evidence (*e.g.*, pathway-activity proxies derived from transcriptomic signatures, or targeted perturbations to regulatory modules) to cell behaviors such as growth, differentiation, apoptosis, adhesion, migration, secretion, and force-mediated remodeling. Virtual-Tissue simulations produce interpretable intermediate readouts—cell-state composition, pathway-activity surrogates, geometric and mechanical metrics, and time-resolved morphogenetic trajectories—supporting mechanistic hypothesis testing, sensitivity analysis, and uncertainty quantification. A key enabling component is the development of computable tissue substrates (*e.g.*, a computable epiblast) that make early developmental dynamics executable and testable in silico [1].

3. Results

A central exemplar will be morphogenetic closure processes relevant to neural tube closure defects (*NTDs*), where modest changes in regulatory programs can shift collective dynamics and increase the probability of structural failure. Building on a computational dynamic-systems model of neural tube closure defects, I will highlight how transcriptomics-driven perturbations can be mapped onto conserved pathways represented in the model to enable probabilistic hazard assessment and mechanistic interpretation of closure failure [2].

4. Discussion and Conclusions

Virtual-Tissue NAMs provide a practical bridge from molecular evidence to tissue-scale phenotypes by making assumptions explicit, generating mechanistically interpretable intermediate readouts, and enabling reproducible what-if testing of timing, dose, and susceptible states. The emphasis of this presentation will remain on morphogenesis and neural tube closure as a flagship mechanism-to-phenotype use case. Separate presentations at VPH2026 will report our group's adult-tissue Virtual-Tissue toxicology models of the cornea (vCornea) and skin (vSkin).

5. References

1. Barham K, Spencer R, Baker NC, Knudsen TB. Engineering a computable epiblast for in silico modeling of developmental toxicity. Reproductive Toxicology. 2024;128:108625.
2. Berkhout JH, Glazier JA, et al. A computational dynamic systems model for in silico prediction of neural tube closure defects. Current Research in Toxicology. 2025;8:100210.

Acknowledgements:
The authors would like to thank ONTOX project, Horizon 2020 EC grant agreement No 963845, P&G Corporation and the US National Science Foundation (Grants NSF 2303695 and NSF 2120200) for providing financial support to this project.

VIRTUAL SKIN: A MECHANISTIC VIRTUAL EPIDERMIS WITH APPLICATIONS TOWARDS IN SILICO DERMAL EXPOSURE

Lorenzo Veschini (1, 2), Alison Stephens (2), Emmma-Mary Hull (2), Leigh Knight (2), Catherine Mahony (2), James A Glazier (1)

1. Department of Intelligent Systems Engineering and Biocomplexity Institute, USA; 2. Procter & Gamble Technical Centre, Reading, United Kingdom

1. Introduction

Computational in silico models for dermal exposure must represent not only chemical transport but also the dynamic biology of the epidermal barrier including self-renewal, stratification, hydration gradients, and recovery after perturbation.

We present Virtual Skin, a mechanistic, agent-based model of human interfollicular epidermis developed as a general-purpose digital tissue framework.

2. Materials and Methods

VSkin is implemented in the Cellular Potts framework (CompuCell3D), enabling explicit representation of cell–cell adhesion, proliferation and differentiation rules, and diffusive transport fields within a spatial lattice.

3. Results

VSkin recapitulates epithelial self-renewal and stratification through basal cell proliferation coupled to progressive differentiation toward granular and squamous layers. A parameterised diffusion field models water transport across the tissue, allowing estimation of hydration gradients and a proxy for trans-epidermal water loss (TEWL) under defined environmental boundary conditions. Tissue morphology can be tuned to mimic different epithelial states, including keratinising, non-keratinising, flat, and ridged epithelia, and to evaluate repair upon wounding in different configurations.

4. Discussion and Conclusions

VSkin architecture enables integration with existing exposure modelling. The model has been designed with interoperability in mind, supporting integration with spatial or non-spatial models through modular coupling strategies. The existing transport framework can be adapted to represent solute influx and distribution, grounded in experimental permeability data, while maintaining explicit coupling to tissue turnover and barrier integrity.

Current efforts focus on benchmarking tissue architecture and hydration outputs against published histological and biophysical datasets. Future developments aim to incorporate inflammatory and vascular components, enabling to investigate how epithelial perturbation propagate to downstream biological responses.

Overall, VSkin provides a flexible mechanistic epidermal framework that is broadly applicable to studies of epithelial homeostasis, perturbation, and recovery, and can be tailored to support in silico dermal workflows in a variety of applications.

Acknowledgements:

The authors would like to thank Drs Joel Vanin and Michael Getz for fruitful discussions and contributions to this work. The VSkin project is kindly sponsored by Procter & Gamble, UK.

LLM-BASED PSYCHOLOGICAL DIGITAL TWINS IN SOCIAL RESEARCH: APPLICATION TO ANTI-VACCINATION MOVEMENTS

Pawel Sobkowicz

Sano - Centre for Computational Personalized Medicine, Poland

1. Introduction

Anti-vaccination movements exploit emotional appeals and psychological biases effectively [1, 2], while public health authorities face a critical ethical asymmetry: they cannot conduct large-scale social experiments testing communication strategies on vaccine-hesitant populations. Anti-vaccination activists face no such constraints, continuously optimizing messaging through real-time social media experimentation. While small-scale interventions show promise [3,4], we lack validated approaches for predicting effectiveness at population scales where active propaganda is present. Our goal is to answer the following research questions: How do anti-vaccination communication strategies differ from evidence-based medicine messaging in persuasion tactics, emotional appeals, accessibility, and other aspects? What individual and contextual factors predict susceptibility to anti-vaccination misinformation across the population segments? Which counter-messaging strategies show highest predicted effectiveness for specific population segments in validated simulations?

2. Research Framework

We propose to use an Agent Based Modeling approach combining rule-based ABMs (offering transparency and explainability) with LLM-powered generative agents (offering behavioral realism and complexity[5]). The dual-modeling allows cross-validation between model types, plus experimental validation, addresses limitations inherent in each approach individually.

Methodology combines 4 steps

(1) Systematic analysis (LLM assisted) of chosen health communications originating from government agencies, medical professionals, anti-vaccination sources and social media, detecting source characteristics, linguistic features, emotional content, persuasion tactics, misinformation markers. (2) Dedicated population survey measuring: demographics and health context; vaccination attitudes; information behaviors; trust profiles; Health Belief Model components; and Elaboration Likelihood Model indicators. The results would be used to identify several population segments with distinct susceptibility profiles. (3) Dual ABM development: **Rule-Based ABM**: Influencer agents with communication profiles from step 1; population agents representing segments identified at step 2. **LLM-Powered ABM**: agents created via detailed prompts encoding demographic ("psychological" digital twins, not of individual persons – which would face difficult ethics challenges, but representing relevant segments of society). (4) Simulation scenarios to be tested: current environment, enhanced evidence-based messaging, simplified communication, emotional appeals, trusted messengers, peer testimonials, preemptive inoculation, counter-messaging, hybrid strategies. Statistical comparison identifies optimal approaches overall and per segment.

3. Results and Conclusions

We propose novel dual-validation strategy (rule-based + LLM) for social simulation; offering ethical framework for testing pro-vaccination interventions. The model would use characterization of anti-vaccination vs. evidence-based communication strategies; population segmentation for susceptibility to health misinformation; and evidence-based recommendations for counter-messaging by segment.

4. References

1. Wawrzuta, D., et al.: Vaccines 10(8), 1190 (2022)
2.Ball, H., Wozniak, T.R.: Health Comm. 37(14), 1812–1819 (2021)
3. Horne, Z., et al.: PNAS 112(33), 10321–10324 (2015)
4. Dai, H., et al.: Nature 597(7876), 404–409 (2021)
5. Gao, C., et al.: Humanities and Social Sciences Communications 11(1) (2024)

Acknowledgements:

The publication was supported by Minister of Science and Higher Education "Support for the activity of Centers of Excellence established in Poland under Horizon 2020" on the basis of the contract number MEiN/2023/DIR/3796. This project has received funding from the European Union's Horizon 2020 research and innovation program under grant agreement No. 857533

V-CORNEA: A MULTI-SCALE IN SILICO FRAMEWORK FOR OCULAR TOXICOLOGY AND IVIVE

Joel Vanin (1), Michael Getz (1), Catherine Mahony (2), Thomas Knudsen (1), James Glazier (1)

1. Department of Intelligent Systems Engineering and Biocomplexity Institute, Indiana University, Bloomington, IN, USA; 2. Procter & Gamble Technical Centre, Reading, United Kingdom

Corresponding author: Joel Vanin, jvanin@iu.edu, Department of Intelligent Systems Engineering, Indiana University, Bloomington, IN 47408, USA.

1. Introduction

Predicting injury severity and time-to-recovery after ocular chemical exposure remains a critical industry need for chemical classification and risk assessment. Existing in vitro and ex vivo New Approach Methodologies (NAMs) provide essential data on how toxicants affect cells at specific time points but struggle to predict dynamic, system-level outcomes such as tissue healing trajectories or non-recovery potential. We present V-Cornea, a multi-scale agent-based model (ABM) that serves as an in silico NAM and an engine for in vitro to in vivo extrapolation (IVIVE), bridging the gap between static assay readouts and dynamic tissue-level outcomes.

2. Materials and Methods

V-Cornea decomposes the corneal injury-repair process into interpretable, mechanistic components. First, a homeostatic virtual corneal epithelium self-organizes from defined rules governing cell proliferation, migration, differentiation, and shedding, reproducing baseline tissue turnover and renewal consistent with literature constraints. This validated baseline supports simulation of injury at multiple depths, with time-to-recovery matching clinical data for superficial to mild injuries [1].

Second, a time-resolved, localized-damage framework introduces cell-fate decisions designed as a digital twin of an experimental protocol for localized injury. Each cell executes a stochastic Boolean network governing fate decisions between survival, apoptosis, and necrosis [2] as a function of local chemical concentration.

3. Results

Necrotic cells burst and release damaging signals, driving secondary damage propagation, a behavior observed experimentally and reproduced in silico. This digital twin, once validated against experimental data, serves as a hypothesis generator: through systematic sweeps of concentration and exposure duration, we produced phase diagrams mapping exposure conditions to tissue-level outcome regimes, from containment to catastrophic spread.

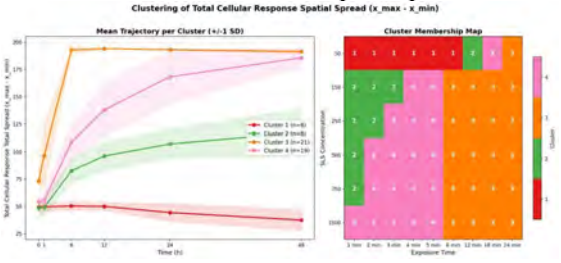


Figure 1: Phase space (exposure time and concentration; right) results of extent of damage. Clustering through k-means allows classification into 4 general outcome regimes.

4. Discussion and Conclusions

Critically, without immune-mediated debris clearance and inflammation resolution, the model's damage-propagation loop has no off-switch, mirroring what in vitro assays observe but diverging from in vivo recovery. This defines the IVIVE boundary. By introducing immune response dynamics into the in silico experiment, we provide the missing recovery signals, enabling the framework to extrapolate from assay-level observations to in vivo-relevant predictions of injury severity and recovery time.

5. References

1. Vanin J, Getz M, Mahony C, Knudsen TB, Glazier JA (2025) V-Cornea: A computational model of corneal epithelium homeostasis, injury, and recovery. PLoS Comput Biol 21(12): e1013410. https://doi.org/10.1371/journal.pcbi.1013410 **2.** Calzone L, Tournier L, Fourquet S, et al. (2010) Mathematical Modelling of Cell-Fate Decision in Response to Death Receptor Engagement. PLoS Comput Biol 6(3): e1000702. https://doi.org/10.1371/journal.pcbi.1000702

Acknowledgements:

This work was supported by Procter & Gamble and conducted through collaboration with Indiana University. "The authors would like to thank the National Science Foundation (NSF 2303695 to JAG; NSF 2120200 to JAG and MG) and from the National Institutes of Health (NIH U24 EB028887 to JAG) for providing financial support to this project".

HOSPITAL-LEVEL PREDICTION OF EMERGENCY ROOM DEMAND DURING PERIODS OF EXTREME HEAT

Giulio Colombini(1,2), Francesco Durazzi (1), Marianna Santoro (3), Anna Vesely (4), Rossella Miglio (4), Paolo Tubertini (3), Daniel Remondini (1), Armando Bazzani (1,2)

1. Department of Physics and Astronomy, University of Bologna, Italy; 2. Centre for Advanced Studies in Tourism, University of Bologna, Italy. 3. IRCCS Sant'Orsola Bologna, Italy; 4. Department of Statistical Sciences, University of Bologna, Italy

1. Introduction

Heatwaves and extreme heat in general are associated with increased mortality and emergency hospitalizations, particularly for cardiovascular and respiratory conditions[1]. In urban settings, healthcare demand during extreme temperature events depends not only on meteorological intensity but also on population exposure. Within a collaboration between the University of Bologna and IRCCS Sant'Orsola, we developed a city-level predictive model integrating local temperature and mobility data to estimate daily emergency room accesses during heatwaves, with the goal of supporting operational hospital planning.

2. Materials and Methods

We developed a linear model predicting daily accesses to emergency room (ER) using a heatwave exposure index (HE) capturing social activity and temperature. As a proxy for social activity and population abundance in the city we used traffic open-data. Temperature data was provided by the local weather agency ARPAE and compared with ECMWF (both open data). Daily accesses to ER have been provided by IRCCS Sant'Orsola, aggregated by diagnosis code (ICD9-CM). The HE index counts the days of statistically critical temperature in the previous 7 days weighted by urban traffic data. We selected relevant diagnosis in a data-driven approach, designing a genetic algorithm to select the combination of diagnoses that correlated the most with the HE.

3. Results

The genetic algorithm selected a list of relevant diagnoses which partially overlapped with a list provided by the medical direction and partially extended it. In Figure 1, we show the prediction results over time, focusing on a test set (summer 2025) which has not been used for model fitting.

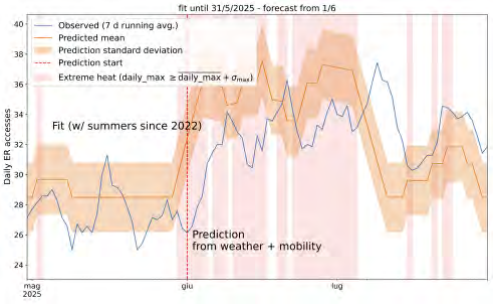


Figure 1. Number of daily ER accesses (blue) and model predictions (orange), with associated standard deviation.

The linear trend in Figure 1 had also been enhanced using the locally measured time series of temperature, which better captured extreme temperature values than the more smoothed ECMWF data. Also, the use of mobility as exposure weight accounts for the smaller amount of observed ER accesses during the August summer holidays, when less people are present in the area.

4. Discussion and Conclusions

The modelling approach we developed sets useful advancements to enhance predictive precision of health risk during heatwaves at single city level. The usage of raw data of local temperature and urban traffic data introduce locally-relevant features, that are crucial to for prediction. Our model also leverages the increase of health risk over time by cumulating the exposure, while many models often relay on point-wise correlation, optionally with delays.

5. References

1. Gasparrini et al., Lancet, 2015, 386(9991):369-75.

Acknowledgements:

The authors would like to acknowledge the funding by Italian Ministry of University and Research within the Complementary National Plan PNC-I.1 "Research initiatives for innovative technologies and pathways in the health and welfare sector", project DARE - Digital Lifelong Prevention project, no. PNC0000002.

PHYSIOLOGICAL AND PHYSICOCHEMICAL DRIVERS OF INHALED VOC DOSIMETRY VIA GLOBAL SENSITIVITY ANALYSIS OF LUNG GAS EXCHANGE MODEL

Robin Curnow (1), Ran Wang (2), Stephen Fowler (2), Waqar Ahamed (2), Carl Whitfield (1)

1. Department of Mathematics, University of Manchester, United Kingdom; 2. Division of Immunology, Immunity to Infection & Respiratory Medicine, University of Manchester, United Kingdom

1. Introduction

Epidemiological studies have identified correlations between respiratory disease and inhaled volatile organic compound (VOC) exposure, with *in-vitro* studies uncovering toxicological mechanisms (Faber et al, 2018). Relating inhaled concentrations to cellular dosimetry requires accounting for diverse gas properties and population-wide physiological differences.

2. Materials and Methods

We build on a computational model of inhaled VOC exchange (Anderson et al, 2003). A global sensitivity analysis highlights the key physiological parameters affecting the extent and location of VOC exchange.

3. Results

We found, large differences in solubility exhibited between VOCs is a key determinant of exchange location in the lungs, with higher blood solubility shifting exchange from the alveoli to conducting airways. By utilizing population-level distributions of physiological data, we identify drivers of tissue-level dosimetry. We demonstrate the extent to which hemodynamic, anatomical and morphometric parameters (e.g. cardiac output, tissue thickness or lung volume) drive inter-individual susceptibility to specific VOC pollutants. Furthermore, we show intra-individual variability is modulated by respiratory patterns.

4. Discussion and Conclusions

Our findings offer a mechanistic framework linking environmental exposure to *in vitro* models of respiratory disease, with external factors like exercise or humidity affecting internal concentrations independent of ambient levels (figure).

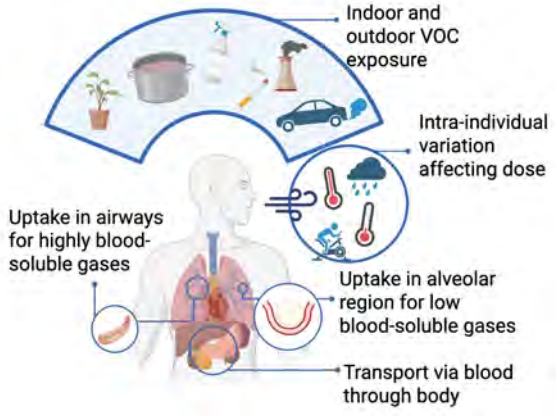


Figure 1: Sources of inhaled VOC.

5. References

1. Faber SC, McCullough SD. Through the Looking Glass: In Vitro Models for Inhalation Toxicology and Interindividual Variability in the Airway. *Applied In Vitro Toxicology*. 2018;4(2):115-128. doi:10.1089/aivt.2018.0002
2. Anderson, J.C., Babb, A.L. & Hlastala, M.P. Modeling Soluble Gas Exchange in the Airways and Alveoli. *Annals of Biomedical Engineering* **31**, 1402–1422 (2003). https://doi.org/10.1114/1.1630600

Acknowledgements:

The research was supported by the Engineering and Physical Sciences Research Council (EPSRC) Network Plus 'BIOREME' (EP/W000490/1). Robin Curnow is supported by the Medical Research Council (MR/W007428/1). Carl Whitfield was supported by a Dame Kathleen Ollerenshaw Fellowship. Ran Wang is funded by NIHR (through NIHR Clinical Lectureship) and received funding from Asthma + Lung UK (ECSG24\28). Waqar Ahmed is funded by the North West Lung Centre Charity; all co-authors are supported by Manchester National Institute for Health and Care Research (NIHR) Biomedical Research Centre (BRC).

CARDIOVERSE: COMPREHENSIVE ASSESSMENT OF CARDIAC RISK THROUGH DATA-DRIVEN IN-SILICO VIRTUAL ECOSYSTEMS

Vincenzo Carbone[1], Candice Baker[2], Nadia Rosenthal[2], Paul Robson[2], Travis Hinson[2,3], Daniel Paull[2,4], Daniel Beard[4], Daniel Röshammar[1], Luca Emili[1], Matt Mahoney[2]

1. InSilicoTrials Technologies, Italy; 2. The Jackson Laboratory, USA; 3. University of Connecticut Health Center, USA, 4. The New York Stem Cell Foundation, USA, 5. University of Michigan, USA

1. Introduction

Cardiotoxicities in the form of arrhythmia, cardiomyopathy, myocarditis, and heart failure are leading causes of drug-candidate failure and account for 10-14% of post-market withdrawals [1]. Non-arrhythmia cardiotoxicities (NACTs) are substantially more heterogeneous events, resulting from toxicities that are often rare and idiopathic and driven by multiple overlapping pathways [2], and therefore may not be detected in the current preclinical pipeline. CARDIOVERSE project aims to develop a hybrid AI–mechanistic (HAIM) platform to identify poorly predicted cardiotoxicity events by integrating genetically heterogeneous in vivo and in vitro data with advanced computational modelling, to simulate drug responses within the human cardiovascular system across human variability.

2. Materials and Methods

Multi-scale training data are generated using genetically diverse J:DO mice and 48 hiPSC-derived cardiomyocyte lines exposed to cardiotoxic and cardiac-safe compounds. Omics profiles, metabolomics, contractility assays, and echocardiography inform digital twin models of heart function. A graph neural network framework aligns omics–to–physiology mappings across species, while chemoinformatic models predict drug mechanisms of action from structure and targets.

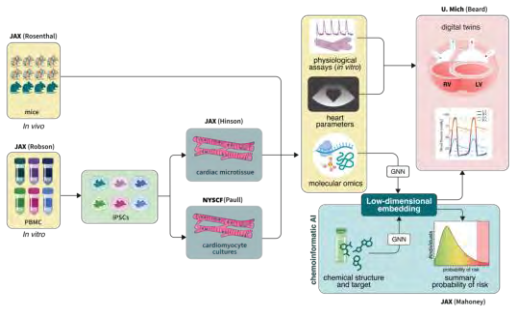


Figure 1: CARDIOVERSE Data Generation and Modeling Overview.

3. Results

CARDIOVERSE HAIM models are integrated into a cloud-based suite of in silico predictive safety pharmacology tools, alongside existing pro-arrhythmia modules developed under the CiPA initiative [3], enabling unified assessment of electrophysiological and non-arrhythmic cardiotoxicities. CARDIOVERSE SUITE is deployed through Modeling and Simulation-as-a-Service (MSaaS) approach, complying with international regulatory guidance, and offering flexibility, scalability and reproducibility. User-friendly graphical interface allows complex simulations to be designed and run by domain specialists that are not computational modeling experts, dramatically lowering the barrier to use.

4. Discussion and Conclusions

CARDIOVERSE aims to establish a scalable, regulatory-ready in silico cardiotoxicity assessment platform capable of generating simulated Phase 1 populations and individualized risk profiles. By embedding genetic heterogeneity, mechanistic interpretability, and explainable AI, the platform will enable safer and more efficient drug development and will support the transition toward fully computational IND-enabling studies, offering a powerful path toward animal-free safety evaluation and accelerated development of safer therapeutics.

5. References

1. Ferri N et al., Pharmacol Ther. 2013 Jun;138(3):470–484
2. Hansen J et al., Nat Commun. 2024 Sep 11;15(1):7968.
3. Li Z et al., Clin Pharmacol Ther. 2019 Feb;105(2):466–475

Acknowledgements:

The authors would like to thank the Advanced Research Projects Agency for Health (ARPA-H) for providing financial support to this project (Grant no: AY2AX000124).

NUMERICAL STUDY OF MAGNETIC MICROBEADS STEERED BY MAGNETIC RESONANCE NAVIGATION FOR TUMOR EMBOLIZATION

Mahdi Rezaei Adariani (1,2), Jiří Pešek (1), Ning Li (2), Cyril Tous(2), Gilles Soulez (2), Irene Vignon-Clementel (1)

1. Inria (Saclay IdF), France; 2. CR-CHUM (Montreal), Canada;

1. Introduction

Magnetic resonance navigation (MRN) of medicinal particles is an emerging technique for liver cancer treatment. MRN relies on particle clusters formed via interactions induced by the MRI scanner's magnetic field. These aggregates are injected into the blood flow, and steered toward the target vessels by blood drag, magnetic gradient forces, and gravity [1]. A critical challenge is understanding the aggregate motion, particularly near vessel walls, which is inadequately addressed by existing models [2]. This study investigates these factors using numerical simulations to provide insights into aggregate behavior, and improve computational models for targeted embolization.

2. Materials and Methods

Magnetic micro-bead aggregates were simulated in a hepatic artery geometry under physiologically relevant flow conditions and validated against in-vitro phantom experiments. Inlet conditions were derived from phase-contrast MRI, with outlet flow rates measured manually. Particle motion was modeled using a Lagrangian point-particle approach based on the Maxey-Riley equation. Drag was estimated by the bead drag model for chain-like aggregates [3], with near-wall corrections available in the literature [4]. While these simplifications neglect shape effects and the complexity of the flow, they provide a framework for analyzing aggregate behavior near vessel walls, which is key for the application. Hydrodynamic forces on individual particles were further analyzed using direct numerical simulation (DNS) to better capture aggregate dynamics near vessel walls.

3. Results

The study began with chains of spherical particles oriented parallel or perpendicular to flow. Total drag predictions were validated against experimental data and the bead-chain drag model. Near-wall corrections were further validated using DNS for a particle moving in stationary flows and a particle fixed in shear flow. Strong agreement between analytical solutions and numerical results confirms the model's accuracy for these configurations. Moving particles in flow were further analyzed.

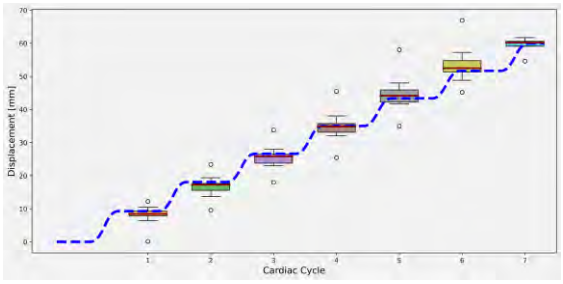


Figure 1: Experimental (box plot) vs. numerical (dashed line) displacement of aggregates.

4. Discussion and Conclusions

The simplified model was verified, and validated against realistic phantom experiments. Preliminary results suggest that the method provides reasonable estimates of aggregate motion. However, the bead drag model is limited to rigid chains of spherical particles, and further research is needed to generalize hydrodynamic effects on aggregates of varying shapes in realistic arterial flow. Ongoing work aims to develop a semi-empirical model to better bridge the gap between one-way coupling simulations and experiments, providing a foundation for optimizing MRN-based tumor embolization in-vivo.

5. References

1. Li,N et al,Science Robotics9.87(2024)eadh8702.
2. Vartholomeos et al, TransBioEng,59(11), 2012.
3. Yang, K et al, PLoSOne,12(11), e0188015,2017
4. Zeng, Lanying, et al. Physics of fluids 21.3 (2009).

Acknowledgements:

Funding by European Research Council (ERC) under the European Union's Horizon 2020 research and innovation program (Grant agreement No. 864313)

A MULTISCALE DIGITAL TWIN FRAMEWORK FOR MECHANISTIC PREDICTION OF CARDIAC ALLOGRAFT VASCULOPATHY

Elisa Serafini[1], Antonio Martino[1], Luca Pasini[2], Maria Sole Lami[2], Diego Amici[1,2], Giuseppe De Nisco[2], Diego Gallo[2], Claudio Chiastra[2], Sadeer Al-Kindi[1], Carly Filgueira[1], Stefano Casarin[1]

1. Houston Methodist Hospital, USA; 2. Polytechnic University of Turin, Italy

1. Introduction

Cardiac allograft vasculopathy (CAV) is the leading cause of late graft failure after heart transplantation (HTx) and remains clinically silent until advanced vascular remodelling and lumen loss occur [1]. Because current surveillance methods detect disease relatively late, improved tools for early, physiology-based risk stratification are needed [2]. We aim to develop a mechanistic, multiscale Digital Twin (DT) that integrates vascular inflammation and coronary hemodynamic to better characterize CAV progression.

2. Materials and Methods

The proposed DT integrates mechanistic models of vascular inflammation and remodeling [3] with subject-specific coronary hemodynamics [4]. Coronary geometries were reconstructed from imaging data, and computational fluid dynamics (CFD) simulations were used to estimate local flow descriptors, including wall shear stress (WSS). These hemodynamic features were coupled with a mechanistic model of inflammatory cell trafficking, endothelial dysfunction, and intimal growth. Model calibration and initial evaluation were performed using longitudinal murine CAV data and applied to six samples to assess feasibility and reproducibility of the integrated framework.

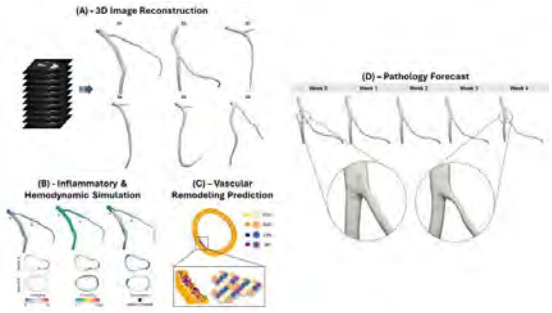


Fig. 1 | Computational pipeline. (A) CT-derived coronary geometry; (B) hemodynamic and inflammatory simulations estimating vascular injury; (C) mechanobiological remodelling model predicting intimal thickening and lumen loss; (D) forecast of CAV severity for risk stratification.

3. Results

A fully integrated DT developed and applied to six murine datasets. The framework effectively coupled subject-specific coronary geometries and hemodynamic simulations with mechanistic representations of inflammatory and vascular remodelling processes. Initial calibration demonstrated that the model can reproduce spatiotemporal patterns of vascular remodelling and progressive lumen narrowing observed in the preclinical data. Across the six samples, the framework generated individualized trajectories of intimal hyperplasia and hemodynamic stress distributions, demonstrating feasibility of the integrated approach. The model architecture allows extraction of mechanistically interpretable features linking inflammatory burden, endothelial dysfunction, and adverse shear environments with structural vascular changes.

4. Discussion and Conclusions

This study demonstrates the feasibility of a mechanistic DT framework that integrates inflammatory and hemodynamic drivers of CAV progression. Initial preclinical implementation in six murine samples supports the ability of the model to reproduce vascular remodelling dynamics and generate interpretable mechanistic features. Ongoing work is expanding this framework toward clinical application using both retrospective imaging datasets and a prospective patient cohort to evaluate its potential for early risk stratification and personalized surveillance in heart transplant recipients.

5. References

1. Ramzy D, et al., Can J Surg. 2005;48(4):319-27
2. Chih S, et al., Seminars in Nuclear Medicine. 2021;51(4):349-56
3. Serafini E, et al. Front. Bioeng. Biotechnol. 2023; 11:1190409
4. Searfini E, Martino A, et al., Comp. in Biol. And Med. 2025; 187:109793

SYNGROW – GLOBAL OPTIMIZATION AS A GOVERNING PRINCIPLE OF VASCULAR DESIGN IN ORGANS

Etienne Jessen (1), Marc Steinbach (2), Dominik Schillinger (1)

1. Institute for Mechanics, Computational Mechanics Group, Technical University of Darmstadt, Germany; 2. Institute of Applied Mathematics, Leibniz Universität Hannover, Germany

Corresponding author: Etienne Jessen, Technical University of Darmstadt, 64289 Darmstadt, Germany, email: etienne.jessen@tu-darmstadt.de

1. Introduction

The vasculature within organs forms hierarchical vessel networks that govern tissue perfusion. Understanding the principles that shape these networks remains limited, yet is essential for the functional assessment of organs. Scaling behaviour at vessel branches is commonly described by Murray's law, which is derived from the assumption that vessels minimize local energy expenditure. However, experimental observations frequently deviate from this prediction, indicating that vascular design is governed by more general scaling laws beyond local optimality. To investigate this hypothesis, we developed SynGROW, a global optimization framework for synthetic vascular tree generation in organs.

2. Materials and Methods

SynGROW formulates the tree generation as a weighted length minimization problem. The weighting function can be prescribed to represent different scaling laws. SynGROW seeks the global optimum of this problem over both topology and geometry [1], while enforcing non-intersecting vascular trees within nonconvex organs [2]. To assess whether global optimality explains vascular design in organs, segmented liver and lung vascular trees were used as anatomical reference data. Root and terminal locations were extracted and used as boundary conditions for tree generation. The weighting function was calibrated to minimize centreline deviation between synthetic and segmented trees.

3. Results

SynGROW achieves more than an order-of-magnitude speedup compared with constrained constructive optimization (CCO) [3], while reducing the energy expenditure of generated trees by up to 24%. In addition, CCO-based methods fail to accurately reproduce segmented vascular trees, as highlighted in Figure 1 for a hepatic vein, whereas SynGROW achieves excellent agreement across all datasets tested. Furthermore, the calibrated scaling laws are in good agreement with experimental data.



Figure 1: Comparison of trees against segmentation data of a hepatic vein (terminal nodes in blue).

4. Discussion and Conclusions

The results establish global optimization as a governing principle of vascular design in organs. Improved agreement with segmented vasculature and distinct organ-specific scaling laws show that local optimality, and consequently methods like CCO, are insufficient to explain vascular architecture. SynGROW provides the first practical framework to utilize this principle for synthetic vascular tree generation.

5. References

1. Jessen E. et al., J. R. Soc. Interface.; 19(191):20220087 (2022).
2. Jessen E. et al., IEEE Trans. Biomed. Eng.; 72(10):2871-2881 (2025).
3. Sexton Z. et al., Science; 388(6752):1198-1204 (2025).

Acknowledgements:

This work was supported by the European Research Council (ERC) through the European Union's Horizon 2020 Research and Innovation Programme under Grant 759001, achieved as part of the ERC Starting grant Project 'ImageToSim'.

COMPUTATIONAL MODELING OF THE CONTRACTILE BEHAVIOR OF ENGINEERED HEART TISSUES

Silvia Spadoni (1), Silvia Todros (2), Josè Manuel Pioner (3), Piero G. Pavan (2,4), Lorenzo Marcucci (1)

1. Department of Biomedical Sciences, University of Padova, Italy; 2. Department of Industrial Engineering, University of Padova, Italy; 3. Department of Biology, University of Florence, Italy; 4. Fondazione Istituto di Ricerca Pediatrica Città della Speranza, Padova, Italy

1. Introduction

Engineered heart tissues (EHTs) are lab-grown constructs that replicate key features of native heart muscle and are used to study cardiac physiology, drug responses, and regenerative therapies. They consist of a cardiac extracellular matrix (cECM) scaffold populated with human-induced pluripotent stem cell–derived cardiomyocytes (hiPSC-CMs), whose spontaneous beating allows investigation of cellular responses to matrix stiffness variations [1]. However, experiments typically measure only the global mechanical response of EHTs, making it difficult to isolate the effects of CMs contractility and ECM stiffness. To address this limitation, Finite Element Method (FEM)-based models are used to evaluate the effects of matrix stiffness on local stresses and strains generated by cardiomyocyte contraction, providing insight into cell-matrix mechanical interactions.

2. Materials and Methods

Immunofluorescence assays on the sample core (length of about 5 mm) are performed to identify contractile (CMs) and non-contractile (fibrin gel mimicking the cECM) regions using laminin and α-actinin staining.

EHT mechanical behavior is described using a constitutive formulation based on an adapted Hill three-element model [2], calibrated to the activation, force–length, and force–velocity relations of hiPSC-CMs. The FE model also includes CM spatial orientation, represented by a 3D distribution around a preferential direction depending on tissue organization and maturation [3]. The model is implemented via user subroutines in ABAQUS (SIMULIA, Dassault Systèmes®). The geometry reproduces the experimental setup, where the EHT forms between two PDMS pillars that support the tissue and allow for contraction measurement through pillar deflection.

3. Results

CMs contraction induces pillar displacement, influenced by activation level, cECM stiffness, twitch stress generated by CMs, and PDMS stiffness. Numerical simulations of pillars deflection are compared with experimental measurements on a specimen-specific basis to minimize uncertainties related to structural variability across different EHT constructs. The FE model, informed by isometric experimental data for CM contractile capacity, captures the experimental deflection with good fidelity (Fig. 1c). Comparative analyses at two different stiffness values enable investigation of the effects of matrix stiffness on CM contractility.

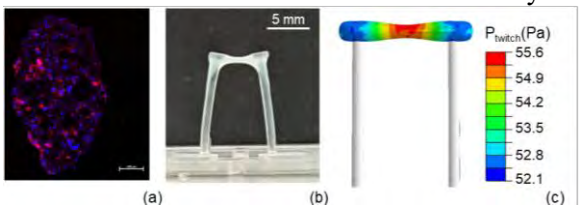


Figure 1: Immunofluorescence cross-section image stained with DAPI and α-actinin (a), EHT geometry (b), preliminary results showing the twitch stress (c).

4. Discussion and Conclusions

Results demonstrate the capability of the proposed approach to evaluate the contractile behaviour of EHT constructs *in vitro* and provide substantial support to the experimental campaign. The model enables the estimation of mechanical quantities that are not easily accessible experimentally and allows investigation of EHT modifications, such as varying cECM stiffness to mimic pathological conditions like fibrotic tissue in Duchenne Muscular Dystrophy.

5. References

1. Querceto et al, J Mol Cel Cardiol, 166:36-49, 2022.
2. Marcucci et al., Biomech Model Mechanobiol, 16: 1833-1843, 2017
3. Holzapfel et al, R. Soc. Interface, 12: 20150188, 2015

USING NEURAL NETWORKS TO DETERMINE CONSTITUTIVE MODEL FORMS FOR MYOCARDIUM IN FULL 3D DEFORMATIONS

Michael Sacks

Willerson Center for Computational Cardiology

Oden Institute for Computational Engineering and Sciences, Department of Biomedical Engineering
University of Texas at Austin, USA

1. Introduction

Development of material models that connect tissue function and local tissue structure require local quantitative structural data, particularly for the fibrous components. Ideally, we are interested in methods for full 3D tissues that can also be potentially used for in vivo studies. Diffusion tensor magnetic resonance imaging (DT-MRI) is a particularly attractive non-invasive method for in vivo tissue structure; based on the observation that the apparent diffusivity of water is greatest along the dominant structural feature orientations (e.g. fibers). DTMRI is particularly attractive in that it produces a symmetric second rank tensor diffusion tensor **D** that represents the local tissue anisotropic structure in a compact form.

2. Materials and Methods

In the present study we developed a universal approach for ex vivo tested 3D myocardium tissue modeling based on use of the full form of **D**, that is all six independent components**,** and not just the eigendirections as in past studies. he approach included separate extensional and compression and shear-like interactions terms. All biomechanical experimental data for the present study were taken from our previous myocardium study. Briefly, passive state myocardial tissue was tested in full 3D mechanical response using our triaxial testing methodology, using pure shear data along the X-Y, X-Z, and Y-Z axes. We first developed a form that incorporated the full diffusion tensor **D**. We take our starting point for model form from related work on meso-structural material models, wherein the response in a direction n is weighted by the mass fraction of material in that direction. To describe the kinematics in tension-compression along n we utilized the pseudo-invariants I4 and I8, the later referred to the n and the material axes. We assumed the form of the mechanical response in any direction n is the same, the tension and compression loading paths will have different material constants. From these considerations, we directly state the 3D general form as

$$\Psi_{AD}(\mathbf{C}) = \int\int \rho(\mathbf{D})\, \Psi_4(I_4)\, dS^2 - p(J-1) \qquad (1)$$

where

$$\rho(\mathbf{D},\mathbf{n},\alpha) = \frac{\mathbf{n}\cdot\mathbf{D}^{\alpha}\cdot\mathbf{n}}{\int\int(\mathbf{n}\cdot\mathbf{D}^{\alpha}\cdot\mathbf{n})\, dS^2} \quad (2)$$

The 3D form for a model form that included extension-shear coupling is

$$\Psi_{FG}(\mathbf{C}) = \int\int \rho(\mathbf{D}) \left[\Psi_4(I_4) + \sum_{i=I}^{III} \Psi_8^{(i)}(I_{8i})\right] dS^2 - p(J-1) \quad (3)$$

Next, to determine the sub-forms of Ψ_4 and Ψ_{8i}, a specialized neural network (NN) training regime was developed. All NN studies were implemented in JAX, a Python library for accelerator-oriented array computation and program transformation, chosen to take advantage of the automatic differentiation tools to minimize the loss functions. Training started with initializing the networks with weights drawn from a normal distribution. After obtaining the gradients, we updated the network parameters, with the cycle repeated until convergence. The optimizer used was stochastic gradient descent (SGD) with an exponential decay learning rate scheduler.

3. Results. The resultant constitutive model was able to simulate the unique anisotropic tension/compression behaviors, including directionally dependent non-linearities. The constitutive model was validated by accurate predictions of tissue in other loading paths not used for parameter estimation.

4. Discussion and Conclusions

The present modeling approach was able to predict myocardial tissue 3D mechanical behavior accurately, as well as shed insight into connections to the underlying myocardial tissue structure via the use of **D**. We are currently incorporating this approach into computation models of the heart that also have the complete **D** data available to demonstrate greater fidelity.

Acknowledgements: NIH R01HL184128

AGENT-BASED MODELING & MACHINE LEARNING TO PREDICT MOLECULAR DETERMINANTS OF FOAM CELL FORMATION

Mané Sarkissian (1), Vicenta Llorente-Cortés (2), Jerome Noailly (1)

1. Pompeu Fabra University, Spain; 2. Spanish National Research Council (CSIC), Spain

Corresponding author: Mané Sarkissian, mane.sargsyan@upf.edu

1. Introduction

Atherosclerosis (AS) is influenced by inflammation and biomechanics and is characterized by foam cell (FC) formation. AS has no cure beyond a very early stage. New approaches are necessary for subclinical characterization. We aimed to create a model of early AS, including key atherogenic processes for improved patient risk stratification and therapeutic target identification.

2. Materials and Methods

A regulatory network model (RNM) was combined with ABM. The RNM was solved with a set of Boolean-based differential equations [1]. It interacted with agent rules integrating oxidative stress; inflammation; LDL modification; wall shear stress (WSS); reverse cholesterol transport (RCT). WSS was either "normal" or "low", as per the activation of endothelial (EC) signaling pathways: normal WSS activated ERK5-KLF2; low WSS activated NF-kB [2]. The model was implemented in BioDynaMo. 18 cases were simulated with 3 HDL levels (low=25 mg/dL, borderline=50 mg/dL and normal=75 mg/dL) combined with the normal and low WSS. Each combination was then simulated with 3 levels of LDL: high (200 mg/dL); borderline (150 mg/dL); normal (90 mg/dL). A sensitivity analysis (SA) explored the effects of the rate of: LDL uptake by CD36, SR-A1 & LRP1 receptors; RCT by ABCA1; LDL modification. Four ensemble models (Random Forest, Gradient Boosting, XGBoost, LightGBM) were trained on 42 model features. Permutation importance analysis (PIA) was conducted on the best-performing model with 100-repeat shuffling and one-sample t-test.

3. Results

Gradient boosting had the best performance on the final year 3 dataset (R^2=1.000, MAE=3.99 FC). PIA revealed no single factor to have an importance above 1.0 showing that the model captured the multi-factorial nature of AS. EC superoxide was the main predictor of FC. High WSS showed a protective role followed by atherogenic MC-CD36 and accumulation of dead MC (Fig. 1).

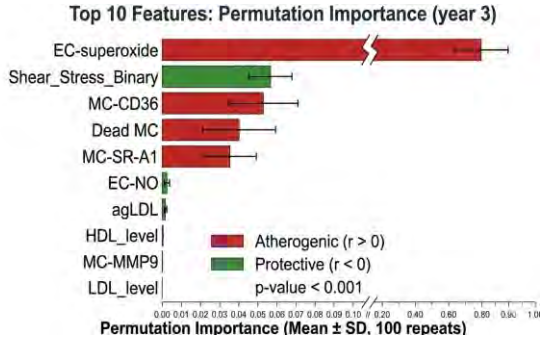


Figure 1: Main AS predictors based on PIA.

4. Discussion and Conclusions

This hybrid AS model uniquely considers the diversity of patient lipid profiles and shows that AS is not caused by a single factor, but by a combination of several conditions (oxidative stress, disturbed WSS, inflammation). The prediction of EC superoxide as a key driver of FC is in line with its literature-established role in triggering inflammation and LDL oxidation. By revealing the role of dead MC in increasing FC (Fig. 1), our model points at an underexplored therapeutic target - MC efferocytosis. Enhanced clearance of dead MC could break the vicious cycle of inflammation and cell death. In the future, the model will be validated by replicating a real cohort of patients on statin treatment.

5. References

1. Mendoza L. et al., J Theor Biol Med Model; 3:13, 2006.
2. Zhao Y. et al., Cell Biochem. Biophys; 78(3):383-389, 2020.

Acknowledgements:
European Research Council (ERC-2021-CoG-O- Health-101044828).

WHOLE BODY HEMODYNAMIC MODEL FOR PATIENTS WITH CIRRHOSIS

Friederike Schäfer* (1), Louis Meyblum* (2), Pavlos Varsos (1), Cristina Ripoll (3), Nicolas Golse (4,5,6), and Irene Vignon-Clementel (1)

1. Inria Saclay Center, France; 2. Department of Interventional Radiology, Pitié-Salpêtrière Hospital, AP-HP, Sorbonne Université, France 3. Internal Medicine IV. Department of Gastroenterology, Hepatology, Infectious diseases and interdisciplinary endoscopy, Jena University Hospital, Germany 4. AP-HP Hôpital Paul-Brousse, France; 5. Inserm UMR-S 1193, France; 6. Université Paris-Saclay, France

**Email: friederike.schaefer@inria.fr, louis.meyblum@aphp.fr*

1. Introduction

Computational models are increasingly applied to support clinical decision-making, but their value depends on reliable predictions across diverse patient populations. Patients with liver cirrhosis pose challenges due to a hyperdynamic circulatory state and a high risk of complications, particularly from portal hypertension. In selected cases, management includes transjugular intrahepatic portosystemic shunt (TIPS) placement. The porto-caval pressure gradient (PPG) is a key risk indicator and is currently measured invasively during TIPS using hepatic venous catheterization. The European ARTEMIs project seeks to improve personalized management of metabolic-associated fatty liver disease (MAFLD) by integrating virtual patient twins into clinical workflows. Here, we present a closed-loop 0D hemodynamic model calibrated with clinical data from patients with cirrhosis, with the goal to enable non-invasive prediction of PPG after TIPS.

2. Materials and Methods

A closed-loop lumped-parameter model of whole-body hemodynamics is presented for patients with liver cirrhosis undergoing TIPS placement. The circulatory system is represented using Windkessel elements to model the pulmonary circulation, digestive organs, liver, and the remaining systemic vasculature. Simulations are conducted using LumpedFlux, a novel in-house framework developed for 0D hemodynamic modelling. The model is calibrated to patients with cirrhosis before TIPS placement. Cardiac function is assessed through pressure-volume loops, stroke volume and cardiac output. Flow rates throughout the porto-mesenteric circulation are non-invasively assessed using 4D flow MRI.

3. Results

Altering model parameters from a healthy population to one with cirrhosis changes the hemodynamic state significantly. Figure 1 shows a representative pressure-volume loop of these two populations, with an increase in preload, a decrease in afterload, and a shift to a higher ventricular volume in patients with cirrhosis compared to the healthy one.

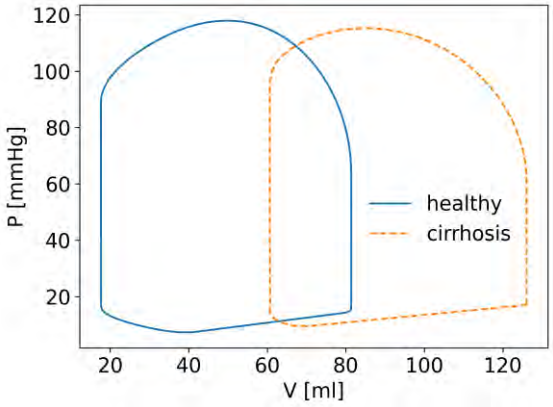


Figure 1: Left ventricle pressure-volume loop with healthy and cirrhosis model parameters.

4. Discussion and Conclusions

The closed loop 0D hemodynamic model is able to replicate the hyperdynamic circulation of patients with cirrhosis observed in clinical practice [1]. Patient-specific calibration will enable post-interventional prediction of hemodynamic quantities like PPG, facilitating hepatic interventional radiology.

5. References

1. Yotti et al., Circ Cardiovasc Imaging, 2014.

Acknowledgements:
The ARTEMIs Project has received funding from the European Union's Horizon 2020 research and innovation programme under grant agreement No 101136299.

BETTER THAN A STAB IN THE SPINE: A COMPUTATIONAL MODEL OF INTRACRANIAL HYPERTENSION

Alireza Sharifzadeh-Kermani* (1, 2), Jet Wright (1, 2), Beatrice Ghitti (2), Finbar Argus (2), Helen Danesh-Meyer (1, 3), Samantha Holdsworth (1), Gonzalo Maso Talou (2)

1. Mātai Medical Research Institute, New Zealand; 2. Auckland Bioengineering Institute, New Zealand; 3. Eye Institute, New Zealand

*Corresponding author. E-mail: alireza.sharifzadeh-kermani@auckland.ac.nz

1. Introduction

Idiopathic intracranial hypertension (IIH) is a serious neurological condition in which intracranial pressure (ICP) increases abnormally without a known cause. IIH requires timely clinical management as it could result in irreversible vision loss. However, its only conclusive diagnosis is via the invasive procedure of lumbar puncture (LP). Current non-invasive alternatives to estimate ICP do not provide clinically accurate estimates to correctly stratify IIH cases. Here, we propose a novel digital twin-based technique that demonstrates stratification in close agreement with the gold standard LP.

2. Materials and Methods

This technique uses a detailed mechanistic model of intracranial pulsatility, incorporating hemodynamics, brain solid mechanics, and cerebrospinal fluid (CSF) flow dynamics [2]. This model is personalised from MRI-based measurements, including brain displacement and blood/CSF flow, to estimate ICP level using a harmonic balance method for efficiency. A sensitivity analysis study was performed to find the minimum anatomical and physiological complexities to be included without affecting ICP level estimations, to accelerate subject-specific model generation.

3. Results

The translational significance of the technique was explored in a prospective clinical study, including 18 cases suspected of IIH, who underwent LP, and 13 age/sex-matched control cases. The ICP predictions of the model demonstrated a close agreement in terms of stratifying IIH and non-IIH cases with LP, quantitatively, a specificity of 100% and sensitivity of 82% (Figure 1).

4. Discussion and Conclusions

Further validation with more cases is ongoing in an extended clinical trial. Preliminary results suggest this safe, cheap, and non-invasive technique could contribute to the clinical diagnosis of individuals with IIH.

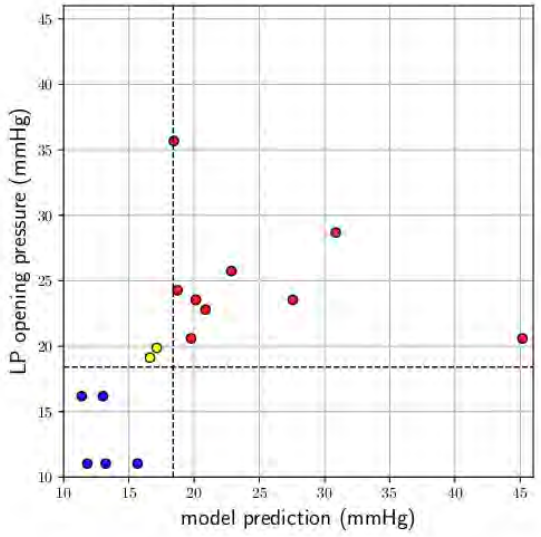


Figure 1: LP opening pressure measurements against model predictions, for subjects suspected of IIH. The black dashed lines are the clinical stratification threshold.

5. References

1. Friedman DI et al., Revised diagnostic criteria for the pseudotumor cerebri syndrome in adults and children (2013).
2. Sharifzadeh-Kermani A et al., Sci Rep; 15(1):42356 (2025).

Acknowledgements:

The authors would like to gratefully acknowledge the generous support of the Royal Society Te Apārangi Marsden Fund (grant number 20-UOA-290), Health Research Council of New Zealand (HRC - grant number 23-293), and an HRC Sir Charles Hercus Fellowship (contract number 24-016).

FMRI-DERIVED OCULOMOTOR SIGNATURES PREDICT VISUAL RECOVERY TRAJECTORIES AFTER STROKE

Jan K. Argasinski (1,2), Mikołaj Turczyniak (1,2), Cemal Koba (1)

1. Sano, Centre for Computational Medicine, Poland; 2. Jagiellonian University, Poland

1. Introduction

Visual deficits are among the most frequent consequences of stroke, yet tools for predicting individual recovery trajectories remain limited. fMRI signals from eye orbits reliably reflect eye movement behaviour, as shown by strong correlations with simultaneously acquired eye-tracking data [1,2]. Here, we test whether eye movements — quantified during resting-state fMRI — capture acute neural disruption indexed by lesion size, stroke severity, and brain network deviation, and whether they track deficit-specific recovery over one year.

2. Materials and Methods

139 stroke patients underwent resting-state fMRI at acute (2 weeks), 3-month, and 1-year timepoints; 28 healthy controls were scanned twice. Patients were classified by visual deficit type: none, perceptual, visual field, eye movement, and multiple. Twelve fMRI-derived oculomotor features were extracted per session: signal amplitude (SD), variability (MSSD), temporal autocorrelation (AC1), and spectral entropy. Brain network functional deviation was computed across seven resting-state networks. Longitudinal trajectories were modelled with GEE; oculomotor–clinical associations with Spearman correlation; all tests FDR-corrected

3. Results

At the acute timepoint, oculomotor features correlated with lesion volume (spectral entropy: r=−0.36, FDR=0.004; AC1: r=+0.30, FDR=0.027; amplitude: r=+0.28, FDR=0.031) and NIHSS (amplitude: r=+0.31, FDR=0.027). Visual field deficit patients showed elevated functional deviation across somatomotor, attention, and control networks (Kruskal-Wallis FDR=0.038; GEE FDR<0.05), with AC1 correlating with ventral attention network deviation (r=+0.28, p=0.001). Longitudinally, AC1 increased across all patients (GEE β=+0.034, FDR=0.043); visual field patients showed the sharpest normalisation of binocular coordination, while eye movement deficit patients exhibited progressive amplitude lateralisation. Spectral entropy and MSSD decreased in tandem, indicating progressive stabilisation of eye movement dynamics.

4. Discussion and Conclusions

Acute oculomotor signatures reflect both structural damage (lesion volume) and functional disruption (brain network deviation, NIHSS), and track distinct recovery trajectories depending on visual deficit type. This positions oculomotor dynamics as accessible, passively acquired predictors of post-stroke visual recovery, a key ingredient for constructing patient-specific models that simulate rehabilitation trajectories from acute-stage measurements. Future work will integrate these oculomotor signatures with network-level deviation scores to build predictive models of behavioural and perceptual recovery after stroke.

5. References

1. Nau, M., et al. Nature Communications; 16(1): 7865 (2025).

2. Koba, C., et al. Network Neuroscience; 5(2): 451–476 (2021).

3. Koba, C., et al. NeuroImage: Clinical; 45: 103755 (2025).

Acknowledgements:

This project was funded by National Science Center, Poland, grant no 2024/55/D/NZ5/02998. National Science Centre, Poland (2024/55/D/NZ5/02998); European Union Horizon 2020 (No 857533); Foundation for Polish Science, International Research Agendas Programme (MAB PLUS/2019/13); Minister of Science and Higher Education, Poland (MEiN/2023/DIR/3796); PLGrid ACK Cyfronet (PLG/2025/018289);

BIOMECHANICAL IMPACT OF INTRAOCULAR PRESSURE ELEVATION ON CRYSTALLINE LENS DYNAMICS

Jorge Grasa (1,2), Agnieszka Boszczyk (3), Agnieszka K. Jóźwik (3), Milad Salimibani (3), Damian Siedlecki (3)

1. Aragón Institute of Engineering Research (I3A), Universidad de Zaragoza, Spain; 2. Centro de Investigación Biomédica en Red en Bioingeniería, Biomateriales y Nanomedicina (CIBER-BBN), Spain; 3. Department of Optics and Photonics, Wrocław University of Science and Technology, Poland

1. Introduction

Elevated intraocular pressure (IOP) modifies the internal fluid environment of the eye, altering the fluid–structure interactions that govern crystalline lens motion [1]. These pressure-driven changes influence how the lens oscillates, displaces, and dynamically responds during eye movements. This work investigates the biomechanical impact of increased IOP on crystalline lens dynamics through fluid–structure interaction (FSI) modelling.

2. Materials and Methods

A 3D idealized eye model was built in COMSOL Multiphysics including the sclera, cornea, zonular fibres, the vitreous humour as part of the solid domain, and a homogeneous crystalline lens. The aqueous humour was defined as the fluid domain to capture fluid–structure interaction under pressure-driven dynamics. Figure 1 shows a section of the finite element mesh of the solid region.

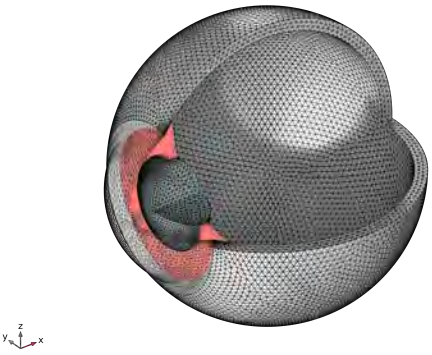


Figure 1: Solid domain of the FSI eye model.

The material properties assigned to the ocular tissues in the model were taken from [1], ensuring consistency with experimentally derived mechanical parameters commonly used in ocular biomechanics simulations.

The model incorporates the acceleration components from [2] to reproduce the dynamics of rapid eye movements. Different intraocular pressure levels were also simulated to assess how pressure variations modify the resulting lens motion.

3. Results

The oscillatory motion of the crystalline lens obtained from the simulations is presented in a form comparable to PIV-PI images, allowing the visualization of lens displacement patterns consistent with those typically captured through Purkinje-based tracking techniques [1].

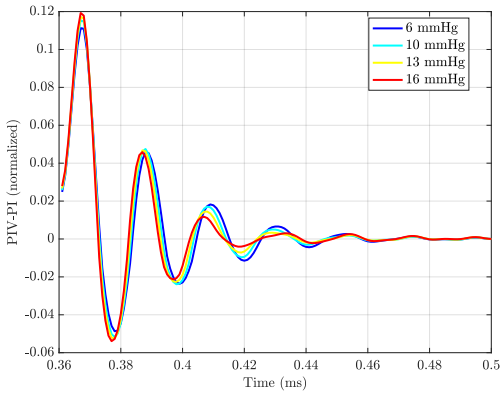


Figure 2: PIV–PI displacement signals for four IOP.

4. Discussion and Conclusions

The simulations show that increasing intraocular pressure alters the amplitude and temporal pattern of crystalline lens oscillations. The FSI model captures these pressure-dependent changes, highlighting the relevance of IOP in shaping lens dynamics and supporting its use for studying ocular mechanical behaviour.

5. References

1. Dahaghin A et al., Front. Bioeng. Biotechnol.; 13:1504769 (2025).
2. Silva AF et al., J. Mech. Behav. Biomed. Mater.; 110:103860 (2020).

TOWARDS A MULTISCALE MODEL OF AGE-DEPENDENT EYE GROWTH

Benedetta Fantaci (1), Elisa Bianchini (3), Jorge Grasa (1, 2), Begoña Calvo (1,2)
1. *Applied Mechanics and Bioengineering (AMB), Instituto de Investigación en Ingeniería de Aragón (I3A), Universidad de Zaragoza, Spain; 2. CIBER-BBN, Spain; 3. Politecnico di Milano, Italy.*

1. Introduction

The human eye undergoes a highly coordinated developmental expansion throughout the first 20 years of life. Disruptions to this biomechanical equilibrium often lead to myopia. To better understand the interplay between tissue mechanics and ocular elongation, a longitudinal multiscale computational model of eye growth is proposed, encompassing prenatal development through to age 20, providing mechanistic insights into the regulatory processes of emmetropization.

2. Materials and Methods

An idealized finite-element (FE) model of the globe (comprising the cornea, limbus, and sclera) was constructed using biometric parameters representative of a 12-week gestation fetus. To simulate developmental expansion, boundary conditions were defined to allow only radial displacements. Growth was modeled via a multiplicative decomposition of the deformation gradient, $\mathbf{F} = \mathbf{F}_e\mathbf{F}_g$, utilizing a local coordinate system to enforce multiple growth directions [1]. The temporal evolution of growth (stretch ratio $\vartheta(t)$) was governed by a dual-phase equation. During the initial phase (prenatal to age three), growth was defined as isotropic in all directions and followed a bi-exponential trajectory to capture rapid early expansion. Subsequently, growth was restricted to the scleral tangential plane, with a single-exponential decay calibrated to the longitudinal data of Rozema et al. [2], reflecting the physiological stabilization of corneal dimensions and scleral thickness.

3. Results

The computational framework successfully captured the age-dependent trajectory of eye expansion as reported in [2], accurately simulating both axial elongation and volumetric ocular growth (Figure 1.a-b). The predicted axial length demonstrated high fidelity when compared against biometric data. Furthermore, the spatial distribution of growth at the terminal stage of development aligned with physiologically observed patterns of eye enlargement, confirming the model's ability to replicate non-uniform expansion across different developmental phases.

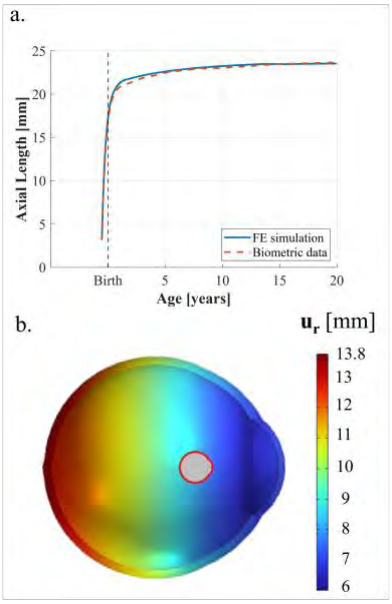


Figure 1.a. Axial Length evolution: experimental vs. simulated; b. radial displacement $\mathbf{u}_r$ at age 20; the initial fetal geometry is shown in grey.

4. Discussion and Conclusions

This work establishes a biomechanically grounded framework for simulating ocular development from early gestation through adulthood, offering a first step toward identifying the mechanical drivers of pathological elongation. Future iterations will integrate biochemical signaling pathways to elucidate the mechanisms of myopic progression.

5. References

1. Fantaci et al., Comp Bio Med, 2024
2. Rozema et al., Ophthalmic Physiol Opt, 2023

Acknowledgements:
This project has received funding from the Department of Industry and Innovation of Aragon through the grant T24–23R and the Spanish Ministerio de Ciencia, Innovación y Universidades. (MICIU/AEI/10.13039/501100011033).

INTEGRATED HYDRAULIC AND SOLUTE TRANSPORT MODELLING IN A SIMPLIFIED LAYERED RETINA–CHOROID SYSTEM

Giulia Sbaruffati (1,3), Riccardo Tripputi (1), Diego Albani (2), Carmen Giordano (1), Rodolfo Repetto (3), Federica Boschetti (1)

1. Politecnico di Milano, Italy; 2. Istituto di Ricerche Farmacologiche Mario Negri IRCCS, Italy; 3. University of Genoa, Italy

Corresponding author: Federica Boschetti, Politecnico di Milano, Italy. Email: federica.boschetti@polimi.it

1. Introduction

Fluid and solute fluxes across the retina and retinal pigment epithelium (RPE) are essential for tissue homeostasis [1]. However, quantitative data on retinal and choroidal permeabilities to fluid and solutes remain limited.

We present an integrated computational–experimental approach to characterise hydraulic behaviour and ongoing solute permeation in a simplified layered retina–RPE–choroid configuration.

2. Materials and Methods

Computational model

A two-dimensional axisymmetric retina-RPE-choroid model, inspired by [2], was implemented in COMSOL Multiphysics. Retina and choroid were described as porous media using a Darcy-Brinkman formulation, with the RPE represented as an internal interface. Physiologically relevant boundary conditions were applied.

The model is modular and structured for progressive integration of solute advection–diffusion transport.

Experimental characterisation

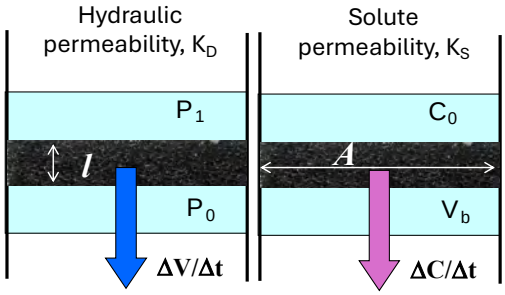
Hydraulic permeability of ex vivo porcine retina–RPE–choroid complex samples was measured using a pressure-driven setup, similarly as in [3], enabling estimation of complex permeability for model parameterisation.

Solute permeation experiments using model molecules of different molecular weights, as reported in [4], are ongoing to support calibration of the coupled transport framework (Figure 1).

3. Results

Experimentally updated choroidal permeability induces redistribution of the pressure field across the layered structure, with a sharp pressure drop at the RPE interface.

The predicted mean trans-RPE flux remains within the physiological order of magnitude (~10^{-8} m/s). Ongoing experiments indicate molecular-weight-dependent solute permeation, supporting extension toward coupled fluid–solute modelling.



$$k_D = \frac{\Delta V \cdot \mu \cdot l}{\Delta t \cdot A \cdot \Delta P} \qquad k_S = \frac{\Delta C \cdot V_b}{\Delta t \cdot A \cdot C_0}$$

Figure 1: Pressure-driven fluid flux (P_1–P_0) and solute permeation configuration (C_0, A, V_β) across the layered retina–RPE–choroid system.

4. Discussion and Conclusions

This study highlights the sensitivity of retinal interstitial flow to experimentally derived hydraulic parameters.

By integrating updated hydraulic measurements and ongoing solute transport characterisation within a structured computational framework, we establish a scalable platform for comprehensive retinal transport modelling.

The modular architecture supports refinement of hydraulic and solute parameters, contributing to experimentally grounded virtual retinal models within the Virtual Physiological Human paradigm.

5. References

1. Antonetti DA, Silva PS, Stitt AW. Nat Rev Endocrinol. 2021;17(4):195–206.
2. Ruffini A et al., Invest Ophthalmol Vis Sci. 2024;65(11):19.
3. Antcliff RJ et al., Arch Ophthalmol. 2001;119(4):539–544.
4. Pitkänen L, Ranta VP, Moilanen H, Urtti A. Invest Ophthalmol Vis Sci. 2005;46(2):641–646.

ANATOMY-DRIVEN MULTIPHYSICS MODELING OF RETINAL LASER TREATMENTS IN HEALTHY AND PATHOLOGICAL CONDITIONS

G Zanellati (1), D Allegrini (2,3), F Auricchio (4), M R Romano (2,3), A Cattenone (4), G Alaimo (4), S Marconi (1,4)

1. Fondazione IRCCS Policlinico San Matteo, Pavia, Italy; 2. Department of Biomedical Sciences, Humanitas University, Milan, Italy; 3. Department of Ophthalmology, Humanitas Gavazzeni–Castelli, Bergamo, Italy; 4. Department of Civil Engineering and Architecture, University of Pavia, Pavia, Italy

1. Introduction

Central Serous Chorioretinopathy (CSC) is a retinal disorder characterized by dysfunction of the retinal pigment epithelium (RPE), accumulation of subretinal fluid, and neuroretinal detachment. While Subthreshold Micropulse Laser Photocoagulation (SMLP) has emerged as an effective treatment that minimizes retinal damage [1], the complex thermal dynamics within ocular tissues are still not well understood. Insufficient understanding of these effects can result in suboptimal or harmful outcomes, depending on the patient's anatomy and device parameters. Although previous research has examined ocular thermal behavior [2], computational modeling of SMLP temperature distributions remains largely unexplored [3], creating a critical gap in treatment optimization.

2. Materials and Methods

The study introduces a computational framework developed in COMSOL Multiphysics 6.1 that combines ray tracing and heat transfer analysis to simulate the entire SMLP procedure. The model includes two main parts: (i) a 3D CAD model of the contact lens employed during treatment, and (ii) a 3D anatomically accurate eye model derived from the Liou & Brennan optical model [4]. The geometry was adapted to also simulate the pathological condition of CSC by including subretinal fluid. Clinically representative SMLP parameters were applied. Ray tracing algorithms determine the laser path and establish a volumetric heat source based on tissue-specific energy absorption. This heat source is directly integrated into the heat transfer solver to produce the full 3D temperature field.

3. Results

The simulation accurately reproduces the propagation of laser beams through the optical system. The resulting thermal maps (Figure 1) reveal a highly localized temperature peak of 44.7 °C on the RPE surface, with thermal diffusion extending into adjacent layers. Cumulative heating across the spot matrix results in a 2 °C increase in temperature at the final spot relative to baseline. Lastly, in the pathological condition, subretinal fluid alters inter-tissue distances, resulting in a decrease in retinal temperature of about 7 °C.

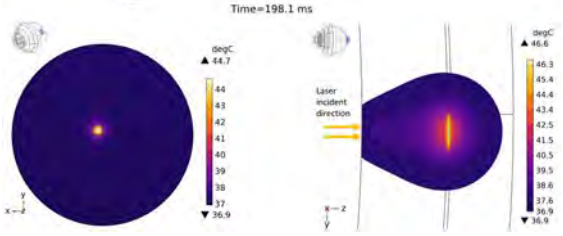


Figure 1: (a) Temperature on RPE surface (b) Temperature distribution in the ocular fundus

4. Discussion and Conclusions

The results demonstrate that anatomy-driven multiphysics modeling enables quantitative investigation of retinal laser–tissue interactions, capturing both localized heating and cumulative multispot effects. The simulated temperature stays within the established therapeutic range [5], reflecting the conservative treatment approach. Comparing healthy and pathological anatomies reveals that subretinal fluid significantly impacts optical energy deposition and heat diffusion, lowering retinal heating and shifting temperature peaks toward deeper layers. The framework provides a physically grounded basis for studying retinal laser treatments in both normal and pathological conditions.

5. References

1. Parodi et al., Pharmaceuticals, 13:359, 2020.
2. J.A. Scott, Phys. Med. Biol., 33:227, 1988.
3. P.H. Zhao et al., Int. J. Therm. Sci., 183:107897, 2023
4. H.L. Liou et al., J. Opt. Soc. Am. A, 14:1684-1695, 1997
5. G. Dorin, Semin. Ophthalmol., 18:147-153, 2003

CONTINUUM AND MICROMECHANICAL MODELLING OF THE RETINA

Damiano Bertolo (1), Federica Boschetti (1), Anna Pandolfi(2)

1. LaBS Department of Chemistry, Materials and Chemical engineering "Giulio Natta", Politecnico di Milano, Italy; 2. Department of Civil and Environmental Engineering Politecnico di Milano, Italy

1. Introduction

The retina is a cellular tissue located in the posterior chamber of the eye, and it is responsible for transducing light into neural signals. The mechanical behaviour of the retina has not been extensively studied due to its fragility, although a few experimental studies have investigated its mechanical behaviour and attempted to describe it using mathematical models [1,2]. Previous investigations revealed that the intricate microstructure of the retina is responsible for a complex nonlinear and time dependent mechanical behaviour that cannot be accurately described with standard continuum mechanics. In this work we propose an innovative model of the retina model that takes into account explicitly its microstructure.

2. Materials and Methods

The proposed finite element model discretizes the retina as an assembly of unit cells, Figure 1, consisting of three layers: an upper network of trusses linking the top of the cells, modelling the internal limiting membrane; an intermediate layer consisting of vertical truss elements, representative of cells such as cones, rods and Muller cells; and a lower network of truss, mimicking the bonds between cells at the interface with retinal pigmented epithelium.

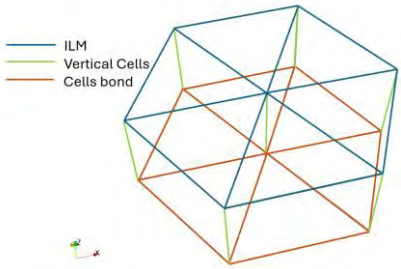


Figure 1: Schematization of the unit cell used for meshing the retinal microstructure.

The unit cell geometry and the discretization of the retinal geometry used in simulations are generated using an ad hoc Matlab code. Numerical simulations are carried out with Abaqus. The truss elements are characterized by a visco-hyperelastic behaviour. Hyperleasticity is accounted for with a Neo-Hookean model, while the viscous behaviour is described through a generalized Maxwell model. The objective of this study was to evaluate the effectiveness of the proposed approach with respect to standard continuum models. To this end, tensile and small punch tests were simulated and compared with experimental data from tests on porcine retinas.

3. Results

Figure 2 presents the results of the numerical simulations of the small punch test comparing the continuum model and the micromechanical model. The micromechanical model provides a superior overall fit of the retina's mechanical response, particularly at low displacements.

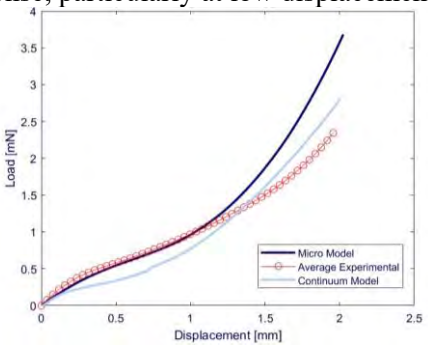


Figure 2: Result of numerical simulations of small punch test with micro and continuum models

4. Discussion and Conclusions

The micromechanical model reveals as a promising alternative approach to continuum models in the description of the mechanical behaviour of the retina. Future work will focus on implementing damage to capture the reduction in stiffness observed at higher strains.

5. References

1. Belgio B et al., Exp Eye Res. 2025; 251:110242
2. Ferrara M et al., Eye, 2021; 35: 1818-1832

Acknowledgements:
Project funded by European Union Next GenerationEU, CUP D43C24001170001.